molecular ce   earch

①

CUG-H05432-1-P25706

SAMPLE COPY

for additional information contact :
ALLIED/ELSEVIER JOURNALS
MARKETING GROUP
30, WEST COTT ROAD, Ph : 82468
MADRAS - 600 014./
750, MOUNT ROAD,
MADRAS - 600 002.

BBA

iochimica
t Biophysica Acta (C)

anaging Editors: P. Borst, P. Cohen,
L.M. van Deenen (Chairman), R.A. Flavell,
K. Radda and E.C. Slater

ol. 804, No. 3, pp. 265–386
ly 20, 1
sevier

SN 0006-3002
0167-4889
BACAQ 804 (3) 265–386 (1984)
AMRDP 804 (3) 265–386 (1984)

PUBLICATION SCHEDULE FOR 1984

BBA is published according to a volume-numbering scheme that embraces all sections of the journal. In addition, each regular section has its own sequential volume-numbering system, running parallel to the overall BBA scheme set out below.

	BIO-ENERGETICS	BIO-MEMBRANES	GENE STRUCTURE AND EXPRESSION	PROTEIN STRUCTURE AND MOLECULAR ENZYMOLOGY	LIPIDS AND LIPID METABOLISM	GENERAL SUBJECTS	MOLECULAR CELL RESEARCH	BBA REVIEWS
Jan.	764/1 = B66/1	769/1 = M115/1 769/2 = M115/2	781/1 = N8/1	784/1 = P19/1 784/2 = P19/2	792/1 = L67/1	797/1 = G109/1	803/1 = C5/1	In addition to the regular volumes of BBA, three volumes of BBA REVIEWS will be published (a) BBA REVIEWS ON BIOENERGETICS Vol. 768 = BR12 (b) BBA REVIEWS ON BIOMEMBRANES Vol. 779 = MR13 (c) BBA REVIEWS ON CANCER Vol. 780 = CR11
Feb.	764/2 = B66/2	769/3 = M115/3 770/1 = M116/1	781/2 = N8/2	784/3 = P19/3 785/1 = P20/1	792/2 = L67/2	797/2 = G109/2 797/3 = G109/3	803/2 = C5/2	
March	764/3 = B66/3	770/2 = M116/2 771/1 = M117/1	781/3 = N8/3	785/2 = P20/2 785/3 = P20/3	792/3 = L67/3 793/1 = L68/1	798/1 = G110/1	803/3 = C5/3	
April	765/1 = B67/1	771/2 = M117/2 772/1 = M118/1		786/1 = P21/1 786/2 = P21/2	793/2 = L68/2	798/2 = G110/2 798/3 = G110/3	803/4 = C5/4	
May	765/2 = B67/2	772/2 = M118/2 772/3 = M118/3	782/1 = N9/1	786/3 = P21/3 787/1 = P22/1	793/3 = L68/3	799/1 = G111/1	804/1 = C6/1	
June	765/3 = B67/3	773/1 = M119/1 773/2 = M119/2	782/2 = N9/2	787/2 = P22/2 787/3 = P22/3	794/1 = L69/1	799/2 = G111/2 799/3 = G111/3	804/2 = C6/2	
July	766/1 = B68/1	774/1 = M120/1 774/2 = M120/2	782/3 = N9/3	788/1 = P23/1 788/2 = P23/2	794/2 = L69/2 794/3 = L69/3	800/1 = G112/1	804/3 = C6/3	
Aug.	766/2 = B68/2	775/1 = M121/1 775/2 = M121/2	782/4 = N9/4	788/3 = P23/3 789/1 = P24/1	795/1 = L70/1	800/2 = G112/2 800/3 = G112/3	804/4 = C6/4	
Sept.	766/3 = B68/3	775/3 = M121/3 776/1 = M122/1		789/2 = P24/2 789/3 = P24/3	795/2 = L70/2	801/1 = G113/1	805/1 = C7/1	
Oct.	767/1 = B69/1	776/2 = M122/2 777/1 = M123/1	783/1 = N10/1	790/1 = P25/1 790/2 = P25/2	795/3 = L70/3 796/1 = L71/1	801/2 = G113/2 801/3 = G113/3	805/2 = C7/2	
Nov.	767/2 = B69/2	777/2 = M123/2 778/1 = M124/1	783/2 = N10/2	790/3 = P25/3 791/1 = P26/1	796/2 = L71/2	802/1 = G114/1	805/3 = C7/3	
Dec.	767/3 = B69/3	778/2 = M124/2 778/3 = M124/3	783/3 = N10/3	791/2 = P26/2 791/3 = P26/3	796/3 = L71/3	802/2 = G114/2 802/3 = G114/3	805/4 = C7/4	
	5 volumes [a]	11 volumes [b]	3 volumes	8 volumes	5 volumes	6 volumes	3 volumes	
	Total 42 volumes [c] plus Cumulative Index (1983).							

Authors should submit their manuscripts (three copies) for publication in BIOCHIMICA ET BIOPHYSICA ACTA by sending them to one of the Managing Editors:

Dr. P. Borst, c/o BBA Editorial Secretariat, P.O. Box 1345, 1000 BH Amsterdam, The Netherlands
Dr. P. Cohen, Department of Biochemistry, Medical Sciences Institute, University of Dundee, Dundee, DD1 4HN, U.K.
Dr. L.L.M. van Deenen, c/o BBA Editorial Secretariat, P.O. Box 1345, 1000 BH Amsterdam, The Netherlands
Dr. R.A. Flavell, c/o BBA Editorial Secretariat, P.O. Box 1345, 1000 BH Amsterdam, The Netherlands
Dr. G.K. Radda, Department of Biochemistry, University of Oxford, South Parks Road, Oxford, OX1 3QU, U.K.
Dr. E.C. Slater, c/o BBA Editorial Secretariat, P.O. Box 1345, 1000 BH Amsterdam, The Netherlands.

Detailed information for contributors may be found in Biochim. Biophys. Acta 715 (1982) 1–23, also published as the 1982 edition of the booklet

INFORMATION FOR CONTRIBUTORS TO BIOCHIMICA ET BIOPHYSICA ACTA

which is available free of charge from the BBA Editorial Secretariat.

P25706

Subscription information

1984 BBA Molecular Cell Research, Volumes 803–805 (3 volumes in 12 issues) Dfl. 645 (US$ 248) + Dfl. 63 (US$ 24) postage, packaging and handling. Total price: Dfl. 708 (US$ 272).
1984 BBA full subscription, Volumes 764–805 (42 volumes in 126 issues), Dfl. 6720 (US$ 2585) + Dfl. 882 (US$ 339) postage, packaging and handling. Total price: Dfl. 7602 (US$ 2924).
The Dutch guilder price is definitive. The U.S. dollar price is subject to exchange-rate fluctuations and is given only as a guide.
Journals are sent by air to North America at no extra charge, and by surface delivery to all other countries. Airmail and SAL (Surface Airlifted Mail) rates for other countries are available upon request.
Subscription orders can be entered only by calendar year (Jan.–Dec.) and should be sent to Elsevier Science Publishers, Journals Department, P.O. Box 211, 1000 AE Amsterdam, The Netherlands, Tel. (020) 5803 642, Telex 18582, or to your usual subscription agent.
Claims for missing issues should be made within 3 months of publication, otherwise they cannot be honoured free of charge.
The Publisher reserves the right to issue additional volumes during the course of the year. Such volumes will be invoiced before publication and delivered after receipt of payment.
In the United States and Canada: for further information concerning this or any other Elsevier Science Publishers journal, contact Elsevier Science Publishers, Journal Information Center, 52 Vanderbilt Avenue, New York, NY 10017, U.S.A., Tel. (212) 867 9040.

Vol. 804, 768, 866, 865
No. 3 [illegible]

Biochimica et Biophysica Acta, 804 (1984) 265–274
Elsevier

BBA 11323

PROSTAGLANDIN MODULATION OF *N*-FORMYLMETHIONYLLEUCYLPHENYLALANINE-INDUCED TRANSMEMBRANE POTENTIAL CHANGES IN RAT NEUTROPHILS

JOSEPH C. FANTONE, RICARDO E DUQUE and SEM H. PHAN

Department of Pathology, University of Michigan Medical School, Ann Arbor, MI 48109 (U.S.A.)

(Received December 8th, 1983)

Key words: N-Formylmethionylleucylphenylalanine, Membrane potential; (Rat neutrophil)

Prostaglandins of the E-series (PGEs) and PGI_2 will inhibit formylmethionylleucylphenylalanine- (f-Met-Leu-Phe) induced lysosomal enzyme release and superoxide-anion (O_2^-) production by neutrophils. The inhibitory effects of PGEs and PGI_2 on neutrophil functional responses have been correlated with their ability to increase intracellular cAMP. In this study we have examined the effects of PGEs and PGI_2 on f-Met-Leu-Phe- and phorbol-myristate-acetate-induced rat neutrophil membrane potential changes using an optical probe of membrane potential 3,3-dipropylthiodicarbocyanine iodide. 15-(*S*)-15-methyl-PGE_1 (15-methyl-PGE_1), a stable analogue of PGE_1 and PGI_2 inhibited f-Met-Leu-Phe-induced transmembrane potential changes in a dose-dependent manner. This inhibition was correlated with the ability of these agents to increase intracellular cAMP levels and inhibit O_2^- production and degranulation. In contrast, 15-methyl-PGE_1 and PGI_2, did not inhibit phorbol-myristate-acetate-induced transmembrane potential changes and O_2^- production. These results suggest independent mechanisms of activation of neutrophils by phorbol myristate acetate and f-Met-Leu-Phe, and they also suggest that the inhibitory effects of prostaglandins and cAMP on f-Met-Leu-Phe-stimulated cells is at a step or steps prior to activation of those processes involved in effecting changes in transmembrane potential, which are common to both stimuli.

Introduction

Stimulation of certain neutrophil functions by f-Met-Leu-Phe is initiated by its binding to a specific formyl peptide receptor on the plasma membrane. One of the early events following the binding of f-Met-Leu-Phe to its receptor is a change in sodium, potassium and calcium ion fluxes across the plasma membrane, associated with a change in the transmembrane potential. These events have been shown to precede the release of superoxide anion and lysosomal degranulation. A high degree of correlation of stimulus-induced changes in transmembrane potential with the production of O_2^- and degranulation has been demonstrated [1–3].

Prostaglandins of the E series (PGEs) and PGI_2 have been shown to inhibit neutrophil-dependant inflammatory reactions in vivo. Systemic treatment of rats with PGE_1 will inhibit immune complex-induced vasculitis in the skin [4], carrageenin-induced inflammation in the rat footpad [5] and adjuvant arthritis [6]. In addition, pretreatment of neutrophils with PGEs or PGI_2 has been shown to inhibit neutrophil chemotaxis [7], aggregation [8] O_2^- production [9–11] and degranulation [12].

The inhibition of neutrophil stimulation by f-

Abbreviations: f-Met-Leu-Phe, *N*-formylmethionylleucylphenylalanine; ΔF, relative fluorescence change; TPCK, tosyl-L-phenylalanylchloromethyl ketone; di(S)-C_3-(5), 3,3′-dipropylthiodicarbocyanine iodide; PGE_1, prostaglandin E_1; 15-methyl-PGE_1, 15-(*S*)-15-methyl-prostaglandin E_1; PGI_2, prostaglandin I_2; $PGF_{2\alpha}$, prostaglandin $F_{2\alpha}$.

0167-4889/84/$03.00 © 1984 Elsevier Science Publishers B.V.

Met-Leu-Phe is thought to be mediated by increases in intracellular cAMP levels induced by PGEs and PGI_2. Studies performed using mast cells and basophil leukemia cells lines have correlated the inhibition effects of prostaglandins and cAMP on calcium release and degranulation with their ability to inhibit cell membrane-associated phospholipid transmethylation reactions [13]. Additional studies suggest that the inhibitory effects of PGE_1, PGI_2 and cAMP on platelet aggregation are secondary to their ability to decrease intracellular free-calcium levels after stimulation [14,15].

In an effort to clarify the mechanisms by which PGEs and PGI_2 modify neutrophil stimulation, we have investigated the effects of these agents on the transmembrane potential change associated with f-Met-Leu-Phe stimulation of rat neutrophils. We have found that PGE's, PGI_2 and other agents which increase intracellular cAMP levels inhibit f-Met-Leu-Phe-induced transmembrane potential changes at concentrations which also inhibit superoxide-anion production and degranulation. The data indicate that these agents can alter an early biophysical response of rat neutrophil plasma membrane to f-Met-Leu-Phe stimulation; and further suggest that this effect may be mediated by increases in intracellular cAMP levels.

Materials and Methods

Animals and chemicals. Adult female Long Evans rats, weighing approx. 400 g, were used throughout this study. All chemicals were purchased from Sigma (St. Louis, MO), unless otherwise noted. Prostaglandins, including 15-(*S*)-15-methyl-PGE_1, were kindly provided by Dr. John Pike of the Upjohn Co. (Kalamazoo, MI). The cyanine dye 3,3′-dipropylthiodicarbocyanine (di(S)-C_3-(5)) was obtained from Molecular Probes Incorporated (Junction City, OR). Prostaglandins were prepared as stock solutions in ethanol (10 mg/ml). Cytochalasin B (5 mg/ml), and *N*-formylmethionylleucylphenylalanine were prepared and stored as $1 \cdot 10^{-2}$ M tock solutions in dimethylsulfoxide at −20 °C.

Preparation of neutrophils and enzyme and O_2^- assays. Cells were suspended in a balanced salt solution consisting of 138 mM NaCl/5.4 mM KCl/1.6 mM $CaCl_2$/0.8 mM $MgSO_4$/0.8 mM Na_2HPO_4/0.8 mM KH_2PO_4/10 mM Hepes (pH 7.4). Neutrophils were obtained from rat peritoneal cavities approx. 16 h after injection of 50 ml of 1.0% oyster glycogen in 0.9% of saline, as previously described [16]. Lysosomal enzyme release was performed by incubating $2 \cdot 10^6$ cells in the presence of 5 μg/ml cytochalasin B at varying concentrations of f-Met-Leu-Phe in a total volume of 250 μl for 10 min at 37 °C. Reactions were terminated by placing the tubes in an ice-bath followed by centrifugation. *N*-Acetyl-β-D-glucosaminidase, lysozyme and lactate dehydrogenase activities were assayed in the supernatant, as previously described [17,18]. All assays were performed in triplicate, and the data are expressed as percentage of maximum (as assessed by using 0.1% Triton X-100 to lyse cells completely) enzyme release (±S.E.). The amount of superoxide anion produced was determined by the superoxide dismutase-inhibitable reduction of ferricytochrome *c* by stimulated cells, as previously described [9], and the results are expressed as nmol $O_2^-/10^6$ cells per 10 min, using an extinction coefficient of 21.2 $cm^{-1} \cdot mM^{-1}$ at 550 nm. All assays were performed in triplicate and data are expressed as mean values ± S.E.

Measurement of membrane potential changes. Membrane potential changes were measured as previously described [3]. Briefly, neutrophils ($2 \cdot 10^6$ cells/ml) were exposed to $2 \cdot 10^{-6}$ M diS-C_3-(5) at 37 °C with constant stirring of the cell suspension, until (usually after less than 5 min) there was no change in the fluorescence intensity as measured using a Varian SF330 spectrofluorimeter. The cells were then stimulated with various concentrations of f-Met-Leu-Phe or phorbol myristate acetate, and the maximum change in fluorescence (excitation at 622 nm, emission as 655 nm and band widths of 10 nm) was determined. The resting membrane potential was determined using the 'null point' method as described previously [3]. Membrane potential changes were expressed as the maximum change in fluorescence (ΔF).

Measurement of cAMP levels. 1.0 ml of rat neutrophils ($5 \cdot 10^6$ cells/ml) were incubated in the presence or absence of prostaglandins for 5 min at 37 °C. The reaction was stopped by the addition of trichloroacetic acid, to a final concentration of 6%. The supernates obtained after centrifugation

(2000 × g for 50 min) were extracted three times with diethylether (1.0 ml vol.) to remove trichloroacetic acid. The aqueous phase was then evaporated to dryness. The dried samples were then resuspended in 0.05 M sodium acetate (pH 6.2), and cAMP levels were determined by radioimmunoassay (New England Nuclear, Boston MA).

Statistical analysis. Student's *t*-test (two-tailed analysis) was used to compare the mean values of the responses of treated cells with those for non-treated control cells. *P* values less than 0.05 were considered statistically significant.

Results

Effects of prostaglandins on f-Met-Leu-Phe-induced transmembrane potential changes

The effect of 15-methyl-PGE$_1$, a stable analogue of PGE$_1$ [4], on f-Met-Leu-Phe-induced changes in ΔF of rat neutrophils incubated with di(S)-C$_3$-(5) was examined. 15-methyl-PGE$_1$ inhibited f-Met-Leu-Phe-induced transmembrane potential changes in a dose-dependent manner (Fig. 1). $1 \cdot 10^{-4}$ M 15-methyl-PGE$_1$ inhibited f-Met-Leu-Phe-induced ΔF by more than 60% over a broad range of concentrations of stimulus. $1 \cdot 10^{-5}$ M 15-methyl-PGE$_1$ was much less effective in inhibiting f-Met-Leu-Phe-induced ΔF at each concentration of stimulus. Increasing concentrations of f-Met-Leu-Phe failed to overcome totally the inhibitory effects of 15-methyl-PGE$_1$, even at concentrations of stimulus as high as $1 \cdot 10^{-6}$ M. The inhibition of the f-Met-Leu-Phe-induced

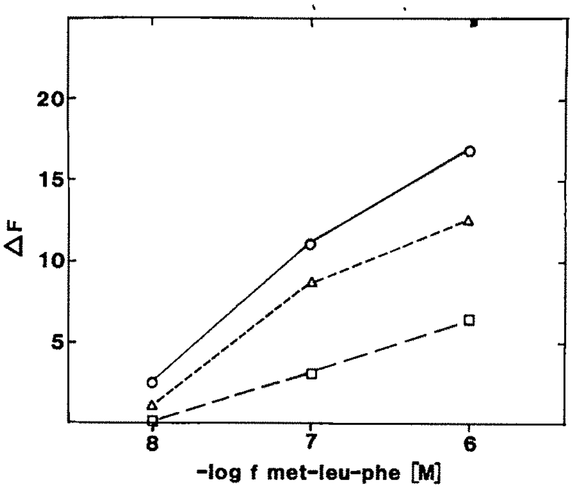

Fig. 1. Inhibition of f-Met-Leu-Phe-induced transmembrane potential changes. $2 \cdot 10^6$ neutrophils/ml were equilibrated with di(S)-C$_3$-(5) (2 μM, final concentration). Varying doses of f-Met-Leu-Phe were added to cells pretreated for 5 min at 37 °C with; ethanol (0.1%, final concentration), (○——○), 15-methyl-PGE$_1$ (10^{-5} M), (△- - -△), and 15-methyl-PGE$_1$ ($1 \cdot 10^{-4}$ M), (□——□). Results are duplicate determinations with variations smaller than 10%.

TABLE I

EFFECT OF PROSTAGLANDINS ON f-Met-Leu-Phe-INDUCED CHANGES IN FLUORESCENCE OF diS-C$_3$-(5)-TREATED RAT NEUTROPHILS.

Rat polymorphonuclear neutrophils were equilibrated with diS-C$_3$-(5) prior to pre-treatment with each reagent (37 °C, 5 min.) Cells were stimulated with f-Met-Leu-Phe, and the maximum change in fluorescent intensity (ΔF) was determined. ΔF values represent means ± S.E. Each experiment shown is a representative example from at least three separate experiments n.s., not significant.

Treatment	ΔF	% inhibition	*P* value
f-Met-Leu-Phe ($1 \cdot 10^{-6}$ M)	19.8 ± 1.6	–	–
f-Met-Leu-Phe + 15-methyl-PGE$_1$ ($1 \cdot 10^{-5}$ M)	11.2 ± 0.2	43.3	< 0.01
f-Met-Leu-Phe + PGI$_2$ (1 10^{-5} M)	12.2 ± 1.9	38.1	< 0.05
f-Met-Leu-Phe + PGF$_{2\alpha}$ ($1 \cdot 10^{-5}$ M)	23.5 ± 5.0	−17.2	n.s.
f-Met-Leu-Phe ($1 \cdot 10^{-7}$ M)	26.0 ± 1.2	–	–
f-Met-Leu-Phe + 15-methyl--PGE$_1$ ($3 \cdot 10^{-5}$ M)	14.8 ± 1.7	43.1	< 0.001
f-Met-Leu-Phe + dibutyryl cAMP ($1 \cdot 10^{-3}$ M)	14.5 ± 2.0	44.2	< 0.001
f-Met-Leu-Phe + isoproterenol ($5 \cdot 10^{-6}$ M) + theophylline ($5 \cdot 10^{-4}$ M)	15.7 ± 0.9	39.6	< 0.001

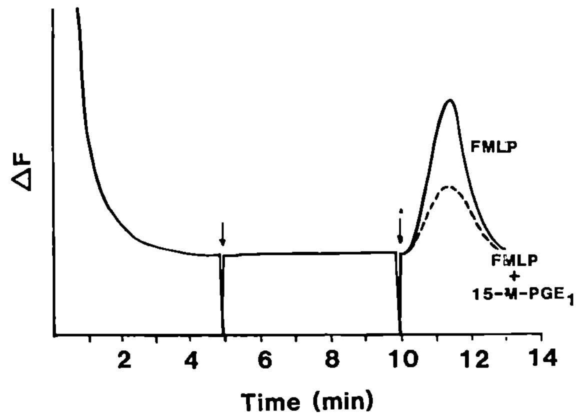

Fig. 2. Effect of 15-methyl-PGE$_1$ on f-Met-Leu-Phe-induced di(S)-C$_3$-(5) fluorescence. $2 \cdot 10^6$ neutrophils/ml were equilibrated with di(S)-C$_3$-(5) (2 μM, final concentration). Cells were pre-treated (↓) with either ethanol (0.1% final concentration) (———) or 15-methyl-PGE$_1$ (10 μM, final concentration) (- - - - -) for 5 min at 37 °C prior to stimulation with f-Met-Leu-Phe ($1 \cdot 10^{-7}$ M, final concentration). The second arrow indicates addition of f-Met-Leu-Phe (FMLP).

transmembrane potential change by 15-methyl-PGE$_1$ demonstrated a molecular class specificity, since PGI$_2$, but not PGF$_{2\alpha}$, also inhibited f-Met-Leu-Phe-induced fluorescence changes (Table I). Although 15-methyl-PGE$_1$ pretreatment of rat neutrophils decreased the maximum f-Met-Leu-Phe-induced transmembrane potential change, it did not alter the lag time to achieve maximal fluorescence (Fig. 2).After a 5 min preincubation of rat neutrophils with 15-methyl-PGE$_1$ ($1 \cdot 10^{-5}$ M), the fluorescence change with f-Met-Leu-Phe occurred rapidly, reaching a maximum within 60 s, followed by a gradual decrease in fluorescence.

Pre-treatment of rat neutrophils with 15-methyl-PGE$_1$ did not significantly alter the baseline fluorescence of di(S)-C$_3$-(5) or the resting membrane potential. The resting membrane potential of rat neutrophils in the absence of prostaglandins was calculated to be −60.2 mV, while in the presence of 15-methyl-PGE$_1$, ($1 \cdot 10^{-4}$ M) the resting membrane potential was −58.0 mV. Both of these values are consistent with previously published values [19,20] and were not significantly different.

The inhibitory effect of 15-methyl-PGE$_1$ on f-Met-Leu-Phe-induced transmembrane potential changes was reversible. Neutrophils which had been washed (twice) with buffered salt solution (see Materials and Methods) at 4 °C and incubated at 37 °C for 10 min after pre-incubation with 15-methyl-PGE$_1$ ($1 \cdot 10^{-5}$ M) showed no inhibition of f-Met-Leu-Phe-induced transmembrane potential changes (data not shown) and O_2^- production [9]. In addition, pre-incubation periods of 30 s with 15-methyl-PGE$_1$ produced reproducible and significant inhibition of f-Met-Leu-Phe-induced transmembrane potential changes and O_2^- production (data not shown). This correlates with the rapid increase in intracellular cAMP levels associated with PGE$_1$ and PGI$_2$ exposure of neutrophils [7,12].

Effect of dibutyryl cAMP and isoproterenol on f-Met-Leu-Phe-induced transmembrane potential changes

Since the inhibitory effects of PGEs and PGI$_2$ on neutrophil functional responses are thought to be mediated by activation of adenylate cyclase and increased intracellular cAMP levels, the effects of other agents known to elevate cAMP levels on f-Met-Leu-Phe-induced fluorescence changes were determined. Both dibutyryl cAMP and isoproterenol in the presence of theophylline inhibited f-Met-Leu-Phe-induced fluorescence changes in a dose-dependent manner (Table I). Preincubation of rat neutrophils with dibutyryl cAMP at a concentration of $1 \cdot 10^{-3}$ M inhibited f-Met-Leu-Phe-induced changes in transmembrane potential by 44.2%. At concentrations of dibutyryl cAMP less than $1 \cdot 10^{-4}$ M no inhibition of transmembrane potential changes was observed (data not shown). Isoproterenol ($5 \cdot 10^{-6}$ M) in the presence of theophylline ($5 \cdot 10^{-4}$ M) (concentrations previously shown to produce significant increases in neutrophil intracellular cAMP levels [7,12]), produced a similar degree of inhibition (39.6%) of f-Met-Leu-Phe-induced transmembrane potential changes. However, in the absence of theophylline or at concentrations of isoproterenol less then $1 \cdot 10^{-6}$ M, minimal inhibition of transmembrane potential changes was observed.

Correlation of inhibition effects of prostaglandins on transmembrane potential changes with functional responses

The dose-dependent inhibitory effect on f-Met-

TABLE II

EFFECT OF PROSTAGLANDINS ON PHORBOL-MYRISTATE-ACETATE-INDUCED CHANGES IN FLUORESCENCE OF di(S)-C_3-(5)-TREATED RAT NEUTROPHILS

Rat polymorphonuclear neutrophils were treated as described in Table I. Cells were stimulated with phorbol myristate acetate, and the maximum change in fluorescent intensity (ΔF) was determined. ΔF values represent means ± S.E. Each experiment shown is a representative example from at least three separate experiments. n.s., not significant.

Treatment	ΔF	% inhibition	P value
Phorbol myristate acetate (100 ng/ml)	16.6 ± 0.2	–	–
Phorbol myristate acetate + 15-methyl-PGE_1 ($1.2 \cdot 10^{-4}$ M)	16.0 ± 0.6	3.6	n.s.
Phorbol myristate acetate + 15-methyl-PGE_1 ($6 \cdot 10^{-5}$ M)	15.7 ± 1.4	5.4	n.s.
f-Met-Leu-Phe ($1 \cdot 10^{-5}$ M)	16.5 ± 0.3	–	–
f-Met-Leu-Phe + 15-methyl-PGE_1 ($6 \cdot 10^{-5}$ M)	10.7 ± 0.9	35.2	< 0.001
Phorbol myristate acetate (100 ng/ml)	19.2 ± 1.3	–	–
Phorbol myristate acetate + 15-methyl-PGE_1 ($1 \cdot 10^{-5}$ M)	20.2 ± 1.3	−1.1	n.s.
Phorbol myristate acetate (10 ng/ml)	17.2 ± 0.6	–	–
Phorbol myristate acetate + 15-methyl-PGE_1 ($1 \cdot 10^{-5}$ M)	16.7 ± 0.3	2.9	n.s.
f-Met-Leu-Phe ($1 \cdot 10^{-6}$ M)	30.0 ± 1.2	–	–
f-Met-Leu-Phe + 15-methyl-PGE_1 ($1 \cdot 10^{-5}$ M)	20.3 ± 1.2	32.6	< 0.01

TABLE III

EFFECT OF PRE-TREATMENT OF RAT NEUTROPHILS WITH 15-METHYL-PGE_1, PGI_2, $PGF_{2\alpha}$, DIBUTYRYL cAMP AND DIBUTYRYL cGMP ON O_2^- SECRETION AND LYSOSOMAL ENZYME RELEASE

Rat polymorphonuclear neutrophils were pre-incubated with the prostaglandins or cyclic nucleotides for 5 min (37 °C) prior to stimulation with f-Met-Leu-Phe. the production of O_2^- and secretion of *N*-acetyl-β-D-glucosaminidase were determined. O_2^- secretion and enzyme release are expressed as the mean ± S.E. n.s., not significant

Treatment	O_2^- (nmol/$2 \cdot 10^6$ cells)	% inhibition	P value	*N*-Acetyl-β-*O*-glucosaminidase % maximum enzyme	% inhibition	P value
f-Met-Leu-Phe ($1 \cdot 10^{-6}$ M)	5.9 ± 0.2	–	–	14.7 ± 0.5	–	–
f-Met-Leu-Phe + 15-methyl-PGE_1 ($1 \cdot 10^{-4}$ M)	2.6 ± 0.2	55.9	< 0.01	8.3 ± 0.3	43.5	< 0.02
f-Met-Leu-Phe + 15-methyl-PGE_1 ($1 \cdot 10^{-5}$ M)	3.3 ± 0.4	44.1	< 0.05	11.2 ± 0.3	23.8	< 0.05
f-Met-Leu-Phe + PGI_2 ($1 \cdot 10^{-4}$ M)	2.5 ± 0.1	57.6	< 0.01	9.2 ± 0.2	37.4	< 0.01
f-Met-Leu-Phe + PGI_2 ($1 \cdot 10^{-5}$ M)	3.7 ± 0.1	37.2	< 0.02	12.3 ± 0.1	16.3	< 0.05
f-Met-Leu-Phe + $PGF_{2\alpha}$ ($1 \cdot 10^{-5}$ M)	5.5 ± 0.2	6.8	n.s.	14.2 ± 0.2	3.4	n.s.
f-Met-Leu-Phe + dibutyryl cAMP ($1 \cdot 10^{-3}$ M)	3.2 ± 0.1	45.7	< 0.02	11.8 ± 0.4	19.7	< 0.05
f-Met-Leu-Phe + dibutyryl cGMP ($1 \cdot 10^{-3}$ M)	5.9 ± 0.2	0.0	n.s.	15.0 ± 0.3	2.0	n.s.

TABLE IV

EFFECT OF PRE-TREATMENT OF RAT NEUTROPHILS WITH 15-METHYL-PGE$_1$ ON PHORBOL-MYRISTATE-ACETATE-INDUCED O_2^- SECRETION.

Rat neutrophils ($2 \cdot 10^6$ cells) were pre-incubated in the presence or absence of 15-methyl-PGE$_1$ ($1 \cdot 10^{-4}$ M) at (37 °C, 5 min) and then stimulated with either phorbol myristate acetate of f-Met-Leu-Phe and incubated for an additional 10 min at 37 °C. The number of nmol of O_2^- produced was determined (see Materials and Methods). Values represent means ± S.E. Each experiment shown is a representative example from at least three separated experiments HBSS, Hanks' balanced salt solution; n.s., not significant.

Treatment	O_2^- (nmol/$2 \cdot 10^6$ cells)	% inhibition	P value
HBSS	3.0 ± 0.4	–	–
Phorbol myristate acetate			
(100 ng/ml)	44.7 ± 0.3	–	–
(10 ng/ml)	39.6 ± 1.0	–	–
(1 ng/ml)	4.3 ± 0.3	–	–
Phorbol myristate acetate			
(100 ng/ml) + 15-methyl-PGE$_1$ ($1 \cdot 10^{-4}$ M)	49.3 ± 1.6	−10.3	n.s.
(10 ng/ml + 15-methyl-PGE$_1$ ($1 \cdot 10^{-4}$ M)	41.9 ± 0.9	−5.8	n.s.
(1 ng/ml + 15-methyl-PGE$_1$ ($1 \cdot 10^{-4}$ M)	4.5 ± 0.1	−4.6	n.s.
HBSS + 15-methyl-PGE$_1$ ($1 \cdot 10^{-4}$ M)	2.7 ± 1.4	10.0	n.s.
f-Met-Leu-Phe ($1 \cdot 10^{-6}$ M)	5.7 ± 0.1	–	–
f-Met-Leu-Phe ($1 \cdot 10^{-4}$ M)	3.1 ± 0.2	45.6	$P < 0.01$

Leu-Phe-induced fluorescence changes by 15-methyl-PGE$_1$ and PGI$_2$ correlated with their inhibitory effects on f-Met-Leu-Phe-induced superoxide anion production and lysosomal enzyme release (Table III). Concentrations of 15-methyl-PGE$_1$ and PGI$_2$ greater than $1 \cdot 10^{-5}$ M and dibutyryl cAMP ($1 \cdot 10^{-3}$ M) consistently inhibited f-Met-Leu-Phe-induced transmembrane potential changes and O_2^- production by approx. 40%. However, these agents appeared to be less effective in inhibiting f-Met-Leu-Phe-induced lysosomal enzyme release. Although 15-methyl-PGE$_1$ and PGI$_2$ at relatively high concentrations ($1 \cdot 10^{-4}$ M) inhibited N-acetyl-β-D-glucosaminidase release to relatively the same degree as O_2^- and transmembrane potential changes, at $1 \cdot 10^{-5}$ M there was only an approx. 20% inhibition of enzyme release compared to a 40% inhibition of O_2^- production and transmembrane potential change. A similar differential effect of dibuturyl cAMP on the functional response of rat neutrophils was observed. Dibutyryl cAMP at $1 \cdot 10^{-3}$ M inhibited lysosomal enzyme release by 19.7%, compared to a 45.7% inhibition of O_2^- production. In contrast, neither PGF$_{2\alpha}$ nor dibutyryl cGMP altered either the functional responses of the cells to f-Met-Leu-Phe or the f-Met-Leu-Phe-induced membrane potential changes. These data suggest a close correlation between changes in transmembrane potential and O_2^- production and a partial dissociation between these two indices of neutrophil stimulation and degranulation.

Effects of prostaglandins on cAMp levels

The ability of 15-methyl-PGE$_1$ to increase rat neutrophil intracellular cAMP levels was verified and was dose-dependent. At a concentration of $1 \cdot 10^{-5}$ M 15-methyl-PGE$_1$ there was a 94% ($P <$ 0.001) increase in intracellular cAMP levels (Table V). This is a similar dose range in which consistent inhibition of f-Met-Leu-Phe-induced changes of both fluorescence and functional responses were observed. However, at concentrations of 15-methyl-PGE$_1$ of $1 \cdot 10^{-6}$ M or theophylline of $5 \cdot 10^{-4}$ M, there was no consistent inhibition of either the f-Met-Leu-Phe-induced changes in transmembrane potential or functional responses, despite a 20–30% increase in intracellular cAMP levels. These observations suggest that significant elevations of intracellular cAMP levels of approx. 100% above baseline levels are necessary for significant inhibition of f-Met-Leu-Phe-induced responses of glycogen elicited rat neutrophils.

TABLE V

EFFECT OF PROSTAGLANDIN E_1 AND THEOPHYLLINE ON INTRACELLULAR cAMP LEVELS OF RAT NEUTROPHILS

0.5 ml of rat polymorphonuclear neutrophils ($1 \cdot 10^7$ cells/ml) were pre-incubated at 37 °C for 5 min. in the presence or absence of 15-methyl-PGE_1 or theophylline. The reactions were terminated by the addition of trichloroacetic acid (final concentration 6%), and the concentrations of cAMP were determined. All assays were performed in triplicate and Student's *t*-test was used to compare treated with nontreated cells. Each experiment shown is a representative example from at least three separate experiments

Treatment	cAMP concentration ($\text{pmol}/5 \cdot 10^6$ cells)	% increase	*P* value
None	4.01 ± 0.07	–	–
15-Methyl-PGE_1 (1.0 μM)	5.15 ± 0.25	28.4	< 0.05
15-Methyl-PGE_1 (10 μM)	7.79 ± 0.32	94.0	< 0.001
15-Methyl-PGE_1 (100 μM)	7.47 ± 0.97	86.2	< 0.05
Theophylline ($5 \cdot 10^{-4}$ M)	4.80 ± 0.06	19.7	< 0.02

Effects of 15-metyl-PGE_1 on phorbol-myristate-acetate-induced responses

In contrast to the inhibitory effects of 15-methyl-PGE_1 on f-Met-Leu-Phe-induced neutrophil responses, no inhibition of phorbol-myristate-acetate-induced membrane potential changes (Table II) and O_2^- production (Table IV) were observed over a range of doses of stimulus. These studies indicate a stimulus-specific inhibitory effect of 15-methyl-PGE_1 on the stimulated neutrophil fluorescence changes of di(S)-C_3-(5)-treated rat neutrophils and O_2^- production.

Discussion

Prostaglandins of the E series and PGI_2 have been shown to inhibit the production of O_2^-, chemotaxis and secretion of lysosomal enzymes by neutrophils in response to a variety of stimuli, including f-Met-Leu-Phe [7–12]. However, there is a paucity of data examining the effect of prostaglandins on the early biochemical and biophysical events associated with stimulus-response coupling in the neutrophil. The data presented here demonstrate an inhibitory effect of 15-methyl-PGE_1 and PGI_2 on f-Met-Leu-Phe-induced membrane potential changes of rat neutrophils. This is correlated with the inhibitory effects of 15-methyl-PGE_1, PGI_2 and other agents known to increase intracellular cAMP levels on f-Met-Leu-Phe-stimulated O_2^- production and lysosomal enzyme secretion. Other authors have demonstrated inhibitory effects of PGEs, PGI_2 and cAMP agonists on neutrophil functional responses in a variety of species [7–12]. This study correlates the inhibitory effects of these agents with their ability to inhibit one of the early events associated with stimulus-response coupling in the neutrophil, i.e., changes in cell transmembrane potential.

Recently, Seligman et al. [21] observed a similar inhibition by histamine of f-Met-Leu-Phe-induced changes in transmembrane potential in human neutrophils. This inhibitory effect by histamine was correlated with its ability to inhibit f-Met-Leu-Phe-induced functional responses of human neutrophils and was blocked by H_1 receptor antagonist. Histamine has been shown by other authors to activate neutrophil-adenylate cyclase and increase intracellular cAMP levels [22]. Therefore, similar mechanisms of inhibition of transmembrane potential may underlie the inhibitory effect of histamine, PGEs and PGI_2. This possibility is supported by the close correlation between intracellular cAMP elevation and inhibition of membrane potential changes.

In contrast to the inhibitory effects of 15-methyl-PGE_1 on f-Met-Leu-Phe-induced O_2^- production and changes in membrane potential, 15-methyl-PGE_1 did not inhibit either phorbol myristate acetate induced membrane potential changes or O_2^- production. These observations further clarify the metabolic events associated with stimulus-response coupling in the neutrophil. Several laboratories have described distinct specific receptors for binding of f-Met-Leu-Phe and phorbol myristate acetate to neutrophils [17,24–27]. After binding of f-Met-Leu-Phe to the formyl peptide receptor on the neutrophil, a complex series of events occurs. One of the earliest events includes changes in Na^+, K^+ and Ca^{2+} fluxes across the cell membrane and changes in transmembrane potential [1–3,28,29]. These changes in transmembrane potential can be monitored by changes in the fluorescence intensity of a variety of cyanine dyes, including di(S)-C_3-(5). Subsequent to changes in ion fluxes and transmembrane potential is the expression of the functional responses of the neutrophil, including O_2^- production. Since neither 15-methyl-PGE_1 nor dibutyryl cAMP altered phorbol-myristate-acetate-induced neutrophil responses, it would appear that the primary inhibitory effect of prostaglandins and cAMP on f-Met-Leu-Phe-stimulated cells is at a step or steps prior to activation of those processes involved in effecting changes in transmembrane potential, which are common to both f-Met-Leu-Phe and phorbol myristate acetate stimulation.

Two mechanisms for the inhibition of inflammatory cell activation by prostaglandins and cAMP have been proposed. Studies performed using mast cells and basophil leukemia cell lines suggest that prostaglandins and adenylate cyclase agonists increase cAMP levels and inhibit cell membrane-associated phospholipid transmethylation reactions that occur subsequent to cell stimulation and prior to calcium release and degranulation [13]. If similar mechanisms occur in f-Met-Leu-Phe-stimulated neutrophils, our data would suggest that phorphol myristate acetate stimulation of neutrophils does not require phospholipid transmethylation reactions for changes in membrane potiential and functional responses to occur; and/or the methyltransferase activities associated with phorbol myristate acetate activation of human neutrophils are not regulated by prostaglandins and cAMP.

The second proposed mechanism for the inhibitory activity of prostaglandins as mediated via cAMP is that these agents alter the availability of intracellular free calcium. Studies performed using platelets in which transmethylation reactions do not appear to be a requirement for biological activity [30] indicate that PGI_2 and increased intracellular cAMP levels decrease intracellular free-calcium levels after stimulation [14,15]. The data suggest that increased cAMP levels activate a calcium-dependent ATPase with increased sequestration of free calcium in the dense tubular system. Stimulation of rabbit and human neutrophils with f-Met-Leu-Phe causes a rapid increase in free intracellular calcium, as determined using the calcium-sensitive fluorescent probe quin-2 [31]. This increase in intracellular calcium correlates with the ability of f-Met-Leu-Phe to induce neutrophil degranulation and O_2^- production. In addition, pretreatment of neutrophils with the intracellular calcium antagonist, 8-(*N*,*N*-diethylamino)octyl-3,4,5-trimethoxybenzoate also inhibits f-Met-Leu-Phe-induced O_2^- production [32]. Thus, there is an abundance of data supporting the importance of intracellular calcium for stimulus-response coupling in the neutrophil. However, the role of intracellular free calcium as a second messenger associated with phorbol myristate acetate stimulation of neutrophils is less clear. Although 8-(*N*,*N*-diethylamino)octyl-3,4,5-trimethoxybenzoate inhibits phorbol-myristate-acetate-induced neutrophil O_2^- production [33], experiments by Sha'afi et al. [31], using quin-2, failed to demonstrate a rise in the level of free intracellular calcium with phorbol myristate acetate stimulation. This latter observation may explain the differential affects of prostaglandins on f-Met-Leu-Phe and phorbol-myristate-acetate-induced O_2^- production. The data support the hypothesis that prostaglandins and cAMP modulate intracellular free calcium levels as their primary mechanism of inhibiting neutrophil biologic responses.

Additional effects of prostaglandins on cell membranes have been described. Kury et al. [34] observed increased deformability of PGE_1-treated red blood cells and correlated these changes with a decrease in orientational relaxation times of fatty acid spin-labeled erythrocytes. They concluded that the fatty acid side chains in cell membrane phospholipids are more liquid or fluid in the presence of PGE_1. Therefore, it is possible that the inhibitory activity of 15-methyl-PGE_1 and PGI_2 toward neutrophils are in part secondary to direct alterations of the neutrophil plasma membrane's physicochemical properties. Three recent studies have described alterations in ligand-receptor interactions in prostaglandin treated platelets [35], macrophages [36] and neutrophils [16]. Of particular interest is the observation that neutrophils isolated from rats treated with 15-methyl-PGE_1 show decreased lysosomal enzyme release and O_2^- production in response to f-Met-Leu-Phe stimulation [16]. This is associated with a 2- to 3-fold decrease in binding affinity of f-Met-Leu-Phe to the formyl peptide receptor on these cells. Alterations in f-Met-Leu-Phe receptor interactions may explain the ability of PGEs and cAMP to inhibit membrane potential changes associated with cell stimulation. Additional studies to examine the specificity of PGE_1 and cAMP modulation of neutrophil ligand receptor interactions in vitro are currently in progress. Although the use of cyanine dyes as indicators of changes in transmembrane potential is an indirect technique for studying electrical potential across cell membranes, several authors have demonstrated a high degree of correlation of stimulus-induced fluorescence changes with other indices of cell activation, suggesting that this technique is indeed a valid measure for examining membrane potential changes [1–3]. The relative contributions of plasmalemmal or intracellular organelle membrane potential changes to the changes in fluorescence intensity of cyanine dyes has been discussed in the recent literature [3,37]. Although it is difficult to exclude the possibility that changes of mitochondrial membrane potentials contribute to the observed fluorescence changes associated with f-Met-Leu-Phe stimulation, it would appear that under our experimental conditions the observed changes in fluorescence of di(S)-C_3-(5)-labeled cells most likely represent changes in plasmalemmal membrane potentials.

In summary, our data indicate that 15-methyl-PGE_1 and PGI_2 inhibit in a dose-dependent manner f-Met-Leu-Phe-induced transmembrane potential changes and functional responses of rat neutrophils. The lack of inhibiting effects of these agents on phorbol-myristate-acetate-induced membrane potential changes and superoxide-anion production suggest that this stimulus does not require the prostaglandin-sensitive step(s) to induce these cellular responses. The results confirm previous observations suggesting a close association, if not tight coupling, between transmembrane potential changes and the functional responses of the neutrophil.

Acknowledgements

This study was supported in part by grants from the National Institutes of Health HL-00905, HL-23192 and HL-28737.

References

1 Whitin, J.C., Chapman, C.E., Simons, E.R., Chovaniec, M.E. and Cohen, H.J. (1980) J. Biol. Chem. 255, 1874–1878
2 Seligmann, B.E., Gallin, E.K., Martin, D.L., Shair, W. and Gallin, J.I. (1980) J. Membrane Biol. 52, 257–272
3 Duque, R.E., Phan, S.H., Sulavik, M.C. and Ward, P.A. (1983) J. Biol. Chem. 258, 8123–8128
4 Kunkel, S.L., Thrall, R.T., Kunkel, R.G., Ward, P.A. and Zurier, R.B. (1979) J. Clin. Invest 64, 1525–1528
5 Fantone, J.C., Weingarten, B. and Kunkel, S.L. (1982) Biochem. Pharm. 31, 3126–3128
6 Zurier, R.B. and Quagliata, F. (1971) Nature 234, 304–306
7 Rivkin, I., Rosenblatt, J. and Becker, E.L. (1975) J. Immunol. 115, 1126–1134
8 O'Flaherty, J.T., Kreutzer, D.L. and Ward, P.A. (1979) Prostaglandins 17, 201–210
9 Fantone, J.C. and Kinnes, D.A. (1983) Biochem. Biophys. Res. Commun. 113, 506–512
10 Sedgwick, J.B., Berube, M.C. and Zurier, R.B. (1983) Fed. Proc. (420A).
11 Wong, K. and Freund, K. (1981) Can. J. Phys. Pharm. 59, 915–920
12 Zurier, R.B., Weissmann, G., Hoffstein, S., Kammerman, S. and Tai, H.H. (1974) J. Clin. Invest. 53, 297–309
13 Ishizaka, T., Hirata, F., Ishizaka, K. and Axelrod, J. (1980) Proc. Natl. Acad. Sci. U.S.A. 77, 1903–1906
14 Feinstein, M.D., Egan, J.J., Sha'afi, R.I. and White, J. (1983) Biochem. Biophys. Res. Commun. 113, 598–604
15 Kaser-Glansmen, R., Jakavobe, M., Georger, J. and Lusetter, E.F. (1979) Biochim. Biophys. Acta 466, 429–440.
16 Fantone, J.C., Marasco, W.A., Elgas, L.J. and Ward, P.A. (1983) J. Immunol. 130, 1495–1497
17 Showell, H.J., Freer, R.J., Zigmond, S.H., Schiffman, E., Aswanikumar, S., Corcoran, B. and Becker, E.L. (1976) J. Exp. Med. 143, 1154–1169
18 Woollen, J.W., Heyworth, R. and Walker, P.G. (1961) Biochem. J. 78, 111–119
19 Freedman, J.C. and Laris, P.C. (1980) Int. Rev. Cytol. Suppl. 12, 177–236
20 Utsumi, K., Sugiyama, K., Miyahara, N.M., Owai, M. and Inore, M. (1977) Cell. Struct. Funct. 2, 203–209
21 Seligmann, B.E., Fletcher, M.P. and Gallin, J.T. (1983) J. Immunol. 130, 1902–1909
22 Anderson, R., Glover, A. and Robson, A.R. (1977) J. Immunol. 118, 1690–1698
23 Kitagawa, S., Takaku, F. and Sakamoto, S. (1980) J. Clin. Invest. 65, 74–81
24 Schiffman, E., Corcoran, B. and Wahl, J.M. (1975) Proc. Natl. Acad. Sci. U.S.A. 72, 1059–1062

25 Marasco, W.A., Showell, H.J., Freer, R.J. and Becker, E.L. (1982) J. Immunol. 128, 956–962

26 Lehrer, R.I. and Cohen, L. (1981) J. Clin. Invest. 68, 1314–1320

27 Goodwin, B.J. and Weinberg, J.B. (1982) J. Clin. Invest. 70, 699–706

28 Naccache, P.H., Showell, H.J, becker, E.L. and Sha'afi, R.I. (1979) J. Cell Biol. 83, 179–186

29 Naccache, P.H., Showell, H.J., Becker, E.L. and Sha'afi, R.I. (1977) J. Cell Biol. 75, 635–649

30 Shattil, S.J., Montgomery, J.A. and Chiang, P.K. (1982) Blood 59, 906–912

31 Sha'afi, R.I., White, J.R., Molski, R.F.P., Shefcyk, J., Volpi, M., Naccache, P.H. and Feinstein, M.B (1983) Biochem. Biophys. Res. Commun. 114, 638–645

32 Becker, E.L., Showell, H.J., Naccache, P.H. and Sha'afi, R. (1981) Biochemistry of Acute Allergic Reactions, pp. 257–278, Alan Liss, New York

33 Smith, R.J. and Iden, J.J. (1979) Biochem. Biophys. Res. Commun. 91, 263–271

34 Kury, P.G., Ramwell, P.W. and McConnell, H.M. (1974) Biochem. Biophys. Res. Commun. 56, 478–483

35 Bennett, J.S., Vilaire, G. and Burch, F.W. (1981) J. Clin. Invest. 68, 981–989

36 Razin, E. and Globerson, A (1979) Adv. Exp. Med Biol. 114, 415–422

37 Korchak, H.M., Rich, A.M., Wilkenfeld, C., Rutherford, L.E. and Weissmann, G. (1982) Biochem. Biophys. Res. Commun. 108, 1495–1501

Biochimica et Biophysica Acta, 804 (1984) 275–284
Elsevier

BBA 11317

METABOLIC STUDIES OF MAMMALIAN CELLS BY ^{31}P-NMR USING A CONTINUOUS PERFUSION TECHNIQUE

RICHARD H. KNOP [c], CHI-WAN CHEN [a], JAMES B. MITCHELL [b],
ANGELO RUSSO [b], SCOTT McPHERSON [b] and JACK S. COHEN [a,*]

[a] Laboratory of Theoretical and Physical Biology, National Institute of Child Health and Human Development, the [b] Radiation Oncology Branch, National Cancer Institute and the [c] National Cancer Institute-Navy Oncology Branch, National Institutes of Health, Bethesda, MD 20205 (U.S.A.)

(Received November 23rd, 1983)

Key words: ^{31}P-NMR; Cell perfusion, ATP; Dinitrophenol; Intracellular pH; P_i; (Fibroblast)

Levels of ATP and P_i in metabolically active Chinese hamster lung fibroblasts were monitored noninvasively by ^{31}P-NMR over many hours and under a variety of conditions. The cells were embedded in a matrix of agarose gel in the form of fine threads which were continuously perfused in a standard NMR tube. The small diameter of the thread allows rapid diffusion of metabolites and drugs into the cells. The changes in ATP and P_i levels were followed as a function of time in response to perfusion with a glucose-containing medium, with isotonic saline and with a medium containing 2,4-dinitrophenol, an uncoupler of oxidative phosphorylation. This gel-thread perfusion method should enable routine NMR studies of cellular metabolism, and may have other potential biological applications.

Introduction

A true understanding of cellular biology requires the ability to monitor metabolism noninvasively. NMR spectroscopy has been applied to the noninvasive study of cellular metabolism [1–3]. However, to obtain sufficient signal NMR experiments on cells requires a densely-packed suspension (approx. 10^8 cells/ml). The problems associated with such dense suspensions of cells include hypoxia, rapid consumption of nutrients and build-up of catabolic end-product. Addition of nutrients to the cell suspension and intermittent bubbling of oxygen partially relieve these problems [4,5]. However, effective application of NMR to study the metabolism of cells under controlled conditions which simulate the physiological state as closely as possible requires continuous perfusion.

NMR studies of various isolated perfused organs have been reported [6–9]. But, perfusion of cells or microorganisms is not straightforward, because they flow with the perfusate and block filters used to restrain them. To perfuse cells, it is necessary to sequester them within a limited volume (that of the receiver coil), while allowing perfusate to flow through, and at the same time ensure that the means used to restrain the cells does not prevent the rapid diffusion of metabolites into the cells. Also, it is important not to reduce the quantity of cells within the coil, since this reduces the signal intensity. Several approaches to cell perfusion have been reported [10–13], all of which have some advantages and disadvantages (see Discussion). We have succeeded in overcoming the difficulties involved in cell perfusion by embedding the

---

[*] To whom correspondence should be addressed at Clinical Pharmacology Branch, NCI, NIH, Bethesda, MD 20205, U.S.A.

Abbreviations: DCCD, dicyclohexylcarbodiimide; Hepes, 4-(2-hydroxyethyl)-1-piperazineethanesulfonic acid.

0167-4889/84/$03.00 © 1984 Elsevier Science Publishers B.V

cells in an agarose gel matrix [14] extruded in the form of a fine thread [15]. Cell densities achieved in the packed gel threads are comparable to those in dense cell suspensions. We have shown that the small diameter of the thread (0.5 mm) enables diffusion of nutrients and drugs into the center of the thread in approx. 1 min, and the spaces between the packed threads allow perfusate to flow between them. Previously, we have briefly described the application of this technique to yeast [15]. Here we characterize the method in more detail and describe its application to the study of the metabolism of mammalian cells under well-controlled conditions.

A preliminary account of some of this work was presented by Cohen et al. at the American Society of Biological Chemists' Meeting, San Francisco, CA, June 5–9, 1983.

Experimental

The apparatus. All glassware was sterilized by autoclaving before use. Both the gel thread casting apparatus and the perfusion system were flushed with citric acid/sodium metabisulfite (0.5 g each in 200 ml), absolute ethanol, sterile water, penicillin/streptomycin (0.2 g each in 200 ml) and the growth medium (see below) prior to each experiment. The gel-thread casting system consists of a 15 ml Falcon 2095 conical tube which is connected to a peristaltic pump via a plastic T-joint, and to Teflon tubing (0.5 mm i.d.) that extends to the bottom of the conical tube. The perfusion system includes a 7 inch long 10 mm o.d. NMR tube with a screw-cap top (Wilmad No. 513-TR) and a hollow insert made of Kel-F. The top of the insert is fitted with Teflon inlet tubing (0.8 mm i.d.) connected to a peristaltic pump (Pharmacia model P-3), outlet tubing and an optional temperature probe (for example, Luxtron model 1000B fluoroptic probe). The inlet tubing reaches to the bottom of the NMR tube through the center of the Kel-F insert and is wrapped around with a piece of sponge inside the insert to restrain the gel threads [15].

Gel-thread preparations. Chinese hamster lung fibroblasts (V79) were grown in 850 cm^2 roller flasks in F12 medium (GIBCO, Grand Island, NY) supplemented with 10% fetal calf serum, penicillin (0.14 g/l), streptomycin (0.20 g/l) and 20 mM Hepes at pH 7.35–7.40. The concentration of P_i in this medium was $1 \cdot 10^{-6}$ M, well below the level of ^{31}P-NMR detection. Cells were harvested at mid-log phase by removing with trypsin and rinsing with the growth medium. Approx. $(1.5–2.0) \cdot 10^8$ cells were centrifuged down to a pellet at 400 g for 3 min and were resuspended in approx. 0.7 ml of the medium, and 0.6 ml of a 1.8% low gelling temperature agarose solution at 37 °C was then added to a final concentration of 0.6%. The cell/gel mixture was thoroughly mixed and, while maintained at 37 °C in a water bath, was extruded under mild pressure through the teflon tubing immersed in an ice/water bath into an NMR tube containing the medium. This gel-casting process usually took up to 10 min. The NMR tube was immediately attached to the perfusion system, and the pump was turned on to allow a flow rate of 2.7 ml/min. After the first 10 ml of effluent was collected and discarded, the clear perfusate was recycled.

pH control. The pH value of the perfusate was constantly monitored and was found to lie between 7.35 and 7.40 for up to 3 h. Therefore, replacing the perfusate with fresh medium once every 2–3 h was sufficient to maintain a constant extracellular pH level. The NMR chemical shifts of the P_i as well as ATP signals change as a function of pH [16]. In order to determine the intracellular pH, titration curves of ^{31}P chemical shifts vs. pH were obtained on fibroblast extracts after sonication (60 s) and centrifugation, as well as on a solution mixture of ATP, AMP and P_i, with 85% H_3PO_4 as the external reference. The two experiments gave identical titration curves for the P_i signal.

Temperature control. Because of the air cooling effect on the perfusion inlet and outlet tubings, it was necessary to set the probe temperature at 50 °C (at a flow rate of 2.7 ml/min) so that the gel threads inside the NMR tube could be maintained at 37 ± 1 °C. These settings were determined using a thermocouple (copper-constantan) attached to a digital thermometer, as well as a Luxtron 1000B fluoroptic probe. However, because the thermocouple interfered with radio-frequency absorption in the NMR measurement, only the fluoroptic probe, which is noninterfering, could be used during NMR accumulations. In experiments where perfusion was turned off, the probe temperature was kept at 37 °C in order to provide the same temperature inside the tube. Similarly, for experiments that were carried out at 25 °C the probe was simply set at that temperature.

NMR measurements and perfusion experiments. The perfused sample tube (10 mm Wilmad screw-cap) was placed into the NMR probe with a special tube holder (8.5 cm long, made of Kel-F or Rulon LD) for proper balance. The shimming of the field homogeneity was achieved, without any deuterium-lock or spinning of the sample, by optimizing the water free induction decay signal through the ^{31}P observe channel. The ^{31}P spectra were recorded at 109.3 MHz with a Bruker superconducting magnet on a Nicolet 293A spectrometer equipped with a Nicolet 1180 computer. All spectra were obtained in 2K data points with a spectral window of ± 3000 Hz and a 78° pulse, and a 30 Hz line broadening was applied before Fourier transformation. In the experiments with glucose-containing medium, 22-min spectra (6000 scans) were acquired with a repetition rate of 220 ms. In the saline and dinitrophenol experiments, 30-min (3800 scans) and 15-min (or 10-min) spectra were collected with a repetition rate of 470 ms. All the data presented in the figures are the cumulative results at the end of the 10, 15, 22 or 30 min acquisition periods. Peak intensities were measured directly from the Nicolet computer after a linear base line correction and are accurate to $\pm 10\%$. In order to be certain that the spectral intensities observed reflect the true cellular concentrations of the ATP present, the pulse-repetition rate was varied over a wide range, and it was found that a recycle time of 470 ms with a 78° pulse provided the best signal-to-noise ratio within the shortest period of time. All ^{31}P chemical shift values in the cell spectra were set relative to fully protonated P_i as an internal standard, by setting the α-ATP signal to -11.30 ppm, since this signal is essentially insensitive to changes in pH [16]. To convert ^{31}P chemical-shift values relative to external 85% H_3PO_4, 0.50 ppm should be added. The saline-perfusion experiment was carried out after the system had equilibrated (typically after about 1 h) by replacing the growth medium with a 0.9% isotonic saline solution containing 20 mM Hepes (pH 7.4). As usual, the first 10 ml of effluent was discarded. The 2,4-dinitrophenol (Sigma) experiment was performed in the same manner, with growth medium containing varying amounts of dinitrophenol (pH 7.4). Whenever possible, if the ATP returned to its original level at the end of the experiment, the sample was perfused with a medium containing 2 mM phosphocreatine. A spectrum with a 67 ° pulse and a repetition time of 2.17 s was recorded to quantitate the amount of ATP present, which is usually between 1 and 1.5 mM. T_1 relaxation times of ATP-α, -β, and -γ resonances in the fibroblasts under equilibrium perfusion conditions at 37 °C were determined to be: γ, 152 ± 18; α, 213 ± 14; and β, 243 ± 36 ms, using the T_1-inversion recovery method with a delay time of 2 s.

Cell viability. Cell viability was determined by the colony forming ability of single cells. Cells were removed from the gel threads by vigorous pipetting. The cell suspension was then passed through a sterile nylon mesh (70 μm diameter) to remove the agarose debris. The cells were then counted, diluted, and plated for macroscopic colony formation. Following 5–8 days of incubation, the colonies were fixed with methanol/acetic acid, stained with crystal violet and scored.

Results

Cell viability in gel threads

Threads made with Chinese hamster lung fibroblasts embedded in agarose gel (Fig. 1A) were examined microscopically. Phase contrast microscopy shows that a very high cell density is achieved (Fig. 1B). Paraffin block sections (Fig. 1C) show intact nuclei with prominent nucleoli. Recovered cells were metabolically functional as demonstrated by both a positive Trypan blue exclusion test and their relatively high colony-forming ability. The colony-forming ability of the cells plated immediately after they were embedded in the gel threads ranged between 50 and 90%. Those plated after 2, 6 and 14.5 h in the gel threads maintained at 37 °C were 88, 67 and 64% (average of 3 replicate experiments), respectively, relative to the 0 h controls. The high cloning efficiency of cells maintained in the gel threads for up to 14 h underscores the feasibility of conducting long-term experi-

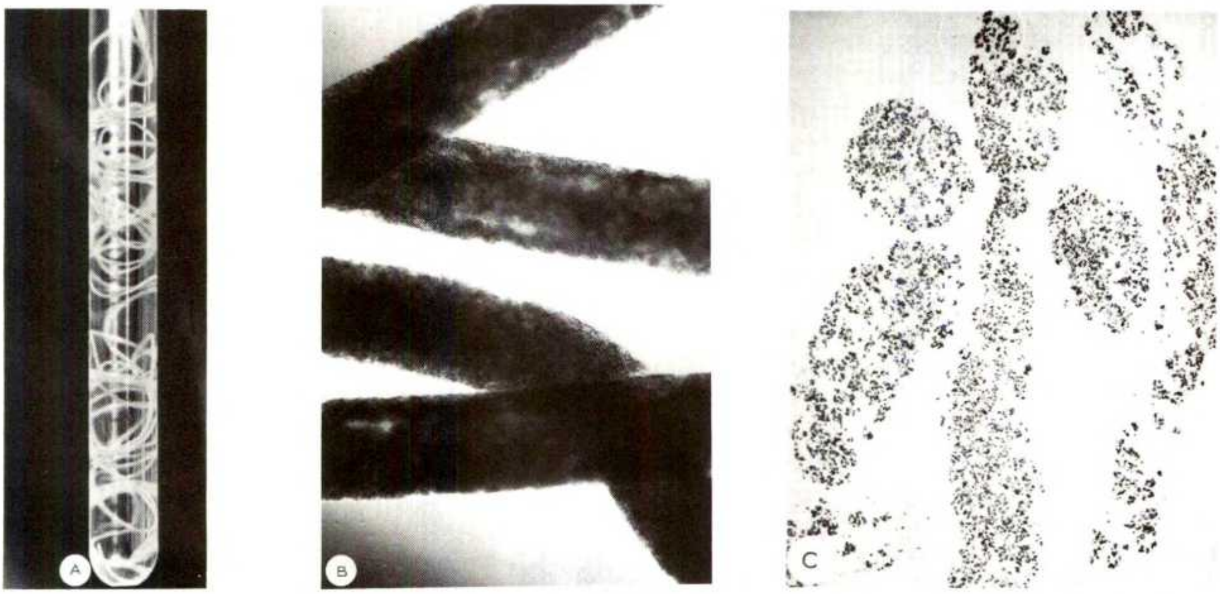

Fig. 1. (A) The gel threads containing the cells were extruded through thin tubing into the growth medium containing 20 mM Hepes buffer which was maintained at pH 7.35–7.40. (B) Phase-contrast microscopy (×100) (presented at a 45% reduction) of the gel threads, showing a high density of fibroblasts throughout the gel matrix. (C) Paraffin-block sections (7–8 μm) of the gel threads, fixed with Bouins stain. Intact nuclei with prominent nucleoli in the cells are visible.

ments on metabolically active, clonable cells. Further, for samples containing less than $1 \cdot 10^8$ cells, the prolonged period of viability in the gel threads upon perfusion allows for adequate signal-to-noise ratios to be obtained, since time is available for a greater number of spectral accumulations.

Perfusion with glucose-containing medium

The metabolic activity of cells embedded in the gel threads can be evaluated by monitoring their ATP levels with ^{31}P-NMR. The ^{31}P-spectra consist of signals from intracellular sugar phosphates, P_i, and ATP [1,15]. Suspensions of fibroblasts without intervention lose all ATP in approx. 1.5 h with a concomitant increase in the P_i level, as indicated by the time-dependent changes in the signal levels [17]. However, colony-forming ability of a sample of cells after 1.5 h in dense suspension in an NMR tube, with loss of ATP signals, was 94%. Thus, these cells were not dead, but were metabolically inactive after 1.5 h in a nonperfused suspension. By contrast, the cells in the gel threads, when perfused continuously with the glucose-containing growth medium, can be maintained in a metabolically active state for 18–24 h at 25 °C, as evidenced by maintenance of their equilibrium ATP levels [17]. The response of the cells in the gel threads to perfusion and stopping of perfusion is shown in a series of sequentially recorded ^{31}P-NMR spectra in Fig. 2A. The relative changes in P_i and ATP intensities as a function of time are presented in Fig. 2B. It should be noted that some intensity in the peaks referred to as γ- and α-ATP could derive from β- and α-ADP, respectively. However, because the relative spectral intensity of the γ and α peaks and the β-ATP peak are approximately equal, the amount of NMR-observable ADP present is negligible. Since the decrease in the intensity of all three ATP peaks appeared to be parallel within experimental error, the calculated ATP levels are the average of all three ATP peak heights.

During continuous perfusion, the chemical-shift values of the ^{31}P-signals remained constant. The signal of P_i at 1.6 ppm reflected an intracellular pH of 7.35. The intracellular pH was estimated using a calibration curve of chemical shift of P_i vs. pH derived from the cell extracts. The ATP phosphate signals were observed at -6.2 and -20.1 ppm for the γ- and β-phosphates, respectively, with the α-phosphate signal set to -11.3 ppm. After the perfusion was stopped, changes were

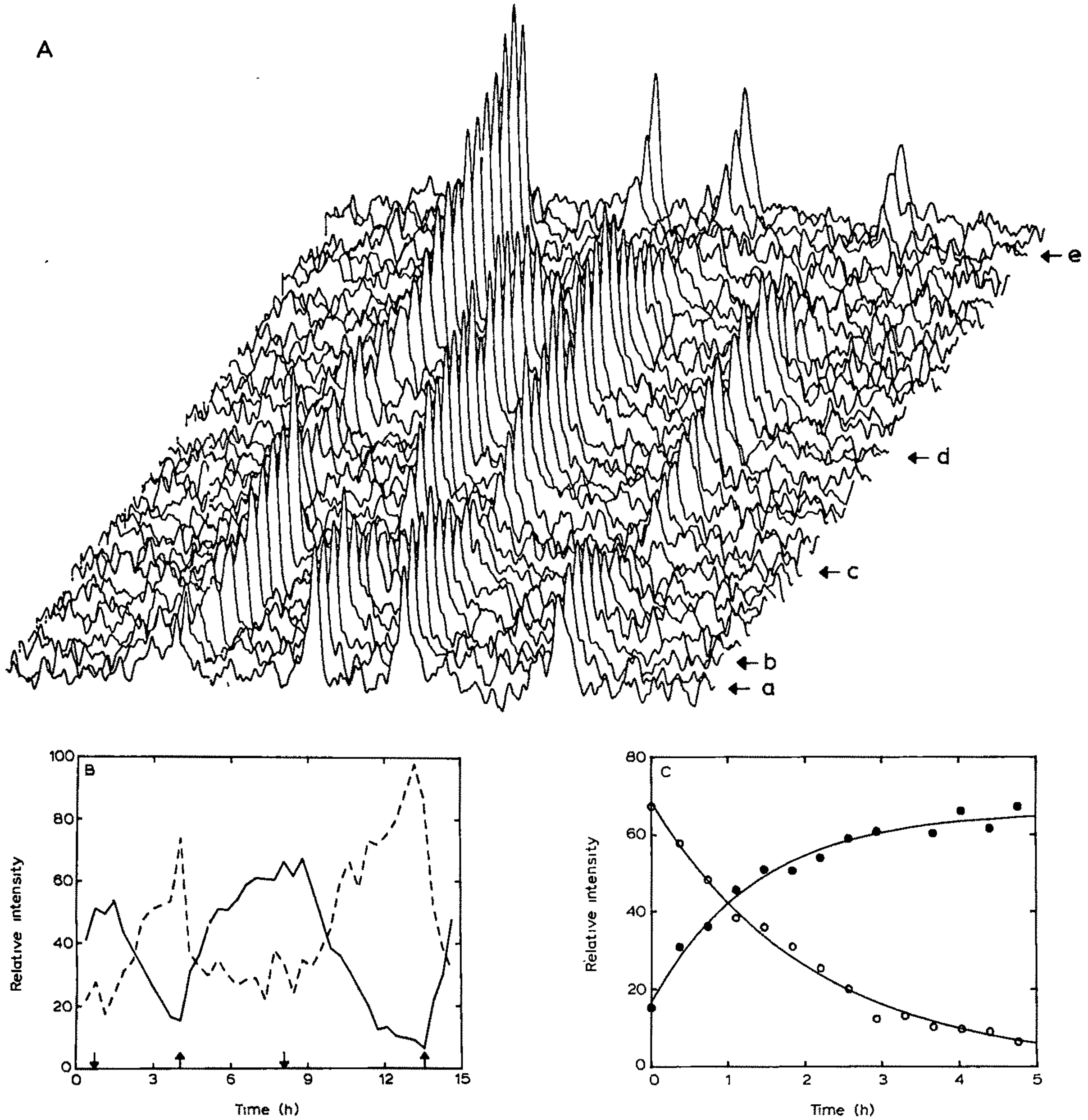

Fig. 2. (A) Stacked plot of ^{31}P-NMR spectra of fibroblasts embedded in agarose gel threads at 25 °C, showing the effects of stopping perfusion and subsequently reperfusing with a glucose-containing medium. The perfusion was started at 0.4 h (a), stopped twice, at 0.7 (b) and 8.1 h (d), and restarted twice, at 4.0 and 13.6 h (e), as shown by the arrows. Each spectrum was a 22 min accumulation. The α-ATP resonance was set to -11.3 ppm in all spectra. (B) Plot of the relative intensities of ATP (———) and P_i (- - - - -) peaks as a function of time from (A). The ATP intensity was the average of α-, β-, and γ-resonances. Each data point was the cumulative result at the end of a 22 min accumulation. Up and down arrows denote when the perfusion was turned on and offf, respectively. (C) Fits to equation $F(x) = a + be^{cx}$ of ATP-relative intensities during the second perfusion (●, 4.0–8.1 h) and nonperfusion (○, 8.1–13.6 h) periods in (B). The time constants (c) derived from the fits are 0.73 ± 0.08 and 0.44 ± 0.04 h^{-1}, respectively.

observed in all of the phosphate signals. The P_i peak shifted upfield until it reached a value corresponding to an intracellular pH of approx. 5.80. The γ-ATP signal shifted gradually to -6.8 ppm, whereas the chemical shift of the β-ATP changed very little. The intensity of the P_i signal continued

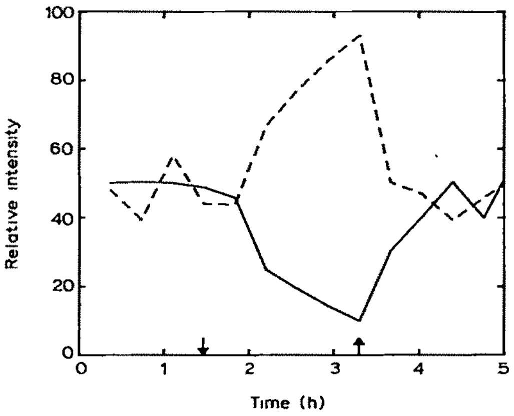

Fig. 3. Plot of the relative intensities of ATP (———) and P_i (------) NMR signals of fibroblasts embedded in gel threads, as a function of time at 37 °C with and without perfusion. Perfusion was turned off and on at times indicated by the up and down arrows.

to increase throughout this time-period, while the signals of the ATP phosphates showed a concomitant decrease (Fig. 2B). Reperfusion of the gel threads resulted in a metabolic response that was the reverse of the effect observed after the perfusion was turned off. However, the P_i peak intensity decreased more rapidly than the concomitant increase in the ATP level. On reperfusion, both the P_i and ATP levels were restored to their original values. When the process was repeated, the cellular response detected by ^{31}P-NMR paralleled that of the initial nonperfusion/perfusion period (Fig. 2A and B). The change in signal intensities for the total ATP during the periods of perfusion and nonperfusion exhibited similar, although opposite, rates (Fig. 2C). Fitting with an exponential function gave exponential time constants of 0.73 ± 0.08 and 0.44 ± 0.04 h^{-1}, respectively. Attempts to fit the P_i data were unsatisfactory.

A similar but faster response in the ^{31}P-NMR signal intensities of P_i and ATP of the cells in the gel threads was also observed on altering perfusion at 37 °C (Fig. 3). There were too few data points at that temperature to fit an exponential function adequately.

Perfusion with isotonic saline

The response of the cells in the gel threads to changing the glucose-containing medium to isotonic saline at 37° was similar to the results of stopping the perfusion. The cells were perfused for 105 min with isotonic saline/Hepes (pH 7.35) at 37 °C. Spectra were obtained every 15 min. Representative spectra are shown in Fig. 4A, and the relative changes in P_i and ATP intensities are presented in Fig. 4B. After 1 h, there was a signifi-

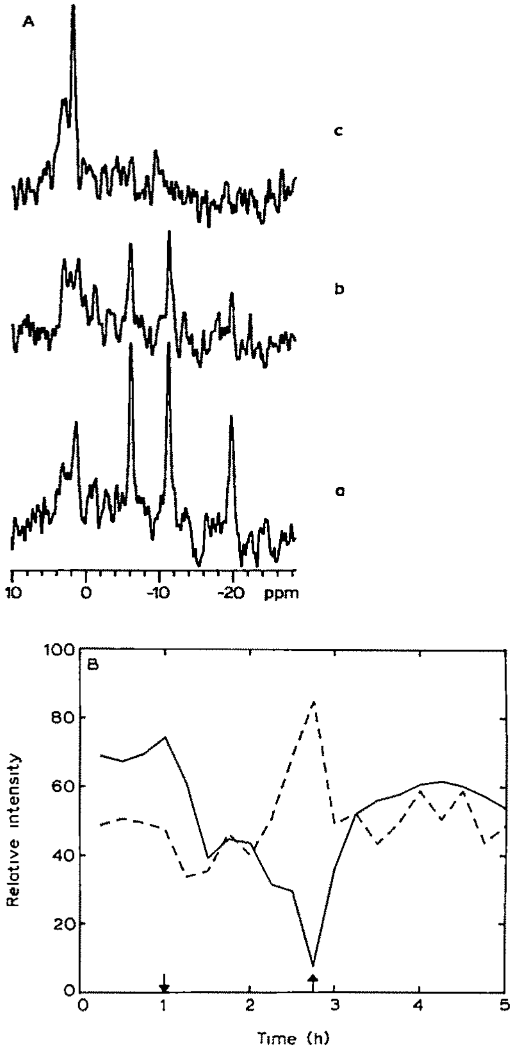

Fig. 4. (A) ^{31}P-NMR spectra of fibroblasts in gel threads during perfusion with isotonic saline/Hepes at 37 °C. A, control at 0.25 h; B and C, at 0.5 and 1.75 h, respectively, after switching to saline solution. Each spectrum was a 30 min accumulation (B) Plot of ATP- (———) and P_i- (------) relative intensities as a function of time on perfusing with isotonic saline solution. Up and down arrows denote when the perfusate was switched to saline solution and back to glucose-containing medium, respectively

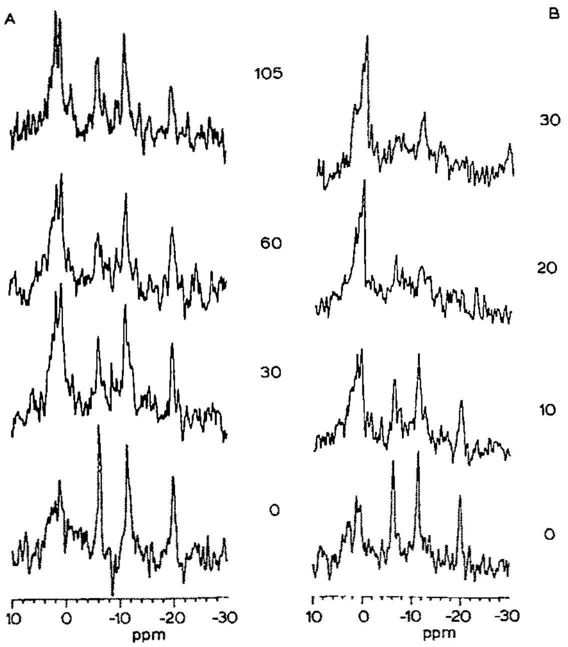

Fig. 5. Responses of fibroblasts in perfused gel threads to dinitrophenol at 37 °C, as monitored by ^{31}P-NMR spectroscopy. The perfusate was switched to a dinitrophenol-containing medium at time zero after the control spectrum had been obtained. A, 10 mM dinitrophenol, 15 min accumulation; B, 25 mM, 10 min accumulations. Times in minutes shown to right of spectra.

cant loss of ATP signal accompanied by an equivalent increase in the intensity of the P_i signal. The chemical shift of the P_i peak during perfusion with the glucose-containing medium and that during perfusion with the isotonic saline (1.33 ppm) were not significantly different. The γ-ATP signal shifted slightly upfield during the isotonic saline perfusion, and the β-ATP signal did not change significantly. When the gel threads were reperfused with glucose-containing medium, the recovery of ATP and the loss of P_i in the cells were seen immediately (Fig. 4A and B). After 30 min of reperfusion, the intensity of the P_i signal was comparable to that of the control spectra prior to isotonic saline perfusion. The recovered levels of ATP and P_i could be maintained for more than 2 h.

Perfusion with dinitrophenol

Dinitrophenol acts as an uncoupler of oxidative phosphorylation (Ref. 18 and references therein). The fibroblasts embedded in gel threads were perfused with growth medium containing several different concentrations of dinitrophenol at pH 7.48 and 37 °C. This caused an increase in intensity of the original P_i peak (at approx. 1.4 ppm), as well as the appearance of a new peak at 0.5 ppm with increasing intensity (Fig. 5). Since this new peak cannot be attributed to AMP (approx. 3.0 ppm), the two peaks at 1.4 and 0.5 ppm appear to represent two P_i signals in separate compartments [19,20] with an estimated pH of 7.2 and 6.4, respectively. An initial decrease of the ATP level was also observed, followed by either a leveling-off of ATP or a slight recovery of ADP (Fig. 5), depending on the dinitrophenol concentration used. The rate of decrease in the ATP level and the rate of increase in P_i were much higher in the presence of 25 mM dinitrophenol (Fig. 5B) than in 10 mM dinitrophenol (Fig. 5A). The ATP level reached a steady-state value after 60 min exposure to 10 mM dinitrophenol; however, in the presence of 25 mM dinitrophenol the ATP intensity dropped to near zero after 20 min. Reperfusion of either of these dinitrophenol-treated cells with fresh growth medium without dinitrophenol reversed the changes caused by dinitrophenol and restored the ATP and P_i signals nearly to their original levels.

The same experiment was repeated with 15 and 35 mM dinitrophenol (data not shown). As expected, the response of embedded cells to 15 mM dinitrophenol fell between that to 10 and 25 mM dinitrophenol, Whereas with 35 mM dinitrophenol present the ATP level dropped almost immediately to zero. As before, a new P_i peak appeared at approx. 0.5 ppm with increasing intensity, while the original P_i peak at approx. 1.3–1.4 ppm grew at a much lower rate.

Other perfusion experiments

The Chinese hamster lung fibroblasts in gel threads have also been subjected to perfusion with a medium containing 2-deoxyglucose instead of glucose, a glucose-depleted medium and a DCCD/cyanide-containing medium at 37 °C (data not shown). When exposed to 2-deoxyglucose instead of glucose, a peak at approx. 4.7 ppm arising from 2-deoxyglucose 6-phosphate appeared within 20 min. The intensities of 2-deoxyglucose 6-phosphate, AMP and P_i signals increased as those of ATP signals decreased with time. Unlike the 2-deoxyglucose experiment, perfusion with glucose-depleted medium or medium containing cyanide (20 mM) or DCCD (2 mM) alone produced little or no effect on the ATP and P_i signals. However, if the cells were perfused with 2 mM DCCD for 1 h, followed by addition of 10 mM NaCN to the perfusate, a total loss of ATP signals occurred immediately.

Discussion

This report describes our first applications of the gel-perfusion method to NMR studies of mammalian cells. We have demonstrated that Chinese hamster lung fibroblasts remain viable in the gel threads over periods of many hours, as evidenced by their colony-forming ability. Cellular energy metabolism remained at equilibrium upon perfusion with glucose-containing medium, as indicated by the maintenance of the ATP level and constant intracellular pH.

Cellular metabolism responded as expected upon stopping perfusion and then reperfusing. Changes in ATP and P_i levels were opposite, and the total phosphate metabolite pool remained approximately constant (Fig. 2B). The overall rates of production and loss of ATP were found to be approximately equal and to fit a simple exponential function (Fig. 2C). There was an acidification of the intracellular pH upon stopping perfusion similar to the response observed for dense suspensions of cells [21]. This arises from the build-up of catabolic end-products, e.g. lactic acid. However, upon perfusion in our system this process was reversible, which emphasizes that acidification and loss of ATP do not in themselves connote cell death as defined in clonogenic cell-culture growth systems. No comparable decrease in intracellular pH was observed when the cells in gel threads were perfused with isotonic buffered saline (Fig. 4A), indicating no build-up of catabolites as long as the cells are continuously perfused. Perfusion with glucose-depleted medium showed no changes in the ^{31}P-NMR spectrum of the cells, indicating that the amino acids in the medium were a sufficient source of energy metabolism. When 2-deoxyglucose was substituted for glucose in the medium, the increase in peaks corresponding to 2-deoxyglucose 6-phosphate, AMP and P_i were similar to the responses observed previously for yeast under the same conditions [15].

Dinitrophenol is an uncoupler of oxidative phosphorylation and stimulates the mitochondrial uptake of oxygen and protons [18]. Thus, the observation of two distinct P_i peaks upon perfusion with dinitrophenol (Fig. 5) can be explained by the acidification of the intramitochondrial compartment, consistent with previous observations on rat liver cells [19]. This process also activates mitochondrial ATPases and results in a loss of ATP, as observed. By contrast, DCCD inhibits membrane-bound ATPases, but has no effect on proton transport. Correspondingly, no change in ATP levels and intracellular pH was seen [22]. Perfusion with cyanide, which blocks respiration, had no effect alone [23], but DCCD combined with cyanide blocks substrate phosphorylation, and total ATP quickly fell to zero. All of these results indicate that rapid diffusion of small molecules occurs into the cells within the threads, and that the system can therefore be applied to other studies of metabolism. Currently, we are investigating the response of fibroblasts to heat, and the metabolic characteristics of several cancer-cell lines grown in culture.

Several other perfusion systems to study cell metabolism by NMR have been described. Beads [11] and hollow fibers [12] have been used as supports on which cells are grown and then placed in the NMR spectrometer. In such systems, the cells form densely packed layers, which results in greatly reduced rates of diffusion and the formation of gradients. The use of a commercial multiple hollow-fiber system [12] or a chamber in which cells may be stirred in suspension [10] requires the construction of a special probe and the use of a wide-bore magnet. An apparatus has also been described in which cells are perfused in suspension, using an insert with hollow fibers within a sealed standard bore NMR tube [13]. In order to obtain flow in this apparatus, there is a build-up of back-pressure, which could affect the cells. Both perfusion and diffusion are much slower in such a system than in in our perfusion apparatus, where there is no appreciable back-pressure. Compared to these other methods our approach is applicable to any cells grown in culture, including surface-independent cultures, allows rapid diffusion of any metabolite, drug or hormone into the whole homogeneous cell sample, and enables long-term monitoring of metabolism under controlled conditions in any NMR spectrometer.

An alternative approach to the study of human cancer cells has been to inject them into mice and monitor the growth of tumor with ^{31}P-NMR using surface coils [24]. While this approach is useful for the study of solid tumors, it does suffer from several disadvantages. In order to obtain sufficient ^{31}P-NMR signal, the surface coil has to be of a certain minimal radius (approx. 2 cm) and this requires a superficial tumor with a minimum size (approx. 500 mg). In this method, one relies on the mouse to vasculate the human tumor cells, in order to supply oxygen and nutrients and remove catabolites. But, such vasculation is generally peripheral, and, unlike homogenous in vitro perfusion, leads to oxygen and nutrient gradients. In tumors of such size, there are interior cores of necrotic tissue, and it was found that the P_i peak increases with tumor size. Contributions of necrotic areas to the P_i signal represent an additional factor that must be taken into account when interpreting therapeutic responses by this approach [25].

The cell-perfusion system we have described is equally applicable to studies of cell metabolism by ^{1}H- and ^{13}C-NMR methods [26,27], as well as ^{31}P-NMR, with due allowance made for such differences as water suppression in ^{1}H-NMR. This perfusion method also has other potential research and biomedical applications. Two methods of trapping cells in gel in order to isolate cellular products have been described. In one case the cells were trapped inside agarose micro-beads made by stirring cells and agarose in an oil suspension [28], and in another method the cells were individually micro-encapsulated [29]. From a technical and quantitative point of view our gel-thread technique would seem to have certain advantages over these methods.

Acknowledgement

We thank Lance Liotta for carrying out the fixing and sectioning (Fig. 1C).

References

1 Shulman, R.G., Brown, T.R., Ugurbil, K., Ogawa, S., Cohen, S.M. and Den Hollander, J.A. (1979) Science 205, 160–166
2 Gadian, D.G. (1982) Nuclear Magnetic Resonance and its Application to Living Systems, Clarendon Press, Oxford
3 Cohen, J.S., Knop, R.H., Navon, G. and Foxall, D.L. (1983) in NMR in Biology and Medicine in Life Chemistry Reports, Vol. 1 (Bannister, J.V. and Michelson, A.M., eds), pp. 281–457, Harwood Academic Press, London
4 Navon, G , Navon, R., Shulman, R.G. and Yamane, T. (1978) Proc. Natl. Acad. Sci. U S.A. 75, 891–895
5 Ogawa, S., Shulman, R.G., Glynn, P., Yamane, T and Navon, G. (1978) Biochim Biophys. Acta 502, 45–50
6 Jacobus, W.E., Taylor, G.J., Hollis, D P. and Nunnally, R.L. (1977) Nature 265, 756–758
7 Garlick, P.B., Radda, G.K., Seeley, P.J. and Chance, B. (1977) Biochem. Biophys. Res. Commun. 74 1256–1262
8 Iles, R A., Griffiths, J.R , Stevens, A.N., Gadian, D.G. and Porteous, R. (1980) Biochem J. 192, 191–202
9 Radda, G.K., Ackermann, J.J.H., Bone, P.J., Sehr, P.A., Wong, G.G., Ross, B.D., Green, Y.L, Bartlett, S. and Lowry, H. (1980) Int. J. Biochem. 12, 277–282
10 Balaban, R.S., Gadian, D.G., Radda, G K. and Wong, G.G. (1981) Anal. Biochem. 116, 450–455
11 Ugurbil, K., Guernsey, D.L., Brown, T.R., Glynn, P., Tobkes, N. and Edelman, I.S. (1981) Proc Natl. Acad. Sci. U.S.A. 78, 4843–4847
12 Gonzalez-Mendez, R., Wemmer, D., Hahn, G., Wade-Jardetzky, N. and Jardetzky, O. (1982) Biochim. Biophys. Acta 720, 274–280
13 Karczmar, G.S., Koretsky, A.P., Bissell, M.J., Klein, M. and Weiner, M.W. (1983) J. Magn. Res. 53, 123–128
14 Jacobson, L. and Cohen, J.S. (1981) Biosci. Rep. 1, 141–150
15 Foxall, D.L. and Cohen, J.S. (1983) J. Magn. Res. 52, 346–349
16 Jacobson, L. and Cohen, J.S. (1982) in Noninvasive Probes of Tissue Metabolism (Cohen, J.S., ed.), pp. 5–24, Wiley, New York
17 Foxall, D.L., Cohen, J.S. and Mitchell, J.B. (1984) Exp. Cell Res., in the press
18 Stryer, L. (1981) Biochemistry, 2nd Edn., pp. 307–331, W.H. Freeman, San Francisco
19 Cohen, S.M., Ogawa, S., Rottenberg, H , Glynn, P., Yamane, T., Brown, T.R., Shulman, R.G. and Williamson, J.R. (1978) Nature 273, 554–556
20 Busby, J.W., Gadian, D.G., Radda, G.K., Richards, R.E. and Seeley, P.J (1978) Biochem. J. 170, 103–114
21 Navon, G., Shulman, R.G., Yamane, T., Eccleshall, T.R., Lam, K.B., Baronofsky, J.J. and Marmur, J. (1979) Biochemistry 18, 4487–4499
22 Navon, G., Ogawa, S., Shulman, R.G. and Yamane, T. (1977) Proc. Natl. Acad. Sci. U.S.A. 74, 888–891
23 Dubyak, G.R. and Scarpa, A. (1983) Biochemistry 22, 3531–3536
24 Ng, T.C., Evanochko, W.T , Hiramoto, R.N., Ghanta, V.K., Lilly, M.B., Lawson, A.J., Corbett, T.H., Durant, J.R. and Glickson, J.D. (1982) J Magn. Res 49, 271–286

P25706

25 Evanochko, W.T., Ng, T.C., Lilly, M.B, Lawson, A.J., Corbett, T H., Durant, J.R. and Glickson, J.D. (1983) Proc Natl. Acad. Sci. U.S.A. 80, 334–338
26 Agris, P.F. and Campbell, I.D. (1982) Science 216, 1325–1327
27 Foxall, D.L., Cohen, J.S. and Tschudin, R.G. (1983) J. Magn. Res. 51, 330–334
28 Nilsson, K., Scheirer, W., Merten, O.W., Ostberg, L, Liehl, E., Katinger, H.W.D. and Mosbach, K. (1983) Nature 302, 629–630
29 Lim, F. and Sun, A.M. (1980) Science 210, 908–910

Biochimica et Biophysica Acta, 804 (1984) 285–290
Elsevier

BBA 11294

TRANSFORMATION-ASSOCIATED CHANGES IN NUCLEAR-CODED MITOCHONDRIAL PROTEINS IN 3T3 CELLS AND SV40-TRANSFORMED 3T3 CELLS

STEVEN H. ZUCKERMAN *, STIG LINDER ** and JEROME M. EISENSTADT ***

Department of Human Genetics, Yale University School of Medicine, New Haven, CT 06510 (U.S.A.)

(Received December 27th, 1983)

Key words: Transformation; Protein composition; Mitochondrial protein; (3T3 cell)

Comparative two-dimensional gel electrophoretic studies were performed on mitochondrial proteins in nontransformed mouse 3T3 cells and in SV40-transformed 3T3 cells, SV-T2. Two polypeptides, of 58 and 40 kDa, were present in increased amounts in SV40-transformed cells. These polypeptides were demonstrated to be nuclear-coded mitochondrial proteins by their absence in mitochondrial preparations, when labeling was performed in the presence of a mitochondrial-specific inhibitor, Rhodamine 6G. Temperature-sensitive mutants for transformation were derived from 3T3 cells by transfection with cloned SV40 DNA containing the ts A58 mutation. Increased amounts of the 58 kDa protein were apparent in these cells at the permissive temperature (33°C) compared to the restrictive temperature (39.5°C).

Introduction

Warburg's hypothesis that cancer cells have an elevated rate of glycolysis due to an impaired respiratory capacity [1] and the finding that mitochondria are the principal site for oxidative phosphorylation and ATP generation in animal cells [2] resulted in extensive investigations of mitochondria from neoplastic cells. Differences in mitochondrial structure and numbers, as well as in mitochondrial enzyme content, membrane lipids, transport mechanisms and substrate specificities, have been reported [3,4]. However, these differences are variable depending on the tumor source, mitochondrial isolation procedures and the in vivo and in vitro growth properties of the tumors. Accordingly, it has been difficult to define which changes are associated with neoplastic transformation. In a different approach, sarcoma-virus-transformed mink fibroblasts were reported to have a decreased mitochondrial membrane potential compared to control, nontransformed mink fibroblasts [5]. These differences in membrane potential were based on the decreased uptake and retention of the mitochondrial-specific cationic dye Rhodamine 123 and were reversible following addition of the ionophore nigericin. Further studies on the retention of Rhodamine 123 in various tumors indicated that many transitional cell carcinomas, adenocarcinomas and chemically transformed epithelial cell lines retained Rhodamine 123 for extended periods, while oat cell carcinomas did not [6]. These results demonstrate that neoplastic transformation is associated with discrete mitochondrial changes.

In the present study, we have performed comparative studies on nuclear-coded mitochondrial proteins in nontransformed 3T3 cells and in

---

* Present address: Department of Immunology, Lilly Research Laboratories, 307 East McCarty Street, Indianapolis, IN 46285, U.S.A.

** Present address: Department of Medical Genetics, The Biomedical Centre, Uppsala University, 75123 Uppsala, Sweden.

*** To whom correspondence should be addressed.

Abbreviation: R6G, rhodamine 6G.

0167-4889/84/$03.00 © 1984 Elsevier Science Publishers B.V.

SV40-transformed 3T3 cells by two-dimensional gel electrophoresis. Increased quantities of two nuclear-coded mitochondrial proteins, of 58 and 40 kDa, were detected in SV40-transformed 3T3 cells. Increased synthesis of the 58 kDa protein was also detected in 3T3 cells transformed with the SV40 ts A58 mutant.

Materials and Methods

Cell culture

Balb/c 3T3 cells clone A31 and SV40-transformed 3T3 cells, SV-T2, were obtained from the American Type Culture Collection. These cell lines were maintained at low density in Dulbecco's modified Eagle's media supplemented with 5% calf sera [7]. Temperature-sensitive transformation mutants of 3T3 were obtained using the ts A58 SV40 mutant inserted in pBR322 (provided by Dr. Charles Cole, Dartmouth College, Hanover, NH). The temperature-sensitive mutation has been mapped within the large T antigen [8]. Calcium phosphate coprecipitates of ts A58 and carrier DNA were incubated with 3T3 cells [9]. Following incubation, cells were seeded in soft agar and incubated at 33°C. Four soft agar clones (3.4, 4.4, 5.1 and 6.1) were isolated, which grew in soft agar at 33°C, but not at 39.5°C.

Mitochondria preparation and gel electrophoresis

$2 \cdot 10^6$ cells were seeded in 25 cm^2 flasks (Falcon) and labeled for 90 min (short pulse) or 18 h (long pulse) with 200 and 40 μCi/ml, respectively, of [^{35}S]methionine (Amersham International) in methionine-free media (GIBCO, Grand Island, NY). In parallel cultures, Rhodamine 6G (Kodak) was present at 2 μg/ml during the overnight labeling [10]. Following labeling, cultures were washed

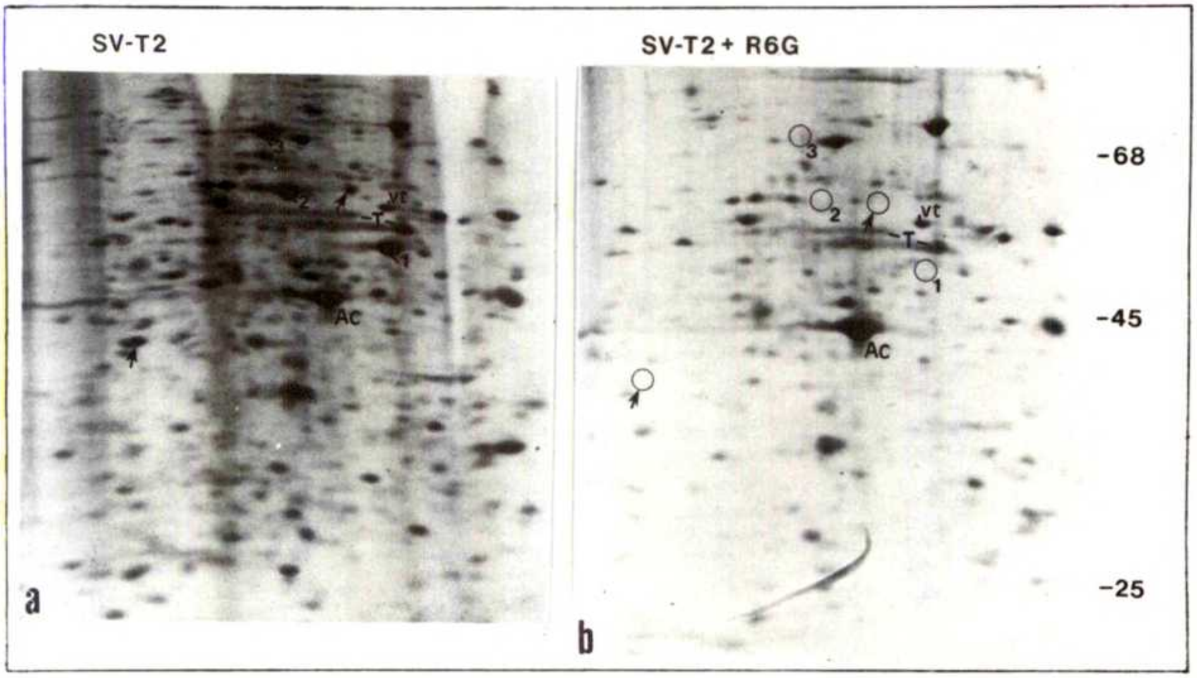

Fig. 1. R6G-sensitivity of nuclear-coded mitochondrial proteins in SV-T2. SV-T2 was labeled for 18 h with 40 μCi/ml of [^{35}S]methionine in the absence (a) or presence (b) of 2 μg/ml R6G. Mitochondria were then isolated, and nuclear-coded mitochondrial polypeptides were resolved by two-dimensional gel electrophoresis. Approx. 30 polypeptides were absent or significantly reduced, including the predominant polypeptides 1, 2 and 3. The position of these polypeptides in R6G-treated SV-T2 is indicated by circles. Two R6G-sensitive polypeptides (arrows) are present in greater quantities in SV-T2 relative to non-transformed 3T3 cells (see Fig. 2). The contaminating cytoskeletal proteins actin (Ac) tubulin (T) and vimentin (vt) are not sensitive to R6G. A pH gradient between 4.0 and 6.5 was generated in the isoelectric-focusing gels. The basic region of the isoelectric-focusing gel is to the left. Molecular weights are indicated in thousands.

and mitochondria were prepared using the procedure of Bogenhagen and Clayton [11]. Unlabeled mitochondria were added as carrier prior to centrifugation in a 1.0–1.5 M sucrose step gradient. The mitochondria were washed and lysed in O'Farrell lysis buffer [12]. Mitochondrial lysates were electrophoresed on two-dimensional gels with isoelectric focusing in the first and SDS-10.5% polyacrylamide gels in the second dimension [12]. The isolation of an inner mitochondrial membrane-enriched preparation was performed by digitonin solubilization of the outer membrane and Lubrol WX fractionation of the inner membrane and matrix [13]. In additional experiments, mitochondria were lysed with 0.5% NP-40 and incubated for 30 min at 37 °C with 10 U of bovine alkaline phosphatase (Sigma, St. Louis, MO) at pH 8.5 in the presence of 2 mM phenylmethylsulfonyl fluoride. Alkaline phosphatase-treated lysates were then subjected to two-dimensional gel electrophoresis. All gels were dried and exposed to Kodak X-Omat film.

Results

Mitochondria prepared from [^{35}S]methionine-labeled 3T3 cells and 3T3 cells transformed with SV40 were lysed and resolved using two-dimensional gel electrophoresis. Preliminary experiments indicated that polypeptides comigrating with cytoskeletal components were abundant in sucrose gradient purified mitochondrial preparations. It was thus necessary to distinguish between mitochondrial specific polypeptides and contaminating cytoplasmic polypeptides. This was achieved by labeling parallel cultures in the presence or absence of 2 μg/ml of R6G, a mitochondrial-specific dye which inhibits oxidative phosphorylation [10]. R6G-treated cells are unable to transport nuclear-cold mitochondrial proteins into and across the inner mitochondrial membrane. Therefore, only polypeptides that were sensitive to R6G were considered for analysis. Fig. 1 shows the polypeptide patterns of SV-T2 cells labeled in the absence (Fig. 1a) or presence (Fig. 1b) of R6G. Approx. 30 polypeptides were absent or significantly diminished in mitochondrial preparations from R6G-treated cells. These polypeptides represent nuclear-coded mitochondrial proteins and differ in their relative abundance, molecular weights and isoelectric points. A number of polypeptides are common to both preparations, notably actin, tubulins and vimentin. The identity of these polypeptides were confirmed by tryptic peptide analysis (not shown). The predominant R6G-sensitive polypeptides 1–3 correspond to the Mitcon 1–3 polypeptides described by Anderson [14].

3T3 and SV-T2 mitochondrial polypeptides were then analyzed by two-dimensional gel electrophoresis in cells labeled for 90 min with [^{35}S]methionine (Fig. 2). Two R6G-sensitive polypeptides, of 58 and 40 kDa, were present in approx. 6- and 3-fold greater quantities respectively in SV-T2 (Fig. 2b) compared to 3T3 cells (Fig. 2a). The 40 kDa polypeptide remained associated with the inner membrane during mitochondrial fractionation with digitonin and Lubrol WX (Fig. 2c). The 58 kDa polypeptide could not be unequivocally assigned to matrix or membrane fractions. Protein 1 (Mitcon 1) was enriched in the inner membrane fraction and was found to react with an anti-F_1 ATPase serum in immunoblot experiments [20]. Mitcon 1 was identified as the β-subunit of the F_1 ATPase complex, based on its molecular weight and isoelectric point [15,16]. Proteins 2 and 3 were enriched in the matrix fraction. Incubation of detergent solubilized mitochondria with alkaline phosphatase resulted in the altered electrophoretic mobility of several polypeptides, presumably due to phosphate removal (Fig. 2d and e). This procedure did not alter the mobility of the 40 kDa polypeptide, suggesting that this transformation-related polypeptide is not phosphorylated. The 58 kDa polypeptide appeared to be more labile and could not be detected after incubating mitochondrial lysates at 37 °C, with or without phosphatase. In further experiments, neither the 40 nor the 58 kDa protein were labeled with [^{32}P]orthophosphate.

In a different series of experiments, four SV40 ts A58-transformed clones of 3T3 were isolated which were capable of growth in soft agar at the permissive temperature of both 33 °C and 39.5 °C. One of these lines, ts 6.1, was labeled with [^{35}S]methionine for 18 h at 33 °C, but not at 39.5 °C. Two-dimensional gel analysis (Fig. 3) indicated that at 33 °C (Fig. 3b) the ts 6.1 line had 5–6-fold greater amounts of the 58 kDa protein

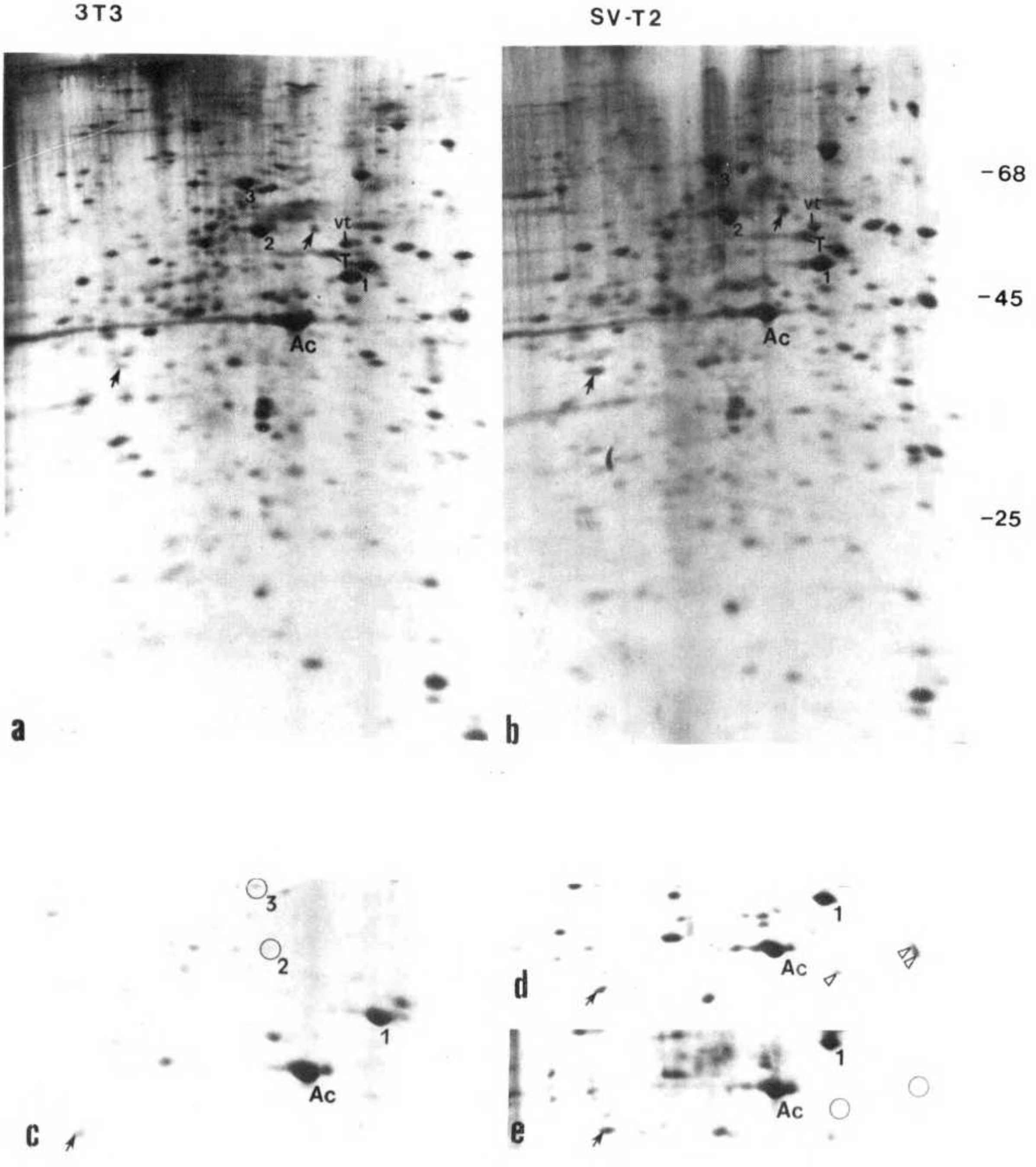

Fig. 2. Transformation-related changes in nuclear-coded mitochondrial polypeptides. 3T3 cells (a) or the SV40-transformed SV-T2 (b) were labeled for 90 min with 200 μCi/ml of [^{35}S]methionine. Mitochondria were then isolated and nuclear-coded mitochondrial polypeptides were resolved by two-dimensional gel electrophoresis. Two R6G-sensitive polypeptides (arrows) of 58 and 40 kDa, were present in greater quantities in SV-T2 compared to 3T3 cells. (c) The 40 kDa polypeptide, actin, and polypeptide 1 fractionate with an inner mitochondrial membrane preparation, while polypeptides 2 and 3 are lost and represent matrix proteins. [^{35}S]Methionine-labeled mitochondrial lysates were incubated in the absence (d) or presence (e) of bovine alkaline phosphatase. The 40 kDa polypeptide (arrow) is not altered by alkaline phosphatase treatment, while the mobility of two other polypeptides (open arrowheads) was altered.

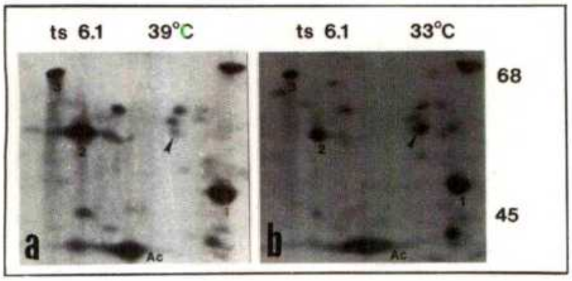

Fig. 3. Temperature-dependent changes in the 58 kDa protein in the ts 6.1 cell line. 3T3 cells were transformed with the ts A58 mutant of SV40, and the 6.1 cell line was isolated. The 6.1 line was labeled with 40 μCi/ml of [^{35}S]methionine for 18 h at the restrictive temperature of 39.5 ° C (a) or permissive temperature of 33 ° C (b) for transformation. Note increased amounts of the 58 kDa protein at the permissive temperature (b).

compared to the same line at 39.5 °C (Fig. 3a). Similar results were observed with the three other temperature-sensitive transformed lines. None of these lines revealed any significant differences in the expression of the 40 kDa protein at the two temperatures.

Discussion

The present experiments suggest that transformation of 3T3 cells with SV40 results in quantitative changes in nuclear-coded mitochondrial proteins. This was evident in both SV-T2 and in the ts A58-transformed mutants at the permissive temperature for transformation. Two proteins, of 58 and 40 kDa, were found in increased quantities in the SV-T2 cells. These proteins were identified as nuclear-coded mitochondrial proteins by their sensitivity to R6G. Increased synthesis of the 58 kDa protein, but not the 40 kDa protein, was also detected in the temperature-sensitive 3T3 transformants. Whether this reflects the variability inherent in different transformed lines is not known.

In additional studies, 3T3 and SV-T2 were labeled with [^{32}P]orthophosphate, and the mitochondrial polypeptides were resolved on two-dimensional gels. A similar pattern of phosphoproteins was observed on two-dimensional gels of 3T3 and SV-T2 cells (data not shown). None of the approx. 50 phosphoproteins that we resolved were R6G-sensitive. This observation could be explained by the phosphorylation of proteins already inside the mitochondria. We were therefore unable to distinguish between nuclear-coded mitochondrial phosphoproteins and cytoplasmic phosphoprotein contaminants.

Biochemical and structural differences have been reported in mitochondria from tumor vs. control cells [1–4]. However, although two-dimensional gel electrophoretic patterns have been reported for mitochondria preparations [14,16–18], we are unaware of any comparative two-dimensional gel studies of mitochondrial proteins between closely related normal and transformed cells. This may in part be related to the problem of cytoplasmic contamination of mitochondrial preparations. The use of the mitochondrial inhibitor rhodamine 6G enabled us to identify nuclear-coded mitochondrial-specific proteins on our two-dimensional gels. The potassium ionophore nonactin has been used in a similar approach to identify nuclear-coded mitochondrial proteins in whole-cell lysates [14]. A nuclear-coded mitochondrial protein (Mitcon 5) was lost in human lymphocytes, following treatment with phorbol ester tumor promoters. Furthermore, this transformation-sensitive protein was not detected in lymphoblastoid cell lines.

Further studies are required to identify other transformation-related changes in nuclear-coded mitochondrial proteins. Recently, Gay and Walker [19] have reported that a portion of p21, the product of the bladder carcinoma oncogene, exhibits significant sequence homology to the nucleotide-binding region of the β-subunit of the nuclear-coded mitochondrial ATP synthase. Clearly, it is necessary to define how transformation-related changes in nuclear-coded mitochondrial proteins affect the function and regulation of the mitochondrial genome.

Acknowledgements

This work was supported by NIH grant GM 21873 awarded to J.M.E. S.H.Z. was supported by a Swebilius Cancer Research Award. S.L. was supported by a James Hudson Brown Postdoctoral fellowship. S.H.Z. would like to thank Dr. Sandra Zuckerman for her stimulating discussions.

References

1 Warburg, O. (1956) Science 123, 309–314
2 Kennedy, E.P. and Lehninger, A.L. (1948) J. Biol. Chem. 172, 847–848
3 Pederson, P.L. (1978) Prog. Exp. Tumor Res. 22, 190–274
4 Spitsberg, V.L. (1979) Arch. Biochem. Biophys. 195, 136–144
5 Johnson, L.V., Summerhayes, I.C. and Chen, L.B. (1982) Cell 28, 7–14
6 Summerhayes, I.C., Lampidis, T.J., Bernal, S.D., Nadakavukaren, J.J., Nadakavukaren, K.K., Shepherd, E.L. and Chen, L.B. (1982) Proc. Natl. Acad. Sci. U.S.A. 79, 5292–5296
7 Aaronson, S.A. and Todaro, G.J. (1968) J. Cell. Physiol. 72, 141–148
8 Lai, C.-J. and Nathans, D. (1975) J. Virol. 66, 70–81
9 Abrahams, P.J. and Van der Eb, A.J. (1975) J. Virol. 16, 206–209
10 Gear, A.R.L. (1974) J. Biol. Chem. 249, 3628–3637
11 Bogenhagen, D. and Clayton, D.A. (1974) J. Biol. Chem. 249, 7991–7995
12 O'Farrell, P.H. (1975) J. Biol. Chem. 250, 4007–4021
13 Greenawalt, J.W. (1979) Methods Enzymol. 31, 310–323
14 Anderson, L. (1981) Proc. Natl. Acad. Sci. U.S.A. 78, 2407–2411
15 Penefsky, H.S. (1979) Adv. Enzymol. 49, 223–280
16 Henslee, J.G. and Srere, P.A. (1979) J. Biol. Chem. 254, 5488–5497
17 Burnett, K.G. and Scheffler, I.E. (1982) J. Cell Biol. 90, 108–115
18 Hare, J.F. and Hodges, R. (1982) J. Biol. Chem. 257, 3375–3580
19 Gay, N.J. and Walker, J.E. (1983) Nature 301, 262–264
20 Ludwig, B. and Capaldi, R.A. (1979) Biochem. Biophys. Res. Commun. 87, 1159–1167.

Biochimica et Biophysica Acta, 804 (1984) 291–300
Elsevier

BBA 11313

α-ADRENERGIC EFFECTS ON $^{86}Rb^+(K^+)$ POTENTIALS AND FLUXES IN BROWN FAT CELLS

EEWA NÅNBERG, JAN NEDERGAARD and BARBARA CANNON

The Wenner-Gren Institute, University of Stockholm, Norrtullsgatan 16, S-113 45 Stockholm (Sweden)

(Received October 18th, 1983)
(Revised manuscript received February 24th, 1984)

Key words. Rb^+ flux, Membrane potential, α-Adrenergic effect, (Brown fat cells)

Net K^+ fluxes in isolated hamster brown fat cells were studied by the use of the K^+ analogue $^{86}Rb^+$. In isolated cells, cold-stored overnight to diminish K^+ gradients, an equilibrium $^{86}Rb^+(K^+)$ clearance value of 27 µl/million cells was obtained after 30 min incubation at 37°C. This corresponds to a 10-fold K^+ gradient over the plasma membrane, and a K^+ potential of about −60 mV. The attainment of this equilibrium was dependent upon the presence of Na^+ in the extracellular medium, and the uptake was fully inhibited by the $(Na^+ + K^+)$-ATPase inhibitor ouabain. Ouabain had, however, no significant acute effect on the maximal rate of thermogenesis achieved after norepinephrine stimulation of the cells, but if the restoration of ionic equilibrium was inhibited by ouabain in prolonged incubations, a decreased thermogenesis was observed. This was probably due to the low cytosolic K^+ content then encountered, and the resulting inhibition of lipolysis. The addition of norepinephrine to cells in which $^{86}Rb^+(K^+)$ equilibrium had been attained resulted in a rapid efflux of $^{86}Rb^+$ and the establishment of a new equilibrium value, at about 65% of the unstimulated value. This corresponds to a decrease in K^+ potential of about 15 mV. The effect of norepinephrine was stereospecific and reversible, and had an EC_{50} value of about 10 nM. As catecholamine effects were much more sensitive to phentolamine than to propranolol, the adrenergically-induced efflux was classified as predominantly α-adrenergic. It is suggested that the norepinephrine-induced K^+ efflux is due to a (probably Ca^{2+}-mediated) opening of K^+ channels in the cell membrane, and that this effect occurs secondarily to the α-adrenergically induced membrane depolarization (and increase in cytosolic Ca^{2+}). The increased P_K over the cell membrane would counteract further depolarization, and the K^+ gradient would then approach the Nernst equilibrium under the new steady-state conditions.

Introduction

The mechanism behind and the significance of hormone-induced membrane depolarization in nonexcitable tissues is not presently known.

In brown adipose tissue, norepinephrine stimulation leads to a membrane depolarization [1–3]. The relationship between this depolarization and the main physiological function of the tissue, nonshivering thermogenesis, is presently discussed (for review see Ref. 4).

By the use of the K^+ analogue $^{86}Rb^+$, we have here followed the K^+ potentials and fluxes in isolated brown fat cells, both in the unstimulated state, and when the cells were adrenergically stimulated.

We found that whereas the maintenance of ionic gradients was beneficial, it was not essential for thermogenesis. The $(Na^+ + K^+)$-ATPase activity was not acutely of thermogenic significance, but chronic inhibition of the pump could lead to diminished thermogenesis, due to unrestored ionic gradients (i.e., low cytosolic K^+ content). α-Adrenergic stimulation led to an efflux of K^+

0167-4889/84/$03.00 © 1984 Elsevier Science Publishers B.V.

from the cells. This efflux probably represents the approach of the K^+ gradient towards the new Nernst equilibrium of the depolarized state induced by norepinephrine.

Some of these results have previously been published in preliminary form [5–7].

Materials and Methods

Isolation of brown fat cells. Brown fat cells were prepared from adult golden hamsters (*Mesocricetus auratus*), mainly females, weighing about 100 g. The animals were kept at room temperature, 22°C, with food (a sunflower-seed-based mixture) and water ad libitum.

The brown fat (interscapular, cervical, axillary and periaortic depots) from 2–4 animals was used for each cell preparation. The cells were isolated by collagenase digestion [3,8,9], then washed three times and stored overnight at 4°C. The following day the pooled cells were washed, filtered again to remove aggregates, and kept on ice.

The cells were counted in a Bürker chamber, and the viability was determined by vital staining with Alcian blue. Only intact cells were counted. The final stock concentration was about 2 million cells/ml.

Measurement of $^{86}Rb^+$ uptake. Cellular K^+ fluxes were followed by the use of the K^+ analogue $^{86}Rb^+$ which, compared to $^{42}K^+$, has the advantage of a longer half-life (19 days vs. 12 h). Use of $^{86}Rb^+$ as a K^+ analogue is a well-documented technique, and there is no reason to assume a significant difference between the behavior of Rb^+ and K^+ [10–13].

All incubations were performed in a Krebs-Ringer bicarbonate buffer (see below).

To this buffer, $^{86}Rb^+$ was added to about 2 kBq/ml (40 nCi/ml). This corresponds to an addition of about 1 μM Rb^+ (cf. the buffer K^+ concentration of 6.0 mM). [^{14}C]Methoxyinulin was used as an extracellular marker (2 kBq/ml).

Routinely, the uptake of $^{86}Rb^+$ was started by addition of 300 000 cells (stored at 4°C overnight) to 3 ml labeled buffer (37°C) in plastic test-tubes at time zero. To recollect the cells, two methods were used. In the filtration technique (which is similar to the filtration technique used by Svoboda et al. [14] for receptor studies in these cells), the incubates were filtered through Whatman GF/C glass-fiber filters (mounted in a Millipore sampling manifold) at 140 mmHg. The total filtration time was less than 10 s. The filters were then washed with 3 ml ice-cold unlabeled Krebs-Ringer bicarbonate buffer (0.1% albumin). Thereafter, the filters were immediately transferred to scintillation vials and dried. 5 ml scintillation fluid (toluene/Triton X-100 (2 : 1), 17% H_2O (v/v), 0.5% (w/v) 2,5-diphenyloxazole (PPO)) was added, and the samples were counted in an Intertechnique scintillation spectrometer. In the oil floatation technique (based on the method of Gliemann et al. [15]), the incubated cells were poured onto 600 μl of a phthalate oil mixture (dibutylphthalate (density 1.046)/bis(2-ethylhexyl)phthalate (density 0.985), 3 : 5, v/v) and centrifuged for 50 s at 1300 × *g* on a Hettich bench centrifuge. After centrifugation, the cells were collected with a 200 μl automatic pipette from the surface of the oil, which now overlayed the buffer. The pipette tip, containing the cells in oil, was placed in a scintillation vial, and the radioactivity was measured as above.

Quantitatively and qualitatively, the two techniques gave near to identical results. As, however, the amount of residual buffer trapped on the filter was about 10 μl, whereas the amount passing with the cells through the oil was only 2 μl, the background was much smaller with the oil floatation technique, and this technique is now used routinely.

For each experimental series, buffer ^{86}Rb and ^{14}C activities and ^{86}Rb spill-over ratio were measured in triplicate samples.

The apparent $^{86}Rb^+$ uptake into the cells was defined as the excess $^{86}Rb^+$ recovered above $^{86}Rb^+$ originating from the residual buffer. This uptake was expressed as a clearance, i.e., as the number of μl buffer/million cells to which it corresponded.

The active uptake at a given time was defined as the apparent uptake at that time minus the apparent uptake at time zero at 37°C in the presence of 1 mM ouabain (see Results). Each experimental point was determined at least in duplicate.

O_2 consumption. In order to monitor hormonal sensitivity of the cells, cell respiration was measured in all preparations with a Yellow Springs Instrument 4004 Clark oxygen electrode mounted in a closed chamber containing 10^5 cells in 1.4 ml Krebs-Ringer bicarbonate buffer at 37°C. Only

cell preparations where 1 µM norepinephrine stimulated the respiration about 10-times over the basal rate, were used for the Rb^+ experiments.

In experiments where thermogenesis and ion flux were studied in parallel, the cells were incubated as described above (Rb^+ uptake), and the incubate was then added directly to the oxygen electrode chamber.

Respiration was calculated in nmol O/min per 10^6 cells, based on an oxygen content of 434 nmol O/ml H_2O at 37°C.

Buffers. Krebs-Ringer phosphate buffer (used only for cell preparation) contained (in mM) 148 Na^+/6.9 K^+/1.5 Ca^{2+}/1.4 Mg^{2+}/117 Cl^-/1.4 SO_4^{2-}/22 phosphate/10 glucose/10 fructose/4% crude bovine serum albumin (pH 7.4).

Krebs-Ringer bicarbonate buffer (used for Rb^+ uptake experiments and respiratory studies) contained (in mM) 145 Na^+/6.0 K^+/2.5 Ca^{2+}/1.2 Mg^{2+}/130 Cl^-/1.2 SO_4^{2-}/1.2 phosphate/25 bicarbonate/10 glucose/10 fructose/4% fatty-acid-free bovine serum albumin (pH 7.4).

Chemicals. ^{86}RbCl was from Amersham International and [^{14}C]methoxyinulin from New England Nuclear. Pentex bovine serum albumin (crude and fatty-acid free) was from Miles Laboratories. Crude collagenase, ouabain octahydrate, L-norepinephrine bitartrate, L-isoprenaline bitartrate and L-phenylephrine-HCl were all from Sigma Chemicals. L-Propranolol HCl was from ICI, phentolamine methansulfonate from Ciba-Geigy, and D-norepinephrine bitartrate was a gift from Pharmacia.

Results

The chemical basis for changes in membrane potential is the membrane permeability to certain ions (especially Na^+ and K^+) and the gradients of these ions over the plasma membrane. We have here followed one of these parameters, the K^+ gradient, by the use of the K^+ analogue $^{86}Rb^+$; intracellular K^+ accumulation has been expressed as a clearance value for $K^+(Rb^+)$.

$^{86}Rb^+(K^+)$ uptake in brown adipocytes

We initially studied the characteristics of the $^{86}Rb^+$ uptake process in isolated brown fat cells.

As shown in Fig. 1, the cells exhibited a high initial rate of $^{86}Rb^+$ uptake during the first 10 min, and an equilibrium level was reached at 30 min. The maximal uptake under control conditions, expressed as microliters clearance, was 27 ± 1 µl/million cells (mean value ± S.E., $n = 58$). This is equivalent to an uptake of 160 nmol K^+/million cells.

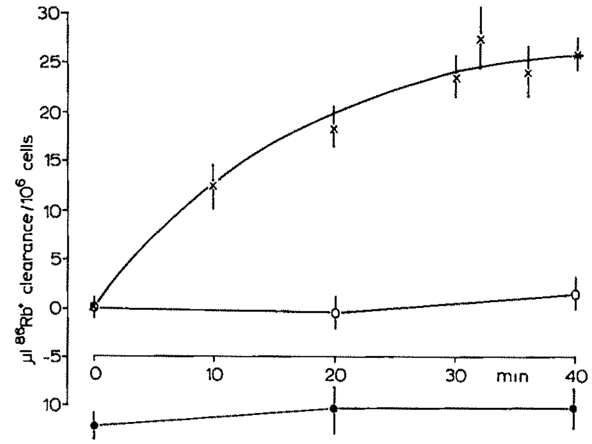

Fig. 1. Active uptake of K^+ ($^{86}Rb^+$). Samples of 300000 cells were incubated at 37°C (×), at 37°C with 1 mM ouabain (○), and at 4°C (no additions) (●). The incubated cells were filtered, and the cellular $^{86}Rb^+$ content was determined at different times between 0 and 40 min. The $^{86}Rb^+$ distribution is expressed as the $^{86}Rb^+$ clearance in µl/million cells. The apparent uptake at time zero at 37°C in the presence of 1 mM ouabain was set to zero and subtracted from all other values. Values are means ± S.E. from at least ten determinations on at least ten different cell preparations.

Prior to the experiments, the cells had been stored overnight at 4°C. This treatment probably resulted in a decreased K^+ gradient over the plasma membrane, due to a reduced $(Na^+ + K^+)$-ATPase activity. The Rb^+ uptake could therefore be considered to be composed of two components: a net influx of $Rb^+(K^+)$, due to the active restoration of the lowered ion gradients over the cell membrane, and a successive exchange of remaining internal K^+ for $^{86}Rb^+$, corresponding to the inherent K^+ leakage of the membrane. The plateau after 30 min would thus represent a steady state between the inherent passive $K^+(Rb^+)$ leakage and the ATPase-dependent uptake at isotopic equilibrium.

To establish the activity of the exchange pathway, cells were preincubated at 37°C, and $^{86}Rb^+$

was subsequently added. Under these conditions, the initial rate of ^{86}Rb uptake was much lower than that seen in Fig. 1 (data not shown). Thus, the main process for the uptake must be considered to be the active restoration of the ion gradients.

In extended incubation periods, 40–90 min, the equilibrium level tended to decline after 40–50 min (not shown). The major reason seems to be that the cells aggregated, became more 'leaky', and lost their viability. Measurements of O_2 consumption showed a parallel loss of norepinephrine response.

As shown in Fig. 1, the presence of the ($Na^+ + K^+$)-ATPase inhibitor ouabain, or incubation at 0°C, completely inhibited the $^{86}Rb^+$ uptake, indicating an active ATPase-dependent uptake mechanism. The value at time zero at 37°C in the presence of ouabain was chosen as zero level for the active uptake (Fig. 1).

When cells were incubated in a modified Krebs-Ringer bicarbonate buffer containing only 25 mM Na^+ (and 120 mM choline$^+$), the final $^{86}Rb^+$ equilibrium was only about 60% of that seen in the normal buffer (data not shown).

Thus, it was concluded that the cells, cold-stored overnight, were markedly depleted in intracellular K^+, but that within a 30 min incubation period they were able to restore their ionic equilibria to steady-state values by active transport processes.

The relationship between $^{86}Rb^+(K^+)$ uptake and the capacity for norepinephrine-induced thermogenesis (oxygen consumption)

In order to elucidate the significance of the K^+ status of the cells on their ability to carry out hormone-stimulated thermogenesis, we have determined the relationship between the cellular K^+ content and the subsequent respiratory response to norepinephrine.

This response was tested in oxygen electrode experiments parallel to the uptake experiments shown in Fig. 1. As seen in Table I, cold-stored cells, transferred to 37°C and incubated for 5 min to observe the basal rate of respiration, responded well to norepinephrine. When ouabain was present during the 5 min incubation, no statistically significant effect was observed on the norepinephrine response. However, the presence of ouabain during a 30 min pre-incubation period (which totally abolished Rb^+/K^+ uptake, cf. Fig. 1) resulted in a 40% reduced respiratory response to a maximal dose of norepinephrine. The enhancement of inhibition seen during the extended ouabain incubation probably indicates that the cells were initially not entirely K^+-depleted, but lost further K^+ when exposed to the higher temperature in the presence of ouabain, and this was reflected in a loss of norepinephrine response. This loss was not due to a direct effect of ouabain on maximal thermogenesis and thus not directly due to ($Na^+ + K^+$)-ATPase inhibition, as addition of ouabain to cells which (according to Fig. 1) had already attained equilibrium, did not have any acute inhibitory effect (Table I). Rather, the effect of ouabain on respiration was probably secondary to the unrestored ion gradients and to the low cytosolic K^+ content. In agreement with this suggestion, it has earlier been observed that incubation of the cells in a low K^+ buffer (which would also result in a decreased cytosolic K^+ content) leads to inhibition of lipolysis [16] and thus to lack of substrate for thermogenesis (respiration).

TABLE I

EFFECT OF OUABAIN ON THE NOREPINEPHRINE-INDUCED RATE OF THERMOGENESIS (RESPIRATION)

Cells were incubated and tested in the oxygen electrode. 1 mM ouabain was added at time zero or at 30 min, and 1 μM norepinephrine at 5 or 35 min The increase in oxygen consumption caused by 1 μM norepinephrine (NE) added after 5 min basal respiration was set to 100% in each preparation (mean value 505 nmol O/min per million cells). The results are the means ± S E. from four determinations on two different cell preparations. [a] indicates a significant effect of ouabain ($P < 0.01$; Student's t-test).

	NE-induced increase in respiration (%)
Time zero preincubation	
no additions	100 ± 6
+1 mM ouabain (0–5 min)	86 ± 9
30 min preincubation	
no additions	108 ± 11
+1 mM ouabain (30–35 min)	106 ± 14
+1 mM ouabain (0–35 min)	63 ± 3 [a]

It may therefore be concluded that restoration of the intracellular ion milieu and the ion gradients were beneficial for thermogenesis, but that such restoration was not essential, and that the direct anti-thermogenic effect of inhibition of the $(Na^+ + K^+)$-ATPase was small.

Effect of norepinephrine on the $^{86}Rb^+(K^+)$ distribution

In order to investigate the effect of norepinephrine on the intracellular $^{86}Rb^+(K^+)$ content, brown fat cells were incubated as in Fig. 1 for 30 min to reach the equilibrium level of intracellular $^{86}Rb^+$. Thereafter, 1 μM norepinephrine was added, and its effect was followed for 10 min (Fig. 2). Already the first sample, about 30 s after norepinephrine addition, showed a very marked decrease in $^{86}Rb^+$ level compared with the control. This lower level was sustained for at least 10 min under these conditions, i.e., in the presence of ascorbate (which was added here in order to counteract oxidation of norepinephrine [17,18]). Unfortunately, the techniques used did not allow the initial time-course of this efflux to be followed in detail.

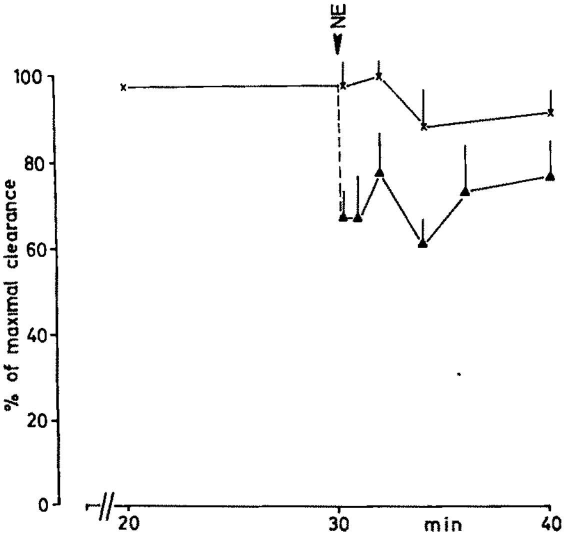

Fig. 2. Effect of norepinephrine on the $K^+(^{86}Rb^+)$ clearance. 1 μM norepinephrine (NE) was added at equilibrium (30 min) and the induced changes in the $^{86}Rb^+$ distribution followed for 10 min Values are expressed as percentage of maximal clearance in each preparation. Points indicate mean±S.E. from 6–14 determinations, performed on 3–7 different cell preparations. The norepinephrine was dissolved in 10 μl of a 0.04% ascorbate solution. ×, control; ▲, 1 μM NE added.

Due to the possible release of stored endogenous norepinephrine by ascorbate [19], dose-response experiments were performed in the absence of ascorbate.

The effect of norepinephrine was, as seen in Fig. 3 (curve '30.5 min'), dose dependent, with an apparent EC_{50} of about 10 nM norepinephrine and a maximal effect at about 1 μM.

However, under these conditions, i.e., the absence of ascorbate, the norepinephrine response was fully reversed after 10 min (in contrast to the results presented in Fig. 2).

As seen in Fig. 4, the effect of norepinephrine was stereospecific. Thus, 10–100-times more D-norepinephrine was needed in order to obtain the same effect as with the natural isomer.

Investigation of the possible involvement of the $(Na^+ + K^+)$-ATPase in the norepinephrine-induced $^{86}Rb^+(K^+)$ efflux

Theoretically, the decrease in intracellular $^{86}Rb^+$ after norepinephrine addition could be due to either an inhibition of the $(Na^+ + K^+)$-ATPase or to a direct or indirect increase in K^+ permeability. In order to distinguish between these possibilities, cells were stimulated with norepinephrine in the presence and in the absence of a concentration

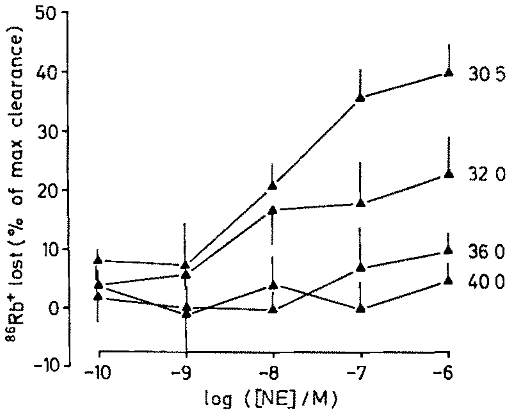

Fig. 3. Dose-response curve for the effect of norepinephrine (NE) on the $^{86}Rb^+(K^+)$ distribution in brown fat cells. Norepinephrine was added at 30 min. The curves indicate the levels at different times (in minutes) measured as demonstrated in Fig. 2, but in the absence of ascorbate (cf., the discussion of ascorbate effects by Mohell et al. [19]). Points indicate the mean decrease (±S.E., $n = 2$–6) in $^{86}Rb^+$ clearance, as compared to control levels.

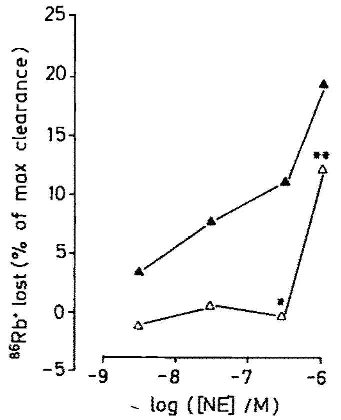

Fig. 4. Stereospecificity of the effect of norepinephrine (NE) on the $^{86}Rb^+$ distribution in brown fat cells. Experiments were performed as in Fig 2 (but in the absence of ascorbate) with indicated concentrations of D- or L-norepinephrine (△ and ▲, respectively) The levels were measured 2 min after norepinephrine addition (cf., 32.0 min in Fig 3) Points are the mean decrease below control levels from 8–10 determinations on four different cell preparations * and ** indicate $P < 0.05$ and 0.01, respectively (analysis of variance on duplicate determinations in four preparations)

of ouabain which fully inhibited the ATPase, cf. Fig. 1. As seen in Table II, the effects of ATPase inhibition and hormone stimulation were additive, indicating that the hormone effect was not due to $(Na^+ + K^+)$-ATPase inhibition.

Further, as the uptake of $Rb^+(K^+)$ is fully dependent on ATPase activity (cf. Fig. 1), we investigated whether the initial uptake rate was influenced by the presence of norepinephrine. As seen in Fig. 5, the presence of norepinephrine was without inhibitory or stimulatory effect.

TABLE II

EFFECT OF OUABAIN UPON CONTROL AND NOREPINEPHRINE-INDUCED $^{86}Rb^+$-DISTRIBUTION

Ouabain (1 mM) was added after 29 min incubation. At 30 min, norepinephrine (1 μM) in ascorbate, or only ascorbate, was added. The effects were measured at 34 min. Values represent the means±S.E. of 4–6 determinations from 2–3 different cell preparations. 100% was defined as the maximal clearance value in each individual cell preparation.

	% of maximal $^{86}Rb^+$ clearance
No additions	88± 8
1 mM ouabain	69± 2
1 μM norepinephrine	66± 5
1 mM ouabain+1 μM norepinephrine	53±15

Thus, in our experimental system, we were unable to obtain any evidence for a direct effect of norepinephrine on the $(Na^+ + K^+)$-ATPase activity.

Pharmacological characterization of the adrenergically induced $^{86}Rb^+(K^+)$ efflux

Norepinephrine at 1 μM binds to both α- and β-adrenergic receptors [14,20], and it is therefore not possible to determine from Fig. 2 whether the response is α- or β-mediated. In order to investigate this, we initially compared the effect of the predominantly α-adrenergic agonist phenylephrine and the predominantly β-adrenergic agonist isoprenaline to that of norepinephrine. The concentrations used (1 and 0.1 μM, respectively) were those shown by Mohell et al. [19] to yield maximal respiratory responses through their respective receptors.

We found that all three agonists induced similar effluxes of $^{86}Rb^+$ (not shown).

However, as shown in Fig. 6, both the response to phenylephrine and that to isoprenaline were much more sensitive to the α-antagonist phentolamine than to the β-antagonist propranolol.

We therefore conclude that the effect of all the

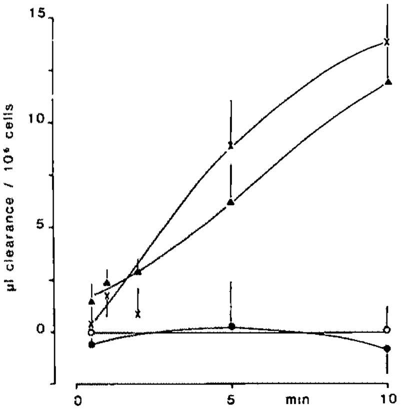

Fig. 5. The effect of norepinephrine on the initial rate of $^{86}Rb^+$ uptake. Cells were incubated as in Fig. 1 in the presence or the absence of ouabain (1 mM) and/or norepinephrine (1 μM), dissolved in buffer. Results are means±S.E from 6–10 determinations from 3–5 different cell preparations. ×, control; ○, ouabain; ●, norepinephrine+ouabain; ▲, norepinephrine

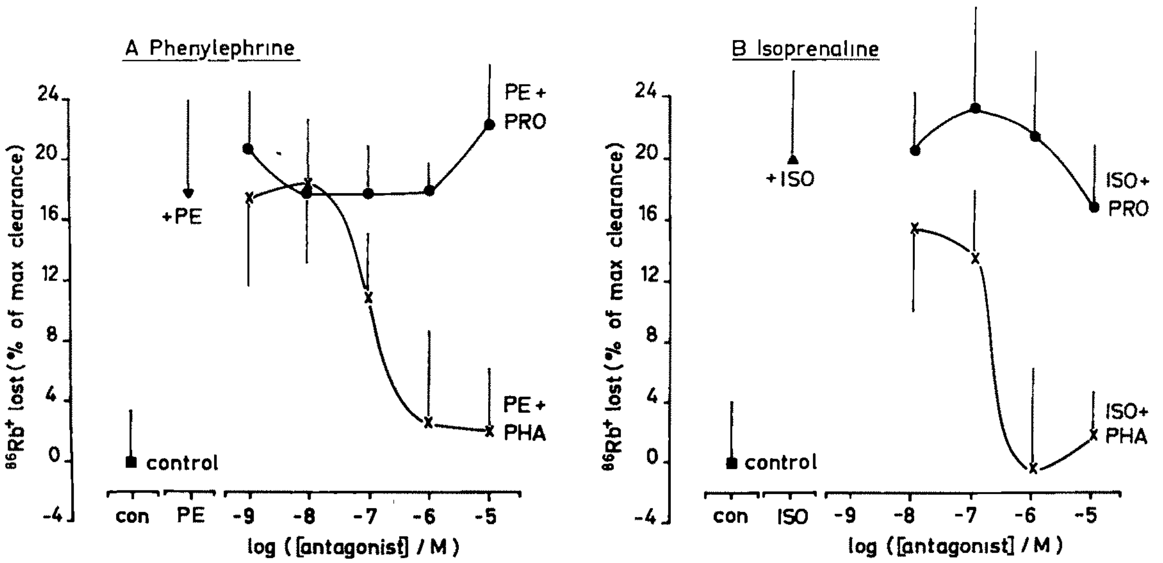

Fig. 6. The effect of α- and β-antagonists on catecholamine-induced $^{86}Rb^{+}$ fluxes. Cells were incubated as in Fig 2, but with varying amounts of the indicated antagonist, phentolamine (PHA) or propranolol (PRO) added at 28 min. At 30 min, 1 μM phenylephrine (PE) or 0 1 μM isoprenaline (ISO) (both dissolved in Krebs-Ringer bicarbonate buffer) were added. After another 2 min the incubation was stopped and the cells were recollected. Points indicate the means ± S.E. from triplicate determinations in 3–4 different cell preparations.

catecholamines is predominantly of an α-adrenergic nature.

Discussion

In the experiments described here, we have shown that brown fat cells, ionically depleted by cold incubation, were able to fully restore their monovalent ion gradients within 30 min, leading to a $K^{+}(Rb^{+})$ clearance of about 27 μl/million cells, equivalent to a K^{+} gradient of some 10-fold (see below). The restoration was fully dependent upon the action of the $(Na^{+} + K^{+})$-ATPase. Further, we found that it was possible to release reversibly a substantial part of the accumulated K^{+} by α-adrenergic stimulation, under conditions where a membrane depolarization has been observed in microelectrode studies.

Differentiation of acute and chronic effects of inhibition of $(Na^{+} + K^{+})$-ATPase

The degree of participation of the $(Na^{+} + K^{+})$-ATPase in the thermogenic mechanism of brown adipose tissue has been widely discussed [4,21–23]. The experiments described here, where ion gradients and thermogenic response have been investigated under parallel conditions, may help to elucidate this question.

The results presented above did not substantiate an acute role of the $(Na^{+} + K^{+})$-ATPase in the thermogenic mechanism of the brown fat cells (i.e., the possibility that a substantial part of the heat production should arise from the ATP breakdown of the $(Na^{+} + K^{+})$-ATPase). During basal respiration, the thermogenic inhibition caused by the addition of the $(Na^{+} + K^{+})$-ATPase inhibitor was small (less than 5%), in agreement with the calorimetric data presented by Chinet et al. [24]. Similarly, during maximal norepinephrine-stimulated respiration, no significant effect of ouabain addition was found (Table I). This may be interpreted so that the mitochondrial capacity for respiration is fully exploited under conditions of maximal stimulation, and extra utilization of ATP for the $(Na^{+} + K^{+})$-ATPase cannot lead to any further respiration. There is, however, good reason to think that the $(Na^{+} + K^{+})$-ATPase is indirectly stimulated by norepinephrine during thermogenesis; this indirect stimulation would be the result of the norepinephrine-induced lowered ion gradients. Thus, some portion of total respiration would naturally result from the synthesis of ATP required for the $(Na^+ + K^+)$-ATPase. In our experimental system we have not been able to observe a direct stimulatory effect of norepinephrine on the $(Na^+ + K^+)$-ATPase (Fig. 5), in contrast to what has been observed with the isolated ATPase [23].

Regarding the effect of prolonged inhibition of the $(Na^+ + K^+)$-ATPase, the comparison between the respiratory data and the ionic accumulation gives a good indication that the inhibitory effect of ouabain on thermogenesis under these circumstances is due to the very low ion gradients then encountered. As seen, a prolonged inhibition of K^+ uptake before norepinephrine addition resulted in a 40% reduction of thermogenesis (Table I).

The most likely explanation for this inhibitory effect of prolonged incubation with ouabain is that lipolysis (and thus provision of substrate for thermogenesis) is dependent upon a physiologically high cytosolic K^+ content. After prolonged incubation with ouabain, this high K^+ content is no longer found, and a situation reminiscent of that observed with incubation of cells in a low-K^+ buffer is created. In both brown [16] and white [25] fat cells, this leads to inhibition of lipolysis.

This clear distinction between the effects observed upon acute and prolonged inhibition of the $(Na^+ + K^+)$-ATPase may help to explain why different estimates of the participation of the $(Na^+ + K^+)$-ATPase in brown fat thermogenesis have been reported, and why, for example, time-dependent effects [26] have been noted.

The K^+ gradient and the membrane potential

In the basal state, a K^+ clearance of about 27 μl/million cells (27 pl/cell) was found. In order to convert this to a K^+ gradient, the cytosolic volume of the brown fat cells must be known. On the basis of a cell concentration of about 100 million/g tissue (for compilation, see Ref. 3), a cellular volume of about 10 pl can be estimated, and with the triacylglycerols being about one-third of the tissue (e.g., Ref. 27), and the mitochondria being a major part of the cytoplasmic space, a cytosolic volume of about 2–3 pl remains. (In preliminary experiments, we have tried to determine the cytosolic space with 3-*O*-D[*methyl*-^{3}H]glucose. This gave values of 4–5 pl/cell.) Thus, the concentration gradient of K^+ is in the order of 10-fold (or more, as full passive ionic distribution was not necessarily assured by the incubation of the cells overnight at 4°C). This gradient – according to the Nernst equation – is equivalent to a K^+ potential of at least −60 mV.

The membrane potential of brown fat cells is about −60 mV, when measured at 37°C (for review, see Ref. 3). There is thus good agreement between the basal membrane potential and the K^+ potential, indicating (in agreement with the calculations of Girardier et al. [1]) that the K^+ potential dominates the membrane potential in the resting state, with P_{Na} being only about 1/25 of P_K. (The K^+ potential is probably somewhat higher than the membrane potential, as addition of the K^+ ionophore valinomycin leads to a hyperpolarization of these cells [28].)

The addition of catecholamines brings about a membrane depolarization of 15–25 mV ([1,2,29], for review see Ref. 3). This membrane depolarization is persistent, as long as the catecholamine is being perfused. It is reported here that after norepinephrine addition, a K^+ efflux occurred from isolated cells (principally in accordance with earlier studies of fractional loss of $^{42}K^+$ from tissue slices [1,30,31]). In the experiments demonstrated here, this efflux led to the loss of 30–40% of the accumulated K^+. In the presence of ascorbate, this decreased K^+ potential was maintained (Fig. 2). However, in the absence of ascorbate, the K^+ potential gradually returned to initial levels (Fig. 3). (Although this is in accordance with a protective antioxidant effect of ascorbate on the added norepinephrine, control oxygen electrode experiments indicated that this simple explanation of ascorbate action could not fully account for the effect of ascorbate.) According to the Nernst equation, the observed (transient or maintained) loss of 30–40% of the accumulated K^+ is equivalent to a decrease in K^+ potential of 15 mV.

There is thus, both in the unstimulated and the norepinephrine-stimulated steady state conditions, rather good agreement between the membrane potential (determined electrophysiologically) and the K^+ potential (determined chemically). Also, both the initial phase of membrane depolarisation [2] and the decreased K^+ potential reported here (Fig. 6) are of an α-adrenergic nature.

Taken together, these observations are indicative of a close relationship between membrane depolarisation and the α-adrenergically-stimulated K^+ efflux, a relationship which has been observed not only in brown adipose tissue, but also in several other nonexcitable tissues, notably parotid gland [10,32,33], lacrimal gland [11], cultured kidney cells [13], guinea-pig and rabbit (but not rat) liver [34–36] and white adipose tissue [37]. The functional relationship between α-adrenergic stimulation and K^+ efflux is presently unknown.

In brown fat cells, the observed K^+ release from the cells is probably not due to an immediate and direct opening of K^+ channels in the plasma membrane, induced by norepinephrine stimulation. Such an increase in P_K would lead to a hyperpolarisation, not to the electrophysiologically observed depolarisation. Rather, we suggest that increase in P_K is involved in a specific pathway for the mediation of α_1-adrenergic signals, as described below.

A possible mechanism for the α-adrenergic stimulation of K^+ efflux

The adrenergic receptors of the brown fat cells have until recently been considered to be exclusively of the β-adrenergic type. The (main part of) thermogenesis is β-adrenergically mediated [19], and is thought to involve the classical β-adrenergic steps: an increase in cyclic AMP; stimulation of protein kinase(s); activation of hormone-sensitive lipase; and release of free fatty acids from the triglycerides (for review see Ref. 3). The free fatty acids themselves [38,39] or their acyl-CoA derivatives [40,41] are then thought to partially uncouple the mitochondria through their interaction with thermogenin, the brown-fat specific [42], 32 kDa purine nucleotide (GDP) binding protein in the mitochondrial membrane (for review see Refs. 3 and 43).

The results presented here accede to an increasing body of evidence that also an α_1-adrenergic mechanism exists in these cells. We suggest that the K^+ efflux observed here is mediated through the following chain of events [44].

Agonist binding to the abundant α_1-adrenergic receptors [19] leads to an increase in plasma membrane conductivity (probably P_{Na}) [45], which is manifested as an α-adrenergic [2,29] membrane depolarization.

Thus, Na^+ enters the cells, and the cytosolic Na^+ concentration increases [30,31]. This leads via the mitochondrial Na^+/Ca^{2+} exchange to a mobilization of mitochondrial Ca^{2+} [9] and to an elevated cytosolic Ca^{2+}. This Ca^{2+} may then activate Ca^{2+}-dependent K^+ channels, of the type described in several nonexcitable tissues [13,36,46,47], and the increased P_K may tend to counteract the membrane depolarization brought about by the increase in P_{Na}. Under the conditions of a decreased membrane potential and an elevated P_K, the K^+ gradient adjusts itself to the new Nernst equilibrium, and a net K^+ efflux is observed.

Thus, in this model, the membrane depolarization in these cells may be understood, not mainly as an electrical/physical phenomenon, but rather as a chemical/metabolical phenomenon, being part of a system which probably has as its purpose to reset intracellular ionic conditions. It is likely that it is the increase in cytosolic Ca^{2+} which is the main mediatory event in this sequence; this Ca^{2+} then has as one of its effects to activate the feed-back increase in K^+ permeability described here, but the Ca^{2+} has presumably additional mediatory effects, as yet unidentified in this tissue.

Acknowledgement

This work was supported by the Swedish Natural Science Research Council. The authors would like to thank Torben Clausen, Jørgen Gliemann and Ole Sonne for advice, discussions and demonstrations.

References

1 Girardier, L., Seydoux, J. and Clausen, T. (1968) J Gen. Physiol. 52, 925–940
2 Girardier, L. and Schneider-Picard, G (1983) J. Physiol. (Lond.) 335, 629–641
3 Nedergaard, J. and Lindberg, O. (1982) Int. Rev. Cytol. 74, 187–286
4 Horwitz, B.A. (1978) Exp. Suppl. 32, 19–23
5 Nedergaard, J., Nånberg, E. and Cannon, B. (1981) Acta Univ. Carol. 1979, 331–333
6 Nånberg, E., Nedergaard, J. and Cannon, B. (1981) Acta Pharmacol. Toxicol. 49, Suppl III, 36
7 Nånberg, E., Nedergaard, J. and Cannon, B. (1982) Acta Pharmacol. Toxicol. 51, Suppl. II, 31
8 Pettersson, B. and Vallin, I. (1976) Eur. J. Biochem. 62, 383–390

9 Connolly, E., Nånberg, E. and Nedergaard, J. (1984) Eur. J. Biochem., in the press
10 Putney, J.W., Jr. (1976) J. Pharm. Exp. Ther. 198, 375–384
11 Parod, R.J. and Putney, J.W., Jr. (1978) J. Physiol. (Lond.) 281, 359–369
12 Resh, M., Nemenoff, R.A. and Guidotti, G. (1980) J. Biol. Chem. 255, 10938–10945
13 Brown, C.D.A. and Simmons, N.L. (1982) Biochim. Biophys. Acta 690, 95–105
14 Svoboda, P., Svartengren, J., Snochowski, M., Houstek, J. and Cannon, B. (1979) Eur. J. Biochem 102, 203–210
15 Gliemann, J., Østerlind, K., Vinten, J. and Gammeltoft, S. (1972) Biochim. Biophys. Acta 286, 1–9
16 Nedergaard, J. (1981) Eur. J. Biochem 114, 159–167
17 Durand, J., Giacobino, J.P. and Girardier, L. (1978) Experientia, Suppl. 32, 45–53
18 Durand, J., Giabocino, J.P., Deshusses, J. and Girardier, L. (1979) Biochem. Pharmacol. 28, 1347–1351
19 Mohell, N., Nedergaard, J. and Cannon, B. (1983) Eur. J. Pharmacol. 93, 183–193
20 Mohell, N, Svartengren, J and Cannon, B. (1983) Eur. J. Pharmacol. 92, 15–25
21 Horwitz, B.A. (1973) Am. J. Physiol. 224, 352–355
22 Horwitz, B.A. (1978) in Strategies in Cold (Wang, L.C H. and Hudson, J.W., eds.), pp. 619–654, Academic Press, New York
23 Hettinger, D.R. and Horwitz, B.A. (1983) Comp. Biochem. Physiol. 74C, 355–360
24 Chinet, A., Clausen, T. and Girardier, L. (1977) J. Physiol. (Lond.) 265, 43–61
25 Mosinger, B. and Vaughan, M. (1967) Biochim. Biophys. Acta 144, 556–568
26 Herd, J.A., Hammond, R.P. and Hamolsky, M.W. (1973) Am. J. Physiol. 224, 1300–1304
27 Nedergaard, J. and Cannon, B. (1984) Am. J. Physiol., in the press
28 Krishna, G., Moskowitz, J., Dempsey, P. and Brodie, B.B. (1970) Life Sci. 9, 1353–1361
29 Fink, S. and Williams, J.A. (1976) Am. J. Physiol. 231, 700–706
30 Girardier, L. and Seydoux, J. (1971) in Nonshivering Thermogenesis (Janský, L., ed.), pp. 255–270, Academia, Prague, and Swetz & Zeitlinger, Amsterdam
31 Girardier, L. and Seydoux, J. (1971) J. Physiol. (Paris) 63, 147–186
32 Strittmatter, W.J., Davis, J.N. and Lefkowitz, R.J. (1977) J. Biol. Chem. 252, 5472–5477
33 Danielsson, Å, and Sehlin, J. (1983) Acta Physiol. Scand. 117, 561–566
34 Haylett, D.G. and Jenkinson, D.H. (1972) J. Physiol. (Lond.) 225, 721–750
35 Haylett, D.G. and Jenkinson, D.H. (1972) J. Physiol. (Lond.) 225, 751–772
36 Burgess, G.M., Claret, M. and Jenkinson, D.H. (1981) J. Physiol. (Lond.) 317, 67–90
37 Perry, M C and Hales, C.N. (1970) Biochem. J. 117, 615–621
38 Cannon, B., Nicholls, D.G. and Lindberg, O. (1973) in Mechanisms in Bioenergetics (Azzone, G.F., Ernster, L., Papa, S., Quagliariello, E., and Siliprandi, N., eds.), pp. 357–364, Academic Press, New York
39 Locke, R., Rial, E., Scott, I.D. and Nicholls, D.G. (1982) Eur. J. Biochem. 129, 373–380
40 Cannon, B., Sundin, U. and Romert, L. (1977) FEBS Lett. 74, 43–46
41 Strieleman, D.J., Edson, C.E. and Shrago, E. (1983) Fed. Proc. 42, 1324
42 Cannon, B, Hedin, A. and Nedergaard, J. (1982) FEBS Lett. 150, 129–132
43 Nicholls, D.G. (1979) Biochim. Biophys. Acta 549, 1–29
44 Nedergaard, J., Connolly, E., Nånberg, E. and Mohell, N. (1984) Biochem. Soc. Trans., in the press
45 Horowitz, J.M., Horwitz, B.A. and Smith, R.E. (1971) Experientia 27, 419–421
46 Atwater, I., Dawson, C.M., Ribalet, B. and Rojas, E. (1979) J. Physiol. (Lond.) 288, 575–588

Biochimica et Biophysica Acta, 804 (1984) 301–307
Elsevier

BBA 11315

PHOSPHOLIPID COMPOSITION OF HUMAN MONOCYTES AND ALTERATIONS OCCURRING DUE TO CULTURE AND STIMULATION BY C3b

FRED F. KENNETT [a], HARVEY A. SCHENKEIN [a,*], THOMAS M. ELLIS [b], and R. BRUCE RUTHERFORD [a,**]

[a] Departments of Periodontics and [b] Microbiology and Immunology, Medical College of Virginia, School of Dentistry, Richmond, VA 23298 (U.S.A.)

(Received December 20th, 1983)
(Revised manuscript received March 20th, 1984)

Key words. Phospholipid composition, Complement component; C3b; (Human monocyte)

The phospholipid composition of human peripheral blood monocytes has not been previously reported, due to difficulty in isolating these cells in a purified state. In this study, monocytes were purified by counterflow centrifugation without selective adherence, and were characterized with the use of fluorescent monoclonal antibodies to T and B lymphocytes and monocytes by flow cytometry. These platelet-free cell preparations contained less than 5% T cells and less than 3% B cells. Isolated monocytes, which were rapidly frozen after isolation, contained phospholipids (in order of decreasing concentrations) as follows: phosphatidylcholine > phosphatidylethanolamine > sphingomyelin > phosphatidylserine > phosphatidylinositol > cardiolipin. A small amount of lyso-PC, but no lyso-PE, phosphatidic acid or lyso-PI, was found. The effect of culturing these cells in the presence or absence of a known stimulant of monocyte prostaglandin E and thromboxane release, the C3b fragment of the third component of human complement (C3), was studied with regard to phospholipid composition. Monocytes cultured without stimulant for 24 h contained 3–4% more sphingomyelin than did uncultured cells, and lyso-PC concentrations were consistently elevated. The addition of the stimulant C3b to cultured cells resulted in enhancement of release of immunoreactive prostaglandin E into culture supernatants, without affecting the release of lysosomal enzymes. Analysis of the phospholipid content of cells cultured in the presence of C3b revealed that there was a significant decrease in total PI compared to cells cultured in the absence of C3b, in addition to an increased concentration of sphingomyelin and lyso-PC when compared to freshly isolated cells. These changes occurred in the absence of elevated concentrations of phosphatidic acid.

Introduction

Cells of the monocytes/macrophage lineage are capable of the enzymatic conversion of polyunsaturated fatty acids, particularly arachidonic acid to the biologically active eicosanoids thromboxane A_2 and prostaglandin E_2 [1]. Amongst the mononuclear leukocytes, the monocyte (macrophage), with a high concentration of arachidonic acid in phospholipid (over 20%) [2,3], is the principle source of eicosanoids. Most, if not all, lymphocytes do not synthesize prostaglandin or thromboxanes, despite the presence of adequate concentrations of arachidonic acid in their membrane phospholipids [4]. A variety of substances, such as zymosan [5], concanavalin A [6], Ca^{2+} ionophore

---

[*] To whom correspondence should be sent.

[**] Current address: University of Connecticut School of Dental Medicine, Department of Oral Biology, Farmington, CT 06032 (U.S.A.)

Abbreviations: PC, phosphatidylcholine; PE, phosphatidylethanolamine; PS, phosphatidylserine; PI, phosphatidylinositol, C3, third component of human complement; C3b, 180 kDa fragment of C3.

0167-4889/84/$03.00 © 1984 Elsevier Science Publishers B.V

[7], aggregated immunoglobulin [8], immune complexes [9], phorbolesters [10], and fragments of the third component of human complement (C3) [11] have been shown to stimulate macrophage prostaglandin release.

It is well established that prostaglandins and thromboxanes are not stored in mammalian tissues, and that the concentration of available unesterified fatty acids in these tissues is insufficient to account for the cell's potential to produce metabolites of arachidonic acid. Therefore, it is generally accepted that the rate-limiting step for the synthesis of these eicosanoids is the release of arachidonic acid from cell phospholipid. It has further been shown that different stimuli induce different pathways of macrophage phospholipid metabolism [7,10].

Until recently, studies of arachidonic acid metabolism and phospholipid composition of human blood monocytes have been hindered by the difficulties in preparing platelet-free cell populations and by the potential alterations that may occur when cells are isolated by selective adherence culturing techniques. We have recently demonstrated that the purified, fluid-phase complement components C3b and iC3b stimulated the release of immunoreactive prostaglandin and thromboxane from human peripheral monocytes that were isolated by counterflow centrifugation [11,12]. This isolation technique provides platelet-free cell preparations that have not undergone an adherence and disadherence phase of purification.

The purpose of the present study was to examine the phospholipid composition of well-characterized preparations of purified human monocytes and the changes that occur during culture of these cells for 24 h. In addition, we examined the effects of C3b, a known stimulant of monocyte prostaglandin release, on phospholipid composition and lysosomal enzyme release during culture.

Methods

Cell isolation and culture

The techniques for the preparation of cells for culture, isolation of C3b and incubation conditions were as reported previously [6]. Briefly, mononuclear cells collected following centrifugation of citrated blood on Ficoll-Hypaque gradients were separated into monocyte and lymphocyte populations by counterflow centrifugation. The monocyte population was cultured in medium MCDB 104 [13] in the absence of serum or protein additives. The C3b utilized for this study was prepared by limited trypsin digestion [14] of purified human C3 [15]. The characteristics of such preparations have been previously published [11].

Monocytes isolated by counterflow centrifugation were characterized as described below, and their concentration was determined by microscopic counts and by analysis on a Coulter cell counter. The monocytes were divided equally into three groups, and were diluted to a final concentration of $1 \cdot 10^6$ cells/ml with culture medium. One group served as a control and was immediately frozen at $-60\,^\circ$C. The other two groups of $(12–24) \cdot 10^6$ cells were cultured for 24 h in the presence or absence of C3b (25 μg/ml).

Extraction of phospholipid and analysis

After the 24 h incubation, the culture media were removed with a Pasteur pipette, and adherent cells were mechanically harvested. Cells were suspended in 0.1 M KCl with a glass-Teflon tissue homogenizer and samples were removed for enzyme analyses (see below) prior to extraction for lipids. The noncultured controls were thawed, and the media from these samples and the experimental cultures were clarified by centrifugation in a Beckman 50.1 rotor. All clarified supernatants were saved for analysis of their lysosomal enzyme activity. Corresponding cells and membrane fragments were extracted for total lipids by the method of Folch et al. [16] as modified by Beckman et al. [17] with re-extraction of the upper phase. 10 vol. chloroform/methanol (2 : 1) were added per volume of cells. Combined chloroform phases were taken to complete dryness and redissolved in 100 μl of chloroform/methanol (9 : 1). Phospholipids were separated according to the method of Turner and Rouser [18] in the presence of butylated hydroxytoluene. Total phosphorous and individual phospholipid phosphorous were determined according to the method of Bartlett [19].

Enzyme and prostaglandin determinations

β-Glucuronidase and N-acetyl-β-glucosaminidase were assayed according to the method of

Ruth et al. [20]. Lysozyme was assayed using micrococcus lysodeiktius as described by Shugar [21]. Immunoreactive prostaglandin was determined by a competitive radioimmunoassay as described previously [11]. Samples or PGE_2 standards were incubated with rabbit anti-prostaglandin E-bovine serum albumin and 3H-labeled prostaglandin E_2. After 90 min, goat anti-rabbit IgG plus pre-immune rabbit serum was added to the incubation mixture. Bound radioactivity in the precipitate was determined by liquid scintillation spectroscopy. The commercial rabbit anti-prostaglandin E serum (Miles Laboratory, Elkhart, IN) displayed the following specificity: prostaglandin E_2, 100%; prostaglandin E_1, 70%; prostaglandin A_1, 1%; prostaglandin F_2, 5%; prostaglandin B_1, 0.6%; and prostaglandin B_2, 0.1%.

Characterization of cell populations

Cell ppopulations were characterized by their reactivity with the following monoclonal antibodies: a-OKT3 and a-OKT11 were the kind gift from Dr. T. Tachovsky. Anti-OKM1 was from Ortho Diagnostic Systems, Inc. (Raritan, NJ), a-B1 was from Coulter Electronics, Hialeah, FL, and a-Mo1 and a-Mac1 were generously provided by F. Todd and T. Mohanakumar, respectively.

Cytometric analysis was performed using an Ortho Spectrum II flow cytometer (Ortho Diagnostic Systems, Westwood, MA) equipped with a Iw argon-ion laser, emitting at a wavelength of 488 nm at an operating power of 30 mW. Forward and right angle (90°) light scatter was measured using photomultiplier gain settings of 27 and 210, respectively, and an integrator gain setting of 5 for both parameters. Green fluorescence was measured using photomultiplier and integrator gain settings of 540 and 15, respectively. Fluorescence-positive cells were expressed as the percentage of total cells which showed staining intensities beyond a window containing 99.5% of control stained cells. Open trigger regions were utilized in all analyses, in order to include all cells present in each sample.

Results

In order to determine the purity of the monocyte preparations, their reactivities with monoclonal antibodies directed against surface antigens of various mononuclear cell types were assessed. The data in Table I show the relative concentrations of T lymphocytes (OKT3- and OKT11-positive cells), B lymphocytes (B1-positive cells) and monocytes (Mac1-, OKM1- and Mo1-positive cells). T lymphocyte markers were present on less than 5% of cells in the monocyte preparations, compared to 60% OKT3 (+) cells and 76% OKT11 (+) cells in unseparated mononuclear cell preparations. B1-positive cells comprised 2.5% of the

TABLE I

FLOW CYTOMETRIC ANALYSIS OF MONOCYTE POPULATIONS PREPARED BY COUNTERFLOW CENTRIFUGATION

Mononuclear cells were prepared by centrifugation on Ficoll-Hypaque gradients. Monocytes were prepared from mononuclear cells by counterflow centrifugation. n.d., not determined

	Mononuclear cells (% positive ± S.D.)	Monocytes (% positive ± S.D.)	Number of determinations
OKT 3	60.0 ± 8.3	4.8 ± 1.1	4
OKT 11	75 7 ± 11.9	2.8 ± 0.3	4
B 1	7 7 ± 2.8	2.5 ± 1.5	2
OKM 1	n.d.	85.0 ± 10.0	2
MO 1	n.d.	77.9 ± 0.9	2
MAC 1	9.5 ± 0.0	84.2 ± 0.3	2

TABLE II

QUANTITATION OF *N*-ACETYL-β-GLUCOSAMINIDASE AND IMMUNOREACTIVE PROSTAGLANDIN IN SUPERNATANTS FROM MONOCYTES CULTURED FOR 24 H WITH OR WITHOUT C3b

Total *N*-acetyl-β-glucosaminidase activity in freshly isolated monocytes was 0.885 ± 0.166 μM/10^6 cells/min. Data are expressed as the mean ± S.D.

	Control ($n = 6$)	C3b, 25 μg/ml ($n = 6$)
N-acetyl-β-glucosaminidase		
Total activity (μM/10^6 cells/min)	0.786 ± 0.296	0.708 ± 0.159
N-acetyl-β-glucosaminidase		
% in supernatants	15.8 ± 7.7	15.9 ± 3.7
Prostaglandin E (ng/10^6 cell)	2 72 ± 2.1	9.44 ± 6.2 [a]

[a] Significantly different from control, $P < 0.05$ as determined by Student's paired *t*-test

monocyte preparations, compared to 7.7% in the mononuclear cell preparations. The monocyte markers (OKM1, Mo1, and Mac1) were present on 78–85% of cells in the monocyte preparations. Mac1-positive cells comprised 9.5% of the mononuclear cells prior to counterflow centrifugation. These data confirm our previous observations on the purity of these cells, which were shown to be over 90% phagocytic and esterase positive [5]. The remaining mononuclear cells in the monocyte preparations are thought to be null cells or promonocytes. Microscopic analysis and size distribution of monocyte preparation revealed a complete absence of platelets, either free or adherent to the monocyte surfaces.

The data in Table II depict the activity of the lysosomal enzyme *N*-acetyl-β-glucosaminidase found in clarified supernatants and in detergent-solubilized cell pellets in six experiments. Despite a decrease in the mean total enzyme activity of the cultured cells as compared to that in noncultured cells that were frozen immediately after isolation, no significant differences were noted between cultures exposed to C3b and those exposed to medium alone. Thus, C3b failed to stimulate release of *N*-acetyl-β-glucosaminidase under these conditions.

Determinations of the enzymatic activities of lysozyme and β-glucuronidase (data not shown) also failed to demonstrate an effect of C3b on these lysosomal enzymes. Lysozyme was slightly more membrane associated, with release of approx. 10% of the activity into the supernatant. β-Glucuronidase was slightly more labile; approx. 20% of the total activity was released into the culture medium.

Table II also demonstrates the release of immunoreactive prostaglandin in these six experiments. As was previously noted, C3b-stimulated prostaglandin production 3- to 7-fold when compared to the corresponding controls. Cultured cells produced prostaglandin at low levels (range 0.54–6.0 ng/10^6 cells), but prostaglandin levels in noncultured cells barely reached reliable limits of detection. In similar preparations, we have shown 5- to 10-times as much thromboxane B_2 release as prostaglandin E_2 [12].

Table III shows the results of the analysis of the monocyte membrane phospholipids expressed as a percentage of total recovered phosphate. Mean recovery was found to be 93.4 ± 7.1% (range 84–111). For all samples, total phosphates were 6.0–7.5 nmol phospholipid P/10^6 cells. No significant differences were noted between experimental groups. The various phospholipids are listed according to their relative concentrations in these membranes. PC was always found to be the major phospholipid, followed by PE and sphingomyelin in each of the preparations. These phospholipids accounted for 70–80% of the total phospholipids.

TABLE III

PHOSPHOLIPID COMPOSITION OF MONOCYTES

Data are expressed as percentage of total recovered phospholipid phosphorus ± S.D. Remaining phospholipid phosphorus is accounted for by unidentified phospholipid plus material remaining at origin of chromatographs. Data represent results of eight different experiments. Numbers in parentheses represent the number of trials in eight experiments in which lyso-PC was detected. In the two trials in which lyso-PC was detected, it accounted for 0 37 and 0.64% of the total phospholipid phosphorus.

Phospholipid	Uncultured cells	24-h cultures	
		control	C3b, 25 μg/ml
Phosphatidylcholine	39.8 ± 4.2	36.8 ± 3.1	35.5 ± 3.2 [a]
Phosphatidylethanolamine	30.4 ± 3.5	29.6 ± 3.4	29.5 ± 5.2
Sphingomyelin	10.9 ± 1.1	14.1 ± 2.1 [a]	16.8 ± 3.3 [a]
Phosphatidylserine	9.5 ± 1.2	7.6 ± 1.6	7.5 ± 1.8
Phosphatidylinositol	6.9 ± 1.1	6.4 ± 1.7	5.0 ± 1.4 [a,b]
Cardiolipin	1.4 ± 0.8	1.2 ± 0.5	1.5 ± 0.8
Lysophosphatidylcholine	< 1.0 (2)	2.4 ± 0.9 (5)	3.7 ± 1.8 (6)

[a] Significantly different from uncultured cells, $P < 0.05$ (Student's paired *t*-test).

[b] Significantly different from cells cultured in the absence of C3b, $P < 0.001$ (Student's paired *t*-test).

A significant decrease in the major phospholipid, PC, was noted only in cultured cells exposed to C3b. Interestingly, the proportion of sphingomyelin was significantly increased in both cultured cell groups. Analysis of the minor phospholipid species failed to demonstrate any lyso-PE or lyso-PI. As has been noted by others [22], the cardiolipin content of these cells is low, less than 2%, and remains low after 24 h of culture. Lyso-PC was found in trace quantities in two of eight uncultured control samples, but was more consistently found in both cultured cell groups (five of eight and six of eight, respectively). Significant decreases in the content of PI were noted only for C3b-treated cells. The decrease was dramatic (over 50%) in four of eight preparations; however, only two preparations yielded any detectable phosphatidic acid after extraction and chromatographic separation.

Discussion

This report confirms the utility of counterflow centrifugation as a means to obtain large numbers of highly pure human peripheral monocytes [6]. This procedure allowed us to examine platelet-free monocyte populations, while avoiding the potential problems of using selective adherence during isolation of our starting material [2]. The purity and uniqueness of these cells have been confirmed by enzyme analysis, microscopy, cell-sizing analysis, and now by immunological techniques (Table I).

The release of prostaglandins and thromboxanes from leukocytes has been demonstrated to occur in response to a variety of stimuli. Elucidation of the phospholipid source of the precursor fatty acid for eicosanoid production has been an active area of study, and is of particular interest with regard to macrophage immunomodulatory functions that may be mediated by metabolites of arachidonic acid.

Although data are available describing the phospholipid composition of certain leukocyte populations and changes that occur during prostaglandin production, to our knowledge our data are the first published which describe the phospholipid content of well-characterized human monocytes. Lipid analysis of human mononuclear cells reported to this point have been performed on cells containing significant numbers of platelets, lymphocytes and monocytes [3,23] or have failed to provide an individual accounting of all phospholipid species [24]. Thus, these data reflect the relative contribution of contaminating cells to total phospholipid analysis, or provide an incomplete or inaccurate picture of phospholipid composition, when only major phospholipids are described. Our choice to examine changes in total cellular phospholipids rather than pulse-labeled phospholipid pools was made to avoid labeling of selected phospholipids during early maturation of the monocyte. In a recent study of platelet-depleted monocyte cultures, the uptake of radiolabeled arachidonic acid into membrane phospholipid pools has been reported [2]. The data reported did not reflect the composition of the monocyte membrane phospholipids, as they are reported in this study. Freshly isolated monocytes contained phospholipids as follows: phosphatidylcholine > phosphatidylethanolamine > sphingomyelin > phosphatidylserine > phosphatidylinositol > cardiolipin. Lyso-PE and phosphatidic acid were not detectable in the cells, and lyso-PC was occasionally present in minute quantities. However, since changes in phospholipids were measured after 24 h in culture, these data do not rule out the possibility that phosphatidic acid was formed early and metabolized further to species not identified by these methods. The same is true for lyso-PC, since these cells are capable of active reacylation when fatty acyl coenzyme A is available as substrate.

Analysis of phospholipid changes due to culture was also performed. It is well known that as monocytes mature in culture, metabolic and structural changes occur [25]. Proliferation of plasma membrane, lysosomes and mitochondria has been shown to occur as early as 24 h after adherence. This has been confirmed microscopically by a number of groups. Biochemical analyses of changes of total and specific activities of organellar marker enzymes also supports these observations [26]. Our study extends these observations by demonstrating that other membrane-associated changes are occurring. The elevation of lyso-PC and sphingomyelin noted in both cultured cell groups may suggest increased membrane turnover in preparation for spreading or maturation. Sphingomyelin is found at high concentration levels in plasma membranes, and to a lesser extent in other organelles [27]. Lyso-PC is one by-product of the action of phospholipase A_2, an initiating step in prostaglandin E production and a means by which the membrane phospholipid can change the fatty acid composition and thus the physical characteristics of the membrane. Lyso-PC is also utilized for de novo synthesis of PC, the major phospholipid of monocyte membranes.

The source of arachidonic acid for production of prostaglandin E and thromboxanes in several other leukocyte systems has been found to be PI and PC, through the use of pulse-radiolabeling techniques. Data that exist demonstrating a predominant pathway for generation of arachidonic acid show a variability that appears to depend on the stimulus utilized and the cell challenged, and it is possible that multiple pathways of arachidonic acid release can be involved [5,7,10]. The degradation of PI and PC and the release of arachidonic acid need not be mutually exclusive; a recent report emphasizes that complex interrelationships may exist between these two processes [31]. In addition, release of lysosomal enzymes in some systems has been reported by others to occur concomitantly with PI turnover [7,28].

We have recently reported that C3b stimulates prostaglandin and thromboxane release from monocytes purified by counterflow centrifugation when they are cultured as described in this study [11,12]. Furthermore, C3b is reported to stimulate release of lysosomal enzymes from rodent macrophages [29,30]. The data reported in the present study indicate that C3b stimulates PI turnover without causing increased release of lysosomal enzymes. In agreement with this concept, others have reported that lysosomal enzyme release and prostaglandin production are not necessarily interdependent processes [5,24]. Our data in Table II demonstrate that human monocytes are capable of prostaglandin production. When stimulated by C3b, a 3- to 6-fold increase in the release of immunoreactive prostaglandin was noted. However, no increase in the release of lysosomal enzymes from these cells was noted after stimulation by C3b. The measurements of lysosomal enzymes did not differ significantly in total activity or in the proportion of activity that remained bound or solubilized for all three enzymes tested. This suggests that, under the conditions reported here, prostaglandin E release and lysosomal enzyme secretion are independent events. We have not studied the influence of cytochalasin B in this system. Examination of the changes in PI for each individual cell preparation from our study alse failed to show any significant correlation between PI turnover and lysosomal enzyme release.

When cultured monocytes were exposed to C3b, changes similar to those seen in nonstimulated cultures were noted in their content of lyso-PC and sphingomyelin. In four of the eight C3b-treated cultures the proportion of lyso-PC recovered was slightly greater than that in corresponding cultured controls, while the increase in sphingomyelin was similar for both groups. Also, in four of the eight C3b treated cultures a large decrease in the content of PI was noted. A similar trend in PI depletion was noted by Serhan et al. [32] following stimulation of human neutrophils. It was thus difficult to segregate changes due to normal membrane turnover of phospholipids and phospholipid changes that may be induced by C3b during prostaglandin E and thromboxane production. This includes the complex metabolic changes that the various intermediates of the major phospholipids may undergo. Our data clearly show that relative changes in phospholipid composition may occur due to culturing conditions, and total quantification of major and minor phospholipid must be performed in order to assess accurately the significance of these changes. Our data are consistent with the interpretation that PI is one possible source of arachidonate for prostaglandin and thromboxane production when the monocyte is activated by C3b. However, these data cannot be interpreted to indicate the presence of a receptor triggered phosphatidylinositol cycle in human monocytes. The decrease in PI could be due to enhanced phospholipase A_1, C or D activity. Data demonstrating the release of arachidonic acid from phosphatidic acid and its conversion to prostaglandin in response to C3b would be required to suggest an active phosphatidylinositol cycle. Experiments to identify the precise source of monocyte arachidonic acid which is converted to thromboxanes, prostaglandins or other metabolites are in progress.

Acknowledgements

This work was supported in part by Grants DE-05512 and DE-05626 from the National institute of Dental Research, National Institutes of Health, and by Biomedical Research Support Grant S07RR-05724. Fred F. Kennett is recipient of Postdoctoral Training Fellowship T32HL-07244, and Harvey A. Schenkein is a recipient of a Research Career Development Award DE-00108, both from the National Institutes of Health.

The authors wish to thank Ms. Debra Bruce, Ms. Lissa Jackson, and Mr. Rennie Berry for their excellent technical assistance.

References

1 Goldyne, M.E. and Stobo, J.D. (1981) CRC Crit. Rev. Immunol. July, 189–223

2 Pawlowski, N., Kaplan, G., Hamill, A., Cohen, Z.A. and Scott, W. (1983) J. Exp. Med. 158, 393–412

3 Stossel, T., Mason, R. and Smith, A. (1974) J. Clin. Invest. 54, 638–645

4 Ferber, E., DePasquale, G. and Resch, K. (1975) Biochim. Biophys. Acta 398, 364–376

5 Bonney, R., Wrightman, P., Davies, P., Sadowski, S., Kuchl, F. and Humes, J. (1978) Biochem. J. 176, 433–442

6 Rutherford, B. and Trummel, C.L. (1983) J. Reticuloendothel. Soc. 33, 175–184

7 Homma, Y., Owozaki, K., Hashimoto, T., Nagai, Y. and Takenawa, T. (1982) J. Immunol. 129, 1619–1626

8 Passwell, J.H., Dayer, J.M. and Merler, E. (1979) J. Immunol. 123, 115–120

9 Rutherford, B. and Schenkein, H.A. (1982) J. Periodontal Res 17, 484–486

10 Humes, J.L., Sadowski, S., Galavage, M., Goldenberg, M., Subers, E., Bonney, R.J. and Kuehl, F.A. (1982) J. Biol. Chem. 257, 1591–1594

11 Rutherford, B. and Schenkein, H.A. (1983) J. Immunol. 130, 874–877

12 Schenkein, H.A. and Rutherford, B. (1984) Immunology 51, 83–91

13 McKeehan, W.L., McKeehan, K.A., Hammond, S.L. and Ham, R.G. (1977) In Vitro 13, 399–416

14 Bokisch, V.A., Muller-Eberhard, H.J. and Cochrane, C.G. (1969) J. Exp. Med. 129, 1109–1132

15 Tack, B.F. and Prahl, J.W. (1976) Biochemistry 15, 4513–4521

16 Folch, J., Lees, M. and Sloane-Stanley, G.H. (1957) J Biol. Chem. 226, 495–509

17 Beckman, J., Owens, K. and Weglicki, W. (1981) Lipids 16, 796–699

18 Turner, J. and Rouser, F. (1970) Anal. Biochem. 38, 423–436

19 Bartlett, G. (1958) J. Biol Chem. 234, 466–471

20 Ruth, R., Kennett, F. and Weglicki, W. (1978) J. Mol. Cell Cardiol. 10, 739–751

21 Shugar, D. (1952) Biochim Biophys. Acta 8, 302–306

22 Gottfried, E. (1967) J. Lipid Res. 8, 321–327

23 Marinetti, G. and Cattieu, K. (1982) Chem. Phys. Lipids 31, 169–177

24 Hseuh, W., Kohn, C. and Needleman, P. (1979) Biochem. J. 184, 345–354

25 Cohen, Z.A (1978) J. Immunol. 121, 813–816

26 Rinehart, J., Wvest, D. and Ackerman, A. (1982) J. Immunol. 129, 1436–1440

27 Rouser, G., Kitchevsky, G. and Kamamoto, A. (1972) Adv. Lipid Res. 10, 261–360

28 Rubin, R., Sink, L. and Freer, R. (1981) Mol. Pharm. 19, 31–37

29 Schorlemmer, H.U., Davies, P and Allison, A.C. (1976) Nature 261, 48–49

30 Schorlemmer, H.U. and Allison, A.C. (1976) Immunology 31, 781–788

31 Seiss, W., Siegel, F. and Lapetina, E. (1983) J. Biol. Chem. 258, 11236–11242

32 Serhan, C., Boekman, M., Korchak, H., Marcus, A. and Weissman, G. (1982) Biochem. Biophys Res. Commun. 107, 951–958

Biochimica et Biophysica Acta, 804 (1984) 308–323
Elsevier

BBA 11309

THE EFFECT OF GLYCERALDEHYDE ON RED CELLS

HAEMOGLOBIN STATUS, OXIDATIVE METABOLISM AND GLYCOLYSIS

P.J. THORNALLEY * and A. STERN

Department of Pharmacology, School of Medicine, New York University Medical Center, 550 First Avenue, New York, NY 10016 (U.S.A.)

(Received November 1st, 1983)

Key words: Glyceraldehyde; Hemoglobin status; Oxidative metabolism, Glycolysis; (Human red cell)

Glyceraldehyde induces changes in the flux of glucose oxidised through the hexose monophosphate pathway, the concentrations of intermediates in the Embden-Meyerhoff pathway, the oxidative status of haemoglobin and levels of reduced and oxidised pyridine nucleotides and glutathione in red cells. Glyceraldehyde autoxidises in the cellular incubations, consuming oxygen and producing glyoxalase I- and II-reactive materials. Major fates of glyceraldehyde in red cells appear to be: (i) adduct formation with reduced glutathione and cellular protein; (ii) autoxidation and reaction with oxyhaemoglobin and pyridine nucleotides, and (iii) phosphorylation of D-glyceraldehyde and entry into the glycolytic pathway as glyceraldehyde 3-phosphate. The production of glycerol from glyceraldehyde by red cell L-hexonate dehydrogenase appears not to be a major reaction of glyceraldehyde in red cells. These results indicate that high concentrations of glyceraldehyde (1–50 mM) may induce oxidative stress in red cells by virtue of the spontaneous autoxidation of glyceraldehyde, forming hydrogen peroxide and α-ketoaldehydes (glyoxalase substrates). The implications of glyceraldehyde-induced oxidative stress for the in vitro anti-sickling effect of DL-glyceraldehyde and for the polyol pathway metabolism of glyceraldehyde are discussed.

Introduction

Glyceraldehyde (used herein to denote features common to D-, L- and DL-glyceraldehyde) is an aldotriose and is one of the simplest monosaccharides found in biology. D-Glyceraldehyde is the biologically important stereoisomer, although L-glyceraldehyde also appears in normal metabolism as a metabolite. The use of glyceraldehyde as an anti-tumour agent, until recently, has been the focus of glyceraldehyde-related research [1].

DL-Glyceraldehyde has recently been shown to inhibit the sickling of sickle cells in vitro. DL-Glyceraldehyde-treated sickle cells showed a small increase in oxygen affinity, a reduction in the Hill coefficient, a substantial increase in the minimum gelling concentration and modification of up to two lysine residues per haemoglobin molecule [2]. DL-Glyceraldehyde did not reverse the sickling of sickle cells when the haemoglobin was in the deoxy state. Other simple monosaccharides were found not to be as effective anti-sickling agents as glyceraldehyde, and there was no stereospecificity with respect to the glyceraldehyde; DL-, D- and L-glyceraldehyde were equally effective. Relatively high concentrations of DL-glyceraldehyde (50 mM) induced cross-linking of cellular haemoglobin and

---

* To whom all correspondence should be addressed at (present address). Department of Pharmacy, University of Aston in Birmingham, Gosta Green, Birmingham, B4 7ET, U.K.

Abbreviations: HMS, hexose monophosphate shunt; Hepes, 4-(2-hydroxyethyl)-1-piperazineethanesulfonic acid.

0167-4889/84/$03.00 © 1984 Elsevier Science Publishers B.V.

membrane proteins. Cells treated with lower concentrations of DL-glyceraldehyde (5–20 mM) showed little change in osmotic fragility, exhibited improved filtration properties and had a lowered viscosity [3]. In an on-going study, the site-specific binding and the formation of ketoamine adducts between haemoglobin and glyceraldehyde have been studied [4–6].

In a recent report [7], we have described the autoxidation of glyceraldehyde and other simple monosaccharides, catalysed by phosphate buffer. DL-, D- and L-glyceraldehyde were shown to autoxidise and form hydroxypyruvaldehyde, hydrogen peroxide, hydroxyl and 1-hydroxylalkyl free radicals. Further studies demonstrated the oxidation of oxyhaemoglobin by autoxidising glyceraldehyde and other simple monosaccharides [8]. D-Glyceraldehyde has been shown to be phosphorylated by red cell triokinase activity [9] and reduced by red cell L-hexonate dehydrogenase activity [10]. The L-hexonate dehydrogenase activity was consistent with the observed stimulation of the hexose monophosphate shunt and oxidation of NADPH in red cells treated with 1.5 mM D-glyceraldehyde. The current interest in the use of high concentrations (up to 50 mM) of DL-glyceraldehyde as a preferred substrate for aldose reductase (alditol: NADPH oxidoreductase, EC 1.1.1.21) in the polyol pathway [11] prompted studies on the oxidative effects of glyceraldehyde on red cell metabolism.

In this report, the effects of glyceraldehyde on red cells, over a concentration range of more than two orders of magnitude, have been studied. Glyceraldehyde induces changes in the flux through the hexose monophosphate pathway, the levels of cellular glycolytic intermediates in the Embden-Meyerhoff pathway, the oxidative status of haemoglobin and the levels of reduced and oxidised pyridine nucleotides and glutathione in red cells. All these changes in red cell metabolism appear to have no gross, acute effects on cellular osmotic fragility (no lysis observed).

Materials and Methods

Red cell preparations. Adult human blood was drawn daily into 3.8% sodium citrate solution. After centrifugation, plasma and white cells were removed and the red cells were washed three times with phosphate-buffered saline (9 parts 0.9% NaCl; 1 part 0.1 M KH_2PO_4/K_2HPO_4 (pH 7.4)) or isotonic saline (0.9% NaCl). A 25% (v/v) suspension of red cells was prepared in Krebs-Ringer phosphate buffer (120 mM NaCl, 4.8 mM KCl, 1.3 mM $CaCl_2$, 1.2 mM $MgSO_4$, 16.5 mM NaH_2PO_4/Na_2HPO_4) using the phosphate-buffered saline washed cells, and a 25% (v/v) suspension of red cells was prepared in Krebs-Ringer glycylglycine buffer (120 mM NaCl, 4.7 mM KCl, 2.5 mM $CaCl_2$, 1.2 mM KH_2PO_4, 1.2 mM $MgSO_4$, 50 mM glycylglycine (pH 7.4)) using the isotonic saline washed cells.

Red cells containing methaemoglobin were prepared by incubating a volume of packed red cells with an equal volume of 0.5% $NaNO_2$ in half-concentrated phosphate-buffered saline for 10 min at room temperature. After this time, the red cells were washed five times in phosphate-buffered saline to remove excess nitrite. A portion of the packed methaemoglobin-containing red cells thereby produced was analysed for methaemoglobin content (see below), to ensure that complete conversion of the native oxyhaemoglobin to methaemoglobin had been achieved. A 25% (v/v) suspension of the packed methaemoglobin-containing cells in Krebs-Ringer phosphate buffer was prepared for all subsequent incubations.

Red cell suspensions containing carbonmonoxyhaemoglobin were prepared by blowing carbon monoxide over 25% suspensions of red cells in Krebs-Ringer phosphate buffer, until haemolysates of a portion of the cells (see below) gave a maximal absorbance at 569 nm. Carbonmonoxyhaemoglobin-containing red cells, thereby produced, were washed once in aerated phosphate-buffered saline.

Enzymes. Fructose-1,6-bisphosphate aldolase (EC 4.1.2.13), glyceraldehyde-3-phosphate dehydrogenase (EC 1.2.1.12) and pyruvate kinase (EC 2.7.1.40) – all from rabbit muscle – triosephosphate isomerase (EC 5.3.1.1) from bakers yeast, lactate dehydrogenase (EC 1.1.1.27) from bovine heart, glycerol kinase (EX 2.7.1.30) from *Candida mycoderma*, glyoxalase I (EC 4.4.1.5) grade IV from yeast, glyoxalase II (EC 3.1.2.6) from bovine liver, glucose-6-phosphate dehydrogenase (EC 1.1.1.49) from bakers yeast, aldehyde dehydrogenase (EC 1.2.1.5) from bakers yeast and glutathione reductase (EC 1.6.4.2) type III from yeast were supplied by Sigma, St. Louis, MO. Glutamate dehydrogenase (EC 1.4.1.3) from bovine liver and alcohol dehydrogenase (EC 1.1.1.2) from yeast were supplied by Boehringer Mannheim. Other materials: DL-glyceraldehyde, D-glyceraldehyde, L-glyceraldehyde, reduced and oxidised pydridine nucleotides NAD(P)$^+$, NAD(P)H, sodium α-ketoglutarate, glucose 6-phosphate, fructose-1,6-bisphosphate and sodium lactate pyruvate were purchased from Sigma.

Glyceraldehyde content of supernatant from red cells incubated with glyceraldehyde. A 25% (v/v) suspension of red cells in Krebs-Ringer phosphate buffer was incubated with 10 mM glyceraldehyde at 37°C for 1 h. Aliquots were withdrawn after 0, 20, 40 and 60 min reaction time and were immediately centrifuged for 5 min at 2000 × g, and the supernatant was analysed for aldehyde content with aldehyde dehydrogenase [12]. The supernatant was diluted 100-fold into the cuvette assay mixture, and the A_{340} was followed with time until no further increase was observed. The cuvette assay mixture comprised 2 mM NAD$^+$, 100 mM KCl, 100 mM K$^+$ Hepes (pH 7.4), 1 mM dithiothreitol and 1% (v/v) cellular supernatant. Control levels of red cell aldehyde detected (less than 50 μM) were subtracted from concentrations of aldehyde found during glyceraldehyde treatment. Data shown are the means of four experiments.

Measurement of flux of glucose through the HMS. The flux of glucose oxidised through the HMS was measured by collecting $^{14}CO_2$ released from D-[U-^{14}C]glucose. D-[U-^{14}C]Glucose rather than D-[1-^{14}C]glucose was used, so that the entire flux was measured, including recycling of pentoses through the hexose monophosphate pathway. 1 ml of 25% red cell suspensions with 5 mM glucose containing 0.33 μCi of D-[U-^{14}C]glucose (supplied by New England Nuclear, Boston, MA), in the presence and absence of glyceraldehyde, were incubated for 1 h at 37°C in 10-ml stoppered Erlenmeyer flasks containing a well of 0.2 ml of 2 M KOH. Procedures of analysis are as described previously [13]. The flux through the HMS was calculated after subtracting blank values and was expressed as μmol of glucose oxidised per h per ml of packed red cells. Results presented are the means of four determinations.

Determination of the levels of glycolytic intermediates. The concentrations of lactate and pyruvate in 25% red cell suspensions with 5 mM glucose, in the absence and presence of 10 mM glyceraldehyde, were determined by previously published methods [14]. Lactate and pyruvate concentrations in red cell suspensions at $t = 0$ and after 1 h incubation at 37°C were determined. Data presented are the means of four determinations. The concentrations of the glycolytic triose pool of intermediates (glyceraldehyde 3-phosphate, dihydroxyacetone phosphate and fructose 1,6-bisphosphate) were determined by previously published methods [14]. 4 ml of 25% suspensions of red cells with 5 mM glucose, in the presence and absence of 10 mM glyceraldehyde, were incubated for 1 h at 37°C. After this time, the red cell suspensions were washed with 5 ml phosphate-buffered saline. The 1 ml pellet of red cells was then treated with 8 ml 4% perchloric acid and centrifuged at 2000 × g for 10 min. 7 ml of the perchloric acid extract supernatant were neutralised with 1 M K_2CO_3, and the neutralised extract was made up to 10 ml with distilled water, The neutralised extract was centrifuged at 2000 × g for 10 min, and the supernatant was analysed for triose pool glycolytic intermediates, following NADH production from NAD$^+$ by fluorescence spectrophotometry with sequential addition of: (i) 8 U/ml glyceraldehyde-3-phosphate dehydrogenase; (ii) 200 U/ml triosephosphate isomerase, and (iii) 0.35 U/ml aldolase, in the presence of the neutralised perchloric acid extract. Data presented are the means of four determinations. Blanks (water substituted for the perchloric acid extract) and standard solutions of fructose 1,6-bisphosphate (after addition of all three enzymes) were analysed for fluorescence changes. The excitation frequency was 340 nm, and the emission band was followed at 460 nm. Fluorescence spectrophotometry was performed on a Perkin-Elmer 650-10S fluorescence spectrophotometer.

Determination of the levels of oxidised and reduced pyridine nucleotides. Cellular levels of NAD$^+$, NADP$^+$, NADH and NADPH, in control and glyceraldehyde-treated cells, were determined by a modification of the ethanolic extraction procedure of Sander et al. [15]. NADH and NADPH concentrations were measured by fluorescence spectrophotometry (see above). The concentrations of pyridine nucleotides were determined in 8.0 ml 25% red cell suspensions at $t=0$ and after incubation for 1 h at 37°C in Krebs-Ringer phosphate buffer (pH 7.4). After incubation, the red cells were washed with 5 ml phosphate-buffered saline, and the 2 ml red cell pellet was then collected by centrifugation. Data presented are the means of four determinations.

For the red cell extraction procedure, 6.0 ml of absolute ethanol and 2.0 ml of 0.2 M K_2HPO_4 (pH 9.0) were pipetted into a 25-ml Erlenmeyer flask and heated to boiling. The 2.0 ml red cell pellets from the incubations with and without glyceraldehyde (see above) were then quickly added to the boiling ethanolic solution. This mixture was quickly brought back to the boiling point (2 s) while shaking. The flask was then cooled on ice, and 2.0 ml 0.1 M $ZnCl_2$ was added to the mixture while shaking. The flask and contents were retained on ice at 0°C for a further 20 min, after which the mixture was centrifuged at $48\,000 \times g$ for 15 min. The supernatant was decanted and kept at 0°C until the time for assay.

The assays for the pyridine nucleotides were essentially those of Segel et al. [16]. In each assay, 1 ml of the ethanolic extraction was added to approx. 2 ml assay buffer plus enzyme. In the NADH assay, 0.2 unit lactate dehydrogenase in 20 μl of extract was added to 2 ml of a solution of 75 mM imidazole/7.5 mM $MgCl_2$/15 mM pyruvate/ 37.5 mM KCl (pH 7.0). In the NADPH assay, 0.5 units glutamate dehydrogenase in 20 μl water were added to cuvettes containing 1.0 ml extract and 2.0 ml of a solution of 75 mM imidazole/7.5 mM $MgCl_2$/7.5 mM α-ketoglutarate/37.5 mM KCl (pH 7.4) (this assay measures both NADH and NADPH; the NADH value obtained above is subtracted to give the NADPH concentration). The decrease in fluorescence emission at 460 nm was recorded. In the NAD^+ assay, 5 units of alcohol dehydrogenase in 20 μl water were added to cuvettes containing 1.0 ml of extract and 2 ml of solution of 30 mM tetrasodium pyrophosphate and 14.25% ethanol. In the $NADP^+$ assay, 0.04 unit of glucose-6-phosphate dehydrogenase in 20 μl water was added to 1.0 ml of extract and 2.0 ml of a solution comprising 120 mM Tris-HCl (pH 7.0)/0.15 mM $MgCl_2$/1.5 mM glucose 6-phosphate. The increase in fluorescence emission at 460 nm was recorded. (Reduced pyridine nucleotide assays were performed on all samples prior to oxidised pyridine nucleotide assays, due to the oxidative instability of NADH and NADPH.)

The reaction between autoxidising DL-glyceraldehyde and pyridine nucleotides in Krebs-Ringer phosphate buffer was followed by a similar enzymatic analysis procedure. Reaction mixtures (5 ml) containing 20 μM of a pyridine nucleotide (NAD^+, $NADPH^+$, NADH and NADPH) and 10 mM DL-glyceraldehyde, were incubated for 1 h at 37°C in Krebs-Ringer phosphate buffer (pH 7.4). The yield of oxidised/reduced/non-intact (enzymically inactive) pyridine nucleotide was determined in all cases by the above procedures. Reaction incubations were terminated by rapid freezing to −40°C and were thawed immediately prior to enzymatic analysis.Data presented are the means of four determinations.

Determination of oxidised and reduced glutathione. The concentrations of oxidised and reduced glutathione (GSSG and GSH, respectively) in red cells were assayed by the methodologies previously described by Beutler [14].

Reduced glutathione (GSH) was assayed in 25% red cell suspensions at 20 min intervals over a 1 h period, for incubations at 37°C, in the absence and presence of 10 and 50 mM DL-glyceraldehyde. Data shown are the means ± S.D. of four independent determinations.

Oxidised glutathione (GSSG) was assayed in sedimented red cells and in the supernatant before and after incubation of 25% red cell suspensions, with and without 10 mM DL-glyceraldehyde, for 1 h at 37°C in a shaking water bath. Data presented are the means ± S.D. of four independent determinations.

Oxygen consumption. The rate of oxygen consumption by autoxidising DL-glyceraldehyde in Krebs-Ringer phosphate and Krebs-Ringer glycylglycine buffers (pH 7.4) at 37°C was followed on a Clark-type oxygen electrode (YSI Model 53, Yellow Springs Instrument Co., Yellow Springs, OH). Data presented are the means of four determinations.

Glyoxalase I- and II-reactive material. Red cell suspensions, incubated in the absence and presence of 10 mM DL-glyceraldehyde, were analysed for glyoxalase I- and II-reactive material by analysis of neutralised trichloroacetic acid extracts with GSH/glyoxalase I and glyoxalase II, in a sequential enzymatic assay system following *S*-glutathione adducts by absorbance at 240 nm [17].

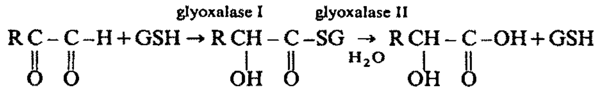

$$\mathrm{R\underset{\displaystyle\overset{\|}{O}}{C}-\underset{\displaystyle\overset{\|}{O}}{C}-H+GSH \xrightarrow{\text{glyoxalase I}} RCH(\underset{}{OH})-\underset{\displaystyle\overset{\|}{O}}{C}-SG \xrightarrow[H_2O]{\text{glyoxalase II}} RCH(OH)-\underset{\displaystyle\overset{\|}{O}}{C}-OH+GSH}$$

1-ml 25% suspensions of red cells, in the absence and presence of 10 mM DL-glyceraldehyde, were incubated at 37°C in Krebs-Ringer phosphate buffer and Krebs-Ringer glycylglycine buffers at pH 7.4 for 1 h. After this time, the red cell suspensions were treated with ice-cold 0.5 ml 30% (v/v) trichloroacetic acid, with constant stirring. The trichloroacetic acid extracts were left on ice for 5 min, then centrifuged at 2000 × *g* for 10 min, and the supernatant was removed. The clear trichloroacetic acid extracts were extracted four times with water-saturated ice-cold diethyl ether (5 ml), and the residual diethyl ether was finally driven off with water-saturated nitrogen. The extracts were now neutral to pH paper and were used in the glyoxalase analyses. Control samples of normal red cell suspensions, without incubation, were also prepared.

Cuvette assay mixtures contained 100 mM sodium phosphate buffer (pH 6.6), 2 mM GSH, 1 mM DETAPAC, with and without 10% neutralised trichloroacetic acid extract. The absorbance at 240 nm was recorded before (baseline) and after the addition of 12.5 U/ml glyoxalase I (to test and reference cuvettes), until a maximum absorbance was attained. A further addition of 2.5 U/ml glyoxalase II was then made. The fall in absorbance at 240 nm was recorded until a minimum was attained. The concentrations of glyoxalase I- and II-reactive material were calculated for the red cell suspensions, using an extinction coefficient from Ref. 17 and appropriate dilution factors.

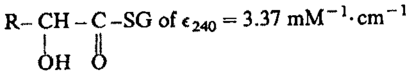

$$\mathrm{R-CH(OH)-\underset{\displaystyle\overset{\|}{O}}{C}-SG}\ \text{of}\ \epsilon_{240} = 3.37\ \mathrm{mM^{-1}\cdot cm^{-1}}$$

Hydroxypyruvaldehyde production from 10 mM DL-glyceraldehyde in Krebs-Ringer phosphate and Krebs-Ringer glycylglycine buffers at 37°C was determined as previously described [7].

Analysis of red cell haemoglobin. 25% red cell suspensions were incubated in Krebs-Ringer phosphate buffer, with or without (a) glyceraldehyde and (b) glyceraldehyde and 5 mM D-glucose, for 1 h at 37°C. After the incubation, the red cells were collected by centrifugation and the resulting 0.25 ml pellets were lysed by addition of 4 ml distilled water and vigorously stirred, and then 1 ml 100 mM potassium phosphate (pH 7.4) was added. In the case of lysates prepared from red cells containing carbonmonoxyhaemoglobin, lysates were futher incubated at 25°C with gentle shaking for 1 h under air until the visible absorption band at 577 nm reached a maximum – showing restoration of oxyhaemoglobin absorption band. The membrane fragments were sedimented by centrifugation (10000 × *g* for 10 min), and the supernatant was diluted 10-fold in the cuvette for spectrophotometric analysis.

The percentage of oxyhaemoglobin, methaemoglobin, intact haemoglobin and non-intact haemoglobin in red cell lysates was determined by the measurement of changes in absorbance of the methaemoglobin 630 nm band, on addition of 0.5 mM potassium cyanide and 0.5 mM potassium ferricyanide (a modification of the methods of Harley and Mauer [18]), as follows. (a) Oxyhaemoglobin – ΔA_{630} with the addition of 0.5 mM potassium ferricyanide. (b) Methaemoglobin – ΔA_{630} with the addition of 0.5 mM potassium cyanide. (c) Intact haemoglobin – addition of 0.5 mM potassium ferricyanide; ΔA_{630} with the addition of 0.5 mM potassium cyanide. Then percentage intact haemoglobin = ΔA_{630} ($t = 60$ min incubation)/A_{630} ($t = 0$ incubation) × 100. (d) Non-intact heamoglobin = 100 – % intact haemoglobin (check: intact haemoglobin = oxyhaemoglobin + methaemoglobin).

Non-intact haemoglobin is defined here as haemoglobin which is oxidised to haemichromes other than methaemoglobin, so that it cannot be oxidised by ferricyanide to methaemoglobin or bind cyanide to form cyanomethaemoglobin. Physiologically, non-intact haemoglobin is irreversible haemichrome and may represent haemoglobin bound to the membrane fragments by processes resulting from the metabolism of glyceraldehyde.

Enzymatic analysis for glycerol. The enzymatic analysis for glycerol production from D-glyceraldehyde-treated red cells was performed as previously described by Beutler and Guinto [10]. However, the apparent glycerol production was found to occur in the absence of red cells (unpublished observations). As the apparent glycerol production was greater than the aldehyde consumption (measured by aldehyde dehydrogenase, see above), the 'glycerol' production may rather appear to be due to isomerisation of D-glyceraldehyde (not a substrate for glycerokinase) to dihydroxyacetone/L-glyceraldehyde [19] which are substrates for glycerokinase [9] and, therefore, give an 'apparent' glycerol production. Since factors other than L-hexonate dehydrogenase appear to be involved in the glyceraldehyde-induced changes in the hexose monophosphate shunt in red cells (see below), glycerol production for glyceraldehyde-treated red cells was not pursued further.

Results

Glyceraldehyde content of supernatant from red cells incubated with glyceraldehyde

The glyceraldehyde content of the extracellular fluid in 25% suspensions of red cells, incubated with 10 mM DL-glyceraldehyde in Krebs-Ringer phosphate buffer at pH 7.4 and 37°C, is shown in Fig. 1. The rate of consumption of DL-glyceraldehyde due to autoxidation in Krebs-Ringer phosphate buffer at 37°C (curve a and corroborative oxygen consumption data, see below) was approx. 0.7 μmol/ml solution per h, whereas, the loss of DL-glyceraldehyde under the same conditions from a 25% suspension of red cells was considerably faster – approx. 5 μmol/ml 25% cell suspension per h (curve c). The rate of DL-glyceraldehyde consumption by carbonmonoxyhaemoglobin-containing red cell suspensions (curve b) was significantly lower than in oxyhaemoglobin- and methaemoglobin-containing cell incubations (curves c and d).

The oxidation of glucose via the hexose monophosphate shunt

The effect of DL-glyceraldehyde on the flux of

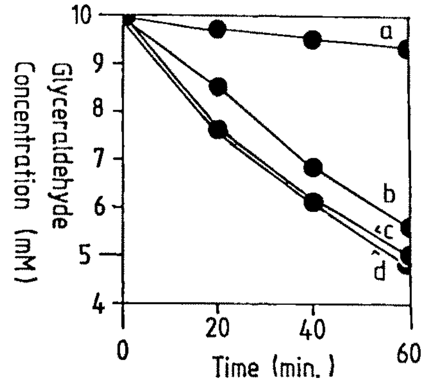

Fig. 1. Glyceraldehyde content of supernatant from red cells incubated with DL-glyceraldehyde. Reaction mixtures all contain 10 mM DL-glyceraldehyde in Krebs-Ringer phosphate buffer (pH 7.4) at 37°C. Further additions were: (a) none (spontaneous autoxidation); (b) 25% (v/v) carbonmonoxyhaemoglobin-containing red cells; (c) 25% oxyhaemoglobin-containing red cells, and (d) 25% methaemoglobin-containing red cells. Incubations were carried out for 1 h at 37°C in a shaking water bath. Data shown are the means ± S.D. (within the size of the data point) of four determinations.

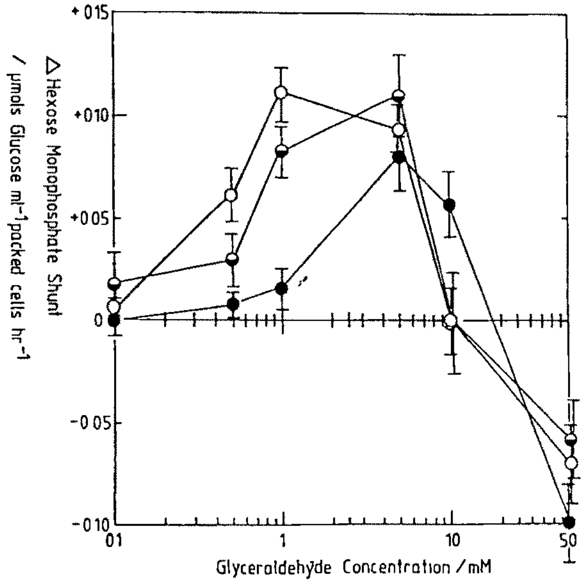

Fig. 2. The effect of glyceraldehyde on the flux of glucose oxidised by the HMS in red cells. The HMS was measured at pH 7.4 and 37°C in Krebs-Ringer phosphate buffer. Data given are the mean ± S.D. of four determinations. ○, oxyhaemoglobin-containing red cells; ◑, carbonmonoxyhaemoglobin-containing red cells; ●, methaemoglobin-containing red cells

glucose oxidised via the HMS, in red cells, is shown in Fig. 2. Curves showing the stimulation and inhibition of the HMS in oxyhaemoglobin-, methaemoglobin- and carbonmonoxyhaemoglobin-containing cells treated with 0.1–50 mM DL-glyceraldehyde are given (the saline concentration in Krebs-Ringer phosphate buffer was decreased by 25 mM and 5 mM for incubations with 50 and 10 mM DL-glyceraldehyde, respectively).

For DL-glyceraldehyde, there is a stimulation in the hexose monophosphate shunt in the concentration range 0.1 to 10 mM. The stimulation is maximised between 1 and 5 mM. The maximum stimulation observed (at 1 mM DL-glyceraldehyde) was $\Delta HMS = +0.11$ μmol glucose/ml cells per h. Above 10 mM DL-glyceraldehyde, the flux through the HMS was decreased by increasing DL-glyceraldehyde concentrations, ($\Delta HMS = -0.07$ μmol glucose/ml cells per h with 50 mM glyceraldehyde). Carbonmonoxyhaemoglobin-containing cell suspensions and methaemoglobin-containing cell suspensions showed similar behaviour, except that for a given stimulation of the HMS, a slightly higher concentration of glyceraldehyde was required. For incubations with 0.5 and 1 mM glyceraldehyde, the relative order of HMS stimulation was:

oxyhaemoglobin > carbonmonoxy- > methaemoglobin
cells haemoglobin cells cells

The control values for the HMS (μmol glucose/ml cells per h) in cell incubations with no added glyceraldehyde were: oxyhaemoglobin-containing cells, 0.17 ± 0.02; methaemoglobin-containing cells, 0.23 ± 0.03; and carbonmonoxyhaemoglobin-containing cells, 0.19 ± 0.02.

D-Glyceraldehyde gave a large stimulation in the HMS when added to red cells at 5 mM, but, as with DL-glyceraldehyde, inhibited the HMS when added to red cells at 50 mM (Table I). L-Glyceraldehyde inhibited the HMS at all concentrations studied, though this effect was minimised at an L-glyceraldehyde concentration of 5 mM and increased below and above this concentration (Table I). These effects on the HMS by addition of D- and L-glyceraldehyde, relative to addition of DL-glyceraldehyde, to red cell suspensions were found in all three red cell systems studied (Table I). Statistical analysis (paired *t*-test) of the individual groups of data (four times D-, L- and DL-treated samples of blood) showed the following order of HMS activity:

D-glyceraldehyde > DL-glyceraldehyde > L-glyceraldehyde
-treated cells -treated cells -treated cells

with the HMS of L-glyceraldehyde-treated cells frequently exhibiting an inhibitory effect.

The stimulation of the HMS in oxyhaemoglobin-containing red cells treated with 5 mM DL-glyceraldehyde was dependent on the supporting buffer medium: in Krebs-Ringer phosphate buffer, a stimulation was observed of $\Delta HMS_p = +0.094 \pm 0.030$ (Table I); in Krebs-Ringer glycylglycylglycine buffer, $\Delta HMS_{GG} = +0.019 \pm 0.010$ μmol glucose/ml per h. The ingibition of the HMS in oxyhaemoglobin-containing red cells treated with 50 mM DL-glyceraldehyde was also dependent on the supporting buffer medium: $\Delta HMS_p = -0.060 \pm 0.030$ (Table I); $\Delta HMS_{GG} = -0.010 \pm 0.11$.

The production of lactate and pyruvate by glycolysis

Incubating red cells with 5 mM glucose in the extracellular fluid for 1 h, increases the concentration of lactate and slightly decreases the concentration of pyruvate in the red cell suspension (Table II). Addition of 10 mM DL-glyceraldehyde to the red cell suspension decreases lactate production; further addition of DL-glyceraldehyde (50 mM) enforces the inhibitory effect on lactate production observed with 10 mM DL-glyceraldehyde. However, addition of L-glyceraldehyde (10 mM) only, gave strong inhibition of lactate production and addition of D-glyceraldehyde (10 mM) only, increased lactate production in the cells suspension. All isomers of glyceraldehyde at 10 mM slightly decreased pyruvate production in red cell suspensions.

The oxidative status of haemoglobin

The incubation of 25% red cell suspensions with 0.1–50 mM DL-glyceraldehyde for 1 h at 37°C in Krebs-Ringer phosphate buffer produced relatively small amounts of methaemoglobin (less than 5% of total haemoglobin) with rather more non-intact haemoglobin (up to 40% of total haemoglo-

TABLE I

THE STEREOISOMERIC DEPENDENCE OF THE GLYCERALDEHYDE-INDUCED CHANGES IN THE FLUX OF GLUCOSE OXIDISED VIA THE HEXOSE MONOPHOSPHATE SHUNT IN RED CELLS

Incubations were carried out as described in Materials and Methods. Data reported are the means ± S.D. for four estimations. The level of significance was determined using a paired *t*-test; statistical comparisons were made between paired D- and L-, D- and DL- and DL- and L-incubations of the same cell type and glyceraldehyde concentration. All data pairings gave a positive significance test ($p > 0.05$) except where indicated by [a].

Glyceraldehyde addition	HMS (μmol glucose/ml packed cells per h)		
	Oxyhaemoglobin-containing cells	Methaemoglobin-containing cells	Carbonmonoxyhaemoglobin-containing cells
0.5 mM			
D-	+0.023 ± 0.010 [a]	+0.067 ± 0.015	+0.011 ± 0.040
DL-	+0.061 ± 0.025 [a]	+0.009 ± 0.010	+0.029 ± 0.020
L-	−0.003 ± 0.020 [a]	−0.021 ± 0.030	−0.045 ± 0.030
5.0 mM			
D-	+0.699 ± 0.025	+0.906 ± 0.200	+0.881 ± 0.100
DL-	+0.094 ± 0.030	+0.082 ± 0.035 [a]	+0.110 ± 0.050 [a]
L-	−0.099 ± 0.020	+0.062 ± 0.020 [a]	+0.010 ± 0.040 [a]
50 mM			
D-	−0.033 ± 0.010	−0.040 ± 0.020	+0.082 ± 0.040
DL-	−0.069 ± 0.030	−0.111 ± 0.030	−0.059 ± 0.040
L-	−0.134 ± 0.020	+0.142 ± 0.050	−0.089 ± 0.030

bin) (Fig. 3). With 5 mM D-glucose in the extracellular medium during the incubation, these changes in the oxidative status of haemoglobin were suppressed in such a way that only in the incubation with 50 mM DL-glyceraldehyde was a change observed in the oxidative state of cellular haemoglobin. Incubation with D-glyceraldehyde gave a greater change in the oxidative status of haemoglobin than did an equivalent incubation with DL-glyceraldehyde. Incubations with L-glyceraldehyde gave changes in the oxidative status of haemoglobin smaller (for 0.5 mM glyceraldehyde) or similar to (for 5 and 50 mM glyceraldehyde) than those occurring with an equivalent incubation with DL-glyceraldehyde.

TABLE II

THE EFFECT OF GLYCERALDEHYDE ON LACTATE AND PYRUVATE PRODUCTION BY RED CELLS

Lactate and pyruvate were measured in 25% (v/v) suspensions before and after incubation for 1 h in Krebs-Ringer phosphate buffer at pH 7.4 and 37°C. Data reported are the means ± S.D. of four independent experiments.

Glyceraldehyde addition	Lactate production (μmol/ml red cells per h)	Pyruvate production (μmol/ml red cells per h)
None (control)	3.05 ± 0.10	0.11 ± 0.04
10 mM DL-	2.34 ± 0.24	0.01 ± 0.02
50 mM DL-	0.86 ± 0.14	−0.02 ± 0.02 [a]
10 mM D-	4.34 ± 0.28	−0.01 ± 0.01 [a]
10 mM L-	1.86 ± 0.34	0.00 ± 0.02

[a] Indicates that the pyruvate concentration was reduced below the initial, $t = 0$, value (0.01 ± 0.01 μmol per ml red cells).

Incubations of glyceraldehyde with methaemoglobin-containing cells (Fig. 4A) produced non-intact haemoglobin. DL-, D- and L-glyceraldehyde produced similar amounts of non-intact haemoglobin. Addition of 5 mM D-glucose to the extracellular medium also had little effect on the methaemoglobin conversion to non-intact haemoglobin.

Incubations of glyceraldehyde with carbonmonoxyhaemoglobin-containing cells (Fig. 4B) produced small amounts of non-intact haemoglobin (up to only 3% of total haemoglobin with 50 mM DL-glyceraldehyde). D- and L-glyceraldehyde incubations gave a similar effect.

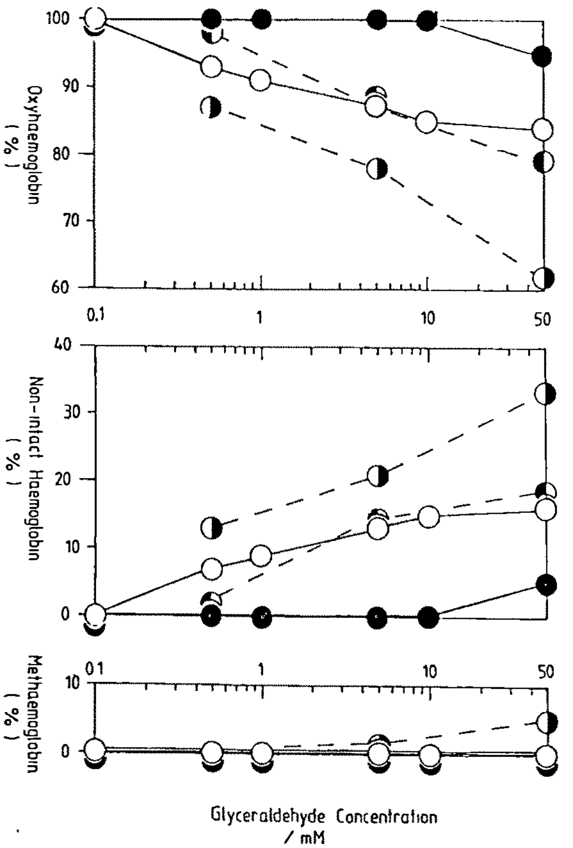

Fig. 3. The effect of glyceraldehyde on the oxidative status of haemoglobin in oxyhaemoglobin-containing red cells. Incubations contained the given glyceraldehyde concentration and 25% (v/v) oxyhaemoglobin-containing red cells in Krebs-Ringer phosphate buffer at pH 7.4 and 37°C. The cell suspensions were incubated for 1 h and then analysed for haemoglobin derivatives. Data are the means ± S.D. (within the data point) of four determinations. ○, red cells + DL-glyceraldehyde; ●, red cells + DL-glyceraldehyde + 5 mM glucose; ◐, red cells + L-glyceraldehyde; ◑, red cells – D-glyceraldehyde.

The effect of glyceraldehyde on the levels of reduced and oxidised pyridine nucleotides and glutathione in the red cell

The cellular levels of reduced and oxidised pyridine nucleotides: NADH, NADPH, NAD^+ and $NADP^+$ are given in Table III. With 10 mM DL-glyceraldehyde, the concentrations of NADH and NADPH are decreased and concentrations of NAD^+ and $NADP^+$ are increased. It appears that cellular concentrations of NADH and particularly NADPH are decreased by treatment with glyceraldehyde, probably by co-autoxidation with

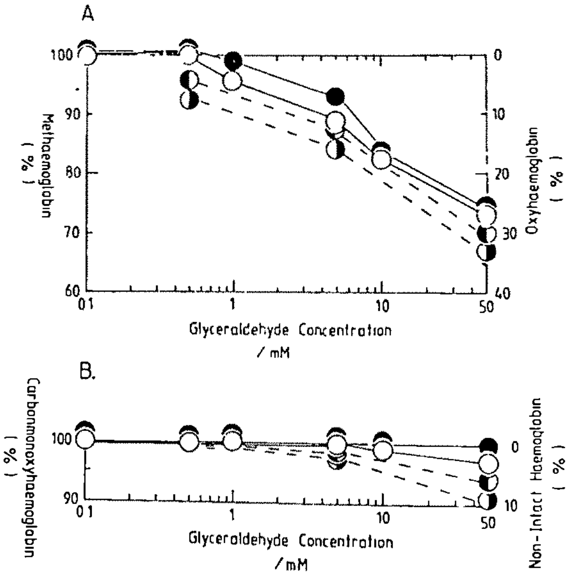

Fig. 4. The effect of glyceraldehyde on the oxidative status of haemoglobin in methaemoglobin- (A) and carbonmonoxyhaemoglobin-containing (B) red cells. Incubation conditions, data analysis and key as for Fig. 3.

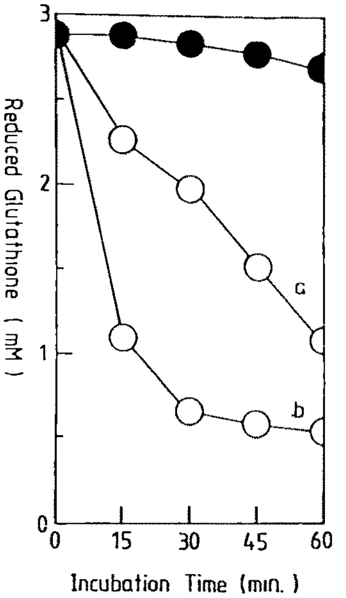

Fig. 5. The effect of DL-glyceraldehyde on reduced glutathione levels in red cells. Incubations contain 25% (v/v) oxyhaemoglobin-containing red cells in Krebs-Ringer phosphate buffer at pH 7.4 and 37°C. Further additions were: none (control, ●), 10 mM DL-glyceraldehyde (a) or 50 mM DL-glyceraldehyde (b). Data are the means ± S.D. (within the data point) of 4 determinations.

TABLE III

GLYCERALDEHYDE-INDUCED CHANGES IN RED CELL CONCENTRATIONS OF REDUCED AND OXIDISED PYRIDINE NUCLEOTIDES AND GLUTATHIONE

Reduced and oxidised pyridine nucleotides (nmol/ml packed red cells) and glutathione (μM) were determined. Data presented are the mean ± S.D. of four determinations. The leakage of GSSG from the red cells was approx. 1 μM (control cells) and 6 μM (glyceraldehyde-treated cells). t, incubation time.

Addition	Concentration			
	[NAD$^+$]	[NADH]	[NADP$^+$]	[NADPH]
None	14.9 ± 0.3	4.2 ± 0.4	3.3 ± 0.3	6.9 ± 0.3
10 mM DL-glyceraldehyde	16.2 ± 0.3	3.1 ± 0.2	8.1 ± 0.2	0.4 ± 0.1
	[GSH]		[GSSG]	
	$t = 0$	$t = 60$ min	$t = 0$	$t = 60$ min
None	2900 ± 50	2720 ± 50	28 ± 6	53 ± 16
10 mM DL-glyceraldehyde	2900 ± 50	1080 ± 50	29 ± 5	203 ± 59

glyceraldehyde autoxidation (cf., glyceraldehyde-induced oxidation of oxyhaemoglobin [8]). A similar effect was observed in the reaction of DL-glyceraldehyde with pyridine nucleotides in Krebs-Ringer phosphate buffer at 37°C (Table IV). DL-Glyceraldehyde oxidises NADH and NADPH to from NAD$^+$ and NADP$^+$, respectively, with some enzymatically inactive (non-intact) pyridine nucleotide formation. DL-Glyceraldehyde also reacts with NAD$^+$ and NADP$^+$ to produce small amounts of non-intact pyridine nucleotide (TAble IV). (Non-intact pyridine nucleotide refers to a pyridine nucleotide metabolite other than NAD(P)$^+$ and NAD(P)H.)

TABLE IV

THE REACTION OF DL-GLYCERALDEHYDE WITH PYRIDINE NUCLEOTIDES IN KREBS-RINGER PHOSPHATE BUFFER UNDER PHYSIOLOGICAL CONDITIONS

All incubations initially contain 20 μM pyridine nucleotide ± 10 mM DL-glyceraldehyde in Krebs-Ringer phosphate buffer at pH 7.4 and 37°C. Samples were incubated for 1 h and analysed enzymatically for pyridine nucleotide at $t = 0$ and $t = 60$ min. Data (μM) presented were calculated as follows: ΔNAD(P)H $=$ NAD(P)H$_{t-0}$ $-$ NAD(P)H$_{t-60}$, ΔNAD(P)$^+$ $=$ NAD(P)$^+_{t-60}$ $-$ NAD(P)$^+_{t-0}$; non-intact $=$ ΔNAD(P)H $-$ ΔNAD(P)$^+$

Initial nucleotide	Nucleotide analysis	Control	+ 10 mM glyceraldehyde
NADH	ΔNADH	1.0 ± 0.3	3.1 ± 0.4
	ΔNAD$^+$	0.7 ± 0.5	1.7 ± 0.4
	non-intact	0.3 ± 0.8	1.4 ± 0.8
NADPH	ΔNADPH	15.2 ± 0.6	18.2 ± 0.6
	ΔNADP$^+$	8.8 ± 0.6	10.4 ± 0.6
	non-intact	6.4 ± 1.2	7.8 ± 1.2
NAD$^+$	ΔNAD$^+$	0.3 ± 0.2	0.9 ± 0.2 [a]
	non-intact	0.3 ± 0.3	0.9 ± 0.3
NADP$^+$	ΔNADP$^+$	0.0 ± 0.1	1.1 ± 0.6 [a]
	non-intact	0.0 ± 0.4	1.1 ± 0.9

[a] No non-enzymatic reduction of NAD(P)$^+$ by DL-glyceraldehyde was observed

Red cells treated with 10 and 50 mM DL-glyceraldehyde undergo a rapid depletion in cellular levels of reduced glutathione (Fig. 5, curves a and b, and Table IV). The rate of depletion of GSH is not significantly decreased by addition of 5 mM glucose in the external medium (data not shown). The production of GSSG under the same conditions was much lower than expected for the oxidation of GSH to its oxidised co-gener GSSG (Table IV). The large decrease in GSH in excess of that expected by the concomitant production of GSSG (approx. 1.5 mM after 1 h with 10 mM DL-glyceraldehyde) suggests that GSH is forming an adduct with DL-glyceraldehyde (e.g., thiohemiacetal [20]).

GSSG was measured in the supernatant of red cell suspensions sedimented after incubation with glyceraldehyde. The GSSG concentration found was approx. 2 μM, i.e., equivalent to a leakage of 6 μM from the red cells, or 12 μM GSH lost from the cells per h.

TABLE V

THE EFFECT OF GLYCERALDEHYDE ON THE CONCENTRATIONS OF THE TRIOSE POOL OF GLYCOLYTIC INTERMEDIATES IN THE RED CELL

25% (v/v) red cell suspensions were incubated in krebs-Ringer phosphate buffer (pH 7.4) for 1 h at 37°C, with and without glyceraldehyde and glucose. The cell suspensions were analysed for triose pool intermediates. Concentrations are expressed as nmol/ml packed cells. Data shown are the mean ± S.D. of four independent determinations [Triose pool] = [GAP]+[DHAP]+2·[F-1,6-BP]; GAP, glyceraldehyde 3-phosphate, F-1,6-BP, fructose 1,6-bisphosphate; DHAP, dihydroxy acetone phosphate

Additions	t (min)	[GAP]	[DHAP]	[F-1,6-BP]	[Triose pool]
None	0	–	10 ± 3	2 ± 1	14 ± 5
5 mM glucose	60	4 ± 1	117 ± 24	46 ± 12	213 ± 49
10 mM DL-glyceraldehyde + 5 mM glucose	60	3 ± 1	76 ± 10	27 ± 8	133 ± 27
10 mM L-glyceraldehyde + 5 mM glucose	60	–	6 ± 1	3 ± 1	12 ± 3
10 mM D-glyceraldehyde + 5 mM glucose	60	22 ± 6	212 ± 11	125 ± 19	484 ± 66

Levels of glyceraldehyde 3-phosphate, dihydroxyacetone phosphate and fructose 1,6-bisphosphate in glyceraldehyde-treated red cells

Table V shows the effect of glyceraldehyde on the production of glycolytic intermediates of the triose pool (glyceraldehyde 3-phosphate), dihydroxyacetone phosphate and fructose 1,6-bisphosphate in red cell suspensions incubated at

TABLE VI

α-KETOALDEHYDE PRODUCTION FROM AUTOXIDISING DL-GLYCERALDEHYDE AND FROM DL-GLYCERALDEHYDE-TREATED RED CELLS

Oxygen uptake and glyoxalase I- and II-reactive materials were measured. n.d., none detected; t, incubation time.

Glyceraldehyde autoxidation	Rate of oxygen uptake (μM/h)		Glyoxalase-reactive material (μM/h)	
10 mM DL-glyceraldehyde in Krebs-Ringer phosphate buffer at pH 7.4 and 37 °C	54 ± 12		54 ± 2	
10 mM DL-glyceraldehyde in Krebs-Ringer glycylglycine buffer at pH 7.4 and 37 °C	14 ± 6		9 ± 2	
Glyceraldehyde-treated red cells	Glyoxalase I-reactive material[a] (μM)		Glyoxalase II-reactive material[a] (μM)	
	t = 0	t = 60 min	t = 0	t = 60 min
25% (v/v) red cell suspension with 10 mM DL-glyceraldehyde in Krebs-Ringer phosphate buffer at pH 7.4 and 37 °C.	n.d.	18 ± 5	n.d	151 ± 9
25% red cell suspension with 10 mM DL-glyceraldehyde in Krebs Ringer glycylglycine buffer at pH 7.4 and 37 °C.	n.d.	n.d.	n.d.	22 ± 5

[a] There was no detectable formation of glyoxalase-reactive material from control red cell suspension (without glyceraldehyde).

37°C with 5 mM glucose. Red cell suspensions incubated for 1 h with 10 mM DL-glyceraldehyde gave a 38% decrease in production of the triose pool glycolytic intermediates relative to control incubations in the absence of glyceraldehyde. Incubations of red cells with 10 mM D-glyceraldehyde under the same conditions, however, showed a greatly enhanced production of all the components of the triose pool (the triose pool overall is up 127%), whereas the production of triose pool glycolytic intermediates was severely inhibited by the incubation of red cells with 10 mM L-glyceraldehyde (the triose pool is decreased by 94% of the control value, Table V).

The production and detoxification of glyoxalase-reactive material in glyceraldehyde-treated red cells

The autoxidation of DL-glyceraldehyde, catalysed by buffer ions, produces hydroxypyruvaldehyde [7,8]. Table VI shows glyoxalase I- and II-active products formed from DL-glyceraldehyde in Krebs-Ringer phosphate and glycylglycine buffers in 37°C in the absence and presence of red cells. Glyoxalase I- and II-active products from the autoxidation of DL-glyceraldehyde were detected for incubations of DL-glyceraldehyde in Krebs-Ringer phosphate and glycylglycine buffers at pH 7.4 and 37°C. A previous report [7] has shown this product to be hydroxypyruvaldehyde. Less hydroxypyruvaldehyde production occurs in Krebs-Ringer glycylglycine buffer than in Krebs-Ringer phosphate buffer, reflecting the lower rate of autoxidation of glyceraldehyde in the former buffer system (see below). Red cells treated with 10 mM DL-glyceraldehyde, appear to accumulate glyoxalase-reactive material, particularly as the *S*-glutathione adducts (which are substrates of glyoxalase II) (Table VI).

Oxygen consumption by autoxidising glyceraldehyde in Krebs-Ringer buffer systems

Table VI shows the observed initial rates of oxygen consumption by autoxidising DL-glyceraldehyde in Krebs-Ringer phosphate and glycylglycine buffers at 37°C and pH 7.4. The rate of oxygen consumption by 10 mM DL-glyceraldehyde in Krebs-Ringer phosphate buffer is approx. 4-times the rate observed for the same autoxidising system in Krebs-Ringer glycylglycine buffer. This is consistent with the previously reported [7] relatively high efficiency with which phosphate buffer catalyses the autoxidation of DL-glyceraldehyde. The products of glyceraldehyde autoxidation, hydrogen peroxide and hydroxypyruvaldehyde [7], are therefore expected to be formed in DL-glyceraldehyde-treated red cell suspensions. Indeed, the production of glyoxalase-reactive material closely parallels oxygen consumption in the two Krebs-Ringer buffer systems used (Table VI).

Discussion

The utilisation of glyceraldehyde-treated red cells

Glyceraldehyde-treated red cells were initially studied with respect to the possibility that glyceraldehyde might aid the maintenance of 2,3-bisphosphoglycerate levels in red cell storage. 20 mM glyceraldehyde did not aid maintenance of cellular levels of 2,3-bisphosphoglycerate and appeared to produce red cell damage [9]. Concurrently, Beutler and Guinto [9,10] reported two enzyme activities, utilising glyceraldehyde as a substrate, in the red cell: (i) triokinase [9], and (ii) L-hexonate dehydrogenase [10]. Current interest in glyceraldehyde-treated and red cells lies in the following. (i) The in vitro anti-sickling properties of relatively high concentrations (5–20 mM) of DL-glyceraldehyde. The antisickling activity appears to be a result of glyceraldehyde-sickle haemoglobin (HbS) adduct formation [2–6]. (ii) The use of the red cell as a model for studying the coupling of NADPH-dependent sugar alcohol formation from monosaccharides via the polyol pathway, with aldose reductase [21]. The polyol pathway is thought to be an important step in the manifestation of chronic diabetic pathogenesis [22].

The effects of glyceraldehyde on red cell metabolism

The stimulation and inhibition of the HMS

The HMS in red cells was stimulated by low concentrations of DL-glyceraldehyde (less than 10 mM) but inhibited at higher concentrations (more than 10 mM). The HMS may be stimulated by the oxidation of NADPH to NADP$^+$ and the oxidation of GSH to GSSG.

The oxidation of NADPH may be induced by the direct reaction of NADPH with xenobiotic agents (e.g., Methylene blue and primaquine) [23,24], by NADPH-dependent dehydrogenases (e.g., glutathione reductase and aldose reductase) [21,25] and by monenzymatic and enzymatic transhydrogenation with NAD^+ [26,27].

The oxidation of GSH may be induced by the direct reaction of GSH with oxidising species (e.g., free radical intermediates and oxidised ascorbate) [28,29], and by glutathione-dependent enzymes (e.g., glutathione peroxidase in the detoxication of hydrogen peroxide and organic hydroperoxides) [30,31].

The major factors operating in the stimulation of the HMS on red cells incubated with glyceraldehyde appear to be: (i) the non-enzymatic direct oxidation of NADPH by autoxidising glyceraldehyde (Table IV); and (ii) The relatively small amount of GSSG formed which may result from the action of glutathione peroxidase on low levels of hydrogen peroxide produced by glyceraldehyde autoxidation and the reaction of glyceraldehyde with oxyhaemoglobin [8].

The stimulation of the HMS by glyceraldehyde was decreased in Krebs-Ringer glycylglycine buffer compared to that in Krebs-Ringer phosphate buffer. That oxidative metabolism stimulated by glyceraldehyde shows this buffer ion dependence correlates with the rates of glyceraldehyde autoxidation in Krebs-Ringer phosphate and glycylglycine buffers (Table VI). This suggests that the oxidative metabolism induced by glyceraldehyde in red cells is related to the autoxidation of glyceraldehyde, rather than due to a depletion of NADPH by the polyol pathway (aldose reductase) – see below.

Factors involved in the inhibition of the HMS in red cells treated with glyceraldehyde are less clear. However, the observation that L-glyceraldehyde at 0.5 and 5 mM is a potent inhibitor of the HMS in all three cell types, compared to stimulation of the HMS by D-glyceraldehyde, suggests some stereospecific requirement for the inhibition of the HMS. L-Glyceraldehyde may combine with dihydroxyacetone phosphate to form sorbose 1-phosphate, which is a competitive inhibitor of hexokinase [32]. Both anaerobic and aerobic glycolysis was inhibited by L-glyceraldehyde, suggesting that the indirect inhibition of hexokinase by L-glyceraldehyde is consistent with the decreased capacity of L-glyceraldehyde-treated red cells to undergo glycolysis. The inhibition of hexokinase activity by L-glyceraldehyde could not be conclusively demonstrated directly, however, as the putative sorbose 1-phosphate is diluted in the haemolysate for the hexokinase assay procedure.

For red cells treated with 50 mM glyceraldehyde, all stereoisomer forms – D-, L- and DL-glyceraldehyde – inhibit the HMS, except for D-glyceraldehyde in carbonmonoxyhaemoglobin-containing cells (Table I). The gradation of inhibitory effect is:

L-glyceraldehyde > DL-glyceraldehyde > D-glyceraldehyde

Carbonmonoxyhaemoglobin-containing cell incubations also appear to exhibit generally a weaker inhibitory effect by the different isomers of glyceraldehyde than do oxyhaemoglobin- and methaemoglobin-containing cell systems. This inhibition of the HMS general to stereoisomeric forms may be due to the stereoisomerisation of sufficient L-glyceraldehyde from D-glyceraldehyde, during the incubation, to inhibit hexokinase. The effect of carbomonoxyhaemoglobin implies that the reaction of glyceraldehyde with the haem groups in haemoglobin [8] makes a minor contribution to inhibition of the HMS.

In principle, the inhibition of glucose-6-phosphate dehydrogenase, glutathione reductase and glutathione peroxidase, or the removal of the oxidised cogeners, $NADP^+$ and GSSG, from the cell, may inhibit the HMS. Reduced glutathione was severely depleted in red cells treated with 50 mM DL-glyceraldehyde after only 30 min incubation time, which, for the most part, was without the concomitant production of GSSG. This may also contribute to the inhibition of the HMS by 50 mM glyceraldehyde.

The stimulation and inhibition of lactate and pyruvate production from glycolysis

Red cells with glucose (5 mM) added in the extracellular medium, and treated with D-glyceraldehyde (10 mM) show enhanced lactate production and decreased pyruvate production over incubation for 1 h at 37°C in Krebs-Ringer phosphate buffer (pH 7.4). Addition of 10 mM DL-glyceraldehyde and L-glyceraldehyde were found to slightly decrease pyruvate production, but also to inhibit lactate production under the same conditions. This suggests D-glyceraldehyde is entering into the lower stages of glycolysis, whereas the L-isomer is inhibiting glycolysis, probably by the inhibition of hexokinase, as discussed above for the HMS. The phosphorylation of D-glyceraldehyde by triokinase was consistent with the enhanced triose pool of glycolytic intermediates (glyceraldehyde 3-phosphate + dihydroxyacetone phosphate + 2 × fructose 1,6-bisphosphate) found in D-glyceraldehyde-treated red cells.

Consequences of glyceraldehyde autoxidation

The autoxidation of glyceraldehyde has been shown [7] to produce hydroxypyruvaldehyde and hydrogen peroxide with the formation of 1-hydroxylalkyl-free radicals at pH 7.4. This rate of oxygen consumption and production of glyoxalase-reactive material by 10 mM DL-glyceraldehyde in Krebs-Ringer phosphate buffer at 37°C was shown to be approx. 6-times faster than the rate of oxygen consumption by DL-glyceraldehyde in Krebs-Ringer glycylglycine buffer. This was expected because of the previously reported relative efficiencies by which phosphate and amine buffers catalyse the autoxidation of monosaccharides [7].

The stimulation of the HMS and the production of glyoxalase I- and II-active material in DL-glyceraldehyde-treated red cells were all decreased in glycylglycine relative to phosphate-buffered systems. This may indicate that the autoxidation of glyceraldehyde is an important contributory factor in mediating the stimulation of the HMS, particularly via the detoxication of hydrogen peroxide (produced in the autoxidation process) and the production of $NADP^+$ (which is produced from NADPH by autoxidising DL-glyceraldehyde).

Hydroxypyruvaldehyde production in red cells may be quenched by the red cell glyoxalase system [33], although high concentrations of hydroxypyruvaldehyde have been shown to inhibit glyoxalase I [24]. The accumulation of glyoxalase II substrate in red cells treated with DL-glyceraldehyde may indicate that the detoxication of α-ketoaldehydes by the glyoxalase system in the red cell is rate-limited by the glyoxalase II step. This is particularly pertinent to the changes in red cell shape in reported cases of glyoxalase II deficiency [35].

Sites of interaction between glyceraldehyde and red cells.

The sites of glyceraldehyde metabolism have been followed in this work. However, the adduct formation of glyceraldehyde with the globin of haemoglobin is also a major fate of glyceraldehyde in red cells. From the work of Manning and co-workers [3–6], it can be deduced that for an incubation of 25% red cell suspension with 10 mM glyceraldehyde for 1 h at 37°C approx. 2.5–5 mM glyceraldehyde is expected to be complexed on the protein of haemoglobin (membrane proteins may also have small amounts of glyceraldehyde adducts).

For a standard incubation of 1 ml of 10 mM DL-glyceraldehyde with a 25% red cell suspension is Krebs-Ringer phosphate buffer (pH 7.4), the major sites of glyceraldehyde metabolism in the first hour of incubation at 37°C appear to be: (i) adduct formation with reduced glutathione, approx. 0.5 μmol (2 μmol/ml packed cells); (ii) phosphorylation of D-glyceraldehyde by triokinase and entry into the triose pool, approx. 30 nmol (121 nmol/ml packed cells); (iii) Autoxidation of glyceraldehyde [7], 54 nmol; (iv) The oxidation of oxyhaemoglobin to non-intact haemoglobin [8], approx. 0.9 μmol glyceraldehyde (assuming one haem group reacts with one glyceraldehyde molecule for the conversion of non-intact haemoglobin).

This accounts for approx. 1.5 μmol glyceraldehyde when approx. 5 μmol glyceraldehyde consumption was observed. The remainder may be accounted for by protein adducts with glyceraldehyde (3.5 μmoles) as observed by Nigen and Manning [3].

The stimulation of the HMS in red cells treated with D-glyceraldehyde has previously been attributed to L-hexonate dehydrogenase activity, utilising NADPH to reduce glyceraldehyde to glycerol [10]. The glycerol-assay procedure employed involved a coupled enzymatic assay system with glycerokinase. It should be noted that at 37°C in phosphate buffer, D-glyceraldehyde isomerises to dihydroxyacetone and L-glyceraldehyde, which, unlike D-glyceraldehyde but like glycerol, are substrates for glycerokinase [9]. This isomerisation of D-glyceraldehyde would therefore give misleading results of glycerol production.

In this report, we have described other processes (glyceraldehyde autoxidation) which appear to be instrumental in the stimulation of the HMS and non-enzymatic oxidation of NADPH. L-Hexonate dehydrogenase activity response in red cells [10] appears to play a minor role in red cell metabolism of glyceraldehyde.

Implications for the utilisation of glyceraldehyde-treated red cells in anti-sickling and polyol-pathway research.

In vitro anti-sickling effects of glyceraldehyde. Red cell metabolism appears to withstand the high concentrations (10–20 mM) of DL-glyceraldehyde necessary to give a beneficial rate of non-enzymatic glyceraldhyde-HbS adduct formation, and prevent sickling. The red cell, however, is severely depleted of reduced glutathione and NADPH: the HMS, initially stimulated in response to glyceraldehyde autoxidation, is passified and inhibited, and the triose pool of glycolytic intermediates is enhanced by phosphorylation of D-glyceraldehyde (catalysed by triokinase), but lactate production is decreased. All these features appear not to have an acute effect on the continued existence of the red cell; although with little GSH, thiol groups in red cell proteins would be expected to be irreversibly oxidised, there being no GSH-dependent repair mechanism operating [36].

Glycerol production from glyceraldehyde in red cells – the polyol pathway. At present, there has been no purification of aldose reductase from the red cell, although aldose reductase-like activity exists [11,21]. Glycerol production from D-glyceraldehyde, reported by Beutler and Guinto [10], is cited [37] as evidence for the red cell polyol pathway. The oxidative effects of glyceraldehyde autoxidation, as expressed in oxidative metabolism of the red cell, imply that no strict coupling of NADPH oxidation to glycerol production exists in glyceraldehyde-treated red cells. The interferences in the glycerol assay, delineated above, suggest that the relevance of the polyol pathway to glyceraldehyde metabolism in red cells must be reserved until an improved method of glycerol detection in red cells is devised.

The oxidative metabolism of glyceraldehyde: what relevance physiologically?

An important feature of glyceraldehyde-treated red cells is the accumulation of glyoxalase-reactive material. This observation was made in spite of an active glyoxalase system detoxifying α-ketoaldehydes during the incubation. α-Ketoaldehydes are known to crosslink proteins [1], and such effects on red cell membrane proteins would reduce the cell deformability and decrease the lifetime of the red cell in the circulation. This may be of importance if DL-glyceraldehyde is to be used as an in vivo anti-sickling agent. Moreover low levels of hydroxypyruvaldehyde 3-phosphate has been detected in red cells [17]. This may be produced by the autoxidation of hydroxyacetone phosphate or glyceraldehyde 3-phosphate, under physiological conditions [7].

The observation that monosaccharide autoxidation is stimulated by phosphate-buffered systems (Refs. 8 and 9 and this work) may prompt concern towards the relevance of this work to the in vivo setting. In defence of monosaccharide autoxidation, the following points should be noted. (i) The mean plasma inorganic phosphate concentration is approx. 4 mM (cf. 16.5 mM in the Krebs-Ringer phosphate buffer) [38]. (ii) It now appears that amine buffers and metal ion chelators (e.g., Tris, glycylglycine and diethylenetriaminepentaacetic acid) form adducts with the ene-diol of glyceraldehyde (an intermediate in the autoxidation reaction [8]) and with hydroxypyruvaldehyde (the α-ketoaldehyde product from glyceraldehyde autoxidation) [39–41]. The decreased production of glyoxalase-reactive material in Krebs-Ringer glycylglycine now appears to be due to the quenching of intermediates and products of glyceraldehyde autoxidation by the glycylglycine buffer (Thornalley and Stern, unpublished observation).

It is not clear if the rates of monosaccharide autoxidation and production of glyoxalase-reactive material observed in these in vitro experiments give a reasonable reflection of the rate of monosaccharide autoxidation/α-ketoaldehyde production in vivo. Yet, in our previous studies [8,9], no effective inhibitor of monosaccharide autoxidation was found; catalase proved most effective. The effects of monosaccharide autoxidation on cellular systems is, however, expected to be chronic rather than acute; if only because, under normal conditions, the resident concentrations of monosaccharides, which autoxidise relatively rapidly, are very low (e.g., triose phosphates). Rather, the monosaccharide stores in the cell are in the form of hexoses which autoxidise relatively slowly [8].

Acknowledgement

The authors thank the NIH for research funding.

References

1 Schauenstein, E., Esterbauer, H. and Zollner, H. (1977) Aldehydes in Biological Systems, pp. 103–111, Pion, London
2 Nigen, A.M. and Manning, J.M. (1977) Proc. Natl. Acad. Sci. U.S.A. 74, 367–371
3 Nigen, A.M. and Manning, J.M. (1978) J. Clin. Invest. 61, 11–19
4 Acharya, A.S. and Manning, J.M. (1980) J. Biol. Chem. 255, 1406–1412
5 Acharya, A.S. and Manning, J.M. (1980) J. Biol. Chem. 255, 7218–7224
6 Acharya, A.S., Sussman, L.G and Manning, J.M. (1983) J. Biol. Chem. 258, 2296–2302
7 Thornalley, P.J., Wolff, S., Crabbe, J. and Stern, A. (1984) Biochim. Biophys. Acta 797, 276–287
8 Thornalley, P J., Wolff, S., Crabbe, J. and Stern, A. (1984) Biochem J. 217, 615–622
9 Beutler, E. and Guinto, E. (1973) Blood 41, 559–568
10 Beutler, E. and Guinto, E. (1974) J. Clin. Invest. 53, 1258–1264
11 Travis, S.F., Morrison, A.D., Clements, R.S., Winegrad, A.I. and Oski, F.A. (1971) J. Clin. Invest. 50, 2104–2112
12 Rendina, A.R. and Cleland, W.W. (1981) Anal. Biochem. 117, 213–218
13 Sullivan, S.G. and Stern, A. (1980) Biochem. Pharmacol. 29, 2351–2359
14 Beutler, E. (1975) Red Cell Metabolism. A Manual of Biochemical Methods. 2nd Edn., 160 pp, Grune & Stratton, New York
15 Sander, B.J., Oelschlegel, F.J. and Brewer, G.J. (1976) Anal. Biochem. 71, 29–36
16 Segel, G.B., Feig, S.A., Baehner, R L. and Nathan, D.G (1971) J. Lab. Clin. Med. 78, 969–976
17 Cogoli-Greuter, M. and Christen, P. (1981) J. Biol. Chem. 256, 5708–5711
18 Harley, J.D. and Mauer, A.M. (1960) Blood 16, 1722–1735
19 Federonko, M. and Konigstein, J. (1969). Collect. Czech. Chem. Commun. 34, 3881–3894
20 Kanchuger, M.S. and Byers, L.D (1979) J Am. Chem. Soc. 101, 3005–3009
21 Malone, J.I., Leavengood, H., Peterson, M.J., O'Brien, M.M., Page, M.G. and Aldinger, C.E. (1984) Diabetes 33, 45–49
22 Jeffry, J. and Jornvall, H. (1983). Proc. Natl. Acad. Sci. U.S.A 80, 901–905
23 Metz, E.N., Balcerak, S.P. and Sagone, A.L. (1976) J. Clin. Invest. 58, 797–802
24 Thornalley, P.J., Stern, A. and Bannister, J.V. (1983) Biochem. Pharmacol 32, 3571–3575
25 Jacob, H.S. and Jandl, J.H. (1966) J. Biol. Chem. 241, 4243–4250
26 Rapoport, I., Elsner, R, and Muller, M. (1979), Acta. Biol. Med. Germ. 38, 901–908
27 Bernofsky, C. and Gallagher, W J. (1981), Biochim. Biophys. Acta 659, 1–6
28 Trotta, R.J., Sullivan, S.G. and Stern, A (1983) Biochem J. 212, 759–772
29 Basu, S., Som, S. and Deb, S. (1979). Biochem. Biophys. Res. Commun. 90, 1335–1340
30 Cohen, G. and Hochstein, P. (1963). Biochemistry 2, 1420–1428
31 Trotta, R.J., Sullivan, S.G , and Stern, A. (1983) Biochem. J. 204, 405–415
32 Kanchuger, M.S., and Byers, L.D. (1979) J. Am. Chem. Soc. 101, 3005–3009
33 Knox, W.E. (1960) in Enzyme (Boyer, P.D., Landy, M. and Myrback, K., eds.), 2nd Edn., Vol. 2, pp. 253–294, Academic Press, New York
34 Iio, M., Okabe, K. and Omura, H. (1976). J. Nutr. Sci. Vitaminol, 22, 53–61
35 Valentine, W.N., Paglia, D.E., Neerhout, R.C. and Konrad, P.N. (1970) Blood, 36, 797–808
36 Armstrong, D.A. and Buchanan, J.D. (1978), Photochem. Photobiol. 28, 743–745
37 Malone, J.I., Leavengood, H., Peterson, M.J., O'Brien, M.M., Page, M.G. and Aldinger, C.E. (1984) Diabetes 33,
38 Lehninger, A.L. (1975) Biochemistry, 2nd Edn., p. 831 Worth, New York
39 Patthy, L. and Smith, E.L. (1975) J. Biol. Chem. 250, 557–564
40 Takahashi, K. (1968) J. Biol. Chem 243, 6171–6179
41 Robertson. P., Jr., Fridovich, S.E., Misra, H.P. and Fridovich, I. (1981) Arch. Biochem. Biophys. 207, 282–288

Biochimica et Biophysica Acta, 804 (1984) 324–330
Elsevier

BBA 11318

PROTON NUCLEAR MAGNETIC RESONANCE SPECTROSCOPY OF ISOLATED RABBIT FUNDIC GLANDS

R.A. LEVINE [a,*], G.D. LEVINE [a], A.P. HEALEY [b], D.I. COOK [b], P.W. KUCHEL [c] and J.A. YOUNG [b]

[a] *Department of Medicine, State University of New York, Upstate Medical Center, 750 East Adams Street, Syracuse, NY 13210 (U.S.A.) and the Departments of [b] Physiology and [c] Biochemistry, University of Sydney, Sydney, NSW 2006 (Australia)*

(Received September 26th, 1983)

Key words: ^{1}H-NMR; Phospholipid; Aminopyrine uptake; Oxygen consumption; Amino acid; (Rabbit fundic glands)

^{1}H-nuclear magnetic resonance spectroscopy (NMR) was adapted to isolated rabbit fundic glands and identification made of compounds responsible for several observed spectral resonances. A minimum gland concentration of 0.5 mg dry weight or 5 mg wet weight per 0.5 ml was needed for adequate signal-to-noise ratio. At physiological temperature and pH, the glands demonstrated reproducible spectra, stability for accumulation times greater than 30 min and responsiveness to histamine stimulation, as measured by oxygen consumption and aminopyrine uptake. The relatively anaerobic conditions favored use of proton compared to phosphorus NMR, since ^{1}H-NMR allowed significantly shorter spectral accumulation times and therefore did not compromise glandular viability to the same extent as ^{31}P-NMR. The most conspicuous resonance in the gland spectrum was assigned to the -N$^+$(CH$_3$)$_3$ protons of choline and related compounds. In membrane-free lysates, several components of the signal were resolvable and assigned to choline, phosphatidylcholine, phosphocholine and L-α-glycerophosphocholine. Thin-layer chromatography verified that phosphatidylcholine and phosphatidylethanolamine were the major phospholipids present in gland lipid. Presumably, they represent the source of the surface-active phospholipids present in gastric juice, which may play a role in gastric cytoprotection.

Introduction

Previously, studies with phosphorus (^{31}P) or proton (^{1}H) NMR have not been applied to gastric tissue. Isolated gastric glands are useful to study the biochemical and secretory responses of the mammalian parietal cell to pharmacologic agents and hormones. Compared with isolated canine parietal cells or glands [1], rabbit glands have the advantages that they are more responsive to the secretagogue histamine, are more representative of an intact system and are relatively viable over 180 min.

We show that ^{1}H-NMR is easily applicable to isolated fundic glands and could be used in the future to study, noninvasively, metabolic responses in unstimulated and stimulated gastric tissue. This preparation holds great promise as an NMR model system because it may be easily prepared in quantities sufficient to permit simultaneous biochemical and physiological measurements.

Materials and Methods

Chemicals and reagents. Histamine acid phosphate was obtained from David Bull Laboratories, Melbourne, Victoria. All chemicals were the highest grade available.

Gastric gland preparation. Isolated fundic glands were obtained using the method of Berglindh and

---

[*] To whom correspondence and reprint requests should be addressed.

Abbreviation: Hepes, 4-(2-hydroxyethyl)-1-piperazineethanesulfonic acid.

0167-4889/84/$03.00 © 1984 Elsevier Science Publishers B.V.

co-workers [2,3]. Rabbits of the New Zealand White strain, weighing approx. 3 kg, were used. Urethane (30%) was the anesthetic given via an ear vein (to a maximum of 5 ml/kg). The gland preparation contained by volume approx. 40% each of chief cells and parietal cells [1,3].

Briefly, the technique involves high-pressure perfusion of the stomach with an oxygenated phosphate-buffered saline, stripping and mincing of the mucosa, and subsequent collagenase digestion (0.1% collagenase, type IV, Worthington Chemical) at 37 °C for 45 min [1]. The glands were then suspended in a respiratory medium, and washed three times. The respiratory incubation medium was gassed with 95% O_2/5% CO_2 and contained, in mM: NaCl, 133; KCl, 5.4; Na_2HPO_4, 5.0; NaH_2PO_4, 0.88; $MgSO_4$, 1.2; $CaCl_2$, 1.0; glucose, 11; and rabbit albumin, 2.0 mg/ml. At the end of the last washing, the settled glands were diluted at a ratio of 10 ml of respiratory medium for each 1 ml of glands. This yielded 10–15 mg wet wt. glands/1 ml respiratory medium. In some experiments glands were prepared in ^2H_2O-based media or glucose-free media before acquisition of NMR spectra. The glands were transferred to centrifuge tubes, top-gassed with 95% O_2/5% CO_2, and allowed to stand at room temperature (approx. 25 °C) or in an ice/water mixture (10 °C) for 20 min before spectral acquisition, where they became loosely packed with a cytocrit of about 15% and a uniform dry weight of 10 ± 3 mg ($n = 12$). In order to prevent cell damage, centrifugation was not used.

Gland lysates were prepared by freezing and thawing fresh cells three or four times, using liquid nitrogen or dry ice/ethanol. Each lysate was centrifuged at $14000 \times g$ (Sorvall SA600 rotor in a RC5B centrifuge at 4 °C), and the supernatant was removed and then stored frozen until required. Samples obtained from ^1H_2O-washed cells were subsequently freeze-dried, then reconstituted in ^2H_2O to 1/5–1/3 of the original volume. The consequently higher glucose and albumin levels were avoided by washing the cells with low glucose (3 mM) and albumin-free medium.

^{31}P-NMR and ^1H-NMR. ^{31}P-NMR spectra were obtained using a Bruker WM 360 wide-bore spectrometer operating at 145.78 MHz in pulsed Fourier transform mode at 25 °C. Glandular suspensions in 10 mM Hepes solution at pH 7.4 were placed in 20 mm (outer diameter) sample tubes and free induction decays were accumulated for 10–20 min. Pulse angle was generally 90 °, spectral width 10 kHz and repetition time 1 s. Creatine phosphate was used as a reference compound. However, despite top-gassing with 95% oxygen/5% CO_2, the intensity of the intracellular inorganic phosphate signal (4–6 ppm) exceeded that of the nonmembrane phospholipids (3–4 ppm), AMP and sugar phosphates (6–8 ppm) and minimally detectable ATP and ADP resonances (-4 to -20 ppm). The loss of nucleotide phosphate resonances suggested some impaired viability of the gland preparation and led to more extensive ^1H-NMR experiments.

^1H-NMR spectra were measured at 400 MHz in the Fourier mode using a Bruker WM 400 spectrometer at 25 °C or 37 °C. The spin-echo pulse sequence [4], $90°-\tau-180°-\tau$ with a delay time $\tau = 0.06$ s preceded by a water irradiation pulse of 0.2–0.5 s (used only on suspensions prepared in a water medium) and a total repetition time of 1–2 s was most successfully employed. This sequence discriminates against acquisition of signals from large immobile species such as proteins and membrane structures. A total of 256 or 512 transients were averaged using a spectral width of 5 kHz and 8K or 16K data points. We also tried variations of the inversion-recovery Carr-Purcell-Meiboom-Gill sequence, but the resulting spectra were less informative. Chemical shifts (in ppm) are quoted relative to 2,2-dimethyl-2-silapentane 5-sulfonate present in a small capillary tube placed coaxially inside the NMR tube.

Just prior to ^1H-NMR measurements, 500 μl of fresh glands or membrane-free lysates were gently mixed in a 5 mm (outer diameter) NMR sample tube and allowed to reach the appropriate experimental temperature (25 or 37 °C). The delay between warming and data acquisition was no longer than 10 min. Spectral accumulation was commenced within 3.5 h after the start of the isolation-preparation procedure.

Aminopyrine determination. An aliquot of stabilized gland preparation containing [^{14}C]aminopyrine (Amersham, 118 mCi/mmol) at a concentration of 1.5 μCi/ml of glands was incubated with histamine for 20 min at 25 or 37 °C. The aminopyrine accumulation was determined as the ratio of intraglandular aminopyrine and extraglandular aminopyrine as described previously [1]. Samples were counted on a liquid scintillation counter (Beckman LS 3800).

Oxygen consumption. Oxygen consumption was measured using an Astrup respirometer (Radiometer, Copenhagen) at 25 and 37 °C, using air as the gas phase. Glands were placed in 3.7 ml reservoir volume with a gland-respiratory medium ratio of 1 : 2. A stirring electrode magnet rod was placed within the reservoir. Histamine was dissolved in the respiratory medium after a 30 min equilibration. The system was allowed to stabilize for 3 min, whereupon recordings were resumed. Oxygen consumption was recorded at 5-min intervals for 60 min. All results were converted to μl O_2/min per mg dry wt. [2]. Oxygen consumption recorded on the manometers was adjusted to standard temperature and pressure. Corrections were made for the solubility of oxygen in respiratory medium at 25 and 37 °C [5]. Rates were calculated in some instances from the slope of graphs of oxygen disappearance versus time.

Assessment of gland viability during NMR experimental conditions. Each preparation was tested for cellular viability at varying times (0–180 min storage) and under different temperature conditions (25 and 37 °C) by Trypan blue exclusion, pH, oxygen consumption and aminopyrine uptake. Only those preparations with greater than 90% dye exclusion were used.

Amino acid and lipid analyses. Perchloric acid extracts of glands were analyzed by automated column chromatography for free amino acids, using a JEOL (JLC-6AH) amino acid analyzer (Tokyo, Japan). Thin-layer chromatography was performed on gland lipid extracted into chloroform from the membrane and nonmembrane fractions of cell lysates. The plates (Merck Kieselgel G60) were placed in chloroform/methanol/water (65 : 25 : 4) at room temperature to separate the phosholipids from fatty acids [6].

Statistical analysis. Data are expressed as mean ± 1 S.E.

Results

Assignments of resonance

Resonance assignments were made on the basis of their chemical shifts measured in membrane-free lysates reconstituted in ^2H_2O, comparison with authentic samples and chemical analysis of amino acid. Selective irradiation experiments were performed to determine the extent of linkage between resonances.

A typical complete ^1H-NMR spin-echo spectrum of a ^1H_2O glandular suspension is shown in Fig. 1. Spectra were reproducible. Spectra of reconstituted ^2H_2O revealed a larger number of well-resolved resonances which were not all apparent in the gland spectrum (Fig. 2).

The most conspicuous glandular resonance at 3.19 ppm was assigned to the $-N^+(CH_3)_3$ protons of choline and related compounds (Fig. 3). In membrane-free lysates, several components of the resonance were resolvable, and those were assigned to choline, phosphatidylcholine, phosphocholine and L-α-glycerophosphocholine (Fig. 4). L-α-Glycerophosphocholine (choline moiety βCH_2) was also seen at 4.26 ppm (see Fig. 2, D_2), linked to αCH_2 at 3.63 ppm, and phosphocholine (βCH_2) was observed at 4.11 ppm (see Fig. 2, D_1), linked to αCH_2 at 3.54 ppm.

Other resonances identified in gland suspensions and lysates consisted of protons of free amino acids or other compounds (Figs. 1–4). Resonances found downfield of water were very small relative to the rest of the spectrum, except for a single peak at 4.83 ppm. The downfield signals may be derived from nucleosides (containing ribose), purines and pyrimidines from nucleotide turnover and breakdown. It is unlikely that NAD, NADH, etc. were present, since no bands were observed at appropriate chemical shieldings. It is also possible that there were some other sugar derivatives present in the lysates, such as amino sugars.

Resonances of the α protons of amino acids, sugars and the hydroxyl groups of keto acids appeared in an as yet unassigned group of peaks between 3.50 and 4.00 ppm. The majority of amino acids detected by chromatography were not seen in the glandular spectrum. The amino acids glutamate, glycine, alanine, lysine, serine and aspartate were present of highest concentration levels in the glands, as measured by chromatographic analysis ($n = 4$), but only alanine and glycine were easily recognized by ^1H-NMR spectroscopy.

In general, top-gassing of glands provided better spectra than relatively anaerobic conditions (i.e., in the absence of top-gassing). The small glandular lactate βCH_3 peak identified at 1.29

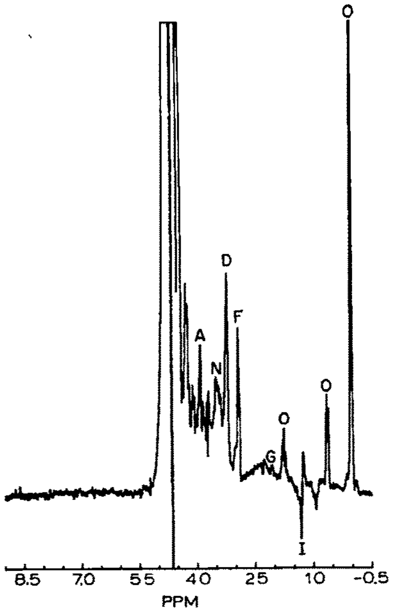

Fig. 1. ^1H-NMR spin-echo spectrum of loosely packed rabbit fundic glandular suspension, of cytocrit 0.15, prepared in respiratory medium (pH 7.4) (top-gassed 95% O_2/5% CO_2) at 37 °C, 512 transients. Abscissa shown in parts per million (ppm) with 2,2-dimethyl-2-silapentane 5-sulfonate used as an external reference standard. The letters adjacent to each resonance denote signals for which assignments have been confirmed. Compounds additional to those identified may contribute to a given resonance. Similar explanation of illustrations applies to Figs. 2–4. Resonances found only in lysates are indicted by *. The method used is included in parentheses so that (dec) = used decoupler transmitter to test linkages; (add) = added compound to gland or lysate. Identified resonances include: A, glycine (αCH_2) (3.50 ppm*) (add); B, *phosphatidylcholine (3.17 pm) (add); C, *choline (-$N^+(CH_3)_3$ (3.14 ppm) (add)); D, *phosphocholine (and D_1) and/or L-α-glycerophosphocholine (and D_2) (-$N^+(CH_3)_3$), (3.16 ppm*) (add/dec) plus part of glucose β anomer H_2 multiplet (N) (3.16–3.20 ppm*); F, creatinine (CH_3) (2.97 ppm) (add); G, acetyl ester (αCH_3) (2.07 ppm); H, alanine (βCH_3) (1.46 ppm) (add/dec); I, lactate (βCH_3) (1.29 ppm) (dec); N, glucose (C2H-C6H_2) (3.20–3.90 ppm); and O, 2,2-dimethyl-2-silapentane 5-sulfonate reference standard.

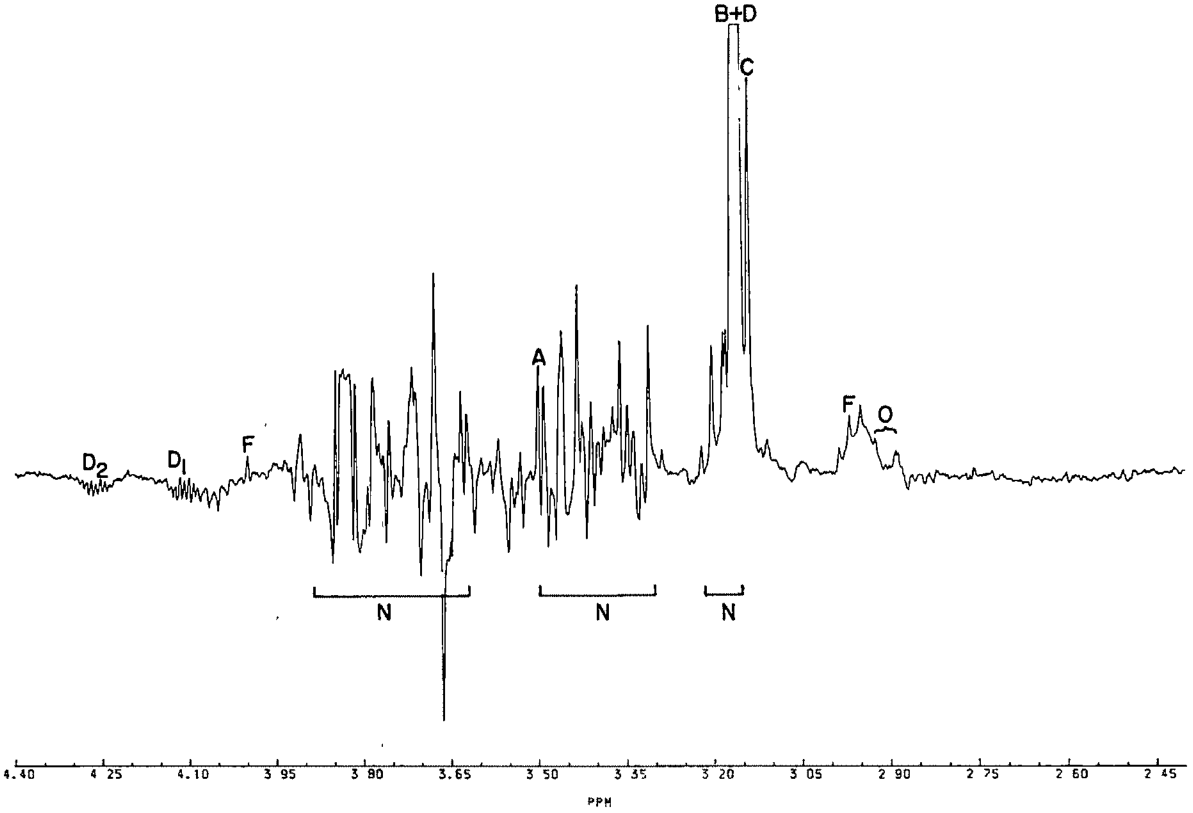

Fig. 2. ^1H spin-echo NMR partial spectra of lysate prepared in ^2H_2O at 37 °C.

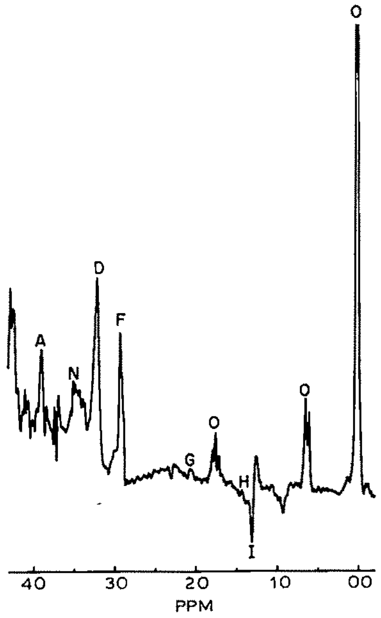

Fig. 3. ^{1}H spin-echo NMR spectra from gland suspensions of Fig. 1, showing expanded scale in aliphatic region of spectrum. Signal D represents composite of B, C and D phospholipid signals shown in Fig 4.

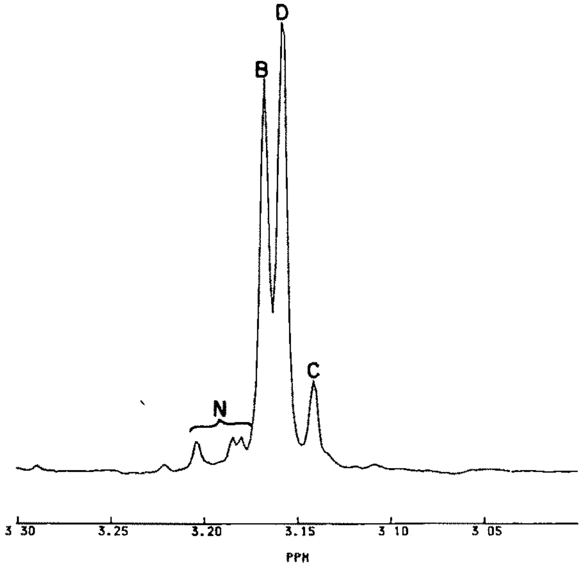

Fig. 4. ^{1}H spin-echo NMR spectra of lysate shown in Fig. 2. Only part of the aliphatic region of the spectrum is reproduced. Note the increased spectral resolution in the phospholipid signal (B + D) with additional resonance peaks being observed as -$N^+(CH_3)_3$ groups of phosphatidylcholine (B) and phosphocholine and/or L-α-glycerophosphocholine (D).

ppm increased minimally with time (over 45 min at 25 or 37 °C).

Glucose presented a complex signal between 3.20 and 3.90 ppm and any other peaks present (i.e., αCH protons of several amino acids) appeared to be masked and complicated by the glucose pattern. In lysates, glucose resonances were present in three groups (3.15–3.20, 3.30–3.51 and 3.60–3.87 ppm), and the resonances of protons attached to the anomeric carbon lay downfield of these groups at 5.18 ppm (α) and 4.59 (β). When glucose was omitted from the incubation and respiratory media during preparation of the glands, almost all resonances were absent (the notable exception belonging to the phospholipid group). The respiratory medium control spectrum showed only glucose resonances with spin-echo NMR, thus demonstrating that the albumin signal was selected against by the multipulse spin-echo sequence. However, rabbit albumin could be seen in the medium by repetitive single-pulse experiments.

Thin-layer chromatography verified that phosphatidylcholine and phosphatidylethanolamine were the major phospholipids present in gland lipid.

The effects of temperature on NMR spectrum

In order to optimize cell viability within the alloted experimental session, initial studies were performed at 25 ° ($n = 14$). However, with top-gassing, similar spectra were acquired at 37 °C ($n = 6$) indicating that there were no demonstrable changes by NMR in the cellular status quo (apart from the increase in lactate formation) at a physiological temperature.

Effect of histamine on oxygen consumption and aminopyrine uptake

Oxygen consumption increased after the addition of histamine (final concentration $1 \cdot 10^{-5}$ M) at 25 and 37 °C almost 70% over control levels (mean 0.013 ± 0.004 μl/min per mg dry., $n = 8$).

Aminopyrine uptake increased after histamine stimulation (final concentration $1 \cdot 10^{-4}$ and $1 \cdot 10^{-5}$ M) by 4- and 6-fold, respectively, at 25 °C ($n = 6$) and 6- and 8-fold, respectively, at 37 °C ($n = 4$), compared to control levels of 11 ± 4 ($n = 10$).

Histamine-stimulated oxygen and aminopyrine uptake were unchanged 15, 30, 60, 120 and 180 min after preparation, and thereafter only minimally diminshed.

Variations of pH with aging glands

A standard pH meter study of a gland suspension (with/without top-gassing) at 25 °C showed that after 60–80 min the pH decreased by 0.1–0.2 units, presumably due to production of lactate as an end product of anaerobic glycolysis. Subsequently, respiratory media were changed after 60 min, and any change in pH was monitored by Phenol red addition to the medium to assure that experimental conditons remained above pH 7.0.

Discussion

This is the first report of NMR analysis of gastric tissue presenting ^{1}H spectra of acceptable signal-to-noise ratio. The fundic glands demonstrated long-term stability for over 30 min in the NMR sample tube. Other whole cells studied predominantly by ^{31}P-NMR techniques include erythrocytes, brain, liver, kidney, plants and micro-organisms, skeletal muscle, sciatic nerve and salivary gland [7–11].

The stomach is one of the most highly aerobic tissues and acid secretion depends upon adequate oxygenation [12]. For that reason limited oxygen delivery can impair function. Similarly, NMR analyses in stomach tissue require physiologic temperature, sufficient tissue oxygenation and adequate pH regulation for proper interpretation of such events as acid secretion. Moreover, if the cytocrit is too high (i.e., over 50%), as often found necessary for ^{31}P-NMR, poor mixing can occur, and excess metabolic end-products may accumulate.

Because of its inherently greater sensitivity, proton NMR allows shorter term experiments and therefore does not comprise glandular viability to the same extent as phosphorus NMR, which demands significantly greater spectral accumulation times. It is possible that the high inorganic phosphate peaks and loss of ^{31}P resonances during phosphorus NMR studies may reflect the relatively anaerobic conditions. For this reason, we assessed viability by direct methods (aminopyrine uptake, oxygen consumption and Trypan blue exclusion) and showed that under the NMR conditions employed the glands appeared to be viable and responsive to histamine stimulation. Our ^{1}H-NMR studies conducted for at least 30 min in a relatively anaerobic preparation showed good spectral resolution, provided the suspension was homogeneous.

A conspicuous resonance at 3.19 ppm was assigned as being due to the protons of quarternary ammonium groups such as choline and related compounds. The large amplitude of this composite. resonance was found to be quite consistent from sample to sample. The phospholipid and choline concentrations were readily measured by the spin-echo technique (see Fig. 4), and the phospholipid composition was confirmed by thin-layer chromatography. In the gland spectrum either phosphatidylcholine, phosphocholine and/or L-α-glycerophosphocholine could be the major components of this resonance. Choline probably was not highly concentrated in the gland system, since in the lysate it was not the dominant peak. It is likely that glycerophosphocholine represented an intermediate of phosphatidylcholine metabolism.

Butler et al. [13] found mucosal surface phospholipids in canine parietal cell locations with phosphatidylcholine and phosphatidylethanolamine being most prominent and representing 38 and 34%, respectively, of the total phospholipid content. These surface-active phospholipids may play a role in gastric cytoprotection, but their source has not been established. The gastric surfactants appear to be derived from the gastric mucosa [13,14]. Our data confirm that these phospholipids are present in the fundic gland and presumably account for the presence of the phospholipids in the gastric juice and on the gastric mucosal lining. Their metabolic significance is unknown. The role of phospholipids in the pathogenesis of acid-peptic disease is open to speculation, but their localized increase in gastric mucosa may mediate, in part, prostaglandin-induced cytoprotection [15]. Additional studies on the relation between ulcerogenesis by damaging agents and alterations in gastric phospholipids are warranted and could be determined by proton NMR.

Acknowledgements

We thank Francis Seow for help with the oxygen consumption experiments. This project was supported by the National Health and Medical Reasearch Council of Australia.

References

1 Levine, R.A., Kohen, K.R., Schwartzel, E.H., Jr. and Ramsay, C E (1982) Am. J. Physiol. 242 (Gastrointest. Liver Physiol. 5), G21–1G26

2 Berglindh, T. and Obrink, K.J. (1976) Acta Physiol. Scand. 96, 150–159

3 Berglindh, T., Helander, H.F and Obrink, K.J. (1976) Acta Physiol. Scand. 97, 401–414

4 Brown, F.F., Campbell, I.D., Kuchel, P.W. and Rabenstein D.C. (1977) FEBS Lett. 82, 12–16

5 Dean, J.A. (1973) Lange's Handbook of Chemistry, 11th Edn., McGraw-Hill, New York

6 Carrol, K.D. (1961) J. Lipid Res. 2, 135–141

7 Kuchel, P.W. (1981) in Critical Reviews in Analytical Chemistry (Campbell, B. and Waites, L., eds.), pp. 155–231, CRC Press, Boca Raton

8 Balaban, R.S., Gadion, D.G., Radda, G.K. and Wong, G.G. (1981) Anal. Biochem. 116, 450–455

9 Young, J.A., Chapman, B.E., Cook, D.I., Healey, A.P., Kuchel, P.W., Lingard, J.M., Nichol. M., Novak, I. and Seow, F. (1982) in Fluid and Electrolyte Abnormalities in Exocrine Glands in Cystic Fibrosis (Quinton, P.M., Martinez, J.R. and Hopfer, U., eds), pp 102–124, San Francisco Press, San Francisco

10 Murakami, M., Imai, Y., Seo, Y., Morimoto, T., Shiga, K. and Warari, H. (1983) Biochim. Biophys. Acta 762, 19–24

11 Ingwal, J.S. (1982) Am. J. Physiol. 242 (Heart Circ. Physiol. 11), H729–H744

12 Hersey, S.J. and Miller, M. (1981) in Membrane Biophysics: Structure and Function in Epithelia (Dinno, M.A. and Callahan, A.B., eds.), pp. 175–187, A.R. Liss, New York

13 Butler, B.D., Lichtenberger, L.M. and Hills, B.A. (1983) Am. J. Physiol. 244 (Gastrointest. Liver Physiol. 7), G645–G651

14 Wassef, M.K., Lin, Y.N. and Horowitz, M.I (1979) Biochim. Biophys. Acta 573, 222–226

15 Lichtenberger, L.M., Graziani, L.A., Dial, E J., Butler, B.D. and Hills, B.A. (1983) Science 219, 1327–1328

Biochimica et Biophysica Acta, 804 (1984) 331–340
Elsevier

BBA 11319

UPTAKE OF L-[*propyl*-2,3-^{3}H]DIHYDROALPRENOLOL BY INTACT HeLa CELLS

KATHRYN E. MEIER * and ARNOLD E. RUOHO

Department of Pharmacology, University of Wisconsin, Madison, WI 53706 (U.S.A.)

(Received January 31st, 1984)

Key words: Adrenergic receptor; Dihydroalprenolol uptake; Binding site; (Hela cell)

This report describes the uptake of L-[*propyl*-2,3-^{3}H]dihydroalprenolol, a β-adrenergic antagonist, by HeLa (human adenocarcinoma) cells. [^{3}H]Dihydroalprenolol binds to sites of high capacity and low affinity in intact HeLa cells. The binding achieves equilibrium rapidly and is rapidly reversible. Bound [^{3}H]dihydroalprenolol is displaceable by β-adrenergic antagonists in a nonstereoselective fashion, but is not displaceable by isoproterenol, an adrenergic agonist. Phentolamine, an α-adrenergic antagonist, and chloroquine, a lysosomotropic amine, also compete for [^{3}H]dihydroalprenolol binding sites. [^{3}H]Dihydroalprenolol binding is inhibited by metabolic inhibitors, but not by cytoskeletal blocking agents. The binding is sensitive to extracellular pH (less binding at lower pH) and is temperature-sensitive (less binding at lower temperatures). The bound radioligand is rapidly reversed following hypotonic lysis of the cells. These [^{3}H]dihydroalprenolol binding sites in intact HeLa cells therefore do not have the characteristics expected for β-adrenergic receptors. Further studies showed that β-adrenergic receptors could be detected in a HeLa membrane preparation using [^{125}I]iodohydroxybenzylpindolol, and that chloroquine had very low affinity for these receptors. We conclude that [^{3}H]dihydroalprenolol diffuses across the plasma membrane of intact HeLa cells and accumulates in acidic intracellular compartments.

Introduction

Identification of β-adrenergic receptor binding sites on intact cells is a useful methodology which allows receptor-ligand interactions to be studied under physiological conditions. Important differences in agonist-receptor interactions have been observed between intact and broken cell preparations [1]. Methods have been described for the detection of receptor-specific binding of several β-adrenergic radioligands in a variety of cell types. Nonspecific binding of the β-antagonist radioligands L-[*propyl*-2,3-^{3}H]dihydroalprenolol and [^{125}I]iodohydroxybenzylpindolol has frequently interfered with the detection of specific binding sites in intact cells, and, to a lesser extent, in membrane preparations [2]. Nonspecific binding of these radioligands to membranes has been attributed to their lipophilicity [3]. However, the nature of the nonspecific binding sites in intact cells has not been carefully delineated. Agents which have been used to reduce nonspecific binding of adrenergic radioligands to intact cells include phentolamine, an α-adrenergic antagonist [4–9], chloroquine, a lysosomotropic agent [10], and valinomycin, a metabolic inhibitor [8]. Prolonged washing protocols [5,7] and hypotonic lysis [11,12,13] have also been utilized to reduce nonspecific binding to intact cells.

In this report, we describe the characteristics of [^{3}H]dihydroalprenolol uptake sites in a human

---

* To whom correspondence should be addressed at: Department of Medicine, Division of Pharmacology, M-013 H, University of California, San Diego, La Jolla, CA 92093, U.S.A.

0167-4889/84/$03.00 © 1984 Elsevier Science Publishers B.V.

adenocarcinoma cell line. As shown by our work and that of previous investigators [14–16], HeLa cells possess isoproterenol-sensitive adenylate cyclase activity and β-adrenergic receptors. However, our attempts to identify these receptors in intact HeLa cells using [^{3}H]dihydroalprenolol revealed a major component of [^{3}H]dihydroalprenolol binding which was not attributable to β-adrenergic receptors. We observed that: (1) [^{3}H]dihydroalprenolol accumulates in the cytoplasmic compartment of HeLa cells; (2) β-adrenergic antagonists, lysosomotropic agents and metabolic inhibitors inhibit [^{3}H]dihydroalprenolol uptake, and (3) [^{3}]dihydroalprenolol uptake is decreased at low temperature or low pH. We conclude that [^{3}H]dihydroalprenolol probably diffuses across the plasma membrane and accumulates in lysosomes or other acidic intracellular compartments.

Materials

(−)-Alprenolol (+)-tartrate, (−)-isoproterenol hydrochloride, (±)-propranolol hydrochloride and valinomycin were obtained from Sigma, St. Louis, MO. L-[*propyl*-2,3-^{3}H]Dihydroalprenolol, [^{3}H]-cAMP and Omnifluor were purchased from New England Nuclear, Boston, MA. ACS scintillation cocktail was from Amersham, Arlington Heights, IL. (±)-Hydroxybenzylpindolol was a gift from Sandoz Pharmaceuticals, Nutley, NJ, and was iodinated using ^{125}I obtained from New England Nuclear. The resulting [^{125}I]iodohydroxybenzylpindolol was purified to a theoretical specific activity of 2200 Ci/mmol as described by Maguire et al. [17] and was used within 2 months after preparation. Phentolamine hydrochloride and (−)- and (+)-oxprenolol were supplied by Dr. Carl Buckner of the University of Wisconsin School of Pharmacy. Hepes was a gift from Research Organics, Cleveland, OH. Powdered media, antibiotics and trypsin solution were obtained from KC Biologicals, Lenexa, KS. Fetal calf serum was purchased from KC Biologicals and Pel-Freez.

HeLa human adenocarcinoma cells were obtained from Dr. Elliot Dick of the Wisconsin State Laboratory of Hygiene. The 'O-HeLa' subline, which was originally adapted for growth on a solid substrate, was used for all experiments unless otherwise mentioned. Cells of the 'L-HeLa' subtype, which were originally adapted for growth in suspension culture, were used in some experiments. The cells were grown in Eagle's minimal essential medium supplemented with 200 U/ml penicillin, 200 μg/ml streptomycin and 10% fetal calf serum, were maintained in a humidified incubator at 37 °C in an atmosphere of 95% air/4% CO_2, and were subcultured using trypsin every 5–8 days.

Methods

Preparation of cell suspensions

HeLa cells were grown to confluence (2 days) in disposable culture dishes (Falcon 3003, 100 × 20 mm) containing 20 ml of complete medium. The medium was removed, and the dishes were rinsed twice with 10 ml of Hanks' balanced salt solution. Hanks' balanced salt solution (5 ml) was added, and the cells were then detached from the dish by gentle scraping with a rubber spatula. The cell suspension was transferred to a plastic test-tube and was centrifuged for 2 min at 200 × *g*. The supernatant was discarded, and the cells were resuspended in 4 ml of Hanks' balanced salt solution. This rinsing procedure was repeated three times, and the cells were finally resuspended in the desired volume of Hanks' balanced salt solution.

[^{3}H]Dihydroalprenolol-binding assays using intact cell suspensions

The incubation was initiated by adding 100 μl of a freshly prepared cell suspension to polystyrene tubes containing [^{3}H]dihydroalprenolol and competing ligands in Hanks' balanced salt solution to give a total volume of 500 μl. Both the assay tubes and the cell suspension were briefly warmed to 37 °C prior to initiation of the assay. The tubes were incubated for 10 min at 37°C with gentle shaking. At the termination of the incubation, 2 ml of ice-cold Hanks' balanced salt solution was added to each tube, the contents of the tube were filtered over Whatman GF/C paper using a vacuum filtration manifold, and each filter was washed with 25 ml of ice-cold Hanks' balanced salt solution. This filtration procedure was completed in less than 1 min. Each dried filter was added to 10 ml of ACS scintillation cocktail and the tritium content was determined using a Packard liquid scintillation counter. The cell concentration of the cell suspensions was determined using a hemacytometer. In most experiments, $2 \cdot 10^5$ cells were added to each assay tube. The properties of the observed [^{3}H]dihydroalprenolol binding were similar at all cell concentrations tested ($2 \cdot 10^4$ to $3 \cdot 10^5$ cells per tube). When (−)-isoproterenol was used as a competing ligand, the incubation mixture contained 0.8 mM ascorbic acid and 3 mM catechol to retard catecholamine oxidation and degradation.

Radioligand-binding assays using intact cells in multiwell culture plates

Cells were grown to confluence in 24-well culture plates containing 1 ml of complete media per well. The medium was removed by aspiration, and the cells were rinsed twice with 1 ml of Hanks' balanced salt solution. A 1 ml aliquot of incubation mixture containing [^{3}H]dihydroalprenolol and competing ligands in Hanks' balanced salt solution was then added to each well. The cells were incubated at 37 °C for 10 min. The incubation mixture was removed, and the cells were rinsed twice with 1 ml of Hanks' balanced salt solution. The cells were then dissolved by the addition of 1 ml of 20% sodium dodecyl sulfate (SDS) to each well. The SDS solution was removed and each well was rinsed with 1 ml of water. The pooled SDS and water washes from each well were added to 10 ml ACS and their tritium content was determined using a Packard liquid scintillation counter.

Preparation of cell membranes

Membranes were prepared from cultured cells by the method of Harden, Su and Perkins [18]. Dishes of confluent cells were rinsed twice with cold 'wash buffer' (2 mM $MgCl_2$/1 mM Tris-HCl (pH 7.5)) and were then incubated with 5 ml wash buffer for 15 min at 4°C. The cells were removed from the dishes using a rubber spatula and each dish was washed once with 2 ml wash buffer. The pooled lysates were centrifuged at $35\,000 \times g$ for 10 min at 5 °C. The pellet was resuspended in 10 ml of wash buffer and was washed twice. The final pellet was resuspended in 1–2 ml of ice-cold 'assay buffer' (2 mM $MgCl_2$/145 mM NaCl/ 20 mM Tris-HCl (pH 7.5)).

The cell concentration was determined at the conclusion of each experiment by adding 100 μl of the membrane suspension to 100 μl of 0.6% Trypan blue in 0.9% NaCl. The intact, Trypan-blue-stained nuclei were counted using a hemacytometer. Estimates of the number of cells per culture dish derived from nuclei counts of the membrane suspension were similar to estimates obtained by counting intact cells removed from the dishes by trypsinization.

Binding of [^{125}I]iodohydroxybenzylpindolol to membrane preparations

Membrane binding assays were performed in polystyrene tubes containing [^{125}I]iodohydroxybenzylpindolol, competing ligands and membranes, to give a total volume of 100 μl. Duplicate of triplicate tubes were prepared for each experimental condition. The assay was initiated by adding the membrane suspension to the the prewarmed assay tubes. The tubes were incubated at 37°C for 30 min. The assay was terminated by adding 1 ml of 37°C assay buffer to each tube, filtering the contents over Whatman GF/A filter paper using a vacuum filtration manifold, and rinsing each filter with 25 ml of 37°C assay buffer. The amount of radioligand retained on each filter was determined using a Searle gamma counter.

Results

[^{3}H]Dihydroalprenolol binding sites in intact HeLa cells were characterized by high capacity, low affinity, and rapid rates of association and dissociation. The radioligand binding represented approx. 50% of the total ligand added to the incubation mixture (Fig. 1). The [^{3}H]dihydroalprenolol binding throughout this concentration range was reduced by approx. 80% in the presence of 10 μM (±)-propranolol (data not shown). The propranolol-protectable binding was not saturable in the range of 0.5–25 nM [^{3}H]dihydroalprenolol. Similar numbers of [^{3}H]dihydroalprenolol-binding sites were observed for control cells and for cells incubated for 18 h with 5 mM sodium butyrate (data not shown). The observed binding reached equilibrium rapidly, and maximal binding was measured after 3 min at 37°C (Fig. 2A). (−)-Isoproterenol (100 μM) did not affect the rate of association or the amount of [^{3}H]dihydroalpre-

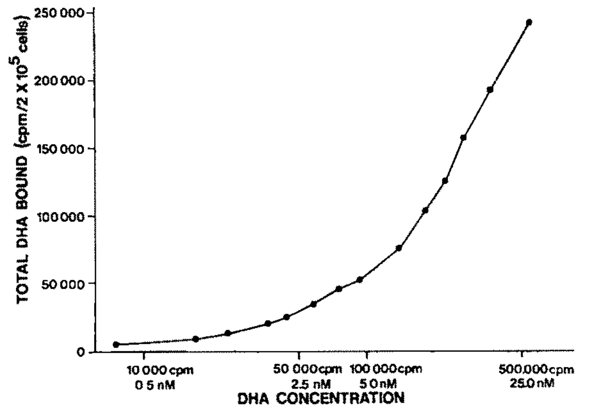

Fig 1. Binding of [^{3}H]dihydroalprenolol (DHA) to intact HeLa cells. HeLa cell suspensions (2.5·10^5 cells/tube) were incubated for 10 min at 37 °C with varying concentrations of [^{3}H]dihydroalprenolol in Hanks' balanced salt solution. The amount of total [^{3}H]dihydroalprenolol binding was determined as described in the text. The [^{3}H]dihydroalprenolol concentration is expressed both as the nanomolar concentration and as the total number of cpm present in each assay tube. Each datum point represents the mean of triplicate determinations.

nolol bound at equilibrium. Following a 5-fold dilution of the incubation mixture, 50% of the bound [^{3}H]dihydroalprenolol dissociated in 3 min, and 85% of the radioligand had dissociated within 15 min (Fig. 2B).

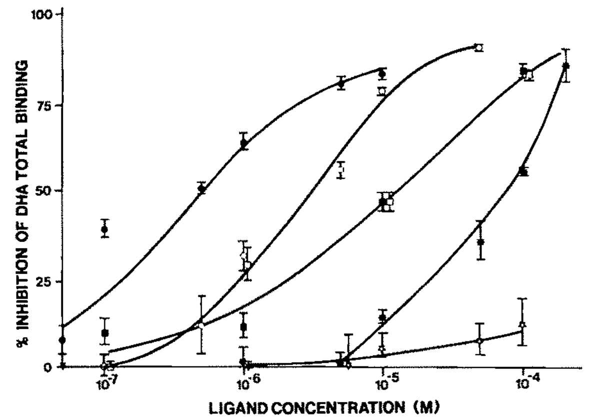

Fig. 3. Competition for [^{3}H]dihydroalprenolol binding to intact HeLa cells by adrenergic ligands. HeLa cell suspensions ((1–2)·10^5 cells per tube) were incubated with 2.5 nM [^{3}H]dihydroalprenolol for 10 min at 37 °C in the absence and presence of varying concentrations of the indicated adrenergic agents. The data are expressed as percentage inhibition of maximal binding observed in the absence of competing ligands. Each datum point represents the mean ± S.E. of triplicate determinations ●, (−)-alprenolol; ○, (±)-propranolol; ■, (−)-oxprenolol; □, (+)-oxprenolol; ★, phentolamine; ☆, (−)-isoproterenol.

The abilities of various adrenergic agonists and antagonists to compete for [^{3}H]dihydroalprenolol binding to intact HeLa cells are shown in Fig. 3. Of the agents tested, the β-adrenergic antagonist

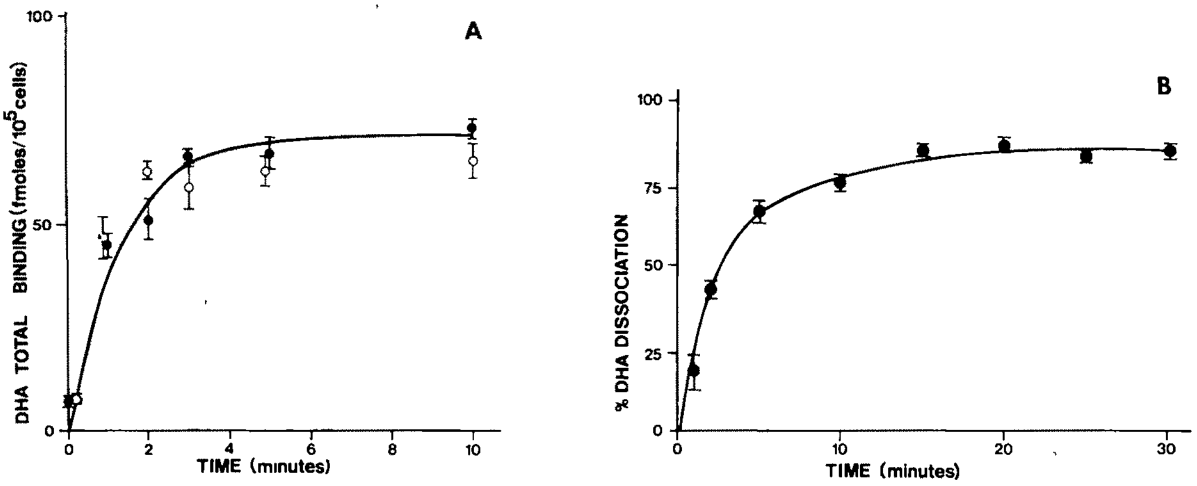

Fig. 2. Time-course of [^{3}H]dihydroalprenolol (DHA) association and dissociation to intact HeLa cells. HeLa cell suspensions (2.5·10^5 cells per tube) were incubated with 2.5 nM [^{3}H]dihydroalprenolol in the absence (●) or presence (○) of 100 μM (−)-isoproterenol at 37 °C. In panel A, the amount of total [^{3}H]dihydroalprenolol binding was measured at varying time points and is expressed as fmol bound/10^5 cells. In panel B, the cells were incubated with 2.5 nM [^{3}H]dihydroalprenolol for 10 min at 37 °C and were then diluted 5-fold by the addition of Hanks' balanced salt solution. The amount of [^{3}H]dihydroalprenolol binding was measured at varying times after dilution and is expressed as percentage dissociation of initial binding. In both panels, each point represents the mean ± S.E. of triplicate determinations.

(−)-alprenolol was the most potent inhibitor of [^{3}H]dihydroalprenolol binding. (±)-Propranolol, another β-adrenergic antagonist, was less effective in inhibiting [^{3}H]dihydroalprenolol binding than was alprenolol. The (+) and (−) isomers of oxprenolol, a β_1-antagonist, were equally potent in inhibiting [^{3}H]dihydroalprenolol binding. Phentolamine, an α-adrenergic antagonist, also competed for the [^{3}H]dihydroalprenolol-binding sites. (−)-Isoproterenol, a β-adrenergic agonist, was an extremely poor competitor for these binding sites. The IC$_{50}$ values for these agents are summarized in Table I.

Chloroquine, a lysosomotropic amine, inhibited [^{3}H]dihydroalprenolol binding to intact HeLa cells (Fig. 4). The dose of chloroquine required to inhibit [^{3}H]dihydroalprenolol binding was similar both for HeLa cell suspensions and for HeLa cells grown in multiwell culture plates, indicating that the preparation of cell suspensions did not alter the properties of [^{3}H]dihydroalprenolol binding. The addition of 50 μM chloroquine to cells which had been preincubated for 10 min with [^{3}H]dihydroalprenolol resulted in 83% dissociation of [^{3}H]dihydroalprenolol within 3 min after chloroquine addition. Methylamine and ammonium chloride, which have chloroquine-like lysosomotropic activities in other biological systems, also inhibited [^{3}H]dihydroalprenolol binding to intact HeLa cells (Table I). The concentrations of these amines which caused maximal inhibition (10 mM) were higher than that required for chloroquine (0.1 mM).

TABLE I

SUMMARY OF IC$_{50}$ VALUES FOR INHIBITION OF [^{3}H]DIHYDROALPRENOLOL BINDING TO INTACT HeLa CELLS

HeLa cell suspensions were incubated with 2.5 nM [^{3}H]dihydroalprenolol in the presence of varying concentrations of the indicated compounds for 10 min at 37°C. [^{3}H]Dihydroalprenolol binding was assessed as described in the text.

Ligand	IC$_{50}$ (μM)
β-Antagonist	
(−)-alprenolol	0.5
(±)-propranolol	3.5
(−)-oxprenolol	15
(+)-oxprenolol	15
β-Agonists	
(−)-isoproterenol	>100
α-Antagonist	
phentolamine	75
Amines	
chloroquine	8.0
methylamine	2500
ammonium chloride	800

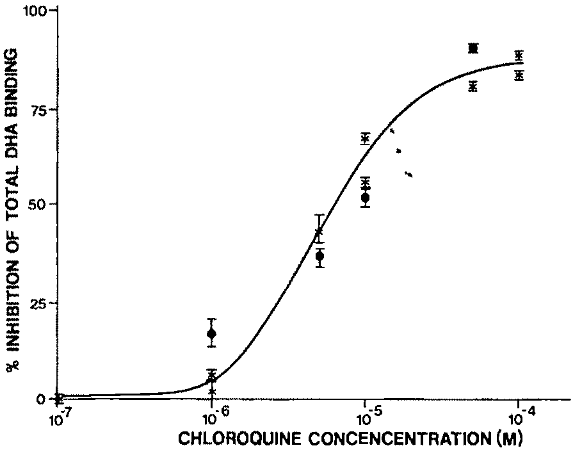

Fig. 4. Inhibition of [^{3}H]dihydroalprenolol (DHA) binding to intact HeLa cells by chloroquine. HeLa cell suspensions (1.2·10^5 cells per tube) (●) or HeLa cells grown in multiwell culture plates (2·10^5 cells per well) (∗) were incubated with 2.5 nM [^{3}H]dihydroalprenolol in the absence and presence of chloroquine at varying concentrations for 10 min at 37 ° C. [^{3}H]dihydroalprenolol binding was assessed as described in the text. Each datum point represents the mean ± S.E. of triplicate (cell suspension) or quadruplicate (multiwell plate) determinations.

The binding of [^{3}H]dihydroalprenolol to intact HeLa cells was dependent on both the pH and the temperature of the incubation medium. The dependence of [^{3}H]dihydroalprenolol binding on the extracellular pH is shown in Fig. 5. The amount of total [^{3}H]dihydroalprenolol binding increased 4-fold as the pH of the incubation buffer was increased from 6.5 to 8.0.

The temperature dependence of [^{3}H]dihydroalprenolol binding is shown in Table II. The amount of binding was decreased by 73% when the cells were incubated for 30 min at 4 ° C, as compared to 10 min at 37 ° C. [^{3}H]Dihydroalprenolol binding did not increase when the cells were incubated at 4 ° C for up to 90 min, indicating that the reduced level of binding was not due to a lower association rate at 4 ° C. When the cells were incubated with

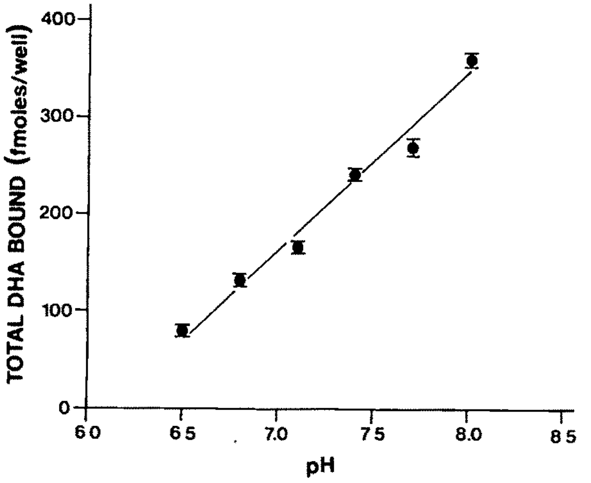

Fig. 5. Effect of pH on [^{3}H]dihydroalprenolol binding to intact HeLa cells. HeLa cells grown in multiwell plates (2·10^5 cells per well) were incubated for 10 min at 37 °C with 2.5 nM [^{3}H]dihydroalprenolol in Hanks' balanced salt solution containing 25 mM Hepes adjusted to various pH values. The cells were then rinsed with buffer at the same pH used for the incubation and [^{3}H]dihydroalprenolol binding was assessed as described in the text. Each datum point represents the mean ± S.E. of quadruplicate determinations.

[^{3}H]dihydroalprenolol for 30 min at 4°C and were then warmed to 37 °C for 10 min, the amount of [^{3}H]dihydroalprenolol binding was similar to that measured in cells which had not been preincubated at 4 °C. When cells were incubated with [^{3}H]dihydroalprenolol at 37 °C and were subsequently cooled to 4 °C, no reduction in the total [^{3}H]dihydroalprenolol binding was observed, indicating that cooling of the cells did not cause dissociation of bound radioligand. In summary, these data show that [^{3}H]dihydroalprenolol uptake occurs at 37 °C but not at 4°.

TABLE II

EFFECTS OF INCUBATION TEMPERATURE ON TOTAL [^{3}H]DIHYDROALPRENOLOL BINDING TO INTACT HeLa CELLS

HeLa cell suspensions (2·10^5 cells per tube) were incubated at 4 °C or 37 °C for varying incubation times with 2.5 nM [^{3}H]dihydroalprenolol ([^{3}H]DHA). [^{3}H]Dihydroalprenolol binding was assessed as described in the text. Each value represents the mean of triplicate determinations ± S.E.

Incubation conditions	Total [^{3}H]DHA bound (% of control)
10 min at 37 °	100.0
30 min at 4 °C	26.8 ± 0.9
30 min at 4 ° C, followed by 10 min at 37 °C	78.4 ± 3.9
10 min at 37 ° C, followed by 20 min at 4 °C	114.6 ± 4.6

TABLE III

EFFECTS OF THE COMPOSITION OF THE WASH BUFFER ON [^{3}H]DIHYDROALPRENOLOL BINDING TO INTACT HeLa CELLS

HeLa cell suspensions (1.4·10^5 cells per tube) were incubated with 2.5 nM [^{3}H]dihydroalprenolol in Hanks' balanced salt solution (HBSS) at 37 °C for 10 min. [^{3}H]Dihydroalprenolol ([^{3}H]DHA) binding was assessed as described in the text, except that during filtration of the incubation mixtures the cells were washed with the indicated buffers. The data are expressed as [^{3}H]dihydroalprenolol binding as percentage of control (HBSS incubation and wash). Each value represents the mean of triplicate determinations ± S.E.

Incubation buffer	Wash buffer	[^{3}H]DHA bound (% of control)
HBSS	HBSS (25 ml)	100
HBSS	10 mM Tris-HCl, pH 7.5 (50 ml)	20.1 ± 2.9
HBSS	H_2O (25 ml)	58.1 ± 1.9
HBSS	H_2O (100 ml)	28.4 ± 2.4

[^{3}H]Dihydroalprenolol binding was reduced when HeLa cells were washed with hypotonic solutions following incubation with the radioligand (Table III). When cells were incubated with [^{3}H]dihydroalprenolol in Hanks' balanced salt solution and were then washed on the filters with either distilled water or 10 mM Tris-HCl (pH 7.4), the amount of radioligand retained on the filter was reduced by 41–80% as compared to control cells washed with Hanks' balanced salt solution. Similar reductions in [^{3}H]dihydroalprenolol binding were observed in cells which were incubated in phosphate-buffered saline and then washed with distilled water (data not shown).

Valinomycin, a K$^+$-ionophore which depletes intact cells of ATP, reduced the binding of [^{3}H]dihydroalprenolol in a dose-dependent manner to a maximum extent of 61% (Table IV). The effectiveness of sub-maximal concentrations of valinomycin was increased by incubating the cells with valinomycin for 5 min prior to addition of [^{3}H]dihydroalprenolol. Sodium azide, another metabolic inhibitor, also inhibited radioligand binding in a concentration-dependent fashion.

Two cytoskeletal-disrupting agents, colchicine and cytochalasin B, had little effect on [^{3}H]dihydroalprenolol binding. Each agent was preincubated with the cells for 15 min prior to addition of the [^{3}H]dihydroalprenolol. Colchicine (1–100 μM) inhibited binding by approx. 30%, but the effect was not dose-dependent. Cytochalasin B had no significant effect (less than 16% inhibition) at concentrations between 1 and 100 μM.

In order to determine whether the component of [^{3}H]dihydroalprenolol binding described above was unique to the O-HeLa cell line used in these experiments, the properties of radioligand binding to another HeLa cell line, L-HeLa, were examined. In L-HeLa cells, [^{3}H]dihydroalprenolol binding was similarly protectable by (±)-propranolol, chloroquine and valinomycin (data not shown).

We next studied the properties of β-adrenergic-binding sites on HeLa cell membranes. Since the intact-cell results had suggested that β-receptors were not present in very high densities on the HeLa cells used for this study, we used [^{125}I]iodohydroxybenzylpindolol as the radioligand in these experiments because its specific activity is higher than that of [^{3}H]dihydroalprenolol. Specific binding of [^{125}I]iodohydroxybenzylpindolol to HeLa membranes was determined in the presence of 10 μM (−)-alprenolol or 100 μM (−)-isoproterenol, and typically represented 60–75% of the total binding. Specific binding achieved equilibrium within 20 min at 37 °C and was stable for at least 45 min (data not shown). Equilibrium binding of [^{125}I]iodohydroxybenzylpindolol to HeLa cell membranes was performed using membranes prepared from cells grown in the absence and presence of 5 mM sodium butyrate. The receptor number of membranes prepared from butyrate-treated cells was increased as compared to control membranes. In a representative experiment, the binding capacity increased from 4.17 to 7.04 fmol/10^6 cells (−butyrate: 2510 receptors/cell; +butyrate: 4238 receptors/cell) following butyrate exposure, as calculated from the linear regression analyses of the data plotted by the method of Schatchard [19]. The K_d values for [^{125}I]iodohydroxybenzylpindolol binding were similar for normal and butyrate-treated cells (200 and 330 pM). The mean increase in receptor number for butyrate-treated cells was 286% (ratio of −butyrate/+butyrate: mean = 0.35 ± 0.04 S.E., $n = 6$).

TABLE IV

EFFECT OF METABOLIC INHIBITORS ON [^{3}H]DIHYDROALPRENOLOL BINDING TO INTACT HeLa CELLS

HeLa cell suspensions ($1 \cdot 10^5$ cells per tube) were incubated with 2.5 nM [^{3}H]dihydroalprenolol in the presence and absence of varying concentrations of valinomycin or sodium azide for 10 min at 37 °C. In some samples, the cells were preincubated with valinomycin for 5 min prior to the addition of [^{3}H]dihydroalprenolol ([^{3}H]DHA). [^{3}H]Dihydroalprenolol binding was assessed as described in the text. Each value represents the mean of triplicate determinations ± S.E.

Compound conc. (M)	Preincubation time (min)	[^{3}H]DHA bound (% of control)
Valinomycin		
$1 \cdot 10^{-7}$	0	72.7 ± 2.2
$1 \cdot 10^{-6}$	0	62.1 ± 2.5
$1 \cdot 10^{-5}$	0	43.9 ± 0.8
$1 \cdot 10^{-7}$	5	52.4 ± 3.2
$1 \cdot 10^{-6}$	5	44.1 ± 0.2
$1 \cdot 10^{-5}$	5	39.0 ± 3.3
Sodium azide		
$1 \cdot 10^{-4}$	0	83.4 ± 3.5
$1 \cdot 10^{-3}$	0	77.3 ± 2.0
$1 \cdot 10^{-2}$	0	64.5 ± 2.1

The abilities of various agents to compete for [^{125}I]iodohydroxybenzylpindolol sites on control and butyrate-treated HeLa cell membranes were examined (data not shown). (−)-Alprenolol and (−)-isoproterenol competed for the [^{125}I]iodohydroxybenzylpindolol-binding sites with high affinity in both normal and butyrate-treated HeLa cell membranes (K_d values of 0.1 and 400 nM, respectively). Chloroquine inhibited [^{125}I]iodohydroxybenzylpindolol binding to membranes by less than 50% at a concentration of 1 mM.

Discussion

Our previous observation [14] that isoproterenol stimulated cyclic AMP accumulation in intact HeLa cells indicated that functional β-adrenergic receptors were present on the cells, confirming observations from other laboratories [15,16]. However, our attempts to detect β receptor-specific [^{3}H]dihydroalprenolol binding to intact HeLa cells yielded results which were initially perplexing. The [^{3}H]dihydroalprenolol-binding sites were protectable by 10 μM propranolol and were characterized by high capacity and by rapid rates of association and dissociation. However, approx. 50% of the added radioligand was bound to the cells and the 'specific' binding was not saturable. These features were not typical of [^{3}H]dihydroalprenolol binding to β-adrenergic receptors, which are saturable and of high affinity.

When we investigated the ligand specificity of the [^{3}H]dihydroalprenolol binding sites, we found that the β-antogonists (−)-alprenolol and (±)-propranolol blocked [^{3}H]dihydroalprenolol binding. However, the binding was nonstereoselective and the concentrations of the antagonists required to inhibit [^{3}H]dihydroalprenolol binding were much higher than expected on the basis of their dissociation constants for β-adrenergic receptors [20]. [^{3}H]Dihydroalprenolol binding was inhibited by phentolamine, an α-adrenergic antagonist, but not by (−)-isoproterenol, a β-adrenergic agonist. These data indicated that the majority of [^{3}H]dihydroalprenolol-binding sites in intact HeLa cells did not represent β-adrenergic receptors.

Observations from further studies were all consistent with our hypothesis that a cytoplasmic uptake process was responsible for the observed [^{3}H]dihydroalprenolol binding. We observed that the [^{3}H]dihydroalprenolol binding to intact HeLa cells was inhibited by lysosomotropic amines and was pH- and temperature-dependent. When cells were washed with hypotonic buffer to induce cell lysis, bound [^{3}H]dihydroalprenolol was removed. Two metabolic inhibitors, valinomycin and sodium azide, suppressed [^{3}H]dihydroalprenolol binding. We feel that the most probable site of [^{3}H]dihydroalprenolol accumulation is the lysosomal compartment. Our model is as follows. (1) Since [^{3}H]dihydroalprenolol is a lipophilic weak base (pK 9.5–10), the neutral form (which is more prevalent at higher pH) diffuses across the plasma membrane and accumulates in the lysosomal compartment (pH approx. 4.5). This process is facilitated by elevated extracellular pH. (2) [^{3}H]dihydroalprenolol uptake is blocked at 4°C because the radioligand cannot diffuse across the plasma membrane at this temperature, due to the altered physical state of the membrane. (3) Other lipophilic amines (i.e., adrenergic antagonists and lysosomotropic agents) compete for binding to the lysosomal compartment and thereby inhibit [^{3}H]dihydroalprenolol uptake. (4) [^{3}H]Dihydroalprenolol retained in the cytoplasmic compartment is washed out during cells lysis, resulting in a decrease in the detectable radioligand binding. (5) Since the lysosomal pH gradient is maintained by an ATP-driven proton pump [21], metabolic poisons abolish the gradient and thereby decrease [^{3}H]dihydroalprenolol entrapment.

Alternative explanations for the observed [^{3}H]dihydroalprenolol binding are as follows. First the ligand might partition into the lipid bilayer of the plasma membrane in a nonspecific fashion. This is unlikely in view of the fact that hypotonic lysis of the cells removes bound radioligand (Table IV). Second, the uptake might be a receptor-mediated accumulation resulting from internalization of the ligand-receptor complex. However, this explanation is inconsistent with our observations that β-agonists have no effect on the amount of uptake or the rate of uptake, and that β-adrenergic antagonists block uptake at concentrations higher than predicted on the basis of their affinities for β-adrenergic receptors as measured in other systems. Finally, the uptake might be due to accumulation of [^{3}H]dihydroalprenolol in nonlysosomal sites. This latter possibility cannot be eliminated without conducting further experiments.

Amine uptake has been observed in a variety of cellular systems. In macrophages, [^{3}H]propranolol uptake is dependent on temperature and pH, and is inhibited by lysosomotropic amines and by metabolic inhibitors, but not by norepinephrine or epinephrine, and is abolished by sonication of the cells [22]. The uptake of dopaminergic radioligands by several types of intact cells is inhibited by chloroquine and alprenolol and is pH-dependent [23]. A study of amine uptake by rabbit lung showed that amines with higher pK_a values are accumulated within cells to a greater extent than those with lower pK_a values and that the physiochemical characteristics of the nonnitrogenous portion of the molecule influence the extent of the uptake [24]. Presumably, β-adrenergic agonists, such as isoproterenol, do not block [^{3}H]dihydroalprenolol uptake because they are more hydrophilic and therefore diffuse across plasma membranes less readily than the more hydrophobic antagonists.

β-Adrenergic-receptor sites were successfully identified and quantitated in membrane preparations of HeLa cells, using [^{125}I]iodohydroxybenzylpindolol as the radioligand. These sites were distinct from the [^{3}H]dihydroalprenolol uptake sites described for intact cells. Chloroquine, an effective inhibitor of [^{3}H[dihydroalprenolol uptake in intact HeLa cells, was a very poor inhibitor of [^{125}I]iodohydroxybenzylpindolol binding to HeLa membranes. The concentrations of chloroquine required to block the binding of 88–160 pM [^{125}I]iodohydroxybenzylpindolol were 100-fold greater than the concentrations required to block the binding of 2.5 nM [^{3}H]dihydroalprenolol to the intact cells. Thus, the effects of chloroquine on [^{125}I]iodohydroxybenzylpindolol binding to membranes are probably due to a mechanism different from that implicated in the intact cell. This was especially evident in the striking differences in the rank order of potencies of alprenolol and chloroquine in the two systems. In intact cells, alprenolol and chloroquine were approximately equipotent in inhibiting [^{3}H]dihydroalprenolol uptake. In the membrane preparation, alprenolol was approx. $2 \cdot 10^{6}$-fold more potent in blocking [^{125}I]iodohydroxybenzylpindolol binding than was chloroquine.

Various strategies may be employed to reduce nonspecific [^{3}H]dihydroalprenolol binding. These include the use of lysosomotropic agents, low temperature, and metabolic inhibitors. While these methods permit the detection of β-adrenergic receptors on the intact cells, they may complicate studies of the dynamics of β-adrenergic receptors in intact cells. For example, metabolic inhibitors may inhibit receptor internalization and receptor turnover, lysosomotropic agents are likely to inhibit degradation of internalized receptors, and low temperature may abolish receptor internalization and receptor-effector interactions. The capability of studying phenomena such as receptor desensitization is one of the major advantages of an intact cell system. Hypotonic lysis of cells following their incubation with radioligand is probably the most benign method for the reduction of nonspecific binding, since it can be accomplished rapidly at the conclusion of the incubation period.

Care must be taken to define 'specific' [^{3}H]dihydroalprenolol binding in intact cells, since other β-antagonists compete for the radioligand uptake. Our results suggest that isoproterenol, which blocks receptor-specific binding, but not radioligand uptake, is an appropriate ligand to use in defining nonspecific binding. Chloroquine is a useful agent for testing the specificity of radioligand binding, since it is much more effective at reducing [^{3}H]dihydroalprenolol uptake than at inhibiting radioligand binding to β-receptors. We recommend that chloroquine be used in preference to phentolamine to inhibit [^{3}H]dihydroalprenolol uptake in intact cell systems, since it is more potent than phentolamine. Ultimately, the use of more polar radioligands may avoid the problem of radioligand uptake. Recently, a hydrophilic β-adrenergic antagonist ([^{3}H]CGP-12177) has been successfully employed for the identification of β-adrenergic receptors on intact cells [13].

The uptake of β-antagonists may be of clinical importance. Other exogenously-administered amines may displace these drugs from the lysosomal compartment and lead to an abrupt increase in plasma drug levels. Also the possibility exists that the adrenergic amines may affect lysosomal function in a manner similar to chloroquine. HeLa cells are a useful model system in which to explore these possibilities.

Acknowledgements

This work was supported in part by a grant from the NIH. Kathryn E. Meier was a recipient of a predoctoral fellowship from the American Association of University Women.

References

1 Porzig, H. (1982) Trends Pharm. Sci., 75–78
2 Dax, E.M., Partilla, J.S. and Gregerman, R.I. (1981) J. Receptor Res. 2, 267–283
3 Dax, E.M. and Partilla, J.S. (1982) Mol. Pharmacol. 22, 5–7
4 Schonberg, M., Krichevsky, A and Bilezikian, J.P. (1980) Life Sci. 26, 1287–1292
5 Pochet, R. and Schmitt, H. (1979) Nature 277, 58–59
6 Pittman, R.M. and Molinoff, P.B. (1980) J. Cyclic Nucleotide Res. 6, 421–435
7 Terasaki, W.L. and Brooker, G (1978) J Biol. Chem. 253, 5418–5425

8 Cabelli, R.J. and Malbon, C.C. (1979) J Biol. Chem. 254, 8903–8908

9 Dibner, M.D. and Insel, P.A. (1981) J. Cell. Physiol. 109, 309–316

10 Dulis, B.H. and Wilson, I.B. (1980) J. Biol. Chem. 255, 1043–1048

11 Paietta, E., Hoyer, D., Engel, G. and Schwarzmeier, J.D (1982) Mol. Cell. Endocrinol. 25, 267–276

12 Insel, P.A. and Stoolman, L.M. (1978) Mol. Pharmacol 14, 549–561

13 Staehelin, M., Simons, P., Jaeggi, K. and Wigger, N. (1983) J. Biol. Chem. 258, 3496–3502

14 Meier, K.E. and Ruoho, A.E. (1983) Biochim. Biophys. Acta 761, 257–261

15 Lin, M.C., Lin, C.-S. and Whitlock, J.P. (1979) J. Biol. Chem 254, 4684–4688

16 Tallman, J.F., Smith, C.C. and Henneberry, R.C. (1977) Proc. Natl. Acad. Sci. U.S.A. 74, 873–877

17 Maguire, M E., Wiklund, R.A. Anderson, H.J. and Gilman, A.G (1976) J. Biol Chem. 251, 1221–1231

18 Harden, T.K., Su, Y.-F. and Perkins, J.P. (1979) J. Cyclic Nucleotide Res. 5, 99–106

19 Scatchard, G. (1949) Ann. N.Y. Acad. Sci. 51, 660–672

20 Minneman, K.P., Hedberg, A. and Molinoff, P.B. (1979) J. Pharmacol. Exp. Ther. 211, 502–508

21 Schneider, D.L. (1981) J Biol. Chem. 256, 3858–3864

22 Vestal, R.E., Kornhauser, D.M. and Shand, D.G. (1980) J Pharmacol. Exp. Ther. 214, 106–111

23 Maloteaux, J.-M., Gossuin, A., Waterkeyn, C. and Laduron, P.-M. (1983) Biochem. Pharmacol. 32, 2543–2548

24 Anderson, M.W., Orton, T.C., Pickett, R D. and Eling, T.E. (1974) J. Pharmacol. Exp. Ther. 189, 456–466

Biochimica et Biophysica Acta, 804 (1984) 341–347
Elsevier

BBA 11324

LOCALIZATION AND IDENTIFICATION OF THE COMPOUND CAUSING PEAK 'X' IN THE ^{31}P-NMR SPECTRUM OF *SACCHAROMYCES CEREVISIAE*

RICHARD A. GAGE [a], WICK VAN WIJNGAARDEN [a], ALEXANDER P.R. THEUVENET [a,*],
GEORGE W.F.H. BORST-PAUWELS [a] and CORNELIS A.G. HAASNOOT [b]

[a] *Department of Chemical Cytology and* [b] *Department of Biophysical Chemistry, Faculty of Science, University of Nijmegen, Toernooiveld, 6525 ED Nijmegen (The Netherlands)*

(Received February 17th, 1984)

Key words: ^{31}*P-NMR, Phosphomannan, (S. cerevisiae)*

The present study is aimed at identifying the unidentified compound which gives rise to the so-called resonance 'X' in the ^{31}P-NMR spectra of yeast cells. In addition, it is attempted to determine the localization of X (inside or outside the cell). Enzymic removal of the cell wall causes resonance 'X' to disappear in the spectra of the cells. This observation indicates an extracellular localization of X. The ^{31}P-NMR spectrum of the phosphomannan extracted from the yeast shows a single resonance at exactly the same position as that of resonance 'X'. Extraction of the phosphomannan from delipidized cells causes resonance 'X' to disappear from the ^{31}P-NMR spectrum of the cells. The intensity of resonance 'X' in the spectrum of the intact cells can be almost quantitatively attributed to the amount of phosphomannan present in the yeast. The present results demonstrate that the resonance 'X' in the ^{31}P-NMR spectrum of yeast cells is caused by phosphomannan in the cell wall.

Introduction

The ^{31}P-NMR spectra of yeasts show a resonance in the phosphodiester range, designated as peak 'X' (see e.g. Refs. 1–3). The compound causing this peak has not yet been identified and also its localization, (e.g., inside or outside the yeast cell) has not been determined.

The cell walls of yeast cells typically contain a compound with phosphodiester bonds, namely phosphomannan (see e.g. Ref. 4). Therefore, it may be considered that the phosphomannan caused peak 'X' in the ^{31}P-NMR spectra of yeast cells.

Here we report on a ^{31}P-NMR study of the yet unidentified phosphorus pool in *Saccharomyces cerevisiae* and we will show that phosphamannan of the yeast cell wall indeed causes peak 'X'.

Materials and Methods

Preparation of cells and protoplasts. Cells and protoplasts of *S. cerevisiae* A294 (Whitbread and Co., Luton, U.K.) were grown and harvested according to the method of Theuvenet and Bindels [5]. Cells and protoplasts were washed and resuspended in 45 mM Tris succinate (pH 4.5) containing 0.82 M sorbitol, 1 mM $CaCl_2$ and 10% (v/v) ^2H_2O. The pellet volume was usually 40% of the total sample volume. Cells and protoplasts were kept on ice until needed.

Preparation of delipidized cells. Cell lipids were extracted according to the method of Wanka [6]. Using *S. cerevisiae* A294, 6 g wet wt. was washed

---

[*] To whom correspondence should be sent.

Abbreviations: TSP, 3-(trimethylsilyl)propionic acid-(d_4) sodium salt; TPP, tetraphenylphosphonium chloride; TMP, trimethylphosphate.

0167-4889/84/$03.00 © 1984 Elsevier Science Publishers B.V.

twice with distilled water. The pellet was then resuspended in 50 ml of an ethanol/diethylether (3 : 1) mixture and heated at 75 °C under reflux for 10 min. The residue was pelleted by slow centrifugation and resuspended in ethanol/diethylether (3 : 1) and the process was repeated three times. For ^{31}P-NMR the residue was resuspended in 15 ml distilled water containing 10% (v/v) ^2H_2O.

Extraction of phosphomannan. The delipidized cells (obtained from 6 g wet wt. of intact cells) were washed with acetone and subsequently with ether and then dried. The pellet was resuspended in 50 ml distilled water and 125 mg pronase (grade B, Calbiochem, La Jolla, U.S.A.) was added. The mixture was stirred thoroughly for 15 min at 37 °C and further incubated for a period of 20 h at 37 °C. The digest was then centrifuged at 1500 × *g* and the phosphomannan isolated following the sodium borate Cetavlon method of Cawley et al. [7]. This phosphomannan extract (yield 100 mg) was stored at 0 °C for a short period until further use.

For ^{31}P-NMR of the phosphomannan extract, 40 mg of the extract was suspended in 15 ml distilled water containing 10% (v/v) ^2H_2O.

Thin-layer-chromatography (TLC) of the phosphomannan extract. TLC was carried out using Cellulose F TLC plates (Merck, Darmstadt, F.R.G.). 3 mg of the phosphomannan extract was dissolved in acetic acid. Two spots were applied to the plates, one at each side of the centre line, and the plates were allowed to develop in propan-2-ol /aqueous ammonia 0.88/distilled water (6 : 3 : 1). The plates were then sprayed with a molybdate spray according to the method of Dittmer and Lester [8] and a sodium periodate rosaniline spray (Schiff's reagent) according to the method of Buchanen et al. [9].

Acid hydrolysis of the phosphomannan extract. An acid hydrolysate of the phosphomannan extract was prepared by dissolving 30 mg of the extract in 1 ml 2 M HCl and by heating the solution for 4 h at 120 °C in a sealed tube. Subsequently, 5 ml distilled water was added and the solution was evaporated to near dryness, distilled water was again added and the process repeated three times until a pH value of 4.5 was reached. The hydrolysate of the extract was then evaporated to dryness on a rotary evaporator and stored at −20 °C until further use.

For ^{1}H-NMR, 0.5 mg of the acid hydrolysate was dissolved in 0.3 ml ^2H_2O with 1% (v/v) TSP as internal standard.

Preparation of phenylhydrazones according to Richtmyer [10]. About 6 mg of the acid hydrolysate of the phosphomannan extract was dissolved in 0.5 ml distilled water. 0.1 ml of a mixture of phenylhydrazine (200 mg/ml) and sodium acetate (120 mg/ml) was added, and the resulting mixture was allowed to stand for 2 h. It was then cooled to 0–4 °C and allowed to stand for a further 2 h. After slow centrifugation the pellet was resuspended in 2 ml distilled water at 0 °C and centrifuged again. The pellet was then washed twice successively with ice-cold ethanol and diethylether and allowed to dry. The resulting crystals (yield 3 mg) had a greyish white colour. The melting point of these crystals was compared to that of a standard of mannose phenylhydrazone, using a Fisher Johns melting point apparatus.

Preparation of derivatives of hexoses and their characterization by gas-liquid chromatography (GLC). The acid hydrolysate of the phosphomannan extract was derivatized to the per-*O*-acetyl aldononitrile, using a variation of the method of Lance and Jones [11] as follows. About 3 mg of the hydrolysate was dissolved in 0.1 ml pyridine provided with 6 mg hydroxylamine hydrochloride. The solution was heated in a sealed tube at 90 °C for 30 min. 0.25 ml acetic anhydride was added, and the mixture was heated at 90 °C for another 30 min. Standards were prepared in the same way, using mannose, glucose and galactose. The resulting derivatives were directly injected in the gas chromatograph. GLC was performed on a Varian 3700 gas-liquid chromatograph using a fused silica capillary column of SE 54 quartz and a temperature program of 2 °C per min in the range of 150–180 °C with helium as carrier at 28 lb/in^2 (2.1 ml per min) and a split ratio 1 : 90. The retention time of the derivatized hydrolysate was compared to that of authentic samples.

^{31}P-NMR. ^{31}P-NMR spectra were recorded on a Bruker WM 200 spectrometer operating in the Fourier transform mode at 81.01 MHz with broad band ^{1}H decoupling at 200 MHz. The pulse length was 28 μs with a relaxation delay of 1 s, and the sweep width was 5000 Hz. Chemical shifts are

given relative to TPP, used as an external reference. All reported shifts are denoted using the δ-convention, i.e., positive values represent shifts to lower field; the chemical shift of TPP compared to TMP is 19.68 ppm.

All samples, containing 10% (v/v) ^2H_2O, had a volume of 15 ml and were measured in Wilmad tubes with a diameter of 20 mm. The spectra represent a time average of 100 scans and were recorded at 22°C. Adjustments of the pH of the medium were carried out by addition of hydrochloric acid or sodium hydroxide.

^{1}H-NMR. ^{1}H-NMR were recorded on a Bruker WM 500 spectrometer operating at 500 MHz in the Fourier transform mode. Spectra were recorded at 24°C in 5 mm Stohler S4 thin-walled tubes; chemical shifts are expressed relative to TSP (1% w/v) added as an internal reference.

Determination of phosphorus pools in intact cells. Ortho- and polyphosphates were extracted from the cells according to Weimberg [12]. The orthophosphate in the fractions was determined according to the method of Fiske and SubbaRow [13] after acid hydrolysis of the fractions with HCl (pH 0–1), for 7 min in a boiling water bath. Also, the orthophosphate content of the acid hydrolysate of the phosphomannan extract was determined in this way.

Spectroscopic detection of polyphosphate. The detection of polyphosphate in the supernatants of suspensions of delipidized cells was performed according to Tijssen et al. [14]. The effect of the supernatants on the fluorescence emission spectrum of 4′,6-diamidino-2-phenylindole was measured with an Aminco SPF 500 spectrofluorimeter, using the excitation wavelength of 340 nm. The spectra were recorded with an Aminco SPF 500 *XY*-recorder.

Results and Discussion

Fig. 1A shows a 81.01 MHz ^{31}P-NMR spectrum of a suspension of the yeast strain A294 under anaerobic conditions. The spectrum is recorded in the absence of an external energy source, pH$_0$ 4.5. Following Navon et al. [2] the resonances marked P$_i$ and PP are the inorganic phosphate and polyphosphate pools present in yeast, respectively. In the suspension only one inorganic orthophosphate pool can be detected. The resonance labeled P$_i$ is assigned to intracellular orthophosphate, as external orthophosphate is not present in detectable amounts. However, to date, one resonance in the yeast NMR spectrum has not yet been assigned (resonance 'X'). In view of the relative position of this resonance and its pH insensitivity, assignment to a phosphodiester moiety has been suggested [2].

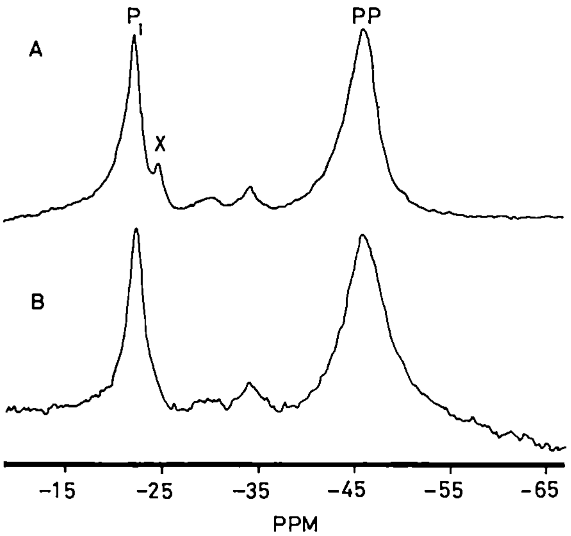

Fig. 1. ^{31}P-NMR spectrum of an anaerobic suspension of *S. cerevisiae* A294 in the absence of substrate. The cells are suspended to a density of 40% wet wt. in a total volume of 15 ml, pH$_0$ 4.5 (A) Intact cells, (B) protoplasts. The spectrum represents a time average of 100 scans. Peak assignments are made by comparison to known spectra [2]. 'X' is the unassigned phosphodiester compound; PP is the resonance caused by the middle phosphate groups of polyphosphates; TPP is used as external standard and assigned arbitrarily at 0 ppm.

Fig. 1B shows the ^{31}P-NMR spectrum of the cells after enzymic removal of the cell wall. It is clear that peak 'X' is absent in the protoplast spectrum. This strongly indicates that the presumed phosphodiester compound X causing the resonance at −24.7 ppm has an extracellular localization. Consequently, X may be associated with the external surface of the plasmamembrane of the cell from which it might have been removed by enzymic breakdown of the cell walls, or it may be an integral part of the cell wall.

Fig. 2 shows that X is not a phospholipid. In ^{31}P-NMR spectra of delipidized cells, peak 'X' is still present. Obviously the delipidized cells also still contain orthophosphate. In agreement with earlier observations (e.g. Ref. 15), the P_i peak shifts down-field on raising pH_o, while peak 'X' stays at −24.7 ppm. It is also of interest to note that the polyphosphate peak (PP), not present at pH 4.2 (Fig. 2A), appears at pH 8.2 (Fig. 2B). Apparently, at the lower pH_o the polyphosphate is not detectable in the ^{31}P-NMR spectrum of these cells. This may be due to a strong binding of polyphosphate to the cell wall of the delipidized cells at the lower pH_o. As a matter of fact, Harold and Miller [16] showed that in another fungus, *Neurospora crassa*, polyphosphate forms strong complexes with the cell walls, upon breaking down the cell membranes by homogenization of the cells. They also showed that the polyphosphate is rapidly solubilized by alkali (pH 9.2). The appearance of the polyphosphate peak in the ^{31}P-NMR spectrum of the delipidized yeast cells at higher pH_o may therefore reflect the solubilization of the polyphosphate initially bound to the cell wall. This is supported by the finding that in the ^{31}P-NMR spectrum of the same cells at pH_o 8.2, after collecting them by centrifugation and resuspension in medium of pH_o 8.2, the polyphosphate peak is strongly reduced in intensity (Fig. 2C), but is found to be present in the spectrum of the supernatant. On lowering the pH_o of this supernatant the polyphosphate peak remains and does not show a shift in position (Fig. 2D). We have also observed a red shift in the fluorescence emission spectrum of the cationic dye 4′,6-diamidino-2-phenylindole in the presence of the supernatant of the delipidized cells at pH_o 8.2 (data not shown). This confirms the presence of polyphosphates in the supernatant [14]. Fig. 2 shows that a single washing of the delipidized cells in medium of high pH_o removed most of the ortho- and polyphosphates. The compound causing peak 'X', however, remains present. As a matter of fact, the original intensity of peak 'X' is not altered by the washing (data not shown). This indicates that X is tightly bound to the cell wall or to remnants of the plasma membrane.

Relatively abundant phosphodiester com-

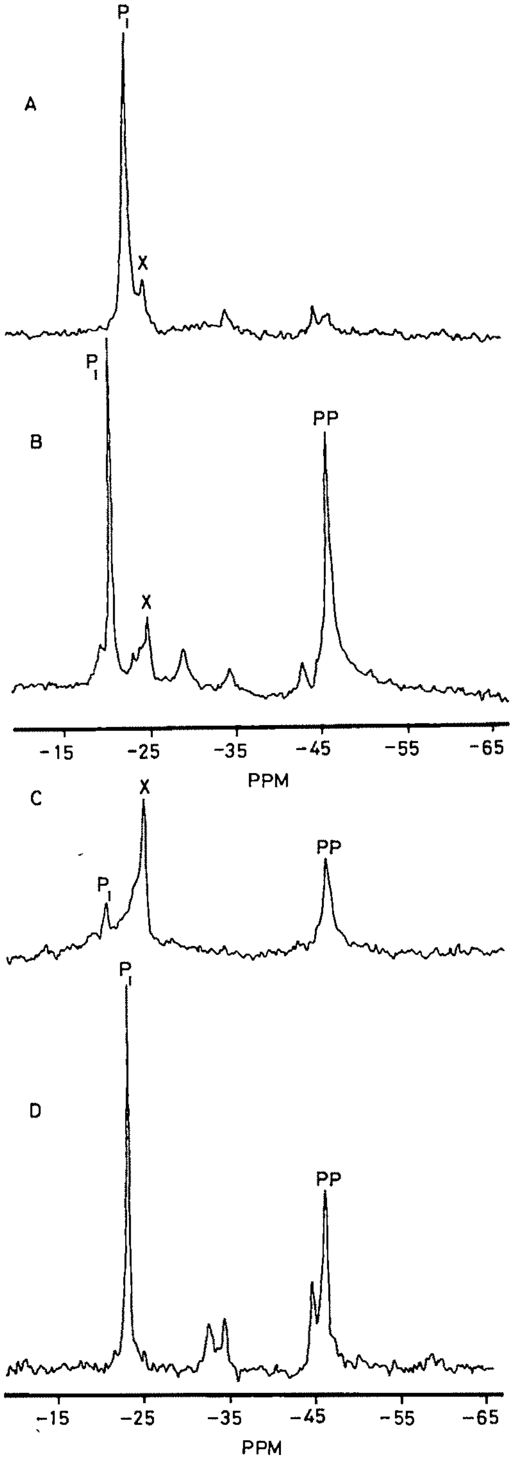

Fig. 2. ^{31}P-NMR spectra of delipidized cells prepared from 6 g wet wt. of cells of *S. cerevisiae* A294, and of the supernatant obtained from the suspension at pH 8.2 and adjusted to pH 4.2. (A) Suspension of delipidized cells after lipid extraction at pH_o 4.2; (B) same as A after adjustment of pH_o to 8.2; (C) cell pellet of B resuspended in medium of pH_o 8.2; (D) supernatant of cells B after adjustment of pH_o to 4.2. See also legend to Fig. 1.

pounds, present in cell walls of yeast, are the phosphomannans [17,18]. We have therefore examined whether X could be a phosphomannan. For that purpose the phosphomannan is extracted from the delipidized cells according to a method described by Cawley et al. [7]. Identification of the phosphomannan is carried out using several methods.

A thin-layer chromatogram of the extract shows only one spot with a positive reaction to molybdate, light blue in colour, indicating the presence of a phosphate ester [8]. In addition, the spot gives a positive reaction to Schiff's reagent, blue-grey in colour, indicating the presence of an α-glycol arrangement [9]. These observations are indicative for the presence of a single phosphorylated hexose compound in the extract.

Different lines of evidence show that the hexose is a mannose. The melting point of the phenylhydrazone of the hexose liberated by acid hydrolysis of the extract is found to be 198 °C and compares favourably with that of a standard mannose phenylhydrazone being 199 °C [19]. Also, a gas-chromatogram of the per-*O*-acetylalodononitrile derivative of the hexose shows a single peak with the same retention time as the mannose derivative (Fig. 3A). A co-injection of the derivatized hexose and a derivatized mannose standard gives a chromatogram with one peak only (Fig. 3B). The good resolution on this system is illustrated by the appearance of three peaks with different retention times on injecting a mixture of the derivatives of mannose, glucose and galactose (Fig. 3C).

Fig. 4, finally, shows that the ^{1}H-NMR spectra of the acid hydrolysate of the extract and that of commercially obtained D-(+)-mannose are identical, which supports the notion that mannose is the

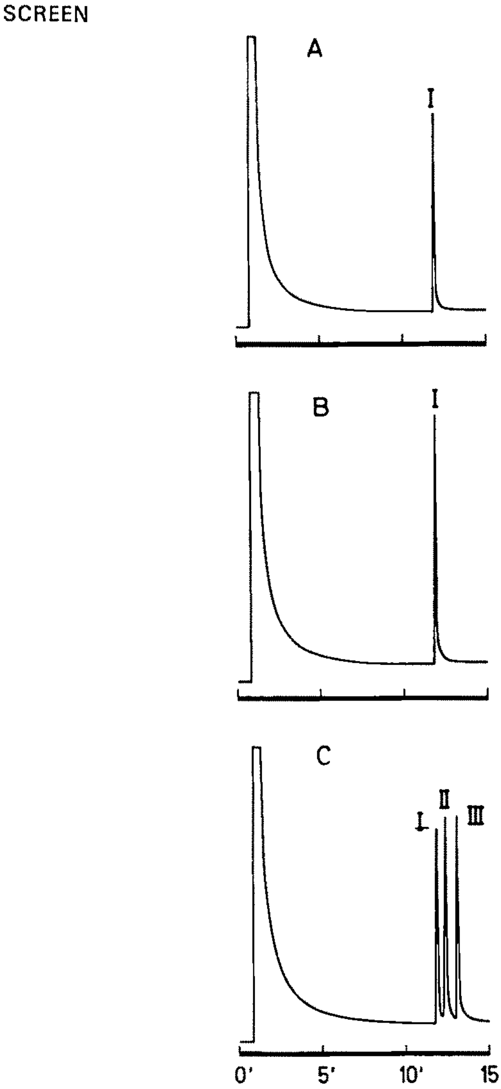

Fig. 3. Gas chromatogram of the per-*O*-acetyl aldononitrile derivative of the acid hydrolysate of the phosphomannan extract from delipidized cells of *S. cerevisiae* A294 and of derivatives of commercially obtained pure hexoses. A, a 1 μl injection of the derivative of the hydrolysate; B, a coinjection of 0.5 μl derivatized hydrolysate with 0.5 μl of a standard pentaacetyl mannononitrile; C, a 1 μl injection of a mixture of the derivatives of mannose (I), glucose (II) and galactose (III).

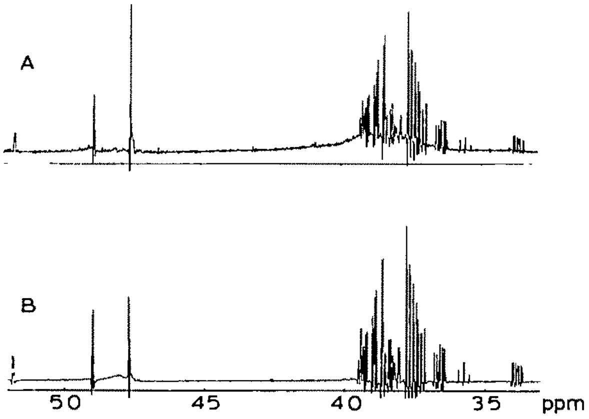

Fig. 4. ^{1}H-NMR spectra of the acid hydrolysate of the phosphomannan extract and of D-(+)-mannose. A, 0.5 mg of the hydrolysate in 300 μl ^2H_2O; B, 1.0 mg of D-(+)-mannose in 300 μl ^2H_2O provided with 1% TSP.

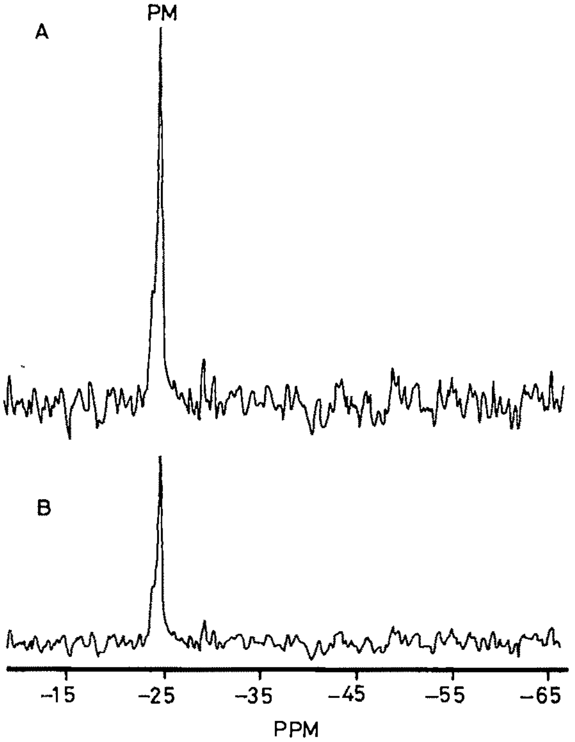

Fig. 5. ^{31}P-NMR spectra of the phosphomannan extract. 40 mg of the extract is dissolved in 15 ml distilled water containing 10% (v/v) ^2H_2O. A, at pH_0 4.2; B, at pH_0 10.2. The attenuation of spectrum B is twice that of spectrum A. PM, phosphomannan. See also legend to Fig. 1

only hexose present in the extract of the delipidized cells.

The yeast used by us contains about 28 mmol of phosphorus present in the phosphomannan and about 810 mequiv. of phosphorus present in the polyphosphates and orthophosphate pools of the cell per kg of dry weight. From these data a molar ratio of phosphorus in phosphomannan and in the remaining phosphorus pools of the cells of 0.035 is calculated. A ratio of 0.041 is calculated from the relative areas of peak 'X' and the sum of areas of the peaks of polyphosphate and cellular orthophosphate in the ^{31}P-NMR spectrum of the intact cells (Fig. 1B). This indicates that peak 'X' may be caused almost entirely by the amount of phosphomannan present in the cell suspension.

Fig. 5A and B shows the ^{31}P-NMR spectra of the phosphomannan extracted from the delipidized cells, at pH_0 4.2 and pH_0 10.2, respectively. The extracted phosphomannan has a resonance at the same position as peak 'X' and, just as for peak 'X', the resonance is pH independent over the range used.

The identity of the phosphomannan as the compound causing peak 'X' is further indicated by the finding that in the ^{31}P-NMR spectrum of the delipidized cells peak 'X' is no longer present after the phosphomannan is extracted from the cell (data not shown).

In summary, it is demonstrated that resonance 'X' in the ^{31}P-NMR spectra of yeast cells originates from the phosphomannan of the cell wall, thus confirming an extracellular localization as indicated earlier.

Acknowledgements

We thank Professor C.W. Hilbers (Department of Biophysical Chemistry) and Dr. G.J.F. Chittenden (Department of Exobiology) for their comments and many helpful suggestions and Mr. P. Peters for determining the polyphosphate content of the yeast cells. NMR experiments were performed at the Dutch National 500/200 hf-NMR facility at Nijmegen (The Netherlands). The technical assistance of Ing. W. Guijt and Ing. P.A.W. Van Dael is gratefully acknowledged. This study was supported in part by grants from the Netherlands Foundation for Chemical Research (S.O.N.) and the Netherlands Foundation for Biophysics under the auspices of the Netherlands Organization for the Advancement of Pure Research (Z.W.O.).

References

1 Salhany, J.M., Yamane, T., Shulman, R.G. and Ogawa, S. (1975) Natl. Acad. Sci. USA 72, 4966–4970
2 Navon, G., Shulman, R.G., Yamane, T., Eccleshall, T.R., Lam, K.B., Baronofsky, J.J. and Marmur, J. (1979) Biochemistry 18, 4487–4499
3 Nicolay, K., Scheffers, W.A., Bruinenberg, P.M. and Kaptein, R. (1982) Arch. Microbiol. 133, 83–89
4 Farkas, V. (1979) Microbiol. Rev. 43, 117–144
5 Theuvenet, A.P.R. and Bindels R.J.M. (1980) Biochim. Biophys. Acta 599, 587–595
6 Wanka, F. (1962) Planta 58, 594–609
7 Cawley, T.N., Harrington, M.G. and Letters R. (1972) Biochem. J. 129, 711–720
8 Dittmer, J.C. and Lester, L. (1964) J. Lipid Res. 5, 126–127

9 Buchanen, J.G., Dekker, C.A. and Long, A.G. (1950) J. Chem. Soc. Lond. 3162–3167

10 Richtmyer, N.K. (1963) in Methods in Carbohydrate Chemistry (Whistler, R.L., Wolfrom, M.L. and BeMiller, J.N., eds.), Vol. II pp. 127–131 Academic Press, New York

11 Lance, D.G. and Jones, J.K.N (1967) Can. J. Chem. 45, 1995–1998

12 Weimberg, R. (1975) J. Bacteriol. 121, 1122–1130

13 Fiske, C.H. and SubbaRow, Y (1925) J. Biol. Chem. 66, 375–400

14 Tijssen, J.P.F., Beekes, H.W and Van Steveninck, J. (1982) Biochim. Biophys. Acta 721, 394–398

15 Barton, J.K., Den Hollander, J A., Lee, T.M., McLaughlin, A. and Shulman, R G. (1980) Proc. Natl. Acad. Sci. USA 77, 2470–2473

16 Harold, F.M. and Miller, A (1961) Biochim. Biophys. Acta 50, 261–270

17 Mill, P.J (1966) J. Gen. Microbiol. 44, 329–341

18 Jayatissa, P.M. and Rose, A.H. (1976) J Gen. Microbiol. 96, 165–174

19 Fischer, E. and Hirschberger, J.H (1888) Ber. Dtsch. Chem. Ges. 21, 1805–1809

Biochimica et Biophysica Acta, 804 (1984) 348–355
Elsevier

BBA 11320

POLYAMINE REQUIREMENT FOR PROLACTIN ACTION ON MACROMOLECULAR SYNTHESIS IN THE MCF-7 HUMAN MAMMARY EPITHELIAL CELL LINE

BRUCE E. LINEBAUGH and JAMES A. RILLEMA *

Department of Physiology, Wayne State University School of Medicine, 540 E Canfield, Detroit, MI 48201 (U.S.A.)

(Received September 6th, 1983)
(Revised manuscript received March 19th, 1984)

Key words: Polyamine requirement; Prolactin action, Macromolecular synthesis, (Human mammary epithelial cell)

The actions of insulin, hydrocortisone, prolactin and growth hormone on the synthesis of macromolecules in MCF-7 cells was determined in a serum-free defined medium. The inclusion of the polyamine spermidine in the medium was shown to enhance the insulin stimulation of the rate of [^{3}H]uridine incorporation into RNA in a manner similar to that demonstrated for hydrocortisone. Spermidine, in addition to insulin and hydrocortisone, was also essential for prolactin to manifest a stimulation of the rate of [^{3}H]uridine incorporation; this effect of spermidine was optimal with spermidine concentrations between 1 and 5 mM. Prolactin also stimulated the rate of [^{3}H]leucine incorporation into total cellular protein and into an isoelectrically precipitable (pH 4.6) phosphoprotein fraction. The actions of prolactin on total protein and phosphoprotein synthesis were only expressed if spermidine, in addition to insulin and hydrocortisone, was contained in the culture medium. All of the prolactin responses were observed employing physiological concentrations of prolactin. Specificity of the prolactin responses was established by demonstrating that porcine growth hormone had no effects on RNA or phosphoprotein synthesis in the MCF-7 cells.

Introduction

The human mammary epithelial cell line MCF-7 has been characterized and studied as an in vitro model of normal and neoplastic mammary cells since its description [1]. The MCF-7 cell line has been shown to possess a specific estrogen receptor [2] with an unusual subcellular distribution [3]. The original description of the cell line [1] reported it to be insulin-dependent for culture growth. Subsequently, it was demonstrated to be biphasic in its response to various estrogen concentrations [4] and responsive to androgens [5]. A receptor for glucocorticoid has also been reported in the MCF-7 cell line [6]. Prolactin has been shown to stimulate the specific intracellular 17β-estradiol binding without any effect on growth rate of the cells [7]. The presence of prolactin receptor in MCF-7 cells and properties of the interaction between prolactin and its receptor have been described [8]. However, the demonstration of a specific lactogenic hormone response by MCF-7 cells and the resultant production of milk components, such as casein, in a defined medium has remained elusive [9]. Accordingly, we have designed and conducted studies attempting to (1) establish serum-free defined medium conditions which are required for continued cellular metabolism without loss of integrity or altered biochemical properties, (2) determine the optimal hormone levels, enzyme cofactors, and metabolic intermediates necessary for cellular synthesis of metabolic products which are quanti-

---

* To whom reprint requests should be addressed.

Abbreviations: I, insulin; H, hydrocortisone; Spd, spermidine; Prl, prolactin

0167-4889/84/$03.00 © 1984 Elsevier Science Publishers B.V.

tatively measurable. and (3) elucidate the time sequences of metabolic parameters which are altered as a result of multiple hormone actions and interactions. The characteristics of the insulin stimulation of DNA, RNA and protein metabolism [10] and hydrocortisone enhancement of insulin's action on the synthesis of these macromolecules in MCF-7 cells [11] have been described. Subsequently, we demonstrated that similar responses could be evoked by insulin and hydrocortisone in primary epithelial cell cultures from mouse mammary glands [12]. The effect of insulin at dilution endpoint concentrations on macromolecular synthesis in the primary mouse mammary and human breast cancer epithelial (MCF-7) cells was recently described [13].

In the current investigation we have characterized the minimal conditions of defined medium necessary for prolactin to stimulate RNA, protein and phosphoprotein synthesis in MCF-7 cells. The role of the polyamine spermidine as a permissive metabolic agent in these processes is evidenced. These results are compatible with our previous findings concerning the relationships the polyamines have to the expression of prolactin's stimulation of casein synthesis in mouse mammary gland explants [14].

Materials and Methods

Materials used in these studies were from the following sources: bovine insulin (lot 9SH35AE, 26.1 USP units/mg), penicillin and streptomycin from Eli Lilly (Indianapolis, IN); hydrocortisone from Pfizer Laboratories (New York, NY); spermidine trihydrochloride from Sigma (St. Louis, MO); Hammersten casein from Nutritional Biochemicals (Cleveland, OH); ovine prolactin (NIH-P-S-12) from the National Institutes of Arthritis and Metabolic Diseases; Porcine growth hormone (P-1120-1) a gift from Dr. Jack Kostyo, University of Michigan, School of Medicine, Department of Physiology (Ann Arbor, MI); Bacto-trypsin from Difco Labs (Detroit, MI); Eagle's minimal essential medium, medium 199 (Earle's salts), Hanks' balanced salts solution, nonessential amino acids, L-glutamine and newborn bovine serum from K.C. Biological (Lenexa, KS); tissue culture plates and flasks from Corning Glass (Corning, NY); and [5,6-^{3}H]uridine (42.0 Ci/mmol), [*methyl*-^{3}3H]thymidine (20.0 Ci/mmol), and L-[4,5(n)-^{3}H]leucine (59.2 Ci/mmol) from New England Nuclear (Boston, MA). The MCF-7 human mammary epithelial cell line was obtained from the Michigan Cancer Foundation (Detroit, MI) and maintained in continuous culture.

The MCF-7 cells were cultured in Eagle's minimal essential medium (E-MEM) supplemented with 2 × nonessential amino acids, L-glutamine (292 mg/l), 10% newborn bovine serum (inactivated), penicillin (100 U/ml), streptomycin (100 μg/ml), and insulin ($1 \cdot 10^{-6}$ M). Cultures in log growth were harvested with 0.25% trypsin in phosphate-buffered saline (pH 7.4). The cells were seeded at a density of $(0.5\text{–}1) \cdot 10^6$ cells/60 mm plate in supplemented Eagle's minimal essential medium (Earle's salts) and incubated at 37°C in a humidified atmosphere of 5% CO_2/95% air. This medium was aspirated and replaced on day 2. On day 4, the medium was removed, the cells were washed with 5 ml Hanks' balanced salts solution per plate (37°C, 30 min) and then incubated for 16–24 h in 5 ml/plate serum and hormone-free medium 199 supplemented with 2 × nonessential amino acids, L-glutamine (292 mg/l), penicillin (100 U/ml) and streptomycin (100 μg/ml), as previously described [10–13].

Experiments concerning hormonal influences on RNA synthesis in MCF-7 cells were performed using the rate of [^{3}H]uridine uptake and incorporation into RNA as a measurement of this parameter. Details of the methods have been previously described [10–13]. Following the depletion period (16–24 h) in serum- and hormone-free medium 199, the cells were incubated in medium 199 containing hormones in the combinations and at the concentrations indicated. A pulse-labeling period with [^{3}H]uridine (1 μCi/ml medium 199) during the final 30 min of incubation was employed. RNA was quantitated by the method of Munro and Fleck [15] and the specific activity of the ^{3}H in the RNA was calculated.

Hormonal influences on protein synthesis were investigated by measuring the rates of [^{3}H]leucine uptake and incorporation into protein. [^{3}H]Leucine (1 μCi/ml) was present in medium 199 for a terminal pulse-labeling period of 1 h. Protein content was quantitated by the method of Lowry et al.

[16], and the specific activity of the ^3H in the protein was determined.

Experiments concerned with hormonal influences on phosphoprotein synthesis in MCF-7 cells were assessed by measuring the rate of cellular [^3H]leucine uptake and incorporation into a phosphoprotein fraction of the cell [17]. The extent of [^3H]leucine incorporation into this phosphoprotein fraction of the cell was measured by a variation of the isoelectric precipitation method of Ashworth [18]. After a terminal 1 h pulse-labeling period with [^3H]leucine (1 μCi/ml medium 199) the cells were washed with 5 ml Hanks' balanced salts solution per plate (0–4°C), overlayed with 1.0 ml homogenization buffer (0.15 M KCl/0.004 M $NaH_2PO_4 \cdot H_2O$/0.1 M imidazole (pH 6.7)) and rapidly frozen in situ. The plates were then thawed, the cells were scraped from the plates, the plates were washed with 3.0 ml homogenization buffer and the combined 4.0 ml were homogenized in a ground glass homogenizer with a motor-driven pestle. A 1.0 ml aliquot of the homogenate was placed in a conical tube and precipitated with 5.0 ml 0.5 M $HClO_4$ (0–4°C) for determination of acid-soluble [^3H]leucine uptake and total DNA content. Methods of DNA extraction and quantitation by the diphenylamine procedure of Burton [19] have been previously described [10–13]. The remaining 3 ml was centrifuged (1000 × *g*, 5 min), and 2.0-ml aliquots of the supernatants were removed for isoelectric precipitation. To each supernatant aliquot, 1 ml of homogenization buffer containing 1 mg/ml bovine casein was added for carrier. To each sample, 17.6 ml distilled H_2O (45°C) was added, followed by 2.5 ml precipitation buffer (25 ml glacial acetic acid, 125 ml 1 M NaOH, 250 ml 95% ethanol, H_2O sufficient to make 1 liter (pH 4.6 ± 0.02)). The samples were mixed, allowed to stand 2–3 h at room temperature, refrigerated overnight, and centrifuged (5000 × *g*, 15 min), the supernatant was decanted, the pellet was dissolved in 2.0 ml 5 M glacial acetic acid, and the radioactivity in a 1.0 ml aliquot was measured by liquid scintillation spectrometry. The ^3H in the isoelectric phosphoprotein precipitate was expressed as dpm of [^3H]leucine incorporated into phosphoprotein per μg cellular DNA per 60 min.

Statistical comparisons were made with the Student's *t*-test when two mean differences were being compared; when more than two means were being compared, the multiple *t*-test was used. Differences were considered significant with $P < 0.05$.

Results

Table I shows the effects of hydrocortisone, spermidine, prolactin and growth hormone in various combinations with insulin, on the rate of [^3H]uridine uptake and incorporation into RNA in MCF-7 cells. The uptake of [^3H]uridine, determined by the quantity of radioactivity in the $HClO_4$-soluble fraction, is not significantly altered by any combination of hormones when tested with insulin. Using the incorporation of [^3H]uridine as a measurement of RNA synthesis, several significant differences are noted. The hydrocortisone enhancement of insulin's action on RNA synthesis, which has been previously demonstrated [11] is evident at the 12 h incubation period. Spermidine, like hydrocortisone, enhances insulin's action on RNA synthesis. The combination of insulin, hydrocortisone, and spermidine was not significantly different from that of insulin and spermidine, suggesting nonadditivity of the hydrocortisone and spermidine enhancements of insulins action on RNA synthesis. Spermidine, like hydrocortisone, had no effect on RNA synthesis when tested without insulin (data not presented). Prolactin by itself, or in combination with insulin, insulin plus hydrocortisone, and insulin plus spermidine, failed to effect any significant increase in the rate of [^3H]uridine incorporation into RNA (data not shown). However, when combined with insulin, hydrocortisone and spermidine, prolactin did significantly increase the rate of [^3H]uridine incorporation into RNA when compared to its control (insulin, hydrocortisone plus spermidine). Growth hormone itself, in combination with insulin, insulin plus hydrocortisone, or insulin plus spermidine, did not influence the rate of [^3H]uridine incorporation into RNA (data not presented). In combination with insulin, hydrocortisone and spermidine, growth hormone also failed to influence the rate of [^3H]uridine incorporation (Table I).

Prolactin at concentrations from 0.1–1000 ng/

TABLE I

EFFECTS OF HYDROCORTISONE, SPERMIDINE, PROLACTIN AND GROWTH HORMONE ON THE RATE OF [^{3}H]URIDINE UPTAKE AND INCORPORATION INTO RNA IN MCF-7 CELLS

MCF-7 cells were exposed to hormones for 12 h at the indicated concentrations: I, insulin ($1 \cdot 10^{-6}$ M); H, hydrocortisone ($1 \cdot 10^{-6}$ M); Spd, spermidine (5 mM); Prl, prolactin (1 µg/ml); and G.H., growth hormone (1 µg/ml). [^{3}H]Uridine (1 µCi/ml) was present during the terminal 0.5 h of incubation. Values given are the mean ± S.E. of five separate culture observations.

Medium (M199+)	$HClO_4$-soluble [^{3}H]uridine (dpm/µg RNA per 30 min)	[^{3}H]Uridine incorporated into RNA (dpm/µg RNA per 30 min)
I	7157 ± 636	1010 ± 43
I, H	6842 ± 173	1152 ± 40 [a]
I, Spd	6646 ± 87	1249 ± 16 [a]
I, H, Spd	6716 ± 302	1294 ± 24
I, H, Spd, Prl	7109 ± 227	1566 ± 5 [b]
I, H, Spd, G.H.	7102 ± 80	1313 ± 37

[a] Greater than I ($P < 0.05$).

[b] Greater than I, H, Spd ($P < 0.05$).

ml elevated the rate of [^{3}H]uridine incorporation into RNA in the MCF-7 cells (Table II), when tested in the presence of insulin, hydrocortisone and spermidine. Over this range, a concentration-response relationship is not apparent, and below 0.1 ng/ml, prolactin is without effect. Concentrations above 1000 ng/ml prolactin do not further increase the rate of [^{3}H]uridine incorporation into RNA.

The effect of spermidine concentration on [^{3}H]uridine incorporation into RNA is demonstrated in Table III. A 5 mM spermidine concentration is optimal for the prolactin stimulation of RNA synthesis, and thus has been employed in prolactin-concentration (Table II) and time-course (Table IV) studies.

The time-course of prolactin stimulation of [^{3}H]uridine incorporation into RNA in MCF-7 cells is shown in Table IV. The [^{3}H]uridine incorporation rates for the control (I, H, Spd) cultures peak at 12–15 h and return to initial levels at 24 h. The prolactin-treated cultures (I, H, Spd, Prl) exhibit a similar pattern, reaching a maximum rate of [^{3}H]uridine incorporation at 12–15 h and returning to the initial levels at 24 h. Further, at 12 and 15 h the rates of [^{3}H]uridine incorporation are significantly elevated in cultures exposed to prolactin. The necessity for both hydrocortisone and spermidine inclusion in the medium is evidenced at the 12 h time period. Cultures containing I, H, Prl and I, Spd, Prl exhibit rates of [^{3}H]uridine incorporation into RNA significantly lower than cultures containing I, H, Spd, ($P < 0.05$).

TABLE II

EFFECT OF PROLACTIN CONCENTRATION ON THE RATE OF [^{3}H]URIDINE INCORPORATION INTO RNA IN MCF-7 CELLS

MCF-7 cells were incubated in medium 199 containing insulin (I, $1 \cdot 10^{-6}$ M), hydrocortisone (H, $1 \cdot 10^{-6}$ M), spermidine (Spd, 5 mM) and prolactin (indicated concentrations) for 12 h with [^{3}H]uridine (1 µCi/ml) present during the terminal 0.5 h. Values in the table represent the mean ± S.E. of five separate culture observations.

Prolactin concn. (ng/ml) added to I, H, Spd	[^{3}H]Uridine incorporated into RNA (dpm/µg RNA per 30 min)
0	1294 ± 24
1000	1566 ± 5 [a]
100	1530 ± 37 [a]
10	1512 ± 15 [a]
1	1407 ± 61 [a]
0.1	1519 ± 45 [a]
0.01	1271 ± 45

[a] Greater than control ($P < 0.05$).

TABLE III

EFFECT OF SPERMIDINE CONCENTRATION ON THE RATE OF [^{3}H]URIDINE INCORPORATION INTO RNA IN MCF-7 CELLS

MCF-7 cells were incubated in medium 199 containing combinations of insulin (I, $1 \cdot 10^{-6}$ M), hydrocortisone (H, $1 \cdot 10^{-6}$ M), prolactin (Prl, 1 µg/ml), and spermidine (indicated concentrations) for 12 h with [^{3}H]uridine (1 µCi/ml) present during the terminal 0.5 h. Values in the table represent the mean ± S.E. of five separate culture observations

Spermidine concn. (mM) added to I, H, Prl	[^{3}H]Uridine incorporated into RNA (dpm/µg RNA per 30 min)
0	1011 ± 25
10	1209 ± 25 [a]
5	1566 ± 5 [a]
1	1438 ± 33 [a]
0.1	1166 ± 77

[a] Greater than control ($P < 0.05$).

TABLE IV

TIME COURSE OF PROLACTIN STIMULATION OF [^{3}H]URIDINE INCORPORATION INTO RNA IN MCF-7 CELLS

MCF-7 cells were incubated in medium 199 containing combinations of: insulin (I, $1\cdot10^{-6}$ M), hydrocortisone (H, $1\cdot10^{-6}$ M), spermidine (Spd, 5 mM), and prolactin (Prl, 100 ng/ml) for the indicated times (h); [^{3}H]uridine (1 μCi/ml) was present during the terminal 0.5 h of incubations. Values in the table represent the mean ± S.E. of five separate culture observations.

Time (h)		[^{3}H]Uridine incorporated into RNA (dpm/μg RNA per 30 min)
0.5	I, H, Spd	994 ± 30
	I, H, Spd, Prl	953 ± 29
3	I, H, Spd	1086 ± 23
	I, H, Spd, Prl	1014 ± 33
6	I, H, Spd	1193 ± 22
	I, H, Spd, Prl	1119 ± 25
9	I, H, Spd	1202 ± 31
	I, H, Spd, Prl	1206 ± 27
12	I, H, Spd	1391 ± 45
	I, H, Spd, Prl	1591 ± 18 [a]
	I, H, Prl	1248 ± 35 [b]
	I, Spd, Prl	1264 ± 23 [b]
15	I, H, Spd	1498 ± 28
	I, H, Spd, Prl	1617 ± 19 [a]
18	I, H, Spd	1320 ± 71
	I, H, Spd, Prl	1368 ± 39
21	I, H, Spd	1063 ± 40
	I, H, Spd, Prl	1108 ± 24
24	I, H, Spd	898 ± 33
	I, H, Spd, Prl	985 ± 27

[a] Greater than I, H, Spd ($P < 0.05$).

[b] Less than I, H, Spd ($P < 0.05$) and I, H, Spd, Prl ($P < 0.01$).

The influences of insulin, hydrocortisone, spermidine and prolactin on [^{3}H]leucine uptake and incorporation into total protein are shown in Table V. As previously demonstrated, insulin stimulates the rate of [^{3}H]leucine incorporation into protein [10], and hydrocortisone enhances insulin's action [11]. Prolactin by itself, combined with insulin, or combined with insulin plus spermidine, failed to increase the rate of [^{3}H]leucine incorporation into protein (data not presented). As shown (Table V), prolactin also failed to increase the rate of [^{3}H]leucine incorporation when combined with insulin and hydrocortisone. Only when combined with insulin, hydrocortisone and spermidine did prolactin stimulate the rate of [^{3}H]leucine incorporation into protein.

The effects of insulin, hydrocortisone, spermidine and prolactin on the rate of [^{3}H]leucine uptake and incorporation into phosphoprotein in MCF-7 cells was studied using the hormones individually and in various combinations. In studies not presented, we found the following: (a) insulin stimulates the rate of [^{3}H]leucine incorporation into the phosphoprotein fraction; (b) hydrocortisone and spermidine individually enhance insulin's action on phosphoprotein synthesis; (c) prolactin, by itself or in combination with insulin, insulin plus hydrocortisone, or insulin plus spermidine, does not significantly elevate the rate of [^{3}H]leucine incorporation into phosphoprotein. Table VI shows the effects of various concentrations of prolactin on the rate of [^{3}H]leucine uptake and incorporation into the isoelectrically precipitable phosphoprotein fraction in MCF-7 cells. Prolactin concentrations between 10 and 1000 ng/ml stimulated the rate of [^{3}H]leucine incorporation into the phosphoprotein fraction. Prolactin concentrations of 1 ng/ml or less had no effect on the rate of phosphoprotein synthesis. A 16 h incubation period was chosen for the concentration studies, after obtaining the results of a series of time-course experiments.

Fig. 1 shows the time-course of the prolactin

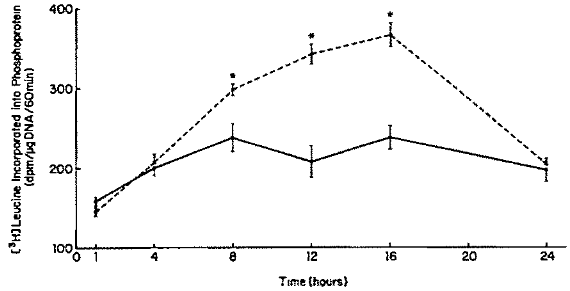

Fig. 1. Time-course of prolactin stimulation of [^{3}H]leucine incorporation into phosphoprotein in MCF-7 cells. MCF-7 cells were incubated in medium 199 containing: I ($1\cdot10^{-6}$ M), H ($1\cdot10^{-6}$ M), Spd (5 mM) (O———O) or I, H, Spd and prolactin (1 μg/ml) (O------O) for the time periods indicated. [^{3}H]Leucine was present during the terminal 1 h of incubation. Values in the figure represent the mean ± S.E. * Greater than control ($P < 0.05$).

TABLE V

[^{3}H]LEUCINE UPTAKE AND INCORPORATION INTO PROTEIN IN MCF-7 CELLS: THE EFFECTS OF INSULIN, HYDROCORTISONE, PROLACTIN AND SPERMIDINE

MCF-7 cells were incubated for 24 h in medium 199 containing combinations of: I, insulin ($1 \cdot 10^{-6}$ M); H, hydrocortisone ($1 \cdot 10^{-6}$ M); Spd, spermidine (5 mM); and Prl, prolactin (1 μg/ml); [^{3}H]leucine (1 μCi/ml) was present during the terminal 1 h of incubation. Values given are the mean ± S.E. of five separate culture observations.

	HCl_3O_2-soluble [^{3}H]leucine (dpm/μg protein per 60 min)	[^{3}H]Leucine incorporated (dpm/μg protein per 60 min)	Total protein (μg/plate)
E-M199	44.1±1.3	24.9±0.8	2009±143
I	44.1±1.2	31.5±1.0 [a]	2422± 88
I, H	48.9±0.8	40.1±1.0 [b]	2658± 52
I, H, Prl	48.3±1.9	42.4±0.7	2654± 96
I, H, Spd	48.8±1.8	37.1±0.7	2724±120
I, H, Spd, Prl	48.7±1.0	47.9±0.7 [c]	2826± 90

[a] Greater than E-M199 ($P < 0.05$).
[b] Greater than I ($P < 0.05$).
[c] Greater than I, H, Spd ($P < 0.05$).

response over a 24 h period. Prolactin elevates the rate of [^{3}H]leucine incorporation into phosphoprotein at 8 h, reaches a maximum at 16 h, and by 24 h the rate returns to control levels. Table VII shows the time-course for the effects of (a) I + H, (b) I + H + Prl, (c) I + H + Spd, and (d) I + H + Spd + Prl on the rates of [^{3}H]leucine incorporation into phosphoprotein, [^{3}H]leucine uptake into the $HClO_4$-soluble fraction, and the total DNA (μg/plate). Clearly, prolactin stimulates the rate of [^{3}H]leucine incorporation into the isoelectrically precipitable phosphoprotein fraction only when spermidine is present in the incubation medium (I, H, Spd, Prl vs. I, H, Spd). Also evident is an increased amount of [^{3}H]leucine present in the $HClO_4$-soluble fraction of the MCF-7 cells exposed to medium containing I, H, Spd vs. I, H. Prolactin did not affect the amount of [^{3}H]leucine present in the $HClO_4$-soluble fraction either in the presence or absence of spermidine. The amount of DNA present in MCF-7 cultures (μg/plate) was not significantly different between groups at each time point, but an increased amount of DNA was present in all groups after 16 and 24 h in culture, as previously reported [10,11,13].

TABLE VI

EFFECT OF PROLACTIN CONCENTRATION ON THE RATE OF [^{3}H]LEUCINE UPTAKE AND INCORPORATION INTO PHOSPHOPROTEIN IN MCF-7 CELLS

MCF-7 cells were incubated for 16 h in medium 199 containing insulin (I, $1 \cdot 10^{-6}$ M), hydrocortisone(H, $1 \cdot 10^{-6}$ M), spermidine (Spd, 5 mM), and prolactin at the concentrations indicated; [^{3}H]leucine (1 μCi/ml) was present during the terminal 1 h of incubation. Values given are the mean ± S.E. of five separate culture observations.

Prolactin concn. (ng/ml) added to I, H, Spd	$HClO_4$-soluble [^{3}H]leucine (dpm/μg DNA per 60 min)	[^{3}H]Leucine incorporated into phosphoprotein (dpm/μg DNA per 60 min)	Total DNA μg/plate
0	664±21	108±4.3	350.4± 8.4
1000	682± 9	140±2.5 [a]	342.4± 4.8
100	642±15	130±2.7 [a]	348.8± 9.6
10	696±16	138±4.2 [a]	328.0± 8.0
1	657±18	118±6.8	349.6± 9.6
0.1	704±20	119±7.6	328.8± 4.8
0.01	697±20	94±5.7	340.8±12.4

[a] Greater than control ($P < 0.05$).

TABLE VII

TIME-COURSE FOR PROLACTIN STIMULATION OF [^{3}H]LEUCINE UPTAKE AND INCORPORATION INTO PHOSPHOPROTEIN IN MCF-7 CELLS

MCF-7 cells were exposed to the hormone combinations indicated: I, insulin ($1 \cdot 10^{-6}$ M), H, hydrocortisone ($1 \cdot 10^{-6}$M), Spd, spermidine (5 mM), Prl, prolactin (1 µg/ml). [^{3}H]Leucine was present during the terminal 1 h of incubation. Values given are the mean ± S.E. of five separate culture observations.

	[^{3}H]Leucine (dpm/µg DNA per 60 min)					
Time (h):	1	4	8	12	16	24
[^{3}H]Leucine incorporation into phosphoprotein						
I, H	153 ± 5.6	194 ± 7.7	226 ± 23.7	183 ± 16.7	176 ± 11.9	186 ± 14.2
I, H, Prl	143 ± 5.1	206 ± 7.6	273 ± 14.4	184 ± 26.8	238 ± 20.6	201 ± 12.8
I, H, Spd	157 ± 5.9	199 ± 9.9	238 ± 17.1	207 ± 21.7	238. ± 15.8	198 ± 14.3
I, H, Spd, Prl	144 ± 4.6	208 ± 12.3	297 ± 7.1[a]	342 ± 12.0[a]	366 ± 13.0[a]	205 ± 7.1
[^{3}H]Leucine $HClO_4$-soluble						
I, H	486 ± 22	578 ± 16	753 ± 26	876 ± 49	689 ± 15	715 ± 8
I, H, Prl	499 ± 20	621 ± 16	850 ± 15	805 ± 14	684 ± 20	726 ± 17
I, H, Spd	507 ± 16	598 ± 10	973 ± 18[b]	1020 ± 17[b]	866 ± 11[b]	1032 ± 6[b]
I, H, Spd, Prl	472 ± 9	678 ± 18	970 ± 69	1047 ± 9	901 ± 11	1041 ± 18
Total DNA (µg/plate)						
I, H	131.6 ± 5.6	131.2 ± 6.8	128.0 ± 4.0	135.6 ± 6.0	164.4 ± 2.0	168.8 ± 2.0
I, H, Prl	130.8 ± 4.8	133.6 ± 1.2	126.4 ± 4.0	136.4 ± 2.8	150.4 ± 2.4	162.0 ± 8.0
I, H, Spd	123.6 ± 4.4	137.6 ± 4.4	131.6 ± 1.2	140.8 ± 4.8	158.0 ± 2.0	166.4 ± 3.2
I, H, Spd, Prl	132.0 ± 4.8	124.0 ± 2.8	128.4 ± 3.6	138.8 ± 2.4	153.6 ± 4.8	162.8 ± 1.6

[a] Greater than I, H, Spd ($P < 0.05$).

[b] Greater than I, H ($P < 0.05$).

Discussion

The role of polyamines in cellular growth and differentiation has been studied in numerous biological systems, The increase in RNA content during cellular growth and reproduction is often paralleled by an increase in spermidine content. This process is proceeded by a marked increase in the activity of the enzyme ornithine decarboxylase and the intracellular concentration of the polyamine putrescine [14,20]. The hormonal regulation of polyamine transport and metabolism in the mouse mammary gland explant system was characterized, and it was also demonstrated that 90% of the spermidine taken up by mammary epithelial cells remains chemically unchanged [21]. The control of polyamine release from growing and serum-deprived cells (BHK-21/C13) suggests that growth arrest is accompanied by a decrease in the cell content and an increase in the release of polyamines from the cells into the culture medium [22]. Moreover, studies on the effects of extracellular serum (at concentrations as low as 0.5%) on the stimulation of ornithine decarboxylase activity and polyamine biosynthesis in normal and transformed cells indicated that intracellular polyamine levels may influence other characteristics of cells in culture, in addition to the functions related strictly to growth [23].

We have demonstrated in this study that when the polyamine spermidine is present in a serum-free defined medium, prolactin stimulates the rates of synthesis of specific macromolecules associated with phosphoprotein formation in mammary epithelial cells. The concentrations of spermidine employed in these studies resulting in the prolactin stimulation of RNA and phosphoprotein synthesis, are in millimolar levels. These concentrations are typical of those in most eukaryotic tissues [20], including the mammary gland [14]. The optimal concentration range of spermidine necessary for prolactin to stimulate the synthesis of these metabolic products is 1–5 mM. This concentration of the polyamine was found in mammary gland explants from mice, when stimulated with the three hormone combination of insulin, hydrocortisone and prolactin [14]. It has furthermore been demonstrated that spermidine cannot substitute for hydrocortisone in the prolactin stimulation of RNA and phosphoprotein synthesis in MCF-7 cells incubated in serum-free defined medium. The necessity for the presence of both hydrocortisone and spermidine for the prolactin stimulation of RNA and phosphoprotein synthesis has been demonstrated. The concentrations of prolactin which stimulate RNA and phosphoprotein synthesis in MCF-7 human mammary epithelial cells are similar to those which stimulate the same activities in mouse mammary gland explants [24]. The hormone specificity of prolactin's actions in the MCF-7 mammary cells has been established by showing that growth hormone has no effect on RNA and phosphoprotein synthesis.

Acknowledgements

This investigation was supported by grant number HD06571 from NICHD.

J.A.R. is the recipient of faculty research award FRA 186 from the American Cancer Society.

References

1 Soule, H.D., Vazquez, J., Long, A. and Brennan, M. (1973) J. Natl. Cancer Inst. 51, 1409–1416
2 Brooks, S.C., Locke, E.R. and Soule, H.D. (1973) J. Biol. Chem. 248, 6251–6253
3 Zava, D.T. and McGuire, W.L. (1977) J. Biol. Chem. 252, 3703–3708
4 Lippman, M.E. and Bolan, G. (1975) Nature 256, 592–593
5 Lippman, M.E., Bolan, G. and Huff, K. (1975) Nature 258, 339–341
6 Horwitz, K.B., Costlow, M.E. and McGuire, W.L. (1975) Steroids 26, 785–795
7 Shafie, S. and Brooks, S.C. (1977) Cancer Res. 37, 792–799
8 Shiu, R.P. (1979) Cancer Res. 39, 4381–4386
9 Monaco, M.E., Bronzert, D.A., Tormey, D.C., Waalkes, P. and Lippman, M.E. (1977) Cancer Res. 37, 749–754
10 Rillema, J.A. and Linebaugh, B E (1977) Biochim. Biophys. Acta 475, 74–80
11 Linebaugh, B.E. and Rillema, J.A. (1977) Mol. Cell. Endocrinol. 7, 335–343
12 Linebaugh, B.E. and Rillema, J.A. (1979) Endocrinology 105, 806–811
13 Linebaugh, B.E. and Rillema, J.A. (1982) Biochim. Biophys Acta 720, 346–355
14 Rillema, J.A., Linebaugh, B.E. and Mulder, J A (1977) Endocrinology 100, 529–536
15 Munro, H.N. and Fleck, A. (1966) Analyst 91, 78–88
16 Lowry, O.H., Rosebrough, N.J., Farr, A.L. and Randall, R.J. (1951) J. Biol. Chem. 193, 265–279
17 Juergens, W.G., Stockdale, F.E., Topper, Y.J. and Elias, J.J. (1965) Proc. Natl. Acad. Sci. U S A. 54, 629–634
18 Ashworth, U.S. (1965) J. Dairy Sci. 48, 537–543
19 Burton, K A. (1956) Biochem. J. 62, 315–323
20 Cohen, S.S. (1977) Cancer Res. 37, 939–942
21 Kano, K. and Oka, T. (1976) J. Biol. Chem 251, 2795–2800
22 Melvin, M.A. and Keir, H.M. (1977) Biochem. Soc. Trans. 5, 711–712
23 O'Brien, T.G., Saladik, D. and Diamond, L. (1980) Biochim. Biophys. Acta 632, 270–283
24 Rillema, J.A., Wing, L.Y.C. and Cameron, C.M. (1981) Horm. Res. 15, 133–140

Biochimica et Biophysica Acta, 804 (1984) 356–360
Elsevier

BBA 11321

GLUTATHIONE DEPLETION INCREASES CHEMILUMINESCENCE EMISSION AND LIPID PEROXIDATION IN THE HEART

RENATA BARSACCHI [a,b], GUALTIERO PELOSI [a], PAOLO CAMICI [a], LUCIANO BONALDO [c], MATILDE MAIORINO [c] and FULVIO URSINI [c,*]

[a] *C.N.R. Institute of Clinical Physiology, Pisa,* [b] *Institute of Biological Chemistry, University of Pisa, Pisa and* [c] *Institute of Biological Chemistry, University of Padova, Via F. Marzolo 3, 35131 Padova (Italy)*

(Received December 1st, 1983)

Key words: Glutathione depletion; Chemiluminescence, Lipid peroxidation; (Rat heart)

Diamide, CDNB and phorone were used to deplete glutathione in retrogradely perfused rat hearts. Following glutathione depletion the spontaneous chemiluminescence increased by 70%, irrespective of the agent used. The glutathione depletion and the chemiluminescence emission were associated to an increase of malondialdehyde content in the heart, as determined by HPLC. Under these conditions the heart function was impaired and histological examination showed a coagulative myocytolysis, a pattern already described in human and experimental pathology, where a key role is attributed to a Ca^{2+} homeostasis impairment.

Introduction

The role of lipid peroxidation in the pathogenesis of the ischemic damage of heart membranes has been recently postulated [1]. Moreover, some antioxidants seem to exert a protective effect against myocardial damage following post-ischemic reoxygenation [1,2]. In a recent paper [3] we have investigated the effect of an oxidative stress, induced by the infusion of hydroperoxides, on the perfused rat heart function, taking advantage of the very sensitive technique of organ chemiluminescence detection to monitor the oxidative radical reactions. The oxidative stress caused morphological and functional changes resembling those of the so called ‘stone heart’, a pathological feature probably related to a sudden impairement of intracellular Ca^{2+} regulation [4,5].

However, since the infused hydroperoxides may act both as peroxidation sparkers and glutathione depletors, in the present work we sought to evaluate more specifically the role of glutathione depletion on chemiluminescence emission, lipid peroxidation and morphological and functional alterations of the heart.

Part of this work has been previously presented in abstract form [27].

Materials and Methods

Rat hearts were perfused retrogradely according to the method of Langendorff, and the chemiluminescence emission was recorded as previously described [3]. The GSH depletors were added to the Krebs-Henseleit buffer gassed with 95% O_2/5% CO_2 or, in some experiments, with 95% N_2/5% CO_2. The perfusion with GSH depletors started after a 20 min equilibration period with the Krebs-Henseleit buffer alone. The GSH depletors used were: 0.2–0.8 mM diamide, 0.1–0.5 mM CDNB and 1–5 mM phorone [6]. The electrocardiogram was continuously monitored by an epicardial electrode. The GSH and GSSG content of the hearts was determined by an HPLC procedure [7], following derivatization with iodoacetate and

---

[*] To whom correspondence should be addressed.
Abbreviation: CDNB: 1-chloro-2,4-dinitrobenzene.

0167-4889/84/$03.00 © 1984 Elsevier Science Publishers B.V.

1-fluoro-2,4-dinitrobenzene. The results were expressed as μmoles of GSH or GSSG per gram of fresh tissue. An HPLC method for the determination of malondialdehyde as thiobarbituric acid-reactive material in tissues has been reported [8]. We have modified this procedure in two respects: (1) an antioxidant (butylated hydroxytoluene) was included in the homogenization and reaction media to prevent further peroxidation; (2) esansulfonic acid was used as counter ion in the HPLC elution mixture, since it appeared to improve the resolution by increasing the affinity of the malondialdehyde-thiobarbituric acid chromogen for the stationary phase. In this way the retention time could be modulated by the gradient and the overlapping of the peak with those of 535 nm-absorbing contaminants was avoided. The hearts were homogenized with a Polytron apparatus in 5 ml of 180 mM KCl/10 mM EDTA/50 mM Tris buffer containing 0.02% butylated hydroxytoluene. 2 ml of the homogenate were added to a mixture of 0.67% thiobarbituric acid (2 ml)/20% trichloroacetic acid (5 ml)/10% butylated hydroxytoluene in ethanol (0.1 ml). After boiling for 15 min the mixture was centrifugated at 3000 × *g* for 10 min. 1 ml of the supernatant was then extracted with 1 vol. of *n*-butanol, and the organic phase was evaporated under a N_2 stream using a plate warmed at 60°C. The residue was then resuspended in a small volume of HPLC solvent A (described below) and injected. The column used as an Ultrashere ODS (Beckman Co., Berkeley, CA). The detection was carried out at 535 nm using a Beckman Mod. 165 detector. The chromatographic mobile phase consisted of 10 mM esansulfonic acid (pH 3), as solvent A, and methanol as solvent B. The percentage of B rised from 20 to 70% within 15 min and the flow rate was 0.7 ml/min. The quantitation was carried out against a standard curve obtained using malondialdehyde tetraethylacetal as a generator of malondialdehyde. The results were expressed as nmol of malondialdehyde per mg of homogenate protein. The protein concentration was evaluated by the biuret method [9]. After 20 min perfusion with GSH depletors, some hearts were processed for conventional light microscopy, using hematoxilin-eosin staining. All reagents were of analytical grade.

Results

The glutathione content of isolated perfused rat hearts was lowered by adding diamide, CDNB or phorone to the perfusion medium (Fig. 1). The concentrations of diamide and CDNB used were the minimal necessary to obtain the complete disappearance of GSH within 5 min. This was never obtained with phorone, even when its concentration was 5 mM. Diamide, which is a typical thiol oxidant, induced an early increase of GSSG followed by a decrease apparently related to losses through the sarcolemma. Such GSSG increase did not occur with CDNB or phorone, which enzymatically couple with GSH [6]. GSSG disappeared much more slowly than GSH. It is worth

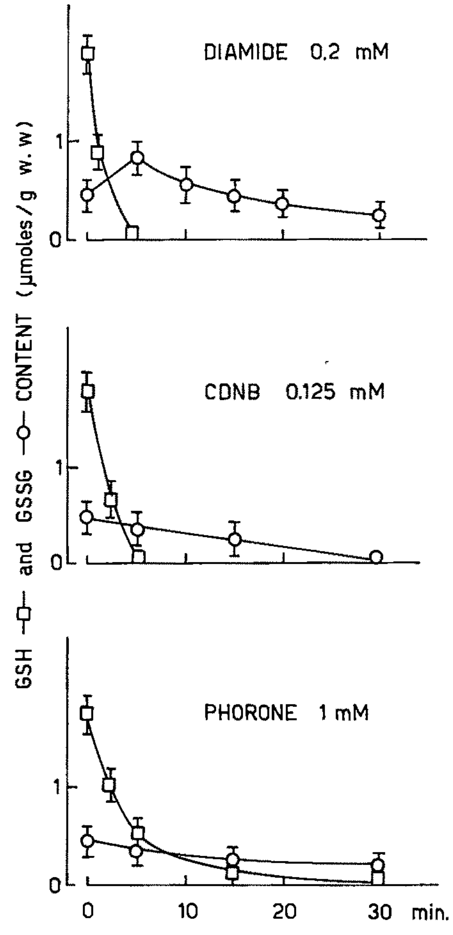

Fig. 1. GSH and GSSG content of rat hearts perfused with GSH depletors. The means and the S.D. of three independent determinations are reported.

noting that if the perfusion was continued in the absence of depletors after the complete disappearance of GSH, GSSG slowly reappeared, suggesting that resynthesis can take place and that GSH is immediately oxidized (data not shown).

The chemiluminescence emission progressively increased following perfusion with glutathione depletors, and reached a maximum 70% higher than the basal level (Fig. 2). The extent of the increase of chemiluminescence was the same, irrespective of the depletor used. A plateau was reached when the concentration of GSH in the heart was reduced practically to nil. The slope of the increase of chemiluminescence emission was roughly proportional to the concentration of the depletor. When the glutathione depletors were added to a perfusion medium where N_2 was substituted for O_2 the chemiluminescence increase did not occur, and when O_2 was readmitted a burst of chemiluminescence took place followed by a plateau 70% above the basal level (results not shown). The chemiluminescence remained high also in experiments where the perfusion was continued for variable times without the depletor after the complete disappearance of GSH. The malondialdehyde content of the hearts following perfusion with CDNB is reported in Fig. 3. It is worth noting that the lag phase of malondialdehyde production was shorter than the time required for the complete disappearance of GSH (cf. Fig. 1), indicating that also a partial GSH depletion may induce the onset of lipid peroxidation.

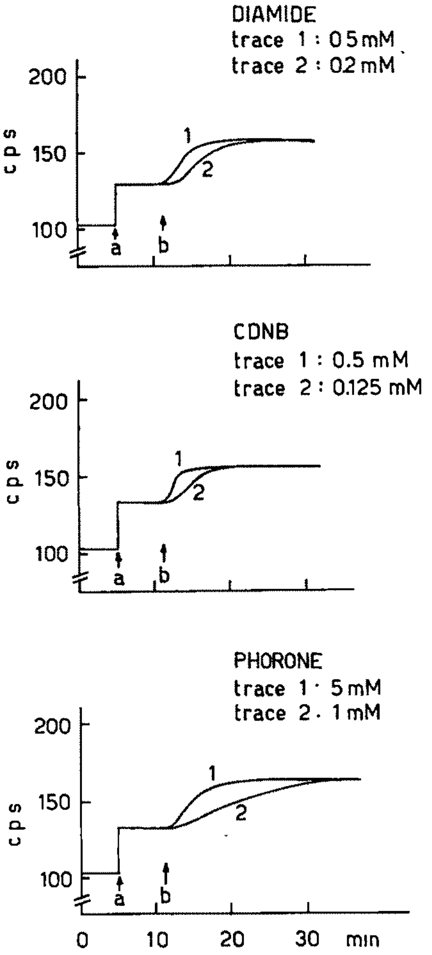

Fig 2. Chemiluminescence of rat hearts upon perfusion with GSH depletors At time *a* the shutter in front to the photomultiplyer was opened; at time *b* the perfusion with GSH depletors started.

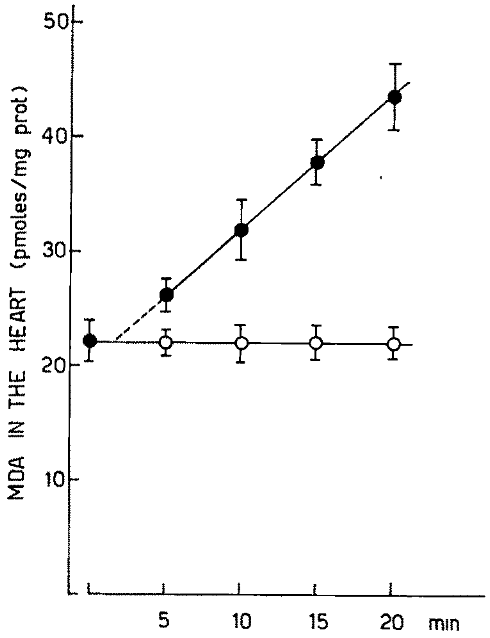

Fig. 3. Malondialdehyde content of rat hearts perfused with 0.125 mM CDNB (●) and control hearts (○). The means and the S D of five independent determinations are reported.

The heart function was strongly affected by GSH depletors. The functional impairement was similar to that observed after perfusion with hydroperoxides, though less dramatic. The heart rate progressively declined and the heart stopped after 30 min. Macroscopically evident hypercontracture was present after 30 min. The histological examination carried out after 20 min of perfusion showed a contraction band necrosis (coagulative myocytolysis) involving 50% of the tissue, identical to that reported for hydroperoxide perfusion [3], which constitutes the typical hystological finding of the 'stone heart' [5].

Discussion

The role of GSH as a factor in the multilevel protection system against free radical damage of biomembranes is well established. GSH plays a protective role in radiation and oxygen toxicity [10], as a substrate for peroxidases [11–13], and it was postulated to increase the antioxidant activity of vitamin E [14]. Moreover, the GSH depletion leads to lipid peroxidation in isolated hepatocytes and in homogenates [15,16].

We show in this paper that the chemiluminescence emission of the perfused rat heart is increased following perfusion with GSH depletors. A direct effect of these agents on chemiluminescence emission should be excluded, since (i) similar increases were observed with different GSH depletors, and (ii) the high chemiluminescence emission did not require the continuous presence of the depletor as shown inexperiments where, after an initial perfusion with these agents, the perfusion was continued with depletor-free media. Moreover, the chemiluminescence emission depends on the aerobic metabolism [10], as confirmed here by the decrease following the substitution of N_2 for O_2 in the perfusion medium. The relationship between the formation of chemiluminescent species and the process of lipid peroxidation was well established and discussed by Boveris et al. [17] and Cadenas et al. [18]. Chemiluminescence of intact organs or isolated cells involves photoemissive reactions of species which are formed in essential steps of lipid peroxidation, in particular dimol emission of singlet oxygen generated by the reaction of peroxy radicals and the emission of excited carbonyl groups. In the present work, photon emission from the perfused heart was too low to allow spectral identification of photoemissive species. However, their being identical to those involved in lipid peroxidation was established by the detection of lipid peroxidation products through a highly sensitive and specific HPLC analysis of the thiobarbituric acid-malondialdehyde chromogen. The increased chemiluminescence emission and the conocmitant malondialdehyde production upon GSH depletion indicate that this condition leads to an imbalance between the peroxidation-sparking reactions and the antioxidant capacity of the cells. The constant level of malondialdehyde in the control heart, in front to the continuous chemiluminescence emission, may indicate that the amount of lipid peroxides in the cells represents a steady state between formation and degradation and that the GSH depletion alters this steady state.

A functional derangement of the heart follows GSH depletion: the hystological examination shows a contraction band necrosis identical to that observed upon perfusion with hydroperoxides. This contraction band necrosis represents the morphological counterpart of the damage following post-ischemic reoxygenation, where a sudden increase of the cytosolic Ca^{2+} is supposed to play a key role [5]. Therefore, a complex relationship between GSH levels, lipid peroxidation and Ca^{2+} regulation can be envisaged from the above experiments and from the following results reported by other authors:

(a) the GSH depletion of liver cells is associated with lipid peroxidation [15,16];
(b) the GSH depletion is associated with morphological changes (bleb formation) in the hepatocyte membranes [19], and this fact was related to altered Ca^{2+} levels in the cytosceletal environment;
(c) bleb formation takes place in isolated myocytes following incubation in the presence of cumene hydroperoxide or diamide [20];
(d) the lipid peroxidation alters the cation permeability through lipid bilayers [21];
(e) GSH oxidation and the consequent high $NAD(P)^+/NAD(P)H$ ratio stimulates Ca^{2+} efflux in liver mitochondria [22,23];
(f) the oxidative stress inhibits the ATP-dependent Ca^{2+} uptake by rat liver microsomes [24];
(g) lipid peroxidation inhibits the Ca^{2+} uptake from sarcoplasmic reticulum [25].

Finally, in the light of these observations, also the evidence that ischemia depletes the GSH of the heart [26] is in agreement with the hypothesis that the 'stone heart', consequent to the post-ischemic reoxygenation damage, can be due to an impairment of regulation of the endocellular Ca^{2+} caused by lipid peroxidation.

Acknowledgments

The Authors wish to thank Professor C. Gregolin for helpful discussion and revision of the manuscript, and drs. U. Bottigli, R. Bellina and A. Benassi for setting up the electronic equipment and the computer programs.

References

1 Meerson, F.Z., Kagan, V.E., Kozlov, Yu P., Belinka, L.M. and Arkhipenko, Yu.V. (1982) Basic Res Cardiol. 77, 465–485

2 Guarnieri, C., Ferrari, R., Visioli, O , Caldarera, C.M. and Nayler, W.G. (1978) J. Mol. Cell. Cardiol 10, 893–906

3 Barsacchi, R., Camici, P., Bottigli, V., Salvadori, P A., Pelosi, G., Maiorino, M. and Ursini, F. (1983) Biochim. Biophys. Acta 762, 241–247

4 Baroldi, G , Milam, I.D., Wukasch, D.C., Sandiford, F.M., Romagnoli, A. and Cooley, D.A. (1974) J Mol. Cell. Cardiol. 6, 395–399

5 Ganote, C.E. (1983) J. Mol. Cell Cardiol. 15, 67–73

6 Plummer, J.L., Smith, B.R., Sies, H. and Bend, J.R. (1981) Methods Enzymol. 77, 50–59

7 Reed, C.J., Babson, J.R , Beatty, P.W., Brodie, A E., Ellis, W.W. and Potter, D.W. (1980) Anal. Biochem. 106, 55–62

8 Bird, R.P., Hung, S.O., Hadley, M and Draper, H.H. (1983) Anal. Biochem 128, 240–244

9 Gornall, A.G., Bardawill, C.J and David, M.M. (1949) J Biol. Chem. 177, 751–760

10 Meister, A. and Anderson, M.E. (1983) Annu. Rev. Biochem. 52, 711–760

11 Little, C. and O'Brien, P.I. (1968) Biochem. Biophys. Res. Commun. 31, 145–150

12 Ursini, F., Maiorino, M., Valente, M., Ferri, L. and Gregolin, C (1982) Biochim. Biophys. Acta 710, 197–211

13 Maiorino, M., Ursini, F., Leonelli, M., Finato, N. and Gregolin, C. (1982) Biochem. Int. 5, 575–583

14 Pryor, W.A (1976) in Free Radicals in Biology, Vol. I (Pryor, W.A., ed.), pp. 1–49, Academic Press, New York.

15 Stacey, N. and Priestly, B G (1978) Toxicol. Appl Pharmacol. 45, 41–46

16 Younes, M and Sierges, C.P. (1980) Res. Commun. Chem. Phatol. Pharmacol. 27, 119–124

17 Boveris, A , Cadenas, E , Reiter, R., Filipkowski, M., Nakase, Y. and Chance, B. (1980) Proc. Natl. Acad. Sci USA 77, 347–351

18 Cadenas, E., Wefers, H. and Sies, H. (1981) Eur. J. Biochem. 119, 531–536

19 Jewell, J.A , Bellomo, G., Thor, H., Orrenius, S. and Smith, M T. (1982) Science 217, 1257–1279

20 Noronha-Dutra, A.A. and Steen, E.M. (1982) Lab. Invest. 47, 346–353

21 Lebedev, A.V., Levitsky, D.O. and Loginov, V.A. (1983) in 'Advances in Myocardiology (Charof, E., Sminof, V and Dhalla, N.S., eds.), Vol. III, pp. 425–438, Plenum Medical Book Co., New York

22 Lotschen, H.R., Winterhalter, K., Carafoli, E. and Richter, C. (1980) J. Biol. Chem. 255, 9325–9330

23 Moore, G.A., Jewell, S.A., Bellomo, G. and Orrenius, S. (1983)FEBS Lett. 153, 289–292

24 Jones, D.P., Thor, H., Smith, M.T., Jewell, S.A. and Orrenius, S. (1983) J. Biol. Chem. 258, 6390–6393

25 Player, T J. and Hultin, H.O. (1978) Biochem. J. 174, 17–22

26 Guarnieri, C., Flamigni, F. and Rossoni-Caldarera, C. (1979) Biochem Biophys. Res. Comm. 89, 678–684

27 Barsacchi, R. (1983) Third International Conference on Oxygen Radicals in Chemistry and Biology, Munchen (F.R.G.), July 10–15, 1983, Abs. P. 65

Biochimica et Biophysica Acta, 804 (1984) 361–369
Elsevier

BBA 11316

ISOLATION OF A STORAGE AND SECRETORY ORGANELLE CONTAINING VON WILLEBRAND PROTEIN FROM CULTURED HUMAN ENDOTHELIAL CELLS

JAN HENDRIK REINDERS, PHILIP G. DE GROOT, MERVIN D. GONSALVES, JOKE ZANDBERGEN, CORNELIA LOESBERG and JAN A. VAN MOURIK

Central Laboratory of the Netherlands Red Cross Blood Transfusion Service, P.O. Box 9190, 1006 AD Amsterdam (The Netherlands)

(Received January 20th, 1984)

Key words: Von Willebrand factor; Secretory organelle, (Human endothelium)

Von Willebrand protein was synthesized and secreted by human endothelial cells in culture. Ca^{2+} ionophore A23187 and phorbol myristate acetate stimulated the release of Von Willebrand protein from the cultured cells. Stimulated release was accompanied by the disappearance of rod-like structures from the cultured endothelial cells immunostained for Von Willebrand protein, suggesting the existence of a storage organelle for Von Willebrand protein in these cells (Loesberg, C., Gonsalves, M.D., Zandbergen, J., Willems, C., Van Aken, W.G., Stel, H.V., Van Mourik, J.A. and De Groot, P.G. (1983) Biochim. Biophys. Acta 763, 160–168). Cultured human endothelial cells were fractionated on a density gradient of colloidal silica. Von Willebrand protein was found in two organelle populations: a buoyant one sedimenting with a variety of cell organelle marker enzymes, including those of the Golgi apparatus, mitochondria, lysosomes, peroxisomes, endoplasmic reticulum and plasma membrane fragments (peak density of this fraction: 1.08 $g \cdot ml^{-1}$), and a dense one with a peak density of 1.12 $g \cdot ml^{-1}$. The dense organelles containing Von Willebrand protein were apparently free of other organelles. Stimulating Von Willebrand protein release with phorbol myristate acetate or Ca^{2+} ionophore A23187 resulted in a decrease or even complete disappearance of Von Willebrand protein from the high-density organelle fraction, implying a role of this organelle in the stimulus-induced release of Von Willebrand protein. The Von Willebrand protein content of the buoyant fraction was lowered to some extent or did not change upon incubation of the cells with ionophore A23187 and phorbol myristate acetate. Restoration of Von Willebrand protein content of the dense organelle fraction after stimulation occurred within 2 days; this was accompanied by recurrence of immunostaining of rod-shaped structures in cells and an increase in cellular Von Willebrand protein. The excretion of restored Von Willebrand protein could be stimulated again.

Introduction

Von Willebrand protein is the moiety of the plasma protein factor VIII-Von Willebrand factor complex (reviewed in Refs. 1 and 2) that has a key role in the adhesion of platelets to subendothelium after micro-vascular injury [3,4]. The bleeding disorder Von Willebrand disease is a result of absence of, or defect in, Von Willebrand protein.

Vascular endothelial cells [5] and megakaryocytes [6] synthesize Von Willebrand protein. Cultured human endothelial cells enable the in vitro study of Von Willebrand protein biosynthesis [5,7–9]. The excretion of Von Willebrand protein from cultured human endothelial cells is a continuous process. Besides this basal secretion, transient extra release of cellular stored Von Willebrand protein can be provoked by a variety of stimulants like thrombin [10,11], Ca^{2+} ionophore A23187 and phorbol myristate acetate [11]. The

---

Abbreviation: PMA, phorbol myristate acetate.

0167-4889/84/$03.00 © 1984 Elsevier Science Publishers B.V.

stimulated Von Willebrand protein release depends on the presence of extracellular Ca^{2+} ions [11]. Immunofluorescence studies with cultured endothelial cells stained for Von Willebrand protein show that part of the cellular Von Willebrand protein is localized in rod-shaped structures [9], which disappear upon stimulation [11]. Immunoelectron microscopy studies suggested that these rod-shaped structures are identical with Weibel Palade bodies [9], endothelial cell-specific organelles of unknown function [12].

So far, the presence of Von Willebrand protein in subcellular compartments of endothelial cells was demonstrated by immunohistochemical techniques. In this study, we describe the isolation of an organelle containing Von Willebrand protein by colloidal silica density gradient centrifugation. This isolated organelle might function in the endothelial cell as a storage pool for Von Willebrand protein and is involved in the stimulus-induced Von Willebrand protein release.

Part of the results described here have been presented at the IXth International Congress on Thrombosis and Haemostasis, Stockholm, July 1983 and appeared abstracted in Ref. 31.

Methods

(1) Cell culture

Endothelial cells were isolated from human umbilical cord vein according to the isolation method originally described by Jaffe et al. [7], with some modifications [13]. The cells were identified as endothelial cells by their typical characteristics [7]. Cells were cultured in plastic flasks precoated with fibronectin or on glass coverslips coated with glutardialdehyde-fixed gelatin. Culture medium consisted of an equal mixture of RPMI 1640 and Medium 199 (both from Gibco, Paisley, U.K.), 20% human serum (pool of 24 healthy male donors), 2 mM glutamin and the antibiotics penicillin (100 units · ml^{-1}), streptomycin (100 $\mu g \cdot ml^{-1}$) and amphotericin B (5 $\mu g \cdot ml^{-1}$) (Gibco). When human serum had to be omitted from the medium, 1% human serum albumin, insulin from bovine pancreas (10 $\mu g \cdot ml^{-1}$, Sigma, St. Louis, MO) and human transferrin (20 $\mu g \cdot ml^{-1}$, Sigma) were added instead [14] to this serum free medium. Cells were used in experiments after the third passage when the culture had reached confluency.

(2) Cell fractionation

(2.1) Harvesting of the cells. Cells were harvested with trypsin/EDTA (Gibco) after rinsing the monolayer of cells gently with phosphate-buffered saline (150 mM NaCl/10 mM sodium phosphate buffer (pH 7.4)). Immediately after all cells had detached, as judged by microscopy, 3 vol. of ice-cold 20 mM Tris-HCl (pH 7.4)/0.2 M sucrose/1 mM EDTA/0.2 mg · ml^{-1} soybean trypsin inhibitor (Sigma) were added. The culture flask was rinsed with another 3 vol. of this buffer. The combined cell suspension was centrifuged for 10 min at 900 × *g*, the pellet was resuspended in the same buffer, but without soybean trypsin inhibitor.

(2.2) Cell homogenate. 5 ml of cell suspension was homogenized at 4°C in a 10 ml potter; pestle speed at 100 rpm and 20 strokes.

(2.3) Fractionation of cell homogenate on a colloidal silica density gradient was performed essentially as described elsewhere [15–17]. A 38 ml centrifuge tube was filled with a 2 ml cushion of 2.5 M sucrose, 24 ml of the colloidal silica material and 4 ml of cell homogenate, which was carefully layered on top. The colloidal silica material was 7% Ludox HS40 (a generous gift from Du Pont et de Nemours, Wilmington, U.S.A.), supplemented with 5% polyvinylpyrrolidone K30 (Fluka, Buchs, Switzerland) and 0.25 M sucrose. The pH was adjusted carefully to 7.2 with approx. 2 ml 1 M HCl per 500 ml gradient material. The material was subsequently filtered over a Schleicher & Schüll paper filter No. 595 1/2.

The self-generating density gradient of the colloidal silica material was allowed to adjust itself for 75 min at 100000 × *g* at 4°C (Sorvall 625 angle rotor, Kontron ultracentrifuge). 1-ml fractions were collected and frozen until analysis. For microscopy, gradient fractions were diluted, and organelles were spun down by centrifugation for 15 min at 4000 × *g* on slides for microscopy. Density of gradient fractions was assessed by weighing.

(3)Enzymes and Von Willebrand protein

Lactate dehydrogenase and malate dehydrogenase were measured according to Bermeyer and Bernt [18]. Pyruvate, malate and β-NADH were from Boehringer, Mannheim (F.R.G.)

β-Hexosaminidase was assayed as described by de Groot et al. [19]; substrate *p*-nitrophenyl-2-acetamido-2-deoxy-β-D-glucopyranoside was from Koch-Light (Colnbrook, U.K.). UDPgalactosyltransferase and 5′-nucleosidase were assayed as described by Brew et al. [20] and Avruch and Hoelzl Wallach [21], respectively; UDP[^{14}C]galactosyl and [^{3}H]adeninemonophosphate were from Amersham International, Amersham, U.K. NADPH-cytochrome *c* reductase and catalase were assayed according to the method of Phillips and Langdon [22] and Meerhof and Roos [23], respectively. Protein was estimated according to Bradford [24], with human albumin as standard.

Von Willebrand protein was determined by an immunoradiometric assay as factor-VIII-related antigen, essentially following the method described by Ruggeri et al. [25]; instead of purified polyclonal IgG monoclonal antibodies [26] CLB-Rag-21, CLB-Rag-35 and CLB-Rag-201 were used as indicator antibodies. Polyclonal rabbit-Rag antibodies serves as the solid phase. Pooled normal plasma served as standard. The lower detection limit of this Von Willebrand protein assay was to 10^{-4} units · ml^{-1}. 1 unit of Von Willebrand protein is the amount present in 1 ml pooled normal plasma (approx. 20 μg · ml^{-1}).

(4) Immunofluorescence

Cells were extensively washed with phosphate-buffered saline (Methods, section 2.1) and fixed with methanol for 15 min at room temperature, incubated with murine monoclonal antibody CLB-Rag-1 against human Von Willebrand protein [26] and subsequently incubated with FITC-labeled goat anti-mouse IgG. Preparations were embedded in 10% glycerol.

(5) Miscellaneous

Ca^{2+} ionophore A23187 (Boehringer, Mannheim, F.R.G.) and 4-β-phorbol 12-myristate 13-monoacetate (Sigma) were dissolved in dimethylsulfoxide (Merck, Darmstadt, F.R.G.). Dimethylsulfoxide concentration in the medium did not exceed 0.1% (v/v).

Results

(1) Isolation of an organelle containing Von Willebrand protein

(1.1) Latency of Von Willebrand protein in cultured endothelial cells. In Fig. 1., sedimentability of Von Willebrand protein, lactate dehydrogenase and β-hexosaminidase is given. Endothelial cells were homogenized in a Potter-Elvejhem; cells were broken up readily under these conditions, since most of the lactate dehydrogenase – a cytosolic marker – was relased after a few strokes with the Potter-Elvejhem homogenizer. Von Willebrand protein and β-hexosaminidase – a lysosomal marker – could be sedimented, except for a minor part, which was released gradually during pottering. This indicates that in endothelial cells, Von Willebrand protein was present in organelle-like structures.

(1.2) Density gradient fractionation of endothelial cell homogenate. On a colloidal silica density gradient, endothelial cell homogenate was found to contain two distinct populations of cell constituents containing Von Willebrand protein (Fig. 2A). One population of cell particles with Von Willebrand protein sedimented to high density in

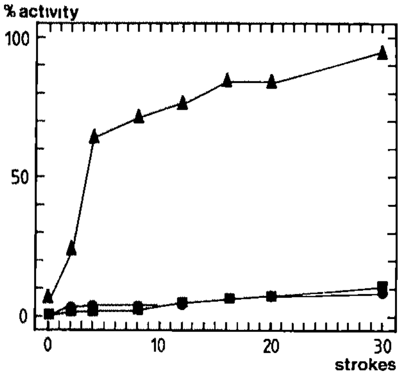

Fig. 1. Sedimentability of Von Willebrand protein (■——■), β-hexosaminidase (●——●) and lactate dehydrogenase (▲——▲) in cultured human endothelial cells. Cell suspension was homogenized in a Potter-Elvejhem instrument, aliquots of the homogenate were withdrawn and centrifuged for 5 min at 8000 × g. Supernatants were assayed for Von Willebrand protein, β-hexosaminidase and lactate dehydrogenase; percentage of total activity liberated from cell structures was determinated. Data represent the mean of two experiments, two determinations per experiment.

the colloidal silica gradient; they had a density ranging from 1.11 to 1.18 g · ml^{-1} with the peak at approx. 1.12 g · ml^{-1}. No substantial activity of other known organelle marker enzymes could be found at this density. Also, the protein concentration was below the detection limit (Fig. 2B). Von Willebrand protein contents in the high-density particles accounted for 20–65% of the total amount of Von Willebrand protein recovered from the gradient (Table I). The second Von Willebrand protein containing population of cell constituents was present at a peak density of 1.08 g · ml^{-1}. In contrast to the dense fraction, this buoyant fraction with Von Willebrand protein contained enzyme activities for mitochrondria (malate dehydrogenase), lysosomes (β-hexosaminidase), endoplasmic reticulum fragments or microsomes (NADPH-cytochrome *c* reductase), the Golgi apparatus (UDPgalactosyltransferase), plasma membrane fragments (5′-nucleosidase), peroxisomes (catalase), DNA from nuclei (ethidium bromide fluorescence, results not shown) and considerable amounts of protein (Fig. 2). Lactate dehydrogenase, marker of the soluble cell constituents or cytoplasma, stayed in the top fractions. Considerable amounts of the cell protein and 5–20% of the Von Willebrand protein (Table I) were also recovered from the soluble fraction (Fig. 2). A minor part of soluble marker enzymes from disrupted organelles was also found in the top fractions.

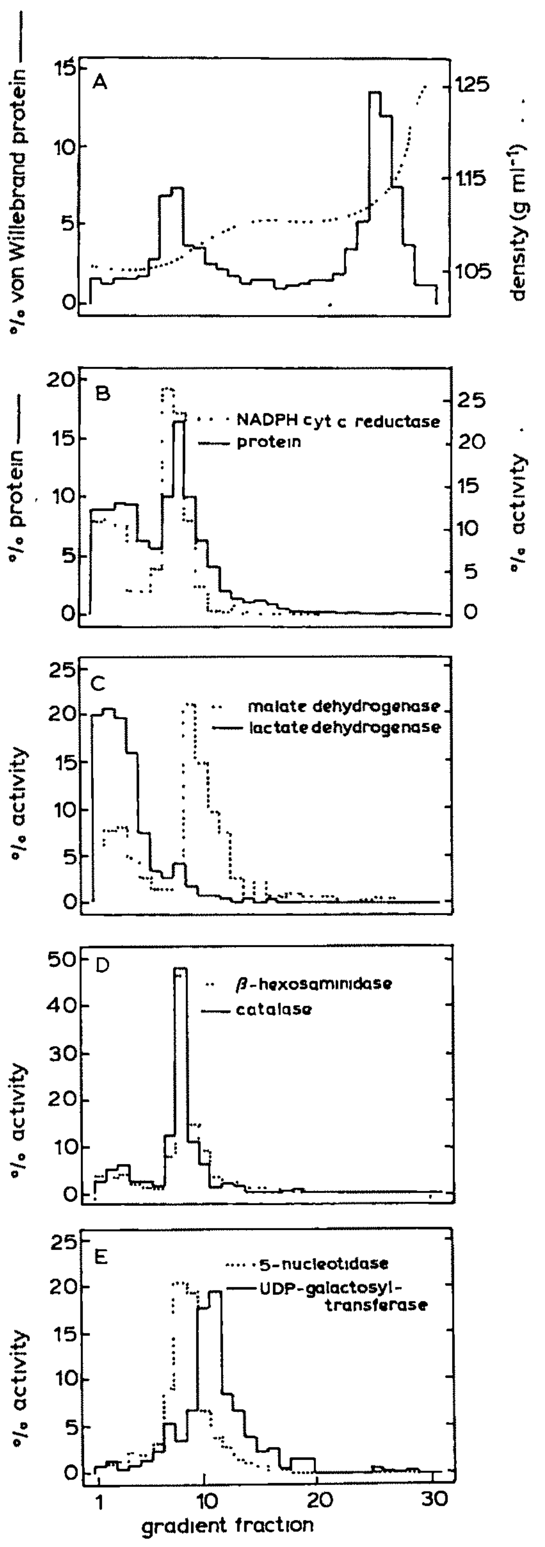

Fig. 2. Von Willebrand protein and cell-organelle markers in fractionated endothelial cell homogenate. Fractionation was on a density gradient of colloidal silica. (A) Von Willebrand protein (———) in gradient fractions and density (- - - - -) of colloidal silica after centrifugation. (B) Protein (———) determined according to Bradford [22] and NADPH-cytochrome *c* reductase (- - - - -) (microsomes, endoplasmic reticulum). (C) Lactate dehydrogenase (———) (cytosol) and malate dehydrogenase (- - - - -) (mitochrondria and cytosol). (D) Catalase (———) (peroxisomes) and β-hexosaminidase (- - - - -) (lysosomes). (E) UDP-galactosyltransferase (———) (Golgi apparatus) and 5′-necleotidase (- - - - -) (plasma membrane). Von Willebrand protein and marker enzyme activity are presented as percentage of total activity recovered from the colloidal silica gradient. Recoveries from gradients were within 70 to 130% of applied cell homogenate; interference of gradient material was corrected for. The marker-enzyme profiles were typical for at least three experiments; the ones shown here were not from the same run.

TABLE I

DISTRIBUTION OF VON WILLEBRAND PROTEIN IN ENDOTHELIAL CELL HOMOGENATE FRACTIONATED ON A COLLOIDAL SILICA DENSITY GRADIENT

Von Willebrand protein distribution is given as percentage of total amount recovered from the gradient. Recovery was 70–90% of the amount applied on the gradient. The soluble fractions were defined as those fractions containing more than 95% of the lactate dehydrogenase activity and having a density lower than 1.06 g·ml^{-1}; the buoyant fractions with cell organelles had a density around 1.08 g·ml^{-1}, and the high-density organelle fractions sedimented to a peak density around 1.12 g·ml^{-1} (see also Fig. 2A).

Experiment	Von Willebrand protein (%)		
	Soluble fraction	Buoyant fraction	Dense fraction
1	17.5	50.1	32.4
	16.0	51.3	32.7
2	12.7	72.9	14.4
	8.9	66.2	24.9
3	2.6	35.7	61.7
4	16.3	37.9	45.8
5	13.5	41.6	44.9
6	11.5	22.7	65.8
7	15.2	31.4	53.4
8	18.2	32.7	49.1
9	5.7	51.7	42.6
10	7.0	49.1	43.9
11	6.6	67.7	25.7
12	13.4	71.7	14.9
13	10.7	40.7	48.6
14	8.4	34.8	56.8
15	6.7	59.5	33.8
16	3.6	26.3	70.1
17	11.0	49.1	39.9

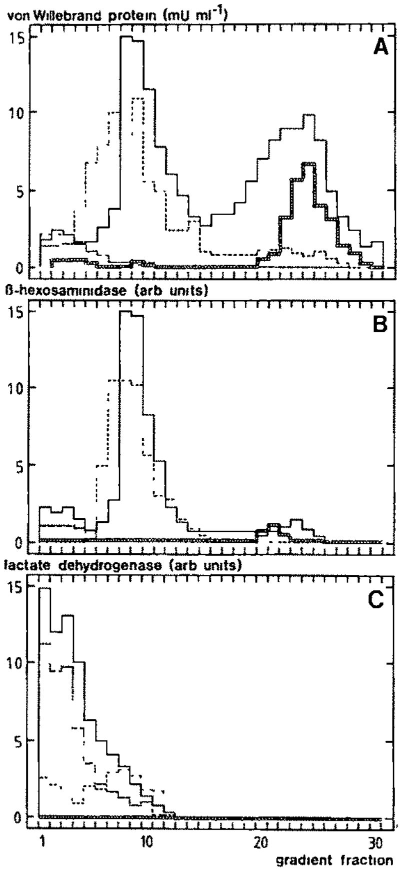

Fig. 3. Recentrifugation of buoyant and dense particles with Von Willebrand protein obtained with a colloidal density gradient. Fractions indicated were pooled, diluted 1 : 1 with homogenizing buffer (Methods 2.1), applied on fresh colloidal silica material and centrifuged (A) Von Willebrand protein in endothelial cell homogenate fractionated on a colloidal silicia density gradient (———); recentrifuged buoyant particles (- - - -); dense particles (∞∞∞) and soluble fraction (······). (B) β-Hexosaminidase as in A. (C) Lactate dehydrogenase as in A. Amounts of proteins were corrected for dilution of recentrifuged fractions.

At a density of 1.11 g·ml^{-1} minor amounts of β-hexosaminidase activity were recovered occasionally, most likely from residual bodies, as reported by Rome et al. [15]. When a detectable amount of β-hexosaminidase activity at 1.11 g·ml^{-1} was found, it did not comprise more than 5% of total β-hexosaminidase activity recovered from the density gradient (Fig. 3).

After recentrifugation of gradient fractions on fresh colloidal silica gradients, fractions reappeared at the same density. Lactate dehydrogenase, β-hexosaminidase and Von Willebrand protein were evaluated in these recentrifugation experiments (Fig. 3). No shift of Von Willebrand protein from the dense pool of particles to the buoyant and soluble fraction was observed. Part of the Von Willebrand protein from the buoyant fraction appeared at high density, presumably derived from membrane encapsulated organelles freed before the second centrifugation.

Immunofluorescent staining for Von Willebrand protein of the dense organelle fraction showed, similar to the endothelial cells [9,11], that the dense fraction contained rod-like structures. Von Willebrand protein in cell homogenate and in the buoyant gradient fraction was present both in vesicles and in a few rod-shaped structures (data not shown).

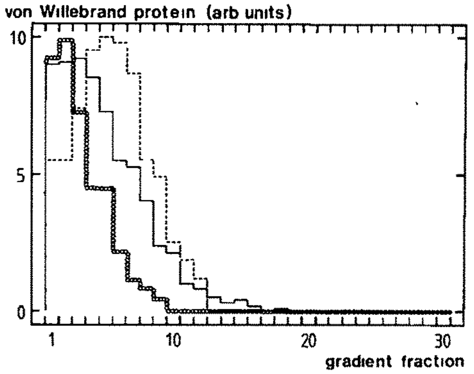

Fig. 4. Solubilized Von Willebrand protein from endothelial cells, buoyant and dense particles on colloidal silica density gradient. Endothelial cell homogenate was freeze-thawed twice in the presence of 0.2% Triton X-100 and applied on a colloidal silica density gradient (———). Buoyant and dense particles were obtained by fractionating endothelial cell homogenate, as shown in Fig. 2, freeze-thawed and applied on a colloidal silica density gradient; buoyant (- - - - - -) and dense (ooooo) particles.

TABLE II

EFFECT OF IONOPHORE A23187 AND THE PHORBOL ESTER PMA ON THE SUBCELLULAR LOCALIZATION OF VON WILLEBRAND PROTEIN

Endothelial cells were incubated for 1 h with ionophore A23187 or PMA. Cell homogenates were subsequently fractionated by colloidal silica density centrifugation. Von Willebrand protein is expressed as the percentage of total content recovered from gradient on which a parallel control incubation was fractionated. Fractions are defined as in Table I

Stimulus, concn	Von Willebrand protein (%)		
	Soluble fraction	Buoyant fraction	Dense fraction
A23187, 10 μM	7.1	43.6	28.8
Control	13.5	41.6	44.9
A23187, 20 μM	7.0	34.6	1.7
Control	16.7	50.7	32.6
A23187, 20 μM	3.0	31.0	1.6
Control	8.9	66.4	24.7
PMA, 100 ng·ml^{-1}	3.0	36.5	0.0
Control	6.0	60.0	34.0
PMA, 100 ng·ml^{-1}	1.6	35.7	0.0
Control	6.6	67.7	25.7

To exclude the possibility that the dense fraction with Von Willebrand protein arose from precipitation of free Von Willebrand protein, solubilized Von Willebrand protein was centrifuged on colloidal silica density gradients (Fig. 4). Solubilized Von Willebrand protein from endothelial cells that had been freeze-thawed in the presence of 0.2% Triton X-100 stayed in top fractions when centrifuged on a colloidal silica density gradient. Lactate dehydrogenase and β-hexosaminidase showed the same behavior (data not shown). Von Willebrand protein from freeze-thawed buoyant and dense organelle fractions stayed in top fractions (Fig. 4), as did Von Willebrand protein purified from plasma.

(2) Characterization of the high-density Von Willebrand protein organelle

Homogenates of cultured endothelial cells, which had been treated with PMA or Ca^{2+} ionophore A23187, were centrifuged on colloidal silica density gradients. Stimulation of Von Willebrand protein excretion with PMA or Ca^{2+} ionophore A23187 resulted in decrease of the Von Willebrand protein content of both buoyant and dense fractions (Table II). Loss of Von Willebrand protein was preferentially from the high-density organelle fraction. With Ca^{2+} ionophore A23187, a dose-dependent removal of Von Willebrand protein fromt he high-density particle fraction was observed. Treatment of the cells with PMA resulted in a complete or near complete disappearance of Van Willebrand protein from the high-density fraction. Von Willebrand protein content of the buoyant fraction was not reduced after treatment of cells with 10 μM ionophore A23187 and reduced to 50% of control after treatment with 20 μM Ca^{2+} ionophore A23187 or 100 ng·ml^{-1} PMA.

Culturing endothelial cells after a 1 h PMA pretreatment for 2 days in serum-free medium resulted in a recovery of the Von Willebrand protein content in the high-density fraction (Fig. 5A). No detectable amount of Von Willebrand protein was left in the dense organelle fraction after the 1 h incubation of endothelial cells with PMA (Fig. 5A). The Von Willebrand protein content in high-density organelles, which was restored with 2 days of culturing, could be reduced by a second PMA treatment (Fig. 5B). This suggested release of a newly formed storage pool of Von Willebrand protein in high-density organelles. Immunofluorescence studies carried out concurrently with the density gradient experiments showed disap-

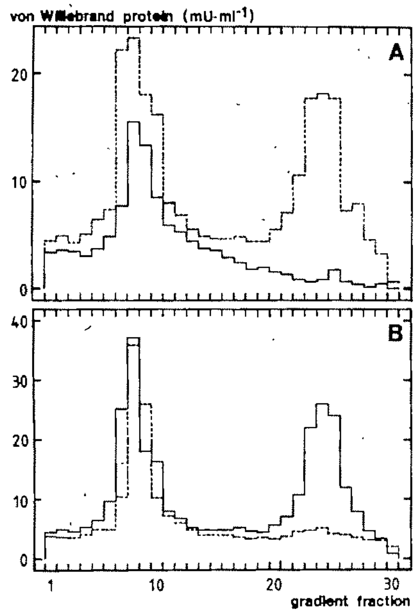

Fig. 5. Von Willebrand protein in endothelial cell homogenate fractionated on a colloidal silica gradient; influence of the phorbol ester PMA. Cultured endothelial cells were treated with PMA, 100 ng·ml^{-1} for 1 h and subsequently cultured for 2 days with serum-free medium. PMA-treated cultures were again stimulated with PMA, 100 ng·ml^{-1} for 1 h. Homogenates of cultures were fractionated on a colloidal silica density gradient. (A) PMA-treated at day 0 (———), PMA pretreated at day 0 and cultured for 2 days (- - - - - -). (B) PMA pretreated at day 0, subsequently cultured for 2 days (———) and again stimulated for 1 h with PMA (- - - - - -).

pearance of the rod-shaped structures with Von Willebrand protein from the cultured endothelial cells after a 1 h treatment with PMA (Fig. 6 A and B). Within 2 days of culturing the cells after PMA pretreatment, these rod-shaped structures with Von Willebrand protein reappeared (Fig. C and D).

Discussion

It was shown previously [9,11] that Von Willebrand protein in cultured endothelial cells was located in distinct vesicular structures. Further, it has been demonstrated that upon stimulation with various stimuli, including thrombin, ionophore A23187 and the phorbolester PMA, endothelial cells in culture rapidly release their Von Willebrand protein content, independent of protein synthesis [10,11].

It has been suggested that the vesicular structures seen in endothelial cells by immunostaining for Von Willebrand protein are secretory in nature [9,11]. This seems likely, but has never been demonstrated. Here, we provide evidence that these structures containing Von Willebrand protein are associated with stimulus-induced secretion.

Upon fractionation of an endothelial cell homogenate by colloidal silica density gradient centrifugation, two fractions of cell particles were obtained which contained Von Willebrand protein (Fig. 2). A fraction with relatively high density (1.12 g·ml^{-1}) apparently containing only Von Willebrand protein, and a more buoyant fraction (1.08 g·ml^{-1}) with Von Willebrand protein associated with a number of enzymes that are markers for well-defined subcellular structures including lysosomes, mitochrondria, Golgi apparatus, peroxisomes, fragments of plasma membrane and endoplasmic reticulum and nuclei.

A number of observations suggest that the dense organelles containing Von Willebrand protein are secretory granules. Upon stimulation, the Von Willebrand protein content of the dense fraction decreased concomitantly with a decrease of granular fluorescence in the cells. This was accompanied by accumulation of Von Willebrand protein in the medium. Restoration of granular appearance of Von Willebrand protein immunofluorescence following stimulus-induced degranulation was associated with an increase of Von Willebrand protein content of the dense organelle fraction. The newly formed granules again were secretory in nature (Fig. 5B).

Immunoelectron microscopy studies suggested that the rod-like organelles containing Von Willebrand protein were identical to Weibel Palade bodies [9]. As demonstrated by electron microscopy, the endothelial-cell-specific Weibel Palade bodies appeared to be secretory in nature [27,28], although the content of the Weibel Palade body was not identified. These findings provide tentative evidence that the secretory granules containing Von Willebrand protein, isolated from cultured endothelial cells, might be identical with Weibel Palade bodies. However, definite proof must be obtained by electron microscopy studies. Problems were encountered in preparation of gradient fractions for electron microscopy because of the presence of silica.

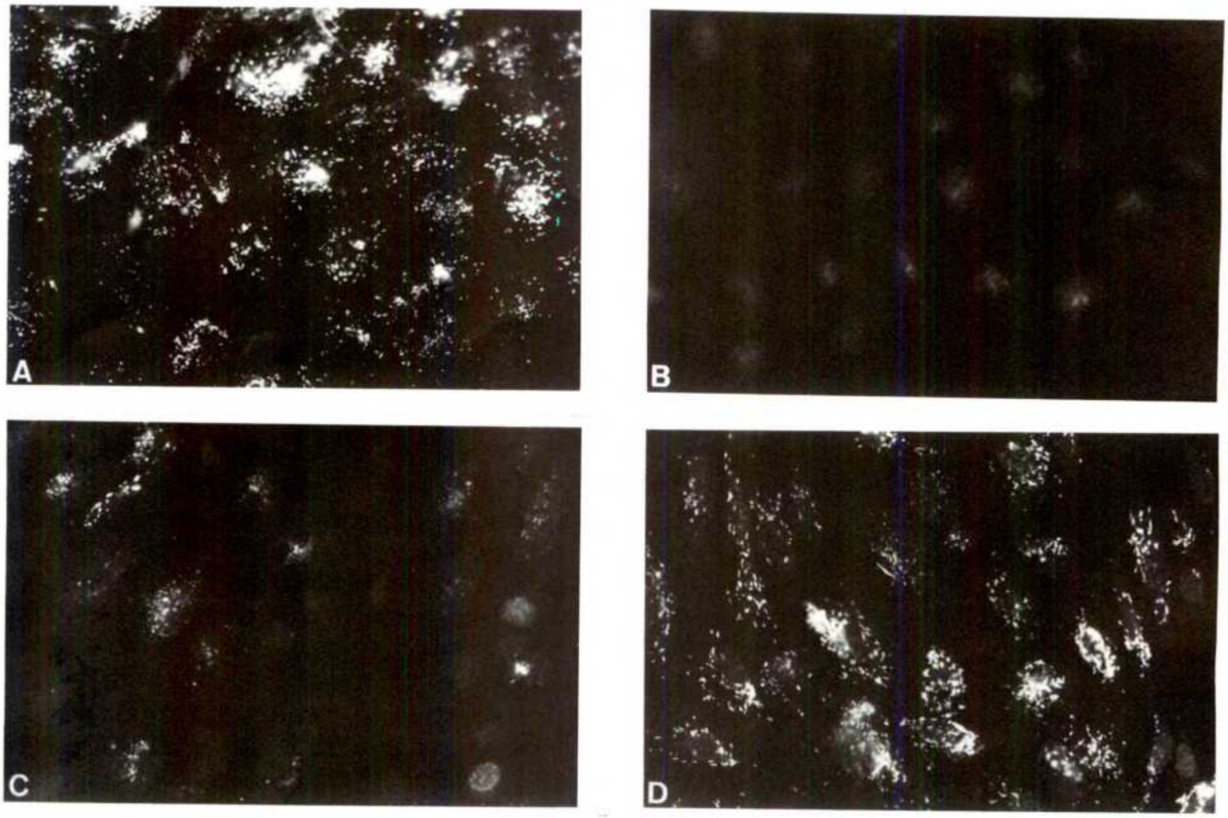

Fig. 6. Von Willebrand protein in cultured human endothelial cells. Indirect immunofluorescence pattern with a monoclonal antibody to von Willebrand protein and FITC-labeled goat anti-murine IgG. Endothelial cells were grown on coverslips. (A) Endothelial cells. (B) Endothelial cells treated with the phorbol ester PMA, 100 ng · ml^{-1} for 1 h. (C) and (D) Endothelial cells incubated with phorbol ester PMA as in B and subsequently incubated with serum free medium for 1 and 2 days, respectively.

The buoyant fraction of the colloidal silica density gradient contained most of the cell organelles, as demonstrated by the presence of the different markers. Von Willebrand protein in the buoyant fraction might originate from the endoplasmic reticulum system, remnants of the extracellular matrix [29], dense organelles entrapped in membrane vesicles during homogenation and possibly residual whole cells. Loss of Von Willebrand protein from the buoyant gradient fraction after stimulation of cells with PMA could be explained by taking into account the presence of incompletely broken cells and entrapped secretory granules in this fraction. Indicative of this phenomenon was the finding that Von Willebrand protein organelles were found at high density when the buoyant fraction was recentrifuged (Fig. 3). It could not be excluded, however, that the endothelial cells in culture contained two pools of secretory granules with Von Willebrand protein which differed in density. Since poly(vinyl pyrrolidone) formed part of the gradient material and may precipitate the factor-VIII complex [30], it was necessary to exclude the possibility that the high-density fraction with Von Willebrand protein was due to artifactual precipitation. However, soluble Von Willebrand protein from disrupted endothelial cells, buoyant and dense organelle fractions, and Von Willebrand protein purified from plasma stayed in top fractions when centrifuged on colloidal silica (Fig. 4).

The technique described in this paper not only provides a means to identify further and characterize the structural organization of the secretory granules and their content, but also to study in more detail the biosynthetic pathway, assembly and intracellular storage of Von Willebrand protein.

Acknowledgements

This study was supported in part by grants from the Foundation for Medical Research (FUNGO) which is subsidized by the Netherlands Organization for the Advancement of Pure Research (ZWO) (grant no. 13-30-31) and the Netherlands Heart Foundation (grant no. 28.004). The authors greatfully acknowledge the secretarial assistance of Ms. E. Van Rijn.

References

1 Hoyer, L.W. (1981) Blood 58, 1–12

2 Zimmerman, T.S. and Meyer, D. (1981) in Haemostasis and Thrombosis (Bloom, A.L. and Thomas, D.P., eds.), pp. 111–123, Churchill Livingstone, Edinburgh

3 Tschopp, T., Weiss, H.J. and Baumgartner, H.R. (1974) J. Lab. Clin. Med. 83, 296–300

4 Sakariassen, K.S., Bolhuis, P.A. and Sixma, J.J (1979) Nature 279, 636–638

5 Jaffe, E.A., Hoyer, L.W. and Nachmann, R.L. (1973) J. Clin. Invest. 52, 2757–2764

6 Nachmann, R.L., Levine, R. and Jaffe, E.A. (1977) J. Clin. Invest. 60, 914–921

7 Jaffe, E.A., Nachmann, R.L., Becker, C.G. and Minick, C.R. (1973) J. Clin. Invest. 52, 2745–2756

8 Wagner, D.D. and Marder, V. (1983) J. Biol. Chem. 258, 2065–2067

9 Wagner, D.D.. Olmsted, J.B. and Marder, V. (1982) J. Cell Biol. 95, 355–360

10 Levine, J.D., Harlan, J.M., Harker, L.A., Joseph, M.L. and Counts, R.B. (1982) Blood 60, 531–534

11 Loesberg, C., Gonsalves, M.D., Zandbergen, J., Willems C., Van Aken, W.G., Stel, H.V., Van Mourik, J.A. and De Groot, P.G. (1983) Biochim. Biophys. Acta 763, 160–168

12 Weibel, E.R. and Palade, G.E. (1964) J. Cell Biol. 23, 101–112

13 Willems, C., Astaldi, G.C.B., De Groot, P.G., Janssen, M.C., Gonsalves, M.D., Zeijlemaker, W.P., Van Mourik, J.A. and Van Aken, W.G. (1982) Exp. Cell Res. 139, 191–197

14 De Groot, P.G., Willems, C., Gonsalves, M.D., Van Aken, W.G. and Van Mourik, J.A. (1983) Thromb. Res. 31, 623–634

15 Rome, L.H., Garvin, A.J., Allietta, M.M. and Neufeld, E.F. (1979) Cell 17, 143–153

16 Wolff, D.A. (1975) in Methods in Cell Biology, Vol. 10 (Prescott, D.M., ed.), pp. 85–104, Academic Press, New York

17 Pertoft, H., Wärmegård, B. and Höök, M. (1978) Biochem. J. 174, 309–317

18 Bergmeyer, H.V. and Bernt, E. (1970) in Methoden der Enzymatischen Analyse, Vol. 1 (Bergmeyer, H.V., ed.) pp. 533, Verlag Chemie, Weinheim

19 De Groot, P.G., Strijland, A., Kalsbeek, R., Meera Khan, P., Westerveld, A., Hamers, M.N. and Tager, J.M. (1980) Exp. Cell Res. 126, 207–216

20 Brew, K., Shaper, J.H., Olsen, K.W., Trayer, I.P. and Hill, R.L. (1975) J. Biol. Chem. 250, 1434–1444

21 Avruch, J. and Hoelzl Wallach, D.F. (1971) Biochim. Biophys. Acta 233, 334–347

22 Phillips, A.M. and Langdon, R.G. (1962) J. Biol. Chem. 237, 2652–2660

23 Meerhof, L.J. and Roos, D. (1980) J. Reticuloendothel. Soc. 28, 419–425

24 Bradford, M.M. (1976) Anal. Biochem. 72, 248–254

25 Ruggeri, Z.M., Mannucci, P.M., Jefcoate, S.L. and Ingram, G.I.C. (1976) Br. J. Haematol. 33, 221–232

26 Stel, H.V., Sakariassen, K.S., Scholte, B.J., Veerman, E.C.I., Van Der Kwast, T.H., De Groot, P.G., Sixma, J.J. and Van Mourik, J.A. (1984) Blood, in the press

27 McNiff, J.M. and Gil, J. (1983) J. Appl. Physiol. Respir. Environ. Exercise Physiol. 54, 1284–1286

28 Sengel, A. and Stoebner, P. (1970) J. Cell Biol. 44, 223–226

29 Rand, J.J., Sussman, I.I., Gordon, R.E., Chu, S.V. and Solomon, V. (1980) Blood 55, 752–756

30 Casillas, G. and Simonetti, C. (1982) Br. J. Haematol. 50, 665–672

31 Reinders, J.H., De Groot, P.G., Scholte, B.J., Gonsalves, M.D., Loesberg, C., Willems, C., Over, J. and Van Mourik, J.A. (1983) Thromb. Haemostasis 50, 25

Biochimica et Biophysica Acta, 804 (1984) 370–376
Elsevier

BBA 11322

MULTIPLE EFFECTS OF INTERFERON ON MYOGENESIS IN CHICKEN MYOBLAST CULTURES

YOSHIMI TOMITA [a] and SHUJI HASEGAWA [b]

[a] *Department of Microbiology and* [b] *Brain Research Institute, School of Medicine, Chiba University, Chiba 280 (Japan)*

(Received November 23rd, 1983)

Key words: Interferon; Myogenesis; (Chicken myoblast)

Effects of chicken interferon on the differentiation of chicken skeletal muscle in vitro were examined. Continuous treatment of chicken myoblast culture with 200 IU/ml of interferon (10 IU/mg protein) resulted in significant inhibition of cell fusion and subsequent myotube formation. However, treatment of myoblast culture with 2 to 200 IU/ml of interferon increased activities of creatine kinase and myokinase in 4- or 6-day cultured muscle cells in a dose-dependent fashion. The effect of interferon on myokinase was less than on creatine kinase. Three-fold increase in creatine kinase activity induced by interferon was not accompanied by the accelerated transition of creatine kinase isozyme from BB- to MM-type. On the other hand, accumulation of acetylcholinesterase in interferon-treated cells at day 6 was suppressed to nearly half the level of control cells. Rates of actin and myosin synthesis in 4-day cultures estimated by pulse-labelling with [^{35}S]methionine were also suppressed to 85% of control cultures. However, a proportion of ^{35}S-labelled actin and myosin in labelled proteins associated with glycerinated cells was not changed by interferon treatment. These results indicate that partially purified interferon has multiple effects on the process of the myogenic differentiation of chicken myoblast in vitro.

Introduction

Interferon exerts various non-antiviral effects on cells, such as the reduction of growth rate [1] and the suppression of virus-induced fusion of cells [2–5] by inducing alterations in plasma membranes, cytoskeletal structures and metabolic activities [6–11]. Interferon is also known to modulate cell differentiation in vitro [12–15]. Myogenesis in vitro seems to be suitable for the study of non-antiviral actions of interferon on cell fusion and differentiation. Myoblasts from chicken and mammalian embryos proliferate, differentiate and fuse in culture, to form multinucleated myotubes. During the myogenic process the amount of contractile proteins and enzymic activities of creatine kinase (EC 2.7.3.2) myokinase (EC 2.7.4.3) and acetylcholinesterase (EC 3.1.1.7) rapidly accumulate in cells to a high level [16–19]. Recently, Lough et al. [20] reported inhibitory effects of chicken interferon on myogenic events during the differentiation of skeletal muscle in vitro.

In this paper we report that chicken interferon has multiple effects on the differentiation of cultured chicken myoblasts. Namely, interferon enhances the accumulation of creatine kinase and myokinase in muscle cells in a condition in which the fusion of myoblasts and the accumulation of acetylcholinesterase are markedly inhibited.

Materials and Methods

Cell cultures. Muscle cell cultures were prepared from thigh muscles of 11- or 12-day-old chick embryos, as described previously [21]. Briefly,

---

Abbreviation: Hepes, 4-(2-hydroxyethyl)-1-piperazineethanesulphonic acid.

0167-4889/84/$03.00 © 1984 Elsevier Science Publishers B.V.

$(1.5-2.2) \cdot 10^7$ cells were seeded on a gelatin-coated 150 mm petri dish and maintained in Eagle's minimal essential medium, containing 15% horse serum and 5% chick embryo extract, for 16 to 18 h. Secondary cell suspension was prepared from primary cultures to eliminate fibroblasts and to enrich myogenic cells in culture. About $3.2 \cdot 10^5$ cells were inoculated on a gelatin-coated 35 mm dish, unless otherwise stated, and were grown in the nutrient medium described above. Cultures were fed fresh nutrient medium every 2 days. When cultures were treated with interferon from day 1, interferon was added 6 h after plating.

Interferon. Partially purified chicken interferon, which was induced by ultraviolet-inactivated Newcastle disease virus in chicken embryo fibroblasts in primary culture, was kindly supplied by Dr. M. Kohase, National Institute of Health, Japan. The specific activity of interferon was $1.0 \cdot 10^6$ IU/mg protein.

Fusion index. Duplicate cultures treated with or without interferon were fixed with 100% methanol for 10 min and stained with 10% Giemsa solution in phosphate-buffered saline (pH 6.8) for 20 min. Nuclei were counted under a microscope with an eyepiece grid. For each dish, 20 randomly selected microscopic fields were examined, and in total 1600–2500 nuclei were counted. The extent of cell fusion is expressed as a fusion index, i.e., the percentage of nuclei found in multinucleated cells.

Assay of enzyme activities and contents of DNA and protein. Cells were scraped from dishes with a rubber policeman, washed by suspending in Eagle's minimal essential medium and dispersed in 0.5 ml of 20 mM mM Tris-HCl buffer (pH 8.0). The cells were disrupted by brief sonication. Creatine kinase activity and myokinase activity were measured by the method described by Kuby et al. [22] and Shainberg et al. [18], respectively. For determination of activity of acetylcholinesterase, Triton X-100 was added to cell homogenates to a concentration of 0.1%. The enzyme activity was measured in the presence of 0.1 mM tetraisopropylpyrophosphoramide, according to the procedure described by Ellman et al. [23]. One unit of enzyme activity is the amount which catalyzes the formation of 1 μmol product/min at 30 °C for creatine kinase and at 37 °C for the other two enzymes. 2-5A synthetase activity was estimated as described previously [4]. For 2-5A synthesis assay, cells detached from three dishes were sonicated in 0.15 ml of 20 mM Hepes-KOH buffer (pH 7.4)/60 mM magnesium acetate/0.2 M KCl, and 80 μl of the sonicate was used for enzyme assay. DNA content of cell homogenates was measured by indole reaction [24], and protein content was determined by the method of Lowry et al. [25].

Zone electrophoresis. Electrophoresis was performed in 0.05 M barbital/0.01 M 2-mercaptoethanol (pH 8.6) on cellulose acetate strips at 0.6 mA/cm for 120 min. The strips were stained for creatine kinase activity as described previously [26].

Actin and myosin synthesis. Muscle cultures were washed with Eagle's minimal essential medium and labelled for 90 min with [^{35}S]methionine (20 μCi/ml; Amersham) in minimal essential medium with 200-fold reduction in the methionine concentration. The cultures were rinsed with minimal essential medium and kept in 50% glycerol/50% standard salt solution at 4 °C for 4 days [27]. Standard salt solution consisted of 0.1 M KCl/5 mM $MgCl_2$/6 mM sodium phosphate buffer (pH 7.0). The glycerol solution was removed, and the preparations were rinsed with standard salt solution, scraped into standard salt solution and precipitated by centrifugation at 3000 rpm for 5 min. The pellets were solubilized with 100 μl of sample buffer for electrophoresis, 0.15 M Tris-HCl (pH 6.8)/30% sodium dodecyl sulphate (SDS)/3% 2-mercaptoethanol/30% glycerol, and were applied on a gel for electrophoresis. Slab gel electrophoresis was done in gel of 12.5% acrylamide containing 0.1% SDS. Bands of actin (molecular weight 43 000) and myosin heavy chain (molecular weight 200 000) were located by fluorography [28]. Radioactivities in these bands were determined by cutting the dried gel and counting the activities in ACS II scintillant (Amersham).

Results

Effects of interferon on myotube formation

Myoblast fusion and morphological changes during myogenic differentiation in control and interferon-treated cultures were studied by determining fusion indexes and by microscopic observation. As shown in Fig. 1, morphological differences between control and interferon-treated cultures were observed by day 4 after the beginning of interferon treatment. Many long and thick myotubes having cluster of nuclei at their peripheral or branching regions developed in control cultures (Fig. 1c), but short and thin myotubes were formed in interferon-treated cultures (Fig. 1d). At day 6, myotubes in control cultures became longer and wider, whereas the development of myotubes in interferon-treated cultures remained inhibited (Fig. 1e and f). Fig. 2a shows that myoblast fusion was initiated at 48 h and completed by 80 h after plating in high-density cultures. The addition of interferon (100 IU/ml) to cultures resulted in a reduction of their fusion indexes to about 40% of those of control cultures at 90–117 h after plating. However, when the interferon-treatment started after the onset of fusion (at day 3), subsequent fusion was not inhibited significantly (Fig. 2b), suggesting that the anti-fusion state is efficiently induced in myoblasts prior to fusion. To confirm that diminished formation of myotubes can be attributed to an action of interferon, we examined responsiveness of muscle culture to interferon by estimating 2-5A synthetase activity induced by interferon. Myoblast cultures were treated with interferon from 48 to 72 h after the time of plating. Synthesis of radioactive 2-5A in extracts of cells treated with 10 and 100 IU/ml of interferon was 190 and 2909 cpm/80 μl per 25

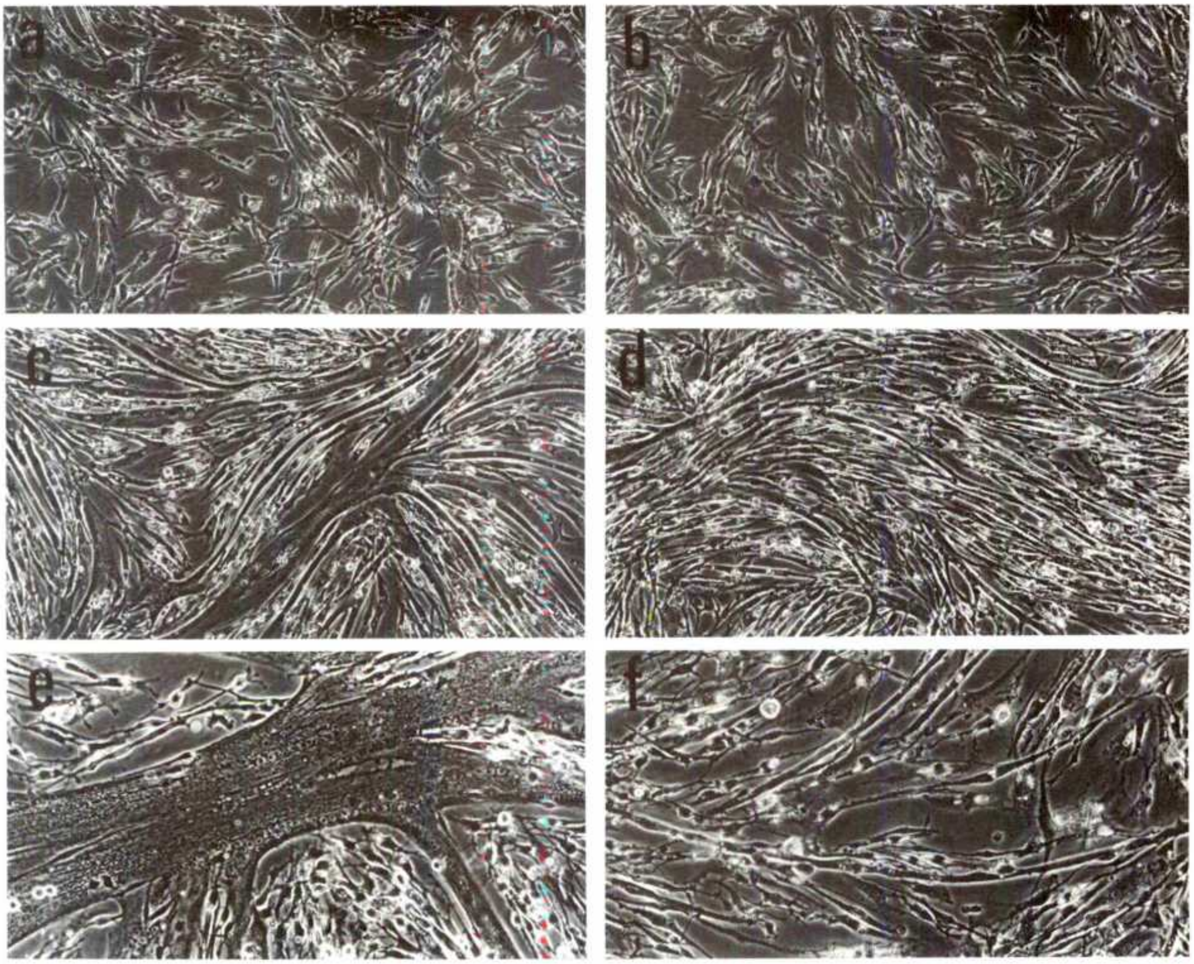

Fig. 1. Inhibition of myotube formation by interferon-treatment. Myoblasts were cultured for 2 days (a, b) or 4 days (c, d) in the absence (a, c) or presence (b, d) of 100 IU/ml of interferon, and photographs were taken under phase-contrast microscope (× 62.5). Myotubes formed after 6-days cultivation in a control dish (e) and in a dish treated with 200 IU/ml of interferon (f) (× 125).

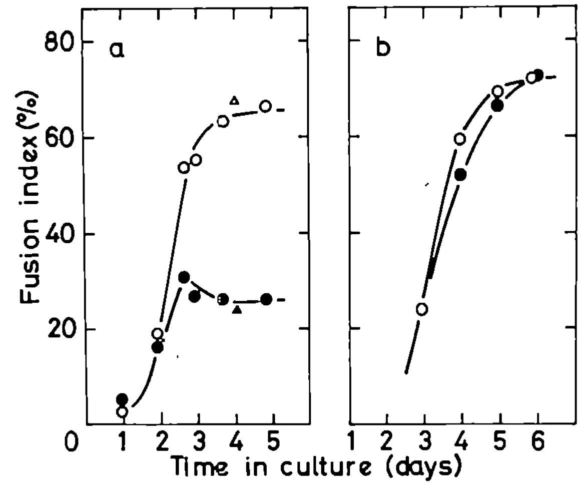

Fig. 2. Myoblast fusion in interferon-treated and untreated cultures. Interferon (100 IU/ml) was added to cultured 6 h (a) or 3 days (b) after plating and culture medium with or without interferon was changed at 2-day intervals. Inoculum size was $3.2 \cdot 10^5$ cells (a) and $6.4 \cdot 10^4$ cells (b) per dish. ○ and △, untreated control cultures; ● and ▲, interferon-treated cultures. Triangle symbols represent a separate experiment.

A_{260}, respectively, whereas synthesis of 2-5A in control extract was hardly detectable.

Enhanced accumulation of creatine kinase and myokinase in interferon-treated cells

Interferon stimulated the accumulation of both creatine kinase and myokinase activities in myotube cultures. Interferon treatment at 200 IU/ml for 4 days from 48 h after plating resulted in three fold increase of the specific activity of creatine kinase; creatine kinase activities of interferon-treated cultures and control cultures were 72.4 ± 1.9 and 23.8 ± 2.4 mU/mg protein (mean ± S.D. for three independent experiments), respectively. As shown in Table I, the effect of interferon on creatine kinase activity was dose-dependent. A 1.5-fold enhancement of creatine kinase level in cultured muscle cells was observed even after 2-days treatment from day 2 to day 4 with 100 IU/ml of interferon. But 1-day treatment from day 5 to day 6 was not enough to ensure the significant enhancement of creatine kinase level (data not shown), suggesting that interferon accelerates creatine kinase accumulation at a relatively early stage of myotube formation in vitro. Myokinase activity was also stimulated by interferon treatment, but less effectively as compared to creatine kinase activity. Enzyme activity of myokinase in interferon-treated cultures (100 IU/ml) was 122.5% of control (Table I).

Creatine kinase isozymes

To determine whether the enhanced accumulation of creatine kinase activity by interferon was

TABLE I

DOSE-DEPENDENT EFFECTS OF INTERFERON TREATMENT ON ENZYME ACTIVITIES IN CULTURED MYOTUBES

Myotube cultures obtained from a single muscle cell preparation were treated with interferon (IFN) for 4 days from 48 h after plating, harvested and subjected to simultaneous analysis of enzyme activities and DNA and protein content in Expt. 1. Myotube cultures obtained from another muscle cell preparation were treated with interferon for 6 days from day 1, harvested and subjected to measurement of myokinase in Expt. 2.

IFN (IU/ml)	DNA (μg/dish [a])	Protein (μg/dish [a])	Creatine kinase		Acetylcholinesterase		Myokinase	
			mU/mg protein [a]	%	mU/mg protein [b]	%	mU/mg protein [a]	%
Expt. 1								
0	7.38 ± 0.94	223 ± 6.6	27.1 ± 4.4	100	32.6	100.0		
2	7.70 ± 1.15	256 ± 13.9	42.8 ± 7.7	157	25.0	76.7		
20	6.51 ± 1.01	240 ± 1.4	50.5 ± 5.4	186	24.6	75.5		
200	6.91 ± 0.74	235 ± 16.0	73.1 ± 6.2	270	17.7	54.3		
Expt. 2								
0		345 ± 14.1					80.0 ± 6.9	100.0
10		315 ± 4.1					87.5 ± 3.3	109.4
100		411 ± 2.8					98.8 ± 8.7	122.5

[a] Each value is the mean ± S.D. for three dishes.

[b] Aliquots of homogenates obtained from three dishes were pooled for determination of enzyme activity.

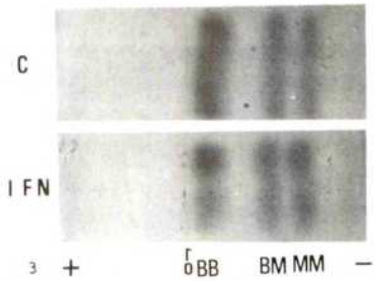

Fig. 3. Electrophoretic patterns of creatine kinase isozymes. Extracts were prepared from 6-day cultures of muscle cells grown in the presence or absence of interferon (200 IU/ml). C, control; IFN, interferon-treated.

accompanied by an accelerated transition in creatine kinase isozyme from BB-type to MM-type, we examined the isozyme patterns of creatine kinase in cell homogenates prepared from interferon-treated and untreated cultures on day 6. As shown in Fig. 3, both preparations contained BB-, BM- and MM-type creatine kinases, and the electrophoretic pattern of the interferon-treated preparation was extremely similar to that of control, suggesting that interferon equally stimulated the accumulation of both B- and M-type subunits of creatine kinase.

Suppression of acetylcholinesterase accumulation in interferon-treated cells

We examined the effect of interferon on acetylcholinesterase accumulation in cultured muscle cells. As shown in Table I, in contrast to the effects on creatine kinase and myokinase, interferon treatment suppressed acetylcholinesterase accumulation in a dose-dependent fashion. Acetylcholinesterase activity in cultured cells which were treated with 200 IU/ml of interferon for 4 days before harvesting was 54.3% of that in control cultures.

Effect of interferon on actin and myosin synthesis

Muscle cells were grown in the presence or absence of interferon (200 IU/ml) and the rates of actin and myosin heavy chain synthesis were determined on day 4 by pulse labelling of cells with [^{35}S]methionine followed by glycerination and analysis with SDS-polyacrylamide gel electrophoresis. Table II shows that, although total protein content in interferon-treated culture was higher than that in control culture (121.3%), an incorporation of [^{35}S]methionine into trichloroacetic acid-insoluble materials of glycerinated cells in interferon-treated culture was lower than that in control culture (86.9%). An almost similar gel-electrophoretic pattern was observed in both samples (Fig. 4). Radioactivities incorporated into actin and myosin heavy chain bands in interferon-treated culture were also lower than those in control culture (86.8 and 82.2% of control, respectively). However, the sum of the radioactivities recovered in actin and myosin bands was 57.2% of trichloroacetic acid-insoluble radioactive materials applied on gel in the control preparation and 56.3% in the interferon-treated preparation. These results sug-

TABLE II

EFFECT OF INTERFERON-TREATMENT ON THE INCORPORATION OF [^{35}S]METHIONINE INTO ACTIN AND MYOSIN IN CULTURED MUSCLE CELLS

Muscle cells were grown with or without interferon (IFN), pulse-labelled with [^{35}S]methionine, glycerinated and solubilized. Radioactivities of myosin and actin bands in gels shown in Fig. 3 were determined after cutting the gels. TCA, trichloroacetic acid.

	TCA-insoluble radioactivity in glycerinated cells		Radioactivity recovered			
			in actin		in myosin	
	cpm/dish	% control	cpm	% recovery [a]	cpm	% recovery [a]
Control	114 370	100.0	4613	40.3	1937	16.9
IFN-treated	99 340	86.9	4003	40.3	1592	16.0

[a] Percentage of radioactivity applied on the gel.

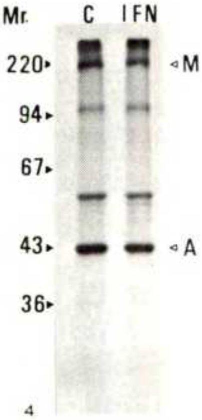

Fig. 4. SDS-polyacrylamide gel electrophoresis of [^{35}S]methionine-labelled materials in glycerinated muscle cells. Myoblasts were grown in the absence or presence of interferon (200 IU/ml) for 4 days. For analysis, radioactive materials from control and interferon-treated cells (11 437 and 9 930 trichloroacetic acid-precipitable cpm, respectively) were applied on the gel. Electrophoresis was carried out at 160 V for 3.5 h. C, control; IFN, interferon-treated; A, actin; M, myosin-heavy chain. M_r ($\times 10^{-3}$): 220, ferritin half unit; 94, phosphorylase *b*; 67, albumin; 43, ovalbumin; 36, lactate dehydrogenase.

gest that interferon decreased the rate of synthesis of proteins associated with glycerinated cells by nearly 15% in 4-day cultures of muscle cells, but did not change the proportion of synthesis of actin and myosin in those proteins. Similar results were obtained in experiments using 6-day cultures (data not shown).

Discussion

Recently we have shown that interferon inhibits cell fusion of human transformed cells which are induced by ultraviolet-inactivated retrovirus [2] and Sendai virus [3,4]. This action of interferon was further confirmed by Chatterjee et al. [5] using human and monkey cells. In the studies reported here, interferon at concentrations up to 200 IU/ml inhibited cell fusion in chick embryonic myoblast cultures and affected the accumulation of some muscle-specific proteins in cultured cells. Interferon increases the rigidity of plasma membrane lipid bilayers in mouse sarcoma S-180 cells [10] and the reorganization of actin-containing microfilaments in cells, which may result in the suppression of redistribution of some cell surface components [9]. It is likely that the similar alterations in plasma membrane and submembraneous cytoskeletal components are induced in interferon-treated myoblasts. The inhibition of myoblast fusion by interferon treatment could be a result of an antagonistic effect of interferon on the rapid increase in the membrane fluidity in myoblast, which precedes the membrane union [29]. Myoblast fusion is a multistep process, including at a minimum two phases: (i) cell migration, recognition and alignment and (ii) membrane union [30]. An alternative explanation of fusion-blocking action of interferon is that the interferon-induced suppression of synthesis or redistribution of cell surface components which are required for cell migration, recognition and alignment might result in blockade of the fusion process.

Originally, Lough et al. [20] tested effects of chicken interferon on the chicken myogenesis in vitro and reported that interferon inhibits myogenesis in terms of morphology and isozyme transition from BB-creatine kinase to MM-creatine kinase. In our present work, we confirmed the inhibitory action of interferon on myotube formation under light-microscopic observation. However, we found that, up to 200 IU/ml, chicken interferon enhances the accumulation of creatine kinase and myokinase in muscle cells, even in a condition in which interferon inhibits the fusion of myoblasts, the accumulation of acetylcholinesterase and the synthesis of contractile proteins. We also found that the transition of BB-creatine kinase to MM-creatine kinase is not inhibited by interferon treatment. It may be argued that the diminished formation of myotubes and the alterations in enzyme activities are due to an action of some components other than interferon, which were produced by chicken embryonic fibroblast cells and coexisted in our interferon preparation. This is unlikely, since myoblasts were grown in nutrient medium supplemented with the supernatant of homogenate of whole chick embryos. Our observations that in primary muscle cultures the enzyme activity of creatine kinase and myokinase was elaborated in fusion-blocked myoblast cells agree with the findings reported in non-fusing muscle cell line M3A [31] that the synthesis of creatine kinase and the progress of cell fusion are regulated independently in myogenesis in vitro.

While our experiments were in progress, Fisher et al. [32] reported an acceleration of myoblast fusion and creatine kinase isozyme transition by human leukocyte interferon in human myoblast culture. In chicken myoblast culture, we observed a slight acceleration in myoblast alignment in early stage of cultures which were treated with relatively high titre of interferon (1000 IU/ml), even though following fusion was markedly inhibited. Long-term treatment with 1000 IU/ml of interferon was toxic for culture, and many unfused cells were detached from a dish by days 5 to 6 after the beginning of treatment. At present, we cannot propose a reason for the discrepancy observed on the effects of interferon on myoblast fusion in human and chicken cultures. In our system, it is conceivable that interferon has divergent effects on myogenic process of chicken skeletal muscle in vitro.

Acknowledgments

We wish to thank Dr. M. Kohase for kindly suppling chicken interferon. This study was supported by grants from National Center for Nervous, Mental and Muscular Disorders and the research committee of CNS degenerative diseases of the Ministry of Health and Welfare, Japan and a grant from the Ministry of Education, Science and Culture, Japan.

1 Stewart, W.E. II (1981) The Interferon System, Springer-Verlag, Wien
2 Tomita, Y. and Kuwata T. (1979) J. Gen. Virol. 43, 111–117
3 Tomita, Y. and Kuwata T. (1981) J. Gen. Virol. 55, 289–295
4 Tomita, Y. Nishimaki, J., Takahashi, F. and Kuwata T. (1982) Virology 120, 258–263
5 Chatterjee, S., Cheung, H. and Hunter, E. (1982) Proc. Natl. Acad. Sci. USA 79, 835–839
6 Friedman, M.R. (1979) in Interferons (Gresser, I., ed.), Vol. 1, pp. 53–74, Academic Press, New York
7 Pfeffer, L.M. Wang, E. and Tamm, I. (1980) J. Cell Biol. 85, 9–17
8 Wang, E., Pfeffer, L.M. and Tamm, I. (1981) Proc. Natl. Acad. Sci. USA 78, 6281–6285
9 Tamm, I., Wang, E., Landsber, F.R. and Pfeffer, L.M. (1982) UCLA Sym. Mol. 25, 159–179
10 Chandrabose, K. and Cuatrecasas, P. (1981) Biochem. Biophys. Res. Commun. 98, 661–668
11 Apostolov, K. and Barker, W. (1981) FEBS Lett. 126, 261–264
12 Keay, S. and Grossberg, S.E. (1980) Proc. Natl. Acad. Sci. USA 77, 4099–4103
13 Rossi, G.B., Matarese, G.P., Grappelli, C. and Benedetto, A. (1977) Nature 267, 50–52
14 Tomida, M., Yamamoto, Y. and Hozumi, M. (1982) Biochem. Biophys. Res. Commun. 104, 30–37
15 Fisher, P.B., Mufson, R.A. and Weinstein, I.B. (1981) Biochem. Biophys. Res. Commun. 100, 823–830
16 Paterson, B. and Strohman, R.C. (1972) Develop. Biol. 29, 113–138
17 Whalen, R.G., Butler-Browne, G.S. and Gros, F. (1976) Proc. natl. Acad. Sci. USA 73, 2018–2022
18 Shainberg, A., Yagil, G. and Yaffe, D. (1971) Dev. Biol. 25, 1–29
19 Prives, J.M. and Paterson, B.M. (1974) Proc. Natl. Acad. Sci. USA 71, 3208–3211
20 Lough, J., Keay, S., Sabran, J.L. and Grossberg, S.E. (1982) Biochem. Biophys. Res. Commun. 109, 92–99
21 Konigsberg, I.R. (1979) Methods Enzymol. 511–527,
22 Kuby, S.A., Noda, L. and Lardy, H.A. (1954) J. Biol. Chem. 209, 191–201
23 Ellman, G.L., Courtney, K.D., Andres, V., Jr. and Featherstone, R.M. (1961) Biochem. Pharmacol. 7, 88–95
24 Keck, K. (1956) Arch. Biochem. Biophys. 63, 446
25 Lowry, O.H., Rosebrough, N.J., Farr, A.L. and Randall, R.J. (1951) J. Biol. Chem. 193, 265–275
26 Turner, D.C., Maier, V. and Eppenberger, H.M. (1974) Dev. Biol. 37, 63–89
27 Schroeder, T.E. (1973) Proc. Natl. Acad. Sci. USA 70, 1688–1692
28 Laskey, R.A. and Mills, A.D. (1975) Eur. J. Biochem. 56, 335–341
29 Prives, J. and Shinitzky, M. (1977) Nature 268, 761, 763
30 Nameroff, M. and Munar, E. (1976) Dev. Biol. 49, 288–293
31 Tarikas, H. and Schubert, D. (1974) Proc. Natl. Acad. Sci. USA 71, 2377–2381
32 Fisher, P.B., Miranda, A.F., Babiss, L.E., Pestka, S. and Weinstein, I.B., (1983) Proc. Natl. Acad. Sci. USA 80, 2961–2965

Biochimica et Biophysica Acta, 804 (1984) 377–385
Elsevier

BBA 11325

EFFECT OF ADRENALECTOMY ON CELLULAR CALCIUM METABOLISM AND ON THE RESPONSE TO ADRENERGIC STIMULATION OF HEPATOCYTES ISOLATED FROM MALE AND FEMALE RATS

REBECCA K. STUDER and ANDRÉ B. BORLE *

Department of Physiology University of Pittsburgh School of Medicine, Pittsburgh, PA 15261 (U.S.A.)

(Received January 16th, 1984)

Key words: Adrenalectomy; Ca^{2+} metabolism; Adrenergic stimulation, (Rat hepatocyte)

The effects of adrenalectomy on cell calcium metabolism and on the effects of epinephrine on cAMP, phosphorylase *a* activity, and calcium efflux were studied in hepatocytes isolated from adult male and female rats. Adrenalectomy increased the total calcium of hepatocytes, all exchangeable calcium pools, and all calcium fluxes between the cellular pools in both sexes. After adrenalectomy, basal cAMP was elevated, phosphorylase *a* + *b* was decreased, but basal phosphorylase *a* activity was not changed. In adrenalectomized males and at all concentrations of epinephrine studied ($1 \cdot 10^{-8}$–$1 \cdot 10^{-5}$ M) stimulation of calcium efflux was decreased and cAMP accumulation was enhanced, while the resulting phosphorylase *a* activation was depressed. In hepatocytes from adrenalectomized females there was a similar increase in cAMP accumulation induced by epinephrine, and a decrease in the stimulation of calcium efflux; however, the depression in phosphorylase *a* activation was much less and was significant only at $1 \cdot 10^{-8}$ and $1 \cdot 10^{-5}$ M epinephrine. In the male, while activation of phosphorylase *a* shifted from a pure α-adrenergic response mediated by calcium to one also involving a cAMP-mediated β-adrenergic response, the contribution of the attenuated calcium signal was still significant. Hepatocytes from female rats did not show a comparable α- to β-shift, since the relative contribution of calcium and cAMP to phosphorylase activation was similar in sham-operated and adrenalectomized animals.

Introduction

Adrenalectomy or corticosteroid deficiency interferes with systemic glucose homeostasis [1] and several specific defects in the regulation of hepatic glucose release are well documented [2]. The stimulation of glucose production from glycogenolysis and gluconeogenesis evoked by epinephrine or glucagon is depressed in hepatocytes of adrenalectomized rats [3–5]. Since α-adrenergic stimulation of glycogenolysis in the adult male rat is triggered almost exclusively by an increase in cytosolic calcium which activates phosphorylase *b* kinase and increases phosphorylase *a* activity [6], a change in cell calcium metabolism following adrenalectomy could well be a contributing factor. Although it has been reported that in some species adrenalectomy alters systemic calcium homeostasis [7,8] and increases calcium transport by the small intestine [9], the effects of corticosteroid deficiency on hepatic calcium metabolism have never been documented. One of the goals of our investigations was to determine whether adrenalectomy influences the calcium metabolism of isolated hepatocytes.

In male rats, adrenalectomy also changes the pathway of adrenergic activation of hepatic glycogenolysis from a predominantly α-mediated

---

* To whom correspondence should be addressed.

0167-4889/84/$03.00 © 1984 Elsevier Science Publishers B.V.

calcium-dependent mechanism to one in which the β-mediated cAMP-dependent pathway is also involved. We have recently shown that hepatocytes from adult female rats normally exhibit a mixed α- and β-adrenergic response to epinephrine, and show differences in basal calcium metabolism when compared with cells isolated from males [10,11]. A second goal of our investigations was to compare males and females after adrenalectomy with respect to possible changes in cellular calcium, and to determine whether the shift from an α- to a β-receptor pathway during the adrenergic response occurs in the female as well as in the male.

We found that adrenalectomy caused significant changes in both sexes in the total and exchangeable calcium of hepatocytes and in the kinetically defined calcium pools and fluxes. After adrenalectomy, epinephrine caused a greater rise in cAMP, but a lesser increase in cytosolic calcium as measured by calcium fractional efflux. Phosphorylase *a* stimulation was significantly depressed, especially in hepatocytes isolated from male adrenalectomized rats. In males, adrenalectomy induced a shift from a pure α- to a mixed α-, β-adrenergic response to epinephrine. In females, however, the relative importance of the α- and β-components of the adrenergic activation of phosphorylase remained qualitatively the same.

Methods

Adult female and male Sprague-Dawley rats were adrenalectomized or sham-operated 7–13 days before being used. The adrenalectomized animals were given a 0.9% NaCl solution as their drinking water. Hepatocytes were prepared from fed rats as previously described [10], using a modification of the collagenase perfusion method of Berry and Friend [12]. The isolated hepatocytes were incubated with gentle stirring in Krebs-Henseleit bicarbonate buffer/1.3 mM Ca^{2+}/5 mM glucose/1% bovine serum albumin (buffer 1) with a gas phase of 95% oxygen/5% CO_2. Measurements of ^{45}Ca efflux, cAMP, and phosphorylase *a* activity were done on separate aliquots of the same hepatocyte preparation.

^{45}Ca fractional efflux ratio. Liver cells were labeled with ^{45}Ca and desaturated with buffers containing 1.3 mM Ca^{2+} as previously described [10]. The ^{45}Ca fractional efflux is calculated as the radioactivity released per unit time expressed as a percentage of the average cell radioactivity during the collection period [13]. The ^{45}Ca fractional efflux ratio is the fractional efflux of stimulated cells divided by the fractional efflux of control cells perfused concurrently. An increase in ^{45}Ca fractional efflux ratio may be caused by a rise in cytosolic free calcium, by an increase in active transport across the plasma membrane, or by mobilization of an intracellular pool of calcium with a specific activity greater than that of cytosol. We assume that the increase in ^{45}Ca fractional efflux observed in response to epinephrine stimulation reflects a rise in cytosolic calcium activity [10,11].

Phosphorylase activity. Aliquots of the hepatocyte suspension were added to the ice cold buffer described by Hutson et al. [14], homogenized, and frozen until assayed in the direction of glycogen synthesis by the method of Stalmans and Hers [15]. Phosphorylase *a* was assayed in the presence of 0.5 mM caffeine to minimize any contribution of phosphorylase *b* activity. Phosphorylase $a + b$ was assayed in the absence of caffeine with 3 mM AMP present and 80 mM glucose 1-phosphate as substrate [16]. In both cases, the [^{14}C]glucose 1-phosphate converted to glycogen was precipitated on filter paper with 66% ethanol [17]. Phosphorylase activity is expressed as $nmol \cdot min^{-1} \cdot mg^{-1}$ cell protein, with the protein concentration being determined by the method of Lowry et al. [18].

Hepatocyte cAMP. The concentration of cAMP in the cells was determined by radioimmunoassay as previously described on acetylated acetate buffer extracts [10]. Values are reported as $pmol \cdot mg^{-1}$ cell protein.

Hepatocyte calcium content and steady-state kinetic analysis of cell calcium pools and fluxes. Liver cells from adrenalectomized or sham-operated rats were incubated for 120 min in buffer 1 with 1.3 mM Ca^{2+}. ^{45}Ca was added during the last 60 min to label the cells. Aliquots of the cell suspension were rapidly centrifuged in 40 ml of unlabeled calcium-free phosphate-buffered saline, the pellet was sonicated in deionized water and analyzed for ^{45}Ca and ^{40}Ca content by standard methods [19]. Calcium pools and fluxes were measured by steady-state analysis of ^{45}Ca desaturation. After 60 min labeling, desaturation was accomplished by perfusion at 0.6 ml/min for 180 min with nonradioactive buffer 1, 1.3 mM Ca^{2+}, and the efflux curves were analyzed as previously published [20]. The justification for modeling the data to a three-compartment catenary system, and the assumptions and equations for calculating the kinetic parameters have been published [21–24].

Materials. Collagenase, 3-isobutyl-1-methylxanthine, L-epinephrine bitartrate and DL-propanolol hydrochloride, were obtained from Sigma. Phenoxybenzamine was purchased from Smith, Kline and French, and 2-*O*-[^{125}I]succinyladenosine-3′,5′-cyclic phosphoric acid, $^{45}CaCl_2$ and [^{14}C]glucose 1-phosphate from New England Nuclear. The cAMP antibody was generously provided by Dr. F. DeRubertis, VA Hospital, Pittsburgh, PA.

Statistics. Statistical analyses were made by first determining the equality of variances between groups by the F-test criterion, and the significance of the results were calculated accordingly either by F-statistics or by Student's *t*-test. All values presented are expressed as the mean ± S.E.

Results

Effect of adrenalectomy on hepatocyte calcium content, calcium pools and steady-state calcium fluxes

Table I shows the changes in hepatocyte calcium metabolism measured 1–2 weeks after adrenalectomy. The effects of adrenalectomy are similar in males and females; in both sexes there are significant increases in both ^{40}Ca cell content and in the 60 min exchangeable ^{45}Ca. Kinetic analysis showed that this increase was shared by all three exchangeable cellular pools, with the largest being seen in S_3, the mitochondrial pool. The value for S_3 was increased 139% in the male and 245% in the female. In the male, the calcium fluxes occurring between all the pools were significantly increased: extracellular exchange (ρ_{01}) increased 57%, plasma membrane transport (ρ_{12}) increased 79% and the cytosol-mitochondrial exchange (ρ_{23}) increased 119%. In the female, only the plasmalemmal exchange and cytosol-mitochondrial exchange were increased, 50 and 241% respectively. The difference usually observed between males and females with respect to the mitochondrial pools and fluxes were abolished in the sham-operated animal [11,25]. The values for S_3 and ρ_{23} in the sham-operated female were decreased to the levels usually found in the male.

Effects of adrenalectomy on basal phosphorylase a, total phosphorylase and basal cAMP in hepatocytes from male and female rats

In sham-operated females, the basal phosphorylase *a* concentration, shown in Table II, was lower than the value we previously measured in hepatocytes isolated from normal female rats [10,11,25]. Thus, there was no difference in enzyme level between sham-operated males and females: the value measured in females was reduced to that found in the male. The values we previously measured in unoperated females were 12.2 ± 0.75 [10], 12.7 ± 1.3 [11] and 10.3 ± 0.67 [25], all significantly different from the value of 7.7 ± 0.4 obtained in sham-operated females. Adrenalectomy had no effect on basal phosphorylase *a* activity; it was 8 nmol/min per mg protein in all four groups. The total phosphorylase $a + b$ concentration in hepatocytes was decreased 31 and 28%, in males and females respectively. The basal cAMP concentration was increased in adrenalectomized animals, 30% in males and 34% in females. There was also a large and significant difference between males and females in the basal concentration of cAMP both in sham-operated and adrenalectomized animals: at rest, cAMP in the male was more than twice that of the females.

Influence of adrenalectomy on the response to adrenergic stimulation

Fig. 1 shows the effects of $1 \cdot 10^{-7}$ M epinephrine on cAMP, phosphorylase *a* and fractional calcium efflux in hepatocytes isolated from sham-operated and adrenalectomized male and female rats. Following adrenalectomy, the rise in cAMP was significantly enhanced: in females, 1 min after adrenergic stimulation, the peak cAMP levels were increased 5-fold compared to a 2-fold rise in sham-operated animals; in males, the peak 1 min stimulation represented in 2.5-fold increase after adrenalectomy, while there was only a 1.4-fold rise in sham-operated rats. Conversely, adrenalectomy significantly depressed the rise in ^{45}Ca fractional efflux, 30% in females and 40% in males. The net

TABLE I

EFFECTS OF ADRENALECTOMY ON HEPATOCYTES CALCIUM METABOLISM

Values are the mean ± S E. n = number of experiments.

	Females			Males		
	sham	adrenalectomized	% change	sham	adrenalectomized	% change
Total cell calcium (nmol·mg^{-1} protein)	6.29 ± 0.47(9)	8.10 ± 0.31(12)	+29	7.23 ± 0.31(17)[a]	9.47 ± 0.41(17)	+31
Exchangeable cell ^{45}Ca (nmol·mg^{-1} protein)	2.46 ± 0.10(9)	3.40 ± 0.19[a](15)	+38	3.55 ± 0.26(16)	4.59 ± 0.22[a](18)	+29
Calcium pools (nmol·mg^{-1} protein)	$n = 6$	$n = 4$		$n = 7$	$n = 10$	
S$_1$ (glycocalyx)	1.84 ± 0.11	2.88 ± 0.08[a]	+56	1.41 ± 0.22	2.04 ± 0.14[a]	+45
S$_2$ (cytosol)	0.94 ± 0.05	1.71 ± 0.21[a]	+82	1.16 ± 0.12	1.90 ± 0.15[a]	+64
S$_3$ (mitochondria)	0.33 ± 0.02	1.14 ± 0.15[a]	+245	0.28 ± 0.03	0.67 ± 0.12[a]	+139
Calcium fluxes (pmol·min^{-1}·mg^{-1} protein)						
ρ_{10} (exchange with glycocalyx)	749 ± 56	788 ± 39	–	663 ± 110	1043 ± 95[a]	+57
ρ_{21} (plasmalemmal transport)	50 ± 4	75 ± 11[a]	+50	41 ± 6	73 ± 4[a]	+78
ρ_{23} (mitochondrial exchange)	1.7 ± 0.1	5.8 ± 0.6[a]	+241	1.6 ± 0.2	3.5 ± 0.3[a]	+119

[a] $P < 0.05$ adrenalectomized vs. sham-operated animals.

result was an inhibition of phosphorylase *a* activation induced by $1 \cdot 10^{-7}$ M epinephrine: although the rise in phosphorylase was only slightly attenuated in females, the depression was significant in the male. Fig. 2 presents the dose-response curve of epinephrine on cAMP, phosphorylase *a* and calcium efflux in sham-operated and adrenalectomized male and female rats. In females, adrenalectomy enhanced the increase in cAMP evoked by adrenergic stimulation, while it depressed the rise in calcium efflux induced by $1 \cdot 10^{-7}$ M and $1 \cdot 10^{-6}$ M epinephrine; as a result,

TABLE II

BASAL LEVELS OF PHOSPHORYLASE *a*, PHOSPHORYLASE *a* + *b*, AND cAMP IN HEPATOCYTES FROM ADRENALECTOMIZED AND SHAM-OPERATED MALE AND FEMALE RATS

Values are the mean ± S.E. n = number of experiments.

	Females			Males		
	sham	adrenalectomized	% change	sham	adrenalectomized	% change
Phosphorylase *a* + *b* (nmol·min^{-1}·mg^{-1} protein)	79.1 ± 2.2(22)	57.2 ± 3.5[a](14)	−28	75.0 ± 1.6(32)	51.9 ± 2.1(32)	−31
Phosphorylase *a* (nmol·min^{-1}·mg^{-1} protein)	7.7 ± 0.4(22)	7.9 ± 0.8(14)	–	7.8 ± 0.4(32)	8.2 ± 0.6(32)	–
cAMP (pmol·mg^{-1}·protein)	2.3 ± 0.2(25)	3.1 ± 0.2[a](28)	+34	5.0 ± 0.2(34)	6.5 ± 0.2[a](32)	+30

[a] $P < 0.05$ adrenalectomized vs. sham-operated animals.

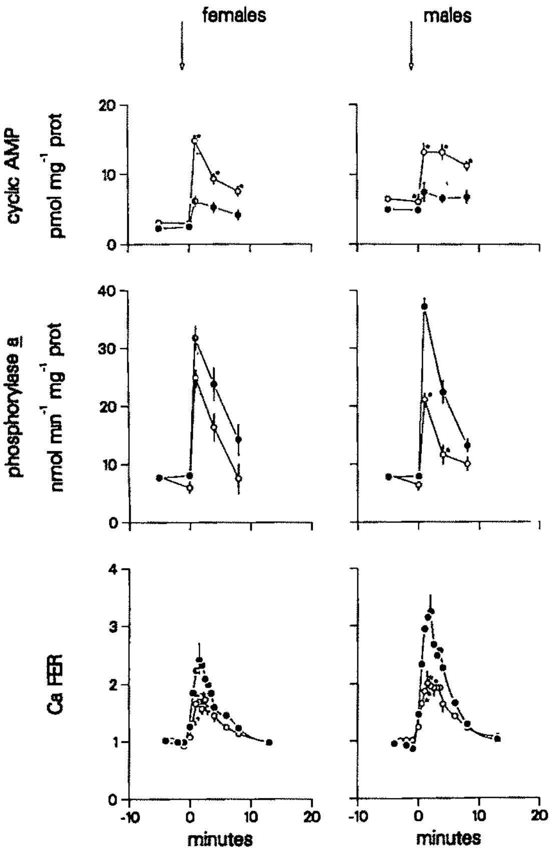

Fig. 1 Effects of $1 \cdot 10^{-7}$ M epinephrine on cAMP, phosphorylase *a* activity and calcium efflux in hepatocytes isolated from sham-operated (●) and adrenalectomized (○) male and female rats. Hepatocytes were incubated for 150 min in buffer 1, 1.3 mM Ca^{2+}, aliquots were taken for determination of basal phosphorylase *a* and cAMP, $1 \cdot 10^{-7}$ M epinephrine was then added, and the cells sampled at the time indicated. The cells used for the determination of ^{45}Ca efflux were incubated for 45 min, labeled with ^{45}Ca (5 μCi/ml) for 60 min, separated from the labeling medium and placed into perfusion chambers. After 50 min of perfusion, the medium perfusing the 'experimental' chamber was changed to one containing $1 \cdot 10^{-7}$ M epinephrine. Data from 55–75 min of the desaturation is shown. Values are mean ± S.E. of 3–8 experiments. * $P < 0.05$ comparing sham-operated with adrenalectomized rats FER, fractional efflux ratio.

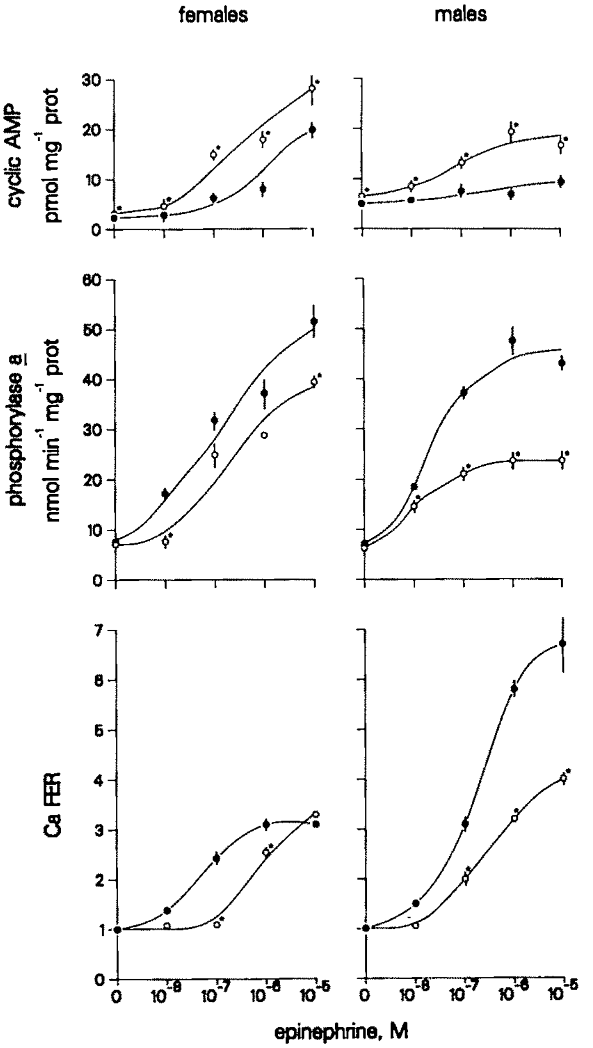

Fig. 2. Epinephrine dose-response curves of hepatocytes from sham-operated (●) and adrenalectomized (○) male and female rats. The conditions of incubation were as described in Fig. 1. Values are mean ± S.E. of the maximum response defined by the time-course shown in Fig. 1. Values are mean ± S.E. of 3–8 experiments. * $P < 0.05$ when comparing sham-operated with adrenalectomized animals. FER, fractional efflux ratio.

the stimulation of phosphorylase *a* tended to be smaller in adrenalectomized females, the difference being significant at $1 \cdot 10^{-8}$ and $1 \cdot 10^{-5}$ M epinephrine. In the male, adrenalectomy restored the β-adrenergic stimulation of cAMP, which was absent in sham-operated or normal animals. The inhibition by adrenalectomy of the rise in calcium efflux caused by epinephrine was much greater than in females, especially at high concentrations of the hormone. As a result, the activation of phosphorylase *a*, in the male, is consistently and significantly decreased by adrenalectomy at all concentrations of epinephrine.

TABLE III

ADRENERGIC ACTIVATION OF HEPATOCYTES OF ADRENALECTOMIZED MALE RATS IN THE PRESENCE OF α- AND β-BLOCKERS

Values are the mean ± S.E. *n* and numbers in parentheses represent the number of experiments.

Additions (M)	Fractional calcium efflux (experimental/control ratio)		cAMP (pmol mg^{-1} protein)		phosphorylase *a* (nmol·min^{-1}·mg^{-1} protein)	
	sham	adrenalectomized	sham	adrenalectomized	sham	adrenalectomized
None	–	–	5.03±0.20(34)	6.54±0.22 [b](32)	7.20±0.27(26)	6.27±0.35(36)
Epinephrine, $1 \cdot 10^{-7}$	4.55±0.89(5)	2.00±0.20 [b](6)	7.52±1.3(6)	13.2 ±1.6 [b](6)	37.2 ±1.62(4)	21.1 ±1.18 [b](6)
Epinephrine, $1 \cdot 10^{-7}$ + propranolol, $1 \cdot 10^{-5}$	5.22±0.40(3)	1.62±0.12 [b](4)	5.81±0.70(6)	6.30±0.43 [a](6)	41.3 ±2.2(6)	14.6 ±0.66 [ab](4)
Epinephrine, $1 \cdot 10^{-6}$	5.81±0.26(5)	3.24±0.24 [b]	6.86±0.10(2)	19.3 ±2.6 [b](4)	47.6 ±6(4)	23.7 ±1.8 [b](8)
Epinephrine, $1 \cdot 10^{-6}$ + phenoxybenzamine, 10^{-5}	1.24±0.07 [a](3)	1.10±0.06 [a](3)	6.46±0.26(2)	20.9 ±5.0 [b](4)	10.7 ±1.5 [a](4)	12.0 ±1.2 [a](4)

[a] $P < 0.05$ when compared to epinephrine alone.

[b] $P < 0.05$ when compared to sham-operated animals

Influence of α- and β-adrenergic antagonists on the response of hepatocytes from adrenalectomized male and female rats to epinephrine

In sham-operated males, the expected inhibition by the adrenergic antagonist phenoxybenzamine of the rise in calcium efflux caused by epinephrine is shown in Table III. As a result, phosphorylase stimulation was suppressed. In contrast, the β-adrenergic antagonist propranolol did not alter any of the responses in sham-operated males, indicating the absence of a β-adrenergic pathway in this group. On the other hand, in adrenalectomized males, propranolol did suppress the rise of cAMP and caused a 30% reduction in the stimulated phosphorylase activation, thus showing that a significant β-component in response to adrenergic stimulation is present in adrenalectomized males. Nevertheless, the inhibition caused by phenoxybenzamine after adrenalectomy is even more striking, since the increase in phosphorylase activity evoked by $1 \cdot 10^{-6}$ M epinephrine is reduced 50%, suggesting that even though the α-

TABLE IV

ADRENERGIC ACTIVATION OF HEPATOCYTES OF ADRENALECTOMIZED FEMALE RATS IN THE PRESENCE OF α- AND β-BLOCKERS

Values are the mean ± S.E. *n* and numbers in parentheses represent the number of experiments.

Additions (M)	Fractional Calcium Efflux (experimental/control ratio)		cAMP (pmol·mg^{-1} protein)		phosphorylase *a* (nmol·min^{-1}·mg^{-1} protein)	
	sham	adrenotectomized	sham	adrenalectomized	sham	adrenalectomized
None	–	–	2.28±1.8(25)	3.08±0.18 [b](28)	7.64±0.23(4)	7.10±0.77(6)
Epinephrine, $1 \cdot 10^{-7}$	2.42±0.27(4)	1.69±0.11 [b](5)	6.15±0.58(8)	14.85±0.83 [b](8)	37.8 ±1.8(6)	30.8 ±1.5(4)
Epinephrine, $1 \cdot 10^{-7}$ + propranolol, $1 \cdot 10^{-5}$	2.83±0.46(7)	2.08±0.39(5)	2.89±0.22 [a](4)	3.40±0.28 [a](6)	28.5 ±1.7(6)	26.3 ±2 [b](4)
Epinephrine, $1 \cdot 10^{-6}$	3.12±0.07(5)	2.54±0.24 [b](5)	5.70±1.2(2)	17.8 ±1.3 [b](10)	41.7 ±7.3(4)	37.3 ±2.3(2)
Epinephrine, $1 \cdot 10^{-6}$ + phenoxybenzamine, $1 \cdot 10^{-5}$	1.21	1.21±0.06 [a](2)	5.10±0.10(2)	14.8 ±0.05 [b](2)	29.1 ±6(4)	29.2 ±3.6(4)

[a] $P < 0.05$ when compared to epinephrine alone.

[b] $P < 0.05$ when compared to sham-operated animals.

adrenergic calcium-mediated pathway for phosphorylase is attenuated by adrenalectomy, it is still responsible for a significant part of the activation. Table IV shows data obtained from similar experiments in hepatocytes isolated from sham-operated and adrenalectomized females. As expected [10,11], the stimulation of hepatic phosphorylase *a* activity in the sham-operated adult female was mediated by both α- and β-adrenergic pathways involving respectively calcium and cAMP, and neither propranolol nor phenoxybenzamine, when administered singly, effectively blocked the phosphorylase activation induced by epinephrine. In contrast to the male, in which adrenalectomy caused a significant shift from a pure α- to a mixed α- and β-mediated adrenergic stimulation of phosphorylase, there was no difference between sham-operated and adrenalectomized females in the inhibition of phosphorylase activation by propranolol and phenoxybenzamine.

Discussion

These studies show that 1–2 weeks after adrenalectomy there are striking changes in hepatocyte calcium metabolism both in males and in females. The total ^{40}Ca as well as all of the kinetically defined calcium pools and fluxes are significantly increased. These results are consistent with the observations of Chambaut et al. [26], who showed that adrenalectomy causes an increase in liver plasma membrane calcium binding, seen in our studies as an increase in the glycocalyx pool S_1. On the other hand, studies with subcellular organelles have shown that adrenalectomy decreases the capacity of hepatic microsomes to accumulate calcium [27] and inhibits the increase in mitochondrial calcium accumulation and retention caused by glucagon [28], while corticosteroid administration causes a decrease in mitochondrial calcium uptake and retention [29]. Obviously, studies done with cell-free systems cannot be readily compared with results obtained in intact cells. But they do suggest an influence of corticosteroids on cell calcium. Recently, Chan et al. [5] concluded that adrenalectomy did not alter cell calcium metabolism. These conclusions were based on the observation that adrenalectomy does not influence the total cell calcium and the stimulation of phosphorylase *a* activity by vasopressin and ionophore A23187. However, these studies were performed only 3–5 days after adrenalectomy; the changes in cell calcium metabolism may require a longer period of corticosteroid deficiency to develop.

The lack of difference in cell calcium metabolism between sham-operated males and females is intriguing. Over a period of 3 years, this is the only group of animals kept in our laboratory in which no sex differences were observed. Moreover, this is the only group in which basal phosphorylase *a* levels were not greater in females than in males [10,11,25], an observation which supports our hypothesis that the enzyme difference is partly due to a difference in cell calcium metabolism. We have no explanation for the abolition of all the sex differences previously reported. Perhaps, the trauma of the sham operation may have disrupted the estrous cycles of the females and thus abolished the sex difference usually observed. Whether the calcium metabolism of hepatocytes changes during the estrous cycle has yet to be determined.

The decrease in total phosphorylase *a* + *b* activity has already been documented, however there are disagreements as to the changes in basal phosphorylase *a* activity after adrenalectomy [1,3,5]. The studies which reported a depressed basal phosphorylase *a* activity were done less than a week after adrenalectomy when the basal cAMP levels were not found to be elevated, suggesting that the alterations in hepatic metabolism continue to evolve after 5 days of adrenalectomy. Perhaps the elevated levels of basal cAMP may be a compensation for the decrease in total phosphorylase *a* + *b*; this may restore the normal resting phosphorylase *a* activity which can be detected in longer-term studies.

Figs. 1 and 2 clearly show that adrenalectomy altered the response to epinephrine in both males and females. It depressed the increase in calcium efflux and enhanced the accumulation of cAMP. In females, the net result is a tendency of phosphorylase *a* to be depressed (significant only at $1 \cdot 10^{-8}$ and $1 \cdot 10^{-5}$ M epinephrine), while in the male, phosphorylase *a* activity is markedly depressed at all doses of epinephrine. Thus, as far as phosphorylase *a* activity is concerned, the female appears to be affected less than the male. Whether this is translated into less severe perturbations of glucose homeostasis is unknown.

The enhanced accumulation of hepatic cAMP in response to adrenergic agonists after adrenalectomy has been well documented in male rats [2,3]. However, this is the first report that adrenalectomy induces changes in the cAMP content of hepatocytes in females. The increased cAMP appears to be caused by an enhanced adenyl cyclase activity, and not by a change in phosphodiesterase activity [30–32]. A 2–3-fold increase in the number of hepatic β-receptors (but not in their affinity) has been reported in plasma membranes from adrenalectomized female [33,34] and male rats [32]. Although no decrease in α-receptor number was ever observed [34], at least in membranes from females, Goodhardt et al. [35] have recently shown that adrenalectomy does decrease the affinity of α-receptors for epinephrine in membranes from male rats. This could contribute to the decreased α-adrenergic activation reported in this paper.

The shift from a pure α- to a mixed α-, β-adrenergic regulation of phosphorylase *a* in adrenalectomized males may represent an important adaptive advantage: since adrenalectomy decreases the total phosphorylase $a + b$ concentration and depresses the calcium signal which mediates the α-adrenergic pathway, adult male rats, which usually utilize exclusively the α-route, would be less able to mobilize effectively glucose by glycogenolysis if they did not regain the capacity, lost as adults [36], to activate phosphorylase by the cAMP-dependent β-adrenergic pathway. However, in spite of the significant β-blockade observed with propranolol, in adrenalectomized males, there is an even more striking inhibition by the α-blocker, phenoxybenzamine. Thus it appears that even though the α-mediated calcium signal is significantly inhibited by adrenalectomy, it is still responsible for much of the phosphorylase activation. In females, even though cAMP accumulation is enhanced, and the rise in Ca efflux somewhat reduced, the relative effectiveness of α- and β-blockers on phosphorylase activation remains the same in sham-operated and adrenalectomized animals.

Our studies do not provide conclusive evidence as to whether the changes in phosphorylase *a* activation are causally related to the changes in cell calcium metabolism which occur after adrenalectomy. The decrease in total phosphorylase, as well as the changes reported in other enzymes of the glycogenolytic cascade, undoubtedly contribute significantly to the effects of adrenalectomy [5]. However, the marked reduction in phosphorylase *a* activity, when the calcium signal depressed by adrenalectomy is further abolished by the α-blocker phenoxybenzamine, underline the importance of calcium in enzyme activation in the adrenalectomized animal. Chan et al. [3] proposed that adrenalectomy may primarily affect the elusive intracellular messenger, the 'putative signal' transducing α-adrenergic receptor binding into a rise in cytosolic calcium, because they found no significant alteration in cell calcium or in α-receptor binding, 3–5 days after the operation. However 7–14 days after adrenalectomy, we found significant changes in cell calcium metabolism; whether or not these changes have any relationship to the alterations in adrenergic phosphorylase activation after adrenalectomy requires further investigation.

Acknowledgements

The technical assistance of Pamela Cardillo, Philip Messer and Glenn Fleet is gratefully acknowledged. The PROPHET computer system which was used in these investigations was made available by the Division of Research Resources of the National Institutes of Health. This work was supported by United States Public Health Service Grant 1 RO1 AM26089 and 2 RO1 AM07867 from the National Institutes of Health.

References

1 Schaeffer, L.D., Chenoweth, M. and Dunn, A. (1969) Biochim. Biophys. Acta 192, 292–303

2 Exton, J.H., Friedman, N., Wong, E., Brineaux, J., Corbin, J. and Park, C. (1972) J. Biol. Chem. 247, 3579–3588

3 Chan, T., Blackmore, P., Steiner, K. and Exton, J. (1979) J. Biol. Chem. 254, 2428–2433

4 Exton, J., Miller, T., Harper, S. and Park, C (1976) Am. J. Physiol. 230, 163–170

5 Chan, T., Steiner, K. and Exton, J. (1979) J. Biol. Chem. 254, 11374–11378

6 Exton, J (1981) Mol. Cell. Endocrinol. 23, 233–264

7 Eliel, L., Thomsen, C. and Chanes, R. (1965) J. Clin. Endocrinol. 25, 457–464

8 Kimberg, D.V., Baerg, R., Gershon, E. and Graudusius, R. (1971) J. Clin. Invest. 50, 1309–1321

9 Kimberg, D.V., Schacter, D. and Schenker, J. (1961) Am. J. Physiol. 200, 1256–1262

10 Studer, R. and Borle, A. (1982) J. Biol. Chem. 257, 7987–7993

11 Studer, R. and Borle, A. (1983) Biochim. Biophys. Acta 762, 302–314

12 Berry, M. and Friend, D. (1969) J. Cell. Biol. 43, 506–520

13 Borle, A., Uchikawa, T., and Anderson, J. (1982) J. Membrane Biol 68, 37–46

14 Hutson, H., Brumley, F., Assimacopoulos, F., Harper, S. and Exton, J (1976) J. Biol. Chem. 251, 5200–5209

15 Stalmans, W. and Hers, H.B. (1975) Eur J Biochem 54, 341–350

16 Tan, A and Nuttall, F. (1975) Biochim. Biophys. Acta 410, 45–60

17 Gilboe, D., Larson, K and Nuttall, F. (1972) Anal. Biochem. 47, 20–27

18 Lowry, O., Rosebrough, N., Farr, A. and Randall, R. (1951) J. Biol Chem. 193, 265–275

19 Borle, A. and Briggs, F. (1968) Anal. Chem. 40, 339–344

20 Uchikawa, T. and Borle, A. (1978) Am. J. Physiol. 234, R29–R23

21 Jacques, J.A. (1972) Compartmental Analysis in Biology and Medicine, p. 109, Elsevier, New York

22 Sheppard, C. (1962) Basic Principles of the Tracer Method, pp. 63–64, John Wiley and Sons, New York

23 Borle, A. (1972) J. Membrane Biol. 10, 45–66

24 Borle, A. and Uchikawa, T. (1978) Endocrinology 102, 1725–1732

25 Studer, R. and Borle, A. (1984) J. Biol. Chem., 259, 3596–3604

26 Chambaut, A.-M , Leray-Pecker, F., Feldmann, C. and J. Hanoune (1974) J. Gen. Physiol. 64, 104–126

27 Friedman, N. and Johnson, F. (1980) Life Sci. 27, 837–842

28 Hughes, B. and Barritt, G. (1979) Biochem. J. 180, 291–295

29 Kimura, S. and Rasmussen, H. (1977) J. Biol. Chem. 252, 1217–1225

30 Bitensky, M., Russell, V. and Blanco, M (1970) Endocrinology 86, 154–159

31 Leray, F., Chambaut, A.-M., Perrenoud, M.-L. and J. Hanoune (1973) Eur. J. Biochem 38, 185–192

32 Wolfe, B., Harden, T. and Molinoff, P. (1976) Proc. Natl. Acad. Sci. U.S.A. 73, 1343–1347

33 Munnich, A., Geynet, P., Schmelck, P.-H. and J. Hanounce (1981) Horm. Metab. Res. 13, 18–21

34 Guellaen, G., Yates-Aggerbeck, M., Vauquelin, G., Strosberg, D. and Hanoune, J. (1978) J. Biol. Chem. 253, 1114–1120

35 Goodhardt, M., Ferry, N., Geynet, P. and Hanoune, J. (1982) J. Biol. Chem. 257, 11577–11583

36 Blair, J., James, M. and Foster, J. (1979) J. Biol. Chem. 254, 7579–7584

ANNOUNCEMENT

KEY-WORD SYSTEM OF INDEXING

Authors are requested to select a maximum of six key words (or short phrases) and include them with the submitted typescript. These will be used in the compilation of the annual cumulative index and will be printed on the title page of the published article. (Authors should note that American spelling will be used.)

Important factors of the investigation as a whole should be selected as key words and general terms like enzyme, rat, spectroscopy, etc. should be avoided. In some cases, the general term can be used when qualified; e.g. synaptic membrane, salicylate transport, etc. The key words should be chosen so that the combination of these (as they will appear in the published index) will give the reader sufficient direct information as to the relevance of a given article to his/her particular field.

Example:
Title: Oestrogen-induced synthesis of riboflavin-binding protein in immature chickes. Kinetics and hormonal specificity

Key words: Riboflavin-binding protein; Estrogen induction; Hormonal specificity; Clomiphene; (Immature chick)

The submitted list may be amended by the editorial office to ensure that index entries are consistent throughout the cumulative index. If the list appears with words in parentheses, this indicates that these words are appropriate to the article, but are not of sufficient indexing value; these words will not appear as individual index entries, but will be printed each time a key-word index entry appears.

PLANT SCIENCE LETTERS

An International Journal of Experimental Plant Biology

Editors-in-Chief
J.A. SCHIFF, Waltham, MA, U.S.A. and **J.H. WEIL**, Strasbourg, France
Associate Editor
O. CIFERRI, Pavia, Italy

Plant Science Letters publishes in the minimum time, papers recommended by its referees in all areas of experimental plant biology.
Papers describing experimental work with multicellular plants and plant-like microorganisms (protists, including algae and fungi and blue-green algae (cyanobacteria) are appropriate. Submission of manuscripts in the broad areas of biochemistry (including enzymology), bioenergetics, cell biology, development, genetics, molecular biology, physiology and structure in relation to function as well as fundamental work in these areas related to agriculture and phytopathology is invited.
The following examples of areas covered by Plant Science Letters are not exhaustive; original work of high quality in any area of experimental plant biology, broadly construed, will be welcome.
Examples of areas covered by Plant Science Letters:
Cell and tissue culture, protoplasts, cell fusion, Cell organelles including development of plastids and mitochondria, cell walls, Cellular and molecular genetics
Enzymology and intermediary metabolism
Inorganic metabolism including nitrate reduction, nitrogen fixation, sulfur metabolism, other macro and micro elements
Molecular biology of plant cells
Nucleic acids, proteins and their metabolism
Nucleocytoplasmic interactions
Photosynthesis, respiration and carbon metabolism
Phytochemistry and secondary plant products
Pigments, including biochemistry, metabolism, and biosynthesis of chlorophylls, anthocyanis, etc.
Regulation of growth, development and differentiation
Ultrastructure and cellular fractionation
Viruses
Water relations, transport of solutes etc.

Editorial Board
J. Amesz, *Leiden*
C.J. Arntzen, *East Lansing, MI*
P. Benviste, *Strasbourg*
S. Bonotto, *Mol*
G.M. Cheniae, *Lexington, KY*
R. Chollet, *Lincoln, NE*
R.E. Cleland, *Seattle, WA*
E.C. Cocking, *Nottingham*
R. Douce, *Grenoble*
E. Epstein, *Davis, CA*
G.L. Farkas, *Szeged*
L.J. Feldman, *Berkeley, CA*
G. Forti, *Milan*
M. Furuya, *Tokyo*
J. Gressel, *Rehovot*
J. Hall, *Southampton*
R.B. Hallick, *Boulder, CO*
Hu Han, *Beijing, China*
W. Haupt, *Erlangen*
R. Herrmann, *Düsseldorf*
E.J. Hewitt, *Bristol*
L. Hirth, *Strasbourg*
H. Kaldewey, *Saarbrucken*
H.W. Kohlenbach, *Frankfurt-am-Main*
A.B. Legocki, *Poznan*
F.A. Leowus, *Pullman, WA*
M.M. Margulies, *Rockville, MD*
E. Marrè, *Milan*
P. Mazliak, *Paris*
L. Mets, *Chicago, IL*
B. Parthier, *Halle, (Saale)*
P.E. Pilet, *Lausanne*
S. Puisieux-Dao, *Paris*
J. Ricard, *Marseille*
H. Stafford, *Portland, OR*
G.A. Strobel, *Bozeman, MT*
W. Tanner, *Regensburg*
L. van Vloten-Doting, *Leiden*
D.P.S. Verma, *Montreal, PQ*
C.F.L. Woodcock, *Amherst, MA*
K. Zetsche, *Giessen*

1984 - Volumes 33-37 (5 volumes in 15 issues)
Subscription price: US $ 570.00 including postage and handling
ISSN 0304-4211

ELSEVIER

Send Your orders to:
Elsevier Scientific Publishers Ireland Ltd., P.O. Box 85, Limerick, Ireland

Requests for free sample copies should be sent to

In the U.S.A and Canada
JOURNAL INFORMATION CENTER
Elsevier Science Publishing Co., Inc
P O Box 1663, Grand Central Station, New York, NY 10163, U.S A

In all other countries,
ELSEVIER SCIENTIFIC PUBLISHERS IRELAND LTD,
P.O Box 85,
Limerick, Ireland

BP 080

ADVANCES IN BIOPHYSICS

Editor: MASAO KOTANI
Associate Editor: HARUHIKO NODA

Advances in Biophysics is an international review journal to be published this year in two hardback volumes. The individual reviews are well-organized and well-documented contributions presenting a complete account of the particular author's work on a specific topic. The whole of Volume 18 is devoted to the Dynamics of Protein Folding. They aim to be understandable to the interested reader without the necessity of referral to previously published work. Therefore, pertinent background information and a short review of related studies by other scientists are also included.

1984 Volume 17
Discovery of the Role of Ca^{2+} in Muscle Contraction: The Days with the Late Professor Kamada, *H. Kinoshita.* Photophysiological Function of Visual Pigment, *T. Yoshizawa.* A Hypothesis for Neural Control of the Speed of Muscle Contraction in the Mammals, *M. Kuno.* Molecular Organization in the Head of Bacteriophage T_{eve}: Underlying Design principles, *M. Yanagita.* Dynamic Structure of Biological and Model Membranes – A Nanosecond Fluorescence Depolarization Study, *K. Kinosita.*

Volume 18
Dynamics of Protein Folding
(special editor, N. Go).
Experimental Elucidation of Pathways and Mechanisms of Protein Folding, *T. E. Creighton.* Self Assembly of Oligomeric Proteins, *A. Ikai* and *J.-R. Garel.* Dynamics of Proteins, *M. Karplus.* Prediction of Packing of Secondary Structure, *K. Nagano.* Multiple Pathways of Folding of Ribonuclease, *H. A. Scheraga.* Kinetic Intermediates of the Protein Folding, *F. X. Schmid* and *K. Kuwajima.* Liquid-like State of Side Chains at the Intermediate Stage of Protein Denaturation, *M. Oogushi* and *A. Wada.* Theoretical Studies of Folding-unfolding Dynamics, *N. Go.*

Subscription Information:
1984 Vols. 17 & 18 (2 volumes in 2 issues).
Price: US$96.00 including postage and handling.

ELSEVIER
SCIENCE
PUBLISHERS

Send your orders to:
Elsevier Scientific Publishers Ireland, Ltd. P.O. Box 85, Limerick, Ireland.
Orders from Japan and Asia between Pakistan and Korea should be sent to
Japan Scientific Societies Press, 2-10 Hongo, 6-chome, Bunkyo-ku,
Tokyo 113, Japan.

FL 37A 263

Biochimica et Biophysica Acta
Molecular Cell Research, C6(3)

Vol. 804, No. 3
July 20, 1984

Contents

Regular papers

Prostaglandin modulation of *N*-formylmethionylleucylphenylalanine-induced transmembrane potential changes in rat neutrophils (BBA 11323)
by J.C Fantone, R E Duque and S H. Phan (Ann Arbor, MI, U S A.) 265

Metabolic studies of mammalian cells by ^{31}P-NMR using a continuous perfusion technique (BBA 11317)
by R H. Knop, C.-W. Chen, J B. Mitchell, A. Russo, S. McPherson and J S Cohen (Bethesda, MD, U S.A.) 275

Transformation-associated changes in nuclear-coded mitochondrial proteins in 3T3 cells and SV40-transformed 3T3 cells (BBA 11294)
by S H Zuckerman, S Linder and J M Eisenstadt (New Haven, CT, U S A) 285

α-Adrenergic effects on ^{86}Rb^{+} (K^{+}) potentials and fluxes in brown fat cells (BBA 11313)
by E. Nånberg, J Nedergaard and B Cannon (Stockholm, Sweden) 291

Phospholipid composition of human monocytes and alterations occurring due to culture and stimulation by C3b (BBA 11315)
by F F Kennett, H.A. Schenkein, T.M. Ellis and R.B Rutherford (Richmond, VA, U S.A.) 301

The effect of glyceraldehyde on red cells. Haemoglobin status, oxidative metabolism and glycolysis (BBA 11309)
by P J Thornalley and A. Stern (New York, NY, U S.A.) 308

Proton nuclear magnetic resonance spectroscopy of isolated rabbit fundic glands (BBA 11318)
by R A. Levine, G.D. Levine, A P Healey, D.I Cook, P.W Kuchel and J.A. Young (Syracuse, NY, U.S A , and Sidney, Australia) 324

Uptake of L-[*propyl*-2,3-^{3}H]dihydroalprenolol by intact HeLa cells (BBA 11319)
by K.E. Meier and A.E Ruoho (Madison, WI, U.S.A) 331

Localization and identification of the compound causing peak 'X' in the ^{31}P-NMR spectrum of *Saccharomyces cerevisiae* (BBA 11324)
by R A Gage, W. Van Wijngaarden, A.P.R. Theuvenet, G W.F.H. Borst-Pauwels and C.A G. Haasnoot (Nijmegen, The Netherlands) 341

Polyamine requirement for prolactin action on macromolecular synthesis in the MCF-7 human mammary epithelial cell line (BBA 11320)
by B E. Linebaugh and J.A. Rillema (Detroit, MI, U.S.A.) 348

Glutathione depletion increases chemiluminescence emission and lipid peroxidation in the heart (BBA 11321)
by R. Barsacchi, G Pelosi, P. Camici, L Bonaldo, M. Maiorino and F. Ursini (Pisa and Padua, Italy) 356

Isolation of a storage and secretory organelle containing Von Willebrand protein from cultured human endothelial cells (BBA 11316)
by J.H. Reinders, P G De Groot, M.D. Gonsalves, J Zandbergen, C. Loesberg and J.A Van Mourik (Amsterdam, The Netherlands) 361

continued

Cited in. Current Contents Life Sciences - Biological Abstracts - Chemical Abstracts - Index Chemicus - Index Medicus - Excerpta Medica

INFORMATION FOR CONTRIBUTORS TO BIOCHIMICA ET BIOPHYSICA ACTA

The 1982 edition of this booklet, offering detailed guidance to authors, is available free of charge from the BBA Editorial Secretariat, P.O. Box 1345, 1000 BH Amsterdam, The Netherlands. It is also published as Biochim. Biophys. Acta 715 (1982) 1–23.

Multiple effects of interferon on myogenesis in chicken myoblast cultures (BBA 11322)
by Y Tomita and S. Hasegawa (Chiba, Japan) 370
Effect of adrenalectomy on cellular calcium metabolism and on the response to adrenergic stimulation of hepatocytes isolated from male and female rats (BBA 11325)
by R K Studer and A B Borle (Pittsburgh, PA, U S.A) 377

BIOCHIMICA ET BIOPHYSICA ACTA
International Journal of Biochemistry and Biophysics
Founded in 1947 by H G K Westenbrink, Managing Editor 1947–1964

© 1984, Elsevier Science Publishers B V
Printed in The Netherlands

All rights reserved No part of this publication may be reproduced, stored in a retrieval system, or transmitted, in any form or by any means, electronic, mechanical, photocopying, recording or otherwise without the prior permission of the copyright owner Submission to this journal of a paper entails the author's irrevocable and exclusive authorization of the publisher to collect any sums or considerations for copying or reproduction payable by third parties (as mentioned in article 17 paragraph 2 of the Dutch Copyright Act of 1912 and in the Royal Decree of June 20, 1974 (S. 351) pursuant to article 16b of the Dutch Copyright Act of 1912) and/or to act in or out of Court in connection therewith

Special regulations for readers in the U.S.A This journal has been registered with the Copyright Clearance Center, Inc. Consent is given for copying of articles for personal or internal use, or for the personal use of specific clients This consent is given on the condition that the copier pays through the Center the per-copy fee stated in the code on the first page of each article for copying beyond that permitted by Sections 107 or 108 of the U S. Copyright Law. The appropriate fee should be forwarded with a copy of the first page of the article to the Copyright Clearance Center, Inc , 21 Congress Street, Salem MA 01970, U S.A. If no code appears in an article, the author has not given broad consent to copy and permission to copy must be obtained directly from the author. Any articles published prior to 1980 may be copied for a per-copy fee of US$ 2.25, also payable through the Center. This consent does not extend to other kinds of copying, such as for general distribution, resale, advertising and promotion purposes, or for creating new collective works Special written permission must be obtained from the publisher for such copying.

Special regulations for authors. Upon acceptance of an article by the journal, the author(s) will be asked to transfer copyright of the article to the publisher. This transfer will ensure the widest possible dissemination of information.

Biochimica et Biophysica Acta, 768 (1984) 81–112
Elsevier

BBA 86109

THE DYNAMIC BASIS OF ENERGY TRANSDUCTION IN ENZYMES

BÉLA SOMOGYI [a], G. RICKEY WELCH [b,*] and SÁNDOR DAMJANOVICH [a]

[a] *Department of Biophysics, Medical University of Debrecen, H-4012 Debrecen (Hungary) and* [b] *Department of Biological Sciences, University of New Orleans, New Orleans, LA 70148 (U.S.A.)*

(Received December 16th, 1983)

CONTENTS

I. Introduction 81

II. Protein dynamical models of enzyme action 82
  A. Thermodynamic basis of the dynamical view 82
  B. Empirical foundation 85
  C. Protein-dynamical models 87
    1. Group-transfer-hydration model 87
    2. Mobile-defect model 87
    3. Electro-mechano-chemical models 87
    4. Statistical time-correlation model 88
    5. Transient-strain model 88
    6. Molecular enzyme kinetic model 88
    7. Molecular-dynamics approach 89

III. The nature of thermally-based enzyme action 90
  A. Arrhenius Law as a focal point 90
  B. The 'local' view of enzyme catalysis 91
  C. The energy-transduction modality: the 'zymon' 95

IV. Nonthermal enzyme systems 100
  A. A deeper look at the structural-functional design of the enzyme molecule 102
  B. Protein dynamics in organizd states 104
  C. Kinetic features of nonthermal enzyme systems. 105

Summary 107

knowledgements 109

Note added in proof 109

References 109

I. Introduction

In bioenergetics, one is usually concerned with modalities underlying the transduction (coupling)

---

[*] To whom all correspondence should be addressed.

Abbreviations: E, enzyme; S, substrate; P, product; T, transition.

0304-4171/84/$03.00 © 1984 Elsevier Science Publishers B.V.

of free energy between such 'sources' as (photo)redox reactions and such 'sinks' as ATP synthesis, ion pumps, metabolite transport, inter alia. Yet, as phrased by Nicholls [1], "all biochemical reactions involve energy changes, so the term 'bioenergetics' could be ap-plied to the whole of biochemistry". Extending this ratiocination one step further, we approach *the enzyme molecule* – the very catalyst of biochemical rate processes. Teleonomy has charged enzymes with the task of catalyzing material/energetic transformations at rates, and under appropriate conditions, commensurate with the vitality of the cell. Most importantly, the enzyme acts to reduce the activation energy for the respective (electro)chemical reaction. Frugality dictates this role, in view of the restricted temperature range suitable for living cells, as well as limitation on intracellular reactant concentrations posed by consideration of cytosolic solvent capacity [2,3].

The striking feature of enzyme action, as observed in vitro, is its manifestation in a *random-field environment*. There is an emergent view, that the enzyme molecule is a beautifully intricate energy transducer, serving as a 'deterministic mediator' between the molecular chaos of the environment and the localized chemical-reaction coordinate [4]. Moreover, there are growing indications that metabolic enzymes *in organized states* are designed to 'plug into' long-range energy continua in vivo, serving as devices to channel non-thermal energy coherently to the bound chemical subsystem [5,6]. (Of course, this scheme is familiar in the well-known enzyme systems (e.g., F_0F_1-H^+ ATP synthetase) of bioenergetics [7,8].) The basis for this modality lies in the structure/function relationship of the individual protein molecule.

In the past 100 years of enzymology [9], much concerning the role of enzymes in catalysis has been elucidated. Binding substrates and prosthetic groups at specific positions within their structure, they provide the optimal three-dimensional constellation for effectuation of the chemical reaction. And, their presence in membranes generates, for example, coupling between transmembrane fluxes and chemical reactions [10]. Yet, for most of these catalytic functions, the enzyme protein seems ostensibly, to be *too big*. Consequently, the question has arisen [4], whether perhaps an important aspect (indeed, maybe the 'secret of enzymes' [11]) has been overlooked: *enzyme catalysis cannot be based on a static picture of the protein.*

The old notion, that the overall structure of an enzyme serves the singular role of maintaining statically a requisite three-dimensional arrangement of active-site residues, has become outmoded [12–18]. Accumulating evidence has revealed a rich variety of internal motions in globular proteins, spanning a virtual gamut of time-domains and encompassing essentially every part of the protein structure. Of particular interest are frequencies outside the range of the well-known folding-unfolding transitions and gross conformational changes. Cognition of the dynamic nature of the protein matrix has spawned the development of a number of theoretical models of enzyme action [19]. These dynamical models propose, that particular classes of motions in the protein structure provide means for collimating energy to produce high free-energy events for passage of the bound chemical subsystem into the transition state. For enzymes operating in bulk solution, the source would be fluctuations in the protein molecule, as it exists at thermodynamic equilibrium with the solvent (heat bath). In the case of organized enzyme assemblages, the enzyme may actually function in the performance of net work on the surroundings – serving to transduce energy from an external (nonequilibrium) source to the chemical subsystem.

In the present article, we shall review the basic tenets of the dynamical models of enzyme action in bulk solution. We shall attempt to glean common threads permeating all of these models, and to abstract a generalized view which may gi[illegible] some degree of unification. Then, we exceed t[illegible] level of the isolated protein molecule and explo[illegible] the relevance of the 'dynamic view' to non-therma[illegible] systems in organized states.

II. Protein dynamical models of enzyme action

IIA. Thermodynamic basis of the dynamical view

Traditional analytical methods of *averaging* over time and over ensembles of protein molecules give the superficial picture of a static structure. However, in the thermodynamic sense, individual protein molecules are quite small systems consisting of relatively few particles. Hence, statistical fluctuations in thermodynamic properties assume much greater importance. For example, consider the mean square fluctuation of internal energy, E, given by:

$$\sigma_E^2 = kT^2 mC_v \tag{1}$$

where m is the mass, C_v is the heat capacity (at constant volume), k the Boltzmann constant and T the absolute temperature. For typical values of the parameters, Cooper [20] has calculated the root-mean-square fluctuation in E to be $2.7 \cdot 10^{-19}$ J *per protein molecule*. (If all protein molecules in the solution were to fluctuate *in synchrony*, this value would correspond to an energy fluctuation of about 160 kJ/mol!) Despite the results from time-averaged studies of ensembles of proteins, which indicate a static and compact structure, sizeable variance in a number of thermodynamic properties is possible (see also Refs. 21 and 22). Of course, extremes of the fluctuational spectrum are relatively rare. And, the time-scale of the fluctuations for many thermodynamic quantities is very short. Hence, proteins do not denature appreciably at a given physiological temperature!

The energy-transduction aspect of thermally based enzymes, as it relates to the Second Law of Thermodynamics, has been discussed by a number of authors [4,23,24]. Enzymes operating in bulk solution achieve catalysis by generating locally high free-energy events (at the active site). Notwithstanding, the protein molecule – at thermal equilibrium with a reservoir at constant temperature and pressure – does not use heat energy to perform net work on the surroundings (i.e, thermally based enzymes do not affect chemical equilibria). Now, the Second Law of Thermodynamics says that the Gibbs free-energy function, $G = H - TS$, for the protein cannot increase (where H is the enthalpy and S is the entropy). However, if before transduction, $G_1 = H_1 - TS_1$, and afterwards, $G_2 = H_2 - TS_2$, then, the Second Law of thermodynamics allows $\Delta G = G_1 - G_2 = 0$, if the enthalpy and entropy changes are compensated (i.e., $\Delta H - T\Delta S = 0$). As stated by Kemeny [23], "this does not mean that heat energy is turned into free energy but rather that the transduction of internal energy and heat exchange with the reservoir are part of the same mechanism". The fluctuations, necessary for proteins to function, not only do not contradict the Second Law of Thermodynamics, but are *a consequence of its statistical nature.*

Any functional feature of the enzyme molecule *in bulk solution* will be based on the thermal properties of the system at equilibrium with the solvent phase (see Section III). *We define 'thermally-based enzyme action' in the following way*: because of its size (with much greater density of energy levels), the bulk reservoir controls the situation through its energy-level density (its entropy) and forces upon the system the *canonical distribution* of states (within the internal constraints on the atomic particles in the folded globular protein). Free-energy linkage in the protein is based on the equilibrium fluctuational character of the system under this condition. In order to define 'conformational free energy', one notes that a macroscopically observed conformation of a protein corresponds to *a mixture* of a number of instantaneous (microscopic) conformational states in thermal equilibrium [29,30]. Each of these states represents a point (P,R) in the phase space of momenta (P) and generalized coordinates (R) of the protein. The probability of a given state is determined by the Boltzmann factor, exp $(-E(P,R)/kT)$, where $E(P,R)$ is the total (kinetic plus potential) energy of the protein in the state (P,R). One can define the statistical-mechanical *partition function*, Z, for the protein as:

$$Z = (\text{constant}) \cdot \int \exp(-F(R)/kT)\, \mathrm{d}R$$

where $F(R)$ is the potential energy [29]. $F(R)$ is a sum of two terms: the intramolecular interaction energy of the macromolecule in the absence of solvent *and* the free energy of solvation. $F(R)$ represents a 'potential of mean force' operative on the protein molecule for various configurations of the solvent particles. Then, the (Hemholtz) *free energy* of the protein conformation is defined as $-kT$ ln Z [29,30]. If a number of microscopic states contribute to the partition function, then any 'property' of the system, A (e.g., substrate binding, catalytic constant), will be a weighted average over all such states, as follows:

$$\langle A \rangle = \int A \cdot \exp(-F(R)/kT)\, \mathrm{d}R$$

with integration performed over the accessible conformational (coordinate) space [31]. This situation indicates that, in the event a given function of the enzyme requires *fluctuation* between specific microstates, it will not be revealed in studies of the macroscopic conformation.

Lumry and coworkers [25–27] have developed in great detail the *enthalpy-entropy compensation* concept, as the root of free-energy linkage in enzymic processes. In attempting to grasp the thermodynamic basis of enzyme action, as it relates to the macromolecular properties of proteins, we will pursue Lumry's idea. We begin by distinguishing, that in a system such as a protein molecule, G, P and T must be constant (to a very high order), in contrast to H, S and V. It is in fluctuations of the latter quantities that one must seek the dynamical features of enzyme catalysis. In particular, as suggested by Lumry [26], "there is increasing evidence that enthalpy (H) fluctuations have been exploited by nature in the evolution of many biological functions".

Lumry has elaborated his 'motive' view of enzyme dynamics from a *composite representation* of the equation for free energy, $G(T)$, due to Max Planck (*Treatise on Thermodynamics*), as stated more recently by Benzinger [28]. At issue is the fundamental point, that *G and ΔG (under isothermal conditions) can contain no heat terms.* One decomposes the enthalpy part into a sum of two terms: $H(0)$, which is the potential energy and zero-point vibrational kinetic energy; and $\langle Q(T) \rangle$, the *mean heat* contained in the system, obtained by integrating the constant-pressure heat capacity, C_p, from 0 K to T. This pure heat part, $\langle Q(T) \rangle$, is called a *compensation enthalpy*, H_{comp}. It describes the fluctuations of internal energy and volume between the system and environment, as can be seen from the relation, $C_p(T) = \sigma_H^2/kT^2$, with $\sigma_H^2 = \sigma_E^2 + P^2\sigma_V^2 + T\sigma_{EV}$ [26]. (This term has negligible influence for small-molecule systems.) In principle (although rarely in reality), any system in equilibrium with a reservoir could, via a fluctuation, temporarily lose its total heat energy (Q). For a chemical change involving the system, the part ΔH_{comp} has nothing to do with the actual mechanism of the chemical reaction; this is specified only by $\Delta H(0)$, the 'motive' part [28]. In fact, the Second Law of Thermodynamics requires that, in the overall expression of ΔG, ΔH_{comp} be negated (compensated) by a term $T\Delta S_{\text{comp}}$ due to a *compensation entropy*. One finds that S_{comp} is just equal to $\langle Q(T) \rangle / T$ [26].

A crucial message from this representation is that the enzyme molecule cannot effect catalysis (i.e., lower the activation energy) by serving as a reservoir of excess heat [27]. Moreover, the enzyme cannot collimate *heat* energy (i.e., that from individual molecular, collisional events at the protein-solvent interface) *directly* to the active site, for the performance of work. If a fluctuation delivers a certain enthalpy to a region of the protein (e.g., active center), it is 'paid for' by an entropy change elsewhere in the macromolecule. The role of fluctuations is just to set the *course* of free-energy transfer and storage in the enzyme. The 'motive' part of the transition-state ΔG corresponds to the *mise en scène* of enzyme catalysis, while the 'compensation' (fluctuation) part is the *mise en train*.

As indicated by Lumry (unpublished data), "the dynamical features of proteins are manifestations of enthalpy and entropy fluctuations between protein and environment, and of redistributions of H and S within the protein". Most globular proteins exist in solution as an equilibrium mixture of a number of different conformational states of approximately the same free energy. An enzyme function may depend on fluctuation among these states (as well as fluctuation between protein and solvent), as a means of attaining the proper enthalpy-entropy arrangement defining the transition-state passage (see subsection IIC-2). Lumry and Biltonen [25] designated this idea, the 'free-energy complementarity principle', whereby the enzyme macromolecule and its bound chemical subsystem engage in a fluid and variable exchange of free energy during the course of catalysis (see Fig. 1). That is, the protein matrix serves as a fluctuating free-energy 'reservoir' in the generation of the catalytic configuration.

The consonance of the energy-transduction idea and the Second Law of Thermodynamics is demonstrated further in an approach, taken by Careri et al. [11,24], based on tenets of *near-equilibrium* (linear) *thermodynamics*. For a system of composite flows, J_i, and conjugate forces, X_i, operating close to equilibrium, we may write:

$$J_i = \sum_j L_{ij} X_j \tag{2}$$

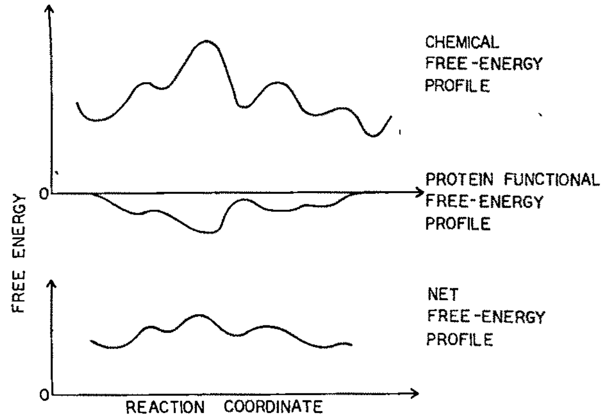

Fig. 1. Simplified example of the flattening of the net free-energy profile through 'complementarity' developed between the chemical parts of the protein-supported process and the conformational contribution from the functional conformation process of the protein. (Reproduced from Ref. 25 with the kind permission of the publisher and of the authors.)

where the phenomenological coefficients L_{ij} form the so-called 'Onsager matrix'. Coupling of various composite processes is potentiated by nonzero off-diagonal elements in this matrix. Since enzymes must function reversibly around equilibrium, this formalism might be applied to the coupling between protein-surface events and active-center processes. To wit, Careri et al. [11,12,24] maintain that statistical fluctuations, e.g., in the density of bound water are coupled to position-fluctuations of active center groups (see Section IIC). The only thermodynamic requirement, owing to the equilibrium character, is that the time-average of the *dissipation function*, ϕ, vanish, i.e,:

$$\bar{\phi} = \overline{J_i X_i} = 0 \tag{3}$$

which assumption seems justifiable in the overall operation of the enzyme. Moreover, when the equilibrium relaxation times of the coupled processes are similar transduction can be very efficient [12].

In summary, we can state that *fluctuational behavior is the direct mechanism for free-energy linkage in the enzyme* [11]. The foregoing considerations raise a question, as to how much of the free-energy configuration of the enzyme transition-state arises from heat exchange with the solvent (bath) and how much is 'borrowed' from the protein macromolecule (see Section III). Also, the physical nature of the 'heat exchange' between protein and medium, and, as well, how it affects the internal redistribution providing for free-energy transduction, are subjects of concern (see Ref. 32 and Section IV).

IIB. Empirical foundation

In principle, the internal (e.g., vibrational) motions of large molecules like proteins, interacting thermally with their environment, can be predicted by quantum-statistical laws. The population of the nth level of molecular vibrations is calculated as:

$$P(n) = \frac{e^{-nh/\lambda kT}}{\sum\limits_{n=0}^{\infty} e^{-nh/\lambda kT}} \tag{4}$$

as discussed for example by Peticolas [33]. (Here, λ is the wave-length and h is the Planck constant – see subsection IIIB). Some features of protein dynamics (particularly, the large-scale, slower motions of whole segments of the protein) can be studied with existing experimental technology. However, an unequivocal correlation of such motions with functional properties of a protein is one of the most difficult problems in molecular biology [11,12]. The empirical basis of the protein-dynamical view of enzyme action is, presently, rather inferential.

Well-known methods for studying protein dynamics include hydrogen-deuterium exchange [34], NMR (and ESR) [35], laser-excited luminescence techniques [36–42]. subnanosecond-scale fluorescence depolarization [43], and light scattering [44]. Frauenfelder and coworkers [21] have developed elegant means for looking at protein motions, through temperature-dependent X-ray crystallography (cf. Ref. 22). And, they [18] have provided a model system for examining the role of protein fluctuations in ligand binding, using flash photolysis. In particular, fluorescence-quenching methods have found increasing usage in the elucidation of protein motions [13,45,46]. The possibilities of participation of nanosecond-scale motions in enzyme activity have been revealed for particular enzymes [41,46]. (However, some quenching data have been interpreted also in an alternative way [47].) Recent refinements of this technique include *double-*

quenching methods, for distinguishing between surface fluorophors (e.g., tryptophan) and those buried within the globular protein [42]. Förster-type resonance energy transfer has also been applied to the analysis of protein fluctuations [48]. Virtually all of these many approaches share the common characteristic, unfortunately, that functional properties (e.g., catalytic action) can very rarely be examined *simultaneously* with the actual study of the protein dynamics.

Kinetic experiments, following ligand-binding and catalytic activity as a function of varying environmental conditions (e.g., viscosity), have given *suggestive evidence* for the general role of protein dynamics [4,18,41,42,49–52]. Likely candidates for direct verification are those enzymes, whose active regions operate in a 'hinge-bending' manner [53]. Following the course of such motion, parallel to ligand association/dissociation and/or catalysis, may yield clear evidence. Positive results from these relatively simple systems will give more validity to the various indirect evidences and to the theoretical modeling.

Direct measurement of protein fluctuations in the microsecond or millisecond time-range, more closely relevant to that of most enzyme catalytic-turnover number, has not been possible. However, recently developed techniques using time-resolved phosphorescence anisotropy, delayed fluorescence, and ground-state depletion may yield such a time-window [38–40,54].

There must be given increased attention in the future to the nature of events occurring *at the protein-solvent interface.* As stressed so cogently by Careri et al. [12], the coincidence of the time-domains of enzyme-catalytic processes with the time-domains of many internal protein motions seems beyond fortuity. This is especially important for the case of *water-protein interaction* [12,24–27, 55–57]. Kinetic and thermodynamic studies have suggested that protein hydration plays a critical role in the dynamics and energetics of enzyme action.

There have been virtually no attempts, thus far, to study internal protein motions *during the course of enzyme action.* Experimental verification, of the direct participation of protein dynamics, is a challenging task and of fundamental importance to our understanding of the mechanism of enzymes. Although recent advances in experimental techniques hasten the attainment of that goal, such efforts remain hindered by a number of difficulties. Even the most sensitive methods demand a certain critical subpopulation of active enzyme molecules in a given sample. Association/dissociation conditions, for example, make it difficult to realize the requisite ligand-saturated concentration of active enzyme and, concomitantly, the perceptible rate of product formation (or substrate consumption). It is hoped that these technical difficulties will be overcome with advancing methodologies.

Experimental thermodynamics (e.g., calorimetry) may yield some useful avenues into the energy-transduction problem. However, conventional thermodynamic analyses of enzyme reactions yield little insight in this regard. This is particularly applicable to measurements of overall ΔG values. As discussed in subsection IIA, G and ΔG contain no information about the 'heat' and, thus, no information about fluctuations. Moreover, in systems (such as protein-based reactions) with large ΔC_p, ΔG does not relate in a straightforward manner to ΔH and ΔS [25,26,28]. As stressed by Lumry (unpublished data), "if the fluctuational basis for biological function proves to be correct, we have been in the extraordinary position of making all the measurements but whose we need the most". In principle, heat-capacity studies over wide temperature ranges (ideally, down to 0 K) are necessary, in order to separate the 'motive' and 'compensation' (fluctuation) parts of ΔG. Yet, such approach is difficult in practice [26]. Other authors (e.g., Refs. 23, 52, 63) have discussed the applicability and limitations of thermodynamic analyses in the study of enzyme reactions.

The dynamical nature of enzyme action is rapidly gaining firm theoretical foundation; and, there is a clear and present challenge in the experimental realm. The 'message' emerging from the energy-transduction aspect implies, as phrased by Lumry (unpublished data), "a harder and longer road to understanding of biological mechanisms than has been generally anticipated. However, the devil we know is better than the devil we don't, or so stills appears to be the case in science".

IIC. Protein-dynamical models

Let us look briefly at the features of the thermally based protein-dynamical models of enzyme action (see Refs. 4 and 19). What differentiate the various models are the types of *surface phenomenon* assumed to serve as the source of the energy and the suggested *mode of linkage* between the ambient source and the enzyme active-site.

IIC-1. Group-transfer-hydration model

Low and Somero [55,56] have offered a mechanism of enzyme action, involving the hydration properties of residues on the protein surface. The model proposes that the transfer of surface amino-acid groups into or out of the protein interior, during rate-limiting steps of enzymic processes, may modify the energetic characteristics of catalysis. These energy changes are due to alteration in the organization of water around surface side-chains. The observed perturbing influence of neutral salts on enzyme catalysis is considered in support of this notion. The *temporal connection*, between the surface-group transfers (which, in reality, are probably slight 'flickers') and specific catalytic events, may be part-and-parcel of other energy-transduction models below.

IIC-2. Mobile-defect model

Lumry and Eyring [58] suggested long ago, that many protein functions might be based on energy (and volume) fluctuations, due to extremes in vibrational and bond-rearrangement features. More recently, Lumry and Rosenberg [59] formalized this notion into a specific model – the 'mobile-defect hypothesis'. Local regions of the globular protein where distortions and poor secondary (e.g., hydrogen) bonding occur are termed 'defects'. The previous authors [59] proposed that, "proteins are selected to have a considerable amount of free volume which migrates, collecting to form moderately large cavities on occasion and dispersing into small vacuoles continuously without appreciable change in free energy among the conformers so produced by the migration of these 'mobile defects' "(see Fig. 2). These 'defects' are interconnected in a highly cooperative manner, correlated by atomic packing and bonding patterns in the protein fabric [14]. Their occurrence implies local, transient increases in free energy, which, in the vicinity of the enzyme active center, could direct mechanical strain along reaction coordinates relevant to catalysis.

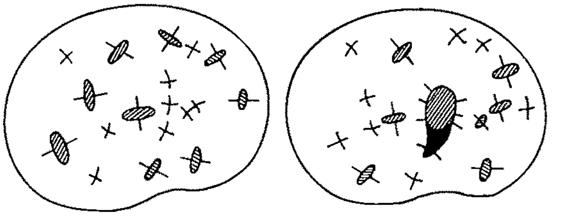

Fig 2. A rough two-dimensional projection of channel production by rearrangement of the free-volume increments associated with mobile defects. Channel is shown in the right figure. Crosses represent regions of good bonding which are potential defects. Cross-hatched ellipsoidal symbols are defects showing broken hydrogen bonds. (Reproduced from Ref. 59 with the kind permission of the authors.)

IIC-3. Electro-mechano-chemical models

Electro-mechano-chemical models view the enzyme specifically as a thermally activated inducer of substrate-bond polarization or distortion. This view has been developed by a number of workers. Green et al. [60] suggested that oscillatory motion of the protein generates, transiently, a stabilized conformational state in which the bound substrate is subjected to directional (local) electric fields relevant to catalytic events. This electro-mechano-chemical view assumes that critical active-site coordinates are coupled specifically to low-frequency,

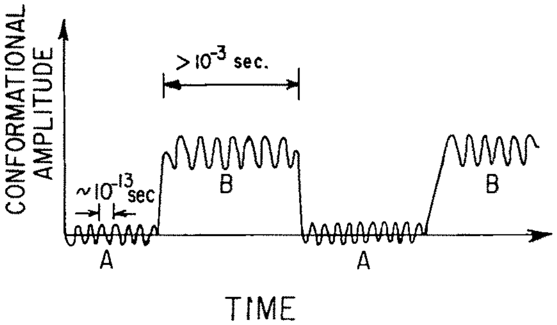

Fig. 3. Diagrammatic representation of the periodic flip of a protein from one conformation (A) to another (B), in the 'electro-mechano-chemical' model of Green (Ref. 60). The oscillatory motions of the protein due to atomic vibrations are orders of magnitude faster than the conformational fluctuations. (Reproduced by kind permission of the author and of the publisher.)

collective vibrational modes of the protein structure (see Fig. 3). In order for the critical, internal protein coordinates to be strained long enough for initiation of the catalytic process, the electro-mechano-chemical model proposes that intramolecular interactions (e.g., hydrogen bonds) would stabilize, intermittently, the protein conformation at extremes of the oscillatory motion. Fröhlich [61,62] has cast the electro-mechano-chemical model into a rigorous physical form, relating to the dielectric properties of proteins. Here, metastable conformational states are assumed to be coupled to giant dipole oscillations in the protein. Alternatively, Blumenfeld [63] proposed that enzyme catalysis might be linked to a protein-conformational *relaxation* – as opposed to a transient *strain*.

IIC-4. Statistical time-correlation model

A statistical model, developed by Careri et al. [11,24,65], proposes that the 'secret of an enzyme' lies in its ability to let the relevant conformational fluctuations occur with a well-defined *time correlation*. This does not mean a *rigid coupling* between conformational variables, rather a statistical correlation in their rate of change around equilibrium. From typical numerical values of enzyme-catalytic constants and of associated activation-energies, the previous author [11] determined that 'active' conformational fluctuations must originate from that part of the frequency spectrum which is centered around 10^8 s^{-1}. Canvassing the literature, concerning the various kinds of fluctuations which occur within globular proteins and at the solvent interface, one notes the occurrence of quite a number of different statistical events (e.g., relaxation of bound water, proton-transfer reactions, local conformational motion (breaking of hydrogen bonds), solvent charge-density fluctuations), having a similar correlation time in the range 10^{-9}–10^{-7} s. In this view, it is proposed that the internal enzyme structure is 'programmed', such that the temporal course of catalytic events is governed through the spacetime fluctuating nature of solvent-surface interactions.

IIC-5. Transient-strain model

The transient-strain model was constructed by Gavish [66,67] and later by Frauenfelder's group [18,52]. It also focuses on a critical active-center coordinate(s) and assumes, as above, that enzymatic function is governed by transient strains developed during conformational transitions. Physically, the model views the structural fluctuations of the enzyme-substrate complex, around the critical reaction coordinate, as the motion of a particle connected to a spring imbedded in a viscous liquid and acted on by a random force (i.e., the protein matrix is considered a 'Fokker-Planck fluid'). Interacting with the impinging solvent molecules through random collisions and frictional forces, the fluctuating protein structure has a certain probability of reaching a given degree of internal strain (see Fig. 4). Basing the model on the *Kramers theory of chemical kinetics,* Gavish [66,67] and Beece et al. [52] obtained an explicit formulation of the enzyme catalytic rate constant, k_{cat}, as:

$$k_{\text{cat}} = \left(A/\eta_s^{\epsilon} + A'\right)e^{-\Delta/kT} \tag{5}$$

where Δ is the 'activation energy' (enthalpy), η_s is solvent viscosity, A is a function of structural parameters characterizing the potential-energy profile, the exponent ϵ (where $0 < \epsilon \leqq 1$) relates the attenuating influence of the protein matrix on solvent viscosity, and A' is an empirical (viscosity-independent) parameter.

IIC-6. Molecular enzyme kinetic model

This model, developed by Somogyi and Damjanovich [4,68–72], also focuses on the issue of 'energization' at the protein-solvent interface. It is supposed that there is a specific statistical coupling of events at the interface with the catalytic process. However, no explicit assumption has been made regarding the manner of coupling to 'reaction-center coordinates'. Originally, it was proposed that the energy for catalytic events is exchanged between the protein and its environment, by means of interaction patterns with solvent/solute particles, and that this energy-exchange is correlated in some way to the active site. Broadly, the term 'collision' can be interpreted as direct momentum transfer *or* as a local binding/relaxation impulse (see subsection IIC-4). The model proposes that catalytic processes demand 'collisional' excitation on the protein surface, with well-defined organizational patterns *in space, time, and energy*. The model yields an explicit form of the enzyme-catalytic constant, as:

$$k_{cat} = \frac{\tilde{P}}{\eta_s} e^{-\tilde{E}_c/kT} \tag{6}$$

where η_s is solvent viscosity; $\tilde{E}_c$ is a composite symbol, representing a method of averaging and conditional probability according to the manner by which the enzyme molecule progressively accumulates the requisite energy; and $\tilde{P}$ contains probability factors defining formally the specific pattern of interaction between the protein and the solvent/solute system [69].

IIC-7. Molecular-dynamics approach

In recent years, *molecular dynamics* has emerged as a powerful method for computing the average and time-dependent properties of protein systems [15–17,73]. Basically, this involves computer-integration (for a finite time period) of the classical equations of motion for all the atoms of the molecule. Such approach has yielded significant conclusions apropos of enzyme function. For example, it has been found that the most important influence of the *solvent* is on the dynamic average structure of the protein [74]. The magnitudes of atomic fluctuations in the interior of the protein are little influenced by the presence of solvent (as compared to that in vacuo), while there is an increase in the relaxation times of these fluctuations. However, for atomic groups *at the protein surface*, the solvent alters both the magnitude and the time-course of the fluctuations. The motions of surface atoms are found to have a more *correlated, diffusive character* in the presence of solvent, than for the in vacuo case. A study [75] of the time-dependence of the atomic motions indicates that *groups of atoms in the protein move ('diffuse') collectively*, as single 'quasi-particles'. These collective, low-frequency

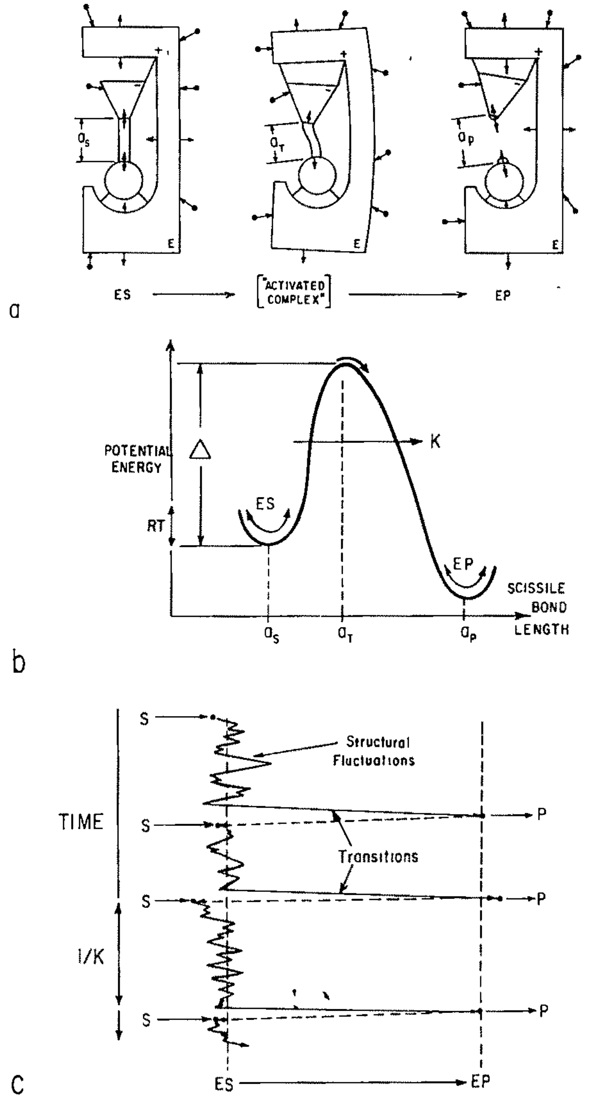

Fig. 4. Transient-strain model of enzymic catalysis (see Ref. 51) (a) Discrete catalytic steps during the cleavage of a specific bond in a substrate S, which forms a complex with the enzyme E to give a product P. The binding of E to either S or P may include electrostatic interaction between charges. The bond breaking occurs during the transition through the 'activated complex', shown during its decay to EP (note the distortion in E and S). The latter dynamic process is the result of structural fluctuations. These originate from the collisions of the solvent's molecules (black circles with arrows) with the complex, accompanied by various modes of motion of parts of the complex through the solvent (small arrows), which acts to dissipate their kinetic energy. a_S, a_T and a_P are the lengths of the scissile bond at the discrete states shown above. (b) Description of the catalysis by means of potential energy vs. scissile length. Structural fluctuations (double-edge arrows) possess an average thermal energy, RT. The conformational transitions ES → EP occur at rate k by overcoming an energy barrier of height Δ. (c) The evolution in time of structural fluctuations and conformational transitions. The horizontal dashed lines represent the assumption that after releasing the product the enzyme rapidly reaches its initial state. The steps of formation or breaking the complex (denoted by points) are assumed to be relatively rapid processes. (Reproduced with kind permission of the authors and of the publisher.)

'modes' have an inhomogeneous character and, because of their extended nature, would be more sensitive to the solvent environment. Indeed, Swaminathan et al. [75] suggested the possibility, that such 'quasi-paricles' are involved in transmitting solvent effects to the protein interior (e.g., enzyme active-site). Very recently, Northrup et al. [76] described a molecular-dynamics rate-constant formulation, applicable to reaction rates of activated process in globular proteins (see Section III).

III. The nature of thermally based enzyme action

IIIA. Arrhenius Law as a focal point

Clearly, the central theme of Section II is the idea that the enzyme is an energy transducer, in the sense that spatiotemporal ordering of the fluctuational behavior of the protein molecule serves an integral role in catalysis. The great number of atomic components in a protein molecule and the stochastic nature of their thermal motions dictate that meaningful theoretical modeling must ultimately employ the tools of statistical mechanics – in particular, a *correlation-function* formulation (see subsection IIIC). It is not possible at present to pursue this course with great precision, due to the paucity of information on the dynamic nature of the protein interior. From the standpoint of free-energy transduction (as distinct from the matter of mere structural stability), there appear to be two relevant pictures of the protein matrix: (i) *a dense, hard-sphere fluid* [15,16] and (ii) *a fluctuating network of hydrogen-bonded particles* [12,59,62,65, 77,78]. Thus far, both representations have contributed to our (rather crude) understanding of the energy-transduction process. Probably, a given enzyme protein employs some combination of the two in its catalytic function. (Perhaps, we might avoid the distinction and simply designate the protein a 'liquid crystal' [79].)

Progress, in the dialectical course toward elucidation of the dynamical 'secret' of enzymes, may be fostered by recognition and unification of common features in the various models above. Here, we present a generalized view which embraces ideas from all of the models. Our approach is a purely formal one, as none of the models have yet to acquire a sufficiently rigorous mathematical rate-constant formulation (cf. subsections IIC-5, IIC-6 and IIC-7 above).

We begin, by considering the protein (transducing unit) as a structure imbedded in (and at equilibrium with) a large thermal reservoir at constant temperature and pressure, as per the discussion in subsection IIA above. We make the usual assumption that the enzyme-substrate complex, ES, proceeds toward product in the manner, $\mathrm{ES} \rightleftarrows (\mathrm{ES})^{\ddagger} \rightleftarrows \mathrm{EP} \rightleftarrows \mathrm{E} + \mathrm{P}$, where $(\mathrm{ES})^{\ddagger}$ represents the 'activated complex' (transition state, or saddle point). We suppose that the transition ES → EP is rate-determining on the forward pathway. The rate constant, k_{cat}, characterizing this step is our concern. The overall free-energy change associated with the transition state may be decomposed into two contributions: that from *chemical processes* (e.g., E-S binding, solvation/desolvation effects) localized specifically at the active site, and that from the *protein matrix* interacting with the bound chemical subsystem [4,51,52]. We shall consider only the latter contribution. We assume any rate process involving the protein to be characterized by a *fluctuation enthalpy*. Hence, if a catalytic event demands an enthalpy $h^{\ddagger}$ in the protein, the rate (following the aforementioned treatment by Kemeny [23]) will be given by the *rate of occurrence of fluctuations:*

$$k'_{\mathrm{cat}} = k_{v} \cdot W(h^{\ddagger},T) \tag{7}$$

where k_v is a frequency factor and $W(h^{\ddagger},T)$ is a probability distribution describing the fluctuating enthalpy of the protein at temperature T. (The 'prime' on k_{cat} reminds us that we are considering only the *protein contribution* to the transition-state passage.) This distribution has the form:

$$W(h^{\ddagger},T) = \exp\left(- \frac{(h^{\ddagger} - H) - T(s - S)}{kT} \right) \tag{8}$$

where H and S are mean enthalpy and mean entropy, respectively, of the protein body. The factor s is a fluctuation entropy defined by:

$$s(h^{\ddagger}) = k \ln g(h^{\ddagger}) \tag{9}$$

with $g(h^{\ddagger})$ the density of states (or statistical weight).

One might make the correspondence to the usual transition-state formalism, by defining an 'activation enthalpy', $\Delta H^{\ddagger} = h^{\ddagger} - H$, and an 'activation entropy', $\Delta S^{\ddagger} \leq s - S = \Delta S^{0}$, where ΔS^{0} represents an *upper limit*. The latter identification comes from the realizaton, that not all states with the requisite energy fluctuation will be effective in the given rate process. That is, the energy must appear *in the proper degrees of freedom.* Accodingly, we may rewrite Eqn. 8 as:

$$k'_{\mathrm{cat}} = k_{\upsilon}\, \mathrm{e}^{\Delta S^{\ddagger}/k}\, \mathrm{e}^{-\Delta H^{\ddagger}/kT}$$

$$= k_{\upsilon\epsilon}\, \mathrm{e}^{-\Delta H^{\ddagger}/kT} \tag{10}$$

We have a modified frequency factor, $k_{\upsilon\epsilon}$, which defines the rate of energy uptake (transfer), *as well as* the probability that it occurs in the appropriate degrees of freedom. The chemical mechanism of catalysis, specified by the active-site configuration (in conjunction with the bound substrate), dictates the energy $\Delta H^{\ddagger}$ (or the 'motive' part thereof – see subsection IIA). *It is the protein matrix (in communication with the ambient medium) which determines the rate at which the active site obtains that energy, through the factor $k_{\upsilon\epsilon}$.* And, this is a major distinguishing factor in the various models in Section II.*

In the ensuing development, we first consider a 'local' view of the enzyme-catalytic process, with the enzyme-substrate complex regarded as quasi-independent thermally from the surrounding medium (i.e., high-viscosity limit). Then, we proceed to the complete picture of the protein matrix, as a free-energy transducer between the solvent phase and the active-center (i.e., low-to-moderate viscosity range). Viscosity is an appropriate parameter relating to the modality of thermal interaction (at a given temperature) between the protein ans solvent medium. At the microscopic level, the *mobility* of the particles composing the system is proportional to $1/\eta$ [80]. The thermal '(de)energization' of an enzyme-substrate complex is determined by that 'mobility' – whether it specifies direct diffusional/collisional interaction of the solvent molecules with the protein *or* binding/relaxation of the solvent/solute particles with the protein, according to the particular assumptions of the theoretical models in Section II.

IIIB. The 'local' view of enzyme catalysis

It is well-known, that an enzyme effectively enhances the reaction rate by lowering the activation energy. This is accomplished, not by the utilization of the many degrees of freedom of the protein as a 'reservoir of excess thermal energy' (see Section IIA), rather by the creation of an alternative mechanistic pathway under special microenvironmental conditions at the active-center [81]. Stereospecificity, as well as elaboration of the reaction mechanism, demand that *the substrate must be bound to the enzyme active-site at multiple (usually many) points*. The enzyme-substrate interactions (most of which are electrostatic in nature) are very strong in the active-site, owing to the low dielectric constant in the hydrophobic core of the protein [81,82]. Thus, we can assume tight coupling of the bound substrate to the immediate (local) region of the protein and regard the enzyme-substrate complex as a single entity.

Of course, many of these contact interactions between the enzyme active-site and the substrate play roles in the facilitation of catalysis. Hence, we can specify them as 'relevant active-site variables (coordinates)' [11]. These 'coordinates' may be key bond-lengths, charge-separations, charge-transfer parameters, etc. (see Fig. 5). It is the configuration of these 'coordinates' which actually defines the chemical mechanism of the catalytic reaction and, concomitantly, the value of the energy, $\Delta H^{\ddagger}$, in Eqn. 10. Yet, these 'coordinates' are not static – nor can they be, since in general a multi-step catalytic process would require spatiotemporal change in their configuration. On a relatively short time-scale, these 'coordinates' (more specifically,

---

* When applying the Arrhenius rate law (and its transition-state form) to enzyme-catalyzed reactions, one must exercise great care Consideration of the contributions of the protein matrix to the $\Delta H^{\ddagger}$ and $\Delta S^{\ddagger}$ terms can lead to gross misinterpretation, as stressed by Blumenfeld [63]. Eqn 7 is perhaps more general. In the present treatise, we employ the transition-state theory in a purely formal sense, for intercomparison of the tenets of the various protein-dynamical models (see Ref. 4). In view of the relatively imprecise form of the rate constants at this stage in the development of the models, the transition-state theory may be beneficial in allowing a preliminary discussion of the physical foundations, using familiar thermodynamic and statistical-mechanical concepts.

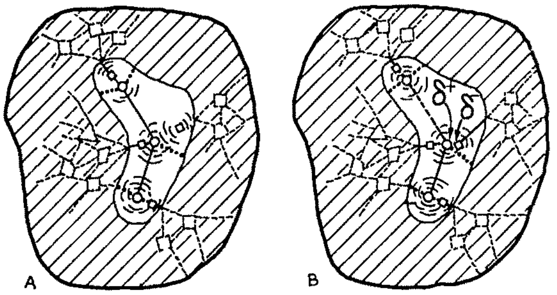

Fig. 5. Simple representation of the active-site configuration of an enzyme-substrate complex, in the ground state (A) and transition-state (B). In the trnasition state, bonds in the substrate may become labilized and/or transient charges (δ^+, δ^-) may develop The critical active-site groups (which are interconnected to the ensemble of particles in the protein matrix) are in constant thermal motion (see text).

the particles relating to them) are subject to stochastic motion, due to their interaction with the ensemble of particles composing the surrounding protein matrix.

We arrive at a crucial point regarding the 'local' nature of enzyme catalysis – a point which may be obvious, yet demands emphasis here. An enzyme lowers the activation energy of a given reaction (and enhances the rate by many orders of magnitude), *while increasing the number of degrees of freedom (viz., the 'relevant active-site coordinates') directly involved in the chemical reaction.* This is a seemingly incompatible combination, as the probabilistic problem of coordinating the behavior of an increased number of constituent variables would tend to *decrease* the rate constant (see below). The multi-point interaction between E and S, which defines the stereospecificity and the very reaction mechanism, necessarily engenders an increase in the number (and kinds) of critical degrees of freedom relevant to the chemical reaction. In turn, these 'critical variables' interact dynamically with the collection of particles composing the remainder of the protein structure. Thus one must logically conclude that the surrounding protein matrix is uniquely 'designed' to be able to correlate the spatiotemporal behavior of these active site 'coordinates', at least over some time-scale that is relevant to the catalytic process [11]. This idea is basic to any protein-dynamical view of enzyme action and, indeed, explains (at least partially) why enzymes must be so 'big' (and globular in shape).

In terms of energy exchange, we see that the bound substrate is interacing with two thermal reservoirs. There is the immediate protein body and, indirectly, the surrounding solvent medium. Accordingly, the enzyme 'active-site' is subject to Langevin dynamics, as influenced by the fluctuating nature of the protein body. The protein (at least, the surface portion thereof), in turn, is subject to Langevin dynamics, as influenced by the fluctuating nature of the solvent system at the interface.

In this section we shall take a 'local' view of the enzyme-substrate complex, imagining it as 'isolated' from the solvent medium. To construct this situation, we take the enzyme molecule to be at thermal equilibrium in a bath having very high viscosity. The rate of energy-exchange at the protein-solvent interface would be greatly diminished (let us assume infinitely slow) here. Adding substrate, we somehow follow (in our 'thought experiment') the course of events in a typical enzyme-substrate complex, as it executes the catalytic process. Observing the same enzyme molecule through many such catalytic cycles (or, alternatively, sampling many enzyme-substrate complexes), we would be able to follow the ergodicity of the collection of particles in the protein body, as it generates the proper configuration for the catalytic process. We would find, that the 'local' dynamics of the enzyme active-center (with bound substrate) are specified by the internal motions of *the protein matrix itself* (at the given temperature).

We want to consider the general form of the catalytic rate constant for a simple, one-step chemical process in this 'local' situation (i.e., quasi-independent of the solvent medium). Following the approach in subsection IIIA, we now assume that the *active-site* itself (with bound substrate) is a 'body' immersed in a thermal reservoir represented by the *protein matrix*. In order to relate this role of the protein as a 'solvent' for the chemcial reaction, let us start from first principles. When we have an ensemble of systems at equilibrium with a thermal reservoir at temperature T, elementary physical chemistry tells us that the probability $P(E_a)$ of finding a system with energy E_a is:

$$P(E_a) = e^{-E_a/kT} / \sum_a e^{-E_a/kT} \tag{11}$$

which is just the canonical-ensemble distribution.

The simplistic picture, represented by Eqn. 11, shows us the manner of 'energization' of the enzyme active-site by the remainder of the protein 'solvent'. To see this, we suppose that the protein, when 'decoupled' from its natural solvent medium, does not manifest the energy-transduction modes which are present when it interacts normally with the solvent (see subsection IIIC). Thus, we assume as an approximation that the 'relevant active-site variables (coordinates)' (as well as the remainder of the 'diffusional' and 'hydrogen-bond' degrees of freedom in the two pictures noted in subsection IIA) are not correlated (or only weakly so) and sample the dimensionality of the protein-ensemble 'phase-space' independently of each other (at least on a time-scale short compared to that of the catalytic cycle). Suppose the ith 'relevant active-site variable' of the enzyme-substrate complex must have an energy E_i in the range $E_{i1} \leqq E_i \leqq E_{i2}$ for catalysis to proceed. Treating the complex in this limiting 'local' case as an equilibrium system following a Maxwell-Boltzmann distribution, the probability P_{E_i} for this event is obtained directly from Eqn. 11 as follows:

$$P_{E_i} = \int_{E_{i1}}^{E_{i2}} \frac{1}{kT} \mathrm{e}^{-E_a/kT} \mathrm{d}E_a$$

$$= \mathrm{e}^{-E_{i1}/kT}(1 - \mathrm{e}^{-\Delta E_i/kT}) \tag{12}$$

where $\Delta E_i = E_{i2} - E_{i1}$. (One replaces the summation in Eqn. 11 by an integration over E_a from zero to infinity, giving a value of unity. One notes, that in the event E_{i2} can go to infinity, P_{E_i} takes the familiar form, $\exp(-E_{i1}/kT)$.) And, there are n such 'relevant active-site variables', *each* of which must satisfy the condition of Eqn. 12. In general, it is not enough that each of the n 'variables' simply satisfy this energy condition. Because of stringent requirements on the coordinated motion of the critical 'variables' during catalysis, there would be additonal probability factors relating to proper orientation, synchronization, etc., of these 'variables'. Let us fomally include all such factors into one term, P_{S_i}, for each of the n 'variables'.

Finally, we can write a simple expression for the 'local' form of the catalytic constant, $\tilde{k}'_{\mathrm{cat}}$, as:

$$\tilde{k}'_{\mathrm{cat}} = k_v \mathrm{e}^{-\Delta\tilde{H}/kT} \prod_{i=1}^{n} (1 - \mathrm{e}^{-\Delta E_i/kT}) P_{S_i} \tag{13}$$

where:

$$\Delta\tilde{H} = \sum_{i=1}^{n} E_{i1}$$

Eqn. 13 indicates that the rate of the reaction is proportional to the probability that each of the separate 'variables' *simultaneously* possesses an energy within a certain range. This probability is just the mathematical product of the *individual* probabilites for each 'variable'. The value for the frequency factor, k_v, depends on the actual nature of the energy exchange between the active-site and the protein body. The limiting value, of course, would be the frequency of atomic vibrations (approx. kT/h). Obviously, this is many orders of magnitude greater than typical values of enzyme-catalytic constants. However, the energy-transfer modes, in the pictures of the protein interior indicated in subsection IIIA, entail frequencies considerably lower than for atomic vibrations. Additionally, the frequency factor in Eqn. 13 is tempered by the aforementioned probability factors, P_{S_i}. Following Eqn. 10, we have:

$$k_{v\epsilon} = k_v \prod_{i=1}^{n} P_{S_i} \tag{14}$$

The fundamental form of Eqn. 13 (which is analogous to Eqn. 10) is at the heart of the stochastic nature of the 'energization' of the enzyme active-site by the transducing protein matrix – whether the protein be viewed as a dense hard-sphere fluid *or* a hydrogen-bond network, according to subsection IIIA. The application of the fomulation in Eqns. 11–13 to these detailed pictures of the protein *milieu intèrieur* demands more specific elaboration of the probability distribution in Eqn. 7. Fittingly, $W(h^{\ddagger},T)$ can be expressed in precisely the (integral) form of Eqn. 11, so that:

$$W(h^{\ddagger},T) = \frac{g(h^{\ddagger}) \exp(-h^{\ddagger}/kT)}{\int_0^{\infty} g(h) \exp(-h/kT)\, \mathrm{d}h} \tag{15}$$

where, as in subsection IIIA, $g(h^{\ddagger})$ is specified as $\exp(s(h^{\ddagger})/k)$ [23]. The most general way to pursue $W(h^{\ddagger},T)$, applicable to all models of protein dynamics, is to cast it into a 'coordinate-space' form. Let us label the n 'relevant active-site coordinates' as $\boldsymbol{r}_1$, $\boldsymbol{r}_2$, ,...,$\boldsymbol{r}_n$. Then we can assign a density function, $P(\boldsymbol{r}_1, \boldsymbol{r}_2, ,\ldots,\boldsymbol{r}_n)$, to this collection of coordinates, corresponding to the probability of finding a given configuration in a statistical (canonical) ensemble of all the *other* internal coordinates. We suppose, that 'energization' of the enzyme active-site for catalysis requires a configuration wherein the coordinates $\boldsymbol{r}_1$, $\boldsymbol{r}_2$, ,...,$\boldsymbol{r}_n$ all have a specific range, corresponding to a defined n-dimensional volume element $V^{\ddagger}$. Then the probability of finding an enzyme-substrate complex in this state will be:

$$W(\zeta^{\ddagger}) = \frac{\int_{V^{\ddagger}} P(\zeta)\,\mathrm{d}\zeta}{\int_{V^{\infty}} P(\zeta)\,\mathrm{d}\zeta} \tag{16}$$

where ζ symbolizes the composite reaction coordinate $(\boldsymbol{r}_1, \boldsymbol{r}_2, ,\ldots,\boldsymbol{r}_n)$. The numerator is integrated just over the 'transition-state volume', $V^{\ddagger}$, whereas the denominator is integrated over the entire space available to the coordinates (denoted V^{∞}). We can now apply Eqn. 16 to the two (transducing) pictures of the protein matrix:

Case 1. Dense, hard-sphere fluid

Using the molecular-dynamics paradigm of subsection IIC-7, Northrup et al. [76] employed the 'phase-space trajectory method' of Eqn. 16 to formulate rate constants for reactions in proteins. Their rate constant has the general form:

$$k = \tfrac{1}{2}\kappa\langle|\dot{\zeta}|\rangle\rho(\zeta^{\ddagger})/\int_{i} P(\zeta)\,\mathrm{d}\zeta \tag{17}$$

where, as above, ζ represents a composite reaction-coordinate of a *localized* region of the protein. $\rho(\zeta^{\ddagger})$ corresponds to the numerator in Eqn. 16. Here, $P(\zeta)$ is normalized around the initial-state 'valley' preceding the transition state, and the integral in eqn. 17 is performed over all possible values of ζ in the configurations of this 'valley'. The quantity $\langle|\dot{\zeta}|\rangle$ is the average (absolute) value of the 'crossing velocity' (evaluated at $\zeta^{\ddagger}$), and κ is a 'transmission coefficient' (by analogy to the transition-state theory formalism).

Northrup et al. [76] used this rate-constant form to describe rotational isomerization of an aromatic ring in the small protein, bovine pancreatic trypsin inhibitor. The molecular dynamics (computer simulation) approach of subsection IIC-7. is employed, with empirical energy functions assigned to the various particle interactions inside the protein. For determination of the rate constant k (more specifically, $\rho(\zeta^{\ddagger})$), the protein is prepared by 'heating' it to a given temperature, prescribing a Maxwellian distribution of particle velocities. The numerical results from this simulation demonstrate the feasibility of the molecular-dynamics method of calculating rate constants for reactions in proteins.

As detailed by the previous authors [76], we may associate with $P(\zeta)$ a 'potential of mean force', $F(\zeta)$, defined by the relation (see subsection IIA):

$$F(\zeta) = -kT \ln P(\zeta) \tag{18}$$

And, by virtue of the correspondence between $F(\zeta)$ and the Helmholtz free-energy change, we have $F(\zeta) = \Delta E(\zeta) - T\Delta S(\zeta)$. Assuming the pV term is negligible, $E \equiv \Delta H$ [76]. Thus, from Eqn. 17 we recover the form of Eqns. 10 and 15.

Case 2. Hydrogen-bond network

In order to derivatize Eqns. 15 and 16 for this picture, we follow in extenso a protein-fluctuation model proposed by Ikegami [77]. The dynamical structure of the protein is characterized by the fluctuating state of secondary bonds between unique pairs of sites in the polypeptide. The instantaneous free-energy of the protein 'structural state' is then defined by the fraction (Y) of secondary bonds in the bonded state. Ikegami [77] developed an explicit form for the Gibbs free energy of the protein molecule, $G(T, Y)$, as a function of temperature and 'structural state' (defined by Y). For simplicity, it was assumed that all of the possible secondary bonds have the same properties (e.g., bond energy, number of nearest-neighbor bonds, energy loss per bond-pair in different states), and that the *number of conformations* produced when a single bond breaks is the same for all bonds. Accordingly, the previous author defined the probability density of the system, $W(T,Y)$, as:

$$W(T,Y) = \frac{\exp(-G(T,Y)/kT)}{\int_0^1 \exp(-G(T,Y)/kT)\,\mathrm{d}Y} \tag{19}$$

with the standard state for G set at 0 K (i.e., $Y = 1.0$). Using an explicit expression for $G(T,Y)$, Ikegami [77] applied Eqn. 19 to the study of overall protein structure, gross structural changes (e.g., denaturation) and average values of processes dependent on specific structural states.

No rate-constant formalism, based on this 'secondary-bond network' picture, has yet been developed. In order to pursue this, one might suppose that 'energization' of the enzyme active-site requires a certain number of bonds (say, hydrogen bonds) in the protein matrix to be in the bonded (or unbonded) state. Then, one would express the catalytic rate constant, k'_{cat}, in terms of the type of probability function in Eqn. 19, multiplied by an appropriate frequency factor (k_υ). As an upper limit, this factor might be approximated as the vibrational frequency of hydrogen bonds.

Before the Ikegami approach can be applied to the kinds of protein-dynamical models in Section II (especially IIC-2 and IIC-4), additional entropic considerations are necessary. As indicated above, expediency in calculating the entropy part of $G(T,Y)$ demanded some simplifying assumptions – viz., isotropy in the hydrogen-bond network. Evidently, active-site processes would require anisotropy in the spatiotemporal behavior of these bond patterns. From the theoretical viewpoint, the most appropriate route here might be the development of an internal coordinate system which represents the various secondary bonds as vectors. Then, one could construct Eqn. 16 or 19 according to the probability that these various vectors (of stochastic magnitude) 'project' (as their vector dot product) in a specific way onto the 'relevant active-site coordinates' [83].

From the foregoing, we see that a conceptual framework may be gradually emerging, for modeling the 'local' interaction between the protein matrix and the active-site of an enzyme. In all likelihood, the formal distinction between the two cases above will break down. The scheme of *Case 1* is the more general. Potential-energy functions for hydrogen bonds, for example, can be included in the molecular-dynamics simulation [84]. Should such bonded interactions dominate the 'energization' of the active-site of a given enzyme, then, the molecular-dynamics approach would, in principle, reveal this feature. Reification of this theoretical modeling, of course, must await additional information on the nature of protein dynamics (especially the role of the 'external' solvent), as well as further studies from X-ray crystallography (in defining the proper 'coordinate spaces' inside the enzyme).

Concluding our 'local' view of enzyme catalysis, let us return to the simple representation of Eqn. 13. It is important to reiterate, that enzyme catalysis, as a dynamic process, demands of the protein matrix (the 'local' solvent) more than simply an *energetic fluctuation*. It requires a specific configuration in the 'phase space' (i.e., a definite pattern for the coordinates *and* momenta) of the 'relevant active-site variables'. This, in turn, entails steric positioning, synchronization, etc. – all lumped into the probability factors P_{s_i} in Eqn. 13. If the critical 'variables' all behaved independently, in their interactions with the protein matrix, one sees from Eqn. 13 that the rate constant would be quite small. For example, suppose that there are four critical 'variables' ($n = 4$), and that for each the value of P_{s_i} is $1 \cdot 10^{-2}$. This, in itself, would lower the rate by an overall factor of $1 \cdot 10^{-8}$ (see Eqn. 14).

Certainly, the protein matrix must be designed, not only to present the active-site with the actual three-dimensional arrangement of requisite atomic groupings (as per the classical view of the enzyme), but, also, to correlate *dynamically* their motions during the catalytic process. To avoid the apparent entropic cost (e.g., P_{s_i}) of this motive design, as it relates to the large number of particles in a protein molecule (see Eqn. 10), one is led to assume that many of the degrees of freedom in the enzyme are coupled dynamically – at least on some time-scale relevant to catalysis [11]. In order to understand this aspect, we must exceed the 'local' level and consider the general role of the enzyme molecule as an energy transducer mediating between the ambient medium and events at the active-site.

IIIC. The energy-transduction modality: the 'zymon'

Now, we must relax the high-viscosity restriction of subsection IIIB and consider the enzyme-substrate complex interacting freely with the solvent (i.e., low-to-moderate viscosity range). It is in this range that we would expect the energy-transduction modes, as suggested in Section II, to be manifest. Based on the reasoning of subsection IIIB, we will take a 'leap in logic' and assume that such modes exist in enzymes [4]. It will be our task in this section to examine the evidence (such as there is) for the functional nature of these modes.

Basically, the protein molecule is viewed as interacting (stochastically) with the medium in such a way, that energy is 'borrowed' (as a fluctuation) from the reservoir and transduced 'somehow' through the matrix to the active-site. (The *net* free-energy change at the end of transduction is zero, so the Second Law of Thermodynamics is inviolate – see subsection IIA). We concluded in subsection IIIB that the various critical 'coordinates' at the enzyme active-site must be dynamically correlated (at least on a time-scale relevant to the catalytic process). This feature intimates, that 'something' at the protein-solvent interface, acting through the protein 'mediator', induces the proper correlation of active-site variables (see subsection IIC). It is important to stress the point that this correlation phenomenon does not imply a rigid structural coupling among degrees of freedom in the protein, rather a (relatively) long-time statistical effect (see Fig. 6). (In fact, on time-scales much shorter than that of the catalytic cycle, we might expect the critical active-site 'variables' to perform apparently uncorrelated dynamics.)

In principle, the probability distribution for the population of the (ES)‡ state is a function of the complete phase space (i.e., the generalized coordinates and momenta of all the particles composing the ES complex and the solvent). In order to pursue a completely rigorous description of the enzymic rate process, one must integrate the classical equations of motions for *all* the atoms of the protein molecule, including the various interaction potentials for the protein interior and for the solvent-protein interface. *Molecular-dynamics simulations* [15,16,73–76] along this line have revealed important information on protein motions (see subsections IIC-7 and IIIB). Yet, present limitations on computer-time requirements preclude such a *general approach*, except for small proteins with integration over relatively short time-span. Here, we construct the rate process approximately, by viewing the protein matrix at a higher hierarchical level than the constituent atoms. One may expect the *individual atoms* to perform rather high-frequency motion, the character of which is uniform throughout the protein structure [75]. A common denominator of all the existing theoretical models in subsection IIC (see Ref. 4) is the basic postulate, that the protein is designed to communicate with the medium in such a manner as to correlate the motions of the requisite atomic groupings during the catalytic process. Clearly, the protein-dynamical basis of enzyme action must be sought in lower-frequency *collective motions*, having an inhomogeneous distribution in the protein.

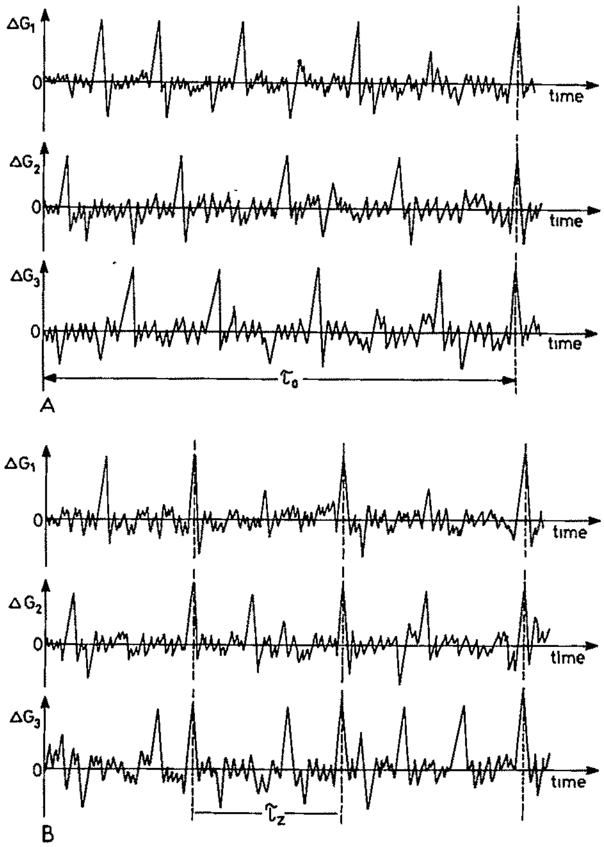

Fig. 6. Local free-energy fluctuations in the enzyme-substrate complex. A catalytic step might require coordinated fluctuations at, say, points 1, 2 and 3 in the complex. This fluctuational pattern would occur with a recurrence time τ_0 when the system is 'de-coupled' from the solvent medium (A) and with τ_z when 'coupled' appropriately to the solvent (B) (cf. Fig. 4).

In this vein, we can narrow our concern to two aspects.

(1) In order to bring the critical 'variables' into the proper phase relation, with a 'coherence time'

commensurate with typical catalytic turnover-rates of enzymes, the protein matrix must be viewed as a highly *inhomogeneous* 'fluid' *or* as an *anisotropic* secondary-bond 'network' (depending on one's disposition toward the two cases in subsections IIIA and IIIB).

(2) Interacting with the random generator in the surrounding medium, these 'collective' degrees of freedom must be able to screen (select from) the ambient 'noise' according to specific 'excitation patterns'.

Let us consider the first aspect. Recalling our discussion from Section IIIB, this stems from the entropic 'cost' of the 'energization' process. From a functional perspective, the number of internal degrees of freedom in the whole protein which *effectively* participates in 'energization' of the active-site must be rather small. That is, the *individual* active-site 'variables' (or specific subsets thereof) are each correlated ('coupled') to a certain *group of atomic degrees of freedom* in the protein – each 'unit' (group) behaving as a singular degree of freedom on some time-scale relating to catalysis. Experimental and theoretical studies thus far suggest two physical ways of understanding this collective behavior. First, there are the 'mobile defects' proposed by Lumry and coworkers (see subsection IIC-2). These are small cavities (or 'vacuoles'), created by local disruption of secondary bonds, which migrate throughout the protein matrix. This mobility would be highly cooperative, correlated by atomic packing and overall bonding patterns in the protein [14,59]. Events at the enzyme active-site would depend on the probability (and frequency) of coalescence of certain such 'defects' at this spatial location – mediated by an intrinsic (teleonomically designed) anisotropy in the cooperativity of the secondary-bond network in the protein. The applicability of this transducing mode is especially clear for the models in subsection IIC-2 and IIC-4, and, possibly, part-and-parcel of the others as well.

A second physical means of such collective behavior has been suggested, most clearly from molecular-dynamics simulation [17,75]. Recall, that this approach regards the protein matrix, roughly, as a dense hard-sphere fluid. Done in the presence of solvent, such simulation has revealed the existence of *highly correlated, diffusion-like motion of groups of atoms* in the protein. These *transient* groupings were designated as 'quasi-particles' [75]. And, these 'particles' are found to be inhomogeneously distributed in the protein structure. This inhomogeneity, particularly in larger proteins, might arise from 'built-in' cooperativity in the conglomeration of interaction potentials defining the dynamics of such a 'dense fluid' [17]. This view seems fitting, particularly for the models in subsection IIC-5 and IIC-6.

Now, we ponder the *second major aspect* listed above, viz. the interaction with the solvent (thermal reservoir). All of the authors of the various models in subsection IIC stress the importance (and nature) of surface events in the energy-transduction process. The difficulty lies in establishing the proper interaction mode (if, indeed, it is possible to specify *just one*). Clearly, there are *two general modes*: direct collisional interchange of energy between the protein and solvent/solute species *or* binding/relaxation of solvent/solute particles on the protein surface. The nature of energy (momentum) transfer in the former case is perhaps obvious (e.g., see subsections IIC-5–7). It is more subtle (and complex) in the latter case. First, consider the binding/relaxation of water molecules. Owing to the prevalence of hydrophilic groups on their surfaces, globular proteins in aqueous solution have a number of tightly bound water molecules and also are covered with a mobile layer ('swarming cloud') of associated water [57,85 86]. The binding/relaxation of this water might affect internal protein dynamics in a number of ways. For example, it can produce local perturbations in the protein conformation (e.g., due to the influence on the planarity of the amide group and also due to effects on local electric fields in the protein) [65]. And, by virtue of the extended nature of hydrogen-bond chains in globular proteins, binding/relaxation of water on the surface could play a 'deterministic' role in the generation of internal hydrogen-bond 'defects' [6,59,87]. Similar considerations apply to the binding/relaxation of ions (see subsection IIC-1 and Refs. 12 and 65). Of particular importance may be *proton-transfer processes* at the protein surface, as regards the introduction of fault ('defect') states in internal hydrogen-bond chains [87]

Once one has identified the transducing mode *and* the relevant surface phenomenon, there remains the question: how does the dynamical interaction between the two provide the correlated 'energization' pattern at the enzyme active-site? Most likely, this involves correlation (synchronization) of molecular events over extensive regions of the protein surface. The spatial extent of such regions may relate to the size (and nature) of the kinds of 'quasi-particles' specified in the two transduction pictures of the protein matrix. We might apply the term 'quasi-particle' to *both* cases – using it in reference to the 'collective-diffusional' motion in the dense-fluid picture, as well as to the 'mobile-defect' modality in the secondary-bond network representation. For economy of thought (and expression), let us give these 'quasi-particles' a name and call them *zymons*, with the symbol 'Z_{H}' for hydrogen-bond 'mobile-defect' *zymons* and 'Z_{F}' for 'fluidized' collective-diffusional *zymons*. (In a sense, the distinction into two *zymons* may be superfluous. For the transient formation of a Z_{H}-*zymon* may entail creation of a Z_{F}-*zymon*, and vice versa.) We reiterate the previous point, that these 'particles' represent *transient correlated motions ('excitations') of groups of particles in the protein matrix,* and that the dynamics (and energetics) of individual active-site 'coordinates' (or subsets thereof) are *causally linked (coupled) to specific zymons* (see Fig. 7). Again, the *zymons* are the *effective* degrees of freedom, in the enzyme molecule, to which the active-site 'energization' is geared.

Regarding Z_{F}-*zymons*, we find from the molecular-dynamics simulations [17,75] that the solvent plays a vital role in their generation. Thus far in these simulation studies, the solvent has been modeled as a rather simple Van der Waals medium; so, the observed thermal 'excitation' of the Z_{F}-mode is apparently due to collisional-frictional interaction of the protein and solvent. As the previous authors [75] noted, formation of such 'particles' encompasses significant regions of the protein surface; and, consequently, they indicated that 'particle-formation' might be quenched if the solvent phase becomes immobile (e.g., frozen). This basic idea is maintained, explicitly or implicitly, in the models of subsections IIC-2 and IIC-4–6.

Similar considerations apply to Z_{H}-*zymons*. Lumry and Rosenberg [59] have stressed, that the number (and mobility) of the internal 'defects', as well as their ordering on a free-energy scale, are critically dependent on protein-water interactions, solvent composition, inter alia. Strong suggestion comes also from changes in bound-water density on the protein surface, implicated during the course of catalysis [25,27,57]. A similar notion is entailed in the models of subsections IIC-1 and IIC-4 (see Refs. 9 and 19).

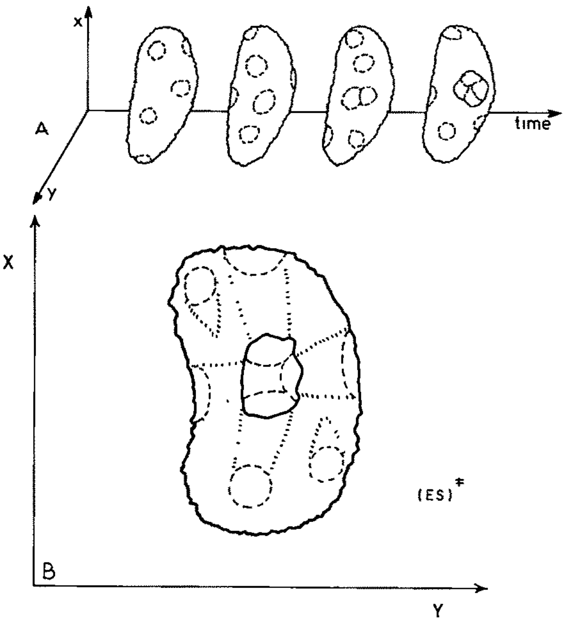

Fig. 7. Simplistic coordinate-space representation of the *zymon* scheme for activation of the enzyme-substrate complex. As the complex interacts stochastically with the solvent medium, these 'quasi-particles' are constantly forming, decaying and diffusing in the macromolecular matrix. Enzyme catalysis would demand a certain pattern of coalescence among a number of such *zymons*. Part A represents the course of catalysis as a diffusion process in the *zymon* 'coordinate space' (for simplicity, in two dimensions) (In principle, the course would involve the complete phase space of *zymon* coordinates and momenta. Part B shows the course of catalysis viewed along the time axis, as the 'quasi-particles' form, decay, and diffuse in the structure (cf. Fig. 6B).

We might consider the solvent-induced 'excitation' of *zymon*-modes analogous to a harmonic-oscillator system subject to Langevin dynamics. We suppose, that the *zymon* 'particle' can be approximated as a large oscillator. And the solvent particles can be viewed as a 'reservoir' of very many small oscillators which act on the 'large' one (e.g., see Ref. 88). The *zymon*-oscillator will have a characteristic frequency, and the reservoir oscillators will have a given range (bandwidth) of frequencies. (The energies of the reservoir particles would follow a Boltzmann distribution, while their amplitudes would follow, say, a Gaussian distribution.) One assumes, that a given *zymon*-oscillator is coupled preferentially to a narrow portion of this reservoir bandwidth [88]. Thus, proper 'excitation' of the *zymon*-mode might require that a certain region on the protein surface suffers a specific pattern of interactions (e.g., collision, binding/relaxation) with the bath particles. This would not imply that these molecular events on the surface must occur at precisely the same time. There might be a finite time-domain, during which the 'excitation' of the *zymon*-mode could be progressively achieved. Once 'excitation' is attained, one must presume that the mode-lifetime is sufficiently long (in the appropriate solvent-viscosity range), for a given *zymon* to have a fairly high probability of *coming into phase with other zymons* at the enzyme active-site. That is, the frictional forces inside the protein must not 'damp' the *zymon* too quickly. (Results from molecular-dynamics simulation suggest rather long lifetimes [75]). The extent, to which this damped-oscillator picture reflects the nature of *zymon*-modes, remains to be defined.

Thus far, there has been only one attempt to formulate mathematically this kind of 'excitaiton' at the protein-solvent interface. Somofi and Damjanovich [69] developed an expression for k_{cat}, whose preexponential factor contains terms relating to the probability that *specific sites* on the protein surface undergo a steric, energetic, and temporally assigned interaction with solvent/solute particles (see subsection IIC-6). This model originally assumed that the 'excitation' is collisionally induced. But its formalism is readily adaptable to binding/relaxation phenomena as well (see subsection IIC-4). Similarly, Careri et al. [65] have suggested that a stochastic *master-equation* approach might be suitable for modeling the 'surface-excitation' process. It is hoped that further attention to this aspect will be forthcoming.

The '*zymon*-approach' to the protein-dynamical models of enzyme action illustrates, once again, the recurrent theme that the *enzyme plus solvent* must be viewed as a single unit, if we are to understand how enzymes have evolved to function in situ [4,25]. Some of the models in subsection IIC (at the present stage in their development) have addressed the energy-transduction process by looking at the protein interior, whereas others have focused on the protein-solvent interface. We see that elements of *both* kinds of model relate to the 'whole picture'. For the two approaches are *complementary aspects* of the same thing.

Stemming from this *zymon* view, we may condense the foregoing description of *thermally based* enzyme action as follows. The rate process is at the whim of a Maxwell-Boltzmann type distribution, as seen, for example, in Eqns. 10 and 13 (see subsection IIA). The value of the requisite energy comes from the nature of the chemical reaction. The rate at which that energy is taken-up by the protein (as a fluctuation), and delivered to the proper degrees of freedom, is dictated by the preexponential factor, $k_{\nu\epsilon}$. *This 'energization' (at a given temperature) must depend explicitly on the medium viscosity*, η_s. Not only does the solvent '(de)energize' the ES complex, but, also complements the protein structure in generating the transducing modality.

In order to formalize this general viscosity-dependence, Whittenburg, S.L., Wan, W. and Welch, G.R. (unpublished data) related the constant $k_{\nu\epsilon}$ to the underlying protein dynamics by the theory of *time-correlation functions*, that is:

$$k_{\nu\epsilon} = \int_0^\infty \mathrm{d}t \, \langle \dot{N}^{\ddagger}(0) \dot{N}^{\ddagger}(t) \rangle \tag{20}$$

where $\langle \dot{N}^{\ddagger}(0) \dot{N}^{\ddagger}(t) \rangle$ is the time-correlation function for the flux (time derivative) of the number ($N^{\ddagger}$) of ES complexes in the transition state. At time $t = 0$, we have a flux $\dot{N}^{\ddagger}(0)$ entering the saddle-point ((ES‡) surface from the equilibrium reactant (ES) state. And $\dot{N}^{\ddagger}(t)$ is the outgoing flux to the (EP) state at time t. The time integral in Eqn. 20 just sums all the reactive flux, into the (EP) state, which occurs during the mean time that an ES complex is in the transition-state region. Following the preceding discourse, we postulate that $N^{\ddagger}$ will depend on the positions (r_i) and momenta (p_i) of the *zymon* quasi-particles. Assuming that there are *n zymons* defining the transition state, we expand the flux $\dot{N}^{\ddagger}(t)$ in the phase space (r_i, p_i) to give:

$$\dot{N}^{\ddagger}(t) = \sum_{i=1}^{n} \frac{\partial N^{\ddagger}}{\partial p_i} F_i + \sum_{i=1}^{n} \frac{\partial N^{\ddagger}}{\partial r_i} V_i + \frac{\partial N^{\ddagger}}{\partial t} \tag{21}$$

where F_i is the force on the ith 'particle' and V_i the velocity. Using a linear harmonic approximation, the previous authors (Whittenburg, S.L., Wan, W. and Welch, G.R., unpublished data) derived the following form for Eqn. 20:

$$k_{\nu\epsilon} \cong \left(\frac{n+1}{n} + 4\frac{\zeta_s}{\zeta_p} \right) 3kT\zeta_s Z(p) + \frac{3kT}{n}\frac{1}{\zeta_s} Z(r) \tag{22}$$

where ζ_s is a solvent friction (proportional to η_s) and ζ_p an intrinsic protein 'viscosity'. A *zymon structure factor*, $Z(r)$, is defined by:

$$Z(r) = \sum_{i=1}^{n} \left(\frac{\partial N^{\ddagger}}{\partial r_i} \right)^2 \tag{23}$$

and a *zymon momentum factor*, $Z(p)$, by:

$$Z(p) = \sum_{i=1}^{n} \left(\frac{\partial N^{\ddagger}}{\partial p_i} \right)^2 \tag{24}$$

As detailed elsewhere (Whittenburg, S.L., Wan, W. and Welch, G.R., unpublished data), a Stokes-force interpretation of the *zymon* motions in the solvent reveals a $(1/\zeta_s)^2$-dependence for $Z(p)$. (These two *zymon* 'factors' must be evaluated for particular enzyme mechanisms.) Accordingly, Eqn. 22 yields a viscosity-dependence of the form seen in Fig. 8. At intermediate viscosity, Eqn. 22 predicts an approximate $(1/\eta_s)$-dependence for $k_{\nu\epsilon}$, as is observed experimentally (see subsections IIC-5 and IIC-6). At very high viscosity the plot in Fig. 8 plateaus. Here, the solvent becomes 'rigidified' (and the *zymon* modes damped), whereby *intrinsic* protein motions ('viscosity') now dictate the transition-state passage (see subsection IIIB and Ref. 52). (By virtue of the $(1/\zeta_s)^2$-dependence on $Z(p)$, in the high-viscosity limit Eqn. 22 approximates to the form $k_{\nu\epsilon} \propto (1/\zeta_p)$.)

The form of Eqn. 22 (and the approximate forms in subsections IIC-5 and IIC-6) may be taken as the hallmark of the rate process for *thermally based* enzyme catalysis, as it relates to solvent-protein dynamics. And the inherent *zymon* modality points toward the nature of enzyme action in *nonthermal* systems.

IV. Nonthermal enzyme systems

In recent decades electron microscopy has revealed a complex and richly diverse particulate infrastructure in living cells – especially larger eukaryotic cells. This structure encompasses the extensive membraneous reticulation (e.g., plasmalemma, endoplasmic reticulum, mesosomes (bacteria)), as well as the hyaloplasmic space. The latter region, containing the so-called 'ground substance', is laced with a dense array of various cytoskeletal elements (e.g., microtubules, microfilaments, intermediate filaments) and an interlocking microtrabecular lattice [90,91].

Accumulating empirical and theoretical considerations indicate that the majority (if not all) of the enzymes of intermediary metabolism operate in vivo in association with particulate structures [92–95]. A persual of the literature reveals evidence for enzyme organization in virtually all major metabolic pathways. The organizational mode may entail formation of protein-protein complexes and/or adsorption to cytological substructures. Experimental and theoretical calculations [96,97] of protein 'concentrations', in association with cytomembranes and organelles, indicate high, crystal-like densities of protein molecules in (on) particulate structures of the cell. There is a remarkable homology, in the surface area-to-volume ratio for *all* membraneous cytological substructures. Such considerations led Sitte [96] to propose

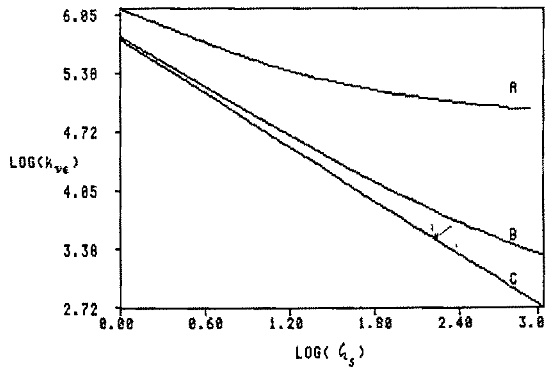

Fig. 8. Viscosity (friction)-dependence of the catalytic rate constant predicted by Eqn. 22, for the following cases: (A) $Z(r) = 10^3\ Z(p)$; (B) $Z(r) = 10^4\ Z(p)$; and (C) $Z(r) = 10^6\ Z(p)$. (Scales are in arbitrary units.) (See Whittenberg, S.L., Wan, W. and Welch, G.R., unpublished data).

that all cytomembraneous elements have evolved in a common fashion to function as effective 'protein collectors' in the operation of cell metabolism. And recent work from Porter's group [98] shows the microtrabecular lattice itself to be 'dressed' with a multitude of (as yet unidentified) proteins. It has even been suggested [5,95] that multienzyme systems form an integral part of this lattice (see Fig. 9).

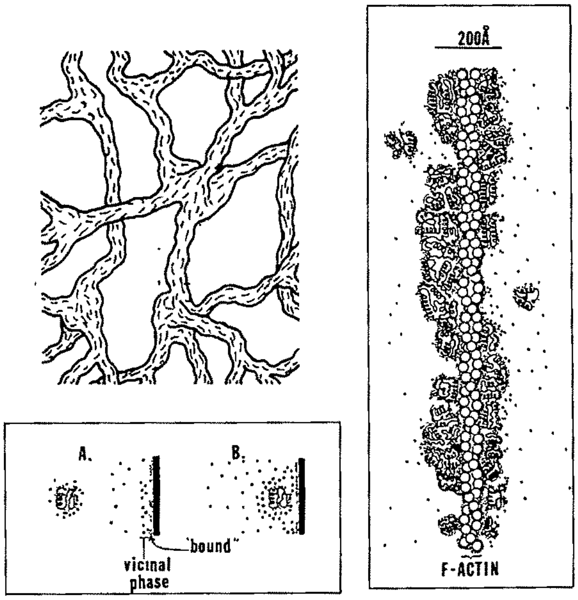

Fig. 9. Diagrammatic representation of the microtrabecular lattice. Inset at right depicts the hypothetical composition of a small region of the lattice. It is suggested that multienzyme systems may be adsorbed to the surface. (The basic unit of at least some trabeculae is considered to be an F-actin element.) Parts A and B show a hydrated globular protein free in solution and adsorbed to the lattice, respectively. 'Bound' and 'vicinal' refer to water (dots) immediately next to the surface and farther away, respectively. (Adapted from Ref. 95. Generously furnished by Prof. J.S. Clegg.)

Thus, cell biology presents us with a rather simple, biphasic view of cellular infrastructure: *a solid phase*, encompassing extensive membrane surfaces and the fibrous lattice-work; and *a soluble, aqueous phase* (albeit containing a considerable amount of 'structured' water [95].) We must focus on the solid phase as the primary site of intermediary metabolic processes, with the soluble phase functioning largely in such subservient roles as thermal buffering, distribution of common substrates, regulatory substances, and salt ions, etc.

There are compelling kinetic and thermodynamic reasons for abandoning the traditional 'macroscopic' view of intermediary metabolism, in favor of a local 'molecular-energy machine' picture engendering long-range energy continua [6,32,92,94,99]. As discussed elsewhere [6,32], this conclusion comes from a combination of the following factors: (1) the *reactivity of the very protein fabric* of the enzyme molecule (as per the preceding sections herein), (2) the *material substratum* (organized states) in which most metabolic processes are imbedded in vivo, and (3) the essence of (long-range) *energy-transduction modalities* permeating cytological substructures. The third factor is the most important, as regards the development of a theoretically consistent, holistic view of cellular metabolism. And because of its (presently) weak empirical base, its general acceptance demands the greatest 'leap in logic'. Yet, many lines of evidence – including the observed properties of the individual protein and of multienzyme complexes, as well as of the well-known energy-transduction modalities of 'bioenergetics' – betoken the existence of motive 'energy continua' in the function of much of intermediary metabolism.

One of the most important holistic 'integrative principles' in cell biology, potentially widely applicable to material flow in organized enzyme systems, was proposed some 25 years ago. Indeed, the very inception of the concept of 'vectorial metabolism' dates to the pioneering work of Mitchell [10], in the late 1950s, dealing with group-translocation and chemiosmotic reaction systems. A basic motif in Mitchell‘s work has been the elucidation of general mechanisms of linkage between metabolism and transport. This 'vectorial idea' found one of its earliest, and most notable, applications in the bioenergetics of electron-transport phosphorylation. Most importantly, this work spawned the concept of 'proticity' and the role of the proton gradient as a bioenergetic transducing principle. The 'proton gradient' (or proton-motive 'force') has emerged as a central, interconvertible form of energy – interconnecting such diverse entities as electron transport, ATP-bond energy, transhydrogenation reactions, flagellar (mechanical) motion, pH regulation, active transport and heat production. When the cell must ensure flow of a substance in a preferred direction *across the* *organized phase of a membrane*, transport is coupled to a local, redox proton-motive force generator *or* to an ion-translocating ATPase.

Organization of enzyme sequences at cytosol-particulate interfaces juxtaposes them to sources of proton (and, possibly, electron) gradients and significant (local) electric fields. Is this juxtaposition fortuitous? Are the localized enzymic processes in vivo functionally independent of those energy-transducing elements? We suggest not. Here, we will review this topic just briefly, indicating possible correlations of such energy states with the dynamical properties of the enzyme-protein.

IVA. A deeper look at the structural-functional design of the enzyme molecule

As is apparent from the preceding sections, the protein *as* a whole is designed to provide a specific (anisotropic) *solvent medium* for a given chemical reaction. Wherein, the combined chemical and protein subsystems engage in a fluid exchange of free energy, facilitating the entrance of the bound chemical subsystem into its transition state. From the enthalpic ($\Delta H^{\ddagger}$) side, one finds in the enzymology literature a number of catalytic factors which lead to a decrease in $\Delta G^{\ddagger}$. Generally, these fall into one of the following categories: (1) catalysis by *'rack' mechanisms* (whereby the bound, ground-state substrate is strained or distorted), (2) *general acid-base catalysis* (involving proton-transfer to or from the transition state), and (3) *electrophilic/nucleophilic catalysis* (usually involving covalent stabilization of the transition state) (see Fig. 5). Underlying these various catalytic modes is the importance of *local electric fields*, in the microenvironments of enzyme active centers. It has been suggested, that the geometry of active-center dipole groups is engineered in evolution to provide optimal 'solvation' (electrostatic stabilization) of polar transition states [82].

What of the role(s) of the protein matrix in active-center events? Viewing the enzyme as a macromolecular free-energy transducer, an immediate question concerns the *kinds of useful energy* which are transduced. It is quite clear from the foregoing, that *mechanical* (i.e., potential/kinetic) *forms* are involved. Considering, the predominance of activated protonic/electronic states during catalytic events at the active center, it is natural to ponder a role of the protein molecule as a *protical/electrical transducer*. There is an increasing indication, from both experimental and theoretical fronts, that such transduction does, indeed, occur in *individual* proteins, and that it may be involved in catalytic processes [100,101]. Interest in this type of energy transduction is heightened further, when we relate the cytological juxtaposition of organized enzyme systems and sites of protonic/electronic sources (see above). It is quite plausible that, in many cases, the enzyme molecule not only connects the active center *mechanically* to the surroundings, but, also, protically/electrically. That is, many enzymes may operate as *biochemical electrodes and protodes* [5].

Let us look at elements of protein structure which suggest such energy-transduction design. The obvious possibilities are regions of local secondary structure, viz., α-helix and β-structure. First, we consider the α-helix. The α-helix possesses a marked *dipole moment*, originating in the alignment of the dipole moments of the individual peptide units [102]. The helix dipole generates a considerable electric field, whose strength increases with helix length – particularly in a medium (viz., the interior of a globular protein or a membraneous phase) with low dielectric constant.

Hol et al. [102] suggested that the electric field of the α-helix is "a significant factor which must be included in the discussion of the properties of proteins". The previous authors proposed three possible functional roles of this field in enzyme activity: (i) binding of charged substrates or coenzymes; (ii) long-range attraction and/or orientation of charged substrates; and (iii) contribution to catalytic events. Several widely diverse types of enzymes are known from structural studies to bind negatively charged compounds at the N-terminal-region of an α-helix. Moreover, Hol et al. [102] specify a number of different kinds of enzymes (e.g., NAD-dehydrogenases), whose active sites are known to be located at the N-terminus of an α-helix. Moieties at such helix termini appear to function in proton-transfer networks which 'activate' (deprotonate) catalytic nucleophiles and/or in stabilization of negatively-charged (e.g., oxyanion) transition states.

Other, interesting roles of α-helical elements have been suggested. Types of α-helices may constitute the framework through which proton transport occurs in the well-known, membraneous proton 'pumps' [103–105]. Also, the α-helix seems appropriately designed for vectorial conduction of *soliton* energy impulses (i.e., phonon wave-packets), from sites of energy release (e.g., ATP hydrolysis, redox reactions) to sites of utilization (see below) [106,107].

Regular β-structures in some enzymes (e.g., serine proteases) most likely contribute to local fields, involved in substrate-binding and/or catalytic events. It appears that β-structures provide an additional way of integrating the substrate into the protonic 'circuitry' of the protein matrix [101].

Another structural array, which may be particularly important in proton semiconduction, is a hydrogen-bonded network (see Fig. 10), formed by interdigitated R-groups of parallel α-helix segments *or* parallel β-structures [108]. Obviously, such a network could function efficiently as a proton conductor only within a relatively hydrophobic environment (viz., a membrane phase *or* inside a globular protein). As shown by Nagle et al. [109], this design can be a modus operandi for proton 'pumps', protochemical reactions, and, even, proton-driven mechanical work (e.g., cyclic conformational changes, generated by migrating 'faults' which follow proton 'hopping' – see below).

Long-range, mobile protonic states are finding increasing relevance to many cellular processes, stemming from the original pioneering suggestion as to the role in electron-transport phosphorylation [10]. As indicated above, this kind of energy continuum is emerging as a unifying theme in cell metabolism. The importance of this theme demands that we begin looking at enzyme structure/function with new perspectives. Relating to basic enzyme action, as expressed by Wang [100], mobile protonic states may represent "a broad catalytic principle which transcends the idiosyncracies of individual enzymes". The three enthalpic catalytic factors discussed above may all be subservient to this 'principle'. That is to say, *facilitated proton transfer*, in the enzyme-substrate complex, plays a key role in most enzyme catalyses. (This is obvious in the case of acid-base catalysis. It is more subtly involved in 'rack' and covalent mechanisms. For example, nucleophilic (e.g., hydroxyl, sulfhydryl) groups at the active center usually require 'activation' by proton shuttles or charge-relay networks.)

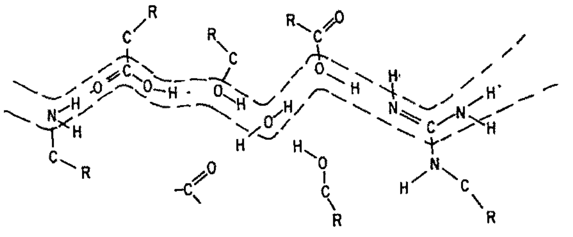

Fig. 10. Hydrogen-bonded chain formed from amino acid side chains from conjoined proteins and some bound water molecules. The symbol R refers to the remainder of the amino acid side chains leading to the protein backbone. The proton channel containing the hydrogen-bonded chain is outlined with dashed lines. (See Ref. 108.)

A similar notion has been advanced forcefully by Metzler [101], in a review on tautomerism in enzyme catalysis. As noted by the previous author, "the rapid equilibration of isomers in which one or more hydrogen atoms change positions is a prevalent phenomenon among biochemical substances". He proposed that enzyme molecules have evolved generally *to conjugate with such protonic/electronic chemical configurations*, and that tautomeric effects in enzyme-substrate complexes probably play basic roles in catalysis and regulation. As discussed by Metzler [101], proteins contain many tautomeric groups, such as the peptide/amide groups and many of the amino-acid side-chains, as well as bound coenzymes. The non-polar nature of the protein interior favors the formation of extended hydrogen-bonded networks (and ensuing charge mobility) among these various groups. Charge transfer through these chains is likely to be fundamentally important to enzyme action. In particular, addition or removal of a proton, at one end of a chain of such hydrogen-bonded groups, will produce a local field-effect *at a distance* (and vice versa), via the 'continuum' of the network (see also Ref. 117).

Superimposed on these designs may be long-range *electronic semiconduction* states which may be important in some enzymes, especially in organized states in vivo [111]. Various modes of electronic (and electron-phonon) coupling between enzyme and substrate have been offered as theoretical possibilities (see below) [63,112,113].

IVB. Protein dynamics in organized states

Naturally, the question arises, as to the *interaction* between excited conformational (e.g., vibrational) states and excited protonic/electronic states in the enzyme molecule. This consideration is particularly important, when one notes that virtually all enzymatic mechanisms ultimately involve some kind of *mechanical force*, acting through electrostatic interactions, generated across chemical bonds in the substrate [25,63]. The discourse in the preceding sections would suggest that the enzyme molecule is capable of achieving the proper configuration, through equilibrium-fluctuational interaction with the surrounding bath. All would seem to be well, as we reckon that biological evolution has apparently come to grips, in this way, with the random field in the medium. Notwithstanding, there is something deceptive and misleading about this developing picture. It bears a taint of reductionism. Accepting the premise that many enzymes of intermediary metabolism operate in organized regimes in vivo, there is a certain degree of artificiality in our construction of general theoretical models which attempt to 'unify' the dynamical protein molecule *with a bulk aqueous medium*.

One indication, for example, is seen from the in vitro viscosity dependence of protein function. Studies, using the kind of plot as in Fig. 8, imply that some proteins do not quite manifest maximal function (e.g., k_{cat}) even at viscosities as low as that of *pure water* (e.g., Refs. 51 and 52). Considering the relatively high viscosities potentially extant in cellular microenvironments [72, 95], many enzymes, by extrapolation from in vitro data, would be operating at rather low rate – if their 'energization' is by simple *thermal* means. We contend that by probing the theoretical models in subsection IIC more deeply, we discover a hint – from the fluctuational behavior of the isolated protein in bulk solution – as to *nonthermal modes* of operation in organized states in vivo.

The key feature, in the nonthermal 'excitation' of organized enzyme systems, may lie in the lattice structure and dynamical properties of *hydrogen-bond chains* in proteins (and in supramolecular assemblages). External *and* internal hydrogen-bonding plays an integral role in the dynamic (and quaternary) structure of globular proteins [59,77]. Following tenets of certain of the dynamical enzyme models (e.g., subsection IIC-2), one sees that Z_H-*zymons* (i.e., gaps, defects) in the internal-bonding arrangement might elevate *locally* the free-energy of the system – electrostatically and mechanically, as well as 'protonically' (see subsection IVA). Such Z_H-*zymons* arise, in a protein dissolved in aqueous solution, in conjunction with binding/relaxation of bound water, fluctuating proton-transfer processes, charge-density fluctuations at the surface, etc. Inside the protein, these 'faults' can migrate, for example, by proton hopping [108]. The energy required for a single 'hop' is about kT, i.e., *thermal energy*. This characteristic explains why certain enzymes, which might be designed to function in conjunction with external, nonequililbrium excitation modes (e.g., protonic 'energy continua') in vivo, can work (at least, in some fashion) when isolated in bulk aqueous solution. For the Z_H-*zymons* can be thermally (albeit ramdomly) activated.

Berry [5,114] has offered a novel *electrochemical interpretation of metabolism*, which advances the idea that proton current ('proticity'), generated by local redox (or photoredox) processes and ATP-cleavage reactions, flows through 'intracellular circuits' in structured matrices, specific for various metabolic functions in the cell. 'Structural' proteins in membranes (e.g., 'protoneural' proteins [115]) and microtrabecular lattices, as well as multienzyme systems adsorbed thereto, might sustain this proton transmission. Recently, Welch and Berry [6] extended this view, drawing further attention to a possible physiological connection, between the central bioenergetic concept of 'proticity' *and* the universal role(s) of 'mobile protons' in enzyme structure, function, and evolution. It was suggested, that organized proton flow in *localized* enzyme aggregates can coordinate protochemical, as well as conformational-dynamical, aspects of enzyme catalysis – in the manner of a 'molecular-energy machine' [32]. This approach embraces the Nagle-Morowitz model of proton-semiconduction in extended hydrogen-bond chains [108]. Accordingly, such organized enzyme systems are supposed to be 'plugged into' a protonic 'continuum' (e.g., at a membrane interface), so that the action of a given enzyme may be 'driven' dynamically by a steady-state proton flow (in conjunction with

reviews on bioenergetics

SAMPLE COPY

for additional information contact:
ALLIED/ELSEVIER JOURNALS
MARKETING GROUP
30, WEST COTT ROAD, Ph: 82468
MADRAS - 600 014./
750, MOUNT ROAD,
MADRAS - 600 002.

BBA
Biochimica et Biophysica Acta (BR)

Editor for Reviews on Bioenergetics P.L. Dutton and M. Wikström

ors: P. Borst, P. Cohen,
Chairman), R.A. Flavell,
ter

Vol. 768
No. 2
1984

ISSN 0006-3002
0005-2728
BBACAQ 768 (2) 81-200 (19
BRBMC 5 768 (2) 81-200 (1984)

PUBLICATION SCHEDULE FOR 1984

BBA is published according to a volume-numbering scheme that embraces all sections of the journal. In addition, each regular section has its own sequential volume-numbering system, running parallel to the overall BBA scheme set out below

	BIO-ENERGETICS	BIO-MEMBRANES	GENE STRUCTURE AND EXPRESSION	PROTEIN STRUCTURE AND MOLECULAR ENZYMOLOGY	LIPIDS AND LIPID METABOLISM	GENERAL SUBJECTS	MOLECULAR CELL RESEARCH	BBA REVIEWS
Jan	764/1 = B66/1	769/1 = M115/1 769/2 = M115/2	781/1 = N8/1	784/1 = P19/1 784/2 = P19/2	792/1 = L67/1	797/1 = G109/1 797/2 = G109/2	803/1 = C5/1	In addition to the regular volumes of BBA, three volumes of BBA REVIEWS will be published (a) BBA REVIEWS ON BIOENERGETICS Vol 768 = BR12 (b) BBA REVIEWS ON BIOMEMBRANES Vol 779 = MR13 (c) BBA REVIEWS ON CANCER Vol 780 = CR11
Feb	764/2 = B66/2	769/3 = M115/3 770/1 = M116/1	781/2 = N8/2	784/3 = P19/3 785/1 = P20/1	792/2 = L67/2	797/3 = G109/3	803/2 = C5/2	
March	764/3 = B66/3	770/2 = M116/2 771/1 = M117/1	781/3 = N8/3	785/2 = P20/2 785/3 = P20/3	792/3 = L67/3 793/1 = L68/1	798/1 = G110/1	803/3 = C5/3	
April	765/1 = B67/1	771/2 = M117/2 772/1 = M118/1		786/1 = P21/1 786/2 = P21/2	793/2 = L68/2	798/2 = G110/2 798/3 = G110/3	803/4 = C5/4	
May	765/2 = B67/2	772/2 = M118/2 772/3 = M118/3	782/1 = N9/1	786/3 = P21/3 787/1 = P22/1	793/3 = L68/3	799/1 = G111/1	804/1 = C6/1	
June	765/3 = B67/3	773/1 = M119/1 773/2 = M119/2	782/2 = N9/2	787/2 = P22/2 787/3 = P22/3	794/1 = L69/1	799/2 = G111/2 799/3 = G111/3	804/2 = C6/2	
July	766/1 = B68/1	774/1 = M120/1 774/2 = M120/2	782/3 = N9/3	788/1 = P23/1 788/2 = P23/2	794/2 = L69/2 794/3 = L69/3	800/1 = G112/1	804/3 = C6/3	
Aug	766/2 = B68/2	775/1 = M121/1 775/2 = M121/2	782/4 = N9/4	788/3 = P23/3 789/1 = P24/1	795/1 = L70/1	800/2 = G112/2 800/3 = G112/3	804/4 = C6/4	
Sept	766/3 = B68/3	775/3 = M121/3 776/1 = M122/1		789/2 = P24/2 789/3 = P24/3	795/2 = L70/2	801/1 = G113/1	805/1 = C7/1	
Oct	767/1 = B69/1	776/2 = M122/2 777/1 = M123/1	783/1 = N10/1	790/1 = P25/1 790/2 = P25/2	795/3 = L70/3 796/1 = L71/1	801/2 = G113/2 801/3 = G113/3	805/2 = C7/2	
Nov	767/2 = B69/2	777/2 = M123/2 778/1 = M124/1	783/2 = N10/2	790/3 = P25/3 791/1 = P26/1	796/2 = L71/2	802/1 = G114/1 802/2 = G114/2	805/3 = C7/3	
Dec	767/3 = B69/3	778/2 = M124/2 778/3 = M124/3	783/3 = N10/3	791/2 = P26/2 791/3 = P26/3	796/3 = L71/3	802/3 = G114/3	805/4 = C7/4	
	5 volumes [a]	11 volumes [b]	3 volumes	8 volumes	5 volumes	6 volumes	3 volumes	
	Total 42 volumes [c] plus Cumulative Index (1983)							

Authors should submit their manuscripts (three copies) for publication in BIOCHIMICA ET BIOPHYSICA ACTA by sending them to one of the Managing Editors

Dr. P Borst, c/o BBA Editorial Secretariat, P O. Box 1345, 1000 BH Amsterdam, The Netherlands
Dr P. Cohen, Department of Biochemistry, Medical Sciences Institute, University of Dundee, Dundee, DD1 4HN, U K.
Dr. L L M van Deenen, c/o BBA Editorial Secretariat, P O. Box 1345, 1000 BH Amsterdam, The Netherlands
Dr R.A Flavell, c/o BBA Editorial Secretariat, P.O. Box 1345, 1000 BH Amsterdam, The Netherlands
Dr. G K. Radda, Department of Biochemistry, University of Oxford, South Parks Road, Oxford, OX1 3QU, U K
Dr E.C Slater, c/o BBA Editorial Secretariat, P O Box 1345, 1000 BH Amsterdam, The Netherlands

Detailed information for contributors may be found in Biochim Biophys Acta 715 (1982) 1–23, also published as the 1982 edition of the booklet

INFORMATION FOR CONTRIBUTORS TO BIOCHIMICA ET BIOPHYSICA ACTA

which is available free of charge from the BBA Editorial Secretariat.

Subscription information

1984 BBA Reviews on Bioenergetics, Volume 768 (1 volume in 4 issues) Dfl 215 (US$ 83) + Dfl 21 (US$ 8) postage, packaging and handling Total price Dfl 236 (US$ 91).
1984 BBA full subscription, Volumes 764–805 (42 volumes in 126 issues), Dfl 6720 (US$ 2585) + Dfl 882 (US$ 339) postage, packaging and handling. Total price Dfl 7602 (US$ 2924)
The Dutch guilder price is definitive The U S dollar price is subject to exchange-rate fluctuations and is given only as a guide.
Journals are sent by air to North America at no extra charge, and by surface delivery to all other countries Airmail and SAL (Surface Airlifted Mail) rates for other countries are available on request
Subscription orders can be entered only by calendar year (Jan -Dec) and should be sent to Elsevier Science Publishers, Journals Department, P.O Box 211, 1000 AE Amsterdam, The Netherlands, Tel (020) 5803 642, Telex 18582, or to your usual subscription agent
Claims for missing issues should be made within 3 months of publication, otherwise they cannot be honoured free of charge
The Publisher reserves the right to issue additional volumes during the course of the year Such volumes will be invoiced before publication and delivered after receipt of payment
In the United States and Canada for further information concerning this or any other Elsevier Science Publishers journal, contact Elsevier Science Publishers, Journal Information Center, 52 Vanderbilt Avenue, New York, NY 10017, U S.A , Tel. (212) 867 9040

local field effects acting, for example, through α-helix dipoles). This flow would serve, in some instances, a 'stoichiometric' role, as a source/sink of protons for protochemical events at active-centers [100]. And, generally, the 'energy continuum' of the mobile protonic state, by virtue of *proton-conformational-interaction* [108], would serve to 'energize' the ES complex (i.e., toward defined transition states) (see also Ref. 63).

And, there is the possible relevance of mobile *electronic* states, in relation to protein dynamics. Interaction of electronic and nuclear degrees of freedom is well-known in solid-state physics. An example is electron-phonon coupling in crystal-lattice dynamics. The possible roles of such modes in enzyme action have been discussed by others [63,112,113,116]. Generally, the idea of electron semiconduction has not been taken seriously in cellular processes (at least over large distances), because of the gap in the band structure of proteins, problems of insulating the flow, etc. However, in organized states in vivo such problems may be obviated [17,111].

Fröhlich [61,62,117] has developed the notion that the activities of localized enzymes couple to electric fields (and other energy sources) via excitaion of metastable states in the protein. The modality involves longitudinal electric dipolar oscillations of *hydrogen-bond units*, which are modeled as active *phonons* (i.e., quasi-particle lattice vibrations). Such systems can store external energy in specific modes (and subsequently do work with it), via a phonon-condensation phenomenon (analogous to the condensation of a Bose-Einstein gas), if the energy is 'pumped' into them above a acritical rate. It was proposed [61,62], that this modality may be involved in driving the conformational dynamics of organized enzyme systems, as well as substrate-translocation processes. This scheme might also involve a cyclic conformational-relaxation in nonequilibrium states [63,64].

Coherent hydrogen-bond phonons (e.g., in α-helical regions), arising from external energy 'pumps', can propagate under some conditions in the form of dispersionless wave-packets termed *solitons*. These soliton modes have been suggested as transduction devices in the operation of proton-motivated 'molecular engines', ATP-linked muscle contraction, inter alia [105–107,118–121].

With these nonthermal systems, one sees perforce a *direct* correspondence between the *zymon* entity and 'quasi-particles' (e.e., mobile protonic states, phonons, solitons) which are well known in quantum physics. And, by vitrtue of their operation in conjunction with an 'external' (nonequilibrium) energy source, these enzyme systems can actually use the *zymon* modality to perform work on the surroundings (e.g., alteration of chemical equilibria). The enzyme simply transduces the energy coherently, from the 'source' to the bound chemical subsystem. The *zymon* modes represent the modus operandi of the transduction process – for thermal as well as for nonthermal systems.

Empirical data in support of these long-range energy-transduction modalities (as they apply to *intermediary metabolism*) are, presently, rathere sparse. Nonetheless, there are some preliminary indications thereto [120,122–124]. It should be emphasized that direct experimental evidence for these modalities is likely to be unobtainable by the more conventional techniques. Although we have gained some clues from enzymes isolated in vitro, as to their roles in 'molecular-energy machines' [32], the holistic transduction designs must be studied with whole cells and cytological substructures.

IVC. Kinetic features of nonthermal enzyme systems

The operation of enzymes in organized states requires a refinement in our understanding of the dynamical nature of chemical process in vivo. Customarily, the laws of chemical kinetics tell us, that the rate (velocity) of a reaction in bulk solution is given as the product of a concentration and a unitary rate constant. Of course , this product is just the probability of *finding* a reactant molecule (or an encounter pair, in the case of a bimolecular reaction) in solution, multiplied by the probability that such a molecule (or encounter pair) actually *reacts*. We usually think of the term 'concentration' very simplistically, as a scalar quantity reflecting the random statistical distribution of solutes in the bulk phase. However, the concept of 'concentration', in the usual macroscopic sense, breaks down for organized enzyme systems. Notionally, one must define 'concentration' (or, more appropriately, the *chemical poten-*

tial) according to the physical *context* in which a given reaction occurs [32,92,94,125,126]. A similar status rerum is found for the case of *local proton flow* in energy-transducing membrane systems [7,8,127].

And, the *rate constant* takes new meaning for nonthermal systems. The most familiar depiction of the rate constant (for thermal systems) is the Arrhenius form discussed in subsection IIIA. Of course, the probability function, W, in Eqn. 7 reflects a *Maxwell-Boltzmann distribution* for the energy states of the reactant species (see Eqns. 11, 12 and 15). This statistical distribution pertains to the so-called 'classical limit', at high temperature *or* at low density (i.e., where the number of available molecular-quantum states is much greater than the number of particles in the system). This condition applies to the vast majority of physico-chemical systems studied under laboratory conditions, including isolated enzymatic processes in vitro. However, there are indications [32] that nonthermal enzyme systems, functioning in organized states, maintain an inherent restriction on molecular degrees of freedom [63]. Indeed, many of these systems have a *quantal nature* which requires some more exact fomalism than that of Maxwell-Boltzmann statistics.

In quantum physics, all particles (and quasi-particles) are categorized as 'fermions' *or* as 'bosons', depending on whether the particles fit Fermi-Dirac *or* Bose-Einstein statistics, respectively. (Both go over to Maxwell-Boltzmann in the 'classical limit'.) For example, electrons and protons are fermions, whereas photons and phonons are bosons. The quantum-statistical counterpart of the equilibrium distribution function, W, in Eqn. 7 is found in the following form:

$$\bar{n}_i = \frac{\lambda e^{-\epsilon_i/kT}}{1 \pm \lambda e^{-\epsilon_i/kT}} \qquad (25)$$

where $\bar{n}_i$ is the average number of particles in the ith quantum state, ϵ_i the energy of the ith state, and λ an absolute activity given as:

$$\lambda = e^{\mu/kT} \qquad (26)$$

with μ the chemical potential. With (+) in Eqn. 25 we have Fermi-Dirac and with (−) Bose-Einstein statistics. (Electromagnetic radiation and electrons in metals are two well-known phenomena which are described by such quantum statistics.)

The various 'bio-quanta' discussed in subsection IVB are, in principle, amenable to quantum-statistical description. However, one cannot proceed by simple substitution of Eqn. 25 into Eqn. 7. For the distribution in Eqn. 25 – just as that in the Maxwell-Boltzmann form used in Eqns. 11, 12 and 15 – represents an *equilibrium situation*. In many of the 'molecular-energy machines' in vivo [32], the particles are not allowed to sample an equilibrium distribution of energy states at a given temperature, because of nonequilibrium constraints imposed by the organizational mode of the system and/or by external energy sources. Thus, for nonthermal systems plugged into external energy sources ('pumps'), one must obtain W of Eqn. 7 (i.e., the fraction of reactant species possessing some critical energy) by solving (for $\bar{n}_i$) *a stationary-state equation* containing source and sink terms for the relevant quanta. Fröhlich [62] has given a cogent discussion of such calculations for phonon modes in proteins. A similar approach is available for soliton behavior [107,119]. And, such calculations might be possible for other 'bio-quanta' (e.g., 'active' protons [87]), insofar as they are energetically separable from protein modes [126].

One might approach the *frequency term*, k_υ, in Eqn. 7 in a like manner. As indicated in Section III, the frequency factor, for an enzyme-protein in bulk solution, will depend on transient, *thermal excitation* of the relevant quanta (*zymons*). Within certain organized regimes in vivo, the conformational-dynamical participation of the protein matrix may be driven by a cyclical (external) flow of quanta (see subsection IVB). Hence, the 'kinetics' of such organized enzyme systems may be governed entirely by the 'kinetics' of the external energy 'pump'. Possible advantages of this 'master-slave' relationship have been discussed by others [6–8,32,99,109,117]. Blumenfeld [63,64] has elaborated a number of aspects of protein-conformational dynamics in nonequilibrium states, particularly applicable to electron-transport phosphorylation.

Although the nature of enzyme action in these organized states is far from clear, its microscopic *quantum-mechanical character* is becoming increasingly apparent. The nature of the *zymon* modality, as it is manifested in both thermal and nonthermal systems, points to this realization. This situation will necessitate a dramatic shift in our thinking, as regards both kinetic *and* thermodynamic aspects of (electro)chemical processes in vivo [5–8]. This subject is treated in more detail elsewhere [32].

V. Summary

The most important idea underlying our treatment herein is *the unity of the enzyme molecule and the medium.* Appreciation of this relationship is vital, if enzymology is to graduate from its present reductionistic status to a more holistic posture. Enzymes are *biological* entities firstly, and isolated objects of physicochemical analysis secondly. Perhaps the most crucial 'biological lesson', particularly apropos of enzymes *in intermediary metabolism*, concerns the 'cytosociology' of enzyme action in vivo [94,128]. The natural habitat of many enzymes in the living cell is far different from that in bulk aqueous solution in vitro. In order to obtain a real grasp of the nature of enzyme function, one must ultimately couch enzymology in concepts emerging from contemporary cell biology [95].

Notwithstanding, analysis precedes synthesis; and one must needs begin with the individual enzyme molecule. The trenchant efforts of the physical chemist and the organic chemist have produced a wealth of information on the nature of the binding and catalytic events at the enzyme active site. While it is not yet possible to explain *precisely* the complete sequence of events in the catalytic process, nevertheless, the basic mechanisms by which enzymes effect catalysis (i.e., reduce activation energy) now seem apparent [81,129]. The new frontier is to be found, in exploring the dynamic role of the protein matrix [17]. Not only does the protein provide the 3-D scaffolding for active-site processes, but, more importantly, it serves as the *local solvent* for the bound chemical subsystem. Thus, the dynamical aspects of enzyme catalysis (for thermally based systems) must arise from the fluctuational properties of the protein molecule. This notion is the common denominator in all of the models in subsection IIC. It is the anisotropic nature of this fluctuational behavior, which would characterize the energy-transduction phenomenon leading to localized catalytic events at the active-site. In Section III we attempted to show that all of the various enzyme models contribute pieces to a single, all-embracing jig-saw puzzle. Some models focus on the dynamical properties of the protein per se, whereas others deal with the stochastic aspects of protein-solvent interaction. The two approaches are complementary, as are mutually interlocking pieces of a puzzle.

The ultimate picture depicted by this 'jig-saw puzzle' is still somewhat vague – owing to the present paucity of empirical information on protein motions. Nevertheless, accumulating experimental data, computer-simulation studies, and theoretical models indicate that *solvent interaction* plays an important role in inducing the reactive modes in the enzyme molecule. And, it is apparent that the protein-dynamical basis of enzyme action must be sought in slower, collective motions distributed inhomogeneously in the protein. This is obvious, when we compare the values of typical enzyme catalytic constants and the vibrational frequency (and number) of *individual* atoms in the protein. For economy of thought, we have termed these 'quasi-particles' as *zymons*. Although their exact physical character remains to be elucidated, there can be no doubt that *zymon* modalities exist in enzymes. Most likely, the lattice structure and dynamical properties of *hydrogen-bond chains* are at the root of such collective motions in the protein.

Yet, this thermally-based dynamical view of enzyme action leads to some problems, when we consider the enzyme molecule in its natural setting in vivo. It appears that most enzymes (at least those of intermediary metabolism) operate in organized states, probably in association with particulate structures. A discordant note is found in the observed *viscosity-dependence* of enzymes in vitro. Viscosity is an appropriate parameter characterizing the '(de)energization' of an enzyme-substrate complex, as it relates to the transfer of momentum between protein and solvent. When studied in isolation, many enzymes apparently obey Eqn. 22 (see Fig. 8). If we extrapolate this observed viscosity-dependence to the kinds of high-viscosity microenvironments extant in vivo, we realize that such enzymes would operate in a rather depressed state – assuming thermal 'energization' is the modus operandi. For, the internal *zymon* modes would be overdamped.

Mitchell [130] defined 'molecular mechanical lubricity', as "the effective smoothness and slipperiness of the molecular articulations" involved in the ligand-conduction processes catalyzed by enzymes, carrier proteins, etc. He suggested, that this "lubricity ... presumably plays a vital part in keeping down the energetic cost of transmitting chemicals and energy from one place to another in living organisms. Therefore, we may expect that the orderliness and lubricity of the working configurational or conformational cycles of catalytic ligand-conducting proteins, and of other components catalysing vectorial metabolism, may have become highly developed by natural selection" *. The role of organized multienzyme systems in this regard has been discussed widely (see Refs. 92 and 131 and others cited therein). At the level of the individual enzyme molecule, one sees (Fig. 1) a beautiful example of 'lubricity' in the free-energy complementarity idea of Lumry and Biltonen [25]. Indeed, such a fluid-like exchange of free energy between protein and chemical subsystems is central to all the dynamical models presented in subsection IIC.

However, natural selection can go only so far in designing the *isolated* enzyme molecule to work against the 'random field', especially for enzymes of intermediary metabolism. The conditions (e.g., viscosity) of the ambient 'aqueous phase' in the localized microenvironments in vivo are rather imposing. Mitchell [130] suggested that, "one reason for the evolution of dimeric or polymeric enzymes and osmoenzymes (e.g., F_0F_1-ATPase) that work by alternating site mechanisms may be that the changes of volume and shape of the monomers can be partially compensatory in the dimer or polymer, so that the frictional losses through environmental viscosity can be mitigated." This contention may be valid to some extent. Nevertheless, one finds [130] for example that the mitochondrial F_0F_1-ATPase, when decoupled functionally from its endogenous 'energy source' and assayed in vitro in the direction of ATP hydrolysis, exhibits the kind of viscosity dependence indicated by Eqns. 5, 6 and 22 (see also Ref. 132). Yet, the conformational dynamics of the F_0F_1-ATPase – as for many enzymes of intermediary metabolism functioning in vivo (as discussed in Section IV) – may be *driven* by external 'pumps' engendered by long-range energy continua.

Once the 'lubricational' device of the free-energy 'complementarity principle' [25] was pushed to its limits in the evolution of the individual enzyme molecule, perhaps the only recourse was to 'plug' many enzymes into such 'energy continua' (e.g., local electric fields, mobile protonic states). Consistent with this view is the emerging notion (see Section IV), that *cell metabolism is largely a surface (2-D) phenomenon* [95,133].

There is the equally plausible view, that 'surface activity' was the rule from the earliest stages of cellular evolution, and that free-energy 'complementarity' manifest in many enzymes reflects just their capability of linking chemical reactions to *external* energy sources. It is widely held among molecular evolutionists, that biochemical processes took place, under primordial conditions, in association with adsorptive clay surfaces (and the ambience of structured, polarized water layers), followed by formation of coacervates, microspheres and the like. It is likely that *mobile protons* were intimately involved in the catalytic activity of these surface states [134,135]. And, it has been proposed [6,136] that present-day enzyme molecules are 'microcolloids' reminiscent of this primordial condition. Thus, it is natural to ponder a possible connection between the central bioenergetic concept to 'proton-motive force', on the one hand, and the roles of mobile protons in enzyme structure, function and evolution, on the other hand. The theoretical considerations of Section IV would suggest that the enzyme molecule – in many more systems than the well-known H^+-F_0F_1 ATPase and porter enzymes – may serve to connect a specific chemical reaction-coordinate to this 'active' protonic state.

---

* In attempting to give a microscopic explanation for the observed linear relationship between the velocity and the driving force in ligand-conduction systems (which apparently occur far from thermodynamic equilibrium (e.g., in mitochondria)), Mitchell [130] equated the viscosity (or friction) coefficient to a 'microscopic irreversibility coefficient'. However, this approach is questionable. In order to describe rigorously the stochastic influence of the medium on these molecular systems, one must construct a generalized Langevin equation, as opposed to a simple Stokes-force relation (which the previous author [130] used). The whole issue of the microscopic basis of irreversibility may not be explainable by conventional statistical-mechanical laws [137]. Moreover, the organizational character of biological energy-transducing systems, at the molecular level, may not fit the usual paradigm of macroscopic thermodynamics [7,8,32,99,127].

The subject of 'nonthermal' enzyme systems, as it relates to long-range energy-transduction modalities in the living cell, is fertile ground for both experimental and theoretical pursuit. Not only are there many unanswered questions in this area, but, also, the proper questions may have yet to be posed. The nature of enzyme action within the microscoping confines of organized states is a subject of increasing interest in contemporary enzymology. The theoretical investigations reviewed in Section IV would indicate that many enzymes in such organized regimes are not 'free-wheeling engines', completely at the whim of a random-field environment. Rather, they may operate as 'molecular-energy machines' [32], with a *quantum-mechanical essence* of the form suggested by McClare [99].

When we regard the connection between 'bioenergetics' and 'intermediary metabolism', we traditionally think of ATP – that stable, diffusible carrier of free energy. ATP is considered the primary 'functional coupling agent' [2], between energy-generation processes and anabolic metabolism. With the advent of such 'bioenergetic' principles as the H^+-electrochemical potential difference (and proton-motive energy coupling), in conjunction with the increasing focus on cytological surfaces as the operational site of most multienzyme systems of cell metabolism, we are forced to infer a much more intimate link between 'bioenergetics' and 'intermediary metabolism' [5]. As stated so appropriately by Harold [138], "to find the secret of life we shall have to marry the study of macromolecules and genes with that of the vectorial flux of ions, molecules, and chemical groups in fields of force". Study of the dynamical properties of proteins should ultimately reveal the true nature of the enzyme as an energy transducer, in equilibrium as well as in nonequilibrium states.

Acknowledgements

G.R.W. thanks appreciatively the following, for their constructive input to the development of ideas presented herein: Prof. M.N. Berry, Dr. D.B. Kell, Prof. R. Lumry and Dr. H.V. Westerhoff. Also, G.R.W. gratefully acknowledges the United States National Academy of Sciences and the Hungarian Academy of Sciences, for grants in support of this work.

Note added in proof (Received May 4th, 1984)

The term 'zymon', introduced in subsection IIIC, was chosen by analogy to the quantum-gravitational fluctuations in the metric of space-time. The latter fluctuations, dubbed 'instantons' [139] or 'fluctuons' [140], permeate the vacuum of space and are scaled by the so-called Planck mass (approx. 10^{-5} g) and Planck length (approx. 10^{-33} g). Particles of matter embedded in space are likened to localized perturbations (or exciton-like changes in the phase relations) of this pervasive, rippling microstructure [140]. By analogy, the generation of 'hot spots' (at the active center) in an enzyme molecule may be regarded as local excitations of the fluctuating microstructure of the globular protein. In the Lumry model [25], the flow of an enzyme-catalyzed process along the reaction coordinate is characterized by a dynamic, compensatory enthalpy-entropy 'phase relation' in the protein matrix. It is interesting to note that the geometrodynamical 'fluctuons' in the vacuum state also exhibit a collective 'compensation', via the negatory influence of gravitational coupling [140].

Since the completion of the present review, the detailed molecular dynamics of an actual bond-breaking event in a fluctuating enzyme-substrate complex has been simulated [141]. The fluctuations of the enzyme electrostatic potential, as related to protein motions, were found to be a key dynamical factor in reactions involving large change in bond-polarity.

References

1 Nicholls, D.G. (1982) Bioenergetics, Academic Press, New York

2 Atkinson, D.E. (1977) Cellular Energy Metabolism and Its Regulation, Academic Press, New York

3 Pollard, E.C. (1963) J. Theor. Biol. 4, 98–112

4 Welch, G.R., Somogyi, B. and Damjanovich, S. (1982) Progr. Biophys. Mol. Biol. 39, 109–146

5 Berry, M.N. (1981) FEBS Lett. 134, 133–138

6 Welch, G.R. and Berry, M.N. (1983) in Coherent Excitations in Biological Systems (Frohlich, H and Kremer, F., eds.), pp. 115–140, Springer-Verlag, New York

7 Kell, D.B. and Hitchens, G.D. (1983) in Coherent Excitations in Biological Systems (Frohlich, H. and Kremer, F., eds.), pp. 205–226, Springer-Verlag, New York

8 Westerhoff, H.V., and Van Dam, K. (1984) Mosaic Nonequilibrium Thermodynamics and (the Control of) Biological Free-Energy Transduction, Elsevier, Amsterdam

9 Gutfreund, H. (1976) FEBS Lett. 62 (Suppl.), E1–E2

10 Mitchell, P. (1979) Eur. J. Biochem. 95, 1–20

11 Careri, G. (1974) in Quantum Statistical Mechanics in the Natural Sciences (Kursunoglu, B., Mintz, S.L. and Widmayer, S.M., eds.), pp. 15–35, Plenum Press, New York

12 Careri, G., Fasella, P. and Gratton, E. (1975) CRC Crit. Rev. Biochem. 3, 141–164

13 Lumry, R. and Hershberger, M. (1978) Photochem. Photobiol. 27, 819–840

14 Gurd, F.R.N. and Rothgeb, T.M. (1979) Adv. Protein Chem. 33, 73–165

15 McCammon, J.A. and Karplus, M. (1980) Annu. Rev, Phys. Chem. 31, 29–45

16 Karplus, M. and McCammon, J.A. (1981) CRC Crit. Rev. Biochem. 9, 293–349

17 Karplus, M. and McCammon, J.A. (1983) Annu. Rev. Biochem. 53, 263–300

18 De Brunner, P.G. and Frauenfelder, H. (1982) Annu. Rev. Phys. Chem. 33, 283–299

19 Welch, G.R. (ed.) The Fluctuating Enzyme (1984) Wiley-Interscien, New York, in the press

20 Cooper, A. (1976) Proc. Natl. Acad. Sci. U.S.A. 73, 2740–2741

21 Frauenfelder, H., Petsko, G.A. and Tsernoglou, D. (1979) Nature (Lond.) 280, 558–563

22 Artymiuk, P.J., Blake, C.C.F., Grace, D.E.P., Oatley, S.J., Phillips, D.C. and Sternberg, M.J.E. (1979) Nature (Lond.) 280, 563–568

23 Kemeny, G. (1974) Proc. Natl. Acad. Sci. U.S.A. 71, 2655–2657

24 Careri, G. and Gratton, E. (1977) Biosystems 8, 185–186

25 Lumry, R. and Biltonen, R. (1969) in Structure and Stability of Biological Macromolecules (Timasheff, S.N. and Fasman, G.D., eds.) p. 65, Dekker, New York

26 Lumry, R. (1980) in Bioenergetics and Thermodynamics. Model Systems (Braibanti, A., ed.), pp. 405–423 and 435–452, Reidel, Dordrecht

27 Lumry, R. (1971) in Electron and Coupled-Energy Transfer in Biological Systems (King, T. and Klingenberg, M., eds.), p. 1, Dekker, New York

28 Benzinger, T.H. (1971) Nature (Lond.) 229, 100–102

29 Gō, N. and Scheraga, H.A. (1969) J. Chem. Phys. 51, 4751–4767

30 Gō, N. and Scheraga, H.A. (1976) Macromolecules 9, 535–542

31 Pincus, M.R. and Scheraga, H.A. (1981) Acc. Chem. Res. 14, 299–306

32 Welch, G.R. and Kell, D.B. (1984) Not Just Catalysts – Molecular Energy Machines in Bioenergetics, in The Fluctuating Enzyme (Welch, G.R , ed.), Wiley-Interscience, New York, in the press

33 Peticolas, W.L. (1979) Meth. Enzymol. 61, 425–458

34 Linderstrom-Lang, K.U. and Schellman, J.A. (1959) in The Enzymes (Boyer, P.D., Lardy, H. and Myrbäck, K , eds.), 2nd Edn., Vol. 1, pp. 443–510, Academic Press, New York

35 Campbell, I.D., Dobson, C.M., Williams, R.J.P. and Xavier, A.V. (1973) Ann. N.Y. Acad. Sci. 222, 163–174

36 Austin, R.H., Chan, S.S., and Jovin, T.M. (1979) Proc Natl. Acad. Sci. U.S.A. 76, 5650–5654

37 Cherry, R J. (1979) Biochim. Biophys. Acta 559, 289–327

38 Jovin, T.M., Bartholdi, M., Vaz, W.L.C. and Austin, R.H. (1981) Ann. N.Y. Acad. Sci. 366, 177–196

39 Damjanovich, S., Trón, L., Szollosi, J., Zidovetzki, R., Vaz, W.L.C., Regateiro, I., Arudt-Jovin, D. and Jovin, T M. (1983) Proc. Natl. Acad. Sci. U S.A., 80, 5985–5989

40 Eisinger, J. and Flores, J. (1983) Biophys. J. 41, 367–379

41 Matkó, J., Trón, L., Balázs, M., Hevessy, J., Somogyi, B. and Damjanovich, S. (1980) Biochemistry 19, 5782–5786

42 Papp, S., Seres, I., Matkó, J. and Somogyi, B. (1984) Biophys. Chem., in the press

43 Munro, I., Pecht, I., and Stryer, L. (1979) Proc Natl. Acad. Sci. U.S.A. 76, 56–60

44 Pilz, I., Glatter, O., and Kratky, O. (1979) Meth. Enzymol 61, 148–249

45 Lakowicz, J.R. and Weber, G. (1973) Biochemistry 12, 4171–4179

46 Eftink, M.R. and Ghiron, C.A (1977) Biochemistry 16, 5546–5551

47 Eftink, M.R. and Selvidge, L.A. (1982) Biochemistry 21, 117–125

48 Somogyi, B., Matkó, J., Papp, S., Hevessy, J., Welch, G.R. and Damjanovich, S. (1984) Biochemistry, in the press

49 Damjanovich, S., Bot, J., Somogyi, B , Sümegi, J. (1972) Biochim. Biophys. Acta 284, 345–348

50 Damjanovich, S. and Somogyi, B. (1978) in New Trends in the Description of the General Mechanism and Regulation of Enzymes (Symp. Biol. Hung.), Vol. 21, (Damjanovich, S., Elödi, P. and Somogyi, B., eds.), pp. 159–179, Akadémiai Kiadó, Budapest

51 Gavish, B. and Werber, M.M. (1979) Biochemistry 18, 1269–1275

52 Beece, D., Eisenstein, L., Frauenfelder, H., Good, D., Marden, M.C., Reinisch, L., Reynolds, A.H., Sorensen, L.B. and Yue, K.T. (1980) Biochemistry 19, 5147–5157

53 McCammon, J.A., Gelin, B.R., Karplus, M. and Wolynes, P.G. (1976) Nature (Lond.) 262, 325–326

54 Garland, P.B. and Moore, C.H. (1979) Biochem. J., 183, 561–572

55 Low, P.S. and Somero, G.N. (1975) Proc. Natl. Acad. Sci. U.S.A. 72, 3014–3018 and 3305–3309

56 Low, P.S. (1978) in New Trends in the Description of the General Mechanism and Regulation of Enzymes (Symp. Biol. Hung.), Vol. 21, (Damjanovich, S., Elodi, P. and

Somogyi, B., eds.), pp. 217–248, Akadémiai Kiadó, Budapest

57 Rupley, J.A., Gratton, E. and Careri, G. (1983) Trends Biochem. Sci. 8, 18–22

58 Lumry, R and Eyring, H. (1954) J. Phys. Chem. 58, 110–120

59 Lumry, R. and Rosenberg, A. (1975) Colloques Internationaux du C.N.R.S. (No. 246, L'Eau et Les Systèmes Biologiques), pp. 53–62

60 Green, D.E. (1974) Ann. N.Y. Acad. Sci. 227, 6–45

61 Frohlich, H. (1975) Proc. Natl. Acad. Sci. U.S.A. 72, 4211–4215

62 Frohlich, H. (1968) Int. J. Quant. Chem. 2, 641–649

63 Blumenfeld, L.A. (1981) Problems of Biological Physics, Springer-Verlag, New York

64 Blumenfeld, L.A., Burbajev, D.S. and Davidov, R.M. (1984) Processes of Conformational Relaxation in Enzyme Action, in The Fluctuating Enzyme (Welch, G.R., ed.) Wiley-Interscience, New York, in the press

65 Careri, G., Fasella, P. and Gratton, E. (1979) Annu. Rev. Biophys. Bioenerg. 8, 69–97

66 Gavish, B. (1978) Biophys. Struct. Mech. 4, 37–52

67 Gavish, B. (1980) Phys. Rev. Lett. 44, 1160–1163

68 Somogyi, B. and Damjanovich, S (1971) Acta Biochim. Biophys. Acad. Sci. Hung. 6, 353–364

69 Somogyi, B. and Damjanovich, S. (1975) J Theor Biol. 48, 393–401

70 Damjanovich, S. and Somogyi, B. (1973) J. Theor. Biol. 41, 567–569

71 Somogyi, B., Karasz, F.E., Trón, L. and Couchman, P.R. (1978) J. Theor. Biol. 74, 209–216

72 Welch, G.R., Somogyi, B., Matkó, J. and Papp, S. (1983) J. Theor. Biol. 100, 211–238

73 Berendsen, H.J.C. (ed.) (1976) Models for Protein Dynamics, CECAM, Orsay

74 Van Gunsteren, W.F. and Karplus, M. (1982) Biochemistry 21, 2259–2274

75 Swaminathan, S., Ichiye, T., Van Gunsteren, W. and Karplus, M. (1982) Biochemistry 21, 5230–5241

76 Northrup, S.H., Pear, M.R., Lee, C.-Y., McCammon, J.A., and Karplus, M. (1982) Proc. Natl. Acad. Sci. U.S.A. 79, 4035–4039

77 Ikegami, A. (1977) Biophys. Chem. 6, 117–130

78 Gavish, B., A Correlation Between Proteins Main-Chain Atomic Displacements and Density of Hydrogen Bonds, preprint No. ILL-(EX)-81-4, Department of Physics, University of Illinois, Urbana, IL

79 Brown, G.H. and Wolken, J J. (1979) Liquid Crystals and Biological Structures, Academic Press, New York

80 Chandler, D. (1978) Annu. Rev. Phys. Chem. 29, 441–471

81 Fersht, A. (1977) Enzyme Structure and Mechanism, Freeman, San Francisco

82 Warshel, A. (1978) Proc. Natl. Acad. Sci. U.S.A. 75, 5250–5254

83 Cantor, C.R. and Schimmel, P.R. (1980) Biophysical Chemistry, Part III, The Behavior of Biological Macromolecules, W.H. Freeman, San Francisco

84 Levitt, M. (1982) Annu. Rev. Biophys. Bioeng. 11, 251–271

85 Hopfinger, A.J. (1977) Intermolecular Interactions and Biological Organization, Wiley, New York

86 Hagler, A.T. and Moult, J. (1978) Nature (Lond.) 272, 222–226

87 Nagle, J.F. and Morowitz, H.J. (1978) Proc. Natl. Acad. Sci U.S.A. 75, 298–302

88 Haken, H. (1977) Synergetics, Springer-Verlag, New York

89 Kramers, H.A. (1940) Physica 7, 284–304

90 Porter, K.R. and Tucker, J.B. (1981) Sci. Am. 244, 56–67

91 Clegg, J.S. (1983) in Coherent Excitations in Biological Systems (Fröhlich, H and Kremer, F., eds.), pp. 189–204, Springer-Verlag, New York

92 Welch, G.R. (1977) Prog. Biophys. Mol. Biol. 32, 103–191

93 Kell, D.B. (1979) Biochim. Biophys Acta 549, 55–99

94 Welch, G.R. and Keleti, T. (1981) J. Theor. Biol 93, 701–735

95 Clegg, J.S. (1983) Am. J. Physiol., 246, R133–R151

96 Sitte, P. (1980) in Cell Compartmentation and Metabolic Channeling (Nover, L., Lynen, F. and Mothes, K., eds.) pp. 17–32, Elsevier/North-Holland, New York

97 Srere, P. (1981) Trends Biochem. Sci. 6, 4–7

98 Schliwa, M., Van Blerkom, J. and Porter, K.R. (1981) Proc. Natl. Acad. Sci. U.S.A. 78, 4329–4333

99 McClare, C.W.F. (1974) Ann. N.Y. Acad. Sci. 227, 74–97

100 Wang, J.H. (1968) Science 161, 328–334

101 Metzler, D.E. (1979) Adv. Enzymol. 50, 1–40

102 Hol, W.G.J., Van Duijnen, P.T. and Berendsen, H.J.C. (1978) Nature (Lond.) 273, 443–446

103 Van Duijnen, P.T. and Thole, B.T (1981) Chem Phys. Lett. 83, 129–133

104 Krimm, S. and Dwivedi, A.M. (1982) Science 216, 407–408

105 Dunker, A.K. (1982) J. Theor. Biol. 97, 95–127

106 Davydov, A.S. (1981) Physica 3D, 1–22

107 Scott, A.C. (1981) in Nonlinear Phenomena in Physics and Biology (Enns, R.N., Jones, B.L., Miura, R.M. and Rangnekar, S.S., eds.), pp. 7–82, Plenum Press, New York

108 Nagle, J.F. and Tristram-Nagle, S. (1983) J. Memb. Biol. 74, 1–14

109 Nagle, J.F., Mille, M. and Morowitz, H.J. (1980) J. Chem. Phys. 72, 3959–3971

110 Banacky, P. (1981) Biophys. Chem. 13, 39–47

111 Lewis, T.J. (1979) in Submolecular Biology and Cancer (Ciba Foundation Symposium, No. 67), pp. 65–78, Excerpta Medica, New York

112 Volkenstein, M.K. (1981) J. Theor. Biol. 89, 45–51

113 Conrad, M. (1979) J. Theor. Biol. 79, 137–156

114 Berry, M.N., Grivell, A.R. and Wallace, P.G. (1983) in Comprehensive Treatise on Electro-chemistry, Vol. 10, Bioelectrochemistry (Srinivasan, S. and Bhizmadzhev, Y.A., eds.), Plenum Press, New York

115 Kell, D.B. and Morris, J.G. (1981) in Vectorial Reactions in Electron and Ion Transport in Mitochondria and Bacteria (Palmieri, F., Quagliariello, E., Siliprandi, N. and Slater, E.C., eds.), pp. 339–347, Elsevier/North-Holland, Amsterdam

116 Caserta, G. and Cervigni, T. (1974) Proc. Natl. Acad. Sci. U.S.A. 71, 4421–4424

117 Frohlich, H. (1980) Adv. Electron. Electron Phys. 53, 85–152

118 Bilz, H., Buttner, H. and Frohlich, H. (1981) Z. Naturforsch. 36B, 208–212

119 Davydov, A.S. (1982) Biology and Quantum Mechanics, Pergamon Press, Oxford

120 DelGiudice, E., Doglia, S. and Milani, M. (1982) Phys. Scripta 26, 232–238

121 Layne, S.P. and Scott, A.C. (1983) in The Neurobiology of Pain (Holden, A.V. and Winlow, B., eds.), Springer-Verlag, New York

122 Frohlich, H. and Kremer, F. (eds) (1983) Coherent Excitations in Biological Systems, Springer-Verlag, New York

123 Webb, S.J. (1980) Phys. Rep. 60, 201–224

124 Lomdahl, P.S., MacNeil, L. and Scott, A.C. (1982) Phys Lett. 92A, 207–210

125 Sols, A. and Marco, R. (1970) Curr. Top Cell. Regul. 2, 227–273

126 Hill, T.L. and Eisenberg, E. (1981) Quart. Rev. Biophys. 14, 463–511

127 Westerhoff, H.V., Melandri, B.A., Venturoli, G., Azzone, G.F. and Kell, D.B. (1984) FEBS Lett., 165,1–5

128 Welch, G.R. and DeMoss, J.A. (1978) in Microenvironments and Metabolic Compartmentation (Srere, P.A. and Estabrook, R.W., eds.) pp. 323–344, Academic Press, New York

129 Walsh, C. (1979) Enzymatic Reaction Mechanisms, Freeman, San Francisco

130 Mitchell, P. (1981) in Chemiosmotic Proton Circuits in Biological Membranes (Skulachev, V.P. and Hinkle, P.C., eds.), pp. 611–633, Addison-Wesley, Reading, MA

131 Welch, G.R. (1977) J. Theor. Biol. 68, 267–291

132 Ando, T. and Asai, H. (1977) J. Bioenerg. Biomemb. 9, 283–288

133 Clegg, J.S. (1979) in Cell-Associated Water (Drost-Hansen, W. and Clegg, J.S., eds.), pp. 363–413, Academic Press, New York

134 Fripiat, J.J. and Cruz-Cumplido, M.I. (1974) Annu. Rev. Earth Plan. Sci. 2, 239–256

135 Mortland, M.M. and Raman, K.V. (1968) Clays and Clay Miner. 16, 393–398

136 Good, W. (1973) J. Theor. Biol. 39, 249–276

137 Prigogine, I. (1980) From Being to Becoming. Time and Complexity in the Physical Sciences, Freeman, San Francisco

138 Harold, F.M. (1982) Curr. Top. Membrane Transp. 16, 485–516

139 Carr, B.J. and Rees, M.J. (1979) Nature (Lond.) 278, 605–612

140 Wheeler, J.A. (1968) in Topics in Nonlinear Physics (Zabusky, N.J., ed.), pp. 615–724, Springer-Verlag, New York

141 Warshel, A. (1984) Proc. Natl. Acad. Sci. U.S.A. 81, 444–448

Biochimica et Biophysica Acta, 768 (1984) 113–163
Elsevier

BBA 86110

THE BIOENERGETICS OF METHANOGENESIS

LACY DANIELS [a], RICHARD SPARLING [a] and G. DENNIS SPROTT [b]

[a] *Department of Microbiology, University of Iowa, Iowa City, IA 52242 (U.S.A.) and* [b] *Division of Biological Sciences, National Research Council of Canada, Ottawa, Ontario, K1A 0R6 (Canada)*

(Received July 18th, 1983)

Contents

I. Introduction 114

II. Biochemistry and enzymology of methanogenesis 117
- A. Pathway of methanogenesis 117
  - 1. Whole cell work 117
  - 2 Cell extract work 118
  - 3. Coenzymes and related components in methanogenic bacteria 119
    - a. Electron transport 119
    - b. Carbon transfer 123
    - c. Unknown function 126
  - 4. Enzyme studies 127
    - a. Hydrogenase 127
    - b. Formate dehydrogenase 128
    - c. Methyl transferase reactions 130
    - d. Methyl CoM reductase 131
    - e. Carbon monoxide dehydrogenase 132
    - f. NADP-F_{420} oxidoreductase 133
    - g. Methylene-formaldehyde-activating factor oxidoreductase 133
  - 5. The RPG effect 134
  - 6 Summary of the methanogenesis pathway 134
  - 7. Cytoplasmic membrane components 135
- B. The ATP requirement in methanogenesis 136
- C. Carbon fixation into cell material 137
- D. Y_{ATP} studies 138
- E. Scheme of bioenergetic coupling 140

III. Energy conservation and use 140
- A. The protonmotive force ($\Delta\bar{\mu}_{H^+}$) 140
- B. The methanochondrion controversy 142
- C. Transport in methanogens 144

Abbreviations: CCCP, carbonyl cyanide *m*-chlorophenylhydrazone; HS-CoM, 2-mercaptoethanesulphonate; DCCD, *N,N′*-dicyclohexylcarbodiimide; FCCP, carbonyl cyanide *p*-trifluoromethoxyphenylhydrazone; F_{342}, degradation product of carboxymethanopterin that fluoresces at 342 nm; F_{420}, a 8-hydroxy 5-deazaflavin; F_{430}, nickel tetrapyrrole cofactor of the methyl reductase; $\Delta G^{0\prime}$, Gibbs free energy; TCS, tetrachlorosalicylanilide; TPB^-, tetraphenylboron anion; $TPMP^+$, triphenylmethylphosphonium cation; Y_{ATP}, gcell produced per mol ATP; YFC, yellow fluorescing compound = carboxymethanopterin, or formylmethanopterin; FAF, formaldehyde activating factor; CDR, methanofuran, carbon dioxide reduction factor; X_i, intracytoplasmic X; X_o, exocellular X.

0304-4173/84/$03.00 © 1984 Elsevier Science Publishers B.V.

D. ATPase and ATP synthesis 145
E. Inhibitors of methanogenesis 146
F. Sodium requirement for CO_2 respiration 148
G. Discussion of bioenergetic relationships in methanogenesis 149
  1. Proton ionophores 149
  2. Valinomycin (a K^+ ionophore) and K^+ 149
H. Models for generation of $\Delta\bar{\mu}_{H^+}$ and ATP during methanogenesis 151
  1. Formation of $\Delta\bar{\mu}_{H^+}$. Internal membrane required (the methanochondrion hypothesis) 152
  2. Formation of $\Delta\bar{\mu}_{H^+}$ Internal membranes *not* present 152
    a. Methanogenesis from H_2/CO_2 or formate 152
    b. Methanogenesis from acetate 153
    c. Methanogenesis from methanol 153
    d. Methanogenesis from $H_2 + CH_3OH$, but not from methanol alone 154
I. Cautions on methanogen diversity 154

IV. Summary 155

Acknowledgements 156

References 156

I. Introduction

The biosynthesis of methane is limited to a rather specialized group of bacteria, the methanogens, that live in waterlogged soils, guts of animals, sewage sludge, manure piles, marine and fresh water sediments, and hot springs [1–4]. They are obligate anaerobes that produce methane as an end-product of their metabolism.

Phylogenetic analysis based on ribosomal RNA sequence characterization places the methanogens in the recently proposed grouping, or urkingdom, of archaebacteria [5–9], distinct from both the eubacterial urkingdom (composed of the 'typical bacteria') and the urkaryotic urkingdom (representing the cytoplasmic component of the eukaryotic cell). With the eubacteria, they share similar size, absence of cellular organelles, ribosomal subunit sizes, etc. Features in common with urkaryotes include insensitivity to vancomycin, penicillin and kanamycin [10,11], absence of formyl-methionine in protein synthesis, and ADP-ribosylation of the peptide elongation factor EF2 by diphtheria toxin [12,13].

Apart from r-RNA sequence homology, other important distinctly archaebacterial features include: ether-linked poly-isoprenoid glycerol lipids [14–16] as opposed to ester-linked alkanelipids; non-peptidoglycan cell walls [17–19] of various types containing peptides and/or carbohydrates; absence of thymidine in the 'common arm' of the t-RNA [20]; absence of dihydrouracil [8], and distinct transcription systems [21–23]. Translation too is distinctive [24], and the shape of the ribosome itself is different from that in the other two urkingdoms [25–27].

The archaebacteria are, however, a heterogeneous group. Besides the methanogens, this group includes heterotrophic, aerobic extreme halophiles (e.g., *Halobacterium*), thermophilic acidophiles (e.g., *Thermoplasma* and *Sulfolobus* [8]) and thermophilic anaerobes (e.g., *Thermoproteus* [28,29] and *Desulfurococcus* [30]). The recently discovered archaebacterium *Pyrodictium occultum* is able to reduce S^0 to H_2S with H_2 a property also described in the methanogens [31]. *P. occultum* grows optimally at 105°C [32,33]. Metabolic abilities in this urkingdom range from aerobic respiration of sugars, to the respirations of elemental sulfur and CO_2. Fermentation occurs in a few of these organisms. Discussions of the interesting properties of the archaebacteria can be found in several recent reviews and papers [1,5,7,8,22,34,35].

We will now consider the general properties of the methanogens, but once again, more extensive coverage of the biology and general physiology may be obtained in recent papers and reviews [1,2,3,36–42].

For obligate anaerobes, oxygen is toxic [43]. All methanogens are obligate anaerobes and are thus killed by exposure to air. Among the methanogens marked differences occur in oxygen sensitivity [44–46]. *Methanospirillum hungatei* *, *Methanobacterium thermoautotrophicum* and *Mb. bryantii* showed [45] viability reductions after aeration similar to non-methanogenic anaerobes; *Methanobrevibacterium arboriphilus* AZ can survive for up to 2 h in 10–20% O_2 without significant loss in viability [46]. *Mb. thermoautotrophicum, Mbr. arboriphilus* and *Methanosarcina barkeri* can survive exposures up to 30 h [44], but loss of colony-forming units occurs thereafter. In contrast, *Methanococcus vannielii* and *Mc. voltae* are killed without lag upon exposure to air [44]. Methanogenesis, however, is extremely oxygen-sensitive due to oxygen lability of certain of the methanogenic cofactors (e.g., component B and formaldehyde activating factor) such that exposure to very low concentrations of O_2 is bacteriostatic rather than bacteriocidal and cells can recover.

Recent technical advances in the culture of anaerobes [47–49] have allowed the convenient growth of methanogens. Under appropriate conditions yields of 3–8 g wet weight per l can be obtained with some of the organisms. Many have doubling times of less than 10 h, but optimal doubling times vary from weeks [50] for *Methanothrix soehngenii* to 30 min with *Mc. jannaschii* [51]. Optimal growth temperatures of pure cultures vary from 30 to 95°C [52].

Recent observations of samples from deep-sea hydrothermal vents imply that some methanogens may grow at temperatures well in excess of 100°C [53,54]. Baross and Deming [54] have recently reported bacterial growth and methanogenesis at 250°C by a mixed culture of bacteria obtained from deep-sea hydrothermal vents. Little is known of the bacteria present, but this phenomenon is unprecedented, and may represent another archaebacterial habitat. Several points need to be made regarding the unusual claim of bacterial growth at super-thermophilic temperatures: (1) due to the unusually extreme temperature, exhaustive control experiments are needed to rule out artifacts arising from the conditions; (2) many biological molecules would not ordinarily be expected to survive at the described temperatures (Stetter, K.O., White, R. and Yayanos, A., personal communications); (3) this phenomenon requires the use of specialized and sophisticated equipment, and growth measurement will be somewhat unusual and difficult. Despite these cautions concerning the interpretation of this work, the scientific community must remain open-minded to such unusual possibilities.

Though most workers report preferred growth at a near-neutral pH, growth between 5.5 and 6.0 is not uncommon (Belay, N. and Daniels, L., unpublished data), and biologically produced CH_4 has been reported from alkaline lakes (pH 9.7, however, the pH of the bacterial environment might be lower) [55]. Fresh-water and marine species have been isolated.

Substrates that can be used as both carbon and energy sources include H_2/CO_2, formate, methanol, carbon monoxide, methylamines and acetate. Virtually all methanogens can grow on H_2/CO_2 (except for four: a coccoid methanogen growing only on H_2 plus methanol [56], *Methanosarcina strain* TM1 [57], *Mtx. soehngenii* [50] and *Methanolobus tindarius* [58]). About half the genera can use formate. Only *Mtx.* and *Ms.* species can use methanol, methylamine and acetate, but these cannot use formate. Growth on CO [59] is slight but mixotrophic conversion of CO [60,61] with a preferred substrate may be of ecological or industrial significance.

Genetic analysis of methanogens is still in its infancy: only three plasmids [62,63] and one phage [381] have been found associated with the methanogens. Transposition (transposons) appears to be a relatively frequent event [64]. Though the natural resistance of the methanogens to most

---

* The methanogens are a diverse group of organisms presently composed of 12 genera. All genus names begin with the letter *M*, and thus the convention of expressing genus and species (after textual introduction of the full genus name) as *M.* followed by species name could become quite confusing to the reader, in particular, since some species names are similar. We adopt for this review the following abbreviation scheme for genus names, and recommend its use in future multi-genus papers: *Methanobacterium* (*Mb.*), *Methanobrevibacterium* (*Mbr.*), *Methanogenium* (*Mg.*), *Methanospirillum* (*Msp.*), *Methanosarcina* (*Ms.*), *Methanococcus* (*Mc.*), *Methanothrix* (*Mtx.*), *Methanoplanus* (*Mpl.*), *Methanothermus* (*Mt.*), *Methanolobus* (*Ml.*), *Methanococcoides* (*Mcc.*).

TABLE I

COMMONLY STUDIED METHANOGENIC BACTERIA

Organism	Growth substrates	Relevant properties	Isolation Ref.
Mb. thermoautotrophicum (ΔH and Marburg strains)	$H_2 + CO_2$	thermophile; rapid growth; high yields	69
Ms. barkeri (Schnellen strain)	$H_2 + CO_2$; CH_3OH; acetate; methylamine	meophile; slow growth; high yields	70
Mc. thermolithotrophicus	$H_2 + CO_2$; formate	thermophile; halophile; rapid growth; very little cell wall; fragile	71
Mbr. ruminantium (Strain M-1)	$H_2 + CO_2$; formate	mesophile; requires exogenous coenzyme M	72
Mc. vannielii	$H_2 + CO_2$; formate	mesophile; very little cell wall; fragile	73
Msp. hungatei	$H_2 + CO_2$; formate	mesophile; sheath largely protein; inner cell wall, probably protein rich polymer; can spheroplast	74
Mb. bryantii	$H_2 + CO_2$	mesophile, possible Ni^{2+} bonding in cell wall; can form protoplasts	75

antibiotics makes classical genetic screening difficult, transfer of genetic material to *Escherichia coli* and *Bacillus subtilis* has been accomplished [65–67]. Physical organization of genes for ribosomal RNA has been studied in *Mc.* [68].

For the reader's convenience in interpreting the work discussed below, Table I gives a listing of the more commonly discussed methanogens, the substrates they use and other relevant properties. Table II shows the energy-yielding reactions used by the methanogens, and the energy available in each.

If one assumes that about −37 kJ/mol of energy are needed to produce one ATP [76], a maximum of two to three ATP could be produced per methane evolved from all substrates in Table II, except for acetate. Not surprisingly, growth on acetate is quite slow, since less than one ATP is available per methane. We should point out that the values in Table II are at standard conditions (pH 7.0, 1 atm of gases and 1 M solute concentration, 25°C). These are far from natural conditions, where all the substrates are at much lower concentrations (e.g., less than 0.001 atm H_2 in lake sediments, marine sediments and rumens [3,76]). Though low methane concentrations help the thermodynamic situation of these organisms in nature, they must compete with other organisms (e.g., sulphate reducers) [77–79] for potential energy sources, e.g., H_2.

There is controversy regarding the terminology to be used in referring to the reactions described in Table II. Traditionally, respiration has been defined as "an ATP-generating process ... in which electrons are passed through an electron transport chain" [80], and fermentation as "an ATP-generating process in which organic compounds serve both as electron donors and electron acceptors; the electrons are not passed through an electron transport chain" [80]. In certain contexts, e.g., industrial microbiology jargon, fermentation is simply growth. In considering the chemiosmotic

TABLE II

ENERGY-YIELDING REACTIONS USED BY METHANOGENIC BACTERIA

Values are calculated from Gibbs free energy of formation values at pH 7 in water [76].

Reaction	$\Delta G^{0\prime}$ per reaction (kJ)	$\Delta G^{0\prime}$ per CH_4 (kJ)
$4H_2 + CO_2 \rightarrow CH_4 + 2H_2O$	−138.8	−138.8
$4HCOOH \rightarrow 3CO_2 + CH_4 + 2H_2O$	−119.5	−119.5
$4CH_3OH \rightarrow 3CH_4 + CO_2 + 2H_2O$	−310.5	−103.5
$4CH_3NH_3^+ + 2H_2O \rightarrow 3CH_4 + CO_2 + 4NH_4^+$	−225.7	−75.2
$4CO + 2H_2O \rightarrow CH_4 + 3CO_2$	−185.6	−185.6
$CH_3COOH \rightarrow CH_4 + CO_2$	−27.6	−27.6

theory we propose the following definitions, which wil lbe used in this review, and which we feel simplify the confusion over these two very basic terms; our definitions are really only a modification of the older definitions given above, to accommodate a variety of newly studied anaerobic bacteria (e.g., SO_4^{2-} reducers, S^0 reducers, methanogens, and fumarate reducers), which in some cases do not fit into either of the above definitions [76]. *Fermentation* is any process used by a cell to obtain energy that involves substrate-level phosphorylation; the chemiosmotic gradient in such cells is maintained at the expense of ATP already produced. *Respiration* is any process used by a cell to obtain energy that involves the use of electron transport phosphorylation and the chemiosmotic process (i.e., a separation of charge across a biological membrane). Such definitions can be expressed in this manner:

$$\text{Protonmotive force} \underset{\text{fermentation}}{\overset{\text{respiration}}{\rightleftarrows}} \text{ATP} \qquad (1)$$

Thus, such processes as glucose conversion to pyruvate and further conversion to end-products like butyric or acetic acids are fermentations, whereas the oxidation of pyruvate to CO_2 and the reduction of CO_2 to CH_4 by H_2 are considered respiratory processes. Likewise, since energy generation by all the substrates in Table II is also likely to involve electron transport phosphorylation and not substrate level phosphorylation, it should be considered respiration.

In the sections that follow, we will discuss the biochemical basis for methanogenesis, the involvement of the chemiosmotic process in ATP formation and the relation of these processes to cell growth. We will clarify some seeming inconsistencies in the literature, provide several heuristic models for the relationship of methanogenesis to ATP formation, and suggest several experimental approaches that might be of use in improving the understanding of methane production.

II. Biochemistry and enzymology of methanogenesis

This section will deal with the work done on the biochemical steps of methane production and their relationship to one another and to energy utilization and production.

IIA. Pathway of methanogenesis

IIA-1. Whole-cell work

Earlier this century, it was suggested by H.A. Barker [81] that methanogens could reduce carbon dioxide with a source of electrons (e.g., H_2) to form methane. This was confirmed in 1940 by Barker [82] using radioactive carbon (^{11}C) in one of its first applications. He showed CO_2 to be a source of cell carbon as well. Further experiments with ^{14}C verified these findings and also showed methane formation from methanol and the methyl group of acetate in *Ms. barkeri* [83].

Deuterium experiments in the 1950's demonstrated that the hydrogens on those latter methyl moieties are transferred directly to methane [84,85]. Recently, it was proven that when CO_2 is reduced by hydrogen, the 'H' on methane arises not from hydrogen gas, as was previously reported [86], but rather from the protons in water [87,88]. H_2 then serves only as a source of electrons (protons serve in the membrane gradient, as we will see later).

As for formate, a substrate used by half the genera of methanogens, initial evidence was that it is not directly used in methanogenesis, but instead is first cleaved to H_2 and CO_2, which are then used [89]. However, present interpretation [37,90,91] is that formate (25%) could enter the methane pathway directly at the formate oxidation level with subsequent reductions by H_2 or reduced intermediates (F_{420}) formed by the oxidation of formate to CO_2 (see Table II).

Optimal whole-cell methane production rates vary considerably, although few quantitative measurements have been made. Rates range from 50 nmol/min per mg protein for *Mtx. soehngenii* on acetate [50] to 14000 nmol/min per mg protein for *Mb. thermoautotrophicum* strain Marburg [92] on H_2/CO_2.

Ms. barkeri can grow mixotrophically [93–96]. Certain interesting metabolic traits were demonstrated in these mixotrophic studies. When grown on acetate under N_2 gas, about 80% of the methane arises from acetate; the remainder comes from the organic compounds in the medium (low levels of trypticase and yeast extract greatly stimulate this organism during growth on acetate [94,95]). Methane in this case comes predominately from the methyl group of the acetate. If excess H_2/CO_2 is present (instead of N_2), 42% of the methane arises from the methyl group of acetate, while in the presence of methanol (under an N_2 atmosphere) only 5% of the methane produced arises from acetate. Methanol stimulates the oxidation of the acetate methyl group; i.e., acetate provides a source of electrons for the reduction of methanol to methane and provides little methanogenic carbon.

Whole-cell studies of methanogens cannot tell us much more about the biochemistry of methane formation, except for inhibitor studies which will be discussed later. We will now describe what is observed when cells are cracked open for a look inside.

IIA-2. Cellextract work

Successful demonstration of methanogenesis in cell-free systems was not accomplished until 1963 with *Mb. bryantii* [104] (then called *Mb. omelianskii*) and with *Ms. barkeri* [105].

Extracts of the former would, under a H_2 atmosphere, reduce CO_2 as its preferred substrate (30 nmol/min per mg protein) and also CH_3-B_{12}, serine, pyruvate, methyl tetrahydrofolate and formate to methane [105]. Extracts of the latter converted methanol to methane best (6 nmol/min per mg protein), as well as (but with lower rates) CO_2, CH_3-B_{12}, methyltetrahydrofolate, formaldehyde and pyruvate. In both extract systems, ATP was required for methanogenesis. Coenzyme A was additionally required in *Ms.* [106].

Since this early work, a detailed description of the reduction of CO_2 to methane by crude extracts of *Mb. thermoautotrophicum* strain ΔH has been completed by Romesser et al. [97–99,380] and other workers in Wolfe's lab [100–103a]. The effects of adenosyl nucleotides, cofactors, tricarboxylic acid cycle intermediates, buffers, pH, Mg^{2+} concentration and temperature were studied. Optimal rates obtained were about 20 nmol/min per mg protein, well below that of whole-cell rates (about 7000 nmol/min per mg protein).

Several other groups [86,107,108], including the authors of this review [379], have studied methane production rates in this and other methanogens from CO_2 in cell-free extracts, but several observations common to all studies still return to haunt us:

(1) very high protein concentrations are required (10–30 mg/ml);

(2) rates of methane synthesis are quite low compared to those in whole cells (e.g., 50 nmol/min per mg protein vs. 7000 nmol/min per mg protein in extracts and whole cells, respectively, of *Mb. thermoautotrophicum* strain ΔH, [100,380];

(3) the process is very oxygen-sensitive, even though many of the enzymes and cofactors involved in methanogenesis are oxygen-stable.

The requirements for high protein levels in extracts from thick cell slurries (0.5–1.0 g.wet weight cells mixed with 1 ml buffer) and low overall activities are puzzling. These could be explained in several ways.

Soluble cofactors essential for the reaction series may be diluted out in the extract-making process. However, successful use of dialyzed extracts [380] that can produce CH_4 at rates comparable to crude extracts makes it unlikely that dilution of soluble cofactors would be the cause.

Activity could also be impaired if the salt content or ionic strength were drastically different in the crude extract from that within the cell. Indeed, the cells maintain high internal potassium levels (0.1–1.2 M K^+ [109–111]). At least one enzyme, the 5-deazaflavin reducing hydrogenase from *Mb. thermoautotrophicum,* requires high salt concentration for activity [112].

If the methanogenic enzymes were freely soluble in the cytoplasm one would expect that their activities should not be greatly impaired by dilution and that specific activities should not vary greatly with dilution; however, if for activity one required these proteins to have a certain physical arrangement that cell lysis could disrupt, then only those enzymes which had maintained·the proper physical relationship to one another would still function. In such cases, the extract-making procedure would destroy much of the methanogenic apparatus.

One cell structure which could hold the methanogenic enzymes in close proximity to one another is a membrane; in making cell-free extracts, membranes are disrupted radically and reassembled in a variety of shapes and sizes. Activity

($CO_2 \rightarrow CH_4$) can still be found in supernatants of lysates centrifuged at 30000–100000 × g; this does not exclude the presence of membranes and membrane-bound proteins [86,113,114]. The increase of methane activity in pellets with increasing centrifugation is consistent with this idea [86]. One could even speculate that closed vesicles may be required for methanogenesis, since both methane production and vesicle formation are concentration-dependent. The strongly inhibitory effects of membrane-solubilizing agents (deoxycholate) and uncouplers (2,4-dinitrophenol (DNP) and carbonyl cyanide *m*-chlorophenylhydrazone (CCCP)) suggest that membranes could be involved [86]. The use of different cell-breakage procedures (e.g., French press, Ribi cell breakage, osmotic lysis and sonication) may yield different size distributions and orientation of membrane structures [115]. That membranes are involved in methanogenesis is reasonable, since the reduction of CO_2 is an energy-producing redox process producing a separation of charge and chemiosmotic production of ATP, as will be discussed in a later section.

Another process that may be at work is protein-protein interaction. Higher protein concentrations may favor multimer or aggregate formation, with or without membrane association. Such physical interactions may be essential for some electron- or carbon-transferring reactions. One such enzyme in methanogens is the 5-deazaflavin reducing hydrogenase, which is hydrophobic and forms high-molecular-weight (approx. 10^6) aggregates with a variety of proteins [112].

The explanation of oxygen sensitivity is found in further study of the purified systems (see below). At least two components of the reaction series (component B and the formaldehyde-activating factor [103,116,117]) are rapidly destroyed by O_2, but many of the other enzymes (e.g., hydrogenase and CH_3-CoM reductase) and cofactors (e.g., CoM) are O_2 stable.

The involvement of membranes, lipids or protein aggregates makes separation of components and elucidation of the individual reactions involved in this process difficult. This is a partial explanation of why few of the enzymes or cofactors related to methane production are fully understood.

IIA-3. Coenzymes and related components in methanogenic bacteria

The methanogens have provided a wealth of new coenzymes for biochemical studies. A variety of novel, heretofore undescribed coenzymes have been demonstrated to occur only (or predominately) in these bacteria. Most have known structures and functions; some are obviously involved in the methane production path. We will discuss each described novel cofactor in turn, and point out information on the use of the traditional widespread coenzymes. A compilation of quantitative information on most of these is provided in Table III. Figs. 1–3 give the structures of many methanogen coenzymes.

IIA-3a. Electron transport

(i) 5-Deazaflavin (F_{420}). The first naturally occurring 5-deazaflavin (F_{420}) was discovered in methanogens [138,139,119]. It has the structure shown in Fig. 1a, and is found in all methane-pro-

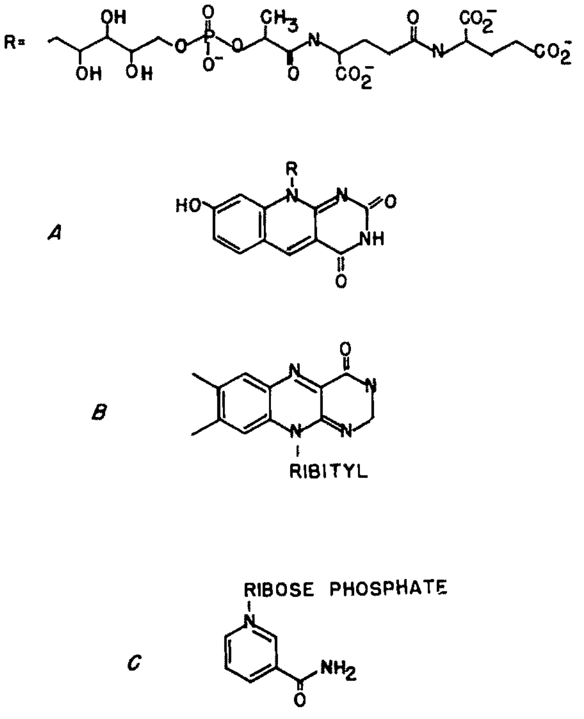

Fig. 1 Structures of electron-transferring coenzymes in methanogens. (A) F_{420} (*N*-(*N*-L-lactyl-γ-L-glutamyl)-L-glutamic acid phosphodiester of 7,8-didemethyl-8-hydroxy-5-deazariboflavin 5′-phosphate) [139]; (B) riboflavin; (C) nicotinamide mononucleotide.

TABLE III

COENZYME CONTENT OF METHANOGENIC BACTERIA

Coenzyme levels were calculated from the indicated references assuming dry weight = 0.2 wet weight, and that protein contributes 50% to the cell's dry weight. The methods used in the references included a wide variety of coenzyme estimation techniques, including bioassays, purification and weighing, spectroscopy and HPLC

Coenzyme	Molecular weight [Ref.]	Levels of coenzymes (nmol/mg protein)					
		Methanobacterium thermoautotrophicum	Ref.	Other methanogen	Ref.	Eubacterial comparison	Ref.
Electron transfer							
5-Deazaflavin (F_{420})	843 [118]	≈1.2	118	≈1.2 – *Ms. barkeri*	118	none, *E. coli*, *Acetobacterium woodii*; 0.08 – *Streptomyces griseus*	119 120
Nicotinamides (as nicotinic acid)	123 [121]	0.44	122	3.6 – *Mc. voltae*	122	6.6 – *E coli*	122
Flavins (as riboflavin)	376 [121]	0.19	122	0.20 – *Mc. voltae*	122	1.65 – *E coli* 0.19 – *B subtilis*	122 122
Quinones: menaquinones	≈ 600 [121]	none	76	not determined	–	35 – *Vibrio succinogenes*	123
α-Tocopheroquinones	448 [124]	0.03	124	0.03 – *Mb. bryantii*	124	0.05 – *E. coli*	124
Cytochrome *b*	unknown	none	76	0.30 – *Ms. barkeri*	125	0.11 – *Pseudomonas* AM1	126
Cytochrome *c*	unknown	none	76	0.02 – *Ms barkeri*	125	0.46 – *Pseudomonas* AM1	126
Carbon transfer							
Coenzyme M	141 [127]	3.0–12.1	127	15.0–50.0 – *Ms. barkeri*	127	none	127
Corrinoids	≈1400 [121]	1.3	128	3.2–8.2 – *Ms barkeri*	128	1.4 – *Acetobacterium woodii*, < 0.01 – *E coli*	128 129
Methanopterin	757 [391]	≈ 3.2 ≈ 4.2	130 118	≈ 4.2 *Ms. barkeri*	118	unknown	–
YFC (tentatively formyl-methanopterin)	≈ 725 [131]	≈ 0.3	131	–	–	unknown	–
Methanofuran (CDR)	564 [132]	≈ 3	132	–	–	–	–
FAF	≈ 700 [133]	≈1.4	133	–	–	–	–
Biotin	244 [121]	0.0003	122	not determined	–	0.0018 – *E. coli*	122
Folic acid	443 [121]	0.00004	122	0.0001 – *Mc. voltae*	122	0.005 – *E. coli*	122
Thiamine	337 [121]	0.0066	122	0.0096 – *Mc. voltae*	122	0.044 – *E coli*	122
Pantothenic acid	219 [121]	0.077	122	0.012 – *Mc. voltae*	122	1.55 – *E. coli*	122
Unknown function							
F_{430}	977 [134]	1.2	134	1.6 – *Ms barkeri*	134	none – *Acetobacterium woodii*, *E coli*	134
		≈ 3.6	118	≈ 3.6 – *Ms barkeri*	118	–	–
Component B	≈1000	7	392	≈ 3.5 – *Ms. barkeri*	392	none	392

ducing bacteria (approx. 1.1–4.7 nmol/mg protein). Interestingly, it is involved in at least two reactions in *Streptomyces* species [120,140], photoreactivation and chlorotetracycline biosynthesis, its only non-methanogen occurrences in the literature. In these non-methanogens, the levels are about 15-fold lower (See Table III). Recent work in our lab (Daniels, L. and Harmon, K., unpublished data) suggests it is widespread among the streptomyces. The structural similarity to a flavin (Fig. 1b) is obvious, but actual chemical properties make it more similar to nicotinamide (Fig. 1c); it has a portion of the nicotinamide in the central ring of its structure, and is chemically restricted to only $2e^-$ transfers like other 5-deazaflavins and unlike flavins, which can carry out both one- and two-electron processes [141–144]. Prior to the structural elucidation of F_{420}, deazaflavins had been widely used as model reactants to study flavin and nicotinamide enzymes [141–145]; some of these organically synthesized compounds were useful in the original structural work, and in the later synthesis of F_0. F_0 is an abbreviated molecule of F_{420}, containing only the ribityl and not the entire R group shown in Fig. 1a. F_0 has full catalytic capacity in the redox reactions used by F_{420} in methanogens [139,119,145–148]. An interesting comparison of the evolution of flavins, deazaflavins and nicotinamides has been made [149].

The function of F_{420} is the transfer of electrons. It is reduced by H_2 via hydrogenase (see also below, enzymes) and can transfer electrons to NADP but not NAD using NADP-F_{420} oxidoreductase [1,112,150–153]. Evidence from isotopic methane experiments suggests it accepts $2e^-$ from H_2 and $2H^+$ from water [87,88]; it can then transfer the H at position 5 directly and stereospecifically to the NADP [154]. Formate (via formate dehydrogenase), CO and possibly methanol and acetate also donate electrons to F_{420} [90,155–157]. Its function in other redox reactions (e.g., pyruvate or α-ketoglutarate dehydrogenases, assayed only in crude extracts [158]) in methanogens is not clear. The direct electron donors for methanogenesis are unknown; F_{420} is a likely candidate, since in partially purified methyl reductase systems (see below), either F_{420} reduced by NADPH-F_{420} oxidoreductase [116] in the assay mixture or prereduced F_{420} is required for methyl reductase activity. It is not known if F_{420} is bound to one or more proteins in the cell, or is a freely diffusable cofactor. However, in a more purified system, hydrogenase or chemically reduced F_{420} did not reduce methyl-CoM to methane through the methylreductase enzyme (Nagle, D., personal communication). Its use in cell carbon biosynthesis has not yet been fully studied. However, it is clear that it is a central redox cofactor for the oxidation of H_2, and probably many of the electrons used by methanogens pass through it.

(ii) Nicotinamides, flavins and folates. The ubiquitous nicotinamide precursor, nicotinic acid (and presumably NAD and NADP), flavins and folic acid are found in methanogens [122,159]; see Table III. The levels of these coenzymes are comparable to those in eubacteria, except for low amounts of folic acid. It is of interest that the organisms have both nicotinamides and F_{420} (discussed above), since they carry out similar $2e^-$ transfer reactions [112,141–144,160]. NADP can be reduced through NADP-F_{420} oxidoreductase; NAD, however, cannot be reduced via F_{420} [151,158] nor directly from hydrogenase [1,150,158] or formate dehydrogenase [91]. The reduction pathway for NAD is not known. Moreover, NADPH : NAD transhydrogenase activity has not been detected in crude extracts [161]. NAD is the preferred cofactor of the malate dehydrogenases of *Mb. thermoautotrophicum* [158], *Ms. barkeri* [95] and *Msp. hungatei* [162]. The isocitrate dehydrogenase of *Ms. barkeri* [95] requires NADP; however, either NADP or NAD can function in gluconeogenesis reactions [158].

Since certain enzymes have an absolute requirement for NADH, a way must exist to reduce NAD. Though none has yet been found, one can conceive that those enzymes which can use either nicotinamide could act as electron transferases. One example is glyceraldehyde-3-phosphate dehydrogenase. In the reducing direction it has a 10-fold greater affinity for NADPH, while in the oxidizing direction NAD or NADP have the same affinity [158]. Since the NADP can be reduced by F_{420}, the concentration of NADP should be quite low, while NAD should be higher, such that NADPH could reduce 3-phosphoglyceric acid to glyceraldehyde 3-phosphate. NAD could then be reduced to

NADH. From this one could conceive a regulatory role for NADH in metabolism whereby the NAD : NADP ratio might act as a sensor of cell production of reducing equivalents (i.e., F_{420}-reduced). However, experiments along this line have not been conducted.

Flavins (FMN, FAD or riboflavin) can be reduced by hydrogenase or formate dehydrogenase, but at a slower rate than F_{420} [91,150,157]. In *Msp. hungatei*, flavin-dependent NADH oxidase activity has also been described [161]. Also, FAD acts as a prosthetic group of the F_{420}-reducing hydrogenase of *Mb. thermoautotrophicum* [112], and FAD is required for the formate dehydrogenase in *Mb. formicicum* [163,164]. FMN is found on a flavoprotein in *Mb. thermoautotrophicum* ΔH (Hausinger, R., personal communication).

Methyl tetrahydrofolate can serve as a low-rate methanogenic substrate in crude extracts, probably indirectly [104,106,165,166]. Although a variety of reactions using folic acid derivatives have been discussed or demonstrated, the relevance of this cofactor group in methanogenesis is not clear (see also below under carbon transfer cofactors).

(iii) Quinones. Quinones, namely menaquinone, are used in the electron transfer chain of most eubacteria; they are lacking in *Mb. thermoautotrophicum* (Kröger, A., unpublished data; see also Ref. 76), the only methanogen in which they were looked for. However, in a recent study [124] a new class of these cofactors, the α-tocopheroquinones and α-tocopheroquinols (Fig. 2), were found in a variety of eubacteria, eukaryotes and the archaebacteria. *Mb. thermoautotrophicum*, *Mb. bryantii* and *E. coli* all had roughly the same levels (0.03 nmol/mg protein); see Table III. The function of these electron carriers is known only for a few organisms, including a *Butyribacterium* sp. that use it in the biohydrogenation of unsaturated fatty acids. Their role in redox reactions may vary in other organisms.

It is doubtful that the methanogens would use these in the methanogenic pathway. In *Vibrio succinogenes*, which uses menaquinones as obligate redox mediators of formate-fumarate reductase, the level of the menaquinones is 35.0 nmol/mg protein [123], a concentration more comparable to that of F_{420} (1.9 nmol/mg protein) than of α-tocopheroquinones (0.03 nmol/ mg protein) [124]. It is thus unlikely that the α-tocopheroquinones are involved in a high-flux pathway such as methanogenesis.

(iv) Ferredoxins. Four different laboratories have reported the presence of ferredoxin in *Ms. barkeri* [167–170]. Though easily contaminated by heterotrophs, microbiological plating and microscope examinations revealed none; it thus seems the ferrodoxin is from the methanogen. Its structure at the N-terminal end shows protein sequence homologies with ferredoxins from *Clostridium* and *Desulfovibrio* species [167,168]. It was shown to act in *Ms. barkeri* as a cofactor in the pyruvate dehydrogenase system, whereas F_{420} did not; thus, it may be important in cell biosynthesis reactions. Precedence for involvement in such reactions is found in pyruvate and formate biosynthesis in *Clostridium pasteurianum* [170–174]. Ferredoxin has also been found in a thermoacidophilic archaebacterium, where it acts as electron acceptor for 2-oxoacid : ferredoxin oxidoreductases [175].

Attempts to isolate ferredoxin in other methanogens have not yet been successful (unpublished data). It is not clear whether this protein can play any part in methanogenesis, even in *Ms.*

(v) Cytochromes. Few methanogens have been examined thoroughly for cytochromes. Four strains of *Ms.* were shown to contain both cytochromes *b*-559 and *c* [176,125]; see Table III. *Ms. barkeri* strain Fusaro contains two cytochrome *b* species when grown on methanol or methylamine, and possibly a third when grown on acetate. The levels of *b* type cytochromes (0.3 nmol/mg protein) are similar to those of aerobic methylotrophs [126]. Low levels of cytochrome *c* (0.016–0.075 nmol/mg protein) were found in all *Ms.* strains. The care in checking against contamination and the high levels of cytochrome *b* indicates contaminants cannot account for the findings.

Phylogenetically and on the basis of nutritional versatility, the *Ms.* stand apart from the other methanogens [36]; thus, it is not unreasonable that

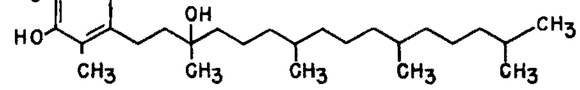

Fig. 2. Structure of α-tocopheroquinone [124].

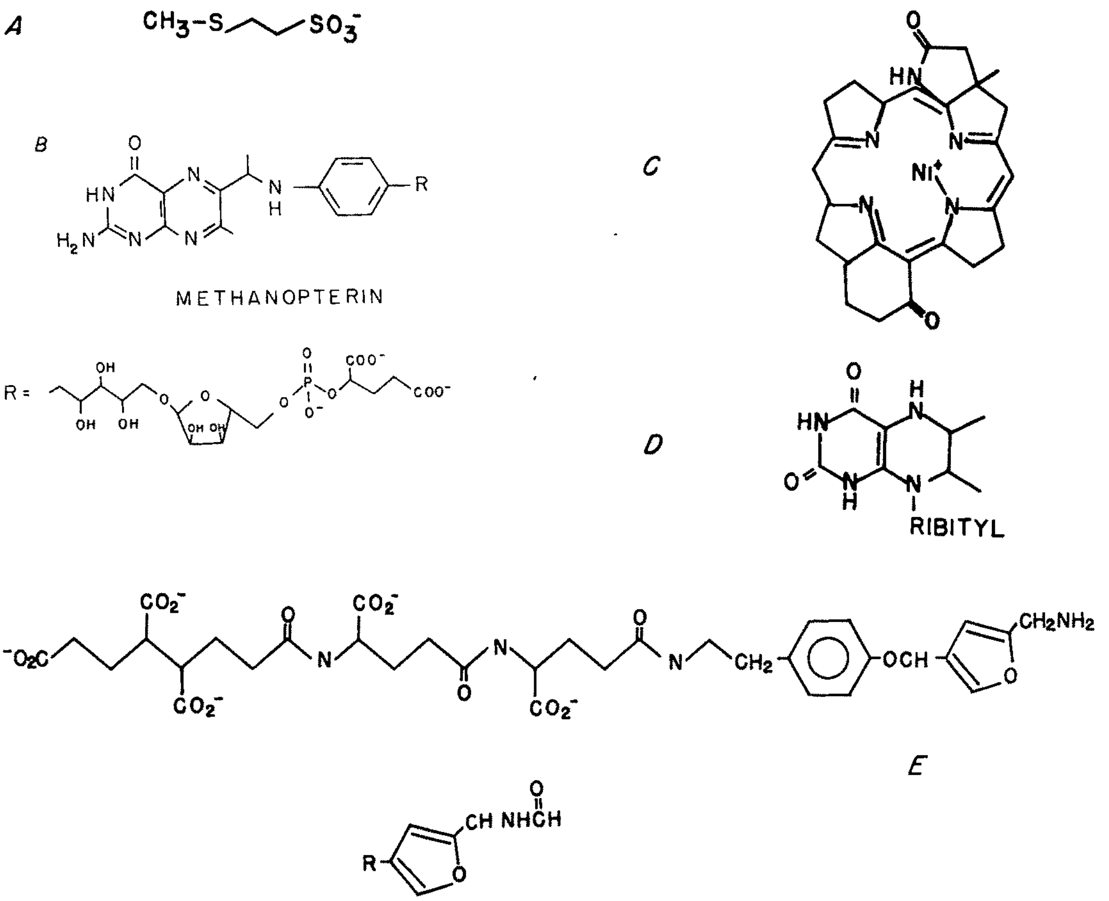

Fig. 3. Structures of coenzymes in methanogens that are used in carbon transfer or reduction reactions: (A) methyl coenzyme M (2-(methylthio)ethane sulfonate) [135]; (B) methanopterin [391]; (C) chromophore of F_{430}, a nickel corrinoid [136,196]; (D) a tetrahydrolumazine found associated with F_{430} (6,7-dimethyl-8-ribityl-5,6,7,8-tetrahydrolumazine) [137]; (E) CDR (methanofuran above and formyl methanofuran below) [132].

cytochromes are found only in this group. Another unusual methanogen recently isolated, *Mtx. soehngenii,* has been reported to contain two different types of membrane-bound cytochrome [50]. *Mb. thermoautotrophicum,* an obligate CO_2 respirer, does not possess cytochromes [76,2]. It is interesting that all the above-mentioned cytochrome containing methanogens are the only ones that reduce methyl groups to methane. It will be interesting to see whether the recently isolated *Ms. mazei,* which respires methanol, also contains cytochromes. *Ml. tindarius,* which cannot grow on H_2/CO_2, but on methanol, contains cytochromes (Stetter, K.O. and Kühn, W., unpublished data). New strains of *Mtx. soehngenii* isolated by Fathepure [177] and Patel (Patel, G.B., personal communication) grow much faster than the original strain, and may offer some advantages for the study of cytochromes in methanogens.

The function of these cytochromes is not yet known. They could be involved in electron transfer steps akin to those involved in oxygen respiration, since reduction of oxygen and of oxidized C_1-sources are analogous. On the other hand, if cytochromes are limited to methyl-group metabolizers, they might be involved in electron transfer from methyl-group oxidation to CO_2, similar to methyl oxidation in aerobic methylotrophs. However, these same cytochromes are present at the same level even when the methanogen is grown with H_2/CO_2 [125]; this might only represent a lack of control rather than function under both conditions.

IIA-3b. Carbon transfer

(i) Coenzyme M. Coenzyme M (2-mercaptoethanesulfonic acid) was the first novel cofactor described in the methanogens (Fig. 3a). It has not been found in any other organisms [127]. The mercapto end carries a methyl group in the last two-electron reduction step in methanogenesis. This reaction is catalyzed by CH_3-S-CoM reductase (see enzyme section below) [135,178]. It is present in levels of 3–50 nmol/mg protein in methanogens (see Table III). *Mb. ruminantium* M1 is an auxotroph for this vitamin [47,179].

Various derivatives of coenzyme M have been synthesized with several substitutions of the methyl group at the mercapto end in an attempt to study the methanogenic pathway [101,108]. Hydroxymethyl, formyl, acetyl, dimethyl and others have been made. Few of these derivatives act as methanogenic substrates in crude extract or the methyl reductase assay. Recently, we have synthesized selenium containing coenzyme M (H-Se-CoM and CH_3-Se-CoM) (Ruhe, R. and Daniels, L., unpublished data).

Bromoethane sulfonate ($Br-CH_2-CH_2-SO_3^-$, also called Br-CoM), a starting material that can be used for the organic synthesis of CH_3-S-CoM, is a strong inhibitor of growth and methanogenesis [98,165]; mutants resistant to Br-CoM have been isolated [180].

Coenzyme M has been reported as part, on a 1:1 ratio, of the component CoM-F_{430} (a nickel corrinoid cofactor to be discussed below) of CH_3-S-CoM reductase [181]. Other more recent work (Hausinger, R., personal communication) suggests that coenzyme M is attached in some manner to the enzyme methyl reductase (see below) but to a portion of the molecule other than F_{430}. Thus the structural and functional relationship between these two coenzymes is unknown. The nature of the binding and actual structure of this prosthetic group is unknown. Its binding is stable, suggesting that CoM may not necessarily be a freely diffusing cofactor but may be permanently bound near the active site of the CH_3-S-CoM reductase [182] or that there may be two populations of HS-CoM in the cell, accounting for the ease of reduction of added free methyl CoM to methane, and the participation of free CoM in crude extract methanogenesis. The fact that dialized extracts work in methanogenesis [98] suggests that only a bound population is necessary.

(ii) Corrinoids. Blaylock and Stadtman [106] were the first to report high contents of corrinoids in *Ms. barkeri*, originally suggested by the redness of their extracts. However, only recently, using a bioassay system, have the levels of this coenzyme been examined in this and other methanogens [128]; see Table III. Four *Mb.* species examined had 1.3–1.8 nmol/mg protein and *Ms. barkeri* had 3.2–8.2 nmol/mg protein (depending on growth substrate). Roughly comparable levels, based on spectrophotometric assays on the latter organism, where reported by Shapiro [183]. These levels are moderately high compared to other organisms, indicating an important metabolic role. Note here that the organisms with the highest levels of corrinoids are those that can use methyl groups.

Early work using sewage sludge [184] (methanogens are generally found in high numbers in sludge) and a mixed methanogenic culture [186] had shown the corrinoids present to possess an α-ligand composed of 5-hydroxybenzimidazole instead of the 5,6-dimethylbenzimidazole commonly found in bacteria and eukaryotes. Recently, 5-hydroxybenzimidazole has been found in *Ms. barkeri* [187]. Methanol grown *Ms. barkeri* is shown to contain two derivatives of 5-hydroxylbenzimidazolylcobamide (factor III) as the major natural corrinoids [185]. Of the total corrinoids, these are 70–80% as comethyl-factor III and 20–30% as coaquo-factor III [185]. No other pure culture isolation of corrinoids in methanogens has yet been carried out.

Involvement of corrinoids in methanogenesis was suggested when crude extracts of both *Ms. barkeri* and *Mb. bryantii* [105,188] were shown to convert the methyl group of CH_3-B_{12} to methane. Since then, the enzymatic transfer of methyl from CH_3-B_{12} to HS-CoM has been demonstrated [178]; this reaction, however, may not be relevant to

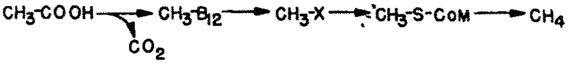

$$CH_3\text{-}COOH \xrightarrow[CO_2]{} CH_3\text{-}B_{12} \longrightarrow CH_3\text{-}X \longrightarrow CH_3\text{-}S\text{-}CoM \longrightarrow CH_4$$

Fig. 4. Proposed path for acetate metabolism to methane [60,61]. CH_3-B_{12} indicates a corrinoid protein; CH_3-X is an unknown methyl-transferring protein.

methane production [2,183]. Recently, Shapiro [183] presented evidence that corrinoids do not function in the conversion of methanol to methane; his data only allow the conclusion that *free corrinoids* are not involved in methanogenesis. However, a *protein-bound corrinoid* does participate, as discussed in both the methyl transferase and methyl reductase sections.

That B_{12} or corrinoids are involved in metabolic processes distinct from, but related to methanogenesis has been proposed by Kenealy and Zeikus [189,61]. They suggest CH_3-B_{12} is involved in acetate formation (Fig. 4) in *Ms. barkeri.* They hypothesize CH_3-B_{12} and cell-carbon synthesis, and CH_3-S-CoM and cell bioenergetics to be linked via a possible common intermediate, 'CH_3-X'.

If this path is correct, energy production from acetate could simply proceed via the reversal of the reactions producing acetate. The search for the elusive acetate cleavage enzyme might fruitfully begin with the 'CO dehydrogenase' [59–61]. This model also explains the production of methane from CH_3-B_{12} in cell free extracts; excess CH_3-B_{12} shifts the equilibrium back towards CH_3-X, CH_3-S-CoM and CH_4. This would be part of a cell-carbon-regulating mechanism; high CH_3-B_{12} levels might shift metabolism toward higher methane production.

(iii) Methanopterin, formylmethanopterin (YFC), F_{342} and FAF. In $^{14}CO_2$- and $^{14}CH_3OH$-labeling experiments, it was observed that, in addition to cell-carbon precursors (e.g., alanine, glutamic acid and aspartic acid) and CH_3-S-CoM, a previously undescribed compound was highly labelled at early times (2–10 s) [190]. Kenealy and Zeikus [61] also have reported this intermediate. This compound, originally termed YFC (yellow fluorescing compound), fluoresces yellow under ultraviolet light when in a dry state. Spectral properties resembled those of pterin or folic acid derivatives but did not match that of any reported compound; it contained neither sulfur nor phosphatase-sensitive phosphate; folic acid bioassays were negative [190]. Decomposition studies showed that the products of acid, base or NH_4^+ treatments still had ultraviolet-visible and fluorescent spectra resembling pterins [131,190].

Extraction of cells and purification of this carbon carrying cofactor yielded only 12 mg/kg wet weight of cells [131]. However, it was observed that YFC was enzymatically converted to a non-carbon carrying blue-fluorescent compound. This cofactor, methanopterin, was present in levels of 150–200 mg/kg wet weight of cells, and structural studies indicate it is a pterin [391]; see Table III and Fig. 3b. Methanopterin was usually isolated aerobically in contrast to the FAF discussed below. However, one study, conducted anaerobically, showed enzymatic conversion concomitant with methanogenic conditions [191]. Structural work is not yet complete on this compound, since organic synthesis have not been completed. The carbon-carrying cofactor (YFC) is thought to carry a methanogenic carbon two electrons reduced from CO_2; this derivative, initially was thought to be a carboxymethanopterin [131], is now thought to be either a formyl- or methenyl-methanopterin [253].

Although the precise function of methanopterin is unknown, it is clearly a carbon-carrying cofactor or prosthetic group, since it is labelled so rapidly [190]. Labelling experiments by Kenealy and Zeikus [61] with $^{14}CH_3OH$ in the absence or presence of hydrogen suggest it is involved in the earlier CO_2 reduction steps, since the presence of hydrogen reduces $^{14}CH_3OH$ to $^{14}CH_4$ and prevents the appearance of [^{14}C]-methanopterin [61]. This hypothesis is also suggested by recent results in Wolfe's lab indicating that it is a component of the originally described CDR factor (to be discussed below) required for CO_2 reduction to methyl-CoM (Nagle, D., personal communication).

Gunsalus and Wolfe have described a strongly blue-fluorescent compound with an absorbance maximum at 342 nm, which they named F_{342} [192]. It may be a metabolic variation of methanopterin, or a decomposition product.

Recently, the original CDR factor has been resolved into two components, both needed for methanogenesis from CO_2: CDR itself, a CO_2 binding non-pterin cofactor described below [132], and FAF a pterin-like 'formaldehyde-activating factor' [133]. FAF spectrally resembles a pterin (absorption maxima at 247 and 302 nm at pH 7) and thus methanopterin; it also has a similar size [133], but its structure is unknown. FAF is isolated from cells anaerobically, and when exposed to air cannot work as a methanogenic cofactor [133], even after a long incubation under reducing conditions, whereas methanopterin can replace FAF in methanogenesis assays after a long lag when allowed to incubate under similar reducing conditions. FAF participates in two separated two-electron reductions, and can carry carbon at the formyl, hydroxymethyl and methyl levels: it may thus be one of the most versatile of the methanogenic intermediates [133]. Further work on the structures and enzymatic conversions of YFC, methanopterin and FAF will be essential to understand the metabolism of methanogens. It should be kept in mind that these various pterins may be interconvertable forms of the same coenzyme used in methanogenesis, or may represent structurally similar compounds with distinctly different functions, for example in acetate synthesis (discussed below in cell carbon biosynthesis) instead of methane production.

(iv) CDR factor (methanofuran). The CDR factor is a CO_2-binding cofactor essential for methanogenesis from CO_2 [99,103a]. It has a biologically unusual furan structure, as shown in Fig. 3 [132]. The structure of the carbon-carrying form is also shown; the formation of this latter intermediate involves the first two-electron reduction in the path of methanogenesis from CO_2. Table III gives an estimated value for the amount present in cells [132].

(v) Biotin, folic acid, thiamine and pantothenic acid. Many of the conventional carbon transferring coenzymes have also been found in methanogens [122,128]; see Table III. They could possibly be involved in the reduction of CO_2 to CH_4 as well as in the other traditional functions of carboxyl and other C_1 transfer reactions.

Biotin content of *Mb. thermoautotrophicum* is about 0.0003 nmol/mg protein, 3–20-times less than the levels in non-methanogens [122]. These levels are reasonable for use in biosynthetic paths but hardly enough for methanogenesis.

Folic acid levels in *Mb. thermoautotrophicum* and *Mc. vannielii* (0.04 and 0.1 pmol/mg protein, respectively) are 80–400-times lower than in non-methanogens. Thus, its use is probably restricted to the biosynthesis of specialized products such as serine or purines. Other pterins, such as methanopterin, (see above) may be involved in similar reactions.

Both *Mb. thermoautotrophicum* and *Mc. vannielii* have about 0.01 nmol thiamine/mg protein [122], roughly 20% of that found in other bacteria examined. These levels are consistent with its function in specific biosynthetic pathways, and not in methanogenesis.

Likewise, pantothenic acid (a component of coenzyme A) is found in methanogens in levels 2–5% of those in a variety of eubacteria [122].

Thus, none of these cofactors is likely to play a role in methanogenesis, and their low levels could imply that other, unique methanogen cofactors may play some part in certain one-carbon transfer reactions.

IIA-3c. Unknown function

(i) Component B. Methyl-CoM reductase catalyzes the last step of the methanogenic path, converting methyl-CoM to methane [103]. This enzyme has been purified and further discussion of it is given in a subsequent section. Methane production by the purified system requires a variety of proteins and cofactors (to be discussed below) including component B [116,117,193]. Little is known of this component's structure or function. It is highly polar, highly ionic, acid labile and oxygen sensitive [382]. The molecular weight is about 1000. Analysis shows approx. 2P and 3N per molecule, as well as an aldopentose. There is no visible absorbance, but component B has ultraviolet maxima at 267 and 233 nm. From 1 kg (wet cells) of *Mb. thermoautotrophicum* 100 mg were recovered; see also Table III. Its presence is essential for enzyme activity, and this assay is the only means of identification.

(ii) F_{430}. Methanogens contain a variety of colored and/or fluorescent materials of more or less known functions. The better known cofactors have already been mentioned. One component of crude extracts of methanogens was originally designated F_{430} for its absorbance at 430 nm [192]. It is a brightly yellow colored, non-fluorescent, Ni containing compound [134,194,195]. The labs of Thauer and Eschenmoser determined the structure [136,196] and part of the biosynthetic pathway leading to the formation of F_{430} [134,194,197–203]. It is a nickel-containing tetrapyrrole (Fig. 3c) possessing a chromophore system not previously encountered in natural products. The native cofactor is the pentacid derivative [197] of the originally

studied F_{430}M. This cofactor is not found in acetogens (other anaerobic bacteria requiring Ni), nor in any other organism tested [136,204]; see Table III.

The last enzyme of the methanogenic pathway, methyl-CoM reductase (from *Mb. thermoautotrophicum*), has been found to contain 2 mol F_{430}/mol enzyme [205] to which is associated a bound form of CoM [181,206]. In looking for enzymes containing F_{430}, a chromophoric protein 'P_{425}' (or 'P_{445}') has been purified from both *Mb. thermoautotrophicum* and *Ms. barkeri* [207]. It contains 1 mole F_{430}/mole protein. Though enzymatic activity of this protein has not yet been examined, it is suggested that it is the methyl reductase, implying that F_{430} may only be found in this enzyme.

The function of F_{430} is not known. It possibly acts as a methyl transferring prosthetic group in concert with CoM. Alternatively, it could participate solely as an electron transfer agent for the reduction of the methyl group to methane. Other Ni-containing enzymes are known to act in redox reactions (e.g., hydrogenase in several bacteria [112,208–213]) or in carbon-binding reactions (e.g., CO dehydrogenase in many bacteria [214,215] and urease in plants [216]). In no instance is the catalytic role of Ni fully understood. Thus, a thorough study of redox and other reactions of the Ni in F_{430} during catalysis will be required to determine its role in methanogenesis.

Possibly associated also with the F_{430} of methylreductase is another compound of unknown function: 6,7-dimethyl-8-ribityl-5,6,7,8-tetrahydrolumazine (Fig. 3d) [137]. It had been thought that bound CoM, F_{430} and the lumazine form a complex called CoM-F_{430}. More recently, other workers have not been able to demonstrate the presence of these cofactors on F_{430} [217]. It is currently thought that coenzyme M may be bound to the methyl reductase at a site distinct from F_{430} (Ref. 217 and Hausinger, R., personal communication). The possible attachment of a lumazine is less clear, and may represent an unfortunate copurification.

(iii) Cyclodiphosphoglycerate. A new phosphogenic compound has recently been found in *Mb. thermoautotrophicum,* independently by Kanodia and Roberts [218] and Seeley and Fahrney [218a]. ^{31}P-NMR and organic synthesis by Kanodia and Roberts have demonstrated that it is 2,3-cyclodiphosphoglycerate (see Fig. 5) [218]. Using ^{31}P-NMR of stationary phase cells, the largest signal (far greater than that of the nucleotide phosphates) was due to this compound. The authors have suggested it could serve as a reserve source of phosphate or energy, but its true function is not yet known. *Mbr. ruminantium* has also been observed to contain the diphosphoglycerate (Roberts, M., Kanodia, S. and Daniels, L., unpublished data). A variety of other unusual ^{31}P signals are also observed in several methanogens (Roberts, M. and Fahrney, D., unpublished data).

IIA-4. Enzyme studies

IIA-4a. Hydrogenase

Early work on the hydrogenases of methanogens indicated that a variety of electron acceptors could be used and that there was a great heterogeneity of molecular weights [112,209,219–221]. In most methanogens, H_2 can serve as an electron source for the reduction of C_1 units to methane and cell carbon (See Tables I and II). Labeling experiments indicate the enzyme hydrogenase normally splits H_2 into protons and electrons, the electron carrier F_{420} taking its protons from water in the medium rather than from hydrogen [87,88]; hydrogenase is not a hydride transferring enzyme. Deuterium isotope experiments indicate that some of the protons released from H_2 gas end up in methane, simply because the hydrogenase releases these protons into a somewhat confined space close to the methanogenic apparatus that is using protons. As will be discussed below in the energy conservation portion, protons might be released on the outside, in the membrane, or inside the cyto-

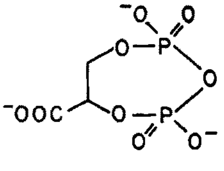

2,3- CYCLOPYROPHOSPHOGLYCERATE

Fig. 5. Structure of a cyclic diphosphoglycerate found in *Mb. thermoautotrophicum* [218,218a].

plasm. Hydrogenase can also make H_2 from protons and electrons, but any physiological importance of this reverse reaction is unclear.

The hydrogenase from *Mb. thermoautotrophicum* ΔH has been purified [112,209]. There are two chromatographically distinct hydrogenases: a higher molecular weight one that can reduce F_{420}, other deazaflavins, flavins and methyl viologen, and a smaller one that can reduce only methyl viologen. The 5-deazaflavin-competent protein has three subunits (M_r 40 000, 31 000 and 26 000) and contains iron, sulfur, nickel and FAD (about 20, 20, 2 and 2 g atoms per mole of enzyme of 170 000, respectively); the FAD most probably interacts with the 5-deazaflavin and flavins. The methyl viologen-only enzyme contains Fe, S and Ni, but no FAD, and has two subunits (M_r 40 000 and 52 000) [208]. The evidence to date suggests the 40 kDa subunits are not identical (Fox, J., personal communication). The smaller hydrogenase may represent protein that has lost its deazaflavin interacting subunit during extraction. Alternatively, it may actually interact with an electron carrier other than F_{420}, e.g., a ferredoxin, flavodoxin or similar protein; thus they may perform distinct physiological functions. The possibility that one or more of the reduction steps in methanogenesis does not involve electrons from the deazaflavin-hydrogenase, but rather the other enzyme should be considered.

Ni has been shown to be a component of the enzyme; since its discovery in this organism, Ni has been reported in hydrogenases from *Desulfovibrio gigas* [211,222,223] (an anaerobic sulfate reducer), *Alcaligenes eutrophus* [212,224] (an aerobic H_2 oxidizer), and *Chromatium vinosum* (a photosynthetic bacterium) [225]. It may be that Ni is involved in most or all hydrogenases.

The role of Ni in catalysis or electron transfer is not understood. EPR studies have shown that Ni is responsible for the oxidized protein's signal, and that the Ni undergoes a Ni^{II}-Ni^{III} transition [208,210,226]. It is interesting to note that Lancaster [210,226] first suggested that Ni^{III} was present in methanogenic bacteria based on theoretical considerations of EPR spectra of whole cells. The catalytic significance of this redox reaction is not known. The flavin and Fe-S centers are also reduced by H_2 [208].

Hydrogenase from *Mb. thermoautotrophicum* strain Marburg (an organism very different from *Mb. thermoautotrophicum* strain ΔH [227]) has been purified 12-fold. It contains Ni and gives EPR spectra similar to those of ΔH [209,228]. Two chromatographic species were observed during hydroxylapatite chromatography. Distinct hydrogenases have also been observed in *Mb. formicicum* [229] and *Mc. vannielii* [152]. The enzyme from *Mc.* contains selenocysteine, but metal and flavin content are unknown; growth of this organism on formate is stimulated by the simultaneous presence of selenite and tungstate [154]. This same stimulation is observed for both H_2/CO_2 and formate growth of *Mc. thermolithotrophicus* [379]. It is possible that the substitution of S by Se in such proteins as hydrogenase or formate dehydrogenase allows better function. The hydrogenase from *Mb. formicicum* contains a flavin (FMN) which may be partly lost during purification but can be reconstituted (Ferry, J.G., personal communication).

Mb. formicicum also has two different hydrogenase forms that, as in *Mb. thermoautotrophicum,* react with methyl viologen, but only one reacts with F_{420} [230]. The subunit patterns and peptide mapping indicate they are distinct enzymes. As with other methanogen hydrogenases, preincubation under reducing conditions is essential.

The location of the hydrogenase is not known with certainty. The large size (M_r, approx. 10^6) of all the purified 5-deazaflavin-reducing hydrogenases indicates aggregation into a multi-enzyme structure, indicating a 'sticky' hydrophobic nature. This has led to difficulties in purification, suggesting a membrane origin for the enzyme. Doddema has presented electron micrographs of redox dye binding experiments suggesting association of the hydrogenase to internal membranes [231]. Though we feel there is no firm evidence for the location of the hydrogenase on internal or other membranes, it is an excellent candidate for a proton pump by which the separation of charges occurs for the chemiosmotic generation of energy (which is the sole mode of energy production these cells possess).

IIA-4b. Formate dehydrogenase

Formate dehydrogenases are found in both aerobic and anaerobic organisms. Aerobes commonly use the enzyme to oxidize formate to CO_2. Some anaerobes reduce CO_2 to formate, while others convert formate to $H_2 + CO_2$ [172,232]. Reaction 2 and Fig. 6 describe the role of this enzyme in formate metabolism:

$$HCOOH \xrightarrow{\substack{\text{formate}\\\text{dehydrogenase}}} 2H^+ + 2e^-$$

$$+ CO_2 \xrightarrow{\text{hydrogenase}} H_2 + CO_2 \qquad (2)$$

The overall process uses two enzymes, formate dehydrogenase and hydrogenase, to carry out the function of 'formate-hydrogen lyase'.

Although few of these enzymes have been examined closely, they appear quite diverse in size, cofactors required and metal content [232,233]. All are inhibited by azide. Most have been demonstrated to contain iron-sulfur centers, and molybdenum; many contain selenium and tungsten. Cofactors commonly used include NAD, NADP, ferredoxin or cytochromes; artificial electron-accepting dyes, e.g., methyl viologen, are commonly used in spectrophotometric assays.

About half the methanogens can convert formate to methane, as indicated in Table II. Little work has been done on the purification and study of this enzyme in these organisms. Formate dehydrogenase has been demonstrated in crude extracts of three methanogens: *Mbr. smithii* [91], *Mb. formicicum* [90,157,234] and *Mc. vannielii* [155].

Crude extract work with *Mbr. smithii* shows that the enzyme is very oxygen sensitive. F_{420}, FMN and FAD can serve as electron acceptors. The specific activity with F_{420} as acceptor in crude extracts was about 110 nmol/min per mg protein; the formate hydrogen lyase reaction (H_2 production) was much slower, 2 nmol/min per mg protein [91], and was dependent on exogenously added F_{420}. Ferredoxin from *C. pasteurianum* would not replace F_{420} in either reaction.

Formate dehydrogenase from *Mb. formicicum* has been purified 71-fold [157]. Azide (10 mM) was used to stabilize the enzyme during purification. The protein has a molecular weight of 288 000 and can use F_{420}, F_0, FMN and FAD as electron acceptors. It contains approx. 2.5 Mo per molecule of protein. An EPR study of this enzyme [163] revealed an unusual molybdenum signal as well as a more typical iron-sulfur signal. The enzyme had an extractable chromophore which exhibited an interesting fluorescence spectrum: excitation occurred at 385 nm (max), 302 nm and 277 nm; emission was at 455 nm. Johnson et al. [235] suggest the formate dehydrogenase contains a novel pterin, since its spectrum is similar to spectra seen in a variety of pterin-containing molybdoenzymes (sulfite oxidase, xanthine oxidase, nitrate reductase).

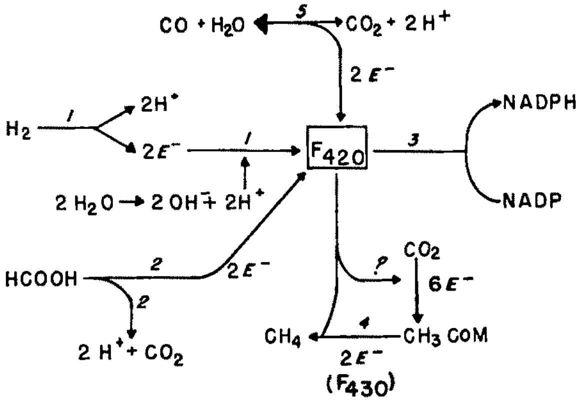

Fig. 6. Major electron transfer reactions in methanogens. (1) Hydrogenase; (2) formate dehydrogenase, (3) NADP-F_{420} oxidoreductase; (4) methyl CoM reductase; (5) CO dehydrogenase

Formate dehydrogenase from *Mc. vannielii* has also been purified [155]. When cells are grown on formate without exogenously added selenium or tungsten, Celite chromatography of the extract reveals only one formate dehydrogenase activity peak, termed peak I. When crude extract formate dehydrogenase was assayed during Celite chromatography of Se/W-grown cell extracts, two distinct peaks were seen: peak I was stable (but very oxygen sensitive); peak II was unstable to the attempted purification procedure and was not isolated.

Peak I formate dehydrogenase was a 105 kDa protein that contained iron and acid labile sulfide (6 gatom per mol enzyme of each) and molybdenum (1 gatom per mol enzyme), but did not contain selenium. However, the amount of this protein was stimulated by addition of Se to growing cells.

Peak II was a higher molecular-weight aggregate composed of iron, sulfur, molybdenum, selenium and tungsten; the Se was in the form of Se-Cys. It occurred only in the Se-grown cells. Tungsten stimulated formation of this peak as well as replaced some of the molybdenum in this protein. Whether this second activity peak may include enzyme from peak I, in an aggregate, is unclear.

The route of formate entry into the methanogenesis pathway is not known. Formate could be split to $H_2 + CO_2$, and these substrates converted to methane. Alternatively, formate could be oxidized by formate dehydrogenase and the electrons transferred to F_{420}, which would then reduce formate (bound in the methanogenic path) to CH_4. Crude extract work with *Mbr. smithii* [91] showed that formate could lead to H_2 production with F_{420} or methyl viologen as the electron-transferring agent, but how the process proceeds under physiological conditions is unknown. If H_2 is produced, then hydrogenase could be involved in the production of a transmembrane H^+ gradient (see also below, Section III). However, if H_2 is not produced, but rather F_{420} accepts electrons from formate and uses them directly to reduce carbon to CH_4, then formate dehydrogenase could be involved in the production of the gradient, or a hydrogenase activity associated with the formate dehydrogenase. A potential problem with this idea is that the formate dehydrogenase in methanogens appears to be soluble [155,157] implying it could be cytoplasmic or loosely bound to the membrane. Another question worth considering is whether formate dehydrogenase could be part of the direct methanogenic pathway of CO_2 to CH_4, in such case formate-utilizing organisms would have an enzyme capable of binding and transforming free formate as well as a carrier-bound formate redox level carbon unit.

IIA-4c. Methyl transferase reactions

In the late 1960's Blaylock and Stadtman [105] observed the formation of methane from added methylcobalamin in cell-free extracts of *Ms. barkeri*; this reaction required ATP. The B_{12}-containing protein was then partially purified [106] and shown to have an M_r of about 200000. In the presence of methanol, this protein could be methylated; the methyl of methyl-B_{12} could then be reduced to methane in crude extract. This methanol-B_{12}-methyl transferase had four components: a corrinoid protein, a second unidentified protein, a ferredoxin and a heat-stable dialyzable cofactor (HS-CoM probably).

It was later shown that methyl-CoM is the methyl donor for crude and purified methyl reductase (see below). This does not prevent consideration of B_{12} as an intermediate. Taylor and Wolfe [135,178] reported methyl group transfer from methylcobalamin to HS-CoM in *Mb. bryantii* and purified the enzyme activity 100-fold. This enzyme does not require ATP, but little more is known. Recently, Wood et al. [236] have purified a B_{12}-containing protein from *Ms. barkeri*, grown on methanol. This enzyme has a molecular weight of 200000 and consists of subunits of 44000. The enzyme's structure resembles that of the transmethylase that participates in acetate synthesis from methylcobalamin and pyruvate in *C. thermoaceticum* [215,237]. The *Ms. barkeri* protein, when methylated and added back to crude extracts, will donate its methyl group for the formation of methane. Since methyl cobalamin can transfer (slowly) its methyl group non-enzymatically to HS-CoM [238], these workers assumed that the B_{12} protein possesses this methyl transferase activity; however, the only activity assayed was the conversion of CH_3-B_{12} to methane in cell-free extracts, which could still require many steps.

Blaylock and Stadtman also suggested [105,106,169,239] a methanol-to-B_{12}-methyl transferase. *Ms. barkeri* has 10-times as much corrinoid as other methanogens [128,183], implying that it has a prominent role in this organism. Recently, Shapiro and Wolfe [240] have found that the conversion of methanol to methane is constitutive in both H_2/CO_2 and methanol-grown cells. They show methanol to be converted to CH_3-S-CoM at the same rate under both conditions and in a 1 : 1 ratio. This reaction required ATP and Mg for activation. This work does not exclude the possibility of a bound corrinoid being an integral part of the methyl transferase.

Using bromoethane sulfonate, Van der Meijden et al. [182] have been able to inhibit methyl reductase activity without altering the methanol HS-CoM transferase, thus permitting direct monitoring of CH_3-S-CoM formation from methanol in cell-free extracts. This reaction required preincubation in H_2 and Mg-ATP for optimal activity. Shapiro [241] has demonstrated this same phenomenon of activation of the methanol-CoM transferase by ATP; after activation, ATP can be removed without effect. Stimulation by H_2 [182,242] can be replaced in crude extracts by pyruvate oxidation to acetyl-CoA, suggesting the effect is reduction; however, added NADPH does not activate the system. FAD and FMN can partially inhibit the activation.

Methyl transferase is inhibited by cyanide, azide, dithionite and pyridoxal 5-phosphate [182]. This later inhibition is similar to that of dioldehydrase [243] in which a B_{12} protein participates. A possible role for B_{12} is consistent with the findings of Wood et al. [236] and Blaylock and Stadtman [106].

Shapiro [183] has tried to disprove the involvement of corrinoids in the methyl transferase from methanol in *Ms. barkeri* using free [*methyl*-^{14}C]-B_{12} and [^{3}H]-CH_3OH. Alkyl-B_{12} derivatives inhibited methyl transfer from B_{12} to HS-CoM, but not the formation of CH_3-S-CoM or CH_4 from methanol. Also, using [^{3}H]CH_3OH, [^{3}H]CH_3-B_{12} could not be detected, whereas [^{3}H]CH_3-S-CoM was as mentioned in Ref. 183. This agrees with earlier $^{14}CO_2$- and $^{14}CH_3OH$-short-term labelling studies of *Mb. thermoautotrophicum, Mbr. ruminantium* and *Ms. barkeri* in which no [^{14}C]CH_3-B_{12} was detected [190]. B_{12} can donate methyl groups to HS-CoM for methanogenesis, but this reaction is not essential [178]. Addition of alkyl-B_{12} did not hinder the reaction, but instead inhibited the CH_3-B_{12}-HS-CoM methyl transferase activity. In the presence of excess methanol ($[CH_3OH]:[\text{HS-CoM}] = 8.6$) and added labelled CH_3-B_{12}, all the CH_3-S-CoM was derived from methanol and not CH_3-B_{12}.

From these data it is clear free corrinoids are not involved in the methyl transferase from methanol; however, it is possible a tightly bound, not freely exchangeable, corrinoid is part of the enzyme. Data of Wood et al. [236] support this possibility, since the corrinoid isolated in their work required ethanol denaturation for release.

Iodopropane and iodobutane are inhibitors of corrinoid mediated methylations. Hydridocobalamins are powerful nucleophiles and react rapidly with alkyl halides to give alkyl-cobalamins [183], inhibiting the corrinoid proteins. The iodoalkyls did not inhibit methyl transferase activity to CH_3-B_{12}, but rather inhibited the methyl reductase, a nickel corrinoid (F_{430}) protein. This evidence indicates an involvement of the F_{430} directly in the transfer of the methyl group of CH_3-S-CoM to methane. It is also the only evidence against the involvement of a hydridocobalamin or B_{12} in the methyl transferase. It is unfortunate that Wood et al. [236] did not assay methanol to HS-CoM methyl transferase activity with their purified protein.

Recently, Van der Meijden et al. [242] have purified an oxygen-sensitive cobalamin protein (methanol : 5-hydroxybenzimidazolylcobamide methyltransferase) which will accept a methyl group from methanol and transfer it to HS-CoM via a second, non-corrinoid protein (methyl-5-hydroxybenzimidazolylcobamide : HS-CoM methyltransferase). Free CH_3-5,6-dimethylbenzimidazole-B_{12} or free methylhydroxybenzamidazole-B_{12} can transfer their methyl group to HS-CoM through the methylhydroxybenzamidazole-B_{12} : HS-CoM methyltransferase. The cobalamin protein requires reductive activation with hydrogen and ATP, confirming previous observations in crude extract [241,242]. Spectrophotometric and ^{14}C-labeling experiments suggest the cobalamin is catalytically active during the reaction [244].

As for the free CH_3-B_{12} : HS-CoM transferase reaction, it could be the reverse of the normal reaction (see Fig. 7): B_{12} is involved as a methyl carrier for acetate synthesis [61]. Since enzymes transfer methyl from CH_3-B_{12} directly to HS-CoM, the methyl-X of the Kenealy and Zeikus model [61] may be free CH_3-S-CoM, as described in Fig. 7.

IIA-4d. Methyl-CoM reductase

A variety of methanogens can reduce methyl CoM to methane in cell-free extracts. This reaction is dependent on added Mg : ATP or any of several nucleotide triphosphates. ATP is used in catalytic amounts; extracts from *Mb. thermoautotrophicum* ΔH produce 15 CH_4 per ATP added [102] and 85 CH_4/ATP in *Ms. barkeri* [240]. CO_2 can act as a positive effector [98].

This activity is fully inhibited by a variety of compounds including chloramphenicol, chloroform, azide, 2,4-DNP, methyl viologen and nitromethane but not by CO, cyanide, nitrous oxide or dithionite [102]. These compounds, some of which are known to inhibit also methanogenesis from $H_2 + CO_2$ (e.g., nitrous oxide) may be of great value in blocking the pathway of methanogenesis at different sites, thus allowing the build-up of methanogenic intermediates. As well, the use of dithionite as an electron source for reduction of C_1 units (via F_{420}) should be examined.

The enzyme in this last step of methanogenesis:

$$CH_3\text{-S-CoM} \underset{2H^+}{\overset{2e^-}{\rightarrow}} CH_4 + \text{HS-CoM} \quad (3)$$

has been purified from the 30 000 × *g* supernatant of cell free extracts of *Mb. thermoautotrophicum* [117] (see also Fig. 6). The purified enzyme (component C) is a yellow protein with an absorption maximum of 425 nm and a shoulder at 455 nm. It is oxygen stable, and has a molecular weight of 300 000 assembled from three different pairs of subunits. There are roughly 2 mol F_{430} per mol enzyme and 1 mol bound CoM per mol F_{430} [181]. This protein may comprise as much as 12% of the total cell protein [117]. For activity the methyl reductase also requires a source of reducing power via hydrogenase (in component A) [103,117,193] and an oxygen-labile cofactor of unknown function (component B) [103,193,382]. This is the only enzyme definitively involved in methanogenesis to be purified.

Recently, component A has been resolved into four components by Nagle and Wolfe [193]. There are three protein fractions A_1, A_2, A_3 and FAD; A_1 contains F_{420}-reducing hydrogenase similar to that purified by Jacobson et al. [112]. Mg-ATP and component B were also required for component C to convert CH_3-S-CoM to CH_4. Although some preparations were stimulated by the addition of low levels of F_{420}, a requirement for this coenzyme was not established. This latter point is puzzling in light of the abundance of the deazaflavin-reducing hydrogenase [112]. Perhaps F_{420} does not donate electrons at the methyl reductase level, but at prior reduction steps? Or, perhaps F_{420} is protein-bound in the enzymes?

NADPH, under N_2, served as an electron donor for the methylreductase in a crude preparation of component C [116]. This enzyme mixture contained the methyl reductase and NADP-F_{420} oxidoreductase. In view of the above-discussed requirements for A_2 and A_3 [193], this preparation of component C probably also contained these two proteins.

The purified protein also requires Mg : ATP for activity [102]. Assay conditions have been optimized with respect to ATP and Mg concentrations, pH and temperature in crude extract systems. However, both crude extract and purified specific activities are very low (20–170 nmol/min per mg protein) compared to whole-cell methanogenesis rates of about 7000 nmol/min per mg protein [102,117,193]. In cell-free extracts, drops in activity may result from dilution of necessary cofactors; alternatively, the reaction conditions are either very unfavorable due to the lack of some component or condition, or a great deal of the enzyme has been damaged during cell breakage or manipulation. In view of the requirements for high salt concentrations for the hydrogenase of this organism [112], the high natural internal salt levels (0.78–1.1 M K^+) [109,111], and the Na^+ requirement for methanogenesis in whole cells [245,246], the ionic strength of the assay media tried to date may not be optimal. Since CO_2 acts as a positive effector of this enzyme, it is possible that there are other activator sites on the enzyme (e.g., for cell carbon intermediates) that may stimulate methyl reductase activity.

IIA-4e. Carbon monoxide dehydrogenase

Carbon monoxide dehydrogenase catalyzes the oxidation of CO:

$$CO + H_2O \rightarrow CO_2 + H_2 \quad (4)$$

(see also Fig. 6). Several aerobes can use CO (in the presence of O_2) as their sole carbon and energy source [247,248]. *Pseudomonas carboxydohydrogena,* for example, uses this reaction to reduce FAD, which then donates its electrons to the respiratory chain at the quinone level [247]. The anaerobic acetogenic clostridia can use CO [215] as well. *Clostridium pasteurianum* and *C. thermoaceticum* have nickel-containing CO dehydrogenases [214]; the enzyme from the former organism can reduce FAD, FMN, methylene blue or viologen dyes, but not NAD(P). It has recently been reported that some clostridia may grow on CO [37,249]. Indeed, the acetogenic anaerobes *Butyribacterium methylotrophicum* [250], *Acetobacterium woodii* [37] and *Eubacterium limosum* can grow well in a 100% CO gas phase [251]. A recent review deals more thoroughly with CO metabolism [248].

Kluyver and Schnellen [70] were the first to report methanogenesis from CO (Table II) in pure cultures. More recently, Daniels et al. [59] investigated this phenomenon with whole cells of 6 methanogenic species and with both growing cells and extracts of *Mb. thermoautotrophicum*. On CO, all cells produced CO_2 and CH_4, and *Mb. thermoautotrophicum* grew very slowly (approx. 1% of the rate seen on H_2/CO_2). In cell-free extracts, CO could reduce F_{420} and methyl viologen; the K_m for CO was quite high (more than 1 mM). This enzyme shares properties with that from *C. pasteurianum*: reversable inactivation by cyanide, inactivation by mercurials, extreme oxygen sensitivity and viologen reduction; however, the clostridial K_m was much lower (5 μM).

Krzycki et al. recently reported that *Ms. barkeri*, growing on acetate as sole energy source has CO dehydrogenase 5-fold higher than when grown on H_2/CO_2 or methanol; this activity was not induced by CO, and was always present [96]. Because of this and the high K_m, it is thought that CO mimics an intermediate in acetate metabolism to CH_4, or in the synthesis of acetate. This is supported by the observation that ^{14}CO is specifically incorporated into acetate [60,61]; in crude extracts, this incorporation is stimulated by B_{12}.

The activity is also found in methanogens unable to use acetate in methanogenesis, such as *Mb. thermoautotrophicum* ΔH discussed above [59]. *Mb. thermoautotrophicum* Marburg incorporates ^{14}CO (in the presence of H_2/CO_2) specifically into the carboxyl moiety of acetyl CoA [60]. The specific activity of the acetyl group was 15% of that of the ^{14}CO, indicating that CO is in equilibrium with a bound form of carbon at the same oxidation level, and not freely exchangeable with atmospheric CO.

From the above data, it appears that CO dehydrogenase activity results from a CO_2 reductase involved specifically in the transfer of the carboxyl in acetyl-CoA, an intermediate of which is in equilibrium with free CO. The CO dehydrogenase activity is simply the reversal of the normal reaction, resulting in formation of $H_2 + CO_2$. In *Mb. thermoautotrophicum* the CO is not a preferred substrate and its oxidation is probably fortuitous.

IIA-4f. NADP-F_{420} oxidoreductase

F_{420} can be reduced by hydrogenase, formate dehydrogenase or carbon monoxide dehydrogenase (Fig. 6). These reduced equivalents can then supply reducing power for CO_2 reduction through the methanogenic and cell-carbon synthesis pathways. In crude extracts of *Mb. thermoautotrophicum* [158] F_{420} was specifically reduced by pyruvate and α-ketoglutarate dehydrogenases; NAD, NADP or ferredoxin could not replace F_{420}. These enzymes were measured in the direction of reduced F_{420} synthesis, but in whole cells, the reactions are in the direction of reductive carboxylations, using reduced F_{420}.

Other oxidoreductases in methanogens have requirements for NADPH or NADH (e.g., glyceraldehyde-3-phosphate dehydrogenase and malate dehydrogenase). While the mechanism of NAD reduction is unknown NADP is specifically reduced by reduced F_{420} in methanogens, using NADP-F_{420} oxidoreductase.

The enzyme from *Mc. vannielii* has been purified to homogeneity [153]. This enzyme catalyzes the reduction of NADP optimally at a pH of about 7.9, and in the opposite direction at a pH optimum of about 4.9. The enzyme is optimally active at 20°C, and is inactivated by warmer temperatures. In its active form it is a dimer composed of two 43 kDa subunits. Zinc is associated with the enzyme and may be a component. The enzyme is estimated to be 0.09% of the soluble protein in the cell. FAD, FMN, riboflavin or NAD are not reduced by reduced F_{420}, nor with NADPH. A variety of deazaflavins can serve as electron acceptors [252].

The NADP-F_{420} oxidoreductase from *Mb. thermoautotrophicum* was partly purified [383]. Maximal activities were observed at pH 8–9 (reduced $F_{420} \rightarrow$ NADP) and pH 5 (NADPH $\rightarrow F_{420}$). The temperature optimum was 20°C, and the enzyme was also sensitive to warmer temperatures, like *Mc. vannielii*.

IIA-4g. Methylene-FAF oxidoreductase

This enzyme is postulated to be involved in the methanogenic pathway, partaking in the reduction of formyl-FAF to methylene-FAF [384] (see Fig. 7). It was used as a catalyst in the spectrophotometric assay for FAF which has been developed by J. Escalante-Semerena. This assay involves the chemical reaction of FAF with formaldehyde to form methylene FAF, followed by observation at 340 nm to monitor the formation of formyl-FAF, an oxidation that occurs using an unknown electron carrier in the enzyme preparation, and results in H_2 production. Aminopterin, a folate analog and common folate enzyme inhibitor, inhibits methylene-FAF oxidoreductase; this is consistent with the idea that FAF (as well as YFC, methanopterin, and F_{342}) is a pterin-like compound. It is interesting to note that (probably using this enzyme) formaldehyde oxidation can drive methane production from CH_3-S-CoM.

IIA-5. The RPG effect

R.P. Gunsalus and Wolfe [100] were the first to report a stimulation of CO_2 reduction to methane by addition of CH_3-S-CoM to cell-free extracts of *Mb. thermoautotrophicum.* This stimulation was dependent on the presence of catalytic amounts of Mg-ATP, in the same manner as the methyl reductase discussed previously. The rate of methane production from CO_2 is increased 30-fold over extracts not supplemented with CH_3-S-CoM. This stimulation is transient, stopping upon depletion of the added CH_3-S-CoM; subsequent additions reinitiate the stimulation such that CO_2 reduction is proportional to the CH_3-S-CoM added.

Romesser and Wolfe [97,98] have expanded this original work, optimizing conditions for maximal stimulation. Maximal rates of CH_4 production in H_2/CO_2 incubated cell-free extracts with the addition of 500 nmol CH_3-S-CoM had specific activities of 18 nmol/min per mg protein compared to 0.65 nmol/min per mg protein without. Yields ranged between 2 and 24 CH_4 per CH_3-S-CoM reduced. ATP was required in catalytic amounts: 17 mol CO_2 was reduced per mol ATP added; data similar to these are found in the ATP needed for methyl reductase activity (15 mol CH_4/mol ATP [102]).

Pyruvate, serine, formaldehyde and CH_3-CH_2-S-CoM also induced this effect, i.e., transient, reinitiable stimulation of CO_2 reduction, but not HS-CoM, other CoM derivatives, lactate, methanol, formate, acetate or serine derivatives. Romesser [380] also mentions stimulation of CO_2 reduction by oxaloacetate, L-malate, fumarate and glyoxalate in cell free extracts, these Krebs cycle intermediates giving a ratio of CO_2 reduced per mole carboxylic acid reduced 10-times greater than for CH_3-S-CoM; thus these compounds are more potent in the RPG effect. In dialyzed extract, all the above-mentioned stimulants were again effective except for L-serine and glyoxalate. It is important to note that even though stimulation of $CO_2 \rightarrow CH_4$ was observed, the phenomenon of repeated stimulation has not been reported; this experiment has only been described with CH_3-S-CoM in *Mb. thermoautotrophicum* [100].

Activation of CO_2 reduction by CH_3-S-CoM was also tested in undialyzed extracts of other methanogens: *Mb. bryantii* and *Msp. hungatei* were stimulated but not *Mb. formicicum, Mbr. ruminantium* or *Ms. barkeri. Mb. bryantii* also exhibited a stimulation with added serine but not pyruvate, acetate or glyoxalate [385]. Other stimulatory compounds were not tested in any of the other methanogens.

From these data, one can derive two classes of stimulants: biosynthetic intermediates and CH_3-S-CoM or CH_3-CH_2-S-CoM. These different stimulants may act at two different sites in CO_2 reduction. (1) The Krebs cycle intermediates are possibly interconvertable such that the addition of one may result in formation of the others. It is possible that one (a) acts as a positive effector for an enzyme involved in one of the first steps of CO_2 reduction or (b) produces a product that can act as an effector. Such a stimulation is reasonable, since it would indicate to the methanogenic machinery that there was much cell carbon, and that the cell thus needed more energy. (2) For methanogenesis, CH_3-S-CoM must be produced, yet its addition stimulates CO_2-reduction to CH_4. Romesser and Wolfe [98] suggested that reduction of CH_3-S-CoM will result in formation of a free radical (•S-CoM) such that it will activate an enzyme further up the methanogenic path. As CH_3-S-CoM produces methane, the radical concentration will rise, first increasing $CO_2 \rightarrow CH_4$, then reacting with other molecules of the same species, forming CoM-S-S-CoM. CO_2 reduction will then slow down.

The real reasons for the RPG effect are unknown. Further work is needed to compare the two classes of effects, and to determine if free radicals are involved, e.g., using EPR and radical trapping agents.

IIA-6. Summary of the methanogenesis pathway

The scheme of methanogenesis described in Fig. 7 depicts the most recent developments in methanogenesis research. The cofactors for most of the steps have been identified, although some structures are not yet known. The actual reactions and enzymes involved have not been studied in any detail. The process consists of the binding of CO_2 to CDR (carbon dioxide reduction) factor, also called methanofuran, and the transfer of the one-carbon unit (after a two electron reduction) to FAF (formaldehyde activating factor); FAF carries the carbon through three oxidation states and transfers a methyl group to CoM. Note that Fig. 7 also indicates the involvement of part of the methanogenic pathway in cell-carbon synthesis. Reference to the above sections on cofactors and enzymes explains this scheme more fully.

An alternative scheme for methanogenesis has been proposed recently [253]; it consists of both several features in common with the above scheme and of several speculative elements. Some aspects of this alternative view, (e.g., a transcarboxylation from a lactylpterin carboxyl to yield the carbon in methane; the formation of ethenylpterin and acetylpterin intermediates) should be examined experimentally, since they are as yet only hypothesized.

IIA-7. Cytoplasmic membrane components

Methanogens, as will be discussed later, are expected to conserve energy in the form of a transmembrane electrochemical ion gradient for performance of useful work (i.e., motility, certain active transport mechanisms, ATPase-associated ATP synthesis, etc.). For understanding these cells' energetics, knowledge about the composition and structure of the cytoplasmic membrane is necessary.

Interest in archaebacterial lipids has flourished, since the discovery of isoprenoid diphytanyl glycerol diethers (see Fig. 8) in *Halobacterium* [254] and dibiphytanyl diglycerol tetraethers [255,256] in *Thermoplasma* and *Sulfolobus*. The structures of these lipids have been reviewed [257,258]. Since not all methanogens contain both diether and tetraether types of lipid, this information can be useful in descriptions of new isolates. The data are obtained easily by thin-layer chromatography of the lipid fraction subjected to acid

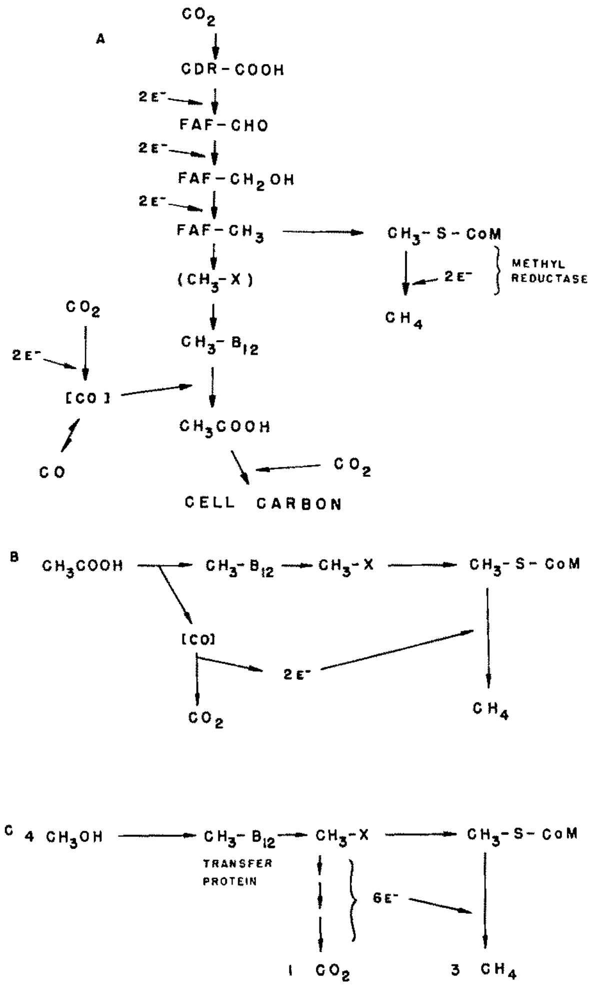

Fig. 7. Overview of methanogenesis carbon path and its relation to cell carbon production. CH_3-X, a postulated, unknown intermediate between FAF-CH_3 and methyl-B_{12}; [CO] indicates a bound carbon group at the carbon monoxide level; CoM, coenzyme M. (A) Path of CO_2 to CH_4; (B) path of acetate to CH_4; (C) path of methanol to CH_4, see text for details.

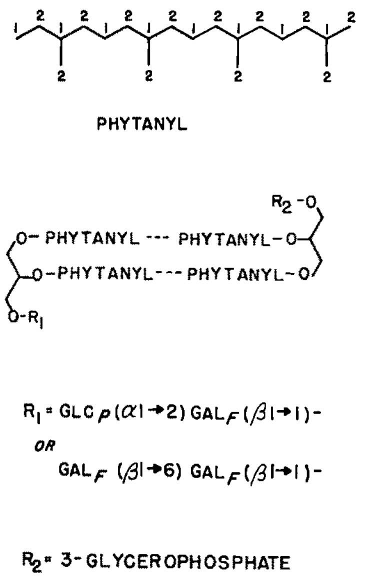
PHYTANYL
R2-O
O-PHYTANYL --- PHYTANYL-O
O-PHYTANYL --- PHYTANYL-O
O-R1
R1 = GLCp(α1→2)GALf(β1→1)-
OR
GALf(β1→6)GALf(β1→1)-
R2 = 3-GLYCEROPHOSPHATE

Fig. 8. Structural components of lipids in methanogenic bacteria [14–16,258,262,263].

methanolysis. Diether lipids account for all of the polar lipids of *Methanococcus* strain PS, *Mc. vannielii, Ms. barkeri* [16], *Mtx. soehngenii* [50] and *Mcc. methylutens* [259]. Other methanogens contain both diether and tetraether lipids, but none has yet been reported with exclusively the tetraether variety. A novel macrocylic alkylglycerol diether, i.e., a bis(phytanyl) glycerol diether with the two phytanyl moieties joined together end-to-end to form a C_{40} ring, has been found [260] in *Mc. jannaschii*. This lipid form comprises 95% of the polar lipids of this organism. It could not be found in the other methanogens surveyed.

The total lipid of methanogenic bacteria extracted by the method of Bligh and Dyer [261] accounts for 2–5.5% of the cell dry weight. Of this, polar lipids comprise 70–94% [16,262,263]. In *Msp. hungatei*, these are either phosphatidylglycerol, diglycosyldiphytanylglycerol diethers or diglycosyldibiphytanyl glycerol tetraethers (see Fig. 8). The hexose sugars of these lipids are often of the furanose form, and an unusual linkage Gal_f (β1 → 6)-$\beta\mathrm{Gal}_f$ is found in one of the two families of structures. The orientation in the membrane of the carbohydrate moiety is unknown. By ^{13}C-NMR analysis each carbon on the phytanyl chain of *Msp. hungatei* has been assigned as originating from either the C-1 or C-2 of acetate and none from CO_2 [264] (see Fig. 8). Completed structures of the polar lipids of other methanogens have not been presented yet, although it appears from thin-layer chromatograms of lipids extracted from several different genera that each has ether lipids of differing mobilities (Kushwaha, Sprott and Kates, unpublished data). The neutral lipids are mainly C_{30} (squalene) hydrocarbons, comprising 6–30% of the total cell lipid (see references mentioned in Refs. 36, 265). A possible role for squalene in proton regulation has been suggested [15,258].

How these lipids may alter the cell membrane properties and functionality is largely unknown. The dimensions of C_{40} lipids appear sufficient to span the cytoplasmic membrane, which would result in a lipid monolayer rather than a bilayer structure [258]. Speculations may be made that ether lipids may impart rigidity and stability to archaebacterial membranes often exposed to the harsh environments of extreme pH, temperature, or high salt concentrations.

The study of the composition of the membranes of methanogens has an inherent problem of the difficulty of separating cell wall and cytoplasmic membrane, since conventional methods do not produce spheroplasts. *Msp. hungatei* can be induced to form osmotically sensitive spheroplasts by treating the cells with dithiothreitol [266]. Following osmotic lysis of the spheroplasts, Sprott et al. [267] were able to isolate and study the chemical composition of the cytoplasmic membrane. It contains 45–50% protein, 36% glycolipid and lipid, and 5–7% non-lipid carbohydrate as galactose, glucose, rhamnose and mannose. Potassium represents 1.1% of the cytoplasmic membrane dry weight, nickel 0.16% and Mg^{2+} 0.04%. Amino acid analysis of cytoplasmic membrane proteins reveal 37% hydrophobic amino acids, 39% neutral and 24% charged. Low amounts of hydrophilic amino acids are characteristic of cell membranes.

Nickel levels in the cell membrane are surprisingly high, suggesting their role might be more than that of cofactor components. They may also be involved in membrane stability as in the case for the cell wall of *Mb. bryantii* [268].

IIB. ATP requirement for methanogenesis

How methanogenesis results in ATP production is the main thrust of this review; the exergonic reactions provide the energy necessary for ATP formation. As early as 1970, whole cell ATP production was found to be concurrent with methanogenesis. However, in the earliest work on cell-free extract methanogenesis by *Mb. bryantii* [104] and *Ms. barkeri* [105] from H_2/CO_2 or methanol, ATP addition was required for methane production. More work [108,240,241] has confirmed these previous observations.

Roberton and Wolfe [269,270] showed that the ATP requirement was not stoichiometric with respect to the CH_4 produced, and that ATP was involved in a preactivation step, since its removal using a hexokinase trap (added after preincubation) did not alter methanogenic rates.

Other workers have shown methanogenesis in cell-free extracts in the absence of exogenously added ATP, using *Mb. thermoautotrophicum* (Ref. 380; Sparling, R. and Daniels, L., unpublished data) and *Mc. thermolithotrophicus* [379]. The addition of ATP over a certain level can be inhibitory. Sauer et al. [86] also demonstrated with *Mbr. ruminantium* that methanogenesis in crude extracts or washed crude membrane preparations does not require added ATP. However, they did show substantial endogenous ATP levels (2.4 and 0.11 nmol/mg protein, respectively) in the preparations. Indeed, ATP can be produced in cell-free extracts under H_2 [113]. However, the rate of production must be greater than the rate of ATPase activity or ATP destruction by chemical processes. That hydrolysis of ATP occurs under assay conditions was demonstrated by Sauer et al. [86]; ATP had a $T_{1/2}$ of about 23 min at 37°C. In another study, the half-life of ATP in soil was less than 1 h [271]. Non-enzymatic catalysis in ATP solutions at 70°C results in ATP hydrolysis with $T_{1/2}$ values of 6–20 h [272]; enzymatic ATP hydrolysis may be much faster [86,113]. The half-life of ATP in 60°C methanogenesis assays may thus be quite short; this hydrolysis problem makes the examination of ATP regeneration systems essential.

Though some organisms require the addition of exogenous ATP for cell-free extract methanogenesis, those that do not still have ATP present endogenously. The varying requirements for ATP may suggest differences in ATP pool sizes rather than demand. Specific methanogenic enzymes in all methanogens require ATP for activity: methyl-CoM reductase and the methanol-CH_3-B_{12} methyltransferase [102,182,241,273].

The last step of methanogenesis, catalyzed by methyl CoM reductase (see above) requires catalytic amounts of ATP for activity when assayed using cell-free extracts under H_2, and with CH_3-S-CoM as substrate. This requirement has been found in all methanogens examined [102]. In such assays the CH_4/ATP ratios were determined for *Ms. barkeri* (85 CH_4/ATP) and *Mb. thermoautotrophicum* (15 CH_4/ATP). The purified enzyme also requires ATP [117,193].

Recently, Shapiro [241] and Van der Meijden et al. [182] have shown an ATP requirement by the methanol : methyl CoM methyltransferase. In both of these enzymes, ATP is only used in catalytic amounts.

The function of ATP in these reactions is not clear. There are several explanations of the ATP effect: (1) a protein is phosphorylated or adenylated; (2) ATP acts as an effector; (3) ATP modifies cofactors used in the reactions. Data at present do not allow a decision between these possibilities. However, since methanogenesis is exergonic in the cells, and ATP production results from it, the rationale for the ATP effect is not obvious.

IIC. Carbon fixation into cell material

Methanogens cannot only derive energy from the production of methane but virtually all of them can derive their cell carbon from single carbon precursors. The biosynthesis of cell carbon has been studied in several genera of methanogens. Since methanogenesis and cell carbon biosynthesis probably have at least one common intermediate (see Fig. 7), a brief discussion of this topic is appropriate here.

Although many of the methanogens are autotrophs, they do not fix CO_2 by the Calvin cycle [60,61,93–95,190,274–280] unlike most photosynthetic and chemotrophic organisms. Instead they have a modified reversed citric acid cycle as shown in Fig. 9. Evidence for this pathway was first

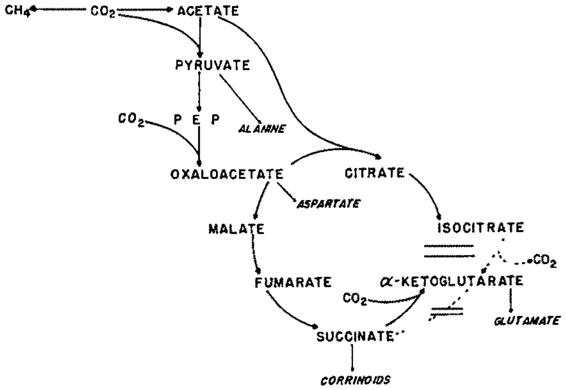

Fig. 9. Pathway of CO_2 assimilation of methanogenic bacteria. In most genera, α-ketoglutarate is produced via succinyl CoA; in *Ms.*, it is produced via isocitrate, as shown in dashed lines

obtained by one of the authors [386], but further work by Zeikus, Weimer, Kenealy, Thauer and especially Fuchs has confirmed and extended the experimental support for this reaction series. Evidence for the scheme in Fig. 9 has arisen from the lack of Calvin cycle enzymes, lack of Calvin cycle $^{14}CO_2$ fixation products, short-term and long-term labelling with $^{14}CO_2$, [^{14}C]acetate and [^{14}C]succinate, and enzyme assays demonstrating the presence of the needed enzymes. By assigning complete labelling patterns for many of the organic compounds synthesized during mixotrophic growth on CO_2 and acetate, ^{13}C-NMR studies have further confirmed and extended information on the assimilatory pathways in methanogens [264].

The scheme in Fig. 9 is largely complete, but the initial production of acetate occurs via a relatively unstudied reaction series. Present evidence suggests a $C_1 + C_1$ condensation. Kenealy and Zeikus [61] and Stupperich et al. [60] have recently proposed a common intermediate between methanogenesis and the methyl group of acetate, presenting experimental evidence for the unification of methane and cell-carbon production paths. Stupperich et al. [60] have shown that acetate is synthesized by $C_1 + C_1$ condensation of carbons at different oxidation states; the carbon forming the carbonyl group is derived from an intermediate in equilibrium with carbon monoxide, and the carbon forming the methyl group is derived from a methanogenic intermediate. A very similar method of acetate formation is thought to occur in a variety of acetogens [37,215,237,281–284]; further, recent work by Eden and Fuchs suggests the method of CO_2 fixation into cell material is similar to that of methanogens [285].

The biosynthesis by methanogens of all amino acids except isoleucine appears to be the same as in typical bacteria (see above) [286]. Three pathways for isoleucine biosynthesis are found among the methanogens examined. First, rather than threonine serving as an intermediate, acetyl-CoA and pyruvate are precursors via the citramalate pathway [264,287]. Second, propionate is incorporated from the growth medium into α-ketobutyrate; thus the C-1 of propionate appears exclusively in the α-C of isoleucine [288,289]. This pathway utilizing propionate and acetate could proceed either by reductive carboxylation of propionyl-CoA to α-ketobutyrate or through 2-methylbutyrate via 2-methylacetoacetyl-CoA [289]. The first possibility is the only pathway presented which explains the labeling pattern completely [288]. Because for maximum assimilation a concentration of exogenous propionate in the millimolar range is required in *Mb. thermoautotrophicum,* the existence of a carrier-mediated transport system seems unlikely [289]. Finally, 2-methylbutyrate is a precursor forming isoleucine probably by carboxylation [41,288,289]. In *Mc. voltae* an exogenous supply of 2-methylbutyrate substitutes for isoleucine for growth [290], and as expected the citramalate pathway from acetyl-CoA and pyruvate is inoperative (Ekiel, I. and Sprott, G.D., unpublished data). The three pathways for isoleucine biosynthesis are subject to metabolic controls, since, for example, 2-methylbutyrate is utilized in preference to propionate [288,289]. Completed labeling patterns for each pathway, including the relative contribution of each to isoleucine biosynthesis, has been measured by ^{13}C-NMR methods [288]. The possibility of a carrier-mediated transport system for 2-methylbutyrate has not been explored.

Since methane production and cell carbon production are related, so are the growth yields related to methanogenesis via ATP production.

IID. Y_{ATP} studies

Quantitative growth studies on methanogens have been conducted. A comparative table (Table

IV) is given, listing the methanogens and their growth yields on various substrates. From the literature values of growth yields, Y_{CH_4} (g cell produced/mol CH_4 produced), we have calculated values for the Y_{ATP} (g cells produced/mol ATP) of methanogens. The values for the energy available in a given redox reaction ($\Delta G^{O\prime}$) were taken from Table II and the value for the energy required to form ATP was taken to be -37 kJ/mol [76]. We assume a 25% energy efficiency for conversion of energy of the reaction into ATP.

The different labs reporting on the Y_{CH_4} of the same organism gave comparable results (see Table IV). Y_{ATP} values range from near 1 for *Mb. thermoautotrophicum* grown under H_2/CO_2 to 7.4 for *Ms. barkeri* on H_2/CO_2; the Y_{ATP} varying according to the organism under consideration, and not much according to the substrate used. (For example, *Ms.* has Y_{ATP} values under H_2/CO_2, CH_3OH, CH_3NH_2, or CH_3COOH of about 8; see Table IV.)

Interestingly, all these values are in general lower than the Y_{ATP} values determined for other organisms. Heterotrophs growing on glucose have been calculated to have maximal Y_{ATP} values as high as 29 [299] and experimental values range from 15–24 [76]. Heterotrophic growth on acetate yields a calculated Y_{ATP}^{max} of 10–15 and autotrophs using the Calvin cycle have a calculated value of about 5. In the absence of firm theoretical ATP consumption steps in methanogen biosynthesis, and, as discussed above, in methanogenesis itself, these figures must be interpreted with caution.

As specified in Table IV, certain of these organisms have been grown for these experiments in complex medium containing yeast extract and

TABLE IV

QUANTITATIVE GROWTH STUDIES ON SEVERAL METHANOGENS

Organism	Substrate	Reference	Organic supplement [a]	Yield (g cell/mol CH_4)	Y_{ATP} [b] (g cell/mol ATP)
Mb. thermoautotrophicum	H_2+CO_2	[92]	none	1.6–3	1.8–3.4
	H_2+CO_2	[291]	none	0 6–1.6	0.7–1.8
	H_2+CO_2	[A]	none	1.6	1.8
Mb bryantii	H_2+CO_2	[270]	0.2% T+2% r.f.	2.4	2.8
Mb. str AZ	H_2+CO_2	[46]		2 5	2.9
Mtx. soehngenii	CH_3COOH	[292]	none	1.1–1.4	4.6–5.9
Ms. barkeri	H_2+CO_2	[93]	none	6.4	7.4
	CH_3COOH	[94,95]	0.2% T+0.2% YE	1.6–1.9	6.7–8.0
	CH_3COOH	[108]		1.1	4.6
	CH_3COOH	[293]	none	1.8–2.7	7.5
	CH_3COOH	[294]	0.1–0.5% YE or 0.2% YE+0.2% T	2.8–3.1	11.7–13.0
	CH_3COOH	[57]		2.1	8 8
	CH_3OH	[295]		6	8.5
	CH_3OH	[93]	none	6	8.5
	CH_3NH_2	[296]		6	8.5
Ml. tindarius	CH_3OH	[58]	none	4.1	6.0
Mb. formicicum	H_2+CO_2	[234]	0.05% YE+0.05% T	3.5	3.6
	HCOOH	[234]	0.05% YE+0.05% T	4 8	6.0
	HCOOH [c]	[297]	none	5.8	7.3
Coccoid isolate	H_2+CO_2	[298]	0.02% YE+0.02% T+10% r.f.	0.9	0.96

[A], Daniels, L., Ph.D. Thesis, University of Wisconsin, 1978.

[a] YE = yeast extract; T = trypticase; r.f. = rumen fluid.

[b] Calculated from $\Delta G^{O\prime}$ values for the reaction, assuming a 25% efficiency for conversion of the available energy into ATP.

[c] Chemostat culture, formate-limited growth.

hydrolyzed protein. Although few active transport systems have been uncovered for organic molecules (exceptions are described later), a certain amount of cell carbon can come from organic molecules penetrating into the cell by passive diffusion, thus lowering the amount of energy needed to build cell mass, and thus rasing the experimentally observed values for Y_{ATP}. However, the Y_{ATP} values for *Ms.* grown with organic supplements does not significantly vary from those obtained with non-supplemented media [293,294].

It is interesting to note that the highest Y_{ATP} values are observed with *Ms. barkeri,* and *Mtx. soehngenii*; both of these organisms contain cytochromes (see above). Since it is not known what the true efficiency for ATP production from the reactions are in each organism, we cannot claim that the cytochromes allow more ATP to be produced. However, the increased Y_{ATP} values suggest that (1) more ATP is produced per reaction, or (2) the cell carbon-fixation path proceeds with less energy consumption. The similarity of the CO_2-fixation pathways [93–95] suggests that possibility (2) is unlikely. Thus, these organisms may extract more of the energy available by virtue of a more efficient ATP-producing system.

IIE. Scheme of bioenergetic coupling

Methanogenesis is the reaction causing proton flux in methanogens, and for that reason, much of the physiology and biochemistry of methane production has been described in the preceding sections. This proton flux drives the chemiosmotic generation of ATP; however, little is known about the actual coupling of ATP synthesis to methanogenesis.

Fig. 10 is a general scheme showing this process in its most simplistic terms; a source of electrons for the reduction of C-1 units to methane (H_2 and CO_2 are shown here, but other methanogenic substrates are also applicable). The following sections will describe a variety of experiments ultimately aimed at understanding the energy-coupling process.

III. Energy conservation and use

IIIA. The protonmotive force ($\Delta\bar{\mu}_{H^+}$)

According to the chemiosmotic theory [300–303], bacterial cells can expel protons from their cytosol using the energy derived from the hydrolysis of ATP or by using light energy in the case of photosynthetic organisms and halobacteria, or oxidation of an electron donor by membrane bound respiratory chains. This process results in energy conservation in the form of a membrane potential, interior negative ($\Delta\psi$), and an osmotic component (ΔpH), inside-alkaline. The protonmotive force, expressed in millivolts, is the summation of the membrane potential and chemical potential:

$$\Delta\bar{\mu}_{H^+} = \Delta\psi - Z\Delta\text{pH} = \text{protonmotive force} \qquad (5)$$

$$Z = 2.3\ RT/F \qquad (6)$$

$$\text{at } 35°\text{C},\ \Delta\bar{\mu}_{H^+} = \Delta\psi - 61\Delta\text{pH} \qquad (7)$$

(F is the Faraday constant, R is the gas constant, and T is the temperature in Kelvin; Δ values are $X_{in} - X_{out}$ [304]).

While the Mitchellian chemiosmotic theory of energy coupling is widely accepted [300–303], the degree to which the ejected protons equilibrate with bulk phase water is disputed [305–310]. Measurements of $\Delta\bar{\mu}_{H^+}$ as a function of the pH of the medium have been reported for a wide range of microorganisms. We limit ourselves here to studies with archaebacteria, and to methanogens utilizing H_2/CO_2 in particular.

Before determinations of $\Delta\bar{\mu}_{H^+}$ are possible, it is necessary to select suitable compounds for the measurement of internal volume. Recently, it was shown for *Msp. hungatei, Mb. thermoautotrophicum* [109], and several other methanogens [111,311] that [^{14}C]glucose provides an excellent non-metabolized marker for extracellular volume, apparently penetrating through the cell wall to the cytoplasmic membrane. Either a gravimetric method or penetrations of [^{14}C]urea give comparable results for the total fluid space (intracellular + extracellular). Urea penetrates the cytoplasmic membrane without concentration or metabolism in all of those methanogens tested [111]. Thus, [^{3}H]urea and [^{14}C]glucose may be mixed with the methanogen suspension in a sealed centrifuge tube * containing H_2/CO_2, the cells centrifuged at ambient temperatures, and the intracellular space in the cell pellet determined as the difference in the space occupied by the two labels [109]. This same centrifugation methodology, or flow dialysis [107], can be used with labelled weak acids or bases to provide measurements of internal pH [301]. Numerous detailed reviews have appeared on the methodology of measuring ΔpH by these methods, or of $\Delta\psi$ using permeant cations [304,313,314].

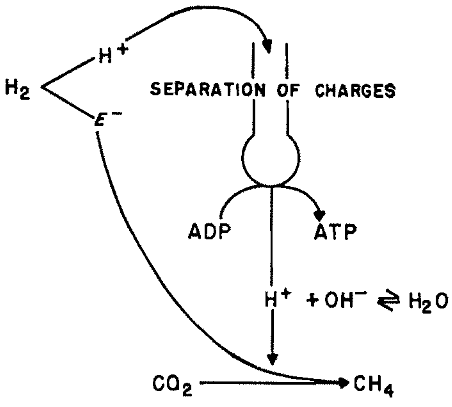

Fig. 10. Scheme of bioenergetic relationships. This figure emphasizes that a charge separation must occur, ATP is produced as a result, and methane is used to remove protons and electrons from the system.

Methanogenic bacteria are capable of maintaining a transmembrane H^+-gradient, although the intracellular pH is sometimes influenced more by the pH of the medium than is the case for several eubacteria including *Micrococcus lysodeikticus* [315], *Escherichia coli* [316,317] and *Staphylococcus aureus* [318]. Another obligate anaerobe *Clostridium pasteurianum* was similar to *Msp. hungatei* in this respect [319,312]. The isopH (the pH value at which the internal and external pH are equal) was about 6.7 for *Mb. thermoautotrophicum* [312], spheroplasts of *Msp. hungatei* [320] and *Mb. bryantii* [321]. Cells of *Mb. thermoautotrophicum* incubated under H_2 at pH 7.5 take up H^+; the internal pH was later estimated to be pH 6.6 in medium of pH 8.9 [107]. Quantitatively similar estimates of internal pH were obtained when several weak acids (5,5-dimethyloxazolidine-2,4-dione (DMO), propionate or butyrate) were compared [312]. Measurements of ΔpH (inside-acid) using methylamine gives large methylamine gradients in *Mb. thermoautotrophicum* ΔH relative to *Msp. hungatei* [107,312]. Other workers [107] found that the label was released from *Mb. thermoautotrophicum* when the pH of the medium was acidified; however, chromatography of the label accumulated by these cells indicated that significant metabolism of the methylamine could invalidate these calculations of ΔpH [312]. Doddema et al. [113] reported an internal pH of 7.6 in cells of *Mb. thermoautotrophicum* suspended in medium of pH 7.5. While it is not entirely clear, these cultures may have been killed by air, a condition which in *Mb. bryantii* dispels ΔpH (inside-alkaline) [321].

Some dispute exists concerning whether methanogens develop a membrane potential. Early attempts to measure $\Delta\psi$ in *Mb. thermoautotrophicum* by $TPMP^+$ distribution were not successful, and explained by attributing CH_4 and ATP synthesis activities to specialized intracellular membranes [107,322], a topic for later discussion. More recently, $\Delta\psi$ in *Mb. thermoautotrophicum* (inside negative) was found to be 120–140 mV using distributions of $TPMP^+$ (in the presence of the hydrophobic counter ion tetraphenylboron) or $^{86}Rb^+$ (in the presence of valinomycin) [312]. It appears that the apparent discrepancy in these results can be explained, since Sauer et al. [322] did not include tetraphenylboron in their assay. A $\Delta\psi$ was also observed in *Msp. hungatei* where tetraphenylboron was absolutely required to obtain $TPMP^+$ uptake, although attempts to demonstrate $\Delta\psi$ by the ^{86}Rb (in the presence or absence of valinomycin) assay were not successful [312]. Likewise, valinomycin in the $^{86}Rb^+$ assay with

---

* Although not commercially available, they may be prepared from Corex 15 ml centrifuge tubes by working the top of the Corex glass tube into the shape of serum-bottle tops. The commonly employed fluted butyl stoppers with metal seals are then suitable. Breakage is rare if forces no greater than 9000 × g are used; stringently anaerobic conditions are maintained throughout by providing a positive pressure of H_2/CO_2 [109,312]. Annealing is avoided, since heating at 600°C results in frequent breakage upon centrifugation (Sprott, G.D., unpublished data).

Halobacterium halobium is ineffective [323]. The failure of valinomycin to work in *Msp. hungatei* may result from an inability to penetrate the outer cell wall, since it functions well in spheroplasts [320]. Additional proof for a membrane potential (negative inside) in *Mb. thermoautotrophicum* has come from using an electrode, sensitive to TPP^+ [324]. Recently, $\Delta\psi$ has been demonstrated in *Mb. bryantii* using both $TPMP^+$ and $^{86}Rb^+$ assays [311,321]. The success of the valinomycin-$^{86}Rb^+$ method with this methanogen may relate to the pronounced cell-wall lesions which occur during growth in S medium [268]. $^{86}Rb^+$ rapidly reached a steady-state equilibrium; protonophores or gramicidin dissipated $\Delta\psi$. This assay system has advantages for further studies of $\Delta\psi$, since, unlike the situation with phosphonium cations, only a very small amount of nonspecific binding occurs. Studies are lacking on the membrane potential in other methanogens, and on the means by which these organisms establish and maintain $\Delta\psi$.

Table V summarizes the data currently available on the protonmotive force in methanogens. All three species examined have $\Delta\psi$ as the major contributor toward the total $\Delta\bar{\mu}_{H^+}$; in some cases ΔpH does not contribute in a positive manner. There is a decrease in ΔpH contribution as the medium pH rises. The total $\Delta\bar{\mu}_{H^+}$ ranges from 85 to 150 mV.

In *H. halobium* the membrane potential is strongly pH dependent, increasing greatly as the external pH is increased from 6 to 8 [325,326].

Thermoplasma acidophila is an archaebacterium which is mycoplasma-like and grows optimally at 59°C and pH 2. A large pH gradient (pH inside of 6.4–6.9) is passively maintained, partially balanced by the membrane potential, inside positive [327]. In contrast, no large pH-dependent change in $\Delta\psi$ was found in *Mb. thermoautotrophicum* [312] or *Mb. bryantii* [321]. Consequently, the decline in the chemical potential occurring as the external pH was increased resulted in a lowered $\Delta\bar{\mu}_{H^+}$. This finding predicts that those functions directly dependent on $\Delta\bar{\mu}_{H^-}$ may occur best in media more acidic than pH 7.0. It would be useful to compare $\Delta\bar{\mu}_{H^+}$ and CH_4 synthesis in relation to the pH of the medium. It is of interest to note that all methanogens grown on H_2/CO_2 may always be growing at pH 5.8–6.8, due to the acidification of the medium by CO_2 (Daniels, L. and Belay, N., unpublished data), unless proper steps are taken during medium preparation. Although the pH optima for growth have often been reported, seldom have the further difficulties been adequately controlled, i.e., sulfide loss and increased redox potentials at acidic pH, and of changes in total CO_2 concentrations.

Although some methanogens are motile [1], no studies have been reported on the energetics of flagella movement.

TABLE V

CONTRIBUTIONS TO THE PROTONMOTIVE FORCE IN METHANOGENS: THE IMPORTANCE OF $\Delta\psi$

Organism	pH_o	pH_i	(61)ΔpH (mV)	$\Delta\psi$ (mV)	Total proton motive force (mV)	Ref.
Mb. thermoautotrophicum	6.8	6.8	0	135 [a]; 119 [b]	135 [a]; 119 [b]	312
	6.5	–	–	173 [c]	173	324
Mb bryantii	5.5	6.6	67	92 [b]	159	321
	7.0	7.0	0	133 [a]; 103 [b]	133 [a]; 103 [b]	311, 321
	7.3	7.1	−12	105 [b]	93	321
Msp. hungatei (spheroplasts)	5.5	6.6	67	102 [b]	169	320
	6.5	6.5	0	108 [b]	108	320
	7.0	6.5	−31	112 [b]	81	320

[a] Measured by ^{86}Rb accumulation.

[b] Measured by $TPMP^+$ uptake, in presence of TPB^-.

[c] Measured by TPP^+ sensitive electrode.

IIIB. The methanochondrion controversy

That specialized intracellular vesicles, probably formed as invaginations of the cytoplasmic membrane, could be the site of ATP and CH_4 synthesis was first suggested by Zeikus and Wolfe [69,328]. The concept was tentative, based only on electron micrographs of thin sections, but has later been expanded by Doddema et al. [231], Spencer et al. [88], Sauer et al. [107] and Kell et al. [329], who coined the term methanochondrion in analogy to the mitochondria of eukaryotes. Although CH_4 synthesis activity from CO_2 in extracts is particulate and may require the presence of sealed membrane vesicles [88,166,322], it has not yet been proven that these membranes are in the form of specialized organelles with a $\Delta\bar{\mu}_{H^+}$ separate from that across the cytoplasmic membrane. The methanochondrion concept has proven convenient in explaining some biochemical data (reviewed in Ref. 329) in *Mb. thermoautotrophicum* such as uncoupler-insensitive ATP synthesis [113], the partial sensitivities of CH_4 synthesis found to various uncouplers [107] and the presence in vesicles of an ADP/ATP translocase activity [354,387]. Support for specialized intracellular membranes was obtained by cytochemical staining, suggesting that all of the hydrogenase activity in *Mb. thermoautotrophicum* may be localized on these membranes [231]. Those not convinced of the requirement for internal membranes in CH_4 synthesis may question the specificity of such dye-coupled reactions. Alternatively, invaginations of the cytoplasmic membrane induced by the handling procedures could form a pocket where the reaction product would accumulate. Such membrane pockets have been observed in isolated cytoplasmic membrane vesicles of *Msp. hungatei* [267].

Recently, the electron microscopic evidence for methanochondria has been thoroughly examined [330]. Large internal vesicles often composed of several membrane layers are frequent in sections of *Mb. thermoautotrophicum* [231,328,330,331]. Both the strain of methanogen [330,332,333] and the conditions of growth [330] markedly influence the frequency of sightings. In general, conditions allowing for rapid growth including optimal temperature and increased availability of H_2/CO_2 result in the production of increased amounts of internal membrane. Such a response suggests a role to provide extra membrane for the incorporation of additional methanogenic enzymes, rather than in providing a specialized role in methanogenesis.

In most other methanogens, there is little electron microscopic evidence for methanochondria. Thin sections of several mesophilic methanogens and freeze fractures of *Mb. bryantii* showed only a low incidence of mesosomes usually located near the polar regions or at new division sites. Thus, any invaginations of the cytoplasmic membrane were similar to the controversial division mesosomes of the gram-positive eubacteria [334–336]. The importance of the study by Sprott et al. [330] is in showing that several methanogens can generate CH_4 at high rates in the absence of appreciable numbers of internal membranes, but their conclusions did not rule out the presence of such membranes under certain specific conditions or in different methanogens. Micrographs of thin sections of *Mb. bryantii* are shown in Fig. 11, illustrating

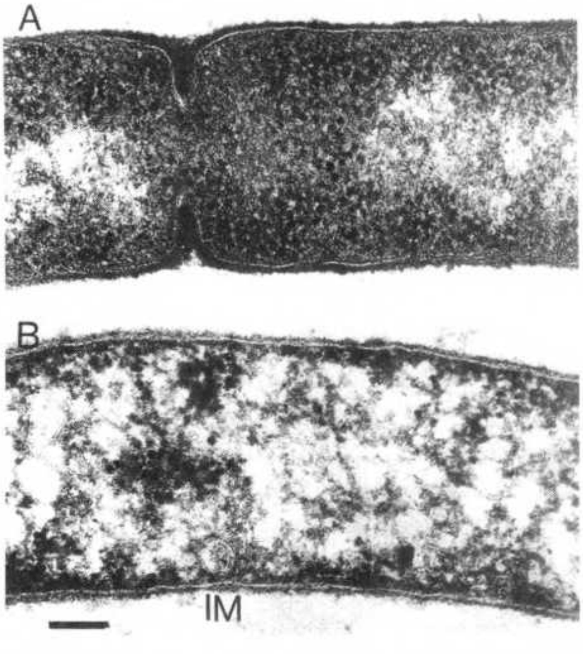

Fig. 11. Electron micrographs of *Mb. bryantii* M.O.H. A typical longitudinal section (A) revealing no intracellular membranes (IM); in less than 1% of such sections an IM was seen (B). The bar represents 0.1 μm. Micrograph A is shown with permission from J.R. Colvin; B, with permission from T.J. Beveridge.

the typical absence of internal membranes (A) and a case (less than 1% of micrographs examined) where an internal membrane is seen (B). Internal membrane fractions that are purified free from cytoplasmic membrane are not available to test the issue. In fact, during purification of the cytoplasmic membrane of *Msp. hungatei*, no bands were found in the sucrose gradients which could be assigned as internal membranes [267]. One methanogen in which internal membranes are consistently found is *Ms. vacuolata* [337], where the structures are known to be gas vacuoles.

Regardless of the outcome of the methanochondrion controversy, the cytoplasmic membrane of methanogens must be an energy-transducing membrane; however an alternate view has been given [107]. Evidence for energy conservation across the cytoplasmic membrane comes from studies of $\Delta\bar{\mu}_{H^+}$ (see preceding section), and of active transport systems (described later). Also, intracellular K^+ reaches concentrations in the cytoplasmic space of up to 1.2 M in *Mbr.* species (Table VI). Only a small part of this K^+ could remain in solution within the relatively small volume of the postulated methanochondrion, proving that concentration occurs across the cytoplasmic membrane. The data does not allow any conclusion with respect to the K^+ concentrations in the methanochondrion, when present.

IIIC. Transport in methanogens

Unfortunately, not many studies have been done on the energy requirements of carrier-mediated transport systems in methanogens. In part, this can be attributed to the narrow range of substrates capable of supporting growth, and to the fact that the gases H_2, CO_2, CO and CH_4 are expected to pass freely through the membrane [243]. We are left with the option of studying transport systems for ions (i.e., K^+, PO_4^{3-}, Mg^{2+}, Ni^{2+}, Co^{2+}, Na^+, etc.), vitamins or cofactors.

The usual substrates supporting growth, such as formate, acetate or methylamines, do not require specific transport systems because they are weak acids and bases which distribute across the cytoplasmic membrane to give a gradient (in/out) according to the ΔpH. Methylamine can be an exception, since carrier mediated transport (pH optimum near neutrality) occurs in several N_2-fixing bacteria, via the naturally occurring ammonium carrier in *Rhizobium* sp. Strain 32H1 [345]. Moreover, *Pseudomonas* sp. MA can transport short-chain alkylamines independent of the ammonium system [346]. At neutral pH, methylamine did not concentrate appreciably within cells of *Msp. hungatei* [312], *Mb. thermoautotrophicum* [312] or *Mb. bryantii* [321]; however, it could be fruitful to look for a methylamine transport system in *Ms. barkeri* following growth on methylamine. Often compounds which stimulate growth are present in rumen fluid [347] or sludge fluid [1]. Unfortunately, these possible transport substrates are unidentified. Prolonged exposures (up to 2 h) of *Msp. hungatei* or *Mb. thermoautotrophicum* to phenylalanine [109] or growth of *Mb. thermoautotrophicum* with cysteine or serine [388] resulted in only small accumulations, as expected for transport-negative cells. Under some conditions *Mb. thermoautotrophicum* strain Marburg can assimilate high levels of pyruvate [348] and incorporate threonine from the medium into protein [287].

The first transport system described in a methanogen was that of HS-CoM in a strain of *Mbr. ruminantium* which required an exogenous supply of the cofactor for growth [179]. Uptake required both CO_2 and H_2, was optimal at pH 7.1, and showed saturation kinetics. Either HS-CoM or CH_3-S-CoM could be transported, but the carrier specificity was restricted to a limited range of HS-CoM analogues. Metabolism of HS-CoM was extensive, but analysis of the pool established that HS-CoM was concentrated against a gradient. Sodium azide, 2,4-dinitrophenol, iodoacetate and air inhibited uptake. Further studies with this methanogen could be valuable with respect to the energetics of HS-CoM transport. No measurements of $\Delta\bar{\mu}_{H^+}$ have been reported.

Methanogenic bacteria require nickel for growth [134,349] and have developed an effective means of scavenging the trace amounts of exogenous nickel normally found in the growth medium. A high-affinity active transport system for nickel (apparent K_m, 3.1 μM) has been described in *Mb. bryantii* [350]. Like the HS-CoM transport system [179], for maximum transport rates both CO_2 and H_2 were required, and air was an inhibitor. However, the pH optimum was 4.9 with little activity

TABLE VI

INTRACELLULAR ATP, K^+ AND Na^+ IN METHANOGENS

Organism	ATP content (nmol/mg protein)	Ref.	Na^+ [a] (mM)		Ref.	K^+ [b] (mM)		Ref.
			Na_i	Na_o		K_i	K_o	
Mb. thermoautotrophicum	7	338	4.2–4.6	1.2	109	780 [c]	14	109
	1–4	339	24–33	14.5	109	1103 [c]	80	111
Thermophile MT1	1–15	339	–	–	–	–	–	–
Mb bryantii	3–12	338, 321	–	–	–	–	–	–
	2–8	270	–	–	–	861	80	111
Mb. str. G2R	5	338	–	–	–	886	80	111
Ms. barkeri MS	3	338	–	–	–	183	80	111
Msp hungatei JF1	23	338	–	–	–	172	80	111
Msp hungatei GP1	20	338	0.9–1.7	1.2	109	150	14	109
	–	338	0–3 6	29.5	109	218	80	111
Mbr arboriphilus	–	–	–	–	–	1225	80	111
E. coli AN180	17.4	340	–	–	–	–	–	–
E coli	–	–	80	145	341	277	5	341
Halobacterium halobium	2.4	325	1200	3900	342	3700	4	342
Halobacterium cutirubrum	–	–	800	3330	343	5320	40	343
Halobacterium salinarium	–	–	1370 [d]	4000	344	4570 [d]	32	344

[a] $Na_i = Na^+$ inside; $Na_o = Na^+$ outside

[b] $K_i = K^+$ inside; $K_o = K^+$ outside

[c] Differences in K_i are primarily the result of a smaller intracytoplasmic volume measured in Ref. 111 as opposed to Ref. 109.

[d] Stationary phase cells.

found at neutral pH or above, suggesting a probable nickel limitation of growth at alkaline pH. Interestingly, nickel was not taken up as an alternate substrate of the Mg^{2+} transport system; Co^{2+} was the only cation found to compete effectively for nickel transport. Once transported, nickel became distributed among the protein fraction, F_{430} and a pool of Ni^{2+}. Large concentration gradients of free Ni^{2+} (in/out) were achieved. The ionophores gramicidin, nigericin and monensin all served as inhibitors of transport. Conditions resulting in depletion of intracellular ATP (e.g., acetylene) [338] or the membrane potential (valinomycin + KCl) [320,321] had little effect on transport, apparently precluding the direct involvement of these possible energy sources. An artificial transient ΔpH, established by injection of HCl into a cell suspension incubated in a N_2 atmosphere, caused the concentrative uptake of Ni^{2+}. While a model based on these results seemed premature, largely because of the unexpected lack of inhibition of transport by the protonophore CCCP, the transport of Ni^{2+} seemed to be coupled to an influx of H^+ [350].

Mc. voltae has provided the only system to date for amino acid transport studies [351]. Isoleucine is concentrated against a gradient via an energy-dependent, carrier-mediated system of high affinity (K_m 4.5 μM). Only valine and leucine effectively compete with [^{14}C]isoleucine for transport. This finding provides the first Na^+-dependent transport system for study in a methanogen.

Methanogens are capable of accumulating K^+ at concentrations well above those in the media (Table VI). The wide range of intracellular K^+ concentrations is especially interesting when compared to the phylogenetic tree of Fox et al. [8,352]. The related *Msp. hungatei* (strains GP1 and JF1) and *Ms. barkeri* contain similar low K^+ contents. *Mbr. arboriphilus* and *Mbr. smithii,* closely related to the halophiles on the basis of 16 S rRNA sequence data [8] have high K^+ contents [110,111]. Studies of K^+ transport have not been reported for a methanogen.

An adenine nucleotide (ADP/ATP) translocase, not previously reported in a prokaryote (except for the parasite *Rickettsia* [353]), was found in membrane vesicles of *Mb. thermoautotrophicum.* Mitochondrial ADP/ATP translocase inhibitors atractyloside and carboxyatractyloside slightly inhibited ATP synthesis, ATP hydrolysis and ADP uptake. One of the inhibitors, atractyloside, bound to a membrane protein [354]. These results have such important implications in arguments favoring the methanochondrion concept that extensions to this work are essential.

IIID. ATPase and ATP synthesis

While little is known about the mechanism of coupling ATP synthesis to CO_2 reduction in methanogens, the current evidence suggests an absence of substrate level phosphorylation, and synthesis of ATP via an ATPase, coupled directly or indirectly to $\Delta\mu_{H^+}$. ATPase activity has been found in particulate extracts of *Mb. thermoautotrophicum* strain ΔH [113] and detectable much lower activities in extracts of *Ms. barkeri* MS [61], *Mb. thermoautotrophicum* Marburg [227], and *Msp. hungatei* [338]. In the latter case, no activity was found unless triton X-100 was included in the assay. Cryptic ATPase activity in *Halobacterium saccharovorum* was similarly expressed only in the presence of Triton X-100 [389]. The failure to detect ATPase activity in the absence of detergent was attributed to the 'right-side-out' orientation of the vesicles, so ATP did not reach the ATPase. If a similar explanation can apply to the low-ATPase activities described above for several methanogens, this may indicate that *Mb. thermoautotrophicum* ΔH is the exception in containing an ADP/ATP translocase function. In the absence of a translocase the rates of ATP hydrolysis in vesicles should reflect the degree to which the vesicles sealed with right-side-out orientation.

Synthesis of ATP is thought to occur according to chemiosmotic principles [300]. In cells of *Ms. barkeri* net synthesis of ATP occurred in response to an acid pH shift (pH 8.2–2.5), which was sensitive to proton conductors and the ATPase inhibitor DCCD [355]. Valinomycin induced a transient synthesis of ATP through electrogenic K^+ efflux in cells of *Mb. thermoautotrophicum*; an acid pulse also induced ATP synthesis, although the kinetics were unusual in showing a lag period and synthesis was not subject to inhibition by DCCD [113,231]. Further evidence in accord with chemiosmotic coupling in ATP synthesis comes from the dramatic declines in intracellular ATP contents in *Msp. hungatei* treated with DCCD, and in *Mb. bryantii* treated with gramicidin, nigericin, monensin or CCCP (Table VII).

The correlation found by Roberton and Wolfe [270] between the rate of CH_4 synthesis and the level of ATP found in *Mb. bryantii,* suggested that ATP was generated during CH_4 synthesis. It was suggested further that ATP or AMP concentrations might control CH_4 production. A recent study of membrane ionophores in *Mb. bryantii* supports this concept in general, but exceptions are noted. Nigericin and monensin (at pH 5.2) virtually eliminated CH_4 synthesis, while ATP levels declined only 24 and 59%, respectively [321]. In contrast, appropriate concentrations of DCCD added to *Msp. hungatei* caused a marked decline in intracellular ATP content without affecting CH_4 synthesis greatly [357]. Apparently, much has yet to be learned about the coupling of methanogenesis to ATP synthesis.

IIIE. Inhibitors of methanogenesis

As described previously, the cell-wall and cytoplasmic membrane structures of methanogens differ markedly in several important aspects from the eubacteria. Consequently, analogies should be avoided regarding penetration and mode of action of inhibitors and membrane ionophores. In *Mb. bryantii* monensin, normally associated with Na^+-H^+ exchange, induced a large efflux of K^+ [321]; see Table VII. Also, the K^+-ionophore valinomycin induced K^+-H^+ exchange in *Mb. thermoautotrophicum* [322]. Care in using ionophores should be exercised with respect to the composition of the external medium, since pH, ionic environment and reducing conditions can be crucial to observing inhibitions. For example, in *Mb. thermoautotrophicum* monensin was a much more effective inhibitor of CH_4 synthesis in medium of acid pH and low Na^+ content [246]. This effect was confirmed in *Mb. bryantii* where monensin was shown to dispel ΔpH at acid pH (inside-alkaline) but to dispel ΔpH at pH 7.6 (inside-acidic) only partially [321]. It follows that the different inhibitions of CH_4 synthesis at acidic and alkaline pH do not necessarily indicate different mechanisms of energy coupling.

Methanogen media are often reduced with cysteine and Na_2S to obtain the low redox potentials associated with growth. The reaction of CCCP with thiols [358] renders this protonophore ineffective; large inhibitions of CH_4 synthesis occurred in *Mb. bryantii* only when cysteine was omitted from the medium [321]. Other inhibitors may be chemically altered, as in the reduction of 2,4-dinitrophenol by *Mb. bryantii* [270]. The importance of inhibitor concentration was illustrated for DCCD with *Msp. hungatei* cells, low concentrations (20 μM) specifically inhibited ATP synthesis, but high levels (500 μM) inhibited CH_4 synthesis and caused K^+ efflux [320,357]. A tabulation of inhibitors of CH_4 synthesis and related effects is shown in Table VII, and will be discussed further in relation to models for CH_4 and ATP synthesis.

IIIF. Sodium requirement for CO_2 respiration

There are many eubacteria that require Na^+ [359–361] for growth, and, indeed, the majority of eubacteria prefer having Na^+ in the medium for optimal growth [362]; it is not surprising that methanogens as well would require sodium for growth and methanogenesis [245]. It is noteworthy that Na^+ is inhibitory at elevated concentrations [363].

Perski et al. have found a K_{Na^+} for growth and methanogenesis of between 0.4 and 1.1 mM, values similar to those calculated from Kodama and Taniguchi [364] for *Pseudomonas stutzeri* (K_{Na^+}, approx. 1.1 mM). Also the observation by Perksi et al. [245] that growth in higher K^+ concentrations requires more Na^+ than in low K^+ media was seen with *P. stutzeri* [365].

The function of Na^+ in these cases is not known. Three hypotheses may be proposed: (1) it is needed for specific enzyme functions; (2) it participates in essential symport activities; (3) it is involved directly in respiration (note that CO_2 respiration by methanogens is analogous to O_2 respiration by aerobes). The first two hypotheses may not explain the interactions of Na^+ and K^+. The third idea has been further studied in *P. stutzeri* [365].

Using Na^+-starved cells to which Na^+ was then added, Kodama and Taniguchi [365] found that activation of respiration and phosphate uptake exhibited a sigmoidal kinetic effect; this effect was temperature-dependent. In the presence of Na^+, respiration is more sensitive to polymyxin B, an antibiotic that perturbs the packing of the lipid molecules by binding to phosphatidylethanolamine. FCCP [365] and 2,4-dinitrophenol stimulated respiration of Na^+-deficient cells but not of cells in the presence of 5 mM Na^+, suggesting that Na^+ is involved in coupling of respiration to growth. The polymyxin B data suggest membranes are involved, which is also consistent with a respiration effect. Further experimentation with methanogens is necessary to see if any of these ideas will apply. One possible explanation (Racker, E., personal communication) of Na^+ effects might be that phosphate entry is facilitated.

Msp. hungatei maintains outwardly directed Na^+ gradients [109]. Their maintenance should be either driven by a Na^+-H^+ antiport using a $\Delta\bar{\mu}_{H^+}$, or by direct Na^+ pumping; neither activity has yet been demonstrated. The most common mechanism for Na^+ extrusion is an exchange with H^+ [366]. Sodium-dependent oxaloacetate decarboxylase from *Klebsiella aerogenes* and methylmalonyl-CoA decarboxylase from *Micrococcus lactolyticus* have been implicated as Na^+ pumps [367,368]. *Vibrio alginolyticus* has an electron transport chain which pumps Na^+ instead of H^+ at alkaline pH_0 [369]. An Na^+-stimulated ATPase activity is linked to Na^+ efflux in *Mycoplasma mycoides* [370], *Acholeplasma laidlawii* [371] and *Streptococcus faecalis* [372].

It therefore appears that Na^+ plays in methanogens no more special a role than in eubacteria. The Na^+ effect on membranes and respiration warrants further study, especially in

TABLE VII

INHIBITORS OF METHANOGENESIS FROM H_2/CO_2

Expected mode of action	Methanogenesis inhibitor	Test system	Related observations [a]	References
Protonophore	CCCP	*Mb. bryantii*-cells	ATP pool declined	270
		Mbr. ruminantium-extracts	–	86
		Mb. thermoautotrophicum-cells	ATP pool declined	107
		Mb bryantii-cells	abolished ΔpH (inside alkaline); decline in $\Delta\psi$ and ATP pool, inhibitions most pronounced at pH_o acidic	311, 321
	TCS	*Msp hungatei*-cells and spheroplasts	$\Delta\psi$ increased	320
		Mb. bryantii-cells	$\Delta\psi$ dissipated	311
	pentachlorophenol	*Mb. bryantii*-cells	ATP pool declined;	270
			methyl reductase inhibited	273
		Ms. barkeri-cells	ATP pool declined	355
	2,4 dinitrophenol	*Mb. bryantii*-cells	ATP pool declined;	270
			methyl reductase inhibited	273
		Ms. barkeri-cells	ATP pool declined	355
		Mb. thermoautotrophicum-cells	ATP pool declined	107
		Msp hungatei-cells and spheroplasts	–	320
	FCCP	*Mb. bryantii*-extracts	prevents activation of methyl reductase by depletion of ATP	273
K^+ ionophore	valinomycin	*Mb. thermoautotrophicum*-cells	pH gradient (interior acid) discharged	322
		Msp. hungatei - + KCl, cells	drop in CH_4	320
		– KCl, cells	no change in CH_4	
		– spheroplasts	decrease in $\Delta\psi$	
Na^+/H^+ antiport	monensin	*Mb. thermoautotrophicum* – Na^+, cells	drop in CH_4	246
		+ Na^+, cells	smaller drop in CH_4	246
		Mbr arboriphilus-cells	–	246
		Mb. bryantii-cells	ATP pool declined; pH gradient (interior alkaline) abolished; K^+ efflux; $\Delta\psi$ increased	321
		Msp hungatei-cells	no effect	320
K^+/H^+ antiport	nigericin	*Msp. hungatei*-spheroplasts	K^+ efflux; decline $\Delta\psi$	320
		Mb. bryantii-cells	ATP pool declined; pH gradient (inside alkaline) abolished; K^+ efflux; $\Delta\psi$ increased	321
General ionophore	gramicidin	*Msp. hungatei*-spheroplasts	K^+ efflux	320
		Mb. bryantii-cells	ATP pool declined; K^+ efflux; H^+ influx; decline in $\Delta\psi$	311, 321
Hydrophobic cations	$TPMP^+$	*Mbr. ruminantium*-extract	presumed decline in $\Delta\psi$	86
		Msp. hungatei-cells and spheroplasts	–	320
	tetraphenyl phosphonium	*Mb. bryantii*-cells	parallel stimulation or inhibition of ATP pool and $\Delta\psi$ depending on inhibitor concentration	311
	tetrabutyl ammonium	*Mb. ruminantium*-extract	–	86
Electron transport inhibitor	*o*-phenanthroline	*Ms. barkeri*-cells	presumed to bind to non-heme iron centers	355
Analogs	bromoethane sulfonate and chloroethane sulfonate	*Mb. thermoautotrophicum*-extracts	inhibition of methyl CoM reductase	101

Table VII, continued

Expected mode of action	Methanogenesis inhibitor	Test system	Related observations	References
	Bromoethane sulfonate	*Ms. barkeri*	–	108, 180
Chlorinated hydrocarbons	chloroform	*Mb bryantii*-cells	ATP pool declined; presumed methyl reductase inhibition	270
		Mb. thermoautotrophicum-cells	ATP pool declined; presumed methyl reductase inhibition	107
	chloroform, carbontetrachloride, methylene chloride	'*Methanobacillus omelianskii*'-extract	–	356
Corrinoid antagonist	iodopropane	*Mb thermoautotrophicum*-cells	growth inhibitor	189
		Mb. formicicum-cells	growth inhibitor	189
		Ms. barkeri-cells	growth inhibitor; by-passed if acetate supplied	189
ATPase inhibitor	DCCD	*Msp. hungatei*-cells	ATP pool declined; CH_4 synthesis affected only at high concentrations	357
Detergents	deoxycholate	*Mbr. ruminantium*-extract	–	86
	Triton-X-100	*Msp hungatei*-spheroplasts -cells	lysis no lysis	320
		Mc. thermolithotrophicus-extracts	–	[b]
		Mb. thermoautotrophicum-extracts	–	[b]
Miscellaneous	acetylene	All examined methanogens -cells	ATP pool declined, pH gradient (inside alkaline) abolished	338
	air (oxygen)	All examined methanogens -cells and extracts	inhibits F_{420}-linked functions; destroys component B	1

[a] Unless otherwise stated, all inhibitors caused a drop in methanogenesis.

[b] Sparling, R. and Daniels, L., unpublished data.

light of the similar effects observed in *P. stutzeri.*

Two organisms, *Mb. thermoautotrophicum* [109] and *Mbr. arboriphilus* [390] can accumulate Na^+ against its gradient when Na^+ concentrations in the medium are below 50 mM. The reason for such a phenomenon is not yet known.

IIIG. Discussion of bioenergetic relationships in methanogenesis

The previous section has dealt with some problems that arise in the study of chemiosmotic-energy production in methanogens, such as differences of permeability of inhibitors through the cell wall, alteration by the reduced environment, and unexpected sites of inhibition. A compilation of the results of diverse uncouplers and methanogenesis inhibitors is given in Table VII. From a discussion of such data, we hope to arrive at models for the physical arrangement of the energy-yielding components of the cell.

IIIG-1. Proton ionophores

All protonophores examined (CCCP, TCS, PCP and 2,4-DNP) (see Table VII) caused a drop in both intracellular ATP levels and methanogenesis. The drop in ATP levels through the disruption of the transmembrane protonmotive force is the expected mode of action; decrease in methanogenesis is probably the result of the methyl reductase requirement for ATP, although an additional requirement for electrochemical ion gradients is possible in reducing the one-carbon unit to formaldehyde [329,76] *. Assuming this last step in methanogenesis is the only one requiring ATP, one should see a build-up of methyl-CoM analogous to the uncoupling of ATP production and respiration in eubacteria. Alternatively, ATP formation may be inhibited indirectly; if methyl reductase (or any other methanogenic enzyme) is blocked (e.g., by 2,4-dinitrophenol), no protons are consumed in the cell interior by the methanogenesis process, and, thus, no H^+ will come through the ATPase; likewise, reduced 5-deazaflavin is not oxidized, and the hydrogenase will stop oxidizing hydrogen. This is similar to respiratory control in aerobes.

---

* The process of methanogenesis is often described as $CO_2 \xrightarrow{1} HCOOH \xrightarrow{2} HCHO \xrightarrow{3} CH_3OH \xrightarrow{4} CH_4$, in which the formal free intermediates are used. $\Delta G^{0'}$ values can be assigned to these two electron steps (1–4: −1.3, +23.4, −44.8, and −112.5 kJ/mol, respectively) [76,329]. However, it should be emphasized that the coenzyme-bound intermediates expected in most or all of these steps will not have the same thermodynamics; extrapolation of these formal values to physiological systems should be done with caution.

In these protonophore experiments $\Delta\psi$ does not drop, implying that it alone is not sufficient for ATP synthesis. Those methanogens investigated do not show a ΔpH at neutral pH [107,320]. However, acid pulsing of *Mb. thermoautotrophicum* and *Ms. barkeri* [113,355] has been shown to induce ATP synthesis. It is likely that most methanogens live in slightly acidic environments and maintain an inside-basic pH (relative to the outside), and use both $\Delta\psi$ and ΔpH to contribute to the $\Delta\bar{\mu}_{H^+}$ (see also Table V).

IIIG-2. Valinomycin (a K^+-ionophore) and K^+

At pH 7.5, cells of *Mb. thermoautotrophicum* ΔH are interior acid [322]. As noted above, this is a pH at which growth is suboptimal. Treatment of the cells with valinomycin in the presence of 0.1 M KCl causes an efflux of H^+ and a drop of methanogenesis [322]. This apparent antiport activity is not expected with valinomycin, since it is not known to elicit K^+-H^+ exchange. Such an exchange function is also suggested by a lack of both CH_4 inhibition and H^+ efflux when 0.1 M NaCl is used to replace KCl. *Mb. thermoautotrophicum* has a high (0.8–1.1 M) cellular K^+ concentration, and a K^+ efflux would be expected rather than the exchange of extracellular K^+ with cellular H^+. The implications of this work are not clear to us, but were interpreted by other workers [322] to favor the methanochondrion concept.

The effects of valinomycin and K^+ on methanogenesis by *Msp. hungatei* whole cells have been studied at a physiologically relevant pH of 6.9 [320]. High medium K^+ concentrations cause a drop in methanogenesis independent of the presence of valinomycin. K^+ may simply enter the cells through leaks or via the K^+ transport carrier, thus decreasing $\Delta\psi$. At pH 6.9, $\Delta\psi$ is the major contributor to the $\Delta\bar{\mu}_{H^+}$ [320]; see also Table V. Alternatively, very high K^+ may cause a Na^+ efflux, or some similar antagonism toward Na^+-dependent systems; this is consistent with the Na^+ requirement for methanogenesis and the observed effect of K^+ on the levels of Na^+ needed for methanogenesis [246].

Valinomycin reacts differently with cells and spheroplasts of *Msp. hungatei* (Table VII) [320]. However, spheroplast experiments with valinomycin in medium of low K^+ concentrations show a rapid efflux of K^+ and a large decrease in methanogenesis accompanied by a slight $\Delta\psi$ loss; this is possibly explained by the potential role of valinomycin as a K^+-H^+ antiporter (as discussed above), in this case emitting K^+ and accumulating H^+. Valinomycin-treated spheroplasts treated in high external K^+ exhibit a collapse in $\Delta\psi$, but not in low or moderate K^+ concentrations; this is consistent with its normal use as a K^+ ionophore.

With spheroplasts of *Msp. hungatei,* the cation-exchanging ionophores monensin and nigericin and the general ionophore gramicidin (at pH 6.9, 47 mM K^+, 13 mM Na^+) all cause a K^+ efflux, resulting in little $\Delta\psi$ change. Presumably, a H^+ influx occurs, as predicted by their properties with other membrane systems, and a drop of the pH_i occurs. Nigericin and gramicidin caused little $\Delta\psi$ drop, but about 60–80% drop of the methanogenesis. Monensin experiments with *Mb. thermoautotrophicum* Marburg at differing pH values has revealed that its effect is pH dependent. In both high and low extracellular Na^+ levels, monensin is much more effective as an inhibitor of methanogenesis at low pH (inhibitions observed at pH 6.0 and somewhat at 6.7) [246]. The efflux of K^+ was not examined in this latter work, but the marked efflux observed from spheroplasts of *Msp. hungatei* [320] and cells of *Mb. bryantii* [321], and the relationships of Na^+ and K^+ [245,246] suggest that the concentrations of both ions could be important.

An inhibition of methanogenesis by phosphonium cations suggests $\Delta\psi$ involvement in methane production. However, the true effects of the hydrophobic cations on the enzymes themselves (e.g., those of the methanogenic path) are not yet known.

The inhibition of methanogenesis by compounds thought to act principally on enzymes in the methanogenic path (for example HS-CoM analogs and chlorinated hydrocarbons) also cause ATP drops (see Table VII). This emphasizes that energy generation is coupled to methane production, even if another enzyme is responsible for the direct generation of a ΔpH (e.g., hydrogenase) and is not inhibited by these compounds.

Both acetylene and air cause a loss of ΔpH (inside alkaline) [321,338]. These effects were not the result of non-specific changes in membrane permeability, since $\Delta\psi$ persists following exposure to either inhibitor.

The pH values at which methanogens grow should be briefly discussed here. Many otherwise excellent publications on the isolation or growth of methanogens describe pH growth curves or cell growth conditions that are in error. Since H_2/CO_2 atmospheres are commonly used for growth, the buffer is often overcome by the production of protons upon CO_2 entry into the medium, with an accompanying pH drop (i.e., $CO_2 + H_2O \rightarrow HCO_3^- + H^+$). Our unpublished experiments (Belay, N., Sparling, R. and Daniels, L., unpublished data) suggest that many methanogens grow well at pH values of 5.5–6.8, but poorly at values above 7.0. This is consistent with a ΔpH (alkaline-inside) being important in ATP formation.

Thus, the evidence discussed above with ionophores and inhibitors suggest that both ΔpH and $\Delta\psi$ can be important components for ATP synthesis. Measurements of internal pH in growing cultures of *Msp. hungatei, Mb. thermoautotrophicum* [312], and *Mb. bryantii* [321] show that ΔpH is negligible or slight (acidic-inside) in growth media of pH 6.8–7.2 (Table V). Hence, under these conditions of growth, ATP synthesis is expected to be driven exclusively by $\Delta\psi$; indeed a close parallel is found between the magnitude of $\Delta\psi$ and the ATP pool size in *Mb. bryantii* treated with varying amounts of tetraphenylphosphonium cation [311]. This is consistent with observations that growth occurs in media of neutral to slightly basic pH.

The protonmotive force has not been measured yet for a growing culture as a function of a range of pH values used for growth. These studies would be helpful to measure the capacity of methanogens to regulate their cytosolic pH, as opposed to past studies documenting their ability to maintain an imposed pH gradient (as shown in Table V).

IIIH. Models for generation of $\Delta\tilde{\mu}_{H^+}$ and ATP during methanogenesis

We would like to present here models descriptive of the possible architecture of the methanogenic and energy-coupling enzymes in light of the above ionophore studies. These models are necessarily speculative, incorporating existing knowledge, but with the intent of stimulating relevant experimental design. We accept the principles of Mitchell's chemiosmotic hypothesis whereby a separation of charge can drive transport and ATP synthesis. However, we do not know whether the protons are extruded to the 'outside' of the membrane where they are freely exchangeable with the external bulk water phase; or if they are *not* freely exchangeable by virtue of association with a space near to the outside of the membrane, as proposed by Kell [373] and Haines [374]; or by association in proton 'pockets' and channels, as proposed by Williams [305,306]. These three views (variations on the same theme) about the physical locations of the protons partaking in the protonmotive force are described in Fig. 12; these are not mutually exclusive. The anionic lipids found in methanogens, although unusual when compared to eubacterial lipids, have the necessary anionic properties to be involved in proton conductance along the membrane surfaces, as proposed by Haines [374]. Some recent work on *Halobacterium halobium* suggests that ATP is produced by proton pumping, where protons do not enter the bulk phase [325]. This may be analogous to some of the work on methanogens as discussed below.

There is indication that either of the last two models of transmembrane proton phenomena would more easily fit data addressing where the 'H' of methane arises. Though most of the 'H' comes from water, $^2H_2$ labelling shows too much '^{2}H' coming from $^2H_2$ to account for free equilibrium with bulk water by the extruded $^2H^+$ pumped by the hydrogenase. The data were originally interpreted as support for either an enclosed membrane (i.e., a methanochondrion) or an invagination open to the bulk water via a narrow aperture [88]. We suggest here that these data are

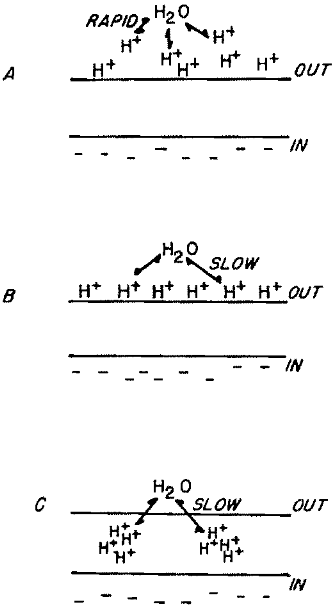

Fig. 12. Different perceptions of a transmembrane proton gradient. (A) Traditional Mitchell view [300], with clearcut separation of protons from membrane, with all protons readily exchangeable with bulk water. (B) Kell [373] and Haines [374] view, with protons as a thin layer, close to the membrane, not readily exchangeable with bulk water. (C) Williams view [306], with protons often associated with pools or channels actually inside the membrane, and not rapidly exchangeable with bulk water. These two latter views suggest that a ΔpH can thus be established either from the surface or within regions of the membrane.

also consistent with the Kell, Haines and Williams variations. Phenomena in a variety of other bacteria are also consistent with these hypotheses (Refs. 374,305–307,373 and references therein). Direct evidence for these views have not yet been obtained; this is likely due to the inherent difficulties in such experiments. The reader is encouraged to consider these three alternate views in reading our discussion of transmembrane phenomena, although we will not extensively deal any further with their subtle distinctions.

IIIH-1. Formation of $\Delta\bar{\mu}_{H^+}$. Internal membrane required (the methanochondrion hypothesis)

This model incorporates the concept that energy generation occurs solely within closed membrane systems (called methanochondria) in the cell cytoplasm [88,113,231,329]. It was proposed that the transmembrane $\Delta\bar{\mu}_{H^+}$ is established between the inside of the methanochondrion and the cytosol (acid in the cytosol, comparatively). ATP would be produced inside the vesicles and be transported to the cytoplasm through the ATP/ADP translocase. (Arguments suggesting the methanochondrion space is more acid than the cytoplasm have also been given [107]; if this were so, the ATPase would be oriented such that ATP would be produced in the cytoplasm, and hence there would be no need for a translocase.) The first model accounts for growth and thus ATP production despite an absence of a ΔpH across the cytoplasmic membrane under neutral conditions. A diagram of this model is given in Fig. 13, and is similar to that described previously as a possible explanation of deuterium labeling studies discussed above [88].

Evidence in the recent thorough electron microscopy study by Sprott et al. [330] suggests that this model is not likely; many methanogens simply lack internal membranes under certian conditions of growth. The hypothesized methanochondrion should be large enough to be easily seen, since the hydrogenase and methanogenic enzymes may account for 15–25% of the cell protein [112,117]. The redox dye evidence for the exclusive location of the hydrogenase on internal membranes, and evidence for an ADP-ATP translocase is not strong, and has not been examined in any other organism besides *Mb. thermoautotrophicum*.

Unfortunately, the ionophore and inhibitor studies cannot yet provide evidence for or against this model.

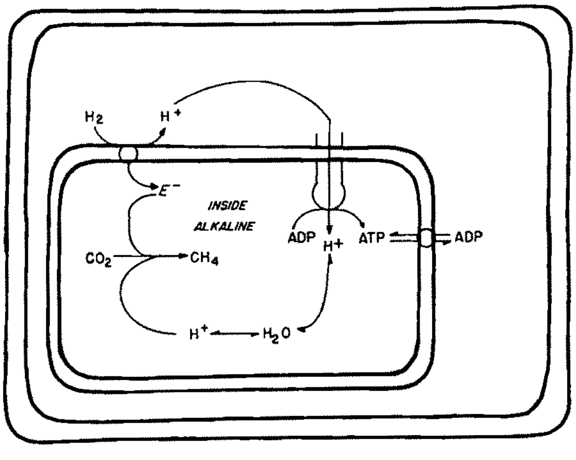

Fig 13. The methanochondrion model of methanogenesis.

IIIH-2. Formation of $\Delta\tilde{\mu}_{H^+}$. Internal membranes not present

IIIH-2a. Methanogenesis from H_2/CO_2 or formate

There are two general models (proton pump vs. sodium pump) that fit the data on H_2/CO_2 or formate grown cells. Since these two substrates are metabolized in much the same way, the same models will be used for both.

(i) Hydrogenase as primary proton pump. As described recently by Sprott et al. [330] internal membranes are not a prerequisite for growth of methanogens on H_2/CO_2. The model for this case is shown in Fig. 14. Hydrogenase acts as a H^+ pump, creating a pH gradient that drives ATP formation. This is supported by acid pulse experiments on whole cells, where external acid additions produced ATP [113,355]. This model also includes the possible involvement of a $K^+(Na^+)/H^+$ symport, suggested by the obligate requirement of Na^+ for methanogenesis [245,246] and the accumulation of Na^+ above the external concentration in *Mb. thermoautotrophicum* [109] and *Mbr. arboriphilus* [246]. The accumulation of K^+ by symport with protons [323,375] or Na^+ [376,377] has been proposed in other prokaryotes. The requirements for Na^+ or K^+ may be no different than those for ordinary bacteria, as discussed above.

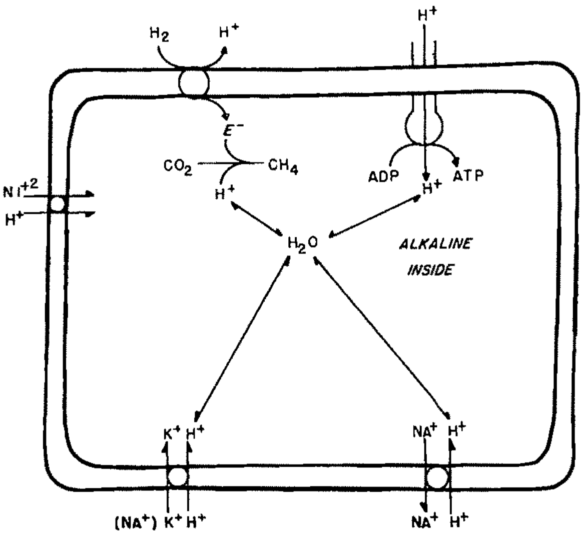

Fig. 14. Model of methanogenesis using hydrogenase as a proton pump, and with no enclosed membrane systems.

A Na^+-H^+ antiporter is included to account for the gradient of Na^+ (inside low) found in *Msp. hungatei* [109]. The apparent Na^+ requirement for growth by methanogens in general and the requirement for higher Na^+ concentrations in the medium in the presence of higher K^+ might be explained if the K^+-H^+ symport could also, though with lower frequency, take in Na^+. This would explain both the concentration of Na^+ by some methanogens and the coupling of Na^+ and K^+ effects.

(ii) Sodium pumping as primary gradient forming event. Perski et al. [245,246] have suggested that Na^+ pumping may be the primary event in the creation of transmembrane motive force. In Fig. 15, we describe a model illustrative of this possibility. The $\Delta\tilde{\mu}_{Na^+}$ would be responsible for the generation of $\Delta\tilde{\mu}_{H^+}$ via a Na^+/H^+ antiporter, and would explain the Na^+ requirement by methanogens and its accumulation by some species. There are two possible sites for this pumping: the hydrogenase or a component of the methanogenic pathway. In the latter case, the reaction could be directly coupled to Na^+ extrusion.

IIIH-2b. Methanogenesis from acetate

The production of CH_4 from acetate by *Ms.*

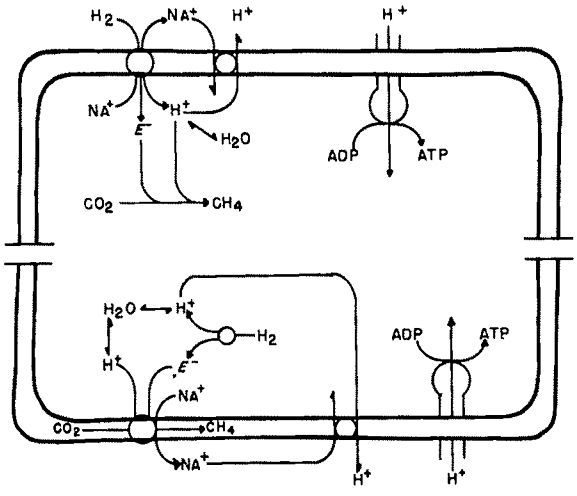

Fig. 15. Model of methanogenesis using a sodium pump, with no enclosed membrane systems. The upper half is one where the sodium pump must be on the membrane, while the methanogenic pathway can be cytoplasmic. The lower half represents a model whereby the methanogenic pathway acts as a sodium pump as suggested by Perski et al. [245,246] and must therefore be on the membrane; in this case the hydrogenase need not be on the membrane.

barkeri and *Mtx.* provides an example of the simplest model requirements. Assuming that internal membranes are not involved (as discussed above) and ignoring the possible role of Na^+ as an intermediate in generation of $\Delta\bar{\mu}_{H^+}$, we can consider Fig. 16a to represent the architecture of an acetate-using methanogen. (Note, however, that Na^+ is required for methanogenesis from acetate [246].) A hydrogenase is not involved; indeed, hydrogenase is not found in *Ms.* TM1, but it grows on acetate alone [57]. Acetate is simply split to CO_2 and CH_4, the oxidation of the acetate's carboxyl by CO dehydrogenase leading to a $\Delta\bar{\mu}_{H^+}$. This model does not require that the methyl reductase be on the membrane. As mentioned earlier, cytochromes are potentially involved in the oxidation step. Alternate models of methanogenesis from acetate have been given by Zehnder and Brock [378] prior to the description of the involvement of CO dehydrogenase in acetate metabolism.

IIIH-2c. Methanogenesis from methanol

The production of CH_4 from methanol is similar to acetate metabolism. Methanol is oxidized to CO_2, creating a $\Delta\bar{\mu}_{H^+}$, possibly using an electron-transfer chain composed partly of cytochromes, or a reversal of the methanogenic pathway. Production of methane from methanol alone requires oxidation of a portion of the substrate to provide protons to maintain $\Delta\bar{\mu}_{H^+}$. There are several possibilities. (1) The proton pumping mechanism here may use cytochromes in some way analogous to the aerobic electron transfer chain, using reduced F_{420} produced by reversal of a cytoplasmic CO_2 reduction chain. (2) Another model would require part of the methanogenic path to be located on the membrane and act as a proton pump; this would produce separation of charge and a reduced electron carrier, probably F_{420}. (3) A third alternative would be that a cytoplasmic hydrogenase would produce H_2, and a membrane-bound hydrogenase would split it and create a proton gradient.

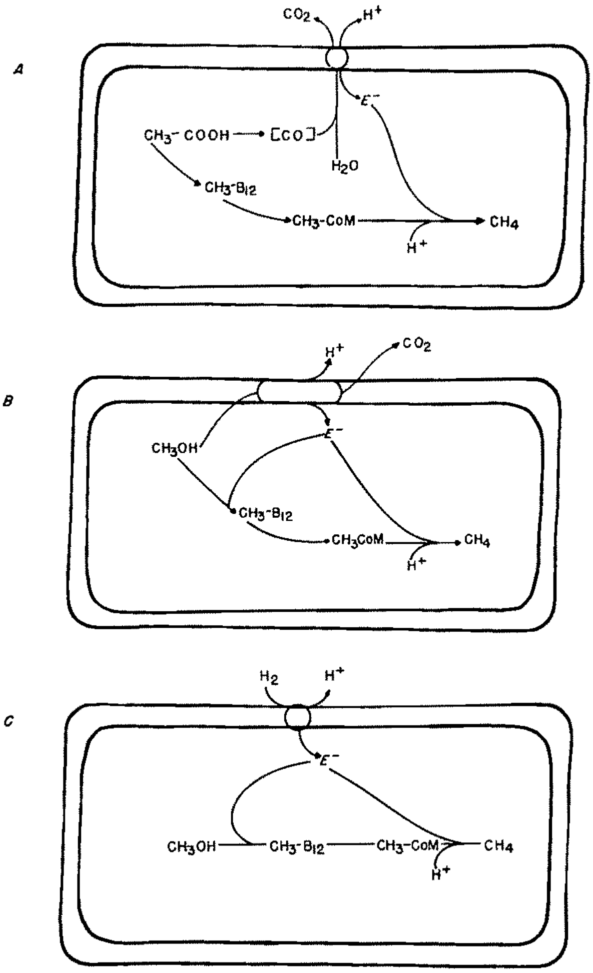

Fig. 16. Models of methanogenesis using a proton pump and substrates other than $H_2 + CO_2$ or formate. (A) Methanogenesis from acetate; (B) methanogenesis from methanol; (C) methanogenesis from H_2 + methanol, but not methanol alone.

That *Ms. barkeri* strain TM1 [57] has very weak hydrogenase activity (and cannot grow on H_2/CO_2), but yet grows well on methanol and suggests that possibility (3) is unlikely. The scheme we present (Fig. 16b) does not require either hydrogenase or methyl reductase to be on the membrane. The possibilities that either cytochromes or part of the methanogenic pathway are on the membrane appear to be most likely; these ideas are, however, as yet speculative.

IIIH-2d. Methanogenesis from H_2 + CH_3OH, but not from methanol alone

The organism growing only on these two substrates together [56] provides an interesting example of cooperation between the methyl reductase and hydrogenase. Fig. 16c shows that there is no need for cytochromes, and that hydrogenase can establish the $\Delta\bar{\mu}_{H^+}$ and provide electrons for the methyl reductase.

III I. Cautions on methanogen diversity

As seen above, energy-conservation models can take on different architectures depending on the methanogen studied. Through this review, we have seen how diverse the methanogens are. That metabolic features may vary significantly between methanogens only reflects the phylogenetic diversity within the group; for example, 16 S rRNA sequencing information suggests that the different orders of methanogens are as related to one another as *Bacillus* sp. are to enterics or cyanobacteria [36]. With such phylogenetic diversity, it is only normal that there be variations between organisms in even the most intrinsic of pathways of methanogenesis and cell carbon synthesis, such that results from work on one methanogen will not always be applicable to another.

IV. Summary

The reduction of CO_2 or any other methanogenic substrate to methane serves the same function as the reduction of oxygen, nitrate or sulfate to more reduced products. These exergonic reactions are coupled to the production of usable energy generated through a charge separation and a protonmotive-force-driven ATPase.

For the understanding of how methanogens derive energy from C-1 unit reduction one must study the biochemistry of the chemical reactions involved and how these are coupled to the production of a charge separation and subsequent electron transport phosphorylation.

Data on methanogenesis by a variety of organisms indicates ubiquitous use of CH_3-S-CoM as the final electron acceptor in the production of methane through the methyl CoM reductase and of 5-deazaflavin as a primary source of reducing equivalents. Three known enzymes serve as catalysts in the production of reduced 5-deazaflavin: hydrogenase, formate dehydrogenase and CO dehydrogenase. All three are potential candidates for proton pumps. In the organisms that must oxidize some of their substrate to obtain electrons for the reduction of another portion of the substrate to methane (e.g., those using formate, methanol or acetate), the latter two enzymes may operate in the oxidizing direction. CO_2 is the most frequent substrate for methanogenesis but is the only substrate that obligately requires the presence of H_2 and hydrogenase.

Growth on methanol requires a B_{12}-containing methanol-CoM methyl transferase and does not necessarily need any other methanogenic enzymes besides the methyl-CoM reductase system when hydrogenase is present. When bacteria grow on methanol alone it is not yet clear if they get their reducing equivalents from a reversal of methanogenic enzymes, thus oxidizing methyl groups to CO_2. An alternative (since these and acetate-catabolizing methanogens possess cytochrome *b*) is electron transport and possible proton pumping via a cytochrome-containing electron transport chain.

Several of the actual components of the methanogenic pathway from CO_2 have been characterized. Methanofuran is apparently the first carbon-carrying cofactor in the pathway, forming carboxy-methanofuran. Formyl-FAF or formyl-methanopterin (YFC, a very rapidly labelled compound during ^{14}C pulse labeling) has been implicated as an obligate intermediate in methanogenesis, since methanopterin or FAF is an essential component of the carbon dioxide reducing factor in dialyzed extract methanogenesis. FAF also carries the carbon at the methylene and methyl oxidation levels. Methyl-CoM is involved in the final enzymatic step in methanogenesis, a reaction catalyzed by the Ni-corrinoid (F_{430})-containing methyl reductase.

CO dehydrogenase, implicated in methanogenesis from both CO and acetate, is actually a catalyst in the pathway of C-1 + C-1 condensation to form acetate. This reaction is a key step in the biosynthesis of C ell material.

The only enzymes required to be on the membrane of the methanogens are those acting as proton pumps. All others could be cytoplasmic, although the complexity of, for example, the methyl reductase, and the low methanogenic rates in cell free extracts, imply close association of the different components.

The relationship of these enzymes to the maintenance of chemiosmotic gradients and electron transport phosphorylation has been studied with ionophores and other uncouplers and inhibitors. Such inhibitor work has been problematic for several reasons: the reduced environments found in suspensions of methanogens affect ionophores and inhibitors (e.g., CCCP); some (e.g., 2,4-dinitrophenol) act as enzyme inhibitors.

Protonophores cause a drop in intracellular ATP and also reduce the rate of methanogenesis, probably due to the ATP requirement for methanogenesis. Valinomycin, in high external K^+ caused a disruption of $\Delta\psi$, as well as stopping methanogenesis; once again, the effect on methane production may be via ATP levels. Work with monensin and the Na^+ requirement for growth of methanogens suggest Na^+ is somehow involved in methanogenesis, but the site of action is not known.

The ionophore and inhibitor work to date suggest a ΔpH-driven ATPase at external acid pH; energy can also be conserved as $\Delta\psi$, becoming more important particularly at external pH values larger than 6.8. In most cases there is substantial inhibition of methanogen growth at alkaline pH, perhaps largely due to loss of the chemical potential (inside alkaline). The contribution of membrane surface layer protons and intramembrane protons (as proposed by Kell, D.B., Haines, T.H. and Williams, R.J.P., see Refs. 373, 374, 305 and 306) should be considered as alternatives to the simpler 'in' or 'out' proton gradient models; these, however, are simply extensions of the Mitchellian hypothesis.

We disagree with the necessity for a methanochondrion as sole site of electron-transport driven ATP synthesis, since the frequency of electron microscopy sightings of such internal vesicles can be of a rarity such that they could not be in all cells of a growing culture. Evidence for methanochondria as obligatory organelles for CH_4 synthesis (e.g., ATP/ADP translocase, or hydrogenase stains in electron microscopy) is not compelling. This does not exclude a role for intracytoplasmic membrane to provide the membrane surface area (additional to the cytoplasmic membranes) needed for increased rates of methanogenesis during rapid growth. The true role of these structures has yet to be determined.

Our preferred model for the physical arrangement of energy-producing proteins for CO_2 respiring methanogens is one with a proton pumping hydrogenase, providing the electrochemical ion gradients required to perform essential functions including ATP synthesis. Although evidence for a Mitchellian transmembrane gradient is good, there is merit in models that involve a proton layer or pool that is not in equilibrium with bulk phase water. ATP production is coupled to the methanogenic enzymes which could be cytoplasmic, but which are most likely aggregated and membrane associated. There are, however, many unsolved problems remaining for a complete understanding of the bioenergetics of the methanogens.

Acknowledgements

We thank the members of our laboratories (Duane Wessels, Ken Jarrell, Negash Belay and Rod Ruhe) for discussion and constructive criticism. We also thank the many workers in the field of methanogens who provided us with papers prior to their publication date. We greatly appreciate the comments of Efraim Racker on the bioenergetics portion. A special thanks is due to Mary Smithson for her excellent secretarial help. Portions of the work described here are supported by grants to L.D. from the American Chemical Society (14062-AC5), NIH (GM30868) and NSF (PCM-8207809), and by a fellowship to R.S. from the Natural Sciences and Engineering Council of Canada.

References

1 Zeikus, J.G. (1977) Bacteriol. Rev. 41, 514–541
2 Wolfe, R.S. and Higgins, I.J. (1979) International Review on Biochemistry in Microbial Biochemistry (Quayle, J.R., ed), Vol. 21, pp. 267–352, University Park Press, Baltimore, MD
3 Zehnder, A.J.B., Ingvorsen, K and Marti, T. (1982) in Anaerobic Digestion (Hughes, D.E., Stafford, D.A., Wheatley, B.I, Baader, W., Lettinga, G., Nyns, E.J., Verstraete, W. and Wentworth, R.L., ed.), pp. 45–68, Elsevier Biomedical Press, Oxford
4 Zeikus, J.G., Ben-Bassat, A. and Hegge, P.W. (1980) J. Bacteriol. 143, 432–440
5 Woese, C.R. and Fox, G.E (1977) Proc. Natl. Acad. Sci. U.S.A. 74, 5088–5090
6 Balch, W.E., Magrum, L.J., Fox, G.E., Wolfe, R.S. and Woese, C.R. (1977) J. Mol. Evol. 9, 305–311
7 Woese, C.R., Magrum, L.J. and Fox, G.E (1978) J. Mol. Evol. 11, 245–252
8 Fox, G.E., Stackebrandt, E., Hespell, R.B., Gibson, J., Maniloff, J., Dyer, T.A., Wolfe, R.S., Balch, W.E., Tanner, R.S., Magrum, L.J., Zablen, L.B., Blakemore, R., Gupta,

R., Bonen, L., Lewis, B.J., Stahl, D A., Luehrsen, K.R , Chen, K.N. and Woese, C R. (1980) Science 209, 457–463

9 Tu, J , Prangishvilli, D., Huber, H., Wildgruber, G., Zillig, W. and Stetter, K O. (1982) J. Mol Evol. 18, 109–114

10 Hilpert, R , Winter, J , Hammes, W. and Kandler, O. (1981) Zbl. Bakt Hyg , I. Abt., Orig. C 2, 11–20

11 Elhardt, D and Bock, A. (1982) Mol. Gen. Genet. 188, 128–134

12 Kessel, M. and Klink, F (1980) Nature 287, 250–251

13 Pappenheimer, A.M., Dunlop, P.C., Adolph, K.W. and Bodley, J.W. (1983) J. Bacteriol. 153, 1342–1347

14 Kates, M., Wassef, M.I. and Pugh, E L (1970) Biochim Biophys. Acta 202, 206–208

15 Tornabene, T.G., Wolfe, R.S., Balch, W.E., Holzer, G , Fox, G E. and Oro, J. (1978) J. Mol. Evol. 11, 259–266

16 Tornabene, T.G. and Langworthy, T.A. (1979) Science 203, 51–53

17 Kandler, O. and Hippe, H. (1977) Arch. Microbiol. 113, 57–60

18 Kandler, O. and Konig, H. (1978) Arch. Microbiol 118, 141–152

19 Konig, H., Kralik, R. and Kandler, O (1982) Zbl Bakt. Hyg., I. Abt., Orig. C 3, 179–191

20 Best, A.N. (1978) J. Bacteriol. 133, 240–250

21 Zillig, W. and Stetter, K.O. (1980) in Genetics and Evolution of RNA Polymerase, tRNA and Ribosomes (Osawa, S., Ozeki, H., Uchida, H. and Yura, T , eds), pp. 525–538, University of Tokyo Press

22 Zillig, W., Stetter, K.O., Schnabel, R., Madon, J. and Gierl, A. (1982) Zbl. Bakt. Hyg., 1. Abt., Orig. C. 3, 218–227

23 Zillig, W., Schnabel, R , Tu, J and Stetter, K.O. (1982) Naturwissenschaften 69, 197–204

24 Schmid, G., Pecher, T.H. and Bock, A. (1982) Zbl. Bakt. Hyg., I. Abt., Orig. C. 3, 209–217

25 Matheson, A.T. and Yaguchi, M (1981) in International Cell Biology (Schweiger, H G., ed.), pp. 103–110, Springer-Verlag, Berlin

26 Matheson, A.T., Yaguchi, M. (1982) Zbl Bakt. Hyg., I. Abt., Orig. C. 3, 192–199

27 Lake, J.A., Henderson, E., Clark, M.W. and Matheson, A.T (1982) Proc. Natl. Acad. Sci. U.S.A. 79, 5948–5952

28 Zillig, W., Stetter, K O., Schäfer, W., Janekovic, D., Wunderl, S., Holz, I and Palm, P. (1981) Zbl. Bakt. Hyg., I. Abt., Orig. C 2, 205–227

29 Zillig, W., Tu, J. and Holz, K. (1981) Nature 293, 85–86

30 Zillig, W., Stetter, K.O., Prangishvilli, D., Schafer, W., Wunderl, S., Janekovic, D., Holz, I. and Palm, P. (1982) Zbl. Bakt. Hyg., I. Abt., Orig. C 3, 304–317

31 Stetter, K.O. and Gaag, G. (1983) Nature 305, 309–311

32 Stetter, K.O. (1982) Nature 300, 258–260

33 Fisher, F., Zillig, W., Stetter, K.O. and Schreiber, G. (1983) Nature 301, 511–513

34 Woese, C.R. (1979) J. Mol. Evol. 13, 95–101

35 Woese, C.R. (1981) Sci. Am. 244, 98–122

36 Balch, W.E., Fox, G.E., Magrum, L.J., Woese, C.R. and Wolfe, R.S. (1979) Microbiol. Rev. 43, 260–296

37 Zeikus, J.G. (1983) Adv. Microbiol. Physiol. 25, 215–299

38 Wolfe, R.S. (1980) in Diversity of Bacterial Respiratory Systems, Vol. 1C (Knowles, J., ed.), CRC Press, Cleveland, OH

39 Mah, R.A (1981) Trends in Biological Fermentations (Hollaender, A , ed), pp. 357–374, Plenum Press, New York

40 Mah, R.A., and Smith, M R. (1981) in Prokaryotes (Starr, M.P., Stolp, H., Trüper, H.G., Balows, A. and Schlegel, H.G., eds.), pp 948–977, Springer-Verlag, Berlin

41 Taylor, G.T. (1982) in Progress in Industrial Microbiology, Vol. 16 (Bull, M.J., ed), pp. 231–320, Elsevier Science Publishers, Amsterdam

42 Mah, R.A., Ward, D.M., Baresi, L. and Glass, T.L. (1977) Annu Rev. Microbiol. 31, 309–341

43 Morris, J G. (1979) in Strategies of Microbial Life in Extreme Environments (Shilo, M., ed.), Vol. 13, Verlag Chemie Life Sci. Report, pp. 149–162, Springer-Verlag, Berlin

44 Kiener, A. and Leisinger, T. (1983) System Appl. Microbiol. 4, 305–312

45 Patel, G.B., Roth, L.A. and Agnew, B.J. (1984) Can. J. Microbiol 30, 228–235

46 Zehnder, A J.B. and Wuhrmann, K. (1977) Arch. Microbiol. 111, 199–205

47 Balch, W.E. and Wolfe, R.S. (1976) Appl. Environ. Microbiol 32, 781–791

48 Teather, R.M. (1982) Appl. Environ. Microbiol. 44, 499–501

49 Hook, L.A., Corder, R.E., Hamilton, P.T., Frea, J.I. and Reeve, J.N. (1984) in Microbial Chemoautotrophy (Strohl, W.R. and Tuovinen, O H., eds.), pp. 275–289, Ohio State University Press, Columbus

50 Huser, B.A., Wuhrmann, K. and Zehnder, A J.B. (1982) Arch. Microbiol. 243, 1–9

51 Jones, W.J., Leigh, J A., Mayer, F., Woese, C.R. and Wolfe, R.S. (1983) Arch. Microbiol. 136, 254–261

52 Stetter, K.O., Thomm, M., Winter, J., Wildgruber, G., Huber, H., Zillig, W., Janécovic, D., Konig, H., Palm, P. and Wunderl, S. (1981) Zbl. Bakt. Hyg., I. Abt., Orig. C 2, 166–178

53 Baross, J.A., Lilley, M.D. and Gordon, L.I. (1982) Nature 298, 366–368

54 Baross, J.A and Deming, J.W. (1983) Nature 303, 423–425

55 Oremland, R.S , Marsh, L. and DesMarais, D.J. (1982) Appl. Environ. Microbiol. 43, 462–468

56 Miller, T.L and Wolin, M.J. (1983) J. Bacteriol. 153, 1051–1055

57 Zinder, S.H. and Mah, R.A. (1979) Appl. Environ. Microbiol. 38, 996–1008

58 Konig, H. and Stetter, K.O (1982) Zbl. Bakt. Hyg., I. Abt., Orig. C 3, 478–490

59 Daniels, L., Fuchs, G., Thauer, R.K and Zeikus, J.G. (1977) J. Bacteriol. 132, 118–126

60 Stupperich, E., Hammel, K.E., Fuchs, G. and Thauer, R.K. (1983) FEBS Lett. 152, 21–23

61 Kenealy, W R. and Zeikus, J.G. (1982) J. Bacteriol. 151, 932–941

62 Meile, L., Kiener, A. and Leisinger, T (1983) Mol. Gen. Genet. 191, 480–484

63 Thomm, M., Altenbuchner, J. and Stetter, K.O. (1983) J. Bacteriol 153, 1060–1063

64 Morris, C. and Reeve, J. (1983) Proceedings of the Fourth International Symposium on Microbial Growth on C-1 Compounds (Hansor, R.S. and Crawford, R., eds.), American Society for Microbiology, Washington, D.C.

65 Wood, A.G., Redborg, A.H., Cue, D.R., Whitman, W B. and Konisky, J. (1983) J. Bacteriol. 156, 19–29

66 Bollschweiler, C. and Klein, A. (1982) Zentralbl Bakteriol. Parasitenkd. Infectionskr. Hyg. Abt. 1, Orig. C 3, 101–109

67 Hamilton, P.T. and Reeve, J.N. (1984) in Microbial Chemoautotrophy (Strohl, W.R. and Tuovinen, O.H., eds.), pp. 291–308, Ohio State University Press, Columbus

68 Jarsch, M., Altenbuchner, J. and Bock, A. (1983) Mol. Gen. Genet 189, 41–47

69 Zeikus, J.G. and Wolfe, R.S. (1972) J. Bacteriol. 109, 707–713

70 Kluyver, A.J. and Schnellen, C.G.T.P. (1947) Arch. Biochem. 14, 57–70

71 Huber, H., Thomm, M., König, H., Thies, G. and Stetter, K.O. (1982) Arch. Microbiol. 132, 47–50

72 Smith, P.H. and Hungate, R.E. (1958) J. Bacteriol. 75, 713–718

73 Stadtman, T.C. and Barker, H.A. (1951) J Bacteriol. 62, 269–280

74 Ferry, J.G., Smith, P.H. and Wolfe, R.S. (1974) Int. J. Syst. Bacteriol. 24, 465–469

75 Bryant, M.P., Wolin, E.A., Wolin, M.J. and Wolfe, R.S. (1967) Arch. Microbiol. 59, 20–31

76 Thauer, R.K., Jungermann, K. and Decker, K. (1977) Bacteriol. Rev. 41, 100–180

77 Kristjansson, J.K., Schonheit, P. and Thauer, R.K. (1982) Arch. Microbiol. 131, 278–282

78 Abram, J.W. and Nedwell, D.B. (1978) Arch. Microbiol. 117, 89–92

79 Winfrey, M.R. and Zeikus, J.G. (1977) Appl. Environ. Microbiol. 33, 275–281

80 Stanier, R.Y., Adelberg, E.A., Ingraham, J.L. and Wheelis, M.L. (1979) Introduction to the Microbial World, Prentice-Hall, Englewood Cliffs, NJ

81 Barker, H.A. (1936) Arch. Mikrobiol. 7, 404–419

82 Barker, H.A., Ruben, S. and Kamen, M.D. (1940) Proc. Natl. Acad. Sci. U.S.A. 26, 426–430

83 Stadtman, T.C. and Barker, H.A. (1949) Arch. Biochem. 21, 256–264

84 Pine, M.J. and Barker, H.A. (1956) J. Bacteriol. 71, 644–648

85 Pine, M.J. and Vishniac, W. (1957) J. Bacteriol. 73, 736–742

86 Sauer, F.D., Erfle, J.D. and Mahadevan, S. (1979) Biochem. J. 178, 165–172

87 Daniels, L., Fulton, G., Spencer, R.W. and Orme-Johnson, W.H. (1980) J. Bacteriol. 141, 694–698

88 Spencer, R., Daniels, L., Fulton, G. and Orme-Johnson, W.H. (1980) Biochemistry 19, 3678–3683

89 Hungate, R.E., Smith, W., Bauchop, T., Yu, I. and Rabinowitz, J.C. (1970) J. Bacteriol. 102, 389–397

90 Schauer, N.L., Brown, D.P. and Ferry, J.G. (1982) Appl. Environ. Microbiol. 44, 549–554

91 Tzeng, S.F., Bryant, M.P. and Wolfe, R.S. (1975) J. Bacteriol. 121, 192–196

92 Schönheit, P., Moll, J. and Thauer, R.K. (1980) Arch. Microbiol. 127, 59–65

93 Weimer, P.J. and Zeikus, J.G. (1978) Arch. Microbiol. 119, 49–57

94 Weimer, P J. and Zeikus, J.G. (1978) Arch Microbiol. 119, 175–182

95 Weimer, P J. and Zeikus, J G. (1979) J Bacteriol. 137, 332–339

96 Krzycki, J.A., Wolkin, R H. and Zeikus, J.G. (1982) J. Bacteriol. 149, 247–254

97 Romesser, J.A. and Wolfe, R.S. (1981) Biochem J. 197, 565–571

98 Romesser, J.A. and Wolfe, R.S. (1982) J. Bacteriol. 152, 840–847

99 Romesser, J A. and Wolfe, R.S. (1982) Zb. Bakt. Hyg., I Abt., Orig. C. 3, 271–276

100 Gunsalus, R.P. and Wolfe, R.S. (1977) Biochem Biophys Res. Commun. 76, 790–795

101 Gunsalus, R.P., Romesser, J.A. and Wolfe, R S. (1978) Biochemistry 17, 2374–2377

102 Gunsalus, R.P. and Wolfe, R.S. (1978) J. Bacteriol. 135, 851–857

103 Gunsalus, R.P. and Wolfe, R.S. (1980) J. Biol. Chem 255, 1891–1895

103 Leigh, J.A. and Wolfe, R.S. (1983) J Biol. Chem. 258, 7536–7540

104 Wolin, E.A., Wolin, M.J. and Wolfe, R.S. (1963) J. Biol. Chem. 238, 2282–2286

105 Blaylock, B.A. and Stadtman, T.C. (1963) Biochem. Biophys Res. Commun. 11, 34–38

106 Blaylock, B.A. and Stadtman, T.C. (1966) Arch. Biochem. Biophys. 116, 138–158

107 Sauer, F.D., Erfle, J.D. and Mahadevan, S. (1981) J. Biol Chem. 256, 9843–9848

108 Hutten, T.J., De Jong, M.H., Peeters, B.P.H., Van der Drift, C. and Vogels, G.D. (1981) J. Bacteriol. 145, 27–34

109 Sprott, G.D. and Jarrell, K.F. (1981) Can. J. Microbiol. 27, 444–451

110 Jarrell, K.F. and Sprott, G.D. (1982) Abstracts of the XIIIth International Congress of Microbiology, Boston, MA, p. 5:1, p. 61

111 Jarrell, K.F., Sprott, G.D. and Matheson, A.T. (1984) Can. J. Microbiol., 30, 663–668

112 Jacobson, F.S., Daniels, L., Fox, J.A., Walsh, C.T. and Orme-Johnson, W.H. (1982) J. Biol. Chem. 257, 3385–3388

113 Doddema, H.J., Hutten, T.J., Van der Drift, C. and Vogels, G.D. (1978) J. Bacteriol. 246, 19–23

114 Racker, E. (1964) Biochem. Biophys. Res. Commun. 14, 75–78

115 Reenstra, W.W., Patel, L., Rottenberg, H. and Kaback, H.R. (1980) Biochem. 19, 1–9

116 Ellefson, W.L. and Wolfe, R.S. (1980) J. Biol. Chem. 255, 8388–8389

117 Ellefson, W.L. and Wolfe, R.S. (1981) J. Biol. Chem. 256, 4259–4262

118 Van Beelen, P., Geerts, W.J., Pol, A. and Vogels, G.D. (1983) Anal. Biochem. 131, 285–290

119 Eirich, L.D., Vogels, G.D. and Wolfe, R.S. (1979) J. Bacteriol. 140, 20–27

120 McCormick, J.R.D. and Morton, G.O. (1982) J. Am. Chem. Soc 104, 4014–4015

121 Dawson, R.M.C., Elliott, D.C., Elliott, W.H. and Jones, K.M. (eds.) Data for Biochemical Research (1969) Clarendon Press, Oxford

122 Leigh, J.A. (1983) Appl. Environ. Microbiol. 45, 800–803

123 Kroger, A. and Innerhofer, A. (1976) Eur. J. Biochem. 69, 497–506

124 Hughes, P.E and Tove, S.B. (1982) J. Bacteriol. 151, 1397–1402

125 Kuhn, W. and Gottschalk, G. (1983) Eur. J. Biochem 135, 89–94

126 Widdowson, D. and Anthony, C. (1975) Biochem. J. 152, 349–356

127 Balch, W.E. and Wolfe, R.S. (1979) J. Bacteriol. 137, 256–263

128 Krzycki, J. and Zeikus, J.G. (1980) Curr Microbiol. 3, 243–245

129 Tanner, R.S., Wolfe, R.S. and Ljungdahl, L.G. (1978) J. Bacteriol. 134, 668–670

130 Keltjens, J T., Huberts, M.J., Laarhoven, W.H. and Vogels, G.D. (1983) Eur. J. Biochem. 130, 537–544

131 Keltjens, J.T., Daniels, L., Jannsen, H.G., Borm, P.J. and Vogels, G.D (1983) Eur. J. Biochem. 130, 545–552

132 Leigh, J., Rinehart, K.L. and Wolfe, R.S. (1984) J. Amer. Chem Soc., to be published in Vol. 106

133 Escalante-Semerena, J., Leigh, J. and Wolfe, R.S. (1984) Proceedings of the Fourth International Symposium on Microbial Growth on C-1 Compounds (Hanson, R.S. and Crawford, R.A., eds.), Amer. Soc. Microbiol., Washington, D.C., in the press.

134 Diekert, G., Konheiser, U., Piechulla, K. and Thauer, R.K. (1981) J. Bacteriol. 148, 459–464

135 Taylor, C.D. and Wolfe, R.S. (1974) J. Biol. Chem. 249, 4879–4885

136 Pfaltz, A., Juan, B., Fassler, A., Eschenmoser, A., Jaenchen, R., Gilles, H.-H, Diekert, G. and Thauer, R.K. (1982) Helvet. Chim. Acta 65, 828–865

137 Keltjens, J.T., Caerteling, C.G., Van Kooten, A.M., Van Dijk, H.F and Vogels, G.D. (1983) Biochim. Biophys. Acta 743, 351–358

138 Cheeseman, P., Toms-Wood, A. and Wolfe, R.S. (1972) J. Bacteriol. 112, 527–531

139 Eirich, L.D., Vogels, G.D. and Wolfe, R.S. (1978) Biochemistry 17, 4583–4592

140 Eker, A.P.M., Pol, A., Van der Meijden, P. and Vogels, G.D. (1980) FEMS Microbiol. Lett. 8, 161–165

141 Hemmerich, P., Massey, V. and Fenner, H. (1977) FEBS Lett. 84, 5–21

142 Fisher, J. and Walsh, C., (1974) J. Am. Chem. Soc. 96, 4345–4346

143 Fisher, J., Spencer, R. and Walsh, C. (1976) Biochemistry 15, 1054–1064

144 Walsh, C., Jacobson, F. and Ryerson, C.C. (1980) in Biomimetic Chemistry, Adv. Chem. Ser. 191, 119–138

145 Spencer, R., Fisher, J. and Walsh, C. (1976) Biochemistry 15, 1043–1053

146 Pol, A., Van der Drift, C., Vogels, G.D., Cuppen, T.J.H.M. and Laarhoven, W.H. (1980) Biochem Biophys Res. Commun. 92, 255–260

147 Ashton, W.T., Brown, R.D., Jacobson, F and Walsh, C. (1979) J. Am. Chem. Soc. 79, 4419–4420

148 Ashton, W.T. and Brown, R.D. (1980) J. Heterocycl. Chem. 17, 1709–1712

149 Visser, C M. (1982) Origins Life 12, 165–179

150 Tzeng, S.F., Wolfe, R S. and Bryant, M.P. (1975) J. Bacteriol. 121, 184–191

151 Yamazaki, S and Tsai, L. (1980) J. Biol. Chem. 255, 6462–6465

152 Yamazaki, S. (1982) J. Biol Chem. 257, 7926–7929

153 Yamazaki, S., Tsai, L., Stadtman, T.C., Jacobson, F. and Walsh, C. (1980) J. Biol. Chem. 255, 9025–9027

154 Jones, J.B. and Stadtman, T.C. (1977) J. Bacteriol. 130, 1404–1406

155 Jones, J.B. and Stadtman, T.C. (1980) J Biol. Chem. 255, 1049–1053

156 Jones, J.B. and Stadtman, T.C. (1981) J. Biol. Chem. 256, 656–663

157 Schauer, N.L. and Ferry, J.G. (1982) J. Bacteriol. 150, 1–7

158 Zeikus, J.G., Fuchs, G., Kenealy, W. and Thauer, R K. (1977) J. Bacteriol. 132, 604–613

159 Lancaster, J.R. (1981) Biochem. Biophys. Res. Commun. 100, 240–246

160 Schneider, K. and Schlegel, H.G. (1976) Biochim Biophys. Acta 452, 66–80

161 McKellar, R.C., Shaw, K.M. and Sprott, G.D. (1981) Can. J. Biochem. 59, 83–91

162 Sprott, G.D., McKellar, R.C., Shaw, K.M., Giroux, J. and Martin, W.G. (1979) Can. J. Microbiol. 25, 192–200

163 Barber, M.J., Siegel, L.M., Schauer, N.L., May, H.D. and Ferry, J.G. (1983) J. Biol. Chem. 258, 10839–10845

164 Schauer, N.L. and Ferry, J.G. (1983) J Bacteriol. 155, 467–472

165 McBride, B.C. and Wolfe, R.S. (1971) Biochemistry 10, 2317–2324

166 Sauer, F.D., Bush, R.S., Mahadevan, S. and Erfle, J.D. (1977) Biochem. Biophys. Res. Commun 79, 124–131

167 Hausinger, R.P., Moura, I., Moura, J.J.G., Xavier, A.V., Santos, M.H., LeGall, J. and Howard, J.B. (1982) J. Biol. Chem. 257, 14172–14194

168 Hatchikian, E.C., Bruschi, M., Forget, N. and Scandellari, M. (1982) Biochem. Biophys. Res. Commun. 109, 1316–1323

169 Blaylock, B.A. (1968) Arch. Biochem. Biophys. 124, 314–324

170 Mortenson, L.E., Valentine, R.C. and Carnahan, J.E. (1962) Biochem. Biophys. Res. Commun. 7, 448–452

171 Bachofen, R., Buchanan, B.B. and Arnon, D.I. (1964) Proc. Natl. Acad. Sci. U.S.A 51, 690–694

172 Thauer, R.K., Rupprecht, E. and Jungermann, K. (1970) FEBS Lett. 8, 304–307

173 Yoch, D.C. and Valentine, R.C. (1972) Annu. Rev. Microbiol. 26, 139–162

174 Jungermann, K., Kirchniawy, H. and Thauer, R.K. (1970) Biochem. Biophys. Res. Comm. 41, 682–689

175 Kerscher, L., Nowitzki, S and Osterhelt, D. (1982) Eur. J Biochem. 128, 223–230

176 Kuhn, W., Fiebig, K., Walther, R. and Gottschalk, G. (1979) FEBS Lett. 105, 271–274

177 Fathepure, B.Z. (1983) FEMS Microbiol. Lett. 19, 151–156

178 Taylor, C D. and Wolfe, R.S. (1974) J Biol. Chem. 249, 4886–4890

179 Balch, W.E. and Wolfe, R.S (1979) J. Bacteriol. 137, 264–273

180 Smith, M.R. and Mah, R.A (1981) Curr. Microbiol. 6, 321–326

181 Keltjens, J.T., Whitman, W.B., Caerteling, C.G , Van Kooten, A.M., Wolfe, R.S. and Vogels, G.D. (1982) Biochem. Biophys. Res. Commun. 108, 495–503

182 Van der Meijden, P., Heythuysen, H.J., Sliepenbeek, H.T., Houwen, F.P., Van der Drift, C. and Vogels, G D. (1983) J. Bacteriol. 153, 6–11

183 Shapiro, S. (1982) Can J. Microbiol 28, 629–635

184 Friedrich, W. and Bernhauer, K. (1953) Angew Chem. 65, 627

185 Hollriegl, V., Scherer, P. and Renz, P (1983) FEBS Lett. 151, 156–158

186 Lezius, A.G. and Barker, H.A. (1965) Biochemistry 4, 510–517

187 Pol, A., Van der Drift, C. and Vogels, G.D. (1982) Biochem. Biophys. Res. Commun. 108, 731–737

188 McBride, B.C. and Wolfe, R.S. (1971) Adv. Chem. Ser. 105, 11–22

189 Kenealy, W. and Zeikus, J.G. (1981) J Bacteriol. 146, 133–140

190 Daniels, L. and Zeikus, J.G. (1978) J. Bacteriol 136, 75–84

191 Van Beelen, P., Thiemessen, H.L., DeCock, R.M. and Vogels, G.D. (1983) FEMS Microbiol. Lett. 18, 135–138

192 Gunsalus, R.P. and Wolfe, R.S. (1978) FEMS Microbiol. Lett. 3, 191–193

193 Nagle, D.P. and Wolfe, R.S. (1983) Proc. Natl. Acad. Sci. U.S.A. 80, 2151–2155

194 Diekert, G., Jaenchen, R. and Thauer, R.K. (1980) FEBS Lett. 119, 118–120

195 Whitman, W.B. and Wolfe, R.S. (1980) Biochem. Biophys Res. Commun. 92, 1196–1201

196 Von Fassler, A., Pfaltz, A., Muller, P.M., Farooq, S., Kartky, C., Kräuter, B. and Eschenmoser, A. (1982) Helvet. Chim. Acta 65, 812–827

197 Livingston, D.A., Pfaltz, A., Schreiber, J., Eschenmoser, A., Ankel-Fuchs, D., Moll J., Jaenchen, R. and Thauer, R.K. (1984) Helv. Chim. Acta 67, 334–351

198 Diekert, G., Gilles, H.-H., Jaenchen, R. and Thauer, R.K. (1980) Arch. Microbiol. 128, 256–262

199 Diekert, G., Klee, B. and Thauer, R.K. (1980) Arch. Microbiol. 124, 103–106

200 Jaenchen, R., Diekert, G. and Thauer, R.K. (1981) FEBS Lett. 130, 133–136

201 Jaenchen, R., Gilles, H.-H. and Thauer, R.K. (1981) FEMS Microbiol. Lett. 12, 167–170

202 Gilles, H., Jaenchen, R. and Thauer, R.K. (1983) Arch. Microbiol. 135, 237–240

203 Gilles, H. and Thauer, R K. (1983) Eur. J Biochem 135, 109–112

204 Thauer, R.K. (1982) Zbl. Bakt. Hyg., I. Abt., Orig C. 3, 265–270

205 Ellefson, W.L., Whitman, W.B. and Wolfe, R.S. (1982) Proc. Natl. Acad. Sci. U.S.A. 79, 3707–3710

206 Keltjens, J.T., Caerteling, C.G., Van Kooten, A.M., Van Dijk, H.F. and Vogels, G.D. (1983) Archiv. Biochem. Biophys. 223, 235–253

207 Moura, I., Moura, J.J.G., Santos, H., Xavier, A V., Burch, G., Peck, H.D. and LeGall, J. (1983) Biochim. Biophys. Acta 742, 84–90

208 Kojima, N., Fox. J.A., Hausinger, R.P., Daniels, L., Orme-Johnson, W.H and Walsh, C.T. (1983) Proc. Natl Acad. Sci. U.S.A. 80, 378–382

209 Graf, E.-G., Thauer, R.K. (1981) FEBS Lett. 136, 165–169

210 Lancaster, J.R. (1982) Science 216, 1324–1325

211 LeGall, J., Ljungdahl, P O., Moura, I., Peck, H.D., Xavier, A.V., Moura, J.J.G., Teixera, M., Huynh, B.H. and DerVartanian, D.V. (1982) Biochem. Biophys Res. Commun. 106, 610–616

212 Friedrich, C.G., Schneider, K and Friedrich, B. (1982) J. Bacteriol. 152, 42–48

213 Thauer, R.K., Diekert, G. and Schonheit, P. (1980) Trends Biochem. Sci. 5, 304–306

214 Diekert, G.B., Graf, E.G. and Thauer, R.K. (1979) Arch. Microbiol. 122, 117–120

215 Drake, H.L. (1982) J. Bacteriol. 149, 561–566

216 Dixon, N.E., Gazzola, C., Blakeley, R.L. and Zerner, B (1975) J. Am. Chem. Soc. 97, 4131–4133

217 Thauer, R.K. (1983) Proceedings of the 4th International Symposium on Microbial Growth on C-1 Compounds (Hanson, R.S. and Crawford, R.A., eds.), Am. Soc. Microbiol., Washington DC, in the press

218 Kanodia, S. and Roberts, M.F. (1983) Proc. Natl. Acad. Sci. U.S.A. 80, 5217–5221

218 a. Seeley, R J. and Fahrney, D.E. (1983) J. Biol. Chem. 258, 10, 835–838

219 McKellar, R.C. and Sprott, G.D. (1979) J. Bacteriol. 139, 231–238

220 Fuchs, G., Moll, J., Scherer, P. and Thauer, R.K. (1978) in Hydrogenases, their catalytic activity, structure and function (Schlegel, H.G. and Schneider, K., eds.), pp 83–92, E. Goltze, Gottingen

221 LeGall, J., Moura, J.J.G., Peck, H.D. and Xavier, A.V. (1982) in Iron Sulfur Proteins, Vol. 4 (Spiro, T.G., ed.), pp. 177–248, John Wiley and Sons, New York

222 Cammack, R., Patil, D., Aguirre, R. and Hatchikian, E.C. (1982) FEBS Lett. 142, 289–292

223 Moura, J.J.G., Moura, I., Huynh, B.H , Kruger, H.J., Teixeira, M., DuVarney, R.C., Der Vartanian, D.V., Xavier, A.V., Peck, H.D. and LeGall, J. (1982) Biochem Biophys. Res. Commun. 108, 1388–1393

224 Friedrich, B., Heine, E., Finck, A. and Friedrich, C.G. (1981) J. Bacteriol. 145, 1144–1149

225 Albracht, S.P.J., Kalkman, M.L. and Slater, E.C. (1983) Biochim. Biophys. Acta 724, 309–316

226 Lancaster, J.R. (1980) FEBS Lett. 115, 285–288

227 Brandis, A., Thauer, R.K and Stetter, K.O (1981) Zbl. Bakt. Hyg., I. Abt, Orig. C 2, 311–317

228 Albracht, S.P.J., Graf, E.G. and Thauer, R.K. (1982) FEBS Lett. 140, 311–313

229 Adams, M.W.W., Mortenson, L.E. and Chen, J S. (1981) Biochim. Biophys. Acta 594, 105–176

230 Jin, S.-L C., Blanchard, D.K. and Chen, J.-S. (1983) Biochim. Biophys. Acta 748, 8–20

231 Doddema, H.J., Van der Drift, C., Vogels, G.D. and Veenhuis, M. (1979) J. Bacteriol. 140, 1081–1089

232 Thauer, R.K., Fuchs, G. and Jungermann, K. (1977) in Iron-Sulfur proteins (Lovenberg, W., ed.), Vol III, pp 122–156, Academic Press, New York

233 Ljungdahl, L.G. (1980) in Molybdenum Chemistry of Biological Significance (Newton, W.E. and Sei Otsuka, eds.), pp. 129–137, Plenum Press, New York

234 Schauer, N.L. and Ferry, J.G. (1980) J. Bacteriol. 142, 800–807

235 Johnson, J.L., Hainline, B.E. and Rajagopalan, K.V. (1980) J. Biol. Chem. 255, 1783–1786

236 Wood, J.M., Moura, I., Moura, J J.G., Santos, M.H., Xavier, A.V., LeGall, J. and Scandellari, M. (1982) Science 216, 303–305

237 Drake, H.L., Hu, S.-I. and Wood, H.G. (1981) J. Biol. Chem. 256, 11137–11144

238 Schrauzer, G.N., Grate, J H. and Katz, R.N. (1978) Bioinorg Chem. 8, 1–10

239 Blaylock, B.A. and Stadtman, T.C. (1964) Biochem. Biophys. Res. Commun. 17, 475–480

240 Shapiro, S. and Wolfe, R.S. (1980) J. Bacteriol. 141, 728–734

241 Shapiro, S. (1982) Can. J. Microbiol. 28, 1409–1411

242 Van der Meijden, P., Heythuysen, H.J., Pouwels, A., Houwen, F., Van der Drift, C. and Vogels, G.D. (1983) Arch. Microbiol. 134, 238–242

243 Kuno, S., Toraya, T. and Fukui, S. (1981) Arch. Biochem. Biophys. 211, 722–730

244 Van der Meijden, P., Jansen, L.P.J.M., Van der Drift, C. and Vogels, G.D. (1983) FEMS Microbiol. Lett. 19, 247–251

245 Perski, H.J., Moll, J. and Thauer, R.K. (1981) Arch. Microbiol. 130, 319–321

246 Perski, H.J., Schonheit, P. and Thauer, R K. (1982) FEBS Lett. 143, 323–326

247 Kim, Y.M. and Hegeman, G.D. (1981) J. Bacteriol. 148, 904–911

248 Hegeman, G. (1980) Trends Biochem. Sci. 5, 256–259

249 Kerby, R and Zeikus, J.G. (1983) Curr. Microbiol. 8, 27–30

250 Lynd, L., Kerby, R. and Zeikus, J.G. (1982) J. Bacteriol. 149, 255–263

251 Genthner, B.R.S. and Bryant, M.P. (1982) Appl. Environ. Microbiol. 43, 70–74

252 Yamazaki, S., Tsai, L. and Stadtman, T.C. (1982) Biochem. 21, 934–939

253 Vogels, G.D. and Visser, C.M. (1983) FEMS Microbiol. Lett. 20, 291–297

254 Kates, M., Yangoyan, L.S. and Sastry, P.S. (1965) Biochim. Biophys. Acta 98, 252–268

255 Langworthy, T.A. (1972) J. Bacteriol. 112, 1193–1200

256 Langworthy, T.A., Mayberry, W.R. and Smith, P.F. (1974) J. Bacteriol. 119, 106–116

257 Kates, M., Kushwaha, S.C and Sprott, G.D. (1982) Methods Enzymol. 88, 98–111

258 Langworthy, T.A., Tornabene, T.G. and Holzer, G. (1982) Zbl. Bakt. Hyg., I. Abt., Orig. C 3, 228–244

259 Sowers, K.R. and Ferry, J.G. (1983) Appl. Environ. Microbiol. 45, 684–690

260 Comita, P.B. and Gagosian, R.B. (1983) Science 222, 1329–1331

261 Bligh, E.G. and Dyer, W.J. (1959) Can. J. Physiol. 37, 911–917

262 Kushwaha, S.C., Kates, M., Sprott, G.D. and Smith, I C.P. (1981) Science 211, 1163–1164

263 Kushwaha, S.C., Kates, M., Sprott, G.D. and Smith, I.C.P. (1981) Biochim. Biophys. Acta 664, 156–173

264 Ekiel, I., Smith, I.C.P. and Sprott, G.D. (1983) J. Bacteriol. 156, 316–325

265 Tornabene, T.G., Kates, M., Gelpi, E. and Oro, J. (1969) J. Lipid Res. 10, 294–303

266 Sprott, G.D., Colvin, J.R. and McKellar, R.C. (1979) Can. J. Microbiol. 25, 730–738

267 Sprott, G.D., Shaw, K.M. and Jarrell, K.F (1983) J. Biol. Chem. 258, 4026–4031

268 Jarrell, K.F., Colvin, J.R. and Sprott, G.D. (1982) J. Bacteriol. 149, 346–353

269 Roberton, A.M. and Wolfe, R S. (1969) Biochim. Biophys. Acta 192, 420–429

270 Roberton, A.M. and Wolfe, R.S. (1970) J. Bacteriol. 102, 43–51

271 Conklin, A.R. and MacGregor, A.N. (1972) Bull. Environ. Contamin. and Toxicol. 7, 296–300

272 Ramirez, F., Marecek, J.F. and Szamosi, J. (1980) J Org. Chem. 45, 4748–4752

273 Whitman, W.B. and Wolfe, R.S. (1983) J. Bacteriol. 154, 640–649

274 Fuchs, G. and Stupperich, E. (1978) Arch. Microbiol. 118, 121–125

275 Fuchs, G., Stupperich, E. and Thauer, R K. (1978) Arch. Microbiol. 117, 61–66

276 Fuchs, G. and Stupperich, E. (1980) Arch. Microbiol. 127, 267–272

277 Fuchs, G. and Stupperich, E. (1982) Zbl. Bakt. Hyg., I. Abt., Orig. C 3, 277–288

278 Kenealy, W.R. and Zeikus, J.G. (1982) FEMS Microbiol. Lett. 14, 7–10

279 Jansen, K., Stupperich, E. and Fuchs, G. (1982) Arch. Microbiol. 132, 355–364

280 Storer, A.C., Sprott, G.D. and Martin, W.G. (1981) Biochem. J. 193, 235–244

281 Balch, W.E., Schoberth, S., Tanner, R.S. and Wolfe, R.S. (1977) Int. J. Syst. Bacteriol. 27, 355–361

282 Braun, M. and Gottschalk, G. (1982) Zbl. Bakt. Hyg., I Abt., Orig. C 3, 368–376

283 Wiegel, J., Braun, M. and Gottschalk, G. (1981) Curr. Microbiol. 5, 255–260

284 Eden, G. and Fuchs, G. (1982) Arch. Microbiol. 133, 66–74

285 Eden, G. and Fuchs, G. (1983) Arch. Microbiol. 135, 68–73
286 Bakhiet, N., Forney, F.W., Stahly, D.P. and Daniels, L (1984) Curr. Microbiol 10,195–198
287 Eikmanns, B., Linder, D. and Thauer, R.K. (1983) Arch. Microbiol. 136, 111–113
288 Ekiel, I., Smith, I.C.P. and Sprott, G.D (1984) Biochemistry 23, 1683–1687
289 Eikmanns, B., Jaenchen, R. and Thauer, R.K. (1983) Arch. Microbiol. 136, 106–110
290 Whitman, W.B., Ankawanda, E. and Wolfe, R.S. (1982) J. Bacteriol. 149, 852–863
291 Taylor, G.T. and Pirt, S.J. (1977) Arch. Microbiol. 113, 17–22
292 Zehnder, A.J.B., Huser, B.A., Brock, T.D. and Wuhrmann, K. (1980) Arch. Microbiol. 124, 1–11
293 Smith, M.R. and Mah, R.A. (1978) Appl. Environ. Microbiol. 36, 870–879
294 Smith, M.R. and Mah, R.A. (1980) Appl. Environ. Microbiol. 39, 993–999
295 Stadtman, T.C. (1967) Annu. Rev. Microbiol. 21, 121–142
296 Hippe, H., Caspari, D., Fiebig, K. and Gottschalk, G. (1979) Proc. Natl. Acad. Sci. U.S.A. 76, 494–498
297 Chua, H.B. and Robinson, J.P. (1983) Arch. Microbiol. 135, 158–160
298 Ferguson, T.J. and Mah, R.H. (1983) Appl. Environ. Microbiol. 45, 265–274
299 Stouthamer, A.H. (1973) Anton. Leeuwenhoek 39, 545–565
300 Mitchell, P. (1966) Biol. Rev. 41, 445–502
301 Mitchell, W.J., Booth, I.R. and Hamilton, W.A. (1979) Biochem. J. 184, 441–449
302 Green, D.E. and Van de Zande, H.D. (1981) Proc. Natl. Acad. Sci. U.S.A., 78, 5344–5347
303 Haddock, B.A. and Jones, C.W. (1977) Bacteriol. Rev. 41, 47–99
304 Padan, E., Zilberstein, D. and Schuldiner, S. (1981) Biochim. Biophys. Acta 650, 151–166
305 Williams, R.J.P. (1972) Biochem. Soc. Trans. 5, 29–32
306 Williams, R.J.P. (1978) Biochim. Biophys. Acta 505, 1–44
307 Kell, D.B. and Morris, J.G. (1979) FEBS Lett. 108, 481–484
308 Skulachev, V.P. (1982) FEBS Lett. 146, 1–4
309 Westerhoff, H.V. (1983) Trends Biochem. Sci. 8, 77
310 Robertson, R.N. and Boardman, N.K. (1975) FEBS Lett. 60, 1–6
311 Jarrell, K.F. and Sprott, G.D. (1983) Biochim. Biophys. Acta 725, 280–288
312 Jarrell, K.F. and Sprott, G.D. (1981) Can. J. Microbiol. 27, 720–728
313 Rottenberg, H. (1975) Bioenergetics 7, 61–74
314 Rottenberg, H. (1979) Methods. Enzymol. 55, 547–569
315 Friedberg, I. and Kaback, H.R. (1980) J. Bacteriol. 142, 651–658
316 Zilberstein, D., Schuldiner, S. and Kaback, H.R. (1979) Biochemistry 18, 669–673
317 Kashket, E.R. (1981) J. Bacteriol. 146, 369–376
318 Kashket, E.R. (1981) J. Bacteriol. 146, 377–384
319 Riebeling, V., Thauer, R.K. and Jungermann, K. (1975) Eur. J. Biochem. 55, 445–453
320 Sprott, G.D and Jarrell, K.F. (1984) in Microbial Chemoautotrophy (Strohl, W.R. and Tuovinen, O.H., eds.), pp. 255–273, Ohio State University Press, Columbus
321 Jarrell, K.F. and Sprott, G.D (1983) Arch. Biochem Biophys 225, 33–41
322 Sauer, F.D., Mahadevan, S. and Erfle, J.D. (1980) Biochem. Biophys. Res. Comm. 95, 715–721
323 Bakker, E.P., Rottenberg, J. and Caplan, S.R. (1976) Biochim Biophys. Acta 440, 557–572
324 Butsch, B. and Bachofen, R. (1982) Experientia 38, 1377
325 Michel, H. and Osterhelt, D. (1980) Biochemistry 19, 4607–4614
326 Michel, H. and Osterhelt, D. (1980) Biochemistry 19, 4615–4619
327 Hsung, J.C. and Haug, A. (1977) FEBS Lett. 73, 47–50
328 Zeikus, J.G. and Wolfe, R.S. (1973) J. Bacteriol. 113, 461–467
329 Kell, D.B., Doddema, H.J., Morris, J.G. and Vogels, G.D (1981) in Proceedings of the Third International Symposium on Microbial Growth on C-1 Compounds (Dalton, H., ed.), pp. 159–170, Heyden & Sons Ltd., London
330 Sprott, G.D., Sowden, L.C., Colvin, J.R., Jarrell, K.F. and Beveridge, T.J. (1984) Can. J. Microbiol. 30, 594–604
331 Sauer, F.D., Erfle, J.D. and Mahadevan, S. (1980) Biochem. J 190, 177–182
332 Langenberg, K.F., Bryant, M.P. and Wolfe, R S (1968) J. Bacteriol. 95, 1124–1129
333 Zeikus, J.G. and Bowen, V.G. (1975) Can. J. Microbiol. 21, 121–129
334 Nanninger, N. (1971) J. Cell. Biol. 48, 219–224
335 Higgins, M.L., Isien, H C. and Daneo-Moore, L. (1976) J. Bacteriol. 127, 1519–1523
336 Higgins, M.L., Parks, L.C. and Daneo-Moore, L (1981) in Organization of Prokaryotic Cell Membranes, Vol. II (Gosh, B.K., ed.), pp. 75–94, CRC Press, Boca Raton, FL
337 Zhilina, T.N. and Zavarzin, G.A. (1979) Mikrobiol. 48, 279–285
338 Sprott, G.D., Jarrell, K.F., Shaw, K.M. and Knowles, R. (1982) J. Gen. Microbiol. 128, 2453–2462
339 Gunnarsson, L.A.H. and Ronnow, P.H. (1982) FEMS Microbiol. Lett. 14, 317–320
340 Sprott, G.D., Dimock, K., Martin, W G. and Schneider, H. (1975) J. Bacteriol. 123, 828–836
341 Schultz, S.G., Norman, N.L. and Epstein, W. (1962) J. Gen. Physiol. 46, 159–165
342 Ginsburg, M., Sachs, L. and Ginzburg, B.Z. (1970) J. Gen. Physiol. 55, 187–207
343 Matheson, A.T., Sprott, G.D., McDonald, I.J. and Tessier, H. (1976) Can. J. Microbiol. 22, 780–786
344 Christian, J.H.B. and Waltho, J.A. (1962) Biochim. Biophys. Acta 65, 506–508
345 Gober, J.W. and Kashket, E.R. (1983) J. Bacteriol. 153, 1196–1201
346 Bellion, E., Alikhan, M.Y. and Romano, M.J. (1980) J. Bacteriol. 142, 786–790
347 Bryant, M.P., Tzeng, S.F., Robinson, I.M. and Joyner, A.E., Jr. (1971) Advances in Chem. Series, No. 105, Anaerobic Biological Treatment Processes, pp. 23–40

348 Huster, R. and Thauer, R.K. (1983) FEMS Microbiol. Lett 19, 207–209

349 Schonheit, P., Moll, J. and Thauer, R.K. (1979) Arch. Microbiol. 123, 105–107

350 Jarrell, K.F. and Sprott, G.D. (1982) J. Bacteriol. 151, 1195–1203

351 Jarrell, K.F., Bird, S.E. and Sprott, G.D. (1984) FEBS Lett. 166, 357–361

352 Fox, G.D., Magrum, L.J., Balch, W.E., Wolfe, R S. and Woese, C.R. (1977) Proc. Natl. Acad. Sci. U.S.A 74, 4537–4541

353 Winkler, H.H. (1976) J. Bacteriol. 251, 389–396

354 Doddema, H.J., Claesen, C.A., Kell, D.B., Van der Drift, C. and Vogels, G.D. (1980) Biochem. Biophys. Res. Commun. 95, 1288–1293

355 Mountfort, D.O. and Asher, R.A. (1979) Appl Environ. Microbiol. 37, 670–675

356 Wood, J.M., Kennedy, F.S. and Wolfe, R.S. (1968) Biochemistry 7, 1707–1743

357 Sprott, G.D. and Jarrell, K.F (1982) Can. J. Microbiol. 28, 982–986

358 Heytler, P.G. (1963) Biochemistry 2, 357–361

359 Gow, J.A., MacLeod, R.A., Goodbody, M., Frank, D. and DeVoe, L (1980) Can. J. Microbiol. 27, 350–357

360 Morishita, H. and Takada, H. (1976) Can. J. Microbiol. 22, 1263–1268

361 Rüger, H. and Hentzschel, G. (1980) Arch. Microbiol. 126, 83–86

362 Brown, A.D. (1976) Bacteriol. Rev. 40, 803–846

363 Patel, G.B. and Roth, L.A. (1977) Can. J. Microbiol. 23, 893–897

364 Kodama, T. and Taniguchi, S. (1976) J. Gen. Microbiol. 96, 17–24

365 Kodama, T. and Taniguchi, S. (1977) J. Gen. Microbiol. 98, 503–510

366 Niven, D.F. and MacLeod, R.A. (1978) J. Bacteriol. 134, 737–743

367 Dimroth, P. (1980) FEBS Lett. 122, 234–236

368 Hilpert, W. and Dimroth, P. (1982) Nature 296, 584–585

369 Tokuda, H. and Unemoto, T. (1982) J. Biol. Chem. 257, 10007–10014

370 Benyoucef, M., Rigaud, J.-L. and Leblanc, G. (1982) Biochem. J. 208, 539–547

371 Jinks, D.C., Silvius, J.R. and McElhaney, R.N. (1978) Bacteriol. 136, 1027–1036

372 Heefner, D.L. (1982) Mol Cell. Biochem 44, 81–106

373 Kell, D.B. (1979) Biochim. Biophys Acta 549, 55–99

374 Haines, T.H. (1983) Proc. Natl. Acad. Sci. U S.A. 80, 160–164

375 Harold, F.M. (1972) Bacteriol. Rev. 36, 172–230

376 Sedgwick, E.G. and MacLeod, R.A. (1980) Can. J. Biochem. 58, 1206–1214

377 Sorenson, E.N. and Rosen, B.P. (1980) Biochemistry 19, 1458–1462

378 Zehnder, A.J.B. and Brock, T.D. (1979) FEBS Lett. 107, 1–3

379 Daniels, L., Sparling, R., Wessels, D. and Belay, N. (1983) Annu. Meet. Am Soc. Microbiol. 198

380 Romesser, J. (1978) Ph.D. Thesis, University of Illinois

381 Baresi, L and Bertani, G. (1983) Abstr. Annu. Mett. Am. Soc. Microbiol. 142

382 Tanner, R.S. (1982) Ph.D. Thesis, University of Illinois

383 Jacobson, F. (1981) Ph.D. Thesis, MIT, Cambridge, MA

384 Escalante-Semerena, J. (1983) Ph.D. Thesis, University of Illinois

385 McBride, B.M. (1970) Ph.D. Thesis, University of Illinois

386 Daniels, L. and Zeikus, J.G. (1976) Annu. Meet. Am. Soc. Microbiol. 121

387 Doddema, H.J. (1980) Ph.D. Thesis, University of Nijmegen, The Netherlands

388 Daniels, L. (1975) M.Sc. Thesis, University of Wisconsin

389 Kristjansson, H., Ponnamperuma, C.P. and Hochstein, L.I. (1983) Abstr. ASM 83rd Annu. Meet. (New Orleans) 198

390 Perski, H.J. (1982) Ph.D. Thesis, University of Marburg

391 Van Beelen, P., Stassen, A.P.M., Bosch, J.W.G., Vogels, G.D., Guijt, W. and Haasnoot, C.A.G. (1984) Eur. J. Biochem. 138, 563–571

392 Tanner, R.S. (1983) Ph.D. Thesis, University of Illinois

Biochimica et Biophysica Acta, 768 (1984) 164–200
Elsevier

BBA 86111

THE *UNC* OPERON

NUCLEOTIDE SEQUENCE, REGULATION AND STRUCTURE OF ATP-SYNTHASE

JOHN E. WALKER, MATTI SARASTE * and NICHOLAS J. GAY

Laboratory of Molecular Biology, The Medical Research Council Centre, Hills Road, Cambridge CB2 2QH (U.K.)

(Received November 1st, 1982)

Contents

I Introduction 165

II Nucleotide sequence 166

III Interpretation of the DNA sequence 170
- A. Identification of genes 171
- B. Translational signals 174
  - 1. Initiation 174
  - 2. Termination 176
- C. Transcriptional signals 176
  - 1. The *unc* promoter 176
  - 2. Internal promoters 176
  - 3. Transcription terminator 176
  - 4. Intercistronic sequences 176

IV Regulation of the *unc* operon 178
- A. Transcription regulation of the *unc* operon 178
- B. Uncoordinacy 179

V Interpretation of protein sequences 183
- A. F_0 subunits 185
  - 1. Subunit *a* 185
  - 2. Subunit *c* 186
  - 3. Subunit *b* 187

---

* Present address: Department of Medical Chemistry, University of Helsinki, Helsinki, Finland.

Abbreviations: H^+-ATPase, H^+ translocating ATPase complex or ATP-synthase; F_1, extrinsic membrane sector of H^+-ATPase; F_0, intrinsic membrane sector of H^+-ATPase; oscp, oligomycin sensitivity conferral protein; DCCD, *N,N'*-dicyclohexylcarbodiimide.

The *unc* operon has also been renamed the *atp* operon. This name has a number of advantages; for instance, mutations in gene 1 are not uncoupled. This may also apply to mutations in the δ subunit, since no mutants in the gene for this subunit have been detected by lack of growth on succinate. The alternative name *pap* has also been suggested. However, despite its limitations, *unc* is widely recognised, and so for historical reasons we have preferred it in this review. Where possible, we have attempted to avoid the use of *unc*B, etc. to describe the genes, preferring to use terms such as 'the gene for the β subunit' as this causes fewer difficulties of understanding to the non-specialist in this area.

Abbreviation: oscp, oligomycin sensitivity conferral protein.

0005-2728/84/$03.00 © 1984 Elsevier Science Publishers B.V.

B. F_1 subunits 188
   1. α and β subunits 189
   2. γ, δ and ε subunits 194
   3. Subunit equivalence 194
C. Assembly 194
   1. Gene order and assembly of ATP-synthase 194
   2. Does gene 1 product influence assembly? 197

VI Conclusions and future prospects 198

Acknowledgements 198

References 198

I. Introduction

Bacterial proton translocating ATP-synthase couples the electrochemical potential difference for H^+ across the cytoplasmic membrane to synthesis of ATP from ADP and P_i [1,2]. It also functions in the reverse direction by coupling hydrolysis of ATP to proton translocation across the membrane in the outward direction, thereby generating an electrochemical membrane potential essential for driving other cellular functions (e.g., transport and motility). The enzyme is bound to the inner membrane of *Escherichia coli.* As depicted in Fig. 1, it is made of two sectors, commonly called F_1 and F_0. F_1 is an ATPase. It is on the cytoplasmic surface of the membrane, from which it can be easily dislodged. F_0, the membrane sector, contains a transmembrane proton channel. F_1 is composed of five different polypeptides α, β, γ, δ and ε assembled with stoichiometries of $3\alpha:3\beta:1\gamma:1\delta:1\varepsilon$ [3,4]. F_0 comprises three proteins, a, b and c. A range of stoichiometries has been proposed (see Ref. 4). A recent estimate is 1a : 2b : 10c [5].

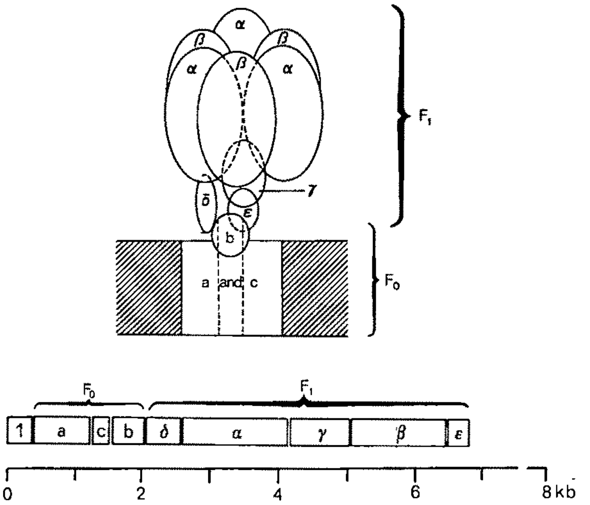

Fig. 1. Arrangement of subunits in the *E. coli* H^+-ATPase complex: (adapted from Ref. 86) δ and ε are both required for binding α, β, γ to F_0 [125]. δ interacts with the N-terminal region of α [90]. Subunit b provides a highly charged membrane-bound α-helical structure to which F_1 may bind via ionic interactions [24,35,83]. Both a and c are essential components of the proton channel [118] (dashed) through the lipid bilayer (hatched). The number of copies of a, b and c in the complex is not firmly established but may be 1a : 2b : 10c [4,5].

Mitochondria and chloroplasts also contain proton-translocating F_1F_0 ATP-synthases with many structural features in common with the bacterial enzyme (for reviews see Refs. 6–8). However, the mitochondrial enzyme is more complex than the bacterial one. A number of extra subunits have been characterised; a protein inhibitor binds to the F_1 portion and at least two extra subunits are associated with F_0, the oligomycin sensitivity conferral protein (oscp) [9–12] and factor 6 (F_6) [13]. The genetics of the *E. coli* enzyme have been investigated for more than a decade (for recent accounts see Gibson [14,15] and Fillingame [4]). Mutants with defects in the enzyme have been selected by lack of growth on nonfermentable carbon sources such as succinate. Some 40% respire normally but are unable to couple oxidation of respiratory substrates to phosphorylation. They are uncoupled and the phenotype has been called *unc.* All mutants mapped at around 83 min between the loci *bgl*R and *asn* on the linkage map of *E. coli* [16]. Seven complementation groups A, B, C, D, E, F and G were defined. By complementation analysis of *unc* mutants induced by bacteriophage Mu17, the known *unc* genes were proposed to be in a single transcriptional unit (or operon) read in the order B(E, F)AGDC in the direction *asn* to *bgl* [14,15,17]. Gene-product relationships have been established for *unc*B = Δ, *unc*A = α, *unc*G = γ, *unc*D = β and *unc*C = ε [14,15,18,19].

In the course of studies of the origin of replication *ori*C of *E. coli*, a λ-transducing phage λ*Asn*5 was isolated that contained a region of the bacterial chromosome including the *unc* locus [20]. Restriction analysis of this region was performed by a number of workers [21,22]. This has enabled restriction fragments from the *unc* locus to be cloned into plasmids and into bacteriophage M13 [23–25] and has facilitated the DNA sequence analysis of this part of the bacterial chromosome.

This review describes the DNA sequence of the *unc* operon and its interpretation. It discusses how the major features of the operon (the promoter, the genes) have been identified and how the operon may be regulated. The protein sequences of the individual proteins are examined in detail and provide many clues to the structure and function of the enzyme complex.

II. Nucleotide sequence

A key to the rapid determination of the DNA sequence of the *unc* operon was the availability of a transducing phage λ*Asn*5 containing a segment of about 30 kb of the *E. coli* chromosome including the *unc* locus (Fig. 2). Restriction analysis coupled with genetic analysis had indicated that the operon would lie at least in part in two adjacent *Eco*RI fragments R_1 and R_2, 2.5 and 4.5 kb in length, respectively. These fragments were recloned, giving rise to plasmids pNR_1 and pNR_2, and sequenced by the combined M13 cloning dideoxy DNA sequencing method [23–25]. Other relevant fragments of λ*Asn*5 were cloned directly into M13 and similarly sequenced. These experiments are summarised in Fig. 2c. Parts of sequence have also been sequenced independently by the chemical sequencing method. The sequence of Nielsen et al. [26] covering bases 870–3370 (Fig. 3) agrees exactly with that presented here. Futai and coworkers [27–31] have presented sequences covering most of the operon. Major discrepancies have been noted, particularly in the regions of gene 1, protein a, in the γ subunit and between α and γ genes. In the first two, Futai has published revised se-

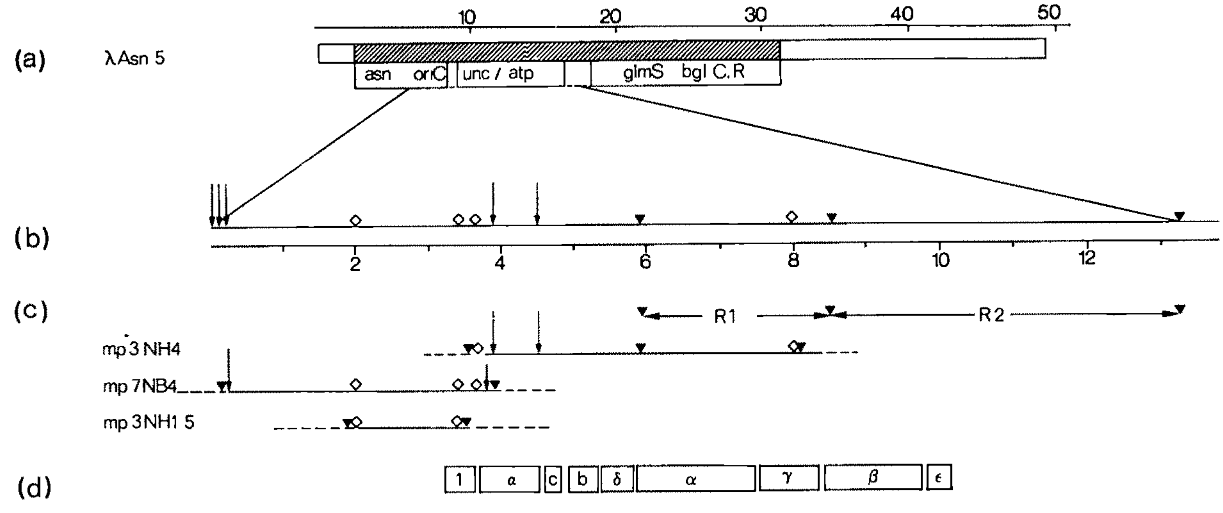

Fig. 2. Genetic and physical maps of the *E. coli* chromosome in the vicinity of the *unc* operon. (a) The extent of the *E coli* chromosome (hatched) in λ*Asn*5 showing genetic markers. The scale is in kilobases. (b) Restriction map of part of this region redrawn from Ref. 85. Arrows denote restriction sites for *Bam*HI, *Eco*RI (▼) and *Hin*dIII (◇). (c) Alignment of EcoRI fragments R_1 and R_2 and primary fragments used for sequence analysis in clones mp3·NH_4, mp7·NB4 and mp3·NH1·5 (d) Alignment of the nine genes of the *unc* operon with restriction map. Transcription is from left to right.

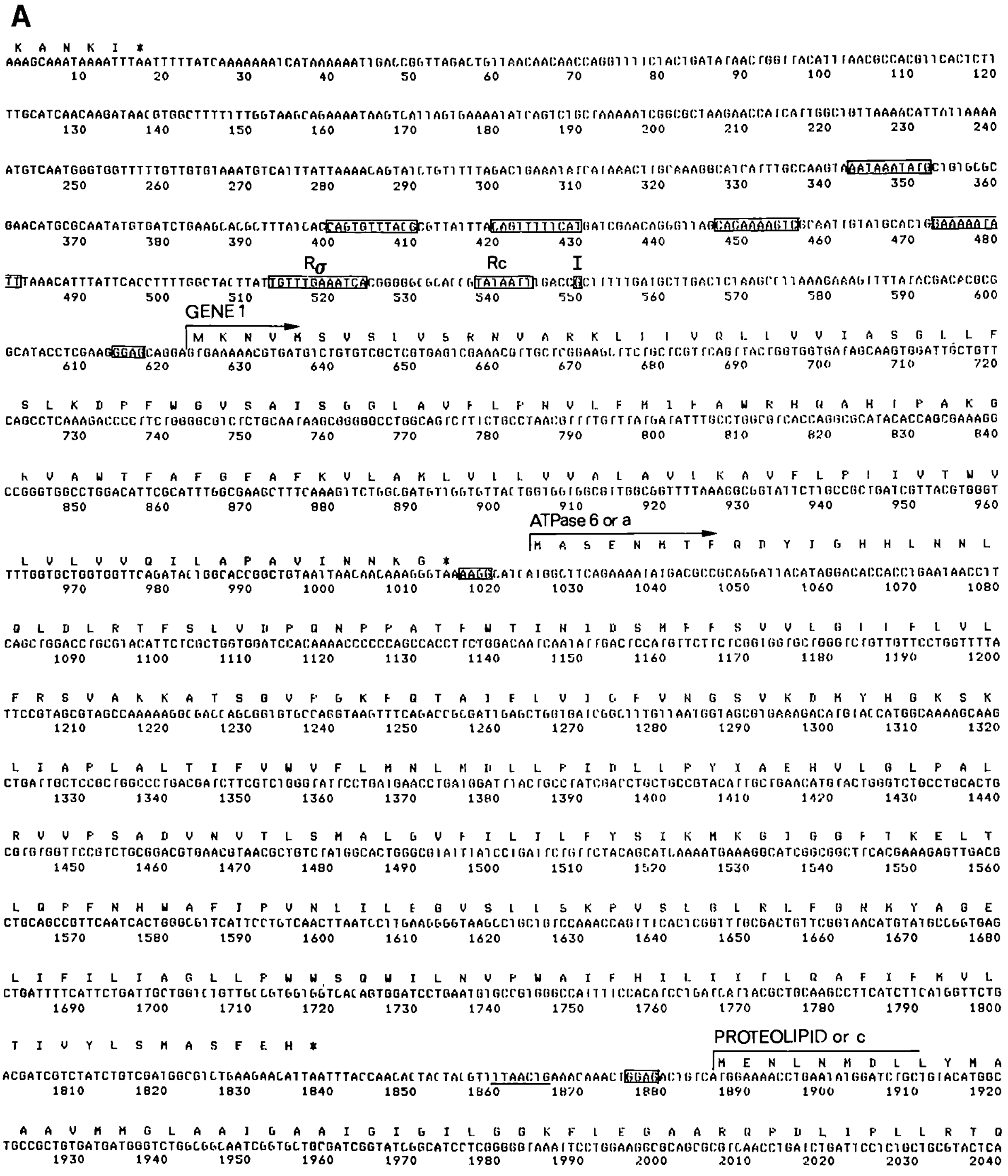

Fig. 3. Nucleotide sequence of the *unc* operon. The sequence is that described in the text it differs from this sequence in one position; an additional c residue is added at nucleotide 7492. The numerous discrepancies between this and those described by Futai and colleagues [27–33] have been annotated in Ref. 34 with experimental evidence in each case to support the sequence described here.

quences, now in broad agreement with those presented here [32,33]. although many minor, single base differences still exist. These differences have been annotated, and detailed experimental data for each difference has been presented that justify the sequence in Fig. 3 [34]. The sequence in this

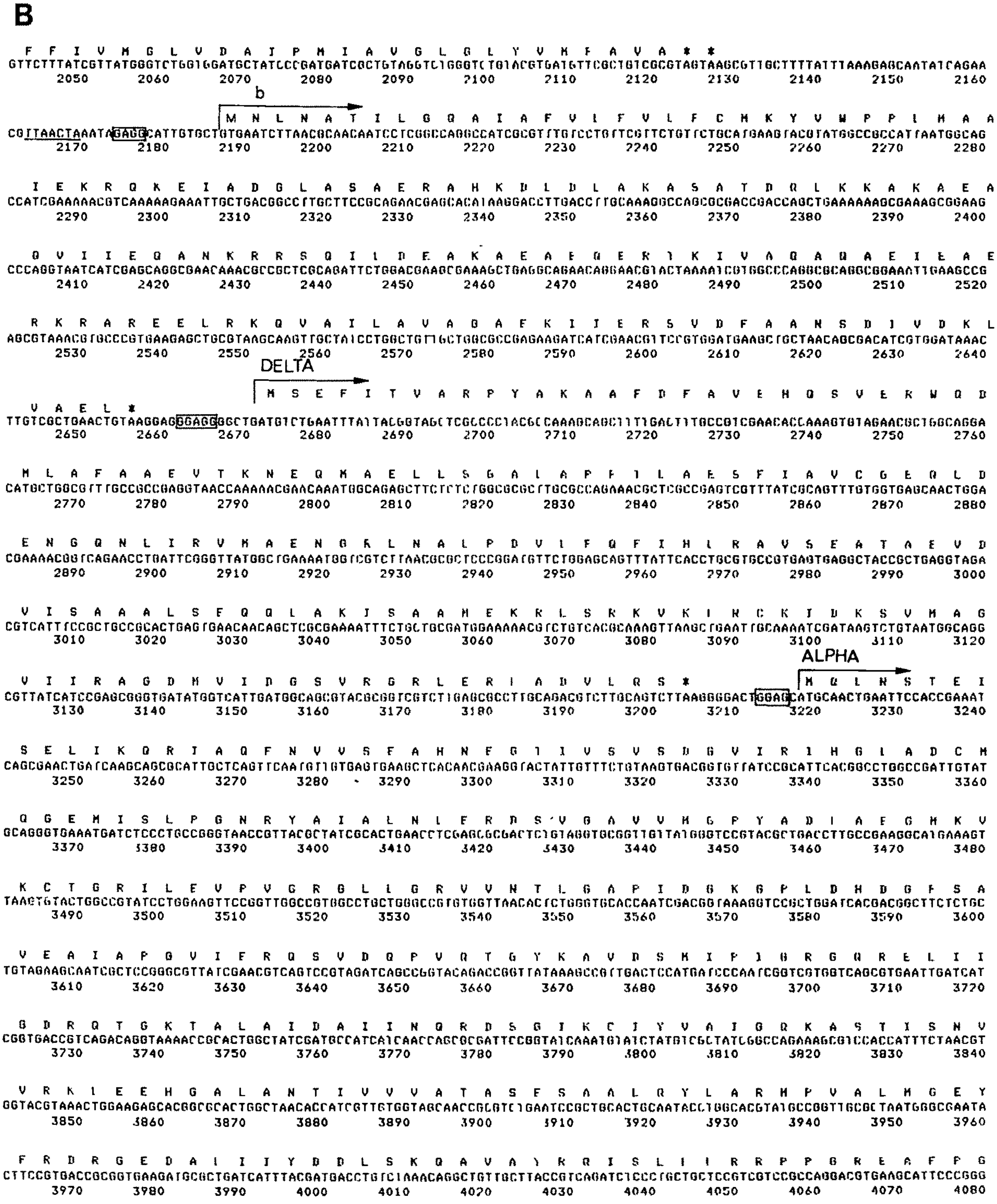

C

```
  D  V  F  Y  L  H  S  R  L  L  E  R  A  A  R  V  N  A  E  Y  V  E  A  F  T  K  G  E  V  K  G  K  T  G  S  L  T  A  L  P
CGACGTTTTCTACCTCCACTCTCGTCTGCTGGAGCGTGCTGCACGTGTTAACGCCGAATACGTTGAAGCCTTCACCAAAGGTGAAGTGAAAGGGAAAACCGGTTCTCTGACCGCACTGCC
      4090      4100      4110      4120      4130      4140      4150      4160      4170      4180      4190      4200

  I  I  E  T  Q  A  G  D  V  S  A  F  V  P  T  N  V  I  S  I  T  D  G  Q  I  F  L  E  T  N  L  F  N  A  G  I  R  P  A  V
GATTATCGAAACTCAGGCGGGTGACGTTTCTGCGTTCGTTCCGACCAACGTAATCTCCATTACCGATGGTCAGATCTTCCTGGAAACCAACCTGTTCAACGCCGGTATTCGTCCTGCGGT
      4210      4220      4230      4240      4250      4260      4270      4280      4290      4300      4310      4320

  N  P  G  I  S  V  S  R  V  G  G  A  A  Q  T  K  I  M  K  K  L  S  G  G  I  R  T  A  L  A  Q  Y  R  E  L  A  A  F  S  Q
TAACCCGGGTATTTCCGTATCCCGTGTTGGTGGTGCAGCACAGACCAAGATCATGAAAAAACTGTCCGGTGGTATCCGTACCGCTCTGGCACAGTATCGTGAACTGGCAGCGTTCTCTCA
      4330      4340      4350      4360      4370      4380      4390      4400      4410      4420      4430      4440

  F  A  S  D  L  D  D  A  T  R  K  Q  L  D  H  G  Q  K  V  T  E  L  L  K  Q  K  Q  Y  A  P  M  S  V  A  Q  Q  S  L  V  L
GTTTGCATCCGACCTTGACGATGCAACACGTAAGCAGCTTGACCACGGTCAGAAAGTGACCGAACTGCTGAAACAGAAACAGTATGCGCCGATGTCCGTTGCGCAGCAGTCTCTGGTTCT
      4450      4460      4470      4480      4490      4500      4510      4520      4530      4540      4550      4560

  F  A  A  E  R  G  Y  L  A  D  V  E  L  S  K  I  G  S  F  E  A  A  L  L  A  Y  V  D  R  D  H  A  P  M  M  Q  E  I  N  Q
GTTCGCAGCAGAACGTGGTTACCTGGCGGATGTTGAACTGTCGAAAATTGGCAGCTTCGAAGCCGCTCTGCTGGCTTACGTCGACCGTGATCACGCTCCGATGATGCAAGAGATCAACCA
      4570      4580      4590      4600      4610      4620      4630      4640      4650      4660      4670      4680

  T  G  G  Y  N  D  E  I  E  G  K  L  K  G  I  L  D  S  F  K  A  T  Q  S  W  *
GACCGGTGGCTACAACGACGAAATCGAAGGCAAGCTGAAAGGCATCCTCGATTCCTTCAAAGCAACCCAATCCTGGTAACGTCTGGCGGCTTGCCTTAGGGCAGGCCGCAAGGCATTGAG
      4690      4700      4710      4720      4730      4740      4750      4760      4770      4780      4790      4800
       GAMMA
          M  A  G  A  K  E  I  R  S  K  I  A  S  V  Q  N  T  Q  K  I  T  K  A  M  E  M  V  A  A  S  K  M  R  K  S  Q  D
GAGAAGCTCATGGCCGGCGCAAAAGAGATACGTAGTAAGATCGCAAGCGTCCAGAACACGCAAAAGATCACTAAAGCGATGGAGATGGTCGCCGCTTCCAAAATGCGTAAATCGCAGGAT
      4810      4820      4830      4840      4850      4860      4870      4880      4890      4900      4910      4920

 R  M  A  A  S  R  P  Y  A  E  T  M  R  K  V  I  G  H  L  A  H  G  N  L  E  Y  K  H  P  Y  L  E  D  R  D  V  K  R  V  G
CGCATGGCGGCCAGCCGTCCTTATGCAGAAACCATGCGCAAAGTGATTGGTCACCTTGCACACGGTAATCTGGAATATAAGCACCCTTACCTGGAAGACCGCGACGTTAAACGCGTGGGC
      4930      4940      4950      4960      4970      4980      4990      5000      5010      5020      5030      5040

 Y  L  V  V  S  T  D  R  G  L  C  G  G  L  N  I  N  L  F  K  K  L  L  A  E  M  K  T  W  T  D  K  G  V  Q  C  D  L  A  M
TACCTGGTGGTGTCGACCGACCGTGGTTTGTGCGGTGGTTTGAACATTAACCTGTTCAAAAAACTGCTGGCGGAAATGAAGACCTGGACCGACAAAGGCGTTCAATGCGACCTCGCAATG
      5050      5060      5070      5080      5090      5100      5110      5120      5130      5140      5150      5160

 I  G  S  K  G  V  S  F  F  N  S  V  G  G  N  V  V  A  Q  V  T  G  M  G  D  N  P  S  L  S  E  L  I  G  P  V  K  V  M  L
ATCGGCTCGAAAGGCGTGTCGTTCTTCAACTCCGTGGGCGGCAATGTTGTTGCCCAGGTCACCGGCATGGGGGATAACCCTTCCCTGTCCGAACTGATCGGTCCGGTAAAAGTGATGTTG
      5170      5180      5190      5200      5210      5220      5230      5240      5250      5260      5270      5280

 Q  A  Y  D  E  G  R  L  D  K  L  Y  I  V  S  N  K  F  I  N  T  M  S  Q  V  P  T  I  S  Q  L  L  P  L  P  A  S  D  D  D
CAGGCCTACGACGAAGGCCGTCTGGACAAGCTTTACATTGTCAGCAACAAATTTATTAACACCATGTCTCAGGTTCCGACCATCAGCCAGCTGCTGCCGTTACCGGCATCAGATGATGAT
      5290      5300      5310      5320      5330      5340      5350      5360      5370      5380      5390      5400

 D  L  K  H  K  S  W  D  Y  L  Y  E  P  D  P  K  A  L  L  D  T  L  L  R  R  Y  V  E  S  Q  V  Y  Q  G  V  V  E  N  L  A
GATCTGAAACATAAATCCTGGGATTACCTGTACGAACCCGATCCGAAGGCGTTGCTGGATACCCTGCTGCGTCGTTATGTCGAATCTCAGGTTTATCAGGGCGTGGTTGAAAACCTGGCC
      5410      5420      5430      5440      5450      5460      5470      5480      5490      5500      5510      5520

 S  E  Q  A  A  R  M  V  A  M  K  A  A  T  D  N  G  G  S  L  I  K  E  L  Q  L  V  Y  N  K  A  R  Q  A  S  I  T  Q  E  L
AGCGAGCAGGCCGCCCGTATGGTGGCGATGAAAGCCGCGACCGACAATGGCGGCAGCCTGATTAAAGAGCTGCAGTTGGTATACAACAAAGCTCGTCAGGCCAGCATTACTCAGGAACTC
      5530      5540      5550      5560      5570      5580      5590      5600      5610      5620      5630      5640

                                                            BETA
 T  E  I  V  S  G  A  A  A  V  *                            M  A  T  G  K  I  V  Q  V  I  G  A  V  V  D  V  E  F  P  Q  D
ACCGAGATCGTCTCGGGGGCCGCCGCGGTTTAAACAGGTTATTTCGTAGAGGATTTAAGATGGCTACTGGAAAGATTGTCCAGGTAATCGGCGCCGTAGTTGACGTCGAATTCCCTCAGG
      5650      5660      5670      5680      5690      5700      5710      5720      5730      5740      5750      5760

   A  V  P  R  V  Y  D  A  L  E  V  Q  N  G  N  E  R  L  V  L  E  V  Q  Q  Q  L  G  G  G  I  V  R  T  I  A  M  G  S  S  D
ATGCCGTACCGCGCGTGTACGATGCTCTTGAGGTGCAAAATGGTAATGAGCGTCTGGTGCTGGAAGTTCAGCAGCAGCTCGGCGGCGGTATCGTACGTACCATCGCAATGGGTTCCTCCG
      5770      5780      5790      5800      5810      5820      5830      5840      5850      5860      5870      5880

   G  L  R  R  G  L  D  V  K  D  L  E  H  P  I  E  V  P  V  G  K  A  T  L  G  R  I  M  N  V  L  G  E  P  V  D  M  K  G  E
ACGGTCTGCGTCGCGGTCTGGATGTAAAAGACCTCGAACACCCGATTGAAGTCCCGGTAGGTAAAGCGACTCTGGGCCGTATCATGAACGTACTGGGTGAACCGGTCGACATGAAAGGCG
      5890      5900      5910      5920      5930      5940      5950      5960      5970      5980      5990      6000

   I  G  E  E  E  R  W  A  I  H  R  A  A  P  S  Y  E  E  L  S  N  S  Q  E  L  L  E  T  G  I  K  V  I  D  L  M  C  P  F  A
AGATCGGTGAAGAAGAGCGTTGGGCGATTCACCGCGCAGCACCTTCCTACGAAGAGCTGTCAAACTCTCAGGAACTGCTGGAAACCGGTATCAAAGTTATCGACCTGATGTGTCCGTTCG
      6010      6020      6030      6040      6050      6060      6070      6080      6090      6100      6110      6120
```

D

```
   K  G  G  K  V  G  L  F  G  G  A  G  V  G  K  T  V  N  M  M  E  L  I  R  N  I  A  I  E  H  S  G  Y  S  V  F  A  G  V  G
CTAAGGGCGGTAAAGTTGGTCTGTTCGGTGGTGCGGGTGTAGGTAAAACCGTAAACATGATGGAGCTCATTCGTAACATCGCGATCGAGCACTCCGGTTACTCTGTGTTTGCGGGCGTAG
      6130      6140      6150      6160      6170      6180      6190      6200      6210      6220      6230      6240

   E  R  T  R  E  G  N  D  F  Y  H  E  M  T  D  S  N  V  I  D  K  V  S  L  V  Y  G  Q  M  N  E  P  P  G  N  R  L  R  V  A
GTGAACGTACTCGTGAGGGTAACGACTTCTACCACGAAATGACCGACTCCAACGTTATCGACAAAGTATCCCTGGTGTATGGCCAGATGAACGAGCCGCCGGGAAACCGTCTGCGCGTTG
      6250      6260      6270      6280      6290      6300      6310      6320      6330      6340      6350      6360

   L  T  G  L  T  M  A  E  K  F  R  D  E  G  R  D  V  L  L  F  V  D  N  I  Y  R  Y  T  L  A  G  T  E  V  S  A  L  L  G  R
CTCTGACCGGTCTGACCATGGCTGAGAAATTCCGTGACGAAGGTCGTGACGTTCTGCTGTTCGTTGACAACATCTATCGTTACACCCTGGCCGGTACGGAAGTATCCGCACTGCTGGGCC
      6370      6380      6390      6400      6410      6420      6430      6440      6450      6460      6470      6480

   M  P  S  A  V  G  Y  Q  P  T  L  A  E  E  M  G  V  L  Q  E  R  I  T  S  T  K  T  G  S  I  T  S  V  Q  A  V  Y  V  P  A
GTATGCCTTCAGCGGTAGGTTATCAGCCGACCCTGGCGGAAGAGATGGGCGTTCTGCAGGAACGTATCACCTCCACCAAAACTGGTTCTATCACCTCCGTACAGGCAGTATACGTACCTG
      6490      6500      6510      6520      6530      6540      6550      6560      6570      6580      6590      6600

   D  D  L  T  D  P  S  P  A  T  T  F  A  H  L  D  A  T  V  V  L  S  R  Q  I  A  S  L  G  I  Y  P  A  V  D  P  L  D  S  T
CGGATGACTTGACTGACCCGTCTCCGGCAACCACCTTTGCGCACCTTGACGCAACCGTGGTACTGAGCCGTCAGATCGCGTCTCTGGGTATCTACCCGGCCGTTGACCCGCTGGACTCCA
      6610      6620      6630      6640      6650      6660      6670      6680      6690      6700      6710      6720

   S  R  Q  L  D  P  L  V  V  G  Q  E  H  Y  D  T  A  R  G  V  Q  S  I  L  Q  R  Y  Q  E  L  K  D  I  I  A  I  L  G  M  D
CCAGCCGTCAGCTGGACCCGCTGGTGGTTGGTCAGGAACACTACGACACCGCGCGTGGCGTTCAGTCCATCCTGCAACGTTATCAGGAACTGAAAGACATCATCGCCATCCTGGGTATGG
      6730      6740      6750      6760      6770      6780      6790      6800      6810      6820      6830      6840

   E  L  S  E  E  D  K  L  V  V  A  R  A  R  K  I  Q  R  F  L  S  Q  P  F  F  V  A  E  V  F  T  G  S  P  G  K  Y  V  S  L
ATGAACTGTCTGAAGAAGACAAACTGGTGGTAGCGCGTGCTCGTAAGATCCAGCGCTTCCTGTCCCAGCCGTTCTTCGTGGCAGAAGTATTCACCGGTTCTCCGGGTAAATACGTCTCCC
      6850      6860      6870      6880      6890      6900      6910      6920      6930      6940      6950      6960

   K  D  T  I  R  G  F  K  G  I  M  E  G  E  Y  D  H  L  P  E  Q  A  F  Y  M  V  G  S  I  E  E  A  V  E  K  A  K  K  L  *
TGAAAGACACCATCCGTGGCTTTAAAGGCATCATGGAAGGCGAATACGATCACCTGCCGGAGCAGGCGTTCTACATGGTCGGTTCCATCGAAGAAGCTGTGGAAAAAGCCAAAAAACTTT
      6970      6980      6990      7000      7010      7020      7030      7040      7050      7060      7070      7080
                        EPSILON
                       M  A  M  T  Y  H  L  D  V  V  S  A  E  Q  Q  M  F  S  G  L  V  E  K  I  Q  V  T  G  S  E  G  E  L
AACGCCTTAATCGGAGGGTGATATGGCAATGACTTACCACCTGGACGTCGTCAGCGCAGAGCAACAAATGTTCTCTGGTCTGGTCGAGAAAATCCAGGTAACGGGTAGCGAAGGTGAACT
      7090      7100      7110      7120      7130      7140      7150      7160      7170      7180      7190      7200

  G  I  Y  P  G  H  A  P  L  L  T  A  I  K  P  G  M  I  R  I  V  K  Q  H  G  H  E  E  F  I  Y  L  S  G  G  I  L  E  V  Q
GGGGATCTACCCTGGCCACGCACCGCTGCTCACCGCCATTAAGCCTGGTATGATTCGCATCGTGAAACAGCACGGTCACGAAGAGTTTATCTATCTGTCTGGCGGCATTCTTGAAGTGCA
      7210      7220      7230      7240      7250      7260      7270      7280      7290      7300      7310      7320

  P  G  N  V  T  V  L  A  D  T  A  I  R  G  Q  D  L  D  E  A  R  A  M  E  A  K  R  K  A  E  E  H  I  S  S  S  H  G  D  V
GCCTGGCAACGTGACCGTTCTGGCCGACACCGCAATTCGCGGCCAGGATCTCGACGAAGCGCGAGCCATGGAAGCGAAACGTAAGGCTGAAGAGCACATTAGCAGCTCTCACGGCGACGT
      7330      7340      7350      7360      7370      7380      7390      7400      7410      7420      7430      7440
                                                                                            Transcription  termination
  D  Y  A  Q  A  S  A  E  L  A  K  A  I  A  Q  L  R  V  I  E  L  T  K  K  A  M  *
AGATTACGCTCAGGCGTCTGCGGAACTGGCCAAAGCGATCGCGCAGCTGCGCGTTATCGAGTTGACCAAAAAAGCGATGTAACACCGGCTTGAAAAGCACAAAAGCCAGTCTGGAAACAG
      7450      7460      7470      7480      7490      7500      7510      7520      7530      7540      7550      7560

GCTGGCTTTTTTTTGCGCGTGTGACCCGTCCTGAATAGCGTTCACATAGATCCTGCTGATATAAAACCCCCCTGTTTTCCTGTTTATTCATTGATCGAAATAAGAGCAAAAACATCCACC
      7570      7580      7590      7600      7610      7620      7630      7640      7650      7660      7670      7680

TGACGCTTAAATTAAGGTACTGCCTTAATTTTCTGCAGACAAAAGGCGTGACGATGGTCGAAAATGGCGCTTTCGTCAGCGGGGATAATCCGTTATTGAACAATTTATCCTCTGTCCATT
      7690      7700      7710      7720      7730      7740      7750      7760      7770      7780      7790      7800
                                                                           GlmS?
                                                                           M  L
TCACGATGAAAAAAATGTAGTTTTTTCAAGGTGAAGCGGTTTAAATTCGTTCTCAAATTACAGTCAGGACGCGTATGTTGA
      7810      7820      7830      7840      7850      7860      7870      7880
```

figure differs in only one base from the sequence summarised by Walker et al. [35]. An extra C residue has been found at position 7492 close to the C-terminus of ε. This makes the sequence of ε consistent with the C-terminal residue methionine determined by Dunn [36] and causes the sequences of the nine C-terminal amino acids to be changed from that presented originally [25].

III. Interpretation of the DNA sequence

Two methods were applied for the identification of reading frames (genes) in this DNA sequence, visual inspection and computer analysis with the program FRAMESCAN [37]. In both methods a reading frame is defined a a sequence of nucleotide triplets coding for amino acids starting with an initiation codon (ATG, GTG or rarely TTG, recognised in mRNA by N-formylmethionyl tRNA) and ending with a termination codon (TAA, TGA or TAG). The initiation codon is preceded by a potential ribosome binding site with sequence complementary to the 3′ end of 16 S ribosomal RNA (also called the Shine and Dalgarno sequence [38]). By visual inspection, nine consecutive reading frames can be discerned in the *unc* region. FRAMESCAN additionally makes use of codon frequency data to assess reading frames. Analysis of the *unc* region shows eight genes with related codon frequencies the ninth, the first in the operon, being clearly different in this respect (Fig. 4); particularly noteworthy is the presence in gene 1 of four of the six AUA codons to be found in the entire operon (see subsection IVB).

IIIA. Identification of genes

Protein sequences of *E. coli* ATP-synthase subunits have been used to identify seven of the genes in the *unc* operon and so to establish the gene order shown in Fig. 3. These sequences [39] are summarised in Table I. In addition, protein sequences in bovine mitochondrial α [34] and β [40] subunits helped to identify reading frames for the corresponding *E. coli* proteins. Dunn has independently determined N-terminal protein sequences for the α, [41], δ and ε [36] subunits and C-terminal residues for α (tryptophan) [41], γ (valine) and ε (methionine) that have proved helpful for establishing the termination codons of these proteins and of ε in particular [36]. It was noted that the F_0 subunit *c* is N-formylated and N-formylmethionine is removed from the β, γ and ε subunits by post-translational processing [39]. In the case of the α subunit, formyl or, alternatively, N-formylmethionine, were found to have been removed in two independently isolated samples of F_1-ATPase [41].

An eighth ATP-synthase subunit, the F_0 subunit *a*, is identified by homology with counterparts of the mitochondrial ATP-synthase (see Fig. 5). These homologies are strongest in the C-terminal portion of the polypeptide chains and are weak towards

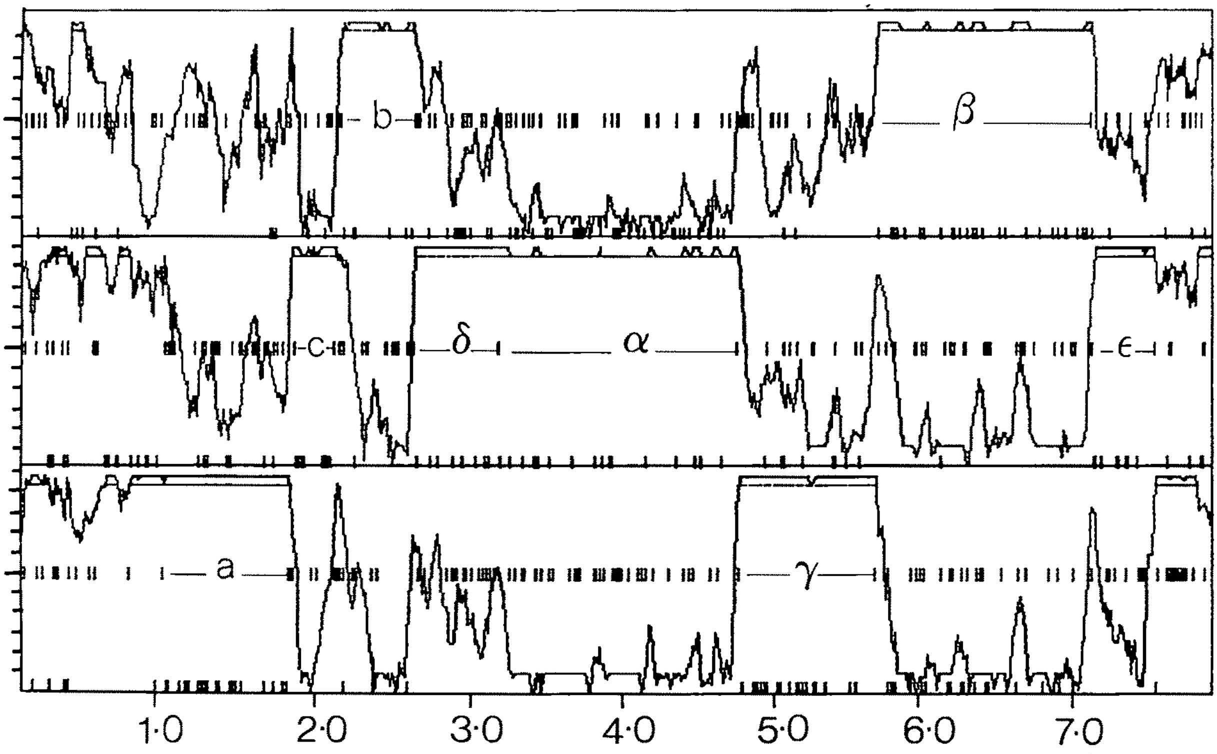

Fig. 4. Identification of reading frames in the *unc* operon with FRAMESCAN. The three boxes represent the three phases of the nucleotide sequence (horizontal scale). The vertical scale is a measure of the similarity of codon usage when compared with the α gene with a window of 45 bases. The vertical bars across the middle of each box are the positions of termination codons. Initiation codons (ATG only) are plotted across the bottom of each box. The positions of *unc* genes are indicated.

TABLE I

AMINO TERMINAL SEQUENCES OF PROTEINS DETERMINED BY PROTEIN SEQUENCE ANALYSIS OF ISOLATED *E COLI* ATP-SYNTHASE SUBUNITS

Subunit		Sequences	Ref
c	Protein	f M E N L N , etc. to C-terminus	79
	DNA	C T G G A G A C T G T C ATG GAA AAC CTG AAT	
b	Protein	M N L N A T I L G Q A , etc.	26
	DNA	T A G A G G C A T T G T G C T GTG AAT CTT AAC GCA ACA ATC CTC GGC CAG GCC	
δ	Protein	M S E F I	26,28
	DNA	G G G A G G G G C C T G ATG TCT GAA TTT ATT	
α	Protein	M Q L N S T E I S E L I K Q R I A Q , etc.	26,39
	DNA	G G G G A C T G G A G C ATG CAA CTG AAT TCC ACC GAA ATC AGC GAA CTG ATC AAG CAG CGC ATT GCT CAG	
γ	Protein	A G A K E I X S K I A S V Q N	36,39
	DNA	T G A G G A G A A G C T C ATG GCC GGC GCA AAA GAG ATA CGT AGT AAG ATC GCA AGC GTC CAG AAC	
β	Protein	A T G K I V Q V I G A V V D V E F P Q D	39
	DNA	T A G A G G A T T T A A G ATG GCT ACT GGA AAG ATT GTC CAG GTA ATC GGC GCC GTA GTT GAC GTC GAA TTC CCT CAG GAT	
ε	Protein	A M T Y X L D V V S A E	36,39
	DNA	A A T C G G A G G G T G A T ATG GCA ATG ACT TAC CAC CTG GAC GTC GTC AGC GCA GAC	

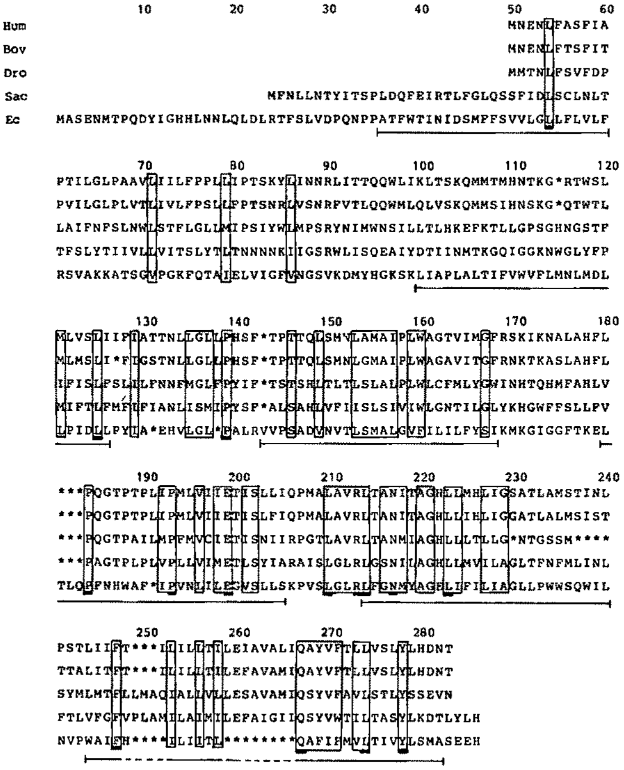

Fig. 5. Sequences of the *E. coli* F_0 subunit a compared with its counterparts encoded in mitochondrial DNA. ***Hum**an* [126], ***Bov**ine* [123], *Mouse* [127], ***Dro**sophila melanogaster* (de Bruijn, M.H.L., unpublished data), ***Sac**charomyces cerevisiae* [124].

the N-terminus. The lack of homology in the N-terminal regions of the *E. coli* and human proteins has led Nielsen et al. [26] to propose that the initial translation product is *a′*, processed to give the smaller product *a″* which is then incorporated into the ATPase complex. It is further suggested that *a* might correspond to a 31 kDa outer membrane protein. However, comparison of the proteins from mitochondrial sources indicates a similar lack of homology in the N-terminal regions, making the suggestion of Nielsen et al. [26] somewhat implausible. Also in the ribosome binding site for the *a″* the initiation codon GTG to nine bases is rather distant from the Shine and Dalgarno box. However, the precise sequence of the mature *a* protein can only be settled by protein sequence analysis.

A summary of the amino acid compositions and molecular weights of the eight subunits of *E. coli* ATP-synthase is presented in Table II.

Gene 1. The function of the region of DNA named gene 1 is a mystery. This sequence has many of the features characteristic of regions of DNA encoding a protein (viz. an initiation codon preceded by a potential ribosome binding site and followed by a coding sequence ending by a termination codon). However, the frequency of codons in this reading frame is markedly different from the genes identified as coding for structural components of ATP-synthase. The relatively higher frequency of rare codons suggests that the gene may be poorly expressed (see subsection IVB-4) and so it could encode a protein involved in regulation of expression or of assembly of the enzyme. In order to study the function of this region of DNA, a strain of *E. coli* has been con-

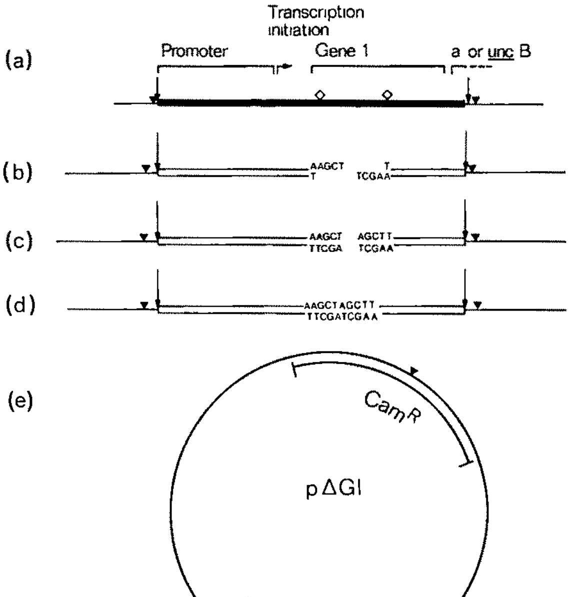

Fig. 6. Construction of a deletion mutant in gene 1 [42]. (a) M13mp RF containing a 920 bp insert from *Hae*II site (nucleotide 159) to *Bam*HI site (nucleotide 1063) was digested with *Hin*dIII releasing a 199 bp fragment of gene 1 and so linearising the fragment (b). (c) The *Hin*dIII cohesive ends will filled in using Klenow polymerase. (d) The modified fragment was then religated and transfected into *E. coli* JM101. Then the mutagenised fragment was released from RF with *Bam*HI ligated into pACYC184 and transformed into *E. coli* HB101. (e) Transformants were selected on media supplemented with chloramphenicol and recombinants identified by insertional activation of tetracycline resistance *Hin*dIII (◇), *Eco*RI (▼) *Bam*HI (↓).

TABLE II

AMINO ACID COMPOSITIONS OF PROTEINS ENCODED BY THE *unc* OPERON

Amino acid	Protein								
	1 [a]	a	c	b	δ	α	γ	β	ε
Aspartic acid	1	8	3	8	9	28	17	27	6
Asparagine	5	12	2	4	6	16	12	11	1
Threonine	3	12	1	3	4	23	13	24	6
Serine	7	17	0	5	12	32	21	25	8
Glutamic acid	1	8	2	18	17	31	15	39	13
Glutamine	3	7	2	10	9	28	14	20	8
Proline	5	15	3	2	3	18	9	20	4
Glycine	7	17	10	3	8	47	20	45	12
Alanine	16	17	13	31	27	57	27	34	17
Cysteine	0	0	0	1	2	3	2	1	0
Valine	24	23	6	11	16	41	25	47	10
Methionine [b]	3	11	8	2	7	11	13	15	6
Isoleucine	6	25	8	13	10	40	13	27	11
Leucine	23	45	12	14	18	47	29	42	12
Tyrosine	0	6	2	1	1	15	11	15	4
Phenylalanine	9	20	4	3	6	14	4	14	2
Histidine	2	7	0	1	2	7	4	7	6
Lysine	7	10	1	15	8	24	23	20	8
Arginine	4	4	2	10	11	30	13	26	5
Tryptophan	4	7	0	1	1	1	2	1	0
Molecular weight	14055 [c]	30285 [c]	8264 [c]	17230 [c]	19328	55282	31559	50286	15051
Polarity index	25	31	16	47	44	43	46	43	44

[a] Assumes GTG initiation codon (see Fig. 10).

[b] Assumes no post-translational removal of methionine.

[c] Includes N-terminal formyl group.

structed by site-directed mutagenesis in which a large segment of the polypeptide chain has been deleted from the core of the putative protein (Fig. 6). This strain retains the ability to grow on non-fermentable carbon sources (*unc*$^+$ phenotype); its rate of growth on minimal succinate medium and anaerobically with glucose is indistinguishable from an isogenic normal strain but its growth yield is lower, possibly because of inefficient use of available energy sources [42]. This could be due to either (a) inefficient assembly resulting in a fraction of inactive enzyme complexes with a compensating increase in transcription of the *unc* operon, or (b) inefficient assembly resulting in loss of chemiosmotic energy through passive proton-conducting pores. The properties of this mutant show that it is most likely that gene 1 is not an essential component for ATP-synthase function, having no discernible effect on qualitative expression of *unc* genes, but that it may affect their quantitative expression.

The putative protein encoded in gene 1 has a number of features that may be helpful in determining its function. The protein would be hydrophobic but would have a net positive charge of +11 (assuming a charge of +0.5 for each histidine). A hypothetical structure for this protein is discussed in subsection VB-5.

IIIB. Translational signals

IIIB-1. Initiation

A ribosome binding site on a messenger RNA includes the initiation codon and the Shine and

TABLE III

RIBOSOME BINDING SITES OF GENES IN THE *unc* OPERON

Each sequence ends with the initiation codon (boxed) preceded by boxed sequences complementary to the 3′ end of 16 S ribosomal RNA; four cistrons have two such sequences and the gene for the γ subunit has three. In some cases termination codons of previous cistrons have dotted underline.

Subunit		DNA sequence	No. of subunits
γ		AGGCCGCAAGGCATTGAGGAGAAGCTCATG	1
δ		CGCTGAACTGTAAGGAGGGAGGGGCTGATG	1
ε		ACTTTAACGCCTTAATCGGAGGGTGATATG	1
c		TTTAACTGAAACAAACTGGAGACTGTCATG	6–10
α		GTCTTGCAGTCTTAAGGGGACTGGAGCATG	3
β		AACAGGTTATTTCGTAGAGGATTTAAGATG	3
a		CAACAAAGGGTAAAAGGCATCATG	1
b		ACGTTAACTAAATAGAGGCATTGTGCTGTG	2
1	(i)	ACGCGGCATACCTCGAAGGGAGCAGGAGTG	–
	(ii)	AGGGAGCAGGAGTGAAAAACGTGATG	–

Canonical ribosome binding site: T*AAGGAGG*TGTTC

Dalgarno box found 5–9 bases upstream of the initiation codon. The initiation codon is usually predominantly ATG (97.5% of observed cases). GTG (2%) is also used [43] and in one case TTG has been observed [44]. Despite this strong bias in favour of ATG, in vitro binding experiments with fMet-tRNA do not show strong discrimination against GTG [45], and so the significance of the occasional use of GTG as initiation codon remains a mystery. It is used at least once and possibly twice in the *unc* operon. As shown in Table III, GTG is the initiation coding for the protein *b* gene and is one of the two possible initiation codons for gene 1. This table also shows the similarity in the sequence of the Shine and Dalgarno boxes and the constancy of the distance between this box and the initiation codes for genes for γ, δ, ε and c. An additional feature of the γ and δ sequences is that they each contain a second Shine and Dalgarno sequence overlapping the other alternative. Two overlapping Shine and Dalgarno sequences also are to be found in one of the possible initiation sequences for gene 1. Of the two possibilities (i) and (ii) in Table III (i) could be preferred on the grounds that the S and D sequence in (ii) is separated from the initiation codon by 11 bases, greater than the usual span of 5–9 bases [43]. Alternative, but non-overlapping, S and D sequences are found in the vicinity of the initiation codons for the genes α and a. In the case of α neither sequence lies within the usual distance (5–9 bases) of the initiation codon. The more distant possibility is separated from the initiation codon by ten bases and additionally partially overlaps the termination codon of δ; the nearer possibility is but one base from the ATG codon. In the case of the protein a gene the more distant possibility is entirely within the proposed coding sequence of gene 1 and separated from the initiation coding by 12 bases; the nearer alternative has a four base spacer sequence.

The significance of these multiple Shine and

Dalgarno sequences is unclear. However, the inadequacy is recognised of the simple model of the ribosome binding site (an initiation codon separated from a Shine and Dalgarno sequence by a spacer sequence). It is clear that the region of interaction with ribosomal RNA is much more extensive and encompasses regions both upstream of the Shine and Dalgarno sequence and also in the coding sequence [46]. In the *unc* operon, as in ribosomal protein genes [46], a preference is found for G in the first position after the initiation codon. Of the structural genes only that for protein b has an A as the fourth base and in this case following a GTG initiation codon. A similar situation may be found at the beginning of gene 1. Evidence has been presented by Taniguchi and Weissmann [47] that the base after the initiation codon is important in determining efficiency of a translation initiation site in binding ribosomes. They found that affinity of the initiation site and ribosomes increased with A in the first position after the initiation codon. This was explained by base pairing the A with the U preceding the anticodon in formylmethionyl tRNA.

IIIB-2. Termination

With the exception of the protein c gene the only termination codon employed in the *unc* operon is TAA, thought to be the major termination codon in *E. coli*. The protein c gene ends with tandem termination triplets TAG · TAA, a combination of tandem termination codons that has not been observed previously [48]. The combination UAA · UAG was observed in coat protein genes of the RNA phages MS2, R17 and f2 [48] and TGA · TAA terminates gene F of ϕX174 [49]. It has been estimated that approx. 13% of all *E. coli* genes contain termination signals TAG or TAA in tandem with a second nonsense triplet [50]. It is generally thought that the feature serves to ensure that read through ('leakiness') does not occur.

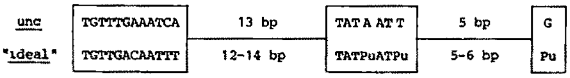

Fig. 7. Comparison of the 'ideal' promoter sequence [51] and the proposed *unc* promoter [24]. I is the base at which transcription initiates.

IIIC. Transcriptional signals

IIIC-1. The unc promoter

The proposed promoter for the *unc* operon (see Fig. 7) contains sequences that resemble the canonical 'Pribnow box' and −35 region derived by comparison of all known promoters [51,52]. The presence of an active promoter in this region was confirmed in vitro by measuring the length of run-off transcripts (see Fig. 8) [53]. These experiments argue against the presence of an active promoter in the region designated gene 1 as proposed by Kanazawa et al. [30]. A mutant SD42, in which a region of 199 bases of gene has been deleted and four inserted, is still viable against the proposal of Kanazawa et al. [30] of a promoter in the region of nucleotide 800.

The possible significance in transcription of the 5′ non-coding region adjacent to the *unc* promoter is discussed in subsection IVA.

IIIC-2. Internal promoters

Evidence has been obtained from *lac*Z fusions for a weak internal promoter approx. 100 basepairs upstream of the start of the protein a gene. It is estimated to be 10-times weaker than the main promoter [54]. Its significance is unknown.

IIIC-3. Transcription terminator

A sequence following the gene for the ε subunit (see Fig. 3) has characteristics of a strong rho-independent transcription termination signal with a G–C rich stem followed by the sequence T_6 as depicted in Fig. 9 [25]. However, experiments to verify this suggestion have not been performed.

IIIC-4. Intercistronic sequences

Attention has been drawn to the presence of only three intercistronic regions of significant length in the *unc* operon [24,25] (Fig. 10). Two surround the protein c gene and the third is between the genes for α and γ. In the first two of these regions, the presence of sequences has been noted that are closely related to the Pribnow box of the Trp-promoter [51]; although homology with the −35 box is absent. The significance, if any, of these sequences is not understood; no experiments have been reported that demonstrate whether or not they represent significant sites for RNA polymerase binding.

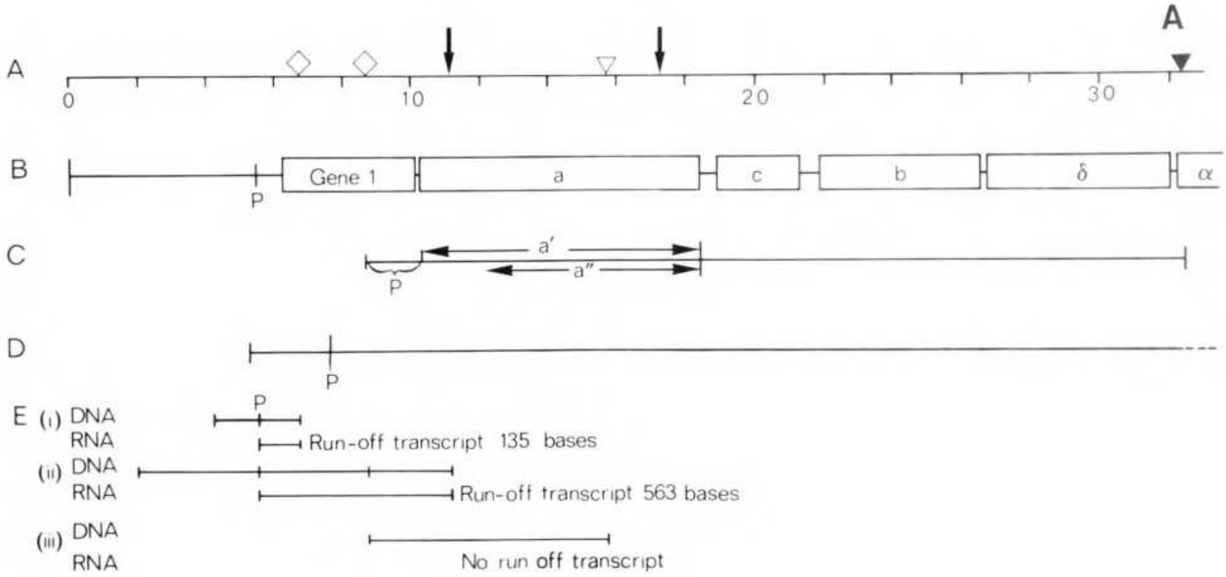

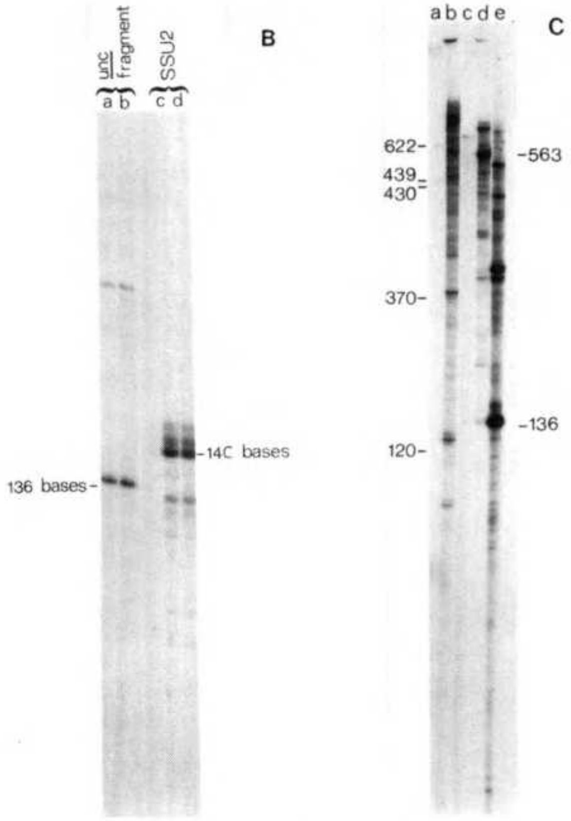

Fig. 8. Experiments to detect the promoter for the *unc* operon. *Part I.* (A) Physical map, *Hin*dIII (◇), *Bam*HI (↓), *Hae*III (▽), *Eco*RI (▼) restriction sites. (B) Genes drawn to scale. P represents the site of initiation of transcription proposed by Gay and Walker [24] and verified as described. (C) P represents the location of a weak promoter proposed by Nielsen et al. [26]. (D) P is the position of a promoter proposed by Kanazawa et al. [31] and disproved by Gay [42]. (E) (i)–(iii) Predicted lengths of in vitro transcripts from various DNA fragments. *Part II.* Autoradiograph of gel showing in vitro transcript of DNA fragment containing proposed promoter (see Fig. 7, Part 1B and E(i)) compared with transcript made from the SSU2 promoter [53]. *Part III.* Products of in vitro transcription of fragments derived from the proximal part of the *unc* operon [53]. (a) pBR322 DNA digested with *Hae*II. (b) Transcription products of a 1675 basepair fragment from *Pst*I site to *Eco*RI site (nucleotides 1563–3228). (c) Transcription products of a fragment from *Hin*dIII site to *Pst*I site (nucleotides 872–1563). (d) Transcription products of a 909 basepair fragment from *Hae*II site to *Bam*HI site (nculeotides 203–1112). (e) Transcription products of *Sau*3A-*Hin*dIII fragment (nucleotides 432–673).

The intercistronic space between the genes for α and γ contains no apparent promoter, but an inverted repeat has been noted [24] that could form a very stable hairpin structure (Fig. 12, see subsection IIIC).

IV. Regulation of the *unc* operon

IVA. Transcriptional regulation of the unc operon

Little is known about the qualitative and temporal control of genes encoding central metabolic processes. Expression of these functions is probably controlled by a complex set of interacting effectors. In the *unc* operon, these effectors could include nucleotides, oxygen, intracellular pH, extracellular metabolites, such as amino acids that require a proton potential gradient to drive their uptake. The H^+-ATPase of *E. coli* is necessary during both aerobic growth, to mediate oxidative phosphorylation of ATP, and anaerobic growth, when it mediates ATP driven membrane energisation [4].

DNA sequence analysis (see Fig. 3) has revealed a very long (400 bp) 5′ non-coding region adjacent to the promoter. Other genes and operons which encode important metabolic processes such as ribosomal proteins, ribosomal RNAs and tRNAs, have similarly extended promoter control regions [55]. These regions are generally characterised by a very high content of A and T. Analysis of these sequences has led to the identification of five homologous 10 bp sequences which have an homology between 60 and 100%, with the consensus sequence C-A-G-A-A-A-A-A-T-C (see Figs. 3 and 11). A possible function for these sequences is that they act as 'locator' sites for RNA polymerase which is proposed to interact weakly with DNA in these regions. Thus RNA polymerase would become concentrated locally in the vicinity of the promoter. This idea has several attractions. Free RNA polymerase is known to exist in at least two different conformations and the equilibrium between these forms is thought to be modulated by nucleotides, specifically by GTP, ATP, ADP, ppApp and ppGpp. For example, during the stringent response evoked by amino acid starvation, the intracellular ppGpp concentration rises from 20 μM to 1 mM. This is accompanied by a dramatic reduction in synthesis from a subset of promoters. This effect has been correlated with a change in the free polymerase from 'dimer' to 'monomer' [56]. Thus the 'locator' sequences have different affinities for different conformation forms of free RNA polymerase and the equilibrium between these forms is modulated by the metabolic status of the cell, then qualitative variations in transcription will result. The variations would reflect the complex and dynamic equilibrium of the cell and the number of permutations would be very large. Another consequence of this idea is that protein-DNA interactions which altered the affinity of the RNA-polymerase for the locator sequences would also result in qualitative differences in transcription. This is in contrast to other control sequences and control proteins such as the *lac* repressor/operator which effects a quantitative switch in transcription.

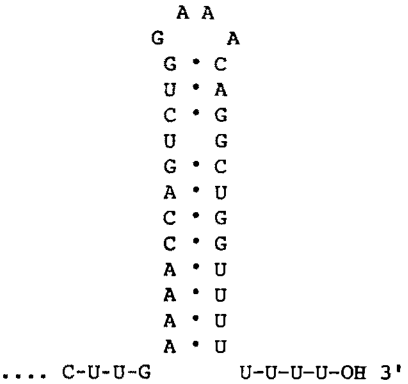

Fig. 9. Proposed structure of RNA at the transcription termination site of the *unc* operon [25].

IVB. Uncoordinacy

The stoichiometry of subunits and the order of the genes in the *unc* operon raises the question of how the synthesis of different amounts of the various proteins from a polycistronic message is achieved. This problem has been encountered previously in other transcriptional units. The term 'non-coordinacy' or 'uncoordinacy' has been coined to describe the phenomena [57]. A most striking example is provided by the morphogenetic genes A–J of bacteriophage λ which form a single transcriptional unit with an 870-fold molar difference between the least and most abundant proteins produced from this operon [58]. Other examples are to be found in the RNA phages. In R17, for example, the middle of three cistrons (encoding the coat protein) is translated about 20-times more

1-a TAAAAGGCATCATG

a-c TAATTTACCAACACTACTACGTTTTAACTGAAACAAACTGGAGACTGTCATG

c-b TAGTAAGCGTTGCTTTTATTTAAAGAGCAATATCAGAACGTTAACTAAATAGAGGCATTGTGCTGTG

b-δ TAAGGAGGGAGGGGCTGATG

δ-α TAAGGGGACTGGAGCATG

α-γ TAACGTCTGGCGGCTTGCCTTAGGGCAGGCCGCAAGGCATTGAGGAGAAGCTCATG

γ-β TAAACAGGTTATTTCGTAGAGGATTTAAGATG

β-ε TAACGCCTTAATCGGAGGGTGATATG

Fig. 10. Intercistronic non-coding regions in the *unc* operon. Each sequence starts with a termination codon and ends with the initiation codons of the following gene. Initiation codons are preceded by proposed ribosome binding sites. Underlined in a–c and c–b are two regions related in sequence to the Pribnow box of the *Trp* promoter (see Ref. 51). Inverted repeats in α–γ are underlined [128].

frequently than its neighbours, the A protein (before) and replicate (after) [59].

A simple explanation is that the subunits are produced in equimolar quantities and unassembled excesses removed by proteolysis. In the absence of any information whatever concerning rates of synthesis of individual subunits of ATP-synthase and their pool sizes, this explanation cannot be formally discounted. However, it would create considerable waste: with a stoichiometry of

Bases before I	tyrT promoter		Bases before I	unc promoter	
-55	CATTTTTCTC (10/10)	→		no homology	
-77	GATGAAAATT (7/10)	←	-76	GAAAAATATT (6/10)	←
-109	CAAAAATAAC (7/10)	←	-103	CAGAAAAGTC (8/10)	←
-129	GATTATTCTT (7/10)	→	-128	CAGTTTTTCAG (7/10)	→
-150	CTTTGTTTAC (6/10)	→	-150	CAGTGTTTACG (6/10)	→
-200	CAGAAAAACG (9/10)	←	-207	AATAAATATG (7/10)	←

Fig. 11. Conserved sequences in the non-coding region 5′ to the *unc* promoter that may serve as locator signals for RNA polymerase [55] compares with sequences 5′ to the tRNA Tyr promoter.

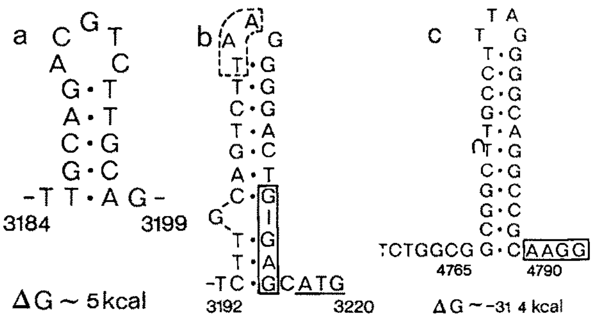

Fig. 12. Possible secondary structures in intercistronic regions of the *unc* operon [67]. The stabilities were calculated by the method of Tinoco et al. [12]. In (b) termination codon of δ is in the dotted box, initiation codon of α is underlined and S and D sequence is boxed. In (c) S and D sequence of γ is boxed.

TABLE IV

CODON USAGE IN THE *unc* OPERON

Codon	Amino acid	Protein									Σ
		a	c	b	δ	α	γ	β	ε	Gene 1	
AAU	Asn	6	1	1	2	2	3	2	0	0	17
AAC		6	1	3	4	14	9	9	1	5	52
AAA	Lys	7	1	10	6	19	17	17	6	5	88
AAG		3	0	5	2	5	6	3	2	2	28
GAU	Asp	3	4	2	4	12	9	6	2	0	41
GAC		5	0	6	5	16	8	21	4	1	66
GAA	Glu	5	2	13	9	27	10	27	8	1	102
GAG		3	0	5	8	4	5	12	5	0	42
UGU	Cys	0	0	0	1	3	0	1	0	0	5
UGC		0	0	1	1	0	2	0	0	0	4
UGA	Term.	0	0	0	0	0	0	0	0	0	0
UGG	Trp	7	0	1	1	1	2	1	0	4	17
CGU	Arg	3	2	7	4	25	9	21	1	1	63
CGC		0	0	2	5	5	4	5	3	0	24
CGA		1	0	1	1	0	0	0	1	1	5
CGG		0	0	0	1	0	0	0	0	2	3
AGU	Ser	0	0	0	3	2	1	0	0	2	8
AGC		6	0	2	1	2	7	2	4	2	26
AGA	Arg	0	0	0	0	0	0	0	0	0	0
AGG		0	0	0	0	0	0	0	0	0	0
GGU	Gly	9	7	0	5	29	6	29	5	0	90
GGC		6	2	3	3	16	12	14	6	4	66
GGA		1	0	0	0	1	0	2	0	1	5
GGG		1	1	0	0	1	2	0	1	2	8
UUU	Phe	3	1	1	6	1	1	3	1	4	21
UUC		17	3	2	0	13	3	11	1	5	55
UUA	Leu	3	0	1	0	0	1	0	0	3	8
UUG		4	0	0	1	2	5	1	1	6	20
CUU		2	0	5	5	3	2	3	1	1	22
CUC		1	1	1	4	4	2	3	2	3	21
CUA		0	0	0	0	1	0	0	0	0	1
CUG		35	11	7	8	37	19	35	8	10	170
AUU	Ile	11	1	3	6	10	6	4	5	1	47
AUC		13	7	10	4	30	6	23	6	1	100
AUA		1	0	0	0	0	1	0	0	4	6
AUG	Met	11	8	2	7	11	13	15	6	3	76
GUU	Val	5	1	3	5	24	8	12	2	8	68
GUC		3	1	2	4	2	6	6	3	2	29
GUA		6	1	2	6	9	2	19	2	2	49
GUG		9	3	4	1	6	9	10	3	12	57

TABLE IV (continued)

Codon	Amino acid	Protein									Σ
		a	c	b	δ	α	γ	β	ε	Gene 1	
UCU	Ser	3	0	0	5	11	2	7	4	2	34
UCC		2	0	2	1	16	5	14	0	0	40
UCA		3	0	0	1	0	1	2	0	0	6
UCG		3	0	1	1	1	5	0	0	1	12
CCU	Pro	3	2	0	0	1	3	4	3	1	17
CCC		1	0	0	1	0	1	0	0	1	4
CCA		4	0	1	1	3	0	0	0	1	10
CCG		7	1	1	1	14	5	16	1	2	48
ACU	Thr	0	1	1	0	4	2	5	1	0	14
ACC		3	0	1	2	17	10	18	4	0	55
ACA		2	0	1	0	2	0	0	0	2	7
ACG		7	0	0	2	0	1	1	1	1	13
GCU	Ala	4	6	9	7	17	2	7	2	3	57
GCC		6	1	8	7	8	12	6	4	2	54
GCA		2	2	6	6	20	6	8	4	5	59
GCG		5	4	8	7	12	7	13	7	6	67
UAU	Tyr	2	0	0	0	4	4	4	1	0	15
UAC		4	2	1	1	11	7	11	3	0	40
UAA	Term.	1	1	1	1	1	1	1	1	1	9
UAG		0	1	0	0	0	0	0	0	0	1
CAU	His	3	0	1	0	0	1	0	0	1	6
CAC		4	0	0	2	7	3	7	6	1	30
CAA	Gln	2	1	2	4	4	2	2	2	0	19
CAG		5	1	8	5	24	12	18	6	3	82

a_1c_1-$b_2\delta_1\alpha_3\gamma_1\beta_3\varepsilon_1$ about two thirds of the synthesised protein would not be assembled into the enzyme complex. So this explanation seems to be unlikely on the teleological grounds of economy in a rapidly growing prokaryote.

Non-coordinacy cannot be explained in terms of internal promoters. These would give rise to shorter transcripts; this would lead to greater numbers of proteins encoded in the distal part of the operon. Nor can it be explained by a fraction of the ribosomes falling off the transcript as they move alone as this would favour production of proteins in the proximal part of the operon. Another transcriptional regulation model proposed that non-coordinacy in λ morphogenetic genes could be explained by selective inactivation either by differential chemical decay or differential functional inactivation of transcripts. However, both possibilities were subsequently eliminated [58,60].

It is more likely that regulation occurs post-transcriptionally [61]. A priori a number of regulatory mechanisms operating at the level of translation can be envisaged. They are discussed below in relation to the *unc* operon.

Regulation during initiation of translation. The importance of mRNA-rRNA interactions in initiation of translation has been emphasised by Steitz

[59]. Efficiency of translation has been correlated with the stability of the interaction and the spacing between initiation codon and Shine and Dalgarno sequence. The features of these regions in the *unc* operon have been described above (subsection IIIB-1), but comparison of them provides no coherent explanation of uncoordinacy. The interaction between mRNA and rRNA can be influenced by secondary structures in rRNA, which may be long range and so difficult to analyse. However, local interactions (hairpins) in the vicinity of the ribosome binding site have been shown to influence translation initiation strongly. For example, a mutation in expression of he lambda receptor resulting in a 10-fold decrease in its expression has been shown to stablise an mRNA secondary structure that sequesters the initiation codon [62].

In the *unc* operon possible hairpin secondary structures in mRNA are found in the vicinity (-20 basepairs) of the initiation codon of the α and γ genes. These are illustrated in Fig. 12. Two structures could form upstream of the α gene. One (Fig. 12a) is within the δ coding region; the other (Fig. 12b) is more extensive ($\Delta G_1 = -131.1$ kJ) and encompasses the δ termination codon as well as the Shine and Dalgarno sequence. Its influence (if any) in translational of this part of the *unc* operon is unclear. However, if it were to stabilise mRNA : rRNA interaction, then it might be expected to increase translation efficiency of the γ gene.

In the RNA phage R17 an intercistronic hairpin structure is the site of recognition of a protein acting as a translational repressor: coat protein stabilises a preformed RNA secondary structure in which replicase initiation codon and Shine and Dalgarno sequence are sequestered [59]. Similar examples are found in Qβ [59]. However, in order to be recognised by protein translational repressors a segment of RNA need not necessarily form a hairpin; gene 32 protein in phage T4 represses its own translation probably by competing for ribosome attachment [63].

Another possible function for secondary structures in translation initiation is to serve as RNAseIII processing sites. In bacteriophage T7 it is thought that the secondary structures surrounding these sites prevent ribosomes from attaching to this region. Attack by RNAseIII makes them accessible to ribosomes and allows translation to proceed [59]. The role of the secondary structures in the *unc* operon (Fig. 12) is as yet undefined. However, it seems likely that they are important in regulation of the operon.

Regulation during elongation. Differences in the rate of elongation of polypeptide chains from different cistrons during protein synthesis would lead to the synthesis of unequal amounts of proteins from a polycistronic message. How can this be arranged?

Ikemura [64] has shown that the abundancies of tRNAs and the frequency of most cognitive codons correlate in *E. coli.* The most frequently used codons correspond to the most abundant tRNA species and vice versa. Furthermore, a linear relationship is found between the relative usage of codons within a codon family and the relative abundancies of the corresponding anticodons. Grantham [65] has proposed that the genomic strategy of a bacterial cell is probably a reflection of this correlation: the protein synthesising machinery as a whole has evolved to maximise when necessary the efficiency of output. Gouy and Grantham [66] have presented a dynamic model of protein synthesis which emphasises the importance of codon/anticodon recognition, and of their relative concentrations, for the general efficiency of the process. Bacterial genes which produce different amounts of proteins seem to use the degenerate genetic code in quantitatively different ways. Thus the use of the genetic code (and the tRNA pool) may constitute a means of modulation of gene expression. The presence of rare codons will slow down the elongation process, leading to stuttering; their absence ensures a smooth synthesis.

We have tested this model by examination of codon usage (Table IV) in some of the *unc* genes [67]. The codons of genes for γ, δ and ε (one copy of each per ATP-synthase complex) were summed and compared with the genes for the α and β subunits (three copies of each per ATP-synthase complex). In twelve codon families (for the amino acids arginine, leucine, serine, threonine, proline, glycine, isoleucine, lysine, glutamic acid, asparagine, glutamine and phenylalanine) a strong preference for particular codons and a clear avoidance

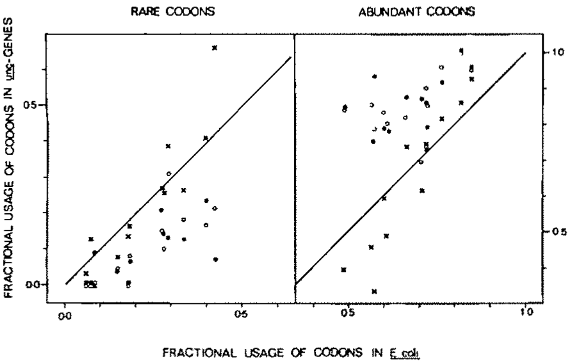

Fig. 13. Comparison of fractional usages of selected rare and abundant codons in the genes for α, β, γ, δ and ε subunits of *E coli* ATP-synthase with fraction usage of the same codons in 49 *E. coli* genes [65,67]. The straight line represents the mean *E coli* usage Codons in genes for α (●); β (○); $\gamma + \delta + \varepsilon$ (×).

of others was noted. (In the remaining codon families no polarisation was observed and so these families were omitted from calculations.) This allowed us to define two categories of codon 'abundant' and 'rare' (see legend to Fig. 13). As observed previously abundant codons correspond to the most abundant iso-accepting tRNAs and vice versa. The abundance or rarity of a codon or tRNA does not, of course, tell us anything about the kinetics of the codon/anticodon interaction; however, as Grantham et al. [65] have pointed out, the most abundant codons often have U or A in the variable third position, which could result in 'intermediate' binding energies and a rapid turnover. Grosjean and Fiers [68] have emphasised that efficient translation requires codon/anticodon interaction with intermediate strength (optimal energy). In MS2 this is a strong influence in selection of synonymous codons.

Fig. 13 shows a comparison of fractional codon usage for twelve amino acids in the genes for F_1 polypeptides compared with the fractional usage of the same codons in 49 published *E. coli* genes. The γ, δ and ε genes seem to use codons in much

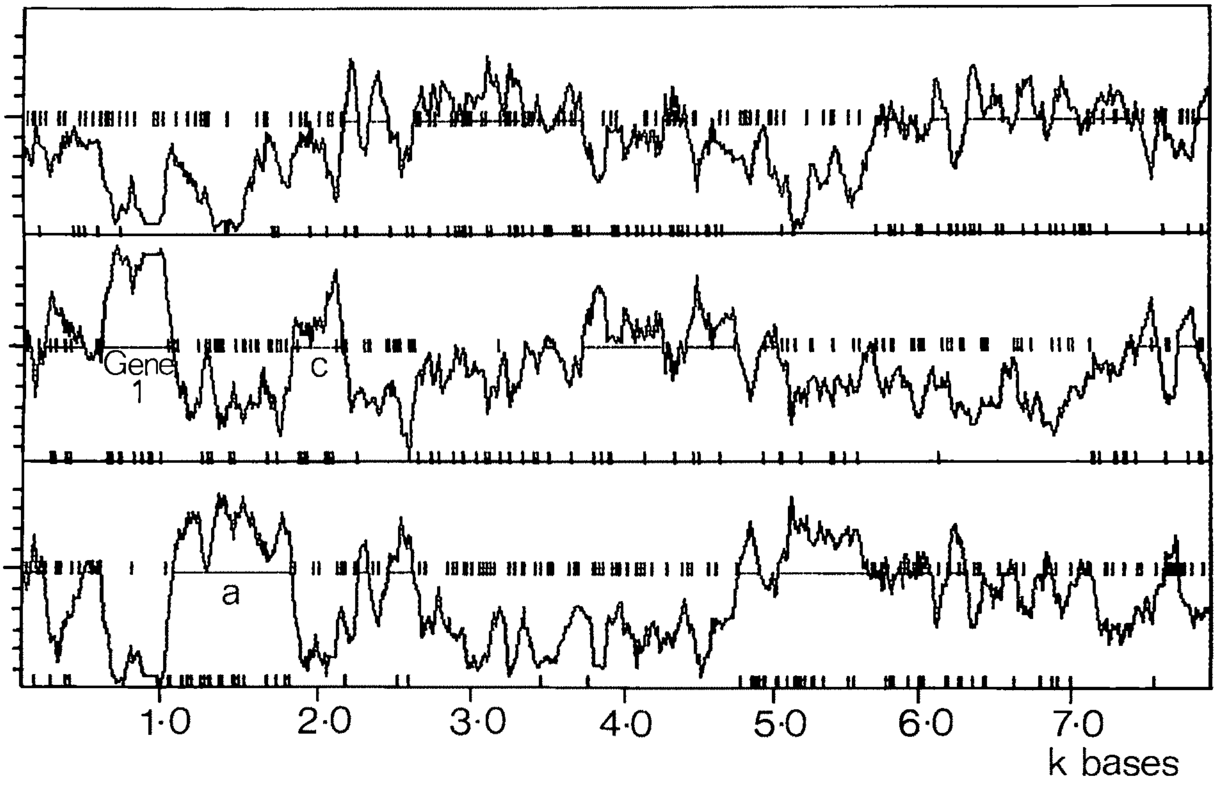

Fig. 14. Comparison of codon usage in gene 1 with other genes in *unc* operon using FRAMESCAN (see Fig. 4) [67].

the same way as an average *E. coli* gene. By contrast, the codon usage in the genes for α and β subunits shows a statistically significant preference for the most abundant variant of the codons and conversely an avoidance of the rare ones [67]. So this analysis suggests codon usage may influence the rates of production of the F_1 subunits. At our present level of understanding it does not provide a clear quantitative explanation for unco-ordinary in the genes for F_1 units.

Another aspect of codon usage is the use of very rare codons, gene 1 being very remarkable in this respect. For example, it contains four AUA isoleucine codons and two CGG arginine codons (Table IV). This difference in its codon usage as compared with the rest of the *unc* operon is illustrated by the two FRAMESCANS calibrated for the α gene and gene 1, respectively. Gene 1 is not well detected in the former, and much of the rest of the operon is not clearly detected by the latter (Fig. 14). It has been suggested that genes that need not be highly expressed might have accumulated rare codons. Other examples are the genes for *Eco*RI endonuclease and methylase [69,70].

V. Interpretation of protein sequences

A summary of the known functions of the various subunits of ATP-synthase is presented in Table V.

In an attempt to understand more about the structure and function of the enzyme we have used a number of computer methods as an aid to interpretation of the protein sequences of the eight subunits [67]. These include a method described by McLachlan [71] employed to predict secondary structures for the F_1 subunits and for the F_0 subunit b, the majority of which appears not to be buried in the lipid bilayer. We have not applied it to the hydrophobic subunits a and c nor to the gene 1 product which is also hydrophobic. Experience has shown that this and related methods that depend upon a database derived from globular proteins are unreliable and misleading when applied to membrane proteins (e.g., they wrongly predict extensive β structures in bacteriorhodopsin). Here we have preferred to inspect the sequences in order to try and discern segments of sequence, for example, that might form α-helices to span the lipid bilayer (as in bacteriorhodopsin [72] and cytochrome oxidase subunit II [73]). These segments would typically contain about 25–30 largely non-polar amino acids. This can form an α-helix sufficiently long to traverse a membrane 6 nm thick [72,74]. These helical segments tend to be bounded by proline residues, and polar residues are most often found in the intervening segments near the membrane boundaries. Latterly, we have also applied to the membrane proteins a computer program HYDROPLOT using an algorithm described by Kyte and Doolittle [75] to calculate the hydropathy along the sequence. These calculations are consistent with assignments made by visual inspection. A third program, DIAGON [76], has been employed to search for internal protein sequence duplications, to look for homologies between subunits and in the case of the α and β subunits to search for homologies with other enzymes that employ nucleotides in catalysis. The results of these calculations and conclusions based upon them are discussed in the following section.

TABLE V

FUNCTIONS OF ATPase SUBUNITS

Subunit	Function	Reference
α	Nucleotide binding	97–99
β	Nucleotide binding, catalysis	4,85,97–99
γ	Gates proton channel	86,87
δ	Interacts with α and possibly b	83,87–90
ε	Interacts with γ and possibly b	36,83
a	Proton channel? part of	118
b	Proton channel/, binds F_1	83,84
	membrane sector	79
c	Proton channel	

VA. F_0 subunits

VA-1. Subunit a

The largest F_0 subunit, *a*, is homologous to the mitochondrially coded ATP-synthase subunit ATPase-6. Alignment of the four mitochondrial proteins with the *E. coli* subunit *a* (Fig. 5) demonstrates that homology is confined to the C-terminal region of the proteins, and no convincing sequence homology can be detected in the N-terminal regions. Nonetheless, both bacterial and mitochondrial proteins have remarkably similar hydropathy profiles (Fig. 15) throughout their sequences. That for the *E. coli* protein shows seven distinct hydrophobic regions I–VII; all except II have counterparts in the mitochondrial proteins. In the latter proteins, region II appears to be less hydrophobic than in the bacterial protein. Regions I and III–VI are of lengths (27–28 residues) consistent with their being able to form transmembranous α-helices and the mitochondrial proteins would be expected to be similarly folded. Region II is less clear. It is conceivable that it also could traverse the membrane, although this would place a number of charged residues within the bilayer. Alternatively, it could form an external loop near the surface of the membrane. An important consequence of this uncertainty is that it is not possible to decide if the amino and carboxyl terminals are on the same or opposite sides of the bilayer.

The bacterial protein also appears to be significantly longer than the mitochondrial homologues, on the basis of its gene sequence. However, until the amino terminal sequence of protein *a* has been established, uncertainty must persist about the significance of this extension in the bacterial ATP-synthase complex.

A number of amino acids (underlined in boxes in Fig. 5) are conserved in all five proteins. Presumably, they must be particularly important for structural integrity in making important contacts or for the function of the enzyme, or both. Of particular interest among these is glutamic acid-198 (Fig. 5) which, according to the folding model (Fig. 16), would be within the bilayer possible able to contribute to proton translocation. Another residue that conceivably could be important is Tyr-278, given that tetranitromethane and iodination have been reported to abolish proton translocation [77,78]. Other conserved residues cluster in helices VI and VII and may be important in contacting conserved regions in other subunits.

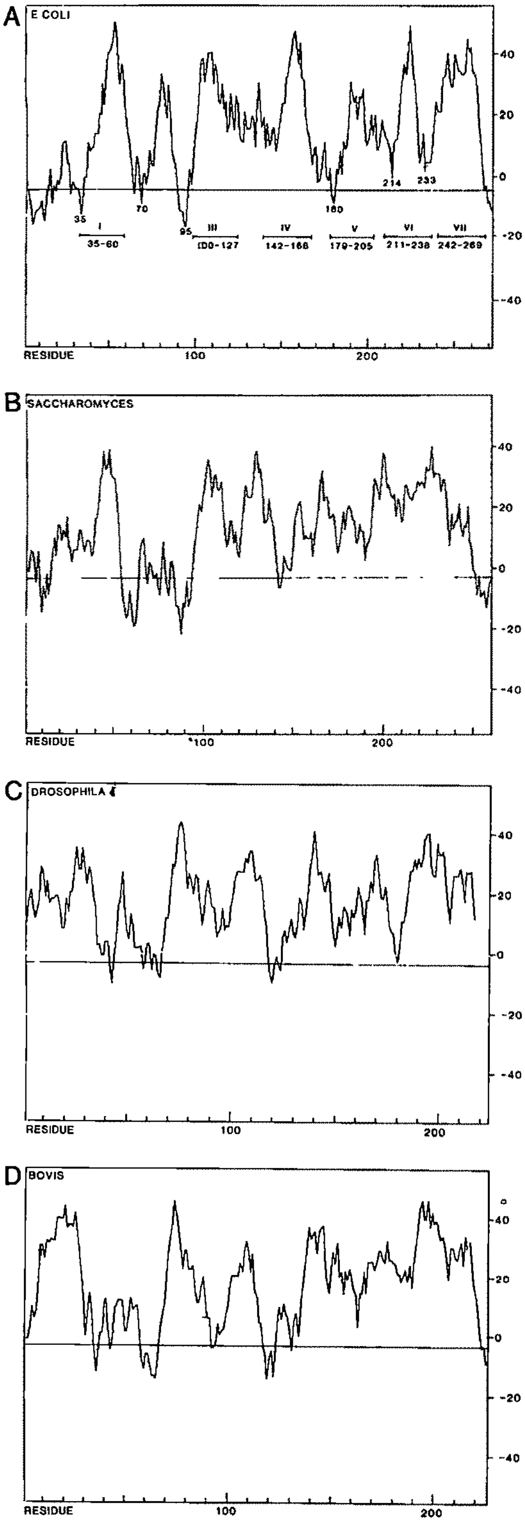

Fig. 15. Hydropathy profiles of (A) *E. coli* subunit a compared with those of equivalent subunits from three mitochondria [67]. (B) *Saccharomyces cerevisiae*, (C) *Drosophila melanogaster*, (D) cow. The sequence is plotted along the horizontal axis. The vertical axis is a measure of hydrophobicity [75] calculated with a span of 11. In (A) I and III–VII represent regions of sequence proposed to form transmembrane α-helices.

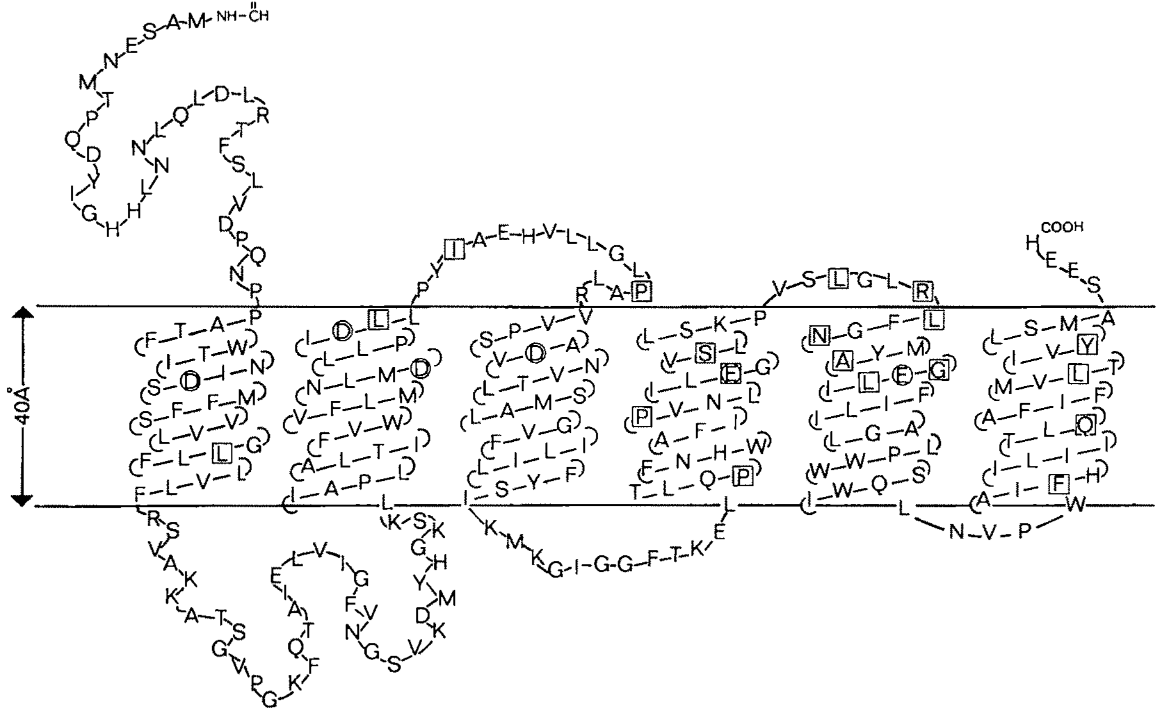

Fig. 16. Proposed path of polypeptide in *E. coli* subunit a [67]. The horizontal lines represent the extent of the lipid bilayer. Proposed transmembranous segments are plotted on α-helical surfaces with 3.5 residues per turn. The segments within the bilayer correspond to segments I and II–VII in Fig. 15. Segment II is shown here outside the membrane, but may also form a transmembrane helix (see text). Residues conserved in all species are boxed, charged residues within the bilayer are encircled

The model for bacterial protein *a* also places six acidic residues (Fig. 15) within but near to the surface of the membrane. However, this feature is not found in the mitochondrial subunit (ATPase-6) and so may not be of functional significance.

VA-2. Subunit c

Comparison of the sequence of *E. coli* subunit c with counterparts from mitochondrial and chloroplasts (Fig. 17) demonstrates a wide sequence diversity similar to that described above in subunit *a*. Although the proteins are clearly homologous, sequence is strictly conserved in only six places (see Fig. 17). However, residue 66 (Asp or Glu) is functionally most important; in the native complex this acidic residue reacts with DCCD [79], thereby blocking proton translocation. That a carboxyl moiety at this point is essential for proton translocation has been emphasised by the finding that a substitution of aspartic acid to asparagine in the *E. coli* protein leads to a non-functional proton channel [80].

Evidence for the oligomeric nature of protein c is derived from inhibition experiments with DCCD and from measurements of radioactivity incorporated into subunit c relative to other subunits. Sebald and Hoppe [79] estimate five to seven copies of the c subunit in the mitochondrial enzyme complex and favour a hexameric arrangement. Recent measurements with the bacterial complex indicate 10 ± 1 copies of c per complex [5]. An interesting observation is that modification by DCCD of a sixth of the total potential sites causes total inhibition of the enzyme. This can be interpreted as showing that the oligomer and not the monomer is essential for proton translocation. Other authors have suggested that subunit c folds into a hairpin structure in the membrane (see [79]), an idea supported by the hydropathy profile (Fig. 18). This illustrates that the sequence has two

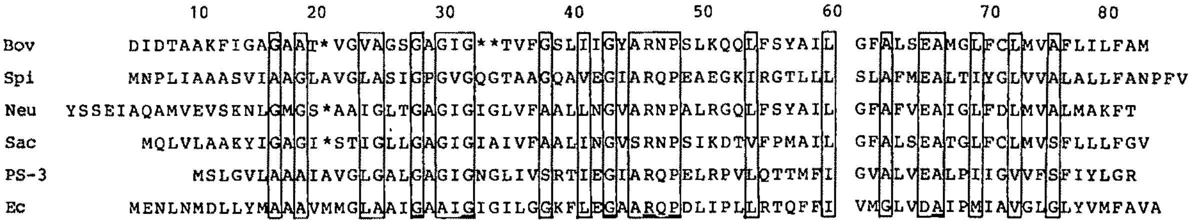
10
20
30
40
50
60
70
80
Bov DIDTAAKFIGAGAAT*VGVAGSGAGIG**TVFGSLIIGYARNPSLKQQLFSYAIL GFALSEAMGLFCLMVAFLILFAM
Spi MNPLIAAASVIAAGLAVGLASIGPGVGQGTAAGQAVEGIARQPEAEGKIRGTLLL SLAFMEALTIYGLVVALALLFANPFV
Neu YSSEIAQAMVEVSENLGMGS*AAIGLTGAGIGIGLVFAALLNGVARNPALRGQLFSYAIL GFAFVEAIGLFDLMVALMAKFT
Sac MQLVLAAKYIGAGI*STIGLLGAGIGIAIVFAALINGVSRNPSIKDTVFPMAIL GFALSEATGLFCLMVSFLLLFGV
PS-3 MSLGVLAAAIAVGLGALGAGIGNGLIVSRTIEGIARQPELRPVLQTTMFI GVALVEALPIIGVVFSFIYLGR
Ec MENLNMDLLYMAAAVMMGLAAIGAAIGIGILGGKFLEGAARQPDLIPLLRTQFFI VMGLVDAIPMIAVGLGLYVMFAVA

Fig. 17. Comparison of the sequence of *E. coli* subunit c with counterparts from other sources, *Bov*ine mitochondria, *spi*nach chloroplasts, *Neurospora crassa* and *Saccharomyces cerevisiae* mitochondria, thermophile PS-3 and *E. coli* [79]. Conservative substitutions preserved in all species are boxed, identities are underlined.

hydrophobic segments linked by a conserved hydrophilic sequence containing proline. The other two conserved sequences are found in the middle of the two arms. The C-terminal arm may well form a transmembrane α-helix (boxed residues in Fig. 19) but the secondary structure of the N-terminal arm is more problematical. The alternation of glycine and alanine residues is more reminiscent of a β-sheet than an α-helix. If so, the carbonyls and amides in the polypeptide backbone would need to accept and donate hydrogen bonds, preferably with another β-sheet structure. This may be of greater significance when it is remembered that the enzyme complex probably contains 6–10 copies of protein [5,79]. Six β-strands, for example, could form a β-barrel motif similar to that found in immunoglobulins and Cu/Zn superoxide dismutase [81].

Loo and Bragg [82] have provided evidence that part of protein c is exposed in F_1 depleted membrane. This site appears to be close to the F_1 binding site and so is on the cytoplasmic surface of the membrane. It seems likely that this exposed region corresponds to the N- or C-terminal region (or both) or the proposed bend in the middle of the polypeptide chain.

VA-3. Subunit b

The sequence of the *E. coli* protein is very striking and shows it to be an amphiphilic protein [24]. It is hydrophobic around the N-terminus and highly charged in the remainder (Fig. 20). We have proposed a model in which the N-terminal segment lies within the membrane and the rest outside [83]. In this model the N-terminal region forms a single transmembrane α-helix making contacts with *a* and *c*. The extramembrane section contains two adjacent stretches of 31 amino acids

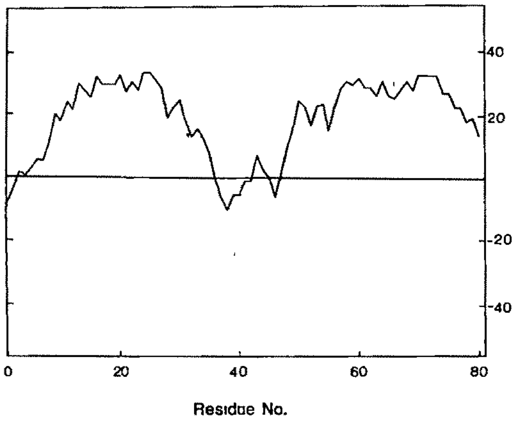

Fig. 18. Hydropathy profile of subunit *c* of *E. coli* ATP-synthase [67].

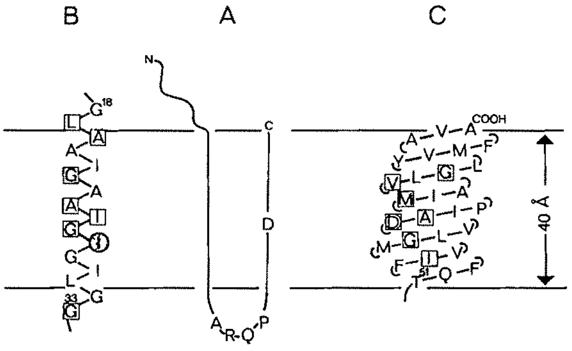

Fig. 19. Path of the polypeptide in *E coli* ATP-synthase subunit c. (A) The hydropathy profile suggests a hairpin structure with N- and C- terminals on the same side of the membrane. (B) Residues 18–33 are drawn as a single strand of a β-sheet. (C) shows the C-terminal part plotted on an α-helical surface. Residues in boxes are conserved. The encircled aspartic acid residue is that modified by DCCD.

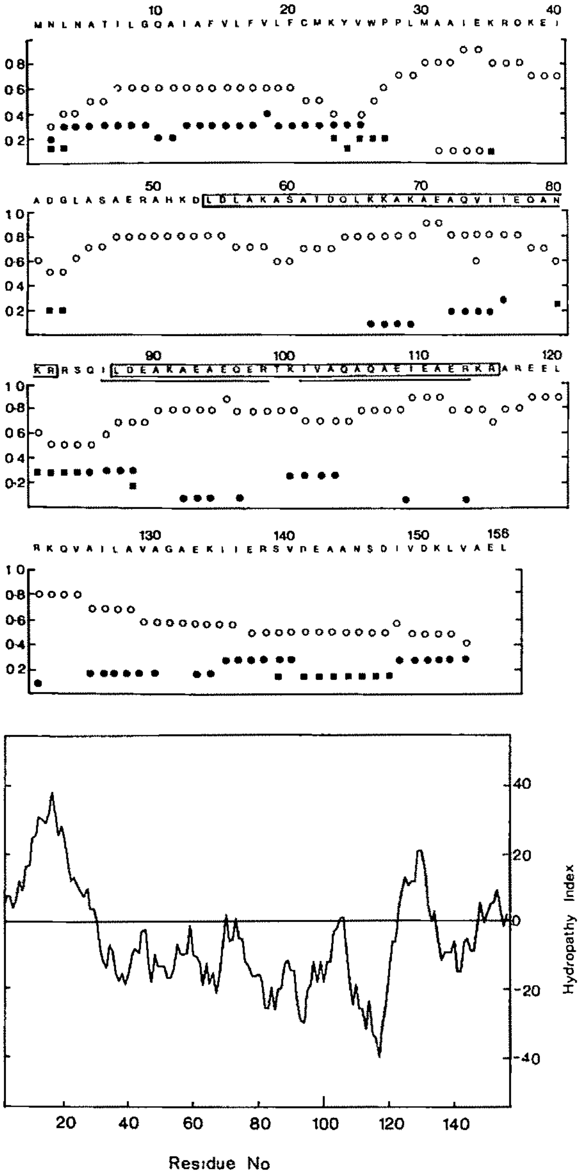

Fig. 20. (a) Amino acid sequence of subunit *b* and its predicted secondary structure. The secondary structure is predicted from the primary sequence using a program described by McLachlan [71]. The boxes under the sequence show probabilities (vertical scale) of residues forming an α-helix (●), β-sheet (○) or β-bend (△). Boxed sequences represent related sequences (the long repeat); underlined segments in the second box are also related to each other (the short repeat). (b) Hydropathy profile of subunit *b*.

of related sequence (the long repeat); within the second of these a further internal homology has been detected (the short repeat, see Fig. 21). It is proposed that these duplicated stretches of polypeptide fold into two α-helices with many common features able to make contacts with F_1 subunits. It would be expected to make important contacts with the δ and ε subunits in particular, since it is known that they are required for binding of F_1 to F_0. The amino acid compositions of these interacting segments in b support the view that their interactions with F_1 will be α-helix rather than α-helix to β-sheet. This is consistent with the high α-helicity of δ proposed from optical measurements of the subunits from thermophile PS3 F_1-ATPase and also predicted from its primary sequence (see below). Hoppe et al. [84] reported that *E. coli* protein b in F_1-depleted membranes is very sensitive to proteolytic degradation and F_1 protects b in these membranes from proteolysis. Additionally, a photoreactive hydrophobic phospholipid derivative reacts with Lys-21. These experiments support the model for b proposed above.

Thus, protein b appears to occupy a central position in the ATP-synthase complex in providing a structural link between F_1 and F_0. In this position it may also be important in H^+ translocation as well as in biosynthetic assembly.

VB. F_1 subunits

The functional properties of F_1 subunits have been discussed recently by Fillingame [4] and are summarised in Table V. Briefly, α and β both contain nucleotide binding sites. It has been suggested that β contains the catalytic sites of the enzyme (evidence summarised by Futai and Kanazawa [85]). However, point mutations in α or β result in loss of ATPase activity, and so α also plays an important role. This is emphasised by the finding that the sequences of α and β are homologous and therefore will have very similar protein folds. In the following section we discuss the significance of this homology and describe attempts to delineate sequences important for binding nucleotides.

On the basis of protein sequences little can be said either about the role proposed for γ as a gate for H^+ flux [86,87] or about its function as an organiser of assembly of γ and β subunits [86]. Both δ and ε are required for binding F_1 to F_0 and in *Thermus* PS3 bind in an unordered sequence to

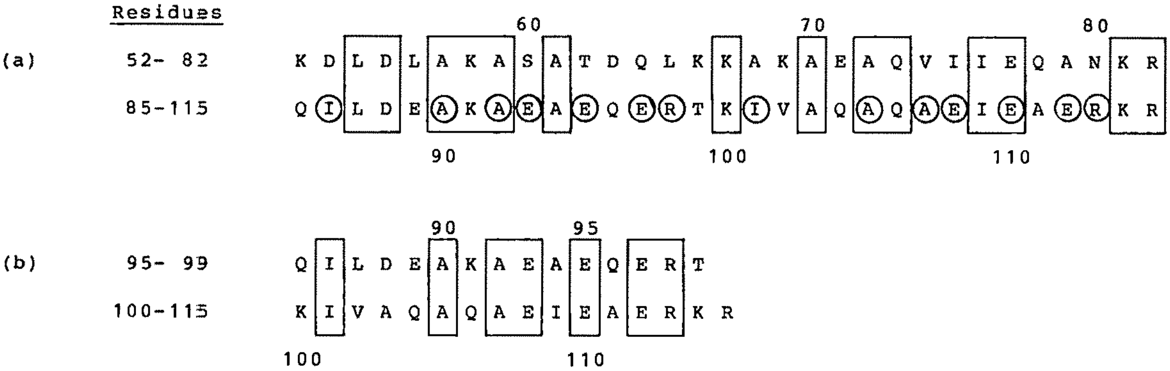
Residues
60
70
80
(a)
52- 82
K D L D L A K A S A T D Q L K K A K A E A Q V I I E Q A N K R
85-115
Q I L D E A K A E A E Q E R T K I V A Q A Q A E I E A E R K R
90
100
110
90
95
(b)
95- 99
Q I L D E A K A E A E Q E R T
100-115
K I V A Q A Q A E I E A E R K R
100
110

Fig. 21. Alignment of repeated sequences in protein b. (a) The long repeats, (b) the short repeats; identities are boxed. In (a), the 14 residues conserved in (b) are encircled; of these, four residues are conserved in both (a) and (b).

$\alpha\beta\gamma$ to form F_1 now able to bind to F_0 [87–90]. This function is discussed below in relation to the way in which they may interact with the F_0 subunit b.

VB-1. α and β subunits

The importance of the β subunit in the F_1-ATPase complex is emphasised by the high degree of sequence conservation between *E. coli* bovine mitochondria and maize and spinach chloroplasts (see Fig. 22 and Table VI). These include conserved residues identified in chemical labelling studies as being important in catalysis. Thus labelling of Tyr-385 (see Fig. 22) of the bovine enzyme with *p*-fluorosulphonyl [^{14}C]benzoyl-5′-adenosine inactivated F_1-ATPase [91]. The F_1-ATPase is also inactivated by DCCD. In the bovine enzyme, the label was located at Glu-215 [92]; the label in TF_1 inactivated with DCCD was localised to a glutamic acid residue in a peptide identical to residues 200–205 of the *E. coli* protein [93].

Sequence studies of the bovine α subunit show

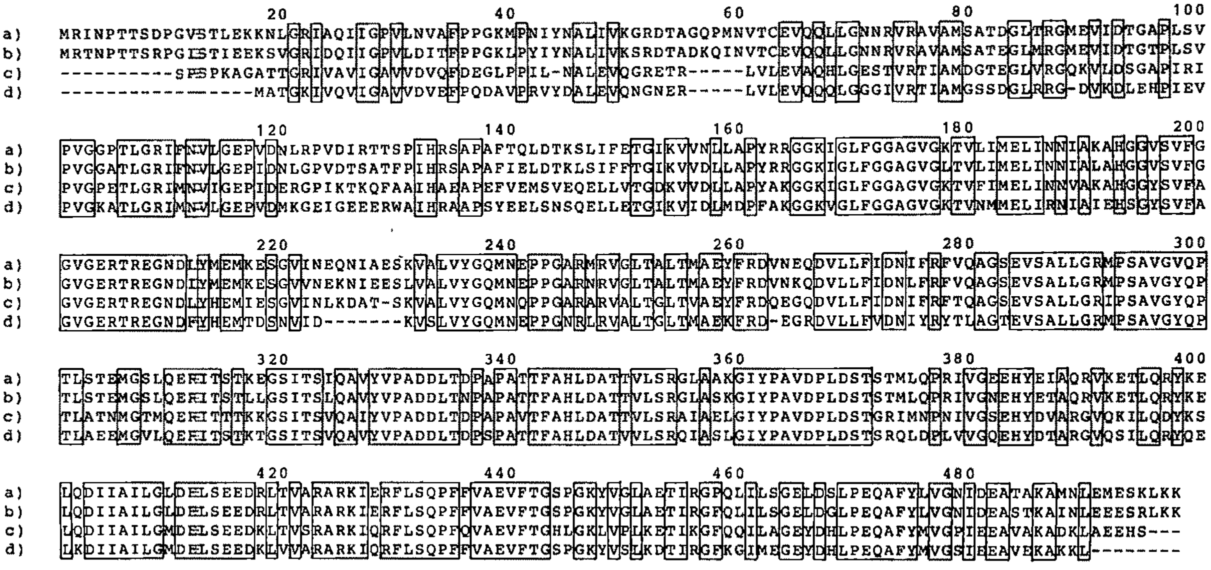
20 40 60 80 100
a) MRINPTTSDPGVSTLEKKNLGRIAQIIGPVLNVAFPPGKMPNIYNALIVKGRDTAGQPMNVTCEVQQLLGNNRVRAVAMSATDGLTRGMEVIDTGAPLSV
b) MRTNPTTSRPGISTIEEKSVGRIDQIIGPVLDITFPPGKLPYIYNALIVKSRDTADKQINVTCEVQQLLGNNRVRAVAMSATEGLMRGMEVIDTGTPLSV
c) ----------SFSPKAGATTGRIVAVIGAVVDVQFDEGLPPIL-NALEVQGRETR-----LVLEVAQHLGESTVRTIAMDGTEGLVRGQKVLDSGAPIRI
d) ------------------MATGKIVQVIGAVVDVEFPQDAVPRVYDALEVQNGNER-----LVLEVQQQLGGGIVRTIAMGSSDGLRRG-DVKDLEHPIEV
120 140 160 180 200
a) PVGGPTLGRIFNVLGEPVDNLRPVDIRTTSPIHRSAPAFTQLDTKSLIFETGIKVVNLLAPYRRGGKIGLFGGAGVGKTVLIMELINNIAKAHGGVSVFG
b) PVGGATLGRIFNVLGEPIDNLGPVDTSATFPIHRSAPAFIELDTKLSIFFTGIKVVDLLAPYRRGGKIGLFGGAGVGLTVLIMELINNIALAHGGVSVFG
c) PVGPETLGRIMNVIGEPIDERGPIKTKQFAAIHAEAPEFVEMSVEQELLVTGDKVVDLLAPYAKGGKIGLFGGAGVGKTVFIMELINNVAKAHGGYSVFA
d) PVGKATLGRIMNVLGEPVDMKGEIGEEERWAIHRAAPSYEELSNSQELLETGIKVIDLMDPFAKGGKVGLFGGAGVGKTVNMMELIRNIAIEHSGYSVFA
220 240 260 280 300
a) GVGERTREGNDLYMEMKESGVINEQNIAESKVALVYGQMNEPPGARMRVGLTALTMAEYFRDVNEQDVLLFIDNIFRFVQAGSEVSALLGRMPSAVGVQP
b) GVGERTREGNDIYMEMKESGVVNEKNIEESLVALVYGQMNEPPGARNRVGLTALTMAEYFRDVNKQDVLLFIDNLFRFVQAGSEVSALLGRMPSAVGYQP
c) GVGERTREGNDLYHEMIESGVINLKDAT-SKVALVYGQMNQPPGARARVALTGLTVAEYFRDQEGQDVLLFIDNIFRFTQAGSEVSALLGRIPSAVGYQP
d) GVGERTREGNDFYHEMTDSNVID-------KVSLVYGQMNEPPGNRLRVALTGLTMAEKFRD-EGRDVLLFVDNIYRYTLAGTEVSALLGRMPSAVGYQP
320 340 360 380 400
a) TLSTEMGSLQERITSTKEGSITSIQAVYVPADDLTDPAPATTFAHLDATTVLSRGLAAKGIYPAVDPLDSTSTMLQPRIVGEEHYEIAQRVKETLQRYKE
b) TLSTEMGSLQERITSTLLGSITSLQAVYVPADDLTNPAPATTFAHLDATTVLSRGLASKGIYPAVDPLDSTSTMLQPRIVGNEHYETAQRVKETLQRYKE
c) TLATNMGTMQERITTTKKGSITSVQAIYVPADDLTDPAPAVTFAHLDATTVLSRAIAELGIYPAVDPLDSTGRIMNPNIVGSEHYDVARGVQKILQDYKS
d) TLAEEMGVLQERITSTKTGSITSVQAVYVPADDLTDPSPATTFAHLDATVVLSRQIASLGIYPAVDPLDSTSRQLDPLVVGQEHYDTARGVQSILQRYQE
420 440 460 480
a) LQDIIAILGLDELSEEDRLTVARARKIERFLSQPFFVAEVFTGSPGKYVGLAETIRGPQLILSGELDSLPEQAFYLVGNIDEATAKAMNLEMESKLKK
b) LQDIIAILGLDELSEEDRLTVARARKIERFLSQPFFVAEVFTGSPGKYVGLAETIRGFQLILSGELDGLPEQAFYLVGNIDEASTKAINLEEESRLKK
c) LQDIIAILGMDELSEEDKLTVSRARKIQRFLSQPFQVAEVFTGHLGKLVPLKETIKGFQQILAGEYDHLPEQAFYMVGPIEEAVAKADKLAEEHS---
d) LKDIIAILGMDELSEEDKLVVARARKIQRFLSQPFFVAEVFTGSPGKYVSLKDTIRGFKGIMEGEYDHLPEQAFYMVGSIEEAVEKAKKL--------

Fig. 22. Alignment of sequences of β subunits of ATP-synthase from *E. coli* [25], bovine mitochondria [40] and maize [109] and spinach [110] chloroplasts.

TABLE VI

ALIGNMENT OF HOMOLOGOUS SEQUENCES IN α AND β SUBUNITS OF ATP-SYNTHASE AND OTHER ADENINE NUCLEOTIDE BINDING PROTEINS [94]

In A, boxes sequences are identical; in B, the boxes contain either conserved basic or conserved hydrophobic residues The significance of encircled residues is discussed in the text. Ref. a, M. Elzinga, personal communication.

Protein	Residues	Sequence	Ref.
		1 10 20 30	
A Bovine ATPase β	144–173	L A P Y A K G G Ⓚ I G L F – G G A G V G K T V F I M E L I N	40
E coli ATPase β	137–165	M C P F A K G G Ⓚ V G L F – G G A G V G K T V N M M E L I R	25
E. coli ATPase α	156–184	M I P I G R G Q Ⓡ E L I I – G D R Q T G K T A L A I D A I I	23
Adenylate kinase	1–30	M E E K L K K S Ⓚ I I F V V G G P G S G K G T Q C E K I V Q	100
RecA protein	52–84	G A G G L P M G Ⓡ I V E I Y G P E S S G K T T L T L Q V I A	119
Myosin, nematode	156–184	M L Q D H E N Q S M L I T – G E S G A G K T E N T K K V I C	120
Myosin, rabbit	165–193	M L T D R E N Q S I L I T – G E S G A G K T V N T K R V I Q	a
		1 10 20 30	
B Bovine ATPase β	241–270	V A E Y F R D Q E G Q D V L L F I Ⓓ N I F R F T Q A G S E V	40
E coli ATPase β	227–255	M A E K F R D – E G R D V L L F V Ⓓ N I Y R Y T L A G T E V	25
E. coli ATPase α	265–293	M G E Y F R D – R G E D A L I I Y Ⓓ D L S K Q A V A Y R Q I	23
ATP/ADP translocase	275–297	S N V L – R G M G G A F V L V L Y Ⓓ E I K K F V	121
Adenylate kinase	102–130	G E E F E R K – I G Q P T L L L Y V Ⓓ A G P E T M T K R L L	100
Phosphofructokinase	85–113	G I E Q L K K – H G I Q G L V V I G G Ⓓ G S Y Q G A K K L T	122

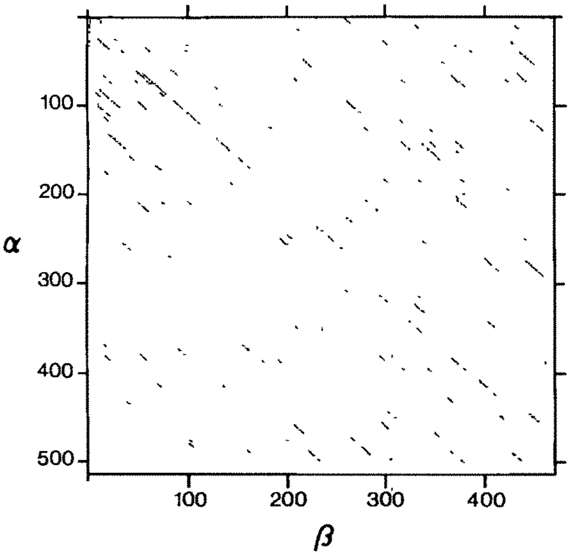

Fig. 23 Comparison of the sequences of the α and β subunits from *E. coli* ATP-synthase [94]. Spans of 19 were used in the calculation with DIAGON.

that it also is very similar to its bacterial counterpart (Tybulewicz, V.L.J. and Walker, J.E., unpublished data).

In contrast, the homology detected between *E. coli* α and β subunits [94] is weak (Fig. 23). It persists throughout most of their peptide chains but is strongest from residues 101–208 (Fig. 24). This homology was not wholly unexpected: antibodies raised to purified β subunits cross-reacted also with α subunits (Gay, N.J., unpublished data), and the similarity of amino acid compositions of α and β had led Harris [95] to postulate sequence similarity between the two proteins.

Studies of other classes of protein, e.g., cytochromes *c*, globins [96] indicate that proteins with related sequences have similar folds. So it is reasonable to expect that α and β will also conform to this rule. Their secondary structures predicted from primary sequences are not entirely concordant, but are generally very similar and support this idea (Fig. 25).

Since α and β have related sequences, and probably a common fold, it is highly likely that they will have common functions. The best defined biochemically is that they both bind adenine nucleotides (for reviews see Refs. 97–99). Therefore, we have tried to identify sequences in α and β that contribute to nucleotide binding by comparison of their sequences with other proteins that employ ATP in catalysis [94]. In this search we

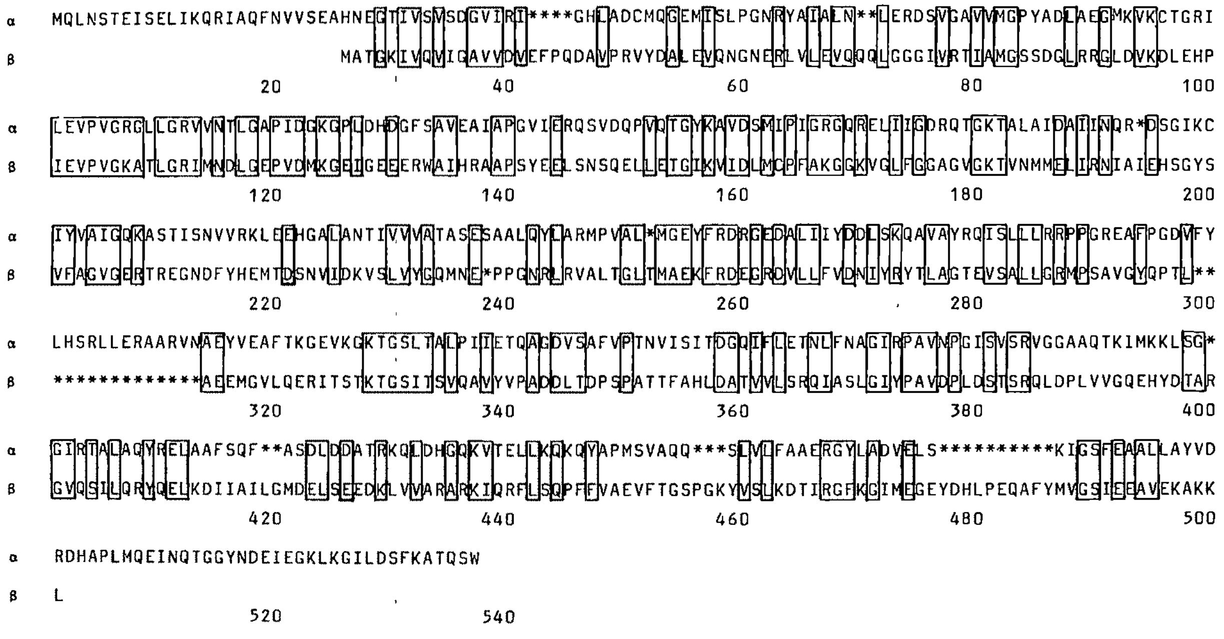

```
α   MQLNSTEISELIKQRIAQFNVVSEAHNEGTIVSVSDGVIRI****GHLADCMQGEMISLPGNRYAIALN**LERDSVGAVVMGPYADLAEGMKVKCTGRI
β                              MATGKIVQVIGAVVDVEFPQDAVPRVYDALEVQNGNERLVLEVQQQLGGGIVRTIAMGSSDGLRRGLDVKDLEHP
                       20                     40                  60                 80                   100

α   LEVPVGRGLLGRVVNTLGAPIDGKGPLDHDGFSAVEAIAPGVIERQSVDQPVQTGYKAVDSMIPIGRGQRELIIGDRQTGKTALAIDAIINQR*DSGIKC
β   IEVPVGKATLGRIMNDLGEPVDMKGEIGEEERWAIHRAAPSYEELSNSQELLETGIKVIDLMCPFAKGGKVGLFGGAGVGKTVNMMELIRNIAIEHSGYS
                      120                    140                 160                180                   200

α   IYVAIGQKASTISNVVRKLEEHGALANTIVVVATASESAALQYLARMPVAL*MGEYFRDRGEDALIIYDDLSKQAVAYRQISLLLRRPPGREAFPGDVFY
β   VFAGVGERTREGNDFYHEMTDSNVIDKVSLVYGQMNE*PPGNRLRVALTGLTMAEKFRDEGRDVLLFVDNIYRYTLAGTEVSALLGRMPSAVGYQPTL**
                      220                    240                 260                280                   300

α   LHSRLLERAARVNAEYVEAFTKGEVKGKTGSLTALPIIETQAGDVSAFVPTNVISITDGQIFLETNLFNAGIRPAVNPGISVSRVGGAAQTKIMKKLSG*
β   *************AEEMGVLQERITSTKTGSIITSVQAVYVPADDLTDPSPATTFAHLDATVVLSRQIASLGIYPAVDPLDSTSRQLDPLVVGQEHYDTAR
                      320                    340                 360                380                   400

α   GIRTALAQYRELAAFSQF**ASDLDDATRKQLDHGQKVTELLKQKQYAPMSVAQQ***SLVLFAAERGYLADVELS***********KIGSFEAALLAYVD
β   GVQSILQRYQELKDIIAILGMDELSEEDKLVVARARKIQRFLSQPFFVAEVFTGSPGKYVSLKDTIRGFKGIMEGEYDHLPEQAFYMVGSIEEAVEKAKK
                      420                    440                 460                480                   500

α   RDHAPLMQEINQTGGYNDEIEGKLKGILDSFKATQSW
β   L
                      520                    540
```

Fig. 24. Alignment of *E. coli* ATP-synthase α and β subunits.

used DIAGON to look for the most similar regions between pairs of proteins. In this way we detected related sequences in α, β and adenylate kinase. Importantly, the sequences in adenylate kinase form part of the AMP binding pocket [100]. Related sequences were also detected in a number of other proteins (Table VI) including myosin in the 25 kDa peptide. This peptide forms part of the S_1 head [101]; chemical labelling studies and proteolysis studies have implicated sequences in it as being important for binding ATP (Ref. 102; see also Yount, R., personal communication). In a third example, phosphofructokinase, the related sequences also form the part of the catalytic site

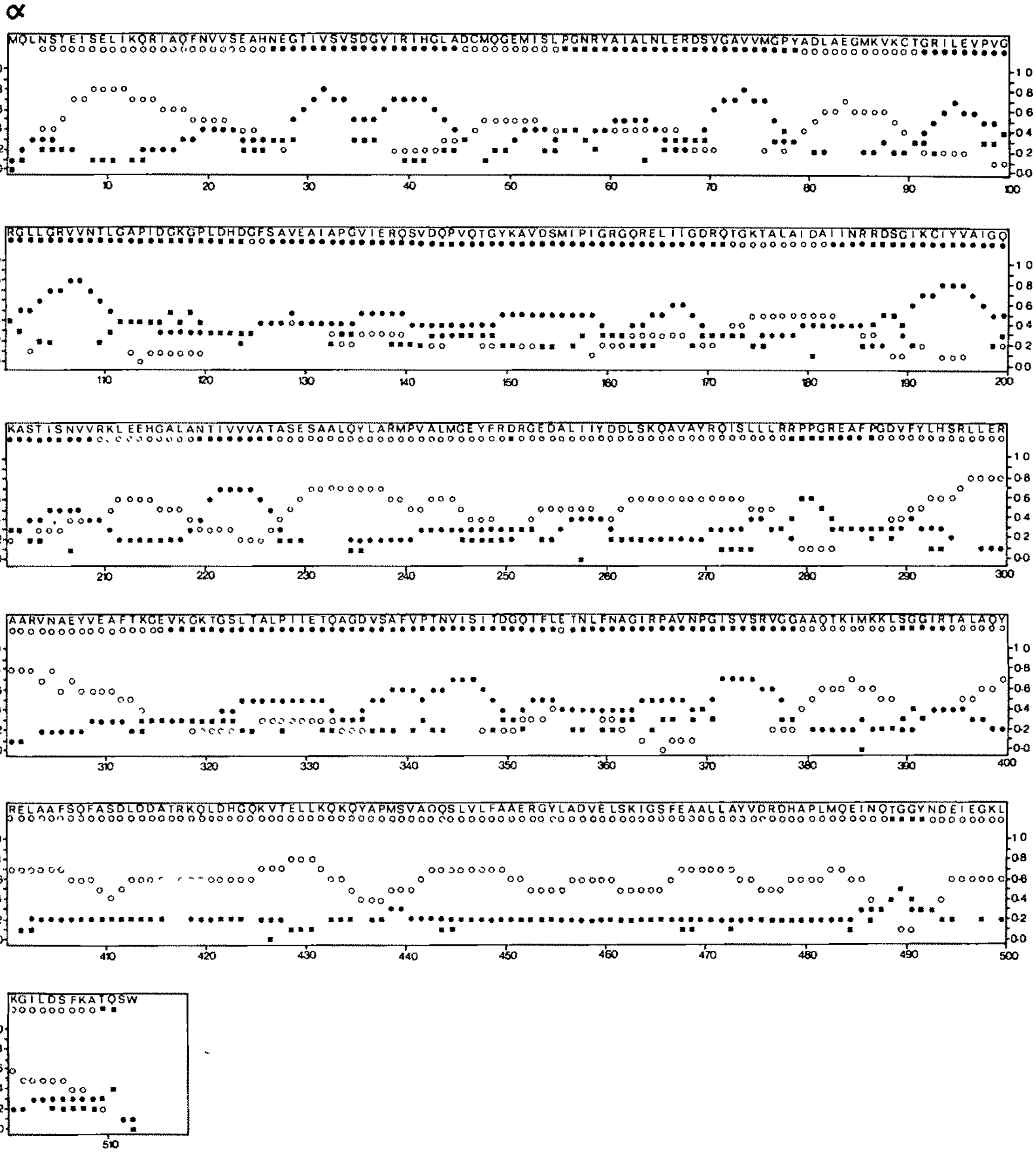

Fig. 25. Secondary structures of *E. coli* ATP-synthase α and β subunits predicted from primary sequence by McLachlan's method [71].

believed to bind ATP [103].

The homologous sequences in α and β detected in this study (listed in Table III) clearly are not the only residues involved in binding adenine nucleotides. This is illustrated by a recent photoaffinity labelling study of F_1-ATPase with 8-azido ATP and 8-azido ADP [104]. Under particular conditions the label can be localised predominantly (about 85%) on the β subunit and causes total inactivation of ATP hydrolysis [105]. Excess of ATP protects against reaction. By chemical degradation the label has been localised in two specific sites. One is in the vicinity of lysine residues 317 and 318 in the bovine enzyme, the other is in the amino terminal arginine peptide (residues 11–22 in Fig. 22c). The region corresponding to N-terminal region of the bovine β protein is largely absent from the bacterial enzyme. It can be removed from the bovine protein by limited proteolysis of BF_1 (Walker, J.E., unpublished data) and so appears to be an exposed tail presumably able to be near the nucleotide binding site of the enzyme. It is not inconceivable that it could be involved in binding the inhibitor protein.

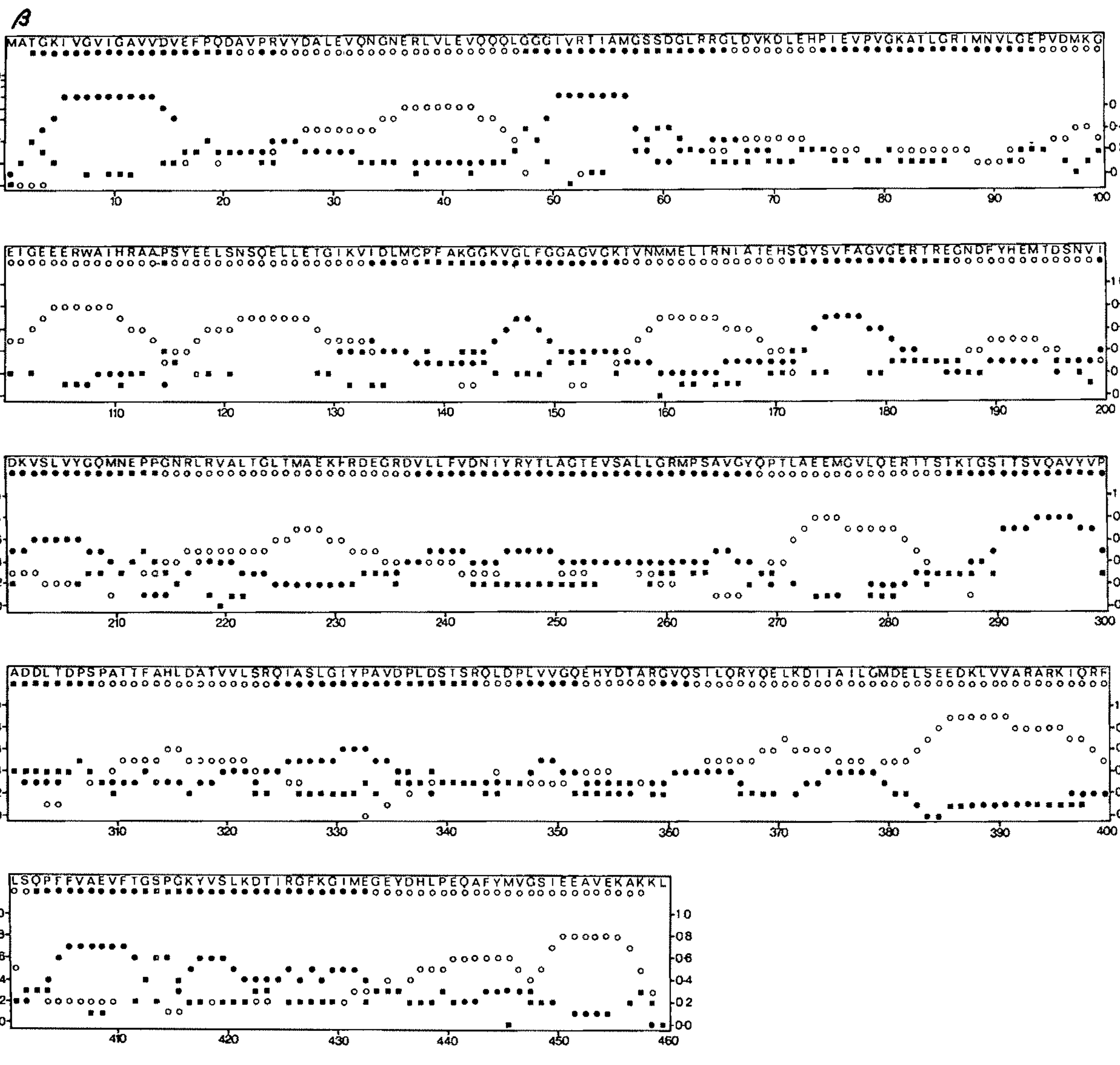

TABLE VII

COMPARISON OF SEQUENCES OF SUBUNITS OF ATP-SYNTHASE FROM *E. COLI* WITH THOSE OF BOVINE MITOCHONDRIA AND CHLOROPLASTS

References: bovine β [40], chloroplast β and ε [109,110], bovine a [123], bovine c [79], chloroplast c [79].

Subunit	Percentage identity	
	E. coli and mitochondria	*E coli* and chloroplast
β	70	65
ε	–	25
a *	24	–
c	21	–

* The bovine mitochondrial subunit a is encoded in mt-DNA and is known also as the ATPase-6 protein. Whilst the region coding for this protein has been identified (by homology with the yeast gene [124]), the N-terminus of the mature protein has not been established, and which of two possible gene starts is actually used remains unknown. In this calculation we have used the gene start point suggested by Anderson et al. [123].

VB-2. γ, δ and ε subunits

Their predicted secondary structures (Fig. 26) are consistent with estimates of α-helicity based upon optical measurements of isolated TF_1 subunits [106]. The high α-helical content of the δ subunit is particularly interesting in relation to subunit interactions with the b protein.

Also of significance is the sequence homology between the C-terminal region of ε, which appears to be α-helical and the repeated sequences in protein b (Fig. 27). Given stoichiometries of $\varepsilon_1 b_2$, this means that the F_1F_0 assembly probably contains five structurally related helices in the region of interaction between F_1 and F_0.

Small regions of homology between γ and ε are also apparent but their significance is obscure. There is, however, no evidence for extensive homologies between the γ, δ and ε subunits.

VB-3. Subunit equivalence

Equivalence of subunits with the same names (α–ε) in *E. coli* and mitochondria is often assumed despite considerable size differences between the δ subunits and between the ε subunits.

Sequence analysis has shown that the δ subunits are not related to each other and so are probably not equivalent in function. Similarly, ε subunits are probably non-equivalent [107]. The available sequence information suggests that the counterpart of the *E. coli* δ subunit is the bovine mitochondrial oscp, a basic protein known to play an important part in binding F_1 to F_0 (Fig. 28) (see Ref. 6). The bacterial δ subunit has a similar role [1]. It is noteworthy that rat liver F_1 and bovine F_1 have been prepared with six subunits [108]. The extra subunit in the rat liver enzyme has a molecular weight of 26500 and has properties in common with the bovine oscp. Complexes diminished in δ have been prepared from *E. coli* [87] and chloroplasts [8]. So it appears that the partitioning of the δ subunit in *E. coli* and chloroplasts or of the oscp in bovine heart (and other) mitochondria during extraction of F_1 is dependent upon the experimental conditions.

The counterpart of bovine δ is probably *E. coli* ε (Fig. 29). Recently, the sequences of a protein homologous to *E. coli* ε has been determined by sequence analysis of fragments of DNA isolated from maize [109] and spinach [110] chloroplasts (Fig. 30). By protein sequence analysis the wheat chloroplast ε protein has been shown to be homologous to these sequences providing confirmation of their identification as CF_1 ε subunits (Fearnley, I.M., Howe, C.J., Gray, J.G. and Walker, J.E., unpublished data). Comparison of the sequences of the bacterial and chloroplast ε proteins (Table VII) shows that they are much less conserved than the β subunits from the same species.

VC. Assembly

VC-1. Gene order and assembly of ATP-synthase

The order of genes in the *unc* operon is striking. It is related to the structure of ATP-synthase in so far as genes for F_0 components a, c and b are clustered at the promoter proximal end and are followed by genes for F_1 subunits in the order $\delta:\alpha:\gamma:\beta:\varepsilon$. It is noteworthy that the order $\beta:\varepsilon$ is also found in chloroplasts [107,108]. Clustering of genes with related functions is a feature of the genetic maps of coliphages (T4, lambda and other phages [111]); in lambda [112], morphogenetic genes for head proteins form a cluster adjacent to a cluster for tail genes; in T4, genes for baseplate head and tail also form clusters. It has been sug-

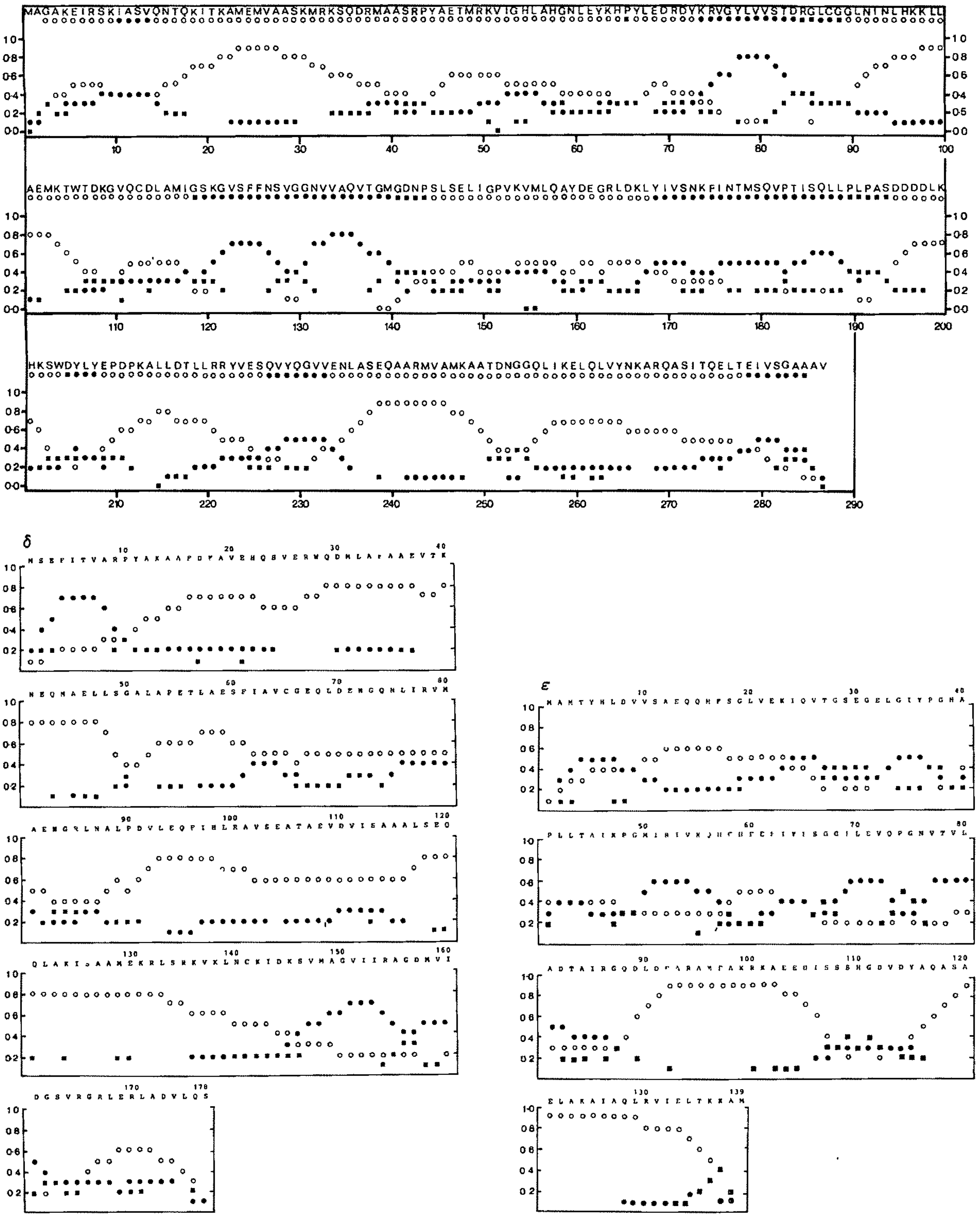

Fig. 26. Secondary structures of *E. coli* ATP-synthase γ, δ and ε subunits calculated from primary sequences as in Fig 22.

gested that these gene clusters might reflect the evolutionary origin of present day assembly genes by tandem duplication and divergence of ancestral assembly genes [113]. In addition, or alternatively, clustering could reflect the selective advantage of minimising recombination between genes for proteins that interact structurally so as to decrease the probability of non-viable hybrids in interstrain matings [113–115]. In lambda, the similarity between the order of action of gene products during assembly (*J, I, L, K, H, G, M, V, U, Z*) and the arrangement of genes in the lambda genome (*J, I, K, L, M, H, G, V, U, Z*) is a particularly

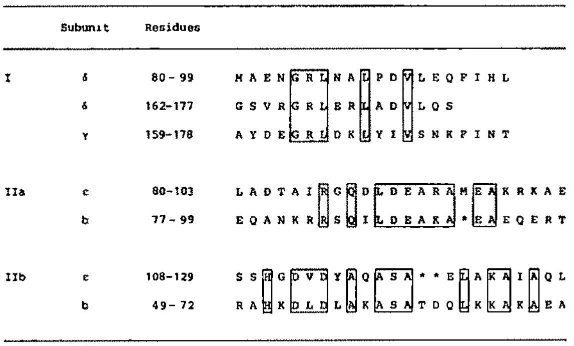

	Subunit	Residues	
I	δ	80 - 99	M A E N G R L N A L P D V L E Q F I H L
	δ	162–177	G S V R G R L E R L A D V L Q S
	γ	159–178	A Y D E G R L D K L Y I V S N K F I N T
IIa	ε	80–103	L A D T A I R G Q D L D E A R A M E A K R K A E
	b	77 - 99	E Q A N K R R S Q I L D E A K A * E A E Q E R T
IIb	ε	108–129	S S H G D V D Y A Q A S A * * E L A K A I A Q L
	b	49 - 72	R A H K D L D L A K A S A T D Q L K K A K A E A

Fig. 27. Homologies between minor subunits of *E coli* ATP-synthase [67].

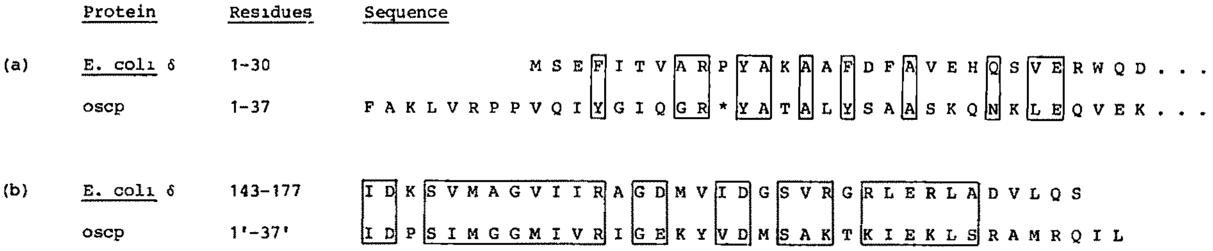

	Protein	Residues	Sequence
(a)	E. coli δ	1–30	M S E F I T V A R P Y A K A A F D F A V E H Q S V E R W Q D . . .
	oscp	1–37	F A K L V R P P V Q I Y G I Q G R * Y A T A L Y S A A S K Q N K L E Q V E K . . .
(b)	E. coli δ	143–177	I D K S V M A G V I I R A G D M V I D G S V R G R L E R L A D V L Q S
	oscp	1'–37'	I D P S I M G G M I V R I G E K Y V D M S A K T K I E K L S R A M R Q I L

Fig. 28. Homologies between *E coli* δ subunit and bovine mitochondrial oligomycin sensitivity conferral protein of F_1F_0 ATPase [107]. In (a) the N-terminal sequences and in (b) the C-terminal sequences are aligned. Identities and conservative substitutions are boxed. *, deletion. Sequences of *E. coli* ε are from [25] and oscp from [130].

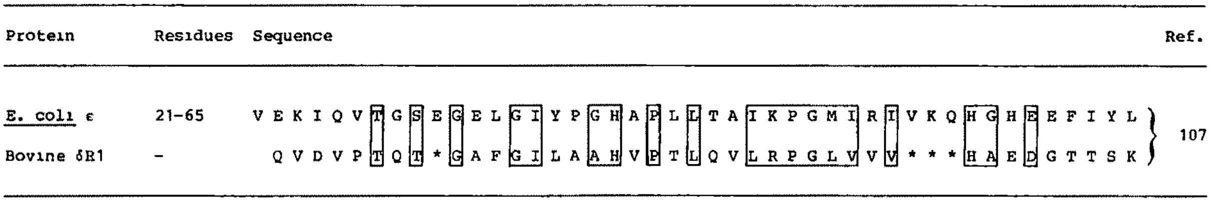

Protein	Residues	Sequence	Ref.
E. coli ε	21–65	V E K I Q V T G S E G E L G I Y P G H A P L L T A I K P G M I R I V K Q H G H E E F I Y L	107
Bovine δR1	–	Q V D V P T Q T * G A F G I L A A H V P T L Q V L R P G L V V V * * * H A E D G T T S K	

Fig. 29. Homology between the *E. coli* ε subunit and bovine mitochondrial δ subunit of F_1F_0 ATPase. *, deletion.

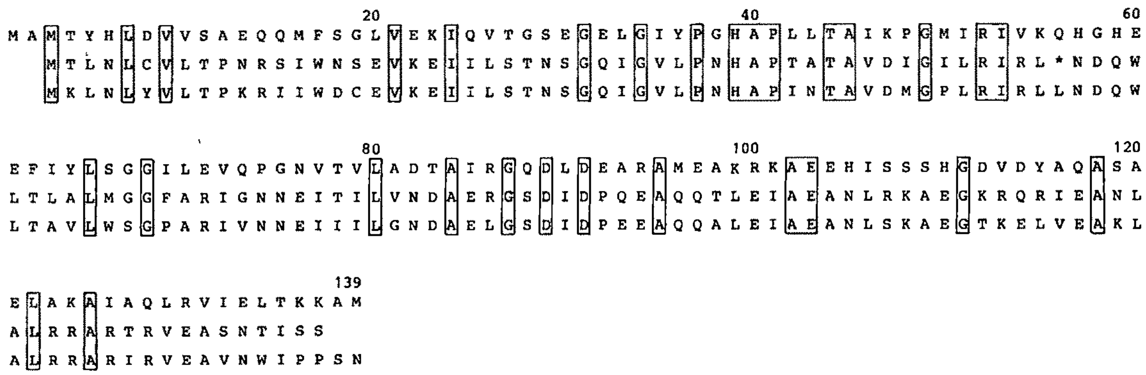

```
                                         20                                      40                                      60
a)  M A M T Y H L D V V S A E Q Q M F S G L V E K I Q V T G S E G E L G I Y P G H A P L L T A I K P G M I R I V K Q H G H E
b)      M T L N L C V L T P N R S I W N S E V K E I I L S T N S G Q I G V L P N H A P T A T A V D I G I L R I R L * N D Q W
c)      M K L N L Y V L T P K R I I W D C E V K E I I L S T N S G Q I G V L P N H A P I N T A V D M G P L R I R L L N D Q W

                                         80                                     100                                     120
a)  E F I Y L S G G I L E V Q P G N V T V L A D T A I R G Q D L D E A R A M E A K R K A E E H I S S S H G D V D Y A Q A S A
b)  L T L A L M G G F A R I G N N E I T I L V N D A E R G S D I D P Q E A Q Q T L E I A E A N L R K A E G K R Q R I E A N L
c)  L T A V L W S G P A R I V N N E I I I L G N D A E L G S D I D P E E A Q Q A L E I A E A N L S K A E G T K E L V E A K L

                                      139
a)  E L A K A I A Q L R V I E L T K K A M
b)  A L R R A R T R V E A S N T I S S
c)  A L R R A R I R V E A V N W I P P S N
```

Fig. 30. Alignment of ε subunits of ATP-synthase [67]. (a) *E. coli*, (b) spinach chloroplast [110], (c) maize chloroplast [109].

good example in support of this idea. A third possibility is that proteins that interact with each other are synthesised near to each other in the cell [112]. All of these possibilities also apply to the *unc* operon. For example, evolutionary relationships between genes are apparent, α being related to β (see Fig. 24) and related sequences being present in δ and ε, and ε and b (see Fig. 27), and evidence has been presented for interaction between subunits from all adjacent pairs of genes in the *unc* operon. However, the gene order is not in accord with the order of action of gene products proposed by Cox et al. [18], summarised in Fig. 31 and discussed below. A fourth explanation for the gene order in the lambda morphogenetic locus was advanced by Parkinson [116], namely that the genes might be arranged in such a way that their temporal sequence of expression would parallel their requirement during morphogenesis. Subsequently, in lambda, this explanation was discounted [112]. The sequence of assembly proposed by Cox et al. [18] suggests that the first events are association of β and then α with the membrane already containing *a*. Only after association of one α subunit and one β subunit can b enter the membrane. This is based upon the finding that a mutant in the α subunit did not contain *b* in its membranes. Mutants in the α subunit exerted a similar effect. An alternative interpretation to these results is that in the absence of α or β, F_1 cannot assemble and that incorporation of b is dependent upon an assembled F_1. F_0 assembles subsequent to this event. A further β subunit is then added. γ, δ and ε associate with the $2\beta:1\alpha$ structure before addition of further α and β subunits. The terminal stages of the pathway are described as tentative [14].

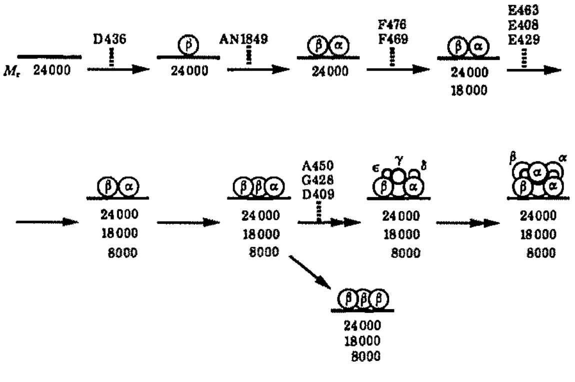

Fig. 31. Proposed sequence for assembly of *E. coli* F_1F_0 ATPase. The mutant allele number a strain number indicates the point at which assembly is interrupted in particular strains. Terminal stages are tentative [18].

VC-2. Does gene 1 product influence assembly?

Although the region of the *unc* operon called gene 1 [24] has the characteristics of a gene (discussed in Section IIIA) convincing in vivo evidence of the gene product is still lacking. Also, the gene does not hyper-express when cloned into an expression vector [34,42]. Schneider and Altendorf [117] have demonstrated the presence of small amounts of a 14 kDa protein in preparations of F_0 and have suggested that it might correspond to gene 1 product. However, protein sequence information to confirm this suggestion is lacking at present.

These difficulties notwithstanding it is possible from the putative gene sequence to make predictions about the structure of its gene product. The protein would have a net positive charge of +11 although the protein overall is rather hydrophobic. Analysis of its sequence with HYDROPLOT (Fig. 32) suggests the presence of transmembrane α-helical segments and a folding pattern based upon this has been proposed [67] (see Fig. 32). This speculative model is of a membrane protein in which the positive charges cluster to one side of the membrane. On the basis of these criteria it was suggested that the protein might fulfil a role in assem-

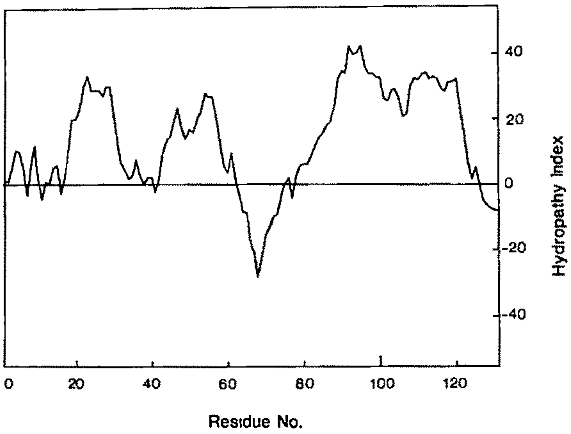

Fig. 32. Hydroplot of putative protein derived from gene 1 [67].

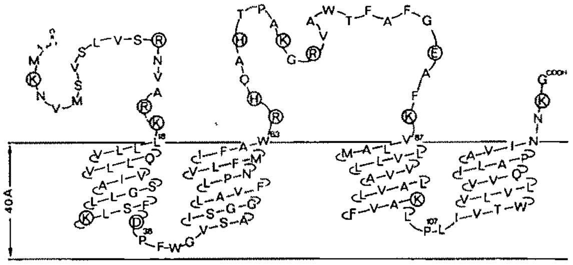

Fig. 33. Possible secondary structure for gene 1 product [67]. For details see legends to Fig. 16.

bly by providing a site to anchor the *unc* transcript near to its 5′ end, such that the F_0 polypeptide might be produced near to each other and to the membrane. it is envisaged that would aid efficient assembly of the enzyme; this might be important for the organism under difficult growth conditions. This model has little experimental basis. However, a deletion mutant (SD42) of gene 1 was constructed [42] (see subsection IIIA) for which a clear phenotype has not been found. However, its reduced growth yield in comparison with wild type is consistent with a role in efficient assembly of the enzyme complex.

VI. Conclusions and future prospects

No *unc* ATPase mutants in *E. coli* have been shown to map to regions of the *E. coli* chromosome other than the *unc* operon. Therefore, an important conclusion derived from the sequence analysis of the *unc* operon is that the *E. coli* ATP-synthase complex contains eight subunits only. For reasons discussed above, it is unlikely that gene 1 codes for a structural protein. In this respect, the enzyme appears to differ from the mitochondrial and chloroplast enzymes, which appear to be more complex. From work discussed above, it is becoming clear that the mitochondrial enzyme apparently has no counterpart to its ε subunit. In addition, associated with the mitochondrial enzyme is the inhibitor protein, which has a defined physiological role in mitochondria and other low molecular proteins. The best characterised of these is factor 6, although its function is rather unclear. Given that the *E. coli* enzyme can function satisfactorily with eight subunits, a major task will now be to define the role (if any) of the extra subunits in preparations of the mitochondrial complex.

The sequences of the ATP-synthase complex are also important in the context of studies on the structure and function of the enzyme, which ultimately should provide a better understanding of how the enzyme works.

The ease of manipulation of the *E. coli unc* genes also provides a means of introducing site-directed mutations into the proteins and offers the prospect of making large quantities of wild-type and mutant enzymes. In addition, site-directed mutagenesis should be an important tool in the dissection both of the assembly of the enzyme complex and of the regulation of expression of *unc* genes, both poorly understood at present.

Acknowledgements

We thank S.D. Dunn and I. Katsura for providing preprints and M.H.L. de Bruijn for permission to quote an unpublished sequence. M.S. was supported by an EMBO Fellowship and N.J.G. by an MRC Studentship.

References

1 Mitchell, P. (1981) in Mitochondria and Microsomes (Lee, C.P., Schatz, G. and Dallner, G., eds), pp. 427–457, Addison-Wesley, Reading, MA

2 Nicholls, D. (1981) in Bioenergetics. An Introduction to the Chemiosmotic Theory. Academic Press, London

3 Bragg, P.D. and Hou, C. (1975) Arch. Biochem Biophys. 167, 311–321

4 Fillingame, R.H. (1981) Curr. Top. Bioenerg. 11, 35–106

5 Foster, D.L. and Fillingame, R.H. (1982) J. Biol. Chem. 257, 2009–2015

6 Racker, E. (1981) in Mitochondria and Microsomes (Lee, C.P., Schatz, G. and Dallner, G., eds.), pp. 337–356, Addison-Wesley, Reading, MA

7 Senior, A.E. (1979) in: Membrane Proteins in Energy Transduction (Capaldi, R.A., ed.), pp. 233–276, Dekker, New York

8 Nelson, N. (1981) Curr. Top. Bioenerg. 11, 1–34

9 Kagawa, Y. and Racker, E. (1966) J. Biol. Chem. 241, 2461–2482

10 MacLennan, D.H. and Tzagoloff, A. (1968) Biochemistry 7, 1603–1610

11 Tzagoloff, A., MacLennan, D.H. and Byington, K.H. (1968) Biochemistry 7, 1596–1602

12 Senior, A.E. (1971) Bioenergetics 2, 141–150

13 Kanner, B.I., Serrano, R., Kandrach, M.A. and Racker, E. (1976) Biochem. Biophys. Res. Commun. 69, 1050–1056

14 Gibson, F. (1982) Proc. R. Soc. Lond. B. 215, 1–18

15 Downie, J.A., Gibson, F. and Cox, G.B. (1979) Annu. Rev. Biochem. 48, 103–131

16 Bachman, B.J. and Low, B.K. (1980) Microbiol. Rev. 44, 1–56

17 Gibson, F., Downie, J.A., Cox, G.B and Radik, J. (1978) J. Bacteriol. 134, 728–736

18 Cox, G B., Downie, J.A., Langman, L., Senior, A.E., Ask, G., Fayle, D.R.H. and Gibson, F. (1981) J. Bacteriol. 148, 30–42

19 Gunsalus, R.P., Brusilow, W.S.A. and Simoni, R.D. (1982) Proc. Natl. Acad. Sci. USA 79, 320–324

20 Miki, T., Hiraga, S., Nagata, T. and Yura, T. (1978) Proc. Natl. Acad. Sci. USA 75, 5099–5103

21 Kanazawa, H., Miki, T., Tamura, F., Yura, T. and Futai, M. (1979) Proc. Natl. Acad. Sci. USA 76, 1126–1130

22 Von Meyenburg, K. and Hansen, F.G. (1980) in Mechanistic Studies of DNA Replication and Genetic Recombination. ICN UCLA Symposium, Vol. XIX (Alberts, B. and Fox, C.F., eds.), pp. 137–159, Academic Press, New York

23 Gay, N.J. and Walker, J.E (1981) Nucleic Acids Res. 9, 2187–2194

24 Gay, N.J. and Walker, J.E. (1981) Nucleic Acids Res. 9, 3939–3926

25 Saraste, M., Eberle, A., Gay, N.J., Runswick, M.J. and Walker, J.E. (1981) Nucleic Acids Res. 9, 5287–5296

26 Nielsen, J., Hansen, F.G., Hoppe, J., Friedl, P. and Von Meyenburg, K. (1981) Mol. Gen. Genet. 184, 33–39

27 Kanazawa, H., Mabuchi, K., Kayano, T., Tamura, F. and Futai, M. (1981) Biochem. Biophys. Res. Commun. 100, 219–225

28 Mabuchi, K., Kanazawa, H., Kayano, T. and Futai, M. (1981) Biochem. Biophys. Res. Commun. 102, 172–179

29 Kanazawa, H., Kayano, T., Mabuchi, K. and Futai, M. (1981) Biochem. Biophys. Res. Commun. 103, 604–612

30 Kanazawa, H., Mabuchi, K., Kayano, T., Noumi, T., Sekiya, T. and Futai, M. (1981) Biochem. Biophys. Res. Commun 103, 613–620

31 Kanazawa, H., Kayano, T., Kiayasu, T. and Futai, M (1982) Biochem. Biophys. Res. Commun. 105, 1257–1264

32 Mabuchi, K., Kanazawa, H., Kayano, T. and Futai, M. (1981) Biochem. Biophys. Res. Commun. 104, 354

33 Kanazawa, H., Mabuchi, K. and Futai, M. (1982) Biochem. Biophys. Res. Commun. 107, 568–587

34 Gay, N.J. (1982) Ph.D. Thesis, University of Cambridge.

35 Walker, J.E., Eberle, A., Gay, N.J., Hanisch, P., Saraste, M. and Runswick, M.J. (1982) in Methods in Peptide and Protein Sequence Analysis (Elzinga, M., ed.), pp. 337–354, Humana, Clifton, NJ

36 Dunn, S.D. (1982) J. Biol. Chem. 257, 7354–7359

37 Staden, R. and McLachlan, .D. (1982) Nucleic Acids Res. 10, 141–156

38 Shine, J. and Dalgarno, L. (1974) Proc. Natl. Acad. Sci. USA 71, 1342–1346

39 Walker, J.E., Auffret, A.D., Carne, A., Gurnett, A., Hanisch, P., Hill, D. and Saraste, M. (1982) Eur. J. Biochem. 123, 253–260

40 Runswick, M.J. and Walker, J.E. (1983) J. Biol. Chem. 258, 3081–3089

41 Dunn, S.D., Heppel, L A. and Fullmer, C.S. (1980) J. Biol. Chem. 255, 6891–6896

42 Gay, N.J. (1984) J. Bacteriol. 158, 820–825

43 Gold, L., Pribnow, D., Schneider, T., Shinedling, S., Singer, B.S and Stormo, G. (1981) Annu. Rev. Microbiol. 35, 365–403

44 Young, I.G., Rogers, B.L., Campbell, H.D., Jaworowski, A. and Shaw, D.C. (1981) Eur. J. Biochem. 116, 165–170

45 Marcker, K.A., Clark, B.F.C. and Anderson, J.S. (1966) Cold Spring Harbor Symp. Quant. Biol. 31, 279–285

46 Stormo, G.D., Schneider, T.D. and Gold, L.M. (1982) Nucleic Acids Res. 10, 2971–2995

47 Taniguchi, T. and Weissmann, C. (1978) J. Mol. Biol. 118, 533–565

48 Steege, D.A. and Soll, D.G. (1979) in Biological Regulation and Development, Vol. I (Goldberger, R.F., ed.), pp. 433–485, Plenum Press, New York

49 Fiddes, J.C. (1976) J. Mol. Biol. 107, 1–24

50 Lu, P. and Rich, A. (1971) J. Mol. Biol. 58, 513–531

51 Pribnow, D. (1978) in Biological Regulation and Development, Vol. I. (Goldberger, R.F., ed.), pp. 219–277, Plenum Press, New York

52 Rosenberg, M. and Court, D. (1979) Annu. Rev. Genet. 13, 319–353

53 Gay, N.J. and Walker, J.E. (1980) J. Mol. Biol., in the press

54 Nielsen, J , Jorgensen, B.B., Hansen, F.G., Petersen, P.E. and Von Meyenburg, K. (1982) EBEC Rep. 2, 611–612

55 Travers, A.A., Lamond, A.I., Mace, H.A.F. and Berman, M.L. (1984) Cell 35, 265–273

56 Travers, A.A., Kari, C. and Mace, H.A.F. (1981) Soc. Gen. Microbiol. Symp. 31, 111–130

57 Goldberger, R.F. (1979) in Biological Regulation and Development, Vol. I (Goldberger, R.F., ed.), p. 15, Plenum Press, New York

58 Ray, P.N. and Pearson, M.L. (1974) J. Mol. Biol. 85, 163–175

59 Steitz, J. (1979) in Biological Regulation and Development, Vol. I, (Goldberger, R.F., ed.), pp. 349–399, Plenum Press, New York

60 Ray, P.N. and Pearson, M.L. (1976) Virology 73, 381–388

61 Ray, P.N. and Pearson, M.L. (1975) Nature 253, 647–650

62 Hall, M.N., Gabay, J., Debarbouillé, M. and Schwartz, M. (1982) Nature 295, 616–618

63 Rusel, M., Gold, L., Morrisset, H. and O'Farrell, P.Z. (1976) J. Biol. Chem. 251, 7263–

64 Ikemura, T. (1981) J. Mol. Biol. 146, 1–21

65 Grantham, R., Gautier, C., Gouy, M., Jacobzone, M. and Mercier, R. (1981) Nucleic Acids Res. 9, r43–r74

66 Gouy, M. and Grantham, R. (1980) FEBS Lett. 115, 151–155

67 Walker, J.E., Gay, N.J., Saraste, M. and Eberle, A.N. (1984) Biochem. J., in the press

68 Grosjean, H. and Fiers, W. (1982) Gene 18, 199–209

69 Newman, A.K., Rubin, R.A., Kim, S.H. and Modrich, P. (1981) J. Biol. Chem. 256, 2131–2139

70 Greene, P.J., Gupta, M., Boyer, H.W., Brown, W.E. and Rosenberg, J.M. (1981) J. Biol. Chem. 256, 2143–2153

71 McLachlan, A.D. (1977) Int. J. Quantum. Chem. 12, Suppl. 1, 371–385
72 Engleman, D.M., Henderson, R., McLachlan, A.D. and Wallace, B.A. (1980) Proc. Natl. Acad. Sci USA 77, 2023–2027
73 Bisson, R. and Capaldi, R A. (1981) J. Biol Chem 256, 4362–4367
74 Walker, J.E, Carne, A.F. and Schmitt, H.W. (1979) Nature 278, 653–654
75 Kyte, J. and Doolittle, R.F. (1982) J. Mol. Biol. 157, 105–132
76 Staden, R. (1982) Nucleic Acids Res. 10, 2951–2961
77 Guerrieri, F. and Pappa, S. (1980) EBEC Rep. 1, 207–208
78 Sone, N., Hamamoto, J. and Kagawa, Y. (1981) J. Biol. Chem. 256, 2873–2877
79 Sebald, W. and Hoppe, J. (1981) Curr. Top. Bioenerg. 12, 2–64
80 Hoppe, J., Schairer, H.U., Friedl, P. and Sebald, W. (1982) FEBS Lett. 145, 21–24
81 Richardson, J.S., Thomas, K.A., Byron, H.R. and Richardson, D.C. (1975) Proc. Natl. Acad. Sci USA 72, 1349–1353
82 Loo, T.W. and Bragg, P.D. (1982) Biochem. Biophys Res. Commun. 106, 400–406
83 Walker, J.E., Saraste, M. and Gay, N.J. (1982) Nature 298, 867–869
84 Hoppe, J., Brunner, J., Friedl, P., Lincoln, D., Von Meyenburg, K., Michelsen, O., Montecucco, C. and Sebald, W. (1982) EBEC Reports 2, 85–86
85 Futai, M. and Kanazawa, H. (1980) Curr. Top. Bioenerg. 10, 181–215
86 Yoshida, M., Okamoto, H., Sone, N., Hirata, H. and Kagawa, Y. (1977) Proc. Natl. Acad. Sci. USA 74, 936–940
87 Kagawa, Y. (1978) Biochim. Biophys. Acta 505, 45–93
88 Futai, M., Sternweis, P.C. and Heppel, L.A. (1974) Proc. Natl. Acad. Sci. USA 71, 2725–2729
89 Smith, J.B. and Sternweis, P.C. (1977) Biochemistry 16, 306–311
90 Sternweis, P.C. (1978) Biochemistry 253, 2123–3128
91 Esch, F.S. and Allison, W.S. (1978) J. Biol. Chem. 253, 6100–6106
92 Yoshida, M., Poser, J.W., Allison, W.S. and Esch, F.S. (1981) J. Biol. Chem. 256, 148–153
93 Yoshida, M., Allison, W.J. and Esch, F.S. (1981) Fed. Proc. 40, 1734
94 Walker, J.E,, Saraste, M., Runswick, M.J. and Gay, N.J. (1982) EMBO J. 1, 945–951
95 Harris, D.A, (1981) Biosystems 14, 113–121
96 Dayhoff, M.O. (1972) Atlas of Protein Sequence and Structure, Vol. 2, p.D8
97 Harris, D.A. (1978) Biochim. Biophys. Acta 463, 245–273
98 Slater, E.C., Kemp, A., Van der Kraan, I., Muller, J.L.M., Roveri, O.A., Verschoor, G.J., Wagenvoord, R.J. and Wielders, J.P.M. (1979) FEBS Lett. 103, 7–11
99 Cross, R.L. (1981) Annu. Rev. Biochem. 50, 681–714
100 Pai, E.F., Sachsenheimer, W., Schirmer, R.H. and Schultz, G.E. (1977) J. Mol. Biol. 114, 37–45
101 Bálint, M. Sréter, F.A., Wolf, I., Nagy, B. and Gergely, J. (1975) J. Biol. Chem. 250, 6168–6177
102 Szilagyi, L., Bálint, M., Sréter, F.A and Gergely, J. (1979) Biochem. Biophys. Res. Commun. 87, 936–945
103 Evans, P.R., Farrants, G.W. and Hudson, P.J. (1981) Phil Trans R. Soc. Lond. B. 293, 5B–62
104 Hollemans, M., Runswick, M.J. and Walker, J.E. (1980) J. Biol. Chem., in the press
105 Wagenvoord, R.J., Kemp, A. and Slater, E.C. (1980) Biochim. Biophys. Acta 593, 204–211
106 Yoshida, M., Sone, N., Hirata, H., Kagawa, Y. and Ui, N. (1979) J. Biol. Chem. 254, 9525–9533
107 Walker, J.E., Runswick, M.J. and Saraste, M. (1982) FEBS Lett. 146, 393–396
108 Fisher, R.J., Liang, A.M. and Sundstrom, G.C. (1981) J. Biol. Chem. 256, 707–715
109 Krebbers, E T., Larrinua, I.M., McIntosh, L. and Bogorad, L. (1982) Nucleic Acids Res. 10, 4985–5002
110 Kurawski, G., Bottomley, W. and Whitfeld, P.R. (1982) Proc. Natl. Acad. Sci. USA 79, 6260–6264
111 Wood, W.B. and King, J. (1979) Compr. Virol. 13, 581–633
112 Katsura, I. (1980) in Lambda II (Hendrix, R.W., Roberts, J.W. and Stahl, F.W., eds.), Cold Spring Harbor, in the press
113 Casjens, S. and Hendrix, R. (1974) J. Mol. Biol. 90, 20–23
114 Kikuchi, Y. and King, J (1975) J. Mol. Biol. 99, 695–716
115 King, J. and Laemmli, U.K. (1973) J. Mol. Biol. 75, 315–337
116 Parkinson, J.S. (1968) Genetics 59, 311–325
117 Schneider, E. and Altendorf, K. (1982) Eur. J. Biochem. 126, 149–153
118 Friedl, P., Bienhaus, G., Hoppe, J. and Schraier, H.U. (1981) Proc. Nat. Acad. Sci. USA 78, 6643–6646
119 Sancar, A., Stachelek, C., Konigsberg, W. and Rupp, W.D. (1980) Proc. Natl. Acad. Sci. USA 77, 2611–2615
120 Karn, J., Brenner, S., and Barnett, L. (1983) Proc. Natl. Acad. Sci. USA 80, 4253–4257
121 Aquila, H., Misra, D., Eulitz, M. and Klingenberg, M. (1982) Hoppe-Seyler's Z. Physiol. Chem. 363, 345–349
122 Kolb, E., Hudson, P.J. and Harris, J.I. (1980) Eur. J. Biochem. 108, 587–597
123 Anderson, S., De Bruijn, M.H.L., Coulson, A.R., Eperon, I.C., Sanger, F. and Young, I.G. (1982) J. Mol. Biol. 156, 683–717
124 Macino, G. and Tzagoloff, A. (1980) Cell 20, 507–517
125 Dunn, S.D. and Futai, M. (1980) J. Biol. Chem. 255, 113–118
126 Anderson, S., Bankier, A.T., Barrell, B.G., de Bruijn, M.H.L., Coulson, A.R., Drouin, J., Eperon, I.C., Nierlich, D.P., Sanger, F., Schreier, P.H., Smith, A.J.H., Staden, R. and Young, I.G. (1981) Nature 290, 457–465
127 Bibb, M.J., Van Etten, R.A., Wright, C.T., Walberg, M.W. and Clayton, D.A. (1981) Cell 26, 167–180
128 Yanofsky, C., Platt, T., Crawford, I.P., Nichols, B.P., Christie, G.E., Horowitz, H., Van Cleemput, M. and Wu, A.M. (1981) Nucleic Acids Res. 9, 6647–6668
129 Tinoco, I., Borer, P.N., Dengler, B., Levine, M.D., Uhlenbeck, O.C., Crothers, D.M. and Gralla, J. (1973) Nature New Biol. 246, 40–41
130 Grinkevich, V.A., Modyanov, N.N., Ovchinnikov, Y.A., Hundal, T. and Ernster, L. (1982) EBEC Reports 2, 83–84

Biochimica et Biophysica Acta
Reviews on Bioenergetics, BR12(2)

Vol. 768, No. 2
September 6, 1984

Contents

The dynamic base of energy transduction in enzymes (BBA 86109)
by B. Somogyi, G.R. Welch and S. Damjanovich (Debrecen, Hungary and New Orleans, LA, U.S.A.) 81
The bioenergetics of methanogenesis (BBA 86110)
by L. Daniels, R. Sparling and G.D. Sprott (Iowa City, IA, U.S.A. and Ottawa, Canada) 113
The *unc* operon. Nucleotide sequence, regulation and structure of ATP-synthase (BBA 86111)
by J.E. Walker, M. Saraste and N.J. Gay (Cambridge, U.K.) 164

Cited in: Current Contents Life Sciences - Biological Abstracts - Chemical Abstracts - Index Chemicus - Index Medicus - Excerpta Medica

---

INFORMATION FOR CONTRIBUTORS TO BIOCHIMICA ET BIOPHYSICA ACTA

The 1982 edition of this booklet, offering detailed guidance to authors, is available free of charge from the BBA Editorial Secretariat, P.O. Box 1345, 1000 BH Amsterdam, The Netherlands. It is also published as Biochim. Biophys. Acta 715 (1982) 1–23.

BIOCHIMICA ET BIOPHYSICA ACTA
International Journal of Biochemistry and Biophysics
Founded in 1947 by H.G.K. Westenbrink, Managing Editor 1947–1964

© 1984, Elsevier Science Publishers B.V.
Printed in The Netherlands

All rights reserved. No part of this publication may be reproduced, stored in a retrieval system, or transmitted, in any form or by any means, electronic, mechanical, photocopying, recording or otherwise without the prior permission of the copyright owner Submission to this journal of a paper entails the author's irrevocable and exclusive authorization of the publisher to collect any sums or considerations for copying or reproduction payable by third parties (as mentioned in article 17 paragraph 2 of the Dutch Copyright Act of 1912 and in the Royal Decree of June 20, 1974 (S. 351) pursuant to article 16b of the Dutch Copyright Act of 1912) and/or to act in or out of Court in connection therewith

Special regulations for readers in the U.S.A. This journal has been registered with the Copyright Clearance Center, Inc. Consent is given for copying of articles for personal or internal use, or for the personal use of specific clients. This consent is given on the condition that the copier pays through the Center the per-copy fee stated in the code on the first page of each article for copying beyond that permitted by Sections 107 or 108 of the U.S. Copyright Law. The appropriate fee should be forwarded with a copy of the first page of the article to the Copyright Clearance Center, Inc, 21 Congress Street, Salem, MA 01970, U.S.A. If no code appears in an article, the author has not given broad consent to copy and permission to copy must be obtained directly from the author. All articles published prior to 1980 may be copied for a per-copy fee of US$ 2.25, also payable through the Center. This consent does not extend to other kinds of copying, such as for general distribution, resale, advertising and promotion purposes, or for creating new collective works. Special written permission must be obtained from the publisher for such copying.

Special regulations for authors. Upon acceptance of an article by the journal, the author(s) will be asked to transfer copyright of the article to the publisher. This transfer will ensure the widest possible dissemination of information.

gene structure and expression

SAMPLE COPY

for additional information contact :

ALLIED/ELSEVIER JOURNALS
MARKETING GROUP
30, WEST COTT ROAD, Ph : 82468
MADRAS - 600 014./
750, MOUNT ROAD,
MADRAS - 600 002.

BBA

Biochimica et Biophysica Acta (N)

Managing Editors: P. Borst, P. Cohen,
K. van Dam, L.L.M. van Deenen (Chairman),
E.P. Kennedy and G.K. Radda

Honorary Managing Editor. E.C. Slater

Vol. 866, No. 1, pp. 1–92
February 24, 1986
Elsevier

ISSN 0006-3002
0167-4781
BBACAQ 866(1) 1–92 (1986)
BBGSD5 866 (1) 1–92 (1986)

PUBLICATION SCHEDULE FOR 1986

BBA is published according to a volume-numbering scheme that embraces all sections of the journal In addition, each regular section has its own sequential volume-numbering system, running parallel to the overall BBA scheme, as set out below
Full subscription 42 volumes plus Cumulative Index 1985

	BIO-ENERGETICS 6 Volumes [a]	BIO-MEMBRANES 11 volumes [b]	GENE STRUCTURE AND EXPRESSION 3 volumes	PROTEIN STRUCTURE AND MOLECULAR ENZYMOLOGY 6 volumes	LIPIDS AND LIPID METABOLISM 5 volumes	GENERAL SUBJECTS 5 volumes	MOLECULAR CELL RESEARCH 5 volumes	BBA REVIEW SECTIONS
Jan	848-1 = B75-1	854-1 = M135-1 854-2 = M135-2	866-1 = N14-1	869-1 = P33-1	875-1 = L77-1	880-1 = G121-1	885-1 = C12-1	BBA REVIEWS ON BIOENERGETICS
Feb	848-2 = B75-2	855-1 = M136-1 855-2 = M136-2	866-2 = N14-2	869-2 = P33-2 869-3 = P33-3	875-2 = L77-2	880-2 = G121-2	885-2 = C12-2	853-1 = BR14-1 853-2 = BR14-2 853-3 = BR14-3 853-4 = BR14-4
March	848-3 = B75-3	855-3 = M136-3 856-1 = M137-1	866-3 = N14-3	870-1 = P34-1	875-3 = L77-3	880-3 = G121-3	885-3 = C12-3	
April	849-1 = B76-1 849-2 = B76-2	856-2 = M137-2 856-3 = M137-3	866-4 = N14-4	870-2 = P34-2 870-3 = P34-3	876-1 = L78-1 876-2 = L78-2	881-1 = G122-1 881-2 = G122-2	886-1 = C13-1 886-2 = C13-2	
May	849-3 = B76-3	857-1 = M138-1 857-2 = M138-2	867-1 = N15-1	871-1 = P35-1	876-3 = L78-3	881-3 = G122-3	886-3 = C13-3	BBA REVIEWS ON BIOMEMBRANES
June	850-1 = B77-1	858-1 = M139-1 858-2 = M139-2	867-2 = N15-2	871-2 = P35-2 871-3 = P35-3	877-1 = L79-1	882-1 = G123-1	887-1 = C14-1	864-1 = MR15-1 864-2 = MR15-2 864-3 = MR15-3 864-4 = MR15-4
July	850-2 = B77-2 850-3 = B77-3	859-1 = M140-1 859-2 = M140-2	867-3 = N15-3	872-1 = P36-1	877-2 = L79-2 877-3 = L79-3	882-2 = G123-2 882-3 = G123-3	887-2 = C14-2 887-3 = C14-3	
Aug	851-1 = B78-1	860-1 = M141-1 860-2 = M141-2	867-4 = N15-4	872-2 = P36-2 872-3 = P36-3	878-1 = L80-1	883-1 = G124-1	888-1 = C15-1	BBA REVIEWS ON CANCER
Sept	851-2 = B78-2	860-3 = M141-3 861-1 = M142-1	868-1 = N16-1	873-1 = P37-1	878-2 = L80-2	883-2 = G124-2	888-2 = C15-2	865-1 = CR13-1 865-2 = CR13-2 865-3 = CR13-3
Oct	851-3 = B78-3	861-2 = M142-2 861-3 = M142-3	868-2 = N16-2	873-2 = P37-2 873-3 = P37-3	878-3 = L80-3	883-3 = G124-3	888-3 = C15-3	
Nov	852-1 = B79-1 852-2 = B79-2	862-1 = M143-1 862-2 = M143-2	868-3 = N16-3	874-1 = P38-1	879-1 = L81-1 879-2 = L81-2	884-1 = G125-1 884-2 = G125-2	889-1 = C16-1 889-2 = C16-2	
Dec	852-3 = B79-3	863-1 = M144-1 863-2 = M144-2	868-4 = N16-4	874-2 = P38-2 874-3 = P38-3	879-3 = L81-3	884-3 = G125-3	889-3 = C16-3	

[a] This includes BBA Reviews on Bioenergetics, Vol 853 [b] This includes BBA Reviews on Biomembranes, Vol 864

Authors should submit their manuscripts (four copies) for publication in BIOCHIMICA ET BIOPHYSICA ACTA by sending them to one of the Managing Editors.

Dr P Borst, c/o BBA Editorial Secretariat, P O Box 1345, 1000 BH Amsterdam, The Netherlands
Dr P Cohen, Department of Biochemistry, Medical Sciences Institute, University of Dundee, Dundee, DD1 4HN, U K
Dr K van Dam, c/o BBA Editorial Secretariat, P O. Box 1345, 1000 BH Amsterdam, The Netherlands
Dr L L M van Deenen, c/o BBA Editorial Secretariat, P O Box 1345, 1000 BH Amsterdam, The Netherlands
Dr E P Kennedy, c/o BBA Editorial Secretariat (Boston), Box C 9123, Brookline, MA 02146, U S A
Dr G K Radda, Department of Biochemistry, University of Oxford, South Parks Road, Oxford, OX1 3QU, U K

Detailed information for contributors may be found in Biochim Biophys Acta 715 (1982) 1–23, also published as the 1982 edition of the booklet
INFORMATION FOR CONTRIBUTORS TO BIOCHIMICA ET BIOPHYSICA ACTA
which is available free of charge from the BBA Editorial Secretariat

---

Subscription information

1986 BBA Gene Structure and Expression, Volumes 866–868 (3 volumes in 12 issues), Dfl 705 (US$ 261 00)+Dfl 72 (US$ 26 75) postage, packaging and handling Total price: Dfl 777 (US$ 287 75)

1986 BBA full subscription, Volumes 848–889 (42 volumes in 125 issues), Dfl 7476 (US$ 2769 00)+Dfl 1008 (US$ 373 25) postage, packaging and handling Total price Dfl 8484 (US$ 3142 25)

The Dutch guilder price is definitive The U S dollar price is subject to exchange-rate fluctuations and is given only as a guide

Journals are sent by surface delivery to all countries, except the following countries where SAL air delivery (Surface Airlifted Mail) is ensured U.S A , Canada, Japan, Australia, New Zealand, P R China, India, Israel, South Africa, Malaysia, Singapore, South Korea, Taiwan, Pakistan, Hong Kong, Brazil Airmail rates for other countries are available on request

Subscription orders can be entered only by calendar year (Jan -Dec.) and should be sent to Elsevier Science Publishers, Journals Department, P O Box 211, 1000 AE Amsterdam, The Netherlands, Telex 18582 ESPA NL, or to your usual subscription agent Claims for missing issues should be made within 3 months of publication, otherwise they cannot be honoured free of charge The Publisher reserves the right to issue additional volumes during the course of the year Such volumes will be invoiced before publication and delivered after receipt of payment

In the U S A. and Canada for further information concerning this or any other Elsevier Science Publishers journal, contact Elsevier Science Publishers, Journal Information Center, 52 Vanderbilt Avenue, New York, NY 10017, U S A , Tel (212) 370-5520

Biochimica et Biophysica Acta

BIOCHIMICA ET BIOPHYSICA ACTA

MANAGING EDITORS

L L M van Deenen (Utrecht)
(Chairman)
P Borst (Amsterdam)
P Cohen (Dundee)
E P Kennedy (Boston, MA)
K. van Dam (Amsterdam)
G K. Radda (Oxford)

HONORARY MANAGING EDITOR

E.C Slater (Southampton)

EDITORS

J Amesz (Leiden)
H R.V Arnstein (London)
J Barber (London)
I Björkhem (Huddinge)
B Borgström (Lund)
J Brachet (Brussels)
A E Braunstein (Moscow)
J Bremer (Oslo)
R. Burgess (Madison, WI)
E Carafoli (Zurich)
J E Cleaver (San Francisco)
C Crane-Robinson (Portsmouth)
M P Czech (Worcester, MA)
J W Daly (Bethesda, MD)
E A Dawidowicz (Boston, MA)
B de Kruijff (Utrecht)
J G Demaille (Montpellier)
J.J H H M de Pont (Nijmegen)
K T Douglas (Colchester)
S Ebashi (Tokyo)
L Ernster (Stockholm)
S Ferguson (Birmingham)
J Gergely (Boston, MA)
F Gibson (Canberra)
W B Gratzer (London)
M. Hamberg (Stockholm)
T E Hardingham (London)
J L Harwood (Cardiff)
E. Heinz (Dortmund)
E J M Helmreich (Würzburg)
S B Hladky (Cambridge)
M D Houslay (Glasgow)
R C Hughes (London)
J B Jackson (Birmingham)
O Jardetzky (Stanford)
P Jollès (Paris)
P L Jørgensen (Aarhus)
Y Kagawa (Tochigi-ken)
K -A Karlsson (Gothenburg)
M Kates (Ottawa)
J Kay (Cardiff)
Y Kaziro (Tokyo)
R Kinne (Dortmund)
C Klee (Bethesda)
A Kleinzeller (Philadelphia)
A G. Lee (Southampton)
D M Lee (Oklahoma City, OK)
F Maley (Albany, NY)
D Marsh (Göttingen)
V Massey (Ann Arbor, MI)
D J Morré (Lafayette)
J F Morrison (Canberra)
L E Mortenson (Athens, GA)
G Nelsestuen (St Paul, MN)
D G. Nicholls (Dundee)
C Nicolau (Orleans)
Y Nishizuka (Kobe)
R C Nordlie (Grand Forks, ND)
S. Numa (Kyoto)
C Pace-Asciak (Toronto)
P G W Plagemann (Minneapolis, MN)
I. Ragan (Southampton)
P Randle (Oxford)
A Razin (Jerusalem)
A M Scanu (Chicago, IL)
H J Schatzmann (Bern)
G.L Scherphof (Groningen)
J Seelig (Basel)
N Sharon (Rehovot)
G.G Shipley (Boston, MA)
D Shugar (Warsaw)
W D Stein (Jerusalem)
J.M Tager (Amsterdam)
T Taniguchi (Tokyo)
J.P Thornber (Los Angeles, CA)
I. Tinoco (Berkeley, CA)
K.F Tipton (Dublin)
I P Trayer (Birmingham)
I Trowbridge (San Diego, CA)
C L Tsou (Beijing)
D E Vance (Vancouver)
T Vänngård (Gothenburg)
A Watts (Oxford)
C Weissmann (Zürich)
M K F Wikström (Helsinki)
R J P Williams (Oxford)
R Williamson (London)
C Wraight (Urbana, IL)
K Wüthrich (Zürich)
R F A Zwaal (Maastricht)

ELSEVIER SCIENCE PUBLISHERS B.V.
AMSTERDAM

BIOCHIMICA
ET BIOPHYSICA ACTA

INTERNATIONAL JOURNAL OF BIOCHEMISTRY AND BIOPHYSICS

gene structure and expression

866 (1986)
(N14)

ELSEVIER SCIENCE PUBLISHERS B.V.
AMSTERDAM

PUBLICATION SCHEDULE FOR 1986

BBA is published according to a volume-numbering scheme that embraces all sections of the journal In addition, each regular section has its own sequential volume-numbering system, running parallel to the overall BBA scheme, as set out below
Full subscription 42 volumes plus Cumulative Index 1985

	BIO-ENERGETICS 6 Volumes [a]	BIO-MEMBRANES 11 volumes [b]	GENE STRUCTURE AND EXPRESSION 3 volumes	PROTEIN STRUCTURE AND MOLECULAR ENZYMOLOGY 6 volumes	LIPIDS AND LIPID METABOLISM 5 volumes	GENERAL SUBJECTS 5 volumes	MOLECULAR CELL RESEARCH 5 volumes	BBA REVIEW SECTIONS
Jan	848-1 = B75-1	854-1 = M135-1 854-2 = M135-2	866-1 = N14-1	869-1 = P33-1	875-1 = L77-1	880-1 = G121-1	885-1 = C12-1	BBA REVIEWS ON BIOENERGETICS
Feb	848-2 = B75-2	855-1 = M136-1 855-2 = M136-2	866-2 = N14-2	869-2 = P33-2 869-3 = P33-3	875-2 = L77-2	880-2 = G121-2	885-2 = C12-2	853-1 = BR14-1 853-2 = BR14-2 853-3 = BR14-3 853-4 = BR14-4
March	848-3 = B75-3	855-3 = M136-3 856-1 = M137-1	866-3 = N14-3	870-1 = P34-1	875-3 = L77-3	880-3 = G121-3	885-3 = C12-3	
April	849-1 = B76-1 849-2 = B76-2	856-2 = M137-2 856-3 = M137-3	866-4 = N14-4	870-2 = P34-2 870-3 = P34-3	876-1 = L78-1 876-2 = L78-2	881-1 = G122-1 881-2 = G122-2	886-1 = C13-1 886-2 = C13-2	
May	849-3 = B76-3	857-1 = M138-1 857-2 = M138-2	867-1 = N15-1	871-1 = P35-1	876-3 = L78-3	881-3 = G122-3	886-3 = C13-3	BBA REVIEWS ON BIOMEMBRANES
June	850-1 = B77-1	858-1 = M139-1 858-2 = M139-2	867-2 = N15-2	871-2 = P35-2 871-3 = P35-3	877-1 = L79-1	882-1 = G123-1	887-1 = C14-1	864-1 = MR15-1 864-2 = MR15-2 864-3 = MR15-3 864-4 = MR15-4
July	850-2 = B77-2 850-3 = B77-3	859-1 = M140-1 859-2 = M140-2	867-3 = N15-3	872-1 = P36-1	877-2 = L79-2 877-3 = L79-3	882-2 = G123-2 882-3 = G123-3	887-2 = C14-2 887-3 = C14-3	
Aug	851-1 = B78-1	860-1 = M141-1 860-2 = M141-2	867-4 = N15-4	872-2 = P36-2 872-3 = P36-3	878-1 = L80-1	883-1 = G124-1	888-1 = C15-1	BBA REVIEWS ON CANCER
Sept	851-2 = B78-2	860-3 = M141-3 861-1 = M142-1	868-1 = N16-1	873-1 = P37-1	878-2 = L80-2	883-2 = G124-2	888-2 = C15-2	865-1 = CR13-1 865-2 = CR13-2 865-3 = CR13-3
Oct	851-3 = B78-3	861-2 = M142-2 861-3 = M142-3	868-2 = N16-2	873-2 = P37-2 873-3 = P37-3	878-3 = L80-3	883-3 = G124-3	888-3 = C15-3	
Nov	852-1 = B79-1 852-2 = B79-2	862-1 = M143-1 862-2 = M143-2	868-3 = N16-3	874-1 = P38-1	879-1 = L81-1 879-2 = L81-2	884-1 = G125-1 884-2 = G125-2	889-1 = C16-1 889-2 = C16-2	
Dec	852-3 = B79-3	863-1 = M144-1 863-2 = M144-2	868-4 = N16-4	874-2 = P38-2 874-3 = P38-3	879-3 = L81-3	884-3 = G125-3	889-3 = C16-3	

[a] This includes BBA Reviews on Bioenergetics, Vol 853 [b] This includes BBA Reviews on Biomembranes, Vol 864

© 1986, Elsevier Science Publishers B V (Biomedical Division)

All rights reserved No part of this publication may be reproduced, stored in a retrieval system, or transmitted, in any form or by any means, electronic, mechanical, photocopying, recording or otherwise without the prior written permission of the publisher, Elsevier Science Publishers B V (Biomedical Division), P O Box 1527, 1000 BM Amsterdam, The Netherlands Submission of a paper to this journal entails the author's irrevocable and exclusive authorization of the publisher to collect any sums or considerations for copying or reproduction payable by third parties (as mentioned in article 17 paragraph 2 of the Dutch Copyright Act of 1912 and in the Royal Decree of June 20, 1974 (S 351) pursuant to article 16b of the Dutch Copyright Act of 1912) and/or to act in or out of Court in connection therewith.

Special regulations for readers in the U S A This journal has been registered with the Copyright Clearance Center, Inc Consent is given for copying of articles for personal or internal use, or for the personal use of specific clients This consent is given on the condition that the copier pays through the Center the per-copy fee stated in the code on the first page of each article for copying beyond that permitted by Sections 107 or 108 of the U S. Copyright Law The appropriate fee should be forwarded with a copy of the first page of the article to the Copyright Clearance Center, Inc , 27 Congress Street, Salem, MA 01970, U S A. If no code appears in an article, the author has not given broad consent to copy and permission to copy must be obtained directly from the author. All articles published prior to 1980 may be copied for a per-copy fee of US$ 2 25, also payable through the Center. This consent does not extend to other kinds of copying, such as for general distribution, resale, advertising and promotion purposes, or for creating new collective works. Special written permission must be obtained from the publisher for such copying

Special regulations for authors Upon acceptance of an article by the journal, the author(s) will be asked to transfer copyright of the article to the publisher. This transfer will ensure the widest possible dissemination of information

Printed in The Netherlands

EDITORIAL

Since the 1982 Editorial by the Board of Managing Editors of *Biochimica et Biophysica Acta* [1], there have been a number of alterations in the Board's composition. Because of other duties, M. Gruber and R.A. Flavell retired in 1982 and 1985, respectively. In this period, the team was joined by P. Borst (1982) and K. van Dam (1985). Furthermore, P.W.J. Rigby was appointed as a (second) Managing Editor of *BBA Reviews on Cancer*. In 1983, L.L.M. van Deenen succeeded E.C. Slater as Chairman.

Following his retirement from the Chair of Biochemistry at the University of Amsterdam, E.C. Slater has decided to reduce his activities on behalf of *Biochimica et Biophysica Acta* from 1986 onwards. In 1957, E.C. Slater joined the founder of *Biochimica et Biophysica Acta*, H.G.K. Westenbrink, and has been largely responsible for the successful development and functioning of the Journal for nearly three decades. Fortunately, Dr. Slater has agreed to accept the appointment of Honorary Managing Editor and in that function he will continue to advise the Journal.

In 1986, E.P. Kennedy, Professor in Biological Chemistry at Harvard University Medical School, will also assume the position of Managing Editor for *Biochimica et Biophysica Acta*. Manuscripts can now also be submitted to the new office in Boston, MA, U.S.A., at the address given below, thus extending the number of BBA offices to four receiving centres (Amsterdam, Boston, Dundee and Oxford). The experience of the past three years has demonstrated that decentralization facilitates the contact between authors and Managing Editors, and allows potential authors the advantage of more choice when submitting papers. Authors should send their manuscripts (four copies) to one of the Managing Editors at the following addresses:

Dr. P. Borst, c/o BBA Editorial Secretariat, P.O. Box 1345, 1000 BH Amsterdam, The Netherlands.

Dr. P. Cohen, Department of Biochemistry, Medical Sciences Institute, University of Dundee, Dundee, DD1 4HN, United Kingdom.

Dr. K. van Dam, c/o BBA Editorial Secretariat, P.O. Box 1345, 1000 BH Amsterdam, The Netherlands.

Dr. L.L.M. van Deenen, c/o BBA Editorial Secretariat, P.O. Box 1345, 1000 BH Amsterdam, The Netherlands.

Dr. E.P. Kennedy, c/o BBA Editorial Secretariat (Boston), Box C 9123, Brookline, MA 02146, U.S.A.

Dr. G.K. Radda, Department of Biochemistry, University of Oxford, South Parks Road, Oxford, OX1 3QU, United Kingdom.

As previously announced [2], the section **Molecular Cell Research** includes a subsection covering papers dealing with investigations of hormones and neurotransmitters at the molecular level. In order to avoid confusion with existing journals for both authors and abstracting services, this subsection is now renamed: **Hormone and Neurotransmitter Action.** The scope of this subsection encompasses articles in the fields of receptor structure and function, transmembrane signalling systems, biological action of second messengers, and protein phosphorylation.

References

1 Editorial (1982) Biochim. Biophys. Acta 714, 1–5
2 Editorial (1985) Biochim. Biophys. Acta 844(3), i

Biochimica et Biophysica Acta 866 (1986) 1–14
Elsevier

BBA 91526

Immunological identification of rat tissue kallikrein cDNA and characterization of the kallikrein gene family

William L. Gerald [a], Julie Chao [b] and Lee Chao [a,*]

Departments of [a] Biochemistry and [b] Pharmacology, Medical University of South Carolina, Charleston, SC 29425 (U.S.A.)

(Received August 12th, 1985)

Key words: Kallikrein gene, cDNA; Nucleotide sequence, (Rat)

A tissue kallikrein cDNA was identified by direct immunological screening with affinity-purified anti-rat tissue kallikrein antibody from a rat submandibular cDNA library constructed with the expression vector pUC8. Sequence analysis of the kallikrein cDNA revealed an encoded protein 97% homologous to the partial amino acid sequence of rat submandibular kallikrein. This cDNA was used to hybrid-select kallikrein-specific RNA from submandibular gland. Translation of the hybrid-selected RNA in a cell-free assay system resulted in the production of a 37 kDa peptide representing the preproenzyme. In addition, hybrid-selection of RNA under less stringent conditions showed cross-hybridization with other submandibular gland mRNA species. In correlation with these results, analysis of rat genomic DNA showed extensive hybridization, suggesting a family of closely related kallikrein-like genes. Consequently, a Charon 4A rat genomic library was screened for kallikrein genes by hybridization with rat tissue kallikrein cDNA. Thirty-four clones were isolated and found to be highly homologous by hybridization and restriction enzymes analyses. Fourteen unique clones were identified by restriction enzyme site polymorphisms within DNA segments which hybridized to the kallikrein cDNA probe and it was estimated that at least 17 different kallikrein-like genes are present in the rat. Sequence and structural analysis of one of the genomic clones revealed a gene structure similar to that of other serine proteinases. Comparison of the partially sequenced exon regions of the gene with the sequence of rat tissue kallikrein cDNA reveals 89% identity when aligned for the greatest homology. However, the genomic sequence predicts termination codons in all three translational reading frames, implying that this gene is nonfunctional, i.e., a pseudogene. Comparison of the rat genomic sequence to a kallikrein-like gene from the mouse reveals extensive preservation of exons, less identity within introns and no significant homology between extragenic regions.

Introduction

Tissue kallikreins (EC 3.4.21.8) are serine proteinases which are able to generate biologically active kinin peptides from kininogen substrates by limited proteolysis [1]. Kallikreins have been found in diverse tissues such as kidney [2], salivary gland [3], pancreas [4], gastrointestinal mucosa [5], and recently in brain [6] and spleen [7]. Kallikrein from any one organ within a species is nearly identical to the enzyme at any other organ within the same species; however, isozymes are recognized [8] and may represent either different protein modifications or separate gene products. Quantitatively, the level of kallikrein differs markedly from tissue

---

[*] To whom correspondence should be addressed at: Department of Biochemistry, Medical University of South Carolina, 171 Ashley Avenue, Charleston, SC 29425, U.S.A.

Abbreviations. SSC, 0.15 M NaCl, 0.015 M sodium citrate, pH 7.0; Pipes, 1,4-piperazinediethanesulfonic acid

0167-4781/86/$03.50 © 1986 Elsevier Science Publishers B.V. (Biomedical Division)

to tissue [9] and seems to be differentially regulated by hormones [10].

Structural, antigenic and functional similarities exist among tissue kallikreins and several other serine proteinases such as epidermal growth factor binding protein, γ subunits of nerve growth factor, tonin, γ-renin and esterase A [11–14]. In addition, several other closely related serine proteinases have been predicted to exist by sequence analysis of cDNA molecules and genes [15–19]. Interestingly, these molecules are found to have extensive amino acid sequence homology and vary at amino acid residues implicated in substrate specificity [20]. Thus it appears that these enzymes have different specificity with regard to the zymogen substrate while maintaining the structure and function of the charge relay system of the serine proteinases. This has led to the popular concept of a serine proteinase subfamily of kallikrein-like enzymes which fucntion to process inactive precursor proteins to produce biologically active peptides by highly specific proteolytic cleaveage [18]. In addition, recent investigations have shown that kallikrein is a member of a large multigene family in the mouse [18]. The complexity of the kallikrein gene system and its tissue-specific regulation poses interesting questions concerning the evolution, structure and function of kallikrein-like genes and gene products. We describe here the isolation and analysis of a cDNA molecule corresponding to rat submandibular kallikrein and we have used this molecule to isolate a large group of closely related but non-identical kallikrein-like genes from the rat. A more detailed analysis of one member of this group reveals strong conservation of sequence in the presence of significant alteration in coding capacity.

Experimental procedures

RNA isolation, cDNA synthesis and cloning. Organs were removed from anesthetized Sprague-Dawley rats, rapidly frozen in liquid nitrogen and then pulverized with a mortar and pestle. Total RNA was prepared from the homogenate by the guanidinium thiocyanate extraction procedure [21] and polyadenylated RNA was isolated by two cycles of chromatography on an oligo(dT)-cellulose column. DNA complementary to rat submandibular gland poly(A)$^+$ RNA was synthesized by using Avian Myeloblastosis virus reverse transcriptase in a reaction mixture containing 100 μg/ml poly(A)$^+$ RNA, 100 mM Tris-HCl (pH 8.3), 10 mM $MgCl_2$, 140 mM KCl, 100 μg/ml oligo$(dT)_{12-18}$, 20 mM 2-mercaptoethanol, 500 units/ml RNAase, 1 mM each of dATP, dTTP and dGTP, 0.5 mM dCTP, 100 μCi [α-^{32}P]dCTP and 800 units/ml reverse transcriptase. Incubation was carried out at 42°C for 2 h. Sodium EDTA and sodium hydroxide were added to 0.02 M and 0.05 M, respectively, and the solution was heated to 65°C for 1 h to hydrolyze RNA. The solution was neutralized by adding Tris-HCl (pH 8.0) to 0.1 M and HCl to 0.02 M. Complementary DNA was separated from unincorporated dNTPs by gel filtration on Sephadex G-50 in spun column chromatography [22]. The second strand was synthesized using the same conditions as for first-strand synthesis with the omission of oligo(dT). Single-stranded DNA was digested for 20 min at 37°C with 50 units S_1 nuclease in a volume of 0.1 ml containing 0.2 M NaCl, 0.05 M sodium acetate (pH 4.5), 1 mM zinc sulfate and 5% glycerol. Staggered ends were filled in by incubating 100 ng of cDNA with 2 units of Klenow fragment of DNA polymerase I in 0.05 M Tris-HCl (pH 7.4), 7 mM MgCl, 1 mM dithiothreitol and 150 nM of each dNTP for 1 h at room temperature. The blunt-ended cDNA molecules were phosphorylated with T_4 polynucleotide kinase. 50 ng of cDNA were ligated to 1 μg of *Sma*I-cleaved, bacterial alkaline phosphatase-treated pUC8 [23] using T_4 DNA ligase. The reaction contained 50 mM Tris-HCl (pH 7.4), 10 mM MgCl, 10 mM dithiothreitol, 0.25 mM spermidine, 1 mM ATP, 50 μg/ml bovine serum albumin and 5 units of ligase. Incubation was carried out at 12°C for 14 h. The ligation reaction mixture was used to transform *Escherichia coli* JM83 [23].

Immunological screening of cDNA library. Immunological screening was carried out by a modification of the method of Helfman et al. [24]. Following lysis of colonies on nitrocellulose filters and incubation with lysozyme and DNAase, the filters were rinsed twice for 15 min each with Tris-buffered saline (50 mM Tris-HCl (pH 7.5), 150 mM NaCl). The filters were then incubated for 2 h at room temperature with affinity-purified rabbit anti-kallikrein antibody (5 μg/ml) in saline plus 3% bovine serum albumin. Filters were washed for 30 min with saline, twice for 30 min each time with saline containing 0.5% Nonidet P-40 and once more with saline for 30 min. The filters were then incubated for 1 h with 100 ml of 3% bovine serum albumin in saline containing $1 \cdot 10^7$ cpm of ^{125}I-labeled protein A [6]. Final washing was carried out with 50 mM Tris-HCl (pH 7.5), 150 mM NaCl, 5 mM EDTA, 0.1% sodium dodecyl sulfate, 0.5% Triton X-100 and 0.25% gelatin for 2 h twice. The filters were dried and used to expose radiographic films.

Hybrid-selected translation assay. 20 μg of single-stranded DNA from M13 bacteriophage were dissolved in water at a concentration of 0.5 mg/ml and heated to 100°C for 10 min. The solution was rapidly chilled on ice and NaOH was added to 0.5 M. After incubation at room temperature for 20 min, the solution was neutralized by the addition of Tris-HCl (pH 8.0) to 0.15 M, concentrated HCl to 0.33 M, NaCl to 0.33 M and sodium citrate to 0.1 M. The neutralized DNA was spotted onto 1-cm^2 strips of nitrocellulose filter paper and the filters were allowed to dry. The filters were washed twice with 6 × SSC, dried in room air and then baked for 2 h at 80°C in a vacuum oven.

For hybridization of RNA, the filters were boiled in water for 1 min and then placed in 50–100 μl of hybridization solution which contained 100–200 μg/ml total tissue RNA, 65% formamide, 20 mM pipes (pH 6.4), 0.2% sodium dodecyl sulfate, 0.4 M NaCl and 100 μg/ml yeast tRNA which had been heated to 70°C for 10 min. Hybridization was carried out for 3 h at the temperature indicated in the figure legends. Following hybridization the filters were washed 10 times with a solution containing 10 mM Tris-HCl (pH 7.6), 0.15 M NaCl, 1 mM EDTA and 0.5% sodium dodecyl sulfate at 65°C, then twice with the same buffer without sodium dodecyl sulfate. The filters were then placed in 300 μl of water containing 30 μg of yeast tRNA, boiled for 1 min and then rapidly chilled in a solid CO_2/ethanol bath. The samples were thawed on ice, and the filters were removed. After extraction of the sample with phenol/chloroform/isoamyl alcohol (25 : 24 : 1, v/v) the RNA was ethanol-precipitated. The precipitate was washed with 70% ethanol, dried and dissolved in water for translation. Cell-free translation was carried out using rabbit reticulocyte lysates [6]. For SDS-polyacrylamide gel analysis of proteins, 1.5 mm linear gradient separating slab gels containing 8% to 16% acrylamide were used in the discontinuous buffer system of of Laemmli [25] with a 4% acrylamide stacking gel.

Rat genomic library construction and screening. Charon 4A phage was kindly supplied to us by F. Blattner. The procedures for Charon phage arm isolation and rat submandibular DNA purification were those described by Maniatis et al. [26]. The purified rat submandibular DNA was partially digested with *Eco*RI and separated in 0.45% agarose gels [26]. Regions of the agarose gel containing DNA fragments between 16 and 20 kb were excised and the DNA was recovered by buffer elution [27]. The in vitro packaging procedure was as described in Maniatis et al. [22]. The library was amplified once by plating the packaged phage using LE 392 as the plating bacteria. A plate lysate was made and stored in SM buffer [22] as the library stock. The amplified rat genomic library was screened using the in situ plaque hybridization technique of Benton and Davis [28]. Approx. 450000 plaque forming units were screened at high density. The positive plaques were purified and rescreened at low-density plating conditions.

DNA and RNA hybridization analyses. The procedures for DNA hybridization were according to those described by Maniatis et al. [22]. RNA filter hybridization was carried out by the method of Thomas [29].

DNA sequence analysis. The dideoxy method of Sanger et al. [30] was used for DNA sequencing with the M13 vectors of Messing [31] and commercially available primers.

Results

Construction of rat submandibular gland cDNA library

Double-stranded cDNA was synthesized by using female Sprague-Dawley rat submandibular gland poly(A)$^+$ RNA as template. The blunt-ended cDNA molecules were ligated into the *Sma*I site o pUC8 [23], a bacterial expression cloning plasmid. This site is located within the *lacZ* coding portion of the vector, making expression of the cDNA insert possible. Production of the appropriate translation product in bacterial transformants is dependent on the proper orientation and frame of cDNA insertion. Under the conditions used for production of the submandibular gland cDNA library, for any particular cDNA molecule one out of six possible orientations of insertion would allow cDNA expression. Transformation of *E. coli* strain JM83 with these recombinant molecules yielded approx. 2400 individual ampicillin-resistant colonies, 80–90% of which contained plasmids bearing inserts.

Screening of the cDNA library

1600 colonies from the cDNA library were replica-plated onto ampicillin plates and grown to a colony size of 1–2 mm. The colonies were then transferred to nitrocellulose paper and processed for immunological screening [24] by using affinity-purified rabbit anti-rat kallikrein antibody followed by ^{125}I-protein A binding [6] Fig. 1 shows the autoradiograph of the two filters that contained colonies synthesizing protein immunologically related to kallikrein. One of these colonies (carrying a cDNA insert designated RSK1105) gave a stronger signal and was further analyzed. The RSK1105 cDNA insert was excised by using the adjacent *Eco*RI and *Bam*HI restriction endonuclease sites within the cloning vector. The released fragment was purified by agarose gel electrophoresis, then labeled by nick-translation and used as a probe to screen the library for homologous inserts. A number of clones were isolated that contained partial homology with RSK1105; however, further analysis revealed that only about 0.4% of clones in the cDNA library hybridized to RSK1105 under stringent conditions. None of these homologous inserts were longer than the insert of RSK1105.

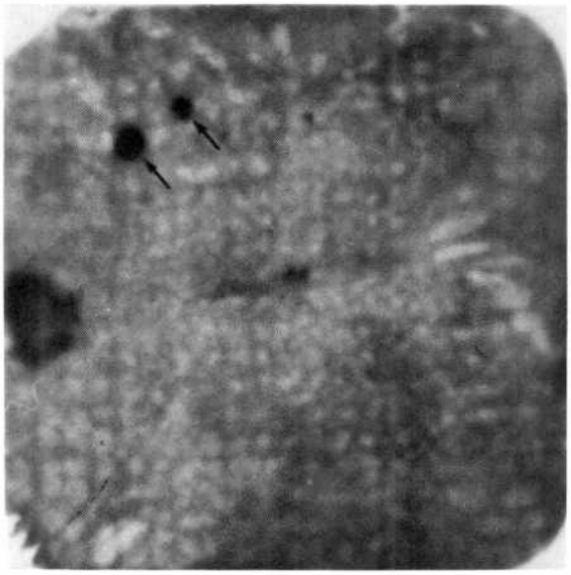

Fig. 1. Immunological detection of bacterial colonies expressing cloned kallikrein cDNA. 1600 cDNA-bearing bacterial colonies on nitrocellulose filter paper were screened for production of kallikrein-like peptides by using affinity-purified anti-rat tissue kallikrein antibody and ^{125}I-protein A as described in Materials and Methods. The figure shows autoradiograms of one filter that contained positive colonies. The clone with a stronger signal corresponds to RSK1105.

Nucleotide sequence of RSK1105

Fig. 2 shows the complete nucleotide sequence of the 534-basepair cDNA insert from RSK1105, the strategy used to determine the nucleotide sequence, and a schematic diagram of this molecule. In order to completely sequence both strands of the insert the large *Eco*RI-*Bam*HI fragment was cleaved with *Hae*III and the resulting fragments were treated with Klenow fragment of DNA polymerase I to fill in recessed ends. The resulting blunt-ended molecules were then cloned in both orientations into the *Sma*I site of M13mp8 for sequencing. Computer analysis of the sequence [31] revealed an open reading frame beginning at the β-galactosidase initiation codon within the pUC8 vector and extending to position 455 of the cDNA insert. This is followed by 46 nucleotides in the 3′ untranslated region and a poly(A) tail of 33 nucleotides. Comparison of the nucleotide sequence of RSK1105 with the sequence of kallikrein-like cDNA from rat pancreas [15] reveals complete homology except for the site of poly(A) tail addition. In the submandibular gland polyadenylation takes place following a C residue 13 bases 3′ to the canonical AAUAAA sequence often present 11–30 bases preceding poly(A) tails of eucaryotic mRNA. In the pancreatic sequence polyadenylation takes places following a C residue 15 bases 3′ to the polyadenylation signal. This difference may simply be the result of heterogene-

```
                                                                              60
   Arg Gln Pro Gly Asp Asp Tyr Ser Asn Asp Leu Met Leu Leu His Leu Ser Gln Pro Ala
CC CGA CAA CCT GGG GAC GAC TAC AGC AAT GAT TTG ATG CTG CTC CAC CTC AGC CAG CCT GCG

                                                                          120
Asp Ile Thr Asp Gly Val Lys Val Ile Asp Leu Pro Ile Glu Glu Pro Lys Val Gly Ser Thr
GAC ATC ACA GAT GGT GTG AAG GTC ATC GAT CTG CCC ATT GAG GAG CCC AAG GTG GGG AGC ACC

                                                                      180
Cys Leu Ala Ser Gly Trp Gly Ser Ile Thr Pro Asp Gly Leu Glu Leu Ser Asp Asp Leu Gln
TGC CTT GCC TCG GGC TGG GGC AGC ATC ACA CCT GAC GGA TTG GAA TTA AGT GAT GAT CTC CAG

                                                                  240
Cys Val Asn Ile Asp Leu Leu Ser Asn Glu Lys Cys Val Glu Ala His Lys Glu Glu Val Thr
TGT GTG AAC ATC GAT CTT CTG TCT AAT GAG AAG TGC GTC GAG GCA CAC AAA GAA GAG GTG ACA

                                                              300
Asp Leu Met Leu Cys Ala Gly Glu Met Asp Gly Gly Lys Asp Thr Cys Lys Gly Asp Ser Gly
GAT CTC ATG CTG TGT GCA GGA GAG ATG GAT GGG GGC AAA GAC ACT TGC AAG GGT GAC TCA GGA

                                                          360
Gly Pro Leu Ile Cys Asn Gly Val Leu Gln Gly Ile Thr Ser Trp Gly Phe Asn Pro Cys Gly
GGC CCC CTC ATC TGT AAT GGT GTG CTC CAA GGC ATC ACG TCC TGG GGC TTT AAC CCA TGC GGT

                                                      420
Glu Pro Lys Lys Pro Gly Ile Tyr Thr Lys Leu Ile Lys Phe Thr Pro Trp Ile Lys Glu Val
GAA CCC AAG AAG CCA GGC ATC TAC ACC AAA CTT ATT AAG TTC ACC CCC TGG ATA AAA GAA GTT

                                          480
Met Lys Glu Asn Pro STOP
ATG AAG GAA AAC CCC TGA GTGTCACACAGTCCCCTGGTCTCAATAAAACCCACCATGCAGCpoly(A)33
```

A

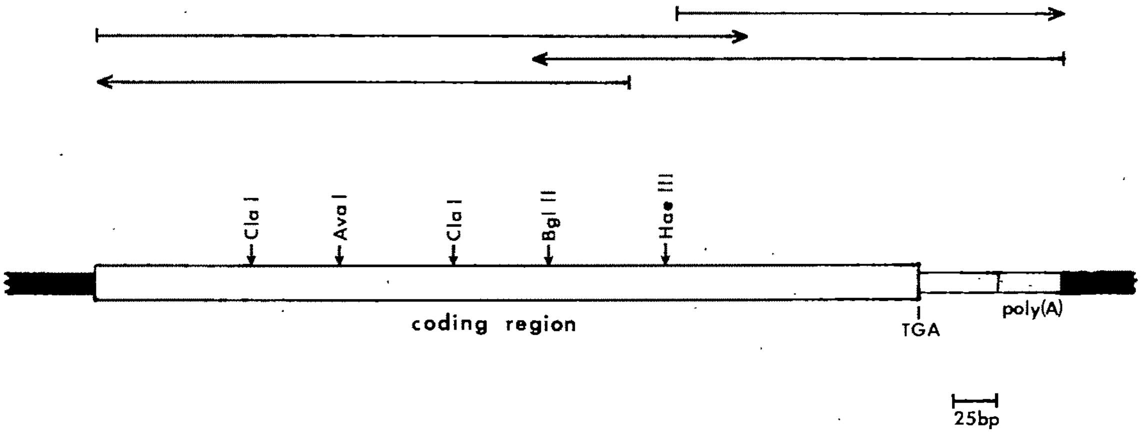

Fig. 2. Schematic diagram and nucleotide sequence of the RSK1105 cDNA insert. A. The nucleotide sequence determination was by the M13 dideoxynucleotide method [30]. Commercially available primers to the M13 cloning vectors of Messing [31] were used. Both strands were sequenced and in most cases at least two analyses were performed. The deduced amino acid sequence is also shown. The conserved sequence AATAAA in the 3′ noncoding region is underlined. B. Schematic representation of the cDNA insert of RSK1105. The open bar represents the cloned cDNA inserted at the *Sma*I site of the pUC8 plasmid (solid bar). Sites for restriction enzymes are depicted by vertical arrows. The horizontal arrows above the restriction map represent the strategy for sequence determination and the extent of the analysis.

ity in the site of polyadenylation, as has been noted for other mRNA species [32,33], or genic variation in the rat. However, the different sites for polyadenylation may be due to tissue-specific or sex-related differences in either the kallikrein gene or in the processing of the kallikrein precursor RNA. In further investigation of this minor discrepancy, a second kallikrein cDNA from the rat submandibular gland cDNA library was identified by colony hybridization and subjected to partial sequence analysis revealing a site of polyadenylation identical to that found in RSK1105.

The predicted amino acid sequence derived from submandibular kallikrein cDNA represents the C-terminal 151 residues of the enzyme and has partial overlap with the incomplete amino acid sequence of rat submandibular kallikrein [15]. 40 of 41 overlapping amino acids are homologous with the single residue difference being a glutamine in the cDNA sequence (position 6–8, Fig. 2A) for a phenylalanine in the amino acid sequence. From comparison of sequence data and the immunoreactivity of the cDNA clone, we conclude that the insert in RSK1105 corresponds to rat tissue kallikrein mRNA. Additional evidence for this conclusion comes from in vitro translation of RNA selected by RSK1105 and will be described below.

Hybrid-selection and translation of rat submandibular gland kallikrein mRNA

Kallikrein-specific mRNA from rat submandibular gland was isolated by hybrid selection using the non-coding strand of RSK1105. The cDNA molecule was ligated into the M13 bacteriophage cloning vector mp9 and single-stranded DNA was isolated from lysates of the recombinant phage. The DNA was bound to nitrocellulose paper and hybridized to total RNA isolated from rat submandibular gland. Results of this experiment are shown in Fig. 3. When RNA selected by hybridization under moderately stringent conditions (50 to 55°C, 65% formamide) was translated in vitro, at least two proteins were produced with approximate M_r of 32 000 and 37 000 (Fig. 3, lanes c–f). Under more stringent hybridization conditions (65°C, 65% formamide) only one protein was produced by translation of the hybrid-selected RNA (lanes g and h). This protein is a single chain with an apparent molecular weight of 37 000 as estimated by SDS-polyacrylamide gel electrophoresis. This probably represents the preproenzyme and is of sufficient length to account for the 33.8 kDa enzyme (molecular weight derived from amino acid composition analysis) isolated from rat urine [34]. The finding that other mRNA species cross-hybridize with kallikrein cDNA is not surprising considering the strong homology between several serine proteinases isolated from rat submandibular gland.

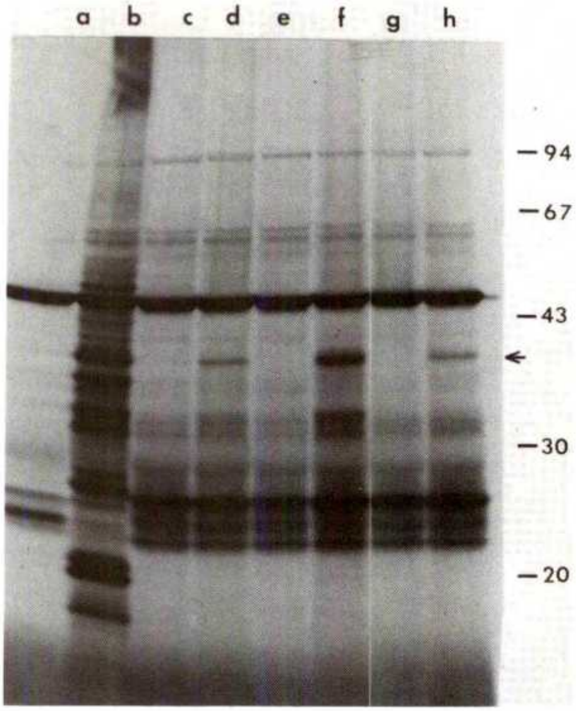

Fig. 3. Translation of rat submandibular gland mRNA selected by hybridization to RSK1105. Hybrid-selection, in vitro translations and SDS-polyacrylamide gel electrophoresis were carried out as described in Experimental procedures. Shown is a fluorogram of the dried gel. Lane a: endogenous protein synthesis in the absence of added mRNA. Lane b: proteins synthesized in the presence of rat submandibular total RNA. Lane c: proteins synthesized in the presence of RNA hybrid-selected by mp9 (cloning vector) ssDNA at 50°C. Lane d: proteins synthesized in the presence of RNA hybrid-selected by mp9RSK1105 ssDNA at 50°C. Lanes e and f: same as c and d, respectively, except hybrid-selection was carried out at 55°C. Lanes g and h: same as c and d, respectively, except that hybrid-selection was carried out at 65°C. The translation product of kallikrein in mRNA is indicated by an arrow. Migration positions of molecular mass markers are indicated at the right in kilodaltons.

Hybridization analysis of kallikrein genes in the rat

Our detection of several closely related kallikrein-like mRNA species in rat and the recent identification [18] of a kallikrein-like multi-gene family in the mouse led us to search for the presence of kallikrein-like sequences in rat genomic DNA. Fig. 4 shows the hybridization pattern obtained when kallikrein cDNA was used as a probe for *Eco*RI-cleaved rat genomic DNA from liver, submandibular gland, pancreas, and kidney. Approximately eight DNA fragments were identified, comprising greater than 50 kilobases of DNA. Such extensive hybridization suggests the existence of multiple kallikrein-like genes in the rat. Furthermore, the analysis showed no gross rearrangements of kallikrein-like genes in the four tissues examined. To explore further the rat kallikrein multigene family, individual genes were isolated as described below.

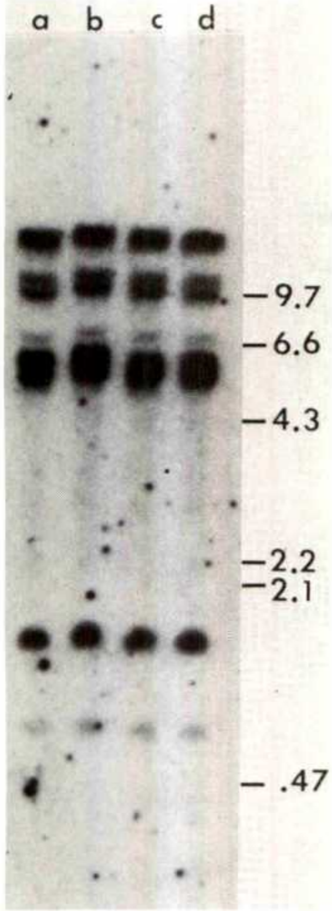

Fig. 4. Hybridization analysis of rat genomic DNA using RSK1105 cDNA probe. Rat genomic DNA was isolated from various tissues. 15 μg of DNA were exhaustively digested with *Eco*RI and the fragments were electrophoretically separated on a 0.8% agarose gel. The DNA was transferred to nitrocellulose paper and hybridized to the cDNA insert from RSK1105 which had been labelled by nick translation in the presence of [α-^{32}P]dCTP [22]. After washing, the filter was dried and used to expose radiographic film with an intensifying screen. Lane a: DNA isolated from liver. Lane b: DNA from submandibular gland. Lane c: DNA from pancreas. Lane d: DNA from kidney. The migration position of DNA fragment markers of defined size is indicated in kilobasepairs.

Screening of the rat genomic library for kallikrein gene sequences

The rat submandibular gland kallikrein cDNA molecule was used as a hybridization probe to screen the rat genomic library for kallikrein genes. The hybridization conditions used for screening (50% formamide, 0.8 M NaCl, 42°C) are considered moderately stringent and should detect only DNA sequences which contain a high degree of homology with the kallikrein cDNA. From screening of approx. 450 000 plaques from the genomic library, 34 clones were isolated and purified by repated screening with low-density plating. Assuming an average insert size of 17 kb and a rat genome size of $3 \cdot 10^9$ bp, only 1 in 180 000 plaques will carry a particular single copy sequence. That being the case, then approx. 17 kallikrein-like clones per genome equivalent of DNA were found, implying 17 unlinked genes per genome. However, linkage has been found in the mouse [18,19] and is probable in the rat, which means that more than one gene could be carried on a single clone causing an underestimation of the number of rat kallikrein genes.

Restriction enzyme digestion and filter hybridization analysis of rat kallikrein-like genes

In an effort to identify the genomic clone with the greatest homology to rat tissue kallikrein cDNA, nitrocellulose filter hybridization was carried out. DNA was prepared from each of the genomic clones and examined by agarose gel electrophoresis, transfer to nitrocellulose paper, and hybridization analysis using kallikrein cDNA as probe. The results are shown in Fig. 5. Hybridization under moderately stringent conditions (0.8

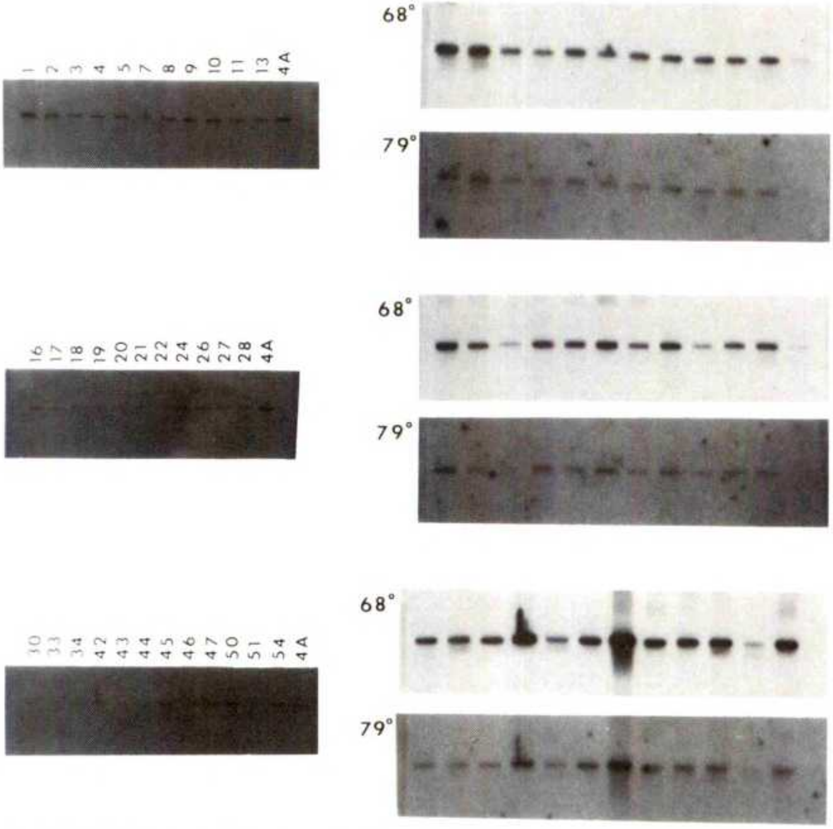
1 2 3 4 5 7 8 9 10 11 13 4A
68°
79°
16 17 18 19 20 21 22 24 26 27 28 4A
68°
79°
30 33 34 42 43 44 45 46 47 50 51 54 4A
68°
79°

Fig. 5. Hybridization analysis of rat kallikrein-like genomic clones using kallikrein cDNA as probe. The small panels on the left show negatives from photographs of ethidium bromide-stained agarose gels on which genomic clones had been electrophoresed. The numbers above the gel columns are designations for individual clones. 4A refers to the cloning vector charon 4A which contains weakly cross-hybridizing sequences within one of the internal fragments. The panels on the right are autoradiograms of DNA transfers from the corresponding agarose gel after hybridization to the radioactive probe. The hybridization conditions are as described in Experimental procedures and carried out at the temperature indicated beside the autoradiogram.

M NaCl, 68°C) yielded little differential hybridization among the isolates except that RSKG18, RSKG26 and RSKG51 showed very weak signals. The signal strengths of all other clones were proportional to the amount of DNA input. Rehybridization under extremely stringent conditions (0.8 M NaCl, 79°C, a temperature approx. 5–9 degrees below the theoretical T_m for our kallikrein cDNA probe) resulted in much weaker signals but again differential hybridization among the clones was minimal. This result suggests that a group of closely related genes had been isolated and filter hybridization was unable to identify the genomic clone most homologous to the kallikrein cDNA. We then carried out restriction enzyme digestion along with hybridization analysis to better characterize the clones. The chart depicted in Fig. 6 shows the results of this examination. It should be noted that in this analysis very small DNA fragments and the *Hin*dIII fragments which remained attached to the vector arms may have been missed. The analysis reveals a high degree of conservation of some restriction sites, again emphasizing the close relationship of this gene family. Fourteen genomic clones were found to be different by polymorphisms of sites for the two restriction enzymes within hybridizing segments of DNA. Comparison of rat genomic DNA hybridization (Fig. 4) with the hybridizing fragments isolated from the genomic library shows that almost all fragments are represented by the genomic clones.

A. EcoRI Digestion of Genomic Clones

Clone															
11	**14000**														
18	**14000**														
21	14000														
27	14000														
30	14000														
33	**14000**														
42	**14000**														
43	**14000**														
44	**14000**														
45	14000														
3		**12000**											2000		**1000**
4		**12000**												1400	600
26		12000												1400	600
28		12000													
64		**12000**												**1400**	
1			**9000**						4000		3000				
5			**9000**								3000		2000		
8			9000						**4000**	3200					
10			**9000**						4000						
13			**9000**						4000						**500**
16			**9000**						4000						
24			**9000**						4000						**800**
34			**9000**						4000				2000		
47			**9000**								3000	**2200**			
2				8500											**500**
17				8500					4000						**700**
20				8500					**4000**						
50				8500					4000				1900		**800**
51				**8500**					4000						
19					7200		**5000**								
7						**6000**		4100			3000			**1500**	
9						**6000**		4100			3000		2000	**1500**	
22						**6000**					3000	2200		1500	
46						**6000**		4100						1500	

B. Hind III Digestion of Genomic Clones

Clone												
3					**8800**			4000				1750
4				10000	**8800**							700
26				10000	**8800**							700
28	**20000**					6500		4000				1750
64				9300	**8800**							700
1			16000				4400			**2000**	1500	
5				10000			4400			**2000**	1500	
8			15000				4400			**2000**	1500	
10				10000			4400			**2000**	1500	
13		19000								**2000**		
16	**20000**	19000										
24		18000								2000		
34						6500	**4400**		2200	**2000**	1200	
47			12000				4400		2200	**2000**	1500	
2			16000							**2000**		
17										**2000**		
20					**7200**							
50										**2000**		
51	**20000**	19000										
19						**6400**						
7				9600	**7000**				**2100**		1500	
9					7000				**2100**		1200	
22										**2000**		
46				10000					**2100**		1200	

Fig. 6. Restriction enzyme digestion and hybridization analysis of rat kallikrein-like genomic clones. DNAs from genomic clones were digested to completion with the indicated restriction enzyme, electrophoresed on agarose gels, transferred to nitrocellulose filter paper and hybridized with radioactive kallikrein cDNA as probe. The approximate size of restriction fragments in basepairs from inserted DNA is depicted and hybridization to the probe is indicated by bold print. The clone designation number is listed on the left. Clones which did not contain *Eco*RI sites within inserted DNA were not subjected to *Hin*dIII analysis. A, *Eco*RI digestion, B, *Hin*dIII digestion.

Structure of RSKG-9

In an effor to characterize further the kallikrein-like gene family, we have analyzed one of the genomic clones, RSKG-9, in detail. RSKG-9 contains more than 16 500 bp of genomic DNA and has one *Hin*dIII and two *Eco*RI fragments which hybridize to the kallikrein cDNA probe. *Eco*RI fragments of the genomic clone were used in hybridization to rat submandibular gland RNA in an effort to identify the locations of other portions of the kallikrein gene. The upper panel of Fig. 7 shows the results of this experiment. Three of the five fragments hybridized to an RNA species of the same size as kallikrein mRNA. Based on these results we identified a fragment which hybridized to messenger RNA but not to the partial kallikrein cDNA. The fragment was approx. 4100 bases in length and apparently contains the 5′ end of the gene. Restriction mapping, hybridization and sequence analysis was used to construct the partial structural map of the kallikrein-like gene in RSKG-9. This is depicted in Fig. 7. The 5′ end of the gene is located in an unsequenced portion of the 4.1 kb *Eco*RI restriction fragment and the 3′ end of the gene is located in an unsequenced portion of the 2 kb *Hin*dIII restriction fragment. One complete exon and a portion of another is located within the 1.5 kb *Eco*RI restriction fragment and were completely sequenced. A small portion of DNA measuring 250–500 bp is located between the 1.5 and 4.1 kb *Eco*RI fragments and is only partially characterized. The gene is less

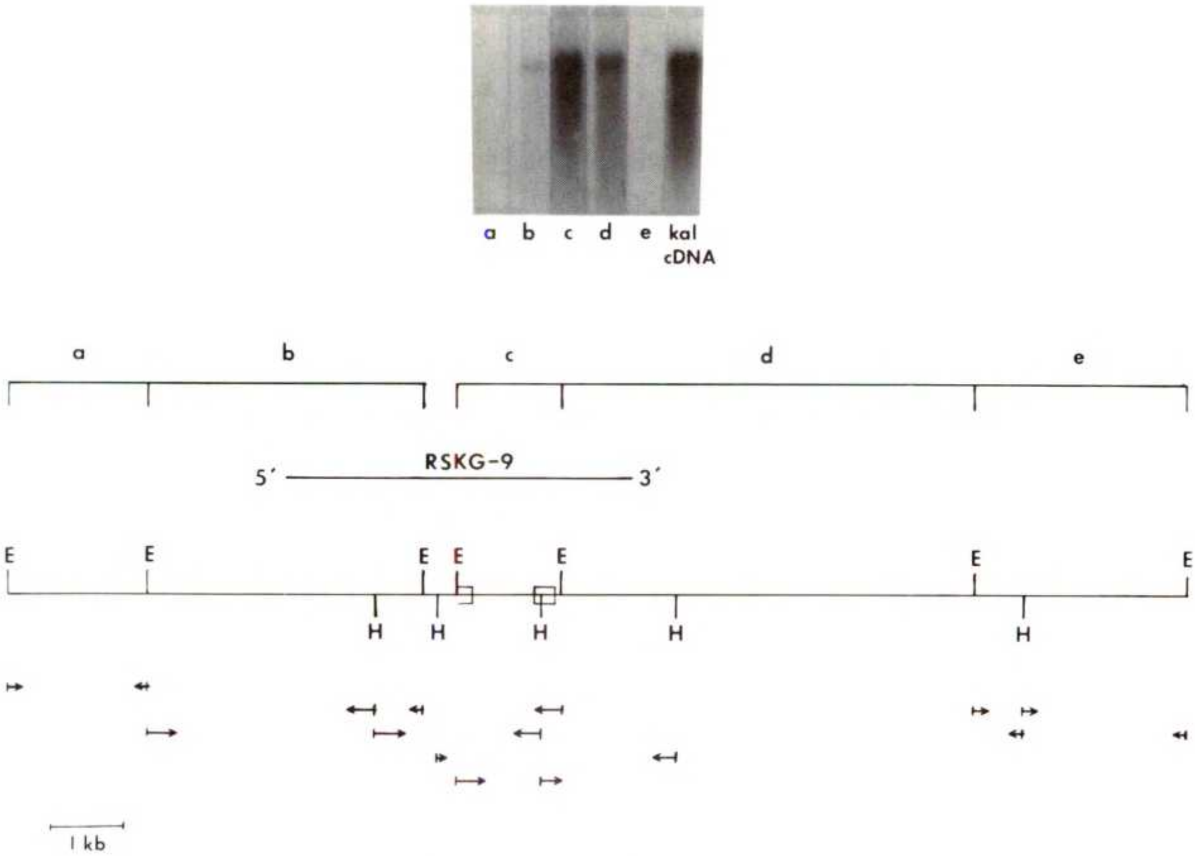

Fig. 7. Partial structural map and mRNA hybridization analysis of RSKG-9. Rat submandibular gland RNA was electrophoresed on agarose gels, transferred to nitrocellulose paper, and hybridized to the indicated restriction fragments (a–e) from the genomic clone. The upper panel is the autoradiogram of the hybridized blot. The diagram depicts the restriction map of the genomic clone (E, *Eco*RI; H, *Hin*dIII). The boxed regions are the positions of exons derived from sequence analysis. The location of the gene is depicted by the line designated RSKG-9 above the restriction map. The 5′ and 3′ ends are indicated. Portions of the clone which have been sequenced are indicated by the arrows below the restriction map.

than 6.5 kb in length and seems to have an intron exon structure similar to that of rat trypsin [35] and mouse kallikrein-like [18] genes, which both have 5 exons and the 2nd and 3rd exons map similar to the positions of the exons located here.

Portions of the genomic clone were subcloned into the M13 vectors of Messing [31] for sequence analysis. More than 3000 bases from the clone were sequenced, of which 2692 bases are mapped as to position (data not shown). A comparison of the RSKG-9 exons with the sequence of rat kallikrein cDNA is shown in Fig. 8. There is approx. 89% identity between the two sequences when aligned for the greatest homology. Four deletions, three insertions, and 34 substitutions exist within the 376 nucleotides from gene exons compared to rat kallikrein cDNA and are dispersed throughout the sequence. When the coding capacity for the exons of RSKG-9 were examined all three possible reading frames contained termination codons created by the sequence differences. Although the sequence analysis is incomplete it suggests that this gene is nonfunctional, i.e. a pseudogene.

A comparison of the exon region of the rat genomic sequences with that of the kallikrein-like gene from the mouse [18] reveals a remarkable sequence homology of 83% (Fig. 9). There is little homology when the introns of the rat genomic

```
                                                                                50
Kallikrein - G AAT TCC CAA CCC TGG CAA GTG GCT GTG TAC TAC TTC GGC GAA  TAC CTA TGT
                                                                      ‡
RSKG-9     - * *** *** *** *** *** *** *** *** C*A *** AG* *** A * ***A *** **C **C

                                                                           100
Kallikrein -   GGG GGT GTC CTG ATA GAC CCC AGC TGG GTG ATC ACA GCT GCT CAC TGC GCA ACC

RSKG-9     -   *** *** *** *** *** *** *** *** ***  ** *** **G *** **C *** *** T*T *G*

                                                                   150
Kallikrein -   GAC AAT TAC CAG GTT TGG CTG GGC CGA AAC AAC CTA TAT GAA GAT GAA CCC

RSKG-9     -   A** *** *** *** *** **  *** *** *** *** *** *** *TA *** *** *** **A

                                                                   200
Kallikrein -   TTT GCT CAG CAC CGG CTT GTC AGC CAA AGC TTC CCT CAC CCC GGT TTC  AAC
                                                                              ‡
RSKG-9     -   *** *** *** *** *** *** *** **T *** *** *** *** *** **T *AC ***A ***

                                                                   250
Kallikrein -   CAG GAC CTC ATA TGG AAC CAC ACC CGA CAA CCT GGG GAC GAC TAC AGC AAT GAT

RSKG-9     -   **  TT* *** **G A** *** *** *** *** A** *** **C **T *** C** *** *** ***

                                                                300
Kallikrein -   TTG ATG CTG CTC CAC CTC AGC C AG CCT GCG GAC ATC ACA GAT GGT GTG AAG
                                            ‡
RSKG-9     -   C** *** *** **A **T *** *** *G** *** *** *** *** *** *** **G *** ***

                                                           350
Kallikrein -   GTC ATC GAT CTG CCC ATT GAG GAG CCC AAG GTG GGG AGC ACC TGC CTT GCC TCG

RSKG-9     -   *** *** *** *** *** *C* *** *** *** *** *** *** *** *** *** *** *** **A


Kallikrein -   GGC TGG GGC A

RSKG-9     -   *** *** *** *
```

Fig. 8. Comparison of RSKG-9 exons with kallikrein cDNA sequence. The upper sequence is rat tissue kallikrein cDNA and the lower sequence is from exon regions of the rat genomic clone RSKG-9. The sequences are aligned for the greatest homology. Identical bases are indicated by *. Insertions are designed by ‡, while deletions are left blank.

clone are compared with that of the mouse genomic clone (data not shown). Taken together these results indicate that a stringent conservation of the exons and a rapid drift of the intron sequences have occurred since the divergence of the two species.

Discussion

We have used direct immunological screening to identify a rat submandibular gland cDNA corresponding to a kallikrein-like mRNA. Several lines of evidence indicate that this cDNA clone encodes rat tissue kallikrein. First, when cloned into an expression vector, the cDNA produces a peptide which is recognized by affinity-purified antibody

```
                                                                   50
MGK1         AGAACTCCCA GCCCTGGCAT GTGGCTGTGT ACCGCTACAA GGAATATATA

RSKG9        ****T***** A********A ******C*A* **A***T**C *A****CC*C

                                                           100
TGCGGGGGAG   TCCTGTTGGA TGCCAACTGG GTTCTCACAG CTGCCCACTG CTATTATGAA

********T*   *****A*A** CC******** T GA****G* ********** ******CA**

                                                150
AAGAACAACG   TTTGGCTGGG CAAAAACAAC CTATACCAAG ATGAACCCTC TGCTCAGCAC

**TT****G*   ****C **** **G******* ******G*** *******A*T **********

                                    200
CGA TTAGTCA G CAAAAGCTT CCTTCACCCT TGCTACAACA TGAGCCTCCA TCGGAACCGC

**GC******* *T*** ***** **C******* ********AC CATT****AT GA******A*

                        250
AT CCAAAATC CTCAGGACGA CTACAGCTAT GACCTGCTGC TGCTCCGACT CAGCA AGCCT

**C******** **GG***T** *C*****A** **T***A*** ****A*AT** ****CC*****

            300                                                    350
GCTGACATCA CAGATGTTFT GAAGCCCATC GCCCTGCCCA CTGAGGAGCC CAAGCTGGGG

**G******* ******GG** *****T**** *AT******* ********** **********


AGCACATGCC TTGCCTCAGG CTGGGGCAG

********** ********** *********
```

Fig. 9. Comparison of the exon regions of a mouse kallikrein gene with that of RSKG9. The upper sequence is from mouse kallikrein gene exons 2 and 3. The lower sequence is the counterpart in RSKG9. The two sequences are aligned for the greatest homology by introducing seven single base gaps. Identical bases are indicated by *.

to rat tissue kallikrein. Second, there is a strong homology between the deduced amino acid sequence of this cDNA and the known partial amino acid sequence of rat submandibular gland kallikrein [12,15]. Third, when RNA from rat submandibular gland is selected by RSK1105 under stringent conditions only one protein is produced on in vitro translation. This protein has an approximate molecular weight of 37000, which is adequate to account for the molecular weight of tissue kallikrein derived from amino acid composition ($M_r = 33\,800$) [34] and to account for pre- and pro-peptides known to exist for most secreted proteinases [36,37]. This is the first time a translation product corresponding to a tissue kallikrein cDNA has been identified and it is interesting to note that the preproenzyme migrates as a much larger molecule than previously predicted by cDNA sequence analysis [15]. The 37 kDa preprokallikrein is also larger than the 32 kDa protein coded for by a cross-hybridizing mRNA species, which may represent a closely homologous preproenzyme. It will be interesting to obtain and compare the complete sequences of rat tissue kallikrein and other members of the kallikrein-like family of serine proteinases in order to evaluate their structure-function relationships. The particular amino acid sequence differences found in the larger tissue kallikrein protein may give insight into the regulation, processing or function of this enzyme.

The existence of a family of kallikrein-like enzymes has been indicated by structural and functional similarities of tissue kallikrein, tonin, epidermal growth factor binding protein, γ subunit of nerve growth factor, and esterase A [11–14,38]. In addition, a family of 25–30 kallikrein-like gene sequences have been identified in the mouse [18]. Our findings support the existence of a kallikrein-like family of genes in the rat by cross-hybridization of the kallikrein cDNA with other mRNA species from rat submandibular gland and by extensive hybridization to rat genomic DNA. We therefore used the kallikrein cDNA molecule to isolate individual kallikrein-like genes from a rat genomic library.

The kallikrein-like gene family is an example of variant repitition with many related but nonidentical members. It is estimated that slightly more than 17 kallikrein-like genes exist in the rat. This is deduced from the finding of 17 clones per genome equivalent of DNA and the possibility of linkage. The number of genes found here agrees well with the number of members of the mouse kallikrein gene family [20]. In fact it is possible that a much larger family of genes with greater variation exists and was not detected due to the stringency of the screening conditions. However, the genomic clones isolated account for practically all of the hybridizing *Eco*RI fragments detected by filter hybridization of DNA isolated from rat tissues.

The screening conditions used for identification of kallikrein-like genes resulted in the selection of a group of genes with strong homology to our kallikrein cDNA probe. Although it is difficult to predict the course of a hybridization reaction involving imperfect hybrids and solid-phase reactions, a rough assumption is that the T_m of an imperfect hybrid decreases 1 Cdeg for every 1% of mismatch. That being the case, the hybridization conditions used in analysis of the genomic clone should have allowed discrimination of clones with coding sequences whichv ary by more than 10% from the kallikrein cDNA sequence. Because there was little differential hybridization among the clones we can assume that the original screening conditions resulted in identifying only clones which differed by not more than about 10–15% in sequence. The sequence analysis of RSKG-9 has so far revealed 1% difference in coding portions of the gene.

Another indication of close homology among the members isolated is the conservation of restriction endonuclease sites among the clones. In particular, a hybridizing *Hin*dIII fragment of approx. 2000–2100 bp is present in 15 of 24 clones analyzed. Ten of the 34 clones contain a single hybridizing *Eco*RI fragment of 14000 bp, nine contain a hybridizing *Eco*RI fragment of 9000 bp and 14 contain a nonhybridizing 4000–4100 bp *Eco*RI fragment. This indicates that not only is there a conservation of coding sequence, there is also a conservation of gene structure among the family members.

This preservation of gene structure indicates either recent divergence of this family or homogenization of its members by gene conversion or multiplication. The relationship of the rat and mouse genes, although they are probably not allelic, reveals that certain portions of the kallikrein-like genes have been conserved more stringently than others. In particular the gene exons show extensive preservation of sequence over the period of evolution since these two species diverged. The introns show significant homologies but are less preserved and correspondence between flanking regions was not found. This seems to imply that preservation of the coding portions of the kallikrein gene family is most important to the maintenance of their function.

A high degree of sequence conservation is observed whent he coding region of the kallikrein pseudogene RSKG-9 is compared against the kallikrein cDNA. It is interesting to note that none of the base substitutions generated termination codons. In fact, among the 34 total substitutions, 18 are silent. The inactivation of RSKG-9 was apparently caused by base insertions and deletions which generated frame-shifts and premature terminations. Such changes can coexist with alterations in sequences involved in transcription and processing of transcripts [39]. Whether this is the case for RSKG-9 awaits further analysis. The presence of pseudogenes in such a large gene family is expected from similar findings in other groups of related genes [39–42]. In fact the creation of pseudogenes may be an inevitable result of the mechanisms for creation of gene families with variant repetition.

Acknowledgements

We thank Harry Margolius for helpful discussions, F.K. Lin for his assistance in constructing the genomic library, John Thomas for excellent technical help and Joan Eynon for preparation of the manuscript. This work was supported by United States Public Health Services Grants from the NIH. J.C. is a Research Career Development Awardee of the National Heart, Lung and Blood Institute.

References

1 Schachter, M. (1980) Pharmacol. 31, 1–17
2 Nustad, K., Vaaje, K. and Pierce, J. (1975) Br. J. Pharmac. 53, 229–234
3 Brandtzaeg, P., Gantvik, K.M., Nustad, K. and Pierce, J.V. (1976) Br. J. Pharmacol. 56, 155–167
4 Kutzbach, C. and Schmidt-Kastner, G. (1972) Hoppe-Seyler's Z. Physiol. Chem. 353, 1099–1106
5 Moriwaki, C., Fujimori, H., Toyono, Y. and Nagai, T. (1980) Chem. Pharm. Bull. 28, 3612–3620
6 Chao, J., Woodley, C., Chao, L. and Margolius, H.S. (1983) J. Biol. Chem. 258, 15173–15178
7 Chao, J., Chao, L. and Margolius, H.S. (1984) Biochim. Biophys. Acta 801, 244–249
8 Chao, J. and Margolius, H.S. (1979) Biochem. Pharmacol. 28, 2071–2079
9 Miller, D., Chao, J. and Margolius, H. (1984) Biochem. J. 218, 37–43
10 Chao, J. and Margolius, H.S. (1983) Endocrinology 113, 2221–2225
11 Bothwell, M.A., Wyndham, H. and Shooter, E.M. (1979) J. Biol. Chem. 254, 7287–7294
12 Lazure, C., Leduc, R., Seidah, N.G., Thibault, G., Genest, J. and Chretien, M. (1984) Nature 307, 555–558
13 Poe, M., Wu, S.K., Forance, J.R., Rodkey, J.A., Brennen, C.D. and Hoofsten, K. (1973) J. Biol. Chem. 258, 2209–2216
14 Chao, J. (1983) J. Biol. Chem. 258, 4434–4439
15 Swift, G., Dagorn, J., Ashley, P., Cummings, S. and MacDonald, R. (1982) Proc. Natl. Acad. Sci. USA 79, 7263–7267
16 Nordeen, S., mason, A., Richards, R., Baxter, J. and Shine, J. (1982) DNA 1, 309–311
17 Richards, R., Catanzaro, D., Mason, A., Morris, B., Baxter, J. and Shine, J. (1982) J. Biol. Chem. 257, 2758–2761
18 Mason, A., Evans, B., Cox, D., Shine, J. and Richards, R. (1983) Nature 303, 300–307
19 Howles, P., Dickinson, D., DiCaprio, L., Woodworth-Gutai and Gross, K. (1984) Nucleic Acids. Res. 12, 2791–2805
20 Shine, J., Mason, A.J., Evans, B.A. and Richards, R. (1983) Cold Spring Harbor Symp. Quant. Biol. 48, 410–426
21 Chirgwin, J.M., Przybyla, A.E., McDonald, R.J. and Rutter, W.J. (1979) Biochemistry 18, 5294–5299
22 Maniatis, T., Fritsch, E. and Sambrook, J. (1982) In Molecular Cloning, a Laboratory Manual, pp. 455–467, 382–389, 109–112, Cold Spring Harbor Laboratory NY
23 Vieira, J. and Messing, J. (1982) Gene 19, 259–268
24 Helfman, D., Feramisco, J., Fiddes, J., Thomas, G. and Hughes, S. (1983) Proc. Natl. Acad. Sci. USA 80, 31–35
25 Laemmli, U.K. (1970) Nature 227, 680–685
26 Maniatis, T., Hardison, R.C., Lacy, E., Lauer, J., O'Connell, C., Quon, D., Sim, D.K. and Efstratiadis, A. (1978) Cell 15, 687–701
27 Southern, E. (1979) Methods Enzymol. 68, 152–176
28 Benton, W.D. and Davis, R. (1977) Science 196, 180–182
29 Thomas, P. (1983) Methods Enzymol. 100, 255–266
30 Sanger, F., Nicklen, S. and Coulson, A. (1977) Proc. Natl. Acad. Sci. USA 74, 5463–5467
31 Messing, J. (1983) Methods Enzymol. 101, 325–331
32 Sasavage, N., Smith, M., Gillam, S., Woychik, R. and Rottman, F. (1982) Proc. Natl. Acad. Sci. USA 79, 223–227
33 Ahmed, C., Chanda, R., Stow, N. and Zain, B. (1982) Gene 19, 297–301
34 Chao, J. and Margolius, H.S. (1977) Fed. Proc. 36, 1014
35 Craik, C.S., Rutter, W.J. and Fletterick, R. (1983) Science 220, 1125–1129
36 Blobel, G. and Sabatani, D.D. (1971) in Biomembranes, Vol. 2 (Manson, L.A., ed.), pp. 193–195, Plenum, New York
37 Neurath, H. and Walsh, K. (1976) Proc. Natl. Acad. Sci. USA 73, 3825–3832
38 Lezure, C., Seidah, N.G., Thibault, G., Boucher, R., Genest, J. and Chretien, M. (1981) Nature 292, 383–384
39 Proudfoot, N. (1980) Nature 286, 840–841
40 Little, P.F.R. (1982) Cell 28, 683–684
41 Brach, C., Nagata, S., Mantei, N. and Weissmann, C. (1981) Gene 15, 379–394
42 Lemischka, I. and Sharp, P.A. (1982) Nature 300, 330–335

Biochimica et Biophysica Acta 866 (1986) 15–18
Elsevier

BBA 91528

Regulation of acetohydroxy acid synthase activities in *Escherichia coli* K-12 by small metabolites

Arthur L. Williams

School of Biological Sciences, University of Kentucky, Lexington, KY 40506 (U.S.A.)

(Received September 3rd, 1985)

Key words: cyclic AMP; Indole acetic acid; Acetohydroxy acid synthase; Gene expression; (*E. coli*)

The effects of several metabolites (indole acetic acid, imidazole acetic acid and indole) on acetohydroxy acid synthase activities have been examined in both *cya*$^+$ and *cya*$^-$ strains. Specifically, indole acetic acid caused an increase in the rate of acetohydroxy acid synthase synthesis under both in vivo and in vitro conditions. Taken together, these data suggest that small metabolites, other than cAMP, can alter acetohydroxy acid synthase gene expression.

Introduction

In *Escherichia coli* K-12, three acetohydroxy acid synthase genes are present which catalyze the first step common to the biosynthesis of both isoleucine and valine [1]. Each of the acetohydroxy acid synthase genes (*ilvB* (AHASI), *ilvG* (AHAS II) and *ilvIH* (AHAS III)) is regulated by separate end-product repression patterns [2]. Additionally, it has been reported that regulation of the *ilvB* gene in *E. coli* K-12 is subjected to catabolite repression [3–6].

Regulation of *ilvB* operon is complex, involving negative control by attenuation [7] and positive by a number of factors [3,8], including cAMP-CRP [9]. A recent report by Friden et al. [10] presented evidence that cAMP-CRP greatly increased transcription when restriction fragments carrying the *ilvB* promoter were used as templates. However, cAMP had little or no effect on the percentage of attenuated transcripts.

In this communication, evidence is reported that other small metabolites, in addition to cAMP, can affect total acetohydroxy acid synthase activities in *E. coli* K12.

Materials and Methods

Organisms. The *E. coli* K-12 strains used, their relevant genotypes and sources are given in Table I.

Media. The minimal medium used was that described elsewhere [11] modified by omitting citrate and increasing the glucose concentration to 0.5%. Amino acid supplements were added at 0.5 mM, unless otherwise indicated; thiamine was 12 mg per liter.

Growth of cells. Batch cultures were prepared by inoculating from nutrient agar slants into 5 ml of Luria broth. These tubes were shaken on a Brunswick Gyrotory water bath-shaker model G76 at 37°C and incubated until stationary phase was attained. The cells were centrifuged and the pellets were resuspended in minimal medium with 0.5%

Present address: Department of Biology, Atlanta University, Atalanta, GA 30314, U.S.A.

Abbreviations: cAMP, cyclic adenosine 3′,5′-monophosphate; cGMP, cyclic guanosine 3′,5′-monophosphate; *cya*, adenyl cyclase gene; *A*, absorbance; SSC, 0.15 M NaCl, 0.015 M sodium citrate; AHAS, acetohydroxy acid synthase; CRP, cAMP receptor protein.

0167/4781/86/$03.50 © 1986 Elsevier Science Publishers B.V. (Biomedical Division)

TABLE I

ORGANISMS USED

Strain	Genotype	Source
AB1053	*ilvCZ, ilvB196, ilvP270, argE3, thi-1, lacY1, galK2, xvl-5, tfr-3, tsx-6*	B. Bachmann
CA8300	*Hfr, Sm*^{s}*, thi-1*	W.S. Rexnikoff
CA8306	*Hfr, Sm*^{s}*, thi-1, cya*$^-$	W.S. Reznikoff
MI253	*ilvI614, ilvH612, thr-10, thi-1, relA1, ara-14*, λ^-	B. Bachmann
MI262	*leuB6, ilvI614, ilvH612, ilvG603, ilvG605 (am), thi-1*, λ^-	B. Bachmann
Phage	λ*CI857*, λ*CI857dilvB*	Laboratory collection

glucose, minimal-glucose supplemented with L-valine ($1 \cdot 10^{-3}$ M), L-leucine and L-isoleucine ($4 \cdot 10^{-4}$ M), or minimal-glucose medium supplemented with casamino acids (0.4%). Growth of the cultures was monitored by measuring the absorbance of the cultures at 420 nm in a Spectronic 20 spectrophotometer.

Enzyme assay. The acetohydroxy acid synthase assay was performed as previously described [12]. Protein content of extracts was measured by the method of Lowry et al. [13] with bovine serum albumin (100 μg/ml) as the standard; specific activities are expressed as μmoles of products formed per minute per mg protein unless otherwise indicated.

Phage DNA extraction. The procedure of James et al. [14] employing phenol/chloroform/isoamyl alcohol was used to extract DNA from specialized transducing phage carrying the *ilvB* region. The $A_{260\text{nm}}$ and $A_{280\text{nm}}$ of the DNA suspension were measured with a Beckman Model DBG spectrophotometer.

In vitro transcription assay. The transcription reactions were carried out as described by Majors [15]. The electrophoretic fractionation of RNA transcripts was performed as described by Moore et al. [16].

DNA-RNA hybridizations. The procedure used was as described by Vonder Haar and Umbarger [17], with slight modifications.

Growth of cells, labeling and extraction of RNA. Cells to be labeled with [^{3}H]uridine were grown in minimal medium containing supplements to an A_{420} of 0.8. The labeling and extraction of RNA were as described elsewhere [17].

Dot blot hybridization. A dot blot assay of RNA was carried out according to the procedures of Thomas [18] and Aiba [19]. Total cellular RNAs from *ilvB*$^-$ and *ilvB*$^+$ strains were incubated in 0.55 M formaldehyde and 7.5 mM sodium phosphate buffer (pH 7.0), at 65°C for 7 min. The reaction mixture was cooled on ice and the denatured RNAs were spotted onto dry nitrocellulose paper which had been treated with H_2O and then 20 × SSC. The nitrocellulose paper was baked for 2 h at 80°C and hybridized with nick-translated DNA probe.

Results and Discussion

The effects of several small metabolites on acetohydroxy acid synthase activities

The effects of several small metabolites on expression of acetohydroxy acid synthase activities were examined in isogenic *cya*$^+$ and *cya*$^-$ derivatives of *E. coli* K-12. As shown in Table II,

TABLE II

THE EFFECTS OF SMALL METABOLITES ON ACETOHYDROXY ACID SYNTHASE ACTIVITIES IN *ESCHERICHIA COLI* K-12

Specific activity is expressed as μmol product/min per mg protein. Experiments were carried out in minimal-glucose medium supplemented with 20 amino acids.

Strain	Effector (1 mM)	Total activity/spec. act.
CA8300 (*cya*$^+$)	none	0.014
	cAMP	0.069
	imidazole acetic acid	0.032
	indole acetic acid	0.082
	tryptophan	0.017
	indole	0.054
	histidine	0.016
	cGMP	0.010
CA8306 (*cya*$^-$)	none	0.012
	cAMP	0.057
	imidazole acetic acid	0.025
	indole acetic acid	0.090
	tryptophan	0.017
	indole	0.082
	histidine	0.015
	cGMP	0.009

acetohydroxy acid synthase activities were increased by, in addition to cAMP, indole acetic acid, imidazole acetic acid and indole in both mutant and wild-type strains. Indole acetic acid was the most potent effector as determined by the standard in vitro acetohydroxy acid synthase assay. Conversely, histidine, tryptophan and cGMP apparently had no effect on acetohydroxy acid synthase activities. Actually, cGMP caused a slight decrease in activity.

Effect of indole acetic acid on acetohydroxy acid synthase gene(s) expression

To determine whether indole acetic acid (the most potent effector) affects the activity or synthesis of acetohydroxy acid synthase, activity was measured at various stages for growth. As shown in Fig. 1, the differential rate of acetohydroxy acid synthase synthesis was significantly elevated in cultures grown in the presence of indole acetic acid. The magnitude of elevation by indole acetic acid was equivalent to that found using cAMP (a known regulatory effector of acetohydroxy acid synthase genes). Thus, these data suggest that at least indole acetic acid can alter acetohydroxy acid synthase gene(s) expression. The effects of this small metabolite appear to be specific, as essentially no effect was observed in several *crp* mutant strains (data not shown). Kline et al. [20–22] reported evidence for a positive effect of imidazole 4-acetic acid and indole acetic acid (i.e. two of the metabolites employed in this study) on the induction of L-arabinose isomerase synthesis.

Effect of indole acetic acid on ilvB (AHASI) gene transcription

The dot blot assay was employed to determine the effect of indole acetic acid on *ilvB* gene transcription. As shown in Table III, these preliminary results indicate that indole acetic acid did indeed stimulate *ilvB* mRNA transcription. These findings are in total agreement with the increased level of acetohydroxy acid synthase synthesis. To couple the data reported herein with previous results, it is clear that certain small metabolites, other than cAMP, are critical in directing gene expression at least in *E. coli*. The use of *E. coli* plasmids harboring the acetohydroxy acid synthase genes should help in assessing the direct role(s) of small

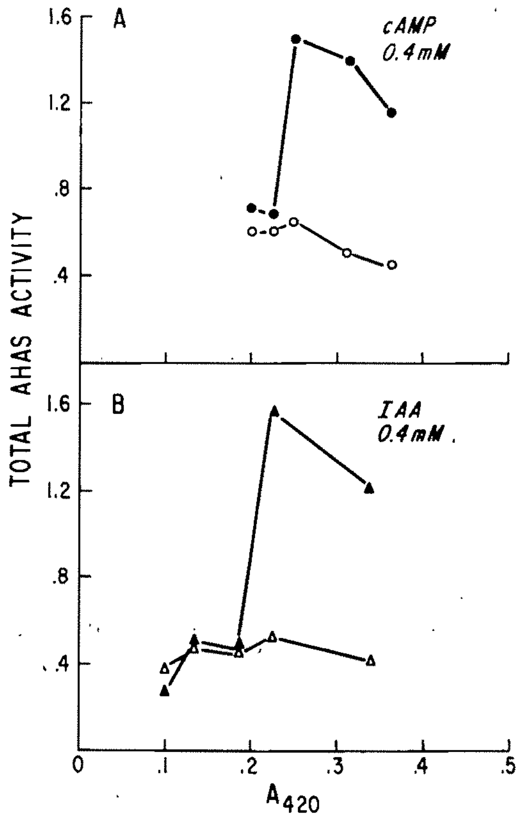

Fig. 1. Differential rate of synthesis of acetohydroxy acid synthase in the presence and absence of cAMP and indole acetic acid (for details see text). Total activity = spec. act. (μmol product formed/h per mg protein) × A_{420}.

TABLE III

EFFECTS OF INDOLE ACETIC ACID ON *ilvB* GENE TRANSCRIPTION

Denatured cellular RNAs (7.5 μg) from *ilvB*⁻ and *ilvB*⁺ strains were spotted on the nitrocellulose paper and hybridized with 100 ng of the *ilvB* gene DNA. All other conditions were as described in the text. cmps were obtained from the decay spots as revealed by the autoradiograms.

DNA source	Effector	[^{3}H]RNA	cpm
ilvB DNA	−	AB1053(*ilvB*$^-$)	371
	+	AB1053(*ilvB*$^-$)	413
*ilvB*DNA	−	MI253(*ilvB*$^+$)	1711
	+	MI253(*ilvB*$^+$)	4003
ilvB DNA	−	none	57
	+	none	60

metabolites on acetohydroxy acid synthase gene(s) expression at the molecular level.

Acknowledgement

This study was supported in part by NSF Grant PRM-8212383.

References

1 Umbarger, H.E. (1978) Annu. Rev. Biochem. 47, 533–606

2 Sutton, A. and Freundlich, M. (1980) Mol. Gen. Genet. 178, 179–183

3 Freundlich, M. (1977) Cell 12, 1121–1126

4 Newman, T., Friden, P., Sutton, A. and Freundlich, M. (1982) Mol. Gen. Genet. 186, 378–384

5 Polglase, W.J. and Whitlow, K.J. (1974) FEBS Lett. 43, 64–66

6 Williams, A.L. (1983) Mol. Gen. Genet. 191, 353–357

7 Hauser, C.A. and Hatfield, G.W. (1983) Nucleic Acids Res. 11, 127–139

8 Friden, P., Voelkel, K., Sternglanz, R. and Freundlich, M. (1984) J. Mol. Biol. 172, 573–579

9 Friden, P., Newman, T. and Freundlich, M. (1982) Proc. Natl. Acad. Sci. USA 79, 6156–6160

10 Friden, P., Tsui, P., Okamoto, K. and Freundlich, M. (1984) Nucleic Acids Res. 12, 8145–8160

11 Davis, B.D. and Mingioli, E.S. (1950) J. Bacteriol. 60, 17–28

12 Stormer, F.C. and Umbarger, H.E. (1964) Biochem. Biophys. Res. Commun. 17, 587–592

13 Lowry, O.H., Rosebrough, N.J., Farr, A.L. and Randall, R.J. (1951) J. Biol. Chem. 193, 265–275

14 James, P., Sens, W., Natter, W. and James, E. (1976) J. Bacteriol. 126, 487–500

15 Majors, J. (1975) Proc. Natl. Acad. Sci. USA 72, 4394–4398

16 Moore, S.K., Garvin, R.T. and James, E. (1981) Gene 16, 119–132

17 Vonder Haar, R. and Umbarger, H.E. (1974) J. Bacteriol. 120, 687–696

18 Thomas, P.S. (1980) Proc. Natl. Acad. Sci. USA 77, 5201–5205

19 Aiba, H. (1985) J. Biol. Chem. 260, 3063–3070

20 Kline, E.L., Bankaitis, V., Brown, C.S. and Montefiori, D. (1979) Biochem. Biophys. Res. Commun. 87, 566–574

21 Kline, E.L., Brown, C.S., Bankaitis, V. and Montefiori, D. (1980) Proc. Natl. Acad. Sci. USA 77, 1768–1772

22 Kline, E.L., Bankaitis, V.A., Brown, C.S. and Montefiori, D. (1980) J. Bacteriol. 141, 770–778

Biochimica et Biophysica Acta 866 (1986) 19–25
Elsevier

BBA 91527

Conserved restriction sites within the ribosomal RNA genes of vertebrates

Susan M. Tanhauser [a], William W. Hauswirth [b] and Philip J. Laipis [a,*]

[a] *Department of Biochemistry and Molecular Biology, and* [b] *Department of Immunology and Medical Microbiology, College of Medicine. University of Florida, Gainesville, FL 32610 (U.S.A.)*

(Received July 16th, 1985)

Key words: rRNA gene; Restriction enzyme; Cleavage site; Evolution

We have mapped the cleavage sites of four restriction enzymes which recognize six-base sequences within the nuclear ribosomal (rRNA) genes of twelve vertebrates, including several placental mammals (*Homo sapiens*, man; *Bos taurus*, cow; *Equus caballus*, horse; *Sus scofra*, pig; *Ovis aries*, sheep; *Rattus rattus*, rat), a marsupial (*Didelphis marsupialis*, opossum), a bird (*Gallus domesticus*, chicken), an amphibian (*Xenopus laevis*), a reptile (*Alligator mississipiensis*), a bony fish (*Cynoscion nebulosus*, sea trout), and a cartilagenous fish (*Carcharhinus* species, requiem shark). These animals represent a span of approx. 400 million years of evolutionary divergence. Our data identify restriction sites in the rRNA genes which are highly conserved among higher vertebrates and therefore are likely to be in functionally important regions. Additionally, the restriction enzyme sites identified will be useful in cloning and sequencing the rRNA genes in any vertebrate. Finally, the consistent size and conserved sequence homology suggests that these rRNA gene segments will be useful as internal controls in hybridization experiments involving other genomic regions in vertebrates.

Introduction

Many copies of the small (17–18 S) and large (25–28 S) ribosomal RNA (rRNA) genes are present in the nuclear DNA of eukaryotes [1]. One copy each of a small and a large rRNA gene together constitute a single transcription unit. These units are tandemly repeated and separated by spacer DNA, most of which is not transcribed. Throughout evolution these genes have remained more highly conserved than most other genes. While the functional importance of the rRNAs is undoubtedly responsible for much of their conservation, their repeated organization has also been suggested to play an important role [2].

Direct nucleotide sequence comparison is an unambiguous way to determine the degree of conservation between species and to predict functional domains of the rRNA. To date, however, only four eukaryotic small rRNA genes [3–6] and five eukaryotic large genes [7–12] have been fully sequenced. The sequence comparisons made have been among extremely divergent species, and the suggested secondary structures have been based on those proposed for the *Escherichia coli* 16 S and 23 S rRNA. While the overall sequences of the rRNA genes are conserved, a number of changes have occurred during evolution, and the restriction enzyme maps of these genes are sufficiently different that they are not directly useful in recognizing ribosomal RNA gene domains on genomic DNA blots from many other vertebrate species. To help alleviate this situation we have examined, using restriction enzymes, a wide range of vertebrate species. Additionally, we have assessed the degree

---

[*] To whom correspondence should be addressed at: Department of Biochemistry and Molecular Biology, Box J-245, JHMHC, University of Florida, Gainesville, FL 32610, U.S.A.

0167-4781/86/$03.50 © 1986 Elsevier Science Publishers B.V. (Biomedical Division)

of conservation of these restriction sites (and their usefulness), and attempted to detect conserved sites among the higher eukaryotes which are not shared with lower organisms and therefore could indicate functionally important domains which differ between these groups.

Materials and Methods

Extraction of nuclear DNA from tissue. Common vertebrate species were obtained from laboratory supply companies, the University of Florida Meat Laboratory, or the College of Veterinary Medicine. Dr. C. Buergelt provided alligator tissue, the authors procured the bony fish, shark (an immature requiem shark (*Carcharinidae*), probably *Carcharhinus limbatus*), and the opossum.

Liver samples were used for all DNA preparations except for human (cultured HeLa cells), trout and shark (sperm sac). Samples were obtained from freshly killed animals. 6–10 g of tissue were chopped very finely using an electric knife fitted with razor blades in place of knife blades. The tissue was homogenized in phosphate-buffered saline (0.14 M NaCl, 0.01 M phosphate buffer (pH 7.4), 4.5 mM KCl, 0.9 mM $CaCl_2$, 0.5 mM $MgCl_2$) first using a ground-glass homogenizer and then a Dounce homogenizer with a loose-fitting pestle. Nuclei were pelleted by centrifugation at 5000 rpm (Sorvall SS-34 rotor) for 10 min at 4°C, then resuspended in 1 × standard saline citrate (SSC: 0.15 M NaCl, 0.015 M sodium citrate, pH 7.2), 10 μg/ml Pronase (Sigma) (pre-digested at 37°C for 60 min) and 1% sodium dodecyl sulfate (SDS), and incubated overnight at 37°C. This mixture was extracted twice with phenol (saturated with 1 × SSC) and three times with ether. Pancreatic RNAase (Sigma) was added, followed by incubation at 37°C for 60 min. The digestion mixture was extracted twice with phenol and three times with ether. DNA was precipitated by addition of 2.5–3 vol. of cold (−20°C) ethanol.

Digestion with restriction enzymes. Each reaction consisted of approx. 20 μg of total nuclear DNA digested with commercial restriction enzymes (Bethesda Research Laboratories or N.E. Biolabs) using the conditions suggested by the supplier. Restrictions sites were mapped using the results of complete, partial and multiple digests.

Agarose gel electrophoresis and transfer to nitrocellulose filters. Restriction enzyme digests of nuclear DNA were analyzed by electrophoresis on 1.5% agarose gels (Marine Colloids) using 0.05 M Tris, 0.02 M sodium acetate, 0.018 M NaCl, 0.002 M EDTA (pH 8.2) as the gel and tank buffer. Digests of pBR322 or bovine mitochondrial DNA were used as size markers.

DNA was transferred from agarose gels to 0.45 μm nitrocellulose filters (Schleicher and Schull) as previously described [13].

Iodination of ribosomal RNAs. 18 S and 28 S rRNA (a gift from G. and J. Stein) from HeLa cell polysomes were isolated as previously described [14]. Polysomes were pelleted from a post-mitochondrial supernatant and extracted with 1 vol. phenol plus 1 vol. chloroform/isoamyl alcohol (24 : 1, v/v). RNAs were ethanol-precipitated and fractionated by zonal gradient centrifugation in a 5–30% sucrose gradient. The size and purity of 18 S and 28 S rRNAs were confirmed on agarose-CH_3HgOH gels. The rRNA was iodinated using a modification [15] of the procedure of Comerford [16]. Briefly, the RNA was incubated at 70°C in aqueous thallic trichloride (ICN Pharmaceuticals, Inc.) plus ^{125}I (Amersham, IMS.300) at pH 5.0. We achieved specific activities of approx. $(1-2) \cdot 10^8$ cpm/μg RNA.

Filter hybridizations and autoradiography. DNA-RNA hybridizations were carried out in plastic bags (Seal-a-Meal; Dazy) containing 10 ml of hybridization solution (2 × or 5 × SSC, depending on the stringency desired, 0.2% SDS, 50 μg/ml tRNA (boiled and quick-chilled), and 20 ng of ^{125}I-labeled rRNA). The bag was incubated at 64°C for 12–36 h. Following hybridization, the filters were washed in 2 × SSC at 50°C, in 1 × SSC plus 50 μg/ml pancreatic RNAase (Sigma) at 37°C for 30–60 min, and two to four times in 1 × SSC at room temperature.

Results

Nuclear DNA was isolated from twelve vertebrate species and digested with restriction endonucleases which recognize six-base sequences within the DNA. Digested DNA was then electrophoresed on 1–1.5% agarose gels, transfered to nitrocellulose filters, and hybridized to either ^{125}I-

labeled 18 S or 28 S rRNA. HeLa rRNA proved to be a convenient probe for all the vertebrate genes. DNA fragment sizes were determined by comparison with appropriate size markers. Restriction sites were mapped using the results of complete, partial and multiple digests, as previously described [17].

Figs. 1 and 2 summarize the restriction size mapping data for the vertebrate rRNA gene region. The restriction sites within the genes are shown in Fig. 1; a high degree of conservation is evident when the genes are aligned. Fig. 2 shows all the restriction enzyme sites mapped in the rRNA gene region of each animal. Neither the length of the spacer regions nor the positions of restriction sites in the spacer DNA have been conserved, as noted by others.

18 S rRNA genes

Sites for three restriction enzymes (*Eco*RI, *Bam*HI and *Pst*I) were mapped in the 18 S rRNA genes of twelve vertebrates. The hybridization patterns of these species, produced by digestion of their nuclear DNA with *Eco*RI and *Pst*I, followed by hybridization to ^{125}I-labeled HeLa 18 S rRNA, are shown in Fig. 3. One fragment of approx. 1050 base pairs or $0.69 \cdot 10^6$ Da was present in digests of all the warm-blooded vertebrates. This fragment was only slightly larger (1980 base pairs or $0.7 \cdot 10^6$ Da) in digests of the amphibian (*Xenopus*) and fish (*Cynoscion*), and was somewhat smaller (915 base pairs or $0.6 \cdot 10^6$ Da) in the shark (*Carcharhinidus*). *Pst*I and *Ec*$_0$RI each cut only once within the 18 S gene, together generating this common internal fragment and variably sized terminal fragments. These two sites were always present at the same positions in all animals examined, as determined by other restriction digest experiments (data not shown). The inter-specific differences in size of the internal 18 S gene fragment between these two conserved sites could be due to small insertions or deletions. Alternatively, differences in DNA concentration, salt, or other experimental

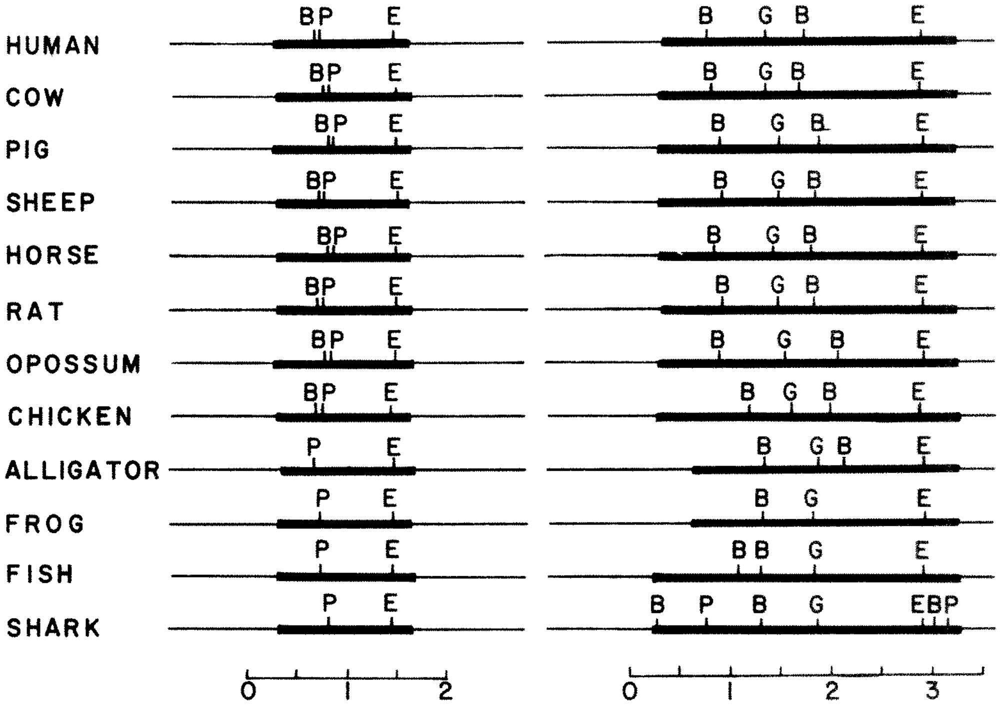

Fig. 1. Restriction site map of the 18 S and 28 S rRNA genes of twelve vertebrates. Enzyme recognition sites were mapped using data from single, double and triple digests and comparison with appropriate size standards. The scale at bottom is in units of 10^6 Da. It should be noted that the methods used do not determine the exact boundaries of the genes. The size shown represents the minimum extent of the gene (except for HeLa 28 S, rat 18 S and 28 S, and *Xenopus* 18 S and 28 S, which have been determined by others).

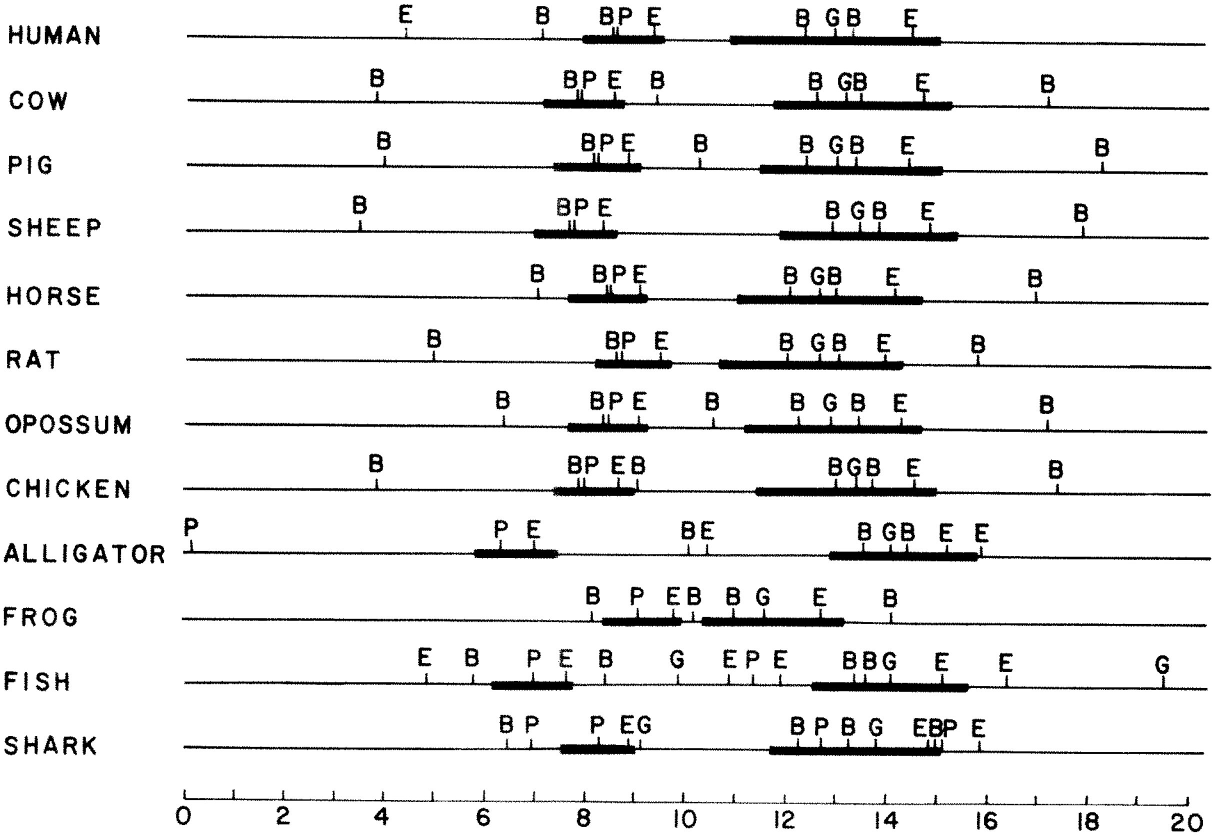

Fig. 2. Restriction site map of the rRNA genes and flanking regions. Additional sites for mapped enzymes may exist distal to the rRNA genes or between them. The ends of the rRNA genes are not exact (see Fig. 1). The scale at bottom is in units of 10^6 Da.

variability between lanes could explain some of the migration-rate variability. A maximum error of up to 4% was occasionally visible in the migration of the same fragment from lane to lane across a gel. A *Bam*HI site was present in all the 18 S rRNA genes of warm-blooded vertebrates, approx. 100 nucleotides 5′ to the *Pst*I site; it was absent in all the lower vertebrates.

28 S rRNA genes

Sites for three restriction enzymes (*Bam*HI, *Bgl*II and *Eco*RI) were mapped within the 28 S rRNA genes of the same organisms. Simultaneous digestion of nuclear DNA with these three enzymes, followed by transfer to nitrocellulose and hybridization with ^{125}I-labeled HeLa 28 S rRNA gave the patterns shown in Fig. 4. Three conserved fragments $((1.07 \pm 0.08) \cdot 10^6$, $(0.61 \pm 0.05) \cdot 10^6$, $(0.36 \pm 0.02) \cdot 10^6$ Da) were present in digests of all of the placental mammals; two of these were also present in the opossum ($0.64 \cdot 10^6$, $0.36 \cdot 10^6$ Da). Other mapping data showed that the sites which flank the $1.07 \cdot 10^6$ Da fragment were present in the same relative location in the opossum 28 S rRNA gene, although the distance between them was reduced to $0.84 \cdot 10^6$ Da. A series of single, double and triple digests was carried out to determine the location of each restriction site in the rRNA gene; the conserved fragments were indeed created by cutting at restriction sites that map to the same relative position in the rRNA genes of all the animals.

Several of these restriction sites were conserved in all species examined. An *Eco*RI site was present at the 3′ end of all of the 28 S rRNA genes studies (Fig. 1). The *Bgl*II site in the middle of the 28 S rRNA gene was also highly conserved. Only one of the several *Bam*HI sites found in the 28 S rRNA genes of vertebrates appears to be highly conserved; it was located approx. 850 basepairs 5′

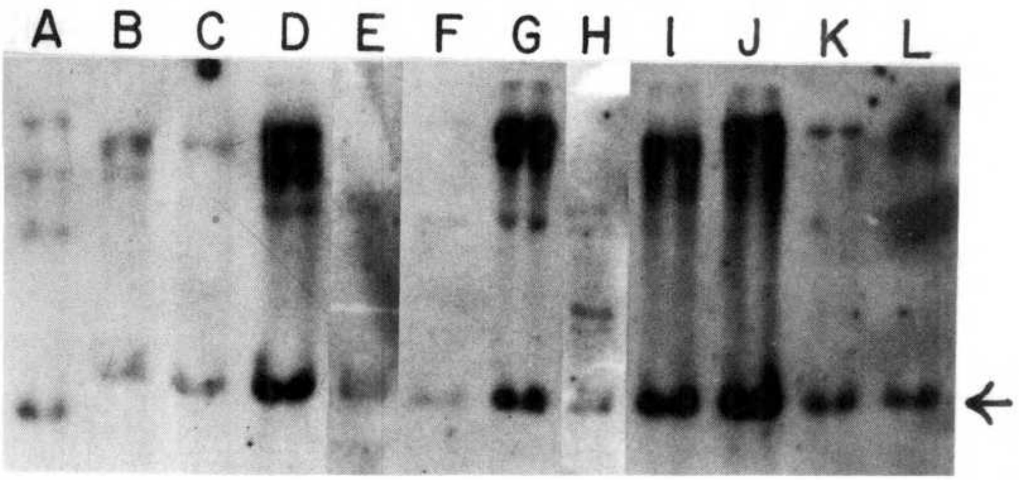

Fig. 3. An *Eco*RI-*Pst*I fragment of $0.69 \cdot 10^6$ Da in the 18 S rRNA gene has been conserved in vertebrates throughout evolution. Nuclear DNA indicated was digested with both *Eco*RI and *Pst*I and electrophoresed on a 1.5% agarose gel. (Horse DNA was digested with *Eco*RI, *Pst*I and *Bam*HI. This does not, however, affect the presence or size of the conserved fragment.) DNA was transferred to a nitrocellulose filter and hybridized with ^{125}I-labeled 18 S rRNA from HeLa cells. Bands were visualized by autoradiography; sizes were determined using appropriate size standards. The arrow indicates the conserved $0.69 \cdot 10^6$ Da fragment. Lane A, shark; lane B, fish; lane C, frog; lane D, alligator; lane E, chicken; lane F, opossum; lane G, rat; lane H, horse; lane I, sheep; lane J, pig; lane K, cow; lane L, human. Lane H is from a *Bam*HI + *Pst*I + *Eco*RI triple digest of horse DNA, rather than a *Pst*I + *Eco*RI double digest.

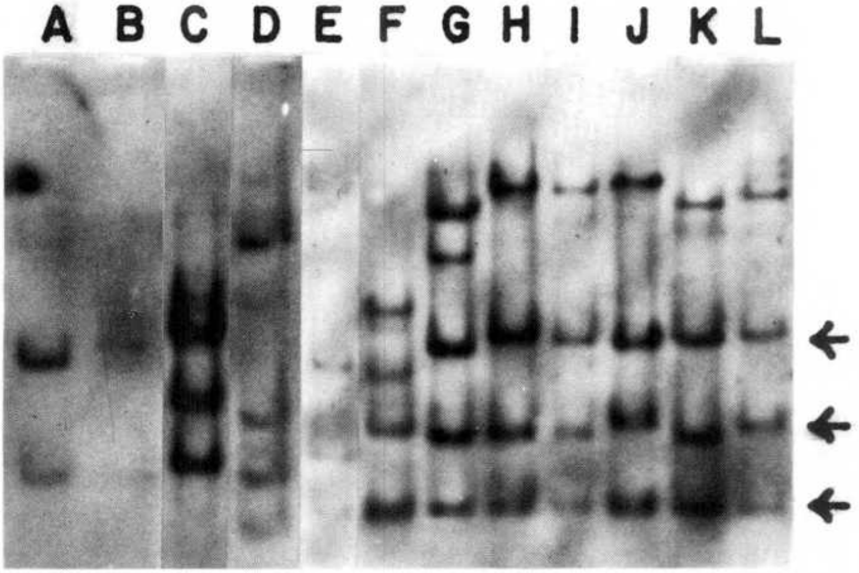

Fig. 4. *Bam*HI + *Bgl*II + *Eco*RI digest of 28 S rDNA of vertebrates. Several fragments are conserved throughout the higher vertebrates. Nuclear DNA was digested simultaneously with *Bam*HI, *Bgl*II and *Eco*RI, and electrophoresed on a 1.5% agarose gel. DNA was transferred to a nitrocellulose filter, and hybridized with ^{125}I-labeled 28 S rRNA from HeLa cells; bands were visualized by autoradiography and sizes were determined using appropriate size standards. The arrows indicate the three fragments conserved in placental mammals. Lane A, shark; lane B, fish; lane C, frog; lane D, alligator; lane E, chicken; lane F, opossum; lane G, rat; lane H, horse; lane I, sheep; lane J, pig; lane K, cow; lane L, human.

to the *Bgl*II site (Fig. 1). The remaining *Bam*HI sites were variable in their presence and position. A *Bam*HI site was located between the highly conserved *Bgl*II and *Eco*RI sites in the 28 S rRNA gene of all warm-blooded animals as well as the alligator (Fig. 1). In *Xenopus* and the fishes, this *Bam*HI site was absent and another *Bam*HI site was present instead near the 5′ end of the gene. In shark, a *Bam*HI site was present at the 3′ end of the gene as well. DNA sequencing around these sites would be required to determine whether these changes are the result of DNA rearrangement, insertion, deletion, or simple base changes.

Discussion

Our results agree with the hypothesis that the rRNA genes of vertebrates have remained conserved throughout evolution. Four of the mapped restriction sites are present at the same positions in all animals examined. Others are more variable. However, there is clearly considerable sequence homology in the actual DNA sequences, since the HeLa rRNA probe hybridized to even the most distant species examined. The stringency of our hybridization conditions requires approx. 12–18 continuous homologous bases for hybridization to occur. Our blots were then washed extensively and incubated with pancreatic RNAase to remove non-homologous single-stranded RNA. Our results thus indicate a high degree of sequence conservation across a broad range of very divergent species. While this is evolutionarily important, it gives the rRNA genes a practical importance as well. Since the internal restriction enzyme sites are so highly conserved, almost any vertebrate 18 S or 28 S rRNA could be used as a probe to provide, for example, internal size markers. The rRNA genes may also serve as internal standards for complete digestion, and they could be useful in determining the copy number of another gene or family of genes.

These sites also provide an easy means of isolating conserved DNA fragments that may be examined to assess evolutionary relatedness in a wide array of divergent vertebrates. Many nuclear genes have diverged sufficiently to make this sort of comparison technically difficult. These conserved DNA fragments, with defined ends and homology to easily obtained probes, could be ideal for such studies.

It is possible to ask if the highly conserved mapped sites fall in areas where a specific secondary structure has been predicted. The *Eco*RI site at the 3′ end of the 18 S gene and the *Pst*I site in the middle of the gene are present in all of the species surveyed. The *Eco*RI site is present in the published *Saccharomyces cerevisiae, Xenopus* and rat small rRNA sequences at a highly conserved stem-loop junction in the two models of rRNA secondary structure proposed for these organisms [6,18]. The *Eco*RI site and corresponding structure are present in *E. coli* as well. The *Pst*I site is present in *Xenopus* and rat, but not in the yeast 18 S rRNA gene, due to a single nucleotide difference (C → U) within the enzyme-recognition site, in a region of otherwise high homology. The *Bam*HI site that we mapped in the 18 S gene is present in all of the homotherms we examined, but not in any of the lower vertebrates in our survey. The *Bam*HI site lies in a region that is not base-paired in the rat 18 S rRNA model [6]. A single base change (T → C at position 544) would create a *Bam*HI site in *Xenopus*, and a second change (a T → A at position 542) would create a *Bam*HI site in the *S. cerevisiae* sequence, in a region analogous to the rat structure.

A secondary structure has recently been proposed for rat 28 S rRNA [10]. It is based on nucleotide sequence analysis as well as structures proposed for *E. coli* [19,20] and yeast [8]. The *Eco*RI site at the 3′ end of vertebrate 28 S gene (Fig. 1) is part of a stem-loop junction in this rat 28 S rRNA secondary structure [10]. An analogous structure is present in yeast [8] and *E. coli* [19,20]. The conserved *Bgl*II site in the 28 S rRNA gene is found adjacent to a conserved stem in the secondary structures proposed for both rat and yeast. The structure, but not the site, is also present in the *E. coli* molecule [19,20]. The *Bam*HI sites in the 28 S rRNA gene are more variable. These sites are present in both basepaired stems and regions with no assigned structure, and it is difficult to correlate them with any conserved structural feature.

Finally, the degree of conservation seen in nuclear rRNA genes differs from that observed in mitochondrial rRNA genes. The mitochondrial rRNA genes have been sequenced in mouse [21,22], human [23] and cow [24]. Although regions of the genes are highly conserved, many nucleotide differences are seen, by both restriction-site analysis and direct nucleotide sequencing. The mouse and human mitochondrial 12 S and 16 S rRNA genes are 75% and 74% homologous, respectively [22]; the corresponding genes of cow and human are 77% and 76% homologous [25]. In contrast, the nuclear 28 S rRNA genes of *Xenopus laevis* and rat are about 75% homologous [9], and *Xenopus* and yeast are about 69% homologous [12]. The mitochondrial rRNA sequences have diverged as much between three orders of mammals as have the nuclear genes of mammals and amphibians. A difference in the stringency of functional constraints, the higher overall rate of mitochondrial DNA sequence divergence, and the correction of the repeated nuclear rRNA genes by recombination or gene conversion are all possible explanations for this rapid divergence in mitochondrial rRNA genes. However, these two functionally equivalent gene systems may make measuring the degree of divergence between both closely related and very distant groups of organisms possible.

Acknowledgements

We thank Dr. Claus Buergelt for alligator tissue. This work was supported by NSF grant PCM 8119166 and NIH grant AGO1636.

References

1 Long, E.O. and Dawid, I.B. (1980) Annu. Rev. Biochem. 49, 727–764.

2 Brown, S.D.M. and Dover, G.A. (1981) J. Mol. Biol. 150, 441–466.

3 Rubtsov, P.M., Muskahanov, M.M., Zakharyev, V.M., Krayev, A.S., Skryabin, K.G. and Bayev, A.A. (1980) Nucleic Acids Res. 8, 5779–5794.

4 Salim, M. and Maden, B.E.H. (1981) Nature 291, 205–208.

5 Olsen, G.J., McCarroll, R. and Sogin, M.L. (1983) Nucleic Acids Res. 11, 8037–8049.

6 Chan, Y.-L., Gutell, R., Noller, H.F. and Wool, I.G. (1984) J. Biol. Chem. 259, 224–230.

7 Georgiev, O.I., Nikolaev, N. and Hadjiolov, A.A. (1981) Nucleic Acids Res. 9, 6953–6958.

8 Veldman, G.M., Klootwijk, J., deRegt, V.C.H.F., Planta, R.J., Branlant, C., Krol, A. and Ebel, J.P. (1981) Nucleic Acids Res. 9, 6935–6952.

9 Chan, Y.L., Olvera, J. and Wool, I.G. (1983) Nucleic Acids Res. 11, 7819–7831.

10 Hadjiolov, A., Georgiev, O. and Yavachev, L. (1984) Nucleic Acids Res. 12, 3677–3693.

11 Otsuka, T., Nomiyama, H., Yoshida, H., Kukita, T., Kuhara, S. and Sakaki, Y. (1983) Proc. Natl. Acad. Sci. USA 80, 3163–3167.

12 Ware, V.C., Tague, B.W., Clark, C.G., Gourse, R.L., Brand, R.C. and Gerbi, S.A. (1983) Nucleic Acids Res. 11, 7795–7817.

13 Southern, E.M. (1975) J. Mol. Biol. 98, 503–517.

14 Thrall, C.L., Park, W.D., Rashba, H.W., Stein, J.L., Mans, R.J. and Stein, G.S. (1974) Biochem. Biophys. Res. Commun. 61, 1443–1449.

15 Tereba, A. and McCarthy, B.J. (1973) Biochemistry 12, 4675–4679.

16 Comerford, S.L. (1971) Biochemistry 10, 1993–1999.

17 Laipis, P.J., Hauswirth, W.W., O'Brien, T.W. and Michaels, G.S. (1979) Biochim. Biophys. Acta 565, 22–32.

18 Zwieb, C., Glotz, C. and Brimacombe, R. (1981) Nucleic Acids Res. 9, 3621–3640.

19 Glotz, C., Zweib, C. and Brimacombe, R. (1981) Nucleic Acids Res. 9, 3287–3306.

20 Maly, P. and Brimacombe, R. (1983) Nucleic Acids Res. 11, 7263–7286.

21 Van Etten, R.A., Walberg, M.W. and Clayton, D. (1980) Cell 22, 157–170.

22 Bibb, M.J., Van Etten, R.A., Wright, C.T., Walberg, M.W. and Clayton, D.A. (1981) Cell 26, 167–180.

23 Eperon, I.C., Anderson, S. and Nierlich, D.P. (1980) Nature 286, 460–467.

24 Anderson, S., DeBruijn, M.H.L., Coulson, A.R., Eperon, I.C., Sanger, F. and Young, I.G. (1982) J. Mol. Biol. 156, 683–717.

25 Anderson, S., Bankier, A.T., Barrell, B.G., DeBruijn, M.H.L., Coulson, A.R., Drouin, J., Eperon, I.C., Nierlich, D.P., Roe, B.A., Sanger, F., Schreier, P.H., Smith, A.J.H., Staden, R. and Young, I.G. (1982) in Mitochondrial Genes (Slonimski, P., Borst, P. and Attardi, G., eds.), pp. 5–43, Cold Spring Harbor, New York.

Biochimica et Biophysica Acta 866 (1986) 26–31
Elsevier

BBA 91555

A novel suppressor tRNA from the dimorphic fungus *Candida albicans*

Michael F. Tuite [a], Patricia A. Bower [b] and Calvin S. McLaughlin [b]

[a] *Biological Laboratory, University of Kent, Canterbury, Kent, CT2 7NJ (U.K.) and* [b] *Department of Biological Chemistry, University of California, Irvine, Irvine, CA 92717 (U.S.A.)*

(Received September 9th, 1985)

Key words: Mistranslation; Suppressor tRNA; (*C. albicans*)

Unfractionated tRNAs from a number of prokaryotes and eukaryotes were examined for their ability to promote termination codon readthrough in a cell-free system isolated from *Saccharomyces cerevisiae*. tRNA from the dimorphic fungus *Candida albicans* was found to have significant UGA and UAG readthrough activity and this activity was present in tRNA extracted from both the yeast and the hyphal phase of the fungus. Unusually the efficiency of readthrough activity in vitro was not affected by the [*psi*] determinant. *C. albicans* tRNA was fractionated by one-dimensional and two-dimensional gel electrophoresis and both readthrough activities appeared to be associated with a single species of tRNA.

Introduction

Increasing evidence from both eukaryotic and prokaryotic organisms has suggested that the regulated translational readthrough of termination codons, in particular the UGA codon, may define a novel mechanism for regulating gene expression [1,2]. Transfer RNAs (tRNAs), present in wild-type cells, that are able to translate the UGA codon have been identified in *Escherichia coli* [3], *Saccharomyces cerevisiae* [4,5], rabbit reticulocytes [6], wheat germ [7] and bovine liver [8]. Similarly, wild-type tRNAs able to translate the UAG (amber) codon in vitro have been identified in wheat germ [9], *Drosophila melanogaster* [10] and tobacco plants [11]. We have examined the ability of unfractionated tRNAs, isolated from a number of different organisms, to translate either the UGA codon or the UAG codon, in a cell-free system prepared from *S. cerevisiae*. We report here the identification of a single tRNA from the dimorphic fungus *Candida albicans* that is able to translate efficiently both the UAG and the UGA codon, as well as inducing a more general in vitro mistranslation of natural mRNAs.

Materials and Methods

Cell-free translation. Cell-free lysates were prepared from a haploid strain of *S. cerevisiae* (465/4d: *MATα ade2-1 lys1-1 can 1-100 ura3-1* [*psi*$^+$]). The method of preparation and the conditions used to translate natural mRNAs have been previously described [12]. Cell-free translation products were labelled with [^{35}S]methionine (> 1000 Ci/mmol) and analysed on 17.5% SDS-polyacrylamide gels as previously described [12].

tRNA isolation. tRNA was isolated from stationary-phase yeast cells of *C. albicans* as previously described [13], and separation by two-dimensional polyacrylamide gel electrophoresis was essentially as described by Fradin et al. [14]. Gels were stained with aqueous methylene blue for a short period to visualize the separated tRNAs, which were then eluted as follows; a piece of gel containing the tRNA(s) of interest was cut out, crushed with a sterile glass rod, and resuspended in 0.5% SDS, 0.3 M NaCl, 0.01 M Tris-HCl (pH 7.4). Following incubation at 37°C for 1 h, the gel slurry was centrifuged through siliconized glass wool to remove solid material and the tRNA was

0167-4781/86/$03.50 © 1986 Elsevier Science Publishers B.V. (Biomedical Division)

precipitated with 2.5 vol. of 95% ethanol at −20°C. The precipitated tRNA was taken up in 5 μl of water prior to addition to the translation system.

Results

Total tRNAs, isolated from a number of different organisms, were examined for their ability to allow in vitro translation to continue past natural UGA and UAG termination codons. Such termination readthrough can be assayed in vitro by examining readthrough of the rabbit β-globin UGA terminator [13,15,16] and the Brome Mosaic Virus (BMV) coat protein UAG terminator [13]. In each case an elongated polypeptide is synthesized which can be separated electrophoretically from the normally terminated translation product, and thus allows a quantitation of the efficiency of readthrough. We have previously shown [4,13] that such a system can be used to assay yeast nonsense suppressors in a homologous cell-free system. As shown in Table I, a number of tRNA samples examined contained UGA suppressor activity, with the exception of tRNA from wheat and soybean. The UGA suppressor activities in *E. coli* [3], *S. cerevisiae* [4] and rabbit reticulocyte [6] have been previously described. In *S. cerevisiae* the major endogenous UGA suppressor activity comes from a mitochondrial tRNA^{Trp} [4,5]. tRNAs from both strains of *C. albicans* examined (304 and C9) had significant UGA suppressor activity and were also capable of inducing UAG readthrough (Table I). Of the other tRNAs examined only tRNA from an *S. cerevisiae* strain carrying the *SUP61* amber suppressor mutation gave detectable UAG readthrough.

Fig. 1 shows the in vitro products synthesized in the presence and in the absence of the *C.*

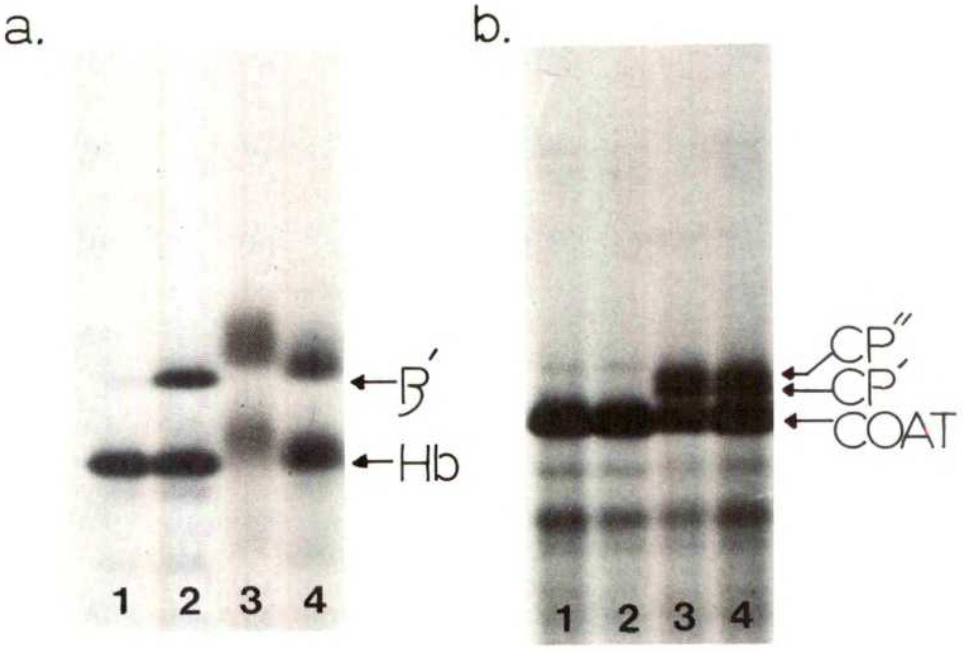

Fig. 1. Readthrough of UAG and UGA natural termination codons induced by *C. albicans* tRNA in a yeast cell-free system. (a) Rabbit globin mRNA (400 μg/ml) was translated in vitro and tRNAs, added at a final concentration of 80 μg/ml, were as follows: lane 1, no tRNA; lane 2, tRNA from a *sup*$^+$ [*rho*$^+$] strain of *S. cerevisiae*; lane 3, tRNA from *C. albicans* strain 304; lane 4, tRNA from *C. albicans* strain C9. Hb is the globin polypeptide and β' is the β-globin-specific, UGA readthrough polypeptide. The lysate used was prepared from a *sup*$^+$ [*rho*^{0}] strain and thus lacked the major endogenous, mitochondrially coded UGA suppressor tRNA activity [4]. (b) BMV RNA (120 μg/ml) was translated in vitro and tRNAs were added at a final concentration of 80 μg/ml as follows; lane 1, no tRNA; lane 2, tRNA from a *sup*$^+$ strain of *S. cerevisiae*; lane 3, tRNA from *C. albicans* strain 304; lane 4, tRNA from *S. cerevisiae* strain carrying the *SUP61* amber suppressor. CP = BMV coat protein; CP' and CP'' are the two BMV-specific amber readthrough polypeptides [13].

TABLE I

ABILITY OF WILD-TYPE tRNA TO TRANSLATE THE UGA AND UAG TERMINATION CODONS IN A YEAST CELL-FREE SYSTEM

Total tRNA was isolated from stationary-phase cells of *S. cerevisiae*, *S. pombe*, *C. albicans* and *E. coli*, as previously described [13]. *Mucor* tRNA was the gift of Professor P. Sypherd (U.C. Irvine), and tRNAs from reticulocyte, soybean and wheat germ were gifts from Dr. N. Wills (University of Utah). tRNA (80 μg/ml) was added to a yeast cell-free system and readthrough of the rabbit β-globin UGA terminator and the Brome Mosaic Virus coat protein cistron UAG terminator was assayed as previously described [17]. The cell-free system was prepared from a sup^+ [psi^+] [rho^0] strain of *S. cerevisiae* to eliminate endogenous UGA readthrough by the mitochondrially-coded $tRNA^{Trp}$ [4]. Spermidine (0.2 mM) was present in all assays [21]. n.t. = not tested.

Source of tRNA	UGA readthrough (%)	UAG readthrough (%)
No tRNA	< 1	< 1
Saccharomyces cerevisiae	37.2	< 1
Schizosaccharomyces pombe	4.1	< 1
Candida albicans (304)	51.6	49.6
Candida albicans (C9)	44.7	45.0
Escherichia coli	18.7	< 1
Rabbit reticulocytes	2.2	< 1
Mucor racemosus	8.1	< 1
Soybean	< 1	< 1
Wheat germ	< 1	< 1
S. cerevisiae (*SUP61-a*)	n.t.	42.0

albicans tRNA. The effect of *C. albicans* tRNA on rabbit globin translation products was dramatic (Fig. 1a). A significant shift in migration of both the globin and the β-globin readthrough polypeptide (β') was observed, with both bands being more disperse in appearance. tRNAs isolated from both *C. albicans* strains examined had this effect (Fig. 1a). We cannot rule out the possibility that some degree of readthrough of the UAA (ochre) terminator of α-globin mRNA is also taking place in the presence of *C. albicans* tRNA; the α-globin readthrough polypeptide (α') normally migrates slightly behind the β-globin readthrough polypeptide, but is normally only synthesized in the presence of ochre suppressor tRNA in the yeast cell-free system if the globin mRNA is heat-denatured prior to translation [13]. In the UAG assay (Fig. 1b) two BMV coat protein readthrough polypeptides are synthesized in the presence of either the *C. albicans* tRNA (lane 3) or the *S. cerevisiae SUP61* tRNA (lane 4); CP′ is synthesized as a result of readthrough of the UAG terminator of the coat protein cistron, and CP″ from the additional readthrough of the next in-phase termination codon (UGA) [13]. A difference in the migration of the BMV coat protein, in the presence of *C. albicans* tRNA only, was reproducibly observed although this was not quite as marked as the mobility shifts observed with the globin polypeptides (see above). This was suggestive of missense errors also being induced by the tRNA from *C. albicans* during in vitro translation, and preliminary peptide analysis has revealed at least one major difference in V8 proteinase digestion products of the BMV coat protein synthesized in the presence of *C. albicans* tRNA compared to coat protein synthesized in the presence of *SUP61* (and sup^+) *S. cerevisiae* tRNA (data not shown).

The in vitro efficiency of all three classes (UAG, UGA and UAA) of yeast tRNA-mediated nonsense suppressors is greatly influenced by the [*psi*] phenotype of the yeast strain used to prepare the lysate [17]. [*psi*] is a cytoplasmic determinant that in vivo modulates the efficiency of yeast ochre suppressors, suppression being much greater in [psi^+] than in [psi^-] lysates, this holding true for both mutant [17] and natural suppressor tRNAs [4]. We therefore examined the efficiency of the *C. albicans* tRNA in both types of lysate, and compared it to a known yeast suppressor tRNA, in this case the *SUP61* amber suppressor tRNA (Fig. 2). Surprisingly, the efficiency of amber readthrough (Fig. 2b) and UGA readthrough (data not shown) induced by the *C. albicans* tRNA was high irrespective of the [*psi*] phenotype of the lysate. The in vitro efficiency of *SUP61* tRNA was clearly [*psi*]-dependent (Fig. 2a). The other heterologous UGA suppressor tRNAs, identified in a [psi^+] lysate (see Table I), had no detectable activity in a [psi^-] lysate (data not shown).

tRNA from *C. albicans* can therefore efficiently translate both the UGA and the UAG termination codons in vitro, and appears to cause some degree of mistranslation of sense codons in natural mRNAs. We have isolated tRNAs from *C. albicans* at various life- and growth-cycle stages, including exponential- and stationary-phase yeast

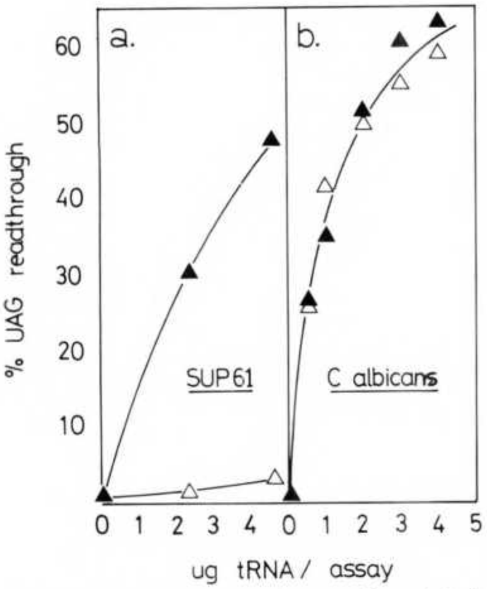

Fig. 2. The efficiency of amber readthrough in [psi^+] and [psi^-] cell-free lysates mediated by either (a) *S. cerevisiae SUP61*-a tRNA or (b) *C. albicans* tRNA. The experiment was carried out as described in the legend to Fig 1, in either a lysate prepared from a sup^+ [psi^+] strain (▲), or in a lysate prepared from an isogenic [psi^-] strain (△) isolated by guanidine hydrochloride mutagenesis [17].

TABLE II

THE EFFECT OF GROWTH PHASE AND DIFFERENTIATED STATE ON *C. ALBICANS* tRNA UAG READTHROUGH ACTIVITY

In each case 2.0 µg of unfractionated tRNA were added per 25 µl translation assay and assayed as described in the legend to Table I.

State of cells	UAG readthrough (%)
Early logarithmic growth : yeast	49.6
Late logarithmic growth : yeast	46.3
Stationary phase : yeast	46.7
Stationary phase : hyphal	42.6

cells, and hyphal cells; in all cases identical 'suppressor efficiences' (defined as percent readthrough per µg tRNA) were observed (Table II), suggesting that this activity probably does not play a role during cell differentiation [19].

Finally, we determined whether one or more tRNA species were responsible for the in vitro

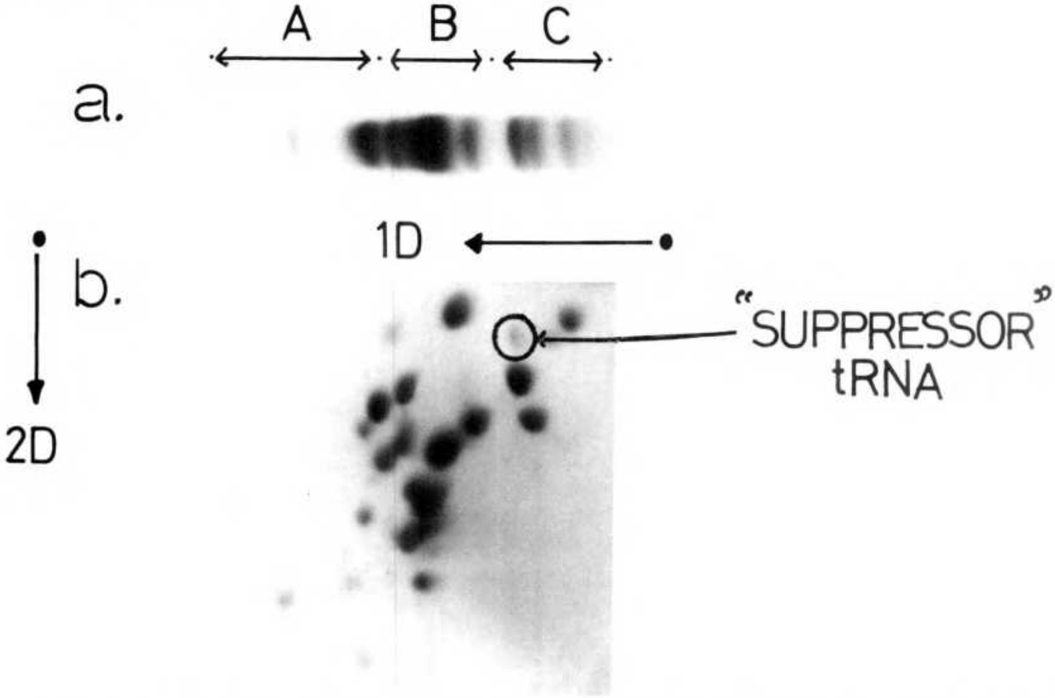

Fig. 3. Separation of *C. albicans* tRNA by one-dimensional and two-dimensional gel electrophoresis: Identification of tRNA able to translate UAG and UGA codons in vitro. (a) One-dimensional separation of *C. albicans* tRNA showing the three fractions (labelled A, B and C) eluted in the preliminary screen; (b) two-dimensional separation of *C. albicans* tRNA. tRNAs were eluted and their suppressor activities were assayed in vitro as described in Materials and Methods. The tRNA with suppressor activity is indicated.

effects of the *C. albicans* tRNA. As a first step, total tRNA from *C. albicans* strain 304 was fractionated on a one-dimensional polyacrylamide gel and the tRNA was eluted from three different regions of the gel (A, B and C; Fig. 3a). Only the tRNA from region C had in vitro readthrough activity. Following a second-dimensional separation step (Fig. 3), tRNA was eluted from the five observable spots (Fig. 3b). Only tRNA from one of these spots induced in vitro readthrough, and was able to induce both UAG and UGA readthrough. It was concluded that most probably a single tRNA species was responsible for the observed in vitro effects of the *C. albicans* tRNA.

Discussion

tRNAs from non-suppressor (wild-type) cells, capable of translating the UGA [3–8] or UAG [9–11] termination codons in vitro have been described. This is the first report of a eukaryotic tRNA species, wild-type or mutant, that is capable of translating both termination codons in vitro. If it is a bona fide suppressor tRNA relying on standard codon : anticodon interactions, it is unusual in that its in vitro efficiency is not influenced by the [*psi*] phenotype of the cell-free lysate; all suppressor tRNAs examined to date in the yeast system are much less efficient in [psi^-] lysates [4,17]. This suggests that it has a significant advantage over the natural termination mechanism, because evidence suggests that termination is very efficient in [psi^-] but not in [psi^+] lysates [17]. The *C. albicans* tRNA can also mistranslate sense codons with high frequency, as judged by the aberrant migration of in vitro synthesized polypeptides on SDS-polyacrylamide gels.

The results presented here are not an artefact of the yeast cell-free system, because similar effects with *C. albicans* tRNA have been observed in both the mammalian system of Schreir and Staehlin [20], and rabbit reticulocyte cell-free translation systems (Wills, N. and Gesteland, R., personal communication). A homologous cell-free system from *C. albicans* has yet to be developed.

Two-dimensional gel fractionation suggests that the tRNA responsible is most likely a single species, and preliminary aminoacylation experiments suggest that the tRNA eluted from the two-dimensional gel (Fig. 3b) can be charged with $[^3H]$leucine, in both *S. cerevisiae* and *C. albicans* cell-free extracts (Bower, P.A. and McLaughlin, C.S., unpublished data). One can only speculate upon the structure and function of a tRNA capable of reading both G and A at the second and third positions of a codon, respectively. Modification of anticodon bases [10] and of bases outside this region [3,8] can significantly alter the coding properties of a tRNA so that it is able to translate a termination codon. We are currently isolating and sequencing this tRNA, both at the RNA and the DNA levels, in order to determine precisely the structure of this novel, naturally occurring suppressor tRNA.

Acknowledgements

This work was supported by a grant from the Cancer Research Co-ordinating Committee of the University of California (79112), and by grant GM28772 from the National Institute of General Medical Sciences.

References

1 Phillipson, L. (1979) in Nonsense Mutations and tRNA Suppressors (Celis, J.E. and Smith, J.D., eds.), pp. 313–319, Academic press, New York

2 Ryoji, M., Hsia, K. and Kaji, A. (1983) Trends Biochem. Sci. 8, 88–90

3 Hirsh, D. and Gold, L. 91971) J. Mol. Biol. 58, 459–468

4 Tuite, M.F. and McLaughlin, C.S. (1982) Mol. Cell. Biol. 2, 490–497

5 Martin, R.P., Sibler, A.P., Dirheimer, G., de Henau, S. and Grosjean, H. (1981) Nature 293, 245–237

6 Geller, A.I. and Rich, A. (1980) Nature 283, 41–46

7 Van Tol, R.G.L., Van Gemeren, R. and Van Vloten-Doting, L. (1980) FEBS Lett. 118, 67–71

8 Diamond, A., Dudock, B. and Hatfield, D. (1981) Cell 25, 497–506

9 Morch, M.-D. and Benicourt, C. (1980) Eur. J. Biochem. 105, 445–451

10 Bienz, M. and Kubli, E. (1981) Nature 294, 188–190

11 Beier, H., Barciszewska, M., Drupp, G., Mitracht, R. and Gross, H.J. (1984) EMBO J. 3, 351–356

12 Tuite, M.F., Plesset, J., Moldave, K. and McLaughlin, C.S. (1980) J. Biol. Chem. 255, 8761–8766

13 Tuite, M.F., Cox, B.S. and McLaughlin, C.S. (1981) J. Biol. Chem. 256, 7298–7304

14 Fradin, A., Gruhl, H. and Feldmans, H. (1975) FEBS Lett. 50, 185–189
15 Kohli, J., Kwong, T., Altruda, F., Soll, D. and Wahl, G. (1979) J. Biol. Chem. 254, 1546–1551
16 Gesteland, R.F. and Wills, N. (1979) in Nonsense Mutations and tRNA Suppressors (Celis, J.E. and Smith, J.D., eds.), pp. 277–284, Academic Press, New York
17 Tuite, M.F., Cox, B.S. and McLaughlin, C.S. (1983) Proc. Natl. Acad. Sci. USA 80, 2824–2828
18 Cox, B.S. (1965) Heredity 20, 505–521
19 Picard-Bennonn, M. (1982) FEBS Lett. 149, 167–169
20 Schreier, M.H. and Staehlin, T. (1973) J. Mol. Biol. 73, 329–338
21 Tuite, M.F. and McLaughlin, C.S. (1983) Curr. Genet. 7, 421–426

Biochimica et Biophysica Acta 866 (1986) 32–36
Elsevier

BBA 91551

Kinetic control of the length of very short homopolymeric additions by terminal deoxynucleotidyltransferase

Karl Sirotkin

Department of Microbiology and Graduate Program in Cellular, Molecular and Developmental Biology, University of Tennessee, Knoxville, TN 37996–0845 (U.S.A.)

(Received July 30th, 1985)

Key words: Terminal deoxyribonucleotidyltransferase; Nucleotide addition; Priming rate; Kinetics

This work is an investigation of the practicality of kinetic control of the length of very short deoxynucleotide homopolymeric additions by terminal deoxynucleotidyltransferase. For such very short additions, the possibility that terminal deoxynucleotidyltransferase acts differently with each deoxytriphosphate, or shows interaction effects when presented with multiple deoxytriphosphates, was investigated. Different relative rates of priming and different relative rates of subsequent additions were found for each deoxytriphosphate. Each triphosphate reacted uniquely, and one case of interaction was found, with adenosine interfering with cytidine addition.

Introduction

Terminal deoxynucleotidyltransferase (EC 2.7.7.31) catalyzes the addition of deoxyribonucleotides to the 3′-OH end of a nucleic acid primer, independently of the template. Primers terminating in DNA are preferred, but since multiple additions of ribonucleotides are also possible [1], the primer can also have RNA at its 3′ end, at least. A previous paper [1] has demonstrated sequence dependence in the primer and measured K_m and V_{max} for the various deoxynucleotides, but since the work was performed before the high-resolution sequencing gels were available, the different addition products could not readily be compared. There have therefore not been any published studies, comparing each nucleotide at early stages in the addition process, in which the various products have been resolved.

My goal was to investigate the difference in the number of additions between each nucleotide. I reasoned that the early stage of the addition process would be the most easily observed. Furthermore, since terminal deoxynucleotidyltransferase probably interacts with multiple bases at the 3′ end of its primer, I suspected that having heteropolymeric 3′ ends would provide more information to terminal deoxynucleotidyltransferase that it might use to exercise a preference. Again, this would only be observable during the early stages of addition.

This work documents that it is possible to generate substrates with very short homopolymeric additions, that each nucleotide is treated somewhat differently by terminal deoxynucleotidyltransferase at the beginning of additions, as well as at later stages, and that there is interaction between nucleotides, even for these short additions.

Abbreviations: dAdo, deoxyadenosine; dCyd, deoxycytidine; dGuo, deoxyguanosine; dThd, deoxythymidine

0167-4781/86/$03.50 © 1986 Elsevier Science Publishers B.V. (Biomedical Division)

Materials and Methods

Enzymes. Terminal deoxynucleotidyltransferase from PL Biochemicals (lot 730-12) was used for all these studies. We have noticed some variations within the same lot in the activity of enzyme from different tubes (data not shown). T_4 polynucleotide 5′-hydroxyl-kinase (EC 2.7.1.78) was used as part of the Bethesda Research Laboratories end-labelling kit.

Nucleotides and primers. [γ-^{32}P]ATP was obtained from ICN, and the nonradiactive dNTPs used were from Sigma or PL Biochemicals. The New England Biolabs 15mer sequencing primer and both the New England Biolabs and the PL Biochemicals 17mer sequencing primers were used for priming terminal deoxynucleotidyltransferase additions of nucleotides.

Initially, primers were separated from reaction mixtures using Schleicher & Schuell Elutip^{TM} Columns. In later experiments, to desalt, concentrate and purify to a greater degree, phenol-extracted reaction mixtures were passed through an 8 ml, 0.5 cm diameter Sephadex G-50 (Sigma) column, previously washed with H_2O. The primers were excluded.

Chemicals. Electrophoresis-grade chemicals were obtained from Bio-Rad, and miscellaneous chemicals were from Fisher or Sigma.

Terminal deoxynucleotidyltransferase buffer. The Mg^{2+}-containing buffer [1] was chosen rather than the Co^{2+} buffer [2], because additions were expected to be slower for the Mg^{2+}-containing buffer [1,2], and I expected that, since Mg^{2+} is the 'natural' cation, more inherent specificity would be observed. Furthermore, the reaction was controlled by increasing the Na^+ concentration, as this is known to be inhibitory [1].

Overview. ^{32}P was added as a 5′-phosphate group to sequencing primers. The purified ^{32}P-labeled primers were used in terminal deoxynucleotidyltransferase reactions. These reactions were terminated by the addition of EDTA to 20 mM, and aliquots were run on 0.35–0.5 mm-thick acrylamide-urea gels. Autoradiography was performed for 12–48 h with one Dupont (lightning plus) intensifier screen.

Results and Discussion

Early addition differences

Early addition differences between the various triphosphates may be due to two factors. One factor could be the different rates at which terminal deoxynucleotidyltransferase interacts with the nucleotide, independently of differences in the DNA sequence of the primer. Since the same primer is used with the different nucleotides, the extent to which the primer is used at all gives a measure of the nucleotide interaction rate. Another factor could be the different rates at which terminal deoxynucleotidyltransferase acts with primers altered by at least one addition: once a nucleotide is added, the primer is altered, in that the 3′ end had a different sequence and, possibly, by the presence of terminal deoxynucleotidyltransferase in activated form. Differences in the pattern of more than one addition would be due to both effects.

Both factors are clearly evident in the data presented in Fig. 1. The figure has three panels, each from a different set of reactions. In all cases, the primer is the New England Biolabs pentadecamer sequencing primer, labelled at the 5′ end with [γ-^{32}P]ATP and T_4 polynucleotide kinase.

Therefore, regardless of length, every molecule contributes the same amount to the resulting signal. The panels contain autoradiograms of polyacrylamide gels of the type used to separate products for DNA sequence determination. In this case, aliquots of the terminal deoxynucleotidyltransferase reactions were electrophoresed. Panel A results from the use of a relatively long reaction time with relatively low amounts of triphosphates and terminal deoxynucleotidyltransferase. The results in panel A seem similar to those in panel B, which resulted from relatively short reaction times and higher concentrations of triphosphates and terminal deoxynucleotidyltransferase. Panel C contains the results of obtained with of longer reactions tunes under the same conditions used to obtain the results in panel B.

The lanes resulting from addition of dGuo show an unexpected result, especially at longer reaction times: the distribution of lengths is trimodal. Modes are observed for the primer with no ad-

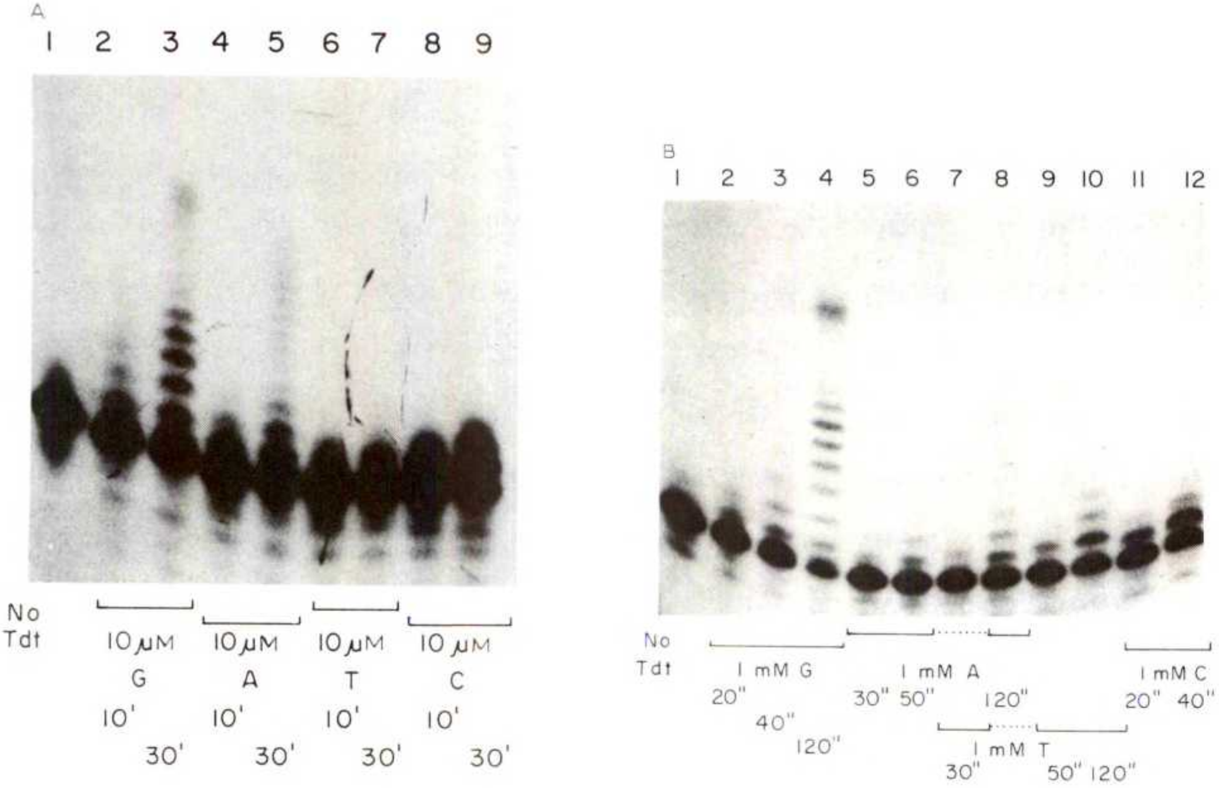

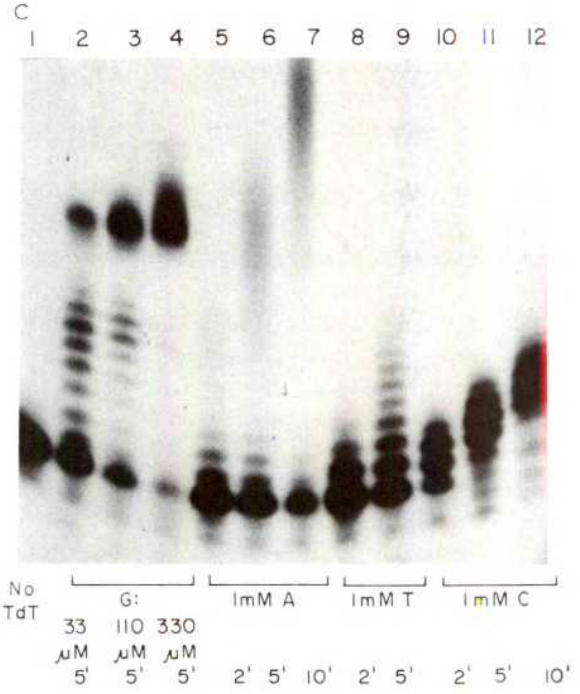

Fig. 1. Early addition of deoxynucleotide homopolymers. Panels A, B and C: lane 1, no terminal deoxynucleotidyl transferase (TdT). Panel A: Lanes 2–9, 6 units TdT per 10 μl reactions mixture, incubation at 37°C, and one of the deoxynucleoside triphosphate at 10 μM; lanes 2 and 3, GTP; lanes 4 and 5, ATP; lanes 6 and 7, TTP; lanes 8 and 9, CTP; lanes 2, 4, 6 and 8, 10-min reaction; lanes 3, 5, 7 and 9, 30-min reaction. Panel B: lanes 2–12, 27 units TdT per 10 μl reaction; incubation at 37°C, and one of the deoxynucleoside triphosphate at 1 mM; lanes 2–4, GTP; lanes 5, 6 and 8, ATP; lanes 7, 9 and 10, TTP; lanes 11–12, CTP; lanes 2 and 11, 20-s reactions; lanes 3 and 12, 40-s reactions; lanes 5 and 7, 30-s reactions; lanes 4, 8 and 10, 120-s reactions; lanes 6 and 9, 50-s reactions. Panel C: lanes 2–12, 27 units TdT per 10 μl reaction, incubation at 37°C with one of the deoxynucleoside triphosphates; lanes 2–4, 5-min reactions with dGTP, lane 2, 33 μM dGTP; lane 3, 110 μM dGTP; lane 4, 330 μM dGTP; latens 5–7, 1 mM dATP; lanes 8–9, 1 mm dATP; lanes 10–12, 1 mM dCTP; lanes 5, 8 and 10, 2-min reactions; lanes 6, 9 and 11, 5-min reactions; lanes 7 and 12, 10-min reactions.

dition, at the addition of five dGuo and approximately at the addition of 12 dGuos. I cannot rule out the possibility that the mode at the +12 position is an artifact due to intra- or intermolecular aggregation mediated by poly(dGuo). In spite of this uncertainty, it is clear that the primer is utilized quickly and, once a dGuo residue is added, the addition of more dGuo residues occurs rapidly (shown in panel B). One difference is apparent between panels A and B. The shorter reaction lacks the mode at +5 (seen in panel A). One explanation for this could be that, with the longer reaction at lower concentrations of dGTP, the 3′ sequence of five dGuos is more likely to terminate additions than in the reactions with a higher dGTP concentration.

The lanes resulting from the additions of dAdo show a different, bimodal distribution. As with dGuo additions, one mode is at the primer alone, implying that for dAdo additions, once a single dAdo is added to a primer, it preferentially receives subsequent additions. The single higher mode, which is only visible in panel C, changes with time. There are two possible explanations for this; either dGuo and dAdo additions are similar, and dGuo causes aggregation, or there are inherent differences in the way terminal transferase adds dGuo or dAdo to a primer that already has a homopolymer extension at the 3′ end. There must be some differences, however, since less of the primer is left in the lanes due to dGuo addition, perhaps because terminal transferase favors addition to long poly(dAdo) rather than to poly(dGuo).

The lanes due to addition of dThd only show one mode, at the primer. The primer is utilized for the first addition about as often for dAdo as for dThd, but subsequent additions occurs more frequently for dAdo. Using the PL Biochemicals heptadecamer sequencing primer, a mode developed at the band due to +3 (dThd) additions, and was maintained until fairly long additions were also present (not shown). This is likely to be a sequence-dependent effect.

The lanes due to addition of dCyd show differences from all the other lanes. In this case, the mode keeps changing and long additions are not favored, the variation in number of additions being small and controllable. The primer is utilized more quickly than with all the other deoxynucleotides except dGuo. All of these results could be explained if terminal transferase were more processive with other deoxynucleotides than with dCyd. In other words, it appears that terminal transferase and the 3′ end of its primer form an activated complex that is more stable after adding other bases than it is after adding dCyd.

I wanted to test whether, when two deoxynucleotides were used at the same time (Fig. 2), the pattern would be as predicted by summation of the two individual patterns. Previous work [1] suggests that a purine would noncompetitively compete with a pyrimidine, at least for long homopolymeric additions. As Fig. 2, lanes 3 and 4, shows, when both dGuo and dCyd were added, the distribution of lengths is no longer trimodal, as it was with dGuo alone. Additionally, lanes 6 and 7 show that when both dAdo and dCyd were added, not only is the the bimodal pattern eliminated, but fewer dCyds are added than when dCTP is used alone. The presence of dATP interfered with the addition of dCyd. This shows competition during the addition of only a few bases, extending the results obtained in previous work.

The data, taken together, are evidence for three complexities in the way terminal transferase interacts with its two substrates. The addition of homopolymer provides evidence that terminal transferase reacts differently with each dNTP (Fig. 1). This is consistent with K_m and V_{max} differences reported previously [1]. Furthermore, the sequence of the primer influences the rate of addition. This has been suspected, but not clearly demonstrated [1]. Additionally, when more than one deoxynucleotide triphosphate is present, complex interactions occur, even for very early additions. This has been reported previously for lengthy products [1], but not for very early additions.

Taken together, these data suggest the following model for terminal deoxynucleotidyltransferase function. Free terminal deoxynucleotidyltransferase, dNTP and primer form a complex. If the rate at which this occurs is slower than the rate at which bases are added once it does occur, this would explain the observations that the primer needs to be activated (this paper and Ref. 1). The rates for the addition of the first base for the deoxynucleotides, from our data, appear to have

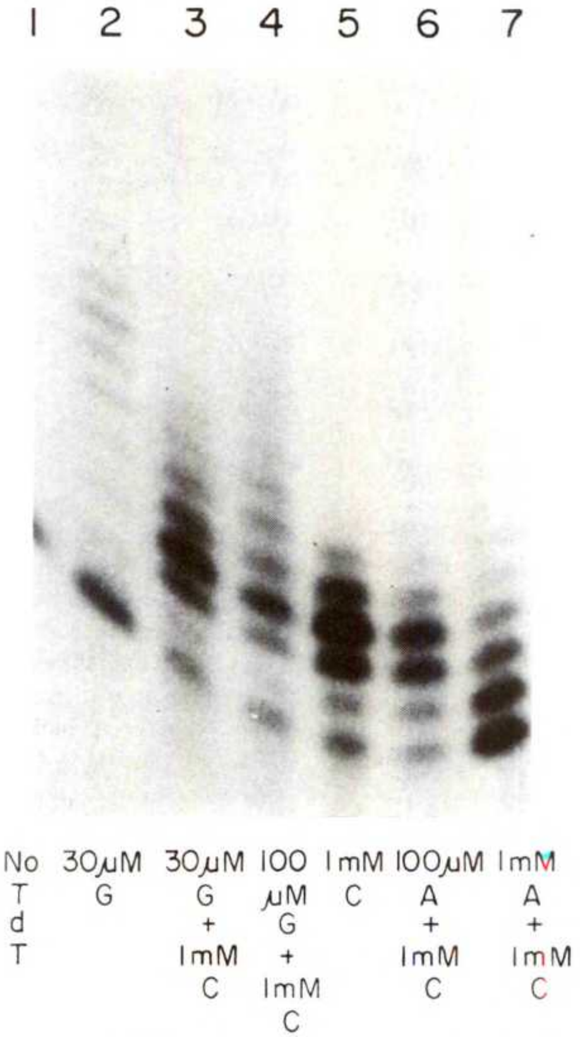

Fig. 2. Addition of very short copolymers of deoxynucleotides. Lane 1, no terminal deoxynucleotidyltransferase (TdT). Lanes 2′, 27 units TdT per 10 μl reaction for 5 min at 37°C; lane 2, 30 μM dGTP; lane 3, 30 μM dGTP plus 1 mM dCTP; lane 4, 100 μM dGTP plus 1 mM dCTP; lane 5, 1 mM dCTP; lane 6, 100 μM dATP plus 1 mM dCTP; lane 7, 1 mM dATP plus 1 mM dCTP.

the following order: dGuo > dCyd > dAdo = dThd. These relative rates would then be, if this model is correct, the relative rates for complex formation. The nucleotide is added, but terminal transferase can sometimes remain in an activated state bound to the primer. This may be visualized formally as follows, where P_i is the primer, of length i, E is terminal transferase, and M is a dNTP.

$$E + P_i \leftrightarrow E \cdot P_i \tag{1}$$

$$E \cdot P_i + M \leftrightarrow E \cdot P_i \cdot M \tag{2}$$

$$E \cdot P_i \cdot M \leftrightarrow E \cdot P_{[i+1]} \tag{3}$$

If this describes what in fact occurs, the pattern of additions would then be influenced by the rate at which the enzyme dissociations from the primer. The faster the dissociation, the fewer the number of bases added to molecules that have been ‘primed’ with at least one addition. The rate at which this dissociation occurs depends on the nucleotide added (and therefore the new 3′ end of the primer) and generally has the order dGuo < dAdo < dThd < dCyd. The K_m and V_{max} values have been measured previously [1] and are in the following order: for K_m, dAdo = dGuo < dThd < dCyd; for V_{max}, dAdo > dGuo ≫ dCyd > dThd. Additionally, there are bases other than the 3′ terminal base that affect the dissociation rate (Ref. 1 and this paper), and the above dissociation rate order may be specific for the sequency of the pentadecamer primer used.

Acknowledgements

Major support from the Department of Microbiology and N.I.H. Biomedical Grant BRSG RR-07088 to the University of Tennessee, and incidental support from NSF grant PCM-8315592 to K.S. and EPA grant CR-810485-01-1 to Dr. Sayler are acknowledged.

References

1 Kato, K.-I., Gonçalves, J.M., Houts, G.E. and Bollum, F.J. (1967) J. Biol. Chem. 242, 2780–2789
2 Roychondhury, R., Jay, E. and Wu, R. (1976) Nucleic Acids Res. 3, 101–116
3 Roychondhury, R. and Wu, R. (1980) Methods Enzymol. 65, 43–64

Biochimica et Biophysica Acta 866 (1986) 37–43
Elsevier

BBA 91552

The role of upstream sequences in determining the strength of an rRNA promoter of *E. coli*

Árpád Pethő *, Jörn Belter **, Imre Boros and Pál Venetianer

Institute of Biochemistry, Biological Research Center, P.O. Box 521, Szeged, H-6701 (Hungary)

(Received November 18th, 1985)

Key words: rRNA promoter; Transcriptional activity; Upstream region; (*E. coli*)

In vitro transcription experiments were carried out with recombinant plasmids containing the promoters of the *rrnB* gene of *Escherichia coli*, and with deletion mutants lacking various lengths of the AT-rich sequence upstream from the P_1 promoter of that gene. The main conclusions are as follows: (a) The in vitro transcriptional activity of the P_1 and P_2 promoters of the *rrnB* gene are an order of magnitude higher on closed-circular (supercoiled) templates than on linear DNA; (2) the strong P_1 and P_2 promoters are heparin-sensitive on linear templates, and on circular DNA only P_2 is heparin-resistant; (3) removal of the upstream AT-rich region did not decrease the apparent in vitro strength of the P_1 promoter under standard conditions (50 mM KCl, high RNA polymerase/DNA ratio); (4) at higher salt concentrations, or with a lower RNA polymerase/DNA ratio, the deletion mutants displayed much lower in vitro transcriptional activity than the wild-type, and the apparent weakening of the P_1 promoter was roughly proportional to the length of the deleted AT-rich sequence. The implications of these findings for the possible in vivo role of the AT-rich region are discussed.

Introduction

A recent review [1] compiled the sequences of 168 *Escherichia coli* promoters and this list has grown steadily since then. From these sequences, and from the analysis of mutants of several well-known promoters, generated in vivo and in vitro, a general picture of the *E. coli* promoter seems to emerge (see also McClure [2]). The prototype *E. coli* promoter consists of two functionally important parts, the so-called −35 and −10 regions, with TTGACA and TATAAT as the ideal, or consensus, sequences, separated by a 17-bp-long spacer region. All existing promoters differ somewhat from this prototype, but it is generally believed that the functional strength of any individual *E. coli* promoter is correlated with the degree of its similarity to the consensus sequence. The boundaries of a promoter are not always well defined, but experiments with chemically synthesized promoters indicate that 42 basepairs are sufficient to create a very strong functional promoter [3]. This does not necessarily mean that DNA sequences outside this region do not play any role in the proper functioning of a promoter. Several strong promoters have characteristic AT-rich sequences upstream of the consensus sequence. Klein and Wells [4] demonstrated that the insertion of poly(dA)·poly(dT) upstream of the *lacUV5* promoter enhances the binding of polymerase to the promoter. Lamond and Travers [5] removed the DNA between −40 and −98 upstream of the *tyrT* promoter and found that the

---

* Permanent address: Chinoin Pharmaceutical Company, Budapest, Hungary.

** Permanent address: Department of Genetics, Martin Luther University, Domplatz 1, DDR-4020 Halle/Saale, G.D.R.

0167-4781/86/$03.50 © 1986 Elsevier Science Publishers B.V. (Biomedical Division)

activity dropped 10-fold. Travers [6] detected common features in the upstream sequences of several stable RNA gene promoters and suggested that these sequences might play some role in determining their activity. These observations prompted us to investigate the role of such upstream sequences in determining the activity of the very strong promoter (P_1) of an rRNA gene (*rrnB*).

Materials and Methods

Escherichia coli HB101 [7] host was used to maintain recombinant plasmids.

Restrictions endonucleases were prepared in this laboratory and were used according to the recommendations of New England Biolabs. RNA polymerase, T_4 DNA ligase and DNA polymerase Klenow fragment were prepared according to published procedures [8–10]. BAL 31 nuclease was obtained from New England Biolabs.

[α-^{32}P]ATP, [α-^{32}P]dATP] and [α-^{32}P]dCTP were from IZINTA (Budapest). Linkers were obtained from New England Biolabs. All other materials were analytical-grade commercial products.

Recombinant DNA experiments were performed using standard methods, as described in the manual of Maniatis et al. [11].

The structure and construction of the plasmids p511-20 and p408-5 are described in a previous paper [12]. Both of these plasmids carry a shortened *rrnB* operon of *E. coli* between the *Eco*RI and *Pvu*II restriction sites of pBR322 (Fig. 1). Derivatives of the p408-5 plasmid with deletions upstream of the promoter were constructed by cleavage at the unique *Eco*RI site, and after limited BAL 31 nuclease digestion, religation with T_4 DNA ligase. In order to facilitate sequencing, ligation was carried out in the presence of synthetic linkers (*Eco*RI or *Bam*HI) in most experiments. In these cases, ligation was followed by cleavage with the respective restriction endonuclease, and religation. The end-points of the deletions were determined by sequencing the relevant part of the plasmid DNA. DNA fragments were labelled by filling the 3′ ends using DNA polymerase Klenow fragment with [α-^{32}P]dATP or [α-^{32}P]dCTP. DNA sequences were determined by the Maxam-Gilbert procedure [13].

Plasmid DNA was prepared by the method of Clewell and Helinski [14] using CsCl centrifugation or Sephacryl-1000 chromatography in the final purification step. DNA fragments were isolated by agarose gel electrophoresis and electroelution. All DNA electrophoresis was on horizontal agarose slab gel according to Helling et al. [16]. RNA electrophoresis was on denaturing 4% polyacrylamide 7 M urea vertical slab gels according to Maniatis et al. [17].

In vitro transcription was carried out essentially as described by Glaser and Cashel [18].

Results

The seven genes coding for rRNA in *E. coli* have basically similar structures. The promoter regions of six of them have been sequenced [19–22]. They all have two strong promoters, P_1 and P_2, located about 110 basepairs apart. The *rrnB* gene analyzed by us has a distinguishing feature, probably not shared by the other rRNA genes; it is preceded, more than 1 kb upstream, by another pair of promoters 70 basepairs apart (P_3 and P_4). Transcription starting from these promoters proceeds without termination through P_1 and P_2, into the *rrnB* gene [23].

Recently, we cloned all these promoters on a pBR322-derived plasmid and constructed several deletion derivatives by removing one or more of them, changing their relative distances, and removing upstream or downstream regions in the vicinity of the promoters [12]. Two of these plasmids are shown in Fig. 1. Plasmid p511-20 carries all four promoters, while p408-5 contains only P_1 and P_2.

We chose to analyze the role of upstream regions in determining promoter strength by estimating the amounts of specific transcripts synthesized in vitro using purified RNA polymerase holoenzyme. First, we wanted to optimize the assay conditions with respect to the following parameters: concentration of salt (monovalent cation), concentration of heparin (an agent generally used in in vitro transcription experiments for reducing nonspecific transcription), and conformation of template DNA (circular or linear).

As Fig. 2 shows, the behavior of the four promoters of the *rrnB* region is very different with respect to changes in these parameters. The P_3 and

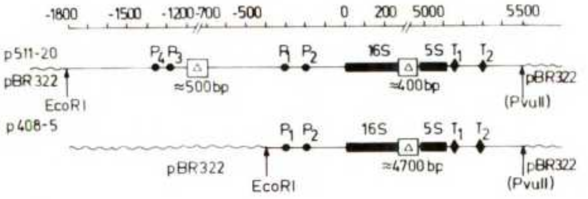

Fig. 1. Schematic structure of plasmids p408-5 and p511-20. Some selected restriction sites are indicated. Black bars, DNA coding for mature rRNA; P and T, promoters and terminators of the *rrnB* gene.

P_4 promoters are relatively much stronger on linear DNA than on circular template and they are also strongly resistant to heparin. Their salt resistance (especially that of P_3) is also much higher than that of P_1 or P_2. On circular template, a high salt concentration markedly increases their strength; 0.2 M appears to be optimal. P_1 and P_2 work much better on circular DNA. On linear template they are heparin- and salt-sensitive. On circular DNA P_2 is heparin-resistant, while P_1 is not, and both are more resistant to salt than on linear template. It must be added that the upper and lower panels depict the results of independent experiments. The autoradiogram in the upper panel was exposed for a shorter time because the overall transcriptional activity (incorporation of the radioactive precursor into trichloroacetic acid precipitable material) is approximately an order of magnitude lower on linear template than on circular, template.

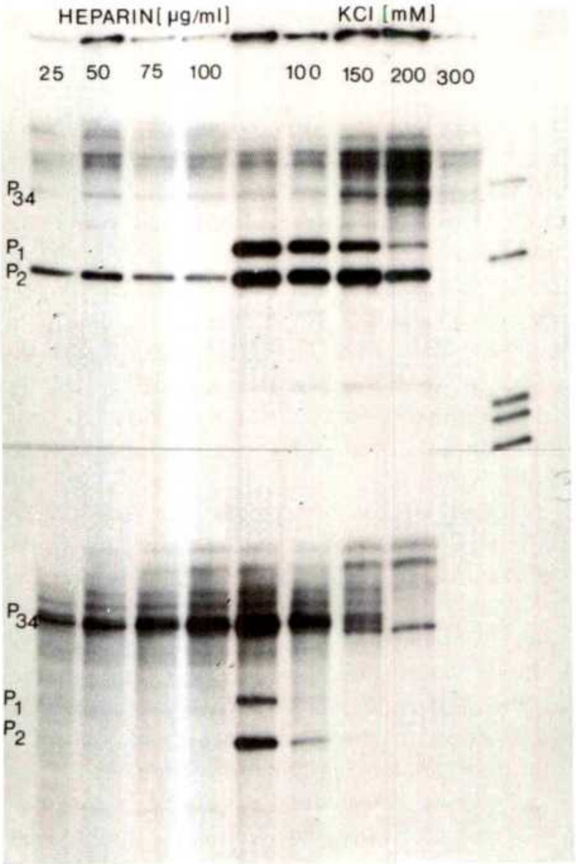

Fig. 2. In vitro transcription on p511-20 plasmid DNA. Upper panel: circular template. Lower panel: DNA linearized with *Hin*dIII digestion. The middle lane represents standard conditions: 50 mM KCl, no heparin. Ratio of RNA polymerase to DNA, 5:1 (weight). In experiments with heparin, DNA + polymerase were preincubated for 5 min, then heparin was added and the reaction was started after 5 min by the addition of nucleoside triphosphates. Reactions were stopped after 20 min by phenolization and transcripts were analysed by electrophoresis on 4% acrylamide-urea gels and autoradiography. The right-most lane in the upper panel contains molecular weight markers.

These results are in complete agreement with earlier data from this laboratory [24] indicating that on linear DNA, the polymerase binding ability of the P_3 and P_4 promoters was much stronger than that of P_1 or P_2. The results shown in Fig. 2 also might serve as a warning; comparison of the strength of different promoters in vitro under any single set of conditions does not necessarily reflect the in vivo activity, and conclusions drawn from such experiments might be misleading.

From the experiments described above, we concluded that for studying P_1 and P_2 promoters, the standard in vitro conditions should be: circular template, low salt concentration (50 mM), no heparin. Under these circumstances the in vitro transcriptional activities of P_1 and P_2 are approximately equal, and both appear to be much stronger than any other promoter present on the pBR322 plasmid. In the next series of experiments, in order to study the role of upstream regions, deletion mutations were introduced by the technique of controlled BAL 31 digestion that removed parts of the upstream region, but left the consensus sequence of the P_1 promoter intact. P_2

```
                                             -35                   -10
rrnB P1   GTTGCGCGGTCAGAAAATTATTTTAAATTTCCTCTTGTCAGGCCGGAATAACTCCCTATAATGCGCC
5d10       CCGGATCCGGAGAAAATTATTTTAAATTTCCTCTTGTCAGGCCGGAATAACTCCCTATAATGCGCC
10d1                   GGAATTCCTTTAAATTTCCTCTTGTCAGGCCGGAATAACTCCCTATAATGCGCC
10d2                     GGAATTCCTAAATTTCCTCTTGTCAGGCCGGAATAACTCCCTATAATGCGCC
5d65                        CCGGATCCGGTTCCTCTTGTCAGGCCGGAATAACTCCCTATAATGCGCC
10d3                            GGAATTCCCCTCTTGTCAGGCCGGAATAACTCCCTATAATGCGCC
10d4                               GGAATTCCCTTGTCAGGCCGGAATAACTCCCTATAATGCGCC
5/55                                 TTTCCCCGTGTCAGGCCGGAATAACTCCCTATAATGCGCC
10d5                                 GGAATTCCTGTCAGGCCGGAATAACTCCCTATAATGCGCC
5d8                                     CCGGATCCGGGGCCGGAATAACTCCCTATAATGCGCC
```

Fig. 3. Sequences of the deletions. *Bam*HI or *Eco*RI linker sequences are underlined. In the case of mutant 5/55 no linker was employed; underlined sequences are of pBR322 origin.

also remained intact, and the amount of P_2 transcript synthesised in each experiment served as an internal control.

The sequences of the deletion mutants are shown in Fig. 3. The left end-points of all deletions lie within the vector DNA.

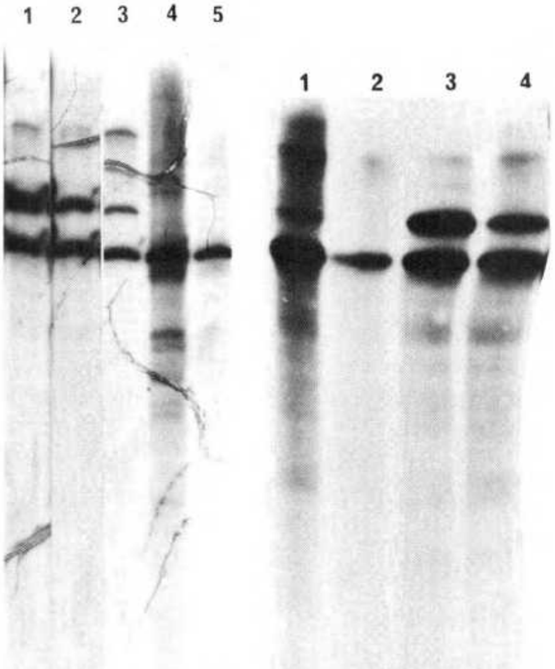

Fig. 4. In vitro transcription on mutant plasmids. Plasmid DNA was in circular form. RNA polymerase: DNA ratio (weight), 5 : 1. Conditions are the same as in the middle lane of Fig. 2. (A) 1, 5d10 DNA; 2, 5d65 DNA; 3, 5/55 DNA; 4, 10d5 DNA; 5, 5d8 DNA. (B) 1, 5/55 DNA; 2, 5d8 DNA; 3, 5d10 DNA; 4, 5d65 DNA.

Fig. 4 shows the results of two in vitro transcription experiments under standard conditions with some selected mutant plasmids. Contrary to our expectations, the removal of most of the AT-rich sequence did not decrease appreciably the apparent strength of P_1 if the -35 region remained intact. It is interesting to note that the intact sequences are identical in mutants 5/55 and 10d5. In both mutants the first (strongly conserved) T of the -35 region is replaced by either G or C. While the G-substitution in mutant 5/55 leads only to the weakening of the P_1 promoter, the C-substitution (in 10d5) completely destroys the activity. However, it should be noted that this is not the only difference between the two mutants; 5/55 was formed by direct ligation after deletion, while in 10d5 an *Eco*RI linker is inserted.

In view of the fact that the reaction conditions employed in the experiments shown in Fig. 4 are optimal in vitro but do not necessarily resemble the in vivo conditions, we compared the in vitro transcription on some of these mutant plasmids at higher monovalent cation concentrations, and at a lower RNA polymerase/DNA ratio.

Figs. 5, 6 and 7 shows the result of these experiments, comparing the wild-type plasmid with a mutant with the AT-rich sequence deleted (10d4) and with a mutant in which approximately half of this sequence is missing (10d1). Table I summarizes the results of these experiments in a quantitative form. It can be seen that, while at a lower polymerase/DNA ratio the wild-type P_1 and

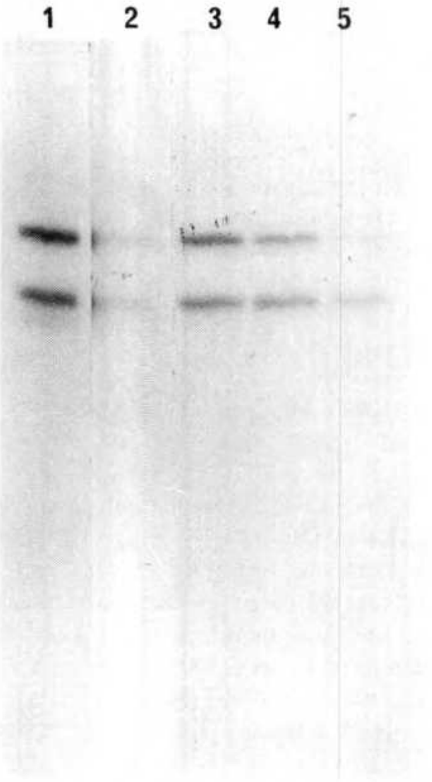

Fig. 5. Transcription on plasmid p408-5 (wild-type). (1) Standard conditions (RNA polymerase/DNA ratio 5:1, 50 mM KCl); (2) RNA polymerase/DNA 1:2, 50 mM KCl; (3) RNA polymerase/DNA 5:1, 100 mM KCl; (4) RNA polymerase/DNA 5:1, 150 mM KCl; (5) RNA polymerase/DNA 5:1, 200 mM KCl.

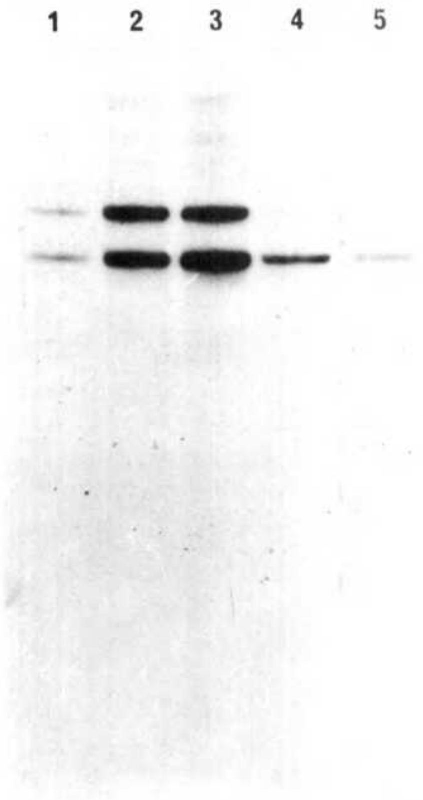

Fig. 6. Transcription on the deletion plasmid p10d1. (1) Standard conditions (RNA polymerase/DNA 5:1, 50 mM KCl); (2) RNA polymerase/DNA 5:1, 100 mM KCl; (3) RNA polymerase/DNA 5:1, 150 mM KCl; (4) RNA polymerase/DNA 5:1, 200 mM KCl; (5) RNA polymerase/DNA 1:2, 50 mM KCl.

P_2 promotors are affected similarly (in other words, the P_1/P_2 ratio remains the same as at a high polymerase concentration), in the deletion mutants the P_1/P_2 ratio drops about 10-fold. Similarly, while the wild-type P_1 promoter retains its relative strength (in comparison to P_2) in 150 mM KCl, and the P_1/P_2 ratio is about 0.6 even at 200 mM, in mutant 10d1 such a decrease is seen at 150 mM and, in the case of 10d4, is already apparent at 100 mM, with proportional decreases at higher salt concentrations.

TABLE I

QUANTITATIVE EVALUATION OF THE AUTORADIOGRAMS BY DENSITOMETRIC SCANNING AND PEAK INTEGRATION

Plasmid DNA	P_1/P_2 transcript ratio				
	standard (50 mM KCl)	100 mM KCl	150 mM KCl	200 mM KCl	1/10 RNA polym.
Wild-type	1.06	1.19	0.94	0.59	1.24
p10d1	0.94	0.96	0.65	0.21	0.09
p10d4	0.71	0.48	0.20	0.07	0.12

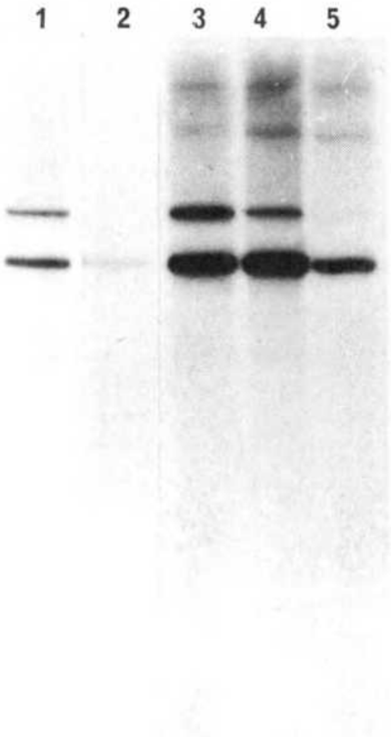

Fig. 7. Transcription on the deletion plasmid p10d4. (1) Standard conditions (RNA polymerase/DNA 5:1, 50 mM KCl); (2) RNA polymerase/DNA 1:2, 50 mM KCl; (3) RNA polymerase/DNA 5:1, 100 mM KCl; (4) RNA polymerase/DNA 5:1, 150 mM KCl; (5) RNA polymerase/DNA 5:1, 200 mM KCl;

Discussion

The main purpose of the work reported here was to analyse the role of upstream sequences in determining the activity of the P_1 promoter of the *rrnB* gene. The results, however, raised some other points worth discussing.

The first notable observation was the dramatic effect of DNA conformation. We compared transcription on linear and circular plasmid DNA. The latter was plasmid DNA isolated from bacterial cells by standard procedures. It contained mostly (more than 80%, data not shown) supercoiled DNA molecules. It can safely be assumed that the effectes observed are due to the supercoiled form of the plasmid. It has long been known that negative supercoiling may increase the efficiency of some promoters [25,26]. This has been shown to be true for the *rrnB* promoters as well [27]. Most of these experiments, however, have been carried out in vivo, or in vitro using crude cell extracts. The effect of supercoiling on transcriptional activity was assessed by employing the gyrase inhibitors, coumermycin or novobiocin; thus the evidence was indirect. The results shown in Fig. 1 give direct evidence for the differential effect of supercoiling on transcription. They might also serve as a warning for caution in the interpretation of in vitro transcription experiments. Looking only at the results with linear template would suggest that P_3 and P_4 promoters are stronger than P_1 or P_2 and, indeed, similar conclusions have been suggested earlier by our electron microscopy and filter-binding studies [23,24]. This conclusion is undoubtedly wrong; in vivo, P_1 and P_2 are the stronger promoters.

The differential effect of conformation on the heparin-resistance of these promoters is also worth noting. It helps to explain an apparent contradiction reported by us earlier, namely that rRNA transcription on carefully prepared, high molecular weight (thus presumably partially supercoiled) bacterial DNA started from multiple, heparin-resistant promoters [28], whereas rRNA transcription on transducing phage DNA, or on restriction fragments, was heparin-sensitive [29]. The heparin-sensitivity of the strong P_1 and P_2 promoters (on linear DNA) is exceptional but not unique, since this is also true for a tRNA promoter [30]. Conclusion, heparin-resistance (assayed on linear templates) cannot be correlated with promoter strength.

As several strong *E. coli* promoters are preceded by AT-rich sequences, we assumed that the AT-rich region in front of the *rrnB* P_1 promoter significantly contributes to its strength. Such a role of the upstream region was verified in the case of the *tyrT* promoter, where its removal resulted in a 10-fold drop in transcriptional activity [5]. The experiments described here demonstrate that, in the case of *rrnB* P_1, the situation is somewhat more complicated. Under optimal in vitro conditions, the removal of the AT-rich region leads to only a slight decrease of transcriptional activity if the -35 region remains intact. In contrast, if the polymerase/DNA ratio is lower, or the concentration of monovalent cations is higher in the reaction mixture, the presence or absence of the AT-rich region has a dramatic effect on transcription.

Although we performed only in vitro experiments, there are good reasons to believe that the conditions used mimic more closely those prevailing in the cell, where the salt concentration is around 0.15 M and the ratio of polymerase to DNA is around 1/2 (total mass). Thus it seems likely that, while under optimal in vitro conditions the contribution of the AT-rich region to promoter strength is only slight, its role is very important in vivo. This conclusion is in accordance with the observations of Gourse et al. (Nomura, M., personal communication), who reported that the removal of the AT-rich region in front of the P_1 promoter strongly reduces the in vivo expression of β-galactosidase if this gene is fused to the P_1 promoter.

References

1 Hawley, D.K. and McClure, W.R. (1983) Nucleic Acids Res. 11, 2237–2254

2 McClure, W.R. (1985) Annu. Rev. Biochem. 54, 171–204

3 Rossi, J.J., Soberon, X., Marumoto, Y., McMahon, J. and Itakura, K. (1983) Proc. Natl. Acad. Sci. USA 80, 3203–3207

4 Klein, R.D. and Wells, R.D. (1982) J. Biol. Chem. 257, 12954–12961

5 Lamond, A.I. and Travers, A.A. (1983) Nature 305, 248–250

6 Travers, A.A. (1984) Nucleic Acids Res. 12, 2605–2618

7 Boyer, H.W. and Roulland-Dussoix, D. (1969) J. Mol. Biol. 41, 459–472

8 Burgess, R.R. and Jendrisak, J.J. (1975) Biochemistry 14, 4634–4638

9 Murray, N.E., Bruce, S.A. and Murray, K. (1979) J. Mol. Biol. 132, 493–505

10 Joyce, C.M. and Grindley, N.D.F. (1983) Proc. Natl. Acad. Sci. USA 80, 1830–1834

11 Maniatis, T., Fritsch, E.F. and Sambrook, J. (1982) Molecular Cloning, Cold Spring Harbor Laboratories, NY

12 Boros, I., Kiss, A., Sain, B., Somlyai, G. and Venetianer, P. (1983) Gene 22, 191–201

13 Maxam, A. and Gilbert, W. (1977) Proc. Natl. Acad. Sci. USA 74, 560–564

14 Clewell, D.B. and Helinski, D.R. (1969) Proc. Natl. Acad. Sci. USA 62, 1159–1165

15 Ginsburg, D. and Steitz, J.A. (1975) J. Biol. Chem. 250, 5647–5654

16 Helling, R.B., Goodman, H.M. and Boyer, H.W. (1974) J. Virol. 14, 1235–1244

17 Maniatis, T., Jeffrey, A. and Van de Sande, H. (1975) Biochemistry 14, 3787–3794

18 Glaser, G. and Cashel, M. (1979) Cell 16, 111–121

19 Young, R.A. and Steitz, J.A. (1979) Cell 17, 225–234

20 Shen, W.F., Squires, C. and Squires, C.L. (1982) Nucleic Acids Res. 10, 3303–3313

21 De Boer, H.A., Gilbert, S.F. and Nomura, M. (1979) Cell 17, 201–209

22 Csordás-Tóth, É., Boros, I. and Venetianer, P. (1979) Nucleic Acids Res. 7, 2189–2197

23 Boros, I., Csordás-Tóth, É., Kiss, A., Kiss, I., Török, I., Udvardy, A., Udvardy, K. and Venetianer, P. (1983) Biochim. Biophys. Acta 739, 173–180

24 Kiss, I., Boros, I., Udvardy, A., Venetianer, P. and Delius, H. (1980) Biochim. Biophys. Acta 609, 435–447

25 Botchan, P. (1976) J. Mol. Biol. 105, 161–176

26 Wells, R.D., Goodman, T.C., Hillen, W., Horn, G.T., Klein, R.D., Larson, J.E., Müller, U.R., Neuendorf, S.K., Panayotatos, N. and Stirdivant, S.M. (1980) Prog. Nucleic Acid Res. Mol. Biol. 24, 167–267

27 Yang, H.-L., Heller, K., Gellert, M. and Zubay, G. (1979) Proc. Natl. Acad. Sci. USA 76, 3304–3308

28 Sümegi, J., Udvardy, A. and Venetianer, P. (1977) Mol. Gen. Genet. 151, 305–312

29 Kiss, I., Slaska, K., Sümegi, J., Udvardy, A. and Venetianer, P. (1978) Biochim. Biophys. Acta 518, 257–266

30 Küpper, H., Contreras, R., Landy, R. and Khorana, H.G. (1975) Proc. Natl. Acad. Sci. USA 72, 4754–4758

Biochimica et Biophysica Acta 866 (1986) 44–52
Elsevier

BBA 91554

Sequence-specific alkali-labile lesions in DNA caused by D-isoglucosamine

Satoshi Nanjou [a], Shoji Fujii [a], Jungi Morita [b], Kazumitsu Ueda [c] and Tohru Komano [c,*]

[a] *Laboratory of Biochemistry, Department of Agricultural Chemistry, Kyoto Prefectural University, Shimogamo, Kyoto 606,*
[b] *Laboratory of Food Chemistry, Department of Food Science, Doshisha Women's College of Liberal Arts, Kyoto 602, and*
[c] *Laboratory of Biochemistry, Department of Agricultural Chemistry, Kyoto University, Kyoto 606 (Japan)*

(Received August 12th, 1985)

Key words: DNA damage; D-Isoglucosamine; Cu^{2+}; Sequence specificity

The site-specific induction of DNA damage by 1-amino-1-deoxy-D-fructose (D-isoglucosamine) was investigated. When ^{32}P-end-labeled DNA restriction fragments of known sequence were reacted with D-isoglucosamine in the presence of Cu^{2+}, and the DNA products were analyzed on high-resolution denaturing polyacrylamide gels after treatment with aqueous piperidine (1 M) at 90°C for 30 min, the DNA strands were cleaved at pyrimidine residues at a statistically significant frequency, and 80.5% of the extensively damaged sites were induced at pyrimidine residues in dinucleotide sequences of pyrimidine-purine (5′ → 3′). These cleavages were scarcely observed without piperidine/heat treatment. The damaged DNA sites increased in proportion to the reaction time and concentration of D-isoglucosamine. Metal-chelating agents (EDTA, diethylenetriaminepentaacetic acid) and some oxygen radical scavengers inhibited the induction of alkali-labile lesions. These results indicate that some oxygen radicals are involved in the induction of alkali-labile lesions.

Introduction

We have investigated the interaction between aminosugars and nucleic acids, and have reported that aminosugars cleaved double-stranded replicative form I DNA (RFI DNA; supercoiled, covalently closed, circular duplex DNA) of bacteriophage ϕX174 more effectively than their corresponding hexose 6-phosphates because the reactivity of aminosugars with DNA was based on amino-reductone structures having higher reducibility [1,2]. Induction of DNA strand breakage by aminosugars was caused by oxygen radicals generated during the autoxidation of aminosugars [3]. It is well known that reducing sugars react nonenzymatically with amines to produce browning substances. Recently, it was reported that a similar reaction occurs between sugars and the amino groups of nucleic acids, and this reaction in organisms might contribute to biological aging [4]. A plausible theory of aging holds that a major source of this damage is oxygen radicals and lipid peroxidation [5]. Oxygen radicals may induce mutation [5] and cancer [6]. Thus, we are interested to determine whether aminocarbonyl reaction products interact with DNA. Aminosugars are distributed widely in organisms as metabolic intermediates, and as constituents of cell membrane and cartilage, but there is little information on the biological activity of aminosugars on genetic materials. Damage to nucleic acid such as DNA strand breakage leads to genetic lesions. Therefore, a study on the interaction between aminosugars

---

* To whom correspondence should be addressed.

Abbreviation: DETAPAC, diethylenetriaminepentaacetic acid.

0167-4781/86/$03.50 © 1986 Elsevier Science Publishers B.V. (Biomedical Division)

and nucleic acids may suggest something about DNA-damageable nonenzymatic browning in organisms as a cause of aging.

We have reported that 1-amino-1-deoxy-D-fructose (D-isoglucosamine), a typical amino-reductone and a model substance produced by an aminocarbonyl reaction through Amadori rearrangement, showed the highest DNA-breaking activity among the sugars so far tested [2,3]. This paper reports that D-isoglucosamine induced the site-specific damage in DNA and that the most extensively damaged site was at the pyrimidine residues in dinucleotide sequences of pyrimidine-purine (5′ → 3′).

Materials and Methods

Chemicals

D-Isoglucosamine hydrochloride was synthesized by the previously described procedure [7]. Diethylenetriaminepentaacetic acid (DETAPAC) was purchased from the Sigma Chemical Co. Other chemicals were obtained from Nakarai Chemicals, Ltd, and were used without further purification.

Enzymes

The restriction enzymes *Eco*RI, *Hae*III, *Tag*I and *Hin*fI, and T4 polynucleotide kinase and the Klenow fragment of DNA polymerase I of *Escherichia coli* were obtained from Takara Shuzo Co. Ltd. Calf intestine alkaline phosphatase was obtained from Boehringer Mannheim GmbH. [α-^{32}P]dCTP, [α-^{32}P]dATP and [γ-^{32}P]ATP (specific activity about 3000 Ci/mmol) were purchased from New England Nuclear, Du Pont, and Amersham International. Superoxide dismutase (EC 1.15.1.1; from bovine blood type I, 2750 units/mg protein) and catalase (EC 1.11.1.6; from bovine liver, 2250 units/mg) were purchased from the Sigma Chemical Co.

Preparation of DNA restriction fragments

Five DNA restriction fragments of defined sequence were prepared from replicative form DNAs of bacteriophages ϕX174 and R199/G4ori.

Bacteriophage ϕX174 RFI was prepared as previously described [8], and digested with *Hae*III. The 310, 234 and 194 basepair restriction fragments designated Z_5, Z_7 and Z_8, respectively, in the map reported by Sanger et al. [9] were purified by electrophoresis on a 4% polyacrylamide gel. Fragments Z_5 and Z_7 were digested with *Taq*I, and were labeled by extension of 3′ termini with Klenow polymerase in the presence of [α-^{32}P]dCTP. Fragment Z_8 was digested with *Hin*fI, and labeled at the 3′ termini with Klenow polymerase in the presence of [α-^{32}P]dCTP and unlabeled dATP. The resulting 3′-end-labeled 257, 178 and 141 basepair fragments (C_{723}–C_{979}, C_{492}–C_{669} and C_{980}–C_{1120}, respectively, in the map reported by Sanger et al. [9]), were purified by electrophoresis on a 6% polyacrylamide gel.

R199/G4ori phage, a chimera of phage R199 [10] with the 274 basepair *Alu*I fragment of G4 DNA containing the origin of complementary strand synthesis, was constructed by G.N. Godson of New York University Medical School, New York, R199/G4ori replicative DNA was digested with *Eco*RI [11]. The resulting DNA fragments were labeled by extension of the 3′ termini with Klenow polymerase in the presence of [α-^{32}P]dATP, and the 3′-end-labeled 144 basepair double-stranded DNA fragment (C_{5727}–C_{5868} in the map reported by Hill and Peterson [12]) was prepared by digestion with *Hae*III. The 274 basepair fragment obtained from R199/G4ori replicative form DNA by digestion with *Eco*RI was dephosphorylated by incubation with intestine alkaline phosphatase, and the 5′ termini were labeled with [γ-^{32}P]ATP and T4 polynucleotide kinase. The doubly end-labeled fragment was then digested with *Hae*III. The resulting singly 5′-end-labeled 98 basepair double-stranded DNA fragment (C_{3797}–G_{3894} in the map reported by Godson et al. [13]) was obtained. Both DNA fragments were purified by electrophoresis on a 6% polyacrylamide gel.

Fragmentation of DNA by D-isoglucosamine

The standard reaction mixture (100 μl) contained a 3′- or 5′-end-^{32}P-labeled DNA fragment (approx. 50 ng; spec. act. $2 \cdot 10^3$ cpm/ng), 1 mM D-isoglucosamine and 10 μM $CuCl_2$ in 10 mM Tris-HCl buffer (pH 7.1), unless otherwise noted. The reaction was carried out for 3 h at 37°C, and stopped by the addition of 150 μl of a mixture that contained 500 mM sodium acetate, 3.3 mM EDTA and 16.5 μg/ml tRNA. The DNA products were first precipitated with ethanol. The pellet was resuspended in 0.3 M sodium acetate and precipitated with ethanol, rinsed in cold ethanol, and dried. The D-isoglucosamine-reacted DNA was treated with 1 M piperidine at 90°C for 30 min. The piperidine/heat-treated DNA was dissolved in 4 μl of loading buffer containing 10 mM NaOH, 1 mM EDTA, 80% (v/v) deionized formamide, and 0.1% (w/v) bromophenol blue/xylene cyanol. The solution was heated for 1 min at 90°C, and was transferred to 6 or 8% polyacrylamide gels for sequence analysis.

Sequence analysis

Autoradiography was carried out by exposing Fuji RX film to the dried polyacrylamide gels for about 3 days. The nucleotide sequence of restriction fragments and the sequence of the oligonucleotides produced by D-isoglucosamine were identified by comparison with the chemically degraded restriction fragments by the method of Maxam and Gilbert [14,15]. The autoradiographs were scanned with a microdensitometer (Joyce Loebl and Co. Ltd. MK II CS double-beam recording microdensitometer), and the relative positions and amounts of the oligonucleotides produced were determined.

To compare the relative extent of cleavage, the following method for normalization was used [16]. The relative peak heights on densitometric scans were measured and normalized relative to the average height of the peaks of products of the deoxyguanylate specific reaction. The normalized relative peak heights, a measure of the relative extent of cleavage at each specific site, were then divided into 10 rankings on a numerical scale. The peak height of the site with the greatest degree of cleavage was taken as 10 and the peak height of the site with the lowest degree of cleavage was taken as 1. On this basis, the sites with rankings from 10 to 8 were regarded as extensively cleaved, from 7 to 4 as moderately cleaved, and from 3 to 1 as weakly cleaved.

Results

Induction of alkali-labile lesions in DNA

Sites and properties of the DNA damage induced by D-isoglucosamine were investigated using a sequencing technique (Fig. 1). When the 178 basepair 3′-end-labeled ϕX174 Z_7-*Taq*I long fragment was reacted with 1 mM D-isoglucosamine in the presence of 10 μM $CuCl_2$, and the DNA product was heat-treated in aqueous piperidine, strong oligonucleotide bands were observed at specific sites (lane 3). No strong site-specific bands but faint random bands were observed without piperidine/heat treatment (lane 8). No oligonucleotides were produced by $CuCl_2$ (lane 4) or D-isoglucosamine (lane 6) alone, but faint bands of oligonucleotides were observed (lanes 5 and 7). When the DNA bands appearing after treatment with D-isoglucosamine (lane 3) were compared with those resulting from the standard chemical procedure (lanes 1 and 2), alkali-labile lesions were seen to be induced at pyrimidine residues. The band position on the gel shows the site of alkali-labile lesions, and the band intensity shows the relative frequency of cleavage at each specific site.

The band intensity of oligonucleotides increased in proportion to the reaction time and concentration of D-isoglucosamine (data not shown). Slight amounts of sequence-specific alkali-labile lesions were produced by reaction with 1 mM D-isoglucosamine for 30 min and subsequent piperidine/heat treatment. However, when the reaction was continued for 3 h, small amounts of sequence-specific alkali-labile lesions were observed even with 100 μM D-isoglucosamine. These results indicate that D-isoglucosamine in the presence of Cu^{2+} induces alkali-labile lesions at specific sites in DNA.

Effects of oxygen radical scavengers and metal chelating agents

Oxygen radicals and metal ions affected the induction of DNA strand scission by aminosugars [3]. We examined the involvement of oxygen radicals and metal ions in the induction of alkali-labile lesions by D-isoglucosamine, and the results are shown in Fig. 2. Metal-chelating agents, EDTA (lane 3) and DETAPAC (lane 4), inhibited the induction of alkali-labile lesions almost completely. Induction of alkali-labile lesions was also inhibited by a singlet oxygen scavenger, 1,4-diazabicyclo[2.2.2]octane (DABCO) (lane 4) and weakly by a superoxide anion scavenger, 1,2-dihydroxybenzene-3,5-disulfonic acid (tiron) (lane 9).

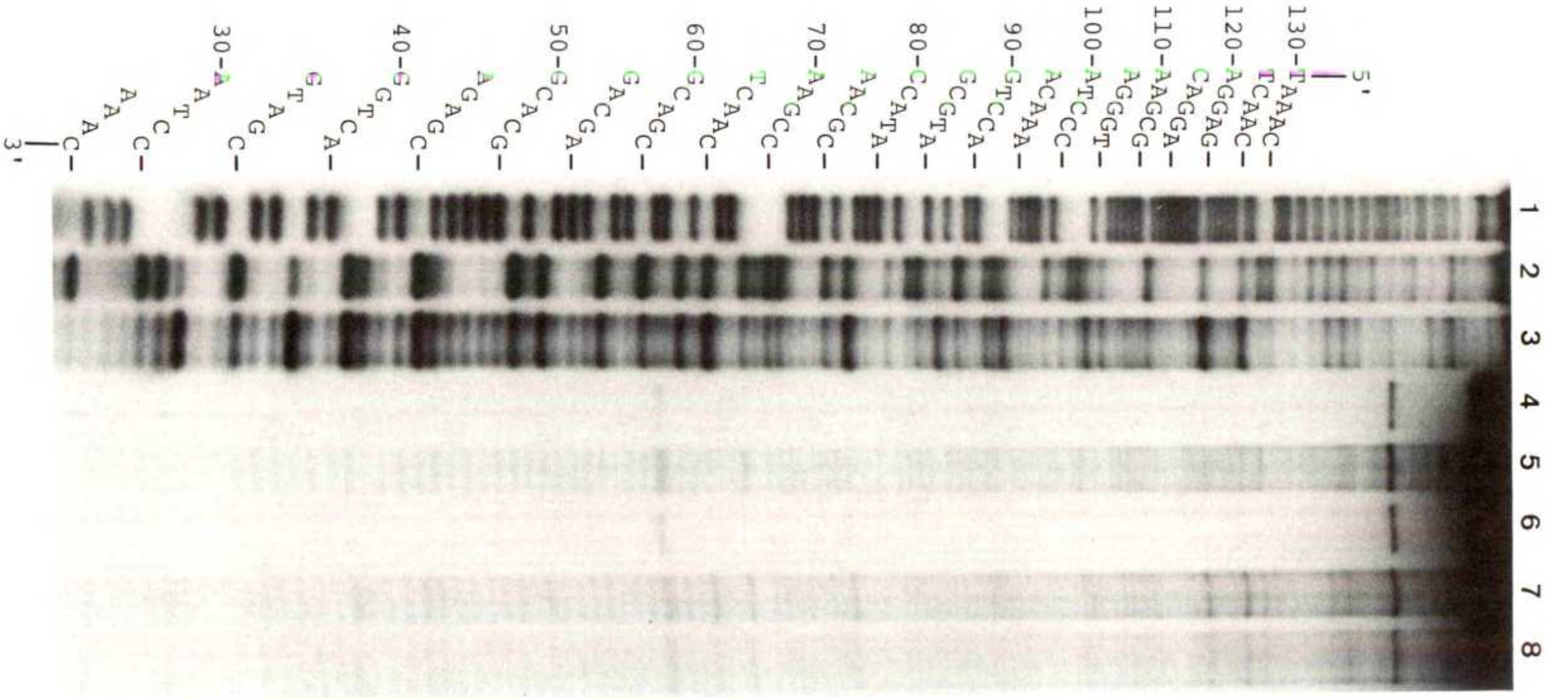

Fig. 1. Site-specific induction of alkali-labile damage by D-isoglucosamine and Cu^{2+}. The 178 basepair 3′-end-^{32}P-labeled Z_7-*Taq*I long fragment of double-stranded φX174 replicative form DNA (C_{492}–C_{669} in the map reported by Sanger et al. [9]) was reacted with D-isoglucosamine (1 mM) in the presence of $CuCl_2$ (10 μM) at 37°C for 3 h. After the reaction and subsequent ethanol precipitation, the D-isoglucosamine-modified DNA was treated with aqueous piperidine (1 M) at 90°C for 30 min. The piperidine/heat-treated DNA was dissolved in 4 μl of loading buffer, and transferred to 6% polyacrylamide gels for sequence analysis. Lane 1, limited DNA cleavage at guanines and adenines by the chemical reaction of the Maxam and Gilbert procedure [14]; lane 2, limited DNA cleavage at thymines and cytosines by the chemical reaction of the Maxam and Gilbert procedure; lane 3, D-isoglucosamine + $CuCl_2$; lanes 4 and 5, $CuCl_2$ control; lanes 6 and 7, D-isoglucosamine control; lane 8, D-isoglucosamine + $CuCl_2$; lanes 4, 6 and 8, the piperidine/heat treatment was omitted. The sequence is indicated on the left of the figure.

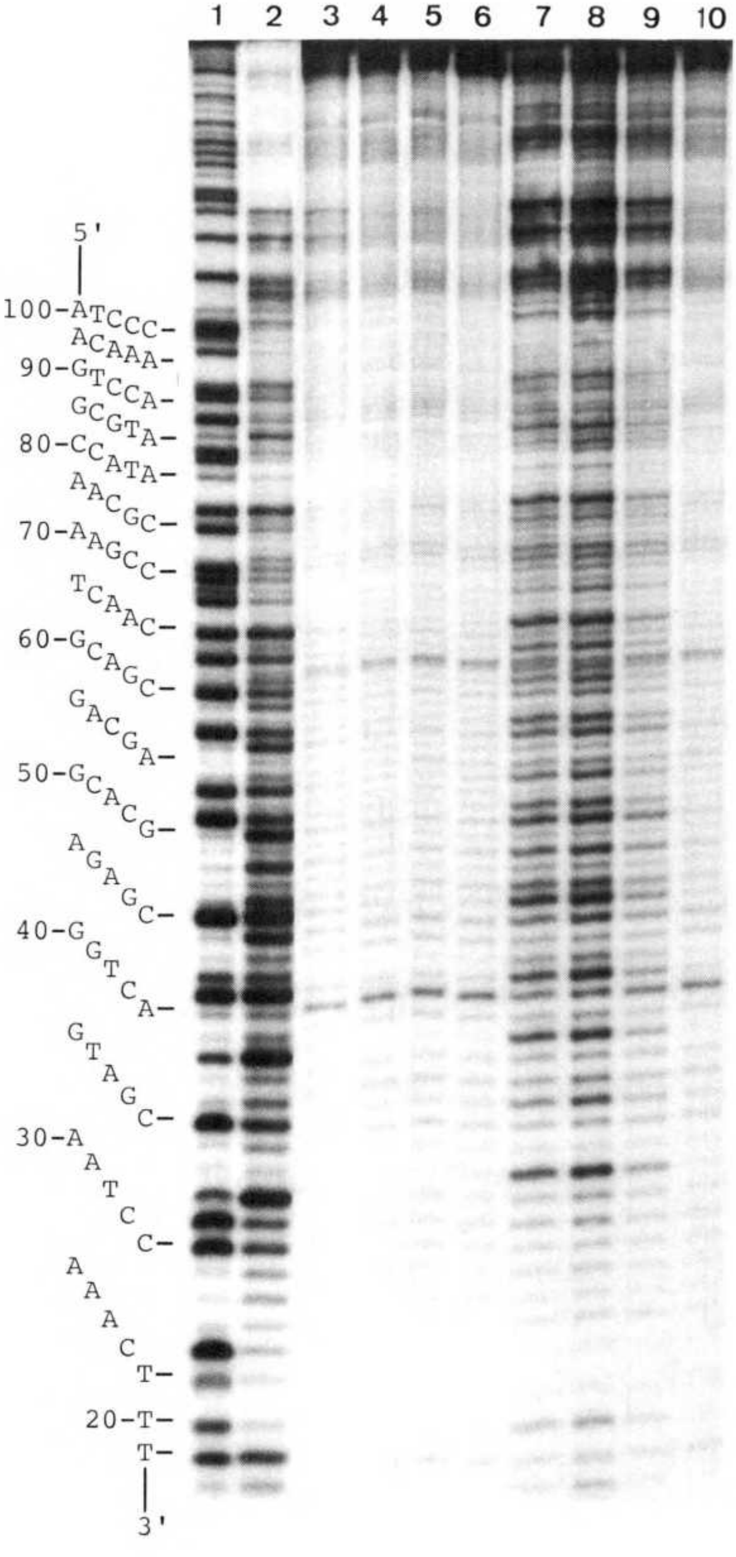

Fig. 2. Effects of metal-chelating agents **and** oxygen radical scavengers on induction of alkali-labile lesions produced by D-isoglucosamine. The 178 basepair 3'-end-^{32}P-labeled Z_7-*Taq*I long fragment of double-stranded φX174 replicative form DNA was reacted with D-isoglucosamine (1 mM) in the presence of $CuCl_2$ (10 μM) with metal-chelating agents or some oxygen radical scavengers at 37°C for 3 h. After the reaction, the DNA products were treated by the procedure described in Materials and Methods. Lane 1, limited DNA cleavage at thymines and cytosines by the chemical reaction of the Maxam and Gilbert procedure [14]; lane 2, D-isoglucosamine + $CuCl_2$; lane 3, 2 + EDTA (50 μM); lane 4, 2 + DETAPAC (50 μM); lane 5, 2 + potassium iodide (50 mM); lane 6, 2 + 1,4-diazabicyclo[2.2.2]octane (50 mM); lane 7, 2 + sodium benzoate (50 mM); lane 8, 2 + 2-aminoethylisothiouroniumbromide-HBr (10 mM); lane 9, 2 + 1,2-dihydroxybenzene-3,5-disulfonic acid (1 mM); lane 10, 2 + 2-mercaptoethylamine (50 mM).

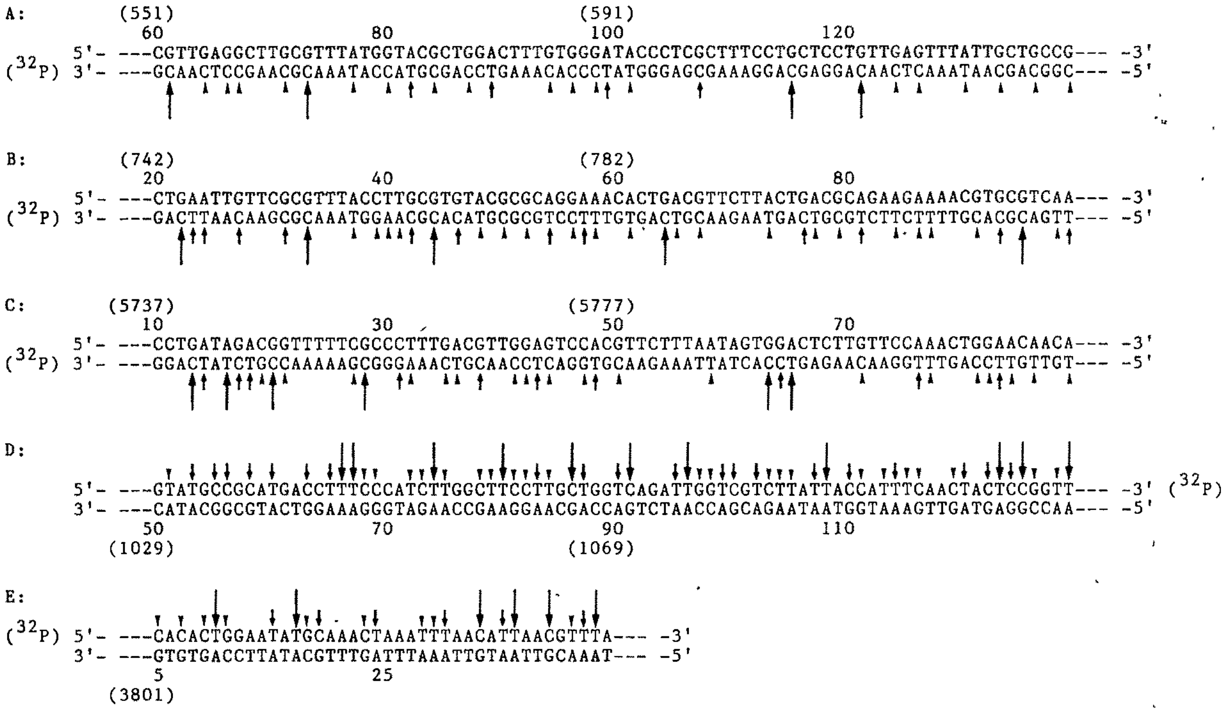
A:
(551)
(591)
60
80
100
120
5'- ---CGTTGAGGCTTGCGTTTATGGTACGCTGGACTTTGTGGGATACCCTCGCTTTCCTGCTCCTGTTGAGTTTATTGCTGCCG--- -3'
(^{32}P) 3'- ---GCAACTCCGAACGCAAATACCATGCGACCTGAAACACCCTATGGGAGCGAAAGGACGAGGACAACTCAAATAACGACGGC--- -5'
B:
(742)
(782)
20
40
60
80
5'- ---CTGAATTGTTCGCGTTTACCTTGCGTGTACGCGCAGGAAACACTGACGTTCTTACTGACGCAGAAGAAAACGTGCGTCAA--- -3'
(^{32}P) 3'- ---GACTTAACAAGCGCAAATGGAACGCACATGCGCGTCCTTTGTGACTGCAAGAATGACTGCGTCTTCTTTTGCACGCAGTT--- -5'
C:
(5737)
(5777)
10
30
50
70
5'- ---CCTGATAGACGGTTTTTCGCCCTTTGACGTTGGAGTCCACGTTCTTTAATAGTGGACTCTTGTTCCAAACTGGAACAACA--- -3'
(^{32}P) 3'- ---GGACTATCTGCCAAAAAGCGGGAAACTGCAACCTCAGGTGCAAGAAATTATCACCTGAGAACAAGGTTTGACCTTGTTGT--- -5'
D:
5'- ---GTATGCCGCATGACCTTTCCCATCTTGGCTTCCTTGCTGGTCAGATTGGTCGTCTTATTACCATTTCAACTACTCCGGTT--- -3' (^{32}P)
3'- ---CATACGGCGTACTGGAAAGGGTAGAACCGAAGGAACGACCAGTCTAACCAGCAGAATAATGGTAAAGTTGATGAGGCCAA--- -5'
50
70
90
110
(1029)
(1069)
E:
(^{32}P) 5'- ---CACACTGGAATATGCAAACTAAATTTAACATTAACGTTTA--- -3'
3'- ---GTGTGACCTTATACGTTTGATTTAAATTGTAATTGCAAAT--- -5'
5
25
(3801)

Fig. 3. Specific sites of alkali-labile lesions. Arrows locate sites determined from sequencing analysis according to the procedure described in Materials and Methods The length of the arrows indicates the relative extents of cleavage (extensive, moderate or weak) at a particular site as measured from densitometric scans of the autoradiographs A, 178 basepair 3′-end-labeled ϕX174 Z_7-*Taq*I long fragment; B, 257 basepair 3′-end-labeled ϕX174 Z_5-*Taq*I long fragment, C, 144 basepair 3′-end-labeled R199/G4ori fragment, D, 141 basepair 3′-end-labeled ϕX174 Z_8-*Hin*fI long fragment; E, 98 basepair 5′-end-labeled G4 Z_{7b}-*Alu*I short fragment.

Some hydroxyl radical scavengers, potassium iodide (lane 5) and 2-mercaptoethylamine-HCl (cysteamine) (lane 10), inhibited the induction of alkali-labile lesions, but other hydroxyl radical scavengers, such as sodium benzoate (lane 7) and 2-aminoethylisothiouroniumbromide-HBr (AET) (lane 8), did not. Catalase, which removes hydrogen peroxide, inhibited the induction of alkali-labile lesions almost completely, but superoxide dismutase, which removes superoxide anion, did not (data not shown). The inhibitory effects of salts seemed negligible when the inhibitors were used below 50 mM, because 50 mM sodium chloride did not inhibit the production of oligonucleotides [17].

The above results suggest that metal ions and oxygen radicals participate in the induction of alkali-labile lesions in DNA modified by reaction with D-isoglucosamine.

Sequence-specificity of damaged sites

To determine the sequence specificity of damaged sites in DNA, we used three more end-labeled DNA restriction fragments of defined sequences as substrates. The sites of alkali-labile DNA damage induced by the reaction with D-isoglucosamine are summarized in Fig. 3. 100% of the extensive degree of damage was induced at pyrimidine residues, and 98.3% of the moderate and 86.4% of the weak degree of damage were also induced at pyrimidine nucleotides in DNA fragments, as shown in Fig. 3 and Table I. Among pyrimidine residues, no distinction is made between thymine and cytosine. Purine residues are rather resistant to damage by D-isoglucosamine and Cu^{2+}.

Table II shows the analysis of the neighboring nucleotides of extensively damaged sites. The analysis demonstrates that purine nucleotides exist at

TABLE I

DAMAGE PATTERNS PRODUCED BY D-ISOGLUCOSAMINE

Nucleotides analyzed in each restriction fragments were taken from Fig. 3 The relative probability of damaged nucleotides is presented in parentheses.

Base	Number in fragments	Number of damaged nucleotides		
		extensive	moderate	weak
A	131	0 (0)	0 (0)	4 (3.9)
G	96	0 (0)	1 (1.7)	10 (9.7)
C	108	23 (56.1)	23 (39.0)	53 (51 5)
T	105	18 (43.9)	35 (59.3)	36 (34 9)
Pur	227	0 (0)	1 (1.7)	14 (13 6)
Pyr	213	41 (100)	58 (98.3)	89 (86.4)
Total	440	41 (100)	59 (100)	103 (100)

TABLE II

ANALYSIS OF NUCLEOTIDES NEIGHBORING EXTENSIVELY DAMAGED SITES

41 damaged sites taken from Fig. 3 were analyzed.

Damaged site ↓ 5′→3′	Frequency	Relative probability (%)
Pyr—Pyr—Pur	17	41.5
Pur—Pyr—Pur	16	39.0
Pyr—Pyr—Pyr	5	12.2
Pur—Pyr—Pyr	3	7.3
Pyr—Pur—Pur	0	0
Pur—Pur—Pur	0	0
Pyr—Pur—Pyr	0	0
Pur—Pur—Pyr	0	0
Total	41	100

the 3′ site of 80.5% (33 out of 41) extensively damaged sites. The nucleotide at the 5′ side of the damaged site did not affect the probability. We could not find a preferred sequence surrounding the extensively damaged sites other than the presence of purine nucleotides at their 3′ sites (data not shown).

Discussion

Damage to nucleic acid such as DNA strand scission introduces genetic lesions. Reducing sugars react nonenzymatically with amines to produce browning substances [18]. This nonenzymatic browning in organisms would contribute to biological aging [19]. A similar reaction occurs between sugars and the amino groups of nucleic acids, and this reaction might be a cause of aging [4]. A plausible theory of aging holds that a major source of this damage is oxygen radicals and lipid peroxides [5]. Thus, we are interested in whether aminosugars interact with DNA to produce genetic lesions in vivo. Actually, various kinds of bacteriophage are inactivated effectively by DNA strand scission [20]. Our results show that D-isoglucosamine specifically produces alkali-labile lesions in the presence of $CuCl_2$, and 80.5% of the extensive degree of damage is induced at pyrimidine residues in the dinucleotide sequence pyrimidine-purine (5′ → 3′). No site-specific extensive bands were observed on autoradiographs without piperidine-heat treatment. D-Isoglucosamine directly breaks RFI DNA in the presence of Cu^{2+} [2,3]. There may be two classes of DNA damage, one being damage to DNA bases which can be cleaved by the piperidine/heat treatment and the other to the DNA backbone, which may correspond to direct breakage.

Induction of alkali-labile lesions by D-isoglucosamine was inhibited by addition of some oxygen radical scavengers or metal-chelating agents. In the absence of $CuCl_2$, alkali-labile lesions were not induced. The active radical species involved in the extent mechanism of the DNA-lesion activity are still unknown. However, structurally diverse antibiotics such as mytomycin C [21] and bleomycin [22], following reduction and reoxidation in vivo, give rise to reactive oxygen radicals including HO_2 (or O_2) and OH [23], and O_2 and H_2O_2 can interact with DNA to produce the reactive radical species, the hydroxyl radical ($OH^{\cdot}$) via the Haber-Weiss reaction [24]. It has been reported [17] that pyrimidine-purine (5′ → 3′) sequences are highly sensitive to oxidative damage [17]. These results and evidence indicate that DNA modification by D-isoglucosamine seems to be concerned with oxygen radicals generated during autoxidation of D-isoglucosamine by the catalysis of Cu^{2+}.

Thornalley et al. [25] reported that simple monosaccharides are autoxidized under physiological conditions, generating 1-hydroxyalkyl free radicals and reduced forms of oxygen: superoxide, hydrogen peroxide and hydroxyl radicals. Reaction of hydrogen peroxide with DNA is known to induce destruction of bases to break the DNA strand [26], and DNA strand scission occurs with enzymically generated oxygen radicals [27]. However, it is not certain whether induction of alkali-labile lesions by D-isoglucosamine is caused indirectly only by oxygen radicals, and we cannot specify the main radical species responsible for the DNA breakage. If the D-isoglucosamine-copper complex binds to DNA directly to form a DNA-D-isoglucosamine-copper complex, where oxygen radicals are generated, this would cause DNA lesions.

We infer that not only does Cu^{2+} act on D-isoglucosamine as a catalyst of autoxydation, but it is also active on DNA, because Cu^{2+} induces alkali-labile lesions by itself at high concentrations (more than 100 μM) (data not shown). Cu^{2+} has also been reported to induce sensitization to the biological damage due to superoxide radicals. The presence of Cu^{2+} and hydrogen peroxide and the binding of the metal ion to the target biomolecules are required for the manifestation of the deleterious role of the superoxide radical [28]. Lesko et al. [29] reported that DNA strand scission by superoxide was catalyzed by adventitious metal ions. Thus, one of the causes of the induction of alkali-labile lesions in the presence of Cu^{2+} seems to result from the attack of reducing radical species on Cu^{2+} bound to DNA.

Acknowledgement

The authors wish to thank Dr. Kunisuke Tanaka for his interest and encouragement.

References

1 Morita, J. and Komano, T. (1983) Agric. Biol. Chem. 47, 11–18

2 Nanjou, S., Fujii, S , Tanaka, K., Ueda, K. and Komano, T (1984) Agric. Biol Chem. 48, 2865–2867

3 Nanjou, S., Fujii, S., Tanaka, K., Ueda, K. and Komano, T. (1985) Agric. Biol. Chem 49, 459–466

4 Bucala, R , Model, P. and Cerami, A. (1984) Proc. Natl Acad. Sci. USA 81, 105–109

5 Levin, D.E., Hollstein, M., Christman, M.F., Schwiers, E.A. and Ames, B.N (1982) Proc. Natl Acad. Sci. USA 79, 7444–7449

6 Ames, B.N. (1983) Science 221, 1256–1264

7 Kuhn, R. and Hass, H.J (1956) Justus Liebigs Ann. Chem. 600, 148–155

8 Ueda, K , Morita, J. and Komano, T. (1981) J. Antibiot. 34, 317–322

9 Sanger, F., Coulson, A.R., Friedmann, T., Air, G.M., Barrell, B.G , Brown, N.L., Friddes, J C., Hutchison, C.A , III, Slocombe, P.M. and Smith, M. (1973) J. Mol. Biol. 125, 225–246

10 Boeke, J D., Vovis, G.F. and Zinder, N.D. (1979) Proc Natl. Acad. Sci USA 76, 2699–2702

11 Ueda, K., Kobayashi, S., Sakai, H. and Komano, T. (1985) J. Biol. Chem., in the press

12 Hill, D.F. and Peterson, G.B (1982) J. Virol. 44, 32–46

13 Godson, G.N., Barrell, B G., Staden, R. and Fiddes, J.C. (1978) Nature 276, 236–247

14 Maxam, A.M. and Gilbert, W. (1977) Proc. Natl. Acad Sci USA 74, 560–564

15 Maxam, A.M. and Gilbert, W. (1980) Methods Enzymol. 65, 499–560

16 Ueda, K., Morita, J. and Komano, T. (1984) Biochemistry 23, 1634–1640

17 Morita, J., Ueda, K., Nanjou, S. and Komano, T. (1985) Nucleic Acids Res. 13, 449–458

18 Maillard, L C. (1912) C.R. Soc. Biol. 72, 599–601

19 Mommier, Y.M. and Cerami, A. (1983) ACS Symposium Series, Am. Chem. Soc., Washington, DC 215, 431–449

20 Morita, J., Kashimura, N. and Komano, T. (1980) Agric. Biol. Chem. 44, 883–890

21 Lown, J W., Begieiter, A , Johnson, D. and Morgan, A R (1976) Can. J. Biochem. 54, 110–119

22 Lown, J.W. and Sim, S. (1950) Biochem. Biophys. Res. Commun. 77, 1150–1157

23 Lown, J.W. (1982) Acc. Chem. Res 15, 381–387

24 Beauchamp, C. and Fridovich, I. (1970) J. Biol Chem. 245, 4641–4646

25 Thornalley, P., Wolff, S., Crabbe, J and Stern, A. (1984) Biochim Biophys. Acta 797, 276–287

26 Rhaese, H., Freese, E. and Meizer, M.S. (1968) Biochim Biophys. Acta 155, 491–504

27 Brawn, K. and Fridovich, I (1981) Arch. Biochem. Biophys. 206, 414–419

28 Samuni, A., Chevion, M. and Czapski, G (1981) J. Biol. Chem. 256, 12632–12635

29 Lesko, S.A., Lorentzen, R.J. and Ts'o P O.P. (1980) Biochemistry 19, 3023–3028

Biochimica et Biophysica Acta 866 (1986) 53–60
Elsevier

BBA 91556

The competitive miscoding of O^6-methylguanine and O^6-ethylguanine and the possible importance of cellular deoxynucleoside 5′-triphosphate pool sizes in mutagenesis and carcinogenesis

Roy Saffhill

Paterson Laboratories, Christie Hospital and Holt Radium Institute, Manchester M20 9BX (U.K.)

(Received July 29th, 1985)

Key words: Transcription; Miscoding; DNA methylation; DNA polymerase

Using initiated poly(dG,O^6-RdG) and poly(dA,O^6-RdG) polynucleotides as templates for DNA polymerase I in vitro the promutagenic potential of O^6-MeG and O^6-EtG has been confirmed, together with the possibility of minor miscoding pathways for O^6-RG. These lead to the incorporation of dAMP and dGMP, which could give rise to some of the limited number of transversions that have been observed arising from the action of alkylating agents. The results are compatible with the current knowledge of oncogenes, explaining the changes in base sequence that have been observed. The competition for the miscoding of O^6-RG which leads to the incorporation of dCMP in addition to the expected dTMP is also shown. The relative amounts of these two nucleotides incorporated depend upon the concentrations of the dCTP and dTTP in the assay. The mutagenic efficiency of O^6-MeG is constant at approx. 0.4 over a wide range of dTTP and dCTP concentrations and only increases when the dCTP in the assay ceases to saturate the polymerizing enzyme, indicating that the DNA polymerase I plays a role in determining the mutagenic efficiency of a modified base. Although the mutagenic efficiency of both O^6-MeG and O^6-EtG depends upon the relative concentrations of dTTP and dCTP in the assay, a reduction in the concentration of dCTP can be more effective at increasing the mutagenic efficiency than a corresponding increase in the concentration of dTTP. These results indicate the importance of cellular dNTP pools in determining the cellular response to agents.

Introduction

Previously we have investigated [1] the modification of the DNA-like alternating co-polymer poly(dC-dG) by the methylating agents *N*-nitroso-*N*-methylurea and dimethyl sulphate, together with the effect of such reactions on the properties of the polynucleotides as templates for *Escherichia coli* DNA polymerase I. The nitrosomethylurea-methylated template led to significant errors (i.e. the incorporation of dTMP) which were attributed to the formation of the promutagenic [2] base O^6-methylguanine (O^6-MeG) in the polynucleotides. Similar observations have been made following modification of the polynucleotide with ethylating, propylating and butylating agents (Hall, J.A. (1981) Ph.D. Thesis, University of Manchester). However, the level of errors produced with the DNA polymerase I was always less than the O^6-MeG content of the polynucleotide used as template, in contrast to O^4-methylthymine (O^4-MeT),

---

Abbreviations: dNMP, deoxynucleoside 5′-monophosphate; dNTP, deoxynucleoside 5′-triphosphate, oligo$(dN)_{12-18}$, oligomer of dNMP 12–18 bases long, O^6-RG, O^6-alkylguanine, O^6-RdG, O^6-alkyldeoxyguanine; O^4-rT, O^4-alkylthymine; poly(dG,O^6-MeRG), polydeoxyguanylic acid containing O^6-Methylguanylic acid residues randomly distributed; R, alkyl group, Me = methyl, Et = ethyl.

0167-4781/86/$03.50 © 1986 Elsevier Science Publishers B.V. (Biomedical Division)

where the error level corresponded to the modified base content [3,4]. For O^6-MeG the error level could be changed by modifying the relative concentrations of dTTP and dCTP in the assay [1]. It was concluded that this arose from a competitive miscoding by O^6-MeG during polynucleotide synthesis leading to the incorporation of both dTMP and dCMP into newly synthesized DNA. These results lead to the proposal that modification of cellular dNTP pools could modulate the mutagenic, and possibly the carcinogenic, effects of alkylating agents and explain [5,6] the synergistic effect of deoxythymidine and deoxycytidine on alkylating agent-induced mutagenesis.

In view of the promutagenic [2] nature of O^6-MeG and its likely importance in the initiation, and probably also in the later stages, of the carcinogenic process induced by alkylating agents [7], together with the role of cellular dNTPs in determining the mutagenic and toxic response of a cell to external agents [7,8], we have further investigated the coding properties of O^6-MeG and O^6-EtG during in vitro DNA synthesis. Polynucleotides containing O^6-MeG and O^6-EtG as the only modified base present have been synthesized and used as templates for DNA polymerase I, in measuring the incorporation of complementary and non-complementary nucleotides into newly synthesized DNA-like material.

Materials and Methods

Materials

Unmodified nucleosides and nucleotides were obtained from the Sigma Chemical Co. Ltd. or the Boehringer Corporation Ltd. Terminal deoxynucleotidyltransferase, oligo(dC)$_{12-18}$ and oligo(dT)$_{12-18}$ were from PL Biochemicals Inc. DNAase I, snake venom phosphodiesterase and *E. coli* alkaline phosphatase were from the Sigma Chemical Co. Ltd. DNA polymerase I was from the Boehringer Corporation Ltd. or the generous gift of dr. L.A. Loeb (Seattle). All radioactive compounds were from Amersham International Ltd. *O*^{6}-Alkyldeoxyguanosine 5′-triphosphates (O^6-RdGTPs) were synthesized from their monophosphates [9] via their phosphoimidazolides as previously described [10]. High-performance liquid chromatography (HPLC) of the products on Partisil-10 SAX showed their purity to be above 97%, contaminants being the corresponding di- and monophosphates.

Synthesis of polynucleotides

Modified polynucleotides containing O^6-RG (R = Me or Et) were synthesized from the appropriate mixture of modified and unmodified dNTPs using terminal deoxynucleotidyltransferase as previously described [4,11] for similar polynucleotides. The O^6-RdG content of the polymers was determined following enzymic hydrolysis using radioimmunoassays [12] specific for O^6-RdG. Poly(dG,O^6-MedG) containing 0.91% and 1.38% O^6-MedG, poly(dG,O^6-EtdG) containing 0.75% O^6-EtdG, poly(dA,O^6-MedG) containing 0.88% O^6-MedG and poly(dA,O^6-EtdG) containing 0.59% O^6-EtdG were synthesized. Poly(dG,dA) containing 1.88% dA and poly(dA,dG) containing 2.01% dG were also synthesized.

DNA polymerase assays

Initiated templates for DNA polymerase I were formed by annealing the polynucleotide with oligo(dC)$_{12-18}$ (for poly(dG,O^6-RdG) templates) or oligo(dT)$_{12-18}$ (for poly(dA,O^6-RdG) templates). The polynucleotide and oligomer were mixed to give a base ratio of 10:1 and heated to 70°C for 5 min and then allowed to cool slowly to 4°C over a period of 1–2 h. The basic DNA polymerase assay (250 μl) contained the appropriate dNTPs at concentrations stated, 2 nmol nucleotide as poly(dN,O^6-RdG):oligo(dN′)$_{12-18}$, 0.3 units DNA polymerase I and was 70 mM in Tris-HCl (pH 7.4) and 3 mM in MgCl$_2$. Complementary nucleotide (dCMP or dTMP with poly(dG,O^6-RdG) or poly(dA,O^6-RdG), respectively) incorporation was determined using [^{3}H]dCTP or [^{3}H]dTTP (0.025 and 0.1 Ci/mmol, depending on the concentration used in the assay) and non-complementary nucleotide (dTMP and dAMP with poly(dG,O^6-RdG) or dCMP and dGMP with poly(dA,O^6-RdG), respectively) incorporation was determined in concurrent assays using the [^{3}H]dNTP (10 or 2 Ci/mmol, depending on the concentration used in the assay). After incubating at 37°C for 30 min the assays were plunged into ice, carrier DNA (100 μg) was added and precipitated by the addition of 5 ml 5% trichloroacetic acid containing 1% $Na_4P_2O_7 \cdot 10H_2O$. The product was collected on glass-fibre GF/C filters, washed with trichloroacetic acid, methylated spirit and dried at 80°C. Radioactivity incorporated into DNA-like material was determined by scintillation counting.

Mutagenic efficiency

Mutagenic efficiency is defined as the number of non-complementary errors produced per modification (i.e. O^6-RG in these studies) present in the template and it is calculated using the formula:

$$\text{Mutagenic efficiency} = \frac{E_n - E_0}{M}$$

where E_n is the error rate for incorporation of nucleotide n with template containing modified base, E_0 is the error rate for template without modified bases and M is the fraction of bases in the template that are modified.

Results

The results obtained with the poly(dG,O^6-RdG) templates are shown in Table I. These templates produced a large incorporation of dTMP and when the ratio of dCTP/dTTP in the assay was reduced the dTMP incorporated increased, confirming the promutagenic nature of O^6-MeG and O^6-EtG along with the earlier indication of a competition between the incorporation of dTMP and dCMP. Since we cannot directly measure the incorporation of dCMP arising from the presence of O^6-RG using these templates we have synthesized the poly(dA,O^6-MedG) polynucleotides for use as templates (see Table II). It can be clearly seen that the presence of both O^6-MeG or O^6-EtG leads to the incorporation of a large amount of dCMP which increases as the ratio of dCTP/dTTP in the assay increases. The results also show that the presence of O^6-MeG and O^6-EtG in the templates can lead to some incorporation of dAMP and dGMP at levels very much less than for the incorporation of dTMP and dCMP. The mutagenic efficiencies that may be calculated from Tables I and II are summarized in Table III. That for the incorporation of dTMP varies from 0.37 to 0.87, whilst that for the incorporation of dCMP varies from 0.5 to 0.07 as the ratio of dTTP/dCTP in the assay increases.

The way that the mutagenic efficiency of O^6-MeG changes with a varying dCTP/dTTP ratio but fixed dTTP or dCTP concentrations is shown in Figs. 1 and 2. If the dTTP concentration in the assay is fixed at 8 or 40 μM the mutagenic efficiency of O^6-MeG does not change significantly from a value of approx. 0.4 over a wide range of dCTP concentrations (approx. 20–80 μM). At dCTP concentrations below approx. 20 μM the mutagenic efficiency increases, particularly with the dTTP concentration fixed at the higher value

TABLE I

WRONG NUCLEOTIDE INCORPORATION WITH POLY(dG,O^6-RdG) TEMPLATES

	O^6-RdG	Errors (dNMP/dCMP) (×10^5)				
	dG (%)	dAMP		dTMP		
		(20/2) [a]	(2/20) [a]	(20/2) [b]	(10/10) [b]	(2/20) [b]
Poly(dG)		12±1.7 [c]	29±3.2 [c]	10±1.3 [c]	17±2.3 [c]	27±2.1 [c]
Poly(dG,O^6-RdG)						
I R = Me	0.91	30	56	348	407	764
II R = Me	1.38	33	83	468	501	1087
III R = Et	0.75	20	52	334		679
Poly(dG,dA)	1.88 [d]	15	30	1767		1853

[a] Ratio (nmol dCTP)/(nmol dATP) in the assay 20 and 2 nmol per assay correspond to 80 and 8 μM, respectively.

[b] Ratio (nmol dCTP)/(nmol dTTP) in the assay.

[c] Averaged over at least three determinations.

[d] dA/dG.

TABLE II

WRONG NUCLEOTIDE INCORPORATION WITH POLY(dA,O^6-RdG) TEMPLATES

	O^6-RdG	Errors (dNMP/dCMP) ($\times 10^5$)			
	dA (%)	dGMP		dCMP	
		(20/2) [a]	(2/20) [a]	(20/2) [b]	(2/20) [b]
Poly(dA)		9 ± 2.7 [c]	19 ± 2.2 [c]	8 ± 2.0 [c]	21 ± 3.9 [c]
Poly(dA,O^6-RdG)					
I R = Me	0.88	61	91	114	461
II R = Et	0.59	39	73	49	287
Poly(dA,dG)	2.01 [d]	13		2038	

[a] Ratio (nmol dTTP)/(nmol dgTP) in the assay. 20 and 2 nmol per assay correspond to 80 and 8 μM, respectively

[b] Ratio (nmol dTTP)/(nmol dCTP) in the assay

[c] Averaged over at least three determinations

[d] dG/dA.

TABLE III

MUTAGENIC EFFICIENCIES OF O^6-MeG AND O^6-EtG

	Mutagenic efficiency [a] for the incorporation of:								
	dAMP [b]		dTMP [b]			dGMP [c]		dCMP [c,d]	
	(20/2)	(2/20)	(20/2)	(10/10)	(2/20)	(20/2)	(2/20)	(20/2)	(2/20)
O^6-MeG	0.02	0.03	0.35	0.4	0.8	0.06	0.08	0.1	0.5
O^6-EtG	0.01	0.03	0.45		0.85	0.05	0.09	0.07	0.45
A [e]	< 0.005		0.95		0.95				
G [f]						< 0.005		1.0	

[a] Errors produced per modification present, calculated to the nearest 0.05 if > 0.1.

[b] Measured using a poly(dG,O^6-RdG) template.

[c] Measured using a poly(dA,O^6-RdG) template.

[d] Not strictly a mutagenic efficiency but included to demonstrate the competition between incorporation of dTMP and dCMP.

[e] Measured using a poly(dG,dA) template.

[f] Measured using a poly(dA,dG) template.

(40 μM). Increasing the dCTP concentration to more than 80 μM produced no decrease in mutagenic efficiency with 40 μM dTTP, whilst with 8 μM dTTP the mutagenic efficiency fell to 0.25 at 200 μM dCTP (see Fig. 1). If the dCTP concentration in the assay was fixed at 40 μM the mutagenic efficiency did not change from approx. 0.4 within the range 4–80 μM dTTP. With 8 μM dCTP the

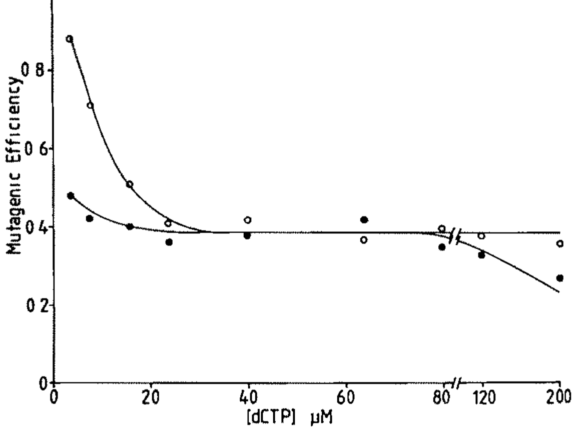

Fig. 1. The mutagenic efficiency of O^6-methylguanine at fixed dTTP concentrations. The dTTP concentration in the assay was fixed at 8 μM (●) or 40 μM (○) and the dCTP concentration was varied within the range 4–200 μM. The poly(dG,O^6-MeG) template contained 0.91% O^6-MeG.

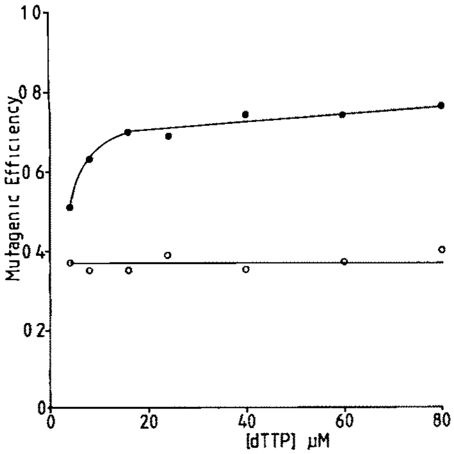

Fig. 2. The mutagenic efficiency of O^6-methylguanine at fixed dCTP concentrations. The dCTP concentration in the assay was fixed at 8 μM (●) or 40 μM (○) and the dTTP concentration was varied within the range 4–80 μM. The poly(dG,O^6-MeG) template contained 0.91% O^6-MeG.

mutagenic efficiency fell from approx. 0.7 at 16 μM dTTP to approx. 0.5 at 4 μM dTTP and at concentrations of dTTP above 50 μM the mutagenic efficiency showed a small increase, with a mutagenic efficiency of approx. 0.8 at 80 μM (see Fig. 2). Fig. 3 shows the effect of reducing the concentration of dCTP in a simple assay with poly(dG) as template. The amount of dCMP incorporated is taken as a measure of the degree of saturation of the DNA polymerase I with the dCTP present in the assay. The incorporation of dCMP only falls off at dCTP concentrations less than approx. 30 μM.

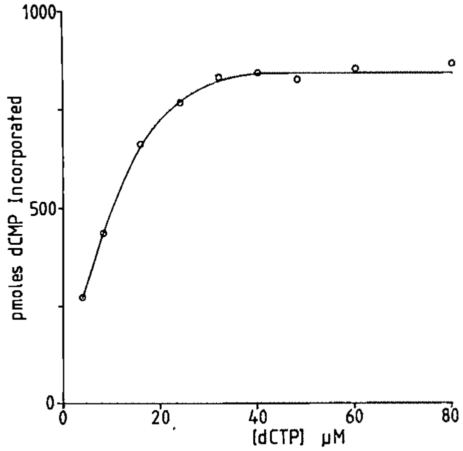

Fig. 3. Effect of varying dCTP concentration on the incorporation of dCMP. The template was poly(dG) The level of dCMP incorporation was taken as a measure of the degree of saturation of the DNA polymerase I with the incoming nucleotide. The only nucleotide in the assay was dCTP

Discussion

The results confirm the promutagenic potential of O^6-MeG and O^6-EtG during DNA synthesis as well as the competitive nature of their miscoding which leads to the incorporation of both dTMP and dCMP. Earlier studies [13] with similar polyribonucleotides containing O^6-MeG as templates for bacterial RNA polymerase have also shown the promutagenic nature of this modified base during RNA synthesis, but there was no indication of competition between the incorporation of UMP and the normal incorporation of CMP. The present results also show minor miscoding pathways for O^6-RG which lead to the incorporation of dAMP and dGMP but with much reduced mutagenic efficiencies (< 0.05 and < 0.1, respectively) compared to that for the incorporation of dTMP (> 0.35). It is not merely the ratio of dTTP/dCTP in the assay that determines the mutagenic efficiency of O^6-MeG, since it can be seen from Figs. 1 and 2 that a decrease in the concentration of dCTP is more effective at increasing the mutagenic efficiency than is a corresponding increase in the concentration of dTTP. From Figs. 1 and 3 it can be seen that the mutagenic efficiency of O^6-MeG is constant at a value of approx. 0.4 over a large range of dCTP and dTTP concentrations, so long as the DNA polymerase I is saturated with dCTP, and only increases (Fig. 1) when the dCTP in the assay ceases to saturate the enzyme, as indicated by a decrease in total incorporation in Fig. 3. This indicates that the affinity of the template/polymerase complex for the incoming nucleotide plays a role in determining the mutagenic efficiency of a modified base. Molecular models have indicated that O^6-MeG–T and O^6-MeG–C basepairs may be constructed [1,7] within the confines of the DNA helix. Although in DNA such modified basepairs may not be hydrogen-bonded (Li, B. and Swann, P.F., personal communication; also see Ref. 7), the various studies [1,3,4,7,11] indicate that an alkylated base will only miscode during DNA synthesis when the appropriate basepair is acceptable to the polymerase. This is likely to be achieved by the polymerase reading and amplifying the tautomeric form and hydrogen-bonding potential of the base within the template, leading to allosteric changes affecting the affinity of the polymerase for the incoming nucleotide. The proof-reading 3′ → 5′ exonuclease activity of DNA polymerase I may also play a role in the selectivity, but using mammalian DNA polymerase α (Saffhill, R., unpublished result), which has no associated exonuclease activities, we have observed similar competition between the incorporation of dTMP and dCMP with O^6-MeG or O^6-EtG in the template. The way that the mutagenic efficiency of O^6-MeG changes with the dTTP/dCTP ratio has been summarized [7] from these results but it is not feasible to cover all combinations of concentrations for all of the four dNTPs in experiments of this type.

The promutagenicity of O^6-MeG has been further demonstrated in vivo by constructing genomes of the bacteriophage M13 mp8 with a single O^6-MeG in place of G at specific locations [14] and, on introduction into *E. coli,* mutated phages were observed. The mutation frequency observed (0.4%0 was lower than might have been expected due to the repair system in *E. coli* demethylating the very small amount of O^6-MeG introduced in the phage DNA. However, by pretreating the host with an alkylating agent the mutated phage progeny were increased to 18%. In this system the mutations arose exclusively by GC → AT transitions. None of the small number of transversions that might be expected from the minor miscoding pathways of O^6-MeG reported here (see Tables I and II) were observed.

It has already been noted [5] that this competition in the miscoding of O^6-RG can, at least in part, explain the synergistic effects of added nucleosides on the mutagenic effects of alkylating agents. Thus low, non-toxic concentrations of deoxythymidine are able to enhance both the toxicity and the mutagenicity of *N*-nitroso-*N*-alkyl-*N′*-nitroguanidine [6] and nitrosomethylurea [15], an effect that may be reversed by the addition of deoxycytidine. The mutagenicity of the alkylating agent ethyl methanesulphonate towards Chinese hamster ovary (CHO) *thy*$^-$ mutator cells, which may be mutated by lower concentrations of the alkylating agent than the wild type, could be modified by varying the ratio of the sizes of the cellular dCTP and dTTP pools [8] by the addition of nucleosides to the cell cultures. In general, the greater the relative concentration of dTTP the more easily were the cells mutated. Also, in the wild-type cells the dCTP/dTTP pool ratio was greater than in the *thy*$^-$ mutants. The role of changes in cellular dNTP pools in determining the mutation frequency is, however, more complex than implied (see above for the changes in mutagenic efficiency), since decreasing the dCTP/dTTP ratio in the pools of the CHO *thy*$^-$ cells did not necessarily increase the maximum mutation frequency produced by increasing doses of ethyl methanesulphonate, but this maximum was reached with a lower concentration of alkylating agent in those cells with a low dCTP/dTTP pool ratio. The toxic effects of the ethyl methanesulphonate in these cells were also related to the dCTP/dTTP pool ratio: the greater the dCTP pool relative to that of dTTP the more resistant the cells were to the ethyl methanesulphonate. Further evidence of the effect of dNTP pool sizes on a cell's response to external agents has been demonstrated using pairs of e$^-$ radiation-sensitive and -resistant cell lines (Booth, J.A., Ockey, C.H. and Saffhill, R., unpublished results). In such comparisons it is observed that the cell line with the higher relative dTTP pool is the least sensitive of the pair, irrespective of whether the difference was pre-existing or was induced by the radiation. Such studies indicate that the sensitivity of a cell depends upon the relative sizes and balance of its dNTP pools. The effectiveness of drug combination chemotherapy may be due in part to changes in the cellular dNTP pools brought about by one or more of the drugs used, such as cytosine arabinoside [16–18] and methotrexate [19]. Although the present results indicate how cellular dNTP pools may influence mutagenicity, their precise role, including their effect on toxicity, has still to be established.

For a long time it has been presumed that there is some relationship between mutagenicity and carcinogenicity which has led to extensive studies on promutagenic lesions and both their formation and repair in the DNA of various tissues [7].

Although a relationship between the formation and persistence of O^6-RG in the DNA of a tissue and its sensitivity to cancer induction has been observed in some systems, a general correlation has not been forthcoming [7], probably due to the complex and multistage nature of the carcinogenic process. Until recently the connection between mutagenesis and carcinogenesis has remained circumstantial, but the recent characterization of oncogenes in both experimental animal and human tumours has provided direct evidence that changes in DNA base sequence, involving a single base, can lead to a change of phenotype from normal to malignant [7]. It is possible to propose that these changes in base sequence can arise from carcinogen-DNA interactions and the formation of specific modified bases with the DNA. Thus, the point mutation observed at codon 12 of the c-Ha-*ras* gene in the nitrosomethylurea-induced rat mammary tumour [20,21] could result from the O^6-MeG formed in that codon miscoding with the incorporation of dTMP leading to a GC → AT transition and the replacement of glycine by glutamine in the gene product. All mutants in codon 12 that have been examined show this transition [21]. Since such a change in sequence would have occurred soon after treatment with the nitrosomethylurea it presumably remained dormant whilst other changes occurred to allow the eventual expression of its oncogenic potential. The base change observed in the same codon of the c-ha-*ras* gene in the human EJ (T24) bladder carcinoma cell line [22–24] may arise as the result of a minor miscoding pathway of O^6-RG or as the result of nonspecific errors induced by other classes of chemical carcinogen, which can induce errors during DNA synthesis [7,25–27]. These can give rise to the GC → AT transversion which gives rise to the replacement of glutamine by valine. Also, the transversion at codon 61 which gives rise to the replacement of glutamine by leucine in the Hs242 c-Ha-*ras* gene from human lung [28] could have arisen from a similar minor miscoding pathway of O^4-RT [4] or as the result of a bulky adduct produced by some other class of carcinogen.

The results demonstrate the promutagenic potential of O^6-MeG and O^6-EtG and they are consistent with current knowledge concerning changes in DNA base sequence that have been observed in certain oncogenes from both human and experimental animal sources. They also indicate the importance of the sizes and balance of the cellular dNTP pools and the role that these may play in determining the response to external agents. Changes in the dNTP pools which effect the toxicity and in particular the mutagenicity of agents may also play a modifying role in carcinogenesis.

Acknowledgements

I thank Dr. J.A. Hall for the synthesis of O^6-MedGTP. This work was supported by the Cancer Research Campaign.

References

1 Abbott, P.J. and Saffhill, R (1979) Biochim. Biophys Acta 562, 51–61

2 Loveless, A. (1969) Nature 223, 206–207

3 Abbott, P.J and Saffhill, R. (1977) Nucleic Acids Res 4, 761–769

4 Saffhill, R. (1985) Chem. Biol. Interact. 53, 121–130

5 Saffhill, R. and Abbott, P.J. (1979) Nature 278, 581

6 Peterson, A.R., Landolph, J.R., Peterson, H. and Heidelberger, C. (1978) Nature 276, 508–510

7 Saffhill, R., Margison, G.P. and O'Connor, P.J. (1985) Biochim. Biophys. Acta 823, 111–145

8 Meuth, M (1981) Somatic Cell Genet. 7, 89–102

9 Saffhill, R. and Hall, J.A. (1981) J. Carbohydr. Nucleosides Nucleotides 8, 573–583

10 Hall, J.A. and Saffhill, R (1983) Nucleic Acids Res 11, 4185–4193

11 Saffhill, R. (1984) Carcinogenesis 5, 691–693

12 Wild, C.P., Smart, G, Saffhill, R and Boyle, J M (1982) Carcinogenesis 4, 1605–1609

13 Gerchman, L L and Ludlum, D B (1973) Biochim. Biophys. Acta 308, 310–316.

14 Essigman, J.M., Loechler, E L. and Green, C.L. (1985) in The Role of Cyclic Nucleic Acid Adducts in Carcinogenesis and Mutagenesis (Singer, B. and Bartsch, H., eds.), IARC, Lyons, in the press

15 Brennand, J, McMillan, S. and Fox, M (1981) Chem. Biol Interact. 38, 89–106

16 Moore, E C. and Hurlbert, R.B. (1966) J Biol Chem. 241, 4802–4809

17 Durham, J.M. and Ives, D.H. (1969) Mol Pharmacol. 5, 538–375

18 Cohen, S.S and Barner, H.O. (1956) Proc. Natl. Acad. Sci USA 40, 885–893

19 Das, S.K., Benditt, E.P. and Loeb, L.A. (1983) Biochem Biophys. Res. Commun. 114, 458–464

20 Sukumar, S., Notario, V, Martin-Zanca, D. and Barbacid, M. (1983) Nature 306, 658–661

21 Zarbl, H., Sukumar, S, Arthur, A.V., Martin-Zanca, D and Barbacid, M. (1985) Nature 315, 383–385

22 Tabin, C J., Bradley, S M., Bargmann, C.I., Weinberg, R A., Papageorge, A.G , Scolnick, E.M., Dhar, R , Lowy, D R and Chang, E.H. (1982) nature 300, 143–149

23 Reddy, E.P., Reynolds, R.K., Santos, E and Barbacid, M. (1982) Nature 300, 149–152

24 Taparowsky, E., Suard, Y , Fasano, O , Shimiza, K., Goldfarb, M. and Wigler, M (1982) Nature 300, 762–765

25 Hall, J A , Saffhill, R., Green, T and Hathway, D.E (1981) Carcinogenesis 2, 141–146

26 Saffhill, R. and Abbott, P.J. (1983) Chem Biol Interact 44, 95–110

27 Chu, Y -H and Saffhill, R. (1983) Carcinogenesis 4, 643–646

28 Yusa, Y., Srivastava, S K , Dunn, C.Y., Rhim, J.S , Reddy, E P. and Aaronson, S.A. (1983) Nature 303, 775–779

Biochimica et Biophysica Acta 866 (1986) 61–67
Elsevier

BBA 91562

Developmental and hormonal regulation of carbamoyl-phosphate synthase gene expression in rat liver: evidence for control mechanisms at different levels in the perinatal period

C.J. de Groot, D. Zonneveld, R.T.M. de Laaf, M.A. Dingemanse, P.G. Mooren, A.F.M. Moorman, W.H. Lamers * and R. Charles

Department of Anatomy and Embryology, University of Amsterdam, AMC,
Meibergdreef 15, 1105 AZ Amsterdam (The Netherlands)

(Received October 15th, 1985)

Key words: Carbamoyl-phosphate synthase; Gene expression, Hormonal regulation; (Rat liver)

Carbamoyl-phosphate synthase gene expression is found to be primarily regulated by conditions that enhance hepatic glucocorticosteroid levels (hormone injections) and cyclic AMP levels (induction of diabetes). After birth, changes in the level of carbamoyl-phosphate synthase protein follow changes in the level of carbamoyl-phosphate synthase mRNA, suggesting a pretranslational control mechanism. In fetal rats, carbamoyl-phosphate synthase gene expression is regulated by the same factors as in adults. However, both the level to which carbamoyl-phosphate synthase mRNA can accumulate and the extent to which mRNA can be translated appear to be limited, indicating control mechanisms at the pretranslational and translational level. Finally, in the immediate postnatal period, a transient but pronounced decrease in the rate of degradation of carbamoyl-phosphate synthase protein may play a role in the accumulation of the enzyme.

Introduction

Carbamoyl-phosphate synthase (EC 6.3.4.16) is an abundant hepatocyte-specific protein [1,2]. It offers an attractive model system for studying the developmental regulation of gene expression, as both the timing and the site of expression within the liver are under developmental control. Rat hepatocytes acquire the capacity to synthesize carbamoyl-phosphate synthase as soon as they differentiate from the embryonic foregut [3], but start to accumulate the enzyme only shortly before birth [4]. After birth, the adult capacity to synthesize carbamoyl-phosphate synthase is acquired [5], as is the typical periportal localization [6].

The factors that regulate carbamoyl-phosphate synthase gene expression at the protein level have been extensively studied, showing glucocorticosteroids and cyclic AMP to be the primary regulatory factors [3,4,7,8]. A preliminary exploration showed that the same factors affected carbamoyl-phosphate synthase mRNA levels [9]. In the present study we have analyzed further the role of hormones in regulating the levels of carbamoyl-phosphate synthase mRNA. Furthermore, we have established a detailed developmental profile of carbamoyl-phosphate synthase mRNA and have compared it to that of carbamoyl-phosphate synthase protein [10]. The results suggest that in the perinatal period, both pretranslational and translational control mechanisms may be operative.

---

* To whom correspondence should be addressed.

0167-4781/86/$03.50 © 1986 Elsevier Science Publishers B V (Biomedical Division)

Materials and Methods

Animals. Wistar rats, obtained from the TNO animal farm in Zeist, The Netherlands, were used. Fetal age was estimated from the time of conception and was accurate to within 12 h; birth normally occurred between 21.5 and 22.5 days after conception. Neonatal age was calculated from the time of birth. Rats were weaned at 4 weeks post partum.

Treatment of animals. For hormonal treatment, either 3–4-month-old adult or 19-day fetal rats were used. Diabetes was induced in adult rats by intraperitoneal injection of streptozotocin (70 mg/kg body weight) after an overnight fast. 24 h later, the animals were checked for glucosuria. Bilateral adrenalectomy and gonadectomy were performed under ether anesthesia and checked for completeness at death. Glucose (5 g/kg body weight) was administered to 24-h-starved rats by gastric gavage. Hormone-treated adult rats received triamcinolone acetonide (4 mg/kg body weight) by intraperitoneal injection. Hormone-treated fetuses received a cocktail of dexamethasone (2.5 mg/kg body weight), triiodothyronine (3.3 mg/kg body weight), dibutyryl cyclic AMP (50 mg/kg body weight) and theophylline (50 mg/kg body weight) by intraperitoneal injection, after laparotomy of the dam. Although triiodothyronine does not have an effect on carbamoyl-phosphate synthase mRNA (see Results) or protein [7] in adult animals, it was included in this cocktail as the hormone does have a stimulatory effect on carbamoyl-phosphate synthase protein before birth [7].

Determination of RNA content. The total RNA content of liver was determined by the orcinol method [11]. RNA was isolated from liver homogenates in guanidinium thiocyanate either by differential precipitation (Ref. 12, as modified in Ref. 9) or by centrifugation through a CsCl cushion [12]. Concentrations were calculated from the absorbance at 260 nm.

The RNA samples were diluted in a high-salt buffer (1.8 M NaCl/100 mM NaH_2PO/10 mM EDTA (pH 7.4)) and aliquots were passed through nitrocellulose filters using a commercial manifold. After heating at 80°C for 2 h, filters were prehybridized and hybridized at 42°C, essentially as described [13]. The cDNA probes for carbamoyl-phosphate synthase mRNA and albumin mRNA [9] and phospho*enol*pyruvate carboxykinase mRNA [14] were labeled by nick translation to a specific activity of approx. 10^8 cpm/μg. In more recent experiments a nearly full-length carbamoyl-phosphate synthase cDNA clone was used (designated pBR-CPS5; insert length, 5.5 kb). After washing, autoradiographs of the filters were made. For quantitative analysis, spots were cut out and radioactivity was determined by liquid scintillation counting.

In the graphs and tables, means ± S.E. of 3–7 independent estimates are given. In Fig. 1, the standard error of the ratio of carbamoyl-phosphate synthase mRNA and carbamoyl-phosphate synthase protein was calculated with the delta method.

Results

Table I describes the effects of long-lasting changes in the levels of glucocorticosteroids and cyclic AMP on the level of carbamoyl-phosphate synthase mRNA. Durable changes in hepatic cyclic AMP concentration were induced by diabetes, starvation, and starvation followed by glucose refeeding [15,16]. As a control, albumin mRNA levels were estimated as well. It is clear that administration of glucocorticosteroids (triamcinolone) enhances carbamoyl-phosphate synthase mRNA levels more than 2-fold after 24 h, whereas a decrease in the levels of circulating glucocorticosteroids as caused by adrenalectomy decreases the mRNA levels to 60% after 96 h. In intact animals, additional glucocorticosteroids have no effect on albumin mRNA levels; however, albumin mRNA levels decrease 2-fold upon removal of the adrenals. Glucocorticosteroids may therefore be necessary for the maintenance of 'normal' levels of albumin mRNA (cf. Ref. 17). Elevated hepatic cyclic AMP levels, as seen in diabetic animals, are associated with a more than 2-fold increase in carbamoyl-phosphate synthase mRNA levels after 24 h. Furthermore, the effects of glucocorticosteroids (triamcinolone treatment) and cyclic AMP (diabetes) are additive, causing a 3.5-fold increase after 24 h. Despite the continued presence of the inducing factors, their effects on carbamoyl-phosphate synthase mRNA levels are transient, showing a 30–40% decrease when effects at 96 h are compared with those at 24 h. No effects of thyroid hormones on carbamoyl-phosphate synthase mRNA levels were observed (data not shown). The diabetic condition causes a decrease in albumin mRNA levels (cf. Ref. 18). Apparently, glucocorticosteroids are able to counteract some of the deleterious effects of diabetes on albumin synthesis. Starvation slightly decreases carbamoyl-phosphate synthase mRNA levels, while glucose refeeding restores the mRNA levels to normal. Starvation for 24 h has little effect on albumin mRNA levels.

Fig. 1a shows the developmental profile of the ratio of the levels of hepatic carbamoyl-phosphate synthase mRNA and total RNA. Between 5 days before birth, when only a very small amount of mRNA can be detected, and 1 day before birth, carbamoyl-phosphate synthase mRNA levels increase 4-fold. Between this time and birth, mRNA levels remain constant, whereas in the first few postnatal days the mRNA levels drop to 50% of those at birth. Thereafter, mRNA levels incrase to attain maximum levels during the weaning period (3rd and 4th postnatal weeks). Adult mRNA levels are approx. 40% of those at weaning. In order to find the relationship between carbamoyl-phosphate synthase mRNA levels and carbamoyl-phosphate synthase protein levels it was necessary to determine the total RNA content per gram liver (Fig. 1b). After birth, the total RNA level was found to be 8–9 mg/g liver. However, before birth much higher RNA contents were found (12–13 mg/g liver at 4–5 days before birth), that rapidly decreased thereafter so that adult values were reached at 1 day before birth. The carbamoyl-phosphate synthase protein content per g liver (Fig. 1c) was recalculated from previously published data [10], taking into account the perinatal differences in immunoreactivity of the enzyme protein. The average of the ratios of the liver content of carbamoyl-phosphate synthase mRNA and carbamoyl-phosphate synthase protein calculated from the data between 5 and 32 days after birth was set arbitrarily at 1 (Fig. 1d). It is clear that large changes in this ratio occur in the perinatal period, decreasing from a high value of 10 at 4 days before birth to a low value of 0.5 at 1–3 days after birth, i.e., a 15–20-fold change. These data may point to an enhanced efficiency of carbamoyl-phosphate synthase protein synthesis from its mRNA and/or a decreased rate of protein degradation in the perinatal period (see Discussion).

For reference, the changes in carbamoyl-phosphate synthase mRNA levels were compared to those of phospho*enol*pyruvate carboxykinase mRNA (Fig. 2a) and albumin mRNA (Fig. 2b). Phospho*enol*pyruvate carboxykinase mRNA levels

TABLE I

EFFECT OF HORMONAL TREATMENT AND STARVATION ON THE LEVELS OF CARBAMOYL-PHOSPHATE SYNTHASE AND ALBUMIN mRNA IN ADULT RAT LIVER

mRNA levels found in control animals ($n = 9$) are regarded as 100%, mRNA levels of experimental animals ($n = 3$–6) are expressed as percentages ± S.E of control values. mRNA levels were determined by hybridization of radioactively labeled cDNA to serial dilutions of purified total RNA that was fixed on nitrocellulose Diabetes was induced with streptozotocin (70 mg/kg), 48 h before the start of the experiment. Triamcinolone acetonide (4 mg/kg) treatment was started at $t = 0$ h and repeated daily Adrenalectomy was performed 48 h before the start of the experiment. Starvation was started at $t = 0$ h Glucose (5 g/kg) was administered by gavage 2 h before death. – = no determination.

Period of treatment	Carbamoyl-phosphate synthase mRNA		Albumin mRNA	
	24 h	96 h	24 h	96 h
Triamcinolone	250 ± 30	170 ± 30	95 ± 5	110 ± 25
Diabetes	220 ± 10	125 ± 15	50 ± 10	60 ± 20
Diabetes + triamcinolone	350 ± 30	230 ± 50	80 ± 10	90 ± 10
Adrenalectomy	–	60 ± 15	–	45 ± 10
Starvation	75 ± 15	–	90 ± 10	–
Starvation + glucose	115 ± 10	–	95 ± 5	–

are extremely low up to parturition. Immediately after birth the levels rapidly accumulate to their developmental maximum (cf. Refs. 14,19 and 20). Thereafter, mRNA levels hardly change. Albumin mRNA levels are relatively low before birth, and increase in the first postnatal week to reach a developmental maximum during the 2nd, 3rd and 4th postnatal weeks. Thereafter, levels decline to adult values (cf. Refs. 21–23).

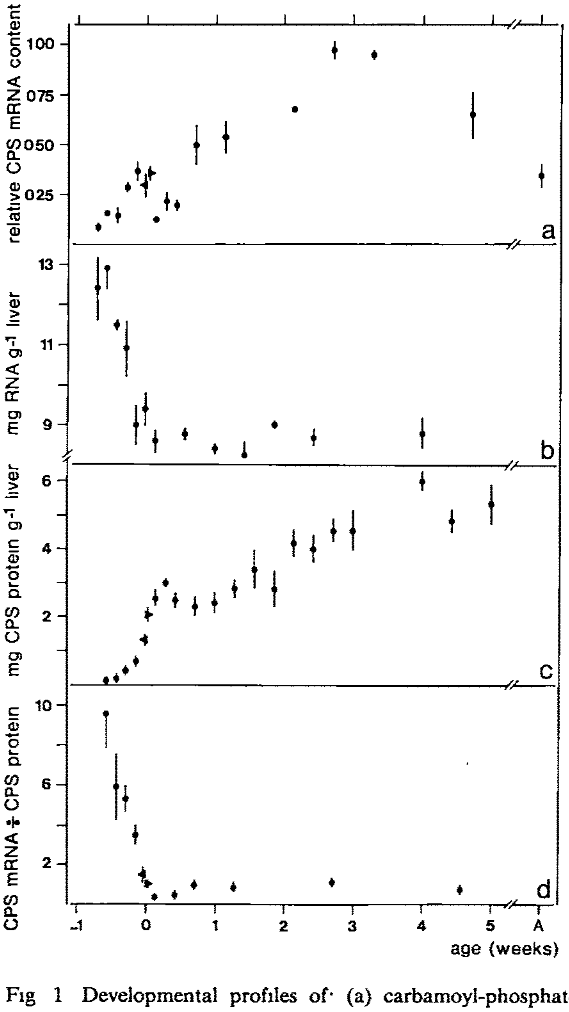

Fig 1 Developmental profiles of· (a) carbamoyl-phosphate synthase (CPS) mRNA, (b) total liver RNA; (c) carbamoyl-phosphate synthase protein and (d) the ratio of carbamoyl-phosphate synthase mRNA and carbamoyl-phopshate synthase protein content (a × b : c). Carbamoyl-phosphate synthase mRNA levels were determined by dot-blot analysis and expressed in arbitrary units per mg total RNA Total liver RNA content was estimated by the orcinol method [11]. Carbamoyl-phosphate synthase protein content was recalculated from previous results [10] The average ratio of carbamoyl-phosphate synthase mRNA and protein between 5 and 32 days after birth was arbitrarily set at 1. Means ± S.E. of 3–7 determinations are depicted.

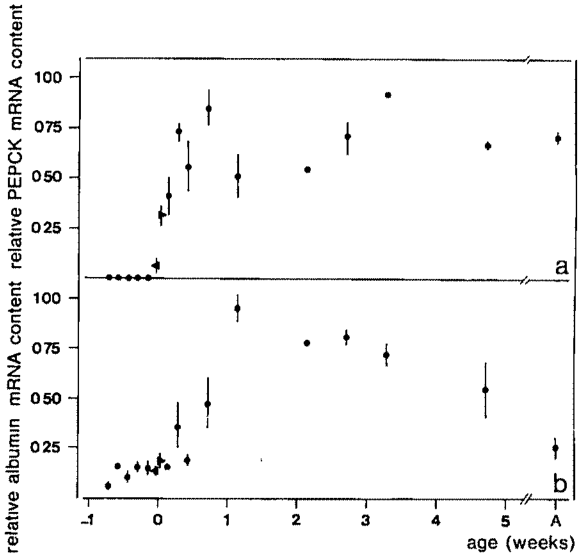

Fig. 2. Developmental profiles of· (a) phospho*enol*pyruvate carboxykinase (PEPCK) mRNA and (b) albumin mRNA. mRNA levels were determined by dot-blot analysis and expressed in arbitrary units per mg total RNA Estimates were derived from the same RNA preparations as used for the determination of carbamoyl-phoshate synthase mRNA content (Fig. 1a)

TABLE II

EFFECT OF HORMONAL TREATMENT ON THE LEVELS OF CARBAMOYL-PHOSPHATE SYNTHASE AND ALBUMIN mRNA IN FETAL RAT LIVER

mRNA levels found in control animals ($n = 3$–9) of the same age are regarded as 100%. mRNA levels of experimental animals (2 pools of 6 fetuses) are expressed as percentage of control values and, between brackets, as a percentage of maximal (inducible) adult values. mRNA levels were determined by hybridization of radioactively labeled cDNA to serial dilutions of purified total RNA that was fixed on nitrocellulose The fetuses were injected 3 days before birth with dexamethasone (2.5 mg/kg), triiodothyronine (3.3 mg/kg), dibutyryl cyclic AMP (50 mg/kg) and theophylline (50 mg/kg) ($t = 0$ h). This treatment was repeated after 24 h for the group examined at 48 h

Period of treatment	Carbamoyl-phosphate synthase mRNA	Albumin mRNA
6 h	420 (16)	80
12 h	210 (12)	80
24 h	145 (11)	80
48 h	120 (11)	50

To find out whether the limited capacity to accumulate carbamoyl-phosphate synthase protein prior to birth [4,5,7,8] is caused by a limited capacity to accumulate carbamoyl-phosphate synthase mRNA, fetal rats were treated with a hormonal cocktail that had previously been found to be optimal for prenatal enzyme induction [8]. Table II shows that, as in adult rats, the effects of hormonal treatment on carbamoyl-phosphate synthase mRNA levels are transient. In fetal rats, the maximal effect (a 4-fold increase over basal levels) is observed after 6 h. Moreover, the maximal levels of carbamoyl-phosphate synthase mRNA that are observed in these fetuses represent only 16% of those observed in adults, showing that the capacity to accumulate carbamoyl-phosphate synthase mRNA is limited prenatally. For comparison, albumin mRNA levels were estimated as well. Table II shows that prolonged hormonal treatment did affect albumin mRNA levels. This effect is presumably due to the cyclic AMP in the hormonal cocktail (cf. Table I).

Discussion

If one assumes that the rate of synthesis of carbamoyl-phosphate synthase protein is a linear function of the concentration of carbamoyl-phosphate synthase mRNA ($V_s = k_s[\mathrm{mRNA}]$) then the change in carbamoyl-phosphate synthase protein level (dE/dt) should equal the difference between the rate of protein synthesis (V_s) and protein degradation ($V_d = k_d[\mathrm{E}]$), i.e. $dE/dt = k_s[\mathrm{mRNA}] - k_d[\mathrm{E}]$ (Ref. 24). The first assumption is allowed when the translational machinery is saturated with mRNAs of different types, while changes in the level of specific mRNAs occur. In steady-state conditions ($dE/dt = 0$), the ratio $[\mathrm{mRNA}]/[\mathrm{E}] = k_d/k_s$. After calculation of dE/dt from the data of Fig. 1c, and assuming that either k_s or k_d is constant, a curve is obtained which is virtually identical to that Fig. 1d. This demonstrates that dE/dt is negligible within the time scale of our observations.

After birth, changes in the level of carbamoyl-phosphate synthase protein usually follow changes in the level of carbamoyl-phosphate synthase mRNA (Fig. 1d; cf., for example, Refs. 25 and 26). The regulation of carbamoyl-phosphate synthase gene expression by glucocorticosteroids and cyclic AMP in rat liver in this period of development is therefore predominantly regulated at the pretranslational level (k_s and k_d constant). Similarly, the effects of different protein contents in the diet on carbamoyl-phosphate synthase gene expression have been localized at this pretranslational level [27]. It is most likely that the effects of protein content in the diet are mediated by cyclic AMP via changes in the rate of glucagon secretion [15,28]. Furthermore, glucocorticosteroids and insulin have been found to affect carbamoyl-phosphate synthase mRNA levels in Reuber hepatoma cells [25].

It was very interesting to find that the carbamoyl-phosphate synthase mRNA/protein ratio is not constant in the perinatal period (Fig. 1d). The differential increase of carbamoyl-phosphate synthase mRNA and protein can in principle be explained by a 10–15-fold difference in the half-life of the mRNA and that of the protein molecule [24]. However, a similar increase in mRNA levels in the postnatal period is followed by a proportional increase in protein levels, as is evident from the constant ratio between both parameters (Fig. 1d). We have already argued that steady-state conditions for carbamoyl-phosphate synthase protein levels can be assumed to exist within the time scale of our observations. This then leaves the possibility that the carbamoyl-phosphate synthase mRNA/protein ratio changes as a result of changes in the half-life of carbamoyl-phosphate synthase protein (k_d) or as a result of changes in the efficiency of protein synthesis from the carbamoyl-phosphate synthase mRNA (k_s). In view of the fact that in cultures of 14-day embryonic hepatocytes the half-life of carbamoyl-phosphate synthase protein is the same as that in adult liver (Van Roon et al., unpublished data), it seems most likely that the changes in the carbamoyl-phosphate synthase mRNA/carbamoyl-phosphate synthase protein ratio in the prenatal period are the result of changes in the efficiency of protein synthesis from the cellular mRNA (translational control). However, in the immediate postnatal period a transient decrease in the rate constant of degradation of carbamoyl-phosphate synthase protein cannot be excluded, as such a phenomenon has been shown to exist for phospho*enol*pyruvate carboxykinase in this period [29]. Therefore, carbamoyl-phosphate synthase gene expression in the prenatal period appears to be characterized by control at the pretranslational (regulation of mRNA levels (Fig. 1a, Table II)) as well as at the translational (regulation of k_s) level, while in the immediate postnatal period, posttranslational (regulation of k_d) control may exist. In view of the long half-life of carbamoyl-phosphate synthase protein under 'normal' conditions [23] and the transient nature of the observed phenomena, it is probably best to verify the nature of the control mechanisms by measuring in vivo the rate of carbamoyl-phosphate synthase protein synthesis as a function of carbamoyl-phosphate synthase mRNA concentration (k_s). The discrepancy between the rates of accumulation of carbamoyl-phosphate synthase mRNA and protein in the perinatal period was not previously observed [30], probably because too few observations were made. Many examples of translational (posttranscriptional) control mechanisms exist. In fact, in some cases, factors such as cyclic AMP can affect both the transcriptional and translational efficiency of genes [31].

The data in Table II clearly show that in order to explain the regulation of carbamoyl-phosphate synthase gene expression in the perinatal period, additional factors have to be identified. In particular, the question arises as to why glucocorticosteroids and cyclic AMP are not able to stimulate gene expression to adult levels. Two still poorly defined factors have been identified by us as responsible for the limited capacity of the fetal hepatocytes to respond to hormones: the intrauterine environment [5] and the degree of developmental maturation of the hepatocytes (Ref. 3, and Van Roon et al., unpublished data). The availability of an in vitro culture system in which maturation towards the adult capacity of gene expression occurs (Van Roon et al., unpublished data) should allow further characterization of these factors and of their effects on carbamoyl-phosphate synthase gene expression.

Acknowledgements

These investigations were supported in part by the Foundation for Medical Research, FUNGO, Grant No. 900-528-038. We want to acknowledge the stimulating discussions with Drs. H. Westerhoff and H. Oosting, the help of Mrs. J.H. van Horssen-Medema and Mr. C. Hersbach in preparing the drawings and photographs and the help of Ms. J. Husslage in preparing the manuscript.

References

1 Charles, R., De Graaf, A. and Moorman, A.F M (1980) Biochim Biophys. Acta 629, 36–49
2 Gaasbeek Janzen, J.W., Lamers, W.H., Moorman, A.F M , De Graaf, A., Los, J.A. and Charles, R. (1984) J Histochem. Cytochem 32, 557–564
3 Lamers, W.H., Zonneveld, D and Charles, R. (1984) Dev Biol. 105, 500–508
4 Lamers, W.H. and Mooren, P.G (1980) Biol. Neonat. 37, 113–137
5 Lamers, W.H., Mooren, P.G., De Graaf, A and Charles, R (1985) Eur. J. Biochem 146, 475–480
6 Gaasbeek Janzen, J.W , Moorman, A F.M., Lamers, W H. and Charles, R. (1985) J. Histochem Cytochem. 33, 1205–1211
7 Lamers, W.H. and Mooren, P.G. (1980) Biol. Neonat 37, 264–284
8 Lamers, W.H and Mooren, P.G. (1981) Mech. Ageing Dev 15, 93–118
9 De Groot, C.J , Van Zonneveld, A.J., Mooren, P.G , Zonneveld, D., Van den Dool, A., Van den Bogaert, A.J.W., Lamers, W.H., Moorman, A.F.M and Charles, R. (1984) Biochem. Biophys. Res. Commun 124, 882–888
10 Charles, R., De Graaf, A., Lamers, W.H. and Moorman, A F M. (1983) Mech Ageing Dev. 22, 193–203
11 Munro, H.N. and Fleck, A. (1966) Methods Biochem. Anal. 14, 113–176
12 Chirgwin, J.M., Przybyla, A.E , MacDonald, R.J. and Rutter, W J. (1979) Biochemistry 18, 5294–5299
13 Meinkoth, J and Wahl, G. (1984) Anal. Biochem 138, 267–284
14 Cimbala, M.A., Lamers, W.H , Nelson, K., Monahan, J E., Yoo-Warren, H and Hanson, R.W (1982) J. Biol Chem. 257, 7629–7636
15 Seitz, H.J., Krone, W. and Tarnowski, W. (1977) Acta Endocrinol. 85, 389–397
16 Seitz, H.J., Luth, W. and Tarnowski, W (1979) Arch. Biochem Biophys. 195, 385–391
17 Moshage, H.J., De Haard, H J W., Princen, H.M G and Yap, S H. (1985) Biochim. Biophys. Acta 824, 27–33
18 Jefferson, L.S., Liao, W.S , Peavy, D.E , Miller, T.B., Appel, M.C. and Taylor, J.M (1983) J Biol Chem. 258, 1369–1375
19 Mencher, D., Cohen, H., Benvenisty, N , Meyuhas, O. and Reshef, L (1984) Eur J Biochem. 141, 199–203
20 Ruiz, J.P.G., Ingram, R and Hanson, R W. (1978) Proc Natl. Acad. Sci. USA 75, 4189–4193
21 Liao, W.S L., Conn, A R and Taylor, J.M. (1980) J. Biol. Chem. 255, 10036–10039

22 Sala-Trepat, J.M., Dever, J., Sargent, T.D., Thomas, K , Sell, S and Bonner, J. (1979) Biochemistry 18, 2167–2178

23 Selten, G.C M , Princen, H M.G., Selten-Versteegen, A.-M E , Mol-Backx, G.P.B.M. and Yap, S.H. (1982) Biochim Biophys Acta 699, 131–137

24 Berlin, C M and Schimke, R.T. (1965) Mol. Pharmacol 1, 149–156

25 Kitagawa, Y , Ryall, J , Nguyen, M. and Shore, G.C (1985) Biochim. Biophys. Acta 825, 148–153

26 Kitagawa, y. and Sugimoto, E (1985) Eur. J. Biochem. 150, 249–254

27 Ryall, J , Rachubinsky, R A., Nguyen, M., Rozen, R., Broglie, K.E. and Shore, G.C. (1984) J. Biol. Chem. 259, 9172–9176

28 Eisenstein, A.B., Strack, I., Gallo-Torres, H., Georgiadis, A. and Miller, O.N (1979) Am. J. Physiol. 236, E20–E27

29 Philippidis, H , Hanson, R.W , Reshef, L., Hopgood, M.F. and Ballard, F J. (1972) Biochem J. 126, 1127–1134

30 Adcock, M.W. and O'Brien, W.E. (1984) J Biol Chem. 259, 13471–13476

31 Noguchi, T , Diesterhaft, M. and Granner, D (1982) J Biol Chem. 257, 2386–2390

Biochimica et Biophysica Acta 866 (1986) 68–74
Elsevier

BBA 91553

Sequence of the cDNA encoding porcine pro-opiomelanocortin

Francis J. Gossard *, Annie C.Y. Chang and Stanley N. Cohen

Departments of Genetics and Medicine, Stanford University School of Medicine, Stanford, CA 94305 (U S A)

(Received September 23rd, 1985)

Key words. Pro-opiomelanocortin cDNA; Nucleotide sequence; Pituitary hormone

Messenger RNA was extracted from porcine pituitary pars intermedia and cloned as cDNA by standard methods. The nucleotide sequence encoding porcine pro-opiomelanocortin was established from analysis of two separate cDNA segments having an overlap of 420 bases. The amino acid sequence for the porcine pro-opiomelanocortin protein, which was inferred from the cDNA sequence, was found to correspond exactly to the sequence determined by direct amino acid analysis of the component peptides of pro-opiomelanocortin; namely, the porcine hormones ACTH, β-lipotropin, γ-MSH and the connecting peptide. We thus find no evidence for the existence of two porcine pro-opiomelanocortin genes that differ in their coding sequences, as was suggested by the in vitro protein synthesis results of others using mRNA obtained from porcine pituitaries.

Introduction

The pituitary hormones β-endorphin and corticotropin are synthesized as a large common precursor protein [1,2] called pro-opiomelanocortin (POMC) [3]. The structure of the POMC protein was first determined from sequence analysis of cloned complementary DNA (cDNA) transcribed in vitro from POMC messenger RNA (mRNA) extracted from bovine pituitary intermediate lobes [4]. Subsequently, the sequences for the human [5–7], rat [8] and mouse [9] POMC genes have been reported. From analysis of the primary structure of the precursor protein that corresponds to the DNA sequences, several conclusions can be reached. First, the sequences of the hormonally active component peptides are flanked in the precursor protein by pairs of basic amino acids that may serve as recognition sequence for a maturation enzyme that cleaves the precursor into its multiple components. Secondly, the sequences that encode known hormones are highly conserved through all of the species studied. Thirdly, the peptide segments that separate those components of POMC that are known to be hormonally active show a high degree of variability from species to species. The selective conservation of specific regions of a multifunctional peptide makes POMC a useful model system for the study of evolution at the genomic level.

Although it is thought that the gene encoding POMC is present as a single copy in the genome, the possibility that multiple POMC genes exist was suggested by the results of rat DNA genomic blots showing multiple POMC-hybridizable bands [8]. Recently, two forms of RNA from the rat pituitary intermediate lobe, both encoding POMC but vary-

---

* Present address: Biotechnology Research Institute, National Research Council, 750 Bel Air Street, Montreal, Quebec H4C 2K3, Canada

Abbreviations: ACTH, adrenocorticotropin; MSH, melanotropin; POMC, pro-opiomelanocortin; SSPC, 0 12 M NaCl/0 015 M sodium citrate/0 020 M KH_2PO_4 (pH 7.2); 1 × Denhardt solution [19], 0.02% Ficoll, polyvinylpyrrolidone, bovine serum albumin; SSC, 0.15 M NaCl/0.015 M sodium citrate (pH 7.0).

0167-4781/86/$03.50 © 1986 Elsevier Science Publishers B V. (Biomedical Division)

ing in the non-coding upstream region, have been identified; however, both of these species seem to arise from differently spliced transcripts of a single gene [29]. In the mouse, a single POMC gene was isolated and sequenced [9]. A second sequence homologous to POMC DNA and present in this species was found to be a pseudogene [10].

While no evidence of multiple copies of the POMC gene has been found by analysis of bovine or human DNA libraries, mRNA extracted from the porcine intermediate lobe and translated in a cell-free system yielded two separate POMC proteins that differed in their primary sequence [11]. This result suggested the existence of two POMC mRNA species that vary in their coding sequence, raising the possibility that two distinct POMC genes are in fact present in the porcine genome. Such an occurrence would make the porcine genome unique among known mammalian systems.

We have cloned POMC cDNA corresponding to a population of mRNA molecules isolated from the porcine pituitary intermediate lobe. We report here the nucleotide sequence of a cDNA species encoding the porcine POMC transcript and our unsuccessful search for a second porcine POMC mRNA species by Northern blot analysis of RNA and by DNA sequencing.

Materials and Methods

Materials. Restriction enzymes were obtained from New England Biolabs or Bethesda Research Laboratories; DNA polymerase Klenow fragment was obtained from Boehringer-Mannheim, and terminal transferase from PL Biochemical. Reverse transcriptase was a gift from Dr. R. Beard. Labeled nucleotides were from Amersham International. pBR322-dG-tailed vector DNA was obtained from New England Nuclear, Bacterial strains were *Escherichia coli* C600 Hfl$^+$ and HB101 [13,15].

mRNA extraction, cDNA synthesis and cloning. mRNA was extracted and purified as described [12]. Synthesis of the first strand of cDNA was initiated by an oligo(dT) primer. Second-strand synthesis was initiated by a self-forming hairpin after boiling of the first strand [12]. After trimming by S_1 nuclease, cDNAs were cloned in two different ways: in the *Pst*I site of pBR322 by the dG-dC tailing method [12] or in the CI gene of bacteriophage λgt-10 after addition of *Eco*RI linker [13].

Analysis of cloned cDNA. Nick-translated [14] DNA corresponding to the pSNAC20 plasmid, which contains the bovine POMC cDNA sequence [4], was used as a probe for colony or plaque hybridization [16,17]. Hybridization was carried out in 50% formamide, 5 × SSPC, 1 × Denhardt solution [18] at 32°C. Sequencing of DNA [19] was done on fragments labeled by the DNA polymerase Klenow fragment.

Northern and genomic blots. RNA samples were denatured in 50% formamide and 2.2 M formaldehyde and run on a 30 cm horizontal 1.4% agarose gel containing 2.2 M formaldehyde [20]. After transfer of RNA to nitrocellulose paper, the blot was hybridized in 5 × SSPC, 50% formamide and 10% dextran sulfate at 42 or 32°C overnight [21]; these conditions should allow for at least 23% mismatch using a probe 750 basepairs in length. The probe used was derived from a nick-translated plasmid (pPIL31) containing part of the porcine cDNA for POMC. Blots were washed for 15 min in 0.1 × SSC, 0.1% SDS at 32 or 42°C [22].

10-μg aliquots of porcine genomic DNA was digested with *Bam*HI, *Hin*dIII or *Eco*RI endonucleases. The DNA digests were electrophoresed on a 1% horizontal agarose gel and transferred to nitrocellulose [22]. Filters were then probed with a nick-translated *Xma*I fragment of pPIL23 in 5 × SSC, 5 × Denhardt solution [18] and 50% formamide for 20 h at 42°C.

Results

Cloning and sequencing

mRNA was extracted from porcine pituitary intermediate lobes, purified by two passages over an oligo(dT)-cellulose column [11], and cDNA was synthesized as indicated in Materials and Methods. The resulting cDNAs were either ligated to *Eco*RI linkers or tailed with dC and reannealled with *Eco*RI-digested λ*gt*10 DNA or dG-tailed pBR322 DNA, respectively. The pBR322 cDNA recombinant was introduced by transformation into *E. coli* strain HB101 host; the efficiency of transformation in this *rec*$^-$ host was about $3 \cdot 10^4$ colonies per microgram DNA. The recombinant λ/cDNA species were packaged and transfected

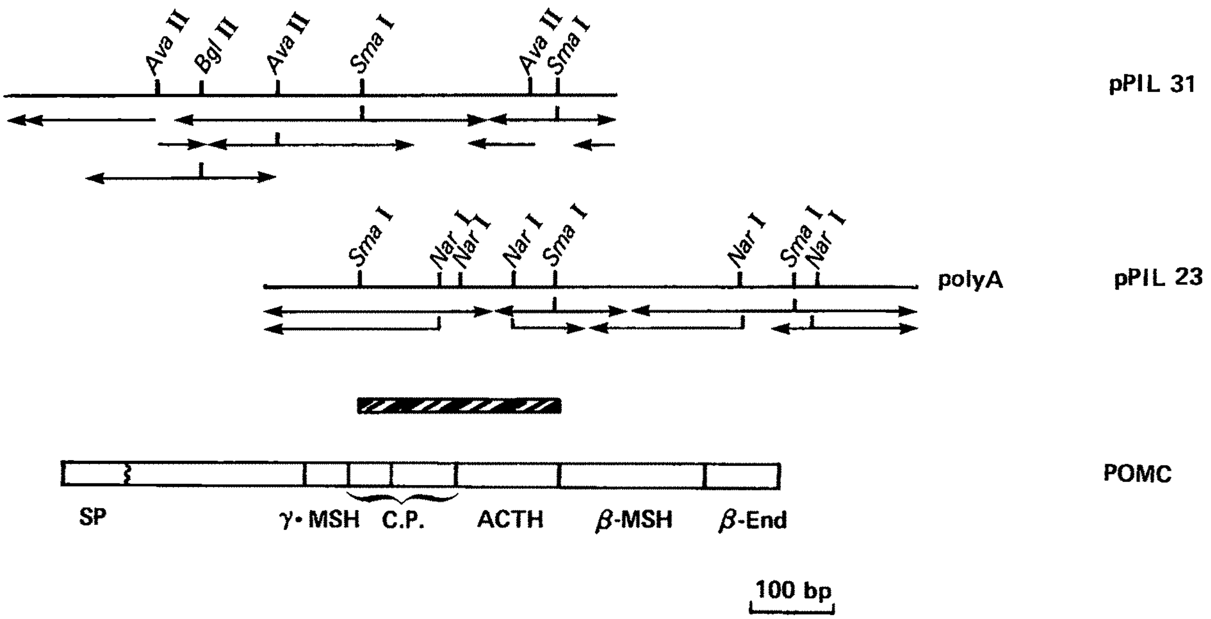

Fig. 1. Strategy for sequencing the two POMC cDNA pPIL31 and pPIL23 are two cDNAs coding for porcine POMC The protein is schematically represented in the lower part. The black vertical lines represent pairs of basic amino acid residues The hatched box represents the *SmaI* fragment used for genomic blot. Arrows indicate the direction of sequencing from relevant restriction enzyme sites. C.P. is connecting peptide

the host C600 Hfl at a frequency of $2 \cdot 10^5$ plaques per μg of cDNA insert.

3% of the colonies or plaques showed hybridization with a nick-translated probe derived from the bovine POMC-containing plasmid. Purification and analysis of these clones showed that most cDNA inserts were short and none contained a full-length POMC cDNA. However, analysis was carried out on two separate clones that spanned the whole porcine POMC sequence (Fig. 1). One of these cDNA inserts (750 bp in length) comprised part of the 5′ non-translated region plus 680 bp of the coding region (pPIL31). The second insert studied (800 bp in length) comprised the entire 3′ non-translated region up to the polyadenylation site, plus 630 bp of the coding region (pPIL23). Both were sequenced by following the strategy shown in Fig. 1; the full sequence is shown in Fig. 2. The overlapping sequence between the two cDNA species is 420 bases long.

Genomic DNA blots

DNA was extracted from porcine liver and aliquots were digested with enzymes, *Eco*RI, *Hin*dIII, and *Bam*HI (Fig. 3). These enzymes do not cut the porcine POMC coding sequence (shown by Fig. 2). More importantly, they do no cut the *Sma*I fragment shown as a hatched box in Fig. 1. In all the genes coding for POMC sequenced thus far (human, rat and bovine [5–7,8,23]) introns occupy corresponding positions: one intron is located in the 5′ non-translated region; the other is present after the codon for the 19th amino acid of the POMC protein. The *Sma*I fragment used to probe the genomic blot does not span either of these two regions. As seen in Fig. 4, two hybridizing bands were observed in every restriction digest. This suggests that two sequences homologous to the central part of POMC cDNA are present in the porcine genome if the porcine POMC gene structure is similar to the structure found in other species. Whether these two sequences represent active genes is not known.

Northern blots

Total RNA (20 μg) from the porcine pituitary pars intermedia lobes were denatured in 50% formamide, 2.2 M formaldehyde and electrophoresed on a horizontal 1.4% agarose gel; a long gel bed (30 cm) was used in order to separate possible

POMC mRNA species that differ only minimally in length. After transfer to nitrocellulose, the RNA blot was hybridized with nick-translated pPIL31 DNA at 42°C. Total RNA yielded a single band representing an RNA species about 1300 bases long (Fig. 4A). On another gel purified mRNA

```
                                    -40
CCGAGTTTCCTGCCTCGCGCAACGGGAGTCGCCCCGAGAGCAGCCTCCCCGCGACAGAGCCTCAGCCTGCTTGGAAG

                                     30                                      60
ATG CCG AGA TTG TGC AGC AGT CGC TCG GGG GCC CTG CTG CTG GCC TTG CTG CTT CAG GCC
Met Pro Arg Leu Cys Ser Ser Arg Ser Gly Ala Leu Leu Leu Ala Leu Leu Leu Gln Ala
 1                                   10                                      20

                                     90                                     120
TCC ATG GAA GTG CGT GGC TGG TGC TTG GAA AGC AGC CAG TGT CAG GAC CTC TCC ACG GAA
Ser Met Glu Val Arg Gly Trp Cys Leu Glu Ser Ser Gln Cys Gln Aps Leu Ser Thr Glu
                                     30                                      40

                                    150                                     180
AGT AAC TTG CTG GCG TGC ATC CGG GCC TGC AAA CCA GAT CTC TCC GCG GAG ACG CCC GTG
Ser Asn Leu Leu Ala Cys Ile Arg Ala Cys Lys Pro Asp Leu Ser Ala Glu Thr Pro Val
                                     50                                      60

                                    210                                     240
TTT CCC GGC AAC GGC GAC GCG CAA CCG CTG ACC GAG AAC CCC|CGG AAG|TAC GTC ATG GGC
Phe Pro Gly Asn Gly Asp Ala Gln Pro Leu Thr Glu Asn Pro|Arg Lys|Tyr Val Met Gly
                                     70                                      80

                                    270                                     300
CAC TTC CGC TGG GAC CGC TTC GGC|CGC CGG|AAT GGC AGC AGC AGC GGC GGC GGT GGC GGT
His Phe Arg Trp Asp Arg Phe Gly|Arg Arg|Asn Gly Ser Ser Ser Gly Gly Gly Gly Gly
                                     90                                     100

                                    330                                     360
GGC GGC GGC GCG GGC CAG|AAG CGC|GAG GAG GAG GAG GTG GCG GCG GGC GAA GGC CCC GGG
Gly Gly Gly Ala Gly Gln|Lys Arg|Glu Glu Glu Glu Val Ala Ala Gly Glu Gly Pro Gly
                                    110                                     120

                                    390                                     420
CCC CGC GGA GAT GGC GTC GCG CCG GGC CCG CGC CAG GAC|AAG CGC|TCC TAC TCC ATG GAG
Pro Arg Gly Asp Gly Val Ala Pro Gly Pro Arg Gln Asp|Lys Arg|Ser Tyr Ser Met Glu
                                    130                                     140

                                    450                                     480
CAC TTC CGC TGG GGC AAG CCC GTG GGC|AAG AAG CGG CGC|CCG GTG AAG GTG TAT CCC AAC
His Phe Arg Trp Gly Lys Pro Val GLy|Lys Lys Arg Arg|Pro Val Lys Val Tyr Pro Asn
                                    150                                     160

                                    510                                     540
GGC GCC GAG GAC GAG TTG GCC GAG GCC TTC CCC CTC GAG TTC|AGG AGG|GAG CTG GCC GGG
Gly Ala Glu Asp Glu Leu Ala Glu Ala Phe Pro Leu Glu Phe|Arg Arg|GLu Leu Ala Gly
                                    170                                     180

                                    570                                     600
GCG CCC CCC GAG CCG GCA CGG GAC CCC GAG GCC CCG GCC GAG GGC GCG GCC GCC CGG GCC
Ala Pro Pro Glu Pro Ala Arg Asp Pro Glu Ala Pro Ala Glu Gly Ala Ala Ala Arg Ala
                                    190                                     200

                                    630                                     660
GAG CTG GAG TAC GGG CTG GTG GCC GAG GCC GAG GCG GCG GAG|AAG AAG|GAC GAA GGG CCC
Glu Leu Glu Tyr Gly Leu Val Ala Glu Ala Glu Ala Ala Glu|Lys Lys|Asp Glu Gly Pro
                                    210                                     220

                                    690                                     720
TAT AAG ATG GAG CAC TTC CGC TGG GGC AGC CCG CCC AAG GAC|AAG CGC|TAC GGC GGC TTC
Tyr Lys Met Glu His Phe Arg Trp Gly Ser Pro Pro Lys Asp|Lys Arg|Tyr Gly Gly Phe
                                    230                                     240

                                    750                                     780
ATG ACC TCC GAG AAG AGC CAG ACG CCC CTG GTC ACG CTG TTC AAA AAC GCC ATC GTC AAG
Met Thr Ser Glu Lys Ser Gln Thr Pro Leu Val Thr Leu Phe Lys Asn Ala Ile Val Lys
                                    250                                     260

                                   810                                     850
AAC GCC CAC AAG AAG GGC CAG TGA GGGTTCAGGGGGCAGGCGCCTCTCACCCCGGAAGCCGACCCCAAAG
Asn Ala His Lys Lys Gly Gln
                        267

                                    890                                    930
CCCCCTCTCCTTGCCTGCCCTCCTGCCGCCTCCAGCCCGGGGTACGCTCAGGCTGTGTGGGCGCCAGATATCCCGCCT
                                    970
CTTACCTGTAGTTAGGAAATAAAACCTTTCAAGTTTGpolyA
```

Fig. 2. Nucleotide sequence of porcine POMC cDNA with the derived protein Pairs of basic amino acid residues are boxed. Nucleotides and amino acid residues are numbered from the initiation methionine codon (upper and lower numbering, respectively).

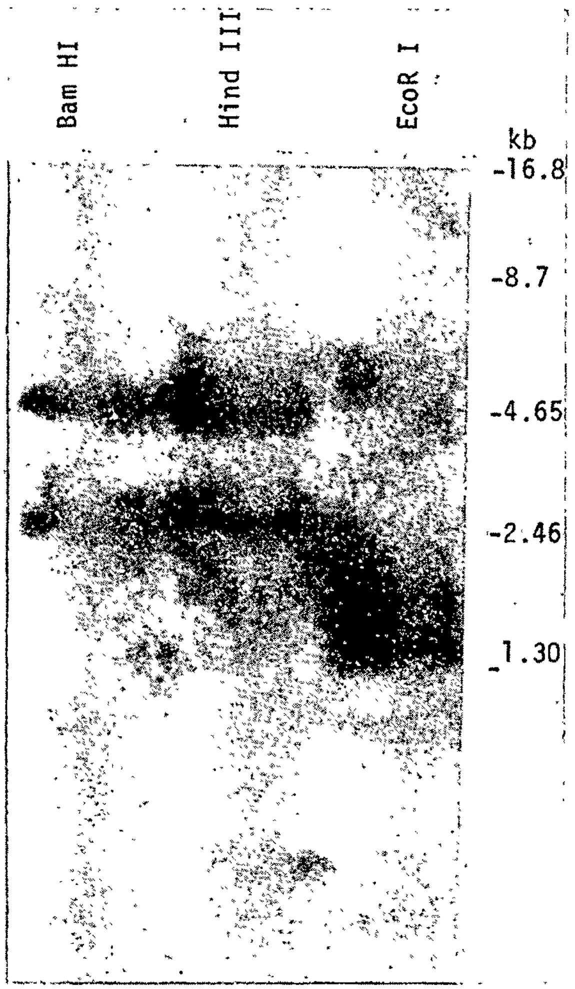

Fig. 3. DNA (10 μg) extracted from porcine liver was digested (lane 1) *Bam*HI (10 units), (lane 2) *Hin*dIII (10 units) or (lane 3) *Eco*RI (10 units) endonuclease The digests were run on a horizontal 1% agarose gel and blotted (see Materials and Methods)

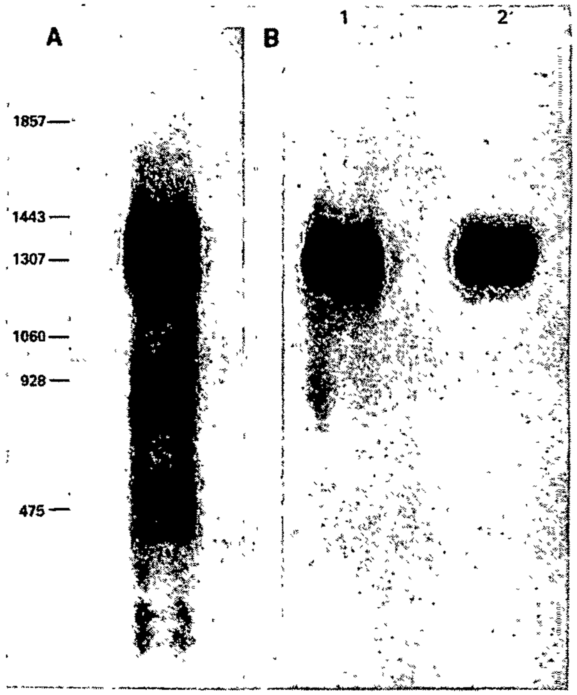

Fig 4 Northern blots of RNAs extracted from porcine pituitary pars intermedia. A. Total RNA (20 μg) was denatured in formaldehyde/formamide, run on a 30 cm horizontal 1.4% agarose gel (see Materials and Methods), blotted and probed with nick-translated pPIL31. The positions of molecular weight markers (denatured pBR322 DNA digested with *Taq*I or *Bst*NI) are shown. B Total RNA (5 μg, lane 1) and purified mRNA (0.3 μg, lane 2) were denatured, run and probed as above.

(0.3 μg) was run and blotted (Fig. 4B, lane 2). Again a single band comigrated with the one observed with total RNA (Fig. 4B, lane 1). Hybridizing this blot at lower temperature (32°C) gave the same results. Denaturation of the RNA by glyoxal [21] prior to electrophoresis also showed identical results (not shown).

Sequencing of different cDNAs encoding Porcine POMC

Both the plasmid and the phage cDNA libraries were probed with nick-translated pSNAC20 or a 5′ *Hinf*/*Ava*II fragment of pPIL31 under low stringency conditions described in Materials and Methods in order to identify several candidates encoding the 5′ end of POMC. Four different clones of various length (350 to 700 bp) were isolated. The POMC amino-terminal coding region of the cDNA insert in each of these clones was sequenced. These sequences encode the signal peptide region of the porcine POMC where recently two different protein sequences have been reported [11]. However, all of them showed the same sequence determined for the cDNA insert of pPIL31.

Discussion

The porcine POMC is different from the previously studied species in the variable region that has been termed the "connecting peptide" (see

Fig. 1); it is more related in this region to human and bovine POMC than to the POMC of rodents. The porcine γ-MSH peptide terminates with an Arg–Arg doublet (at position 89–90) followed by a hypervariable region, then another pair of basic amino acids residues Lys–Arg (position 107–108) followed by the somewhat more conserved region of the connecting peptide. The two rodent species each have an Arg–Arg pair at the end of a longer γ-MSH but lack the Lys–Arg pair further along the precursor protein. The hormone adrenocorticotropin starts at amino acid number 136 of the POMC peptide [24] and is preceded by an Arg–Lys pair that is also present at the same location in all other POMC species sequenced to date; rat [8], mouse [9], bovine [4] and man [5]. Combinations of the basic amino acids arginine and lysine also precede β-endorphin (position 235–236) and the γ-MSH (position 75–76) in all of these species. An arginine doublet occurs in the porcine sequence (position 176–177), as opposed to Lys–Arg in the other species; the effects, if any, of this difference on the maturation of POMC in porcine pituitary are unknown.

The variable region of the porcine POMC connecting peptide is also unusual in its composition as compared with other known POMC sequences. From position 91, a sequence of three serine residues is followed by eight glycines. The latter repetition might have arisen by duplication of the codon GGC in the porcine genome; this codon is slightly degenerate in the third position of some of the glycine-encoding triplets, showing two occurrences of thymine bases instead of cytosine. In the related POMC of human and bovine species, similar but less extensive repetitions of AGC, the codon for serine, occur.

Our analysis of genomic DNA hybridizing with POMC cDNA showed the presence of two separate bands. Analogous results have been observed in several other mammalian species [10], and in at least one species (i.e. the mouse) one of the POMC-hybridizable segments was found to be a pseudogene. Analysis by Northern blotting of RNA obtained from the porcine pars intermedia showed only a single band of 1300 bases. However, when messenger RNA isolated from porcine pituitary pars intermedia was translated in a cell-free system, two proteins bearing antigenic determinants of POMC resulted [11]. These two proteins showed differences in the sequence at the amino terminus. The unique porcine cDNA sequence we have obtained encodes the smaller form of POMC.

In probing through two separate cDNA libraries derived from porcine pars intermedia mRNA under conditions of hybridization allowing for 23% mismatch, we identified four separate clones having cDNA homologous to the 5′ end of the POMC. Nucleotide sequence analysis of these clones in the region corresponding to this segment (which corresponds to the region where differences were found in the porcine POMC protein) showed that all four isolates had a sequence identical to that of pPIL31. While our analysis does not exclude the possibility that two separate POMC mRNA species exist in the porcine pars intermedia, the probability of not finding both of these cDNAs with five separate sequences is small (less than 7%) if both are present in equal amounts as suggested by the results of cell-free translation and immunoprecipitation experiments [11].

While this manuscript was in preparation, Boileau et al. [28] reported a cDNA sequence encoding porcine POMC. The unique sequence shown is identical to ours for most of the coding sequence, with two differences in 700 bases. However, substantial differences were found in the signal peptide region, including our finding of a serine instead of a leucine in position 6, an alanine for a threonine in position 15 and six other silent changes. In all these controversial positions our sequence agrees with the partial one determined by Oates and Herbert [29].

Acknowledgments

We thank Dr. M. Uhler for providing porcine genomic DNA, Drs. E. Oates and E. Herbert for communicating certain of their unpublished results and Ms. Nancy Holt for careful typing of the manuscript. This work was supported by NIH grant GM 27241. F.J.G. was a fellow of the Fond de la recherche en santé du Quebec.

References

1 Mains, R.E and Eipper, B.A. (1976) J Biol. Chem. 251, 4115–4120

2 Roberts, J.L. and Herbert, E. (1977) Proc. Natl. Acad. Sci. USA 74, 4826–4830

3 Chretien, M., Benjannet, S., Gossard, F., Gianoulakis, C., Crine, P., Lis, M. and Seidah, N.G (1979) Can. J Biochem. 57, 1111–1121

4 Nakanishi, S, Inoue, A., Kita, T., Nakamura, M, Chang, A.C.Y., Cohen, S.N. and Numa, S. (1979) Nature 278, 423–427

5 Chang, A.C.Y., Cochet, M. and Cohen, S.N (1980) Proc Natl. Acad. Sci. USA 77, 4890–4894

6 Takahashi, H, Hakamata, Y., Watanabe, Y., Kikuno, R., Miyata, T and Numa, S. (1983) Nucleic Acids Res. 11, 6847–6858

7 Whitfeld, P.L., Seeburg, P H and Shine, J. (1982) DNA 1, 133–143

8 Drouin, J. and Goodman, H.M (1980) Nature 288, 610–613

9 Uhler, M and Herbert, E. (1983) J. Biol Chem. 258, 257–261

10 Uhler, M., Herbert, E., D'Eustachio, P. and Ruddle, F D. (1983) J Biol Chem. 258, 9444–9453

11 Boileau, G, Gossard, F., Seidah, N.G. and Chretien, M. (1983) Can J. Biochem. 61, 333–339

12 Chang, A C.Y., Nunberg, J.H., Kaufman, R.J. Erlich, H.A., Schimke, R.T. and Cohen, S.N. (1978) Nature 275, 617–624

13 Huynh, T.V, Young, R.A. and Davis, R.W. (1984) in DNA Cloning Techniques: A Practical Approach (Glover, D.M., ed), IRL Press, Oxford. in the press

14 Rigby, P.W J. Dieckmann, M., Rhodes, C and Berg, P (1977) J. Mol. Biol. 113, 237–251

15 Boyer, H W and Roulland-Dussoix, D. (1969) J. Mol. Biol 41, 459–472

16 Thayer, R.E. (1979) Anal. Biochem. 98, 60–63

17 Benton, W.D and Davis, R.W. (1977) Science 196, 180–182

18 Denhardt, D. (1966) Biochem. Biophys Res. Commun 23, 641–652

19 Maxam, A.M and Gilbert, W (1980) Methods Enzymol 65, 499–560

20 Maniatis, T., Fritsch, E.F. and Sambrook, J. (1980) Molecular Cloning, pp 202–203, Cold Spring Harbor Laboratory, NY

21 Thomas, P. (1980) Proc. Natl. Acad. Sci. USA 77, 5201–5205

22 Southern, E.M. (1975) J. Mol Biol. 98, 503–517

23 Nakanishi, S, Teranishi, V., Watanabe, Y., Notake, M, Noda, M., Kakidani, H, Jingami, H and Numa, S. (1981) Eur. J. Biochem. 115, 429–438

24 Sheperd, R.G., Willson, S.D, Howard, K.S., Bell, P.H, Davies, D S., Davis, S.B, Eigner, E.A. and Shakespeare, N.E. (1956) J. Am. Chem. Soc. 78, 5067–5076

25 Gilardeau, C. and Chretien, M. (1972) in Chemistry and Biology of Peptides (Proceedings of the Third American Peptide Symposium) pp. 609–611, Ann Arbor Science Pub, Ann Arbor, MI

26 Lariviere, N., Seidah, N G. and Chretien, M (1981) Int. J. Peptide Protein Res. 18, 487–491

27 Boileau, G., Lariviere, N., Hsi, K L., Seidah, N.G and Chretien, M. (1982) Biochemistry 21, 5341–5346

28 Boileau, G., Barbeau, C, Jeannotte, L., Chretien, M and Drouin, J. (1983) Nucleic Acids Res. 11, 8063–8071

29 Oates, E. and Herbert, E (1984) J Biol. Chem 259, 7421–7427

Biochimica et Biophysica Acta 866 (1986) 75–82
Elsevier

BBA 91561

Effects of addition of derived 40 S subunits on translation rate and polysome profile of the reticulocyte lysate

Piet W.L. Tas * and Oskar H.W. Martini

Institute of Virology and Immunology, Versbacher Strasse 7, D-8700 Wurzburg (F R G)

(Received September 19th, 1985)

Key words: 40 S ribosomal subunit; Translation rate, Protein synthesis, Polysome profile, 48 S initiation complex, (Rabbit reticulocyte)

We have investigated the way in which the addition of exogenous 40 S subunits to a reinitiating cell-free translation system, prepared from reticulocytes, may affect translational parameters of the system. The disturbance of the system's subunit stoichiometry resulted in the following changes in the ribosome profile: (1) rapid exhaustion of the pool of native 60 S subunits; (2) appearance of humps on the peaks of the polysome profile, which probably represent unusually long-lived [40 S • polysomal] complexes; (3) at higher doses of exogenous particles, the amount of polysomes decreased. This latter effect reflected a corresponding decrease in the overall translation (i.e. initiation) rate. The phenomena are interpreted as follows: exogenous 40 S subunits combine with 60 S subunits, forming idle 80 S ribosomes. The shortage of 60 S subunits delays the utilization of [40 S • polysomal] complexes, which is compensated for by a pool increase of these complexes. At high 40 S subunit doses this compensatory mechanism fails, and the 60 S shortage begins to determine the overall translation rate. The observations underline that the various translational parameters of the lysate function in an optimally concerted manner, so that only small amounts of derived 40 S subunits are tolerated by the system for analysis.

Introduction

The physiological significance of the phosphorylation of the ribosomal protein S6 located at the mRNA binding site of the 40 S ribosomal subunit [1,2] has remained elusive. On the basis of in vivo observations Duncan and McConkey [3] have claimed that a high degree of 40 S phosphorylation in protein S6 improves the particles' likelihood of becoming engaged in protein synthesis. Attempts to substantiate this claim by in vitro studies using a variety of systems have failed so far [4–7], with the possible exception of one system in which poly(AUG) was employed as message [8]. An obvious approach to arrive at meaningful results would be to add 40 S particles of a defined state of phosphorylation to a reinitiating cell-free translation system and compare the recruitment rates of 40 S subunits of different degrees of phosphorylation.

We have addressed this latter aspect. We noticed, while trying to study the physiological significance of S6 phosphorylation, that the ribosomal subparticle stoichiometry of cell-free translation systems is delicately balanced. A disturbance of this balance by increasing the amount of 40 S subunits in the system will lead to a lag in the utilization of mRNA-bound preinitiation complexes. If the lag increases it will become the rate-limiting step for protein synthesis, as shown here.

---

* To whom correspondence should be addressed

0167-4781/86/$03 50 © 1986 Elsevier Science Publishers B V (Biomedical Division)

Materials and Methods

Materials

Joklik-modified Eagle's medium (JMEM) was obtained from GIBCO. Ingredients for the cell-free system, anisomycin and cycloheximide were purchased from Sigma. Puromycin was obtained from Serva and radioactive methionine (1310 Ci/mmol) from Amersham.

Preparation of derived ribosomal subunits

Young rabbits (approx. 2.8 kg), purchased from farmers, were made anemic by injection of a 2.5% phenylhydrazine solution (0.3 ml/kg on five consecutive days). On the 7th day the anesthetized and heparinized animals were exsanguinated by heart puncture. The blood was collected in ice-cold wash buffer (140 mM NaCl, 5 mM KCl, 5 mM $MgCl_2$) and all further operations were carried out at 0–4°C unless stated otherwise. The cells were sedimented by centrifugation (8 min, 3500 rpm) in a GSA Sorvall rotor and washed three times with 150 ml wash buffer. The cells were weighed and lysed with 2.5 vol. (referring to the weight of packed cells) of lysis medium (4 mM $MgCl_2$, 20 mM β-mercaptoethanol). One-seventh volume (referring to lysate volume) of compensating solution (150 mM KCl, 1.5 M sucrose) was added immediately after lysis. The lysate was centrifuged (15 min, 15000 rpm) in an SS 34 Sorvall rotor, and the postmitochondrial supernatant was layered over a discontinuous sucrose gradient (5 ml of 27% over 5 ml of 45% w/v) sucrose solution in step gradient buffer: 50 mM KCl, 3 mM magnesium acetate, 15 mM β-mercaptoethanol, 20 mM Hepes-KOH (pH 7.4; 18°C) and centrifuged in thick-wall polycarbonate tubes for 6 h at 36000 rpm in a Ti 50.2 Beckman rotor. The supernatant and the top 4 ml of the cushion were discarded.

The ribosomal pellets were suspended in release buffer (500 mM KCl, 3.5 mM magnesium acetate, 20 mM Tris-HCl (pH 7.6), 15 mM β-mercaptoethanol); the suspension was cleared of poorly suspending material by a 5 min centrifugation in an Eppendorf table centrifuge, and the polysomes were incubated for 25 min at 37°C with 1 mM puromycin [9]. The ribosomal subunits were separated by centrifugation in an SW 27 Beckman rotor (18°C, 7 h, 24000 rpm) through an exponential sucrose gradient (formed with 20 ml 10% and 40 ml 50% w/v sucrose solutions) in high salt gradient buffer (500 mM KCl, 5 mM magnesium acetate, 30 mM Tris-HCl (pH7.6), 15 mM β-mercaptoethanol). The gradients were fractionated according to their A_{254} profile so that contamination of 40 S subunits with 60 S subunits was carefully avoided. With 1.6 vol. of compensating buffer (25 mM magnesium acetate, 20 mM KCl, 20 mM Tris-HCl (pH 7.6), 15 mM β-mercaptoethanol) the salt concentrations of the subunit fractions were adjusted to 18 mM magnesium acetate and 200 mM KCl, and the subunits were sedimented in thick-wall polycarbonate tubes in a Ti 50.2 rotor (18 h, 35000 rpm). They were resuspended in ribosome buffer (3 mM magnesium acetate, 80 mM KCl, 15 mM Tris-HCl, pH 7.6) to a concentration of 100 A_{260} units 40 S subunits per ml.

Cell-free system

The rabbit reticulocyte lysate was prepared as described [10]. The reaction mixture for studying endogenous protein synthesis contained in a volume of 50 μl: 35 μl reticulocyte lysate supplemented with hemin (20 μM final) and creatine kinase (EC 2.7.3.2) (50 μg/ml final), 8 μM creatine phosphate, 80 mM KCl, 0.4 mM $MgCl_2$, 200 μM of unlabelled amino acids (without methionine) and 5 μCi of L-[^{35}S]methionine (1310 Ci/mmol). Some lysates showed more linear incorporation kinetics when adenine or 2-aminopurine was added to a final concentration of 6 mM. Incubation was at 30°C; protein synthesis was assayed as described [10].

Gradient analysis of polysome profiles

Incubation mixtures were diluted 1:2 with gradient buffer (20 mM Tris-HCl (pH 7.5), 100 mM KCl, 5 mM magnesium acetate) and loaded onto 12–50% isokinetic sucrose gradients in gradient buffer and centrifuged for 2 h at 36000 rpm in a Beckman SW 41 rotor. After centrifugation the contents of the tube were monitored with an Isco type 4 optical unit connected to a recorder.

For the analysis in Fig. 1 a modified gradient buffer (for details see legend) was used in order to prevent unspecific penetration of radioactive material into the gradient.

Labelled ribosomal subunits

HeLa S3 cells were suspended in 1 litre of a phosphate-free medium which was a modification of JMEM, containing 30 mM Hepes (pH 7.4), twice the normal amount of amino acids and 1.5 g instead of 1 g glucose/l. Carrier-free [^{32}P]orthophosphate (1.5 μCi/ml) was added; this was followed by the addition of 120 ml of horse serum and, 30 min later, by 120 ml of unmodified JMEM. The cell density was $3.8 \cdot 10^5$ cells/ml. The pH of the culture was kept between 7.0 and 7.4, and after 2 days the cells were collected on phosphate-buffered saline-ice. All further preparative work was performed at 4°C unless stated otherwise. The cells were washed three times with phosphate-buffered saline ($1000 \times g$, 5 min) and finally broken by suspension in 6 vol. (referring to weight of packed cells) of lysis medium which contained 5% (w/v) sucrose, 40 mM KCl, 3 mM magnesium acetate, 10 mM KF, 25 mM $KHPO_4$ buffer (pH 7.4), 0.5% (v/v) Triton X-100 and 15 mM β-mercaptoethanol. The supernatant of a 15 min centrifugation at 9000 rpm in an SS 34 Sorvall rotor was adjusted to 1% deoxycholate (using a 10% (w/v) stock solution) and layered over two layers of sucrose (5 ml 27.5% over 5 ml 45% sucrose in 40 mM KCl, 3 mM $MgCl_2$, 10 mM KF, 10 mM $KHPO_4$ buffer, pH 7.4) and centrifuged for 6 h at 36000 rpm in a Ti 50.2 Beckman rotor in thick-wall polycarbonate tubes. The sedimented ribosomes were resuspended in release buffer (480 mM KCl, 7 mM KF, 7 mM $KHPO_4$ buffer, 3.5 mM magnesium acetate, 15 mM β-mercaptoethanol, 20 mM Tris-HCl, pH 7.5) and incubated with 1 mM puromycin for 25 min at 37°C. The HeLa ribosomal subunits were then isolated exactly as described for reticulocyte ribosomal subunits.

Results

Ribosomes, ^{32}P-labelled in their RNA moiety, were prepared from HeLa cells grown in the presence of $^{32}PO_4$. The ribosomes were dissociated into subunits using puromycin in the presence of a high-salt buffer [9]. The biological activity of the 40 S subunits was judged by competition analysis: small amounts of subparticles were added to a cell-free translation system, prepared from rabbit reticulocytes, and allowed to compete with the endogenous unlabelled subunits for recruitment into the polysome fraction (Fig. 1). From the steady-state radioactivity distribution over the ribosomal subpopulations of 40 S, 80 S and polysomal particles, we calculated, by reference to a theoretical model (to be published elsewhere), that 80% of the exogenous 40 S subunits can be regarded as being biologically indistinguishable from the endogenous 40 S subunits of the translation system.

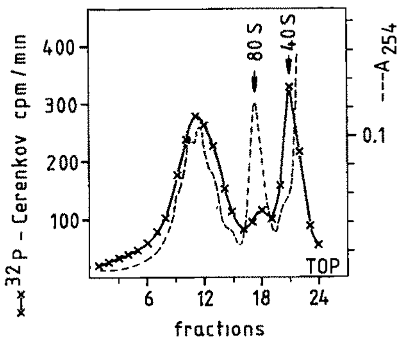

Fig. 1. Distribution of ^{32}P-labelled 40 S over 40 S, 80 S and polysome fractions of a reticulocyte lysate after 4 min incubation at 30°C A reticulocyte lysate (200 μl) supplemented with all the components necessary for protein synthesis was preincubated for 1 min at 30°C to bring the reaction mixture to the desired temperature. Then 0 057 A_{260} units of 40 S particles (labelled with ^{32}P in the rRNA moiety) were added and incubation continued for 4 min The reaction was stopped by the addition of 300 μl cold gradient buffer (50 mM Tris-HCl (pH 7.5), 150 mM KCl, 5 mM $MgCl_2$, 0.1% Triton X-100). The sample was then loaded onto a 10–50% isokinetic sucrose gradient in gradient buffer and centrifuged for 110 min at 36000 rpm in an SW 41 rotor. Fractions of 20 drops were collected from the bottom of the gradient and the absorbance at 254 nm was monitored with an Isco type 4 optical unit connected to a recorder The direction of sedimentation is from left to right.

In order to obtain reliable data on the biological activity of 40 S subunit preparations by this approach, it was important not to exceed a certain critical dose of exogenous particles added to the translation system. This was concluded from the following observation. At low doses of exogenous particles the distribution of the exogenous 40 S subunits over native 40 S and polysome region remained constant (Table I); however, at higher doses the percentage of the 40 S subunits entering the polysome region decreased. At the same time

TABLE I

EFFECT OF THE DOSE OF ^{32}P-LABELLED 40 S SUBUNITS ADDED TO A RETICULOCYTE LYSATE ON THE STEADY-STATE DISTRIBUTION OF RADIOACTIVITY

Increasing amounts of salt-washed 40 S subunits from HeLa ribosomes, labelled during biosynthesis with ^{32}P in the rRNA moiety, were added to a reticulocyte lysate (final volume 200 μl). Incubation was for 6 min at 30°C. The reaction was stopped with 300 μl cold gradient buffer containing 100 μg/ml cycloheximide. The mixture was then analyzed on 10–50% w/v isokinetic sucrose gradients as described in Materials and Methods Using the absorbance profile as guidance, the percentage of the total radioactivity present in the polysomal region of the gradient was calculated The incubation mixture contained 1.87 A_{260} units of reticulocyte ribosomes.

	Dose of 40 S subunits		Radioactivity in polysomes (%)
	as A_{260}	as % of endogenous 40 S	
1	0.023	1.25	47
2	0.046	2.50	47
3	0.092	5	47
4	0.138	7.5	47
5	0.187	10	37
6	0.374	20	13

we observed a decrease in the polysome content of the translation system.

This observation prompted us – because of implications for 40 S subunit activity studies – to examine in more detail the effect of a disturbance of subunit stoichiometry on translational parameters. The first question to be answered was whether the deterioration of the polysome profile reflected an inhibition of translation. Therefore, translation rates were determined as a function of the stoichiometric imbalance of subparticles (Fig. 2) and the results were compared with the changes of the ribosome profile (Fig. 3 and Table II). For this and further analyses unlabelled 40 S subunits derived from reticulocyte ribosomes could be used, since their addition to the translation system had exactly the same dose-dependent effect on the various parameters studied as that of labelled HeLa subunits (data not shown).

Fig. 2 shows that the [^{35}S]methionine incorporation into protein decreased with increasing concentrations of exogenous 40 S particles. The incorporation was reduced to 65–75% of the control when the amount of exogenous particles equalled that of the endogenous 40 S involved in the ribosome cycle (which excludes the 40 S in messenger-free ribosomes from the calculation). Since the polysomes of such lysates (Fig. 3) deteriorated to the same extent as the translation rate, as shown in Table II, we have to assume that initiation is the inhibited process. We wondered whether this effect reflected the presence of damaged particles in our 40 S preparation. If such particles were functional with respect to factor binding but non-functional with respect to mRNP binding or mRNP passage, they might critically reduce the amount of factors available to the fully functional subunits. Addition of purified factors, however, did not have any effect on the level of inhibition (result not shown).

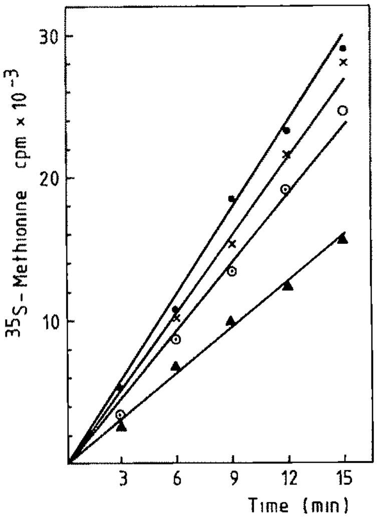

Fig. 2. Effect of the addition of derived 40 S subunits on the [^{35}S]methionine incorporation into protein in a reticulocyte lysate translating endogenous mRNA. Incubation in a final volume of 50 μl was at 30°C. At the start of incubation the following amounts of derived 40 S subunits suspended in 4 μl of ribosome buffer were added: none (●), 0.068 A_{260} (x), 0.136 A_{260} (O) and 0.272 A_{260} (▲). The added 40 S amounted to 40%, 80% and 160%, respectively, of the actively cycling 40 S At intervals of 3 min, samples of 6 μl were withdrawn and processed as described in Materials and Methods.

Interestingly, the quantitative changes of the profile were accompanied by qualitative changes: on the leading edges of the polysome peaks, most clearly visible on those of dimers and trimers, shoulders or even humps could be observed. Con-

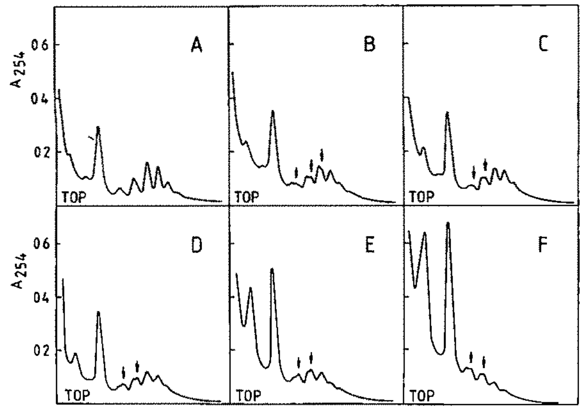

Fig. 3. Effect of the addition of derived 40 S subunits on the polyribosome profile of a reticulocyte lysate. To 96 μl of lysate, supplemented with all the ingredients necessary for protein synthesis, were added, in a volume of 4 μl, the following amounts of derived 40 S subunits: A, none; B, 0.034 A_{260}; C, 0.068 A_{260}, D, 0.136 A_{260}; E, 0.272 A_{260}; F, 0.544 A_{260}. After 9 min at 30°C the reaction was stopped with 200 μl cold gradient buffer (50 mM Tris-HCl (pH 7.5), 100 mM KCl, 5 mM magnesium acetate) containing 100 μg/ml cycloheximide. The mixtures were loaded onto 12–50% isokinetic sucrose gradients in gradient buffer and centrifuged for 2 h at 36000 rpm in a Beckman SW 41 rotor. The direction of sedimentation is from left to right.

comitantly with these changes the peak in the 60 S region, probably mainly representing native 60 S subunits, had begun to dwindle (Fig. 3).

As to the nature of the humps, the *s* values suggested that they might be caused by the binding of 40 S subunits, possibly as preinitiation complexes, to polysomes. We checked for extra 40 S subunits in these polysomes by collecting di-, tri- and tetrasomes with humps and concentrating them by centrifugation. The mRNA was destroyed by limited digestion with RNAase and the material was analyzed on 12–50% sucrose gradients. A small 40 S peak could be detected beside a huge 80 S peak (not shown). This 40 S peak was not present in the gradients when (as a control) polysomes free of humps were subjected to the same analysis.

TABLE II

TRANSLATION RATE AND POLYSOME CONTENT OF A RETICULOCYTE LYSATE TO WHICH INCREASING AMOUNTS OF 40 S SUBUNITS WERE ADDED

The data in the table are derived from Figs. 2 and 3. The [^{35}S]methionine incorporation and polysome content are expressed as percentages of the controls. [^{35}S]Methionine incorporation and polysome content of lysate incubated in the absence of derived 40 S served as controls.

Added 40 S as % of cycling 40 S	[^{35}S]Methionine incorporation (% of control)	Polysomes (% of control
–	100	100
40	90	92.1
80	78.6	76.9
160	54	49.6

Having ascertained that 40 S particles were involved, we considered the nature of their binding to mRNP; were they properly bound as parts of preinitiation complexes or were they only associated with message in a nonspecific manner? The fact that humps survive centrifugation in sucrose gradients containing 100 mM KCl, 5 mM magnesium acetate and 50 mM Tris-HCl points at their stability and argues for specific 40 S subunit binding. The following experiment supports our conclusion; it shows that protein synthesis is a prerequisite for hump formation. We set a complete translation block with $5 \cdot 10^{-4}$ M aniso-

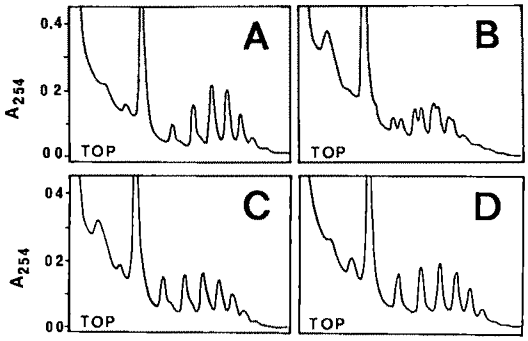

Fig. 4. Effect of the elongation inhibitor anisomycin on the appearance of humps in the polysome profile of a translating cell-free system containing exogenous 40 S subunits. Incubation in a final volume of 100 μl was for 6 min at 30°C without addition of exogenous 40 S subunits (A); with 0.14 A_{260} of 40 S subunits (B); with 0.14 A_{260} of 40 S subunits + $5 \cdot 10^{-4}$ M anisomycin (C), with $5 \cdot 10^{-4}$ M anisomycin but without exogenous 40 S subunits (D). The reaction was stopped with 200 μl cold gradient buffer containing 100 μg/ml cycloheximide. The mixtures were loaded onto 12–50% isokinetic sucrose gradients in gradient buffer and centrifuged for 2 h at 36000 rpm in a Beckman SW 41 rotor. Direction of sedimentation is from left to right

mycin, an inhibitor of elongation, before we added 40 S subunits to the lysate. Humps were barely detectable, although in the control assays which lacked anisomycin but received the same dose of exogenous 40 S subunits humps showed up impressively (Fig. 4). Had hump formation been due to non-specific binding to mRNA of the naked 40 S subunits, we would have expected to find hump formation independently of whether protein synthesis was blocked or not.

The foregoing experiments indicate that the humps represent preinitiation complexes. but they do not allow us to comment on whether these complexes are competent for the last assembly reaction, i.e. 60 S subunit binding. If they simply owed their longevity to the shortage of 60 S particles (we have shown above that appearance of humps coincided with dwindling of 60 S subunits (Fig. 3)) they should vanish upon addition of exogenous 60 S subunits. A reticulocyte lysate was incubated with derived 40 S subunits for 4 min at 30°C, which led to the appearance of humps (Fig. 5A); derived 60 S subunits were added, and the incubation was continued for 1 min. The humps were missing when this incubation mixture was analyzed on a gradient (Fig. 5B). As we found later, addition of 60 S at 0°C suffices to make humps disappear.

We wished to demonstrate that really mRNP-bound 80 S complexes had formed; this would exclude the possibility that 60 S subunits had merely been instrumental in somehow removing the 40 S subunit from the message. We isolated tetra- and pentasomes from a gradient with conspicuous humps. We concentrated the material by centrifugation, resuspended it, added 60 S particles to a portion of it and analyzed this portion and the 60 S-free control on sucrose gradients. Fig. 6 shows the profiles. Apparently material from the lighter peak was chased into the heavier peak and the loss in the tetramer region was only partially compensated for by a gain from the small trimer peak. One may interpret this observation as showing that 80 S initiation complexes were generated by the binding of naked derived 60 S subunits to preinitiation complexes.

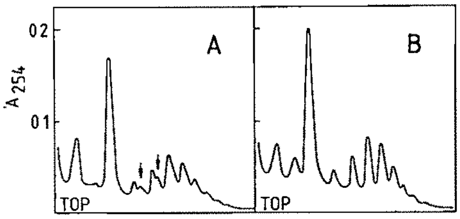

Fig 5. Effect of addition of 60 S subunits on the humps in the polysome profile A reticulocyte lysate (100 μl) was incubated with 0 08 A_{260} of derived 40 S subunits. After 4 min at 30°C the reaction was stopped with 10 μl 10^{-4} M anisomycin followed by the addition of 3 μl ribosome buffer (A) or 0.2 A_{260} 60 S particles in 3 μl ribosome buffer (B). After an additional minute of incubation, the reaction mixtures were diluted with 200 μl cold gradient buffer and centrifuged on 12–50% isokinetic gradients for 2 h at 36000 rpm in an SW 41 rotor. The direction of sedimentation is from left to right.

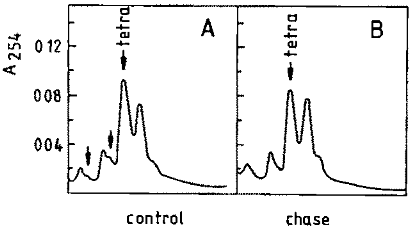

Fig 6 Effect of addition of 60 S subunits on shoulders in the tetra- and pentasome peak. A reticulocyte lysate was incubated for 4 min at 30°C in the presence of 0 08 A_{260} of derived 40 S subunits in 100 μl incubation mixture. This material was centrifuged on 12–50% isokinetic gradients and the tetra- and pentasome peaks of several gradients were collected, diluted 2-fold with ribosome buffer and concentrated for 10 h at 38000 rpm in a Ti 50.1 rotor. Pellets were gently resuspended in ribosome buffer and left standing on ice for 5 h To one part of the resuspended polysomes were added 3 μl ribosome buffer and to the other part 0.2 A_{260} of 60 S subunits in 3 μl ribosome buffer. The material was then loaded on 12–50% isokinetic gradients and centrifuged for 110 min at 36000 rpm in an SW 41 rotor. The direction of sedimentation is from left to right

Since naked 60 S subunits sufficed to convert [40 S · polysomal] complexes into [80 S · polysomal] complexes, the most likely explanation is that eIF-5 had already interacted with the [40 S · polysomal] complex to release eIF-2 and eIF-3 [11].

Discussion

Derived 40 S subunits added to a cell-free translation system interfered with the process of protein synthesis in a dose-dependent manner. Two degrees of severity of this interference could be distinguished. (A) At low doses of exogenous 40 S particles translation was sustained at a normal rate, but the following changes occurred in the ribosome profile: the pool of native 60 S subunits dwindled and humps appeared on the leading edges of the polysome peaks. (B) At higher doses of exogenous 40 S particles, translation rates deteriorated and the amounts of polysomes decreased correspondingly, which identifies initiation as the inhibited process and rules out elongation.

The mechanism leading to shortage of native 60 S subunits

Purified 40 S/60 S subunit couples are known to dissociate readily when exposed to KCl concentrations of 500 mM and higher [12]. The subparticles reassociate upon return to physiological ion concentrations. It is likely that this association reaction can also occur in actively translating lysates. Both reaction partners may have to be naked. The exogenous 40 S particles were added in this state. Cycling 60 S particles may pass through the state of nakedness upon completion of a peptide chain (run-off particles) and before becoming complexed with anti-association factor [13,14]. As a result of the association with 40 S subunits, the 60 S subunits will enter the pool of mRNA-free 80 S ribosomes (note the increase in the monosome peak in Fig. 3E and F). The following observation is consistent with the proposed mechanism, which regards subunit cycling as a prerequisite for the depletion of the pool of native 60 S subunits. The depletion was not observed when the effect of exogenous 40 S subunits was studied at low (4°C) instead of normal (30°C) incubation temperature.

The effect of the shortage of native 60 S subunits on the life span of mRNA-bound preinitiation complexes and on protein synthesis

Situation A. Due to the shortage of 60 S particles the [40 S · polysomal] complexes will have to wait longer than normal for a 60 S partner. This means that the rate of consumption of these complexes is, temporarily, reduced, while the rate of formation remains normal (if it is not even slightly increased, temporarily, due to the abundance of functional 40 S subunits). Since influx of 40 S subunits into the pool of messenger-bound 40 S subunits exceeds efflux, the pool size will grow. As the [40 S · polysomal complexes] become more numerous the chances of run-off 60 S particles hitting such a complex improve. (This implies that 60 S subunits can bypass the native state). The growth of the pool of [40 S · polysomal] complexes comes to a stop when the rate of engagement of 60 S particles is back to normal. Thus under steady-state conditions the rates of initiation and of protein synthesis will be normal, only the pool of [40 S · polysomal] complexes will have expanded, which is what we see.

Situation B. If the dose of exogenous 40 S particles is increased further, their competition for run-off 60 S becomes more severe and the delay of each individual [40 S · polysomal] complex will increase correspondingly. The pool size of these complexes, however, cannot grow indefinitely, since the number of AUG-initiation codons to which these complexes are bound is limited. The critical requirement for the fully adaptive growth of the pool was that the formation rate of [40 S · polysomal] complexes be normal. This condition is no longer fulfilled, perhaps for the simple reason that too many initiation codons are blocked by the lingering 40 S subunits. Thus the utilization of these complexes has become the rate-limiting step for the whole translation process.

Shoulders at undisturbed subunit stoichiometry

Shoulders have been observed in ribosome profiles after incubation of reticulocyte lysates with NaF [15–17]. The inhibitor prevents the 60 S subunit from binding to the preinitiation complex. After removal of the inhibitor 80 S complexes can be formed [16].

Shoulders on di-, tri- and tetrasome peaks, comparable with those described here, can be found elsewhere in the literature [18,19] but have not been discussed by the authors. In the work cited in the appearance of shoulders was not accompanied by a disappearance of the native 60 S peak, which suggests that mechanisms other than those described here were responsible for the effects. The ease with which humps can be generated if one interferes with subparticle stoichiometry and, on the other hand, their rareness in unmanipulated lysates indicate that a number of steps of protein synthesis are delicately balanced in unmanipulated lysates.

Significance of the system for the study of S6 phosphorylation

From the results presented here it is evident that only small doses of 40 S subunits which do not disturb the stoichiometric balance of the lysate should be added for analysis. This approach will allow us to test the postulate of Duncan and McConkey that highly phosphorylated 40 S are preferentially engaged in translation [3]. Because the reticulocyte lysate does not tolerate high doses of 40 S subunits, effects of phosphorylation on overall translation rate cannot be analyzed.

Acknowledgement

We thank Ms. Ute Walter for skillful technical assistance, Mrs. Christel Stoppe for typing the manuscript and Professor E. Wecker for laboratory facilities and discussion. This project was supported by a grant from the Deutsche Forschungsgemeinschaft (SFB 105).

References

1 Terao, K. and Ogata, K. (1979) J. Biochem 86, 605–617.
2 Bommer, U.A., Noll, F, Lutsch, G. and Bielka, H. (1980) FEBS Lett. 111, 171–174
3 Duncan, R. and McConkey, E H (1982) Eur J Biochem. 123, 535–538.
4 Eil, C and Wool, I G (1973) J. Biol. Chem. 248, 5130–5136
5 Krystosek, A., Bitte, L F, Cawthon, M.L. and Kabat, D (1974) in Ribosomes (Nomura, M., Tissières, A. and Lengyel, P., eds.), pp. 850–870, Cold Spring Harbor, New York.
6 Leader, D.P., Thomas, A. and Voorma, H O (1981) Biochim. Biophys. Acta 656, 69–75.
7 Mastropaolo, W. and Henshaw, E.C. (1981) Biochim. Biophys. Acta 656, 246–255.
8 Burkhard, S.J. and Traugh, J A (1983) J Biol. Chem. 258, 14003–14008.
9 Blobel, G. and Sabatini, D. (1971) Proc Natl. Acad. Sci. USA 68, 390–394
10 Pelham, M R.B and Jackson, R.J (1976) Eur. J. Biochem. 67, 247–256.
11 Peterson, D.T., Safer, B and Merrick, W.C (1979) J. Biol Chem 254, 7730–7735
12 Martin, T.E. and Wool, I.G. (1969) J. Mol Biol. 43, 151–161
13 Russell, D W. and Spremulli, L.L (1980) Arch. Biochem. Biophys. 201, 518–526.
14 Valenzuela, D., Chaudhuri, A. and Maitra, U. (1981) Fed. Proc 40, 1749.
15 Hoerz, W. and McCarthy, K.S. (1969) Proc. Natl Acad Sci USA 63, 1206–1213.
16 Hoerz, W. and McCarthy, K.S. (1971) Biochim. Biophys. Acta 228, 526–535
17 Lebleu, B., Marbaix, G., Wérenne, J., Burny, A. and Huez, G. (1970) Biochem. Biophys Res. Commun. 40, 731–739.
18 Safer, B., Kemper, W., and Jagus, R. (1978) J. Biol. Chem 253, 3384–3386.
19 Ranu, R.S. (1983) Proc. Natl. Acad Sci USA 80, 3148–3152.

Biochimica et Biophysica Acta 866 (1986) 83–88
Elsevier

BBA 91529

A *Drosophila* RNA polymerase II cell-free DNA-dependent transcription system

Alan McLachlan * and Patrick Lin

Department of Biochemistry and Molecular Biology, Harvard University, 7 Divinity Avenue, Cambridge, MA 02138 (U.S.A.)

(Received September 13th, 1985)

Key words: RNA polymerase II gene, Transcription; Cell-free system, (*Drosophila*)

A simple procedure is described for the preparation from nuclei of *Drosophila* cells of a soluble system which directs accurate transcription initiation from *Drosophila* RNA polymerase II promoters.

Introduction

Systems capable of faithful transcription in vitro are essential for the identification of transcription factors and regulatory molecules required for expression of RNA polymerase II genes. Three different in vitro transcription extracts made from human cell lines have been described [1–3]. RNA polymerase II in vitro transcription systems prepared from silkworm, chicken and *Drosophila* cells have also been reported [4–7]. Here we report the development and optimization of a particularly simple and reproducible RNA polymerase II in vitro transcription system from *Drosophila* cells, differing in a number of respects, including extraction procedure, from that reported by Parker and Topol [5]. Also, we describe the effects of varying individual parameters of the system on the yield of transcript, using a cloned *Drosophila* tubulin gene as template.

Methods

Preparation of nuclear extract

The cell line used was the K line of Echalier adapted by him to growth without serum [8]. It was obtained from P. Cherbas, designated Kc0% [9]. Soluble extracts were prepared from nuclei using modifications of the procedure described by Dignam et al. for HeLa cells [1]. The cells were grown at 25°C in suspension culture in D-22 medium without serum [8]. Extracts were prepared from batches of cells (1–4 litres) with a density of $(3\text{–}6)\cdot 10^6$ cells/ml. All operations were done at 0–4°C. Cells were harvested from culture by centrifugation for 10 min at 2000 rpm in a Sorvall GS3 rotor ($675\times g$). Pelleted cells were washed once in 40–80 ml of 10 mM sodium phosphate (pH 6.8), 0.14 M NaCl, 1.5 mM $MgCl_2$ by suspension and recentrifugation for 5 min at 3200 rpm in a model CL International Clinical Centrifuge ($1600\times g$). The cell pellet was suspended in 5 vol. of hypotonic buffer (10 mM Hepes-NaOH (pH 7.5), 10 mM KCl, 1.5 mM $MgCl_2$, 0.5 mM dithiothreitol, 0.5 mM PMSF) and allowed to stand for 10 min. Cells were collected by centrifugation for 5 min at 3200 rpm in the clinical centrifuge, suspended in 2 vol. of hypotonic buffer and lysed by 10–15 strokes of an all-glass Dounce Homogeniser (A-type pestle). Cell lysis was more than

---

* To whom correspondence should be sent at (present address). Department of Basic and Clinical Research, Scripps Clinic and Research Foundation, 10666 North Torrey Pines Road, La Jolla, CA 92037, U.S.A.

Abbreviation PMSF, phenylmethylsulfonyl fluoride

90%. The homogenate was centrifuged for 10 min at 5000 rpm in a Sorval SS34 rotor (3000 × g) and the supernatant was carefully poured off to leave a loose nuclear pellet. This was recentrifuged for 20 min at 15 000 rpm in the SS34 rotor (27 000 × g) and the supernatant was decanted. The pellet was resuspended in an equal volume of nuclear extraction buffer (20 mM Hepes-NaOH (pH 7.6), 25% (v/v) glycerol, 0.3 M naCl, 1.5 mM $MgCl_2$, 0.2 mM EDTA, 0.5 dithiothreitol, 0.5 mM PMSF), and the nuclei were lysed with 10 strokes of the homogeniser. The lysate was rocked gently on a shaking platform if the volume was less than 2 ml and stirred gently with a magnetic stirring bar when the total volume was larger. Either procedure was performed for 30 min and then the lysate was centrifuged for 30 min at 15 000 rpm in the SS34 rotor. The supernatant was decanted and dialysed for 5 h against 50 vol. of 20 mM Hepes-NaOH (pH 7.6), 20% (v/v) glycerol, 100 mM KCl, 0.2 mM EDTA, 0.5 mM dithiothreitol, 0.5 mM PMSF. The dialysate was clarified by centrifugation for 20 min at 15 000 rpm in the Sorvall SS34 rotor and the supernatant was frozen in aliquots in liquid N_2 and stored at −80°C.

In vitro transcription analysis

Standard reaction mixtures (25 μl) were made up by combining the following: 10 μl of 20 mM Hepes-NaOH (pH 7.6), 20% (v/v) glycerol, 70 mM KCl, 0.2 mM EDTA, 0.5 mM dithiothreitol, 0.5 mM PMSF; 5 μl of 2.5 mM ATP, 2.5 mM CTP, 2.5 mM GTP, 125 μM UTP containing 10 μCi [α-^{32}P]UTP; 4 μl of 5 mM Tris-HCl (pH 7.5), 1 mM EDTA containing 200–300 pg of template DNA and 1 μl of 0.1 M $MgCl_2$. Transcription reactions were initiated by adding 5 μl of nuclear extract (30–50 μg protein) and were incubated at 20°C for 90 min. The reactions were stopped by adding 375 μl 0.3 M ammonium acetate, 0.1% SDS, 25 μg/ml tRNA and were extracted with an equal volume of phenol/chloroform/isoamyl alcohol (25 : 24 : 1, v/v). After precipitation with 2 vol. of ethanol, the RNA was glyoxalated and analysed by gel electrophoresis in 1.5% agarose [10]. Gels were then dried and autoradiographed for 2–24 h. Transcription products were quantified by densitometry or by cutting out the band representing the specific transcript from the dried gel and counting it in Aquasol scintillation fluid (New England Nuclear). Background corrections were made by using counts from adjacent gel segments. Stable transcription complex formation was assayed by preincubating the nuclear extract with the first DNA template for 30 min at 20°C. The second DNA template was then added and the preincubation continued for 30 min at 20°C. Transcription was initiated by addition of ribonucleoside triphosphates and RNA synthesis was allowed to proceed for 30 min at 20°C.

DNA utilized

The plasmids containing genes cloned from *D. melanogaster* used as templates in in vitro transcription assays were pDmTα1 (tubulin), DmA4 (actin) and pPW229 (hsp70) [11,12,13]. Templates were prepared by cleavage with the indicated restriction enzyme and purified by phenol extraction and ethanol precipitation.

S_1 nuclease analysis

S_1 nuclease mapping was done as described by Merlino et al. [4]. In vitro synthesized RNA was prepared from a standard in vitro transcription reaction except that [α-^{32}P]UTP was omitted, the UTP concentration was 500 μM and the reaction was scaled up 2.5-times. Non-heat-shock RNA was prepared from Oregon R embryos by the method of Maniatis et al. [14]. Heat-shock RNA (kindly provided by R. Cohen) was prepared from adults according to Cohen and Meselson [15]. The 5′-end-labelled fragments used in the S_1 nuclease protection analysis were a 1.8 kb *Pst*I/*Xmn*I fragment of pDmTα1 DNA labelled at the *Xmn*I site, a 306 bp *Hpa*II/*Hin*cII fragment of DmA4 DNA labelled at the *Hin*cII site and a 649 bp *Xho*I/*Xma*III fragment of pPW229 DNA labelled at the *Xma*III site. The sizes of the S_1 nuclease-protected fragments predicted from sequence data are 116, 121 and 462 bases, respectively (Wensink, P.C., Fyrberg, E.A., personal communications, and Ref. 16, respectively). Protected fragments were glyoxalated and analysed by gel electrophoresis in 5% polyacrylamide.

Results and Discussion

Products of the in vitro transcription system

Run-off assays were performed to assess the fidelity of the transcription system for various templates. Table I lists some of the templates used and sizes of the predicted run-off products; examples of the transcripts produced from them are shown in Fig. 1. In each case the run-off transcription product is the predicted size, showing that transcription occurs from the coding strand and is initiated at or close to the in vitro start site. Addition of 1 μg/ml α-amanitin is completely inhibitory, as expected for transcription by RNA polymerase II [17]. To determine more precisely whether in vitro initiation occurred at the correct site, the in vitro RNAs were compared by S_1 nuclease protection mapping with the corresponding RNAs made in vivo. It may be seen in Fig. 2 that both the in vivo and in vitro RNAs protect fragments of the same size, showing that transcription in vitro starts at or within a few nucleotides of the correct initiation site.

Optimization of the system

The optimum NaCl concentration for the nuclear extraction step was determined by lysing nuclei in an equal volume of nuclear extraction buffer containing 0.2, 0.3, 0.4, 0.5 and 0.6 M NaCl. Transcription assays were performed using pDmTα1 DNA/*Pst*I. As shown in Fig. 3, all extracts were active. Maximum activity was observed with 0.3–0.4 M NaCl. Extracts made with buffer containing 0.3 M NaCl were stable for at least 9 months at −80°C.

In order to determine optimum parameters for correctly initiated transcription in vitro, assays were performed using pDmTα1 DNA/*Pst*I as template, varying one parameter at a time, as depicted in Fig. 4. This defined our standard assay conditions for maximum synthesis as 50 mM KCl, 4 mM $MgCl_2$, 500 μM ATP, CTP and GTP and 25 μm UTP, 10 μg/ml DNA and pH 7.6 at 20°C. Similar results were obtained with different tèmplates and with different extract preparations; the variation in optimum parameters was not great. If maximum efficiency is desired, slight variations in the standard conditions should be tested.

TABLE I

TEMPLATE USED FOR TRANSCRIPTION ASSAYS

Based on unpublished sequence and restriction data from Wensink, P.C. and Fyrberg, E.A. (personal communications) and on Ref. 16.

Plasmid DNA	Restriction enzyme cleavage site	Predicted size of run-off transcript (nucleotides)
(a) pDmTα1	*Xba*I	330
(tubulin)	*Pst*I	1 020
(b) DmA4	*Hin*dIII	500
(actin)	*Pst*I	800
(c) pPW229	*Ava*I	590
(hsp 70)	*Bam*HI	1 260

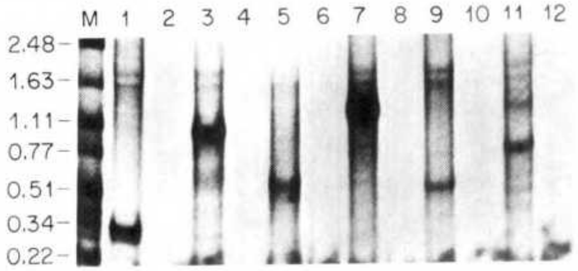

Fig. 1. Gel electrophoretic analysis of run-off transcripts synthesized by *Drosophila* nuclear extracts. Markers (M) are a mixture of the following glyoxalated ^{32}P end-labelled pBR322 DNA restriction enzyme digests: *Bam*HI, *Hin*cII, *Hin*cII + *Ava*I and *Hin*fI. Templates used in standard in vitro transcription reactions: pDmTα1 DNA/*Xba*I (lanes 1 and 2); pDmTα1 DNA/*Pst*I (lanes 3 and 4); pPW229 DNA/*Ava*I (lanes 5 and 6); pPW229 DNA/*Bam*HI (lanes 7 and 8); DmA4 DNA/*Hin*dIII (lanes 9 and 10); DmA4 DNA/*Pst*I (lanes 11 and 12). The reaction mixtures analyzed in lanes 2, 4, 6, 8, 10 and 12 contained 1 μg/ml α-amanitin.

Characterization of the system

The time course of accumulation of in vitro transcripts using pDmTα1 DNA/*Pst*I as template under standard conditions is shown in Fig. 5A. Synthesis is approximately linear for 50 min after a lag period of about 10 min. A similar lag in transcription in vitro is seen in the HeLa cell system. Evidence has been presented that this reflects the time required for formation of transcription complexes prior to initiation [18]. To determine whether the lag period observed here might represent the formation of stable transcription complexes, a mixed template experiment was performed. As illustrated in Fig. 5B (lane 1), when templates pDmTα1 DNA/*Pst*I and pPW229 DNA/*Bam*HI are preincubated together in a tran-

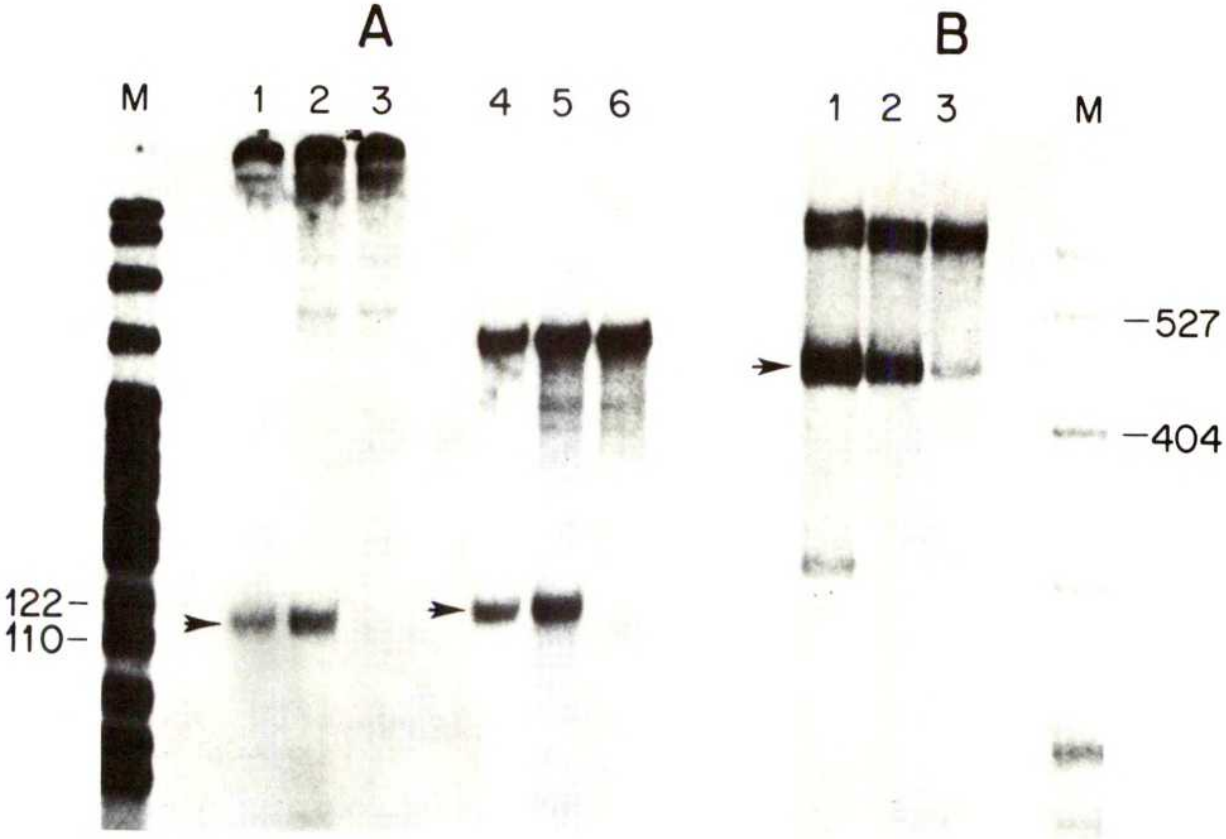

Fig. 2. S_1 protection analysis of transcripts. (M) Markers are glyoxalated ^{32}P end-labelled pBR322 DNA digested with *Hpa*II. RNAs used were (A) 5 μg OreR embryo RNA (lanes 1 and 4), in vitro RNA synthesized from pDmTα1 DNA/*Pst*I (lanes 2 and 3), in vitro RNA synthesized from DmA4/*Hin*dIII (lanes 5 and 6). (B) 5 μg OreR adult heat-shock RNA (lane 1), in vitro RNA synthesized from pPW229 DNA/*Bam*HI (lanes 2 and 3). Lanes 3 and 6 contained 1 μg/ml α-amanitin. DNAs used were (A) 360 ng ^{32}P-pDmTα1 DNA/*Pst*: *Xmn*I fragment (lanes 1–3); 60 ng ^{32}P-DmA4 DNA/*Hpa*II: *Hin*cII fragment (lanes 4–6). (B) 120 ng ^{32}P-pPW229 DNA/*Xho*I: *Xma*III fragment (lanes 1–3). Arrows indicate the position of the protected fragment. The presence of some of the 462 nucleotide protected fragment in lane B suggests the presence of endogenous hsp70 RNA in the nuclear extract.

scription reaction both are transcribed approximately equally. However, as seen in Fig. 5B (lanes 2 and 3), if either template is preincubated with the nuclear extract prior to preincubation with the second template and subsequent addition of ribonucleoside triphosphates, most of the specific transcription occurs on the first template. This is consistent with the possibility that the formation

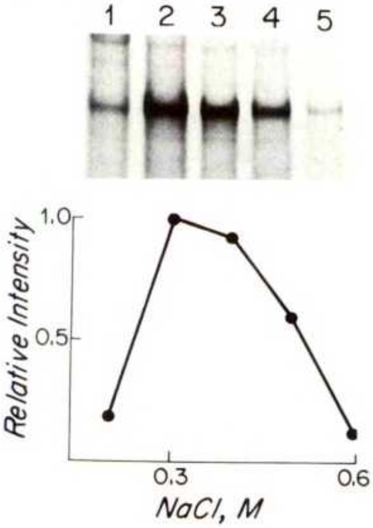

Fig. 3. Run-off transcripts from pDmTα1 DNA/*Pst*I with extracts prepared from nuclei extracted at different NaCl concentrations. Salt concentrations of the nuclear extraction buffer used were 0.2, 0.3, 0.4, 0.5 and 0.6 M (lanes 1–5). Below, the analysis from densitometer scanning is shown.

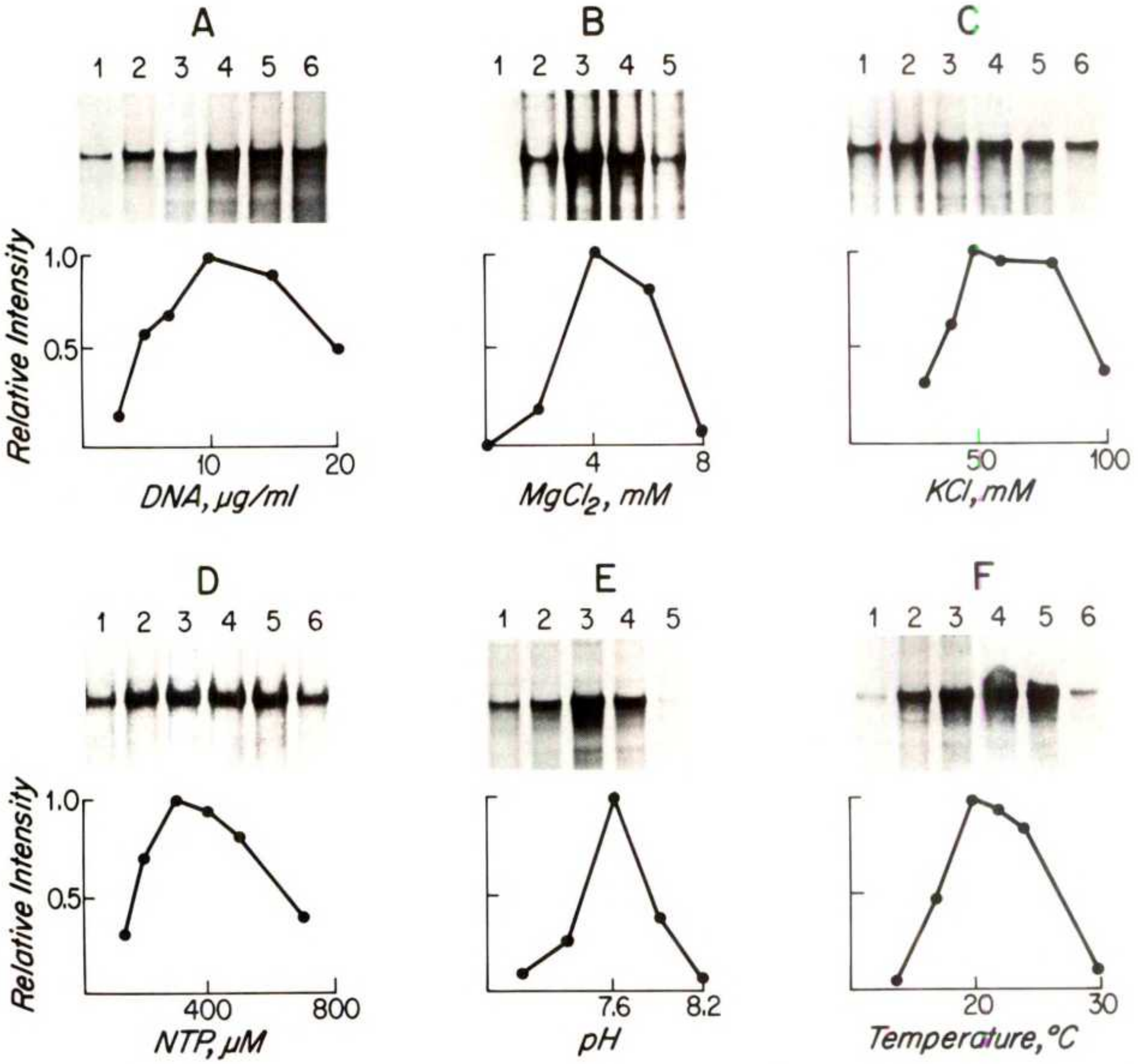

Fig. 4. Optimization of parameters affecting production of in vitro run-off transcripts using pDmTα1 DNA/*Pst*I. (A) Effect of DNA concentration; 3, 5, 7, 10, 15 and 20 µg/ml (lanes 1–6). (B) Effect of $MgCl_2$ concentration; 0, 2, 4, 6, 8 mM (lanes 1–5). (C) Effect of KCl concentration; 30, 40, 50, 60, 80, 100 mM (lanes 1–6). (D) Effect of ribonucleoside triphosphate concentration (UTP concentration was maintained at 25 µM); 100, 200, 300, 400, 500, 700 µM (lanes 1–6). (E) Effect of pH; 7.0, 7.3, 7.6, 7.9, 8.2 (lanes 1–5). (F) Effect of temperature; 14, 17, 20, 22, 24, 30°C (lanes 1–6). Below, the analysis from densitometer scanning is shown.

of a stable transcription complex is an early step in the synthesis of specific RNAs in this *Drosophila* in vitro transcription system.

Quantitation of synthesis from the tubulin template indicates that under standard reaction conditions approx. 0.04 transcripts are produced per template molecule, similar to that found in human cell systems [1,2,3] and the *Drosophila* system of Heiermann and Pong [7] but lower than that reported by Parker and Topol for their *Drosophila* system [5]. Under standard conditions, accurate promotion and synthesis were observed with all *Drosophila* RNA polymerase II templates examined. This includes the tubulin, actin and hsp70

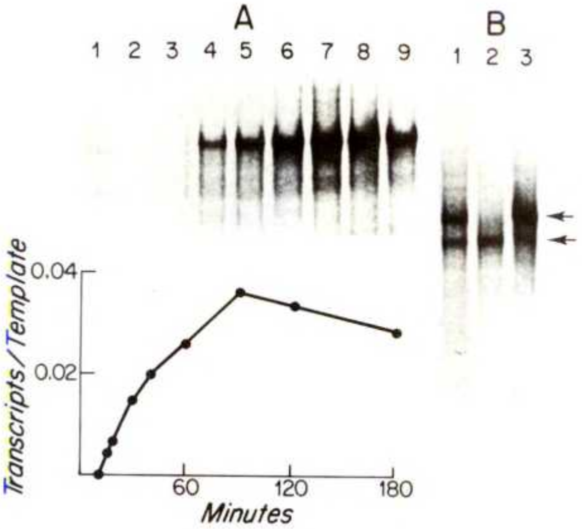

Fig. 5. Time course of accumulation of in vitro transcripts using pDmTα1 DNA/*Pst*I. (A) Synthesis of transcript with time; 10, 15, 20, 30, 40, 60, 90, 120, 180 min (lanes 1–9). Below, the quantitative analysis of this gel is shown. (B) Mixed template experiment. Lane 1. pDmTα1 DNA/*Pst*I + pPW229 DNA/*Bam*HI (8 μg/ml each template) preincubated for 60 min prior to initiation of synthesis by the addition of ribonucleoside triphosphates, and further incubation for 30 min under standard assay conditions. Lane 2, as lane 1, except that pPW229/*Bam*HI was added after pDmTα1/*Pst*I had been preincubated for 30 min. The preincubation was continued for another 30 min and then RNA synthesis was initiated by the addition of ribonucleoside triphosphates. Lane 3, as lane 2, except that pPW229/*Bam*HI was preincubated before pDmTα1/*Pst*I. Arrows show the position of the expected 1020 and 1260 nucleotide run-off transcripts.

genes reported here, cloned in pdmTα1, DmA4 and pPW229, respectively, and two additional templates, DmA2 (actin) and p13XS26 (hsp26) (data not shown). In addition, reproducible transcription from the *Drosophila Adh* promoters has been obtained in another laboratory, using the system described here (P. Macdonald, personal communication).

Recently, the characterization of a similar in vitro transcription extract from *Drosophila* embryos was reported [7]. The parameters affecting transcription efficiencies in these two systems are very similar. The major advantage of the system reported here is the ability to analyze transcription using a simple run-off assay rather than by an indirect S_1 nuclease assay.

Acknowledgements

We are grateful to the MIT Cell Culture Center for preparation of cells, the National Institutes of Health for support and to Matthew Meselson for encouragement and for advice in preparation of the manuscript. A.McL. wishes to thank the Welcome Trust for the award of a Travel Grant. The work of P.L. was in partial fulfillment of requirements for the degree of Bachelor of Arts with Honours (Undergraduate Dissertation, Biochemical Sciences, Harvard University, 1984).

References

1 Dignam, J.D., Lebovitz, P.M. and Roeder, R.G. (1983) Nucleic Acids Res. 11, 1475–1489

2 Manley, J.L., Fire, A., Cano, A., Sharp, P.A. and Gefter, M.L. (1980) Proc. Natl. Acad. Sci. USA 77, 3855–3859

3 Weil, P.A., Luse, D.S., Segall, J. and Roeder, R.G. (1979) Cell 18, 469–484

4 Merlino, G.T., Tyagi, J.S., de Crombrugghe, B. and Pastan, I. (1982) J. Biol. Chem. 257, 7254–7261

5 Parker, C.S. and Topol, J. (1984) Cell 36, 357–369

6 Tsuda, M. and Suzuki, Y. (1981) Cell 27, 175–182

7 Heiermann, R. and Pongs, O. (1985) Nucleic Acids Res. 13, 2709–2730

8 Echalier, G. (1976) in Invertebrate Cell Culture (Kurstak, E. and Maramorosch, K., eds.), pp. 131–150, Academic Press, New York

9 Cherbas, L. and Cherbas, P. (1981) in Advances in Cell Culture (Maramorosch, K., ed.), pp. 91–124, Academic Press, New York

10 McMaster, G.K. and Carmichael, G.G. (1977) Proc. Natl. Acad. Sci. USA 74, 4835–4838

11 Fyrberg, E.A., Bond, B.J., Hershey, N.D., Nixter, K.S. and Davidson, N. (1981) Cell 24, 107–116

12 Kalfayan, L. and Wensink, P.C. (1981) Cell 24, 97–106

13 Livak, K.J., Freund, R., Schweber, M., Wensink,, P.C. and Meselson, M. (1978) Proc. Natl. Acad. Sci. USA 75, 5613–5617

14 Maniatis, T., Fritsch, E.F. and Sambrook, J. (1982) Molecular Cloning, pp. 188–209, Cold Spring Harbor Laboratory, New York

15 Cohen, R. and Meselson, M. (1984) Proc. Natl. Acad. Sci. USA 81, 5509–5513

16 Ingolia, T.D., Craig, E.A. and McCarthy, B.J. (1980) Cell 21, 669–679

17 Greenleaf, A.L. and Bautz, E.K.F. (1975) Eur. J. Biochem. 60, 169–179

18 Fire, A., Samuels, M. and Sharp, P.A. (1984) J. Biol. Chem. 259, 2509–2516

Biochimica et Biophysica Acta 866 (1986) 89–91
Elsevier

BBA 90056

BBA Report

The nucleotide sequence of 4.5 S rRNA from tomato chloroplasts

Cheng Zhen-Qi [a], Xiao Xiao [b] and Wang E-Sheng [b]

[a] *Institute of Biophysics, Academia Sinica, Beijing, and* [b] *Department of Biology, Wuhan University, Wuhan (China)*

(Received April 23rd, 1985)
(Revised manuscript received November 29th, 1985)

Key words: 4.5 S rRNA, rRNA; Nucleotide sequence, (Tomato chloroplast)

The nucleotide sequence of 4.5 S rRNA from tomato (*Lycopersicum esculentum* Mill) chloroplasts has been determined to be: $5'_{\mathrm{HO}}$GAAGGUCAC$\overset{10}{\mathrm{G}}$GCGAGACGA$\overset{20}{\mathrm{G}}$CCGUUUAUC$\overset{30}{\mathrm{A}}$UUACGAUAG$\overset{40}{\mathrm{G}}$UGUCAAGU-G$\overset{50}{\mathrm{G}}$AAGUGCAGU$\overset{60}{\mathrm{G}}$AUGUAUGCA$\overset{70}{\mathrm{G}}$CUGAGGCAU$\overset{80}{\mathrm{C}}$CUAACAGAU$\overset{90}{\mathrm{C}}$GGUAGACUU$\overset{100}{\mathrm{G}}AA\mathrm{C_{OH}}3'$. The 4.5 S rRNA is 103 nucleotides long and has a free 5′-terminal hydroxyl group. It shows at high degree of homology with chloroplast 4.5 S rRNA from other plants.

Since being reported by Dyer and Bowman [1] and Whitfeld et al. [2], the chloroplast 4.5 S rRNA (the only component associated with the large subunit of ribosomes [1–5]) of several higher plants has been sequenced [6–11]. We have determined the nucleotide sequence of tomato chloroplast 4.5 S rRNA, and compared it with that of other 4.5 S rRNAs.

We purified the chloroplast 4.5 S rRNA primarily according to the method described by Wildeman and Nazar [6], with some modification. The mixture of young leaves of tomato, buffer (50 mM sodium acetate (pH 5.0)/0.3% SDS/0.14 M NaCl) and phenol was homogenized in a blender in order to break the chloroplasts. The homogenate was stirred, and centrifuged to remove the debris. The aqueous phase was treated as above in the presence of 2 M LiCl to remove DNA and other high-molecular-weight RNAs and proteins. Then, small RNAs were precipitated by 2.5 vol. of ethanol and were again collected and extracted with phenol. The aqueous phase was precipitated by ethanol, washed with 70% cold ethanol and lyophilized. We obtained the 4.5 S rRNA by using 8% polyacrylamide/7 M urea gel electrophoresis as in Ref. 6.

The 5′-end of the purified 4.5 S rRNA was labeled with polynucleotide kinase and [γ-^{32}P]ATP (Amersham), the 3′-end with RNA ligase and [5′-^{32}P]pCp [12]. The end-labeled RNA was purified as in Ref. 6.

Both 3′- and 5′-end-labeled 4.5 S rRNAs were sequenced using the enzymatic method of Donis-Keller et al. [13,14] with the RNAases T_1, U_2, Phy M and *B. cereus*. The 3′-end-labeled 4.5 S rRNA was also sequenced by the chemical method of Peattie [15]. The sequence was determined from the 5′-end to residue 45 and from residues 102 to 75 by separating the cleavage products in 20% sequencing gel containing 8 M urea. The sequence from residue 40 to 80 was determined in 12% gel.

The 5′- and 3′-terminal residues were respectively identified by PEI-cellulose thin-layer chromatography after complete digestion of the end-labeled RNA with RNAase T_2. On overlapping the autoradiographs from the above-mentioned experiments information on residues 1 to 103 was obtained. The complete nucleotide sequence is shown in Fig. 1.

The 4.5 S rRNA consists of 103 nucleotides and the GC content is 50%. The 5′-terminus is unphosphorylated. The homology comparison of known

0167-4781/86/$03.50 © 1986 Elsevier Science Publishers B.V. (Biomedical Division)

TABLE I

THE HOMOLOGY COMPARISON OF THE 4.5 S rRNAs WHOSE NUCLEOTIDE SEQUENCES ARE KNOWN

Figures represent percent homology.

Species	*L. esc*	*N. Tab*	*S. Ole*	*S. Oli*	*D. acu*	*T. aes*	*Z. Mays*	Refs.
Lycopersicum esculentum (tomato)		99.0	93.4	92.2	86.4	81.7	81.6	
Nicotiana tabacum (tobacco)	99.0		94.3	93.2	87.3	81.7	81.6	7
Spinacia oleracea (spinach)	93.4	94.3		90.6	84.9	79.4	79.2	9
Spirodela oligorrhiza [a]	92.2	93.2	90.6		91.2	82.7	82.5	11
D. acuminata (a fern)	86.4	87.3	84.9	91.2		76.9	77.6	10
Triticum aestivum (wheat)	81.7	81.7	79.4	82.7	76.9		98.0	6
Zea mays (maize)	81.6	81.6	79.2	82.5	77.6	98.0		8

[a] The sequence of *S. oligorrhiza* chloroplast 4.5 S rRNA was deduced from its DNA sequence, determined by Keus et al. [11].

4.5 S RNAs (Table I) shows that the closer the taxonomic affinity, the higher the degree of homology; the nucleotide sequences are conserved strongly. Completely conserved nucleotides account for 73% of these 4.5 S rRNAs. The seven-nucleotide sequence from positions 28 to 34 is noteworthy. It is present in 4.5 S rRNAs of dicotyledonous tomato, tobacco [7] and spinach [9], and pteridophyte *D. acuminata* [10]. It is also present in 4.5 S rRNAs of monocotyledon *Spirodela oligorrhiza* [11] and duckweed (in the RNAase T_2 fingerprint of 4.5 S rRNA from duckweed made by Bowman and Dyer [5], fragment 20 can be seen to be UUUAUCAUUACG, which contains the characteristic sequence UCAUUAC). However, this seven-nucleotide sequence is absent in monocotyledon wheat [6] and maize [8]. Keus et al. [11] considered that the deletion of this fragment must have taken place after the evolutionary separation of dicotyledon and monocotyledon. It might play a particular structural or functional role in one group of ribosomes [16].

In Fig. 1, the nucleotide sequence of tomato 4.5 S rRNA is compared with that of the *E. coli* 3′-terminal region 23 S rRNA, essentially according to the alignment of Edwards and Kössel [17]. The degree of homology between them is 60%. The structural homology suggests that there is some functional homology and relationship between the 4.5 S rRNA and the 3′-terminal region of prokaryotic 23 S rRNA [11,18].

The presence of an unphosphorylated 5′-end is a common characteristic of chloroplast 4.5 S rRNA [1–11]. It suggests that the post-transcriptional process of 4.5 S rRNA might differ from that of other RNAs in chloroplasts.

On analysing the autoradiographs, we found that two regions, from A_8 to C_{12} and from G_{20} to U_{24}, form a hairpin structure. A_8–C_{12} and G_{20}–U_{24} form a double helix by base-pairing and the fragment between them forms a hairpin-loop. The hairpin structure fits well into secondary structure models described by Takaiwa and Sugiura [7], Kumagai et al. [16], and Machatt et al. [18].

The possible secondary structure of the 4.5 S rRNA of tomato (Fig. 2) is deduced mainly according to the base-pairing principle. The calculated free energy release value [19] for this structure is $G = -108.4$ kJ/mol. The value for the Machatt model is $G = -101.7$ kJ/mol. Helix II of

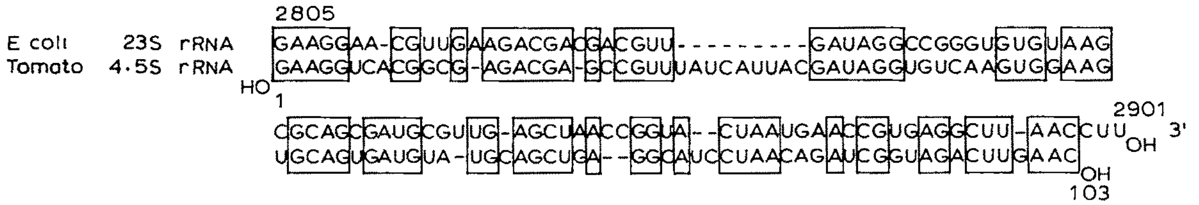
2805
E coli 23S rRNA GAAGGAA-CGUUGAAGACGACGACGUU---------GAUAGGCCGGGUGUGUAAG
Tomato 4.5S rRNA GAAGGUCACGGCG-AGACGA-GCCGUUUAUCAUUACGAUAGGUGUCAAGUGGAAG
HO
1
2901
CGCAGCGAUGCGUUG-AGCUAACCGGUA--CUAAUGAACCGUGAGGCUU-AACCUU
OH
3'
UGCAGUGAUGUA-UGCAGCUGA--GGCAUCCUAACAGAUCGGUAGACUUGAAC
OH
103

Fig. 1. Comparison of tomato chloroplast 4.5 S rRNA with 3′-terminal region of *E. coli* 23 S rRNA.

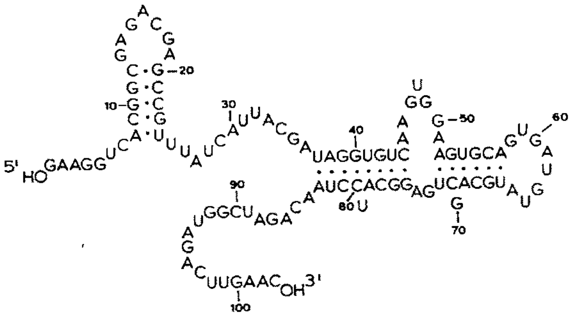

Fig. 2. The secondary structure of tomato chloroplast 4 5 S rRNA

the Kumagai model [16] is not suitable for tomato 4.5 S rRNA.

References

1 Dyer, T.A. and Bowman, C.M (1976) in Genetics and Biogenesis of Chloroplasts and Mitochondria (Bucher, Th., Neupert, W., Sebald, W. and Werner, S., eds), pp. 645–651, North-Holland, Amsterdam

2 Whitfeld, P.R., Leaver, C.J., Bottomley, W and Atchison, B A (1978) Biochem. J. 175, 1103–1112

3 Whitfeld, P.R. (1977) in The Ribonucleic Acids (Stewart, P.R and Letham, D S, eds), 2nd Edn, pp 297–332, Springer-Verlag, Heidelberg

4 Bowman, C M. and Dyer, T.A. (1979) Biochem J. 183, 605–613

5 Hartley, M.R. (1979) Eur. J. Biochem. 96, 311–320

6 Wildeman, A.G. and Nazar, R.N (1980) J. Biol Chem. 255, 11896–11900

7 Takaiwa, F. and Sugiura, M (1980) Nucleic Acids Res 8, 4125–4129

8 Edwards, K., Bedbrook, J., Dyer, T.A. and Kossel, H (1981) Biochem. Int. 2, 533–538.

9 Kumagai, I., Pieler, T, Subramanian, A.R. and Erdmann, V.A. (1982) J. Biol Chem. 257, 12924–12928

10 Takaiwa, F., Kusuda, M and Sugiura, M. (1982) Nucleic Acids Res. 10, 2257–2260

11 Keus, R.J.A., Roovers, D.J., Dekker, A.F and Groot, G.S P (1983) Nucleic Acids Res. 11, 3405–3410

12 Vourbakis, J N, Celantano, J., Finn, M., Lockard, R E, Mitra, T., Pavlakis, G., Troutt, A., Van den Berg, M. and Wurst, R.M. (1981) in Gene Amplification and Analysis, Vol. 2 (Chirikjian, J.G and Papas, T.S., eds), Elsevier/North-Holland, Amsterdam

13 Donis-Keller, H., Maxam, A. and Gilbert, W (1977) Nucleic Acids Res 4, 2527–2538

14 Donis-Keller, H (1980) Nucleic Acids Res. 8, 3133–3142

15 Peattie, D. (1979) Proc. Natl. Acad. Sci. USA 76, 1760–1764

16 Kumagai, I., Bartsch, M., Subramanian, A R. and Erdmann, V.A. (1983) Nucleic Acids Res. 11, 961–970

17 Edwards, K. and Kossel, H. (1981) Nucleic Acids Res. 9, 2853–2869

18 Machatt, M.A., Ebel, J.-P. and Branlant, C. (1981) Nucleic Acids Res. 9, 1533–1549

19 Papanicolaou, C., Gouy, M. and Ninio, J. (1984) Nucleic Acids Res. 12, 31–44

INFORMATION FOR CONTRIBUTORS TO BIOCHIMICA ET BIOPHYSICA ACTA

Biochimica et Biophysica Acta publishes papers reporting advances in our knowledge or understanding of any field of biochemistry or biophysics. Descriptions of new methods valuable for biochemists or biophysicists are also acceptable if their application is made obvious or a new principle is introduced. Negative results will be accepted only when they can be considered to advance our knowledge significantly. Papers providing only confirmatory evidence or extending observations firmly established in one species to another will not normally be accepted.

Two types of paper are published, specified as Regular Papers and BBA Reports. As its name implies, a Regular Paper is the usual medium of publication.

BBA Reports will be restricted to papers describing short, complete studies. They should not exceed three printed pages, including figures and tables, and should be written in a continuous style, without subdivision into Introduction, Methods, Results, Discussion and Acknowledgements. They should always begin with a short summary. A BBA Report, although brief, should be a complete and final publication, and figures and tables should not be included in a later paper.

Papers should be written in English (either American or British spelling is permitted, but only one form should be used in the same paper).

Preparation of papers

Authors and their typists should consult a recent issue of the journal in order to make themselves familiar with the conventions and layout of articles, especially title pages and reference lists. In particular, typists should ensure that the beginning of each new paragraph is clearly indicated, preferably by indentation.

Four copies are required of all material submitted (including the submission letter, if it contains information of relevance to the editors). Legible carbon copies or photocopies are adequate for the second and subsequent copies, except for photographs of electrophoretic patterns, electron micrographs, etc., where high-quality prints must be provided in quadruplicate.

The entire text, including figure and table legends and reference list, should be typed with double or triple spacing on pages of uniform size, on one side of the paper, with a 5-cm margin. All pages should be numbered consecutively.

Title

A paper should be headed by a concise, informative title. Authors are reminded that titles are widely used in information-retrieval systems. The title should be followed by the names of the authors (with first or middle names in full) and by the name(s) and address(es) of the laboratory(ies) where the work was carried out. If the work has been done in more than one laboratory, the one in which each author has worked during the study should be indicated.

Summary

A paper should begin with a summary of 100–200 words for a Regular Paper and approx. 50 words for a BBA Report.

Tables

Tables and their legends should be typed with double or triple spacing.

Figures and illustrations

Legends to figures should not be typed or written on the illustrations but should be typewritten, with double or triple spacing, on separate sheets of paper. The legends should consist of a title followed by a brief description of the way the particular experiment was carried out, and any other necessary material describing the symbols or lines on the figure.

ANNOUNCEMENT

PREPARATION OF FIGURES

A few guidelines are presented which may be of assistance to authors. Detailed suggestions are to be found in 'Information for Contributors' (Biochim. Biophys. Acta 715 (1982) 1–23, also available as a booklet, free of charge, from the BBA Editorial Secretariat, P.O. Box 1345, 1000 BH Amsterdam, The Netherlands).

☐ Note that figures are almost always reduced to fit within the breadth of one column (7.5 cm). You should arrange for letters and symbols to be at least 1.5 mm high *after* reduction.

☐ Electron micrographs should always carry a bar denoting unit length, defined in the figure legend. A minimum essential area of the micrograph should be indicated to aid in reproduction.

☐ For second and third copies of the article, good copies of the original figures are acceptable, but all photographs (gels, electron micrographs, etc.) should be submitted in triplicate.

☐ Use tracing or good quality drawing paper no larger than the paper on which the article is typed. Please do not use heavy card as a mount for photographs. Use black, waterproof ink, or submit sharp, high-contrast, glossy prints. Typewriting and handwriting on figures should be avoided.

☐ On graphs, each trace should be defined using a standard symbol selected from the following: ⌖ △ ⦶ ⬕ ◩ ◪ ⬔ ⬠ ⬡ ◧ ° * ◒ ⦵ ☆ ■ ⊠ □ ● ▲ ▼ ▶ ⊞ ⊟ ⊗ ⊙ ○ ◇ △ ▽ ▷ ◁ ⊕ ⊖ ★ ⊛ Traces may also be labelled, but any abbreviations should be fully defined in the legend. Please avoid bar diagrams, unless they are true histograms. Tables of numerical values are more informative.

☐ Please type the legend(s), using double or triple spacing, on sheets separate from the figures. The actual figure should not bear a title (use A, B, etc. for different panels within a figure). The first sentence of the figure legend should constitute a brief title. Please bear in mind the vertical space occupied by the figure legend, particularly in the case of full-page figures (where 1 cm per 50 words should be allowed). The total typesetting length is 20.5 cm.

Biochimica et Biophysica Acta **Vol. 866, No. 1**
Gene Structure and Expression N14(1) February 24, 1986

Contents

Regular Papers

Immunological identification of rat tissue kallikrein cDNA and characterization of the kallikrein gene family (BBA 91526)
by W.L Gerald, J Chao and L Chao (Charleston, SC, U S A) 1

Regulation of acetohydroxy acid synthase activities in *Escherichia coli* K-12 by small metabolites (BBA 91528)
by A L Williams (Lexington, KY, U S A) 15

Conserved restriction sites within the ribosomal RNA genes of vertebrates (BBA 91527)
by S M Tanhauser, W W Hauswirth and P J. Laipis (Gainesville, FL, U S A) 19

A novel suppressor tRNA from the dimorphic fungus *Candida albicans* (BBA 91555)
by M F. Tuite, P A Bower and C S McLaughlin (Canterbury, U.K , and Irvine, CA, U S A.) 26

Kinetic control of the length of very short homopolymeric additions by terminal deoxynucleotidyltransferase (BBA 91551)
by K Sirotkin (Knoxville, TN, U S A) 32

The role of upstream sequences in determining the strength of an rRNA promoter of *E coli* (BBA 91552)
by Á, Petho, J Belter, I Boros and P Venetianer (Szeged, Hungary) 37

Sequence-specific alkali-labile lesions in DNA caused by D-isoglucosamine (BBA 91554)
by S Nanjou, S. Fujii, J Morita, K Ueda and T Komano (Kyoto, Japan) 44

The competitive miscoding of O^6-methylguanine and O^6-ethylguanine and the possible importance of cellular deoxynucleoside 5′-triphosphate pool sizes in mutagenesis and carcinogenesis (BBA 91556)
by R Saffhill (Manchester, U.K) 53

Developmental and hormonal regulation of carbamoyl-phosphate synthase gene expression in rat liver. evidence for control mechanisms at different levels in the perinatal period (BBA 91562)
by C J de Groot, D Zonneveld, R T M de Laaf, M A Dingemanse, P G Mooren, A.F M Moorman, W H. Lamers and R Charles (Amsterdam, The Netherlands) 61

Sequence of the cDNA encoding porcine pro-opiomelanocortin (BBA 91553)
by F J Gossard, A.C Y Chang and S N Cohen (Stanford, CA, U S A) 68

Effects of addition of derived 40 S subunits on translation rate and polysome profile of the reticulocyte lysate (BBA 91561)
by P W L Tas and O H.W. Martini (Wurzburg, F R G) 75

A *Drosophila* RNA polymerase II cell-free DNA-dependent transcription system (BBA 91529)
by A McLachlan and P Lin (Cambridge, MA, U S A) 83

Report

The nucleotide sequence of 4.5 S rRNA from tomato chloroplasts (BBA 90056)
by Z -Q. Chen, X Xiao and E -S Wang (Beijing and Wuhan, China) 89

Cited in Current Contents Life Sciences - Biological Abstracts - Chemical Abstracts - Index Chemicus - Index Medicus - Excerpta Medica (EMBASE)

INFORMATION FOR CONTRIBUTORS TO BIOCHIMICA ET BIOPHYSICA ACTA

The 1982 edition of this booklet, offering detailed guidance to authors, is available free of charge from the BBA Editorial Secretariat, P.O. Box 1345, 1000 BH Amsterdam, The Netherlands. It is also published as Biochim. Biophys. Acta 715 (1982) 1–23.

BIOCHIMICA ET BIOPHYSICA ACTA
International Journal of Biochemistry and Biophysics
Founded in 1947 by H G.K. Westenbrink, Managing Editor 1947–1964

© 1986, Elsevier Science Publishers B.V (Biomedical Division)
Printed in The Netherlands

All rights reserved. No part of this publication may be reproduced, stored in a retrieval system, or transmitted, in any form or by any means, electronic, mechanical, photocopying, recording or otherwise without the prior written permission of the publisher, Elsevier Science Publishers B.V. (Biomedical Division), P.O. Box 1527, 1000 BM Amsterdam, The Netherlands Submission of a paper to this journal entails the author's irrevocable and exclusive authorization of the publisher to collect any sums or considerations for copying or reproduction payable by third parties (as mentioned in article 17 paragraph 2 of the Dutch Copyright Act of 1912 and in the Royal Decree of June 20, 1974 (S. 351) pursuant to article 16b of the Dutch Copyright Act of 1912) and/or to act in or out of Court in connection therewith

Special regulations for readers in the U S A This journal has been registered with the Copyright Clearance Center, Inc. Consent is given for copying of articles for personal or internal use, or for the personal use of specific clients. This consent is given on the condition that the copier pays through the Center the per-copy fee stated in the code on the first page of each article for copying beyond that permitted by Sections 107 or 108 of the U.S Copyright Law The appropriate fee should be forwarded with a copy of the first page of the article to the Copyright Clearance Center, Inc., 27 Congress Street, Salem, MA 01970, U.S.A. If no code appears in an article, the author has not given broad consent to copy and permission to copy must be obtained directly from the author. All articles published prior to 1980 may be copied for a per-copy fee of US$ 2.25, also payable through the Center. This consent does not extend to other kinds of copying, such as for general distribution, resale, advertising and promotion purposes, or for creating new collective works. Special written permission must be obtained from the publisher for such copying.

Special regulations for authors Upon acceptance of an article by the journal, the author(s) will be asked to transfer copyright of the article to the publisher. This transfer will ensure the widest possible dissemination of information.

reviews on cancer

SAMPLE COPY

for additional information contact:

ALLIED/ELSEVIER JOURNALS
MARKETING GROUP
30, WEST COTT ROAD, Ph: 82468
MADRAS - 600 014./
750, MOUNT ROAD,
MADRAS - 600 002.

BBA
Biochimica et Biophysica Acta (CR)

Managing Editor for Reviews on Cancer P W.J Rigby

Managing Editors: P Borst, P Cohen,
K van Dam, L.L.M van Deenen (Chairman),
E P Kennedy and G K Radda

Honorary Managing Editor E C. Slater

Vol. 865, No. 2, pp. 83–234
October 28, 1986
Elsevier

ISSN 0006-3002
0304-419X
BBACAQ 865 (2) 83–234 (1986)
BBACEU 865 (2) 83–234 (1986)

PUBLICATION SCHEDULE FOR 1986

BBA is published according to a volume-numbering scheme that embraces all sections of the journal In addition, each regular section has its own sequential volume-numbering system, running parallel to the overall BBA scheme, as set out below
Full subscription: 42 volumes plus Cumulative Index 1985

	BIO-ENERGETICS 6 Volumes [a]	BIO-MEMBRANES 11 volumes [b]	GENE STRUCTURE AND EXPRESSION 3 volumes	PROTEIN STRUCTURE AND MOLECULAR ENZYMOLOGY 6 volumes	LIPIDS AND LIPID METABOLISM 5 volumes	GENERAL SUBJECTS 5 volumes	MOLECULAR CELL RESEARCH 5 volumes	BBA REVIEW SECTIONS
Jan	848-1 = B75-1	854-1 = M135-1 854-2 = M135-2	866-1 = N14-1	869-1 = P33-1	875-1 = L77-1	880-1 = G121-1	885-1 = C12-1	BBA REVIEWS ON BIOENERGETICS
Feb	848-2 = B75-2	855-1 = M136-1 855-2 = M136-2	866-2 = N14-2	869-2 = P33-2 869-3 = P33-3	875-2 = L77-2	880-2 = G121-2	885-2 = C12-2	853-1 = BR14-1 853-2 = BR14-2 853-3 = BR14-3 853-4 = BR14-4
March	848-3 = B75-3	855-3 = M136-3 856-1 = M137-1	866-3 = N14-3	870-1 = P34-1	875-3 = L77-3	880-3 = G121-3	885-3 = C12-3	
April	849-1 = B76-1 849-2 = B76-2	856-2 = M137-2 856-3 = M137-3	866-4 = N14-4	870-2 = P34-2 870-3 = P34-3	876-1 = L78-1 876-2 = L78-2	881-1 = G122-1 881-2 = G122-2	886-1 = C13-1 886-2 = C13-2	
May	849-3 = B76-3	857-1 = M138-1 857-2 = M138-2	867-1 = N15-1	871-1 = P35-1	876-3 = L78-3	881-3 = G122-3	886-3 = C13-3	BBA REVIEWS ON BIOMEMBRANES
June	850-1 = B77-1	858-1 = M139-1 858-2 = M139-2	867-2 = N15-2	871-2 = P35-2 871-3 = P35-3	877-1 = L79-1	882-1 = G123-1	887-1 = C14-1	864-1 = MR15-1 864-2 = MR15-2 864-3 = MR15-3 864-4 = MR15-4
July	850-2 = B77-2 850-3 = B77-3	859-1 = M140-1 859-2 = M140-2	867-3 = N15-3	872-1 = P36-1	877-2 = L79-2 877-3 = L79-3	882-2 = G123-2 882-3 = G123-3	887-2 = C14-2 887-3 = C14-3	
Aug	851-1 = B78-1	860-1 = M141-1 860-2 = M141-2	867-4 = N15-4	872-2 = P36-2 872-3 = P36-3	878-1 = L80-1	883-1 = G124-1	888-1 = C15-1	BBA REVIEWS ON CANCER
Sept	851-2 = B78-2	860-3 = M141-3 861-1 = M142-1	868-1 = N16-1	873-1 = P37-1	878-2 = L80-2	883-2 = G124-2	888-2 = C15-2	865-1 = CR13-1 865-2 = CR13-2 865-3 = CR13-3
Oct	851-3 = B78-3	861-2 = M142-2 861-3 = M142-3	868-2 = N16-2	873-2 = P37-2 873-3 = P37-3	878-3 = L80-3	883-3 = G124-3	888-3 = C15-3	
Nov	852-1 = B79-1 852-2 = B79-2	862-1 = M143-1 862-2 = M143-2	868-3 = N16-3	874-1 = P38-1	879-1 = L81-1 879-2 = L81-2	884-1 = G125-1 884-2 = G125-2	889-1 = C16-1 889-2 = C16-2	
Dec	852-3 = B79-3	863-1 = M144-1 863-2 = M144-2	868-4 = N16-4	874-2 = P38-2 874-3 = P38-3	879-3 = L81-3	884-3 = G125-3	889-3 = C16-3	

[a] This includes BBA Reviews on Bioenergetics, Vol 853 [b] This includes BBA Reviews on Biomembranes, Vol 864

Authors should submit their manuscripts (four copies) for publication in BBA Reviews on Cancer by sending them to the following address
BBA Editorial Secretariat, P O Box 1345, 1000 BH Amsterdam, The Netherlands

Managing Editor (Reviews on Cancer) Dr. P W J Rigby, Cancer Research Campaign Laboratory, Department of Biochemistry, Imperial College, London SW7 2AZ, U K

Detailed information for contributors may be found in Biochim Biophys Acta 715 (1983) 1–23, also published as the 1982 edition of the booklet
INFORMATION FOR CONTRIBUTORS TO BIOCHIMICA ET BIOPHYSICA ACTA
which is available free of charge from the BBA Editorial Secretariat

---

Subscription information

1986 BBA Reviews on Cancer, Volume 865, Dfl 235 (US$ 92 00) + Dfl 24 (US$ 9 50) postage, packaging and handling Total price Dfl 259 (US$ 101 50)
1986 BBA full subscription Volumes 848–889 (42 volumes in 125 issues) Dfl 7476 (US$ 2931 75) + Dfl 1008 (US$ 395 25) postage, packaging and handling Total price Dfl 8484 (US$ 3327 00)
The Dutch guilder price is definitive The U S dollar price is subject to exchange-rate fluctuations and is given only as a guide Journals are sent by surface delivery to all countries, except the following countries where SAL air delivery (Surface Airlifted Mail) is ensured: U S A , Canada, Japan, Australia, New Zealand, P R China, India, Israel, South Africa, Malaysia, Singapore, South Korea, Taiwan, Pakistan, Hong Kong, Brazil, Argentina, Mexico, Thailand Airmail rates for other countries are available on request Subscription orders can be entered only by calendar year (Jan –Dec) and should be sent to Elsevier Science Publishers, Journals Department, P O Box 211, 1000 AE Amsterdam, The Netherlands, Telex 18582 ESPA NL, or to your usual subscription agent Claims for missing issues should be made within 3 months of publication, otherwise they cannot be honoured free of charge The Publisher reserves the right to issue additional volumes during the course of the year Such volumes will be invoiced before publication and delivered after receipt of payment
In the United States and Canada for further information contact Elsevier Science Publishers, Journal Information Center, 52 Vanderbilt Avenue, New York, NY 10017, U S A , Tel (212) 370-5520

Biochimica et Biophysica Acta 865 (1986) 83–125
Elsevier

BBA 87156

Gene expression during the mammalian cell cycle

David T. Denhardt, Dylan R. Edwards and Craig L.J. Parfett

Cancer Research Laboratory, University of Western Ontario, London, Ontario, N6A 5B7 (Canada)

(Received January 31st, 1986)

Contents

I. Introduction 84

II Proto-oncogenes and growth control 85
 A c-*myc* 85
 B c-*fos* 87
 C. c-*ras* 88
 D c-*myb* 88
 E p53 89

III The search for cell cycle-regulated genes 90
 A The identification of cDNA clones corresponding to cell cycle-regulated mRNAs 90
 B. Polypeptides synthesized at specific times during the cell cycle 96

IV Some properties of known cell cycle-regulated genes 97
 A Histones 97
 B Enzymes of nucleotide and polyamine metabolism 100
  1 Dihydrofolate reductase (*dhfr*) 100
  2 Thymidylate synthetase (TS) 102
  3. Thymidine kinase (TK) 102
  4 Ornithine decarboxylase (ODC) 103
 C Cyclin, or proliferating cell nuclear antigen (PCNA) 103
 D. Secreted proteins 104
  1 Major excreted protein (MEP) 104
  2 Mitogen regulated protein (MRP, proliferin) 105
  3 Plasminogen activator 105
  4 Interleukin 2 106
  5 Collagen and collagenase 106
  6 Interferons 107

V. Interrelationships of gene expression during the cell cycle 107
 A Cell cycle mutants 108

Abbreviations: kb, kilobase; bp, basepair; hnRNA, heterogeneous nuclear RNA, CHM, cycloheximide; DRB, 5,6-dichlorobenzimidazole riboside; PDGF, platelet-derived growth factor; FGF, fibroblast growth factor; EGF, epidermal growth factor, IL-2, interleukin 2; IGF-1, insulin-like growth factor 1 (or somatomedin C); TPA, 12-*O*-tetradecanoyl phorbol 13-acetate; PHA, phytohemagglutinin; PBL, peripheral blood leukocytes; PBMC, peripheral blood mononuclear cells, ODC, ornithine decarboxylase; TK, thymidine kinase, TS, thymidylate synthetase; *dhfr*, dihydrofolate reductase; LTR, long terminal repeat; BrdUrd, 5-bromodeoxyuridine, mGBG, methylglyoxal bis(guanylhydrazone)

0304-419X/86/$03 50 © 1986 Elsevier Science Publishers B.V (Biomedical Division)

B Timing of gene induction 110
C Control points during the cell cycle 111
D Intracellular metabolites that may orchestrate cell cycle events 113
E Pathways of gene activation and deactivation 114

VI Prospects for the future 116

Acknowledgements 117

References 117

The cell cycle of a growing cell is the period between the formation of the cell by the division of its mother cell and the time when the cell itself divides to form two daughters. It is a fundamental unit of time at the cellular level since it defines the life cycle of a cell.

J.M. Mitchison [1]

I. Introduction

The years since Howard and Pelc [2] introduced the concept of the (deterministic) 'cell cycle' have witnessed a plethora of investigations into the temporal organization of cell division in a wide range of cell types [3]. These studies have revealed that control of vertebrate cell proliferation is principally accomplished in the G_1 phase of the cell cycle, although regulation may occur at other points in the cycle also. G_1 is the period of typically 5–10 h between mitosis and the initiation of DNA synthesis; however, exceptional cell lines (e.g. Chinese hamster V79-8) have a very short G_1 phase (approx. 30 min) [4].

The study of cell cycle-regulated genes (i.e. genes that show variable expression during the cell cycle) has become an important and burgeoning field in modern biology. Not only are such genes intrinsically important, since they identify functions that may enable us to understand better the mechanics of cell replication, but also they are interesting substrates for those wishing to unlock secrets of gene expression in eukaryotes. Eventually, from an elucidation of the functions and modes of regulation of these genes, a coherent picture will emerge of how cell proliferation is controlled.

Consistent with the fact that eukaryotic replication is restricted to a particular period in interphase is the observation that proteins required for DNA replication, such as histones and the enzymes of nucleotide metabolism, are produced in a cell cycle-dependent fashion. The genes encoding some of these proteins have now been cloned, allowing us to address questions about their regulation at the molecular level. Complementary research has identified other genes that also possess the characteristic of cell cycle-dependent expression, but whose functions are as yet obscure. An exciting development has been the overlap of the oncogene field with cell cycle studies; certain cellular proto-oncogenes are expressed transiently when quiescent mammalian cells are stimulated by growth factors and some oncogenes have homologies with growth factors, or growth factor receptors. Much of this information has been acquired since 1981, when an excellent and exhaustive review of gene expression during the cell cycle appeared [5]. The major aim of the present work is to review the research with mammalian cells that has been published between then and late 1985.

We regard G_0, alternatively called resting phase, quiescence, or, in the probabilistic model of cell cycle kinetics, Q-state, as an integral part of the cell cycle [6–8]. Fig. 1 illustrates three ways of conceptualizing the cell cycle. Further details may be found in the legend and the papers by Brooks et al. [8,9]. We leave it to the reader to consider the merits of probabilistic and deterministic models.

Genes whose expression is induced when quiescent mammalian cells are stimulated to reenter the division pathway are classified as 'cell cycle-regulated' genes. This policy has been advocated for such genes by Baserga [10], following the paradigm of the yeast cell division cycle (CDC) genes [11]. By 'induction of expression' we mean the appearance of the gene product (mRNA, or

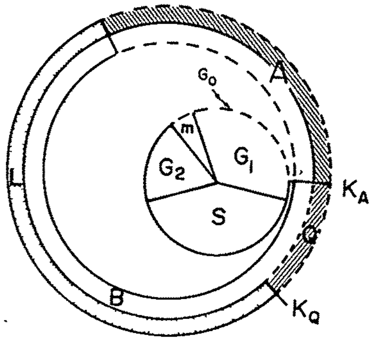

Fig 1 Schematic representations of the mammalian cell cycle The inner acentric ring is the conventional model first proposed in detail by Howard and Pelc [2] Mitosis (M) and the DNA synthesis phase (S) are observable processes, G_1 and G_2 are defined as the gaps between M and S as illustrated. G_0 is a less well-defined state that cells are considered to be in when they are apparently not 'cycling' but still capable of entering the cell cycle (usually to G_1) under appropriate conditions Peripheral blood lymphocytes, quiescent serum-deprived cells, and quiescent confluent cells are considered to be in G_0 The inner and outer concentric rings represent respectively the models of Smith and Martin [7] and Brooks et al. [8] that invoke one or two random transition events K_A is the transition from A phase to either the B state [7] or the Q state [8]. A phase, like G_1, is of indeterminate length and sensitive to external conditions B state is of determinate length largely congruent with $S+G_2+M$ K_Q is a second stochastic event marking the initiation of a process called L [8] It is important to appreciate that L can take place at almost any stage in the 'normal' cell cycle, it is synchronized only when quiescent cells are stimulated to enter the cycle and may involve the maturation of the mitotic centers [8]. These pictorial representations do not do justice to the underlying concepts, and the reader is urged to consult the primary sources

the protein, in the cytoplasm). We expect that a subset of those genes whose expression is enhanced when quiescent cells are stimulated to enter the cell cycle will also be found to be preferentially expressed during the G_1 period in normally cycling cells. It should be appreciated that several 'depths' of G_0 exist, possibly related to the extent of loss of the capacity for protein synthesis, and that results may depend on precisely how the quiescent state has been achieved [12].

In writing this review we have sought to organize the available information on the growing number of known mammalian cell cycle genes. Some of them are of prime importance in controlling cell proliferation. The major focus is on studies done with rodent or primate fibroblast lines, though we have included some material on avian cells and cells of lymphoid origin.

II. Proto-oncogenes and growth control

The functions of most proto-oncogenes have yet to be established, although the unifying theme underlying many investigations is that these genes exert a controlling influence on the molecular events that enable cells to proliferate [13–15]. The evidence in support of this concept may be summarized as follows: (i) the recombinant forms of cellular proto-oncogenes present in acutely transforming retroviruses act as dominant replication-stimulating agents; (ii) evolutionary conservation suggests essential and fundamental roles for these genes in normal cellular metabolism; (iii) numerous studies correlate neoplasia with perturbations of the proto-oncogenes (including translocations, gene amplification, DNA methylation changes and point mutations); (iv) differential expression of some proto-oncogenes during embryonic development and tissue repair or remodeling implicates them in proliferative processes; (v) there are very significant homologies between proteins encoded by certain viral oncogenes and normal cellular growth factors or receptors for growth factors.

Evidence has been accumulating in favour of the hypothesis that at least some proto-oncogenes exert their growth control by regulating processes that directly mediate transit through the normal cell cycle [13–16]. At least five proto-oncogenes (c-*myc*, c-*fos*, c-*ras*, c-*myb*, and p53) have characteristics of such putative controlling genes. For example, expression is enhanced in proliferating cells, and possibly is restricted to the period (or a part thereof) leading up to the onset of DNA synthesis.

IIA. c-myc

The c-*myc* proto-oncogene is the cellular counterpart of the transduced v-*myc* oncogene found in several avian retroviruses and in feline leukemia virus [17]. The gene is transcribed at a low level in most normal cell types into a 2.2–2.4-kb mRNA encoding two related nuclear phosphoproteins around M_r 65 000. Experiments employing quiescent lymphocyte or fibroblast populations stimulated with serum or appropriate mitogens revealed that the level of c-*myc* transcripts in cytoplasmic poly(A) mRNA was modulated in response to these proliferative stimuli. The relative abundance of c-*myc* mRNA was low in both confluent and serum-starved cells, but rose 20–40-fold 3 h after mitogen stimulation [18,19]. There was some increase in c-*myc* transcription after stimulation, but the large increase in the cytoplasmic abundance of c-*myc* mRNA appeared to be achieved through post-transcriptional regulation [20,21].

Direct tests of the c-*myc* gene function as an intracellular mediator of the mitogenic response in G_0' cells have been reported. Expression of the *myc* gene under control of the hydrocortisone-inducible MMTV promoter diminished the requirement for PDGF [22], and microinjected c-*myc* could substantially substitute for PDGF in cooperating with platelet-poor plasma to stimulate DNA replication [22a]. That the full mitogenic response was not obtained, even with hydrocortisone-induced c-*myc* mRNA levels higher than those found in the parental cells stimulated with PDGF, suggested that the c-*myc* gene product was co-ordinated in its actions with other gene products required for the induction of the competent state by PDGF.

In contrast to the rapid increase in c-*myc* mRNA levels when quiescent fibroblasts re-enter the cell cycle, the levels of this transcript and its protein product do not vary greatly throughout the G_1, S and G_2 + M phases in normally cycling cells. When non-synchronized populations were separated into subpopulations of different size and DNA content by counterflow centrifugation (elutriation) or were treated with inhibitors to arrest cells in various stages of the cell cycle, c-*myc* mRNA was observed to vary no more than 2-fold in each cell cycle compartment [23–25]. De novo synthesis occurred at each stage, and the 20–30-min turnover times of both protein and mRNA appeared invariant [25–27]. These studies revealed that c-*myc* protein rapidly accumulated during the G_0 to G_1 transition, and that usually it was continually expressed thereafter during further proliferation, presumably in response to the continued stimulation by growth factors. One exception may be in erythroleukemia cells induced to differentiate; here c-*myc* expression occurred primarily in G_1 [24].

Consistent with a role in cellular proliferation is the reduced c-*myc* transcript level that accompanies differentiation (with the cessation of cell division) induced by a number of chemicals or protein factors in the HL60 promyelocytic human leukemia cell line and mouse erythroleukemia or myeloid leukemia cells [24,28–30]. However, the reduced levels in HL60 cells appeared more related to the differentiation process than to inhibition of proliferation [30a]. In the HL60 cells, which have an amplified c-*myc* locus, the loss of an S_1 nuclease-sensitive site upstream of the first exon correlated with a decrease in the transcriptional activity of the gene [30b]. Growth inhibition after interferon treatment was also associated with reduced c-*myc* mRNA levles [31]. The short half-life of the message [32], possibly mediated by sequences in the first exon of the gene [33,34], may play a significant role in post-transcriptional regulation after interferon treatment [35]; however, transcriptional regulation has been detected after exposure of Daudi Burkitt's lymphoma cells to interferon [36]. Inhibition of protein synthesis in normal bursal lymphoma cells stabilized the c-*myc* mRNA, perhaps by uncoupling a degradative process triggered to begin upon completion of translation of the message [37]. Future studies must assess quantitatively the relative importance of transcriptional and post-transcriptional modes of regulation, both with respect to timing and the cell type (there is considerable variation, cf. Refs. 32 and 36) and under a variety of conditions known to alter c-*myc* mRNA levels.

Recent models of c-*myc* gene regulation have held that the c-*myc* protein is involved either directly or indirectly in a negative feed-back mechanism acting on its own transcription or alternatively on the stability of the transcript [38–41]. Such models are based on the observation that in mouse plasmacytomas and human Burkitt's lymphoma cell lines often only the translocated (often truncated) form of the c-*myc* gene is transcribed, usually in a constitutive and elevated manner. In the presence of the abnormal allele, a *trans*-acting negative regulatory element, possibly the c-*myc* protein itself, or a protein influenced by it, is thought to interact with transcriptional control sequences in the normal gene or with the transcript of the normal allele, suppressing expression of the normal allele. However, it has been argued that at the stage of B-cell differentiation represented by Burkitt's lymphoma cells c-*myc* gene expression is normally suppressed [42]. Experimental support for negative regulation of c-*myc* transcription by its own product has been provided by studies noting the absence of c-*myc* expression in haematopoietic cells or fibroblasts infected with v-*myc* constructs [43]. In this case, v-*myc* mRNA levels were up to 100-fold higher than the normal c-*myc* levels. It is possible that the greatly increased level of v-*myc* product activated a negative control region mapped by DNAase I hypersensitivity about 2 kb upstream of the transcript start site for human c-*myc* [44]. In murine cells, however, the hypersensitive sites were implicated in expression rather than repression of c-*myc* [45].

Studies linking the transient induction of c-*myc* to reinitiation of growth have been reported for regenerating liver [46,47] and stimulated lymphocytes [18,48,49]. c-*myc* can be regulated at several points in the cell cycle of normal lymphocytes by substances as diverse as cyclosporin A, interleukin-2, hydroxyurea and TPA [49]. In exponentially growing A431 human epidermal carcinoma cells, treatment with epidermal growth factor (EGF) inhibited proliferation even though c-*myc* mRNA was induced, suggesting that in this case at least c-*myc* induction was not strictly correlated with the induction of proliferative activity or with the growth state of the cells [50]. The conclusion that different cell types may respond in varying fashions to growth factor stimulation is reinforced by the finding that normal human colon lines, which could be stimulated to re-enter the cell cycle after a period of little growth, exhibited transiently elevated levels of the c-*myc* mRNA [51] rather than the constant elevation seen in continuous growing fibroblasts [23]. Conflicting associations between mitogenesis and c-*myc* induction would be explained if c-*myc* expression were a common response to a diverse group of agents that elicit phosphoinositide turnover and protein kinase C activation, but not necessarily entrance into the cell cycle [49,52].

IIB. c-fos

The c-*fos* product is an M_r 55000 nuclear phosphoprotein ($p55^{c\text{-}fos}$) with unknown function and is encoded by the cellular homologue of the v-*fos* gene present in murine FBJ osteosarcoma virus. The 2.2-kb c-*fos* transcript has been estimated to be maximally expressed at only 0.005% (5–10 copies/cell (= 6 pg RNA)) of NIH 3T3 cell mRNA [53].

In general, the pattern of regulation described for c-*myc* mRNA was also seen for the c-*fos* proto-oncogene. Enhanced expression occurred during liver regeneration, and the levels of c-*fos* mRNA and protein increased rapidly after stimulation of quiescent fibroblasts with serum, TPA or growth factors [53–56]. The peak of expression was followed by a rapid decay in the levels of both mRNA and protein. The appearance of c-*fos* mRNA precedes that of c-*myc* mRNA and is one of the early nuclear events, occurring only 15 min after a proliferative stimulus. Increased transcription accounted for at least part of the increased mRNA level [20].

A 56-bp DNA segment approximately 300 bp upstream of the human c-*fos* mRNA cap site contains a sequence element with enhancer-like properties that is essential for polypeptide mitogen induction of c-*fos* mRNA levels. In addition, sequences at the 3′ end of the gene are required to generate the characteristically rapid breakdown which follows induction during transient transfection assays in fibroblasts [57].

As with the c-*myc* gene, there was no correlation of c-*fos* mRNA induction with the (inhibited) proliferative capacity of A431 human epidermal carcinoma cells exposed to EGF [50]. Rather, the timing of induction appeared to be a primary consequence of growth factor-receptor interaction and did not, itself, lead to the mitogenic response. This view could also apply to c-*fos* induction observed in HL60 cells induced to differentiate into macrophages in response to treatment by phorbol esters [58,59]. A rapid induction of the transcript was followed by a drop in the mRNA level, but in this case the lower level persisted for up to 5 days after TPA treatment, at which time substantial cellular differentiation had taken place. c-*fos* was not induced during DMSO-induced differentiation of HL60 cells into granulocytes [59]. Rat pheochromocytoma cells induced to differentiate to neurons by nerve growth factor treatment expressed elevated levels of c-*fos* and actin transcripts shortly after exposure [60,61]. In each cell type, the induction of the c-*fos* gene may set in motion a unique pattern of gene expression. That the c-*fos* product is functionally involved in such a cascade was shown by experiments in which elevated c-*fos* expression led to cellular differentiation following DNA-mediated gene transfer into the F9 teratocarcinoma stem cells [62,63].

A common feature in the regulation of c-*fos*-related, c-*fos* and c-*myc* mRNAs is that the amount of mRNA induced was increased when cellular protein synthesis was blocked by cycloheximide [18,53,55,56,64]. The magnitude of superinduction ranged from 3- to 20-fold depending on the gene and cell type. These results indicated that the elevated expression of these genes was not the consequence of the induced expression of a new gene. Since inhibition of protein synthesis also blocked G_1 transit [65,66], mRNA superinduction is unlikely to be a secondary effect of continued growth and DNA synthesis. Superinduction of these transcripts when protein synthesis is inhibited by any of a variety of mechanisms suggests a model in which a labile protein(s) regulates the abundance of each mRNA; however, mediation via other changes induced by protein synthesis inhibition should not be ruled out.

IIC. c-ras

The M_r 21000–24000 *ras* proteins are the products of a small family of genes capable, when altered, of causing malignancies. The c-*ras*^{K} and c-*ras*^{H} genes are homologues of the oncogenes of Kirsten and Harvey murine sarcoma virus, respectively. Serum induction experiments have implicated c-*ras*^{K} in the transition from quiescence to proliferation [19], although the approx. 6-fold induction of c-*ras*^{K} mRNA was not as striking as that observed for c-*myc* and c-*fos* mRNA. These studies in cultured cells were mirrored by the pattern of c-*ras*^{H} and c-*ras*^{K} (also c-*myc*, but not c-*abl* or c-*src*) gene expression in normal rat liver regenerating after partial hepatectomy where significant increases in the levels of c-*ras*^{H} and c-*ras*^{K} transcripts were seen to coincide with the peak of DNA synthesis induced by this operation [46,67].

Direct tests for functional involvement of c-*ras* during serum-induced proliferation have involved micro-injection of normal and oncogenic M_r 21000 *ras*^{H} proteins produced in and purified from *Escherichia coli* [68,69]. Only when large amounts of the normal protein were injected into fibroblasts did a portion of the cells made quiescent by serum starvation enter the S-phase of the cell cycle; much lower amounts of the activated *ras*^{H} oncogene protein were able to initiate a round of DNA synthesis. These studies were confirmed by microinjection of monoclonal anti-*ras* antibodies. Inhibition of serum-induced DNA synthesis by anti-*ras* antibody revealed that a functional *ras* protein was required shortly before initiation of S phase [70]. A monoclonal antibody specific for the mutant form of *ras*^{K} protein blocked binding of GTP and caused, after microinjection, transient reversion of the transformed phenotype [71]. In rat pheochromocytoma cells, the *ras* proteins exerted a different biological effect, since neuronal differentiation was induced by introduction of the activated forms c-*ras*^{H} or c-*ras*^{K} [72,73].

The exact role of cellular *ras* proteins in DNA synthesis and cell division continues to be a subject of speculation, and much attention has focused on their high affinity for guanosine nucleotides (GTP or GDP) [74,75], associated GTPase activity [76,77], and cytoplasmic membrane localization possibly due to a post-translational lipid modification [78,79]. The membrane association and GTP-binding capacity, as well as sequence homologies, of the p21 *ras* proteins suggest that they may be related to the G-proteins responsible for stimulation and inhibition of adenylate cyclase following polypeptide hormone interaction with specific cell surface receptors [80,81]. If a similar function can be ascribed to the *ras* proteins, as their ability to activate adenylate cyclase in yeast suggests, then they may represent a branch point for transduction of information across the plasma membrane for the regulation of proteins other than adenyl cyclase [82,83]. The influence that elevated expression of c-*ras* following growth factor stimulation might have on this scenario is unknown.

IID. c-myb

The 4.5-kb transcript from the cellular homologue of the avian myeloblastosis virus oncogene is commonly found in cells of haematopoietic lineage [17]. Its occurrence in immature, proliferating cell populations but not in mature cell types suggests that the expression is regulated in association with growth and cell division [30,84,85]. The appearance of this transcript in mitogen-stimulated T lymphocytes has been correlated with their entry into S phase [86]. In a recent, well-defined series of experiments Thompson et al. [86a] have shown that in chicken embryo fibroblasts and transformed T cells the *c-myb* mRNA levels are regulated post-transcriptionally, in part through changes in stability, with maximal levels in late G_1/S phase of cycling cells; in contrast, the high level found in normal thymocytes was largely the result of tissue-specific enhanced transcription.

IIE. p53

In SV40-transformed mouse cells, virally encoded large T-antigen was found associated with a cellular protein with an apparent M_r in SDS gels of 53 000 [87]. We now know that this normally short-lived nuclear phosphoprotein is stabilized by its association with the viral tumor antigen. The level of p53 in cells is often elevated in cells that have been transformed by a wide range of viral, physical or chemical agents [88–90], and in cells that have suffered certain types of DNA damage [91]. Evidence has accumulated that suggests that p53 plays a role in cell immortalization and transformation [92–96]. In particular, a transcriptionally activated p53 gene can cooperate with activated *ras* oncogenes to transform primary rat fibroblasts [92,93,96]. The mRNA is around 2.5 kb and encodes a polypeptide of predicted M_r 44 000 [96a].

In oncogene complementation systems one group of genes, typified by *myc* and adenovirus E1A, is ascribed establishment/immortalization functions [97]. That p53 is a member of this group is supported by the observation that it was able to immortalize rat chondrocytes that normally senesce after 30 doublings [96]. Other evidence suggests that the contribution of p53 to the process of transformation is not synonymous with immortalization. Already immortalized cell lines (such as Rat-1 cells) can be made highly tumorigenic by overexpression of p53, suggesting that p53 confers a property in addition to immortalization [95]. Also, p53 genes that have been modified by alterations within their coding regions can be shown to immortalize cells while failing to cooperate with an activated *ras* gene to give ‘full-blown’ transformation [98]. Thus, immortalization and *ras* cooperation seem to be separable activities of p53.

A requirement for p53 during the G_0 to S phase transition, but not for the transit of normally cycling cells from mitosis through G_1 to S phase, can be inferred from the effects of monoclonal antibodies directed against p53 on these events after microinjection into cells [99,100]. The amount of cytoplasmic p53 mRNA (approx. 2–3 kb) and the cellular p53 protein level both rose substantially during the transition from G_0 to S in serum-stimulated Swiss 3T3 cells [101]. However, another recent study using Swiss 3T3 cells and C3H10T1/2 cells, while confirming that the absolute level of p53 protein was several-fold lower in quiescent cells compared to exponentially growing cells, also revealed that the relative rate of p53 synthesis was slightly higher in quiescent cells [102]. The increase in the absolute amount of p53 protein per cell after stimulation was correlated with the increase in the rate of total protein synthesis. These authors suggested that, because p53 expression was not selectively shut off in quiescent cells, the p53 protein therefore did not have the characteristics expected for a protein that regulates either the G_0–G_1 or the G_1–S transition [102]. The amount of p53 protein did not vary significantly among G_1, S and G_2 rat 3T3 cells sorted by flow cytofluorimetry and quantified by a radioimmune assay procedure [102a].

Interesting data on p53 expression have been obtained from studies on human peripheral blood lymphocytes (PBL) that had been stimulated with phytohaemagglutinin (PHA) [103]. When depleted of accessory cells (monocytes/ macrophages), PHA-stimulated PBL grew in size but did not replicate their DNA. Entry into the cell cycle was initiated only after the addition of interleukin-2. Thus, growth in size could be distinguished from cell cycle-related events in this system. p53 protein was induced only under conditions leading to a full mitogenic response, and if the response was inhibited by addition of antibody to the interleukin-2 receptor, p53 induction was also inhibited [103]. Although the p53 found in transformed cells was phosphorylated, that found in normal thymocytes was not [90]. Post-transcriptional regulation of p53 levels, likely via protein degradation, is suggested by the observation that cells with high (SV80, Raji) and low (HeLa, normal spleen) amounts of p53 protein had comparable amounts of functional p53 mRNA [103a,b].

On balance it appears that there is good evidence to link p53 expression with cell cycle progression, though its role in this process, and in cellular immortalization, remains obscure. A direct involvement of p53 in cell transformation is suggested by its elevated level in many tumors and the observation that proteins encoded by diverse transforming viruses (SV40, adenovirus) form complexes with it. However, as pointed out by Calabretta et al. [103c], the increased expression of a cell cycle-dependent gene in a tumor may simply reflect an increased proportion of cycling cells. It is intriguing that cell lines exist, such as the human myelocytic leukemia cell line HL60, in which the p53 gene appears to have suffered deletions and is not expressed; however, these cells express *myc* in larger amounts, hinting that this may be one way of compensating for the absence of p53 function [104]. Studies on the content of p53 protein in murine erythroleukemia cells during the chemically induced commitment to terminal cell division and differentiation revealed that lowered p53 levels correlated with terminal G_1 arrest [104a]. When F9 embryonal carcinoma were induced to differentiate there was a 20-fold decrease in the p53 mRNA and protein levels but no change in the (3 h) half-life [104b].

III. The search for cell cycle-regulated genes

In this section we consider proteins and RNA species identified initially by virtue of the cell cycle dependence of their appearance.

Two approaches have been predominant in recent attempts to identify cell cycle-regulated genes. One, employed by several laboratories, is to screen cDNA libraries with probes made from mRNA isolated from cells in two different growth states to identify specific clones that respond differentially [105–110]. Other workers have analysed the proteins (often on two-dimensional SDS-polyacrylamide gels) synthesized by cells at different stages of the cell cycle or after mitogen-stimulation of quiescent cells [111–118]. A derivative of this approach involves looking at the electrophoretic patterns of polypeptides translated in vitro using mRNA isolated from cells in different growth states [119,120]. We will deal with the findings of these two types of studies separately. In studies far too numerous to cite, the ability of various stimuli ranging from tumour promoters and interferons to lectins and growth factors to induce specific proteins or enzyme activities has been examined; however, the focus of these studies has rarely been on cell cycle regulation.

IIIA. The identification of cDNA clones corresponding to cell cycle-regulated RNAs

When filter replicas of a cDNA library are hybridized with radioactive cDNA probes prepared from poly(A) mRNA from cells before and after mitogenic stimulation, differential gene expression (more specifically, altered cytoplasmic abundance of specific RNAs) is reflected by differences in the signal intensities displayed by specific colonies. The virtue of this technique lies in the fact that it permits the isolation of individual genes of interest. Its vices are that artefactual signals are frequently generated, making the work very labour-intensive, and that the level of sensitivity restricts it to the identification of abundant or moderately abundant mRNAs. Stiles and his collaborators have estimated the minimum representation of a particular mRNA detectable in a population to range from 0.01 to 0.1% [106]. Consequently, all of the genes described in this section fall into the category of those that are expressed to reasonably high levels, at least transiently. True low-abundance mRNAs that show cell cycle-dependent patterns of accumulation (e.g. c-*fos* or c-*myc* [53,121]) would not have been detected. However, new approaches to cDNA library generation and colony screening developed in our laboratory [122,123] should yield an increase in the sensitivity of the method; alternatively, subtraction of unwanted clones by repeated hybridization followed by 'brute-force' analysis of the remaining clones also yields interesting clones [124].

As we stated in the introduction, one of the main intentions of this review is to draw together the work on the identification, via cDNA clones, of new genes. These cDNA clones have been obtained from a variety of sources, including mouse, rat and Chinese hamster ovary cells. Published DNA sequence information is available for a few of them, including proliferin [125], JB (r-*fos*) [64] and 49C8, a transcript homologous to B2 repetitive elements [110].

We have compiled data on these genes in Table I. Included in this table are the sources of the various cDNA clones, and (where known) the sizes of their corresponding RNAs and proteins, the specificity of induction by individual growth factors, their times of maximal expression, and the effects of inhibitors of transcription and translation.

The first group, clones KC, JE, C1B, CC, JB (r-*fos*) and MF, contains mRNAs induced by PDGF in BALB/c 3T3 cells [106,126,127]. Three of these clones (KC, JE and JB) have been studied in some detail by Stiles and co-workers. The JB clone has been shown to have homology with the third exon of c-*fos*, hence its designation as r-*fos* [64]. Clone KC corresponds to an mRNA that is superinduced when cycloheximide (CHM) is added along with PDGF, which, as described in section II, is also the case for the PDGF-inducible proto-oncogenes c-*myc* and c-*fos*. In part, the effect of CHM may be attributable to the stabilization of polysomes, thus preventing mRNA turnover. However, this cannot explain the 20-fold superinduction of KC expression by both CHM and puromycin [106]. Possibly the genes are transcriptionally regulated by a labile repressor – either a protein or something keyed to ongoing protein synthesis. KC and JE transcripts were also induced by phytohemagglutinin (PHA) stimulation of normal human peripheral blood mononuclear cells, with times of maximal expression similar to those seen during PDGF-stimulation of quiescent mouse fibroblasts [128]; however, their levels in leukemic cells were reduced [129].

Three clones (18A2, 32A4 and 28H6) described by Linzer and Nathans [107] were derived by comparing cDNA probes from growing BALB/c 3T3 cells to their quiescent, serum-deprived counterparts. One clone, 28H6, showed profound serum- and PDGF-inducibility, with maximal transcript levels 12–18 h after stimulation. Sequence analysis of this clone, subsequently termed proliferin, showed that it encoded a protein containing 30–40% amino acid homology with mammalian prolactins [125]. This gene will be discussed in more detail in section IVD2, since it has been demonstrated that proliferin is identical to the secreted mitogen-regulated protein (MRP) of Swiss 3T3 cells [130]. Clones 18A2 and 32A4 have not been characterized beyond their initial description. From a comparison of the Northern gel patterns, we suggest that 32A4 may be related to clone 49C8, which corresponds to the murine B2 repetitive sequence [110].

Clones of mRNAs whose abundance is enhanced after quiescent mouse fibroblasts are stimulated in the presence of cycloheximide have been isolated by differential screening of a cDNA library made in λgt10 [131]. From 50 000 plaques screened initially, 357 that showed augmented expression were isolated and found to represent between 14 and 41 different mRNAs, some of very low abundance. Five clones (3CH61, 3CH77, 3CH92, 3CH96 and 3CH134) representing five of the families of the more abundant species were studied in detail (Table I). Like c-*fos*, the mRNAs appeared rapidly after stimulation with serum in the absence of cycloheximide, peaking between 40 and 90 min and then decaying with a half-life of about 30 min. The mRNA corresponding to clone 3CH61 increased again after 6–10 h. In the presence of cycloheximide and serum the mRNAs were all stabilized at a high level for at least 3 h; cycloheximide alone had little effect. PDGF, FGF and TPA were each able, alone, to induce expression of the five mRNAs.

Cycloheximide superinduction (or at least stabilization) of mRNA in concanavalin A-stimulated human lymphocytes was used by Forsdyke [132] to obtain clones of mRNAs expressed immediately after entrance of G_0 cells into G_1. The author speculates that certain mRNAs are 'induced' by cycloheximide as the result of a de-

TABLE I

Cell of origin	DNA clone designation	Stimulus when identified	mRNA size (bases)	Encoded protein size ($M_r \times 10^{-3}$)	Time of maximum induction (h)	Effect of transcription inhibition	CHM super-inducibility
BALB/c 3T3	KC	PDGF, 4h	1200	10	1	blocked	yes
	JE	"	990	19	4	blocked	yes
	C1B	"					
	CC	"					
	JB, r-*fos*	"	2000				yes
	MF	"					
BALB/c 3T3	18A2	serum	700		continuous		
	28H6 (proliferin)	"	1000	25	12–18	blocked	
	32A4	"	440–600, 1700, 2900, 5000		12–18		
	3CH61	serum + CHM, 3 h	2700	43	1, 6		yes
	3CH134	"	2800	40	1		yes
	3CH77	"	3600	–	2		yes
	3CH92	"	2200	35	1		yes
	3CH96	"	1600	–	1		yes
*ts*13 hamster	p13-2A8	serum, 6 h	not discrete		6, 24		
	p13-2A9	"	3800, 750		16		yes
	p13-2A10	"	450		16		
	p13-2F1	"	1500		6–16		yes
	p13-4F1	"	1550		6–16		yes
Swiss mouse embryo fibroblast	16C8	serum, 15 h	900	18	6–12	blocked	no
	49C8	"	500	–	S[b]	blocked	yes
	5B10	"	680	7	S[b]		
	31H4	"	2100	48	12		
	33H1	"	2000	42	6–12		
JB6, mouse epidermal	2ar	TPA	1600	60	continuous	blocked	no
Jurkat human leukemic	JD15	TPA	1800–2000	32	2–4	blocked	
Fisher rat 3T3	pTR1	transformation	1900	53	8–24		
Human[a] PBL	7	Con A + CHM, 2h	2150		4		yes
	10	"	2150				
	19	"	980, 1120		4		no
	30	"	3400				

[a] Seven cDNA clones were also isolated after PHA and phorbol ester stimulation of resting human lymphocytes [332,333].

[b] S, the signal reached its highest value during S phase (i.e. 12–24 h after serum stimulation). No subsequent decline was visible, perhaps due to loss of synchrony

crease in the concentration of an autogenously regulated repressor. Four clones identifying at least four mRNAs whose levels were enhanced were partially characterized; whether any of them corresponded to c-*myc* or c-*fos*, which might be found with this methodology, was not determined.

Baserga and his colleagues [108] have described the set of cDNA clones 2A8, 2A9, 2A10, 2F1 and 4F1 corresponding to mRNAs that were induced 6 h after serum stimulation (at 34°C) of quiescent *ts*13 cells, a hamster cell line with a temperature-sensitive mutation blocking passage through G_1. Transcripts corresponding to all of these clones were detectable in cytoplasmic RNA from quies-

Specificity of individual mitogens [c]								Identity	Ref
serum	PDGF	FGF	EGF	insulin	IGF-1	PHA	TPA		
	+ + + +		–	–		+ +			64, 106, 127, 129
	+ + + +	+	+	–		+ +			
	+ + + +		+	–					
	+ + + +								
	+ + + +							3rd exon c-*fos*	
	+ + + +		+	–					
+ +									107, 125, 130, 131
+ + + +	+ + + +							prolactin-like	
+ + + +									
+ +	+ +	+					+		
+ + + +	+ + + +	+					+		
+ + + +	+ + +	+					+		
+ + + +	+ + + +	+ +					+		
+ + + +	+ + +	+ +					+ +		
+ + +									108, 129, 357
+ +						+		c-*fos*-like	
+ + + +									
+ +						+ + +			
+ +						+ + +		Ha-*ras*-like	
+ + + +	+ +	+ +	+	–	–		+ + +		135, 110
+ + + +	+	–	–	–	+		–	B2 element	
+ +									
+ + +									
+ + +									
	+ +		+ + + +		–		+ +		J Smith, unpublished data
						+ + + +	+ + + +		146
–			+ + + +						147
									132

[c] Relative induction of individual genes by purified growth factors estimated from published data for mRNA abundances + + + + represents the maximum induction observed, – indicates no induction

cent cells and were induced 3–6-fold in G_1. The temperature sensitivity of *ts*13 cells, which causes the cells to be blocked 3–5 h prior to the start of S phase, allowed these authors to subdivide the clones into 'early' or 'late' genes. When *ts*13 cells were serum-stimulated at the nonpermissive temperature (39.6 °C), levels of RNA complementary to 2A9 and 4F1 were 10-times those found in quiescent cells, whereas the 2A8 transcript abundance was not altered. Thus the G_1 events that control the expression of the 2A9 and 4F1 genes are not dependent on the function blocked by the *ts*13 mutation.

Transcripts homologous to 4F1 and 2F1 have been detected in human peripheral blood mononuclear cells (PBMC) and shown to be induced after PHA stimulation [129]. No expression of 2A9 could be detected in these cells, though transcripts with 2A9 homology were induced in serum-stimulated human WI-38 fibroblasts, suggesting that the expression of this gene is cell type-specific. The relative abundances of transcripts homologous to 2F1, 4F1, c-*myc*, KC, JE and the gene for the interleukin 2 (IL-2) receptor have been determined in purified preparations of T lymphocytes [128]. In these cells PHA treatment caused expression of 2F1 and the IL-2 receptor, but not expression of c-*myc*, 4F1, JE or KC, which could only be induced in the unfractionated PBMC. Accessory cells in the unfractionated population were necessary for the full proliferative response of lymphocytes to PHA; in their absence the cells grew in size but did not synthesize DNA. These clones may therefore permit dissection of the independent processes of growth in cell size and the preparations for DNA replication [133]. In a comparison of a panel of genes that included c-*myc*, 4F1, KC-1, c-*ras*, 2A9, ornithine decarboxylase, p53, 2F1, thymidine kinase and histone H3, all of which were inducible by serum, it was found that only a subset (the last five named) were activated following adenovirus type 2 infection of cells [134].

We have described five genes isolated from a cDNA library made with poly(A) mRNA from secondary cultures of mouse embryo fibroblasts. The clones were identified via their differential response to probes from quiescent cells and from cells 15 h after serum stimulation [110,135]. Two of these genes (16C8 and 49C8) have been characterized extensively. 16C8 corresponds to a 900-nucleotide mRNA that appears to encode an M_r 22600 secreted protein that may be glycosylated (Edwards et al., unpublished data). The abundance of this mRNA is maximal 6–12 h after serum stimulation of 3T3 fibroblasts, and its expression requires protein synthesis, in contrast to the 'early' class of PDGF-inducible genes [106]. Individual mitogens such as FGF, TPA and PDGF (Fig. 2) caused a partial induction of 16C8, up to 80% of the serum-induced level in the case of TPA. In contrast, other growth factors (EGF, insulin and IGF-I) produced no or very little induction. Transcriptional regulation plays a part in controlling the level of 16C8 mRNA, as shown by a peak in transcription rate at 3 h after serum stimulation in nuclear 'run-off' experiments. However, this is likely not the only level of control, since 16C8 transcripts were found in nuclear RNA from quiescent cells and the steady-state levels in nuclear RNA did not change appreciably after serum stimulation [110].

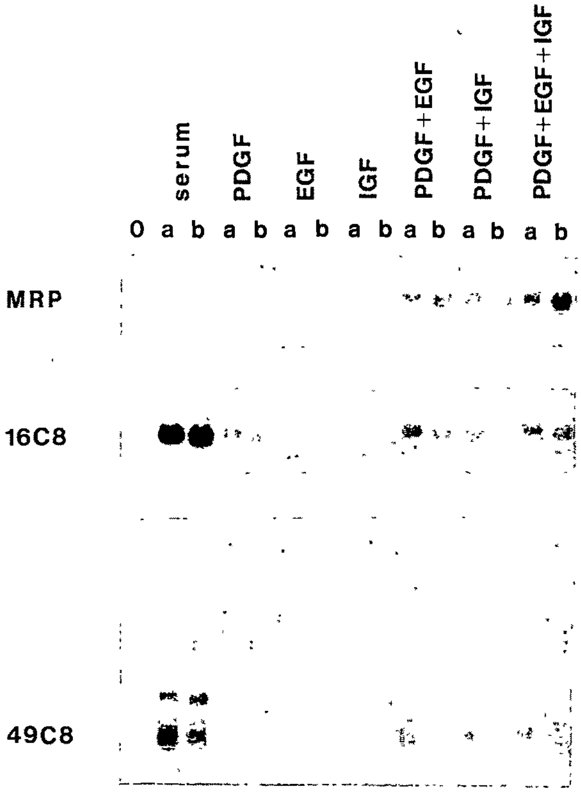

Fig. 2. Induction of cell cycle-dependent genes by various mitogens. Cytoplasmic RNA prepared from quiescent cells (0, in 0.5% fetal bovine serum) and from cells 6 h and 12 h (a and b, respectively) after refeeding with mitogen-supplemented fresh medium was electrophoresed through 1.1% agarose in the presence of formaldehyde and then transferred to nitrocellulose. The blot was hybridized sequentially with three nick-translated plasmids containing a portion of cDNA corresponding to each gene. The band marked with an arrow in the serum-stimulated samples probed with 49C8 derives from some residual 16C8 probe remaining hybridized to the blot. Mitogen supplements were added at the following concentrations. serum, 10%; PDGF, 10 ng/ml; EGF, 20 ng/ml; IGF-(recombinant somatomedin C), 26 ng/ml

Three independent members of the 49C8 class were isolated during the initial screening of the cDNA library. These clones identify a dispersed class of short (approximately 500 nucleotides)

RNA molecules that are not found in polyribosomes and are unable to hybrid-select any translatable mRNAs [110]. The RNAs are homologous to the repetitive element designated B2. The 10^5 members of the 200-bp murine B2 family (B1 is the mouse Alu equivalent) are flanked by inverted repeats and typically contain RNA polymerase III promoter and terminator signals and an oligo(dA) stretch [136–139]. The induction of these short cytoplasmic B2 transcripts after serum stimulation was shown to be sensitive to actinomycin D but not to α-amanitin or 5,6-dichlororibofuranosylbenzimidazole (DRB); in agreement with other studies this suggests that they are products of RNA polymerase III [140,141]. EGF, FGF, insulin and TPA were each poor inducers of the B2-related RNAs when added separately to subconfluent serum-deprived Swiss 3T3 cells [110]. PDGF and IGF-I (somatomedin C) had a modest effect alone (10–20% of that obtained with 10% fetal bovine serum), though combinations of PDGF and EGF or IGF-I were more effective; these same combinations gave the best induction of MRP (proliferin) but not 16C8 (Fig. 2).

The fact that the cytoplasmic B2-related RNAs are induced by mitogens is interesting in the light of other studies showing that the levels of RNAs corresponding to B2 elements show temporal regulation during mouse embryogenesis [142,143]. Genes containing B2 sequences were transcribed extensively, though few cytoplasmic poly(A) mRNAs contained them [137,140]. One such mRNA, encoding an H-2D major histocompatibility gene, was found by Rigby and co-workers in elevated amounts in SV40-transformed 3T3 fibroblasts compared to untransformed cells [144,145]. The short B2 transcripts were also more abundant in these and other SV40-transformed cells [124,141]. The functional involvement, if any, of these sequence elements in the processes of differentiation, cellular transformation and proliferation is not known.

Two other mitogen-inducible genes, JD15 and pTR1, have been identified through cDNA cloning. The JD15 clone was isolated from a human leukemic cell cDNA library and was shown to identify an approx. 1.9-kb mRNA that was inducible by TPA or PHA [146]. Nuclear 'run-off' transcription experiments confirmed that the gene was transcriptionally activated by each agent. The pTR1 cDNA clone was obtained in Breathnach's laboratory by screening a λgt10 library of cDNA prepared from poly(A) mRNA from polyoma virus-transformed Fisher rat 3T3 fibroblasts with a cDNA probe that had been enriched for transformation-specific sequences by 'hybridization subtraction' [147]. The pTR1 gene encodes an M_r 53000 protein unrelated to currently known sequences. In addition to being induced in cells that have been transformed by polyoma virus, Rous sarcoma virus, or the human cellular oncogene *ras*^{H}, pTR1 was induced by EGF at 5 ng/ml. Paradoxically, the presence of 10% fetal calf serum in the growth medium abolished the induction by EGF. This suggests that a component of serum acts to override the induction caused by EGF (cf. also MRP mRNA induction in Fig. 2). Since control of expression of the gene was at the level of transcription, this system offers the possibility of interesting insights into the ways that oncogenes and growth factors control the expression of specific genes.

A relatively small collection of 300 clones was screened using cDNA probes from quiescent serum-starved Rat 1 fibroblast cells and from cells after overnight stimulation with 10 ng/ml EGF in serum-free medium [148]. Fourteen clones yielded an approximately 5-fold elevated signal when probed with cDNA from EGF-stimulated (compared with unstimulated) cells. These clones identified five independent genes. Sequencing of the cDNA inserts revealed that the five families had homologies with lactate dehydrogenase, glyceraldehyde-3-phosphate dehydrogenase, enolase, triosephosphate isomerase and actin. It is likely that the high incidence of positive clones observed in this screen (5% of those analysed) reflected metabolic differences between the quiescent and stimulated cells, particularly as four of the five induced genes encode glycolytic enzymes. In other studies the relative level of glyceraldehyde-3-phosphate dehydrogenase mRNA was found not to vary following serum stimulation of quiescent secondary mouse fibroblasts or Swiss 3T3 fibroblasts [110,135].

Growth-related differences between quiescent and serum-stimulated mouse fibroblasts have been observed previously. There was a doubling in the ratio of mRNA to rRNA in the cytoplasm of exponentially growing or serum-stimulated Swiss 3T3 cells compared to their quiescent counterparts [149]. Protein synthesis is enhanced in proportion to the concentration of serum used to stimulate G_0 cells [149a]. The relative concentrations of transcripts corresponding to mitochondrially-encoded genes decreased 2–3-fold in poly(A) mRNA from mid-S phase fibroblasts compared to unstimulated cells [135]. This suggests that the mitochondrial transcripts accumulate in parallel with the major cytoplasmic RNA species, i.e. rRNA, and therefore reflect growth in cell size.

In addition to the clones described in Table I, differential screening using cDNA probes from unstimulated AKR-2B mouse cells and from cells that had been stimulated by EGF for 6 h showed that a family of retroviral-like sequences called VL30 was induced [105,150]. Murine VL30 mRNAs are 5–6-kb species derived from dispersed, moderately (100 ×) repeated uninterrupted genomic sequences with properties suggestive of an endogenous replication-defective retrovirus related to murine leukemia virus [151]. The VL30 'genes' are bracketed by 600-nucleotide long terminal repeats (LTRs) with all the characteristics of retrovirus LTRs. The polyadenylated RNA encodes no known proteins and is copackaged efficiently by replication-competent retroviruses. Expression of the RNA varies in different murine lines and is substantially increased in cells stimulated by certain growth factors (EGF, TPA); additionally, transformation can cause an increase in VL30 expression under certain conditions [152, 153].

It appears likely that the endogenous VL30 sequences are expressed because they contain a sequence element, presumably in the LTR, that promotes their gratuitous transcription in appropriately stimulated cells. The expression of the LTR of another murine endogenous retroviral element (intracisternal A particle, IAP) has been shown to occur in early G_1 and in density-arrested Friend erythroleukemia cells [154]. There was limited but significant sequence homology between the LTR and the 2A8 clone [108] identified in Syrian hamster cells that corresponded to a repetitive sequence whose expression was highest in the mid G_1 period of serum-stimulated quiescent BHK cells.

IIIB. Polypeptides synthesized at specific times during the cell cycle

One of the reasons for investigating cell cycle-dependent polypeptide synthesis is the particular sensitivity of the G_1 phase of the cycle to inhibitors of protein synthesis [65,66]. Pardee's restriction point model for cell cycle control proposes that commitment beyond a restriction point 'R' in G_1 requires the synthesis of a labile, growth factor-induced protein [66]. Thus proteins that display this characteristic may be especially relevant to cell proliferation studies.

Though the great majority of cellular proteins are synthesized in all stages of the cell cycle, some exceptions have been observed. In general, two-dimensional gel electrophoresis is required to detect these quantitatively minor changes in gene expression [111–113]. In some instances one-dimensional analysis has proved adequate and was used, for example, to demonstrate a peak in actin synthesis in mid G_1 during the transition from G_0 to S phase, but not in the G_1 phase of cycling cells [155]. Lectin activation of lymphocytes increases the cytoplasmic levels of both actin (β and γ) and, to an even greater extent, tubulin (α and β) mRNAs [156].

Five PDGF-inducible proteins (pI to pV with M_r values of 29000, 35000, 45000, 60000 and 70000) whose differential rate of synthesis was raised sufficiently (to roughly 1% of total cellular pulse-labeled protein) have been detected by Pledger et al. on one-dimensional gels [116,157]. One of these proteins (pII) corresponds to the major excreted protein (MEP) of BALB/c-3T3 cells [158] and will be discussed in more detail in section IVD1. The synthesis of the protein pI (M_r 29000) occurs during the first half of G_1 and is thereafter suppressed, indicating a close correlation with the induction of competence by PDGF; it is associated with nuclear material and is stable for 9–12 h [159].

Analysis of SDS gels of proteins translated in vitro from mRNA isolated from PDGF-stimulated BALB/c 3T3 cells revealed four PDGF-inducible mRNAs detected via their translation products (tpI-IV) [119], some of which likely correspond to the proteins (or at least their polypeptide precursors) discussed above. Thus tpI is similar in size to pI (M_r 29 000); however, the PDGF-inducible mRNA has not yet been matched with an mRNA identified by the current collection of PDGF-inducible cDNA clones (Table I). The mRNA encoding tpI reached a maximum 60–90 min after PDGF addition and then declined. The mRNAs corresponding to tpII (M_r 35 000; likely pII/MEP) and tpIII (M_r 55 000) began to accumulate only after 4–6 h and depended upon prior protein synthesis. Only when cycloheximide was added together with PDGF was it possible to detect the mRNA encoding tpIV (M_r 32 000). EGF, but neither insulin nor platelet-poor plasma (containing somatomedin C), was able to induce these mRNAs [119].

Several two-dimensional gel analyses have revealed differences in the patterns of proteins synthesized by quiescent and serum-stimulated cells [111–113,115–118,160]. Four cytoplasmic proteins (26 000, 28 000, 45 000, 47 000) were observed by Thomas et al. [115] to increase in abundance within 1 h of serum stimulation of quiescent Swiss 3T3 cells. Synthesis of three of these proteins was inhibited by actinomycin D treatment. Tubulins increased in abundance during mitosis, while during S there was an increase in an M_r 36 000 'cytoarchitectural' protein [113]. Histones and cyclin (PCNA) are discussed in section IV.

Two dimensional gels were used to unmask proteins that were synthesized at elevated rates 9 h after serum-stimulation, when BALB/c 3T3 cells are approx. 2 h prior to the restriction point R that leads to commitment to cell division [160]. Though several differences were observed, attention was focussed upon an M_r 68 000 protein (p*I* 6.3) because it was synthesized at higher rates in benzo[*a*]pyrene-transformed cells (BPA31) compared to untransformed cells (A31), and because the protein was found to be unstable during a 3 h chase of A31 cells but stable in the BPA31 cells. These characteristics make this protein a candidate for a restriction point control function [161]; however, not all transformed cell lines had elevated p68 levels [160]. Interestingly, the hsp70 family of heat shock proteins contains members that are unstable in vivo and have approximately the same M_r, although p*I* values and half-lives may be somewhat different from p68 [162,163]. The fact that the hsp70 gene of HeLa cells was transcriptionally activated and its mRNA accumulated during G_1 in synchronized cultures [164] is intriguing in view of the identification of human hsp73 as a poly(A)-binding protein with a possible regulatory role in mRNA translation [165].

IV. Some properties of known cell cycle-regulated genes

In this section we review the recent literature concerning cell cycle-dependent expression of genes encoding proteins with (for the most part) defined functions.

IVA. Histones

Histones, the small basic proteins complexed with eukaryotic DNA, have long been known to be synthesized in a cell cycle-dependent manner in most eukaryotic cells. By the mid-seventies it had been established that core histone synthesis in HeLa cells occurred predominately during S phase and that when DNA replication ceased most histone mRNA rapidly disappeared. Coupling of histone synthesis to DNA replication is of course eminently reasonable, since the only time there is a substantial requirement for new histone protein is when new DNA is being made. We discuss below what is generally true in cultured mammalian cells but with the caveat that certain cell types or certain specific histones may constitute exceptions [166].

The core histones H2A, H2B, H3 and H4 are required to form nucleosomes, and because they are needed in equimolar amounts their synthesis is coordinately regulated. H1 serves to link adjacent nucleosomes, and certain H1 subspecies appear to accumulate preferentially in differentiated or quiescent cells, replacing the H1 subtypes synthesized initially [167,168]. There are also several categories of variant replication-independent core histones whose synthesis is not cell cycle-dependent; instead their synthesis either proceeds constitutively in, for example, G_0 lymphocytes at about 3% of the maximal level observed in S phase or occurs only in certain differentiated tissues [166,169]. Mouse L6 myoblasts contain a species of a polyadenylated H4 mRNA whose level in polysomes remains high in the (nonproliferating) myotubes [170].

The role of the replacement core histones is obscure, but may have something to do with DNA repair or with control of gene expression. The particular variants that are synthesized are characteristic of certain phases of the cell cycle, and in particular allow G_0 to be distinguished from G_1; all four H2A variants are synthesized in quiescent cells, while basal (G_1, G_2) synthesis involves only two minor H2A variants [171]. Although $H1^0$ is found almost exclusively in non-proliferating, terminally differentiated cells, its synthesis could be induced by butyric acid in G_2 cells; its presence was not sufficient to prevent cell proliferation [172].

The histone mRNAs are unusual in that almost invariably they are not polyadenylated; also, most histone genes lack introns [166]. (The gene encoding the histone H3.3, which is synthesized in both cycling and quiescent cells, however, is interrupted and produces an mRNA that is polyadenylated [173,174].) The absence of introns and a poly(A) tail may be a 'streamlining' adaptation related to the fact that most histone synthesis is required, and then in massive amounts, only during S phase. In S-phase mammalian cells, some 10% of total protein synthesis is devoted to histone synthesis. There are about 10–20 copies of each major type of histone gene in vertebrate cells. They are clustered, but not tandemly repeated [175]. Although the coding sequences are highly conserved, there has been considerable divergence in the sequence of the noncoding 5′ and 3′ regions [176].

The abundance of the histone mRNAs and their small size have made them an attractive experimental system, and a number of laboratories have investigated the regulation of histone mRNA synthesis in considerable detail. Dominant among these has been the laboratory of G. and J. Stein [177]. These workers [178] and Heintz et al. [179] have isolated and partly characterized genomic clones containing human histone genes.

Using cloned histone genes as probes, several groups have shown that expression of both H1 and the core histones is coordinately regulated both transcriptionally and post-transcriptionally. At the beginning of S phase there is a substantial increment (up to 10-fold, depending on the cells) in the transcription of the histone genes, perhaps coupled to the initiation of their replication; later in S phase the rate of transcription diminishes [180]. This finding, illustrated in Fig. 3, appeared to be valid for all but one of the replication-dependent variants studied, and in most cell types independently of the procedures used to synchronize the cells. Not surprisingly, histone synthesis was blocked at the restrictive temperature by the G_1-specific temperature-sensitive mutation affecting RNA polymerase II in *ts*AF8 BHK cells [181]. It was also blocked by the *ts*K12 mutation that prevents the hamster cells from proceeding past a point about 2–4 h before S phase – neither DNA replication nor the cytoplasmic accumulation of histone mRNA occurs at the restrictive temperature [182]. Curiously, temperature arrest of the *ts*2 derivative of BALB/c 3T3 cells near the G_1/S boundary yielded the anomalous result that his-

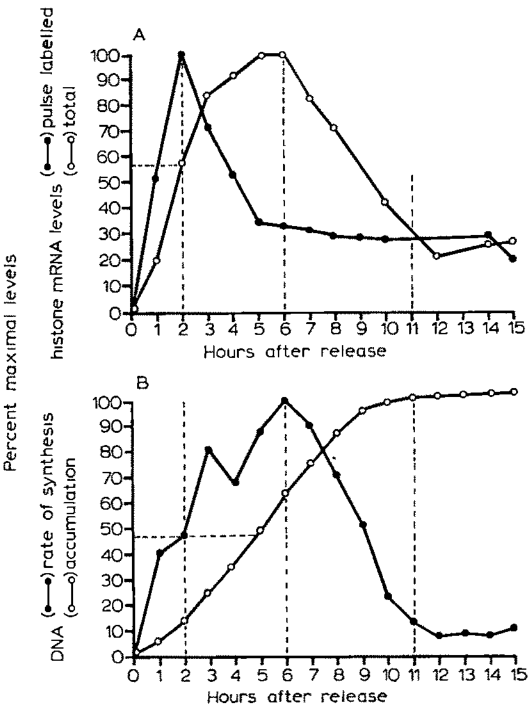

Fig. 3. Cell cycle-dependent expression of the histone genes. (A) ●, rate of histone mRNA synthesis measured by the incorporation of [^{3}H]uridine into histone mRNA during pulse-labeling in intact cells, ○, total amount of histone mRNA in the cell measured by probing Northern blots. (B) ●, rate of DNA synthesis measured by pulse-label incorporation of [^{3}H]thymidine into DNA, ○, accumulation of newly synthesized DNA in the cell. Figure kindly provided by G. Stein.

tone synthesis apparently continued in the absence of DNA synthesis [182a,b].

Changes in the relative amounts of several histone mRNAs after stimulation of quiescent murine 3T6 fibroblasts with serum were studied using an S1 nuclease procedure [183]; H3 transcription increased about 5-fold, even when DNA synthesis was inhibited with cytosine arabinoside. However, the 50-fold increase in the cytoplasmic abundance of the histone mRNA seen during S phase was blocked by the inhibitor. In S-phase HeLa cells, previously synchronized at the G_1/S boundary with thymidine and aphidicolin, there was an increase both in the rate of transcription and in the half-life of the mRNAs encoding the core histones [184]. Alterations in the chromatin structure upstream of an H4 gene in HeLa cells synchronized with a double thymidine block appeared to result from coupled replication and expression of the gene [185]. A study of the cell cycle-dependence of H3 mRNA metabolism in murine erythroleukemia cells fractionated by centrifugal elutriation suggested that the accumulation and decay of the message in the cytoplasm of these normally cycling cells may result from regulation largely in the nucleus at the level of processing or transport rather than transcription or mRNA breakdown [186].

The stability of the histone mRNAs (estimates of the normal half-life range from 20 min to 6 h for different species in various cell lines [187]) is dependent upon ongoing DNA replication [188, 189]. When DNA replication was blocked (e.g. with hydroxyurea, BrdUrd, cytosine arabinoside or aphidicolin) histone synthesis ceased and the histone mRNAs were degraded with a half-life of 10–15 min. For degradation to occur, however, protein (but not RNA) synthesis was necessary; if protein synthesis was blocked at the same time as DNA synthesis then the histone mRNA was not degraded [190]. Inhibition of DNA synthesis was also accompanied by a significant reduction of the rate of transcription of the histone genes, which was again dependent upon ongoing protein synthesis (Refs. 191, 192; but see 187, 190 also). Curiously, novobiocin, which inhibits DNA replication but does not alter the pools of deoxynucleotides (in contrast to hydroxyurea, cytosine arabinoside or aphidicolin), did not reduce the level of histone mRNA [192], Novobiocin, however, has a multitude of effects on mammalian cells, including lowering of the ATP : ADP ratio [193].

When only protein synthesis was inhibited there was an increase in the half-life of histone mRNA from 30 min to more than 2 h with little change in the rate of transcription; resumption of protein synthesis precipitated a rapid breakdown of the excess mRNA [187,190]. Partial inhibition of protein synthesis led to an increase in the cell generation time with little change in the duration of the chromosome cycle ($S + G_2 + M$). Wu and Bonner [194] showed that this chromosome cycle compensation resulted from an increase in the levels of histone (and perhaps other) mRNAs. Although it is possible that a labile protein controls the stability of the histone messenger, the weight of the evidence favors the conclusion that the histones themselves self-regulate their production post-transcriptionally [195]. The argument stems from the thesis that DNA replication is dependent upon and limited by ongoing protein (assumed to be histone) synthesis; inhibition of DNA synthesis leads to an increased concentration of the amount of free histone, which by an unknown mechanism decreases histone mRNA stability. Inhibition of protein synthesis leads to a decrease in the amount of free histone and a concomitant increase in the stability of the mRNA. The stability of the histone message in the absence of protein synthesis is not due to protection by ribosomes, because pactamycin (an inhibitor of initiation) and puromycin (which allows ribosome run-off) show the same effect as cycloheximide [183,190].

All the data are compatible with autogenous regulation of both histone gene transcription and histone mRNA stability by the concentration of histone protein; however, other explanations are not excluded (cf. Ref. 192). Thus Stein and Stein [196] have argued that it is unlikely that transcription of the histone genes is modulated autogenously, rather they favor a more direct coupling to DNA replication [197]. The precedent is provided by yeast, where transcription of the histone genes begins immediately before the initiation of DNA replication, and cessation of transcription in turn depends upon entry into S phase [198].

Sequences in the histone genes and mRNAs that are important for the regulation discussed above are currently being pinpointed. Transcription is presumably modulated by promoter and enhancer sequences near the 5′ end of the gene, and a human histone H4 promoter region 70–100 nucleotides upstream of the transcriptional start site has been characterized [199]. The distal promoter elements are recognized by a factor found preferentially in extracts of S-phase HeLa cells. Capasso and Heintz [200] have reported cell cycle-dependent transcription of a human H4 histone gene transfected into mouse cells; the presence of multiple copies of the human H4 sequence appeared to repress specifically transcription of the endogenous mouse H4 gene – presumably by competing for a *trans*-acting transcriptional factor. The 5′ sequence of a hamster H3 gene has been shown to confer cell cycle-dependent regulation (maximum expression in S phase, blocked by the G_1-specific temperature-sensitive K12 mutation) in hamster cells of an attached sequence encoding neomycin resistance [201].

A 463-bp segment comprising the 3′-terminal half of a mouse histone H4 gene attached to the SV40 early promoter has been shown to be sufficient not only to generate the correct 3′ end of the mRNA but also to allow post-transcriptional cell cycle regulation of expression of the mRNA in a mouse mastocytoma cell-cycle mutant [202]. The distance of the histone sequences from the 3′ end appeared to be important and the authors speculated that the absence of a poly(A) tail and the presence of a conserved palindromic sequence at the 3′ end were important. A conserved stem-loop structure and a nearby CAAGAAAGA spacer sequence in the 3′ region appeared required for processing of sea urchin histone H3 RNA to a form that was stable in frog oocyte nuclei [203]. Sequences near the 3′ end of a human histone H4 gene have been implicated in the generation of a stable transcript in vitro [178].

IVB. Enzymes of nucleotide and polyamine metabolism

During quiescence, mammalian cells economize by reducing their content of many enzymes in the pathways of nucleotide metabolism and DNA replication. Upon reinitiation of growth and DNA synthesis in response to appropriate stimuli, cells in vivo and in vitro elevate nucleotide precursor pools and increase their capacity to incorporate nucleotides into DNA. Known growth-regulated enzymes include thymidine kinase [204], dTMP kinase [205], dCMP deaminase [205], ribonucleotide reductase [206], dihydrofolate reductase [207], thymidylate synthetase [207], ornithine decarboxylase [208], DNA polymerases [209–211], polynucleotide ligase [212], DNA topoisomerase 1 [213] and DNA methylase [214,215].

For some enzymes there are also periodic increases in activity during transit through the cell cycle in exponentially growing cells [216–219]. The shared pattern of increasing activity through S phase, with a maximum near the S/G_2 boundary, suggests pathways for co-ordinate regulation, temporally connected to DNA replication. The exact points of regulation for many of the enzymes mentioned are unknown, but transcriptional and post-transcriptional regulation of mRNA levels are important for dihydrofolate reductase (*dhfr*), thymidylate synthase (TS), thymidine kinase (TK) and ornithine decarboxylase (ODC).

IVB1. Dihydrofolate reductase (dhfr)

Part of the molecular detail of *dhfr* mRNA metabolism is beginning to emerge from studies employing mutant cell lines with multiple copies of the *dhfr* gene selected for their resistance to progressively higher concentrations of the specific inhibitor of *dhfr* enzymatic activity, methotrexate (reviewed in Ref. 207). The increased *dhfr* mRNA content facilitated the molecular cloning of this normally low-abundance species of cytoplasmic 1.6-kb mRNA [220]. Sufficiently high levels of *dhfr* mRNA are present in the variants with the amplified gene to permit direct and sensitive measurements of the transcripts by DNA-excess filter hybridization. Moreover, short pulse-labeling experiments can be used to determine rates for *dhfr* mRNA synthesis, processing, transport and degradation. Inducible gene expression appears to have been preserved faithfully in the mutant cell lines [221].

After mitogen-stimulation of quiescent murine cells, cytoplasmic *dhfr* mRNA levels increased approximately 4-fold 2–6 h before DNA synthesis began [207]. The close correlation between mRNA content and the amount and rate of enzyme synthesis points to the messenger level as being the main factor determining *dhfr* activity during DNA synthesis [222,223]. In contrast to the close association between continued DNA synthesis and histone mRNA transcription, *dhfr* mRNA induction was largely unaffected by inhibitors of DNA synthesis [224].

The nature of the intracellular signal to which the *dhfr* gene responds is unknown, but dibutyryl-cAMP addition to cells during serum-induced S phase rapidly terminated *dhfr* transcription, while permitting DNA synthesis to continue [223,225]. Inhibition of transcription was not observed when dibutyryl-cAMP was added to cells induced to synthesize DNA by polyoma virus infection, suggesting the existence of a second pathway for stimulation of *dhfr* transcription that is independent of the cAMP inhibitory effect [225]. Interpretations regarding the mechanism of regulation by cAMP are difficult, since high levels of intracellular cAMP have many effects on cell growth, including arrest in both the G_1 and G_2 compartments of the cell cycle [226].

The regulation of *dhfr* expression is complex, with evidence for control at both the transcriptional and the post-transcriptional levels. Following serum stimulation of quiescent 3T6 cells, increases in the rates of synthesis of both hnRNA and cytoplasmic mRNA have been observed [225,227]. Although Leys et al. [228] observed increased levels of cytoplasmic *dhfr* mRNA when density-arrested mouse sarcoma cells were replated at a lower density in fresh medium, an increase in the transcription rate could not be measured in nuclear 'run-off' transcription experiments, nor could elevated rates of transport from the nucleus be detected. An increased stability of the message in the nucleus of the freshly plated cells was hypothesized to permit the eventual build-up of cytoplasmic *dhfr* mRNA.

Mouse 3T6 cells may be arrested in the G_1 phase by glutamine starvation, but in this case the resting cells, unlike serum-deprived cells, have levels of cytoplasmic mRNA as high as those found in growing cells [229]. In these cells, the rate at which poly(A) mRNA was labelled by tritiated uridine was decreased 3-fold while there was a concomitant 3-fold rise in the level of *dhfr* hnRNA, pointing to decreased processing or transport from the nucleus. Since cytoplasmic levels of *dhfr* mRNA did not change, it was unclear if this effect represented a form of regulation utilized during normal cellular growth. The delayed processing may simply have been an aberration resulting from protein synthesis inhibition and the presence of an over-abundance of the mRNA due to gene amplification.

Some progress has been made toward an understanding of which regions within the *dhfr* gene are important for post-transcriptional regulation. Kaufman and Sharp [230] constructed *dhfr* 'minigenes' using a mouse *dhfr* cDNA segment and the adenovirus late mRNA promoter. Polyadenylation signals were provided either by the *dhfr* gene, the early or late SV40 polyadenylation sequences, or a CHO sequence. The minigenes were transfected into *dhfr*$^-$ CHO cells and amplified by selection for methotrexate resistance. Growth-dependent accumulation of *dhfr* mRNA, with growing cells containing 10-fold more mRNA than quiescent cells, was found in transformants that used either the *dhfr* or SV40 late polyadenylation signals, but not in transformants that utilized the CHO or the early SV40 signal. Again, 'run-off' transcription experiments revealed only modest increases in de novo transcription between the two states, insufficient to account for the observed effects. Since the *dhfr* gene possesses multiple polyadenylation sites [231], *dhfr* mRNA levels may be controlled in cells in different physiological states by the efficiency of polyadenylation at various termination sites, or by the differential stabilities of the mRNAs produced using these sites [230].

The nucleotide sequence for 1 kb preceding the mouse *dhfr* coding region includes three direct repeats of a 48-bp sequence [232,233]. S1 mapping studies indicated that there were multiple 5′ termini in the *dhfr* mRNA population with a major start site at −115, within the most 3′ of the repeated sequence elements [233,234]. The repeated sequences each contain an AT-rich sequence, CACAAATA, that resembles both the CAAT and TATA 'box' sequences, and approximates the approx. 50-bp separation between the two 'boxes' found in other genes [235]. A region with homology to CAAT and TATA promoter sequences located at -700 also served as an efficient promoter, at least in transfected gene constructs [233]. Each repeat also contains a GC-rich sequence, GGGCGG, similar to single or repeated sequences found in a wide variety of promoter regions from other genes, including the SV40 early region [236], hydroxymethylglutaryl-CoA reductase [237], EGF receptor [238], metallothionein [239] and hypoxanthine–guanine phosphoribosyltransferase [240]. Such genes (except those of SV40) can be considered 'housekeeping' genes, since their transcripts are found in all or nearly all cells and are usually expressed constitutively at much lower levels than many of the tissue-specific genes (e.g. globin, ovalbumin) whose promoters have been well characterized.

A human transcription factor called Spl that binds upstream of cellular and viral promoters containing multiple copies of the sequence GGGCGG has been identified [241]. Close contacts are formed between the Spl protein and the bases of the hexanucleotide. It is tempting to speculate that one way of regulating cell cycle-inducible genes may involve modifications to Spl binding or its subsequent effects on transcriptional initiation. The Spl factor stimulated synthesis of two transcripts that initiate on opposite strands of SV40 DNA in in vitro transcription reactions [242], and it bound to a monkey DNA sequence with in vivo and in vitro promoter activity located between divergent transcriptional start sites [241]. Interestingly, divergent transcripts are produced from the GC-rich *dhfr* promoter region; however, no information is available concerning inducible expression of the opposite strand RNA [243,244].

Recently, evidence for transcriptional regulation of *dhfr* during the cell cycle in exponentially growing mouse 3T6 fibroblasts has been presented [234]. The rates of transcription from the major -115 start site and from a secondary start site at -165 increased 7-fold at the beginning of S phase over the basal rate in G_1, but the proportion of mRNA produced from each start site did not change. Further experiments were needed to define those promoter sequence elements that confer cell cycle-dependent transcriptional activation.

IVB2. Thymidylate synthetase (TS)

The isolation of a fluorodeoxyuridine-resistant mouse cell line with an amplified TS gene facilitated molecular cloning of a cDNA copy of the 1.3-kb mRNA [245]. By several criteria, the structure and regulation of TS appear to be the same in the mutant cells as in the 3T6 line from which it was derived [246,247]. TS mRNA levels peaked at 20–40-fold above those found in the resting state about 20 h after serum-starved cells were re-fed with medium containing 10% serum [248]. The peak of mRNA levels in cycling yeast cells has also been shown to be near the beginning of S period [249]. Since the majority of TS mRNA is associated with polysomes at all times in mouse cells, and there is a good correspondence between TS mRNA and the rate of synthesis of the enzyme, it is doubtful that there are any significant translational controls determining the abundance of the enzyme. However, because the increased rate of transcription (3-fold) and unaltered half-life of the polyadenylated TS mRNA seemed insufficient to account for the rise in cytoplasmic TS mRNA abundance, Johnson and his collaborators have postulated post-transcriptional controls – specifically a differential partition between a relatively stable poly(A)$^+$ species and a labile poly(A)$^-$ species of RNA [248].

IVB3. Thymidine kinase (TK)

The gene for cytoplasmic TK has been cloned by employing DNA-mediated transfection of mouse TK$^-$ cells with DNA from chicken, rodent and human sources [250–254,257]. Molecular probes derived from the genomic clones were subsequently used to demonstrate that the cytoplasmic abundance of this mRNA (1.5 kb in humans) was strictly proliferation-dependent, with essentially undetectable levels in non-cycling cells [134,251,254–256].

TK mRNA levels in continuously growing chicken cells are highest, but not strikingly so, during S phase [23]. Signals governing S-phase induction were closely linked to the DNA segment that was transfected into TK$^-$ cells [250,257]. Those signals that determined the disappearance of the transcript in differentiated chicken muscle cells appeared not to be at either the 5′ or the 3′ end, but in an intragenic location, suggesting that modulation of cytoplasmic abundance was mediated through nuclear processing events in this case

[255]. Post-transcriptional regulation may be central to the regulation of this gene during changes in growth states, since a correlation between the steady-state level of polyadenylated chicken TK mRNA and mitotic activity in cells of several different tissues was not reflected in differential transcriptional activity of the gene; furthermore, nuclear 'run-off' experiments indicated equivalent transcriptional activity in cells with high or low levels of cytoplasmic TK mRNA [256].

In BALB/c cells stimulated from quiescence, the induction of TK mRNA and enzyme activity was blocked by inhibitors of RNA and protein, but not DNA, synthesis [258]. Thus in mouse fibroblasts enhanced TK expression at late G_1/early S required new gene transcription and efficient protein synthesis, but not DNA replication. TK induction was also dependent on prior polyamine accumulation [259].

IVB4. Ornithine decarboxylase (ODC)

Several groups have recently isolated cDNA clones of the mRNA encoding murine ODC [260–263]. This enzyme catalyses the first and rate-limiting step in the synthesis in animal cells of polyamines that are essential for DNA replication and cell proliferation. The protein has an unusually short half-life (10–30 min) and its activity is subject to multiple regulatory controls [208]; its induction (which accompanies the action of most homones and growth factors on their target tissues) is an early response. Inhibition of polyamine synthesis in PHA-stimulated lymphocytes with difluoromethylornithine suppressed the formation of polyribosomes and inhibited both protein and DNA synthesis [263a].

Induction is dependent upon the presence in the medium of a minimal concentration of an ODC-inducing amino acid, such as asparagine, which acts synergistically with the hormone or growth factor [264]. The M_r 51 000–54 000 protein is encoded in a 2–2.6-kb mRNA (there may be several species [260]) whose cytoplasmic abundance is substantially increased by many factors that induce ODC activity [260–263,263b], but only fragmentary information is available on the level(s) at which regulation is accomplished [264–268]. Studies using hydroxyurea to inhibit progression of 'mitotically selected' CHO cells through S phase suggested that ODC induction (which is blocked by hydroxyurea) may be required for passage through, but not entrance into, S phase [269]. There appear to be several ODC-related genes in the mouse genome [270,271].

IVC. Cyclin, or proliferating cell nuclear antigen (PCNA)

Cyclin is an acidic M_r 35 000–36 000 nuclear protein that shows cell cycle-dependent synthesis as seen by high-resolution two-dimensional gel electrophoresis of total cellular proteins [272]. Proliferating cell nuclear antigen (PCNA), which reacts with an antibody generated in the autoimmune disease systemic lupus erythematosus (SLE) [273], has been shown to be identical to cyclin [274]. Using anti-PCNA antibodies, Tan and collaborators showed that PCNA synthesis occurred preferentially in proliferating cells [275,276]. In an analysis of HeLa cell proteins synthesized in different stages of the cell cycle, cyclin was found by Bravo and Celis to increase significantly in S phase [113]. It has been found in various human, mouse, hamster and avian cell lines, where its abundance often correlates with the transformed or proliferative state of the cells [277,278]. (An M_r 50 000 nuclear protein called PSL that was also recognized by an autoimmune serum and showed a cell cycle dependence has also been described [279].)

The extent of the transformation-induced increase in cyclin (PCNA) levels ranges from approximately 1.5-fold to 9-fold, and likely depends on the fraction of cycling cells [264,267,268]. Normal human epidermal basal cells synthesized very low levels of cyclin (PCNA) ($< 0.02\%$ of total protein) compared to SV40-transformed keratinocytes (0.15%); unfortunately the degree to which these cells were proliferating was not reported [280]. Quail embryo fibroblasts that had been transformed with the *myc*-containing MC29 virus displayed only a partially transformed phenotype, being non-tumorigenic in nude mice, but contained significantly increased cyclin (PCNA) levels compared to untransformed fibroblasts. In contrast, cells that had been transformed with the *src*-containing Rous sarcoma virus were tumorigenic and showed no increased cyclin (PCNA) synthesis. The authors concluded that cyclin (PCNA) levels in this system correlated with cell proliferation and not transformation [281].

The addition of serum, FGF or PDGF to quiescent cultures of mouse 3T3 cells induced a 6–7-fold increase in cyclin (PCNA) synthesis which either paralleled DNA synthesis or preceded it by about 2 h [282]. Synthesis of cyclin was uncoupled from DNA synthesis in serum-stimulated cells when DNA replication was inhibited with aphidicolin or hydroxyurea; treated cells maintained high rates of cyclin synthesis, whilst in uninhibited cells the rate decreased dramatically as they left S phase [283,284].

Sequential changes in the nuclear distribution of cyclin (PCNA) during S phase have been observed [284,285]. Early S phase was characterized by immunofluorescent staining throughout the nucleoplasm but not in the nucleoli. As S phase proceeded the staining intensity increased, and prior to maximal DNA synthesis foci appeared in the pattern. The pre-focal stage of cyclin (PCNA) distribution was independent of DNA synthesis, but later stages required replication and an apparent redistribution to the nuclear periphery and nucleoli [276,285]. Since replication of nucleolar and heterochromatic DNA is restricted to late S phase in CHO cells [286], it may be that the pattern of cyclin (PCNA) distribution reflects the temporal order of DNA replication. The fluorescence disappeared as cells left S phase, though this was not due to a disappearance of the protein from the nucleus, since it was shown to be stable in pulse-chase experiments [284]. This suggests that cyclin (PCNA) is modified or becomes incorporated into structures that render it inaccessible to antibody molecules at the end of S phase.

IVD. Secreted proteins

Cells secrete proteins for several reasons. Fibronectin and procollagen are produced in order to create desired extracellular structures, whereas various polypeptide hormones and lymphokines are made to communicate signals to other cells. Some transformed cells generate (autocrine) growth factors which act back on themselves to stimulate proliferation. Proteins destined for secretion, together with proteins destined to enter lysosomes or membrane structures, are synthesized with (usually) an N-terminal leader sequence (signal peptide) that, via an interaction with the signal-recognition particle, directs them into the Golgi system. Concomitant with a series of glycosylations and other modifications, the proteins pass through the Golgi and into secretory vesicles or lysosomes. Although most research in this area has been directed at elucidating the complexities of these pathways, there have been some investigations into the effects of transformation and growth factors on secreted proteins.

In this section we review what is known about selected secreted proteins. Some of the proteins have been studied as molecules with characteristic activities, whereas others have first been seen as labeled proteins in SDS-polyacrylamide gels. Many secreted proteins are produced under hormonal control, and their induction by growth factors or tumour promoters may result from partial overlaps in the pathways of gene activation under the control of each inducer. For example, prolactin gene transcription and prolactin production but not cell proliferation is induced by TPA, EGF or thyrotropin-releasing hormone in a rat pituitary cell line [287]. The secreted proteins considered here are ones for which regulation by factors that concomitantly induce cell proliferation has been demonstrated at the transcriptional, or at least pre-translational, level. Since cell proliferation implies the expansion of a population of cells into a larger environment, it is not unreasonable that the production of proteins affecting the environment of the cell shows cell cycle regulation.

IVD1. Major excreted protein (MEP)

In 1978 Gottesman described a protein of M_r 35 000 that was released into the medium in relatively large amounts (hence the name) by transformed murine fibroblasts [288]. Various immortal, untransformed lines (e.g. Swiss 3T3 cells, 3T6 cells), as well as normal mouse embryo fibroblasts, produced MEP in lesser amounts. MEP is secreted by epidermal cells, both in culture and in vivo (in mouse skin), and in both cases the tumour promoter TPA enhanced production [289]. It is a glycosylated protein and carries the mannose 6-phosphate recognition marker implicated in targeting proteins to lysosomes [290]. Growth factors and tumour promoters stimulate its production, at least in part by increasing transcription of the gene, and most transformed lines tested have higher levels of MEP transcripts than the non-transformed parent [158,291,292]. The PDGF-enhanced synthesis of the 1.8-kb MEP mRNA in density-arrested BALB/c 3T3 cells occurred 6–12 h after stimulation and was dependent upon prior protein synthesis [293]. Many transformed cell lines synthesized MEP constitutively and could not be induced to synthesize more in response to PDGF [158].

MEP (molecular weight revised to 39000) is processed intracellularly into two lower molecular weight forms (M_r 29000 and 22000) [294]. Both are stable, although the M_r 29000 form appeared to be more stable in untransformed cells than in NIH3T3 cells transformed with Kirsten virus. All three forms partitioned in cell fractionation studies with typical precursor and processed lysosomal enzymes; however, only the largest species was secreted. Immunofluorescence and electron microscope immunocytochemistry revealed that the majority of the intracellular MEP was associated with mature lysosomes. The secreted protein was auto-activated at low pH and acquired the ability to cleave various proteins, including extracellular matrix proteins [295]. Retinoic acid reduced the amount of MEP secreted, perhaps by affecting glycosylation [296]. The sequence of a cDNA clone has revealed significant homology with several thiol proteinases, including mammalian cathepsins B and H [297].

IVD2. Mitogen regulated protein (MRP, proliferin)

Nilsen-Hamilton et al. [114] first described a ‘family of proteins’ released into the medium after stimulation of Swiss 3T3 cells with growth factors. Apparently a core protein of M_r 22000 was glycosylated to a variable extent, resulting in a population of molecules ranging in M_r from 30000 to 38000. In contrast to MEP, transformation of immortal lines more often caused a reduction in the level of the secreted protein [114]; Swiss mouse embryo fibroblasts make no detectable MRP (Edwards et al., in preparation). Partial sequence data from a cDNA clone of MRP revealed that it is apparently identical to a prolactin-related protein called proliferin [130].

Proliferin is the name applied to a protein produced by in vitro translation of a mouse mRNA whose abundance was enhanced by stimulation of quiescent cells with serum [125]. The mRNA was discovered via a cDNA clone (28H6, see section IIIA) that was picked out of a library because it showed differential hybridization to labeled cDNA made from RNA from quiescent and serum-stimulated cells [107]. The DNA sequence of the cloned message revealed substantial homology with mammalian pre-prolactins. The protein was found to be secreted as a glycoprotein in the fetal part of mid-gestational mouse placenta, and evidence for two different but related species of mRNA was obtained [298]. An antiserum raised against MRP immunoprecipitated proliferin (encoded by the cDNA and produced in BSC-1 cells using an expression vector) but not prolactin.

The amount of MRP and MEP released into medium after stimulation with growth factors is influenced by substances (monensin, chloroquine, ammonium chloride) that increase the intralysosomal pH and thereby inhibit the hydrolytic activities contained therein [300]. MRP secreted in the presence of the lysosomotropic agents appeared to be less glycosylated. Leupeptin and antipain (inhibitors of thiol-dependent lysosomal proteinases) and 3-methyladenine (an inhibitor of crinophagy – the degradation of secretory vesicles and their contents by lysosomes) also increased MEP and MRP levels 2–6-fold (Nilsen-Hamilton, personal communication). Although the presence of these proteins in secretory granules remains to be directly demonstrated, it is reasonable to infer at the present time that one mechanism of regulation of their intracellular and secreted levels is, like prolactin, by crinophagy. A greater proportion (over 80%) of MRP than of MEP appears to be secreted from cells.

IVD3. Plasminogen activator

Tissue plasminogen activator (t-PA) (M_r 65000–70000), found in serum, and an immunologically unrelated protein, urokinase (u-PA) (M_r 48000–55000), originally isolated from urine, are characterized by their ability to activate plasminogen. They are serine proteinases, secreted in an inactive proenzyme form and often found in cell culture fluids complexed with an inhibitor, a proteinase nexin. A variety of transformed cells produce plasminogen activators, or substances that can induce plasminogen activator production by normal cells [301]; the proteinase is thought to play a role in facilitating the invasion of tissues by tumour cells. Although the principal function of t-PA (when activated by fibrin) may be the conversion of plasminogen to plasmin, which is responsible for the dissolution of blood clots, it (or plasmin) has other activities also – including tissue remodeling and down-regulation of the epidermal growth factor receptor [302]. Tumour promoters, various growth factors, concanavalin A, even DNA damage, have been shown to stimulate the production of plasminogen activator activities in a variety of cell types [303,304].

The stimulation of plasminogen activator synthesis by TPA results from an increase in the amount of its (translatable) mRNA as judged from translation in *Xenopus* oocytes and reticulocyte lysates [305]. Secretion of an M_r 48 000 mouse urokinase proenzyme by a murine sarcoma virus-transformed 3T3 line was enhanced by TPA; the 10-fold increase in production occurring 8–20 h after stimulation correlated nicely with a 6–10-fold increase in the amount of urokinase mRNA [306]. Similarly, TPA increased the urokinase mRNA level in a human kidney carcinoma line [307]. It was not established whether the increased level of plasminogen activator mRNA resulted from increased transcription of the gene, enhanced processing or transport of the mRNA, or prolongation of the life of the functional message.

The TPA-induced increase in the t-PA mRNA in HeLa cells was prevented by cycloheximide; when inhibitor was added after the mRNA had begun to appear it reversed the process, suggesting that an unstable protein was required for the synthesis or stability of the mRNA [308]. In contrast, other workers reported that the increased transcription of a pig kidney urokinase gene induced by calcitonin and vasopressin (presumed to act via stimulation of adenylate kinase) was not blocked by cycloheximide [309]. The TPA- and growth factor-induced stimulation of plasminogen activator synthesis appears to be indirect, perhaps mediated via changes in cAMP levels. Also, metabolites of arachidonate derived via a lipoxygenase pathway have been implicated in the induction of plasminogen activator synthesis [310].

IVD4. Interleukin 2

Interleukin 2 (IL-2), or T-cell growth factor, is produced by certain mature T cells after stimulation with appropriate antigens or lectins and is required for the proliferation of activated normal T cells. In the Jurkat human leukemic T-cell line, TPA plus phytohemagglutinin enhanced the rate of transcription of the IL-2 gene, and transcription was further enhanced by IL-1 [311]. Untreated (unstimulated) cells, and cells treated with TPA or IL-1 alone, contained little, if any, message; however, levels of the message in PHA-stimulated cells were increased by each of these agents in an approximately additive manner.

Inhibition of protein synthesis in PHA-stimulated lymphocytes with cycloheximide, pactomycin or sparsomycin caused superinduction of IL-2 mRNA; these results support the argument that a labile protein regulates the formation of mature IL-2 mRNA [312]. Cyclosporin A inhibited the accumulation of IL-2 mRNA, possibly by destabilizing the message but more likely by interfering with transcription of the gene [313]; in the activated lymphocyte, the induction by TPA of several proteins, including the colony-stimulating factor for granulocytes and macrophages (CSF-GM), was inhibited by cyclosporin [314].

IVD5. Collagen and collagenase

Procollagens $\alpha 1$ and $\alpha 2$ are major high molecular weight secretion products (M_r respectively 180 000 and 150 000) of many cell types, including fibroblasts. They are processed by specific proteinases to generate collagen, which plays a variety of structural roles in the organism. Collagen is degraded by collagenase, either during normally programmed remodeling events and wound healing or in the course of various degenerative diseases. Procollagen mRNA levels did not vary greatly during the cell cycle of normal or transformed mouse fibroblasts in vitro [315,316]; if anything, they are relatively higher in quiescent cells. Synthesis of procollagen by the murine JB6 epidermal cell line was inhibited at a pretranslational level by TPA [317]. TPA inhibited, and retinoic acid enhanced, the production of procollagen, likely by different routes [296]. PDGF increased the amount of collagenase-encoding mRNA in human skin fibroblasts, and the amount of secreted collagenase, 2–3-fold [318].

IVD6. Interferons

This is not the place to review the literature on interferons, or even to discuss them in any depth. Rather we simply mention briefly some evidence suggesting that they may be involved in aspects of cell cycle regulation. (For review see Ref. 319.) Interferons are proteins secreted from cells (lymphocytes, fibroblasts) in response to mitogen stimulation or the appearance of intracellular double-stranded RNA, e.g. as the result of virus infection. The transcription of the gene encoding interferon is substantially enhanced within 1–2 h of induction, apparently by the action of a pre-existing factor modified by the inducer so that it can act on a transcriptional control element regulating the interferon gene [320]. Changes in chromatin structure both upstream and downstream of the mouse β-interferon gene have been detected after induction [321].

Most cells possess receptors for interferon, and the action of interferon on cells is mediated via the receptor. Interferon induces new gene expression, as shown by the isolation of a number of cDNA clones corresponding to mRNAs whose abundance is enhanced by both transcriptional and post-transcriptional mechanisms [322–324]. Protein synthesis was not required. Genes encoding metallothionein II, histocompatibility antigens, and guanylate-binding proteins have been shown to be induced [324–326]. Perhaps the best-known effect of interferon treatment is the induction of 2′-5′ oligo(A) synthetase and a double-stranded RNA-dependent protein kinase. The protein kinase phosphorylates key proteins involved in protein synthesis and inhibits translation of many mRNAs. The synthetase, after activation by dsRNA, polymerizes ATP into 2′-5′-linked oligonucleotides that in turn activate a latent ribonuclease that cleaves single-stranded RNA, both viral and cellular. Two proteins (M_r 30 000 and 63 000) whose secretion from mouse fibroblasts was induced by β-interferon have been described [327].

Interferons can block mitogen-induced replication of lymphocytes and fibroblasts. The expression of certain genes, e.g. thymidine kinase, was inhibited and newly synthesized DNA appeared to be destabilized [328,329]. There was a decreased rate of c-*myc* transcription [36] and the half-life of c-*myc* RNA in Daudi cells was substantially reduced within 3 h of exposure to interferon [35,330]. The induction of competence by PDGF treatment of quiescent bovine aortic smooth muscle cells, and the subsequent progression of the cells to S phase, were each separately inhibited by interferon [331]. We discuss in more detail in section VE the idea that elevated levels of interferon-induced functions are inhibitory to cell cycle progression.

V. Interrelationships of gene expression during the cell cycle

At this early stage in the development of our understanding of gene expression during the cell cycle most investigations have been largely descriptive [3,5,10]. One can ask, for example, at what time during the cell cycle are particular genes expressed, or at what time is the product encoded by a particular gene, defined for example by a temperature-sensitive mutation, required. More revealing, however, are studies that relate specific events to the action of specific genes. The most critical experiments, which fortunately we are now in a position to attempt, will be to engineer the controlled expression (elevated or depressed) of specific genes under defined conditions and ascertain the consequences.

It is self-evident that the ability of the mammalian cell to enter the quiescent state is a sine qua non of our existence. We do not know how the cell accomplishes this. In cell culture cell-cell contact or the deprivation of nutrients or growth factors will push the proliferating cell into quiescence, if not death. Exit from the quiescent state, which can be affected in different cells by things as diverse as transient exposure to high pH or proteinases, or to growth factors, is what much of the preceding material has been about. Cells leaving G_0 typically increase their capacity for RNA and protein synthesis 2–5-fold, and there is a significant increase in the polyadenylated mRNA species in the cytoplasm.

If present indications are any guide, it will turn out that several pathways, or cascades, of gene expression will be discovered – the activation of one gene determining in turn the activation of a second. Normal cells require appropriate input from the environment, whereas transformed cells may not, being somehow 'constitutive' for certain signals. Fluctuations in the intracellular concentrations of key substances, or rate-limiting interactions with extracellular factors, may impose a stochastic nature on the overall process.

VA. Cell cycle mutants

A number of variant temperature-sensitive rodent cell lines have been isolated that at the restrictive temperature express a defect affecting only a particular stage in the cell cycle [5,10,334, 335]. Although in many cases the nature of the defect has not been elucidated, the simplest working hypothesis is that they contain a mutation in a gene affecting (directly or indirectly) a function that is required only at a certain stage (or stages in a few cases) in the cell cycle. Cells of such a mutant placed under restrictive conditions are unable to pass beyond the 'point of arrest' in the cycle; cells that have progressed past the 'execution point' (which is specific for the allele and can be different from the point of arrest) prior to the shift are not blocked [335].

The temperature-sensitive mouse cell cycle mutant *ts*85 arrests in late S or early G_2. Both histone phosphorylation and the addition of ubiquitin to histone H2A were affected at the restrictive temperature [336]. Even more revealing was the finding that the enzyme responsible for activation of ubiquitin had an enhanced heat sensitivity [337]. Since the addition of ubiquitin to proteins is a signal for their degradation [338], a simple interpretation is that one or more protein species must be degraded via an ubiquitin-dependent pathway in order for the cells to pass through G_2. The degradation of abnormal and short-lived proteins is substantially inhibited in this mutant at the restrictive temperature.

The activity of DNA topoisomerase II is affected by the temperature-sensitive lesion in the *ts*A1S9 mouse cell mutant; evidence that the protein itself is affected came from the altered sensitivity of the cells and the enzyme to novobiocin [339]. At the restrictive temperature this mutant was unable to proceed through S phase, and although considerable DNA synthesis occurred, the DNA that was synthesized was not joined into the very large molecules normally made.

The Syrian hamster cell mutant *ts*AF8 has a lesion in RNA polymerase II [340–342]. Starting either from G_0 or from mitosis, this mutant is unable to progress much beyond mid-G_1, apparently because there is an obligatory requirement for transcription at that point. This result clearly establishes a requirement for gene transcription in order for normally cycling cells to progress through G_1 and into S. The nature and function of these genes are of critical importance. It is of interest that the cells continue to grow in size at the restrictive temperature for at least 36 h [133].

DNA polymerase α appears to be altered in the mouse FM3A mammary carcinoma mutant *ts*FT20 [343]. After a shift to the nonpermissive temperature there was a substantial reduction in the rate of synthesis of DNA (but not RNA or protein). The DNA synthetic activity in partially purified preparations of DNA polymerase α from the mutant was also temperature-sensitive. The cells arrested in G_1/S or S phase and rapidly lost viability; there seemed to be an impairment in the ability of the cells to exit G_2 also. An attempt to isolate a temperature-sensitive DNA polymerase α mutant by isolating aphidicolin-resistant mutants at 33.5°C and looking for cells deficient in DNA synthesis activity at 39.5°C yielded mutants with a temperature-sensitive thymidylate synthetase instead [344].

Two other mutants with defects in DNA-synthesizing ability were isolated from the same FM3A line. These are the mutants *ts*131b [345] and *ts*T244 [346]. When transferred to the nonpermissive temperature the cells rapidly reduced their rate of DNA synthesis and mostly accumulated in late S/G_2. The rate of chain elongation was reduced, and there was a loss of DNA polymerase activity from the nucleus. However, the in vitro DNA synthetic capacity of either variant line in crude extracts was not temperature-sensitive.

Two DNA synthesis temperature-sensitive mutants derived from hamster cells are *ts*BN-2 [347] and *ts*C8 [348]. DNA fiber autoradiography suggested that the former mutant was impaired at the restrictive temperature in its ability to initiate new replicons but not in its ability to continue chain elongation; passage through S phase, and perhaps entrance into S, was blocked. Although *ts*C8 showed some of the same properties as *ts*BN-2, it did not (unlike *ts*BN-2) undergo premature chromosome condensation at the restrictive temperature. There is evidence that the *ts*BN-2 product post-transcriptionally regulates the synthesis of an M_r 35 000 protein (cyclin?) that is responsible for chromosome condensation in late G_2 [349,350]. Complementation studies have revealed that at least four or five different CHO mutants defective in DNA synthesis exist [348], but it is not known if any of these affect genes important in cell cycle control.

Chen and Wang [351] have divided the G_1 period into six segments (Fig. 4A) by relating the execution point of three different temperature-sensitive Syrian hamster cell cycle mutants to the arrest points in G_1 induced by serum starvation, by isoleucine deprivation and by hydroxyurea treatment. On the basis of differences in the morphology of prematurely condensed chromosomes, four temperature-sensitive G_1 mouse 3T3 mutants were mapped to different points in G_1 [352]. Although these studies are useful in that they determine the time of action of specific gene products in G_1, they are not informative with regard to the function of the gene product.

A more informative approach is typified by the successful complementation of the cell cycle *ts*24 mutant phenotype by microinjection of mRNA fractionated on agarose gels, indicating a requirement for a 0.9-kb mRNA [353]. This will make it possible to identify the gene product involved and will eventually permit genes identified by *ts* mu-

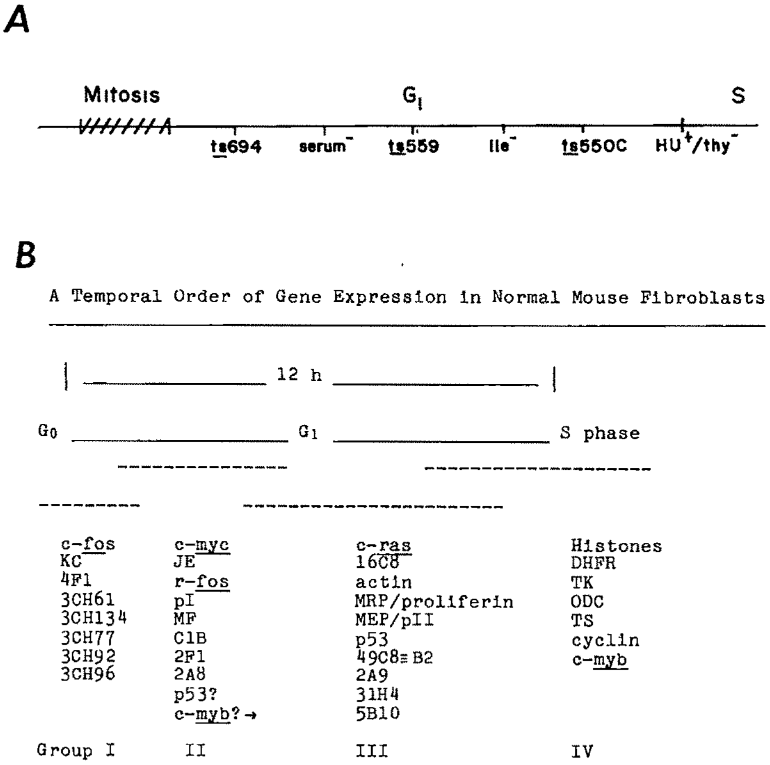
A
Mitosis
G1
S
ts694
serum⁻
ts559
Ile⁻
ts550C
HU⁺/thy⁻
B
A Temporal Order of Gene Expression in Normal Mouse Fibroblasts
12 h
G0
G1
S phase

Group I	II	III	IV
c-fos	c-myc	c-ras	Histones
KC	JE	16C8	DHFR
4F1	r-fos	actin	TK
3CH61	pI	MRP/proliferin	ODC
3CH134	MF	MEP/pII	TS
3CH77	C1B	p53	cyclin
3CH92	2F1	49C8≡B2	c-myb
3CH96	2A8	2A9	
	p53?	31H4	
	c-myb?→	5B10	

Fig. 4. (A) Map of the G_1 period (adapted from Ref. 351). The location of the apparent arrest points of the three temperature-sensitive CHO mutants 694, 559 and 550C are indicated. *ts*694 arrests very early in G_1, apparently before the point of arrest in serum-deprived conditions. Midway through G_1 is a point at which cells can be arrested by isoleucine deprivation; this may correspond more or less to the 'R' restriction point, where efficient protein synthesis is required The block imposed by hydroxyurea and thymidine deprivation is likely in early S phase (B) Approximate time of expression, after serum stimulation of quiescent cells, of the mRNAs identified by various cDNA clones discussed in the text There is considerable overlap between the numbers of various groups, and there is likely to be considerable cell-to-cell variation in the time at which some genes are expressed.

tations to be compared to genes identified by cDNA clones of mRNAs that evince a cell cycle-dependent expression. It does not necessarily follow, however, that a mutation affecting progress through the cell cycle (a defect in any essential gene could do this) will be in a gene expressed in a cell cycle-dependent fashion.

Liu, Baserga and collaborators have pioneered the strategy of using cDNA clones of cell cycle-dependent genes to investigate gene expression in temperature-sensitive cell cycle mutants [354]. They chose to study the expression of *dhfr* and TK in the RNA polymerase II-altered *ts*AF8 mutant and in *ts*13. The latter mutation, which affects an unknown function, has an execution point several hours prior to S. The increase in *dhfr* and TK mRNA, as well as histone mRNA and the transcript corresponding to the cell cycle-dependent clone 2A8 (section IIA), that normally occurs in serum-stimulated cells did not occur in either mutant at the nonpermissive temperature. Astonishingly, *dhfr* enzyme activity increased normally in *ts*AF8 but not *ts*13 at the nonpermissive temperature. The authors attribute this to an increased stability of the mRNA and suggest that this enzyme (or its mRNA) is under both serum and cell cycle control. Some of their data are summarized in Table II.

TABLE II

RNA LEVELS OF VARIOUS GENES AND cDNA CLONES IN G_1-SPECIFIC *ts* MUTANTS OF THE CELL CYCLE (ADAPTED FROM REF 354)

p3C5 and p4A3 are clones that identify mRNAs in the hamster *ts* K12 line that are induced by certain types of stress (high temperature, glucose deprivation). The other genes and cDNA clones are described in the text. ↑, increase; =, no change from G_0; ↓, decrease from G_0. pt and npt, permissive and nonpermissive temperature

Gene or cDNA clone	Cell	Expression at		Ref
		pt	npt	
p2F1	*ts*13	↑ early G_1	↑	108
p4F1	*ts*13	↑ early G_1	↑	108
p2A8	*ts*13	↑ early G_1	=	108
p2A9	*ts*13	↑ mid-G_1	↑	354
TK	*ts*13	↑ late G_1	=	354
Histones	*ts*AF8	↑ G_1/S boundary	=	181
dhfr	*ts*13	↑ S phase	=	354
p3C5	K12	↓ G_1	↑	384
p4A3	K12	↓ G_1	↑	384

VB. Timing of gene induction

The transition from the quiescent, non-proliferating state to the 'active' cell cycle, and to a lesser extent the passage of cycling cells through G_1, is accompanied by temporal patterns of activation of specific genes. Expression of these genes at a higher level is achieved via either elevated transcription or altered post-transcriptional processing, or both, generating increased numbers of their transcripts in the cytoplasm. Changes in mRNA stability are also important. Several different mammalian cell types (e.g. human, mouse, hamster) show similar patterns of activation of genes. Fig. 4B presents a classification of various mammalian cell cycle genes on the basis of the timing of their induction during the G_0 to S phase transition. They are grouped according to the time of maximal transcript abundance, but taking into account the timing of transcriptional activation also.

The proto-oncogene c-*fos* is one of the first genes to be activated, showing increased transcriptional activity within minutes of stimulation of quiescent cells [20,56], followed by a rapid increase in c-*fos* mRNA and protein [55]. In mouse fibroblasts the activation of c-*fos* preceded that of another protooncogene, c-*myc* [20]. c-*myc* is the prototype group II gene. Its activation precedes that of c-*ras*^{H} and c-*ras*^{K}, which may be required for later events in the progression to DNA synthesis [355]. The genes KC [106] and 4F1 [108] join c-*fos* as members of group I since their activation preceded that of c-*myc* [18,128]. Although β-actin synthesis increased within 15 min of serum stimulation of quiescent 3T3 cells, nuclear 'run-off' experiments revealed that activation was biphasic, decreasing from an initial peak at 30 min, then increasing to a second maximum at 2 h [20]. The significance of this early, rapid burst of transcription is uncertain in view of the fact that the concentration of actin transcripts and actin synthesis were maximal in mid G_1, 4–6 h after serum stimulation [19,155]. The cytoplasmic accumulation of β- and γ-cytoskeletal actin, as well as transcription of their genes, is rapidly stimulated in AKR-2B mouse embryo cells by EGF or cycloheximide, and even better by both together [356].

The major distinction between genes in groups III and IV and the 'early' genes in groups I and II is the sensitivity of their induction to inhibitors of protein synthesis [357]. Exposure to cycloheximide causes the content of poly(A) mRNA roughly to double over a 2-h period at any point after serum-induced proliferation of quiescent 3T6 cells [358], so changes in transcript abundance are best normalized to the poly(A) mRNA components. All of the group I and II genes are induced or superinduced when cycloheximide is added along with the growth factors, indicating that these genes are activated as a primary consequence of growth factor stimulation. The genes in groups III and IV require protein synthesis for their full induction, at least in the cells tested, suggesting that the synthesis of specific activators of gene expression is a prerequisite for early G_1 transit. The level of the transcripts of some genes (p53, MRP, histone), once induced, may be increased by cycloheximide because of effects on labile inhibitors or mRNA stability. Cycloheximide also superinduces a number of mitogen-induced secreted proteins [358a] and dsRNA-induced proteins, including interferon [358b].

The cDNA clone 49C8, which detects a family of short RNA polymerase III-derived transcripts from the family of mouse repetitive elements known as B2, does not fit the pattern. These RNAs could be induced by addition of cycloheximide to quiescent Swiss 3T3 fibroblasts, and their levels 6 h after serum stimulation were doubled when cycloheximide was present along with the mitogen [110]. By this criterion they should be placed in the 'early' gene groups; indeed their transcript abundance in some experiments (e.g. Fig. 2) appeared to decrease prior to entry of cells into S phase. The timing and extent of induction of these transcripts may depend critically on the state of quiescence of the cells prior to stimulation.

Assignment of the various genes to different groups based on the precise times at which their cytoplasmic mRNA concentrations peak should be considered tentative because of variations in the cells and synchronization protocols used in different laboratories. In our laboratory, using subconfluent cultures of Swiss 3T3 cells that have been made quiescent in medium containing 0.5% serum, we observe that 16C8 transcript levels generally peak before those of MRP, 49C8 and 5B10, and at around the same time as the actin maximum [19,110,130,155]. Some group III genes (e.g. MRP (proliferin), 49C8, c-*ras* and p53) show no peak accumulation of mRNA followed by a decline, but maintain a high induced level throughout the cell cycle [101,110,130,355].

VC. *Control points during the cell cycle*

Two aspects stand out concerning the G_0 to S phase transition. Firstly, as discussed above, there are obvious temporal patterns of gene expression, and, secondly, there are distinct control points defined by requirements for external signals that punctuate the transition. These, and points defined in cycling cells, are illustrated in Fig. 5.

The first control point is the induction in G_0

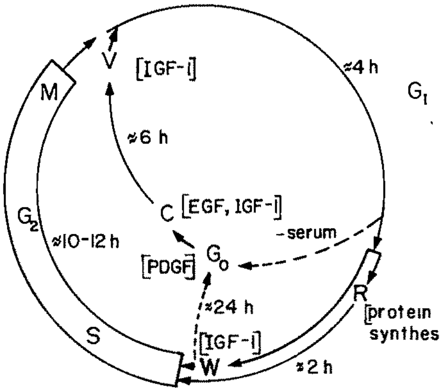

Fig 5 Cell cycle control points in BALB/c 3T3 cells (adapted from Ref 366) The outer circle represents the cell cycle in exponentially growing cells (all required growth factors – PDGF, IGF-1 and EGF in this specific case – and nutrients present). In the absence of required growth factors or certain nutrients (or space to expand into) cells leave the cycle, usually somewhere in mid-to-late G_1 before R or W, to enter the quiescent state G_0 Cells, peripheral blood lymphocytes for example, can remain in G_0 for long periods under favorable conditions Growth factors or conditions required to pass restriction points are indicated in brackets Two signals, one dependent on R, the other on W, are required to initiate DNA synthesis; the two parallel lines indicate the fact that these control points, both of which must be passed, can be reached independently of each other Duration of cell cycle segments are not to scale, but approximate times in hours are indicated

fibroblasts of a state (often called competence) that allows the cells to respond to additional factors, sometimes called progression factors. The state of competence in normal fibroblasts can be induced by PDGF, FGF, calcium phosphate, or even cycloheximide (Refs 157 and 359; and Baserga, R., personal communication); in B lymphocytes, antigen or lipopolysaccharide provides a competence-inducing signal [360]. Various changes have been observed when competence is induced, such as increases in the levels of several mRNAs, including c-*fos* and c-*myc* (Refs. 18–20, 53, 55, 64; see section IIA); c-*myc* has been put forward as an intracellular mediator of the PDGF-induced competent state [22]. The M_r 20000 myosin light chain was phosphorylated and microfilament bundles were disrupted within 5 min of PDGF addition [361]. The cellular protein kinase pp60$^{c\text{-}src}$ was modified, probably by phosphorylation [362]. The competent state, whose induction was blocked by inhibitors of RNA but not protein synthesis, was moderately stable after removal of the inducing factor, and could be transferred to other cells via cytoplasts [363]. Neither maintenance of the competent state nor progression through G_1 required high level expression of c-*myc* or c-*fos* [364]. In cycling cells the induction of competence occurred during the preceding growth cycle [365].

About half-way through the G_1 period of serum-stimulated quiescent fibroblasts is a point, the V point, beyond which cells deprived of key nutrients or growth factors are unable to proceed [366]. Cells can reach this point in less than optimal conditions as long as they have been stimulated to progress by EGF and IGF-1 (somatomedin C; hyperphysiological concentrations of insulin also function) [367]. Progression to the V point in part involves the augmentation (independently of whether the cells have been made competent) of the protein-synthesis capacity of the cell [368,369]. That part of G_1 prior to V is mostly unique to the G_1 period of stimulated quiescent cells. Beyond V, in that part of G_1 that is common with the G_1 period of cycling cells, only IGF-1 and conditions that support efficient protein synthesis appear necessary. New gene transcription is required, whereas late in G_1 IGF-1 mainly influences post-transcriptional events [366]. In B lymphocytes, progress beyond the first restriction point requires alpha-type B-cell growth factors [360].

W is an unstable point immediately before S phase at which cells can be arrested when deprived of growth factors, likely IGF-1 [366,367]. Some 2 h before S phase, at a point called the restriction (R) point, cells appear to commit themselves to enter S [66,161]. Rapid protein synthesis and growth factors are required before, but not after, R. It may be that at this time the concentration of a labile and critical, but as yet hypothetical, protein has built up to the extent required for final entrance into S [160,367]; or requisite multienzyme complexes have been assembled. Transition into and through S phase is also dependent upon an adequate supply of histones. The relation of points like V or R to transitions like K_Q or K_A is not known. Transformed cells, which are generally unable to enter the quiescent state, do not exhibit an exogenous requirement for a competence-inducing signal and do not have an obvious restriction point.

The concepts of competence, progression and restriction point have been derived from an experimental system in which serum-starved confluent BALB/c 3T3 cells were stimulated to synthesize DNA by adding fresh medium with a higher serum content [359,366]. Attempts have been made to compare this organization of growth factor requirements to other cells and culture conditions. Much evidence exists to suggest that such comparisons may not apply in detail. Thus significant variations in the temporal organization of growth factor action have been noted for quiescent subconfluent Swiss 3T3 cells cultured in a defined (serum-free) medium [370]. FGF or PDGF stimulation for 1 h permitted efficient entry into S phase. It may be that inhibitory components in serum or plasma impair key processes. CH3 10T1/2 cells responded to EGF as the sole mitogen, but PDGF potentiated their sensitivity to that factor [371]. In mitogenesis assays with Swiss 3T3 cells there is a marked synergism between two groups of agents: those that elevate intracellular cAMP and those that activate protein kinase C [371a].

T lymphocytes are similar to BALB/c fibroblasts in that they require two signals for entrance into S phase, but differ from them in the nature of the restriction point and the patterns of gene expression caused by each growth factor. The G_0 to G_1 transition in T cells is controlled by antigens or mitogenic lectins that concomitantly induce cell surface IL-2-receptor expression (not found in fibroblasts) and c-*myc* mRNA accumulation [372,373]. Cell surface IL-2-receptor levels were the critical restriction point that controlled entry into S phase after appropriate IL-2 stimulation [372]. T cell c-*myc* accumulation was induced by IL-2 [373], whereas the second mitogenic signal for BALB/c fibroblasts (EGF) had little effect on its expression after the competent state had been established [364]. Thus, the rate-limiting steps during G_1 and the ability of individual growth factors to control those steps might be a function of each cell type and culture condition. Although the pathways leading to DNA synthesis must have underlying similarities at the molecular level in all cell types, it may not be apparent from the perspective of the timing and specificity of growth factor requirements.

VD. Intracellular metabolites that may orchestrate cell cycle events

Besides labile proteins and second messengers such as cyclic nucleotides, what do we know about intracellular, molecular events that could possibly be related to some of these control points? Among compounds implicated in cell cycle events are polyamines, calcium, Ap_4A and mevalonic acid.

As discussed in section IVB4, polyamine synthesis is essential for progression through the cell cycle, and the role of ornithine decarboxylase was reviewed there. Another essential enzyme in polyamine synthesis is *S*-adenosylmethionine decarboxylase, which can be inhibited by methylglyoxal bis(guanylhydrazone) (mGBG). Serum-stimulated quiescent fibroblasts have been shown to be blocked about 4 h before S phase in the presence of mGBG, somewhere between V and W; progression into S after removal of the inhibitor required only activation of the IGF-1 receptor [374]. In the inhibited cell, protein synthesis was reduced (cf. Ref. 263a) and the levels of spermine and spermidine were decreased while that of putrescine was increased. The induction of thymidine kinase in rat embryo fibroblasts was blocked provided that mGBG was added within 3 h of the serum [259].

Calcium deprivation in roughly the first half of G_1 also prevented serum-induced thymidine kinase induction in rat cells, apparently acting at a later stage than polyamine deprivation [259]. Calcium of course is an essential cell constituent required for many diverse processes; transformed cells often evince a diminished requirement [375]. In human WI38 fibroblasts Ca^{2+} was required for the transition out of quiescence and for progression [376]. Ca^{2+} action is usually modulated via calmodulin, whose level is minimal in G_1 and increases when cells enter S or G_0. Calmodulin antagonists prevented cells both from leaving G_0 and from completing a normal cell cycle [377,378]. Very rapidly after the addition to fibroblasts of PDGF or serum, but not other growth stimulants, including EGF, TPA and insulin, there was a decrease in the cell's total calcium content and an approximate 3-fold rise in the concentration of free intracellular Ca^{2+}, apparently released from internal stores [379,380]. Further into G_1, there was a decrease in the content of both calmodulin mRNA and the protein itself, followed by an increase some hours later and just preceding entry of the cells into S phase [378]. However, the calmodulin content normalized to total soluble protein did not vary during the cell cycle, encouraging the authors of a recent review to conclude that changes in calmodulin levels did not play a causative role in cell cycle regulation [375]. Its role as an essential mediator was not challenged.

Two known proteins provide a precedent for the regulation of gene expression by the concentration of calcium ions [381,382]. These proteins (M_r about 100 000 and 80 000) have been designated GRP94 and GRP78 by Lee et al. because their levels were regulated by glucose (as well as by Ca^{2+}) [383]. Stress, nutrient (especially glucose) deprivation, exposure to calcium ionophores, or maintenance of the cell cycle mutant K12 at the nonpermissive temperature enhanced the abundance of the proteins and their mRNAs in the cell [384]. Nuclear 'run-off' experiments showed that the increase was largely due to an increase in their rate of transcription in cells exposed to the calcium ionophore A23187 [383]. A role for calmodulin in the induction of these genes, and their involvement in cell cycle phenomena, remains to be established.

Diadenosine 5′,5‴-P^1,P^4-tetraphosphate (Ap_4A) is formed in the back-reaction of the first step in protein synthesis, the activation of amino acids by aminoacyl-tRNA synthetases. Since its molecular structure is very similar to ATP, it is to be expected that it will have numerous effects mediated via interactions with proteins able to bind ATP. Not only does its intracellular concentration correlate with the proliferative state of cells but also it binds tightly to DNA polymerase α and is capable of priming DNA replication in permeabilized nuclei (see Ref. 385 for review). Grummt and collaborators [386] have made a thorough study of the changes in Ap_4A levels during the cell cycle and have argued strongly for its role as a second messenger crucial to the initiation of S phase. Intriguingly, inhibition of DNA (and protein) synthesis by interferon or cycloheximide was accompanied by decreases in the size of the Ap_4A pools. We wonder whether any of the phenomena that have been attributed to a hypothetical 'labile' protein may instead be due to a decrease in the Ap_4A concentration.

Hydroxymethylglutaryl-coenzyme A (HMG-CoA) reductase, the enzyme that catalyses mevalonate synthesis, is required for entrance into and passage through S phase. That it is the defect in mevalonic acid synthesis that is the problem was shown by the fact that mevalonic acid, or isopentenyladenine (synthesized from mevalonate), could overcome the block to DNA replication induced by blocking HMG-CoA reductase with the competitive inhibitor compactin [387,388]. Mevalonate also reversed the block to DNA replication induced by nalidixic acid. Mevalonate is a key intermediate in the synthesis of isopentenyl pyrophosphate, which in turn is the precursor of numerous important compounds, including isopentenyl-tRNA and cholesterol. Cholesterol seemed to be required, at least under some conditions, in early G_1, whereas the 'isopentenyl effect' was restricted to mid-to-late G_1 [389,390]. Sinensky and Logel [391] have studied a CHO mutant with a defect in mevalonate synthesis and found a close correlation between the decay in the ability to synthesize DNA and the loss of mevalonate-labeled (e.g. terpenylated) proteins. Possibly an isoprenoid-modified protein [392] is essential for progression past a restriction point in G_1.

VE. Pathways of gene activation and deactivation

At this point it is tempting to speculate about possible cascades of gene activations that control the G_0 to S phase transition. The early growth factor-inducible genes may encode functions that in turn activate additional genes, for example those in group IV. The products of the group I and II genes c-*fos* and c-*myc* are both nuclear proteins, and both *myc* and adenovirus transformation protein E1A, which are able to immortalize cells [97,393], are known to induce the transcription of cellular genes, including the M_r 70 000 heat-shock protein [164,394,395]. The requirement for protein synthesis for induction of the group III and IV genes by serum (Fig. 4B) may reflect a requirement for specific *trans*-activating transcriptional factors that are the products of group I or II genes.

A cascade of gene expression may be controlled by β-interferon. The transcript of this growth-regulatory protein accumulates in direct response to PDGF in BALB/c fibroblasts [396] and the protein is secreted into the medium during the G_1 phase of cycling primary cells [397]. The secreted protein presumably interacts with its cell surface receptors in a manner similar to exogenously added interferons and activates a number of genes. Activated genes include those encoding 2′-5′oligo(A) synthetase [330,396], metallothionein-II, class I HLA [326], and several proteins of unknown function [322–324]. The timing of interferon addition is an important aspect in such responses, since addition to quiescent cells at the same time as PDGF reduced accumulation of c-*myc*, c-*fos*, ODC and β-actin mRNAs [398], while in cells pre-treated for 48 h with interferon, c-*myc*, JE and KC mRNAs were slightly 'superinduced' by PDGF [399]. Poly(rI · rC) induction of the interferon β_1 gene in human fibroblasts was similarly controlled by previous interferon treatment, and the 'priming' effect was shown to be the result of increased transcription [400]. Transcriptional modifications under the control of interferon appear to underlie some of these changes in mRNA levels, but post-transcriptional regulation could also be important.

The identities of intracellular components involved in the regulatory events that increase the cytoplasmic concentrations of particular mRNAs in these putative cascades of gene inductions are unknown. It is thus ironic that a mechanism has been discovered for repressing the expression of a class of genes; this is inferred from the cell cycle-associated variations in the activity of the 2′-5′oligo(A) synthetase–RNAase L pathway in synchronized cells. Activation of this pathway sets up a process for the degradation of specific mRNAs and can therefore function as a feed-back regulatory loop to control the levels of growth-regulated transcripts. The members of this pathway include the double-stranded RNA-activated enzymes responsible for synthesis and degradation of ppp$(A2'p)_nA$ – the synthetase and a specific phosphodiesterase that are induced by β-interferon.

The only known function for ppp$(A2'p)_nA$ is to bind to and activate the $2'$-$5'(A)_n$-dependent RNAase (reviewed in Ref. 319). RNAase levels rose about 2-fold during transition from G_1 to S in synchronized murine fibroblasts [397] and 'elutriated' HL60 cells [401] as measured by ppp$(A2'p)_n$A-analogue binding experiments. Even though the activity of the 2′-5′oligo(A) synthetase rose as much as 10-fold [397,402] and that of the phosphodiesterase declined, the amount of 2′-5′oligo(A) in cell extracts remained below detectable limits. Be that as it may, the ability of the activated RNAase to degrade mRNA [403,404] could account for increased c-*myc* mRNA degradation after HL60 cells are treated with interferon [31]. It has been suggested that double-stranded regions of the 5′ end of the c-*myc* mRNA stimulate the activity of the synthetase [330], and c-*myc* may be subject to the same control during the cell cycle.

The increase in interferon activity in the culture medium of cycling G_1-phase cells elicited activation of the 2′-5′oligo(A) synthetase, since interferon-specific antibodies added to the medium reduced synthetase levels in both G_1- and S-phase cells [397]. Similar antibody inhibition experiments have prompted the hypothesis that externalization of an interferon-like molecule may mediate DNA synthesis termination during the cell cycle [402]. It seems that a growth-regulatory system originally discovered by virtue of its ability to confer an anti-viral state is in fact an integral part of cell cycle gene regulation.

We have applied the term cell cycle gene to all of the genes described in Fig. 4. Some of them have been studied in exponentially growing cells that have been fractionated into cell cycle stages, usually by the process of centrifugal elutriation. To date, the only genes that evince cell cycle regulation in such exponentially growing cells appear to fall into group IV, i.e., c-*myb*, the histones and the enzymes of DNA metabolism. Levels of transcripts corresponding to c-*myc* [23–26], 16C8, 49C8(B2), MRP (proliferin) and MEP (our unpublished observations) show no periodic maxima in cycling cells. Obviously, many of the early G_1-specific events that occur as cells exit the quiescent state are specific to that process and apparently are not temporally regulated in exponentially growing cell populations.

The lengthy process 'L' that cells enter when they pass K_A (see Fig. 1) may represent the duplication of mitotic centers [8]. The kinetic analysis suggests that in cycling cells 'L' need not occur at a fixed time relative to mitosis, so that in a population of cycling cells those cells in, say, S phase can consist of cells that are at different positions in L, or perhaps not in L at all. In other words, there may be considerable 'slippage' allowed in the timing of L relative to the replicative and growth cycles. However, centriole duplication and deciliation occur near the G_1/S boundary [405]. According to the 'two-transition' model, cells are synchronized for passage through L when they come out of quiescence, hence some of the new gene expression seen when quiescent cells are stimulated, but not observably synchronized in normally cycling cells, may reflect events in L. The enhanced gene expression seen as cells leave G_0 also includes the 'gearing-up' for an overall increase in the rate of protein synthesis and other anabolic processes as well as the production of the products of 'house-keeping genes' required by cycling cells but not quiescent cells.

VI. Prospects for the future

We are beginning to characterize genes such as *fos*, *myc*, and *ras* that are regulatory, in the sense that they control expression of other genes, as opposed to those (which may be regulated in a cell cycle-dependent fashion) that produce a product required at only one stage in the cell cycle for functional but not regulatory purposes (e.g. histones, dihydrofolate reductase and thymidine synthetase). A principal objective of present-day research is to find out whether the less well-characterized genes are regulatory or operative components in the proliferative cascade, and to distinguish them from genes whose 'induction' is gratuitous and has nothing to do with progress through the cell cycle. Initial efforts in this direction have involved classification of these genes into regulatory 'families' defined by their response to specific perturbations, such as temperature-sensitive mutations or deprivation of essential inducers/mediators. This type of analysis plainly establishes functional separation of early G_1 gene expression from late G_1 gene expression. Induction of TS and TK synthesis appears, like DNA synthesis, to correlate with the presence of a labile protein postulated to accumulate in normal cells after serum stimulation and whose continued synthesis is necessary for G_1 progression [258]. Key questions include the nature of labile regulatory elements and the level of regulation – whether transcriptional or post-transcriptional.

Transformed cells are of particular interest because of the fundamental changes associated with the transformed phenotype and the belief that altered regulation of cell cycle-dependent gene expression is likely to play a pivotal role in aberrant growth control. Thus the proto-oncogene c-*myc* has been thoroughly studied in many tumours and tumour-derived cell lines. The events leading to its activation have been ascribed to retroviral promoter insertion events near the gene or to translocation and truncation events within the genome (see Ref. 17 for a review). Some studies have also revealed elevated and/or constitutive c-*myc* expression in tumours without any detectable gene rearrangements [51], and in cell lines transformed by chemicals [19] or Rous sarcoma virus [405a], indicating that c-*myc* is responsive to alterations in regulatory factors.

In one study, three of five cell cycle-dependent genes examined appeared to be expressed in an altered manner in human leukemias [129]. Elevated expression of the B2 repeat sequence and the VL30 retrovirus-like family occur in mouse cells after mitogen stimulation [110,150] or SV40 transformation [141,153]. Malignant transformation by a variety of retroviruses or retroviral oncogenes increased the level of the transcripts for MEP, a secreted glycoprotein [291,292] and an unidentified transcript, pTR1 [147]. Elevated expression of proliferin (MRP), a mitogen-induced member of the prolactin-growth hormone family, may be linked to the acquisition of immortality by murine fibroblasts [130,297]. Two cell cycle-dependent oncogenes, p53 and activated c-*myc*, can cooperate with the *ras* oncogene, presumably by conferring immortality, to establish tumorigenic lines of normal diploid cells [93,97]. Normal diploid chondrocytes may also be immortalized by the inappropriate expression of the p53 product [96], and the FBR-MuSV p75*gag-fos* protein induced establishment in about one-third of diploid fibroblast transformants [406].

Evidently a number of the cell cycle-regulated (proto-onco) genes are associated with dominant altered regulatory mechanisms in certain transformed cell lines. Complementation studies, on the other hand, suggest that many of the 'mutations' conferring malignancy in human cells are recessive in nature [407]. It is important therefore to learn more about the less well-characterized and still undiscovered cell cycle-regulated genes so that we may eventually comprehend the proliferative process. By employing transformed cells as regulatory mutants (or variants) of growth factor-induced gene expression, not only can we obtain a better understanding of the extent to which gene expression is co-ordinated during the cell cycle, but also we can elucidate those changes in gene expression that contribute to the transformed phenotype. Studies designed to uncover how the regulated expression within this group of genes is disrupted should eventually lead to a coherent picture of the ways in which somatic cells lose control of their growth and the consequences these changes have for cellular behavior.

Although DNA sequence analysis has provided clues to the function of several cloned cell-cycle regulated genes, the function of many remains unknown. Two approaches that may provide the means to assess the contribution of individual gene products in the proliferative response involve genetic manipulations designed specifically either to block their expression or, alternatively, to cause their regulated overexpression. This is done by engineering the production in the cell of copious amounts of a functional mRNA or its complement (anti-sense RNA). Subsequent changes in the molecular biology and physiology of the cell are then assessed, particularly at the level of mRNA production by cell cycle-dependent genes.

Anti-sense RNA has received much attention as an agent useful for suppressing the expression of specific genes in vivo [408]. TK expression was demonstrated to be sensitive to high intracellular levels of anti-sense RNA (10–100-fold excess of anti-sense RNA over mRNA) as measured by reduced [^{3}H]thymidine incorporation, and colony formation in HAT medium was inhibited by blocking endogenous TK mRNA production in CHO cells with enhanced expression of anti-sense TK RNA from chimeric gene constructs [409]. The anti-sense RNA hybridizes to TK mRNA within the nucleus, substantially reducing the amount that is transported to the cytoplasm. Even though up to 10-fold reductions in the level of enzyme activity could be achieved, this was not sufficient to provide resistance to bromodeoxyuridine cytotoxicity, normally mediated by the action of thymidine kinase [410]. Since not all manifestations of the normal phenotype are blocked, the 'null mutation' in this case at least may be considered 'leaky'. However, the anti-proliferative effect and the disruption of the cytoskeleton produced by anti-sense actin RNA indicate that this procedure will find applicability in assessing the contribution of individual genes to the proliferation response, especially if the critical concentration of the gene product falls within the limits of control provided by anti-sense RNA.

The opposite approach, directed expression of the gene in question, has been employed in a number of studies, some of which were described earlier in this review, and additional elaboration of the methodology is unnecessary. We would like to close, however, with a clever technique that exploits the ease with which the *dhfr* gene can be amplified [411]. To obtain permanent cell lines expressing quantities of a heterologous protein, one co-transfects cells with the *dhfr* gene and a 'target' gene. Subsequently, methotrexate-promoted amplification of the copy number of the *dhfr* gene in selected transfected clones will favor co-amplification of sequences adjacent to the *dhfr* construct, including the co-transfected 'target' gene. This approach has been used successfully to obtain CHO cells that express high levels of human tissue-type plasminogen activator [412]. Altered cell morphology was apparently related to the ability of the high-level expression of t-PA to convert serum plasminogen to plasmin, a broad-spectrum proteinase.

Acknowledgements

Research from our laboratory reported herein was supported by the National Cancer Institute of Canada and the Medical Research Council of Canada. D.R.E. and C.L.J.P. were postdoctoral fellows supported by the NCI(C) and the MRC(C) respectively. We thank Linda Bonis for many patient hours on the keyboard preparing the manuscript, Beth Orphan for some of the figures, and Anthony Ridgway and Ann Marie Craig for a careful reading.

References

1 Mitchison, J M. (1971) The Biology of the Cell Cycle, Cambridge University Press, London
2 Howard, A and Pelc, S.R (1953) Heredity 6, 261–273
3 Pardee, A.B., Dubrow, R, Hamlin, J L and Kletzien, R F (1978) Annu. Rev. Biochem 47, 715–750
4 Brooks, R F, Riddle, P N, Richmond, F N and Marsden, J (1983) Exp Cell Res. 127–142
5 Hochhauser, S J, Stein, J.L and Stein, G.S (1981) Int Rev Cytol. 71, 95–243
6 Burns, F.J and Tannock, I F (1970) Cell Tissue Kinet. 3, 321–334
7 Smith, J A and Martin, L. (1973) Proc Natl Acad Sci USA 70, 1263–1267
8 Brooks, R.F., Bennett, D C and Smith, J A (1980) Cell 19, 493–504
9 Brooks, R F, Richmond, F N, Riddle, P N and Richmond, K M V (1984) J Cell Physiol 121, 341–350
10 Baserga, R (1985) The Biology of Cell Rproduction, Harvard University Press, Cambridge, MA
11 Hartwell, L H (1974) Bact Rev. 38, 164–198
12 Miska, D and Bosmann, H B. (1980) Biochem Biophys Res Commun 93, 1140–1145

13 Bishop, J.M and Varmus, H. (1985) in RNA Tumor Viruses Molecular Biology of Tumor Viruses, 2nd Edn (Weiss, R., Teich, N., Varmus, H, and Coffin, J., eds.), pp 249–356, Cold Spring Harbor Laboratory, NY

14 Heldin, C.-H. and Westermark, B (1984) Cell 37, 9–20

15 Weinberg, R.A (1985) Science 230, 770–776

16 Kelly, K and Siebenlist, U (1985) J Clin Immunol 5, 65–77

17 Ratner, L., Josephs, S F. and Wong-Staal, F (1985) Annu Rev Microbiol. 39, 419–449

18 Kelly, K, Cochran, B H, Stiles, C D and Leder, P (1983) Cell 35, 603–610

19 Campisi, J., Gray, H E, Pardee, A.B., Dean, M and Sonenshein, G E (1984) Cell 36, 241–247

20 Greenberg, M E and Ziff, E B. (1984) Nature (Lond) 311, 433–438

21 Blanchard, J-M, Piechaczyk, M, Dani, C, Chambard, J-C, Franchi, A., Pouyssegur, J and Jeanteur, P. (1985) Nature (Lond) 317, 443–445

22 Armelin, H.A, Armelin, M C S., Kelly, K., Stewart, T, Leder, P, Cochran, B H. and Stiles, C D (1984) Nature (Lond) 310, 655–660

22a Kaczmarek, L, Hyland, J.K, Watt, R, Rosenberg, M and Baserga, R. (1985) Science 228, 1313–1315

23 Thompson, C B, Challoner, P B, Neiman, P.E and Groudine, M (1985) Nature (Lond.) 314, 363–366

24 Lachman, H M., Hatton, K S, Skoultchi, A I and Schildkraut, C.L (1985) Proc. Natl. Acad Sci USA 82, 5323–5327

25 Rabbitts, P H., Watson, J V, Lamond, A, Forster, A, Stinson, M.A., Evan, G, Fischer, W, Atherton, E, Sheppard, R and Rabbitts, T H (1985) EMBO J 4, 2009–2015

26 Hann, S R, Thompson, C B and Eisenman, R N (1985) Nature (Lond.) 314, 366–369

27 Persson, H., Gray, H E and Godeau, F (1985) Mol Cell Bio 5, 2903–2912

28 Westin, E H., Wong-Staal, F, Gelmann, E P, Favera, R.D, Papas, T.S., Lautenberger, J A., Eva, A., Reddy, E P, Tronick, S R., Aaronson, S A. and Gallo, R C (1982) Proc Natl. Acad Sci. USA 79, 2490–2494

29 Grosso, L.E and Pitot, H.C (1985) Cancer Res 45, 847–850

30 Gonda, T J. and Metcalf, D (1984) Nature (Lond) 310, 249–251

30a Filmus, J and Buick, R.N. (1985) Cancer Res 45, 822–825

30b Grosso, L E and Pitot, H.C (1985) Cancer Res 45, 5035–5041

31 Jonak, G J and Knight, E, Jr (1984) Proc Natl Acad Sci USA 81, 1747–1750

32 Dani, C, Blanchard, J M, Piechaczyk, M, El Sabouty, S, Marty, L and Jeanteur, P (1984) Proc Natl. Acad. Sci USA 81, 7046–7050

33 Butnick, N.Z, Miyamoto, C, Chizzonite, R, Cullen, B R., Ju, G and Skalka, A.M (1985) Mol Cell. Biol 5, 3009–3016

34 Piechaczyk, M, Yang, J-Q, Blanchard, J.-M, Jeanteur, P and Marcu, K.B. (1985) Cell 42, 589–597

35 Dani, C., Mechti, N, Piechaczyk, M, Lebleu, B., Jeanteur, P. and Blanchard, J M (1985) Proc Natl. Acad. Sci. USA 82, 4896–4899

36 Einat, M., Resnitzky, D. and Kimchi, A (1985) Nature (Lond) 313, 597–600

37 Linial, M., Gunderson, N. and Groudine, M (1985) Science 230, 1126–1132

38 Leder, P., Battey, J, Lenoir, G., Moulding, C, Murphy, W, Potter, H., Stewart, T and Taub, R (1983) Science 222, 765–771

39 Taub, R, Moulding, C, Battey, J, Murphy, W., Vasicek, T, Lenoir, G.M. and Leder, P (1984) Cell 36, 339–348

40 Nishikura, K, Ar-Rushdi, A., Erikson, J, Watt, R, Rovera, G and Croce, C M (1983) Proc Natl Acad Sci USA 80, 4822–4826

41 Rabbitts, T H, Forster, A., Hamlyn, P. and Baer, R (1984) Nature (Lond) 309, 592–597

42 Feo, S, Ar-Rushdi, A, Huebner, K, Finan, J, Nowell, P.C, Clarkson, B and Croce, C M (1985) Nature (Lond.) 313, 493–495

43 Rapp, U.R., Cleveland, J L., Brightman, K, Scott, A and Ihle, J.N. (1985) Nature (Lond) 317, 434–438

44 Siebenlist, U, Henninghausen, L, Battey, J and Leder, P (1984) Cell 37, 381–391

45 Fahrlander, P.D., Piechaczyk, M. and Marcu, K B (1985) EMBO J. 4, 3195–3202

46 Goyette, M, Petropoulos, C.J, Shank, P R and Fausto, N (1984) Mol. Cell Biol. 4, 1493–1498

47 Makino, R., Hayashi, K and Sugimura, T (1984) Nature (Lond.) 310, 697–698

48 Keath, E.J, Kelekar, A and Cole, M D (1984) Cell 37, 521–528

49 Reed, J C., Nowell, P C and Hoover, R G. (1985) Proc. Natl Acad Sci USA 82, 4221–4224

50 Bravo, R, Burchardt, J, Curran, T. and Müller, R. (1985) EMBO J 4, 1193–1197

51 Erisman, M.D, Rothberg, P.G., Diehl, R E, Morse, C.C, Spandorfer, J M. and Astrin, S.M (1985) Mol. Cell Biol 5, 1969–1976

52 Coughlin, S R, Lee, W.M F, Williams, P W., Giels, G M. and Williams, L.T (1985) Cell 43, 243–251

53 Kruijer, W., Cooper, J A, Hunter, T and Verma, I M. (1984) Nature (Lond) 312, 711–716

54 Corral, M., Tichonicky, L, Guguen-Guillouzo, C, Corcos, D, Raymondjean, M., Paris, B, Kruh, J and Defer, N (1985) Exp Cell Res. 160, 427–434

55 Müller, R, Bravo, R., Burckhardt, J. and Curran, T. (1984) Nature (Lond) 312, 716–720

56 Angel, P., Rahmsdorf, H J., Pöting, A and Herrlich, P (1985) in Cancer Cells 3, Growth Factors and Transformation (Feramisco, J., Ozanne, B and Stiles, C., eds), pp. 315–319, Cold Spring Harbor Laboratory, NY

57 Treisman, R (1985) Cell 42, 889–902

58 Müller, R., Curran, T, Müller, D and Guilbert, L. (1985) Nature (Lond) 314, 546–548

59 Mitchell, R.L, Zokas, L, Schreiber, R D. and Verma, I.M. (1985) Cell 40, 209–217

60 Curran, T and Morgan, J I (1985) Science 229, 1265–1268

61 Greenberg, M.E., Greene, L A and Ziff, E.B. (1985) J Biol Chem. 260, 14101–14110

62 Müller, R. and Wagner, E F (1984) Nature (Lond.) 311, 438–442

63 Rüther, U , Wagner, E F and Müller, R (1985) EMBO J. 4, 1775–1781

64 Cochran, B H., Zullo, J., Verma, I.M and Stiles, C.D (1984) Science 226, 1080–1082

65 Brooks, R.F. (1977) Cell 12, 311–317

66 Rossow, P W., Riddle, V.G.H and Pardee, A B. (1979) Proc Natl. Acad Sci USA 76, 4446–4450

67 Goyette, M , Petropoulos, C J , Shank, P R and Fausto, N (1983) Science 219, 510–512

68 Feramisco, J R , Gross, M , Kamata, T , Rosenberg, M. and Sweet, R.W (1984) Cell 38, 109–117

69 Stacey, D W and Kung, H.-F (1984) Nature (Lond) 310, 508–511

70 Mulcahy, L.S , Smith, M.R. and Stacey, D W. (1985) Nature (Lond.) 313, 241–243

71 Feramisco, J R , Clark, R., Wong, G , Arnheim, N , Milley, R. and McCormick, F (1985) Nature (Lond) 314, 639–642

72 Bar-Sagi, D. and Feramisco, J R. (1985) Cell 42, 841–848

73 Noda, M., Ko, M , Ogura, A , Liu, D., Amano, T , Takano, T. and Ikawa, Y (1985) Nature (Lond) 318, 73–75

74 Manne, V , Yamazaki, S and Kung, H.-F. (1984) Proc Natl. Acad Sci USA 81, 6953–6957

75 Poe, M , Scolnick, E.M and Stein, R B (1985) J Biol Chem 260, 3906–3909

76 Manne, V , Bekesi, E. and Kung, H -F (1985) Proc Natl. Acad Sci USA 82, 376–380

77 Sweet, R W , Yokoyama, S., Kamata, T , Feramisco, J R , Rosenberg, M and Gross, M (1984) Nature 311, 273–275

78 Shih, T Y., Weeks, M.O., Gruss, P., Dhar, R., Oroszlan, S. and Scolnick, E M (1982) J. Virol 43, 253–261

79 Sefton, B M., Trowbridge, I S , Cooper, J A. and Scolnick, E.M. (1982) Cell 31, 465–474

80 Gilman, A.G (1984) Cell 36, 577–579

81 Hurley, J B., Simon, M I , Teplow, D B , Robishaw, J.D and Gilman, A G (1984) Science 226, 860–862

82 Broek, D , Samiy, N , Fasano, O , Fujiyama, A , Tamanoi, F., Northup, J and Wigler, M. (1985) Cell 41, 763–769

83 Franks, D.J., Whitfield, J.F. and Durkin, J.P. (1985) Biochem Biophys. Res. Commun 132, 780–786

84 Westin, E.H:, Gallo, R.C , Arya, S.K , Eva, A., Souza, L M , Baluda, M.A., Aaronson, S A , and Wong-Staal, F (1982) Proc. Natl Acad. Sci. USA 79, 2194–2198

85 Sheiness, D and Gardinier, M (1984) Mol Cell Biol 4, 1206–1212

86 Torelli, G., Selleri, L , Donelli, A , Ferrari, S , Emilia, G., Venturelli, D , Moretti, L and Torelli, U (1985) Mol Cell Biol. 5, 2874–2877

86a Thompson, C.B , Challoner, P B , Neiman, P E and Groudine, M (1986) Nature (Lond) 319, 374–380

87 Lane, D P. and Crawford, L.V. (1979) Nature (Lond) 278, 261–263

88 DeLeo, A B., Jay, G , Appella, E , Dubois, G.C., Law, L.W and Old, L J (1979) Proc Natl Acad Sci USA 76, 2420–2424

89 Rotter, V., Witte, O N , Coffman, R. and Baltimore, D (1980) J. Virol 36, 547–555

90 Rotter, V. (1983) Proc Natl Acad Sci USA 80, 2613–2617

91 Maltzman, W. and Czyzyk, L (1984) Mol Cell Biol 4, 1689–1694

92 Eliyahu, D., Raz, A , Gruss, P , Givol D and Oren, M. (1984) Nature (Lond) 312, 646–649

93 Parada, L F , Land, H , Weinberg, R A , Wolf, D and Rotter, V (1984) Nature (Lond.) 312, 649–651

94 Wolf, D , Harris, N. and Rotter, V (1984) Cell 38, 119–126

95 Eliyahu, D , Michalovitz, D and Oren, M (1985) Nature (Lond) 316, 158–160

96 Jenkins, J.R , Rudge, K and Currie, G A (1984) Nature (Lond.) 312, 651–654

96a Zakut-Houri, R., Bienz-Tadmor, B , Givol, D and Oren, M (1985) EMBO J 4, 1251–1255

97 Land, H., Parada, L.F and Weinberg, R A (1983) Nature (Lond) 304, 596–602

98 Jenkins, J.R , Rudge, K., Chumakov, P. and Currie, G A (1985) Nature (Lond) 317, 816–818

99 Mercer, W E , Nelson, D , DeLeo, A B., Old, L J and Baserga, R (1982) Proc Natl Acad Sci USA 79, 6309–6312

100 Mercer, W E , Avignolo, C and Baserga, R (1984) Mol Cell Biol 4, 276–281

101 Reich, N C and Levine, A J (1984) Nature (Lond) 308, 199–201

102 Wynford-Thomas, D , LaMontagne, A , Marin, G and Prescott, D.M. (1985) Exp. Cell Res 159, 191–200

102a Coulier, F , Imbert, J , Albert, J , Jeunet, E , Lawrence, J -J , Crawford, L. and Birg, F (1985) EMBO J 4, 3413–3418

103 Mercer, W E and Baserga, R (1985) Exp Cell Res 160, 31–46

103a Matlashewski, G , Lamb, P , Pim, D., Peacock, J , Crawford, L and Benchimol, S. (1984) EMBO J 3, 3257–3262

103b Rogel, A , Popliker, M , Webb, C G and Oren, M (1985) Mol. Cell Biol. 5, 2851–2855

103c Calabretta, B , Kaczmarek, L , Ming, P -M L , Au, F and Ming, S.-C. (1985) Cancer Res. 45, 6000–6004

104 Wolf, D. and Rotter, V. (1985) Proc. Natl Acad Sci. USA 82, 790–794

104a Shen, D.-W , Real, F X , DeLeo, A B , Old, L J , Marks, P A and Rifkind, R A (1983) Proc Natl Acad Sci USA 80, 5919–5922

104b Reich, N C., Oren, M and Levine, A J (1983) Mol Cell Biol 3, 2143–2150

105 Foster, D N , Schmidt, L J , Hodgson, C P., Moses, H.L and Getz, M J (1982) Proc Natl. Acad Sci USA 79, 7317–7321

106 Cochran, B H., Reffel, A C and Stiles, C D (1983) Cell 33, 939–947

107 Linzer, D I H and Nathans, D (1983) Proc Natl Acad. Sci USA 80, 4271–4275

108 Hirschhorn, R R , Aller, P , Yuan, Z -A , Gibson, C W and Baserga, R. (1984) Proc Natl Acad Sci USA 81, 6004–6008

109 Matrisian, L M, Rautmann, G., Magun, B E and Breathnach, R (1985) Nucleic Acids Res 13, 711–726

110 Edwards, D.R., Parfett, C L.J. and Denhardt, D T (1985) Mol. Cell Biol 5, 3280–3288

111 Milcarek, C and Zahn, K. (1978) J Cell Biol. 79, 833–838

112 Riddle, V G H., Dubrow, R and Pardee, A B (1979) Proc Natl Acad. Sci USA 76, 1298–1302

113 Bravo, R and Celis, J E (1980) J Cell Biol. 84, 795–802

114 Nilsen-Hamilton, M., Shapiro, J M., Massoglia, S.L and Hamilton, R.T (1980) Cell 20, 19–28

115 Thomas, G, Thomas, G and Luther, H (1981) Proc Natl Acad. Sci. USA 78, 5712–5716

116 Pledger, W.J, Hart, C A, Locatell, K L and Scher, C.D. (1981) Proc. Natl. Acad. Sci. USA 78, 4358–4362

117 Adolph, K.W and Phelps, J.P (1982) J Biol. Chem 257, 9086–9092

118 Westwood, J.T, Wagenaar, E.B and Church, R B. (1985) J Biol Chem 260, 695–698

119 Hendrickson, S L and Scher, C D (1983) Mol Cell Biol 3, 1478–1487

120 Forsdyke, D.R. (1984) Can J Biochem Cell Biol 62, 859–864

121 Hayward, W S, Neel, B.G. and Astrin, S M (1981) Nature (Lond.) 290, 475–480

122 Kowalski, J., Smith, J H., Ng, N., and Denhardt, D T (1985) Gene 35, 45–54

123 Edwards, D R, Parfett, C L.J and Denhardt, D.T (1985) DNA 4, 401–408

124 Scott, M.R.D., Westphal, K-H and Rigby, P W.J (1983) Cell 34, 557–567

125 Linzer, D I H. and Nathans, D (1984) Proc. Natl Acad Sci USA 81, 4255–4259

126 Cochran, B.H, Reffel, A C, Callahan, M A., Zullo, J N and Stiles, C D (1984) in Cancer Cells 1, The Transformed Phenotype (Levine, A J., Van de Woude, G F, Topp, W.C. and Watson, J.D., eds), pp 51–56, Cold Spring Harbor Laboratory, NY

127 Hendrickson, S L, Cochran, B H, Reffel, A C. and Stiles, C D (1985) in Mediators in Cell Growth and Differentiation (Ford, R.J and Maizel, A L, eds), pp 71–85, Raven Press, New York

128 Kaczmarek, L., Calabretta, B and Baserga, R. (1985) Proc Natl Acad Sci. USA 82, 5375–5379

129 Calabretta, B, Kaczmarek, L., Mars, W, Ochoa, D, Gibson, C W., Hirschhorn, R R and Baserga, R (1985) Proc Natl. Acad Sci USA 82, 4463–4467

130 Parfett, C L.J., Hamilton, R.T., Howell, B W., Edwards, D R, Nilsen-Hamilton, M and Denhardt, D.T. (1985) Mol. Cell. Biol. 5, 3289–3292

131 Lau, L.F and Nathans, D (1985) EMBO J 4, 3145–3151

132 Forsdyke, D.R (1985) Biochem Biophys Res Commun 129, 619–625

133 Baserga, R (1984) Exp. Cell Res 151, 1–5

134 Liu, H.T, Baserga, R and Mercer, W E (1985) Mol Cell Biol. 5, 2936–2942

135 Edwards, D.R and Denhardt, D.T. (1985) Exp Cell Res 157, 127–143

136 Kramerov, D A, Lekakh, I V, Samarina, O.P and Ryskov, A P. (1982) Nucleic Acids Res 10, 7477–7491

137 Ryskov, A P, Ivanov, P L, Kramerov, D A and Georgiev, G.P (1983) Nucleic Acids Res. 11, 6541–6558

138 Kramerov, D.A., Tillib, S.V, Ryskov, A.P. and Georgiev, G.P (1985) Nucleic Acids Res 13, 6423–6437

139 Bennett, K L, Hill, R E., Pietras, D F, Woodworth-Gutai, M., Kane-Haas, C, Houston, J.M, Heath, J K. and Hastie, N D. (1984) Mol Cell. Biol 4, 1561–1571

140 Kramerov, D A, Tillib, S V, Lekakh, I V, Ryskov, A P and Georgiev, G P (1985) Biochim. Biophys Acta 824, 85–98

141 Singh, K, Carey, M., Saragosti, S and Botchan, M (1985) Nature (Lond) 314, 553–556

142 Murphy, D, Brickell, P M, Latchman, D S, Willison, K and Rigby, P W.J (1983) Cell 35, 865–871

143 Vasseur, M, Condamine, H and Duprey, P (1985) EMBO J 4, 1749–1753

144 Brickell, P M, Latchman, D.S., Murphy, D, Willison, K and Rigby, P W J (1983) Nature (Lond) 306, 756–760

145 Brickell, P M, Latchman, D S, Murphy, D, Willison, K and Rigby, P.W J. (1985) Nature (Lond) 316, 162–163

146 Arya, S K, Wong-Staal, F and Gallo, R C (1984) Mol Cell Biol 4, 2540–2542

147 Matrisian, L.M, Glaichenhaus, N., Gesnel, M-C and Breathnach, R. (1985) EMBO J. 4, 1435–1440

148 Matrisian, L M, Rautmann, G, Magun, B.E and Breathnach, R (1985) Nucleic Acids Res 13, 711–726

149 Johnson, L F., Abelson, H T, Green, H. and Penman, S (1974) Cell 1, 95–100

149a Robinson, J H (1985) Exp Cell Res. 161, 231–241

150 Hodgson, C P., Elder, P K, Ono, T., Foster, D.N. and Getz, M.J (1983) Mol. Cell. Biol 3, 2221–2231

151 Gin, C.P, Hodgson, C P, Elder, P K, Courtney, M.G and Getz, M.J. (1983) Nucleic Acids Res 11, 305–319

152 Courtney, M G, Schmidt, L J and Getz, M.J (1982) Cancer Res. 42, 569–576

153 Singh, K, Saragosti, S. and Botchan, M. (1985) Mol Cell Biol 5, 2590–2598

154 Augenlicht, L H and Halsey, H (1985) Proc Natl Acad Sci. USA 82, 1946–1949

155 Riddle, V G H and Pardee, A B (1980) J Cell Physiol 103, 11–15

156 McCairns, E., Fahey, D, Muscat, G E O, Murray, M and Rowe, P.B (1984) Mol. Cell. Biol 4, 1754–1760

157 Olashaw, N.E and Pledger, W J (1985) in Mediators in Cell Growth and Differentiation (Ford, R.J and Maizel, A.L., eds.), pp 31–44, Raven Press, New York

158 Scher, C.D, Dick, R.L., Whipple, A P. and Locatell, K L. (1983) Mol Cell. Biol 3, 70–81

159 Olashaw, N E and Pledger, W J (1983) Nature (Lond) 306, 272–274

160 Croy, R G. and Pardee, A B (1983) Proc Natl Acad Sci USA 80, 4699–4703

161 Campisi, J, Medrano, E.E, Morreo, G and Pardee, A.B (1982) Proc Natl Acad. Sci USA 79, 436–440

162 Lowe, D.G and Moran, L A (1984) Proc Natl Acad Sci. USA 81, 2317–2321

163 Mitchell, H K, Petersen, N S and Buzin, C H. (1985) Proc. Natl Acad. Sci. USA 82, 4969–4973

164 Kao, H-T., Capasso, O, Heintz, N. and Nevins, J R (1985) Mol Cell. Biol 5, 628–633

165 Schönfelder, M , Horsch, A and Schmid, H.-P. (1985) Proc Natl. Acad Sci USA 82, 6884–6888

166 Old, R.W. and Woodland, H R. (1984) Cell 38, 624–626

167 Pehrson, J R and Cole, R D (1982) Biochemistry 21, 456–460

168 Lennox, R.W. and Cohen, L H (1983) Biol. Chem 258, 262–268

169 Waithe, W.I., Renaud, J , Nadeau, P and Pallotta, D (1983) Biochemistry 22, 1778–1783

170 Bird, R C., Jacobs, F A., Stein, G., Stein, J and Sells, B H (1985) Proc Natl. Acad. Sci. USA 82, 6760–6764

171 Wu, R S., Tsai, S and Bonner, W M (1982) Cell 31, 367–374

172 Chabanas, A , Khoury, E , Goeltz, P., Froussard, P , Gjerset, R , Dod, B., Eisen, H and Lawrence, J J. (1985) J Mol. Biol. 183, 141–151

173 Brush, D., Dodgson, J.B , Choi, O -R., Stevens, P.W and Engel, J D (1985) Mol Cell. Biol. 5, 1307–1317

174 Wells, D and Kedes, J. (1985) Proc. Natl Acad Sci USA 82, 2834–2838

175 Carozzi, N , Marashi, F , Plumb, M , Zimmerman, S , Zimmerman, A , Coles, L S , Wells, J R E , Stein, G and Stein, J (1984) Science 224, 1115–1117

176 Graves, R.A., Wellman, S E , Chiu, I -M and Marzluff, W.F (1985) J. Mol Biol. 183, 179–194

177 Stein, G S , Stein, J L , Park, W D., Detke, S., Lichtler, A.C , Shephard, E A , Jansing, R L. and Phillips, I R (1978) Cold Spring Harbor Symp. Quant Biol 42, 1107–1120

178 Sierra, F., Stein, G and Stein, J (1983) Nucleic Acids Res 11, 7069–7086

179 Heintz, N , Zernik, M. and Roeder, R G (1981) Cell 24, 661–668

180 Plumb, M , Stein, J and Stein, G (1983) Nucleic Acids Res 11, 2391–2410

181 Hirschhorn, R.R , Marashi, F., Baserga, R , Stein, J and Stein, G (1984) Biochemistry 23, 3731–3735

182 Artishevsky, A , Delegeane, A.M and Lee, A S (1984) Mol Cell. Biol. 4, 2364–2369

182a Sheinin, R , Dubsky, M., Naismith, L and Sigouin, J (1985) Exp Cell Res 161, 393–405

182b Sheinin, R and Lewis, P N. (1980) Somatic Cell Gen 6, 225–239

183 DeLisle, A J , Graves, R A., Marzluff, W.F. and Johnson, L.F (1983) Mol Cell Biol 3, 1920–1929

184 Heintz, N , Sive, H.L and Roeder, R.G (1983) Mol. Cell Biol 3, 539–550

185 Chrysogelos, S., Riley, D.E , Stein, G and Stein, J (1985) Proc Natl Acad Sci USA 82, 7535–7539

186 Alterman, R.-B M., Ganguly, S , Schulze, D H , Marzluff, W F , Schildkraut, C.L and Skoultchi, A I. (1984) Mol Cell. Biol 4, 123–132

187 Stimac, E , Groppi, V E., Jr. and Coffino, P (1984) Mol Cell. Biol 4, 2082–2090

188 Baumbach, L L., Marashi, F., Plumb, M., Stein, G and Stein, J (1984) Biochemistry 23, 1618–1625

189 Plumb, M., Marashi, F., Green, L., Zimmerman, A., Zimmerman, S , Stein, J. and Stein, G. (1984) Proc. Natl Acad. Sci. USA 81, 434–438

190 Sive, H L , Heintz, N and Roeder, R G (1984) Mol. Cell Biol. 4, 2723–2734

191 Sittman, D B., Graves, R A and Marzluff, W F (1983) Proc Natl Acad Sci USA 80, 1849–1853

192 Graves, R A and Marzluff, W F. (1984) Mol Cell Biol. 4, 351–357

193 Downes, C S., Ord, M.J., Mullinger, A M , Collins, A R S and Johnson, R T (1985) Carcinogenesis 6, 1343–1352

194 Wu, R S and Bonner, W.M. (1985) Mol Cell. Biol 5, 2959–2966

195 Sariban, E , Wu, R S , Erickson, L C and Bonner, W M. (1985) Mol. Cell Biol. 5, 1279–1286

196 Stein, G S and Stein, J L (1984) Mol Cell. Biochem 64, 105–110

197 Green, L , Stein, G and Stein, J (1984) Mol Cell Biochem. 60, 123–130

198 Hereford, L , Bromley, S and Osley, M A. (1982) Cell 30, 305–310

199 Hanly, S M , Bleecker, G.C. and Heintz, N (1985) Mol Cell Biol. 5, 380–389

200 Capasso, O and Heintz, N. (1985) Proc Natl. Acad Sci. USA 82, 5622–5626

201 Artishevsky, A , Grafsky, A and Lee, A S (1985) Science 230, 1061–1063

202 Lüscher, B., Stauber, C , Schindler, R and Schümperli, D (1985) Proc Natl. Acad Sci. USA 82, 4389–4393

203 Georgiev, O and Birnstiel, M.L (1985) EMBO J 4, 481–489

204 Kit, S (1976) Mol. Cell Biochem 11, 161–182

205 Weber, G (1977) N Engl J. Med 296, 486–493

206 Eriksson, S , Gräslund, A , Skog, S , Thelander, L and Tribukait, B (1984) J Biol Chem. 259, 11695–11700

207 Johnson, L F (1984) in Recombinant DNA and Cell Proliferation (Stein, G S and Stein, J.L , eds), pp 25–47, Academic Press, New York

208 Pegg, A E. and McCann, P P (1982) Am J Physiol 243, 212–221

209 Weissbach, A. (1977) Annu. Rev Biochem 46, 25–47

210 Nakamura, H , Morita, T , Masaki, S and Yoshida, S (1984) Exp Cell Res 151, 123–133

211 Schneider, E , Müller, B. and Schindler, R (1985) Biochim Biophys Acta 825, 375–383

212 Söderhäll, S. (1976) Nature (Lond) 260, 640–642

213 Tricoli, J.V , Sahai, B M , McCormick, P.J , Jarlinksi, S J , Bertram, J S and Kowalski, D (1985) Exp Cell Res 158, 1–14

214 Szyf, M., Kaplan, F , Mann, V., Giloh, H , Kedar, E and Razin, A (1985) J Biol Chem 260, 8653–8656

215 Bestor, T H and Ingram, V M (1985) Proc Natl Acad. Sci USA 82, 2674–2678

216 Brent, T (1971) Cell Tissue Kinet. 4, 297–305

217 Rode, W , Scanlon, K J , Moroson, B A. and Bertino, J R (1980) J. Biol. Chem 255, 1305–1311

218 Mariani, B D , Slate, D L. and Schimke, R T (1981) Proc Natl Acad Sci USA 8, 4985–4989

219 Engström, Y., Eriksson, S , Jildevik, I , Skog, S , Thelander, L and Tribukait, B (1985) J Biol Chem 260, 9114–9116

220 Chang, A C Y., Nunberg, J H, Kaufman, R J, Erlich, H.A., Schimke, R T and Cohen, S N (1978) Nature (Lond) 275, 617–624

221 Wiedemann, L M and Johnson, L F (1979) Proc Natl Acad Sci. USA 76, 2818–2822

222 Kellems, R E, Alt, F W and Schimke, R T. (1976) J Biol Chem 251, 6987–6993

223 Kellems, R E, Morhenn, V B., Pfendt, E A, Alt, F W and Schimke, R.T (1979) J Biol Chem. 254, 309–318

224 Santiago, C., Collins, M and Johnson, L F (1984) J Cell Physiol 118, 79–86

225 Wu, J -S R and Johnson, L.F (1982) J Cell Physiol 110, 183–189

226 Pastan, I.H, Johnson, G S and Anderson, W B. (1975) Annu Rev Biochem 44, 491–522

227 Hendrickson, S.L., Wu, J -S R and Johnson, L F (1980) Proc Natl. Acad Sci USA 77, 5140–5144

228 Leys, E J., Crouse, G F and Kellems, R.E. (1984) J Cell Biol 99, 180–187

229 Collins, M.L, Wu, J -S R, Santiago, C.L., Hendrickson, S L and Johnson, L.F (1983) Mol Cell Biol 3, 1792–1802

230 Kaufman, R.J and Sharp, P A. (1983) Mol Cell Biol 3, 1598–1608

231 Setzer, D R., McGrogan, M, Nunberg, J H and Schimke, R.T (1980) Cell 22, 361–370

232 Crouse, G F, Simonsen, C C, McEwan, R N and Schimke, R T (1982) J Biol Chem. 257, 7887–7897

233 McGrogan, M, Simonsen, C C., Smouse, D.T, Farnham, P J and Schimke, R.T. (1985) J Biol Chem. 260, 2307–2314

234 Farnham, P.J and Schimke, R T (1985) J Biol Chem 260, 7675–7680

235 Breathnach, R and Chambon, P (1981) Annu Rev Biochem 50, 349–383

236 Banerji, J, Rusconi, S and Schaftner, W (1981) Cell 27, 299–308

237 Reynolds, G A., Basu, S K, Osborne, T F, Chin, D J, Gil, G, Brown, M S, Goldstein, J L and Luskey, K L (1984) Cell 38, 275–285

238 Ishii, S, Xu, Y -H., Stratton, R.H, Roe, B A, Merlino, G T and Pastan, I (1985) Proc Natl Acad. Sci USA 82, 4920–4924

239 Richard, R I, Heguy, A and Karin, M. (1984) Cell 37, 263–272

240 Melton, D.W, Konecki, D.S, Brennand, J. and Caskey, C T (1984) Proc Natl Acad Sci USA 81, 2147–2151

241 Gidoni, D, Dynan, W S and Tjian, R (1984) Nature (Lond) 312, 409–413

242 Dynan, W S and Tjian, R (1983) Cell 32, 669–680

243 Farnham, P J ; Abrams, J M and Schimke, R T (1985) Proc Natl. Acad Sci USA 82, 3978–3982

244 Crouse, G F, Leys, E J, McEwan, R N, Frayne, E G and Kellems, R E. (1985) Mol Cell Biol. 5, 1847–1858

245 Geyer, P K and Johnson, L.F (1984) J Biol Chem 259, 7206–7211

246 Jenh, C -H, Geyer, P K, Baskin, F and Johnson, L F (1985) Mol Pharm 28, 80–85

247 Jenh, C -H, Rao, L G and Johnson, L F (1985) J Cell Physiol. 122, 149–154

248 Jenh, C -H., Geyer, P K. and Johnson, L.F (1985) Mol. Cell Biol 5, 2527–2532

249 Storms, R K, Ord, R W, Greenwood, M T, Mirdamadi, B., Chu, F K. and Belfort, M (1984) Mol. Cell Biol 4, 2858–2864

250 Schlosser, C A., Steglich, C, DeWet, J R. and Scheffler, I E (1981) Proc Natl Acad Sci. USA 78, 1119–1123

251 Lewis, J.A, Shimizu, K and Zipser, D. (1983) Mol Cell Biol 3, 1815–1823

252 Merrill, G.F., Harland, R M, Groudine, M and McKnight, S L. (1984) Mol Cell Biol 4, 1769–1776

253 Stuart, P, Ito, M, Stewart, C and Conrad, S.E (1985) Mol Cell Biol 5, 1490–1497

254 Lin, P -F, Lieberman, H B., Yeh, D -B, Xu, T., Zhao, S.-Y and Ruddle, F H (1985) Mol Cell Biol 5, 3149–3156

255 Merrill, G.F., Hauschka, S D and McKnight, S L. (1984) Mol. Cell Biol. 4, 1777–1784

256 Groudine, M and Casimir, C (1984) Nucleic Acids Res. 12, 1427–1446

257 Bradshaw, H.D., Jr (1983) Proc Natl Acad Sci. USA 80, 5588–5591

258 Coppock, D L and Pardee, A B (1985) J. Cell. Physiol 124, 269–274

259 Cheetham, B F. (1983) Mol Cell. Biol 3, 480–483

260 McConlogue, L, Gupta, M., Wu, L. and Coffino, P (1984) Proc Natl Acad. Sci. USA 81, 540–544

261 Berger, F G, Szymanski, P, Read, E and Watson, G (1984) J. Biol Chem. 259, 7941–7946

262 Kontula, K K, Torkkeli, T K, Bardin, C.W and Janne, O A (1984) Proc. Natl. Acad Sci USA 81, 731–735

263 Kahana, C and Nathans, D (1984) Proc Natl Acad Sci USA 81, 3645–3649

263a Hölttä, E and Hovi, T (1985) Eur J Biochem. 152, 229–237

263b Gilmour, S K, Avdalovic, N, Madara, T and O'Brien, T G (1985) J Biol Chem. 260, 16439–16444

264 Rinehart, C.A, Jr and Canellakis, E S (1985) Proc Natl Acad. Sci. USA 82, 4365–4368

265 Erwin, B.G, Seely, J.E and Pegg, A E (1983) Biochemistry 22, 3027–3032

266 Kameji, T, Fujita, K, Noguchi, T., Takiguchi, M, Mori, M, Tatibana, M and Hayashi, S (1984) Eur J Biochem 144, 35–39

267 Feinstein, S C, Dana, S.L, McConlogue, L., Shooter, E M and Coffino, P (1985) Proc Natl Acad. Sci USA 82, 5761–5765

268 Landy-Otsuka, F and Scheffler, I.E (1980) J Cell Physiol. 105, 209–220

269 Cress, A.E. and Gerner, E W (1979) Biochem Biophys Res Commun. 87, 773–780

270 Kahana, C. and Nathans, D (1985) Proc Natl Acad Sci USA 82, 1673–1677

271 Gupta, M. and Coffino, P (1985) J Biol. Chem 260, 2941–2944

272 Celis, J E, Bravo, R, Larsen, P.M and Fey, S J (1984) Leukemia Res 8, 143–157

273 Tan, E M. (1982) Adv Immunol 33, 167–240

274 Mathews, M B, Bernstein, R M, Franza, B.R, Jr and Garrels, J I (1984) Nature (Lond) 309, 374–376

275 Miyachi, K., Fritzler, M J and Tan, E M (1978) J Immunol 121, 2228–2234

276 Takasaki, Y, Deng, J-S and Tan, E M (1981) J Exp Med 1899–1909

277 Bravo, R and Celis, J.E (1980) Exp Cell Res 127, 249–260

278 Bravo, R. and Celis, J E (1982) Clin Chem. 28, 949–954

279 Barque, J.P, Danon, F., Peraudeau, L, Yeni, P and Larsen, C J (1983) EMBO J. 2, 743–749

280 Celis, J.E, Fey, S J., Larsen, P.M. and Celis, A (1984) Proc. Natl. Acad. Sci USA 81, 3128–3132

281 Bravo, R. and Graf, T. (1985) Exp Cell Res 156, 450–454

282 Bravo, R and Macdonald-Bravo, H. (1984) EMBO J 3, 3177–3181

283 Macdonald-Bravo, H. and Bravo, R. (1985) Exp. Cell Res. 156, 455–461

284 Bravo, R. and Macdonald-Bravo, H (1985) EMBO J. 4, 655–661

285 Celis, J E. and Celis, A. (1985) Proc. Natl Acad. Sci USA 82, 3262–3266

286 Yanishevsky, R.M. and Prescott, D M (1978) Proc Natl. Acad Sci USA 75, 3307–3311

287 Murdock, G.H, Waterman, M., Evans, R.M. and Rosenfeld, M G. (1985) J Biol. Chem. 260, 11852–11858

288 Gottesman, M M, (1978) Proc Natl. Acad Sci USA 75, 2767–2771

289 Gottesman, M.M and Yuspa, S (1981) Carcinogenesis 2, 971–976

290 Sahagian, G.G. and Gottesman, M M. (1982) J Biol Chem. 257, 11145–11150

291 Gottesman, M.M and Sobel, M.E. (1980) Cell 19, 449–455

292 Doherty, P J., Hua, L, Liau, G., Gal, S, Graham, D E, Sobel, M. and Gottesman, M M (1985) Mol. Cell Biol 5, 466–473

293 Frick, K K, Doherty, P.J., Gottesman, M.M. and Scher, C D. (1985) Mol Cell Biol. 5, 2582–2589

294 Gal, S, Willingham, M.C. and Gottesman, M.M. (1985) J Cell Biol. 100, 535–544

295 Gal, S and Gottesman, M M (1986) J. Biol. Chem, in the press

296 Jetten, A M and DeLuca, L.M. (1985) Carcinogenesis 6, 337–342

297 Denhardt, D T., Hamilton, R T, Parfett, C L.J, Edwards, D.R., St. Pierre, R., Waterhouse, P and Nilsen-Hamilton, M (1986) Cancer Res., in the press

298 Linzer, D I H, Lee, S.-J., Ogren, L, Talamantes, F and Nathans, D (1985) Proc Natl. Acad. Sci USA 82, 4356–4359

300 Nilsen-Hamilton, M, Hamilton, R T, Allen, W.R. and Massoglia, S L (1981) Biochem Biophys Res Commun 101, 411–417

301 Davies, R L, Rifkin, D.B., Tepper, R, Miller, A and Kucherlapati, R. (1983) Science 221, 171–173

302 Gross, J.L, Krupp, M N, Rifkin, D.B and Lane, M.D (1983) Proc. Natl Acad. Sci USA 80, 2276–2280

303 Eaton, D.L and Baker, J B (1983) J. Cell Biol 97, 323–328

304 Ben-Ishai, R, Sharon, R., Rothman, M and Miskin, R (1984) Carcinogenesis 5, 357–362

305 Opdenakker, G., Ashino-Fuse, H, Van Damme, J, Billiau, A and De Somer, P (1983) Eur J. Biochem. 131, 481–487

306 Belin, D., Godeau, F. and Vassalli, J-D. (1984) EMBO J 3, 1901–1906

307 Ferraiuolo, R, Stoppelli, M P, Verde, P., Bullock, S, Lazzaro, P, Blasi, F. and Pietropaolo, T C (1984) J Cell Physiol 121, 368–374

308 Waller, E K and Schleuning, W.-D (1985) J Biol Chem 260, 6354–6360

309 Nagamine, Y, Sudol, M and Reich, E (1983) Cell 32, 1181–1190

310 Crutchley, D.J and Maynard, J R (1983) Biochim Biophys Acta 762, 76–85

311 Arya, S.K and Gallo, R.C (1984) Biochemistry 23, 6685–6690

312 Efrat, S, Zelig, S, Yagen, B. and Kaempfer, R. (1984) Biochem Biophys Res Commun 123, 842–848

313 Elliott, J.F., Lin, Y, Mizel, S.B, Bleackley, R C, Harnish, D G. and Paetkau, V (1984) Science 226, 1439–1441

314 Paetkau, V (1985) Can. J Biochem Cell Biol. 63, 691–699

315 Parker, I and Fitschen, W (1980) Nucleic Acids Res 8, 2823–2833

316 LaBella, F, Brown, E.H. and Basilico, C (1983) J Cell Physiol. 117, 62–68

317 Sobel, M E, Dion, L D, Vuust, J. and Colburn, N H (1983) Mol. Cell Biol. 3, 1527–1532

318 Bauer, E A, Cooper, T W, Huang, J.S., Altman, J and Deuel, T.F. (1985) Proc Natl Acad Sci USA 82, 4132–4136

319 Lengyel, P (1982) Annu Rev. Biochem 51, 251–282

320 Goodbourn, S., Zinn, K. and Maniatis, T (1985) Cell 41, 509–520

321 Higashi, Y (1985) Nucleic Acids Res 13, 5157–5172

322 Colonno, R.J and Pang, H L (1982) J Biol Chem 257, 9234–9237

323 Larner, A C, Jonak, G., Cheng, Y-S E, Korant, B, Knight, E and Darnell, J.E, Jr. (1984) Proc. Natl Acad Sci USA 81, 6733–6737

324 Friedman, R L., Manly, S.P., McMahon, M, Kerr, I.M and Stark, G R. (1984) Cell 38, 745–755

325 Cheng, Y-S.E, Colonno, R.J and Yin, F.H (1983) J Biol. Chem. 258, 7746–7750

326 Friedman, R.L and Stark, G.R (1985) Nature (Lond) 314, 637–639

327 Tominaga, S, Tominaga, K. and Lengyel, P. (1985) J Biol. Chem 260, 16406–16410

328 Gewert, D.R., Moore, G. and Clemens, M.J (1983) Biochem. J 214, 983–990

329 Clemens, M.J, McNurlan, M.A., Moore, G. and Tilleray, V J. (1984) FEBS Lett 171, 111–116

330 Knight, E., Jr, Anton, E.D., Fahey, D, Friedland, B K and Jonak, G J (1985) Proc Natl. Acad Sci USA 82, 1151–1154

331 Du P Heyns, A, Eldor, A, Vlodavsky, I., Kaiser, N., Fridman, R. and Panet, A (1985) Exp Cell Res 161, 297–306

332 Muscat, G.E O, Caputo, A, McCairns, E. and Rowe, P B (1985) DNA 4, 377–384

333 Chang, N.T , Tam, S H., Kung, P C and Chang, T W (1984) Mol. Biol. Med 2, 151–165

334 Wissinger, W L and Wang, R J (1983) Int Rev Cytol Suppl 15, 91–116

335 Marcus, M , Fainsod, A and Diamond, G (1985) Annu Rev. Genet 19, 389–421

336 Matsumoto, Y , Yasuda, H , Marunouchi, T and Yamada, M (1983) FEBS Lett 151, 139–142

337 Finley, D., Ciechanover, A. and Varshavsky, A (1984) Cell 37, 43–55

338 Ciechanover, A., Finley, D and Varshavsky, A (1984) Cell 37, 57–66

339 Colwill, R.W and Sheinin, R (1983) Proc Natl Acad Sci. USA 80, 4644–4648

340 Rossini, M , Baserga, S , Huang, C H , Ingles, C J and Baserga, R. (1980) J Cell Physiol 103, 97–103

341 Shales, M , Bergsagel, J. and Ingles, C J. (1980) J Cell Physiol 105, 527–532

342 Waechter, D.E., Avignolo, C , Freund, E , Riggenbach, C M , Mercer, W E , McGuire, P M. and Baserga, R (1984) Mol Cell Biochem. 60, 77–82

343 Murakami, Y , Yasuda, H , Miyazawa, H , Hanaoka, F and Yamada, M. (1985) Proc Natl Acad Sci USA 82, 1761–1765

344 Ayusawa, D , Kimiko, I and Seno, T (1980) Biochem. Biophys Res. Commun 96, 1654–1661

345 Hyodo, M. and Suzuki, K (1982) Exp Cell Res 137, 31–38

346 Tsai, Y , Hanaoka, F , Nakano, M.M. and Yamada, M. (1979) Biochem Biophys Res Commun 91, 1190–1195

347 Eilen, E , Hand, R and Basilico, C (1980) J. Cell Physiol. 105, 259–266

348 McCracken, A.A. (1982) Som. Cell Gen 8, 179–195

349 Nishimoto, T., Ishida, R , Ajiro, K , Yamamoto, S and Takahashi, T (1981) J Cell. Physiol 109, 299–308

350 Yamashita, K , Nishimoto, T and Sekiguchi, M. (1984) J Biol Chem 259, 4667–4671

351 Chen, D.J and Wang, R.J. (1984) Exp Cell Res 155, 549–556

352 Naha, P.M (1981) Cell Biol Int. Rep 5, 981–986

353 Fainsod, A , Marcus, M., Lin, P and Ruddle, F H (1984) Proc. Natl. Acad Sci. USA 81, 2393–2395

354 Liu, H T., Gibson, C W , Hirschhorn, R R , Rittling, S , Baserga, R. and Mercer, W.E (1985) J Biol Chem 260, 3269–3274

355 Pardee, A B , Campisi, J., Gray, H E , Dean, M and Sonenshein, G. (1985) Med. in Cell Growth and Differentiation (Ford, R J and Maizel, A L , eds), pp 21–29, Raven Press, New York

356 Elder, P.K., Schmidt, L J , Ono, T and Getz, M J. (1984) Proc Natl Acad. Sci USA 81, 7476–7480

357 Rittling, S R , Gibson, C W., Ferrari, S. and Baserga, R (1985) Biochem Biophys. Res Commun 132, 327–335

358 Meister, R.K., Hulman, S E and Johnson, L F (1979) J Cell Physiol 100, 531–538

358a Hamilton, R T , Nilsen-Hamilton, M and Adams, G (1985) J Cell Physiol 12, 201–208

358b Content, J , De Wit, L , Pierard, D , Derynck, R , De Clercq, E. and Fiers, W (1982) Proc Natl. Acad Sci USA 79, 2768–2772

359 Pledger, W J., Stiles, C D , Antoniades, H.N. and Scher, C.D (1978) Proc. Natl Acad Sci USA 75, 2839–2843

360 Melchers, F. and Lernhardt, W. (1985) Proc. Natl Acad Sci USA 82, 7681–7685

361 Bockus, B J. and Stiles, C D (1984) Exp Cell Res 153, 186–197

362 Ralston, R. and Bishop, J M (1985) Proc Natl Acad Sci USA 82, 7845–7849

363 Smith, J C. and Stiles, C.D (1981) Proc Natl Acad Sci USA 78, 4363–4367

364 Bravo, R., Burckhardt, J and Müller, R (1985) Exp Cell Res. 160, 540–543

365 Scher, C.D., Stone, M E and Stiles, C D (1979) Nature 281, 390–392

366 Campisi, J and Pardee, A B (1984) Mol Cell. Biol 4, 1807–1814

367 Leof, E B , Wharton, W , Van Wyk, J J. and Pledger, W.J (1982) Exp Cell Res 141, 107–115

368 Tushinski, R J. and Warner, J R. (1982) J Cell Physiol 112, 128–135

369 Seuwen, K , Steiner, U and Adam, G (1984) Exp Cell Res 154, 10–24

370 Shipley, R.D. and Ham, R G. (1983) Exp Cell Res 146, 261–270

371 O'Keefe, E J. and Pledger, W.J (1983) Mol Cell Endocrinol 31, 167–186

371a Rozengurt, E (1985) in Molecular Mechanisms of Transmembrane Signalling (Cohen, P and Houslay, M., eds.), pp. 429–452, Elsevier Science Publishers, Amsterdam

372 Cantrell, D A and Smith, K A (1984) Science 224, 1312–1316

373 Reed, J C , Sabath, D E , Hoover, R.G and Prystowsky, M.B (1985) Mol. Cell. Biol. 5, 3361–3368

374 Wharton, W., Van Wyk, J.J and Pledger, W.J (1981) J Cell Physiol. 107, 31–39

375 Veigl, M L., Vanaman, T C and Sedwick, W D. (1984) Biochim. Biophys Acta 738, 21–48

376 Tupper, J.T., Kaufman, L. and Bodine, P V (1980) J. Cell Physiol 104, 97–103

377 Sasaki, Y and Hidaka, H (1982) Biochem Biophys Res Commun. 104, 451–456

378 Chafouleas, J.G , Lagace, L , Bolton, W E , Boyd, A E , III and Means, A.R (1984) Cell 36, 73–81

379 Moolenaar, W H , Tertoolen, L.G J and de Laat, S W (1984) J Biol Chem 259, 8066–8069

380 Frantz, C.N (1985) Exp. Cell Res 158, 287–300

381 Wu, F S , Park, Y -C , Roufa, D and Martonosi, A (1981) J Biol Chem 256, 5309–5312

382 Welch, W.J , Garrels, J I , Thomas, G P , Lin, J J -C and Feramisco, J R (1983) J Biol Chem 258, 7102–7111

383 Resendez, E , Jr., Attenello, J W , Grafsky, A , Chang, C S and Lee, A.S (1985) Mol. Cell Biol 5, 1212–1219

384 Lee, A.S , Delegeane, A.M , Baker, V and Chow, P C (1983) J Biol Chem 258, 597–603

385 Zamecnik, P (1983) Anal Biochem 134, 1–10

386 Weinmann-Dorsch, C., Hedl, A , Grummt, I , Albert, W., Ferdinand, F -J., Friis, R R , Pierron, G , Moll, W and Grummt, F (1984) Eur J Biochem. 138, 179–185

387 Huneeus, V Q , Wiley, M H and Siperstein, M D. (1980) Proc. Natl Acad. Sci USA 77, 5842–5846

388 Habenicht, A J.R , Glomset, J.A and Ross, R. (1980) J. Biol. Chem 255, 5134–5140

389 Quesney-Huneeus, V., Galick, H A , Siperstein, M.D., Erickson, S.K., Spencer, T A and Nelson, J.A (1983) J Biol. Chem. 258, 378–385

390 Fairbanks, K.P , Witte, L.D. and Goodman, D.S. (1984) J Biol Chem 259, 1546–1551

391 Sinensky, M. and Logel, J. (1985) Proc Natl Acad. Sci. USA 82, 3257–3261

392 Schmidt, R.A , Schneider, C J and Glomset, J A (1984) J Biol Chem. 259, 10175–10180

393 Ruley, H E. (1983) Nature (Lond) 304, 602–606

394 Nevins, J R (1982) Cell 29, 913–919

395 Kingston, R.E , Baldwin, A.S , Jr. and Sharp, P.A. (1984) Nature (Lond) 312, 280–282

396 Zullo, J N , Cochran, B H , Huang, A.S. and Stiles, C.D (1985) Cell 43, 793–800

397 Wells, V and Mallucci, L. (1985) Exp Cell Res. 159, 27–36

398 Einat, M , Resnitzky, D. and Kimchi, A (1985) Proc Natl. Acad. Sci USA 82, 7608–7612

399 Tominaga, S and Lengyel, P. (1985) J Biol Chem 260, 1975–1978

400 Nir, U., Maroteaux, L , Cohen, B and Mory, I (1985) J Biol. Chem 260, 14242–14247

401 Heil, M.F , Wu, J M and Chiao, J.W. (1985) Biochim Biophys. Acta 845, 17–20

402 Lin, S L , Ts'o, P O P. and Hollenberg, M.D (1983) Life Sci 32, 1479–1488

403 Baglioni, C , Minks, M.A and Maroney, P.A. (1978) Nature (Lond) 273, 684–687

404 Hovanessian, A.G. and Wood, J.N (1980) Virology 101, 81–90

405 Tucker, R W , Pardee, A.B. and Fujiwara, K. (1979) Cell 17, 527–535

405a Kuchino, Y , Nemoto, K., Sadaaki, S. and Nichimura, S (1985) Jpn. J Cancer Res. 76, 75–78

406 Jenuwein, T., Müller, D., Curran, T and Müller, R. (1985) Cell 41, 629–637

407 Stanbridge, E.J., Der, C.J , Doersen, C.-J., Nishimi, R Y , Peehl, D.M , Weissman, B E and Wilkinson, J.E (1982) Science 215, 252–259

408 Crowley, T.E., Nellen, W., Gomer, R H and Firtel, R.A (1985) Cell 43, 633–641

409 Izant, J G and Weintraub, H (1985) Science 229, 345–352

410 Kim, S K. and Wold, B J. (1985) Cell 42, 129–138

411 Crouse, G F , McEwan, R N and Pearson, M L. (1983) Mol Cell Biol 3, 257–266

412 Kaufman, R.J , Wasley, L C , Spiliotes, A J , Gossels, S D., Latt, S.A., Larsen, G R and Kay, R M (1985) Mol Cell Biol 5, 1750–1759

Biochimica et Biophysica Acta 865 (1986) 127–139
Elsevier

BBA 87159

Idiotypic interactions in immune responses to tumor-associated antigens

Victor K. Lee [a,c], Karl Erik Hellström [a,c] and Gerald T. Nepom [b,c,*]

[a] Oncogen, [b] Genetic Systems Corporation, and [c] Department of Pathology, School of Medicine, University of Washington, Seattle, WA (U.S.A.)

(Received 27 February 1986)

Contents

I. Introduction . . . 127
II. Idiotype–anti-idiotype interactions . . . 128
III. Anti-idiotypic antibodies as internal images of antigens . . . 129
IV. Idiotypic interactions in tumor immunity . . . 130
V. A murine tumor model to evaluate immunity to tumor-associated differentiation antigens . . . 131
VI Generation of anti-6 10 antibodies (Ab2) . . . 132
VII. Testing for the presence of the 6 10 Id in the sera of bladder-tumor-bearing mice . . . 133
VIII Detection of antibody response in mice injected with Ab2 . . . 133
IX. Does selection of 'silent clones' fail in anti-Id immunization to tumor-associated forbidden specificities? . . . 135
X. Conclusions . . . 137
Acknowledgements . . . 137
References . . . 137

I. Introduction

The existence of tumor-specific transplantation antigens was demonstrated more than 30 years ago in experimentally-induced animal tumors [1–4]. During the subsequent years, evidence has accumulated suggesting that human neoplasms also express tumor antigens, since cancer patients sometimes mount immunological responses to their autologous tumors [5,6]. However, the molecular nature and tissue distribution of the target anti-

---

[*] Present address: Virginia Mason Research Center, 1000 Seneca St, Seattle, WA 98101, U.S.A.

Abbreviations: MAb, monoclonal antibodies, TAA, tumor-associated antigens, Id, idiotype; anti-Id, anti-idiotypic antibodies, Ig, immunoglobulin; DTH, delayed-type hypersensitivity; Ts, suppressor T cells; KLH, keyhole limpet hemocyanin; CRI, cross-reactive idiotype, TMV, tobacco mosaic virus; SV40, simian virus 40; HRP, horseradish peroxidase; LAI, leukocyte adherence inhibition BTCC, bladder transitional cell carcinoma; MCA, 3-methylcholanthrene

Correspondence address: Dr V.K. Lee, ONCOGEN, 3005 First Avenue, Seattle, WA 98121, USA

0304-419X/86/$03.50 © 1986 Elsevier Science Publishers B V (Biomedical Division)

gens remained elusive. As the result of the introduction of the hybridoma technology about a decade ago [7], monoclonal antibodies (MAb), mostly of mouse origin, have been made to many types of human cancer [8–10]. Detailed characterization of several of the corresponding tumor markers has been reported [11]. From these analyses, it has become clear that most (and perhaps all) of the markers defined by xenogeneic MAb are not strictly tumor-specific but are differentiation antigens shared by tumors and certain normal and/or fetal tissues. Therefore, they are best referred to as tumor-associated antigens (TAA). Whether human tumor markers detected by xenogeneic responses are capable of evoking an antitumor response in cancer patients, and whether such antigens are indeed related to the response to autologous tumors in cancer patients, remain important questions. Antigens which are either naturally immunogenic in the syngeneic host or can be made immunogenic might potentially be used to induce antitumor immunity for therapeutic and possibly prophylactic benefits.

One approach towards manipulating the immune system is based on idiotypic interactions [12]. This approach has made it possible to direct immune responses toward a predetermined goal, e.g., the protection of animals from lethal viral infections using 'vaccines' in the form of anti-idiotypic antibodies (anti-Id) [13]. In addition, anti-Id can also be used to activate normally silent lymphocyte clones [12]. In this review, we shall address the idiotypic network in relation to tumor immunity emphasizing idiotypic manipulation of immune responses to TAA. We shall begin by reviewing reports from others dealing with this area. This is followed by a presentation and discussion of recent findings from our analysis of specific immune responses to a defined TAA expressed by murine bladder carcinomas; these tumors are useful 'models' for human cancer, since they express differentiation antigens whose degree of tumor specificity is similar to that of most TAA detected in human neoplasms.

II. Idiotype–anti-idiotype interactions

The description of immunoglobulin (Ig) idiotypes has not only contributed knowledge about the heterogeneity of antibody structure, but has also paved the way for new insights into the mechanisms of immune regulation [14,15]. The unique antigenic determinants in and around the antigen-combining site of an Ig molecule which make one antibody distinct from another are defined as idiotopes. The totality of all idiotopes present on the variable portion of a given antibody is referred to as its idiotype (Id). The molecular structure of an Id has been localized to both the complementarity determining regions and the framework regions of the variable domain and is generally but not always contributed to by both the heavy and the light chains in specific association [16]. Several recent studies have attempted to define specific Id through the use of synthetic peptides based on the sequences of the V and J regions of the Ig molecule [17,18].

Idiotypes are serologically defined entities since injection of an antibody (often referred to as Ab1) into a syngeneic, allogeneic, or xenogeneic recipient induces the production of anti-idiotypic antibodies (often referred to as Ab2). When the binding between Ab1 and Ab2 is inhibited by the antigen to which Ab1 is directed, the Id is considered to be binding-site-related, since it may involve a site on the antibody variable domain that is engaged in antigen recognition. There are other interactions that cannot be inhibited by antigen. These may involve idiotopes spatially distinct from the binding site such as those in the framework regions.

Based on the assumption that idiotype–anti-idiotype (Ab1–Ab2) interactions exist physiologically, a receptor-based regulation of the immune system can be envisaged. Niels Jerne [19] postulated such a network theory which views the immune system as a collection of Ig molecules and receptors on T lymphocytes, each capable of recognizing an antigenic determinant (epitope) through its combining site (paratope), and each capable of being recognized by other antibodies or cell-surface receptors of the system through the idiotopes that it displays. A large body of recent studies has indeed demonstrated that Id and anti-Id receptors are present on the surface of both B and T lymphocytes as well as on secreted antibodies [16]. The level of a certain Id is up-regulated by the introduction of the appropriate antigen, and the increased synthesis of the antibody carrying that Id triggers the production of the corresponding anti-Id antibody, and so on.

For the proposed mechanism to satisfactorily explain the regulation of antibody synthesis, at least two requirements should be fulfilled. First, an anti-Id response (Ab2) should follow the formation of antibodies (Abl) to an antigen. Evidence for such Ab2 upon antigen administration was first observed in BALB/c mice hyperimmunized with *Streptococcus pneumoniae* [20]. Antibodies directed against phosphocholine on the *Streptococcus* were found in mice exposed to the bacteria and they expressed a common Id called T15. The titer of antibodies with the T15 Id peaked on day 5 after immunization with *S. pneumoniae,* and auto-antibodies to that Id appeared 3 days later [21]. Second, the introduction of anti-Id antibodies (Ab2) into an animal should influence the course of the relevant immune response. This has been verified in a variety of systems where the in vivo administration of syngeneic, allogeneic and xenogeneic anti-Id antibodies in monoclonal or polyclonal form in the absence of antigen was able to alter the subsequent immune response [16]. For example, in the response of mice to a hapten, nitrophenyl, injection of nanogram doses of a monoclonal antibody specific for a given idiotope enhanced the subsequent expression of this idiotope upon challenge with nitrophenyl, while microgram doses of the same MAb suppressed it [22]. Furthermore, anti-Id can be used to both activate and suppress antibody-producing B cells as well as to induce different T-cell-mediated functions, including help, suppression, cytotoxicity and delayed-type hypersensitivity (DTH) [23–26]. Whether a particular Ab2 will enhance or suppress the immune response appears to depend on its dose, the timing and the route of injection as well as on the nature of the relevant antigen and the particular Id. An early observation suggesting that the isotype of the Ab2 played a contributing role has been questioned as a result of more recent, well-controlled experiments [27,28].

Suppressor T cells (Ts) play an important role in regulating immune responses [29]. In several systems, subsets of Ts appear to interact with each other through idiotypic and anti-idiotypic receptors [30,31]. For example, adoptively transferred Ts (Id^+) can suppress a DTH response to the arsonate hapten by recruiting a population of anti-Id Ts effector cells, and the transfer of anti-Id Ts abrogates antiarsonate responses. Two separate studies have shown that such idiotypic interactions between Ts can occur in the absence of idiotypic responses involving Ig molecules [32,33].

III. Anti-idiotypic antibodies as internal images of antigens

A central question in immunology is the mechanism by which the diversity of antibody specificity is generated. The immune system is apparently capable of responding to antigenic agents that do not even exist naturally. The network hypothesis provides an answer to this question by postulating that each paratope in the immune system recognizes one or a few idiotopes that cross-react with epitopes of 'conventional' exogenous antigens. That is, the antigenic universe of various molecular conformations is reflected within the immune system by the millions of idiotopes expressed by Ig molecules and at lymphocyte surfaces. Those idiotopes which conformationally mimic an antigenic epitope are sometimes called the internal image of that epitope [34,35]. Since both an Ab2 and an antigen bind to the relevant Id^+ Abl, they may share a similar three-dimensional conformation which represents the internal image. Early experimental evidence of this phenomenon came from studies of insulin by Sege and Peterson [36]. These investigators prepared an antiserum containing Ab2 to antibodies specific for bovine insulin and found that this antiserum had the same biological effect as the insulin molecule by triggering the insulin receptor [36]. Another example came from work on reovirus infection in mice [37]. A syngeneic monoclonal Ab2 was raised against a binding site-related determinant of an Abl specific for reovirus type 3 hemagglutinin [38].The Ab2 bound to different cell lines with a degree of reactivity that closely paralleled their ability to bind reovirus type 3 [39]. It also competed with the virus for binding to viral receptors on neuronal cells, and it induced DTH reactions to reovirus type 3 [40]. Furthermore, hybridomas producing the anti-Id antibody could be lysed by T cell clones generated to the virus [41]. Hence, an antibody molecule which was selected from a diverse repertoire could mimic a viral determinant conformationally as an internal image.

The practical implications of these studies for vaccine production are obvious, especially in situations where purified antigen is difficult to obtain or where the antigen is poorly immunogenic in its native form [42]. For example, specific protective immunity could be successfully induced by Ab2 in experimental African trypanosomiasis [43]. Monoclonal Ab1 against three distinct surface glycoproteins of a clone of *Trypanosoma rhodsiense* were chosen as the source of Id, based on the ability of the injected MAb to protect mice from trypanosome infection. Allogeneic anti-Id sera were made to the Id of each of three Ab1, and the IgG1 fractions were purified. Inoculation of mice with an Ab2 serum prior to challenge with the parasite protected them against infection.

Subsequent studies have shown that injection of Ab2 into animals that have never 'seen' an epitope associated with an infectious agent can induce neutralizing antibodies to that antigen. In some cases, specific protection has been demonstrated against challenge with live bacteria, viruses and parasites [44–49]. Monoclonal Ab2 rather than those of polyclonal origin can be used as well. For example, a monoclonal Ab2 was made against the T-15 idiotype, conjugated to keyhole limpet hemocyanin (KLH), and used to immunize BALB/c mice, which subsequently produced Ab1-like antibodies to phosphocholine [45]. When the mice were challenged with a lethal dose of *S. pneumoniae*, they were protected.

In the trypanosomiasis study referred to above, priming with Ab2 gave protective immunity only when certain allotype-linked genes were present in the immunized host [50]. Such genetic restriction is likely to limit the use of an Ab2 in the manipulation of immune responses in outbred populations. However, encouraging results have been reported in that it is possible to use allogeneic and even xenogeneic Ab2 for activating lymphocyte clones which express Id that are not normally detected [51–57]. For example, A/J mice exposed to the hapten arsonate mount an Ab1 response with a cross-reactive Id (CRI) that is not detected in BALB/c mice challenged with the same antigen [58]. Although molecular studies indicated that the genes which encode the CRI in strain A/J are absent from the genome of strain BALB/c, Moser et al. [56] could use anti-Id antibodies against the CRI of A/J mice to induce the same CRI in BALB/c. Francotte et al. [57] extended this observation by demonstrating the activation of silent clones even across species barriers. Antibodies (Ab1) were prepared in rabbits to tobacco mosaic virus (TMV) protein and were used to raise Ab2, also in rabbits. The Ab2 appeared to be directed against a private Id that was not detected on other rabbit antibodies against TMV. The Ab2 was injected into BALB/c mice whose lymphocytes were immortalized by fusion to make MAb. MAb were identified with both the private rabbit Id and the ability to bind to TMV. It is noteworthy that in this situation, an internal image anti-Id was not required for the induction of Ab1-like Ab3.

IV. Idiotypic interactions in tumor immunity

The idiotype regulatory network could conceivably play key roles in regulating immune responses to tumor antigens and this may have many clinical implications. For example, Ab2 might be used diagnostically to detect and monitor antitumor immune responses, as well as therapeutically, and possibly even prophylactically, to induce (or up-regulate) host reactivity to tumors.

In spite of the importance of the problem, the number of published studies in this area is small. Flood et al. [59] induced an immune response to the idiotypes of T lymphocytes generated against a highly immunogenic ultraviolet-induced fibrosarcoma. This led to the suppression of a strong immune response to this specific tumor and permitted the growth of tumor cells in vivo, while an unrelated fibrosarcoma was consistently rejected by similarly treated animals. Furthermore, it was demonstrated that animals developing anti-Id immunity possessed cytolytic T cells capable of lysing tumor specific lymphocytes. Tilkin et al. [60] performed a similar experiment by raising an anti-Id response to suppressor T cells, and they observed inhibition of tumor growth in vivo. Binz et al. [61] showed that anti-Id antibodies could prime for a cytotoxic T cell response against a rat tumor in vitro. However, when rats treated with Ab2 were challenged with a tumor transplant in vivo, tumor growth was enhanced, and this was attributed to the ablation of Id^+ effector cells.

Forstrom et al. [62] hyperimmunized BALB/c mice with cells from a transplanted methylcholanthrene-induced sarcoma and prepared polyclonal antiserum and a MAb from these mice. Both the antiserum and the MAb could prime BALB/c mice for DTH reactions to the sarcoma. The DTH could be transferred by Thy 1^+, Lyt 1^+ lymphocytes to naive mice and was specific for the immunizing tumor as compared to other BALB/c sarcomas. The MAb did not bind to tumor cells, and it could be used to isolate Thy 1^+, Lyt 1^+ cells responsible for DTH to the sarcoma (Nelson et al., unpublished findings). Priming of DTH with the antibody was restricted by allotype-linked genes [62].

Nepom et al. [63] prepared a rabbit anti-Id antiserum (Ab2) against a monoclonal mouse antibody, 8.2 (Ab1), which defined a human melanoma-associated antigen, p97, and showed that the binding between Ab1 and Ab2 could be inhibited by melanoma lysate containing p97. The rabbit antiserum induced specific DTH to human melanoma cells in mice, as well as humoral antibodies which immunoprecipitated the p97 antigen. The authors suggested that a similar approach may be used to induce an active immune response to a variety of TAA.

Kennedy et al. [64] raised rabbit anti-Id antibodies against two mouse MAb which were specific for the amino and carboxyl termini of the T antigen of simian virus 40 (SV40). A small fraction of the T antigen is expressed at the surface of SV40-induced tumor cells and is able to invoke immunity. Priming with a pool of two anti-Id antibodies led to reduced tumor size and increased survival time in approx. 60% of mice upon challenge with syngeneic SV40-induced tumor cells. In some cases, the treated mice showed no detectable tumors whereas all mice of the control group died.

In the experiments reviewed so far, the target antigens on tumors were either not identified [59–62] or they were molecules entirely foreign to the host such as a human antigen (p97) in a mouse or an antigen encoded by a monkey virus (SV40) and introduced into a mouse [63,64]. Whether anti-Id antibodies can induce protective immunity against syngeneic tumors when the target antigens are expressed during certain stages of differentiation remains an open question.

Among the numerous tumor antigens which have been identified by xenogeneic MAb, very few (if any) are entirely tumor-specific because they are often expressed in fetal tissues and in certain normal adult tissues [11]. They are called tumor antigens based upon their association with tumors, yet little information is available as to whether any of these can elicit an immune response in the syngeneic host. We have tested this notion using, as the antigenic target, a defined tumor marker in an animal model, and specific Ab2 to probe and manipulate idiotypic interactions. Our findings are described below.

V. A murine tumor model to evaluate immunity to tumor-associated differentiation antigens

Murine chemically-induced transitional cell carcinomas of the urinary bladder have several advantages as a model [65]. They are transplantable in syngeneic mice for in vivo propagation and can be cultured in vitro as cell lines. They closely resemble human bladder carcinoma in histology and are chemically induced, as human bladder carcinomas are believed to be, and they are, of course, carcinomas, like most human malignancies. They have shared TAA which can elicit specific lymphocyte-mediated immune response in vitro [66,67], and this characteristic is shared with human bladder cancer where lymphocyte-mediated cytotoxicity to autologous and allogeneic bladder carcinoma cells has been reported [68]. Furthermore, the provocative observation has been made that rats immunized with syngeneic bladder tumors and exposed to chemical carcinogen showed a longer latency period before they developed primary bladder tumors [66].

In an attempt to develop xenogeneic MAb to TAA shared by mouse bladder carcinomas, rats were immunized against tumors of BALB/c origin and their spleen cells were hybridized with NS-1 mouse myeloma cells, after which the hybridomas were screened for production of antibodies binding to bladder tumor cells [69–71]. Specificity analysis of selected MAb was then performed by immunohistochemical testing on different normal and neoplastic mouse tissues. The antigenic targets

TABLE I

CHARACTERISTICS OF THE 6 10 Id SYSTEM

	Abl (Id)	Ab2 (anti-Id)	Ab3
	Rat MAb 6 10	(1) Mouse MAb 21D9 and 43A10 (2) Polyclonal rabbit antiserum	Mouse anti-Ab2 antibodies
Specificity	oncofetal antigen p175 on murine bladder carcinoma cells	rat MAb 6 10 Id	unique for each Ab2
Activity	(1) binds bladder carcinomas, some normal and fetal tissues (2) induces Ab2	(1) bind Abl (2) induce Ab3	

of the most specific MAb were studied for their cell-surface association and characterized by immunochemical techniques.

The most specific antibody obtained by this approach was MAb 6.10 [69]. It is a rat IgG2a which defines an antigen expressed by all bladder tumors tested, primary as well as transplanted, in vivo tumors as well as in vitro cell lines and which is also expressed by certain fetal tissues, and, in smaller amounts, by some epithelial cells from the adult host. Thus, MAb 6.10 has approximately the same level of specificity for bladder carcinoma as do many MAb to human TAA. The antigen defined by MAb 6.10 is a monomeric phosphoglycoprotein with a molecular weight of 175 000 (p175) and is located at the cell surface. Serological analysis showed no relationship between this antigen and the independently described molecules p185 or epidermal growth factor receptor (unpublished results; Refs 72,73).

Antibody 6.10 was used as Abl for idiotypic analysis in the studies described below. Monoclonal and polyclonal anti-Id antibodies (Ab2) were generated against the 6.10 idiotype [74]. These antibodies were used as probes for detecting naturally occurring antibodies bearing the 6.10 Id in the sera of mice with tumors and as immunogens for the induction of Ab3. The idiotypic and antigen specificities were examined. Data related to the 6.10 Id system are summarized in detail in Table I.

VI. Generation of anti-6.10 antibodies (Ab2)

Monoclonal anti-Id antibodies (Ab2) were raised against MAb 6.10 by immunizing mice and hybridizing their spleen cells. Out of approximately 2000 hybrids screened, two clones (21D9 and 43A10) were selected, each of which was derived from a different fusion. In immunodiffusion tests, both were found to produce IgM antibodies. Competitive binding inhibition assays showed that antibodies 21D9 and 43A10 bound to idiotopes on MAb 6.10 and not to rat Ig-specific determinants, and preincubation of MAb 6.10 with excess rabbit anti-rat IgG specific for both heavy and light chains did not substantially inhibit the binding of Ab2 to Abl.

To test the relationship between the 6.10 idiotopes and the antigen combining site, a competitive binding assay was performed. Purified MAb2 were adsorbed onto wells of microtest plates, after which different amounts of lysates from cultured cells of bladder carcinoma BTCC-1660 and sarcoma MCA-1511 (as negative control) were added as inhibitors followed by a constant amount of MAb 6.10. The reaction was detected by adding rabbit anti-rat IgG-HRP (horseradish peroxidase) and chromogen. In these experiments, the bladder tumor lysate competitively inhibited the binding of antibody 6.10 to MAb 21D9 and 43A10 in a dose-dependent manner, while the sarcoma lysate showed no significant blocking. Since the observed inhibition of Abl–Ab2 interactions by bladder tumor lysate could be due to steric hindrance upon binding of the p175 to MAb 6.10, the results do not prove that the idiotopes defined by the antibodies 21D9 and 43A10 are the exact determinants involved in antigen recognition. However, they suggest that the Ab2-defined idiotopes are located in close proximity to the antigen combining site.

Polyclonal rabbit Ab2 were also raised to MAb 6.10. This was done in order to increase the probability of obtaining an Ab2 which could act as an internal image. Since rabbit sera have, in many systems [47,64,75], been the most commonly and successfully used anti-Id reagents, a New Zealand White rabbit was immunized with MAb 6.10. After five monthly immunizations, the rabbit serum was exhaustively absorbed on an affinity column prepared with purified normal rat IgG until all detectable reactivity to rat IgG was removed. The rabbit anti-Id antibodies were then obtained from the absorbed serum by chromatography on an affinity column containing MAb 6.10.

In order to characterize the expression of the different idiotopes expressed on MAb 6.10, the two MAb, 21D9 and 43A10, as well as the rabbit polyclonal Ab2 were analyzed for their ability to inhibit each other's binding to MAb 6.10 (Table II). Each Ab2 inhibited, in a dose-dependent fashion, the binding of itself to solid phase MAb 6.10. The two MAb2 also inhibited each other but they did not significantly inhibit the rabbit Ab2. These results suggest that MAb 21D9 and 43A10 recognize idiotopes on antibody 6.10 which are closely related. Since the rabbit Ab2 inhibited MAb 43A10 to a much greater extent than MAb 21D9, the two monoclonal Ab2 are probably not directed to the identical idiotope.

Presumably, therefore, MAb 21D9 and 43A10 recognize closely located idiotopes so that the binding of one Ab2 sterically hinders the subsequent binding of the other. Since MAb 43A10 slightly inhibited the rabbit Ab2, while MAb 21D9 did not, the rabbit Ab2 must recognize more than one idiotope on the MAb 6.10 Id, one of which may be overlapping with the site defined by MAb 43A10. Although the idiotopes recognized by antibodies 21D9 and 43A10 are closely linked, the one defined by 21D9 does not seem to belong to the set of idiotopes reactive with rabbit Ab2. Therefore, it appears that at least three idiotopes on MAb 6.10 have been identified.

TABLE II

SPECIFICITY OF THE Ab2 (ANTI-MAb 6 10) RESPONSE

Ab2 bound to MAb 6 10	Inhibitor	% Inhibition [a]
21D9	21D9	100
	43A10	90
	rabbit Ab2	40
43A10	21D9	100
	43A10	100
	rabbit Ab2	100
Rabbit Ab2	21D9	0
	43A10	22
	rabbit Ab2	100

[a] Maximal inhibition obtained with excess inhibitor at saturated binding conditions.

VII. Testing for the presence of the 6.10 Id in the sera of bladder-tumor-bearing mice

Since MAb 6.10 was obtained from a rat immunized with mouse bladder carcinoma cells, it needed to be determined whether the same Id was also present in BALB/c mice bearing syngeneic bladder tumors. The approach chosen to study this was to search for the 6.10 Id in the immunoglobulin fraction of sera from mice with such tumors. A positive finding would indicate that antibodies bearing the 6.10 Id occur during progression of syngeneic bladder carcinoma in mice; a corollary of such a finding is that mice and rats would have to share the 6.10 Id and that mice could mount an antibody response to p175. Mice were implanted subcutaneously with the BTCC-1660 bladder tumor and their sera were obtained at various subsequent time-points and assayed. Different dilutions of the serum samples were preincubated with ^{125}I-labeled MAb 21D9, 43A10 or rabbit Ab2 and the mixtures were added to MAb 6.10 bound onto a solid phase. Sera from untreated BALB/c mice and from BALB/c mice bearing sarcoma MCA-1511 were used as controls. No significant inhibition was observed with sera obtained at different stages of bladder tumor growth when tested toward MAb 21D9, 43A10 or the rabbit Ab2; that is, the idiotopes on MAb 6.10, as defined by the Ab2 used, were not detected in the mouse sera.

VIII. Detection of antibody response in mice injected with Ab2

Immunization of animals with the proper Ab2 can induce an anti-anti-idiotypic antibody, termed

Ab3 [16]. The Ab3 can resemble the original Ab1 in idiotypic specificity [16], but sometimes lack antigen specificity. To analyze the Ab3 response to Ab2 in the mouse bladder tumor system, MAb 21D9 and 43A10 were used to immunize BALB/c mice and their sera were subsequently assayed for antibodies expressing MAb 6.10 idiotopes and for the ability to bind to the bladder carcinoma-associated p175 antigen. In order to render the MAb2 more immunogenic to the syngeneic mice, the antibodies were copolymerized to the protein carrier KLH using glutaraldehyde [76].

Serum samples from mice injected with a given monoclonal Ab2 were tested along with controls in the form of normal BALB/c serum and sera from mice injected with KLH conjugated to an irrelevant peptide. Figure 1 shows that sera from mice injected with either of the two monoclonal Ab2 completely inhibited the binding of the same Ab2 to MAb 6.10, and the control sera gave no inhibition. Sera from mice injected with both MAb2 inhibited MAb 21D9 and 43A10 equally (not shown).

Immunization with purified polyclonal rabbit Ab2 was also used to raise Ab3 in BALB/c mice, following a protocol published by Bluestone et al. [75]. Mice were injected with rabbit Ab2 in saline on days 0, 3 and 14. As a control, other mice were injected with rabbit anti-rat IgG antibodies which had been isolated from the original immune rabbit serum by affinity purification on a column conjugated with normal rat IgG. The antibody response of the mice was measured by a competitive radioimmunoassay. Sera from mice injected with control antibodies showed a low level of inhibition of ^{125}I-labeled rabbit Ab2 to MAb 6.10, which was probably due to the presence of antibodies to rabbit immunoglobulin (not shown). In contrast, sera from mice given the rabbit Ab2 gave a strong inhibition (Fig. 1).

The sera from mice injected with each of the three Ab2 were then used to inhibit the binding of ^{125}I-Ab2 to Ab1 (MAb 6.10) in a criss-cross manner (Fig. 1). Sera from mice receiving antibody 21D9 completely inhibited the binding of ^{125}I-labeled 21D9 but not that of MAb 43A10, and vice versa (Fig. 1, panels A and B), while sera from neither of these two groups of mice inhibited the binding of iodinated rabbit Ab2. This was unexpected because of the previous demonstration that the Ab1-associated idiotope recognized by MAb 43A10 might constitute a subset of the rabbit Ab2-defined idiotopes. There was thus an exquisite specificity of each Ab3 for its own particular inducing Ab2.

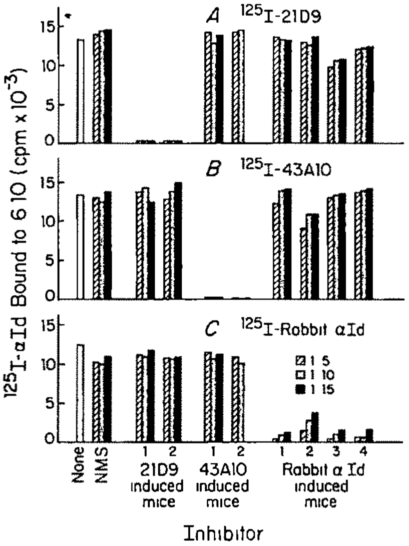

Fig 1 Effect of sera from mice injected with mouse (A and B) or rabbit (C) Ab2 on the binding of the Ab2 to MAb 6 10, showing specificity of Ab3

Ab2 of the internal image type are assumed to share some molecular configuration with the antigenic determinant. In a number of experimental systems (see Section IV above), the Ab3 induced by injection of Ab2 could bind to the original antigen. Therefore, sera containing Ab3 from the three groups of mice injected with the different Ab2 preparations were tested for antigen binding capacity. A competitive radioimmunoassay was used in which the sera were first absorbed on BTCC-1660 (p175 positive) or MCA-1511 (p175 negative) tumor cells. After absorption the sera were used as competitors in the radioimmunoassay, unabsorbed sera were used as control. The rationale for this experiment was the following: If the Ab3 had Ab1-like activities, they should bind to the p175 antigen on tumor cells, so that in the radioimmunoassay, the sera absorbed with BTCC-1660 cells would no longer be able to inhibit the binding between Ab2 and Ab1, while unabsorbed sera or sera absorbed on negative MCA-1511 cells should give similar inhibition. No Ab1-like activity was found in any of the Ab3 sera.

The Ab3 sera were also used in an attempt to immunoprecipitate p175 from [^{35}S]methionine and ^{125}I-labeled BTCC-1660 lysates. No reactivity of Ab3 sera with p175 was found in any of several such experiments. Finally, spleen cells from rabbit Ab2-induced mice were hybridized with NS-1 cells. A total of 800 hybridomas were examined for binding to cultured BTCC-1660 cells by ELISA. Again, no Ab1-like binding to bladder tumor cells was detected. Altogether, these experiments then indicate, within the limitations under which they were carried out, that there is no antibody response involving the 6.10 idiotype in mice with bladder carcinomas, nor is such response inducible by using anti-idiotypic antibodies.

IX. Does selection of 'silent clones' fail in anti-Id immunization to tumor-associated forbidden specificities?

The key findings of our studies as so far presented are summarized by the following three statements. (1) Monoclonal and polyclonal Ab2 made to the 6.10 Id define at least three distinct private idiotopes that are not normally present in the sera of mice exposed to bladder tumors. (2) Each Ab2 elicits an Ab3 response that is strictly specific for unique idiotopes on the inducing Ab2. (3) The Ab3 response shows no reactivity with the tumor antigen defined by MAb 6.10. We shall now discuss the implications of these observations by attempting to answer three questions.

Question 1: Why is the Ab3 specific for each Ab2?

The idiotypic immunization cascade was first used by Urbain and Cazenave to produce four sets of antibodies, Ab4 against Ab3 against Ab2 against Ab1 [77,78]. The results of their studies suggested the circular nature of Id anti-Id interactions in that Ab3 behaves like Ab1 and Ab4 behaves like Ab2 in binding specificity. Since then, Ab2 have been used in many systems to induce the production of Ab1-like Ab3 [44–49]. Furthermore, Ab2 have been used to activate normally silent clones [51–57]. This approach suggests a way of turning on antibody-producing clones in animals that may not normally express them as a part of the natural immune response upon exposure to a given antigen.

Two MAb2 of mouse origin and rabbit affinity-purified polyclonal Ab2 were raised to MAb 6.10 as Ab1. These three antibodies which defined at least three different idiotopes on antibody 6.10 were used as probes for experiments which showed that antibodies with the 6.10 Id are not naturally present in mice with transplanted bladder tumors.

The next step was to inject separate groups of mice with each of the three available sources of Ab2 (the two monoclonal anti-Id and the polyclonal rabbit serum). An Ab3 response was elicited in each of the three groups and was shown to be specific for only the inducing Ab2. Generally, two populations of antibodies capable of binding Ab2 have been described in work performed with non-tumor antigens [79]. One Ab3 population shares Id determinants with Ab1 and may bind antigen. The other Ab3 population is called true anti-anti-Id and it is not idiotypically cross-reactive with Ab1, since it is directed to idiotopes on Ab2. This Ab3 does not bind antigen. Bluestone et al. [80] reported that xenogeneic polyclonal antibodies made to the Id of a MAb defining a H-2 antigen could induce an Ab3 that reacted with a syngeneic MAb2. This indicated that the polyclonal anti-Id antibodies induced Ab1-like molecules. On the other hand, in a study on the mouse myeloma Id ABPC 48, Ab3 were induced and demonstrated to be anti-anti-Id and not Ab1-like [81]. Three monoclonal Ab2 were made to the ABPC 48 Id of the myeloma. Each Ab2 was injected into mice whose serum antibodies were analyzed. The Ab3 responses to the different MAb2 were found to be independent of each other with the majority of the Ab3 binding to only one MAb2, similar to our findings in the mouse bladder system. The co-expression of two ABPC 48 idiotopes on the same Ab3 was rarely found. RNA blotting experiments and sequence comparison of the V_H of Ab1 and Ab3 molecules suggested that the Ab3 formed in response to Ab2 was structurally dissimilar to Ab1 and was probably anti-anti-Id response towards unique idiotopes on each individual Ab2. The Ab3 in the bladder tumor system described here may be similar to the antibodies in the ABPC 48 study.

Question 2: Why were there no antigen-binding Ab3?

As mentioned above, Ab3 produced in response to Ab2 have been demonstrated to sometimes be similar to Ab1 in reacting with the original antigen, and this has been taken as the most definitive demonstration for the presence of internal image antibodies in the Ab2 preparation. If antigen-binding Ab3 could, likewise, be induced in a tumor system, this would be advantageous, since such antibodies may have a therapeutic effect against the tumor, for example by mediating antibody-dependent cellular cytotoxicity, fixing complement or arming macrophages [82]. Therefore, the Ab3 generated in the mouse bladder system were tested for binding to the antigen defined by MAb 6.10. However, no such binding was found.

It is, of course, possible that antigen binding Ab3 were present but in quantities too low to be detected in the serum, for example, as a result of absorption to antigen-positive cells in vivo. The fact that very few tissues in the adult mouse express the p175 antigen defined by MAb 6.10 makes this possibility unlikely [69]. Furthermore, when spleen cells from Ab2-treated mice were converted to hybridomas, none of the hybridomas produced antibodies which bound to bladder tumor cells.

A second possibility is that there are no germline genes in BALB/c mice for the 6.10 Id. Although the germline repertoire may be roughly the same for rats and mice, mutations may have occurred in each species so that BALB/c mice cannot generate antibodies with an Id identical to that of rat MAb 6.10. A recent study of a MAb for nitrophenyl revealed that one amino-acid substitution in the D region can have a profound effect on the Id [83]. While the mutant MAb retained its specificity for nitrophenyl, its Id had been drastically changed from that of the parental antibody, so that an Ab2 made to the wild-type MAb did not react with the mutant antibody.

A third possibility for the absence of antigen-reactive Ab3 is that the Ab2 preparations used did not include any internal image antibodies. This possibility cannot be excluded, although three Ab2 preparations were used, one of which was a rabbit immune serum that contained antibodies reacting with more than one idiotope.

A fourth possibility is that internal image Ab2 were, in fact, present in the anti-Id reagents used but that any lymphocyte clone capable of making Ab1-like antibodies was suppressed (or deleted) in view of the fact that the antibody it made would react with a differentiation or "self" antigen. There may be a need for powerful host mechanisms to suppress the emergence of such clones, since Ab1 specific for self antigens could cause destruction of tissues expressing the antigens as well as other manifestations of autoimmune disease.

Koprowski et al. [84,85] raised a mouse monoclonal antibody to a differentiation antigen associated with human gastrointestinal cancer and infused high doses of antibodies into patients with metastatic colorectal carcinoma. In the sera of several of the treated patients, anti-Id antibodies were detected. These antibodies appeared to be directed to idiotopes closely related to the binding site of the infused MAb, and it was suggested that the presence of anti-Id in the patients' sera correlated with the remission of the disease. However, no evidence was presented that the patients in remission did have an active antibody and/or T cell response to the tumor-related antigen.

Question 3: Are cell-mediated responses involved?

The lack of antigen-binding Ab3 in mice receiving Ab2 may not necessarily mean that an immune response has not been triggered. In many systems, anti-Id reagents raised against Ab1 antibodies have been shown to interact with Id of T cells, and induce cell-mediated immune responses, such as DTH or cytolytic T cells [16]. For example, in the reovirus system [86], a monoclonal Ab2 was made to a monoclonal Ab1 which was specific for the hemagglutinin of reovirus type 3. This MAb2 bound to cytolytic T cells which were generated against reovirus-infected target cells, and it primed for DTH in vivo [40,41]. In the azobenzenearsonate system, an Ab2 was made to a cross-reactive idiotype (CRI) of Ig in A/J mice and shown to induce suppressor T cells in CBA mice. These mice did not produce any antibodies with the CRI, even when hyperimmunized [87].

In a study of chemically induced murine sarcomas, a monoclonal mouse antibody was identified which functioned as Ab2 in the sense that it induced tumor specific DTH mediated by Thy 1^+, Lyt 1^+ cells in an allotype-restricted fashion [62]. Ab2 treatment had an antitumor effect when tested in vivo against transplants of the relevant tumor (Nelson et al., unpublished data). While T cell immunity was induced by Ab2 priming in this study, it is noteworthy that no specific Ab1 activity was identified against this tumor. This suggests that idiotypic interactions of T cells, B cells and Ig molecules may operate independently in terms of regulatory controls, so that an Id^+ T cell may substitute for a 'forbidden' Ab1 upon stimulation by an Ab2 [32].

In a similar study, rabbit Ab2 were made to a MAb specific for the SV40 T antigen and was injected into mice [64]. The primed animals demonstrated protection against challenge with SV40-induced tumors, while no humoral antibody was detected. The authors suggested that cellular mechanisms were responsible for the tumor rejection after anti-Id administration.

Recently, monoclonal Ab2 21D9 and 43A10, referred to above, were used to induce bladder tumor-specific cell-mediated immunity in syngeneic mice, as shown by DTH in vivo and leukocyte adherence inhibition (LAI) reactivity in vitro [74]. MCA-1511 sarcoma and its corresponding MAb2, 5.96, were used as controls. Lymphocytes from mice sensitized with 21D9 or 5.96 specifically recognized antigens in extracts of BALB/c bladder carcinoma BTCC-1660 and sarcoma MCA-1511, respectively. This reactivity was selectively abrogated by prior treatment of the sensitized cells with the appropriate anti-Id antibodies and complement. An antigen recognized in vitro by 21D9-sensitized lymphocytes could be separated from BTCC-1660 extract by immunoadsorption with antibody 6.10 and elution with acidic buffer. These findings suggest that the p175 oncofetal antigen can be recognized by T cells of syngeneic mice after in vivo administration of anti-Id antibodies.

X. Conclusions

From the limited number of reports analyzing the effects of anti-Id in tumor systems, there appears to be a preferential induction of T cell response and an apparent lack of humoral antibodies. Clearly, more data are needed before this observation can be a generalization. However, it is important to determine why a cell-mediated response appears to be favored. Since different T-cell populations have different functions, it is possible that injection of Ab2 can either upregulate or down-regulate the immune responses, dependent on whether the antibody interacts with T helper or T suppressor cells and whether the given cell population is activated or inhibited by the antibody. It is thus crucial to know whether a particular Ab2 reacts with helper or suppressor T cells or both and what the outcome of the interactions is [88]. For example, if an Ab2 could eliminate Id-positive suppressor T cells and stimulate Id-positive helper T cells, this would be advantageous to the host, while the reverse effect could be detrimental. The following two sets of experiments with contrasting results illustrate this point clearly. In the first case, rabbit Ab2 were made to a monoclonal Ab1 against the hepatitis virus and shown to induce virus neutralizing Ab3 [46]. However, an Ab2 prepared in an analogous way by the same group of investigators and used to prime mice to the herpesvirus increased the pathogenicity of the virus so that the Ab2-treated mice had a shorter survival time than the untreated animals [89].

These findings illustrate the importance of selecting the appropriate tumor marker and idiotypic reagents for use as the target for an Ab2-induced response. An approach using naturally occurring Id^+ Ig or T cells in a tumor-bearing host may be advantageous for stimulating antitumor responses with anti-idiotype immunogens.

Acknowledgements

This work was supported by grant CA39211 from the National Institutes of Health and by ONCOGEN. We thank Dr. Karen Nelson for helpful discussions; Ms. Holly Chase and Ms. Phyllis Harps for preparation of the manuscript.

References

1 Gross, L (1943) Cancer Res 3, 326
2 Foley, E J (1953) Cancer Res. 13, 835

3 Prehn, R and Main, D. (1957) J. Natl Cancer Inst 18, 768

4 Klein, G, Sjögren, H.O., Klein, E. and Hellström, K E (1961) Cancer Res 20, 1561

5 Hellström, K.E and Hellström, I. (1969) Adv Cancer Res 12, 167

6 Shiku, H J, Takahashi, T, Resnick, L.A., Oettgen, H F and Old, L.J (1976) J Exp. Med 144, 873

7 Köhler, G and Milstein, C (1975) Nature 256, 495

8 Koprowski, H. and Herlyn, M. (1985) in Molecular Biology of Tumor Cells (Wahren, B, Holm, G, Hammarstrom, S. and Perlmann, P, eds), p 123, Raven Press, New York

9 Reisfeld, R A, Harper, J R and Bumol, T F (1984) CRC Crit. Rev Immunol 5, 27

10 Hellström, K.E., Hellström, I. and Brown, J P (1982) Springer Semin Immunopathol 5, 127

11 Hellstrom, K E and Hellström, I (1985) in Monoclonal Antibodies for Tumour Detection and Drug Targeting (Baldwin, R W. and Byers, V.S, eds), p. 17, Academic Press, London

12 Sacks, D L, Kelsoe, G H and Sachs, D H (1983) Springer Semin Immunopathol 6, 79

13 Finberg, R.W and Ertl, H C J (1986) Immunol Rev 90, 129

14 Oudin, J and Michel, M (1963) C.R Acad Sci 257, 805

15 Kunkel, H G., Mannik, M. and Williams, R C (1963) Science 140, 1218

16 Rajewsky, K. and Takemori, T (1983) Annu. Rev. Immunol 1, 569

17 McMillan, S, Seiden, M V, Houghten, R A, Clevinger, B, Davie, J M and Lerner, R A. (1983) Cell 35, 859

18 Seiden, M V, Clevinger, B, McMillan, S, Srouji, A., Lerner ,R. and Davie, J.M. (1984) J Exp Med 159, 1338

19 Jerne, N K. (1974) Ann Immunol. 125C, 373

20 Kluskens, L and Köhler, H (1974) Proc Natl Acad Sci USA 71, 5083

21 Cosenza, H (1976) Eur. J Immunol. 6, 114

22 Kelsoe, G, Reth, M and Rajewsky, K (1980) Immunol Rev 52, 75

23 Sy, M S, Bach, B.A, Dohi, Y, Nisonoff, A., Benacerraf, B and Greene, M I (1979) J. Exp Med 150, 1216

24 Miller, G G, Nadler, P.I., Asano, Y., Hodes, R.J and Sachs, D H (1981) J Exp. Med 154, 24

25 Thomas, W R, Morahan, G, Walker, I D. and Miller, J F.A P (1981) J Exp. Med 153, 743

26 Ertl, H C.J and Finberg, R W (1984) Proc Natl. Acad Sci. USA 81, 2850

27 Eichmann, K. and Rajewsky, K. (1975) Eur J Immunol 5, 661

28 Muller, C.E and Rajewsky, K (1984) J Exp. Med. 159, 758

29 Green, D R, Flood, P M and Gershon, R K (1983) Annu Rev Immunol. 1, 439

30 Greene, M., Sy, M-S, Nisonoff, A and Benacerraf, B. (1980) Mol. Immunol 17, 857

31 Sy, M.-S, Dietz, M., Germain, R, Benacerraf, B and Greene, M. (1980) J Exp Med 151, 1183

32 Nelson, K and Nepom, G T (1986) in Paradoxes in Immunology (Hoffman, G, Levy, J, Nepom, G T., eds), CRC Press, Boca Raton, in the press

33 Bismuth, G, Somme, G., Roth, C, Gougeon, M.L and Theze, J (1984) Eur. J. Immunol 14, 503

34 Augustin, A.A, Sim, G K and Bona, C.A. (1983) Surv Immunol. Res 2, 78

35 Urbain, J, Slaoui, M and Leo, O. (1982) Ann Immunol 133D, 179

36 Sege. K and Peterson, P.A (1978) Proc. Natl. Acad Sci USA 75, 2443

37 Fields, B N and Greene, M.I (1982) Nature 300, 19

38 Noseworthy, J.H., Fields, B N, Dichter, M S, Sobotka, C, Pizer, E, Perry, L L., Nepom, G T and Greene, M I. (1983) J Immunol 131, 2533

39 Kauffman, R.S., Noseworthy, J.H., Nepom, G T, Finberg, R., Fields, B.N. and Greene, M I (1983) J Immunol. 131, 2539

40 Sharpe, A H., Gaulton, G N, McDade, K.K, Fields, B N. and Greene, M.I. (1984) J Exp. Med. 160, 1195

41 Ertl, H C J., Greene, M.I, Noseworthy, J H, Fields, B N, Nepom, G T, Spriggs, D R and Finberg, R W (1982) Proc. Natl Acad Sci USA 79, 7479

42 Nisonoff, A and Lamoyi, E (1981) Clin Immunol Immunopathol 21, 397

43 Sacks, D L., Esser, K.M. and Sher, A. (1982) J Exp Med 155, 1108

44 Stein, K E and Söderström, T (1984) J Exp Med 160, 1001

45 McNamara, M.K, Ward, R E and Köhler, H. (1984) Science 226, 1325

46 Kennedy, R C and Dreesman, G R (1984) J. Exp. Med. 159, 655

47 Reagen, K J, Wunner, W.H, Wiktor, T J. and Koprowski, H (1983) J Virol 48, 660

48 Uytdehaag, F.G.C.M. and Osterhaus, A.D.M.E. (1985) J. Immunol 134, 1225

49 Grzych, J M., Capron, M, Lambert, P H., Dissous, C., Torres, S and Capron, A (1985) Nature 316, 74

50 Sacks, D L. and Sher, A. (1983) J. Immunol. 131, 1511

51 LeGuern, C., Ben Aissa, F, Juy, D, Mariame, B., Buttin, G and Cazenave, P.-A. (1979) Ann Immunol. 130C, 293

52 Primi, D, Juy, D and Cazenave, P.A. (1981) Eur J Immunol. 11, 393

53 Bona, C A., Heber-Katz, E. and Paul, W E (1981) J Exp Med. 153, 951

54 Hiernaux, J, Bona, C. and Baker, P J (1981) J Exp Med 153, 1004

55 Rubinstein, L.J, Goldberg, B, Hiernaux, J, Stein, K.E. and Bona, C.A (1983) J. Exp Med 158, 1129

56 Moser, M., Leo, O, Hiernaux, J. and Urbain, J. (1983) Proc Natl. Acad Sci USA 80, 4474

57 Francotte, M and Urbain, J (1984) J Exp Med 160, 1485

58 Greene, M I, Nellis, M J, Sy, M-S and Nisonoff, A (1981) Adv Immunol 32, 253

59 Flood, P.M, Kripke, M.L, Rowley, D A and Schreiber, H (1980) Proc. Natl Acad. Sci USA 77, 2209

60 Tilkin, A F, Schaaf-Lafontaine, N, Van Acker, A., Baccardoro, M. and Urbain, J. (1981) Proc. Natl. Acad Sci. USA 78, 1809

61 Binz, H, Meier, B. and Wigzell, H (1982) Int. J. Cancer 29, 417

62 Forstrom, J W., Nelson, K A, Nepom, G T., Hellström, I and Hellström, K E. (1983) Nature 303, 627

63 Nepom, G T, Nelson, K A., Holbeck, S L., Hellström, I and Hellström, K.E (1984) Proc Natl Acad. Sci. USA 81, 2864

64 Kennedy, R.C., Dreesman, G.R., Butel, J S and Lanford, R E (1985) J. Exp. Med. 161, 1432

65 Lee, V.K, See, W.A., Hellström, I. and Hellström, K E (1985) in Immunity to Cancer (Reif, A and Mitchell, M, eds.), p 387, Academic Press, New York

66 Taranger, L.A, Chapman, W H, Hellström, I. and Hellström, K E (1972) Science 176, 1337

67 Hellström, I and Hellstrom, K.E (1972) Natl. Cancer Inst Mongr 35, 125

68 Cooper, E H, and Williams, R.E (eds.) (1975) The Biology and Clinical Management of Bladder Cancer, Blackwell, Oxford

69 Hellström, I., Hellström, K E, Rollins, N, Lee, V K, Hudkins, K. and Nepom, G T. (1985) Cancer Res. 45, 2210

70 Hellström, I, Rollins, N, Settle, S, Chapman, P., Chapman, W H and Hellström, K.E (1982) Int. J. Cancer 29, 175

71 Settle, S, Hellström, I and Hellström, K.E. (1985) Exp Cell Res. 157, 293

72 Drebin, J.A., Stern, D F., Link, V.C., Weinberg, R A and Greene, M.I. (1984) Nature 312, 545

73 Downward, J., Yarden, Y, Mayes, E., Scrace, G, Totty, N, Stockwell, P, Ullrich, A., Schlessinger, J and Waterfield, M. (1984) Nature 317, 521

74 Lee, V.K, Harriott, T.G., Kuchroo, V K, Halliday, W J., Hellström, I., and Hellström, K E (1985) Proc. Natl. Acad. Sci USA 82, 6286

75 Bluestone, J.A., Sharrow, S.O., Epstein, S.L., Ozato, K. and Sachs, D H. (1981) Nature 291, 233

76 Bona, C., Hooghe, R., Cazenave, P.A, LeGuern, C. and Paul, W.E. (1979) J Exp Med 149, 815

77 Cazenave, P-A (1977) Proc Natl Acad. Sci. USA 74, 5122

78 Urbain, J., Wikler, M, Franssen, J.D and Collignon, C. (1977) Proc. Natl. Acad. Sci. USA 74, 5126

79 Köhler, H., Urbain, J and Cazenave, P A (eds) (1984) Idiotypy in Biology and Medicine, Academic Press, London

80 Bluestone, J A, Auchincloss, H., Cazenave, P-A, Ozato, K and Sachs, D H. (1982) J. Immunol. 129, 2066

81 Legrain, P, Sanchez, P. and Buttin, G (1985) Mol Immunol 22, 445

82 Hellström, I, Brankovan, V. and Hellström, K.E (1985) Proc. Natl. Acad Sci USA 82, 1499

83 Radbruch, A., Zaiss, S., Kappen, C, Bruggemann, M, Beyreuther, K. and Rajewsky, K (1985) Nature 315, 506

84 Koprowski, H, Herlyn, D., Lubeck, M., Defreitas, E and Sears, H.F. (1984) Proc. Natl. Acad Sci USA 81, 216

85 Herlyn, M., Steplewski, Z., Herlyn, D. and Koprowski, H (1979) Proc. Natl. Acad. Sci USA 76, 1438

86 Nepom, G T, Weiner, H.L., Dichter, M A, Tardieu, M, Spriggs, D.R, Gramm, C.F., Powers, M.L, Fields, B N and Greene, M.I. (1982) J Exp Med 155, 155

87 Thomas, W R., Morahan, G and Miller, J.F.A.P. (1982) J Immunol. 130, 2079

88 Strauss, H.J. and Schreiber, H. (1984) Cancer Bull. 36, 242

89 Kennedy, R.C, Adler-Storthz, K., Burns, J W, Henkel, R D and Dreesman, G.R. (1984) J. Virol 50, 951

Biochimica et Biophysica Acta 865 (1986) 141–170
Elsevier

BBA 87160

Monoclonal antibody applications in bone marrow transplantation

Christopher L. Reading and Yoichi Takaue

The University of Texas System Cancer Center, M.D. Anderson Hospital and Tumor Institute,
Texas Medical Center, 6723 Bertner Avenue, Houston, TX 77030 (U.S.A.)

(Received 9 December 1985)

Contents

I. Introduction . . . 141

II. Bone marrow transplantation . . . 142
  A. Allogeneic transplantation . . . 142
  B. Autologous transplantation . . . 142

III. Preparation of bone marrow mononuclear cells . . . 143

IV. Elimination of specific cell populations with monoclonal antibodies . . . 144
  A. Monoclonal antibodies . . . 144
  B. Complement-mediated lysis . . . 156
  C. Immunotoxins . . . 157
  D. Physical separations . . . 157

V. Monitoring systems . . . 157

VI. Concluding remarks . . . 164

Acknowledgements . . . 164

References . . . 164

I. Introduction

The purpose of this review is to discuss the current efforts and future potential in the use of monoclonal antibodies to eliminate specific cell populations from bone marrow aspirates used for transplantation. Although bone marrow transplantation (BMT) is used in a number of hematologic disorders, this discussion will be limited to applications in cancer. In the first 10 years of monoclonal antibodies, many clinical applications

---

Abbreviations: BMT, bone marrow transplantation; MA, monoclonal antibodies; GVHD, graft-versus-host disease; MLR, mixed lymphocyte reactions, GM-CFC, granulocyte-macrophage colony-forming cell, BFU-E, burst-forming unit-erythroid, BMBC, bone marrow buffy coat. GEMM-CC, granulocyte,erythroid,macrophage,megakaryocyte-forming cell, HSC, hematopoietic stem cell.

Correspondence address: The University of Texas System Cancer Center, M.D. Anderson Hospital and Tumor Institute, Texas Medical Center, 6723 Bertner Avenue, Houston, TX 77030, U.S.A.

0304-419X/86/$03.50 © 1986 Elsevier Science Publishers B.V. (Biomedical Division)

have met with frustrations. This is partially due to our lack of experience with these new reagents, and partially due to the complexities of applying basic research findings in the clinical setting. We seem to be in a constant dilemma with the clinical applications, since there is an immediate need for therapeutic improvements, but the applications will improve with continued research. We believe that the best approach requires critical analysis of therapeutic applications, along with continuing research. BMT affords us an opportunity to measure the effects of in vitro manipulation that is impossible with in vivo applications of monoclonal antibodies (MA). Careful measurement of the relevant variables in the clinical applications will accelerate successful use of monoclonal antibodies in BMT.

II. Bone marrow transplantation

As cancer chemotherapy and radiation doses are increased to eliminate residual tumor cells in patients, a dose-limiting toxicity is realized, often before eradication of tumor cells is complete [1–5]. Phase I clinical trials have defined agents and combinations of agents which have hematologic toxicity as their dose limitation. BMT allows restoration of hematopoietic function after the use of supralethal doses of radiation and combination chemotherapy [6–12]. There are complications related to the bone marrow cells infused, and MA have been used in a number of ways to eliminate specific cell populations before infusion of the graft. Manipulation of the marrow may increase the risks of complications, which are ever present in BMT [13,14]. There are two types of BMT in clinical use, allogeneic and autologous.

IIA. Allogeneic transplantation

When an apparently histocompatible donor is available, a conventional (allogeneic) transplant can be performed [8,10]. Bone marrow cells ((1–4) $\cdot 10^{10}$ mononuclear cells) are aspirated from the illiac crest of the donor, and are processed for infusing into the recipient. Some of the infused cells are able to re-engraft in the bone marrow and reinitiate hematopoiesis, leading to the formation of stable chimeras. This can be demonstrated with sex-mismatched transplants and with genetic markers [15]. The major complication of allogeneic BMT stems from donor-recipient histoincompatibility. Unmatched marrow grafts lead to severe and usually fatal graft-versus-host disease (GVHD), which results from recognition of recipient tissues as foreign by the transplanted donor lymphocytes [16–20]. This complication does not exist in identical-twin transplants, which represent a very low frequency (1/300 transplants). The use of donors matched at the HLA A, B, C and DR loci, and negative for mixed lymphocyte reactions (MLR) with recipient cells, does not completely overcome this problem: GVHD still occurs in approximately 50% of the cases, and about half of these are fatal. There is a great deal of evidence that transplanted mature donor T lymphocytes are responsible for initiating GVHD, and therefore researchers have attempted to use in vitro methods to eliminate these cells from the graft. These include rosetting with sheep erythrocytes followed by agglutination with soybean agglutinin [21–24], monoclonal anti-T cell MA alone [25–27] or with complement [28–44], toxins [45–49], or physical separation methods [50–53].

IIB. Autologous transplantation

In the absence of a histocompatible donor, bone marrow cells aspirated from the patient at a time when there is no detectable tumor cell contamination can be processed, stored frozen in liquid nitrogen, thawed and reinfused after high-dose cytoreduction. This process of autologous BMT completely overcomes the problem of histocompatibility, but is plagued by the possibility of low levels of cryptic tumor cell contamination in 'remission' bone marrows in leukemia patients, and of undetected metastatic cell contamination in bone marrow aspirates from solid tumor patients [9,12]. Several groups are investigating the potential of MA to eliminate these tumor cells from bone marrow [54–94]. This has been attempted by using complement [54–72], immunotoxins [46,73–87], magnetic microspheres [88,89], magnetic immunocolloids [51,90–93] and drug conjugates [94]. Considerations for the use of monoclonal antibodies with autologous transplantation for ALL patients have recently been reviewed [267].

In either allogeneic or autologous BMT, the treatment must be carefully designed and executed so that the pluripotent hematopoietic stem cells (HSC) are not reduced to a level insufficient for engraftment. Although several in vitro clonogenic assays reflect early hematopoietic progenitor proliferation and differentiation [95–103] the final test of any procedure is engraftment in vivo. When sex-mismatched allogeneic transplants are performed, it is possible to evaluate the origin of the hematopoietic recovery. In the autologous setting, since recovery might stem from incomplete ablation of the in situ HSC, only arguments based on the kinetics of hematopoietic recovery can be made.

Testing of MA and elimination procedures are frequently performed using clonogenic assays in agar or methylcellulose in the presence of a variety of growth and differentiation factors. These assays include analysis of the GM-CFC (granulocyte-macrophage colony-forming cell) [97], the BFU-E (burst-forming unit-erythroid) [95], and the GEMM-CFC (granulocyte, erythroid, macrophage, megakaryocyte colony-forming cell), which give rise to 'mixed-type' colonies [98,100]. An assay which may more accurately reflect the proliferation potential of the HSC is the long-term bone marrow (Dexter) cultures [96,99], which measures renewal of cells giving rise to the above CFCs. This assay is limited, however, by the low frequency of progenitors produced. A newer assay which may prove to be valuable in this analysis is the undifferentiated blast colony assay [104,105].

Hematopoietic recovery is usually measured as the number of days required to reach a certain value of differentiated hematopoietic elements. These include platelets, white blood cells and polymorphonuclear leukocytes. Since delayed engraftment often leads to lethal complications, the relevance of the in vitro assays to predict hematopoietic recovery is of paramount importance. Recovery of immune function is often slow after BMT, even without manipulation of the graft [106–113]. There are no accepted in vitro assays which predict immune recovery. Recovery of immune function is often measured as the period required to obtain a certain response in proliferation assays induced by the mitogens phytohemagglutinin (PHA) or concanavalin A (Con A), or in mixed lymphocyte reactions (MLR). Delayed immune recovery is often associated with lethal complications, including viral, bacterial and fungal infections [13,14].

III. Preparation of bone marrow mononuclear cells

Marrow aspirates contain a large number of erythrocytes and, prior to storage or infusion, a bone marrow buffy coat (BMBC) containing the nucleated cells is usually prepared. A large number of cells must be infused, usually $(1-4) \cdot 10^{10}$, and manipulation of this number of BMBC cells is problematic. Most of the MA treatments require multiple incubations and repeated washing of the cells by centrifugation. Residual platelets and the large number of granulocytes can readily induce clumping and lysis, which in turn results in further clumping and lysis. Addition of DNAase can alleviate some of the problems, but is not always sufficient to avoid clumping, lysis and extensive loss of cell number and progenitors.

Several separation procedures have been attempted in order to obtain a mononuclear fraction from BMBC cells [114–120]. Clinically acceptable results have been obtained with Ficoll/Hypaque gradients and the Haemonetics and IBM blood cell separators. Isopycnic centrifugation on a Ficoll-Hypaque interface ($d = 1.070$) allows removal of the majority of the granulocytes, erythrocytes and platelets, but may lead to losses of progenitors, and the interface cells often clump due to adsorbed platelets. The use of blood cell separators such as the Haemonetics perform most reproducibly with a standard volume and cell concentration, and with small donors has led to variable cell recoveries and losses of progenitors. A further improvement appears to be isopycnic sedimentation on discontinuous Percoll gradients [117], and we have adapted this procedure for preparative use [120]. A preparative discontinuous Percoll gradient and the details of the gradient are depicted in Fig. 1 and typical cell and progenitor yields are presented in Table I. Using this procedure we have been able to reduce the number of BMBC cells to about $(1-4) \cdot 10^9$ and thus the volume of reagents and incubations during treatments with monoclonal antibodies. Furthermore previous problems frequently encountered with

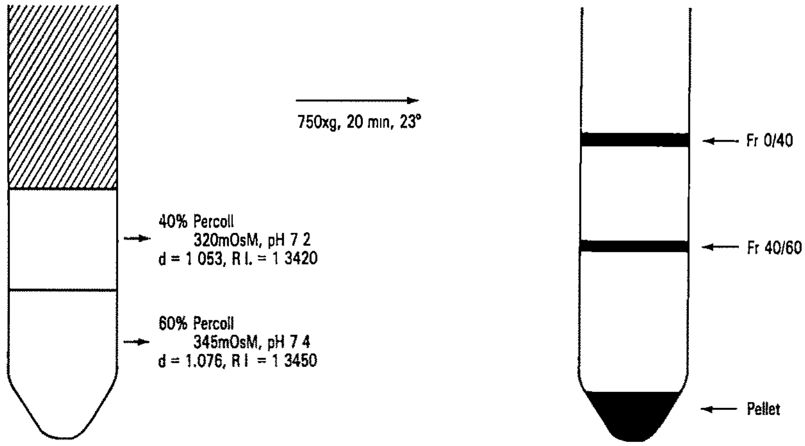

Fig. 1. Preparative two-step discontinuous Percoll gradient for preparation of mononuclear bone marrow cells prior to manipulation with monoclonal antibodies. For details, see the text.

clumping and lysis are virtually eliminated. The yield of progenitors is high, and we have routinely obtained engraftment using this fraction for allogeneic BMT [121].

IV. Elimination of specific cell populations with monoclonal antibodies

IVA. Monoclonal antibodies

A number of MA are available with selective reactivity with hematopoietic elements [122], lymphoid cell subsets [123] and tumor cells [124–129]. Some of the more promising monoclonal antibodies for use in BMT have been the subject of an excellent recent review [56] and these and others are listed in Table II [126–249]. Many of the antibodies reactive with lymphoid and myeloid cell subsets of with acute leukemia cells have been the subject of two intensive workshops [126–129]. These antibodies were examined for similar reactivities and placed in ‘cluster designations’ (CD) as indicated in Table II. A large number of antibodies also presented in Table II were not associated with these clusters. In cases for which the antigen is known, the molecular weight or a description is included. In several cases, additional MA are in the same CD, but additional information is not reported. These are listed next to the antigen descriptions. Reported

TABLE I

DISTRIBUTION OF CELLS AND PROGENITORS IN 0/40/60 PERCOLL GRADIENTS

Analysis	Buffy	Fr 0/40	Fr 40/60	Pellet
Cell recovery [a] (%, $n = 9$)	100	0.3 (0.1–0.4)	11.3 (6.7– 19.3)	74 (54–89)
GM-CFC [b] ($n = 9$)	48 (12–133)		418 (122 –896)	
% recovery	100		98.4 [c]	
BFU-E [b] ($n = 3$)	6.3 (1– 10)		78.6 (7 –120)	
% recovery	100		141 [c]	
GEMM-CFC [b] ($n = 3$)	0.33 (0– 1)		8 (0 – 14)	
% recovery	100		274 [c]	

[a] Mean (range)

[b] Frequency/10^5 (range).

[c] Yields exceeding 100% of the progenitors are commonplace, possibly due to the removal of inhibitory elements in the buffy coat cells. This is especially true with GEMM-CFC

MONOCLONAL ANTIBODIES OF INTEREST FOR BONE MARROW TRANSPLANTATION

Cluster (Antigen) Antibody	Acute leukemias [a]	Cell lines [b]	Progenitors [c]	BMT
CD1 (49 kDa, T1a-like) – (also D47, M24, anti-T6a)				
Leu6	T-ALL [130]			
NA1/34	T-ALL [131]	T, My [131,132]		
OKT6	ATL [133,134]			
CD2 (50 kDa, E_r receptor) – (also D66, HuLy M1, NEI-016, 5FC1, 3pt2H9, a151)				
CT-2				41 pts [41,135]
OKT11	T-ALL, ATL, rare AML [133,136]		not GM-CFC [137]	
anti-T11				10 pts [43,44]
Leu5	T-ALL [130]			
9.6	T-ALL, ATL [131,134]	T [131]		
35.1	not ATL [133]		not GM-CFC, BFU-E, GEMM-CFC [84]	
CD3 (19–29 kDa) – (also 89b1, 38.1, 64.1, anti-T3)				
OKT3	T-ALL, ATL [131,133,134]	T [131]	not GM-CFC [137]	
anti-T3				10 pts [43,44]
Leu4	T-ALL [130]			
UCHT1			not GEMM-CFC [45]	31 pts [138,139]
CD4 (64 kDa) 91D6, anti-T4a				
Leu3A	T-ALL [130]	T, B, My [132]		
OKT4	T-ALL, ATL [131,133,134,140]	T [133]		
CD5 (67 kDa) – (also OKT1, UCHT2, SCI, HH9, IM64, H65, CrisI)				
A50	T-ALL [131]	T, B, My [131,132]		
anti-Leu1				3 pts [141]
T1	ATL [133]			
T2	T-ALL, ATL [134]			
T101		T, B, My [132]	not GM-CFC, BFU-E, GEMM-CFC [45,82,84,85]	39 pts [85,138,139]
10.2	T-ALL [131]	T [131]		
CD6 (100 kDa) – (also 12.1, Leu3a T411, B614, WTG6, anti-T12, Tu33, DGT-3)				
OKT12				1 pt [29]
CD7 (41 kDa) – (also 4a, CL1.3, anti-Leu9, Tu14)				
G3.7			not GM-CFC, BFU-E, GEMM-CFC [84]	
LauA1	T-ALL [142]	T [142]		
3A1	T-ALL, AML [131,143,144]	T, B, My [131,132]		
OKT16	T-ALL [145]		not GM-CFC, BFU-E [145]	
WT1	T-ALL, AUL, AML [146]			
4H9	T-ALL [130]			

Cluster (Antigen) Antibody	Acute leukemias [a]	Cell lines [b]	Progenitors [c]	BMT
CD8 (32–45 kDa) – (also M236, B9.4.1, B9.3.1, B9 7 6, B9.2 4, B9 8 6, B9 1 1, B9 11 10, UCHT4, T811, 51 1, C10, 2D2)				
Leu2a	T-ALL [130]	T, My [132]		
OKT8	T-ALL, ATL [131,133,134,140]	T [131]		
CD9 (p24) – (also FMC8, WB3, CALL1, 3A8, 3A9)				
ALB_6	cALL, B-ALL, AUL, AML [147]			
BA-2	nALL, My-ALL, cALL, T-ALL [148,149]	T, B, My [132]		23 pts [139]
DU-ALL-1	nALL, AML, cALL, T-ALL [150]	T, B, My [132]		
J2			not GM-CFC, BFU-E, GEMM-CFC, LTBMC [62,72,151]	20 pts [152]
SJ9A4	nALL, cALLA, T-ALL, AML [153]	My [153]		
CD10 (100 kDa, CALLA) – (also 24.1)				
ALB_1, ALB_2	cALL, T-ALL, B-ALL [147]			
A12		T, B [142]		
BA-3		T, B, My [132]		23 pts [139,155]
J5	T-ALL, cALL, My-ALL, AUL, rare AML [133,134,148,149,156,157,159]	B [154]	not GM-CFC, BFU-E, CFU-E, GEMM-CFC LTBMC [66,72,151,158]	33 pts [51,61,90,152]
NL-1	cALL, My-ALL, nALL, ATL, AML [132,160,161]	T, B [161]		
VIL-A1	nALL, T-ALL, B-ALL [162]			
CDw11 (95/170 kDa, CR3) – (also M522, B43.4, FK24, MN41, anti-MAC1, CC1 7, M3D11, K1-M5, 44)				
B2.12	AML [163,164]	My [165]		
D12		My [166]	not GM-CFC, BFU-E, GEMM-CFC [166,167]	
Mo1	AML [133,156,163,169]	My [168]	not GM-CFC, GEMM-CFC [168–170]	
OKM1	AML [134,144,163,164,172–174]		not GM-CFC, BFU-E, CFU-E [171]	
VIM12	nALL [85]		unreactive [175]	
60.1	AML [167]		not GM-CFC, BFU-E [167]	
CD12 (NR)				
M-67	AML [163]			
20 2	AML [163]			

CDw13 (160 kDa)				
DU-HL60-4	AML [163]	My [176]	55% GM-CFC [176]	
MCS-2	AML, nALL, rare cALL [163,177,178]	My [132]		
My7	AML, T-ALL [163,170]		50% d7, d14 BM, GM-CFC not PB, GM-CFC, BFU-E, CFU-e [170,179]	
86H1	T-ALL, AML [167,180]	My [166]	? GM-CFC, not BFU-E, GEMM-CFC [166,167]	
CDw14 (85 kDa, 55 kDa) – (also TM18, MA5, SCHL3, Ki-M1, CIM, F13, B44 1, FA6-152)				
AML-2-23	AML [163,169,181]	My [181]	54% d7, 29% d14 GM-CFC, 10% GEMM-CFC [169]	
CRIS-6			15% GM-CFC [166]	
FMC17	AML [163]			
Leu-M3	AML [163,172]			
MoS-1	AML [163]			
MoS-39	AML [163]			
Mo2	AML [156,163,169,174]	My [180]	not GM-CFC, GEMM-CFC [169]	
My3	AML [163,169,174]		not GM-CFC, GEMM-CFC [169]	
My4	AML [163,170,174,181]		unreactive [170]	
M5E2	AML [183]	? My [166,183]	? GM-CFC, 65% Meg-CFC [166,183]	
UCHM1	AML [163,173]		not d14 GM-CFC [166]	
VIM13			unreactive [175]	
5F1	AML, My, ALL [149,163,174,183]	My [165,183]	not GM-CFC, BFU-E, 70% CFU-E [166,183–185]	
20.3	AML [163]			
CDw15 (LeX) – (also LMA-3, HG-2, ANHI-6, WM41, FK32, UM30, G1120, WM38, HG-1, WM37, G9F7, WM27, LMA-1, D-1-36-32, SSEA-1, VEP8, VEP9)				
B4 3	AML [144,163,164]			
B13.9	AML [144,164]			
CBL-gran7	AML [183	My [166,183]	? d14 GM-CFC [166,183]	
Du-HL60-1	AML, ALL [163,176]	My, T, B [176]		
Du-HL60-3	AML, ALL [163,176]	T, B, My [176]		
FMC10	AML [141,163]			
FMC12	AML [163]			
G2	AML, ATL [133,163]			
G7C5		My [166,167]	? GM-CFC, not BFU-E, GEMM-CFC [166,167]	
HLC5		My [166]	not GM-CFC, BFU-E [166,183]	
MCS-1	AML, nALL [163,177]	My [132]		
My1	AML [163]			
M1/N1	AML [144,163,164]			
PM-81	AML, cALL [163,169,186]	My [69,186]	d7, ? d14 GM-CFC, not BFU-E, GEMM-CFC [169,186,187]	7 pts [266]
R1B19	AML [163,188–190]		Portion GM-CFC, ? BFU-E, not GEMM-CFC, LTBMC [187,188,191,192]	

TABLE II (continued)

Cluster (Antigen)				
Antibody	Acute leukemias [a]	Cell lines [b]	Progenitors [c]	BMT
S4-7	AML [163,188–190]		Portion GM-CFC, not BFU-E, GEMM-CFC, LTBMC [187,188,191,192]	
TG-1	AML [163,173]		not GM-CFC, BFU-E, CFU-E [193]	
TG8	AML [163]			
UJ308	AML [144,163,164]			
VIM8		My [166,167]	? GM-CFC, not BFU-E, GEMM-CFC [166,167,175]	
VIMC6		My [166,167]	? GM-CFC, not BFU-E [166,167]	
VIM-D5	AML [144,163,172]		50% d7, not d14 GM-CFC, BFU-E, CFU-E [178]	
WGHS-29-1			Portion of GM-CFC and BFU-E [187,191]	
1/12/13	AML [174]			
1G10	AML, My-ALL [163,174]	My [166]	? GM-CFC, not BFU-E, CFU-E [166,167,184,185]	
28	AML [163,173]	My [166]	d14 GM-CFC [166]	
29		My [167]	not GM-CFC, BFU-E [167]	
80H5	not ALL [180]	My [180]	? GM-CFC, not BFU-E, CFU-E [167,180]	
82H5	not ALL [180]	My [180]	Portion of GM-CFC, ? BFU-E, not CFU-E [166,167,180]	
82H6	not ALL [180]	My [180]	? GM-CFC, not BFU-E, CFU-E [167,180]	
82H7	AML [163,180]	My [180]	GM-CFC, not BFU-E, CFU-E [180]	
CD16 (FcR on granulocytes) – (also CBLFcRgran, BW209/2, CBLgran11, VEP 13, G0226)				
BW 243/41		My [166]	not GM-CFC [166]	
CDw17 (lactosylceramide) – (also G035)				
T5A7	AML (167)		CFU-E, not GM-CFC, BFU-E, GEMM-CFC [166,167,184,185]	
CDw18 (LFA, β chain) – (also MHM23, CBL-LFA-1/1, TSI/18 11, OKTM10)				
TA-1	AML [163,174,194,195]	T [195]	not GM-CFC, BFU-E, GEMM-CFC [45,76]	32 pts [138,139]
60·3			not GM-CFC, BFU-E [167]	
CD19 (24/68 kDa) – (also HD37, 4G7, SG25-C1)				
B4	cALL, nALL [159,196]			
Leu12	nALL [148]			

CD20 (35 kDa) – (also TC3/16, 1F5)				
B1	cALL, B-ALL [134,148,159, 166,174,196,197]	B [198]	not GM-CFC, BFU-E, GEMM-CFC, LTBMC [61,64,151]	8 pts [67]
2H7	cALL [149]			
CD21 (160 kDa) – (also HB5, BL-13)				
B2	some nALL [174,195,199]			
CD22 (135 kDa) – (HD6, HD39, SHCL-1, 29-110, SJ10-1H11) [128]				
CD23 (45 kDa) – (BLAST-2, PL-13, MNM6) [128]				
CDw24 (45/55/65 kDa) – (also HB8, HB9)				
ALB_7,				
ALB_8,				
ALB_9	cALL, B-ALL, AML, AUL [147]			
BA-1	B-ALL, cALL, nALL [148,149, 174,194,200]	B, My [200]		23 pts [139,155]
VIB-C5	cALL, B-ALL, nALL [162]			
CD25 (25 kDa, IL-2 receptor) – (also TAC/1HT4-4H3, T1a, B149 9, 23A9 3, 33B3 1, 39C6 5)				
anti-TAC	ATL [133]			
CD26 (TII19-4-7, TS145, 4EL1C7) [127]				
HLA A, B, C – (also 10H7, 81H2, NC6, 264B8, BB7 7)				
Q1/28			GEMM-CFC [201]	
W6/32		T, B, My [142]		
HLA-DR (28/33 kDa) – (also 3HBB14, 7H3, 8H7, 9-49, NE1-011)				
Various	AML, cALL, nALL, T-ALL, ATL [133,134,148,164,170]		GM-CFC, BFU-E, not CFU-E, ? LTBMC [71,170,202]	2 pts [71]
B5 1			GM-CFC [203]	
B8 11 2			LTBMC [204]	
DA_2	AML [173]			
D4-22		B [142]		
HB10a			GM-CFC, LTBMC recovery slow? [205]	
I2	AML [169]		GEMM-CFC [169]	
L-243			GM-CFC, BFU-E [166,187]	
NC1			GM-CFC, BFU-E	
NL-12	n-ALL,T-ALL, ATL [161]	B [161]		
OKIa-1	AML [144,172,206]			
Q 2/47			GEMM-CFC [201]	
Q 5/13			GEMM-CFC [201]	
RFB-HLA-DR			all GM-CFC, BFU-E, CFU-E, meg-CFC, GEMM-CFC [207]	
S1-19-9	AML [188–190]		GM-CFC, BFU-E, GEMM-CFC, not LTBMC [188,192]	

TABLE II (continued)

Cluster (Antigen) Antibody	Acute leukemias [a]	Cell lines [b]	Progenitors [c]	BMT
YD1/63			marmoset GM-CFC [208]	
YE2/36			GM-CFC [137]	
4.1	nALL, My-ALL, cALL, rare T-ALL [149]			
7.2			81% GM-CFC, delayed LTBMC? [205]	
HLA-DQ				
Tu22			not GM-CFC [166]	
Genox 3.53			not GM-CFC, BFU-E, CFU-E, LTBMC [171,204]	
F-5C9			50% GM-CFC [203]	
IIb.3			not LTBMC [204]	
B_2M (β-2-Microglobulin) – (also M18, M28, BB5, EC3)				
AML-1-201			GM-CFC, BFU-E [186]	
B_2M			LTBMC [151]	
(37 kDa) – (also Tu1)				
BB1	nALL [209]			
IIb/IIIa – (also TD80)				
EDU3, J.15			not GM-CFC [166,167], BFU-E, GEMM-CFC [167]	
C3b/C4b				
E11	AML [163,173]			
E2A7			GM-CFC [166]	
HL-1	AML [160,163]			
HL-21	AML [160,163]			
(95 kDa) – (also B9.8, B13.4, MPA)				
My8	AML [163,170,174]		unreactive [170,210]	
Mo5	AML [168]		not GM-CFC [166]	
(67 kDa)				
My9	AM [163,169,183]	My [183]	? GM-CFC, portion CFU-E, BFU-E, meg-CFC, GEMM-CFC [166,169,183]	
L1B2	AML [183,184]	My [183]	? GM-CFC, portion BFU-E, GEMM-CFC, meg-CFC [166,167,183–185]	
L4F3	AML [183]	My [183]	GM-CFC, portion BFU-E, CFU-E, meg-CFC, not LTBMC [183–185,211]	3 pts [212]

(115 kDa)			
My10	AML, cALL, nALL [213]	My [213]	GM-CFC, BFU-E [213]
12-8			GM-CFC, BFU-E, GEMM-CFC, LTBMC [211,214]
B1-3C5	AUL, AML, nALL, cALL [215]	My [215]	GM-CFC, BFU-E Meg-CFC, GEMM-CFC [216,217]
(Lacto-*N*-neotetraose, I blood group) – (also M39 6, 1B2)			
My28	ALL, AML [218]	My [218]	
(180 kD, 90 kDa, transferrin receptor) – (also B 3/25, 3H2)			
OKT9	T-ALL, some AML [130,157]	T [157]	not GM-CFC, portion BFU-E, CFU-E [157,171,219]
L5-1	AML [188]		portion GM-CFC [188]
5E9	T-ALL [131]		
L22	nALL [220]	T, B, My [132,209]	
(also HeLe 1)			
OKT10	T-ALL, myeloma, AML [130,144,164,221,222]		GM-CFC, BFU-E, CFU-E [168,171]
(Glycophorin) – (also 39)			
R10	AUL, M6-AML [157]		
VIE-G4	M6-AML [144,162,223]	My [223]	
(20 kDa)			
S5-7	AML [163,188]	T, B, My [224]	portion of GM-CFC [188]
K15 1 19		T, My [236]	d7 GM-CFC, BFU-E [236]
(Carbohydrate)			
Tu3	AML [163]		
VIM-2	AML, rare cALL, T-ALL [163,175,183,225]	My [183,225]	portion GM-CFC, BFU-E, ?CFU-E, meg-CFC [175,183]
Unclustered			
AA1 (58 kDa)	T-ALL [226]	T, B, My [227]	
AHN-1	AML, ALL [228]		not GM-CFC [228]
AHN-2			not GM-CFC [228]
AHN-3			not GM-CFC [228]
AHN-7	AML [228]		67% GM-CFC [228]
AHN-8	rare AML [228]		not GM-CFC [228]
ATL27	T-ALL [160,226]		
A9	cALL, B-ALL, AML [229]	B, T [229]	
BL-1 (GL)	cALL [148,220]	B [220]	
BL-2 (68 kDa)	cALL (148,220]	B [220]	
BL-3 (105 kDa)	cALL [148,220]	B [220]	
BL-7 (GL)	rare cALL [148]		
BW 227/19			27% GM-CFC [166]
BW 242/408			not GM-CFC [166]

TABLE II (continued)

Cluster (Antigen)				
Antibody	Acute leukemias [a]	Cell lines [b]	Progenitors [c]	BMT
BW 252/104	AML, T-ALL, cALL [183]	My B [183]	GM-CFC, portion BFU-E, CFU-E, meg-CFC [183]	
B4 3	AML [206]			
B5	ATL [133]			
B7	ATL [133]			
B43	nALL [86]	B [86]	not GM-CFC, BFU-E, GEMM-CFC, LTBMC [86,230]	
CALL-2	T-ALL [231]	T [231]	not GM-CFC [231]	
CAMAL-1 (68 kDa)	AML [232,233]			
CAMPATH-1			unreactive [32]	16 pts [33,36,37]
CA-2-23	AML [163]			
CF-1	AML, ALL [234]	My [92,234]	not GM-CFC, BFU-E, GEMM-CFC, [234]	
C17	AML [144]			
C711	AML [183]	My, B [183]	CFU-E, not BFU-E [183]	
D5	AML [162,174]	My [165]		
D5D6	AML [172,174]			
E10	T-ALL [226]			
FA6-152	AML [235]	My [235]	majority CFU-E, 50% d12, not d16 BFU-E, GM-CFC or meg-CFC [235]	
FMC7	unreactive [174]			
G022b (38 kDa)	My [167]		not GM-CFC, BFU-E, GEMM-CFC [167]	
G7C10			not GM-CFC [166]	
G9F9	AML [183]	My [166,183]	? d14 GM-CFC [166,183]	
HLe-1			GM-CFC (weak) [193]	
H8 4 5 (67–74 kDa)		My [236]	GM-CFC, not BFU-E [236]	
H207 (105 kDa)	T-ALL [226]			
JD2		My [166]	not GM-CFC [166]	
JOAN-1	AML, T-ALL [167,183]	My, T, B [167,183]	GM-CFC, BFU-E, GEMM-CFC, meg-CFC, 76% CFU-E [167,183]	
LB3-45	AML [163,188]		GM-CFC, BFU-E, GEMM-CFC [188,192]	
Leu-M1	AML [163]			
Leu-M2			d14 GM-CFC [166]	
Leu7			d14 GM-CFC [166]	
LB3-37	AML [163,188]		not GM-CFC [188]	

M-G1120	AML [163]		
M-M522	AML [163]		
MAC-120 (120 kDa)	not AML [174]		
MB1		My [166]	25% GM-CFC [166]
MCCH36.71	AML [163]		
MHM31 (190/110 kDa)		My [167]	not GM-CFC, BFU-E, GEMM-CFC [167]
MLR-2			GM-CFC [237]
Mono	AML [140]		
MoP-15	AML [163]		
Mo3	AML [156]		
Mo4 (100 kDa)	AML [156,163]		
Mo6 (80 kDa)	AML [168]		
My901	AML, cALL [170]		unreactive [170]
My906	AML [170]		GM-CFC, BFU-E, CFU-E [170]
M3D11		My [166,167]	not GM-CFC, BFU-E, 50% GEMM-CFC [166,167]
M5D12	AML, cALL [183]	My [166,183]	d7, d14 GM-CFC, portion CFU-E, BFU-E, meg-CFC [166,183]
Nat-9II · 3F-6F (97 4 kDa)	AML [238]	My [238]	not GM-CFC [238]
NHL-30 5 (180 kDa)	AML, ALL [239,240]		CFU-E, BFU-E, GM-CFC [239]
NKH2 (60 kDa)			not GM-CFC, BFU-E, GEMM-CFC [166,167]
NKH1A			not GM-CFC [166]
NL-2	nALL [160]		
NL-4	nALL, rare ATL, AML [161]	My [161]	
NL-8	nALL, T-ALL, ATL, AML [161]	B, My [161]	
NL-9	nALL, ATL, AML [161]	My, T [161]	
NL-22	nALL [161]	B [161]	
NL-25	nALL, T-ALL, ATL, AML [161]	B, T [161]	
NL-30	nALL, ATL, rare AML [161]	My [161]	
N16 (blood group A)			BFU-E, CFU-E, GM-CFC [171]
OKB1	cALL, T-ALL [241]	B, My, T [242]	
OKB2	cALL, AML [148,241]	B, My [242]	
OKB4 (87 kDa)	cALL [241]	B, My [242]	
OKB7 (175 kDa)	unreactive [241]	B, My [242]	
OKT17	T-ALL [143]		
PCA-1, PCA-2 (26 kDa)	myeloma [222]		

TABLE II (continued)

Cluster (Antigen) Antibody	Acute leukemias [a]	Cell lines [b]	Progenitors [c]	BMT
PLT-1	not AML [156]			
P1153/3 (20 kDa)	c-ALL, B-ALL, n-ALL, AUL [174,243]	B [243]		
PMN1	AML [183]	My [183]	46% d7, not d14 GM-CFC [183]	
PMN3	AML [183]	My [166]	not d7, d14 GM-CFC [183]	
PMN 6	AML [163,181]	My [181]		
PMN 29	AML [163,181]	My [181]	unreactive [187]	
RFB-1	cALL [207]		GM-CFC, meg-CFC, BFU-E, CFU-E, GEMM-CFC [207]	
R6A (band 3)			portion of BFU-E, CFU-E, GM-CFC [171]	
RUP1-4	AML [144]			
RUP1-5	AML [144]			
SFL23 6 (neuraminidase-sensitive		My, T [244]	CFU-E, portion of BFU-E, not GM-CFC, GEMM-CFC [244]	
SHCL3 (150/90 kDa)			not BFU-E, GM-CFC [167]	
Sm0	AML [163,173]			
S1-37	AML [188]		not d7, d14 GM-CFC [188]	
S3-13 (29 kDa)	AML [163,188–190]	T, B, My [224]	GM-CFC, BFU-E, GEMM-CFC, LTBMC, 55% CFU-E [187,188,191,192]	
S8-6	AML [163,188–190]		GM-CFC, BFU-E, GEMM-CFC, LTBMC [188,192]	
S16-89	AML [188]		portion of GM-CFC [188]	
S16-109	AML [188]		GM-CFC, BFU-E, LTBMC, 75% CFU-E [188, 192]	
S16-144	AML [163,188–190]		GM-CFC, BFU-E, GEMM-CFC, LTBMC, 64% CFU-E [188,192]	
S17-12	AML [163,188]		? GM-CFC, [188,191]	
S17-14	AML [163,188]		Portion GM-CFC, BFU-E, GEMM-CFC [188,192]	
S17-25			GM-CFC, BFU-E, GEMM-CFC [188,191,192]	
TEPC 183			not GM-CFC [228]	
TM2 (TM3) (120 kDa)	AML, AUL, cALL [245]	My [245]	GM-CFC, not BFU-E, CFU-E [245]	
TM2 26	AML [183]	My, T [167,183]	portion GM-CFC, BFU-E, CFU-E, meg-CFC [183]	

TM18	AML [163]		
Tu2	AML [163]		
Tu5	AML [163]		
Tu9	AML [163]		
T10C6		My [166]	portion GM-CFC [166]
UCHALF (lactoferrin)	AML [163,173]		
UC45 (fibrin)	AML [173]		
VIM-D2	AML [163]		
VIM S8	AML [144]		
VIM10 (165 kDa)			not GM-CFC, BFU-E, GEMM-CFC [167,183]
VIM11 (carbohydrate)			not GM-CFC, BFU-E, CFU-E [175]
VIE-G6	AML [172]		
WBH-A9	cALL, T-ALL [246]		
WBH-H7	nALL, T-ALL [246]	My [246]	
YB5 B8	AML [247]	unreactive [247]	
3-3	T-ALL [248]	T [248]	
3-40	T-ALL, cALL, AML [248]	T [248]	
3C4	AML [163]		
4F2 (40/80 kDa)	T-ALL		
5 5	AML [173]		
9 3 (44 kDa)	T-ALL [131]	T [131]	
63D3 (200 kDa)	AML [163,174]		
75B10	AML [163]		
76/59	AML [249]	My [249]	portion GM-CFC, BFU-E, CFU-E [249]
80H3	AML [163,180]	My [180]	unreactive [180]
82H1	AML [180]	My [180]	GM-CFC, not BFU-E, CFU-E [180]
82H3	AML [180]	My [180]	unreactive [180]
86H3	AML [180]		
80/107	AML [249]	My [249]	
81/24	AML [249]	My [249]	portion GM-CFC [249]

---

[a] T-ALL = T cell acute lymphoblastic leukemia; ATL = adult T cell leukemia; AML = acute myelogenous leukemia, M-6 = acute erythroblastic leukemia, AUL = acute undifferentiated leukemia, cALL = common acute lymphoblastic leukemia, B-ALL = B cell acute lymphoblastic leukemia; nALL, null cell acute lymphoblastic leukemia; my-ALL, 'myeloid' acute lymphoblastic leukemia (ALL with myeloid markers)

[b] T, T cell lines; B, B cell lines; My, myeloid cell lines

[c] LTBMC, long-term bone marrow cultures, CFU-E, colony-forming unit – erythroid; PB, peripheral blood, meg-CFC, megakaryocytic colony-forming cell

reactivities with acute leukemia cells, hematopoietic or leukemia cell lines, hematopoietic progenitors, and applications in allogeneic or autologous bone marrow transplantation are included in the table along with the relevant references. Where discrepancies exist regarding the reactivities, a question mark is printed.

MA by themselves do little to the cells to which they bind, and thus a number of methods for the elimination of monoclonal antibody-reactive cells from aspirated bone marrow have been investigated.

IVB. Complement-mediated lysis

A popular method of eliminating certain cells from marrow aspirates has involved the use of complement. Complement is a series of enzymes in the blood which are activated by interaction with immune complexes and certain nonimmune substances [250], initiating a proteolytic cascade, and result in cell lysis. Although an attractive concept at first sight, a number of complexities arise in the use of complement with murine monoclonal antibodies and human bone marrow cells. In the first place, not all murine monoclonal antibodies fix complement. Only those which perform well in complement-mediated lysis are candidates for this procedure. Secondly, human complement does not work well with many mouse monoclonal antibodies. This dictates the use of a xenogeneic complement source. Purified complement components are not available, which necessitates the use of xenogeneic serum as the source. Complement activity of serum is notoriously unstable, and standardized analysis of its activity after storage is required. The xenogeneic serum contains antibodies of unknown specificity, many of which react with surface components of human cells [250]. While these 'facilitating' antibodies may increase the efficiency of lysis on monoclonal antibody-reactive cells, they increase the possibility of lysis of monoclonal antibody-unreactive or minimally reactive progenitor cells, and leave some degree of uncertainty as to the immunological specificity of the reaction. Since these antibodies cannot be assumed to be constant from each lot of serum used for complement, reproducibility may suffer. Thirdly, high cell number, erythrocytes, and unsubstituted cell surface sialic acid residues inhibit complement activation [250], necessitating large volumes of cells at low concentration. A single incubation is rarely sufficient, and often three cycles of complement-mediated lysis are required. Fourthly, the lysed cells cause clumping and progenitor loss, and are difficult to remove from the remaining live cells. Consequently, the lysed cells are often infused with the live cells. Fifthly, fragments of complement components released during the proteolytic cascade are profound immunoregulators [251] with unknown effects on hematopoietic elements and lymphoid recovery. Finally, it is extremely difficult to reproducibly obtain even two logs of monoclonal antibody-reactive cell removal [252], and while this may be adequate for allogeneic BMT, it is insufficient for autologous BMT.

There are a large number of monoclonal antibodies available for use in BMT (see Table II), and it is possible, for several specificities, to obtain antibodies which fix complement, even human complement in some cses. The nonspecific toxicity of rabbit complement can be decreased by using neonatal rabbit serum, taken at a time when the maternal antibodies have decreased and prior to the maturation of the bunnies' humoral response. These precautions, however, have not always led to a reproducible procedure.

As an example of the irreproducibility of this procedure, several groups have reached divergent opinions about the reactivity of certain monoclonal antibodies with progenitors. Thus, discrepancies exist between reports of the lysis of GM-CFC by 86H1 [166,167], M5E2 [166,183], CBL-gran 7 [166,183], G7C5 [166,167], PM-81 [[169,186], VIM-8 [166,167,175], VIM-C6 [166,167], 80H5 [167,180], 82H5 [166,167,180], 82H6 [167,180], T5A7 [166,167,184], G9F9 [166,183], L1B2 [166,167,183–185] and My9 [166,183].

Another major concern, possibly related to anticomplementarity, is that there are reports that antibodies which fix complement can bind to cells, but the antibody-coated cells are not lysed in some cases [253,254]. These problems have been discussed previously by others [56].

Complement has been used in a number of studies in conjunction with monoclonal antibodies for the removal of T cells, leukemia cells and other tumors (summarized in Table I).

IVC. Immunotoxins

Immunotoxins are often efficient at cell killing, but their biochemical preparation is somewhat complicated. One of the major drawbacks to the use of immunotoxins with acute leukemias can be the number of different immunotoxins which may be required to eliminate heterogeneous leukemia cells such as are present in AML. Immunotoxins can require lengthy periods to exert their effects on target cells, and their activities are dependent on the biochemical preparation as well as incubation conditions. Although GM-CFC and BFU-E were not affected by T101-ricin A chain IT used for treatment of T-NHL and T-ALL marrows, a decreased recovery was observed after freezing. This may indicate that residual IT in treated autologous marrow might be toxic to progenitors after thawing the cryopreserved marrow [85]. Nevertheless, a great deal of effort has been expended in their use with BMT (summarized in Table II). The production and use of immunotoxins has recently been reviewed by Vallera and co-workers [45].

IVD. Physical separation

Other approaches have been based on physical separations of bone marrow cell populations. The first attempts in this vein preceded the advent of monoclonal antibodies. Separation of bone marrow cells on the basis of density was accomplished in discontinuous albumin gradients [255]. Although leukemia cells could be separated from hematopoietic progenitors the separation was only about 90%, and transplantation with this separated marrow could not be expected to have any biological effect [255]. We first attempted to use monoclonals with colloidal gold to alter the density of reactive cell populations [50]. We then realized that a paramagnetic colloidal material with antibody bound to its surface might allow a simplified method for cell separation.

We accomplished initial feasibility trials in 1983 [90] and Kemshead et al. [88] reported a magnetic microsphere separation the same year. Using the anti-CALLA monoclonal antibody J5, we treated four autologous marrows with colloidal cobalt with bound affinity-purified IgG fraction of goat anti-mouse immunoglobulins. The patients transplanted were in second or subsequent remissions, thus making it unlikely that removing leukemia cells from bone marrow could have a biological effect. No toxicity resulted from this procedure, however, and rapid hematopoietic recovery was observed in these transplants. We decided that the results were encouraging enough to warrant optimizing the procedures involved in the production of immunomagnetic fluids and in the procedures used for separation. We have now produced a stable, colloidal cobalt-based immunomagnetic fluid and an improved high magnetic gradient separation column (Reading, Thomas and Chandran, manuscript in preparation). We have started to test this colloid with anti-T cell MAs to remove T cells from an allogeneic marrow (Reading and Dicke, unpublished data).

The magnetic microspheres used by others [88] have been used for the separation of tumor cells from autologous marrows of neuroblastoma patients and recently to remove T cells from marrows used for allogeneic transplants [256]. Immunoabsorption (panning) has also been used to remove lymphocytes from bone marrows (Table III), but dealing with $(2–4) \cdot 10^{10}$ cells may well be beyond the practical capabilities of this technique.

Unlike the procedures involving complement or immunotoxins, the physical methods offer two additional advantages. They can be used to select in a positive sense for monoclonal antibody-reactive cells, and they can be used with other affinity systems such as lectins and receptor-ligand binding.

In certain model systems we have recently demonstrated selective removal of greater than $2\frac{1}{2}$ logs of leukemia cells with retention of 70% of MA-unreactive cells [46,92]. Although this is a relatively new technique, we anticipate efficient removal of monoclonal antibody-reactive cells from both allogeneic and autologous marrows in the near future using magnetic separation with colloidal immunomagnetic fluids.

V. Monitoring systems

The most common analysis of preservation of hematopoietic restoration potential of treated bone marrow has been the use of in vitro clonogenic

TABLE III

ELIMINATION OF CELLS FROM BONE MARROW WITH MONOCLONAL ANTIBODIES AND COMPLEMENT

Abbreviations: BM = bone marrow, SCID = severe combined immunodeficiency disease, NR = not reported, PB = peripheral blood, IF = immunofluorescence, FMF = flow microfluorimetry, CTL = cytotoxic T lymphocytes, ALL = acute lymphoblastic leukemia, ^{125}IUdR = 5-[^{125}I]iodo-2′-deoxyuridine

Antibodies	C′	Cells	Progenitors	Reported efficiency	Monitoring	Ref
T cells						
Anti-Thy-1.2	rabbit	murine BM	no decrease	> 95%	microcytotoxicity	28
Anti-T12	rabbit	SCID	NR	> 99.9%	IF, PHA	29
OKT3, -11A, MBG6	rabbit	human BM	no decrease	> 90% (each Ab), > 99% (combination)	IF, PHA, MLC	31
CAMPATH 1	human	human BM	no decrease	> 99%	IF, PHA, ConA	32
CAMPATH 1	human	human BM	not seriously affected	some detected, 8/10 pts	Er	33
OKT3, Lyt-3, Leu-1	rabbit	human BM	no decrease	89% by Er	IF, Er, FMF, ^{3}H uptake	34
CT-2	human	cadaver BM	no decrease	> 90%	Er, PHA, Con A, MLC	35
CAMPATH 1	human	human BM	no decrease	99.8%–100%	Er, no GVHD in 11 pts, IF	36, 37
MBG6, RFT8	rabbit	human BM	no decrease	> 99%	FMF, no GVHD 11/13, Grade 1 GVHD 2/13	38
35.1, 10.2, etc	rabbit	human BM, PB	no decrease	> 99.9%	IF, IF after culture, T cell clones	39
CT-2	human	cadaver BM	no decrease	94%	IF, Er, T cell clones	40
CT-2	rabbit	human BM	no decrease	97%	IF, Er, PHA	41
OKT3 and OKT11A	rabbit	human BM	no decrease	> 97.5%	IF, CTL	42
OKT-3, OKT-11	rabbit	human BM	54–95% rec.	60–98%	IF, no GVHD	43,44
Leukemia cells						
J5	rabbit	human BM CALLA (+) ALL	NR	NR	^{51}Cr release, IF, FMF, 2 or 4 survived more than 1 yr	54

Anti-cALL	rabbit	human BM 2 ALL pts	no decrease	NR	died days 7, 50	58
Anti-L1210	rabbit	murine BM L1210 leukemia	NR	NR	90% survival of mice	59
J5	rabbit	CALLA (+) ALL	NR	99%	^{51}Cr release	62
BA-1, BA-2	human	human BM + ALL cell lines	NR	98%	dye exclusion, ^{51}Cr release	64
BA-1, BA-2, BA-3	rabbit	human BM + ALL cell lines	no decrease	4 logs	FMF, colony assay	68
PM-81	rabbit	HL-60 + human BM	No effect d14 GM-CFC	3–4 logs	colony assay	69
Ba-1, BA-2, BA-3 + Mafosfamid	rabbit	ALL cell lines + human BM	37–100% rec.	2 1–6 logs	clonogenic assay	70
Anti-HLA DR (5 MA)	rabbit	human BM	29% rec	NR	2/2 pts surviving	71
Other tumors						
Fib-75	rabbit	human BM + carcinoma cells	insignificant decrease	5 logs	colony assay, dye exclusion, ^{51}Cr	60
Various Abs	rabbit	neuroblastoma leukemias	NR	NR	^{51}Cr, ^{125}IUdR, colony growth	63
TFS-2	rabbit	human BM + small cell lung carcinoma	no decrease	> 95%	cloning assay	65
Anti-B1, J-5, J-2	rabbit	Burkitt's tumor cells	no decrease	3 logs	cloning assay	66
Anti-B1	rabbit	human BM + B-cell NHL	NR	95–99%	IF, FMF, promt hematologic and immunologic reconstitution	67
J5, B1, J2 + *4HC*	rabbit	Burkitt's	GM-CFC lost but Dexter culture OK	5 logs	clonogenic assay	72

TABLE IV

IMMUNOTOXINS USED TO ELIMINATE CELLS FROM BONE MARROW ASPIRATES

NR, not reported.

Immunotoxin	Bone marrow	Progenitors	Reported efficiency	Monitoring	Ref
T Cells					
TA-1-ricin, T101-ricin, UCHTI-ricin	human BM	no decrease	NR	PHA assay	45
TA-1-ricin, TA-1-ricin A chain	human PB and leukemic cells	NR	NR	PHA assay, MLR	46
TA-1-ricin, T-101-ricin, UCHTI-ricin	human BM and PB	100-fold less toxic to progenitors than to T cells	NR	cell-mediated lyopholysis	47
TA-1-ricin, T-101-ricin, UCHTI-ricin	human BM	no effect	> 99 5%	PHA, MLR, no GVHD in 2 pts	48
64 1-ricin A	human PB	no toxicity	> 95%	PHA-stimulated protein synthesis	49
Leukemia cells					
TA-1-ricin, TA-1-ricin A chain	human BM, ALL cell line	NR	NR	clonogenic assay	46

W3/25-ricin	murine BM T cell leukemia	NR	99.9%	survival of mouse	73
Anti-mouse Ig-ricin A chain	murine B cell tumor	NR	99.9%	survival analysis	74
Thy 1.1-PAP	murine T cell leukemia cell line	no decrease	unevaluable	protein synthesis	77
SN1-ricin A chain, SN2-ricin A chain	T cell leukemia	NR	nearly complete killing	inhibition of protein synthesis	78
T101- and 3A1-ricin	human BM leukemia cell line	10-fold more resistant	variable (depending on the concentration)	protein synthesis, colony assay	80
T-101-ricin	T cell leukemia cell line	NR	99.99%	colony assay	79
T-101-ricin	T cell leukemia cell line	no toxicity	99.99%	colony assay	82
Anti-Tac-ricin A	adult T cell leukemia	NR	> 99.9%	clonogenic assay, protein synthesis	83
Anti-p67-ricin	T cell leukemia	minimum	6.2 logs	clonogenic assay	84
T-101-ricin A	human BM	15–80% GM-CFC	NR	1/4 remission, 6+ months	85
4 MA-ricin + mafosfamid	T-ALL + human BM	10% rec. GM-CFC	up to 6 logs	clonogenic assay	84
B43-PAP	B-ALL + human BM	50% rec GM-CFC	5.6 logs	clonogenic assay	86
4 MA-ricin	T-ALL + human BM	60% rec GM-CFC	1–4 logs	clonogenic assay	87
T101-ricin A	CEM + human BM	no effect	6 logs	clonogenic assay	82

assays of GM-CFC, BFU-E and GEMM-CFC. The Dexter culture system has only been used in rare instances. The final analysis depends on hematopoietic engraftment after transplantation. It is quite worrying that there is evidence that the in vitro progenitors can be lost after treatment of marrow cells with antibodies and drug treatment without effect on the Dexter cultures, undifferentiated blast colonies [104,105] or on engraftment [72]. We interpret this to mean that the pluripotent hematopoietic stem cell (HSC) is antigenically, metabolically, functionally and probably morphologically distinct from the progenitors measured in the in vitro colony assays. The Dexter system is quite cumbersome and slow to yield the required data, and for these reasons a more rapid clonogenic determination of HSC would be a major step forward in this analysis.

A number of monitoring systems have been used to detect the efficiency of elimination of the unwanted cell population [39,63,252,257,258]. These include dye exclusion or protein synthesis in pure target cell cultrues, ^{51}Cr release, PHA and MLR and Er assays with T cells, in vivo survival analysis in rodents, microscopic indirect immunofluorescence, fluorescent analysis of DNA-stained cells in artificial mixtures, flow cytofluorimetry, and clonogenic analysis of remaining target cells. With the exception of DNA fluorescence, clonogenic analysis and leukemia survival data in rodents, these assays are probably incapable of routinely detecting much less than 1% contamination. This is due to the background levels inherently present in these analyses, and when the level of reactivity is comparable to the background levels the practical limit of the analysis has been reached. These assays certainly cannot compare in sensitivity to the 4–7 log analyses possible with clonogenic assays [61,63,64,74,86,87].

Immunocytochemistry and the dual-marker immunofluorescence technique can in some cases detect as little as 0.1–0.01% residual tumor cell contamination [259] and ultimately these analyses may be the most useful with remission bone marrow samples where the clonogenic fraction of the contaminating tumor cells may be extremely low. Methods for analysis of residual T cells in marrow have recently been reviewed [39]. Clonogenic analysis of tumor cell lines and the DNA fluorescent stain technique for multiple log elimination requires the assumption that all of the tumor cells share the antigen detected by the monoclonal. Due to the instability of the tumor phenotype this may be an unwarranted assumption.

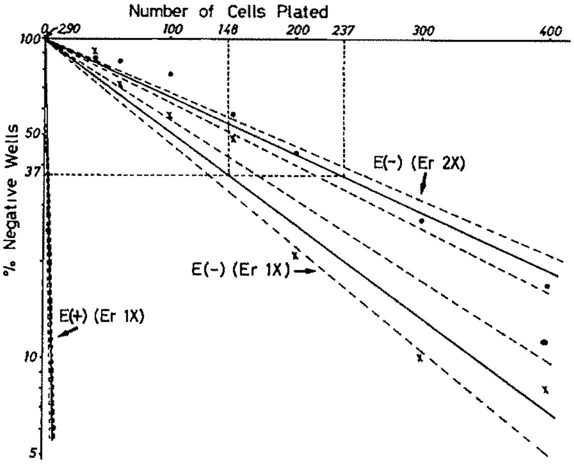

Fig. 2. Limiting dilution analysis of clonogenic T cells after separation by E rosetting. For details, see the text.

We believe that the most valid analysis of efficiency of T cell elimination is the clonogenic analysis of T lymphocytes [39,260–263]. In this analysis, bone marrow cells before and after treatment are stimulated with PHA for 3 days, and cloned at limiting dilution in the presence of interleukin-2. Statistical analysis of the data allows determination of the frequency of remaining clonogenic T cells and analysis of the dependence of clone formation on the presence of helper or suppressor cell types [264].

An example of the application of clonogenic T cell analysis is shown in Fig. 2. Peripheral blood mononuclear cells were rosetted with AET-treated sheep erythrocytes (E) [265] separated on Ficoll-Hypaque and cultured at limiting dilution. The frequency of clonogenic T cells is 1/2.9 for the E(+) fraction, 1/148 for the E(−) fraction after a single rosetting, and 1/237 for the E(−) fraction after two cycles of rosetting. An example of this analysis applied to the elimination of CT-2 positive cells using colloidal immunomagnetic fluid is shown in Fig. 3. In this example clonogenic T cells were reduced to 1/170 bone marrow mononuclear cells. Statistical analysis of the data indicates that there is no deviation from linearity, and thus there are no limiting suppressor or helper cells affecting the analysis.

This analysis has also been applied to elutriation [263], and can detect 1 clonogenic T cell in 10 000 bone marrow cells. Again this analysis was linear, and addition of graded numbers of T cells to this depleted marrow yielded the expected results (data not shown). Beyond 1 clonogenic T cell in 10 000 remaining bone marrow cells, this analysis breaks down because there are too many cells in the 96-well plates to score T cell clones. Adaptation to larger wells in 48- or 24-well plates might overcome this difficulty, but would be substantially more labor-intensive. Others have also concluded that the limiting dilution analysis is the most sensitive method of monitoring T lymphocyte removal [39,260–262].

For any analysis of efficiency of cell removal to be practical it should be performed on a mixture with normal bone marrow cells. This allows concurrent analysis of toxicity to 'bystander' progenitors. The T cell clonogenic analysis currently offers a model to test both elimination and toxicity for

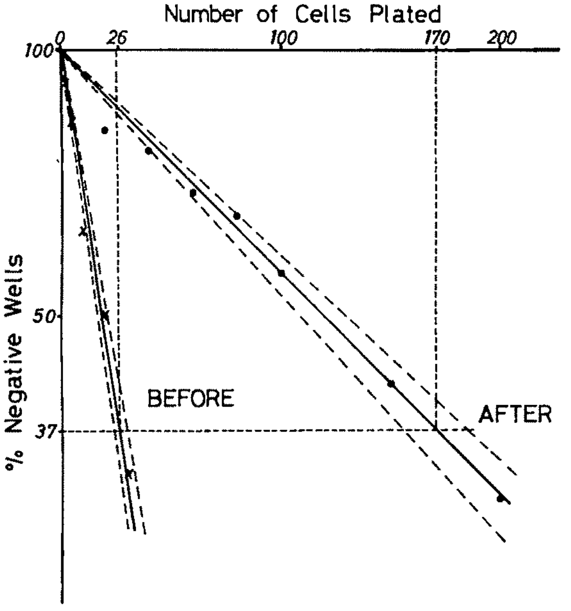

Fig. 3. Limiting dilution analysis of clonogenic T cells before and after separation with monoclonal CT-2 using an immunomagnetic colloidal fluid technique. For details, see the text.

TABLE V

PHYSICAL SEPARATION OF MONOCLONAL ANTIBODY-COATED CELLS IN BONE MARROW ASPIRATES

Antibody	Method	Bone marrow	Progenitor frequency	Reported efficiency	Monitoring	Ref.
6 MA (UJBA, UJ223.8, etc.)	polystyrene magnetic microsphere	human BM neuroblastoma	no significant decrease	99.9%	IF, cloning	89
Leu-1, TM1	panning for T cell removal	human BM	no significant decrease	95%	FMF, PHA, Con A	52
Leu-1, Leu-4	Sepharose 6MB gel	human BM and PB	no significant decrease	98.3%	IF, PHA, FMF	53
J5	cobalt magnetic colloid	2 remission and relapse human BM from CALLA patients	no significant decrease	no positive cells	IF, hematopoietic recovery	90
CF-1	cobalt magnetic colloid	human BM and leukemia cell line	NR	2.5 logs	Clonogenic assay	92
CT-2	magnetite magnetic colloid	PB and BM	no significant decrease	95–99% 97.5%	IF with second T cell antibody T cell colony assay	234

any monoclonal antibody-mediated separation system.

VI. Concluding remarks

As improved cytoreductive regimens are developed, bone marrow transplantation represents an increasingly important method in cancer therapy. One hopes that, some day, less traumatic, more effective therapies will be available for all malignant disease, eliminating the need for such drastic measures as BMT. Until that time we will attempt to increase the survival of BMT patients by eliminating GVHD-reactive cells from allogeneic marrows (estimated at 25% mortality) and by eliminating residual malignant cells from autologous marrow grafts (estimated at 30–40% of the relapse rate). The successful elimination of T cells from allogeneic marrows and the elimination of residual tumor cells from autologous grafts using monoclonal antibodies will be dependent on careful monitoring and incremental increases in efficiency. We currently need improvements in the analyses of hematopoietic restoration potential, immune recovery, and in the detection of minimal residual disease before and after manipulation of autologous marrows.

Acknowledgments

We thank Le Foster for her assistance with the manuscript. This work was supported in part by an NCI grant CA-23077.

References

1 Van Bekkum, D W (1963) Transplantation 1, 39–57
2 Santos, G W. and Haghshenass, M (1968) Blood 32, 629–637
3 Frei, E, III and Canellos, G P (1980) Am J. Med 69, 585–594
4 Herzig, G P (1984) in Advances in Immunobiology Blood Cell Antigens and Bone Marrow Transplantation (McCullough, J and Sandler, S G, eds.), pp 319–335, Alan R Liss, New York
5 Gehan, E.A (1984) Cancer 54, 1204–1207
6 Santos, G W. and Kaizer,. H (9182) Semin. Hematol 19, 227–239
7 Thomas, E D (1983) J. Clin Oncol. 1, 517–531
8 O'Reilly, R J. (1983) Blood 62, 941–964
9 Champlin, R E and Gale, R P (1984) Cancer Treat Rep 68, 145–158
10 Sullivan, K.M. and Storb, R (1984) Cancer Invest 2, 27–38
11 Santos, G W (1984) Cancer 54, 2732–2740
12 Dicke, K.A , Jagannath, S., Spitzer, G , Poynton, C , Zander, A , Vellekoop, L , Reading, C L , Jehn, U.W and Tindle, S (1984) Semin Hematol. 21, 109–122
13 Meyers, J D and Atkinson, K. (1983) Clin Haematol 12, 791–811
14 Deeg, H J. (1984) Br. J Haematol. 57, 185–208
15 Sparkes, M.C , Crist, M.L , Sparkes, R S , Gale, R.P and Feig, S A (1977) Vox Sang 33, 202–205
16 Sprent, J., Von Boehmer, H and Nabholz, M (1975) J Exp Med 142, 321–331
17 Grebe, S C and Streilein, J.W. (1976) Adv. Immunol 22, 120–205
18 Sullivan, K M , Shulman, H M , Storb, R , Weiden, P L , Witherspoon, R P , McDonald, G.B , Schubert, M M., Atkinson, K and Thomas, E.D. (1981) Blood 57, 267–276
19 Korngold, R and Sprent, J (1983) Immunol Rev 71, 5–29
20 Von Melchner, H and Hoffken, K. (1984) Blood 63, 812–817
21 Reisner, Y., Kapoor, N , O'Reilly, R J and Good, R A (1980) Lancet ii, 1320–1323
22 Reisner, Y., Kapoor, N , Kirpatrick, D , Pollack, M S , Dupont, B., Good, R A and O'Reilly, R J. (1981) Lancet ii, 327–331
23 Reisner, Y , Kapoor, N , Kirpatrick, D., Pollack, M S., Cunningham-Rundles, S., Dupont, B , Hodes, M Z., Good, R.A and O'Reilly, R.J. (1983) Blood 61, 341–348
24 Friedrich, W , Goldmann, S.F , Vetter, U., Fliedner, T.M , Heymer, B , Peter, H.H , Reisner, Y and Kleihauer, E (1984) Lancet i, 761–764
25 Rodt, H , Kolb, H J , Netzel, B , Haas, R.J , Wilms, K , Gotze, C.B , Link, H and Thierfelder, S (1981) Transplant. Proc 13, 257–261
26 Prentice, H G., Blacklock, H.A , Janossy, G , Bradstock, K.F., Skeggs, D , Goldstein, G and Hoffbrand, A V (1982) Lancet i, 700–703
27 Filipovich, A H , McGlave, P.B , Ramsay, N K C , Goldstein, G., Warkentin, P I. and Kersey, J H. (1982) Lancet i, 1266–1269
28 Vallera, D A , Soderling, C C B , Carlson, G.J. and Kersey, H (1981) Transplantation 31, 218–222
29 Reinherz, E L., Geha, R , Rappeport, J M , Wilson, M , Penta, A.C., Hussey, R E , Fitzgerald, K.A , Daley, J F , Levine, H , Rosen, F.S and Schlossman, S F (1982) Proc Natl Acad. Sci. USA 79, 6047–6051
30 Hayward, A R , Murphy, S., Githens, J , Troup, G and Ambruso, D (1982) J Pediatr 100, 665–668
31 Granger, S , Janossy, G , Francis, G , Blacklock, H , Poulter, L W and Hoffbrand, A V (1982) Br. J Haematol 50, 367–374
32 Hale, G , Bright, S , Chumbley, G , Hoang, T , Metcalf, D , Munro, A J and Waldmann, H (1983) Blood 62, 873–882
33 Slavin, S , Waldmann, H , Or, R , Cividalli, G , Naparstek, E , Steiner-Saltz, D., Michaeli, J , Galun, E , Weiss, L , Samuel, S , Morecki, S , Bar, S., Brautbar, C , Weshler, Z ,

Hale, G , Rachmilewitz, E A. and Reisner, Y. (1985) Transplant Proc. 17, 465–467

34 Sharp, T G , Sachs, D H., Fauci, A S , Messerschmidt, G L and Rosenberg, S A (1983) Transplantation 35, 112–120

35 Mugishima, H., Terasaki, P I , Sueyoshi, A and Billing, R (1983) Lancet ii, 1194–1195

36 Waldmann, H., Polliak, A , Hale, G , Or, R , Cividalli, G , Weiss, L , Weshler, Z., Samuel, S , Manor, D , Brautbar, C , Rachmilewitz, E.A. and Slavin, S. (1984) Lancet ii, 483–486

37 Hows, J., Parreira, A , Yin, J., Goldman, J and Gordon-Smith, E C. (1984) Exp Hematol. 12, 412 (Abstr)

38 Prentice, H G , Blacklock, H A., Janossy, G., Gilmore, M J M.L , Price-Jones, L , Tidman, N., Trejdosiewicz, L K , Skeggs, D B.L , Panjwani, D , Ball, S , Graphakos, S., Patterson, J , Ivory, K and Hoffbrand, A V. (1984) Lancet i, 472–476

39 Martin, P J. and Hansen, J A. (1985) Blood 65, 1134–1140

40 Mugishima, H , Terasaki, P and Sueyoshi, A (1985) Blood 65, 392–396

41 Mitsuyasu, R.T , Champlin, R E , Ho, W G , Winston, D , Feig, S., Wells, J , Terasaki, P , Billing, R., Weaver, M. and Gale, R P (1985) Transplant Proc 17, 482–485

42 Blazar, B R , Quinones, R R., Heinitz, K.J., Sevenich, E A and Filipovich, A H (1985) Exp Hematol 13, 123–128

43 Herve, P , Racadot, E , Flesch, M., Cahn, J Y., Plouvier, E , Rozenbaum, A , Lamy, B , Noir, A , Leconte des Floris, R. and Peters, A (1984) Exp Hematol 12, 59–60

44 Herve, P , Cahn, J.Y , Racadot, E , Plouvier, E , Flesch, M , Lamy, B and Rozenbaum, A. (1984) Exp. Hematol 12, 412 (Abstr.)

45 Vallera, D A , Ash, R C , Zanjani, E D , Kersey, J.H., LeBien, T.W , Beverley, P.C L , Neville, D M , Jr and Youle, R J. (1983) Science 222, 512–515

46 Vallera, D A., Quinones, R.R , Azemove, S M and Soderling, C.C B (1984) Transplantation 37, 387–392

47 Quinones, R R , Youle, R.J , Kersey, J H , Zanjani, E.D , Azemove, S M , Soderling, C C B., LeBien, T.W., Beverley, P C.L , Neville, D M , Jr and Vallera, D A. (1984) J Immunol. 132, 678–683

48 Filipovich, A H., Vallera, D A , Youle, R J., Quinones, R R , Neville, D.M , Jr and Kersey, J.H (1984) Lancet i, 469–471

49 Martin, P J., Hansen, J A and Vitetta, E S (1985) Blood 66, 908–912

50 Vellekoop, L , Reading, C L , Chandran, M , Tindle, S. and Dicke, K A (1982) Blood 60 (Suppl 1), 174a

51 Poynton, C.H , Reading, C.L. and Dicke, K A (1985) in Autologous Bone Marrow Transplantation (Dicke, K.A , Spitzer, G. and Zander, A R , eds), pp 433–437, The University of Texas M D Anderson Hospital and Tumor Institute, Houston, TX

52 Berenson, R.J , Levitt, L J , Levy, R. and Miller, R A (1984) Transplantation 38, 136–143

53 Greenberg, P L , Baker, S , Link, M and Minowada, J (1985) Blood 65, 190–197

54 Ritz, J. and Schlossman, S.F (1982) Blood 59, 1–11

55 Levy, R. and Miller, R A. (1983) Fed Proc 42, 2650–2656

56 Jansen, J , Falkenburg, J.H.F., Stepan, D E. and LeBien, T W (1984) Semin Hematol. 21, 164–181

57 Treleaven, J G and Kemshead, J T. (1985) Hematol Oncol 3, 65–75

58 Netzel, B., Haas, R.J., Rodt, H , Kolb, H J and Thierfelder, S (1980) Lancet i, 1330–1332

59 Trigg, M.E and Poplack, D G (1982) Science 217, 259–261

60 Buckman, R , McIlhinney, R A J , Shepherd, V , Patel, S , Coombes, R C. and Neville, A M. (1982) Lancet ii, 1428–1430

61 Ritz, J , Sallan, S E , Bast, R C , Jr , Lipton, J M , Clavell, L.A., Feeney, M , Hercend, T , Nathan, D G and Schlossman, S F (1982) Lancet ii, 60–63

62 Bast, R C , Jr , Ritz, J , Lipton, J.M., Feeney, M , Sallan, S E , nathan, D G and Schlossman, S F (1983) Cancer Res. 43, 1389–1394

63 Gee, A P , Graham-Pole, J. and Boyle, M.D P (1983) Exp Hematol 11 (Suppl 14), 7

64 Stepan, D.E , Bartholomew, R.M and LeBien, T W (1984) Blood 63, 1120–1125

65 Okabe, T., Kaizu, T , Ogawa, K , Urabe, A and Takaku, F. (1985) Cancer Res. 45, 1930–1933

66 Bast, R.C , Jr , De Fabritiis, P., Lipton, J , Gelber, R , Maver, C., Nadler, L., Sallan, S and Ritz, J (1985) Cancer Res 45, 499–503

67 Nadler, L.M , Takvorian, T , Botnick, L , Bast, R C , Finberg, R , Hellman, S , Canellos, G P. and Schlossman, S F (1984) Lancet ii, 427–430

68 LeBien, T.W , Stepan, D E., Bartholomew, R.M., Stong, R C and Anderson, J (1985) Blood 65, 945–950

69 Howell, A L and Ball, E D (1985) Blood 66, 649–654

70 LeBien, T W , Andrews, J M , Vallera, D A and Uchun, F M (1986) Leukemia Res 10, 139–143

71 Maraninchi, D., Mawas, C., Mascret, B , Sebahoun, G , Gastaut, J -A., Tublana, N , Perrimond, H , Schavennec, J , Novakovitch, G and Carcossonne, Y. (1985) Exp Hematol 13 (Suppl 17), 28–29

72 De Fabritiis, P , Bregni, M., Lipton, J , Greenberger, J , Nadler, L , Rothstein, L , Korbling, M , Ritz, J and Bast, R C , Jr. (1985) Blood 65, 1064–1070

73 Thorpe, P.E , Mason, D W., Brown, A N F., Simmonds, S J , Ross, W.C J., Cumber, A J. and Forrester, J A (1982) Nature 297, 594–596

74 Krolick, K A , Uhr, J W and Vitetta, E S (1982) Nature 295, 604–605

75 Raso, V , Ritz, J , Busala, M and Schlossman, S (1982) Cancer Res 42, 457–464

76 Vitetta, E S , Krolick, K A , Miyama-Inaba, M , Cushley, W and Uhr, J W. (1983) Science 219, 644–650

77 Ramakrishnan, S and Houston, L L (1984) Science 223, 58–61

78 Seon, B.K. (1984) Cancer Res 44, 259–264

79 Stong, R C , Youle, R J and Vallera, D A (1984) Cancer Res 44, 3000–3006

80 Leonard, J.E , Taetle, R , To, D and Rhyner, K (1985) Blood 65, 1149–1157

81 Vitetta, E.S. and Uhr, J.W (1984) Transplantation 37, 535–538

82 Casellas, P., Canat, X, Fauser, A A, Gros, O., Laurent, G, Poncelet, P. and Jansen, F K (1985) Blood 65, 289–297

83 Kronke, M., Depper, J M, Leonard, W.J., Vitetta, E S, Waldmann, T A and Greene, W.C (1985) Blood 65, 1416–1421

84 Uckun, F M, Stong, R C, Youle, R J and Vallera, D A (1985) J Immunol 134, 3504–3515

85 Gorin, N.C, Dovay, L, Laporte, J P, Lopez, M, Zittoun, R., Rio, B, David, R, Stachowiak, J, Jansen, J, Cazellas, P, Poncelet, P, Liance, M.C., Voisin, G.A, Salmon, C, LeBlanc, G, Deloux, J, Najman, A. and Duhamel, G (1985) Cancer Treat. Rep 69, 953–959

86 Uckun, F.M., Ramakrishnan, G. and Houston, L L (1985) J Immunol. 134, 2010–2016

87 Stong, R C., Uckun, F, Youle, R J, Kersey, J H and Vallera, D A (1985) Blood 66, 627–635

88 Kemshead, J T, Gibson, F J and Ugelstad, J (1983) Proc Am. Assoc Cancer Res 24, 217

89 Treleaven, J G, Gibson, F.M., Ugelstad, J, Rembaum, A, Philip, T., Caine, G D and Kemshead, J T (1984) Lancet i, 70–73

90 Poynton, C H., Dicke, K A., Culbert, S, Frankel, L S, Jagannath, S and Reading, C.L (1983) Lancet i, 524

91 Poynton, C H, Reading, C.L, Chandran, M, Hickey, C M and Dicke, K.A. (1983) Exp Hematol. 11 (Suppl 14), 192

92 Dicke, K.A., Pynton, C H and Reading, C.L (1984) in Minimal Residual Disease in Acute Leukemia (Lowenberg, G. and Hagenbeek, A., eds), pp 209–221, Martinus Nijhoff Publishers, Boston, MA

93 Poynton, C H and Reading, C.L. (1984) Exp Biol. 43, 13–33

94 Davis, M T and Preston, J F. (1981) Science 213, 1385–1388

95 Axelrad, A A., McLeod, D L, Shreeve, M M. and Heath, D.S (1974) in Hemopoiesis in Culture (Robinson, W A, ed), pp. 226–237, US Government Printing Office, Washington DC

96 Dexter, T.M., Allen, T D and Lajtha, L G (1977) J. Cell. Physiol 91, 335–344

97 Metcalf, D. (1979) Clin Haematol. 8, 263–285

98 Fauser, A D and Messner, H A (1979) Blood 53, 1023–1027

99 Gartner, S. and Kaplan, H (1980) Proc. Natl Acad. Sci USA 77, 4756–4759

100 Ash, R.C., Detrick, R A and Zanjani, E D (1981) Blood 58, 309–316

101 Ogawa, M, Porter, P N and Nakahata, T (1983) Blood 61, 823–829

102 Hellman, S., Reincke, U, Botnick, L.E. and Maunch, P M (1983) J Clin Oncol. 1, 277–284

103 Chervenick, P.A (1985) Exp. Hematol 13, 8–15

104 Gordon, M.Y, Hibbin, J A., Kearney, I.U, Gordon-Smith, E C and Goldman, J M (1985) Br J. Haematol 60, 129–136

105 Gordon, M.Y., Goldman, J.M. and Gordon-Smith, E.C. (1985) Leukemia Res 9, 1017–1021

106 Ringden, O., Witherspoon, R, Ekelund, E and Thomas, E D. (1979) J. Immunol 123, 2729–2734

107 Onoe, K, Fernandes, G and Good, R.A (1980) J Exp. Med. 151, 115–132

108 Krown, S E, Coico, R, Scheid, M.P, Fernandes, G. and Good, R.A. (1981) Clin Immunol. Immunopathol. 19, 268–283

109 Lum, L.G, Seugneuret, M.C, Storb, R F., Witherspoon, R.P. and Thomas, E D (1981) Blood 58, 431–439

110 Rappeport, J M, Dunn, M.G. and Parkman, R. (1983) Transplantation 36, 674–680

111 Wood, P J. and Streilein, J W (1984) Transplantation 37, 223–226

112 Witherspoon, R., Lum, L G. and Storb, R. (1984) Semin Hematol. 21, 2–10

113 Friedrich, W, Goldmann, S.F., Vetter, U., Fliedner, T M., Heymer, B., Peter, H.H, Reisner, Y and Kleihauer, E (1984) Lancet i, 761–764

114 Dicke, K.A., McCredie, K B, Spitzer, G, Zander, A, Peters, L., Verma, D S, Stewart, D., Keating, M and Stevens, E E (1978) Transplantation 26, 169–173

115 Gilmore, M.J.M L., Prentice, H G., Blacklock, H.A., Ma, D D F, Janossy, G and Hoffbrand, A.V. (1982) Br J Haematol. 50, 619–626

116 Georgiou, G.M, Roberton, D M., Ellis, W.M., Shen, B J, Ekert, H and Hosking, C S. (1983) Clin Exp Immunol 53, 491–496

117 Ellis, W.M., Georgiou, G M, Roberton, D.M and Johnson, G.R. (1984) J Immunol. Methods 66, 9–16

118 Ho, W G., Champlin, R E., Feig, S.A and Gale, R.P. (1984) Br J. Haematol 57, 155–162

119 Bodger, M.P, Hann, I M., Maclean, R.F. and Beard, M E J (1984) Blood 64, 774–779

120 Dicke, K.A., Reading, C, Jagganath, S, Devaraj, B. and Hickey, C. (1985) Proc. of the 76th Annual Meeting of the Am. Assoc. Cancer Res 26, 180

121 Jagannath, S, Dicke, K.A., Reading, C.L., Tindle, S, Deveraj, B and Spitzer, G. (1986) submitted

122 Robak, T. and Goldman, J M (1985) Br J Haematol 61, 1–9

123 Reinherz, E L and Schlossman, S F (1980) Cell 19, 821–827

124 Feizi, T (1985) Nature 3147, 53–57

125 Reading, C.L. and Hutchins, J T (1985) Cancer Metastas Rev. 4, 221–260

126 Bernard, A, Boumsell, L and Hill, C. (1984) in Leucocyte Typing. Human Leucocyte Differentiation Antigens Detected by Monoclonal Antibodies (Bernard, A., Boumsell, L., Dausset, J, Milstein, C and Schlossman, S F, eds.), pp. 9–142, Springer-Verlag, Berlin

127 Haynes, B F (1986) in Leukocyte Typing II, Vol. 1 (Reinherz, E.L., Haynes, B F., Nadler, L M. and Bernstein, I D, eds), pp 3–30, Springer-Verlag, New York

128 Nadler, L.M. (1986) in Leukocyte Typing II, Vol. 2 (Reinherz, E L, Haynes, B F, Nadler, L M. and Bernstein, I D, eds.), pp 1–43, Springer-Verlag, New York

129 Bernstein, I.D. and Self, S. (1986) in Leukocyte Typing II, Vol. 3 (Reinherz, E.L, Haynes, B.F., Nadler, L M. and Bernstein, I.D, eds), pp 1–25, Springer-Verlag, New York

130 Link, M , Warnke, R., Finlay, J., Amylon, M., Miller, R., Dilley, J. and Levy, R. (1983) Blood 62, 722–728

131 Haynes, B.F., Metzgar, R.S , Minna ,J D and Bunn, P.A (1981) N. Engl J. Med 304, 1319–1323

132 Minowada, J., Tatsumi, E., Sagawa, K., Lok, M.S , Sugimoto, T., Minato, K., Zgoda, K , Prestine, L., Kovy, L. and Gould, D. (1984) in Leucocyte Typing Human Leucocyte Differentiation Antigens Detected by Monoclonal Antibodies (Bernard, A , Boumsell, L., Dausset, J , Milstein, C and Schlossman, S.F , eds), pp 519–527, Springer-Verlag, New York

133 Chen, R -F , Mizutani, S., Sato, H , Ozaki, Y , Ohto, H and Maeda, H. (1984) in Leukocyte Typing. Human Leukocyte Differentiation Antigens Detected by Monoclonal Antibodies (Bernard, A , Boumsell, L., Dausset, J , Milstein, C and Schlossman, S F , eds.), pp 528–533, Springer-Verlag, New York

134 Shimoyama, M., Minato, K , Tobinai, K , Nagai, M., Setoya, T. and Shibata, T (1984) in Leucocyte Typing Human Leucocyte Differentiation Antigens Detected by Monoclonal Antibodies (Bernard, A., Boumsell, L , Dausset, J., Milstein, C and Schlossman, S F , eds.), pp 534–537

135 Trigg, M E , Bozdech, M J , Sondel, P M , Billing, R , Finaly, J L., Peterson, A D., Stuiber, M and Hong, R. (1984) Exp Hematol. 12, 412 (Abstr)

136 Kamoun, M., Martin, P J , Hansen, J.A , Brown, M A , Siadak, A W. and Nowinski, R.C. (1981) J Exp. Med. 153, 207–212

137 Crawford, D H , Francis, G.E., Wing, M A , Edwards, A.J , Janossy, G , Hoffbrand, A.V , Prentice, H G , Secher, D and McConnell, I (1981) Br J Haematol 49, 209–217

138 Filipovich, A H., Vallera, D A , Youle, R.J , Stong, R.C., Neville, D M and Hersey, J.H. (1985) in Autologous Bone Marrow Transplantation Proceedings of the First International Symposium (Dicke, K.A , Spitzer, G and Zander, A R , eds.), pp. 403–407

139 Kersey, J , LeBien, T., Vallera, D , Filipovich, A , McGlave, P., Kim, T and Ramsay, N (1986) in Minimal Residual Disease in Acute Leukemia (Hagenbeek, A. and Lowenberg, B., eds.), pp 275–281, Martinus Nijhoff, The Hague

140 Reinherz, E L., Kung, P.C , Goldstein, G , Levey, R.H. and Schlossman, S F (1980) Proc Natl. Acad Sci USA 77, 1588–1592

141 Kaizer, H., Levy, R and Santos ,G.W. (1982) J. Cell Biochem. Suppl 6, 41

142 Carrel, S., Gross, N., Hermann, D , Sekay, R P , Girardet, C., Schmidt-Kessen, A. and Mach, J -P (1984) Mol. Immunol 21, 831–840

143 Matutes, E., Parreira, A , Foa, R and Catovsky, D (1985) Br J Haematol 61, 649–656

144 Van Rhenen, D G , Van der Reijden, H.J., Van't Veer, M.B , Engelfriet, C.P , Van dem Borne, A E G K and Langenhuijsen, M M A.C (1983) Leukemia Res 7, 357–362

145 Talle, M.A., Rao, P., Makowski, M., Boselli, C , Allegar, N and Goldstein, G (1985) Blood 66, 1124–1132

146 Vodinelich, L., Tax, W., Bai, Y , Pegram, S , Capel, P. and Greaves, M F (1983) Blood 62, 1108–1113

147 Boucheix, C , Perrot, J Y , Mirshahi, M., Giannoni, F , Billard, M., Bernadou, A. and Rosenfeld, C (1985) Leukemia Res 9, 597–604

148 Flug, F., Dodson, L , Wolff, J , Guarini, L , Rausen, A., Wang, C Y and Knowles, D M. (1985) Leukemia Res 9, 1051–1058

149 Dinndorf, P A , Benjamin, D , Ridgway, D and Bernstein, I.D (1985) Leukemia Res 9, 449–461

150 Jones, N H , Borowitz, M.J and Metzgar, R.S (1982) Leukemia Res 6, 449–464

151 Greenberger, J.S., Rothstein, L., DeFabritiis, P , Bragni, M., Bast, R., Ritz, J , Nadler, L M., Lipton, J M and Sakakeeny, M A (1985) Cancer Res. 45, 758–767

152 Takvorian, T , Sallan, S. and Ritz, J (1986) in Minimal Residual Disease in Acute Leukemia (Hagenbeek, A. and Lowenberg, B., eds), pp 266–274, Martinus Nijhoff, The Hague

153 Melvin, S., Yomada, Y , Pelper, S and Metzgar, D (1984) in Leucocyte Typing. Human Leucocyte Differentiation Antigens Detected by Monoclonal Antibodies (Bernard, A , Boumsell, L , Dausset, J , Milstein, C. and Schlossman, S F , eds), pp. 596–599, Springer-Verlag, New York

154 Ritz, J , Pesando, J M., Notis-McConarty, J , Lazarus, H and Schlossman, S F (1980) Nature 283, 583–585

155 Ramsay, N , LeBien, T., Nesbit, M , McGlave, P , Weisdorf, D , Kenyon, P , Hurd, D , Goldman, A , Kim, T and Kersey, J (1985) Blood 66, 508–513

156 Todd, R.F. and Schloss, S.F (1982) Blood 59, 775–786

157 Greaves, M F , Delia, D., Neuman, R and Vodinelich, L (1982) in Monoclonal Antibodies in Clinical Medicine (McMichael, A J and Fabre, J W , eds.), pp 130–165, Academic Press, London

158 Clavell, L.A., Lipton, J M , Bast, R C , Kudisch, M , Pesando, J , Schlossman, S F and Ritz, J (1981) Blood 58, 333–336

159 Nadler, L.M., Korsmeyer, S J , Anderson, K C , Boyd, A.W , Slaughenhoupt, B , Park, E , Jensen, J , Coral, F , Mayer, R J , Sallan, S.E , Ritz, J and Schlossman, S F. (1984) J Clin. Invest. 74, 332–340

160 Ueda, R , Namikawa, R , Ogata, S., Matsuoka, H., Tsuge, I , Minami, S , Nishida, K., Koike, K , Suchi, T., Ota, K and Takahashi, T (1984) in Leucocyte Typing. Human Leucocyte Differentiation Antigens Detected by Monoclonal Antibodies (Bernard, A , Boumsell, L , Dausset, J , Milstein, C and Schlossman, S F , eds), pp 603–608, Springer-Verlag, New York

161 Ueda, R., Tanimoto, M., Takahashi, T , Ogata, S -I , Nishida, K , Namikawa, R., Nishizuka, Y and Ota, K (1982) Proc. Natl Acad Sci. USA 79, 4386–4390

162 Knapp, W., Betterheim, P , Majdic, O , Kiszka, K , Schmidmeier, W and Lutz, D. (1984) in Leukocyte Typing Human Leucocyte Differentiation Antigens Detected by Monoclonal Antibodies (Bernard, A , Boumsell, L , Dausset, J , Milstein, C , and Schlossman, S F , eds), pp 564–573, Springer-Verlag, New York

163 Drexler, H G and Minowada, J. (1986) Leukemia Res. 10, 279–290

164 Van der Reijden, H.J., Van Rhenen, D J, Lansdorp, P M., Van't Veerm, M B., Langenhuijsen, M.A.C, Engelfriet, C P and Von dem Borne, A E.G.K. (1983) Blood 61, 443–448

165 Horton, M A and Cedar, S.H (1984) in Leucocyte Typing, Human Leucocyte Differentiation Antigens Detected by Monoclonal Antibodies (Bernard, A, Boumsell, L, Dausset, J, Milstein, C and Schlossman, S F, eds), pp 395–397, Springer-Verlag, New York

166 Alonso, M.C, Solana, R, Torres, A, Ramirez, R., Navarrete, C, Pena, Y. and Festenstein, H (1986) in Leukocyte Typing II. Human Myeloid and Hematopoietic Cells (Reinherz, E.L., Haynes, B F, Nadler, L.M. and Bernstein, I D., eds.), pp 193–205, Springer-Verlag, New York

167 Janowska-Wieczorek, A., Mannoni, P J, Krantz, M J, Turner, A R and Ture, J.M. (1986) in Leukocyte Typing II Human Myeloid and Hematopoietic Cells (Reinherz, E L, Haynes, B F, Nadler, L M and Bernstein, I D, eds), Springer-Verlag, New York, pp. 171–180

168 Todd, R F., Bhan, A K, Kabawat, S E and Schlossman, S F (1984) in Leucocyte Typing Human Leucocyte Differentiation Antigens Detected by Monoclonal Antibodies (Bernard, A., Boumsell, L, Dausset, J., Milstein, C and Schlossman, S F, eds), pp 424–433, Springer-Verlag, New York

169 Sabbath, K.D, Ball, E.D, Larcom, P, Davis, R.B and Griffin, J D. (1985) J Clin. Invest 75, 746–753

170 Griffin, J D and Schlossman, S F (1984) in Leucocyte Typing, Human Leucocyte Differentiation Antigens Detected by Monoclonal Antibodies (Bernard, A, Boumsell, L, Dausset, J, Milstein, C and Schlossman, S F, eds), pp 404–410, Springer-Verlag, New York

171 Sieff, C, Bicknell, D, Caine, G., Robinson, J, Lam, G and Greaves, M F (1982) Blood 60, 703–713

172 Hermann, F., Komischke, B., Openwald, E and Ludwig, W.D (1983) Blut 47, 157–163

173 Linch, D C., Allen, C., Beverly, P.C.L, Bynoe. A G, Scott, C S and Hogg, N (1984) Blood 63, 566–573

174 Foon, K A., Schroff, R W and Gale, R P. (1982) Blood 60, 1–19

175 Peschel, C, Konwalinka, G, Geisler, D., Majdic, O, Stockinger, H., Braunsteiner ,H and Knapp, W (1985) Exp Hematol. 13, 1211–1216

176 McKolanis, J R, Borowitz, M.J, Tuck, F L. and Metzgar, R S (1984) in Leucocyte Typing. Human Leucocyte Differentiation Antigens Detected by Monoclonal Antibodies (Berrnard, A, Boumsell, L, Dausset, J, Milstein, C. and Schlossman, S F., eds.), pp 387–394, Springer-Verlag, New York

177 Kito, K, Nasu, K, Kamesaki, H, Doi, S, Tezuka, H, Tatsumi, E, Fukuhara, S., Nishikori, M, Uchino, H and Shirakawa, S (1985) Blood 66, 47–52

178 Drexler, H G, Sagawa, K., Menon, M and Minowada, J (1986) Leukemia Res 10, 17–23

179 Griffin, J D., Ritz, J, Beveridge, R P, Lipton, J M, Daley, J F. and Schlossman, S F. (1983) Int. J. Cell Cloning 1, 33–48

180 Mannoni, P, Janowska, A, Fromont, P, Weiblen, B, Turner, A R. and Turc, J M. (1984) in Leucocyte Typing Human Leucocyte Differentiation Antigens Detected by Monoclonal Antibodies (Bernard, A., Boumsell, L, Dausset, J, Milstein, C and Schlossman, S F, eds), pp 410–419, Springer-Verlag, New York

181 Ball, E D, Graziano, R F, Shen, L and Fanger, M W (1982) Proc Natl. Acad Sci. USA 79, 5374–5378

182 Griffin, J.D, Mayer, R J., Weinstein, H J, Rosenthal, D S, Coral, F S, Beveridge, R.P. and Schlossman, S F (1983a) Blood 62, 557–563

183 Peschel, C, Konwalinka, G, Geissler, D., Grunewald, K, Liszka, K, Stockinger, H, Majdic, O., Braunsteiner, H and Knapp, W. (1986) in Leukocyte Typing II. Human Myeloid and Hematopoietic Cells (Reinherz, E L, Haynes, B F, Nadler, L M and Bernstein, I D, eds), pp. 181–192, Springer-Verlag, New York

184 Andrews, R G, Brentnall, T.A, Torok-Storb, B and Bernstein, I.D (1984) in Leucocyte Typing Human Leucocyte Differentiation Antigens Detected by Monoclonal Antibodies (Bernard, A., Boumsell, L, Dausset, J, Milstein, C and Schlossman, S.F, eds), pp 398–404, Springer-Verlag, New York

185 Andrews, R.G, Torok-Storb, B and Bernstein, I D (1983) Blood 62, 124–132

186 Ball, E.D., Graziano, R F and Fanger, M W (1983) J Immunol 13, 2937–2941

187 Robak, T, Nolasco, I, Hibbin, J and Goldman, J M (1985) Leukemia Res 9, 1023–1029

188 Pessano, S., Palumbo, A, Ferrero, D., Pagliardi, G L, Bottero, L, Lai, S K, Meo, P, Carter, G., Hubbell, H, Lange, G and Rovera, G (1984) Blood 64, 275–281

189 Lange, B, Ferrero. D, Pessano, S., Palumbo, A, Faust, J, Meo, P. and Rovera, G (1984) Blood 64, 693–700

190 Lange, B, Ferrero, D., Pessano, S., Hubbell, H., Palumbo, A, Lai, S K. and Rovera, G (1984) in Minimal Residual Disease in Acute Leukemia (Lowenberg, B and Hagenbeek, A., eds), pp 55–65, Martinus Nijhoff, The Hague

191 Ferrero, D, Broxmeyer, H E, Pagliardi, G.L, Venuta, S, Lange, B, Pessano, S and Rovera, G. (1983) Proc. Natl Acad Sci USA 80, 4114–4118

192 Ferrero, D, Gabbianelli, M., Peschle, C, Lange, B and Rovera, G (1985) Blood 66, 496–502

193 Beverley, P.C L, Linch, D. and Delia, D (1980) Nature 287, 332–333

194 LeBien, T, McKenna, R.W, Abramson, C S, Gajl-Peczalska, K J, Nesbit, M E, Coccia, P.F., Bloomfield, C D., Brunning, R.D. and Kersey, J.H (1981) Cancer Res 41, 4776–4780

195 LeBien, T W. and Kersey, J.H. (1980) J. Immunol. 125, 2028–2214

196 Nadler, L M., Anderson, K.C, Bates, M, Park, E, Slaughenhoupt, B. and Schlossman, S F (1984) in Leucocyte Typing Human Leucocyte Differentiation Antigens Detected by Monoclonal Antibodies (Bernard, A, Boumsell, L, Dausset, J, Milstein, C. and Schlossman, S F, eds.), pp 387–394, Springer-Verlag, New York

197 Nadler, L M, Ritz, J, hardy, R, Pesando, J M, Schloss-

man, S F and Stashenko, P (1981a) J Clin. Invest 67, 134–140

198 Stashenko, P., Nadler, L M., Hardy, R and Schlossman, S F. (1980) J Immunol. 125, 1678–1685

199 Nadler, L M, Stashenko, P., Hardy, R, Van Agthoven, A, Terhorst, C and Schlossman, S F (1981) J Immunol 126, 1941–1947

200 Abramson, C.S., Kersey, J.H and LeBien, T W (1981) J Immunol 126, 83–88

201 Fitchen, J.H, LeFevre, C., Ferrone, S and Cline, M J (1982) Blood 59, 188–190

202 Griffin, J D., Sabbath, K D., Herrmann, F, Larcom, P, Nichols, K, Kornacki, M, Levine, H and Cannistra, S A (1985) Blood 66, 788–795

203 Sparrow, R L and Williams, N (1986) Blood 67, 379–384

204 Falkenburg, J H F, Fibbe, W E, Goselink, H M, Van Rood, J.J and Jansen, J (1985) J Exp Med 162, 1359–1369

205 Keating, A, Powell, J, Takahashi, M and Singer, J W (1984) Blood 64, 1159–1162

206 Wouters, R. and Lowenberg, B. (1984) Blood 63, 684–689

207 Bodger, M P, Izaguirre, C.A, Blacklock, H.A. and Hoffbrand, A V (1983) Blood 61, 1006–1010

208 Crawford, D H, Janossy, G., Hetherington, C M, Francis, G E, Edwards, A J, Hoffbrand, A V and Prentice, H G (1981) Transplantation 31, 245–250

209 Clark, E A and Yokochi, T (1984) in Leucocyte Typing Human Leucocyte Differentition Antigens Detected by Monoclonal Antibodies (Bernard, A, Boumsell, L, Dausset, J, Milstein, C and Schlossman, S F, eds.), pp 339–346, Springer-Verlag, New York

210 Griffin, J.D, Ritz, J, Nadler, L M and Schlossman, S F (1981) J Clin Invest 68, 932–941

211 Bernstein, I D and Andrews, R.G (1986) Hybridoma 5, 57 (Abstr.)

212 Bernstein, I (1986) Personal Communication

213 Civin, C I, Strauss, L C, Brovall, C, Fackler, M J., Schwartz, J F and Shaper, J H (1984) J Immunol 133, 157–165

214 Andrews, R G, Singer, J W and Bernstein, I D. (1986) Blood 67, 842–845

215 Tindle, R W., Nichols, R.A B, Chan, L, Campana, D, Catovsky, D and Birnie, G D (1985) Leukemia Res 9, 1–9

216 Katz, F E, Tindle, R., Sutherland, R and Greaves, M F (1985) Leukemia Res 9, 191

217 Katz, F.E, Tindle, R.W., Sutherland, R. and Greaves, M F (1986) in Leukocyte Typing II. Human Myeloid and Hematopoietic Cells (Reinherz, E L, Haynes, B F, Nadler, L M and Bernstein, I D, eds), pp 305–314, Springer-Verlag, New York

218 Spitalnik, S L., Schwartz, J.F, Magnani, J L, Roberts, D D, Spitalnik, P F, Civin, C I and Ginsburg, V (1985) Blood 66, 319–326

219 Greaves, M F. (1981) in Leukemia Markers (Knapp, W, ed), pp 19–32, Academic Press, London

220 Wang, C Y, Azzo, W, Al-Katib, A, Chiorazzi, N and Knowles, D.M. (1984) J Immunol 133, 684–691

221 Nadler, L M, Ritz, J, Griffin, J D, Todd, R F, Reinherz, E L and Schlossman, S F (1981) Prog Hematol XII, pp 187–225

222 Anderson, K C, Park, E K, Bates, M P, Leonard, R C F, Hardy, R, Schlossman, S.F and Nadler, L M (1983) J Immunol 130, 1132–1138

223 Liszka, K, Majdic, O, Bettelheim, P and Knapp, W (1983) Am J Hematol. 15, 219–226

224 Pessano, S, Battero, L, Faust, J., Trucco, M, Palumbo, A, Pegoraro, L, Lange, B, Brezin, C, Borst, J, Terhorst, C and Rovera, G (1983) Cancer Res 43, 4812–4815

225 Majdic, O., Bettelheim, P, Stockinger, H, Aberer, W., Liszka, K., Lutz, D and Knapp, W (1984) Int J Cancer 33, 617–623

226 Hansen, J A, Martin, P J, Beatty, P G, Clark, E A and Ledbetter, J A (1984) in Leucocyte Typing Human Leucocyte Differentiation Antigens Detected by Monoclonal Antibodies (Bernard, A, Boumsell, L, Dausset, J, Milstein, C and Schlossman, S F, eds), pp. 195–212, Springer-Verlag, New York

227 Horibe, K, Knowles, R W, Morishima, Y and Dupont, B. (1984) in Leucocyte Typing Human Leucocyte Differentiation Antigens Detected by Monoclonal Antibodies (Bernard, A., Boumsell, L, Dausset, J, Milstein, C and Schlossman, S.F, eds), pp 212–223, Springer-Verlag, New York

228 Strauss, L C, Skubitz, K.M, August, J T and Civin, C I (1984) Blood 63, 574–578

229 Poulik, M.D, Goodfliesh, R, Hunter, S, Chen, J and Lillehoj, E (1981) in Leukemia Markers (Knapp, W, ed), pp. 73–76, Academic Press, London

230 Uckun, F M, Ramakrishnan, S and Houston, L.L (1985) Cancer Res 45, 69–75

231 Deng, C-T, Chia, J, Terasaki, P and Billing, R (1982) Lancet i, 10–11

232 Levy, J G, Logan, P M, Pearson, D, Whitney, S, Lum, V and Naiman, S (1986) in Leukocyte Typing II Human Myeloid and Hematopoietic Cells (Reinherz, E L, Haynes, B.F, Nadler, L M and Bernstein, I D, eds), pp 267–284, Springer-Verlag, New York

233 Malcolm, A J, Shipman, R C, Logan, P M and Levy, J G (1984) Exp Hematol. 12, 539–547

234 Reading, unpublished observations

235 Edelman, P., Vinci, G, Villeval, J L, Vainchenker, W, Henri, A, Miglierina, R, Rouger, P, Reviron, J, Breton-Gorius, J, Sureau, C. and Edelman, L (1986) Blood 67, 55–63

236 Takaishi, M and Fu, S M (1986) in Leukocyte Typing II Human Myeloid and Hematopoietic Cells (Reinherz, E L, Haynes, B F, Nadler, L M and Bernstein, I D, eds), pp 207–216, Springer-Verlag, New York

237 Bacigalupo, A., Podesta, M., Frassoni, F, Marmont, A, Risso, M and Corte, G (1981) J Immunol 127, 2415–2417

238 Andreasen, R B, Killmann, S-A and Olsson, L (1985) Leukemia Res. 9, 1161–1170

239 Askew, D S., Eaves, A C, Eaves, C J and Takei, F (1986) Blood, 67, 1098–1102

240 Askew, D S, Eaves, A C and Takei, F (1985) Leukemia Res 9, 135–145

241 Knowles, D M., Tolidjian, B , Marboe, C C , Mittler, R S , Talle, M A and Goldstein, G (1984) Blood 63, 886–896

242 Mittler, R S., Talle, M.A , Carpenter, K , Rao, D E. and Goldstein, G. (1983) J Immunol 131, 1754–1761

243 Greaves, M.F , Verbi, W., Kemshead, J and Kennett, R (1980) Blood 56, 1141–1144

244 Gupta, A D , Samoszuk, M.K., Papayannopoulou, T and Stamatoyannopoulos, G. (1985) Blood 66, 5322–526

245 Ohto, H , Maeda, H., Shibata, Y , Chen, R -F , Ozaki, Y , Higashihara, M , Takeuchi, A. and Tohyama, H (1985) Blood 66, 873–881

246 Poulik, M D., Hunter, S V , Chen, J C., Propolec, M and Piston, S (1984) in Leucocyte Typing Human Leucocyte Differentiation Antigens Detected by Monoclonal Antibodies (Bernard, A., Boumsell, L , Dausset, J , Milstein, C and Schlossman, S F , eds.), pp 573–579, Springer-Verlag, New York

247 Gadd, S J and Ashman, L.K (1985) Leukemia Res 9, 1329–1336

248 Naito, K , Real, F X. and Dupont, B (1984) in Leucocyte Typing Human Leucocyte Differentiation Antigens Detected by Monoclonal Antibodies (Bernard, A , Boumsell, L., Dausset, J., Milstein, C and Schlossman, S F , eds), pp 537–543, Springer-Verlag, New York

249 Young, N S. and Huang-Chen, S -P (1981) Proc Natl Acad Sci USA 78, 7073–7077

250 Reading, C L. (1984) in The Biology of Glycoproteins (Ivatt, R , ed), pp 235–321, Plenum Press, New York.

251 Weiler, J M., Ballas, Z.K., Needleman, B W , Hobbs, M V. and Feldbush, T L. (1982) Immunol. Today 3, 238–243

252 Levitt, L , Kipps, T J., Engleman, E G and Greenberg, P L (1985) Blood 65, 663–679

253 Gorb, J.-P., Campana, D , Timms, A , Coustan-Smith, E , Janossy, G and Pretince, H G (1986) J Cell Biochem. Suppl 10D p. 217, Abstr.

254 Ball, E D , Kadushin, J.M., Schacter, B and Fanger, M.W (1982) J Immunol. 128, 1476–1481

255 Dicke, K A , Van Noord, M J., Maat, B , Schaefer, U W and Van Bekkum, D W (1973) Blood 42, 195–208

256 Platsoucas, C.D., Chae, F H , Collins, N., Kernan, N., Lave, J., Ellingsen, T , Stenstad, P., Bjorgum, J., Rembaum, A., Good, R A , O'Reilley, R and Ugelstad, J , submitted

257 Barlogie, B. (1985) in Autologous Bone Marrow Transplantation (Dicke, K A , Spitzer, G. and Zander, A R , eds), pp 351–363, The University of Texas M D Anderson Hospital and Tumor Institute, Houston, TX

258 Reynolds, C.P , Black, A.T and Woody, J.N (1985) in Autologous Bone Marrow Transplantation (Dicke, K A., Spitzer, G. and Zander, A.R., eds), pp 365–369, The University of Texas M D Anderson Hospital and Tumor Institute, Houston, TX

259 Van Dongen, J J.M., Hooijkaas, H , Adriaansen, H J , Hahlen, K and Van Zanen, G E. (1986) in Minimal Residual Disease in Acute Leukemia (Hagenbeek, A and Lowenberg, B , eds), pp 113–133, Martinus Nijhoff, Boston

260 Moreau, J.F and Miller, R G (1983) J Immunol 130, 1139–1145

261 Moretta, A , Pantaleo, G , Moretta, L , Cerottini, J C and Mingari, M C (1983) J Exp Med. 157, 743–754

262 Kernan, N.A , Flomenberg, N , Collins, N.H , O'Reilly, R J and Dupont, B (1985) Transplantation 40, 317–322

263 Takaue, Y , Roome, A J , Turpin, J A and Reading, C.L. (1986) Am J Hematol , in the press

264 Lefkovits, I and Waldmann, H (1979) pp. 1–262, Cambridge University press, New York

265 Falkoff, R., Peters, M and Fauci, A (1982) J Immunol Methods 50, 39–49

266 Ball, E D , Mills, L E , Coughlin, C T., Beck, J.R. and Cornwell, G C III (1986) J. Cell Biochem. p. 238, Abstract P89

267 McIntyre, E A (1986) Clinics Haematol 15, 249–267

Biochimica et Biophysica Acta 865 (1986) 171–195
Elsevier

BBA 87161

The plasma-membrane-associated form of SV40 large tumor antigen: biochemical and biological properties

Janet S. Butel and Donald L. Jarvis

Department of Virology and Epidemiology, Baylor College of Medicine, Houston, TX 77030 (U.S.A.)

(Received 7 April 1986)

Contents

I Introduction 172

II Possible molecular explanations for the multifunctional capacity of T-ag 174
  A Structural diversity 174
  B. Multiple domains 174
  C. Subcellular localization 176

III. The intracellular distribution of T-ag 176
  A. Nuclear T-ag 176
  B Plasma-membrane-associated T-ag 177

IV. Features of the association of T-ag with the plasma membrane 178
  A. Antigenic reactivity of membrane T-ag 178
  B Solubility subclasses of membrane T-ag 179
  C. Stability of membrane T-ag 180
  D Models of membrane insertion 180
  E. Possible existence of T*-ag as membrane T-ag 181

V Cytoplasmic T-ag – a mutant SV40 T-ag defective for nuclear transport 182

VI Individual functions of nuclear and membrane-associated T-ags in transformation 184
  A Transformation domains of T-ag 184
  B Transformation by nuclear-transport-defective mutants 184
  C. Cellular protein p53 185
  D Other evidence for role of membrane T-ag 185

VII Model of mechanism of cell transformation by SV40 186

VIII. The cell biology of T-ag: mechanisms of biosynthesis, sorting and intracellular transport 187
  A Biosynthesis 187
  B Sorting 188
  C Transport 190

Correspondence address: Dr. J.S. Butel, Department of Virology and Epidemiology, Baylor College of Medicine, Houston, TX 77030 U.S.A.

0304-419X/86/$03.50 © 1986 Elsevier Science Publishers B V. (Biomedical Division)

IX Conclusion 191
Acknowledgments 191
References 192

I. Introduction

Simian virus 40 (SV40) ranks among the most well characterized DNA viruses known today. It has been an invaluable tool both for dissecting the molecular details of eucaryotic cell processes and for the development of recombinant DNA technology. First and foremost, however, SV40 continues to serve as a model for the study of basic mechanisms underlying virus-mediated carcinogenesis.

SV40 was originally isolated from cultures of primary rhesus monkey kidney cells [1] and is classified as a member of the papovavirus family [2]. The SV40 genome is a double-stranded, circular DNA molecule, 5243 base-pairs in length, the entire nucleotide sequence of which has been elucidated [3,4]. The genetic map of SV40 defines the virally encoded transcripts and proteins, localized to the regions of the genome responsible for their synthesis (Fig. 1) [3]. Each half of the genome encodes a different set of viral functions

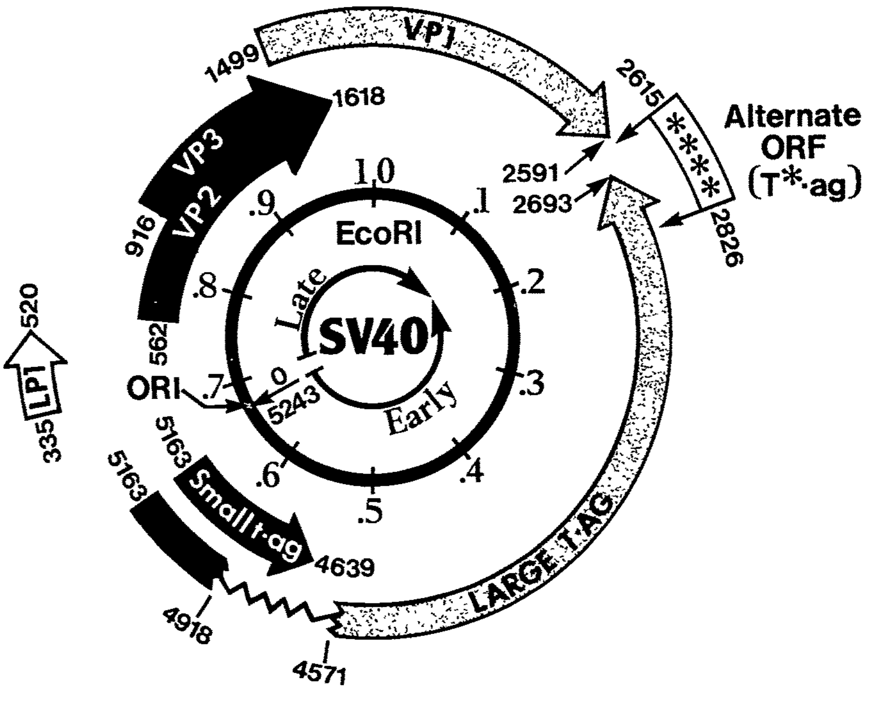

Fig 1 Genetic map of SV40. The thick circle represents the circular SV40 DNA genome, divided into decimal fractions of one map unit The unique *Eco*RI site is shown at map unit 0/1. The origin (ori) of viral DNA replication is marked at the lower left, nucleotide numbers begin and end at this location (0/5243) and proceed in the clockwise direction The boxed arrows indicate the open reading frames that encode the viral proteins Arrowheads point in the direction of transcription, and the beginning and end of each open reading frame is indicated by the corresponding nucleotide numbers. The open, stippled, and shaded areas depict different reading frames for different viral polypeptides or portions thereof The box with the stars indicates the alternate open reading frame that could be used for the unique carboxy terminus of the putative third tumor antigen, T*-ag The genome is divided into 'early' and 'late' regions that are expressed before and after the onset of viral DNA replication, respectively. Only the early region is expressed in transformed cells

that are expressed under temporal regulation in the infected cell. By definition, the 'early' functions are expressed before, and the 'late' functions after, the onset of viral DNA replication. Two unique early mRNA species, generated by differential splicing of the primary transcripts, encode the two early proteins, large tumor antigen (T-ag) and small tumor antigen (t-ag). Both are nonstructural polypeptides, as neither is incorporated into virus particles. Three late mRNAs, also produced by differential splicing, encode the virion structural proteins – VP1, VP2 and VP3. A fourth late protein, LP-1, is encoded by an open reading frame in the 5′ leader region of the mRNA for VP1 [5,6]. LP-1 is a nonstructural protein that appears to function in virion assembly [7]. The region between the sequences encoding the 5′ ends of the early and late transcripts includes the viral origin of DNA replication and the promoter and enhancer sequences involved in the regulation of viral transcription [8].

The biological result of an infection by SV40 depends upon the host cell. African green monkey kidney cells are permissive for SV40 and support a lytic infection. All viral functions are expressed, progeny virions are synthesized, and the cells are lysed, releasing the progeny. Nonpermissive hosts are cell types in which SV40 fails to replicate and some cells, particularly if of rodent origin, may be transformed by the virus. Only early viral functions are expressed in transformed cells: viral DNA is not replicated, progeny virions are not produced, and the cells are not lysed. Instead, the cells acquire an unlimited growth potential (i.e., immortalization), exhibit altered metabolic, morphologic, and growth properties (i.e., phenotypic transformation), and may be tumorigenic in vivo. However, it should be noted that kidney cells derived from the natural host for SV40, the Asian rhesus macaque, respond somewhat differently to virus infection. SV40 establishes a persistent infection in rhesus cells, replicating well and producing normal levels of progeny while the cells suffer only minimal cytopathic effects [8a]. Tumors are not induced in the rhesus monkeys. Therefore, both the dramatic lytic cycles and the transforming infections induced by SV40 in certain cultured cells are invaluable model systems, but they do not reflect the natural virus–cell interactions responsible for the evolution of SV40.

T-ag plays an essential role in both lytic infection and transformation by SV40. The absolute necessity for T-ag was established by studies of temperature-sensitive mutants that mapped to the early region of the viral genome (tsA mutants). At the restrictive temperature, tsA mutants were defective for functions required for the normal progression of a lytic infection, including initiation of viral DNA synthesis [9] and regulation of both early and late viral gene expression [10–12]. The tsA mutants also were incapable of initiating transformation of nonpermissive cells at the restrictive temperature. Further, sustained expression of T-ag was required for the maintenance of at least some characteristics of the transformed phenotype; several growth parameters reverted to normal when cells that had been transformed at the permissive temperature were cultured under restrictive conditions [13–18].

The second early gene product, small t-ag, is dispensable for lytic infection, although mutants lacking t-ag may produce a smaller burst size than wild-type (WT) virus [19]. Small t-ag also is not essential for the initiation and maintenance of cellular transformation. It does, however, facilitate the initiation of transformation in resting cells [20] and exerts an influence over the expression of some characteristics of the transformed phenotype [21,22]. The unique coding domain of small t-ag has been implicated in the ability of the protein to disrupt the actin cytoskeletal network in rat cells (Bikel, I., Mamon, H., Brown, E.L., Boltax, J., Agha, M. and Livingston, D.M., unpublished data). The late proteins are required only for the assembly of progeny virions during a lytic infection. They are not involved in the early phases of virus replication or in cell transformation and are not synthesized in nonpermissive cells [14,15,17, 23,24].

Thus, SV40 T-ag mediates most of the replicative functions required in a lytic infection and can single-handedly induce transformation of nonpermissive cells. The ability of this one protein to trigger such an array of biological effects is rather astounding and suggests that T-ag is an extraordinarily multifunctional protein. Indeed, T-ag exhibits a variety of different activities, as defined by both in vitro and in vivo assays (Table

I) [25]. Some of these activities are directly involved in viral DNA replication, whereas others affect the host cell. A key feature of SV40 infection is that the cell is stimulated to enter S phase, so that the necessary enzymes are available for viral replication. This strategy probably underlies the oncogenic potential of the virus, an unfortunate side-effect of functions that have evolved to maximize virus replication in vivo. The current challenge in the SV40 system is to determine how T-ag accomplishes these various effects. The answers will have an impact on our understanding of basic processes in both normal and transformed cells.

TABLE I

PROPERTIES AND FUNCTIONS OF SV40 T-ANTIGEN

A. Structural properties
  1. Size:
    708 amino acids
    81 632 Da
    M_r 90000–100000
  2. Modifications:
    Phosphorylation
    N-terminal acetylation
    Glycosylation
    Poly-ADP-ribosylation
    Palmitylation
    Adenylation
  3 Supramolecular structure:
    Monomers
    Dimers
    Higher homo-oligomers
    Hetero-oligomer with p53
B. Subcellular distribution
  1. Nuclear:
    Nucleoplasmic
    Chromatin-bound
    Nuclear matrix associated
  2. Plasma membrane.
    NP40 soluble
    NP40 insoluble (plasma membrane lamina)
C Functions
  1. Specific DNA binding (viral origin of replication)
  2. Initiation of viral DNA replication
  3. Autoregulation of viral early transcription
  4 Induction of viral late transcription
  5 Determination of host range
  6. ATPase activity
  7. Tight association with protein kinase
  8 Nonspecific DNA binding (cellular DNA)
  9. Complex formation with cellular protein p53
  10 Initiation of cellular DNA replication
  11 Induction of cellular enzyme synthesis
  12 Reactivation of ribosomal RNA genes
  13. Adenovirus helper function
  14. Initiation and maintenance of cellular transformation
  15 Induction of immunity to SV40 tumor cells
  16 Target for cytotoxic T cells (TSTA)

II. Possible molecular explanations for the multifunctional capacity of T-ag

There are several theoretical molecular bases that might explain the multifunctional capacity of T-ag.

IIA. Structural diversity

The structural diversity of T-ag represents one possible mechanism of multifunctionality. The polypeptide is chemically modified in several ways, including phosphorylation at multiple sites [26–28], N-terminal acetylation [29], poly-ADP-ribosylation [30], glycosylation (Refs. 31, 32; Schmitt, M.K. and Mann, K., personal communication), palmitylation [33], and adenylation [34]. T-ag also assumes different supramolecular structures in the native state, forming monomers, dimers, trimers, and tetramers, and hetero-oligomers composed of T-ag and a cellular protein, p53 [35–39]. Hence, structural variation can generate multiple forms of T-ag, and each form might be capable of providing a separate function. This possibility is supported directly by the observation that different supramolecular forms of T-ag exhibit distinct DNA-binding and ATPase activities [38,39] and, indirectly, by the finding that palmitylation is restricted to the plasma-membrane-associated subpopulation of T-ag [33].

IIB. Multiple domains

A second explanation presupposes the existence of multiple domains within the T-ag polypeptide, each responsible for the provision of one or more distinct functions. There is experimental evidence to support this view, as a few T-ag functions have been mapped to discrete regions of the polypeptide (Fig. 2). For example, the region between amino acids 160 and 272 is involved in stimulation of cell DNA synthesis, nuclear transport is media-

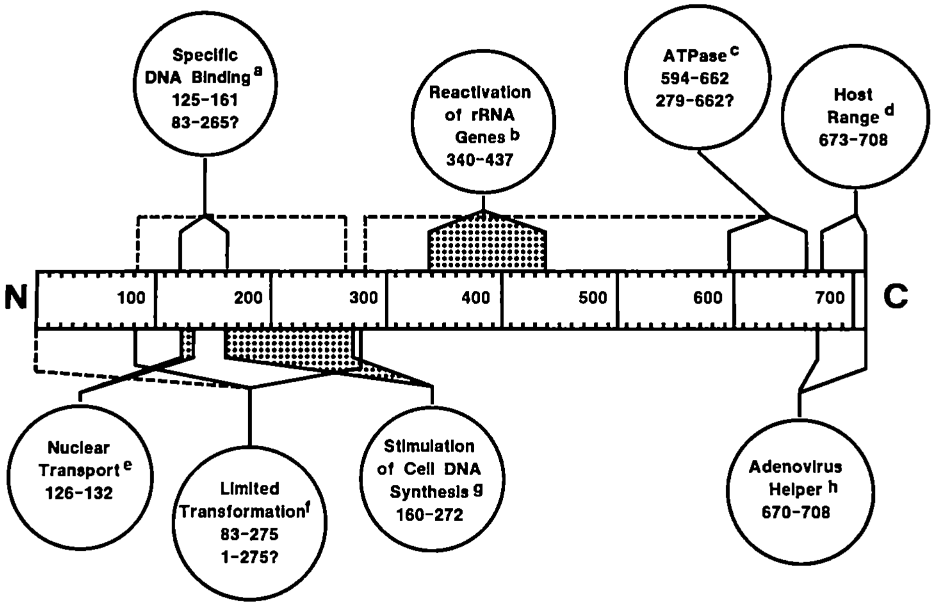

Fig. 2. Functional domains of T-ag. The long box in the center of the figure depicts the 708 amino-acid T-ag. The amino terminus is on the left, the carboxy terminus on the right. Various functions are encircled, and the region of T-ag required for each function is indicated. Solid lines indicate the minimal functional domains, whereas dotted lines indicate reported longer domains The numbers in the circles indicate the amino acid boundaries for the minimal functional domains, and the boundaries for the larger domains indicated by the dotted lines are presented with a question mark The authors emphasize that these numbers should be viewed as approximations and not as precise boundaries for the different functional domains. Data were compiled from the following references: (a) 42, 44, 52, 57, 64, 64a, 166, 211; (b) 50, 55, 59, (c) 42, 44, 212, (d) 53, 54, (e) 66–68, 158; (f) 47–49, 60–62, 164, 165; (g) 50, 58, 59; (h) 43, 213.

ted by amino acids 126–132, and both host range for productive infection and the adenovirus helper function are determined by the carboxy-terminal 35–38 residues.

One approach to delimiting T-ag functional domains has involved the construction of deletion mutants of SV40 that encode different sized fragments of T-ag which can then be assayed for T-ag-specific activities [40–54]. A related approach exploits the nondefective adenovirus-SV40 hybrids, which encode carboxy-terminal fragments of T-ag and which have been used in the same way as SV40 deletion mutants [55–57]. Some investigators have used cloned fragments of SV40 DNA in transfection or microinjection experiments [55, 58–62]. The biological effects induced by individual DNA fragments can be measured and assigned to the appropriate region(s) of T-ag. Alternatively, T-ag fragments have been prepared by proteinase treatment and then analyzed for their functional activities [63,64,64a]. By identifying the region of T-ag from which each fragment is derived, the activities of the fragments can be assigned to those regions of the polypeptide. Finally, numerous naturally occurring or genetically engineered point mutants, insertion mutants, and conditional-lethal mutants have been useful in assigning functions to subregions of T-ag [65–72,166].

It should be emphasized that the study of deleted or truncated polypeptides may suffer a major limitation, as the overall conformation of the molecule may be altered. It is reasonable to assume that the conformational structure of T-ag influences its ability to carry out specific functions or to undergo normal chemical modifications, supramolecular assembly, or intracellular transport. The abolishment of any of the latter events could indirectly prevent the expression of a given function. Therefore, a change in a particular region of T-ag might influence not only the functions encoded within that region, but those of distant regions of the polypeptide as well. Notwithstanding this limitation, the use of mutated genomes has proven that T-ag is a multidomain polypeptide, and this must account for some of its multifunctional capacity.

In this context, it is well to appreciate that T-ag is not a particularly efficient transforming protein; tumor induction by SV40 is usually a slow process, and transformation in vitro produces relatively subtle phenotypic changes in the target cells. It is possible that the evolution of T-ag has involved the assembly of unrelated minimal functional domains from several normal cellular progenitors [73]. Their combination into a single polypeptide, selected for the required replicative functions, may have markedly reduced the efficiency with which cellular transformation functions can be expressed. The involvement of DNA virus transforming proteins in virus replication is a major distinction from the direct-transforming retroviruses that carry transforming genes having no role in virus replication.

IIC. Subcellular localization

A third possible explanation for the multifunctional capacity of T-ag considers its localization to different subcellular compartments. Although the majority of the T-ag is localized within the nucleus of the cell, a small amount is found in association with the plasma membrane and is partially exposed on the cell surface. The nuclear (nT-ag) and plasma-membrane-associated (pmT-ag) forms of T-ag might provide separate functions, based either upon putative structural differences, the influence of local micro-environments, or their interactions with different subcellular targets.

The remainder of this review will focus on the unusual subcellular distribution of SV40 T-ag, with particular emphasis on the structural and functional features of pmT-ag.

III. The intracellular distribution of T-ag

IIIA. Nuclear T-ag

The majority (over 95%) of the intracellular T-ag is localized within the cell nucleus. This distribution was first shown by indirect immunofluorescence (IF) of acetone-fixed cells using sera from SV40 tumor-bearing hamsters (TBS) as the immunological reagent [74,75]. The nuclei exhibited a distinct pattern of granular or particulate staining, with no detectable reactivity in the nucleoli. The presence of T-ag in the nuclei of SV40-infected cells also was demonstrated by immunocytochemistry at the ultrastructural level [76]. T-ag can be extracted and immunoprecipitated from isolated nuclei, prepared by biochemical fractionation of SV40-infected or -transformed cells [10,77,78]. Tegtmeyer and co-workers [10] verified the relationship between the extracted T-ag polypeptide having an apparent molecular mass of about 100 kDa and the nuclear tumor antigen reactivity detected by IF. After treatment of SV40-infected cells with a nonionic detergent at pH 8.0, the 100 kDa polypeptide was released into a post-nuclear supernatant fraction, and tumor antigen reactivity was absent in the residual nuclear structures.

At a more detailed level, T-ag appears to interact with the different structural systems within the nucleus. An isolation procedure developed by Staufenbiel and Deppert [79,80] involves the stepwise biochemical extraction of cultured cells in situ, resulting in the sequential solubilization of nucleoplasmic (soluble nuclear proteins and nuclear membranes), chromatin (chromatin and associated proteins), and nuclear matrix (the residual nuclear structures and cytoskeleton) fractions. T-ag has been found in all three subnuclear fractions prepared from SV40-transformed mouse cells [79,81]. Each fraction appeared to represent a distinct subpopulation of T-ag, as differences were observed in some of their biochemical properties, such as solubility, the amount of bound p53, and the stability of the association with various nuclear substructures [79]. Independent studies have established that T-ag is localized within all three subnuclear fractions of SV40-infected or -transformed monkey cells [82]. Control experiments have shown that the association of T-ag with each of the different subnuclear fractions is specific and not an artifact of the fractionation procedure.

The existence of specific subpopulations of T-ag within the nucleus supports the concept that the multifunctional capacity of T-ag may depend, in part, upon its differential subcellular localization. The movement of T-ag to different sites within the cell would enable it to interact with multiple, independent, subcellular targets.

IIB Plasma-membrane-associated T-ag

Although the majority of the T-ag is found within the nucleus, a small fraction (less than 5%) is localized at the cell surface in association with the plasma membrane.

The transplantation rejection test provided the first demonstration of a tumor antigen in SV40-transformed cells [83–86]. The very nature of that assay implied a cell surface location for the tumor antigen; it had to be exposed for tumor rejection to occur. Although the relationship between the tumor-specific transplantation antigen (TSTA) detected by in vivo tests and the T-ag detected by in vitro methods was unclear, evidence would eventually accumulate which proved that the same viral polypeptide participates in both reactivities. In the process, that same evidence would indicate that T-ag is localized in two different subcellular compartments, in the nucleus and at the plasma membrane.

Nuclei isolated from SV40-transformed cells and known to contain T-ag reactivity were able to induce a TSTA response in vivo [87], suggesting that nT-ag could participate in TSTA. The direct involvement of T-ag in tumor rejection was documented by the demonstration that purified T-ag could immunize mice against tumor cell challenge [88,89]. A purified T-ag-related protein (D2 protein) was used to generate cytotoxic T lymphocytes (CTL) in vivo, and they, in turn, were able to specifically lyse SV40-transformed cells in vitro [90]. In addition, a monoclonal antibody against T-ag was shown to block the lysis of SV40-transformed cells by CTL in vitro [91]. Importantly, the cellular immunology approach rectified what appeared to be a disparity among earlier serological studies. It had been shown that TBS and an antiserum prepared against isolated nT-ag-containing nuclei reacted with both the nucleus and the surface of SV40-transformed cells (supporting a relationship between T-ag and TSTA) [92], while sera from SV40-immunized hamsters that had rejected a tumor cell transplant reacted only with the cell surface (suggesting that T-ag and TSTA might be different) [92–94]. Subsequently, this disparity was further clarified by the finding that the surface-reactive sera from tumor-rejecting animals were able to immunoprecipitate nT-ag [95]. Therefore, T-ag is clearly a component of TSTA. A requirement for the other SV40 early gene product, t-ag, in the expression of TSTA has been ruled out because SV40 deletion mutants unable to express t-ag induced TSTA as efficiently as WT virus [96].

Cellular fractionation studies showed directly that some T-ag is associated with the plasma membrane. Nuclear and membrane fractions were prepared from SV40-infected or -transformed cells, and T-ag could be extracted and immunoprecipitated from both subcellular fractions [78,97]. However, only a minor fraction (less than 5%) of the total T-ag was present in the membrane fraction. A more rigorous fractionation procedure developed by Schmidt-Ullrich and co-workers [98] was used for the isolation of highly purified plasma membrane fractions from normal and SV40-transformed hamster lymphocytes. The plasma membranes from the transformed cells contained proteins that were not found in the normal cells, and the molecular mass of one of those new proteins was consistent with that of T-ag [99–101]. This protein was subsequently identified as T-ag by its reactivity with TBS and by tryptic peptide mapping [31,102]. This same fractionation procedure was used by Soule et al. [92] to confirm the presence of T-ag in the plasma membrane of transformed mouse cells.

Specific antisera directed against partially purified T-ag were used in surface assays, including IF, radioimmunoassay and protein A binding methods. All these approaches showed that T-ag-specific antisera will react with the surface of SV40-transformed cells [92,103–107]. Enzyme-catalyzed radioiodination procedures, designed to label only the proteins exposed on the cell surface, also have demonstrated a surface form of T-ag [108,109]. Cells were surface labeled and extracted; after immunoprecipitation of the extracts with TBS, iodinated T-ag could be visualized by gel electrophoresis. A related method, differential immunoprecipitation, has been used to separate the cell surface T-ag population from nuclear T-ag [110]. This method involves an extracellular reaction between T-ag specific antisera and cell surface proteins, followed by solubilization of the intact cells and recovery and analysis of the immune complexes. Numerous controls established that only surface T-ag was iodinated and immunoprecipitated in these studies.

The idea that a subpopulation of T-ag is specifically localized in the plasma membrane was greeted with a certain amount of scepticism for several years. One reason for this reluctance was that some studies had shown that a minor subpopulation of whole-cell T-ag, when added exogenously, could bind to the cell surface in vitro [111,112]. As only small amounts of pmT-ag were recovered relative to nT-ag and the two were indistinguishable by molecular mass and most immunological and biochemical criteria, pmT-ag might simply have reflected the nonspecific adsorption of small amounts of nT-ag released from dead or dying cells. However, various control experiments showed that the amounts of pmT-ag routinely detected could not be accounted for by cell lysis in transformed cell cultures [109,110,113]. Furthermore, as the specific characteristics of pmT-ag were investigated, certain features were revealed that argued strongly in favor of the existence of pmT-ag as a distinct biochemical entity (see following section for details). Therefore, an accumulation of evidence, derived from multiple experimental approaches, gradually brought about the general acceptance that a specific subpopulation of T-ag exists in association with the plasma membrane of cells. Attention has now shifted to more specific questions concerning the nature of the interaction between pmT-ag and the plasma membrane, the functions of nT-ag and pmT-ag in cell transformation, and the cellular mechanisms that are responsible for the sorting and transport of T-ag to two different subcellular compartments.

IV. Features of the association of T-ag with the plasma membrane

IVA. Antigenic reactivity of membrane T-ag

The interaction between T-ag and the plasma membrane positions pmT-ag in a specific and rather unusual way. Antibodies prepared against a synthetic peptide corresponding to the carboxy-terminal 11 amino acids of T-ag [114] will react with the surface of SV40-transformed cells [115]. Monoclonal antibodies specific for antigenic determinants on the amino- or carboxy-terminal portions of T-ag also will react with the surface of SV40-transformed cells, but some monoclonals that recognize more internal sequences will not [95,116,116a,117]. In addition, cells expressing T-ag fragments derived from the amino- or carboxy-terminal one-third of the molecule can stimulate CTL in vivo and can be recognized and lysed by CTL in vitro [118–120]. A number of individual SV40-specific CTL clones have been isolated and characterized; some recognize amino-terminal sequences, others recognize carboxy-terminal sequences, but none requires the expression of sequences derived from the internal one-third of the T-ag polypeptide [121,122]. These results indicate that both the amino and carboxy termini of T-ag are exposed on the cell surface, while an internal region, encompassing about one third of the molecule, is inaccessible. The reason these internal sequences are unavailable for antibody binding or CTL recognition is not known. They may be buried within the lipid bilayer or may be localized on the cytoplasmic side of the membrane. They might be exposed on the surface, but masked either by chemical modifications or by the conformational or supramolecular structure of the native protein. In any case, the reproducibly specific orientation assumed by pmT-ag argues that it does not simply stick to the membrane in a random fashion and, consequently, probably has a functional role at the cell surface.

An intriguing feature of pmT-ag is that it is oriented slightly differently in the plasma membrane of SV40-transformed or -infected cells [95]. Differential immunoprecipitation of transformed cells revealed that carboxy-terminal epitopes of T-ag were more accessible to antibody binding than amino-terminal epitopes. With infected cells, in contrast, epitopes at both ends of the polypeptide were equally accessible, and certain monoclonals that reacted well with T-ag of transformed cells reacted only poorly with the surface T-ag of infected cells. The pmT-ag in transformed cells is tightly associated with p53 [78,95,97,108,110] and is analogous in that sense to nT-ag [123]. The pmT-ag in infected cells, however, is not detectably complexed with p53 [95]. It is tempting to speculate that the association with p53 may change the conformation of T-ag in the plasma membrane of transformed cells, mediating the subtle changes in antigenic reactivity detected with the monoclonal antibodies. Such a conformational change also might influence the functional capabilities of the T-ag on the surface of transformed cells.

IVB. Solubility subclasses of membrane T-ag

Klockmann and Deppert [33] have presented evidence for the existence of two distinct subclasses of pmT-ag which interact with the plasma membrane in different ways. One subclass, representing about one-third of the total pmT-ag population, could be extracted from the membrane by treatment with the nonionic detergent, Nonidet P40 (NP40). A second subclass was more tightly associated with the membrane and could be extracted only by treatment with a zwitterionic detergent, Empigen BB. Based upon the extraction conditions, it was concluded that the latter subclass of pmT-ag is associated with the plasma membrane lamina (PML), a structure that directly underlies the lipid bilayer of the plasma membrane and connects it to the cytoskeleton [124]. The latter subclass of pmT-ag was shown to be chemically modified by fatty acid acylation, with covalently bound palmitic acid as the acyl group. Palmitylation is the only known structural difference between pmT-ag and nT-ag, as none of the nT-ag populations is modified in this way [33].

The individual roles of the amino-acid sequence and the acyl group in the interaction of T-ag with the plasma membrane have been considered [125]. A 28 kDa carboxy-terminal fragment of T-ag was found to associate with the plasma membrane, but was not acylated and did not interact with the PML. A larger, 42 kDa, carboxy-terminal fragment was acylated and did associate with the PML. It was concluded that the 28 kDa carboxy-terminal amino-acid sequence of T-ag is capable of providing an NP40-soluble interaction with the plasma membrane but not the tighter interaction with the PML. The acyl group is probably required for the interaction between T-ag and the PML, and the acylation site(s) is apparently located within the 160 amino acids between the amino-terminal ends of the 42 and 28 kDa carboxy-terminal fragments of T-ag. It must be appreciated, however, that these results were obtained with truncated, T-ag-related proteins encoded by the nondefective adenovirus 2-SV40 hybrid viruses, ND1 and ND2 (Ad2$^+$ND1 and Ad2$^+$ND2) [126]. Although the ND system has been useful for many studies, the accuracy of these proteins as models for the membrane association of WT T-ag is not certain. For example, the ND proteins are found at the cell surface in much larger quantities than SV40 T-ag [127], and the 28 kDa protein expressed by Ad2$^+$ND1, unlike T-ag, associates with membranes of the rough endoplasmic reticulum (RER) [125] (see below). The 28 kDa protein is apparently synthesized as a 30 kDa precursor which is then proteolytically processed to generate the 28 kDa end-product [128]. It is possible that the ND1 protein is initially synthesized as a chimeric adenovirus-SV40 protein with an adenoviral signal sequence that might mediate the entry of the protein into the secretory pathway [119]. Since this pathway is not utilized for the transport of WT SV40 T-ag (see below), the final interaction of the 28 kDa ND1 protein with the plasma membrane might not precisely mimic that of the intact T-ag polypeptide or even of the T-ag-specific sequences contained within the 28 kDa ND1 protein.

The cell surface disposition of each of the two subclasses of pmT-ag has been analyzed [129]. When SV40-transformed mKSA cells were grown on a plastic substratum, both forms were exposed on the cell surface, as both could be radioiodinated. However, when mKSA cells were grown in suspension or as ascites tumor cells, only the PML-associated subclass was exposed on the cell surface; the NP40-soluble subclass was not available for iodination. It was suggested from these observations that the PML-associated subclass of pmT-ag is normally exposed on the cell surface and is probably a trans-membrane protein, whereas the exposure of the NP40-soluble form is variable and depends upon the shape of the cells, which is dictated, in turn, by culture conditions. However, we have found that at least some of the NP40-soluble subclass of pmT-ag can be radioiodinated under all culture conditions (Butel, J.S., unpublished data). Clarification of these discrepant observations awaits further studies.

IVC. Stability of membrane T-ag

The stability of the membrane association of T-ag remains to be resolved. After radioiodination, the labeled pmT-ag is unstable and disappears from the cell surface during a 2 h chase period at 37°C [109,113,129,130]; the half-life of iodinated surface T-ag appears to be less than 1 h [130]. A portion of the iodinated pmT-ag is shed into the culture medium and can be recovered by immunoprecipitation, but quantitative recovery has never been achieved [109,113]. The pmT-ag lost from the cell surface is rapidly replenished with newly synthesized T-ag molecules that can be iodinated on the 'chased' cells [109,113,130]. These observations suggest that the association of pmT-ag with the plasma membrane is highly dynamic. A valid concern, however, is that the radioiodination procedure may influence the stability of proteins on the cell surface. Accordingly, the stability of pmT-ag has been analyzed by metabolic labeling with [^{35}S]methionine [129,130]. Using differential immunoprecipitation and mKSA cells grown on a plastic substratum, Santos and Butel [130] found that the NP40-soluble subclass of pmT-ag was rather unstable, with a half-life of 1–2 h. By subcellular fractionation of mKSA cells grown in suspension, however, Klockmann and Deppert [129] noted that both subclasses of pmT-ag were stable, with no detectable change in either population during a chase period of 4 h. These results may indicate that the precise interaction of pmT-ag with the plasma membrane depends upon culture conditions that influence the shape of the transformed cells.

IVD. Models of membrane insertion

All available data document that at least a subpopulation of pmT-ag is partially exposed on the cell surface and, therefore, must span the plasma membrane. The precise mechanism by which T-ag is inserted into the membrane and achieves its specific disposition is currently a complete mystery. Models for the insertion of proteins into cellular membranes require either a 'signal' or an 'insertion' sequence [131–133]. The classical signal sequence consists of 16–26 amino acids, with a hydrophilic, basic amino terminus and a central hydrophobic domain. It is usually located at the amino terminus of the protein and is proteolytically removed during biosynthesis. There also are examples of amino-terminal and internal signal sequences that are not removed. The signal sequence mediates the insertion of the protein into the membrane of the RER [134], thereby allowing the protein to enter the secretory pathway with localization at the plasma membrane as one possible result. An alternative mechanism requires an insertion sequence that consists of a stretch of 20 or more hydrophobic amino acids [135] able to accomplish the spontaneous insertion of the protein into a membrane.

A variety of observations strongly suggest that T-ag does not contain a cleavable amino-terminal signal sequence. The molecular mass of T-ag translated in vitro is not different from that of T-ag synthesized in transformed or infected cells [136], and the molecular mass of T-ag is stable in pulse-chase experiments, with no obvious changes during chase times ranging from 5 min to 17 h (Ref. 137; Jarvis, D.L. and Butel, J.S., unpublished data). Although these findings suggest that T-ag does not contain a cleavable signal sequence, the interpretation is complicated by the very anomolous behavior of the protein in acrylamide gels. The calculated molecular mass of T-ag is 81 632 Da [3], but it migrates with an apparent mass of 88–100 kDa, depending upon the gel system used for the analysis. Consequently, it is technically difficult to judge the presence or absence of co- or post-translational modifications of T-ag by electrophoretic analysis. It has been shown that the amino-terminal tryptic peptide of T-ag synthesized in vitro contains a methionine residue donated from initiator tRNA that is identical to the amino-terminal peptide of T-ag isolated from infected cells [29]. In addition, inspection of the primary amino acid sequence of T-ag reveals neither a conspicuous amino-terminal or internal signal sequence nor an ideal insertion sequence (Walter, G., personal communication). An internal stretch of 15 hydrophobic amino acids at positions 568–582 has recently been recognized (Ref. 125; Walter, G., personal communication), a sequence long enough for a membrane-anchoring domain [138], but there is no experimental evidence to suggest that this region can function as an insertion sequence. Analysis of the membrane association characteristics of T-ag mutants lacking this sequence will be most illuminating.

IVE. Possible existence of T-ag as membrane T-ag*

One interesting proposal for the ability of T-ag to insert into the plasma membrane which also could account for its differential subcellular localization is that two closely related, but different, T-ag polypeptides represent the nT-ag and pmT-ag populations. In 1980 Mark and Berg [139] detected a third species of early mRNA similar to that encoding T-ag, but which had undergone an additional splicing event in the 3′ region around 0.20 map units (see Fig. 1). That splice would shift the reading frame of the mRNA so that it could encode a third early protein. The putative product, designated T*-ag, would be derived from the same coding sequences as T-ag, except for the carboxy-terminal 70 amino acids, which would be derived from an alternate open reading frame. The carboxy terminus of T*-ag would be distinctly more hydrophobic than that of T-ag and could provide an internal insertion sequence. T*-ag would thereby have the ability to insert into the RER or plasma membrane post-translationally, as has been proposed for other membrane proteins, such as cytochrome b_5, that have a hydrophobic carboxy-terminal sequence but no other visible means of membrane insertion [133]. The possibility that the 'authentic' T-ag polypeptide represented the abundant nT-ag population, while T*-ag provided the minor pmT-ag population, was attractive. The hypothesis suffered, however, because the existence of the third early mRNA had not been confirmed, and the putative third tumor antigen had not been detected in SV40-infected or -transformed cells. Schmidt-Ullrich and coworkers [31] observed some differences between the tryptic peptide maps of radioiodinated nT-ag and pmT-ag and suggested that those variations might reflect the presence of T*-ag in the plasma membrane fraction. However, recent data now rule out the possibility that T*-ag accounts for the surface-associated form of T-ag.

Denhardt and Crawford [140] defined the reading frame used for T-ag by identification and characterization of its carboxy-terminal tryptic peptide. Their results suggested that the carboxy terminus of T-ag from whole-cell extracts of SV40-infected or -transformed cells was derived from the sequence encoding authentic T-ag and that the alternate open reading frame in the 3′ region had not been utilized. This conclusion is supported by the more recent findings of Klockmann and Deppert [129]. Antisera prepared against a synthetic peptide corresponding to the carboxy terminus of authentic T-ag reacted with both nT-ag and pmT-ag, but antisera against a synthetic peptide corresponding to the carboxy terminus of T*-ag reacted with neither [129]. Other studies have taken advantage of a positive control for T*-ag. SV40 deletion mutants have been constructed such that only the alternate 3′ reading frame can be utilized; these mutants encode polypeptides very similar to T*-ag [45,51]. Direct comparisons have shown that T*-ag migrates faster than authentic T-ag in polyacrylamide gels [45,51,141], whereas pmT-ag and nT-ag from subcellular fractions of SV40-infected or -transformed cells migrate identically [78,97,141]. The structures of nT-ag, pmT-ag and T*-ag encoded by one of the deletion mutants have been compared by peptide mapping [141]. No differences were detected in the overall structures of nT-ag and pmT-ag, and their carboxy-terminal, methionine-containing tryptic peptides were shown to be identical. Importantly, unique peptides were detected in the maps of T*-ag, and its carboxy-terminal, methionine-containing tryptic peptide was distinctly different from that of authentic T-ag. Examination of the pmT-ag maps revealed no evidence of T*-ag-specific peptides; only authentic T-ag-specific peptides were detected. This was not the result of a transport defect, as T*-ag can be expressed at the cell surface and detected by radioiodination or differential immunoprecipitation (Jarvis, D.L. and Butel, J.S., unpublished data) and can induce a TSTA response in vivo and serve as a target for CTL-mediated killing in vitro [142]. Finally, T*-ag appears to be functionally inert, as it is defective for specific DNA binding and ATPase activities [42] and is incapable of immortalizing mouse cells in vitro (Tevethia, M.J., personal communication), suggesting that it is not essential for SV40 replication or transformation.

Thus, all available evidence suggests that T*-ag does not account for pmT-ag. The existence of the alternate open reading frame in the viral genome remains an enigma.

Another hypothesis of note is that the insertion of pmT-ag into the plasma membrane is mediated by its fatty acid modification. This is unlikely, however, as only a subpopulation of pmT-ag has that modification [33]. The NP40-extractable form of pmT-ag, which is not acylated, must traverse the membrane, as evidenced by the fact that it can be radioiodinated on the surface of cells under certain growth conditions [109,129]. It is more likely that acylation is involved in anchoring pmT-ag in the PML, and that the modification occurs after the protein associates with the plasma membrane [129].

V. Cytoplasmic T-ag – a mutant SV40 T-ag defective for nuclear transport

The individual roles of the nuclear and plasma membrane-associated subpopulations of T-ag in virus replication and/or cellular transformation have been difficult to separate. A promising experimental tool has been provided by SV40 variants that encode nuclear-transport-defective forms of T-ag. These mutant T-ags do undergo normal transport to the plasma membrane. (Unfortunately, reciprocal mutants that are nuclear T-ag positive but defective for surface T-ag expression are not available.)

The first variant found to encode a nuclear transport-defective T-ag was isolated from stocks of an SV40-adenovirus (Ad) hybrid virus, PARA-adenovirus 7 [143,144]. The parental hybrid virus, PARA(nT), was isolated from a strain of human Ad7 adapted for growth in monkey kidney cells, and the presence of SV40 genetic information was recognized by its ability to induce the synthesis of intranuclear T-ag [145–147]. The variant, PARA(2cT), was one of the three plaque isolates derived from the parental stock and characterized by the induction of cytoplasmic, but not nuclear, T-ag (cT-ag) reactivity in infected [143] or transformed [148] cells. Subsequently, it was shown that the PARA genome consists of Ad7 DNA with a 16% deletion that is replaced by the entire early region and a small portion of the late region of SV40 [149–151]. As a result of the insert, PARA expresses the functions attributed to the early region of SV40 [25,152].

TABLE II

PROPERTIES OF SV40 WILD-TYPE (WT) AND NUCLEAR-TRANSPORT-DEFECTIVE (cT) LARGE T-ANTIGENS

Property	WT T-ag	cT-ag [a]
Structure:		
1 Apparent molecular mass	90–100 kDa	90–100 kDa
2 Isoelectric point	4.4	4.5
3. Met-containing tryptic peptide maps	WT	WT
4. Palmitylation	+	+
5 Glycosylation	+	+
6. Phosphopeptide maps	WT	cT
7 Amino acid 128	Lys	Asn
8. Oligomerization	+	+ (faster)
Biology.		
1. Subcellular distribution		
Nucleus	+	− or ± [b]
Cytoplasm	−	+
Plasma membrane	+	+
2 Specific DNA binding	+	+
3. Nonspecific DNA binding	+	+
4. Initiation of viral DNA replication in vivo	+	−
5 Autoregulation	+	−
6 Induction of cell DNA synthesis	+	+
7 Adenovirus helper function	+	+
8 p53 binding	+	+
9. Tumorigenicity	+	±
10. Transformation in vitro		
Primary cells	+	± [b]
Established cells	+	+

[a] Properties shown for PARA(cT) and SV40(cT)-3 encoded cT-ag Other transport-defective mutants may vary, depending on their particular alterations

[b] Small amounts of mutant T-ag are detected in the nuclei of some primary cells transformed by the SV40(cT)-3 mutant virus (see text for details)

The cT-ag is similar to WT T-ag in many respects (Table II), having the same apparent molecular mass and methionine-containing tryptic peptide map [153,154]. It expresses the adenovirus helper function [155], binds to cellular DNA [153,155a], viral origin sequences [155a,156], and p53 [72,155a], and is transported normally to the cell surface [113]. However, some subtle structural differences have been identified in cT-ag; it is differentially phosphorylated, as evidenced by its slightly more basic isoelectric point [153] and by its unique phosphopeptide map [154,157]. This difference is not the cause of the nuclear transport defect but, rather, is the result of the inability of cT-ag to reach the nucleus where additional phosphorylation normally occurs [157]. The properties of a different cT-ag described by Vesco and coworkers [158] are dissimilar, undoubtedly due to the large size of the deletion in the mutant viral genome. That transport-defective cT-ag retains the ability to oligomerize, but is dramatically underphosphorylated and lacks specific DNA-binding activity (Fischer-Fantuzzi, L., Scheidtmann, K.H. and Vesco, C., unpublished data).

The structural basis for the nuclear transport defect was elucidated once the SV40 early region sequences were excised from the PARA(2cT) genome and used to construct a recombinant virus [SV40(cT)-3] containing the mutant early region and a WT SV40 late region [68]. Marker rescue experiments mapped the defect between nucleotides 4568 and 4376, and sequence analysis of that region revealed a single point mutation at nucleotide 4434. This mutation resulted in the substitution of an asparagine residue for the WT lysine residue at amino-acid position 128. At about the same time, several additional transport-defective mutants were obtained independently by the deletion of amino acids 110 to 152 [158] or by site-directed mutagenesis of the region around lysine 128 [66]. The latter approach provided a more precise definition of the T-ag domain necessary for nuclear transport; it encompassed amino acids 126–132 (-Pro-Lys-Lys-Lys-Arg-Lys-Val-), a sequence that includes a striking tract of five consecutive basic amino acids [67]. Since the discovery of the nuclear transport signal in T-ag, other nuclear proteins have been surveyed for analogous sequences; some contain the signal but others do not, suggesting that this primary sequence in T-ag is probably not a universal signal [159].

In IF tests, the distribution of cT-ag is usually observed to be diffuse throughout the cytoplasm with no distinct morphological patterns apparent [143,160]. However, in cells infected by the SV40(cT)-3 construct, more intense reactivity is occasionally observed at the cell periphery or in a reticular network throughout the cytoplasm [68]. The ability to detect this defined subcellular distribution in certain cells may be related to the fact that lesser amounts of T-ag are induced by SV40(cT)-3 than by the parental hybrid virus, because the latter synthesis is under the control of the adenovirus late promoter (Ref. 153; Lanford, R.E., Jacob, J.R. and Butel, J.S., unpublished data). Faint nuclear reactivity is very seldom, if ever, observed in infected cells. In contrast, in cells transformed by the mutant virus, occasional cells will exhibit faint nuclear speckling in addition to the diffuse cytoplasmic T-ag reaction typically observed. The significance of this observation is considered below in the context of assigning T-ag functions involved in cell transformation.

A striking phenotype associated with the cT mutation is the dominance of the cytoplasmic localization of T-ag over WT nuclear transport. WT T-ag is retained in the cytoplasm in cells co-infected with mutant and WT virus [160]. The same phenomenon occurs in transformed monkey cells constitutively expressing WT nuclear T-ag following superinfection with cT mutant virus [68,160]. The molecular basis of this effect is not clear, but it may be related to the oligomerization of T-ag molecules [68,160,161]. Not all cT-ag constructs have been analyzed for the 'dominance' phenotype, so it is not known whether this characteristic will be common to all cT-ag mutations.

The SV40(cT)-3 construct is unable to replicate in normal monkey cells [68,156]. This is not an unexpected finding, as T-ag is required for viral DNA replication, which occurs in the nucleus. The replication of SV40(cT)-3 DNA in COS cells ceases in parallel as the dominant effect of newly synthesized cT-ag causes the retention of WT T-ag in the cytoplasm [156]. Although cT-ag may be defective in functions other than nuclear transport, these observations suggest that insufficient mutant cT-ag is transported into the nucleus of monkey cells to support viral DNA replication.

This fact is pivotal to the interpretation of several functional activities attributed to the SV40(cT)-3 mutant. Microinjection of SV40(cT)-3 DNA into quiescent rodent cells resulted in the stimulation of cellular DNA synthesis in transient assays [162]. In addition, the nuclear-transport-defective mutants can mediate some transformation events (considered in detail below). As inadequate levels of cT-ag are transported to the nucleus to sustain viral DNA replication, it is reasonable to assume that the cytoplasmic and/or the plasma membrane-associated form of T-ag is involved in the expression of those functions by the mutant virus that approach WT levels of activity.

VI. Individual functions of nuclear and membrane-associated T-ags in transformation

The expression of T-ag is clearly required for the initiation and maintenance of cell transformation by SV40, but the individual contributions of the nuclear and membrane-associated subpopulations have only recently been explored. The concept that co-operating oncogenes may be required for complete transformation [163] lends credence to the possibility that both forms of T-ag are involved in carcinogenesis. If so, SV40 T-ag would provide both immortalizing and transforming functions which are separated into two polypeptides in the polyoma system and into two or more proteins with the human adenoviruses.

VIA. Transformation domains of T-ag

Deletion mutants have been used in numerous studies to attempt to assign transformation functions to specific domains of the T-ag molecule. However, the identification of sharply demarcated transformation domains has eluded definition. This difficulty may reflect a failure to use the proper assays for the detection of various phenotypic changes, but also may be encountered because protein conformation can be altered significantly by small changes in polypeptide sequence. T-ag conformation may be especially important in the execution of those events resulting in cellular phenotypic changes. Nevertheless, it appears that approximately the amino-terminal half of the molecule is sufficient to immortalize cells [49,60, 61,164,165] (Fig. 2).

The involvement of the carboxy-terminal half of T-ag in transformation is equivocal. The most complete examples of phenotypic transformation seem to require T-ag with an intact carboxy terminus, but some mutants encoding T-ag with carboxy-terminal changes can promote dense focus formation [43,46,62,164]. However, it is evident that ATPase activity [69], specific origin-binding [166], and the ability to initiate viral DNA synthesis [52,70,167,168] are not essential for induction of cell transformation by SV40 T-ag.

The preceding types of study do not address the possible roles of T-ag molecules located in different subcellular compartments. The nuclear-transport-defective mutants of SV40 have been especially valuable for such analyses.

VIB. Transformation by nuclear-transport-defective mutants

Functional analysis of the parental PARA(2cT)-Ad7 was complicated by the presence of excess helper adenovirus particles, and this problem prompted the construction of the cT mutation onto an SV40 background. Nevertheless, early studies with PARA(2cT) had suggested that its transforming potential was impaired. PARA(2cT) could transform hamster embryo fibroblasts, but with a lower efficiency than the parental hybrid virus [148]. The mutant virus was able to induce tumors in newborn hamsters, but at a much reduced frequency and with an extended latent period [169]. The tumor cells that were recovered behaved as minimal transformants, exhibiting reduced growth potential relative to WT transformants under stringent culture conditions [170]. Interestingly, the in vitro conditions appeared to exert a selective pressure for partial reversion of the cT-ag phenotype, as serial subculture of cloned cells containing only cytoplasmic T-ag consistently resulted in the evolution of mixed cultures with many cells showing some T-ag in the nucleus [170].

SV40 nuclear-transport-defective mutants, lacking the adenovirus background of PARA(2cT), can transform previously established (e.g., 3T3) cells in vitro at near WT virus frequencies, and cT-ag is retained in the cytoplasm of the transformed cells [72,171]. This suggests that nuclear T-ag is dispensable for transformation if the cells have already been immortalized by some other means. However, the mutants are markedly impaired in their ability to induce tumors in newborn hamsters and to transform some types of primary cells. Transformation of primary mouse embryo cells was sharply reduced if low serum concentrations were used in focus assays and if anchorage-independent growth assays were utilized [72]. In those primary cells that were transformed, small amounts of cT-ag were transported to the nucleus [72]. Thus, transformation of primary cells by the cT mutant is detectable only under less stringent culture conditions and seems to require the presence of small amounts of T-ag in the nucleus.

One simplistic interpretation of this finding is that nT-ag mediates the immortalizing function(s) of SV40 and pmT-ag provides the transforming function(s). This model represents an important conceptual link between the mode(s) of action of T-ag and other viral transforming proteins. Different transforming proteins appear to mediate distinct, and perhaps co-operating, functions that may correlate with their particular localization within the cell [163,172,173]. In general, it is thought that transforming proteins localized within the nucleus mediate immortalizing functions, while those localized within the cytoplasm or at the plasma membrane mediate transforming functions [163].

VIC. Cellular protein p53

Transforming proteins must mediate biological effects through interactions with cellular substrates. It is important, therefore, to understand those interactions. One substrate has been identified in the SV40 system, a host cell protein designated p53. Large T-ag forms a tight, noncovalent complex with p53 [123].

It is believed that p53 functions in regulation of normal cell proliferation. Its expression is associated with the entry of normal cells from the resting to the growing state [174–176] and when monoclonal antibodies against p53 are microinjected, the entry of cells into S phase is inhibited [177]. Like T-ag, p53 is found in the nucleus and at the plasma membrane, but membrane association is evident only during mitosis [176]. The amount of p53 in normal cells is low, and the protein is quite unstable. Complex formation with T-ag in transformed cells stabilizes p53, extending its half-life and causing an accumulation to elevated levels [178]. There are no changes in the amount of p53 mRNA, so the alteration affecting p53 in transformed cells appears to be post-transcriptional [179].

The potential importance of p53 in cell transformation is strengthened by observations from other systems. The level of p53 is elevated in cells transformed by DNA or RNA tumor viruses or by physical or chemical agents, and higher amounts are found in some human tumor cells [178]. The same p53 is stabilized in adenovirus-transformed cells and is actually bound to an E1B protein in Ad5-transformed cells [180,181]. The placement of a cloned p53 gene under the control of a strong promoter resulted in the production of high levels of p53, which immortalized primary cells and co-operated with the *ras* gene to mediate complete transformation [182–184]. A structural change was detected in p53 that prolonged its half-life in some way, and this was accompanied by an enhancement in immortalizing capability [185].

The p53 protein is complexed with SV40 T-ag in the plasma membrane of transformed cells, as well as with nuclear T-ag [31,78,97,108,110,130]. In cells expressing the mutant cT-ag, cytoplasmic T-ag also is complexed with p53 [72,155a]. It is intriguing that no detectable p53 is complexed with surface T-ag on infected cells [130]. Perhaps the association with p53 changes the conformation of T-ag in the membrane of transformed cells, sparking some transformation-related functional activity. It has recently been shown that T-ag binding induces or stabilizes a particular p53 epitope, indicating that complex formation does have an effect on the conformation of p53 [186]. Finally, recent studies with rat cells transformed by tsA mutants showed that T-ag/p53 complex formation correlates with the transformed phenotype, whereas homo-oligomers of T-ag are not important in maintenance of transformation [187].

These diverse observations combine to suggest that the interaction between T-ag and p53 may play a significant part in the SV40 transformation process.

VID. Other evidence for role of membrane T-ag

The transformation studies with the cT mutants (described above) strongly suggest that membrane T-ag provides a function involved in complete cell transformation. Several lines of more indirect evidence substantiate a role for pmT-ag.

The expression of pmT-ag in SV40-transformed cells is correlated with their growth rate: actively dividing cells consistently express higher levels of pmT-ag than resting cells, and the loss of pmT-ag precedes growth arrest in cells transformed by a tsA mutant of SV40 [188].

The large body of literature on SV40 TSTA [189], coupled with the demonstration that T-ag was part of TSTA, helped prove the existence of a surface form of T-ag. The fact that passage of tumor cells through SV40-immunized mice resulted in the retention of TSTA [190] suggests a requirement for surface T-ag by the tumor cells; otherwise, immune selection would have eliminated pmT-ag-positive cells and allowed the outgrowth of variants lacking TSTA. In more direct support of a role for pmT-ag in cellular transformation, Karjalainen et al. [191] have shown recently that transformation of primary cells by SV40 is inhibited in the presence of an SV40-specific CTL clone.

The observation that certain antisera will react with the surface, but not the nuclei, of SV40-transformed cells [92,93,99] suggests that the native form of pmT-ag might differ from that of nT-ag and that the conformation of T-ag in the nucleus or plasma membrane may influence the way in which it is presented to the immune system. Differences in the native structures of pmT-ag and nT-ag might provide a molecular basis for the ability of each to provide distinct functions, in addition to their particular subcellular localizations per se.

Together, these findings suggest that pmT-ag plays an important role in cellular transformation by SV40.

VII. Model of mechanism of cell transformation by SV40

Carcinogenesis is believed to be a multi-step phenomenon. The examples of cooperating oncogenes in transformation of primary cells in culture [163] are compatible with that concept. In the SV40 system, the steps leading to complete transformation occur concurrently, blurring individual contributions to the process. Experimental evidence is mounting, however, that both nuclear and membrane-associated forms of T-ag are functionally important in mediating phenotypic transformation. A model of how these two forms of T-ag might cooperate is presented in Fig. 3. Although some of the proposed nuclear events are substantiated experimentally, the functions outlined for membrane T-ag are speculative and await experimental confirmation.

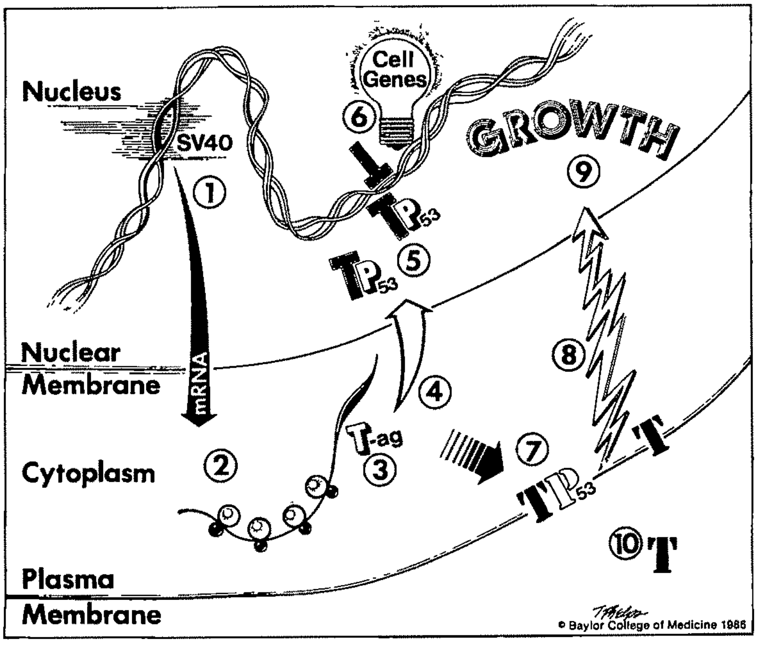

Fig. 3. Model of mechanism of transformation by SV40. This model proposes that the nuclear and plasma membrane forms of T-ag provide separate and cooperative functions necessary to mediate phenotypic transformation. See text for details.

SV40 DNA sequences are integrated in the cellular chromosome and give rise to transcripts encoding T-ag (step 1). Transcripts are transported to the cytoplasm (step 2) where T-ag is synthesized (step 3). The majority of newly synthesized T-ag is rapidly directed into the nucleus (step 4) because of the nuclear transport signal contained in its primary sequence. Nuclear T-ag has a long half-life and accumulates to high levels. Some of the T-ag forms complexes with host protein p53. Free T-ag and/or T-ag/p53 complexes bind to chromatin and the nuclear matrix (step 5), and the expression of cellular genes is activated (step 6). The effect on cellular transcription, and perhaps DNA replication, probably constitutes the T-ag immortalization function; it is essential if the transformation of primary cells is to occur. Although the T-ag function involved in gene activation is presumably derived from a normal cell regulatory protein, regulation of T-ag activity is lost (due either to the absence of regulatory domains on the polypeptide or to the high concentration of nuclear T-ag), and the cell remains continually activated.

A minor fraction of T-ag is transported to the plasma membrane by an unknown pathway (step 7). Some of the pmT-ag population is complexed with p53. It is postulated that the complex, or free pmT-ag, generates a growth signal that gets transmitted to the nucleus by an unknown mechanism (step 8). Membrane T-ag conformation might mimic an activated growth factor receptor or its presence at the cell surface might stimulate outbursts of growth signal 'second messenger' molecules. Nuclear proteins, including nuclear T-ag, respond to the growth signal and promote functions culminating in cell division (step 9). Membrane T-ag would presumably not be responsive to control measures that regulate normal cell growth, so signalling from the cell surface would occur without interruption. This might result in the phenotypic changes characteristic of complete transformation. The signals generated by surface T-ag apparently can function in the absence of nuclear T-ag if the cell has been immortalized in some other way. A relatively weak membrane T-ag activity is probably what makes SV40 less active as a transforming agent than some other tumor viruses. This may be because pmT-ag is not effectively duplicating a cellular growth signal or because the pmT-ag activity was derived originally from some tissue-specific function not common to the cell types routinely employed in laboratory transformation assays, thereby minimizing its phenotypic effects.

The membrane T-ag with its termini exposed on the extracellular face of the cell would be recognized as foreign by host CTL, hence, the involvement of T-ag in SV40 TSTA. Some of the pmT-ag is shed (step 10), with unknown effects on the immune response of the host.

SV40 is unique among known tumor viruses in combining multiple transforming functions into a single protein. If the basic features of this model are correct, T-ag should be considered a 'dual oncogene' protein [73].

VIII. The cell biology of T-ag: mechanisms of biosynthesis, sorting and intracellular transport

In addition to providing a possible molecular basis for its functional diversity, the differential subcellular localization of T-ag poses a unique cell biological problem. T-ag is one of the few proteins known to exist in both the nucleus and plasma membrane of the eucaryotic cell. Consequently, it is of general significance to determine how T-ag molecules are synthesized, sorted, and transported to their ultimate subcellular destinations. It is not yet possible to present a complete and unequivocal description of these processes. However, in light of current data, it is possible to rule out certain mechanisms and to propose working models for future studies (Fig. 4).

VIIIA. Biosynthesis

All proteins are synthesized in the cytoplasm of the cell, but two different mechanisms can be utilized. One involves the translation of mRNA on free polyribosomes with the release of the newly synthesized 'soluble' protein into the cytoplasm. The other involves the translation of mRNA on membrane-bound polyribosomes with the translocation of the nascent polypeptide across the membrane of the RER. The latter mechanism is the first step in the secretory pathway, which is responsible for the biosynthesis and transport of typical plasma membrane-bound proteins.

SV40 T-ag is probably synthesized on free cytoplasmic polyribosomes. Tabuchi and co-workers [76] used peroxidase-labeled Fab′ fragments of antibodies purified from TBS to determine the intracellular distribution of T-ag in infected cells at the ultrastructural level. At early times postinfection, both free and membrane-bound polyribosomes were stained, but because TBS contains a mixture of antibodies, a definitive identification of T-ag at those two sites was not possible. Oren and Levine [192] isolated biologically active T-ag mRNA from a free polyribosome fraction of SV40-transformed cells by an immunoselection procedure. The ability to select that mRNA population with T-ag-specific antisera substantiated the presence of nascent T-ag polypeptides in the free polyribosome fraction, and the specificity of the selected mRNA was proven by in vitro translation. However, the membrane-associated polyribosome fraction was not analyzed. Indirect evidence against a role for membrane-bound polyribosomes in T-ag biosynthesis was provided by Lanford and Butel [113] by immune electron microscopy. The nuclear-transport-defective cT-ag appeared to exist in a soluble form in the cytoplasm and was not detectably associated with any intracellular structures. However, the transport properties of the mutant cT-ag are aberrant, and the influence the mutation might have on its intracytoplasmic distribution is not known.

We have recently completed a study in which the mechanism of T-ag biosynthesis and the role of the secretory pathway were addressed directly (Jarvis, D.L., Chan, W.-K., Estes, M.K. and Butel, J.S., unpublished data). SV40 early mRNA was isolated from infected cells and translated in vitro in the presence of microsomal vesicles; the ability of newly synthesized T-ag to cross the microsomal membrane was assayed by its susceptibility to trypsin digestion. As a positive control, a rotavirus glycoprotein that is normally transported through the secretory pathway was translocated to the interior of the microsomal vesicles where it was protected from the action of exogenous trypsin. In contrast, T-ag remained sensitive to trypsin treatment, suggesting that it did not cross the microsomal membrane. Free and membrane-bound polyribosome fractions were then isolated from SV40-infected cells, and the RNA from each fraction was extracted and translated in vitro; T-ag could be translated only with the RNA from the free polyribosome fraction. Both results suggest that the intracellular site of T-ag biosynthesis is on free cytoplasmic polyribosomes and that T-ag does not enter the secretory pathway at the level of the RER. These findings are consistent with the absence of a signal sequence in T-ag, which would be required to mediate an interaction through the signal recognition particle between nascent T-ag molecules in the translational complex and a receptor in the membrane of the RER [132,133]. Thus, available data suggest that the first step in the T-ag biosynthetic pathway is translation on free polyribosomes, with the release of newly synthesized T-ag molecules into the cytoplasm (Fig. 4, panels A, B, C).

VIIIB. Sorting

A structural difference between nT-ag and pmT-ag could provide a sorting signal for the

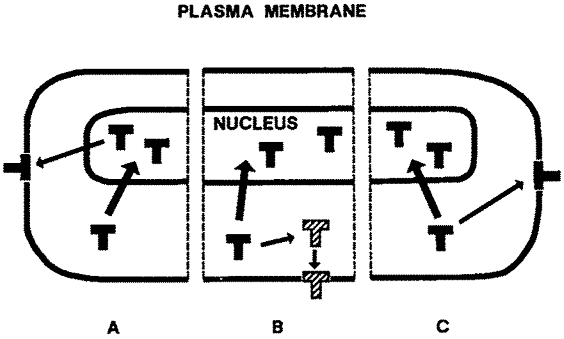

Fig 4 Three possible mechanisms for the intracellular sorting of T-ag molecules destined for the nucleus or the plasma membrane The figure depicts a eucaryotic cell, with the nucleus and plasma membrane shown The 'T's' are T-ag molecules, with the closed T and striated T representing structurally different forms Panel A All newly synthesized T-ag is transported to the nucleus, and a small fraction is subsequently transported to the plasma membrane. Panel B Most of the newly synthesized T-ag is transported to the nucleus, but a minor fraction undergoes a subtle structural modification that allows it to specifically overcome the nuclear transport signal and be transported to the plasma membrane Panel C: Most of the newly synthesized T-ag is transported to the nucleus, but a minor fraction simply 'escapes' the nuclear transport signal and is transported to the plasma membrane. Note that only model B invokes a structural difference between nT-ag and pmT-ag

intracellular recognition and transport of newly synthesized T-ag molecules to either the nucleus or plasma membrane (Fig. 4, panel B). Historically, the best candidate for a unique form of pmT-ag with a difference in its primary structure has been T*-ag, but, as detailed above, its involvement has been ruled out. The possibility that more subtle structural differences in chemical modifications and/or supramolecular structure might act as a sorting signal has not been excluded.

The structures of nT-ag and pmT-ag from subcellular fractions have been compared by a variety of peptide mapping techniques [31,141]. The nT-ag and pmT-ag populations appeared to be structurally homologous, ruling out a mechanism of intracellular sorting based upon a major structural difference [141]. However, only methionine- and proline-containing peptides, encompassing about 60% of the T-ag molecule, were examined. Although this limitation was circumvented by the analysis of V8 proteolytic partial peptides, as the larger digestion products undoubtedly included regions of T-ag lacking those amino acids, it could not be concluded that there were absolutely no structural differences between nT-ag and pmT-ag. Schmidt-Ullrich et al. [31] did detect minor differences between tryptic peptide maps of radioiodinated nT-ag and pmT-ag. It is possible that the use of radioiodinated T-ag permitted the resolution of minor differences that could not be detected by metabolic labeling with amino acids. It should be noted that different sources of T-ag were used in the two studies; Schmidt-Ullrich et al. examined a transformed human cell line (SV80) and Jarvis et al. analyzed SV40-infected monkey cells. This may be important, because the properties of T-ag from different cell lines sometimes differ in characteristics such as specific DNA-binding abilities [193], phosphorylation patterns (Scheidtmann, K.H., personal communication), and cell-surface disposition [95,129]. It can be concluded that, although no major differences exist between the structures of pmT-ag and nT-ag, subtle distinctions have not been ruled out.

Minor structural differences might reflect variable chemical modifications of nT-ag and pmT-ag. Indeed, pmT-ag is differentially modified by palmitylation [33]. Although this modification accounts for minor differences in peptide maps [31], it probably does not provide a sorting signal for the differential localization of nT-ag and pmT-ag. First, only a subpopulation of the total pmT-ag exhibits that modification and, second, palmitylation probably occurs after and is a result of the entry of pmT-ag into its particular transport pathway. Available evidence suggests that palmitylation occurs in the Golgi apparatus [194,195], so that organelle might be involved in the transport of pmT-ag to the plasma membrane. Alternatively, acylation of T-ag might occur at the plasma membrane itself by the acquisition of membrane lipids. The latter possibility is supported by studies which have shown that palmitylation occurs independently of protein synthesis [196,197] and can occur as long as 48 h after the synthesis of some membrane-bound proteins [198]. In addition, exogenously added T-ag can apparently undergo palmitylation by association with the cell surface [199].

Glycosylation may help distinguish nT-ag and pmT-ag. Whole-cell T-ag can be metabolically labeled with radioactive glucosamine or galactose, and control experiments have eliminated the possibility that the labeling occurs nonspecifically after randomization of the sugars to other radioactive precursors (Refs. 31, 32; Schmitt, M.K. and Mann, K., personal communication). However, it is unclear whether glycosylation represents a structural feature limited to any particular T-ag subpopulation. The obvious prediction is that glycosylation would be restricted to pmT-ag, as this modification is a common characteristic of plasma membrane proteins. Schmidt-Ullrich et al. [31] found that only pmT-ag was labeled with [^{14}C]glucosamine and invoked the presence or absence of glycosylation as one possible explanation for the differences in pmT-ag and nT-ag peptide maps. However, on the basis of subcellular fractionation and differential immunoprecipitation of labeled SV40-infected cells, we have found that both nT-ag and pmT-ag populations are labeled with galactose (Jarvis, D.L. and Butel, J.S., unpublished data). We believe that glycosylation per se does not provide a signal for the differential localization of nT-ag and pmT-ag. The incorporation of galactose into T-ag appears to be co-translational, being inhibited in the presence of cycloheximide (Jarvis, D.L. and Butel, J.S., unpublished data).

We also have found that T-ag is glycosylated at multiple sites, with at least two differing size classes of glycopeptides isolable from galactose-labeled T-ag (Jarvis, D.L. and Butel, J.S., unpublished data). Thus, it is possible that one form of T-ag is glycosylated at a subset of sites, while the other is glycosylated at different or additional sites. Additional studies will be necessary to determine whether differential glycosylation provides a structural basis for the intracellular sorting and localization of nT-ag and pmT-ag.

Finally, it is possible that the intracellular recognition of T-ag molecules destined for the nucleus or plasma membrane is based upon differences in their supramolecular structures. T-ag molecules in the cytoplasm of SV40-infected cells reportedly oligomerize more quickly than those within the nucleus, prompting the suggestion that oligomerization might prevent the movement of T-ag into or out of the nucleus [161]. Perhaps premature oligomerization of a small population of newly synthesized T-ag molecules prevents its movement into the nucleus and allows it to enter an alternative transport pathway to the plasma membrane.

VIIIC. Transport

Newly synthesized T-ag is transported out of the cytoplasm very quickly, as it is usually not detectable in cytoplasmic fractions of SV40-infected or -transformed cells [78,97]. Although small amounts of T-ag have been detected in cytoplasmic fractions, the majority of T-ag is transported to the nuclear compartment within 15 min of its biosynthesis [161,200]. The kinetics of transport of T-ag to the plasma membrane have not been determined, but a preliminary experiment suggests that transport is rapid [130].

The precise mechanism of transport of T-ag to the nucleus is unknown. T-ag contains a strong nuclear transport signal that is generated by the primary amino-acid sequence around Lys-128 [66,68]. A stretch of seven predominantly basic amino acids in that region is critical for the expression of the signal and, when fused to certain cytoplasmic proteins, can redirect those proteins to the cell nucleus [67]. In addition, synthetic peptides containing this amino-acid sequence will mediate the nuclear localization of coupled proteins as large as ferritin (465 kDa), while peptides containing the Lys to Asn substitution typical of cT-ag are unable to do so [200a]. Examination of the sequences of other nuclear proteins for the T-ag nuclear transport signal has revealed some similarities but, as yet, a consensus sequence cannot be readily identified [159,201]. The cellular components and processes that recognize the T-ag nuclear transport signal and accomplish its nuclear localization are not understood.

The question of whether pmT-ag expresses a functional nuclear transport signal is central to the eventual solution of the T-ag transport problem. If T-ag is structurally homogeneous at this point in its biosynthetic pathway, the strong nuclear transport signal might dictate the transient localization of plasma membrane-destined molecules (pmT-ag) into the nucleus (Fig. 4, panel A). Although pmT-ag could conceivably be derived from the nT-ag pool, a novel transport mechanism from the nucleus to the plasma membrane would be required. In addition, this proposal is inconsistent with the ability of cT-ag to achieve a plasma membrane localization. An alternative proposal is that the T-ag destined for the plasma membrane undergoes a subsequent subtle structural modification, as discussed above, that negates the nuclear transport signal (Fig. 4, panel B). Finally, there is the possibility that the small amounts of T-ag that associate with the plasma membrane do so by simply escaping the strong nuclear transport signal and entering some other transport pathway (Fig. 4, panel C). However, if pmT-ag provides a critical function at the cell surface, as current data suggest, it is difficult to rationalize such a nonspecific mechanism of transport.

The mechanism by which T-ag is transported to the plasma membrane remains a complete mystery. Typically, plasma membrane-associated proteins are routed through the secretory pathway, entering at the level of the RER and migrating through various compartments of the Golgi apparatus to the plasma membrane [131–133]. However, it is unlikely that this pathway accomplishes the transport of pmT-ag. T-ag does not appear to contain a characteristic signal or insertion sequence that would account for its ability to cross the RER membrane (see above). Furthermore, the majority of plasma-membrane-bound proteins that enter the secretory pathway are modified by cotranslational *N*-glycosylation [202]. T-ag does possess one consensus *N*-glycosylation site [203] at amino acids 156 to 158 (Asn-Arg-Thr), but it does not contain N-linked oligosaccharides [32]. Finally, a chimeric protein, HA-T-ag, was recently designed to force T-ag into the secretory pathway by means of the amino-terminal signal sequence of the influenza hemagglutinin [137]. HA-T-ag entered the secretory pathway and became *N*-glycosylated, but failed to proceed along the pathway to the plasma membrane. These results suggested that the secretory pathway is not normally utilized for the transport of WT T-ag. The authors proposed an alternative model whereby all T-ag molecules are transported into the nucleus by the expression of the nuclear transport signal, a fraction becomes associated with the inner nuclear membrane, and that membrane breaks down during cell mitosis, generating small vesicles that carry the associated T-ag molecules to the plasma membrane [137]. Certain limitations of the use of the HA-T-ag construct to define the involvement of the secretory pathway are evidenced by the results of another study in which a similar chimeric protein was constructed. The signal sequence of the influenza hemagglutinin, which normally utilizes the secretory pathway, was replaced with the signal sequence from the vesicular stomatitis virus G protein [204]. As was observed with HA-T-ag, the heterologous signal sequence mediated the entry of the chimeric protein into the secretory pathway, but interfered with its normal progression to the plasma membrane. Presumably, some undefined change in the overall conformation of the protein produced the adverse effect. Nevertheless, the HA-T-ag observations, together with our in vitro translation experiments with WT SV40 mRNA, strongly suggest that T-ag is synthesized on free polyribosomes and that it does not enter the secretory pathway at the level of the RER.

In view of the inability of T-ag to interact with the RER, a role for the Golgi apparatus in T-ag biosynthesis and transport is doubtful, as proteins typically gain access to the Golgi through the RER. However, as some T-ag molecules are palmitylated [33] and appear to be *O*-glycosylated [32], modifications thought to occur in the Golgi apparatus [194–197,205–208], we considered the possibility that T-ag might enter the Golgi apparatus through some unrecognized alternative pathway. Treatment of SV40-infected cells with monensin, an inhibitor of Golgi function [209], under conditions that inhibited terminal glycosylation of the vesicular stomatitis virus G protein [210], had no specific effect on the glycosylation or cell surface expression of T-ag (Jarvis, D.L. and Butel, J.S., unpublished data). Thus, the Golgi apparatus does not appear to be involved in either the glycosylation or surface transport of T-ag, a finding consistent with the general lack of a role for the secretory pathway. With the elimination of this pathway it becomes difficult to explain how T-ag becomes glycosylated or acylated. We believe that the exciting possibility must be seriously considered that both modifications occur by previously unrecognized mechanisms and that the transport of pmT-ag to the plasma membrane follows a currently unknown route.

IX. Conclusion

In the 25 years since its discovery, studies of SV40 have fostered many technological and intellectual advances in viral oncology and molecular biology. The SV40 system will continue to provide an excellent tool for the investigation of basic cellular processes. In this respect, T-ag is a particularly useful protein; by virtue of its multifunctional nature, it can be applied to the study of such diverse biological phenomena as DNA replication, regulation of gene expression, control of cellular proliferation and the host immune response to tumors. In addition, the unusual subcellular distribution of T-ag presents a unique opportunity for the analysis of cellular mechanisms of protein biosynthesis and trafficking. The next 25 years of investigation promise to be as instructive as the last, with many unexpected revelations sure to ensue.

Acknowledgments

Work in the authors' laboratory was supported in part by grants CA22555 and CA09197 from the National Cancer Institute. Thanks are extended to the many colleagues who kindly shared their unpublished data to facilitate preparation of this review.

References

1 Sweet, B H. and Hilleman, M R (1960) Proc Soc Exp Biol. Med. 105, 420–427

2 Melnick, J.L. (1962) Science 135, 1128–1130

3 Fiers, W., Contreras, R , Haegeman, G , Rogiers, R , Van de Voorde, A., Van Heuverswyn, H., Van Herreweghe, J , Volckaert, G and Ysebaert, M. (1978) Nature 273, 113–120

4 Reddy, V B , Thimmapaya, B , Dhar, R., Subramanian, K N , Zain, B.S , Pan, J , Ghosh, P K , Celma, M.L and Weissman, S.M (1978) Science 200, 494–502

5 Dhar, R , Subramanian, K.N., Pan, J. and Weissman, S.M (1977) Proc. Natl. Acad Sci USA 74, 827–831

6 Jay, G , Nomura, S , Anderson, C W and Khoury, G (1981) Nature 291, 346–349

7 Ng, S -C , Mertz, J E , Sanden-Will, S. and Bina, M (1985) J. Biol. Chem 260, 1127–1132

8 Tjian, R. (1981) Curr. Topics Microbiol Immunol. 93, 5–24

8a Norkin, L C (1982) Microbiol. Rev 46, 384–425

9 Tegtmeyer, P. (1972) J Virol. 10, 591–598

10 Tegtmeyer, P , Schwartz, M., Collins, J K. and Rundell, K (1975) J. Virol. 16, 168–178

11 Cowan, K , Tegtmeyer, P and Anthony, D D (1973) Proc Natl Acad. Sci USA 70, 1927–1931

12 Khoury, G. and May, E (1977) J. Virol 23, 167–176

13 Brugge, J S. and Butel, J S (1975) J Virol 15, 619–635

14 Kimura, G and Itagaki, A '(1975) Proc Natl. Acad. Sci USA 72, 673–677

15 Martin, R G. and Chou, J Y (1975) J Virol 15, 599–612

16 Osborn, M and Weber, K (1975) J. Virol 15, 636–644

17 Tegtmeyer, P. (1975) J. Virol 15, 613–618

18 Brockman, W W (1978) J Virol 25, 860–870

19 Topp, W.C. (1980) J. Virol 33, 1208–1210

20 Seif, R. and Martin, R. (1979) J Virol 32, 979–988

21 Sleigh, M J., Topp, W C , Hanich, R and Sambrook, J.F (1978) Cell 14, 79–88

22 Topp, W.C. and Rifkin, D B (1980) Virology 106, 282–291

23 Anderson, J L. and Martin, R G. (1976) J Cell Physiol 88, 65–76

24 Noonan, C A , Brugge, J S. and Butel, J.S. (1976) J. Virol 18, 1106–1119

25 Rigby, P.W J. and Lane, D.P. (1983) in Advances in Viral Oncology (Klein, G , ed), Vol 3, pp 31–57, Raven Press, New York

26 Tegtmeyer, P , Rundell, K. and Collins, J K (1977) J Virol 21, 647–657

27 Scheidtmann, K -H., Echle, B and Walter, G (1982) J Virol 44, 116–133

28 Van Roy, F , Fransen, L and Fiers, W (1983) J Virol 45, 315–331

29 Mellor, A. and Smith, A E (1978) J Virol 28, 992–996

30 Goldman, N , Brown, M. and Khoury, G (1981) Cell 24, 567–572

31 Schmidt-Ullrich, R , Thompson, W S , Kahn, S J , Monroe, M T and Wallach, D F H. (1982) J Natl. Cancer Inst 69, 839–849

32 Jarvis, D.L and Butel, J S (1985) Virology 141, 173–189

33 Klockmann, U and Deppert, W (1983) EMBO J. 2, 1151–1157

34 Bradley, M K , Hudson, J , Villanueva, M S and Livingston, D M. (1984) Proc Natl Acad Sci. USA 81, 6574–6578

35 McCormick, F and Harlow, E. (1980) J Virol 34, 213–224

36 Fanning, E , Nowak, B and Burger, C (1981) J Virol 37, 92–102

37 Greenspan, D S and Carroll, R B (1981) Proc Natl Acad Sci USA 78, 105–109

38 Bradley, M.K., Griffin, J.D and Livingston, D.M. (1982) Cell 28, 125–134

39 Gidoni, D., Scheller, A., Barnet, B , Hantzopoulos, P , Oren, M and Prives, C (1982) J. Virol 42, 456–466

40 Cole, C N , Landers, T., Goff, S P , Manteuil-Brutlag, S and Berg, P (1977) J Virol 24, 277–294

41 Cole, C.N., Crawford, L V and Berg, P (1979) J. Virol 30, 683–691

42 Cole, C N , Tornow, J , Clark, R. and Tjian, R (1986) J Virol 57, 539–546

43 Polvino-Bodnar, M. and Cole, C.N (1982) J. Virol 43, 489–502

44 Clark, R , Peden, K., Pipas, J.M , Nathans, D and Tjian, R (1983) Mol. Cell Biol. 3, 220–228

45 Lewis, E D , Chen, S , Kumar, A , Blanck, G., Pollack, R.E and Manley, J.L. (1983) Proc Natl Acad. Sci USA 80, 7065–7069

46 Pipas, J.M , Peden, K W.C. and Nathans, D (1983) Mol Cell Biol 3, 203–213

47 Sompayrac, L and Danna, K J (1983) Mol Cell Biol 3, 484–489

48 Sompayrac, L and Danna, K J. (1984) Mol Cell Biol 4, 1661–1663

49 Sompayrac, L. and Danna, K.J (1985) Mol Cell Biol 5, 1191–1194

50 Soprano, K J., Galanti, N , Jonak, G J , McKercher, S , Pipas, J M., Peden, K W C and Baserga, R. (1983) Mol Cell. Biol 3, 214–219

51 Tornow, J. and Cole, C N (1983) J Virol 47, 487–494

52 Peden, K.W.C and Pipas, J M (1985) J Virol. 55, 1–9

53 Pipas, J.M (1985) J Virol 54, 569–575

54 Tornow, J., Polvino-Bodnar, M , Santangelo, G and Cole, C.N. (1985) J. Virol 53, 415–424

55 Soprano, K J , Jonak, G J., Galanti, N , Floros, J. and Baserga, R. (1981) Virology 109, 127–136

56 Montenarh, M , Deppert, W. and Henning, R (1982) FEBS Lett. 142, 129–132

57 Prives, C., Barnet, B , Scheller, A , Khoury, G and Jay, G. (1982) J Virol 43, 73–82

58 Mueller, C., Graessmann, A. and Graessmann, M (1978) Cell 15, 579–585

59 Galanti, N , Jonak, G.J , Soprano, K J , Floros, J , Kaczmarek, L., Weismann, S., Reddy, V B., Tilghman, S M and Baserga, R. (1981) J Biol Chem. 256, 6469–6474

60 Clayton, C E., Murphy, D , Lovett, M. and Rigby, P W J (1982) Nature 299, 59–61

61 Colby, W.W and Shenk, T (1982) Proc Natl. Acad. Sci USA 79, 5189–5193

62 Graessmann, M , Guhl, E , Bumke-Vogt, C. and Graessmann, A (1984) J Mol Biol. 180, 111–129

63 Schwyzer, M , Weil, R , Frank, G and Zuber, H (1980) J Biol Chem 255, 5627–5634

64 Morrisson, B., Kress, M , Khoury, G. and Jay, G. (1983) J. Virol 47, 106–114

64a Simmons, D T (1986) J Virol 57, 776–785

65 Kalderon, D and Smith, A E (1984) Virology 139, 109–137

66 Kalderon, D , Richardson, W D , Markham, A F and Smith, A E (1984) Nature 311, 33–38

67 Kalderon, D , Roberts, B L , Richardson, W D and Smith, A E (1984) Cell 39, 499–509

68 Lanford, R E and Butel, J S. (1984) Cell 37, 801–813

69 Manos, M.M. and Gluzman, Y (1984) Mol. Cell Biol 4, 1125–1133

70 Manos, M.M. and Gluzman, Y (1985) J. Virol 53, 120–127

71 Sugano, S and Yamaguchi, N (1984) J Virol 52, 884–891

72 Lanford, R E., Wong, C and Butel, J S (1985) Mol Cell Biol 5, 1043–1050

73 Butel, J.S (1986) in Cancer Surveys, Vol. 5, No 2 Biochemical Mechanisms of Oncogene Activity (Bishop, J M and Varmus, H E , eds), Oxford University Press, London, in the press

74 Pope, J H. and Rowe, W.P (1964) J Exp. Med 120, 121–128

75 Rapp, F., Butel, J S and Melnick, J L (1964) Proc. Soc Exp Biol Med 116, 1131–1135

76 Tabuchi, K , Lehman, J M and Kirsch, W.M. (1976) J Virol 17, 668–671

77 Tenen, D G , Garewal, H , Haines, L L , Hudson, J , Woodard, V , Light, S and Livingston, D M (1977) Proc Natl Acad Sci USA 74, 3745–3749

78 Soule, H R and Butel, J S. (1979) J. Virol 30, 523–532

79 Staufenbiel, M. and Deppert, W. (1983) Cell 33, 173–181

80 Staufenbiel, M and Deppert, W. (1984) J Cell Biol 98, 1886–1894

81 Verderame, M F , Kohtz, D S and Pollack, R E (1983) J Virol 46, 575–583

82 Covey, L , Choi, Y and Prives, C (1984) Mol Cell. Biol 4, 1384–1392

83 Defendi, V (1963) Proc Soc Exp Biol Med. 113, 12–16

84 Habel, K and Eddy, B.E (1963) Proc Soc. Exp Biol Med 113, 1–4

85 Khera, K S , Ashkenazi, A , Rapp, F and Melnick, J L (1963) J Immunol. 91, 604–613

86 Koch, M A. and Sabin, A B (1963) Proc Soc Exp Biol Med 113, 4–12

87 Anderson, J L , Martin, R.G , Chang, C , Mora, P T and Livingston, D,M (1977) Virology 76, 420–425

88 Chang, C., Martin, R G , Livingston, D M., Luborsky, S W , Hu, C.-P. and Mora, P T (1979) J Virol. 29, 69–75

89 Flyer, D C. and Tevethia, S S (1982) Virology 117, 267–270

90 Tevethia, S S , Flyer, D C and Tjian, R (1980) Virology 107, 13–23

91 Pan, S and Knowles, B B (1983) Virology 125, 1–7

92 Soule, H.R , Lanford, R.E and Butel, J.S (1980) J Virol 33, 887–901

93 Tevethia, S S , Katz, M and Rapp, F (1965) Proc Soc. Exp Biol. Med. 119, 896–901

94 Tevethia, S S , Diamandopoulos, G.T , Rapp, F and Enders, J.F (1968) J Immunol 101, 1192–1198

95 Santos, M and Butel, J S (1984) J Virol 51, 376–383

96 Tevethia, S.S., Flyer, D C , Tevethia, M J and Topp, W.C (1980) Virology 107, 488–496

97 Luborsky, S.W and Chandrasekaran, K (1980) Int J Cancer 25, 517–527

98 Schmidt-Ullrich, R , Wallach, D.F.H. and Davis, F D G , II (1976) J. Natl Cancer Inst 57, 1107–1116

99 Lin, P S , Schmidt-Ullrich, R. and Wallach, D.F H (1977) Proc Natl Acad Sci USA 74, 2495–2499

100 Schmidt-Ullrich, R , Wallach, D.F H and Davis, F D G , II (1976) J Natl Cancer Inst 57, 1117–1126

101 Schmidt-Ullrich, R , Thompson, W S , Lin, P -S and Wallach, D F H (1977) Proc Natl Acad Sci USA 74, 5069–5072

102 Schmidt-Ullrich, R , Kahn, S.J., Thompson, W S and Wallach, D F H. (1980) J Natl. Cancer Inst 65, 585–593

103 Lanford, R E and Butel, J S. (1979) Virology 97, 295–306

104 Deppert, W , Henke, K and Henning, R (1980) J Virol 35, 505–518

105 Henning, R , Lange-Mutschler, J and Deppert, W (1981) Virology 108, 325–337

106 Ismail, A., Baumann, E A. and Hand, R. (1981) J Virol 40, 615–619

107 Ohno, T., Yamaguchi, N and Uchida, S (1985) Microbiol Immunol. 29, 39–46

108 Chandrasekaran, K , Winterbourne, D J , Luborsky, S W and Mora, P T (1981) Int J. Cancer 27, 397–407

109 Soule, H R , Lanford, R E and Butel, J.S. (1982) Int. J Cancer 29, 337–344

110 Santos, M and Butel, J S (1982) Virology 120, 1–17

111 Lange-Mutschler, J and Henning, R (1982) Virology 117, 173–185

112 Lange-Mutschler, J and Henning, R (1983) Virology 127, 333–344

113 Lanford, R E and Butel, J S. (1982) Virology 119, 169–184

114 Walter, G , Scheidtmann, K.-H , Carbone, A , Laudano, A.P and Doolittle, R F (1980) Proc Natl. Acad Sci USA 77, 5197–5200

115 Deppert, W and Walter, G. (1982) Virology 122, 56–70

116 Ball, R K., Siegl, B , Quellhorst, S , Brandner, G and Braun, D G. (1984) EMBO J 3, 1485–1491

116a Gooding, L.R., Gelb, R W , O'Connell, K A and Harlow, E (1984) in Cancer Cells, Vol. 1 The Transformed Phenotype (Levine, A J , Vande Woude, G F., Topp, W C. and Watson, J D , eds), pp. 263–269, Cold Spring Harbor Laboratory, Cold Spring Harbor, NY

117 Whittaker, L , Fuks, A and Hand, R (1985) J Virol 53, 366–373

118 Jay, G., Jay, F.T., Chang, C., Friedman, R.M. and Levine, A.S. (1978) Proc. Natl Acad Sci. USA 75, 3055–3059
119 Gooding, L.R. and O'Connell, K.A (1983) J Immunol 131, 2580–2586
120 Tevethia, S.S., Tevethia, M.J., Lewis, A.J., Reddy, V.B and Weissman, S.M. (1983) Virology 128, 319–330
121 O'Connell, K.A. and Gooding, L.R (1984) J. Immunol. 132, 953–958
122 Tevethia, S.S., Lewis, A.J., Campbell, A.E., Tevethia, M.J and Rigby, P.W.J. (1984) Virology 133, 443–447
123 Lane, D.P and Crawford, L.V. (1979) Nature 278, 261–263
124 Ben-Ze'ev, A., Duerr, A., Solomon, F and Penman, S (1979) Cell 17, 859–865
125 Klockmann, U., Staufenbiel, M. and Deppert, W. (1984) Mol Cell Biol. 4, 1542–1550
126 Lewis, A.M., Jr., Levine, A.S., Crumpacker, C.S., Levin, M.J., Samaha, R.J and Henry, P.H. (1973) J. Virol. 11, 655–664
127 Deppert, W., Walter, G. and Linke, H. (1977) J. Virol 21, 1170–1186
128 Jay, G., Jay, F.T., Friedman, R.M and Levine, A.S. (1978) J Virol 26, 411–419
129 Klockmann, U and Deppert, W. (1985) J. Virol 56, 541–548
130 Santos, M. and Butel, J.S. (1984) J. Virol. 49, 50–56
131 Sabatini, D.D., Kreibich, G., Morimoto, T and Adesnik, M (1982) J. Cell Biol. 92, 1–22
132 Walter, P., Gilmore, R and Blobel, G. (1984) Cell 38, 5–8
133 Wickner, W.T. and Lodish, H.F. (1985) Science 230, 400–407
134 Blobel, G. and Dobberstein, B (1975) J. Cell Biol 67, 852–862
135 Blobel, G (1980) Proc. Natl Acad Sci USA 77, 1496–1500
136 Prives, C., Gilboa, E., Revel, M. and Winocour, E. (1977) Proc. Natl Acad Sci USA 74, 457–461
137 Sharma, S., Rodgers, L., Brandsma, J., Gething, M.-J and Sambrook, J (1985) EMBO J. 4, 1479–1489
138 Adams, G.A. and Rose, J.K (1985) Cell 41, 1007–1015
139 Mark, D.F and Berg, P. (1980) Cold Spring Harbor Symp. Quant. Biol. 44, 55–62
140 Denhardt, D.T and Crawford, L.V (1980) J Virol 34, 315–329
141 Jarvis, D.L., Cole, C.N and Butel, J.S. (1986) Mol Cell Biol. 6, 758–767
142 Tevethia, M.J., Anderson, R.W., Tevethia, S.S., Simmons, D., Feunteun, J. and Cole, C. (1986) Virology 150, 361–372
143 Butel, J.S., Guentzel, M.J. and Rapp, F (1969) J Virol. 4, 632–641
144 Rapp, F., Pauluzzi, S. and Butel, J.S (1969) J Virol. 4, 626–631
145 Huebner, R.J., Chanock, R.M., Rubin, B.A and Casey, M.J (1964) Proc Natl. Acad Sci. USA 52, 1333–1340
146 Rapp, F., Melnick, J.L., Butel, J.S and Kitahara, T (1964) Proc Natl. Acad Sci USA 52, 1348–1352
147 Rowe, W.P. and Baum, S.G. (1964) Proc Natl Acad Sci. USA 52, 1340–1347
148 Duff, R., Rapp, F and Butel, J.S (1970) Virology 42, 273–275
149 Kelly, T.J., Jr. and Rose, J.A (1971) Proc Natl. Acad Sci. USA 68, 1037–1041
150 Kelly, T.J., Jr. (1975) J Virol. 15, 1267–1272
151 Lebowitz, P. and Khoury, G (1975) J Virol 15, 1214–1221
152 Rapp, F (1973) Prog Exp. Tumor Res. 18, 104–137
153 Lanford, R.E and Butel, J.S. (1980) Virology 105, 314–327
154 Jarvis, D.L., Lanford, R.E. and Butel, J.S. (1984) Virology 134, 168–176
155 Guentzel, M.J. and Butel, J.S. (1973) Arch. Ges Virusforsch 43, 74–87
155a Paucha, E., Kalderon, D., Richardson, W.D., Harvey, R.W and Smith, A.E (1985) EMBO J 4, 3235–3240
156 Lanford, R.E. and Butel, J.S (1985) Virology 147, 72–80
157 Scheidtmann, K.H., Schickedanz, J., Walter, G., Lanford, R.E and Butel, J.S (1984) J Virol 50, 636–640
158 Fischer-Fantuzzi, L. and Vesco, C. (1984) FEBS Lett. 170, 125–130
159 Smith, A.E., Kalderon, D., Roberts, B.L., Colledge, W.D., Edge, M., Gillett, P., Markham, A.F., Paucha, E and Richardson, W.D (1985) Proc R Soc Lond B 226, 43–58
160 Lanford, R.E. and Butel, J.S (1980) Virology 105, 303–313
161 Schickedanz, J., Scheidtmann, K.-H. and Walter, G (1986) Virology 148, 47–57
162 Lanford, R.E., Hyland, J.K., Baserga, R and Butel, J.S (1985) Mol. Cell. Biol. 5, 1531–1533
163 Weinberg, R.A. (1985) Science 230, 770–776
164 Hirschhorn, R.R., Mercer, W.E., Liu, H.-T. and Baserga, R (1984) Virology 134, 220–229
165 Asselin, C. and Bastin, M. (1985) J. Virol 56, 958–968
166 Paucha, E., Kalderon, D., Harvey, R.W and Smith, A.E (1986) J Virol 57, 50–64
167 Gluzman, Y. and Ahrens, B (1982) Virology 123, 78–92
168 Stringer, J.R (1982) J Virol. 42, 854–864
169 Richardson, L.S and Butel, J.S. (1971) Int J. Cancer 7, 75–85
170 Lanford, R.E. and Butel, J.S (1981) Virology 110, 147–158
171 Fischer-Fantuzzi, L. and Vesco, C (1985) Proc. Natl Acad. Sci. USA 82, 1891–1895
172 Land, H., Parada, L.F and Weinberg, R.A. (1983) Nature 304, 596–601
173 Ruley, H.E (1983) Nature 304, 602–606
174 Milner, J. and Milner, S (1981) Virology 112, 785–788
175 Reich, N.C and Levine, A.J (1984) Nature 308, 199–201
176 Milner, J and Cook, A (1986) Virology 150, 265–269
177 Mercer, W.E., Avignolo, C. and Baserga, R. (1984) Mol. Cell. Biol. 4, 276–281
178 Crawford, L. (1983) in International Review of Experimental Pathology (Richter, G.W and Epstein, M.A., eds.), Vol 25, pp. 1–50, Academic Press, New York

179 Oren, M , Maltzman, W and Levine, A J. (1981) Mol Cell Biol. 1, 101–110

180 Sarnow, P., Ho, Y S., Williams, J. and Levine, A J. (1982) Cell 28, 387–394

181 Zantema, A., Schrier, P.I., Davis-Olivier, A , Van Laar, T , Vaessen, R.T.M J. and Van der Eb, A.J (1985) Mol Cell Biol 5, 3084–3091

182 Eliyahu, D , Raz, A., Gruss, P , Givol, D and Oren, M (1984) Nature 312, 646–649

183 Jenkins, J.R., Rudge, K. and Currie, G A (1984) Nature 312, 651–654

184 Parada, L.F., Land, H., Weinberg, R.A., Wolf, D and Rotter, V (1984) Nature 312, 649–651

185 Jenkins, J.R., Rudge, K , Chumakov, P and Currie, G A (1985) Nature 317, 816–818

186 Yewdell, J., Gannon, J V and Lane, D.P. (1986) J Virol 59, 444–452

187 Montenarh, M , Kohler, M., Aggeler, G and Henning, R (1985) EMBO J 4, 2941–2947

188 Santos, M and Butel, J S. (1985) Mol Cell. Biol 5, 1051–1057

189 Tevethia, S S (1980) in Viral Oncology (Klein, G , ed), pp. 581–601, Raven Press, New York

190 Flyer, D.C , Pretell, J., Campbell, A E , Liao, W.S L., Tevethia, M.J., Taylor, J M and Tevethia, S S (1983) Virology 131, 207–220

191 Karjalainen, H E., Tevethia, M J and Tevethia, S S (1985) J Virol 56, 373–377

192 Oren, M and Levine, A J (1981) Virology 113, 790–793

193 Burger, C. and Fanning, E. (1983) Virology 126, 19–31

194 Schmidt, M F G. and Schlesinger, M.Y. (1980) J Biol Chem 255, 3334–3339

195 Dunphy, W.G., Fries, E., Urbani, L J. and Rothman, J E (1981) Proc Natl Acad. Sci. USA 78, 7453–7457

196 Magee, A.I. and Courtneidge, S.A (1985) EMBO J 4, 1137–1144

197 McIlhinney, R A J , Pelly, S J., Chadwick, J K. and Cowley, G P (1985) EMBO J. 4, 1145–1152

198 Omary, M B and Trowbridge, I.S (1981) J Biol Chem 256, 12888–12892

199 Lange-Mutschler, J and Henning, R (1984) Virology 136, 404–413

200 Schmieg, F I and Simmons, D.T (1984) J Virol 52, 350–355

200a Lanford, R.E., Kanda, P and Kennedy, R C. (1986) Cell 44, 575–582

201 Richardson, W D., Roberts, B.L. and Smith, A.E (1986) Cell 44, 77–85

202 Rothman, J E and Lodish, H F. (1977) Nature 269, 775–780

203 Hunt, L.T. and Dayhoff, M.O (1970) Biochem Biophys Res Commun 39, 757–765

204 McQueen, N L , Nayak, D P., Jones, L V and Compans, R W (1984) Proc Natl. Acad Sci. USA 81, 395–399

205 Hanover, J A , Elting, J , Mintz, G R and Lennarz, W J (1982) J. Biol Chem. 257, 10172–10177

206 Niemann, H , Boschek, B., Evans, D , Rosing, M , Tamura, T and Klenk, H.-D (1982) EMBO J. 1, 1499–1504

207 Johnson, D C. and Spear, P G (1983) Cell 32, 987–997

208 Roth, J (1984) J. Cell Biol 98, 399–406

209 Tartakoff, A M. (1983) Cell 32, 1026–1028

210 Alonso-Caplen, F V and Compans, R W. (1983) J Cell Biol 97, 659–668

211 Shortle, D.R., Margolskee, R F and Nathans, D. (1979) Proc Natl. Acad. Sci. USA 76, 6128–6131

212 Clark, R , Lane, D.P. and Tjian, R (1981) J. Biol Chem. 256, 11854–11858

213 Fey, G , Lewis, J B , Grodzicker, T. and Bothwell, A. (1979) J. Virol 30, 201–217

Biochimica et Biophysica Acta 865 (1986) 197–231
Elsevier

BBA 87162

Virology, genetics and immunology of murine lymphomagenesis

Maarten Zijlstra * and Cornelis J.M. Melief *

Central Laboratory of the Netherlands Red Cross Blood Transfusion Service, incorporating the Laboratory for Experimental and Clinical Immunology of the University of Amsterdam, Amsterdam (The Netherlands)

(Received 27 March 1986)

Contents

I Characteristics of murine leukemia viruses 198
  A General aspects and scope of review . 198
  B Host-range classes of MuLV 199
  C Endogenous MuLV-related proviral sequences . . 201

II The involvement of different host-range classes of MuLV in lymphomagenesis 202
  A Spontaneous AKR thymomas . . 202
  B Spontaneous HRS/J thymomas 202
  C Spontaneous T, B and non-T/non-B cell lymphomas in mouse strains with a low spontaneous lymphoma incidence 203
  D. Moloney MuLV-induced T-cell lymphomas in mice and rats . . . 203
  E. T, B and non-T/non-B-cell lymphomas induced by AKR-type ecotropic and MCF MuLV in mouse strains with a low spontaneous lymphoma incidence : . . . 204
  F T, B and non-T/non-B cell lymphomas induced by wild mouse-derived ecotropic and amphotropic MuLV 204
  G. Carcinogen and radiation-induced T-cell lymphomas . . . 205
  H. Graft-versus-host (GVH)-reaction-induced B-cell lymphomas 205
  I The involvement of murine mammary tumor viruses (MMTV) in murine thymic lymphomas 206

III Mechanisms of MuLV-induced lymphomagenesis 206
  A. Retroviral insertions in the vicinity of cellular oncogenes 207
  B. Overview of chromosomal aberrations in virus- and non-virus-induced murine lymphomas and of loci important in tumorigenesis 208
  C Other etiologic factors involved in T-cell lymphomas induced by Moloney MuLV in the mouse . 212
  D. Other etiologic factors involved in thymoma development in AKR mice 212
  E Antigen-specific T cells transformed by the radiation leukemia virus (RadLV) . 213

---

* Present address. The Netherlands Cancer Institute, Department of Immunology, Plesmanlaan 121, 1066 CX Amsterdam, The Netherlands

Abbreviations AIDS, acquired immunodeficiency syndrome; CTL, cytotoxic T lymphocyte; DMBA, 7,12-dimethylbenz-[*a*]anthracene, FITC, fluorescein isothiocyanate; FMR, Friend, Moloney and Rauscher; GVH, graft-versus-host; HTLV-I, human T-lymphotropic virus-I, HIV, human immunodeficiency virus; IFN, interferon; IL-3, interleukin-3, Ir, immune response, LTR, long terminal repeat; MCF, mink cell focus-inducing, MHC, major histocompatibility complex, MMTV, murine mammary tumor virus(es), MuLV, murine leukemia virus(es), RadLV, radiation leukemia virus; 20αSDH, 20α-hydroxysteroid dehydrogenase

Correspondence Dr. M Zijlstra, c/o Publication Secretariat, Central Laboratory of the Netherlands Red Cross Blood Transfusion Service, P O Box 9406, 1006 AK Amsterdam, The Netherlands

0304-419X/86/$03 50 © 1986 Elsevier Science Publishers B V (Biomedical Division)

IV. Regulation of anti-MuLV immune responses 213
A The H-2 complex 213
B The antibody response against MuLV virions 214
C The antibody response against MuLV-related cell-surface antigens 215
D Cytotoxic T-cell response against MuLV 216
E NK-cell reactivity with (MuLV-infected) tumor cells 217
F Efects of interferons on the spread of MuLV 217

V. H-2 and MuLV-induced lymphomagenesis 218
A H-2 influence on susceptibility to MuLV-induced lymphomagenesis 218
B Imbalanced expression of MHC molecules on murine lymphomas 220
C Presence of H-2 molecules on MuLV virions 221

VI Conclusions 222

Acknowledgements 223

References 224

I. Characteristics of murine leukemia viruses

IA. General aspects and scope of review

Murine leukemia viruses (MuLV) are members of the group of RNA tumor viruses, which is one of the three subfamilies of Retroviridae [1]. RNA tumor viruses are widespread among many vertebrate species, e.g., birds, rodents and cats, and induce neoplasias of predominantly hemapoietic origin [1–4]. In primates and in man, retroviruses are also found [1,5], as exemplified by human T lymphotropic virus-I (HTLV-I) causing adult T-cell leukemia/lymphoma and human immunodeficiency virus (HIV), the etiologic agent of acquired immunodeficiency syndrome (AIDS) [5]. Characteristically, RNA tumor viruses encode an RNA-dependent DNA polymerase (reverse transcriptase), which enables the virus to generate a double-stranded DNA copy [1,4,6], using the single-stranded viral RNA genome as template. The double-stranded proviral DNA integrates into the cellular DNA, whereafter the provirus is transcribed into genomic RNA which will direct the synthesis of viral proteins, followed by assembly of new virus particles [1,6]. An RNA tumor virus particle (approx. 1000 Å in diameter) consists of an outer lipid membrane with the viral envelope proteins on its surface. The inner core particle contains the gag proteins and two identical single-stranded RNA genomes. On the basis of their ultrastructural morphology, RNA tumor viruses are classified as types A–D [1].

MuLV belong to the type C RNA tumor viruses. The 8.2-kb-long RNA genome encompasses three major regions: 5′-gag-pol-env-3′ [1,4] (Fig. 1). The gag region encodes the 65 kDa gag precursor which is processed into the viral core proteins p15,

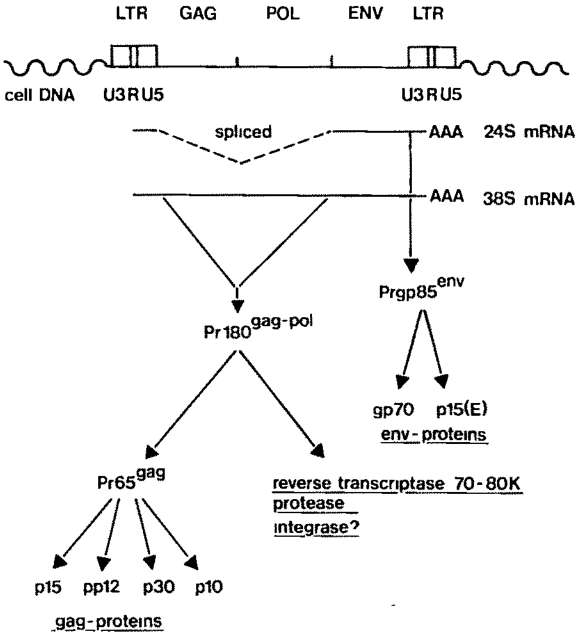

Fig 1. Structure and mode of expression of an integrated murine leukemia provirus

pp12, p30 and p10. The pol region codes for the 75 kDa reverse transcriptase and in addition, this region encodes a proteinase [7] and most likely a protein required for the integration of proviral DNA [8]. The env region encodes the 85 kDa env precursor which is processed into the gp70 and p15(E) envelope proteins.

An important feature of the linear (integrated) proviral DNA is the presence of identical long terminal repeat (LTR) sequences at both termini (Fig. 1). These LTR sequences are generated during the reverse transcription reaction and contain sequences of both the 5′ and 3′ ends of the viral RNA genome [1,4,6]. The LTRs contain sequences unique to the 5′ end of the viral RNA genome (U5 sequences), a repeat sequence (R sequence) present at both ends of the viral RNA genome and sequences unique to the 3′ end of the RNA genome (U3 sequences). In most MuLV, the U3-LTR sequences contain regulatory signals important in viral transcription, such as the 'TATAA' and CCAAT-like boxes, enhancer region and transcription termination signals [1]. The acutely transforming retroviruses (including the MuLV-derived mouse sarcoma viruses and the Abelson virus) contain a fourth gene denoted 'onc', which causes selective transformation of distinct cell types infected with these viruses [2,3,10,11]. In most cases the insertion of the 'onc' gene is accompanied by the deletion of (sections of) viral structural genes. As a result, these acutely transforming retroviruses are mostly replication-defective [2,3,10,11]. For in vivo/vitro spread/transformation, they therefore need a slow acting replication-competent helper virus [2,3,10,11]. Recent reviews concerning the molecular biology of RNA tumor viruses [1–4,9], cellular oncogenes and acutely transforming retroviruses [2,3,10,11] are available.

The induction of lymphomas in the mouse by slow-acting MuLV was first shown in 1951 by the imposing studies of Ludwig Gross [12], whose efforts generated intense interest in the role of MuLV in murine lymphomagenesis, including scrutiny of the role of different host-range classes of MuLV in the process of lymphomagenesis, and characterization of cellular resistance genes [13]. In this review we shall discuss genetically determined resistance mechanisms against lymphomagenesis induced by slow acting MuLV, with emphasis on immune mechanisms and the role of the murine major histocompatibility complex (MHC; H-2 complex). These data will be discussed in the light of recent insights into the cellular events, including onc-gene activation and chromosomal aberrations, involved in malignant transformation of mouse lymphoid cells.

IB. Host-range classes of MuLV

The ability of MuLV to infect cells depends on the viral gp70 envelope protein which determines the interaction with the different cellular receptors for the various host-range classes of MuLV [14–16]. According to their ability to infect and replicate in cells of mouse and/or non-mouse origin, murine leukemia viruses have been divided into four host-range classes (Table I):

(a) Ecotropic. This class of MuLV only infects and replicates in mouse cells. By biochemical and antigenic differences, ecotropic MuLV fall into two main groups: (1) AKR-type virus, which is endogenous to most inbred mice, and (2) FMR-type virus, represented by the exogenous Friend, Moloney and Rauscher species of MuLV.

(b) Xenotropic. This class of MuLV infects and replicates only in certain non-mouse species such as cat, mink, rabbit or man [16]. Xenotropic MuLV is not infectious for cells from all inbred and most wild mice. Recently, cells from some wild mice were found to be susceptible to infection with xenotropic MuLV [17].

(c) Amphotropic. This wild-mouse-derived

TABLE I

HOST-RANGE CLASSES OF MURINE LEUKEMIA VIRUSES

Host-range class of MuLV	Replication in cells of different origin	
	mouse	non-mouse
a Ecotropic	+	–
b Xenotropic	– [a]	+
c Amphotropic	+	+
d Dualtropic MCF	+	+

[a] Recently cells derived from some wild mice were found to be susceptible to infection with xenotropic MuLV [17].

MuLV species is infectious for both mouse and certain non-mouse cells [16].

(d) Dualtropic mink cell focus-inducing (MCF). The MCF viruses, which have been isolated from (pre)leukemic tissue of inbred mice, can also infect and replicate in both murine and certain non-murine cells [16]. They can be clearly distinguished, however, both antigenically [18–20] and biochemically [21] from the wild-mouse-derived amphotropic class of MuLV, because they are recombinants of ecotropic- and xenotropic-like sequences in the viral env region [21–24]. Some MCF isolates preferentially replicate in the thymus and are therefore designated as thymotropic [25,26]. A special feature of MCF viruses is that they induce cytopathologic changes in mink lung cells [27]. Amphotropic and most xenotropic MuLV do not induce these changes, with the exception of certain xenotropic viruses isolated from SL mice [28].

Nature of host-range restriction

Ecotropic, amphotropic and dualtropic MCF viruses appear to infect mouse cells via different cellular receptors [15,16,29,30]. The exact number, identity and mode of action of these cellular receptors is still unknown [29,30]. A locus necessary for replication of ecotropic MuLV, possibly encoding the cellular receptor for ecotropic MuLV has been mapped to chromosome 5 [31]. A gene necessary for replication of amphotropic MuLV has been localized on chromosome 8 [32] and for MCF viruses on chromosome 1 [33]. The identity of the cellular receptor for ecotropic MuLV is still controversial. A receptor for the ecotropic Friend/Rauscher type of MuLV has been characterized as a 10–14 kDa protein which is expressed both on fibroblasts [34] and spleen cells [35]. The receptor for Moloney MuLV solubilized from murine L-cell membranes has an approximate molecular mass of 110 kDa [36]. Binding studies with ^{125}I-labeled gp70 indicate, however, that the cellular receptor for the ecotropic Moloney MuLV on thymocytes consists of a dimer of a 190 kDa protein [37,38]. This putative Moloney MuLV receptor is expressed on the majority of normal thymocytes and to a lesser extent on normal spleen and bone-marrow cells [37]. Despite this fact, normal thymocytes [39] or mitogen/interleukin-2-stimulated T cells [39–41] cannot be productively infected in vitro by ecotropic Moloney virus. It is not clear whether this inability to productively infect T cells is due to a failure to penetrate into the cells, a low level of proviral integration or the result of a transcriptional block for integrated proviruses. Such a transcriptional block has been described for Moloney MuLV-infected embryo carcinoma cells [42,43]. In vitro, only lipopolysaccharide-stimulated B-cell blasts can readily be productively infected by Moloney MuLV [39,40].

Little is known concerning the identity and cell distribution on lymphocytes of the cellular receptors for the other host range classes of MuLV. In vitro, only a small population of thymocytes is susceptible to productive infection by cloned thymotropic oncogenic AKR MCF viruses [25]. In vivo, the thymotropic radiation leukemia virus initially only replicates in a small minority of thymocytes [44].

The Fv-1 gene and other cellular genes regulating MuLV replication

The murine Fv-1 locus on chromosome 4 encodes a product which interferes with productive infection by certain species of MuLV [13,45]. The Fv-1 gene product most likely inhibits the integration of proviral DNA into the cellular genome [46]. The viral structure involved in the determination Fv-1 host range appears to reside in the gag p30 gene of the nonintegrated proviral DNA [47–49]. At least three Fv-1 alleles are known in inbred mice [13]. Homozygous Fv-$1^{n/n}$ cells are much more susceptible (1000-fold) to productive infection by N-tropic MuLV than to B-tropic MuLV, while homozygous Fv-$1^{b/b}$ cells are more susceptible (100-fold) to B-tropic MuLV. Heterozygous Fv-$1^{b/n}$ mice are resistant to both N- and B-tropic viruses [13,50]. A third restriction allele (Fv-1^{nr}) carried by a few inbred mouse strains affects susceptibility to B-tropic viruses as well as certain N-tropic MuLV isolates [50]. Wild mice carry the Fv-1^{nr} or the Fv-1^{o} locus, which does not restrict either N- or B-tropic viruses [50].

A recent study by Levy et al. [51] partially elucidated the mechanism of action of the product of another cellular locus, denoted Gv-1. The Gv-1 locus was shown to coordinately regulate the transcription of multiple endogenous murine retroviruses in 129 mice, most likely by regulating the state of methylation of these proviruses [51].

A third important autosomal gene (Rmcf^{r}) interferes with the infection and spread of MCF viruses in some mouse strains (e.g., DBA/2), presumably because it encodes an MCF MuLV-related env gene product expressed on the surface of lymphoid cells, thus preventing de novo infection by exogenous MCF viruses [52–58].

IC. Endogenous MuLV-related proviral sequences

The genomes of all inbred mice and most wild mice contain a large number of MuLV-related proviral sequences. Both ecotropic and MCF/xenotropic MuLV-related proviral sequences are present in the genome, either as intact inducible proviruses or as non-inducible (probably defective) genomes. All of these MuLV proviral genomes are transmitted as Mendelian genes.

IC-a. Ecotropic MuLV-related proviral sequences

Inbred mice contain variable numbers of ecotropic MuLV genomes as revealed either by the production of (inducible) infectious ecotropic MuLV [59–61] or by the presence in the genome of proviruses annealing with probes specific for the ecotropic gp70 and p15(E) genes [24,62,63]. Some inbred mice, such as high spontaneous leukemia incidence AKR/N, AKR/J and C58/J, mice [61–64], contain several loci of ecotropic MuLV. Different sublines of AKR mice contain variable numbers of proviral ecotropic MuLV [63–66]. Even within one distinct AKR substrain, diversity is sometimes seen among individual animals, reflecting novel germ-line proviral insertions in this strain, with genetically determined highly infectious virus levels persisting throughout its reproductive period [63,66–68]. Other inbred mice, such as C57BL/10, BALB/c and A, with genetically controlled low levels of infectious virus expression, contain a single ecotropic provirus [24,61,62]. These proviruses have been assigned to different chromosomes, e.g., chromosome 8 in C57BL/10 mice and chromosome 5 in BALB/c and A mice [60,61]. Other strains (e.g., NZB, NIH/Swiss and 129 mice) lack an ecotropic MuLV provirus in their genome [62]. In wild mice, ecotropic MuLV genomes have been found only in the DNA of Japanese mice, suggesting an Asian origin of the AKR-type of ecotropic MuLV [69].

The expression of ecotropic MuLV envelope proteins encoded by endogenous provirus(es) could be important in preventing viremia and tumorigenesis induced by horizontal infection with exogenous ecotropic MuLV. An example in favor of this hypothesis is the association between the Fv-4-locus-mediated resistance against Friend virus-induced erythroblastosis and the presence [70,71] and expression [71–74] of ecotropic envelope-related proviral sequences [74].

B10.Y(H-2^{pa}) mice have been reported to possess a high level of expression of endogenous ecotropic MuLV which appears to be regulated by the H-2 complex [75]. The presence in this B10.Y strain of a milk-transmitted MuLV has not completely been ruled out, however [75].

IC-b. Xenotropic/MCF MuLV-related proviral sequences

Hybridization studies with xenotropic/MCF env-specific probes [57,76–80] and molecular cloning of endogenous proviruses [81,82] revealed the presence of multiple copies (15 to 30) of env-related segments in the genome of all inbred and most wild mice. The DNAs of inbred mice most likely contain fewer xenotropic than MCF MuLV env-related sequences [80]. One or more of these loci encode inducible infectious xenotropic MuLV [61,83], others probably represent defective proviruses [61,81]. A number of the xenotropic/MCF-related env sequences have been assigned to chromosomal regions which are tightly linked to loci encoding minor histocompatibility and/or lymphocyte differentiation antigens [60,84–86]. Interestingly, some sequences annealing to a MuLV-specific probe have been localized to the TL region of the major histocompatibility complex, H-2 [87]. One sequence (TLenv1) contains sequences annealing with gag, pol and env AKR MuLV region probes. These MuLV-related sequences are bounded by retrovirus-like, VL30 long terminal repeats [88]. The other sequence (TLenv2) only hybridizes with a probe derived from the pol region of ecotropic AKR MuLV [88]. In certain mouse strains an H-2-linked regulation of xenotropic MuLV expression has been observed [89].

II. The involvement of different host-range classes of MuLV in lymphomagenesis

IIA. Spontaneous AKR thymomas

AKR mice have been selected for a high spontaneous thymoma development (reviewed by Gross [12]). At 6–12 months of age almost all AKR mice develop thymic T-cell lymphomas which sometimes also spread to peripheral lymphoid organs such as spleen and mensenteric lymph nodes [12].

In the process of lymphomagenesis in the thymus, MCF viruses are generated by recombination between the endogenous ecotropic MuLV expressed early in life by AKR mice and endogenous xenotropic-like envelope and LTR proviral sequences [23,24,27,90]. In addition, ecotropic recombinant viruses (ERV) may be generated which have an ecotropic host range but in the env region possess restriction sites characteristic of MCF viruses [91]. Several observations indicate that not only newly generated MCF viruses but also ecotropic MuLV with altered LTR sequences are causative agents in thymoma development:

First, the onset of lymphoma development in the thymus is preceded by the generation and expression of recombinant MCF [26,27,90,92–95] and (recombinant) ecotropic MuLV [23,91,95–102] with acquired xenotropic MuLV-related sequences in the gag-pol, env and/or LTR region.

Second, some of the isolated AKR MCF viruses accelerate thymoma development after inoculation into newborn AKR and C3H mice [26,95,103–106]. Other strains of mice (e.g., DBA/2, NFS), however, are resistant [28,107]. Susceptibility to lymphomagenesis by the highly oncogenic AKR MCF 247 virus in AKR × NFS crosses segregates with the presence of an endogenous ecotropic provirus [108]. This indicates that in these AKR × NFS crosses the AKR MCF 247 virus might need further recombination to create even more oncogenic recombinant viruses. Alternatively, the presence of ecotropic MuLV may facilitate the spread of the AKR MCF 247 virus. Certain ecotropic MuLV isolates with alterations in the p15(E) and/or LTR region are highly oncogenic as well [97,98,100,101,109,110]. However, lymphomagenesis by these altered ecotropic MuLV isolates in AKR mice and most other mouse strains may be associated with the integration and expression of MCF MuLV in the DNA of tumor cells [111,112].

Third, neonatal inoculation of AKR mice with a thymotropic non-oncogenic MCF virus notably delays the onset of spontaneous AKR thymomas [113,114], probably by interference with the spread of oncogenic MCF viruses which are generated de novo later on in the inoculated mice.

Fourth, AKR thymoma DNA contains integrations of predominantly MCF type of MuLV [24,78,115–118]. In 10–15% of the spontaneous and 20–65% of the AKR thymomas induced by oncogenic MCF viruses, MCF proviruses integrate in the vicinity of the cellular oncogenes c-myc [119–122] or pim-1 [120,122,123] and activate the transcription of these genes [119,120,122,123]. At lower frequency, somatically acquired MuLV genomes with ecotropic gp70 sequences are found in tumor DNA [78,98,117,118,124], some of which have been shown to activate c-myc or pim-1 [120,122,123].

The oncogenic potential of MCF and ecotropic AKR MuLV isolates is predominantly determined by structures in the LTR [110,111,125–127]. These LTR sequences contain enhancer regions which cause a tissue-specific transcription preference of the recombinant MuLV [128]. In addition, studies with constructed chimeric viral genomes between non-lymphomagenic and highly oncogenic ecotropic or MCF viruses indicate that the regions encoding gag-pol, gp70 and p15(E) also contribute to the oncogenicity of an ecotropic or MCF MuLV [125–127].

Although AKR mice have been selected for a high spontaneous thymoma development [12], the bone marrow of thymectomized 8–12-mo-old AKR mice contains pre-leukemic B cells [129]. These pre-leukemic B cells become apparent upon transplantation into young recipient AKR mice. This finding exemplifies from another angle the genetic predisposition of AKR mice (chromosome 15?) to lymphoma development.

IIB. Spontaneous HRS/J thymomas

Inbred hairless HRS/J mice carry a mutant autosomal recessive gene (hr) which predisposes hr/hr homozygotes, unlike hr/+ heterozygotes, to the development of thymic T-cell lymphomas

[130] As in AKR mice, thymoma development in HRS/J hr/hr mice is accompanied by the generation and expression of MCF MuLV [130,131]. Neonatal inoculation with some of these MCF viruses accelerates lymphomagenesis in both HRS/J and low spontaneous lymphoma incidence CBA/J mice [130], but not in SWR/J, NIH/Swiss or NFS mice [130,132]. It was suggested that a particular HRS/J hr/hr-derived MCF isolate induces T-cell lymphomas of discrete phenotype [133]. However, the number of lymphomas examined was low. In addition, this finding was not confirmed by other studies in which the Lyt phenotype and I-A/E expression of MCF virus-induced T-cell lymphomas in the AKR mouse [25,134] or C57BL and BALB/c mice were examined [135,136].

IIC. Spontaneous T, B and non-T/non-B cell lymphomas in mouse strains with a low spontaneous lymphoma incidence

Integrations of MuLV in the DNA of spontaneous lymphomas from low leukemia incidence mouse strains have not been extensively examined. In a study with spontaneous lymphomas from H-2 congenic C57BL mice, integrated MuLV genomes could be detected in approx. 50% of the tumors [137]. These C57BL lymphomas arise at low frequency (10–20%) and after a long latency (12–30 months of age). Integrations of several types of MuLV (MCF, ecotropic) were present in the DNA of T, B and non-T/non-B cell lymphomas [137]. No correlation was apparent between lymphoma type and the presence or absence of integrated proviral sequences [137]. The DNA of all spontaneous B-cell lymphomas in CWD/AgL mice contain MuLV integrations, of both ecotropic and MCF MuLV genomes [138,139].

The development of spontaneous B-cell lymphomas in SJL mice is associated with the expression of MCF viruses [140]. Neonatal inoculation of SJL mice with a non-oncogenic MCF virus but not with ecotropic MuLV protects these mice against the development of spontaneous B-cell tumors [141].

IID. Moloney MuLV-induced T-cell lymphomas in mice and rats

T-cell lymphomas can be induced by ecotropic Moloney MuLV in the mouse either by the introduction in the germline of a Moloney MuLV provirus [122,123,142–144] or by inoculation of virus into newborn mice [122,123,144]. In both situations the T-cell lymphomas have acquired integrated MCF MuLV genomes [122,144]. Integrations of ecotropic Moloney proviruses are

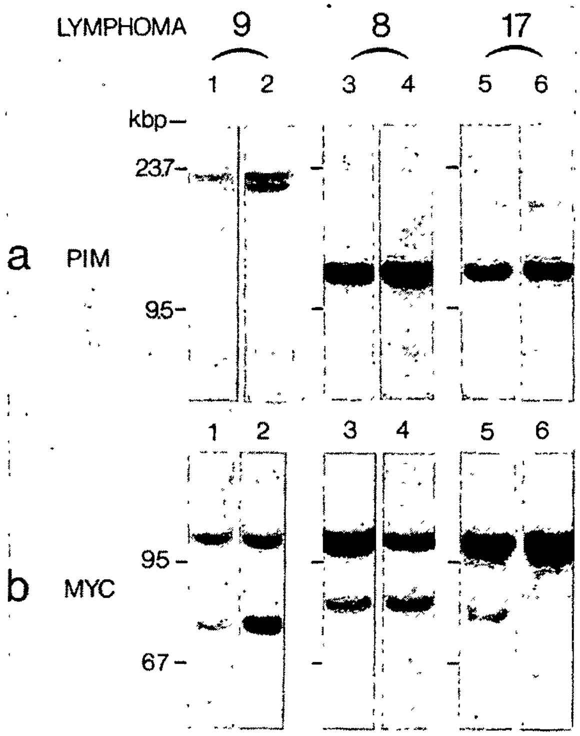

Fig. 2. Segregation of proviral integrations in transplanted Moloney MuLV-induced lymphomas. *Eco*RV (panel a, lanes 1 and 2), *Eco*RI (panel a, lanes 3, 4, 5 and 6) and *Kpn*I (panel b) digests of primary lymphoma DNA from mouse 9, 8 and 17 (lanes 1, 3 and 5 respectively), and the corresponding transplanted tumors (lanes 2, 4 and 6, respectively) (a) Hybridization to pim-1 probe (b) Hybridization to c-myc probe The normal pim-1 allele corresponds to the 22 kbp (*Eco*RV) or the 12 kbp (*Eco*RI) fragment (panel a), the normal c-myc allele corresponds to the 11-kbp fragment (panel b) These analyses indicate that some primary Moloney MuLV-induced lymphomas contain different tumor cell populations. Upon transplantation selection occurs on the subpopulation with a proviral insertion in the vicinity of either c-myc (tumor 8), pim-1 (tumor 17) or a subpopulation of tumor cells with both a c-myc and pim-1 rearrangement (tumor 9) (adapted from [120])

observed as well [122,144]. In approx. 50% of the primary tumor DNAs, integration of either ecotropic or MCF Moloney MuLV is observed in the vicinity of c-myc [120] and/or pim-1 [122,123]. In these cases, either one or both genes are transcriptionally activated by the proviral integrations [120,122,123]. Most primary Moloney MuLV-induced mouse T-cell lymphomas are oligoclonal in origin, as evaluated by transplantation studies which indicated the presence of multiple onc-gene rearrangements in separate primary tumor-cell populations [120,145] (Fig. 2).

A striking feature of Moloney MuLV-induced T-cell lymphomagenesis in the rat is the finding that the DNA of these tumors exclusively contains integrations of ecotropic Moloney MuLV genomes [146,147]. At low frequency these Moloney MuLV genomes integrate in the vicinity of the c-myc locus of the rat [148].

IIE. T, B and non-T/non-B cell lymphomas induced by AKR-type ecotropic and MCF MuLV in mouse strains with a low spontaneous lymphoma incidence

The induction of myeloid leukemias by a horizontally transmitted MuLV in recombinant BXH mice is accompanied by integrations of ecotropic MuLV genomes into the tumor DNA [149,150]. That this DNA also contains somatically acquired MCF proviruses was not excluded [150].

Inoculation of H-2 congenic C57BL or BALB/c mice with ecotropic and/or MCF MuLV induces a variety of lymphoma types [135,136,151–157]. NFS mice congenic for an ecotropic AKV MuLV provirus also develop a wide spectrum of lymphoma/leukemia types [158]. Inoculation, intrathymically or otherwise, with virus stocks containing an oncogenic thymotropic MCF virus induces T-cell lymphomas at a higher frequency [135,136,151,152,159]. The H-2 complex influences both the susceptibility to a particular MuLV isolate [135,136,151–153,155] and the T, B or non-T/non-B cell type of the induced lymphomas [135,136,155]. After neonatal inoculation of the C57BL-derived MCF 1233 virus into H-2-congenic C57BL mice, those H-2-congenic mouse strains (e.g., B10.A, B10.BR) which mount poor antiviral humoral responses predominantly develop lymphomas of T-cell type (Ref. 136; Vasmel et al., unpublished data). In contrast, the H-2-congenic strains with good antiviral antibody responses (e.g., B10, B10.A(5R)) generally develop B or non-T/non-B-cell lymphomas (Ref. 136; Vasmel et al., unpublished data).

The structure of the integrated MuLV genomes present in the DNA of these different types of lymphoma has been examined only to a limited extent. A study of T, B and non-T/non-B cell lymphomas induced with cloned MuLV in H-2 congenic C57BL and BALB/c mice indicates that in these low spontaneous lymphoma incidence mouse strains the process of lymphomagenesis is accompanied by frequent recombination between the inoculated virus and endogenous MuLV [137]. For instance, the DNA of T, B or non-T/non-B cell lymphomas induced by poorly oncogenic MCF viruses often contain integrations of ecotropic MuLV [137]. The DNA of different types of lymphomas induced by inoculation with ecotropic MuLV often contain somatically acquired MCF-related genomes [137]. Radiation leukemia virus-(RadLV)-induced T-cell lymphomas contain somatically acquired RadLV genomes, but the exact structure of these RadLV genomes and the presence of other types of integrated MuLV proviruses has not been examined in detail [160,161].

IIF. T, B and non-T/non-B cell lymphomas induced by wild-mouse-derived ecotropic and amphotropic MuLV

Besides neurogenic hind-limb paralysis [162, 163], wild-mouse-derived MuLV isolates also induce lymphomas in susceptible mice [162,164–166]. Inoculation with the cloned ecotropic Cas-Br-M isolate into NFS/N mice induces a wide spectrum of hematologic neoplasias, including T- and B-cell lymphomas and myelogenous leukemia or erythroleukemia [164]. A study by Jolicoeur and DesGroseillers [167] with in vitro constructed chimeric viral genomes indicates that the oncogenic potential of the ecotropic Cas-Br-E isolate is determined by various regions: gag-pol, pol-env and LTR. This resembles observations made with oncogenic ecotropic and MCF AKR viruses [125–127] (subsection IIA).

In NIH/Swiss mice the induction of splenic non-T/non-B cell lymphomas by the wild-mouse-derived amphotropic 1504A virus is accompanied by the generation of a highly oncongenic recombinant virus [165]. RNAase T_1 oligonucleotide finger printing indicates recombination in the env gene between the parental 1504A virus and endogenous xenotropic-like MuLV sequences of NIH Swiss mice [166].

Although the onset of paralysis induced by infection with wild mice-derived ecotropic MuLV is preceded by the expression of dualtropic MCF virus [162], the paralysis appears to be caused solely by ecotropic MuLV [163].

IIG. Carcinogen and radiation-induced T-cell lymphomas

Although both ecotropic and thymotropic MCF viruses have been isolated from some X-ray-induced thymomas, their causative role in both X-ray- and carcinogen-induced lymphoma development is highly questionable [168–171]. Some studies claim that X-ray-induced thymoma development in C57BL/Ka mice is accompanied by the activation of endogenous ecotropic MuLV [172, 173]. In these studies, however, long-term cocultivations were performed, which favors the possibility that the virus was derived from contaminating non-lymphomatous tissue. Continuous in vitro cell lines derived from the same lymphomas mostly produce ecotropic MuLV, but whether the primary lymphomas already contained such MuLV is uncertain.

The role of MuLV in X-ray-induced lymphomas of BALB/c mice is also unclear. Most lymphomatous tissues contain B-tropic ecotropic MuLV, but no expression of either MCF or xenotropic MuLV is apparent [174,175]. However, expression of this ecotropic MuLV is not prognostic for tumor development in individual mice, and age-matched BALB/c control mice also express ecotropic MuLV to some extent [174]. In X-irradiated NZB mice only xenotropic MuLV was detected [176]. Studies concerning the susceptibility of crosses between mouse strains which either contain (BALB/c, RF mice) or do not contain (129 mice) an infectious endogenous ecotropic MuLV also suggest that infectious ecotropic MuLV is not involved in X-ray- or carcinogen-induced lymphomas [171].

In conclusion, it is unlikely that insertional mutagenesis by MuLV contributes to X-ray- and carcinogen-induced lymphomagenesis. This conclusion has been strengthened by the finding that the DNA of only a minority of primary 3-methylcholanthrene-induced T-cell lymphomas in RF mice [177] and primary radiation-induced BALB/c and C57BL lymphomas [161,178] contain newly acquired MuLV genomes, although in the latter studies the involvement of MCF viruses was not completely excluded. Other mechanisms such as the acquisition of chromosomal aberrations or point mutations in cellular oncogenes are much more likely to play a major role. This is supported by the finding that a high proportion of carcinogen- and X-ray-induced thymomas in (AKR × RF)F_1 mice contain a mutated transforming N-ras or Ki-ras gene [179,180].

Interestingly, genetic studies indicate that (1) loci controlling radiation-induced lymphomagenesis, (2) loci which encode murine histocompatibility or lymphocyte differentiation antigens and (3) endogenous MuLV proviruses are closely linked [57,84,86–88,181–182]. These virus loci were detected with probes specific for the env region of MCF/xenotropic type of MuLV, and were mapped to several chromosomes, including regions on chromosomes 1 and 2 which also code for mouse lymphoid differentiation antigens [57, 181,182].

IIH. Graft-versus-host (GVH)-reaction-induced B-cell lymphomas

The induction of a chronic graft-versus-host (GVH) reaction in certain mouse strain combinations, classically parental BALB/c cells into (BALB/c × A)F_1 hybrid animals, results in the development of lymphomas [183,184]. In most cases these lymphomas develop with a long latency (1–2 years) and constitute predominantly B-cell tumors of host origin [183,184]. H-2 disparity at the left-hand part of H-2 including I-A and/or I-E is necessary for the development of these lymphomas [183].

The role of MuLV in GVH-associated lymphomagenesis is at present still uncertain. One study indicates that during the GVH reaction only the expression of xenotropic MuLV is activated [185].

However, only a relatively short period of time (6 weeks) after the onset of the GVH reaction was examined [186]. In some instances GVH-associated lymphomagenesis may be associated with the generation of MCF MuLV [186,187]. Another study indicated activation of B-tropic ecotropic MuLV in the process of lymphomagenesis in BALB/c → (BALB/c × A)F_1 mice [188]. In this latter study the appropriate controls excluding the possible presence of MuLV in the parental spleen cells inoculated to induce GVH were not performed [183]. More convincing are the findings by Varet et al. [189], which indicate synergism between MuLV infection and GVH reaction in the induction of lymphomas. The phenotype of the lymphomas was not examined in this study.

Southern blot analyses indicate that in the BALB/c → (BALB/c × A)F_1 model integrations of MuLV occur in the DNA of approx. 80% of the lymphomas [184]. These somatically acquired MuLV sequences showed predominantly an ecotropic structure although in some lymphomas deleted MuLV or MCF MuLV genomes were observed. The implications of these MuLV integrations for the mechanism of GVH-induced B-cell lymphomagenesis are still unclear, because they were shown not to have integrated in the vicinity of the cellular c-myc, c-mos or c-myb oncogenes [184]. Thus the concept that these integrated MuLV proviruses contribute to tumor development by insertional mutagenesis has still to be validated.

II-I. The involvement of murine mammary tumor viruses (MMTV) in murine thymic lymphomas

Several studies indicate that in some experimental murine models murine mammary tumor viruses (MMTV), type-B retroviruses, may be involved in the generation of thymic T-cell lymphomas. Generally, the activation of endogenous MMTV or infection with exogenous MMTV is associated with the development of mammary tumors in susceptible strains of mice [190]. In female GR mice, the expression of the endogenous MMTV-2 provirus causes a high incidence of mammary adenocarcinomas [190]. In male GR mice, the expression of this endogenous MMTV provirus is associated with the development, at low incidence, of thymic lymphomas [190]. The DNA of these "spontaneous" thymic lymphomas arising in old male GR mice was shown to contain integrated MMTV proviruses [191]. These integrated MMTV proviruses possess rearranged LTRs which contain novel enhancer-like structures which may allow T-cell-specific replication of the variant MMTV [192]. In the tumor DNAs these variant MMTV genomes do not integrate in the vicinity of known cellular oncogenes (i.e., c-myc, pim-1, int-1, int-2 and others; Michalides, R., personal communication), but other as yet unknown genes may be involved. Studies by Debakan and Ball indicate that thymic lymphoma induction by injection of a virus complex which contains MMTV is also accompanied by integration of MMTV genomes into tumor DNA [193,194]. Finally, the fact that the DNA of a considerable number of transplantable murine T-cell lymphomas contains extra copies of integrated MMTV proviruses [195] may implicate MMTV in lymphoma development or progression.

III. Mechanisms of MuLV-induced lymphomagenesis

In most models which address the question of how slow acting murine leukemia viruses (i.e., viruses without built-in oncogenes) induce lymphomas, chronic immunostimulation caused by MuLV infection is considered as one of the etiologic factors. However, in none of these models has definitive proof been provided. In addition, severe immuno-suppression may also promote oncogenesis in some instances [196,197]. The mechanisms by which oncogenic transformation occurs are clearly diverse, and include insertional mutagenesis by MuLV [119,120,122,123], mutations in cellular oncogenes [179] or the acquisition of chromosomal aberrations [198]. The evidence for these mechanisms, in addition to the data supporting the view that MuLV-specific immune lymphocytes or lymphocytes specifically activated by MuLV infection may be preferential targets for oncogenic transformation, will be reviewed below.

IIIA. Retroviral insertions in the vicinity of cellular oncogenes

Early T-cell lymphomas in mice and rats induced by highly virulent MuLV (Moloney virus and oncogenic AKR viruses)

Mice. In Moloney MuLV-induced C57BL and BALB/c early (latency 2–6 months) T-cell lymphomas [120,122,123], somatically acquired MuLV proviruses are found in the vicinity of pim-1 (approx. 50%) and/or c-myc (approx. 45%). These frequencies are probably overestimated because most of these Moloney MuLV-induced tumors are oligoclonal in origin, as evaluated by transplantation studies which indicated the presence of multiple onc-gene rearrangements in separate primary tumor-cell populations [120,145] (Fig. 2). Although many primary Moloney MuLV-induced early T-cell lymphomas are oligoclonal, serial tumor-transplantation studies unequivocally demonstrated that c-myc and pim-1 can be activated in a single monoclonal tumor line [120,145]. This supports the notion that these oncogenes may act synergistically in transforming lymphoid cells [145]. The product of pim-1 probably belongs to a class of lymphoid-specific protein kinases involved in the activation and/or proliferation of normal lymphocytes [199]. Evidence for deregulation of another lymphocyte-specific protein-kinase gene by insertional mutagenesis of a MuLV provirus was recently obtained from studies of the Moloney MuLV-induced LSTRA thymoma cell line. This gene was termed Isk^{T} [200] or tck [201]. In all cases examined, the proviral insertions are associated with high functional mRNA expression of c-myc, pim-1 or Isk^{T}/tck and, therefore, these viral insertions are probably causative factors in the generation of these tumors. Murine T-cell lymphomas induced by highly oncogenic AKR MCF viruses (latency 2–6 months) also show a high incidence of proviral integrations in the vicinity of c-myc (10–65%) or pim-1 (15–40%) [120–123,202,203]. Some of these tumors may also be oligoclonal [202,203].

Recently a new locus on chromosome 19, denoted Gin-1, was identified which is a common proviral integration site in approximately one-third of the Gross passage A-induced mouse thymomas (Villemur, R., personal communication).

Rats. In approx. 20% of Moloney MuLV-induced T-cell lymphomas in the rat, ecotropic Moloney genomes integrate in the vicinity of c-myc [148]. In addition, five common cellular regions (Mlvi-1, Mlvi-2, Mlvi-3, Mis-1 and dsi-1) for proviral DNA integration in Moloney-induced rat thymomas have been described (Refs. 146, 147, 204, 205; Steffen, D.L., personal communication). The rat Mis-1 locus corresponds with the mouse pvt-1 locus (see below) [206]. In the DNA of some of the monoclonal rat tumors proviral integrations in the vicinity of both Mlvi-1 and Mlvi-2 are observed [204]. In the Mlvi-2 region, a 4 kb mRNA transcript has been identified (Tsichlis, P.N., personal communication). Whether the four other common integration sites contain genes which are transcriptionally active in these tumors has not yet been determined.

Late murine T-cell lymphomas induced by endogenous or exogenous moderately virulent MuLV

In approx. 15% of ‘spontaneous’ AKR thymomas and MCF 1233-induced BALB/c and C57BL T-cell lymphomas (latency 6–12 months), MuLV insertions in the vicinity of pim-1 or c-myc are observed [119–123]. These tumors are predominantly monoclonal in origin [78,137]. Recently in ‘spontaneous’ AKR thymomas insertions of MCF proviruses were also observed in the pvt-1 locus [207], a locus which is defined as a chromosomal breakpoint on chromosome 15 in mouse plasmacytomas carrying the variant 6; 15 translocation [208] (see subsection IIIB).

Early Abelson-Moloney MuLV-induced myeloid tumors

The Abelson-Moloney MuLV complex induces pre-B-cell lymphomas (latency 1–3 months) in susceptible mouse strains [209]. At lower frequency myeloid tumors arise (latency 2–4 months), in which no integrations of the transforming Abelson genome are apparent [210,211]. The DNA of these tumors often contains a rearrangement in the c-myb locus [210,211] caused by the integration of a (deleted) Moloney MuLV provirus [210,211]. These viral integrations are associated with considerable transcription of c-myb and are often accompanied by the presence of c-myb mRNA of aberrant size [209–211] which most likely encodes truncated myb proteins [211]. The lack of p53 expression in the Abelson MuLV-transformed lymphoid cell line L12 is caused by the insertion of a Moloney MuLV provirus into the cellular p53 gene [212]. Reconstitution by transfection of the L12 cell line with a functional p53 gene results in a more malignant phenotype of this cell line in vivo [213]. This fits in with observations made with Friend MuLV-induced erythroleukemias, namely that over-expression of the cellular p53 gene, which was in some cases associated with rearrangements in the p53 gene, seems to enhance the malignant behaviour of tumor cells [214].

Late B and non-T/non-B murine lymphomas

With respect to spontaneous and MuLV-induced B and non-T/non-B cell lymphomas which generally develop after a long latency (6–30 months), no well-established cases of retroviral activation of cellular oncogenes have been reported. In Rauscher MuLV-induced pre-B and B-cell lymphomas rearrangements in c-myc were observed [215] but it was not reported whether retroviral insertions were involved [215]. In a large series of MuLV-induced C57BL and BALB/c B-cell lymphomas no retroviral insertions in the vicinity of c-mos, p53, c-myb or pim-1 were observed (Ref. 137; Zijlstra, M., unpublished observations). The DNA of some of the B-cell lymphomas (5 out of 82) contained an altered c-myc locus, but this could not be correlated with retroviral insertions (Matthews, E., personal communication). At low frequency (4 out of 66) retroviral insertions in the pvt-1 locus are observed in these B-cell lymphomas (Matthews, E., personal communication). The DNA of 4 out of 7 spontaneous SJL/J B-cell lymphomas contained a rearranged c-abl locus, possibly due to MuLV insertional mutagenesis (Chang, K.S.S., personal communication). A striking observation is the high mRNA expression of pim-1 in both normal B-cell blasts and B-cell hybridomas (Selten, G., personal communication).

Other examples of lymphoma/leukemia induction associated with retroviral insertion

Recently, a low frequency common proviral integration region (Fis-1) on mouse chromosome 7 in lymphomas and myelogenous leukemias induced by Friend MuLV has been reported [216]. The enhanced c-Ki-ras expression in the mouse early myeloid cell line 416B is caused by promoter insertion by a deleted Friend provirus within the c-Ki-ras gene [217].

The myeloid cell line WEHI-3B contains an insertion of an endogenous intracisternal A-particle (IAP) genome in the promoter region of the interleukin-3 (IL-3) gene which is associated with a constitutive high level of IL-3 secretion [218]. However, because the WEHI-3B cell line has been selected in vitro for a high level of IL-3 production, the biological significance for the development of this WEHI-3B tumor is presently uncertain.

Conclusions

Activation of cellular oncogenes through retroviral insertional mutagenesis has so far only been well established in MuLV-induced early (latency 2–6 months) murine T-cell lymphomas (i.e., c-myc and pim-1) and MuLV-induced early myeloid tumors (i.e., c-myb). Retroviral insertional mutagenesis involving known cellular oncogenes occurs in only a small percentage of the MuLV-induced T, B and non-T/non-B cell lymphomas which develop after a longer latency (6–30 months). In the remaining overwhelming majority of these tumors, unknown cellular oncogenes may be involved. Alternatively, mutations in cellular oncogenes or the acquisition of chromosomal abnormalities, e.g., translocations activating or deregulating cellular oncogenes (see subsection IIIB) may be more important.

IIIB. Overview of chromosome aberrations in virus- and non-virus-induced murine lymphomas and of loci important in tumorigenesis

Chromosome aberrations, including trisomy and reciprocal translocations, are characteristically found in certain types of both virus- and non-virus-induced mouse lymphomas/leukemias. The chromosomal assignment of the different (putative) mouse cellular oncogenes and of the T-cell receptor and B-cell immunoglobulin genes is shown in Table II. The different cellular oncogenes are spread over many chromosomes of the mouse (Table II). Strikingly, chromosome 15 contains both a considerable number of proven cellu-

TABLE II

CHROMOSOMAL ASSIGNMENT OF CELLULAR ONCOGENES AND THE T AND B CELL RECEPTOR GENES IN THE MOUSE

The chromosomal assignment of the mouse bcl-1, bcl-2, fgr, neu, N-myc, rel, ros, ski and yes loci has not been reported yet

Mouse chromosome no	Putative [a] cellular oncogene	T/B cell receptor genes
1	–	–
2	abl [b],src [c]	–
3	N-ras [d]	–
4	mos [b]	–
5	–	–
6	Ki-ras [c],raf [b]	κ light chain immunoglobulin gene [e], β chain T-cell receptor [f]
7	fes [b],(Fis-1) [g],Ha-ras [c],int-2 [h]	–
8	–	–
9	Ets-1 [i]	–
10	myb [c]	–
11	erb-A [j],erb-B [j],p53 [k]	–
12	fos [l]	heavy chain immunoglobulin [c]
13	–	γ chain T-cell receptor [m]
14	–	α chain T-cell receptor [m]
15	int-1 [n],(Mlvi-1) [o],(Mlvi-2) [p], myc [b],(pvt-1) [q],(Mis-1) [r],sis [b]	–
16	Ets-2 [i]	λ light chain immunoglobulin gene [c]
17	(int-3) [s],pim-1 [t],Tlym-1 [u]	–
18	–	–
19	(Gin-1) [v]	–
X	–	–
Y	–	–

[a] Putative oncogenes are listed in brackets; [b] [219], [c] [220]; [d] [221], [e] [222]; [f] [223]; [g] Friend leukemia virus integration site-1, [216]; [h] ref [224]; [i] [225], [j] [226], [k] [227]; [l] [228]; [m] [229]; [n] [230]; [o] [231], [p] [232]; [q] [208]; [r] Moloney integration site-1, identical to pvt-1 [206]; [s] MMTV, integration site-3, Galahan, D , personal communication; [t] [233]; [u] ref 234, Tlym-1 shares homology with class I MHC genes, formally Tlym-1 has not been assigned to chromosome 17, [v] Gross integration site-1, Villemur, R , personal communication

lar oncogenes (c-sis, int-1 and c-myc) as well as candidate oncogene loci implicated in a breakpoint in variant translocations in plasmacytomas (pvt-1) or as common retroviral insertion sites in T-cell lymphomas (Mlvi-1, Mlvi-2). A listing of the chromosome abnormalities observed in different types of mouse lymphoma/leukemia, is given below (Table III):

Murine T-cell lymphomas. The most common chromosome aberration in murine T-cell lymphomas is trisomy of chromosome 15 [198,235–244] (Table III). Initially trisomy 15 was found in most 'spontaneous' primary AKR/J lymphomas [235]. Subsequent studies indicated that trisomy 15 also occurred at high frequency in primary T-cell lymphomas induced by X-rays [236], RadLV [237], Moloney MuLV [238–240] or carcinogens [241–244]. That trisomy 15 is a causative event in the development of these T-cell tumors is supported by the following observations. First, studies with Moloney MuLV-induced [238] or carcinogen-induced [238,242] tumors showed that in mice that carry chromosome 15 in a Robertsonian translocation a duplication of the Robertsonian chromosome occurred in the tumor cells [238,242]. Second, carcinogen-induced T-cell tumors obtained in crosses with CBAT6T6 mice which possess a T(14; 15)6 chromosome, a nonrandom duplication of chromosome 15 was observed [241]. In (AKR × CBAT6T6)F_1 mice only duplication of the AKR-derived chromosome 15 was observed [241], while in (C57BL ×

TABLE III

CHROMOSOME ABERRATIONS IN MURINE LYMPHOMAS/LEUKEMIA

Tumor Type	Inducing agent	Mouse strain	Chrom aberrations	Ref
T	"Spontaneous" (endogenous MuLV)	AKR/J	Trisomy 15	235
T	X-rays	C57BL, 129	Trisomy 15	236
T	RadLV	C57BL	Trisomy 15,17	237
T	Moloney MuLV	Several	Trisomy 15	238
T	Moloney MuLV	A/Sn, (A × C57BL)F_1	Trisomy 15	239,240
T	Carcinogen	Several	Trisomy 15	241,242
T	Carcinogen	(C57BL/6J × DBA/2)F_1	Trisomy 1,14,15	243
Plasmacytoma	Mineral oil	BALB/c	t 12;15	222,250,251
Plasmacytoma	Mineral oil		t 6;15	208,222,250–252
Plasmacytoma	Mineral oil		t 6;12;15	260
Plasmacytoma	Mineral oil + Abelson virus	BALB/c	t 12;15;t 6,15 Trisomy 11	251
Plasmacytoma	Mineral oil	BALB/c	t 6,10	264
B cell	Miscellaneous	Several	Trisomy 15, others	272,273
Non-T/non-B cell	Carcinogen	SJL	Trisomy 3,12,18	274
Myelocytic	X-rays	C3H,RFM	Deleted chrom 2	275
Erythroid	Rauscher MuLV	BALB/c, DBA/2	Trisomy 3,15, monosomy 6	276

CBAT6T6)F_1 tumors only duplication of the CBAT6T6-derived T(14; 15)6 chromosome occurred [241]. Also in T-cell lymphomas induced by MuLV or by carcinogens in F_1 hybrids between AKR and C57BL mice, a preferential duplication of AKR chromosome 15 is observed, indicating a correlation of the presence of AKR chromosome 15 with lymphomagenesis as opposed to chromosome 15 of low leukemia-incidence C57BL mice [244]. Third, in vitro growth of a spontaneous AKR T-cell lymphoma was shown to be associated with triplication of one chromosome 15 containing an altered c-myc-containing *Eco*RI fragment [245]. Finally, in somatic hybrids between a trisomic AKR lymphoma with normal diploid fibroblasts or lymphocytes, highly tumorigenic hybrids were characterized by the amplification of a lymphoma-derived chromosome 15 [246]. Hence, the genetic content of chromosome 15 appears to be decisive for the preferential duplication in T-cell lymphomas [198].

Other chromosome aberrations have been observed as well. In approx. 50% of transplanted RadLV-induced T-cell lymphomas trisomy 17 is observed, in addition to trisomy 15 which is already present in the majority of the primary lymphomas [237]. In carcinogen-induced tumors trisomy 14 is frequently observed [242,243]. A minority of butylnitrosourea-induced T-cell tumors contain undefined translocations or a trisomy of chromosome 1 [243] (Table III). Strikingly, 3-methylcholantrene-induced T-cell lymphomas of RF mice exhibit a normal diploid complement of chromosomes [247].

Murine plasmacytomas. Murine plasmacytomas can be induced in certain inbred strains by the injection of mineral oil or the implantation of plastic dishes into the peritoneal cavity [248]; BALB/c and NZB mice are most susceptible [248]. In the development of these plasmacytomas (latency 6–12 months) the spread of endogenous infectious ecotropic MuLV is probably not important [249]. The majority of the plasmacytomas carry a reciprocal translocation between the distal portion of chromosome 15 and the distal part of chromosome 12 [222,250,251]. A minority contains a (6; 15) translocation [208,222,250–252].

In most cases the (12; 15) translocation was shown to involve a recombination between c-myc on chromosome 15 and the allelically excluded [222] α heavy-chain immunoglobulin constant region on chromosome 12 [253,254]. Also reciprocal chromosomal translocations between c-myc and the immunoglobulin γ_{2a} [255] or γ_{2b} [256] constant genes have been reported. In general, the translocated c-myc and immunoglobulin genes are found in opposite transcriptional orientation [253,256]. The (12; 15) translocation is in most cases associated with the production of a novel-size approx. 2.1 kb mRNA which lacks sequences of the first non-coding exon of c-myc [253,257,258]. In the plasmacytomas which carry a (12; 15) translocation the level of c-myc mRNA is 30–35-fold greater than in normal, quiescent B cells [259]. Normal B-cell blasts, however, express comparably high levels of c-myc mRNA [259].

In the plasmacytomas which carry the variant (6; 15) translocations the breakpoint on chromosome 6 occurs near the immunoglobulin Cκ gene [208,251,252]. The breakpoint on chromosome 15 in these tumors maps cytogenetically to the same chromosome band as c-myc [208,222, 251,252]. Surprisingly, in 5 out of 9 plasmacytomas examined, this breakpoint on chromosome 15 occurs at least 72 kbp from the c-myc gene in a locus denoted pvt-1 [208,252]. Whether the pvt-1 locus encodes a cellular oncogene or alternatively the pvt-1 locus activates c-myc via long-range effects is uncertain [208,252]. In the other four plasmacytomas examined which carry the variant (6; 15) translocation, neither pvt-1 or c-myc on chromosome 15 was involved [252]. Hence, other pvt-1-like loci may exist.

Also, κ rearrangements which have led to joining of an unknown locus at chromosome 15, the κ gene on chromosome 6 and the Sμ region of chromosome 12 have been reported [260]. In addition, a transposition of a 23 kbp segment of the immunoglobulin heavy chain locus to c-myc has been described [261].

In conclusion, the chromosomal translocations activating c-myc provide an interesting parallel with c-myc activation by retroviral insertion. As in the case of retrovirally activated c-myc the coding second and third exons of c-myc are always intact, despite considerable variability of the translocation breakpoints in or around the c-myc and Ig genes. The c-myc activation probably proceeds by several mechanisms [262], although an IgH enhancer may be the activation element in translocation involving IgH [263].

In the plasmacytoma cell line NS-1 a (6; 10) translocation is observed, in which the immunoglobulin Cκ gene has translocated to an unknown single-copy locus on chromosome 10 [264]. This locus shows no homology with a large number of cellular oncogenes including c-myb which has been localized on chromosome 10 [220].

Plasmacytomas arise in BALB/c mice more rapidly when, in addition to mineral oil, the mice are also inoculated with the Abelson-Moloney MuLV complex [251]. Most of these plasmacytomas carry a (12; 15) or a (6; 15) translocation and integrated v-abl sequences [251]. Interestingly, most of these tumors also contain a trisomy of chromosome 11 [251].

A number of plasmacytoma cell lines [265–269] and hybridomas derived from these plasmacytomas [266,267] contain a rearranged c-mos gene which is transcriptionally active and can transform mouse fibroblasts in transfection assays [265]. The c-mos rearrangement is caused by the integration of an endogenous intracisternal A-particle (IAP) genome in either a head-to-head [268,269] or head-to-tail [269] orientation 5′ to c-mos. The IAP integrations occur in the c-mos coding region and hence most likely result in the production of a smaller c-mos gene product. This is in concordance with the observation that in the XRPC-24 cell line mRNA synthesis starts either in the junction of the IAP-LTR and the 3′ part of the rearranged c-mos or within the IAP-LTR [269]. In this way the IAP integration is most likely bypassing the regulatory function of mouse sequences upstream of the unrearranged c-mos gene which normally prevent expression of c-mos [270].

Other types of mouse leukemia / lymphoma. Abelson-Moloney virus-induced pre-B cell tumors remain diploid, even after a high number of in vivo passages [271]. Most likely the integration and expression of transforming v-abl sequences is sufficient to maintain the transformed status of these tumors [209,271]. In transplanted spontaneous [272,273] and primary DMBA-induced B-cell tumors, which are surface immunoglobulin-positive, no (12; 15) or (6; 15) translocations are found, but trisomy 15 is the most common chromosomal abnormality. However, a considerable number of additional karyotypic abnormalities was observed, including at low frequency trisomy of chromosomes 1, 4, 5, 9, 11, 12, 17, 18, 19, monosomies and the presence of marker chromosomes

[273]. In 13 MuLV-induced B-cell lymphomas of C57BL or BALB/c origin, 8 tumors had an extra chromosome 15. Eight tumors had abnormalities of chromosome 11 (3 with trisomy, 2 with translocations, 3 with insertions of unknown origin). No plasmacytoma-like translocations involving c-myc were seen (Matthews et al., unpublished data).

DMBA-induced SJL non-T/non-B cell lymphomas are often trisomic for chromosomes 3, 12 and/or 18 but not for 15 [274]. Irradiation-induced myelocytic leukemias in C3H and RFM mice carry a partly deleted chromosome 2 [275]. In primary BALB/c and DBA/2 Rauscher MuLV-induced erythroid leukemias no chromosome abnormalities were found [276]. However, in transplanted tumors and cell lines derived from these tumors trisomy 15, trisomy 3 and monosomy 6 were found at high frequency [276]. The karyotype of the cell lines was rather unstable and evolved rapidly [276].

IIIC. Other etiologic factors involved in T-cell lymphomagenesis induced by Moloney MuLV in the mouse

The induction of T-cell lymphomas by Moloney murine leukemia virus is accompanied in most mouse strains by extensive viremia [277]. Another important feature of Moloney MuLV infection is the in-vivo expansion (up to 30–100-fold) of a population of immature T cells responsive to interleukin-3 (IL-3) [278,279]. Production of IL-3 can be induced in vitro in normal spleen cells by the T-cell mitogen concanavalin A or in the spleen cells of Moloney MuLV-infected mice by the addition of the Moloney MuLV gp70 or p12 proteins [280]. IL-3 enables the outgrowth of Lyt 1^-2^- T cells in vitro into continuously growing Lyt 1^+2^- T cells [281]. These Lyt 1^+2^- T cells are marked by their 20α-hydroxysteroid dehydrogenase (20α SDH) content. It is possible that Moloney MuLV infection in vivo expands the population of normal T cells expressing 20αSDH activity [282], although this has not been thoroughly studied. In addition, only approximately one-third of the Moloney MuLV-induced T-cell lymphomas expresses 20αSDH activity [282,284].

The main argument that this IL-3 induced T-cell population expressing 20αSDH activity is essential for oncogenesis comes from the difference in lymphoma incidence between the two closely related CBA/N and CBA/J mouse strains [280]. These closely related strains differ in an X-linked recessive locus which prevents the development of an immune response to certain antigens in the CBA/N mouse. Neonatal inoculation of Moloney MuLV in CBA/J mice is causing early viremia, an in vitro proliferative response to ecotropic Moloney MuLV proteins and the induction of T-cell lymphomas [280]. In neonatally inoculated CBA/N mice extensive viremia also occurs, but no in vitro proliferative response against Moloney MuLV proteins can be measured and in vivo T-cell lymphomas arise after much longer latency [280,283]. However, CBA/J mice carry an endogenous ecotropic provirus which is absent in CBA/N mice [55]. In addition, CBA/N and CBA/J mice differ in the chromosome 5 encoded Rmcf^r locus (see subsection IB) which restricts infection by MCF virus in vitro [55]. In vitro, CBA/N cells show this restriction for MCF MuLV replication but CBA/J cells do not [55]. If this restriction also operates in vivo MCF virus could spread less efficiently in CBA/N mice, leading to a lower susceptibility to T-cell lymphomagenesis.

IIID. Other etiologic factors involved in thymoma development in AKR mice

AKR mice ‘spontaneously’ develop thymomas with an incidence of over 90% within 1 year (average age of death from lymphoma is about 9 months). MCF viruses most likely play an important role in this thymoma development (see subsection IIA). Retroviral insertional mutagenesis as an important etiologic mechanism in the generation of at least a proportion of AKR thymomas was discussed in subsection IIIA. We also discussed the role of chromosome abnormalities including trisomy 15 (subsection IIIB). We shall now discuss the possibility of involvement of specific T-cell receptors for (MCF) viruses as an etiologic factor.

In studies by McGrath and Weissman with MuLV-induced AKR and C57BL thymomas, the binding of different FITC-labeled virions to lymphomas induced by different MuLV isolates was investigated [285,286]. There was a tendency of the lymphomas to preferentially bind the FITC-labeled virion of the MuLV isolate which induced that particular lymphoma. However, the number of lymphomas examined was low. In addition, some appropriate control experiments were not performed. The binding of the FITC-labeled MuLV virions to normal thymocytes was examined and found to be low, but no binding studies were performed with mitogen or interleukin-stimulated normal thymocytes or mature T cells. Nevertheless, the data were interpreted as an argument in favor of lymphoma development as a result of a specific interaction between an antigen-specific T-cell receptor expressed by the individual lymphomas and an antigen present on the viral envelope resulting in an auto-stimulation of the virus-binding (pre)leukemic cells [285,286].

Another argument used by the authors [285,286] to stress the importance of the expression of this virus-binding receptor came from transplantation studies with preleukemic thymuses and their ability to grow out to autonomous lymphomas [286]. By separating virus-binding (receptor$^+$) from non-virus-binding cells (receptor$^-$) a strong enrichment was found in the receptor$^+$ fraction of cells capable of forming tumors upon transplantation into a secondary host [286]. However, this same selection also enriched for large blast cells, which could be a common feature of preleukemic cells. Studies with a larger number of individual lymphomas, appropriate controls and use of probes specific for the T-cell receptor [287] have to be used to further investigate the validity of this auto-stimulation model.

IIIE. Antigen-specific T cells transformed by the radiation leukemia virus (RadLV)

It has been suggested that in-vivo primed antigen-specific helper T-cells [288–290], cytotoxic T cells [291] or suppressor T cells [292,293] are preferential targets for in-vitro transformation by RadLV. In these studies (in vitro selected populations of) T cells which were primed in vivo for DNP-KLH [288], OVA-DNP [289,290], hen egg-white lysozyme [292], syngeneic sarcoma cells [291] or *Torpedo californica* nicotinic acetylcholine receptor [293], were infected with RadLV in vitro, and subsequently injected into irradiated syngeneic recipients. Lymphomas arose in a number of animals after a latency of 3–6 months. Of these tumors 20–80% were shown to be of donor cell type. A number of these donor T-cell derived T-cell lymphomas possessed antigen-specific helper [288–290], cytolytic [291] or suppressor cell activity [292,293], as evaluated from in vitro antigen-specific T-cell proliferation, cytolytic T-cell and in vivo or in vitro antigen-specific plaque-forming cell (PFC) assays. However, the helper cell activity of some tumors was only marginal [288]. In addition, in most experiments it was not completely ruled out that the helper [288–290] or suppressor cell [269] activity was mediated by the production of non-specific mediators such as interleukin-2, interferon-γ, B-cell growth factor or B-cell differentiation factor.

IV. Regulation of anti-MuLV immune responses

IVA. The H-2 complex

The MHC of the mouse (H-2 complex) plays an important role in regulating immune responses to most antigens [294–298], including MuLV proteins. Immune responses which are strongly influenced by the H-2 complex include the magnitude of antibody responses against T-cell-dependent antigens, T and B lymphocyte antigen-presenting cell interactions, the production of lymphokines (e.g., interleukin-2 and γ interferon), delayed hypersensitivity reactions and the strength and specificity of virus-specific cytotoxic T-lymphocyte (CTL) responses [294–298]. The H-2

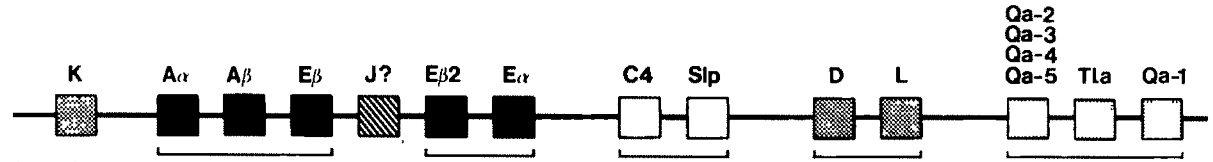

Fig 3 Genetic organization of the H-2 complex (adapted from Ref. 298)

complex is located on chromosome 17 and can be divided into six regions [295,298,299]: K, I, S, D, L and Qa/TL (Fig. 3). The products encoded by the different regions of H-2 are divided both biochemically and functionally into three classes: class I, class II and class III MHC molecules [295,298].

Class I molecules are heterodimers of an H-2 encoded 44K glycoprotein non-covalently associated with β-2 microglobulin on the outer surface of the cell membrane [295,298,299]. The non-polymorphic 12K β-2 microglobulin is encoded by a locus on chromosome 2 [299]. Class I molecules are encoded by the K, D and L regions and are expressed on most nucleated cells in the body. Their main function is specificity direction and regulation of CTL responses [294–298]. CTL directed against viral and other antigens are H-2 restricted, i.e., they recognize specific antigen in association with self class I MHC molecules. This association has been shown to be selective, i.e., a CTL response to a certain antigen occurs only if that antigen is presented in association with certain K, D or L class I MHC products [294–298]. In this way, class I molecules regulate both the magnitude and specificity of CTLs directed against viral antigens [294–298]. The class I-like molecules encoded by the Qa/TL region are only expressed on certain somatic cells including subsets of lymphocytes and their biologic function is presently unknown.

Class II molecules. The I region of the H-2 complex codes for class II MHC products: the I-A and I-E molecules. These class II molecules are membrane-bound heterodimers of non-covalently associated 32 kDa α-chain and 28 kDa β-chain glycoproteins [295,298]. A third polypeptide, which is not encoded by a locus within H-2, has been described, the 31 kDa invariant chain molecule, which occurs in the cytoplasm associated with class II molecules but not with the cell-surface forms of class II molecules [300,301]. The α chains are relatively nonpolymorphic but the β chains are highly polymorphic among different alleles. In contrast to class I molecules, class II MHC products are only expressed on certain cells in the body, e.g., B cells, Langerhans cells in the skin, thymic nurse cells and antigen-presenting cells such as macrophages and dendritic cells [295,302]. Class II molecules function as restricting elements for T-helper cells. Responses of T-helper cells occur only if a particular antigen is presented in association with a certain class II molecule. In this way, T-helper cells influence the magnitude of both CTL and antibody responses [295–297]. The existence of and the exact chromosomal site of the I-J locus which is thought to encode molecules expressed on certain suppressor T lymphocytes is both genetically and biochemically uncertain [295,299,303].

Class III molecules. Although encoded by loci within the H-2 complex, the gene products of the complement encoding loci C4 and Slp do not function as restricting and/or regulating elements for T-cell dependent immune responses and therefore are grouped separately as class III molecules.

IVB. The antibody response against MuLV virions

Most H-2-linked immune response (Ir) gene(s) which regulate anti-MuLV virion antibody responses have been mapped to the I region of the H-2 complex [304,305]. In addition, the subclass of the MuLV-specific immunoglobulins is under H-2 linked Ir gene control. High responder B10 (H-2^b) mice produce predominantly antibodies of IgG class after neonatal infection with MuLV, while low responder B10.A (H-2^a) mice produce predominantly low titer IgM [305,306]. The same Ir gene phenomena are seen after the neonatal inoculation of MCF viruses into B10 and B10.A mice [307]. It is now clear that the I region-encoded molecules responsible for the Ir gene phenomena are synonymous with class II H-2 molecules [295].

The mouse antibodies which are produced after MuLV infection/immunization are directed mainly against the MuLV gp70 and p15(E) env proteins and occasionally against gag proteins [308]. The antibodies can be group- or type-specific, but in general are a mixture of these [309–312]. Type specificity in the gp70, p15(E), gp85 env precursor, p15 and p30 viral proteins has been shown also by monoclonal antibodies specific for ecotropic AKR MuLV [18,313], the ecotropic FMR viruses [19,314–316] and MCF and/or xenotropic MuLV [19,20,317,318]. These MCF and/or xenotropic MuLV-specific antibodies are produced only under certain circumstances, e.g., after inoculation of syngeneic MCF-infected thymocytes [317] or by the induction of a GVH reaction [20,318].

Besides their titer and immunoglobulin class, the fine specificity of MuLV-specific antibodies may also be important in their biological role. Heterologous rabbit or goat anti-gp70 but not anti-p15(E) antibodies are able to neutralize MuLV in the absence of complement [319]. This finding was confirmed in a study with MuLV-specific rat/mouse monoclonal antibodies [14]. Only one monoclonal anti-gp70 antibody neutralized the infectivity of MuLV, while 8 others (5 anti-gp70 and 3 anti-p15(E)), which all recognize different epitopes, were unable to do so [14]. The binding of non-neutralizing anti-gp70 antibodies can be imagined to inhibit the binding of neutralizing anti-gp70 antibodies. This could explain why sometimes mouse sera simultaneously contain anti-gp70 antibodies and infectious MuLV [320, 321].

Other studies with the same monoclonal anti-gp70 and anti-p15(E) antibodies indicate that only the anti-p15(E) antibodies are able to lyse MuLV virions in the presence of complement [322]. This property may reflect the position of the p15(E) molecules embedded into the viral envelope, while the gp70 molecules are expressed more on the outer surface of the virion envelope. This finding is consistent with the observation that many mouse sera which contain anti-MuLV antibodies can neutralize MuLV only to some extent [323]. This neutralization is strongly enhanced, however, by the addition of heterologous guinea pig complement [324].

Of interest is the presence in high titer of a non-immunoglobulin MuLV-inactivating factor in sera of normal uninfected mice. This factor copurifies with the low-density lipoprotein fraction of mouse sera and neutralizes MCF and xenotropic, but not ecotropic MuLV [325]. NIH Swiss mice lack this factor [325].

IVC. The antibody response against MuLV-related cell-surface antigens

In addition to antibodies reactive with MuLV virions, (cytotoxic) antibodies which (exclusively) recognize MuLV-infected (tumor) cells may be an important factor in resistance against MuLV-induced lymphomagenesis [326–329]. Strikingly, a considerable number of both conventional and monoclonal anti-MuLV env-specific antibodies bind to MuLV virions, but poorly or not at all with the cell surface of MuLV-infected cells [330–332]. On the other hand, some monoclonal antibodies which recognize MCF MuLV env-precursor proteins on the cell membrane do not react with purified gp70 and/or p15(E) or intact virions (Refs. 20, 317; Zijlstra, M., unpublished observations). Furthermore, antibodies directed against the $p30^{gag}$ or the glycosylated $Pr65^{gag}$ precursor exclusively react with the outer cell membrane of infected cells, but not with intact virions [333].

Many MuLV-related cell-surface antigens have been described, which are expressed on some tumor cells and/or (subsets of) normal lymphoid cells of certain strains of mice. These antigens are defined either by conventional antibodies, i.e., the X.1 [334], GCSA [335], $G_{(RADA\text{-}1)}$ [336], $G_{(AKSL2)}$ [337], XenCSA [338] and $G_{(B10\,A)}$ [332] antigens, or are defined by monoclonal antibodies, i.e., the G_{IX} [335,339] and $G_{(ERLD)}$ [340] antigens. Detailed reviews describing most of these antigens are available [13,335]. The production of antibodies against some of these MuLV-related cell-surface antigens is under H-2 control [332,334], while in other cases the role of H-2 was not examined. Under certain circumstances (immunization with allogeneic $MuLV^+$ cells) antibodies may be produced which recognize a serologically detectable viral(-induced?) antigen which may be recognized in association with H-2 [341].

The effectiveness of (the different subclasses of) antibodies directed against MuLV-related cell-surface antigens in resistance against MuLV-induced viremia and lymphomagenesis has not been investigated in detail.

IVD. Cytotoxic T-cell response against MuLV

In general, CTL responses against the exogenous ecotropic FMR MuLV can be evoked easily in the appropriate strains of responder mice [342–344]. In contrast, CTL responses against endogenous ecotropic AKR type of MuLV can be elicited only in some strains of mice or under special circumstances, i.e., by immunization with allogeneic virus-positive tumors [345,346].

Moloney MuLV. Priming for CTL responses against this exogenous ecotropic MuLV can be performed either by the induction and subsequent regression of a sarcoma in the thigh by the Moloney-sarcoma complex [38,347,348] or by the inoculation of syngeneic tumor cells expressing Moloney MuLV [342,349]. In vitro restimulation can be performed either by Moloney MuLV-positive syngeneic tumor cells [342,348,349] or by syngeneic Moloney MuLV-infected B-cell blasts [40]. CTL responsiveness is associated with several H-2 haplotyes [343,344,348,350,351]. Mice neonatally infected with Moloney MuLV do not mount to a Moloney MuLV-specific CTL response, probably because they have a much lower Moloney MuLV-specific CTL precursor frequency than uninfected adult mice [352,353], although some weak indications for the presence of suppressor cells were also obtained [354]. Several viral antigens may be recognized by bulk cultures of Moloney MuLV-specific CTL. Cells which are transfected with molecularly cloned Moloney MuLV gp70 and p15(E) sequences are killed by bulk cultures of Moloney-specific CTL to some extent [355]. Studies by Van der Hoorn et al. [356] indicate that the $gp85^{gag}$ precursor is also recognized by CTL clones. The importance of Moloney-specific CTL in either the resistance against Moloney MuLV-induced lymphomagenesis [348] or the regression of Moloney-sarcoma complex-induced sarcomas [357,358] has been questioned. In the latter system mature T cells are necessary for rejection [347,359]. B-cell deprived [360] and natural killer(NK)-cell deprived [361] beige mice still reject the sarcoma. However, the sarcoma also regressed normally in strains of mice which in vitro do not mount a Moloney-specific CTL response [348,357,358,362]. Thus, a delayed type hypersensitivity reaction mediated by Lyt 1^+2^- T cells [347] with involvement of activated, possibly cytotoxic macrophages might play a decisive role in the sarcoma regression [347,357,358,362]. On the other hand, Moloney MuLV-specific CTL clones prevent the outgrowth of transplanted Moloney MuLV-induced lymphomas [356], which may indicate that different immunological mechanisms mediate resistance against sarcoma-versus-lymphoma development.

Friend / Rauscher MuLV. CTL specific for Friend and Rauscher MuLV-induced lymphomas have been generated [342,349,363,364]. In bulk cultures these CTL also recognize syngeneic Moloney MuLV-induced tumor cells but not lymphomas induced by AKR type of ecotropic MuLV [342]. A more complex picture is emerging from studies with individual CTL clones in which reactivity of FMR-specific CTL with AKR MuLV-induced lymphomas is sometimes observed [349]. A drawback in the interpretation of these studies is the lack of knowledge of the viral antigens recognized by the Rauscher/Friend-specific T-helper lymphocytes and CTL. Rauscher MuLV gp70 can stimulate [^{3}H]thymidine uptake by T cells in many mouse strains which indicates that some of the virus-specific T-helper cells can recognize the Rauscher gp70 molecule [365]. Indeed, helper T-cell clones have been described which can be stimulated by the Friend gp70 protein [366]. Studies with tumor cell variants indicate that the gp70 molecule could also be a target antigen recognized by the virus-specific CTL [363,364]. Recent studies by Holt et al. [367] with transfected H-2 and Friend MuLV genes point out that bulk cultures of Friend MuLV-specific CTL recognize both gag and env gene-encoded specificities.

AKR MuLV. CTL responses against ecotropic AKR type of MuLV, which is endogenous to most strains of mice, can be evoked by the inoculation of syngeneic tumor cells only in a few strains of mice [342,349,368,369]. T cells from naive non-immunized mice suppress the in vitro generation of these CTL [370]. In C57BL/6 (H-2^b) mice virus-specific CTL can only be generated under certain circumstances, i.e., by immunization with allogeneic virus-positive tumors [345,346,371]. For in vivo priming the alloantigen and the viral antigens have to be present on the same cell [346] H-2 congenic B6.H-2^k mice are poor responders in this system [372]. The viral antigens recognized by the CTL specific for AKR type MuLV are still uncertain. Initial studies indicated that the viral gag precursor could be the target antigen [371]. This finding was supported by the observation that some monoclonal antibodies directed against the gp70 and p15(E) envelope proteins of ecotropic AKR MuLV could not block the CTL activity [330], while some monoclonal anti-$p30^{gag}$ were able to do so [369]. In addition, CTL lyse cells transfected with a cloned AKV MuLV gag gene [373]. However, studies with tumor cell variants indicate that the gp70 molecule could (also) be a target for CTL [374,375]. Hence, both the gag precursor and gp70 molecule may be targets for virus-specific CTL. Which antigen is preferentially recognized may be dependent on the responder mouse strain (Plata, F., personal communication). Spleen cells of normal AKR Fv-$1^{n/n}$ mice express a CTL target antigen [376]. However, spleen cells of AKR Fv-$1^{b/b}$ mice are found to be negative for this antigen [377,378], probably because the Fv-$1^{b/b}$ genotype interferes with the spread of the N-tropic endogenous ecotropic AKR MuLV [377, 378].

Radiation leukemia virus. In several strains of mice, RadLV-specific CTL can be generated by inoculation of RadLV or RadLV-transformed cells [379–382]. Resistance to lymphomagenesis induced by a certain RadLV isolate correlates with the ability to mount a virus-specific CTL response [381]. However, resistance is also correlated with the capacity to mount a delayed-type hypersensitivity response [383]. In tumorigenesis by highly leukemogeneic RadLV variants such as A-RadLV, tumor-specific immune suppression has been invoked as an important tumor promoting mechanism [380,384].

Xenotropic / MCF MuLV. CTL responses specific for xenotropic or MCF MuLV have not been documented.

IVE. NK-cell reactivity with (MuLV-infected) tumor cells

The involvement of NK cells in resistance to murine (MuLV-induced) lymphomagenesis has been investigated mainly by three sets of experiments. First, mice with the beige (bg) mutation carry a recessive gene which is associated with a severe depression of NK-cell activity [385,386]. This depressed NK-cell activity is accompanied by a somewhat higher susceptibility to tumorigenesis after the inoculation of syngeneic leukemia cells [387,388] and with a slightly enhanced incidence of carcinogen-induced tumors including lymphomas [389]. To our knowledge no studies have been reported in which the susceptibility of bg/bg mice to MuLV-induced lymphomagenesis was examined. Second, in vitro selected NK-sensitive tumor-cell variants grow less efficiently in bg/+ mice in comparison with bg/bg mice [390]. Recent interesting studies with in vitro obtained variants of class I H-2-negative T-cell tumors indicates that these variants are much more sensitive to lysis by NK cells [391–393]. Third, cloned NK cells inhibit radiation-induced thymic leukemia [394].

The interpretation of these findings is difficult, however, because (1) NK cells are heterogeneous both in phenotype and target cell specificity and it is difficult to distinguish at least some of them from T cells [395] and (2) in beige mice not only decreased NK-cell activity but also low allo-specific T-cell responses have been reported [396], which might reflect an additional defect in T-cell function.

IVF. Effects of interferons on the spread of MuLV

Interferons are a family of glycoproteins secreted in response to either viral infection or some non-viral inducers such as double-stranded polyribonucleotides. According to their biochemical and biological properties IFNs have been classified into three categories [397]: (1) IFN-α, acid stable interferon produced by cells (including lymphocytes) in response to a viral infection; (2) IFN-β, acid stable interferon produced by virus-infected fibroblasts; and (3) IFN-γ, acid-labile interferon produced by antigen- or mitogen-stimulated T cells. Although poorly documented at this moment, the production of IFN-α, IFN-β or IFN-γ could all be important in (H-2-linked) resistance against MuLV-induced lymphomagenesis. Interferons can be envisaged to influence the process of lymphomagenesis by two main mechanisms.

First, interferons may influence MuLV replication and/or expression in MuLV-infected cells. Several isolates of MuLV have been shown to induce an uncharacterized 'IFN' in vivo [398]. In vitro studies indicate that IFN-γ inhibits MuLV replication, most likely by inhibiting the integration of proviral DNA in the cellular genome [399,400]. This could be a reflection of the more general property of 'IFN' to inhibit the stable integration of foreign (transfected) DNA [401]. In addition, 'IFN' inhibits the production of infectious MuLV particles in cells which already contain transcriptionally active proviral MuLV [402,403], perhaps as a result of an aberrant processing of some MuLV proteins [404].

Second, interferons could influence the spread of MuLV by affecting the magnitude of anti-MuLV immune responses. Molecularly cloned IFN-γ has been shown to elevate the expression of both class I and class II MHC antigens in the mouse [405,406], and therefore in this way may facilitate the generation of class-I/II-restricted MuLV-specific T-cell responses. Third, molecularly cloned IFN-γ is able to enhance the antibody production by B cells [407,408].

Anti-α/β IFN antibodies enhance in vivo the growth of some transplantable murine tumors [409]. High doses of IFN-β inhibit Rauscher MuLV-induced erythroleukemia [410]. The administration of 'IFN' to pregnant AKR mice inhibits the expression of ecotropic MuLV early in life of their progeny [411]. In all cases several (immunological) mechanisms could play a role and additional studies have to be performed with molecularly cloned IFN and monoclonal anti-IFN antibodies.

V. H-2 and MuLV-induced lymphomagenesis

VA. H-2 influence on susceptibility to MuLV-induced lymphomagenesis

Genetic control by the H-2 complex of susceptibility to MuLV-induced lymphomagenesis was first demonstrated in 1964 by Lilly et al. [412]. In crosses between C3H (H-2^k) and C57BL (H-2^b) mice, susceptibility to lymphomagenesis by the Gross passage A virus was associated with the H-$2^{k/k}$ phenotype [412]. In subsequent studies with H-2 congenic C57BL and BALB/c mice, resistance was mapped to the K-end (including the K, I-A, I-J and I-E regions) of the H-2 complex [413].

Thereafter, several H-2-linked resistance genes were mapped for different types of MuLV (Table IV). In most cases the resistance gene(s) to a particular MuLV was assigned to several regions of H-2 (Table IV), usually including a locus in the

TABLE IV

H-2-LINKED RESISTANCE LOCI IN LEUKEMOGENESIS

Adapted from Ref. 159

Virus	Position within the H-2 complex	Resistant haplotype	Locus	Postulated mechanism of resistance to leukemogenesis/remarks	Ref.
Gross passage A	K,I-A,I-J,I-E	H-2^b	Rgv-1	immunological resistance	413
Friend MuLV	D	H-2^b	Rfv-1	T-cell immunity	414–416
	K,I-A,I-J,I-E	H-2^b	Rfv-2	no explanation	415
Moloney MuLV	K,I-A	H-2^b,H-2^s	Rmv-1	production of anti-virus antibodies	304
Moloney MuLV	I-E,S	H-2^b,H-2^s	Rmv-2	production of anti-virus antibodies	304
Moloney MuLV	D-end	H-2^b,H-2^s	Rmv-3	production of anti-virus antibodies	304
A-RadLV	I-A	H-2^s	Rrv-1	immunological resistance	152,159,423
	I-E,S		Rrv-2	against preleukemic cells	423
D-RadLV	K,I-A	H-2^b	n d *	immunological resistance against preleukemic cells	152,423
RadLV (Kaplan)	K,I-A **	H-2^b	n d	immunological resistance against preleukemic cells	153
RadLV (Kaplan)	D-end	H-2^b,H-2^d	n.d	elevated H-2 expression enhances cellular immune response	151,381,420
RS-RadLV	K,I-A **	H-2^d	n d.	immunological resistance	153
B/TL MuLV	S,D	H-2^b	n d	no explanation	424
MCF 1233	I-A	H-2^b	n d	immunological resistance	Vasmel et al , unpublished data

* Not designated; ** H-2D-linked resistance also observed

I region (Table IV). This indicates that several H-2-linked immune resistance mechanisms play a role. Mapping of resistance to the I region indicates a predominant role for class II MHC-restricted (helper) T cells. These virus-specific (helper) T cells may regulate either the antibody response to virions and/or virus-infected (tumor) cells or may mediate virus-specific delayed-type hypersensitivity reactions, mediated by release of lymphokines from the T-helper cells. However, when class I MHC-restricted virus-specific CTL are involved in resistance, influences of both class I and class II MHC genes can be envisaged [297].

Two H-2-linked resistance genes have been mapped for the splenomegaly induced by the Friend MuLV complex. The first one, Rfv-1, maps to the D region of H-2 and may influence both the level and kinetics of a Friend MuLV-specific T-cell response [414–416]. The second gene, Rfv-2, is located in the K and/or I-A/E regions [414,415]. A third, non-H-2-linked gene (Rfv-3) influences recovery from both viremia and leukemia [417], most likely by regulating the formation of antibodies modulating the expression of viral cell-surface gp70 [418].

Resistance to Moloney MuLV-induced viremia has been mapped to three loci within the H-2 complex. The Rmv-1 gene maps to the K or I-A region [277,419], the Rmv-2 maps to the I-E or S region [277] and Rmv-3 maps to the D end of the H-2 complex [277]. All three Rmv genes act like immune response genes controlling the production of antiviral antibodies [304]. Rmv-1, Rmv-2 and Rmv-3 were also considered to influence the susceptibility to Moloney MuLV-induced lymphomagenesis, but so far data to support this conclusion were mainly mentioned but not shown [277,419]. Thus, the exact role of these three genes in resistance against lymphomagenesis cannot be evaluated and the important question remains whether there is a strict correlation between the magnitude of the antibody response, the level of viremia and the susceptibility to lymphomagenesis [283]. This question is especially relevant because in the same studies it was demonstrated that some non-H-2 gene(s) carried by DBA/2 and A/J mice can confer resistance to lymphomagenesis in spite of a high persisting level of viremia [277]. A sex-dependent gene linked to H-2 has been described which would significantly influence the expression of CBA genes for lymphoma resistance in F_1 hybrids with H-2 congenic BALB/c mice [283].

Susceptibility to thymoma development after intrathymic inoculation of a radiation leukemia virus (RadLV) has been assigned to the D locus of H-2 [420]. Resistance to RadLV-induced thymoma development was accompanied by a rapid increase in expression of H-2D molecules by the thymocytes of resistant mice [151] which correlated with the ability to mount a virus-specific CTL response [381]. In susceptible strains of mice no enhanced H-2D expression or virus-specific CTL were seen [151,420]. To explain this phenomenon the authors propose that a specific integration of RadLV in the vicinity of the H-2D locus occurs, which would enhance the expression of H-2D gene. However, this hypothesis and other possible mechanisms, such as the action of soluble mediators (e.g., interferon) remain to be verified [151,159,420,421]. In addition, the observation of selected enhanced class I MHC expression on MuLV-infected thymocytes of resistant mouse strains was not confirmed by others [159,422].

Lonai and Haran-Ghera investigated tumorigenesis induced by different RadLV variants [152,153]. Resistance genes were localized to the K and/or I-A regions and in addition an influence of the D region was observed [153]. Sometimes a complementation between the I-A and I-E region was apparent in resistance [152]. The mechanism(s) which confers resistance against tumorigenesis induced by these RadLV variants is (are) still unknown but appears to be mediated in some cases by I region-restricted virus-specific T cells [159, 423].

The resistance to cloned MCF 1233 virus-induced early T-cell lymphomas has been localized to the I-A region of the H-2 complex (Vasmel et al., unpublished data). Susceptibility to T-cell lymphoma development is associated with an H-2 I-A-determined high grade of permanent thymus infection (Ref. 136; Vasmel et al., unpublished data). In a comparison of anti-MuLV antibody titers and susceptibility to early T-cell lymphomagenesis induced by MCF 1233 among groups of intra-H-2 recombinant mice, a clearcut overall correlation was observed between resistance to early T-cell lymphomas and the capacity to produce high titers of anti-MuLV envelope antibodies (Ref. 307; Vasmel et al., unpublished data). However, looking at high and low antibody titers of individual mice within a single mouse strain, we found no significant correlation between the H-2-influenced anti-MuLV envelope antibody level at 2 months of age and the time of appearance of a tumor (Ref. 307; Vasmel et al., unpublished data). This implies that either the immunoglobulin subclass [305–307] or the kinetics of the antibody response are most important or alternatively, that other I region-restricted immune responses are operating (e.g., lymphokine release, delayed hypersensitivity reaction).

In conclusion, it seems that both the biological properties of different MuLV isolates and the host resistance towards these isolates are highly polymorphic. This resembles the polymorphism of Ir gene regulation of antibody responses to other viruses, foreign proteins and synthetic peptides and T-helper cell and CTL responses against different viruses and haptens [294–298]. It should be pointed out that in the studies which indicate an H-2D association with lymphomagenesis, involvement of the adjacent Qa and TL regions was not excluded in most cases. In addition, in most studies the mice were probably not examined for the presence of a milk-transmitted ecotropic MuLV or the presence of anti-MuLV antibodies, factors which can influence susceptibility to MuLV-induced lymphomagenesis [136]. The fact that most studies were performed with uncloned in vivo passaged MuLV, which probably contains several host-range classes of MuLV also complicates these studies.

Finally, the important role of non-H-2-linked genes has to be stressed. Some of these genes, such as Fv-1 (see subsection IB), exert a non-immunologic influence on lymphomagenesis by governing virus spread [46,425], while for instance the Rfv-3 gene reportedly regulates the level of anti-viral antibody responses [417,418]. In some situations these non-H-2-resistance/susceptibility genes are clearly the most important factors controlling lymphomagenesis [321,414,426–428].

VB. Imbalanced expression of MHC molecules on murine lymphomas

Class I MHC. Both in spontaneous and MuLV-induced murine lymphomas, imbalanced expression of class I MHC molecules has been observed.

Festenstein and Schmidt have reported that most primary AKR (K^kD^k) thymomas have a low cell surface expression of the K^k molecule, in contrast to a strong D^k expression [429,430]. In more adequate flow cytofluorometry experiments performed by Oudshoorn-Snoek and Demant [431] this finding was not confirmed, however. The AKR thymoma-derived cell line K36-16 lacks expression of K^k on the cell surface [432]. Transfection of this K36-16 cell line with a transcriptionally active K^k gene strongly decreases the transplantability of this cell line [432], perhaps as a result of enhanced susceptibility in vivo to a K^k-restricted MuLV-specific cytotoxic T-cell response [429,430, 432]. On the other hand, studies with variants of T-cell tumors which lack class I MHC expression indicate that these variants are much less tumorigenic due to an enhanced sensitivity to lysis by NK cells [391–393]. Certain RadLV-induced lymphomas lack MHC class I expression associated with hypermethylation of these genes [433]. In the DNA of some of these tumors altered restriction enzyme patterns of MHC class I genes are also observed [433].

Certain Moloney MuLV-induced T-cell lymphomas have also lost expression of certain class I MHC molecules [434]. Strikingly, a recent study by Flyer et al. [435] indicates that Moloney MuLV infection in mouse fibroblasts induces a 10-fold increase of class I MHC cell surface expression. Spontaneous or transplanted SJL/J B-cell lymphomas which have lost H-2D^s expression, are much more aggressive upon transplantation in syngeneic recipient mice [436]. Observations in other rodent tumor models [437–441] also indicate an important role of class I MHC gene expression in tumorigenesis and metastasis.

Class II MHC. Out of a series of 24 primary B10.A (1-A^k, I-E^k) B-cell lymphomas two readily transplantable primary B10.A (I-A^k, I-E^k) B-cell lymphomas with imbalanced class II MHC expression have been observed [442]. Both tumors show strong cell surface I-E^k expression but only minimal I-A^k expression. In one tumor the minimal cell surface I-A^k expression was associated with a strongly reduced level of $A\beta$ mRNA, while the other tumor expressed only a minimal level of $A\alpha$ mRNA [442]. The biological relevance of this finding is presently still uncertain [442].

In conclusion, in some cases immunoselection against MuLV-specific immune responses may lead to an aberrant expression of class I or class II MHC on tumor cells. In other cases, immunoselection may lead to the loss of the viral target antigen involved, as described by Van der Hoorn et al. [356] for the development of variant lymphoma cells which escape from lysis by class I MHC-restricted Moloney MuLV-specific CTL clones.

VC. Presence of H-2 molecules on MuLV virions

Contradictory observations have been made concerning the question whether H-2 molecules (selectively) incorporate into (budding) MuLV virions. Non-random inclusion of certain class I MHC antigens was noted in Friend [443–445] and Rauscher [446] MuLV particles. In immuno-electron microscopy experiments with MuLV producing cell lines, class I MHC molecules at the surface of MuLV particles were found by some [447] but not by others [448]. The latter study also failed to identify a specific association between class I MHC and viral antigens at the cell surface [448]. No studies concerning the presence of class II MHC antigens on MuLV virions have been reported.

TABLE V

SUMMARY OF THE MAIN CHARACTERISTICS OF 'SPONTANEOUS' AND MuLV-INDUCED LYMPHOMAS IN THE MOUSE

Tumor type (latency in months)	Experimental model	Type of MuLV integrations in tumor DNA	Retroviral insertional mutagenesis	Common chromosomal abnormalities
Early T (2–6)	Moloney MuLV-induced	many MCF few ecotropic	c-myc, pim-1	trisomy 15
	oncogenic MCF MuLV-induced	many MCF few ecotropic	c-myc, pim-1	n t [a]
Late T (6–12)	'spontaneous' AKR thymomas	many MCF few ecotropic	c-myc, pim-1	trisomy 15
	'spontaneous' HRS/J thymomas	n t.	n t	n t.
	MCF 1233-induced	many MCF, few ecotropic	pim-1	n t
	X-rays, carcinogens	none	n.t	trisomy 15
Early pre-B (1–3)	Abelson-Moloney MuLV-induced	transforming v-abl sequences	none [b]	none
Late B (6–30)	MuLV-induced C57BL and BALB/c tumors	ecotropic	none [c]	trisomy 15
	'spontaneous' CWD/Agl tumors	ecotropic	n t.	n.t
	GVH reaction-induced	ecotropic	none [c]	n t.
Late plasmacytomas (6–12)	mineral oil-induced	n t.	none [b]	(12;15) and (6;15) chromosome translocations
Early myeloid (2–4)	Abelson-Moloney MuLV-induced	n.t	c-myb	n.t
Later myeloid (6–24)	milk-transmitted MuLV-induced	ecotropic	n t	n t

[a] n.t, not reported; [b] examined for c-myc and c-myb, [c] examined for c-myc, pim-1 and c-myb

VI. Conclusions

The genome of all inbred and most wild mice contains a large number (15 to 30) of MuLV-related proviruses. In most inbred mice ecotropic, dualtropic MCF as well as xenotropic MuLV-related proviral sequences are present in the genome, either as intact inducible proviruses or as non-inducible (probably defective) proviruses.

A summary of the main characteristics of 'spontaneous' and MuLV-induced mouse lymphomas is given in Table V. In high 'spontaneous' lymphoma incidence AKR and HRS/J mice, the development of "spontaneous" T-cell lymphomas (latency 6–12 months) is associated with an early expression of endogenous ecotropic MuLV. Thereafter this activated endogenous ecotropic MuLV recombines with other endogenous MuLV genomes, resulting in the generation of a highly polymorphic group of ecotropic and MCF MuLV with recombinations in the viral gag-pol, gp70, p15(E) and/or LTR regions. In the DNA of these 'spontaneous' T-cell tumors (latency 6–12 months), but also in early T-cell lymphomas induced by highly oncogenic exogenous MuLV isolates (latency 2–6 months), predominantly somatically acquired MCF genomes are found (Table V). In 'spontaneous' C57BL lymphomas, which occur at much lower frequency (10–20%) and after a longer latency (12–30 months), the DNA of approximately 50% of the tumors contains integrated MuLV genomes. In the DNA of MuLV-induced and GVH reaction-induced B-cell tumors (latency 6–24 months) the majority of integrated MuLV genomes are ecotropic.

That integrated MuLV genomes activate cellular oncogenes by insertional mutagenesis has so far only been established in a limited number of experimental models. In Moloney MuLV-induced C57BL and BALB/c early T-cell lymphomas (latency 2–6 months), somatically acquired MuLV proviruses are found in the vicinity of pim-1 (approx. 50%) and c-myc (approx. 45%) (Table V). These frequencies are probably overestimated because most of these Moloney MuLV-induced tumors are oligoclonal in origin. In all cases the proviral insertion is associated with high functional mRNA expression of the cellular oncogene involved and therefore the viral insertion is most likely a causative factor in the generation of these tumors. Also in 'spontaneous' AKR (approx. 15%) and oncogenic AKV-type MuLV-induced early T-cell AKR, BALB/c and C57BL lymphomas (15–65%) MuLV insertions in the vicinity of pim-1 or c-myc are observed (Table V). Myeloid tumors (latency 2–4 months) induced by the Abelson-Moloney complex often contain an insertion of a deleted Moloney MuLV provirus in the vicinity of the c-myb locus and express a high level of functional c-myb mRNA.

With respect to B and non-T/non-B cell tumors which generally develop after a long latency (6–24 months), so far no well-established retroviral activation of known cellular oncogenes has been reported. Thus, the mechanism(s) of in vivo oncogenic transformation in the group of late B and non-T/non-B cell lymphomas and the T-cell lymphomas which do not contain retroviral integrations in the vicinity of c-myc or pim-1 is still uncertain. Unknown oncogenes might have been activated by a retroviral insertion in some of these tumors.

Alternatively, in the group of late T, B and non-T/non-B cell lymphomas a chronic immune stimulation evoked by a persistent MuLV infection is leading to the generation of point mutation in genes of the ras family or the acquisition of chromosomal aberrations which may be more relevant for malignant behavior of these tumors. This is consistent with the observation that in many of the late developing T-cell tumors trisomy 15 is frequently observed (Table V). B-cell lymphomas often contain a trisomic chromosome 15 and trisomy 3, 12 and/or 18 has been described for carcinogen-induced non-T/non-B cell lymphomas. In mineral oil-induced plasmacytomas usually a (12; 15) translocation is found, in which the c-myc gene on chromosome 15 has translocated to one of the heavy chain immunoglobulin loci on chromosome 12. A minority of the plasmacytomas contain a variant (6; 15) translocation, in which a locus on chromosome 15 denoted as pvt-1 is translocated to the κ light chain on chromosome 6. Although the pvt-1 locus cytogenetically maps to the same chromosome band, as c-myc, the pvt-1 locus is localized at least 72 kbp from c-myc.

Oncogenesis by different types of MuLV is clearly modulated by immune mechanisms (Fig.

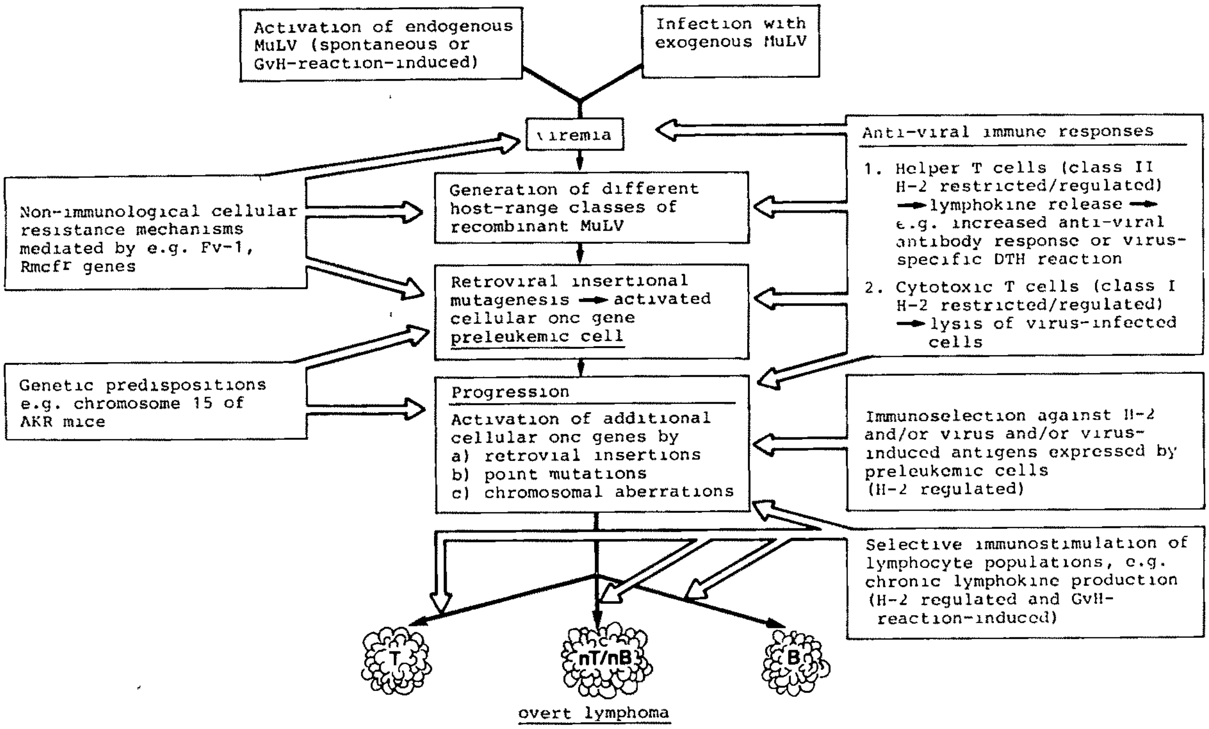
Activation of endogenous MuLV (spontaneous or GvH-reaction-induced)
Infection with exogenous MuLV
Viremia
Anti-viral immune responses
1. Helper T cells (class II H-2 restricted/regulated) → lymphokine release → e.g. increased anti-viral antibody response or virus-specific DTH reaction
2. Cytotoxic T cells (class I H-2 restricted/regulated) → lysis of virus-infected cells
Non-immunological cellular resistance mechanisms mediated by e.g. Fv-1, Rmcf^r genes
Generation of different host-range classes of recombinant MuLV
Retroviral insertional mutagenesis → activated cellular onc gene
preleukemic cell
Genetic predispositions e.g. chromosome 15 of AKR mice
Progression
Activation of additional cellular onc genes by
a) retrovial insertions
b) point mutations
c) chromosomal aberrations
Immunoselection against H-2 and/or virus and/or virus-induced antigens expressed by preleukemic cells (H-2 regulated)
Selective immunostimulation of lymphocyte populations, e.g. chronic lymphokine production (H-2 regulated and GvH-reaction-induced)
T
nT/nB
B
overt lymphoma

Fig. 4 Viral lymphomagenesis in the mouse.

4). The H-2 complex exerts a clear influence on the magnitude of anti-MuLV immune responses. Both the production and (sub)class of antibodies directed against MuLV envelope or MuLV-related cell-surface antigens is regulated by the H-2 complex. The generation and specificity of cytotoxic T lymphocytes specific for MuLV is also under H-2 control. Therefore the marked influence of the H-2 complex on resistance to viral lymphomagenesis is explained most readily by H-2-controlled immunological resistance mechanisms directed against MuLV antigens or MuLV-induced cellular antigens. The assignment of resistance to different H-2 loci (class I and class II) indicates that both class I- and class II-restricted T-cell responses mediate the H-2 influence. Indeed, H-2 controlled immune mechanisms were shown to operate at the level of anti-viral antibodies, virus-specific helper T cells, virus-specific cytotoxic T cells or I region-linked inhibition of the outgrowth of preleukemic cells. Escape from these H-2-controlled immune mechanisms could lie at the base of the imbalanced expression of class I MHC molecules on some T- and B-cell lymphomas and of the imbalanced expression of class II MHC molecules on some B cell lymphomas (Fig. 4).

The clear influence of the H-2 complex on the phenotype of lymphomas induced by neonatal inoculation of MuLV is also explained most readily by differences in H-2-controlled anti-viral immune responses. Mice with poor anti-viral immune responses undergo strong virus spread at an early age, leading to a high level of infection of the thymus and subsequent generation of T-cell lymphomas. H-2 congenic mice with better anti-viral immune responses are partly resistant to T-cell lymphomagenesis but later on, after involution of the thymus develop B-cell lymphomas.

Acknowledgements

We thank Dr. A. Berns, Dr. C.J. Lucas, Dr. P. Ivanyi and Dr. E. Matthews for critical reading of the manuscript, and G. Damhuis for typing this manuscript.

References

1 Weiss, R., Teich, N , Varmus, H and Coffin, J (1982) in RNA Tumor Viruses, 2nd Edn, Cold Spring Harbor Laboratory, NY

2 Bishop, J M. (1982) Adv Cancer Res. 37, 1–32

3 Bishop, J M. (1983) Annu Rev Biochem 52, 301–354

4 Bishop, J M (1978) Annu Rev Biochem. 47, 35–88

5 Wong-Staal, F and Gallo, R C (1985) Blood 65, 253–263

6 Gilboa, E , Mitra, S W , Goff, S and Baltimore, D (1979) Cell 18, 93–100

7 Yoshinaka, Y , Katoh, I , Copeland, T D and Oroszlan, S (1985) Proc Natl Acad Sci USA 82, 1618–1622

8 Schwartzberg, P., Colicelli, J and Goff, S P (1984) Cell 37, 1043–1052

9 Van Zaane, D and Bloemers, H P J (1978) Biochim Biophys Acta 516, 249–268

10 Varmus, H.E (1984) Annu Rev Genet 18, 553–612

11 Bishop, J M (1985) Cell 42, 23–38

12 Gross, L (1970) in Oncogenic Viruses, 2nd Edn. Pergamon Press, Oxford

13 Meruelo, D and Bach, R (1983) Adv. Cancer Res 40, 107–188

14 Nowinski, R C , Pickering, R , O'Donnell, P V , Pinter, A and Hammerling, U (1981) Virology 111, 84–92

15 Rein, A (1982) Virology 120, 251–257

16 Cloyd, M W , Thompson, M M. and Hartley, J W (1985) Virology 140, 239–248

17 Kozak, C (1985) J Virol 55, 690–695

18 Lostrom, M E, Stone, M R , Tam, M , Burnette, W N , Pinter, A. and Nowinski, R.C (1979) Virology 98, 336–350

19 Chesebro, B., Britt, W., Evans, L , Wehrly, K , Nishio, J and Cloyd, M (1983) Virology 127, 134–148

20 Portis, J.L and McAtee, F J. (1983) Virology 126, 96–105

21 Chattopadhyay, S K , Lander, M R , Gupta, S , Rands, E and Lowy, D R (1981) Virology 113, 465–483

22 Fischinger, P J , Nomura, S and Bolognesi, D P (1975) Proc Natl. Acad Sci USA 72, 5150–5155

23 Thomas, C Y and Coffin, J M (1982) J Virol 43, 416–426

24 Quint, W , Boelens, W , Van Wezenbeek, P , Cuypers, T , Robanus-Maandag, E , Selten, G and Berns, A (1984) J Virol 50, 432–438

25 Cloyd, M.W (1983) Cell 32, 217–225

26 Cloyd, M W , Hartley, J W and Rowe, W P (1980) J Exp Med 151, 542–552

27 Hartley, J W , Wolford, N K , Old, L.J and Rowe, W P (1977) Proc Natl Acad Sci. USA 74, 789–792

28 Adachi, A., Sakai, K and Ishimoto, A. (1983) J Virol 45, 447–451

29 Rein, A and Schultz, A (1984) Virology 136, 144–152

30 Chesebro, B and Wehrly, K (1985) Virology 141, 119–129

31 Oie, H K., Gazdar, A F , Lalley, P A , Russell, E K., Minna, J D , Delarco, J , Todaro, G J and Francke, U (1978) Nature 274, 60–62

32 Gazdar, A.F., Oie, H , Lalley, P , Moss, W., Minna, J D and Francke, U (1977) Cell 11, 949–956

33 Kozak, C A (1983) J Virol 48, 300–303

34 Landen, B and Fox, C F (1980) Proc Natl Acad Sci USA 77, 4988–4992

35 Robinson, P.J , Hunsmann, G , Schneider, J. and Schirrmacher, V. (1980) J. Virol 36, 291–294

36 Johnson, P.A and Rosner, M R (1986) J. Virol 58, 900–908

37 Choppin, J , Schaffar-Deshayes, L., Debré, P and Levy, J P (1981) J Immunol. 126, 2347–2351

38 Schaffar-Deshayes, L , Choppin, J. and Levy, J P. (1981) J Immunol 126, 2352–2354

39 Isaak, D D. and Cerny, J (1983) Infect Immun 40, 977–984

40 Stukart, M J., Vos, A. and Melief, C.J M (1981) Eur J Immunol. 11, 251–257

41 Horak, I., Enjuanes, L , Lee, J.C and Ihle, J.N (1981) J Virol 37, 483–487

42 Niwa, O , Yokota, Y , Ishida, H and Sugahara, T (1983) Cell 32, 1105–1113

43 Linney, E , Davis, B , Overhauser, J., Chao, E and Fan, H (1984) Nature 308, 470–472

44 Boniver, J , Declève, A , Honsik, C., Lieberman, M and Kaplan, H S. (1981) J Natl Cancer Inst. 67, 1139–1151

45 Rowe, W P and Sato, H. (1973) Science 180, 640–641

46 Jolicoer, P and Rassart, E (1981) J. Virol 37, 609–619

47 Gautsch, J.W , Elder, J E , Schindler, J , Jensen, F C and Lerner, R A. (1978) Proc Natl Acad Sci USA 75, 4170–4174

48 Ou, C Y , Boone, L R , Kok, C K , Tennant, R W. and Yang, W K. (1983) J Virol 48, 779–784

49 DesGroseillers, L and Jolicoeur, P (1983) J. Virol 48, 685–696

50 Kozak, C A (1985) J Virol 55, 281–285

51 Levy, D E , Lerner, R A and Wilson, M C (1985) Cell 41, 289–299

52 Ishimoto, A , Adachi, A., Sakai, K , Yorifuji, T. and Tsuruta, S (1981) Virology 113, 644–655

53 Ruscetti, S , Davis, L , Feild, J and Oliff, A. (1981) J Exp. Med 154, 907–920

54 Bassin, R H., Ruscetti, S., Ali, I., Haapala, D.K and Rein, A (1982) Virology 123, 139–151

55 Hartley, J W., Yetter, R A. and Morse III, H C (1983) J Exp Med 158, 16–24

56 Johnson, D.A. and Elder, J H (1983) J Exp. Med 159, 1751–1756

57 Wejman, J C., Taylor, B A , Jenkins, N A. and Copeland, N G. (1984) J Virol 50, 237–247

58 Ruscetti, S , Matthai, R and Potter, M (1985) J Exp. Med 162, 1579–1587

59 McCubrey, J and Risser, R. (1982) Cell 28, 881–888

60 Kozak, C A and Rowe, W P (1982) J Exp Med. 155, 524–534

61 Kozak, C A (1985) Adv. Cancer Res. 44, 295–336

62 Jenkins, N.A , Copeland, N G , Taylor, B A and Lee, B K. (1982) J Virol 43, 26–36

63 Moore, J.L and Chan, H W (1982) J Virol. 43, 1038–1045

64 Quint, W , Van der Putten, H , Janssen, F and Berns, A. (1982) J Virol 41, 901–908

65 Buckler, C E , Staal, S P , Rowe, W P and Martin, M A (1982) J Virol 43, 629–640

66 Steffen, D L , Taylor, B A and Weinberg, R A (1982) J. Virol. 42, 165–175

67 Rowe, W P and Kozak, C A (1980) Proc. Natl Acad Sci USA 77, 4871–4874
68 Herr, W and Gilbert, W. (1982) Nature 296, 865–868
69 Steffen, D L., Bird, S and Weinberg, R A (1980) J Virol 35, 824–835
70 Kozak, C A, Gromet, N.J., Ikeda, H and Buckler, C.E (1984) Proc Natl Acad Sci USA 81, 834–837
71 Kai, K, Sato, H and Odaka, T (1986) Virology 150, 509–512
72 Ikeda, H and Odaka, T (1983) Virology 128, 127–139
73 Ikeda, H and Odaka, T (1984) Virology 133, 65–76
74 Ikeda, H., Laigret, F, Martin, M.A. and Repaske, R (1985) J Virol. 55, 768–777
75 Colombatti, A, Dux, A, Berns, A, Démant, P. and Hilgers, J. (1979) J Natl Cancer Inst 63, 869–873
76 Buckler, C E, Hoggan, M.D, Chan, H W., Sears, J F, Khan, A.S, Moore, J L, Hartley, J W, Rowe, W P and Martin, M.A. (1982) J Virol 41, 228–236
77 Hoggan, M D., Buckler, C E, Sears, J F., Chan, H W, Rowe, W P and Martin, M A. (1982) J Virol 43, 8–17
78 Chattopadhyay, S K, Cloyd, M W, Linemeyer, D L, Lander, M R, Rands, E and Lowy, D R (1982) Nature 295, 25–31
79 Hoggan, M D, Buckler, C E, Sears, J F, Rowe, W P and Martin, M.A. (1983) J. Virol 45, 473–477
80 O'Neill, R.R, Khan, A S, Hoggan, M D, Hartley, J W, Martin, M.A. and Repaske, R. (1986) J. Virol. 58, 359–366
81 Rassart, E and Jolicoeur, P (1982) Virology 123, 175–186
82 Khan, A S. (1982) J. Virol 44, 625–636
83 Kozak, C A and Rowe, W P (1982) J Exp Med. 152, 219–228
84 Meruelo, D, Rossomando, A, Offer, M, Buxbaum, J and Pellicer, A (1983) Proc Natl Acad Sci USA 80, 5032–5036
85 Blatt, C., Mileham, K, Haas, M.; Nesbitt, M N., Harper, M E and Simon, M.I (1983) Proc Natl Acad Sci. USA 80, 6298–6302
86 Rossomando, A and Meruelo, D (1986) Immunogenetics 23, 233–245
87 Meruelo, D., Kornreich, R, Rossomando, A, Pampeno, C, Mellor, A L., Weiss, E H., Flavell, R A and Pellicer, A (1984) Proc. Natl Acad. Sci USA 81, 1804–1808
88 Pampeno, C L and Meruelo, D (1986) J Virol 58, 296–306
89 Yetter, R A, Hartley, J.W and Morse III, H C (1983) Proc Natl. Acad. Sci USA 80, 505–509
90 Herr, W and Gilbert, W (1984) J Virol. 50, 155–162
91 Cloyd, M W and Chattopadhyay, S.K (1986) Virology 151, 31–40
92 Yanagihara, K, Hamada, K., Seyama, T, Imamura, N and Yokoro, K. (1982) J Virol 41, 360–366
93 Datta, S K., Thomas, C.Y, Nicklas, J A and Coffin, J M (1983) J Virol 47, 33–45
94 Staal, S P., Hartley, W P and Rowe, W P (1977) Proc Natl Acad Sci. USA 74, 3065–3067
95 Nowinski, R C and Hays, E F (1978) J Virol 27, 13–18
96 Rein, A, Athan, E, Benjers, B M, Bassin, R H and Gerwin, B.I. (1979) Nature 282, 753–754
97 Pedersen, F.S, Crowther, R L, Tenney, D Y, Reimold, A M and Haseltine, W A (1981) Nature 292, 167–170
98 Lenz, J, Crowther, R, Klimenko, S and Haseltine, W. (1982) J. Virol. 43, 943–951
99 Villemur, R, Rassart, E, DesGroseillers, L and Jolicoeur, P (1983) J. Virol 45, 539–546
100 DesGroseillers, L, Villemur, R and Jolicoeur, P. (1983) J Virol 47, 24–32
101 Wolfe, J H and Blank, K J (1983) J Exp Med. 158, 629–634
102 Lenz, J and Haseltine, W A (1983) J Virol 47, 317–328
103 Pedersen, F S, Buchhagen, D L, Chen, C Y, Hayes, E F and Haseltine, W.A. (1980) J Virol 35, 211–218
104 O'Donnell, P V., Stockert, E, Obata, Y and Old, L J (1981) Virology 112, 548–563
105 O'Donnell, P V, Nowinski, R C and Stockert, E (1982) Virology 119, 450–462
106 Lung, M L., Hartley, J W, Rowe, W P and Hopkins, N H (1983) J Virol. 45, 275–290
107 Rowe, W P and Hartley, J W (1983) J Exp Med 158, 353–364
108 Cloyd, M W, Hartley, J W and Rowe, W P (1981) J. Exp. Med 154, 450–458
109 Lenz, J, Celander, C., Crowther, R L., Patarca, R, Perkins, D W and Haseltine, W A (1984) Nature 308, 467–470
110 Hays, E F and Levy, J A (1984) Virology 138, 49–57
111 Famulari, N G, Koehne, C F and O'Donnell, P V (1982) Proc. Natl Acad Sci USA 79, 3872–3876
112 Thomas, C Y. (1986) J Virol 59, 23–30
113 Stockert, E., O'Donnell, P V, Obata, Y and Old, L J (1980) Proc Natl Acad Sci USA 77, 3720–3724
114 Buchhagen, D L and Stockert, E (1984) J Virol 52, 624–629
115 Quint, W, Quax, W, Van der Putten, H and Berns, A (1981) J Virol. 39, 1–10
116 Yoshimura, F K and Breda, M. (1981) J Virol 39, 808–815
117 Yoshimura, F K and Levine, K L (1983) J Virol 45, 576–584
118 Herr, W. and Gilbert, W (1983) J Virol. 46, 70–82
119 Corcoran, L M, Adams, J M., Dunn, A R and Cory, S (1984) Cell 37, 113–122
120 Selten, G., Cuypers, H T, Zijlstra, M, Melief, C and Berns, A (1984) EMBO J. 3, 3215–3222
121 Li, Y, Holland, C.A, Hartley, J W and Hopkins, N (1984) Proc Natl Acad Sci USA 81, 6808–6811
122 Cuypers, H T, Selten, G, Quint, W, Zijlstra, M, Robanus Maandag, E, Boelens, W., Van Wezenbeek, P, Melief, C and Berns, A (1984) Cell 37, 141–150
123 Selten, G., Cuypers, H Th and Berns, A (1985) EMBO J 4, 1793–1798
124 Buchhagen, D L (1984) Virology 134, 287–295
125 DesGroseillers, L and Jolicoeur, P (1984) J Virol 52, 945–952
126 Holland, C A, Wozney, J, Chatis, P A, Hopkins, N and Hartley, J W (1985) J Virol. 53, 152–157
127 Holland, C A, Hartley, J W, Rowe, W P and Hopkins, N. (1985) J Virol 53, 158–165

128 Celander, D. and Haseltine, W.A (1984) Nature 312, 159–162

129 Peled, A and Haran-Ghera, N (1985) J. Exp Med 162, 1081–1086

130 Green, N , Hiai, H., Elder, J H., Schwartz, R S , Khiroya, R.H , Thomas, C Y , Tsichlis, P.N. and Coffin, J M (1980) J Exp Med 152, 249–264

131 Thomas, C Y , Khiroya, R., Schwartz, R S and Coffin, J M (1984) J. Virol 50, 397–407

132 Schwartz, R S and Khiroya, R.H. (1981) Nature 292, 245–246

133 Zielinksi, C C , Waksal, S.D , Tempelis, L D , Khiroya, R H. and Schwartz, R S (1980) Nature 288, 489–491

134 Yetter, R A. and Morse, H.C. III (1984) J. Immunol 132, 2644–2648

135 Zijlstra, M , De Goede, R E Y., Schoenmakers, H J , Schinkel, A H., Hesselink, W G , Portis, J L. and Melief, C J M (1983) Virology 125, 47–63

136 Zijlstra, M , De Goede, R E Y., Schoenmakers. H , Radaszkiewicz, T and Melief, C.J M (1984) Virology 138, 198–211

137 Zijlstra, M., Quint, W , Cuypers, Th , Radaskiewicz, Th., Schoenmakers, H., De Goede, R and Melief, C (1986) J Virol 57, 1037–1047

138 Angel, J.M. and Bedigan, H G. (1984) J Virol 52, 691–694

139 Thomas, C Y , Boykin, B J., Famulari, N G and Coppola, M A (1986) J Virol 58, 314–323

140 De Rossi, A., D'Andrea, E , Colombatti, A , Fischinger, P J. and Chieco-Bianchi, L (1981) J Natl Cancer Inst 67, 1241–1250

141 De Rossi, A., D'Andrea, E., Biasi, G , Collavo, D and Chieco-Bianchi, L (1983) Proc Natl. Acad Sci USA 80, 2775–2779

142 Jaenisch, R (1977) Cell 12, 691–696

143 Vogt, M. (1979) Virology 93, 226–236

144 Van der Putten, H , Quint, W., van Raaij, J , Maandag, E R , Verma, I.M. and Berns, A (1981) Cell 24, 729–739

145 Cuypers, H Th., Selten, G , Zijlstra, M., De Goede, R , Melief, C. and Berns, A (1986) J. Virol , in the press

146 Tsichlis, P N., Strauss, P.G and Hu, L F (1983) Nature 302, 445–449

147 Lemay, G. and Jolicoeur, P (1984) Proc. Natl Acad Sci. USA 81, 38–42

148 Steffen, D. (1984) Proc Natl Acad Sci USA 81, 2097–2101

149 Jenkins, N.A., Copeland, N.G., Taylor, B.A., Bedigan, H.G and Lee, B K (1982) J Virol 42, 379–388

150 Bedigan, H G., Johnson, D.A., Jenkins, N A , Copeland, N G and Evans, R (1984) J. Virol 51, 586–594

151 Meruelo, D (1980) J. Immunogen 7, 81–90

152 Lonai, P and Haran-Ghera, N (1980) Immunogenetics 11, 21–29

153 Lonai, P , Katz, E and Haran-Ghera, N (1980) Immunogenetics 10, 535–543

154 Haas, M and Reshef, T (1980) Eur. J Cancer 16, 909–917

155 Melief, C J M., Vlug, A , De Goede, R.E Y , De Bruyne, C., Barendsen, W. and de Greeve, P. (1980) J Natl. Cancer Inst. 64, 1179–1189

156 Pattengale, P K , Taylor, P , Twomey, P , Hill, S , Jonasson, J , Beardsley, T. and Haas, M. (1982) Am J. Pathol. 107, 362–377

157 Legrand, E , Guilleman, B., Daculsi, R and Laigret, F (1982) Int. J Cancer 30, 241–247

158 Frederickson, T N , Morse, H C., III, and Rowe, W P. (1984) J Natl. Cancer Inst 73, 521–524

159 Lonai, P., Katz, E and Haran-Ghera, N (1982) Springer Semin Immunopathol 4, 373–396

160 Janowski, M., Boniver, J and Maisin, J.R. (1982) Leukemia Res 6, 285–297

161 Newcomb, E W , Binari, R and Fleissner, E (1985) Virology 140, 102–112

162 Hoffman, P.M , Davidson, W F , Ruscetti, S.K , Chused, T M. and Morse, III, H C (1981) J Virol 39, 597–602

163 Oldstone, M.B.A., Jensen, F , Elder, J , Dixon, F.J. and Lampert, P.W (1984) Virology 128, 154–165

164 Frederickson, T N , Langdon, W Y , Hoffman, P.M., Hartley, J W and Morse III, H C. (1984) J. Natl Cancer Inst. 72, 447–453

165 Rasheed, S , Pal, B.K. and Gardner, M B (1982) Int J. Cancer 29, 345–350

166 Lai, M M.C., Rasheed, S , Shimizu, C.S and Gardner, M B. (1982) Virology 117, 262–266

167 Jolicoeur, P. and DesGroseillers, L (1985) J Virol 56, 639–643

168 Ihle, J.N., McEwan, R. and Bengali, K (1976) J Exp. Med 144, 1391–1405

169 Haran-Ghera, N and Peled, A (1979) Adv Cancer Res 30, 45–87

170 Haran-Ghera, N. (1980) in Viral Oncology (Klein, G , ed), pp 161–185, Raven Press, New York

171 Mayer, A and Dorsch-Häsler, K. (1982) Nature 295, 253–255

172 Sankar-Mistry, P. and Jolicoeur, P (1980) J Virol. 35, 270–275

173 Rassart, E , Sankar-Mistry, P , Lemay, G , DesGroseillers, L and Jolicoeur, P (1983) J Virol 45, 565–575

174 Ellis, R.W , Stockert, E. and Fleissner, E. (1980) J Virol. 33, 652–660

175 Tress, E., Pierotti, M , DeLeo, A B , O'Donnell, P V and Fleissner, E (1982) Virology 117, 207–218

176 Harvey, J.J , Tuffrey, M., Holmes, H C and East, J (1979) Int J Cancer 24, 373–376

177 Chinsky, J., Goodenow, M.M., Jackson, M , Lilly, F., Leinwand, L. and Childs, G (1985) J Virol 53, 94–99

178 Jolicoeur, P , Rassart, E and Sankar-Mistry, P (1983) Mol Cell. Biol 3, 1675–1679

179 Guerrero, I , Calzada, P , Mayer, A. and Pellicer, A. (1984) Proc Natl. Acad. Sci USA 81, 202–205

180 Geurrero, I., Villasante, A., Corces, V and Pellicer, A (1985) Proc Natl Acad. Sci USA 82, 7810–7814

181 Meruelo, D , Offer, M. and Flieger, N (1981) J. Exp Med. 154, 1201–1211

182 Meruelo, D., Offer, M and Rossomando, A. (1983) Proc Natl Acad Sci USA 80, 462–466

183 Gleichmann, E , Melief, C J.M and Gleichmann, H. (1978) Rec. Results Cancer Res 64, 292–315

184 Pals, S.T., Zijlstra, M., Radaskiewicz, Th., Quint, W., Cuypers, H.Th., Schoenmakers, H.J., Melief, C.J.M., Berns, A. and Gleichmann, E. (1986) J. Immunol. 136, 331–339

185 Levy, J.A., Datta, S.K. and Schwartz, R.S. (1977) Clin. Immunol. Immunopathol. 7, 262–268

186 Armstrong, M.Y., Weiniger, R.B., Binder, D., Himsel, C.A. and Richards, F.F. (1980) Virology 104, 164–173

187 Cross, S.S., Brede, G., Tucker III, H.S.G., Maloney, M., Montour, J.L. and Hard Jr., R.C. (1983) Infect. Immun. 41, 570–577

188 Armstrong, M.Y.K., Ruddle, N.H. and Richards, F.F. (1977) J. Exp. Med. 145, 1060–1065

189 Varet, B., Cannat, A., Feingold, N., Wechsler, J. and Levy, J.P. (1973) Cancer Res. 33, 759–763

190 Sluyser, M. and Hilgers, J. (eds.) (1981) Mammary Tumors in the Mouse, Elsevier, Amsterdam

191 Michalides, R.E., Wagenaar, E., Hilkens, J., Hilgers, J., Groner, B. and Hynes, N.E. (1982) J. Virol. 43, 819–829

192 Michalides, R., Wagenaar, E. and Weijers, P. (1985) Mol. Cell Biol. 5, 823–830

193 Dekaban, G.A. and Ball, J.K. (1984) J. Virol. 52, 784–792

194 Ball, J.K., Arthur, L.O. and Dekaban, G.A. (1985) Virology 140, 159–172

195 Dudley, J. and Risser, R. (1984) J. Virol. 49, 92–101

196 Mosier, D.E., Yetter, R.A. and Morse, H.C., III (1985) J. Exp. Med. 161, 766–784

197 Bendinelli, M., Matteucci, D.. and Friedman, H. (1985) Adv. Cancer Res. 45, 125–181

198 Klein, G. (1981) Cell 32, 311–312

199 Selten, G., Cuypers, H.Th., Boelens, W., Robanus-Maandag, E., Verbeek, J., Domen, J., Van Beveren, C. and Berns, A. (1986) Cell 46, 603–611

200 Marth, J.D., Peet, R., Krebs, E.G., and Perlmutter, R.M. (1985) Cell 43, 393–404

201 Vorona, A.F. and Sefton, B.M. (1986) Nature 319, 682–685

202 O'Donnell, P.V., Woller, R. and Chu, A. (1984) J. Exp. Med. 160, 914–934

203 O'Donnell, P.V., Fleissner, E., Lonial, H., Koehne, C.F. and Reicin, A. (1985) J. Virol. 55, 500–503

204 Tsichlis, P.N., Strauss, P.G. and Lohse, M.A. (1985) J. Virol. 55, 258–267

205 Jolicoeur, P., Villeneuve, L., Rassart, E. and Kozak, C. (1985) J. Virol. 56, 1045–1048

206 Villeneuve, L., Rassart, E., Jolicoeur, P., Graham, M. and Adams, J.M. (1986) Mol. Cell. Biol. 6, 1834–1837

207 Graham, M., Adams, J.M. and Cory, S. (1985) Nature 314, 740–743

208 Cory, S., Graham, M., Webb, E., Corcoran, L. and Adams, J. (1985) EMBO J. 4, 675–681

209 Mushinski, J.F., Potter, M., Bauer, S.R. and Reddy, E.P. (1983) Science 220, 795–798

210 Shen-Ong, G.L.C., Potter, M., Mushinski, J.F., Lavu, S. and Reddy, E.P. (1984) Science 226, 1077–1080

211 Shen-Ong, G.L.C., Morse, H.C., III, Potter, M. and Mushinski, J.F. (1986) Mol. Cell. Biol. 6, 380–392

212 Wolf, D. and Rotter, V. (1984) Mol. Cell. Biol. 4, 1402–1410

213 Wolf, D., Harris, N. and Rotter, V. (1984) Cell 38, 119–126

214 Mowat, M., Cheng, A., Kimura, N., Bernstein, A. and Benchimol, S. (1985) Nature 314, 633–636

215 Balachandran, R., Reddy, E.P., Dunn, C.Y., Aaronson, S.A. and Swan, D.C. (1984) EMBO J. 3, 3199–3207

216 Silver, J. and Kozak, C. (1986) J. Virol. 57, 526–533

217 George, D.L., Glick, B., Trusko, S. and Freeman, N. (1986) Proc. Natl. Acad. Sci. USA 83, 1651–1655

218 Ymer, S., Tucker, W.Q.J., Sanderson, C.J., Hapel, A.J., Campbell, H.D. and Young, I.G. (1985) Nature 317, 255–257

219 Land, H., Parada, L.F. and Weinberg, R.A. (1983) Science 222, 771–778

220 Sakaguchi, A.Y., Lalley, P.A., Zabel, B.U., Ellis, R.W., Scolnick, E.M. and Naylor, S.L. (1984) Proc. Natl. Acad. Sci. USA 81, 525–529

221 Ryan, J., Hart, C.P. and Ruddle, F.H. (1984) Nucleic Acids Res. 12, 6063–6072

222 Klein, G. (1983) Cell 32, 311–315

223 Caccia, N., Kronenberg, M., Saxe, D., Haars, R., Bruns, G.A.P., Goverman, J., Malissen, M., Willard, H., Yoshikai, Y., Simon, M., Hood, L. and Mak, T.W. (1984) Cell 37, 1091–1099

224 Peters, G., Kozak, C. and Dickson, C. (1984) Mol. Cell. Biol. 4, 375–378

225 Watson, D.K., McWilliams-Smith, M.J., Kozak, C., Reeves, R., Gearhart, J., Nunn, M.F., Nash, W., Fowle, N.R., III, Duesberg, P., Papas, T.S. and O'Brien, S.J. (1986) Proc. Natl. Acad. Sci. USA 83, 1792–1796

226 Zabel, B.U., Fournier, R.E.K., Lalley, P.A., Naylor, S.L. and Sakaguchi, A.Y. (1984) Proc. Natl. Acad. Sci. USA 81, 4874–4878

227 Rotter, V., Wolf, D., Pravtcheva, D. and Ruddle, F.H. (1984) Mol. Cell. Biol. 4, 383–385

228 D'Eustachio, P. (1984) J. Exp. Med. 160, 827–838

229 Kranz, D.M., Saito, H., Disteche, C.M., Swisshelm, K., Pravtcheva, D., Ruddle, F.H., Eisen, H.N. and Tonegawa, S. (1985) Science 227, 941–945

230 Nusse, R., Van Ooyen, A., Cox, D., Fung, Y.K.T. and Varmus, H.E. (1984) Nature 307, 131–136

231 Kozak, C.A., Strauss, P.G. and Tsichlis, P.N. (1985) Mol. Cell. Biol. 5, 894–897

232 Tsichlis, P.N., Strauss, P.G. and Kozak, C.A. (1984) Mol. Cell. Biol. 4, 997–1000

233 Hilkens, J., Cuypers, H.Th., Selten, G., Kroezen, V., Hilgers, J. and Berns, A. (1986) Somat. Cell Mol. Genet. 12, 81–88

234 Lane, M.A., Sainten, A., Doherty, K.M. and Cooper, G.M. (1984) Proc. Natl. Acad. Sci. USA 81, 2227–2231

235 Dofoku, R., Biedler, J.L., Splenger, B.A. and Old, L.J. (1975) Proc. Natl. Acad. Sci. USA 72, 1515–1517

236 Chang, T.D., Biedler, J.L., Stockert, E. and Old, L.J. (1977) Proc. Am. Assoc. Cancer Res. 18, 225

237 Wiener, F., Ohno, S., Spira, J., Haran-Ghera, N. and Klein, G. (1978) J. Natl. Cancer Inst. 61, 227–233

238 Spira, J., Wiener, F., Ohno, S. and Klein, G. (1979) Proc. Natl. Acad. Sci. USA 76, 6619–6621

239 Asjö, B., Fenyö, E.V., Spira, J. and Klein, G. (1980) Leukemia Res. 4, 89–103

240 Spira, J , Asjö, B , Cochran, A , Shen, F.W., Wiener, F and Klein, G (1981) Leukemia Res 5, 113–121

241 Wiener, F , Spira, J , Babonits, M., Haran-Ghera, N and Klein, G. (1980) Int. J Cancer 26, 661–668

242 Wiener, F., Spira, J , Babonits, M and Klein, G (1982) Int J. Cancer 30, 479–487

243 Carbonell, F., Seidel, H J., Saks, S and Kreja, L (1982) Int J Cancer 30, 511–516

244 Wirschubsky, Z , Wiener, F , Bregula, U and Klein, G (1984) Int J Cancer 34, 249–254

245 Wirschubsky, Z , Wiener, F , Spira, J., Sumegi, J and Klein, G (1984) Int J Cancer 33, 477–481

246 Spira, J., Wiener, F., Babonits, M., Gamble, J , Miller, J and Klein, G. (1981) Int J Cancer 28, 785–798

247 Goodenow, M , Kessler, K , Leinwand, L and Lilly, F (1986) Cancer Genet Cytogenet 19, 205–211

248 Potter, M (1972) Physiol Rev 52, 631–719

249 Potter, M., Hartley, J W., Wax, J S and Gallahan, D (1984) J Exp Med. 160, 435–440

250 Wiener, F , Babonits, M , Bregula, U , Klein, G., Leonard, A., Wax, J.S and Potter, M. (1984) J Exp Med 159, 276–291

251 Ohno, S , Migata, S , Wiener, F , Babonits, M , Klein, G , Mushinski, J F. and Potter, M (1984) J Exp Med 159, 1762–1777

252 Webb, E , Adams, J M and Cory, S (1984) Nature 312, 777–779

253 Shen-Ong, G L.C , Keath, E J , Piccoli, S P and Cole, M.D (1982) Cell 31, 443–452

254 Marcu, K B , Harris, L.J., Stanton, L.W , Erikson, J , Watt, R and Croce, C M. (1983) Proc Natl. Acad Sci USA 80, 519–523

255 Harris, L J , Remmers, E F , Brodeur, P , Riblet, R , D'Eustachio, P. and Marcu, K B (1983) Nucleic Acids Res 11, 8303–8315

256 Neuberger, M S and Calabi, F (1983) Nature 305, 240–243

257 Stanton, L.W , Watt, R and Marcu, K B (1983) Nature 303, 401–406

258 Adams, J , Gerondakis, S., Webb, E , Corcoran, L and Cory, S (1983) Proc. Natl. Acad Sci USA 80, 1073–1077

259 Keath, E J , Kelekar, A and Cole, M D (1984) Cell 37, 521–528

260 Van Ness, B G , Shapiro, M , Kelley, D.E , Perry, R P , Weigert, M , D'Eustachio, P and Ruddle, F. (1983) Nature 301, 425–427

261 Corcoran, L., Cory, S and Adams, J M (1985) Cell 40, 71–79

262 Klein, G and Klein, E (1985) Nature 315, 190–195

263 Adams, J M., Harris, A W , Pinkert, C A , Corcoran, L M , Alexander, W S , Cory, S , Palmitter, R D and Brinster, R.L (1985) Nature 318, 533–538

264 Perlmutter, R.M , Klotz, J L , Pravtcheva, D , Ruddle, F. and Hood, L (1984) Nature 307, 473–476

265 Rechavi, G , Givol, D and Canaani, E (1982) Nature 300, 607–611

266 Gattoni-Celli, S , Hsiao, W.L.W and Weinstein, I B (1983) Nature 306, 795–796

267 Cohen, J B., Unger, T , Rechavi, G , Canaani, E and Givol, D (1983) Nature 306, 797–799

268 Canaani, E , Dreazen, O , Klar, A , Rechavi, G , Ram, D , Cohen, J.B and Givol, D. (1983) Proc Natl. Acad Sci USA 80, 7118–7122

269 Horowitz, M., Luria, S , Rechavi, G. and Givol, D (1984) EMBO J 3, 2937–2941

270 Wood, T G , McGeady, M L , Baroudy, B M , Blair, D G and Van der Woude, G.F (1984) Proc Natl. Acad Sci USA 81, 7817–7821

271 Klein, G , Ohno, S , Rosenberg, N , Wiener, F , Spira, J and Baltimore, D. (1980) Int J Cancer 25, 805–811

272 Fialkow, P J., Reddy, A L. and Bryant, J I (1980) Int. J. Cancer 26, 603–608

273 Wiener, F , Babonits, M , Spira, J , Bregula, U., Klein, G., Merwin, R.M , Asofsky, R., Lynes, M and Haughton, G (1981) Int J Cancer 27, 51–58

274 Spira, J , Babonits, M , Wiener, F., Ohno, S , Wirschubski, Z , Haran-Ghera, N and Klein, G. (1980) Cancer Res. 40, 2609–2616

275 Hayata, I , Ishihara, T , Hirashima, K , Sado, T and Yamagiwa, J (1979) J Natl. Cancer Inst 63, 843–848

276 Hagemeyer, A , Smith, E.M E , Govers, F and De Both, N J (1982) J Natl Cancer Int 69, 945–951

277 Debre, P., Gisselbrecht, S , Pozo, F and Levy, J.P (1979) J. Immunol 123, 1806–1812

278 Lee, J C and Ihle, J.N (1981) Proc Natl. Acad Sci USA 78, 7712–7716

279 Fung, M C , Hapel, A J , Ymer, S , Cohen, D R , Johnson, R M , Campbell, H D and Young, I.G (1984) Nature 307, 233–237

280 Lee, J C and Ihle, J N (1981) Nature 289, 407–409

281 Hapel, A J , Lee, J C , Farrar, W L. and Ihle, J N (1981) Cell 25, 179–186

282 Papersack, L , Lee, J C , McEvan, R. and Ihle, J N (1980) J. Immunol 124, 279–285

283 Storch, T G and Chused, T M (1984) J Immunol 135, 2797–2800

284 Asjö, B , Skoog, L , Fenyo, E V and Klein, G (1982) Int J Cancer 29, 163–167

285 McGrath, M.S , Lieberman, M , Decléve, A , Kaplan, H.S and Weissman, I L (1978) J Virol. 28, 819–827

286 McGrath, M.S and Weissman, I L (1979) Cell 17, 65–75

287 Hedrick, S M., Cohen, D I , Nielsen, E A and Davis, M M (1984) Nature 308, 149–153

288 Finn, O J , Boniver, J. and Kaplan, H S. (1979) Proc Natl. Acad Sci USA 76, 4033–4037

289 Yefenof, E., Azar, Y., Eidelstein, P and Ben-Sasson, S.Z (1982) J. Immunol. 128, 625–628

290 Ben-Sasson, S Z , Saito, H , Uchida, T and Dorf, M E (1984) Cell Immunol 89, 290–299

291 Schaaf-Lafontaine, N , Martin, M T and Boniver, J (1986) Eur J Immunol 16, 320–323

292 Ricciardi-Castagnoli, P , Doria, G and Adorini, L. (1981) Proc Natl. Acad Sci USA 78, 3804–3808

293 Sinigaglia, F , Gotti, C , Ricciardi-Castagnoli, P and Clementi, F (1984) Proc Natl. Acad Sci USA 81, 7569–7573

294 Zinkernagel, R M. and Doherty, P C (1979) Adv Immunol 27, 51–117

295 Klein, J, Juretic, A, Baxevanis, C.N and Nagy, Z A (1981) Nature 291, 455–460

296 Wagner, H, Pfizenmaier, K and Röllinghoff, M (1980) Adv Cancer Res 31, 77–124

297 Melief, C J M, Stukart, M.J, De Waal, L P, Kast, W M and Melvold, R W (1983) Transplant Proc 15, 2086–2092

298 Melief, C J.M (1983) Immunol. Today 4, 57–61

299 Steinmetz, M. and Hood, L. (1983) Science 222, 727–733

300 Koch, N, Koch, S and Hämmerling, G J (1982) Nature 299, 644–645

301 Day, C E and Jones, P P (1983) Nature 302, 157–159

302 Nussenzweig, M C and Steinman, R.M. (1982) Immunol. Today 3, 65–68

303 Klyczek, K K, Cantor, H. and Hayes, C E (1984) J Exp Med 159, 1604–1617.

304 Debré, P., Boyer, B., Gisselbrecht, S., Bismuth, A and Levy, J P (1980) Eur J Immunol 10, 914–918

305 Vlug, A., Schoenmakers, H and Melief, C J M (1981) J Immunol 126, 2355–2360

306 Vlug, A, Melief, C.J M., De Bruyne, C, Schoenmakers, H and Molenaar, J L (1980) J Natl Cancer Inst 64, 1191–1198

307 Zijlstra, M, Schoenmakers, H.J and Melief, C J.M (1986) Leukemia Res, in the press

308 Nowinski, R C and Watson, A (1976) J Immunol 117, 693–696

309 Ihle, J N, Lee, J C, Collins, J J, Fischinger, P J, Pazmino, N H., Moennig, V. Schäfer, W, Hanner, M.G Jr and Bolognesi, D P (1976) Virology 75, 88–101

310 Ihle, J N., Domotor, J J Jr and Bengali, K M (1976) J Virol. 18, 124–131

311 Lee, J C, Ihle, J N and Huebner, R (1977) Proc Natl Acad Sci USA 74, 343–347

312 Boiocchi, M and Nowinski, R C (1979) Virology 96, 281–285

313 Pinter, A., Honnen, W J., Tung, J W, O'Donnell, P V and Hämmerling, U (1982) Virology 116, 499–516

314 Chesebro, B, Wehrly, K, Cloyd, M, Britt, W, Portis, J, Collins, J and Nishio, J (1981) Virology 112, 131–144

315 Niman, H L and Elder, J H (1982) Virology 123, 187–205

316 Chesebro, B, Britt, W, Evans, L., Wehrly, K., Nishio, J. and Cloyd, M (1983) Virology 127, 134–148

317 Cloyd, M.W, Chesebro, B, Portis, J L and Weir, M (1982) J Virol 41, 1112–1117

318 Portis, J L, McAtee, F J and Cloyd, M.W (1982) Virology 118, 181–190

319 Fischinger, P J, Schafer, W and Bolognesi, D P (1976) Virology 71, 169–184

320 Nowinski, R C, Kaehler, S.L and Baron, J (1976) Infect. Immun 13, 1091–1097

321 Nowinski, R C., Brown, M, Doyle, T and Prentice, R L (1979) Virology 96, 186–204

322 Orozlan, S and Nowinski, R C (1980) Virology 101, 296–299

323 Ihle, J N and Lazar, B (1977) J Virol 21, 974–980

324 Sarma, P S and Rowe, W.P (1983) J. Virol 45, 956–960

325 Montelarco, R.C, Fischinger, P J, Larrick, S B, Dunlop, N M, Ihle, J N, Frank, H., Schäfer, W. and Bolognesi, D P (1979) Virology 98, 20–34

326 Fischinger, P J, Dunlop, N M, Schwartz, H., Ihle, J N, Weinhold, K., Bolognesi, D P and Schafer, W (1982) Virology 119, 68–81

327 Adams, D O, Hall, T., Steplewski, Z and Koprowski, H (1984) Proc. Natl. Acad Sci USA 81, 3506–3510

328 Liu, W.T, Engelman, R.W., Trang, L Q, Hau, K, Good, R A and Day, N K (1984) Proc Natl Acad Sci USA 81, 3516–3520

329 Weinhold, K J, Hüpper, G., Matthews, T J, Fischinger, P J, Ihle, J N., Schwarz, H, Thiel, H J, Schäfer, W and Bolognesi, D P (1984) Virology 135, 105–117

330 Green, W R, Nowinski, R C and Henney, C S. (1980) J Immunol. 125, 647–655

331 Tam, M R, Green, W R and Nowinski, R C (1980) Cancer Res 40, 3850–3853

332 Vlug, A, Zijlstra, M, De Goede, R E Y, Hesselink, W G, Schoenmakers, H J and Melief, C J M (1983) Int J Cancer 31, 617–626

333 Ledbetter, J and Nowinski, R C (1977) J Virol 23, 315–322

334 Sato, H., Boyse, E.A, Aoki, T, Iritani, C and Old, L J (1973) J Exp Med 138, 593–606

335 Old, L.J and Stockert, E (1977) Annu Rev Genet 17, 127–160

336 Obata, Y, Stockert, E, O'Donnell, P V, Okubo, S, Snijder, H W and Old, L J (1978) J Exp Med 147, 1089–1105

337 Stockert, E, Deleo, A B, O'Donnell, P V, Obata, Y and Old, L.J (1979) J Exp. Med. 149, 200–215

338 Morse, H.C., Chused, T M, Boehm-Truitt, M., Mathieson, B J, Sharrow, S O and Hartley, J W (1979) J Immunol 122, 443–454

339 Pierotti, M., Deleo, A B, Pinter, A, O'Donnell, P V, Hämmerling, U and Fleissner, E. (1981) Virology 112, 450–460

340 Obata, Y, Stockert, E, Deleo, A B, O'Donnell, P V, Snijder, H W and Old, L.J (1981) J Exp Med 154, 659–675

341 Ivanyi, P, Melief, C J M., Van Mourik, P, Vlug, A and De Greeve, P (1979) Nature 282, 843–845

342 Plata, F and Lilly, F. (1979) J Exp Med 150, 1174–1186

343 Duprez, V, Hénin, Y and Levy, J P (1980) J Immunol Methods 37, 249–260

344 Stukart, M J, Vos, A, Boes, J, Melvold, R.W, Bailey, D W and Melief, C J M. (1982) J Immunol 128, 1360–1364

345 Green, W R, Nowinski, R C. and Henney, C S (1979) J Exp Med 150, 51–66

346 Green, W (1982) J Immunol 128, 1043–1049

347 Levy, J P and Leclerc, J C (1977) Adv. Cancer Res 24, 1–66

348 Duprez, V., Debre, P. and Levy, J P (1981) Cell Immunol 65, 317–324

349 Plata, F (1982) J Exp Med 155, 1050–1062

350 Gomard, E, Duprez, V, Reme, T, Colombani, M J and Lévy, J P (1977) J Exp Med 146, 909–922

351 Gomard, E, Hénin, Y, Colombani, M J and Lévy, J P (1980) J. Exp Med 151, 1468–1476

352 Collavo, D , Ronchese, F., Zanovello, P , Biasi, G and Chieco-Bianchi, L. (1982) J Immunol 128, 774–779

353 Ronchese, F , D'Andrea, E., Collavo, De , De Rossi, A , Zanovello, P. and Chieco-Bianchi, L (1984) Cell. Immunology 83, 379–388

354 Tilkin, A.F., Bègue, B., Gomard, E and Levy, J P. (1985) J Immunol. 134, 2779–2782

355 Flyer, D C., Burakoff, S.J. and Faller, D V (1983) Nature 305, 815–818

356 Van der Hoorn, F.A , Lahaye, T , Müller, V , Ogle, M A. and Engers, H D. (1985) J Exp Med. 162, 128–144

357 Stukart, M.J , Boes, J. and Melief, C J M. (1984) Int J Cancer 33, 265–269

358 Becker, S and Klein, E (1980) J Natl Cancer Inst 65, 811–816

359 Stutman, O. (1975) Nature 253, 142–144

360 Gordon, J., Holden, H.T , Segal, S and Feldman, M. (1982) Int. J Cancer 29, 351–357

361 Truesdale, A.T , Johnson, D.A., Bedigan, H.G., Outzen, H.C and Carlson, G.A. (1982) Cell. Immunol. 74, 120–125

362 Becker, S and Haskill, S (1980) J. Natl Cancer Inst 65, 469–475

363 Collins, J.K , Britt, W J and Chesebro, B (1980) J. Immunol 125, 1318–1324

364 Plata, F , Goodenow, M M and Lilly, F (1980) J Exp Med. 151, 726–742

365 Bubbers, J E., Elder, J H. and Dixon, F J (1980) J Immunol 124, 388–394

366 Matis, L.A , Ruscetti, S.K , Longo, D.L , Jacobson, S., Brown, E.J , Zinn, S and Kruisbeek, A.M. (1985) J Immunol. 135, 703–713

367 Holt, C.A , Osorio, K. and Lilly, F (1986) J Exp Med. 164, 211–226

368 Plata, F , Tilkin, A F , Lévy, J.P. and Lilly, F. (1981) J Exp. Med. 154, 1795–1810

369 Plata, F., Kalil, J , Zilber, M.T , Fellows, M. and Lévy, D (1983) J Immunol 131, 2551–2556

370 Tilkin, A F., Gomard, E , Begue, B and Levy, J P (1984) J Immunol 132, 520–526

371 Green, W R (1980) J. Immunol. 125, 2584–2590

372 Green, W R. (1984) J Immunol 132, 2658–2664

373 Abastado, J P., Plata, F., Morello, D., Daniel-Vedele, F. and Kourilsky, Ph (1985) J. Immunol. 135, 3512–3519

374 Green, W.R. (1983) Eur. J Immunol. 13, 863–870

375 Green, W R (1983) Eur. J. Immunol. 13, 871–877

376 Green, W.R. (1983) J Immunol. 131, 3078–3084

377 Green, W.R. (1984) J Immunol. 132, 2665–2671

378 Green, W R (1986) J. Immunol 136, 308–312

379 Yefenof, E , Tchakirov, R. and Kedar, E (1980) Cancer Immunol. Immunother. 8, 171–178

380 Yefenof, E., Meidav, A and Kedar, E (1980) J. Exp. Med. 152, 1473–1483

381 Meruelo, D. (1979) J. Exp Med 149, 898–909

382 Morishita, H., Shiku, H , Horibe, K., Obata, Y , Stockert, E , Oettgen, H F , Old, L.J and Yamada, K. (1986) J Exp. Med 163, 452–457

383 Strassmann, G. and Haran-Ghera, N. (1982) Cell. Immunol. 70, 196–199

384 Yefenof, E and Zilcha, D (1982) Int J Cancer 30, 355–359

385 Roder, J. and Duwe, A K (1979) Nature 278, 451–453

386 Roder, J.C , Lohmann-Matthes, M.L., Domzig, W. and Wigzell, H. (1979) J Immunol 123, 2174–2181

387 Kärre, K , Klein, G.O , Kiessling, R , Klein, G and Roder, J.C (1980) Int J. Cancer 26, 789–797

388 Kärre, K., Klein, G.O , Kiessling, R , Klein, G and Roder, J C (1980) Nature 284, 624–626

389 Argov, S , Cochran, A J , Kärre, K , Klein, G O and Klein, G. (1981) Int J. Cancer 28, 739–746

390 Talmadge, J E , Meyers, K.M., Prieur, D J and Starkey, J.R. (1980) J Natl. Cancer Inst. 65, 929–935

391 Ljunggren, H.G. and Kärre, K (1985) J Exp. Med. 162, 1745–1759

392 Piontek, G E., Taniguchi, K , Ljunggren, H.G , Grönberg, A , Kiessling, R., Klein, G and Kärre, K. (1985) J Immunol 135, 4281–4288

393 Kärre, K., Ljunggren, H G., Piontek, G and Kiessling, R (1986) Nature 319, 675–678

394 Warner, J.F and Dennert, G. (1982) Nature 300, 31–34

395 Minato, N., Reid, L. and Bloom, B.R (1981) J Exp Med 154, 750–762

396 Saxena, R K , Saxena, Q.B. and Adler, W.H. (1982) Nature 295, 240–241

397 Toy, J L. (1983) Clin Exp. Immunol 54, 1–13

398 Blank, K.J. and Murasko, D M (1980) Nature 283, 494–495

399 Huleihel, M and Aboud, M (1983) J Virol 48, 120–126

400 Huleihel, M , Marvitt, J and Aboud, M. (1983) Int J Cancer 31, 737–743

401 Dubois, M.F., Vignal, M , Le Cunff, M and Chany, C. (1983) Nature 303, 433–435

402 Sen, G C. and Herz, R E (1983) J. Virol 45, 1017–1027

403 Sen, G.C and Pinter, A. (1983) Virology 126, 403–407

404 Bilello, J A , Wivel, N A. and Pitha, P M (1982) J Virol 43, 213–222

405 King, D P and Jones, P.P. (1983) J Immunol. 131, 315–318

406 Wong, G H.W., Clark-Lewis, I , Harris, A.W. and Schrader, J.W (1984) Eur. J. Immunol 14, 52–56

407 Leibson, H.J , Gefter, M , Zlotnik, A , Marrack, P and Kappler, J.W. (1984) Nature 309, 799–801

408 Sidman, C.L , Marshall, J.D , Schultz, L.D , Gray, P.W. and Johnson, H.M. (1984) Nature 309, 801–804

409 Gresser, I , Belardelli, F., Maury, C , Maunoury, M.T. and Tovey, M G (1983) J Exp. Med 158, 2095–2107

410 Hekman, R.A.C.P., Prins, M E F , Bosveld, I.J and Trapman, J. (1981) Int. J. Cancer 27, 493–500

411 Murasko, D M and Blank, K J (1980) Virology 106, 148–151

412 Lilly, F., Boyse, E.A. and Old, L J. (1964) Lancet ii, 1207–1209

413 Lilly, F. and Pincus, T (1973) Adv Cancer Res 64, 231–277

414 Chesebro, B., Wehrly, K , and Stimpfling, J (1974) J Exp Med. 140, 1457–1467

415 Chesebro, B and Wehrly, K. (1978) J Immunol. 120, 1081–1085

416 Britt, W.J. and Chesebro, B. (1983) J Exp. Med. 157, 1736–1745

417 Chesebro, B and Wehrly, K (1979) Proc Natl Acad. Sci USA 76, 425–429

418 Doig, D and Chesebro, B. (1979) J. Exp Med 150, 10–19

419 Gisselbrecht, S., Pozo, F., Debre, P., Hurot, A., Lacombe, M J and Levy, J.P (1978) Int J. Cancer 21, 626–634

420 Meruelo, D , Lieberman, M., Ginzton, N., Deak, B and McDevitt, H.O (1977) J. Exp. Med 146, 1079–1087

421 Meruelo, D. and Kramer, J (1981) Transpl. Proc 8, 1858–1862

422 Katz, E , Peled, A. and Haran-Ghera, N. (1985) Leukemia Res. 9, 1219–1225

423 Lonai, P , Katz, E , Peled, A. and Haran-Ghera, N (1981) Immunogenetics 12, 423–432

424 Tennant, J. and Snell, G D (1968) J Natl Cancer Inst. 41, 597–604

425 Suzuki, S and Axelrad, A.A. (1980) Cell 19, 225–236

426 Meruelo, D , Lieberman, M., Deak, B and McDevitt, H O. (1977) J Exp Med. 146, 1088–1095

427 Risser, R., Potter, M. and Rowe, W P (1978) J Exp Med 148, 714–726

428 Chesebro, B , Wehrly, K , Doig, D and Nishio, J. (1979) Proc. Natl Acad Sci. USA 76, 5784–5788

429 Festenstein, H. and Schmidt, W (1981) Immun Rev. 60, 85–127

430 Schmidt, W and Festenstein, H (1982) Immunogenetics 16, 257–264

431 Oudshoorn-Snoek, M. and Demant, P. (1986) Int. J. Cancer 37, 303–310

432 Hui, K.H , Grosveld, F. and Festenstein, H. (1984) Nature 311, 750–752

433 Meruelo, D , Kornreich, R , Rossomando, A , Pampeno, C., Boral, A , Silver, J.L , Buxbaum, J , Weiss, E.H., Devlin, J J., Mellor, A.L , Flavell, R.A. and Pellicer, A. (1986) Proc. Natl. Acad Sci. USA 83, 4504–4508

434 Baldacci, P , Pozo, F , Gisselbrecht, S. and Kourilsky, P. (1983) J Exp. Med 158, 1294–1306

435 Flyer, D C., Burakoff, S J. and Faller, D V. (1985) J. Immunol 135, 2287–2292

436 Rosloniec, E.F., Kuhn, M.H., Genyea, C A , Reed, A H , Jennings, J J., Giraldo, A A , Beisel, K W and Lerman, S P (1984) J Immunol. 132, 945–952

437 Schrier, P I , Bernards, R , Vaessen, R.T M.J , Houweling, A and Van der Eb, A J. (1983) Nature 305, 771–775

438 Bernards, R., Schrier, P I , Houweling, A , Bos, J.L , Van der Eb, A.J., Zijlstra, M. and Melief, C J M (1983) Nature 305, 776–779

439 Tanaka, K., Isselbacher, K.J., Khoury, G. and Jay, G. (1985) Science 228, 26–30

440 De Baetselier, P., Katsav, S., Gorelik, E., Feldman, M and Segal, S. (1980) Nature 288, 179–181

441 Wallich, R., Bulbuc, N , Hämmerling, G.J., Katsav, S., Segal, S. and Feldman, M. (1985) Nature 315, 301–305

442 Zijlstra, M., Vasmel, W.L.E , Voormanns, M , De Goede, R E Y., Schoenmakers, H J., Nieland, J., Slater, R.M and Melief, C J.M. (1986) J Exp. Med 163, 1213–1226

443 Bubbers, J.E. and Lilly, F. (1977) Nature 266, 458–459

444 Bubbers, J.E., Chen, S. and Lilly, F. (1978) J Exp Med 147, 340–351

445 Chen, S and Lilly, F. (1979) Immunogenetics 9, 25–31

446 Schaffar-Deshayes, L., Choppin, J and Levy, J P (1983) Int J. Cancer 31, 329–335

447 Aoki, T and Takahashi, T (1972) J Exp. Med. 135, 443–457

448 Calafat, J , Demant, P. and Janssen, H (1981) Immunogenetics 14, 203–220

Biochimica et Biophysica Acta 865 (1986) 233
Elsevier

ERRATA

BIOCHIMICA ET BIOPHYSICA ACTA, VOL. **865** (1986)

p. 1, right-hand column, line 4 of text:
for 'I' read 'II'

p. 4, left-hand column, lines 8 to 6 from bottom should read:
cells were mostly Lyt-1$^+$,2$^+$ (putative cytotoxic cells; see below) while about 10–15% were Lyt-1$^+$,2$^-$ (putative helper cells) [59]. By day 8, a

p. 6, left-hand column, lines 32 and 38:
for 'B6.CAST.GP1^a' read 'BG.CAST.Gpi.1^a'

Biochimica et Biophysica Acta **Vol. 865, No. 2**
Reviews on Cancer CR13(2) October 28, 1986

Contents

Gene expression during the mammalian cell cycle (BBA 87156)
by D T Denhardt, D.R Edwards and C L.J Parfett (London, Canada) 83

Idiotypic interactions in immune responses to tumor-associated antigens (BBA 87159)
by V K. Lee, K.E. Hellström and G.T. Nepom (Seattle, WA, U S A) 127

Monoclonal antibody applications in bone marrow transplantation (BBA 87160)
by C.L. Reading and Y. Takaue (Houston, TX, U S.A) 141

The plasma-membrane-associated form of SV40 large tumor antigen. biochemical and biological properties (BBA 87161)
by J S. Butel and D L Jarvis (Houston, TX, U S.A.) 171

Virology, genetics and immunology of murine lymphomagenesis (BBA 87162)
by M. Zijlstra and C.J M Melief (Amsterdam, The Netherlands) 197

Errata 233

Cited in. Current Contents Life Sciences - Biological Abstracts - Chemical Abstracts - Index Chemicus - Index Medicus - Excerpta Medica (EMBASE)

INFORMATION FOR CONTRIBUTORS TO BIOCHIMICA ET BIOPHYSICA ACTA

The 1982 edition of this booklet, offering detailed guidance to authors, is available free of charge from the BBA Editorial Secretariat, P.O. Box 1345, 1000 BH Amsterdam, The Netherlands. It is also published as Biochim. Biophys. Acta 715 (1982) 1–23.

BIOCHIMICA ET BIOPHYSICA ACTA
International Journal of Biochemistry and Biophysics
Founded in 1947 by H G.K Westenbrink, Managing Editor 1947–1964

© 1986, Elsevier Science Publishers B V (Biomedical Division)
Printed in The Netherlands

All rights reserved No part of this publication may be reproduced, stored in a retrieval system, or transmitted, in any form or by any means, electronic, mechanical, photocopying, recording or otherwise, without the prior written permission of the publisher, Elsevier Science Publishers B V (Biomedical Division), P O Box 1527, 1000 BM Amsterdam, The Netherlands. Submission of a paper to this journal entails the author's irrevocable and exclusive authorization of the publisher to collect any sums or considerations for copying or reproduction payable by third parties (as mentioned in article 17 paragraph 2 of the Dutch Copyright Act of 1912 and in the Royal Decree of June 20, 1974 (S 351) pursuant to article 16b of the Dutch Copyright Act of 1912) and/or to act in or out of Court in connection therewith

Special regulations for readers in the U S.A. This journal has been registered with the Copyright Clearance Center, Inc. Consent is given for copying of articles for personal or internal use, or for the personal use of specific clients. This consent is given on the condition that the copier pays through the Center the per-copy fee stated in the code on the first page of each article for copying beyond that permitted by Sections 107 or 108 of the U S Copyright Law The appropriate fee should be forwarded with a copy of the first page of the article to the Copyright Clearance Center, Inc , 27 Congress Street, Salem, MA 01970, U S.A. If no code appears in an article, the author has not given broad consent to copy and permission to copy must be obtained directly from the author. All articles published prior to 1980 may be copied for a per-copy fee of US$ 2 25, also payable through the Center. This consent does not extend to other kinds of copying, such as for general distribution, resale, advertising and promotion purposes, or for creating new collective works. Special written permission must be obtained from the publisher for such copying

Special regulations for authors. Upon acceptance of an article by the journal, the author(s) will be asked to transfer copyright of the article to the publisher. This transfer will ensure the widest possible dissemination of information